

[REDACTED]

NASA Conference Publication 2175

Proceedings of the Twelfth Annual Precise Time and Time Interval (PTTI) Applications and Planning Meeting

A meeting held at the
Goddard Space Flight Center
Greenbelt, Maryland
December 2—4, 1980



U. S. AIR FORCE

NASA Conference Publication 2175

Proceedings of the Twelfth Annual Precise Time and Time Interval (PTTI) Applications and Planning Meeting

A meeting held at the
Goddard Space Flight Center
Greenbelt, Maryland
December 2—4, 1980

Sponsored by :
Naval Observatory
NASA Goddard Space Flight Center
Naval Research Laboratory
Defense Communications Agency
Chief of Naval Operations
National Bureau of Standards
and
Army Electronics Technology and Devices Laboratory



National Aeronautics and
Space Administration

Scientific and Technical
Information Office
1981

EXECUTIVE COMMITTEE

**Schuyler C. Wardrip, Chairman
NASA Goddard Space Flight Center**

**Ralph T. Allen
Naval Electronic Systems Command**

**Charles A. Bartholomew
Naval Research Laboratory**

**Andrew R. Chi
NASA Goddard Space Flight Center**

**LCDR Glen E. Eubanks
Chief of Naval Operations**

**Dr. Arthur O. McCoubrey
National Bureau of Standards**

**James A. Murray, Jr.
Naval Research Laboratory**

**Kenneth Putkovich
Naval Observatory**

**Dr. Harris A. Stover
Defense Communications Agency**

**Straton M. Spyropoulos
Naval Observatory**

**Dr. John R. Vig
Army Electronics Technology
and Devices Laboratory**

GENERAL CHAIRMAN

DR. ARTHUR O. McCOUBREY
National Bureau of Standards

TECHNICAL PROGRAM COMMITTEE

CHARLES A. BARTHOLOMEW, CHAIRMAN
Naval Research Laboratory

ROBERT B. MOORE
Naval Research Laboratory

DR. VICTOR S. REINHARDT
NASA Goddard Space Flight Center

DR. FRED L. WALLS
National Bureau of Standards

PAUL F. KUHNLE
Jet Propulsion Laboratory

KENNETH PUTKOVICH
Naval Observatory

EDITORIAL COMMITTEE

L.J. RUEGER, CHAIRMAN
Johns Hopkins University
Applied Physics Laboratory

RALPH T. ALLEN
Naval Electronic Systems Command

SANDRA HOWE
National Bureau of Standards

ERIC BLOMBERG
Smithsonian Astrophysical
Observatory

Dr. HARRIS A. STOVER
Defense Communications Agency

DR. R. GLENN HALL
Naval Observatory

SCHUYLER C. WARDRIP
NASA Goddard Space Flight Center

PAUL F. KUHNLE
Jet Propulsion Laboratory

CHARLOTTE M. HARRIGAN-SECRETARY
Applied Physics Laboratory

SESSION CHAIRMEN

SESSION I

Dr. Gernot M.R. Winkler
Naval Observatory

SESSION IIA

Dr. Martin Levine
Frequency and Time Systems, Inc.

SESSION IIB

Dr. Harris A. Stover
Defense Communications Agency

SESSION III

James A. Buisson
Naval Research Laboratory

SESSION IV

Dr. James Barnes
National Bureau of Standards

SESSION V

David Howe
National Bureau of Standards

ARRANGEMENTS

Shirley E. Darby, GSFC
Donald C. Kaufmann, GSFC
Paul J. Kushmeider, GSFC
William O'Leary, GSFC
Dr. Victor S. Reinhardt, GSFC
Schuyler C. Wardrip, GSFC

FINANCE COMMITTEE

Kenneth Putkovich, USNO
Schuyler C. Wardrip, GSFC

PUBLICATIONS

Schuyler C. Wardrip, GSFC

PRINTING

Charles V. Hardesty, GSFC
Donald E. Ellis, GSFC

RECEPTIONISTS

Charlotte Harrigan, APL
Donna Kline, NBS
Kathy McDonald, NRL
Marie Nader, GSFC
Dorothy Outlaw, USNO
Stella Scates, NRL
Emma Thomas, GSFC

BANQUET SPEAKER

Professor Joseph Weber
University of California, Irvine
and University of Maryland, College Park

CALL TO SESSION

Dr. Arthur McCoubrey
National Bureau of Standards

WELCOME ADDRESS

Dr. John E. McElroy
Deputy Director, NASA Goddard Space Flight Center

OPENING COMMENTS

Rear Adm. R.J. Eustace, Vice Commander,
Naval Electronic Systems Command

Capt. Raymond A. Vohden
Superintendent, Naval Observatory

Capt. E.E. Henifin
Commanding Officer,
Naval Research Laboratory

FOREWORD

These proceedings contain the papers presented at the Twelfth Annual Precise Time and Time Interval (PTTI) Applications and Planning Meeting held December 2-4, 1980, at NASA Goddard Space Flight Center. They also include the discussions following the presentations.

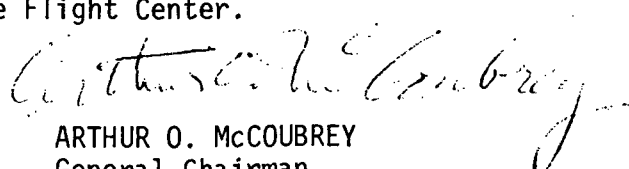
The purpose of the PTTI Applications and Planning Meeting, as defined for 1980, was to give Managers, Systems Engineers, Program Planners, and Industry:

- An opportunity to discuss current and future needs, problems, and programs;
- An overview of state-of-the-art in PTTI applications;
- A review of significant accomplishments in applications;
- A view of important future trends;
- Future applications.

There were 220 registered attendees from government, private industry, universities, and 19 registrants came from foreign countries.

This year, a special emphasis was placed upon the subject of reliability, which has become critically important in the applications of PTTI equipment. With this in mind, speakers were invited to describe their experiences in achieving high levels of reliability in other programs involving high technologies. In addition, the technical program was organized in order to emphasize the importance of views of industry, on one hand, and the views of government officials, on the other hand, in the process of effective planning.

On behalf of the Executive Committee, I particularly want to recognize the excellent efforts of the Session Chairmen and of the Technical Program Committee under the leadership of Mr. C. A. Bartholomew. As in the past, the quality of the technical program was excellent, and the interest in PTTI continues at a high level. I also want to thank the Session Chairmen for their efficient conduct of the Meeting. Finally, it is a pleasure to recognize the contributions of S. Clark Wardrip and the hospitality of NASA Goddard Space Flight Center.


ARTHUR O. MCCOUBREY
General Chairman

CONTENTS

	<u>Page</u>
CALL TO SESSION	1
<i>Dr. Arthur O. McCoubrey</i>	
WELCOME ADDRESS	3
<i>Dr. John McElroy</i>	
OPENING COMMENTS	5
<i>Rear Admiral R. J. Eustace</i>	
OPENING COMMENTS	7
<i>Capt. Raymond A. Vohden</i>	
OPENING COMMENTS	9
<i>Capt. E. E. Henifin</i>	

SESSION I RELIABILITY

Management of Reliability and Maintainability; A Disciplined Approach to Fleet Readiness.	13
<i>W. J. Willoughby, Jr.</i>	
Reliability Achievement in High Technology Space Systems.	57
<i>D. L. Lindstrom</i>	
Approach to Reliability When Applying New Technologies	69
<i>J. C. Bear</i>	
Reliability and the Design Process at Honeywell Avionics Division	81
<i>A. Bezat</i>	
A Space System for High-Accuracy Global Time and Frequency Comparison of Clocks	99
<i>R. Decher, D.W. Allan, C.O. Alley, R.F.C. Vessot and G.M.R. Winkler</i>	

CONTENTS (continued)

Page

SESSION IIA GOVERNMENT PLANNERS

Department of Defense Precise Time and Time Interval Program Improvement Plan.....	115
<i>J. R. Bowser</i>	
A U.S. Navy Precise Time and Time Interval (PTTI) Program Update.....	127
<i>R. T. Allen</i>	
Precise Time Technology for Selected Air Force Systems: Present Status and Future Requirements.....	141
<i>N. F. Yannoni</i>	
NASA PTTI Programs; Present and Future	151
<i>S. C. Wardrip and W. M. Hocking</i>	
Contracting for Research and Development	199
<i>D. H. Weber</i>	

SESSION IIB INDUSTRY VIEWS

Frequency and Time Generation and Control.....	211
<i>M. B. Bloch</i>	
Government and Industry Interactions in the Development of Clock Technology.....	253
<i>H. Hellwig</i>	
Innovation and Reliability of Atomic Standards for PTTI Applications	275
<i>R. Kern</i>	
R & D: To Fund or Not to Fund	281
<i>T. N. Osterdock</i>	
Contractor Point of View for System Development and Test Program	291
<i>F. K. Koide, D. E. Ringer, and C. E. Earl</i>	

CONTENTS (continued)

Page

SESSION III TIME TRANSFER

Progress of the LASSO Experiment.....	307
<i>B. E. H. Serene</i>	
Two-way Sequential Time Synchronization: Preliminary Results from the SIRIO-1 Experiment.....	329
<i>E. Detoma and S. Leschiutta</i>	
Flight and Ground Tests of a GOES Satellite Time Receiver for Satellite Communications Applications.....	351
<i>R. L. Swanson and S. A. Nichols</i>	
PTTI Applications at Hydro-Québec.....	377
<i>G. Missout, J. Béland, and G. Bédard</i>	
USNO GPS Program.....	387
<i>K. Putkovich</i>	
Design Considerations for a Loran-C Timing Receiver in a Hostile Signal to Noise Environment.....	417
<i>J. W. Porter, J. R. Bowell, and G. E. Price</i>	
Short Turn-Around Intercontinental Clock Synchronization Using Very-Long-Baseline Interferometry—A Progress Report.....	445
<i>G. A. Madrid, T. P. Yunck, and R. B. Henderson</i>	

SESSION IV FREQUENCY STANDARDS AND CLOCKS

Recent Progress in the NASA-Goddard Space Flight Center Atomic Hydrogen Standards Program.....	463
<i>V. S. Reinhardt</i>	
Passive Maser Development at NRL.....	495
<i>J. White, A. Frank, and V. Folen</i>	
Reference Clock Parameters for Digital Communications Systems Applications.....	515
<i>P. Kartaschoff</i>	

CONTENTS (continued)

	<u>Page</u>
An Analytic Technique for Statistically Modeling Random Atomic Clock Errors in Estimation	551
<i>P. J. Fell</i>	
Vacuum Pumping System for Spaceborne Passive Hydrogen Masers	581
<i>S. A. Wolf, D. U. Gubser and L. D. Jones</i>	
Frequency and Timing System for the Consolidated DSN and STDN Tracking Network	591
<i>R. C. Coffin, D. E. Johnson, and P. F. Kuhnle</i>	
The Operational Performance of Hydrogen Masers in the Deep Space Network	615
<i>S. C. Ward</i>	

SESSION V ADVANCED TECHNOLOGY

Source Structure Errors in Radio-Interferometric Clock Synchronization for Ten Measured Distributions.	635
<i>J. B. Thomas</i>	
Geodynamics Frequency and Phase.	647
<i>F. O. Vonbun and V. S. Reinhardt</i>	
Time and Frequency Stability for the Crustal Dynamics Project.	649
<i>R. Coates, J. Ryan, and T. Herring</i>	
Optical Fibers for the Distribution of Frequency and Timing References.	663
<i>G. F. Lutes</i>	
On Estimating the Effects of Clock Instability with Flicker Noise Characteristics.	681
<i>Sien-Chong Wu</i>	
NAVSTAR Global Positioning System (GPS) Clock Program: Present and Future	703
<i>Capt. D. M. Tennant</i>	
Development of a Sub-Miniature Rubidium Oscillator for SEEKTALK Application.	719
<i>H. Fruehauf, W. Weidemann, and E. Jechart</i>	

CONTENTS (continued)

	<u>Page</u>
The NATO III 5 MHz Distribution System	743
<i>A. Vulcan and M. Bloch</i>	
The SA-2239/WLQ-4(V) Cutty Sark Distribution System	765
<i>A. Vulcan and J. Ho</i>	
Precision Timekeeping Using a Small Passive Hydrogen Maser	785
<i>F. L. Walls and D. A. Howe</i>	
Statistical Analysis on Three TV-based Time Scales in Italy: Accuracy and Performances	805
<i>L. Mureddu</i>	
Progress Report on Hydrogen Maser Development at Laval University	807
<i>J. Vanier, G. Racine, R. Kanski, and M. Picard</i>	
Some New Results on the Frequency Characteristics of Quartz Crystals Irradiated by Ionizing and Particle Radiations.	829
<i>H. Bahadur and R. Parshad</i>	
Precise Time and Frequency Intercomparison Via VLF Phase Measurements	851
<i>A. S. Gupta, G. K. Goel, and B. S. Mathur</i>	
Precise Time and Frequency Intercomparison Between NPL, India and PTB, Federal Republic of Germany Via Satellite Symphonie-1	863
<i>B. S. Mathur, P. Banerjee, P. C. Sood, M. Saxena, N. Kumar, and A. K. Suri</i>	
List of Attendees	875

CALL TO SESSION

Dr. Arthur O. McCoubrey
National Bureau of Standards

DR. MCCOUBREY: Good Morning. As your General Chairman, it is my pleasure to call to order this 12th Annual Precise Time and Time Interval Applications meeting. I am very pleased to note that the interest in this meeting remains high and that the attendance is already excellent.

Let me remind you of the purpose of the PTTI meeting. It is a meeting to provide managers, system engineers, program directors, and industry with an opportunity to discuss, for planning purposes, current and future needs, problems and programs, to provide for an overview of the state-of-the-art in PTTI applications, to review significant accomplishments in applications, and to review important future trends in applications. I am pleased to say that we have an excellent technical program. The technical interest in this Precise Time and Time Interval Applications meeting remains very high reflecting the rapid advances that continue to emerge.

I want to thank the Technical Program Committee, ably headed by Mr. Charles Bartholomew. They have selected 47 papers from those submitted. Forty-one of these papers will be included in the formal program and a number of additional papers which cannot be included in the formal presentations because of time limitations will be published in the proceedings. Forty-one papers in the formal program exceeds the number presented last year, and I am sure you will appreciate that we have a crowded schedule.

The emphasis which we have selected today for the opening session of the meeting places the subject of reliability up front. PTTI is a field in which applications of very advanced technology are necessary and I am sure you will agree that the questions of reliability is not only important now, but as we apply this technology in more and more demanding situations the importance continues to increase. Therefore, the first session this morning brings a number of speakers from fields in which reliability has been an essential objective for many years; we will have the benefit of their important experience in advanced technology field other than PTTI.

Later today, during this afternoon, the first part of Session II will deal with the perceptions of Government planners; this part of the meeting will be moderated by industry. Later in the afternoon, the second part of the planning session takes up the industry views; this part will be moderated by Government representatives.

Tomorrow we have a session on time transfer. We also have a session on frequency standards and clocks. On Thursday a session on advanced technology is scheduled.

Let me remind you that, as usual, on Wednesday evening we have our informal banquet. This year we are very privileged to have Professor Joseph Webber as a speaker. Professor Webber divides his time between the University of California at Irvine and the University of Maryland here in College Park. His subject tomorrow evening is Listening for Extra Terrestrial Intelligence. Professor Webber is a most interesting speaker and we will have a very interesting evening. I urge you to attend and, in this connection, I also urge you to make your plans early and purchase your tickets.

Next then it is a pleasure for me to call upon officials of our sponsoring agencies to open the meeting. First let me call upon a representative of our host institution, NASA Goddard Space Flight Center. NASA Goddard is also a sponsor of PTTI and it is a pleasure for me to introduce Dr. John McElroy, Deputy Director of NASA Goddard Space Flight Center.

WELCOME ADDRESS

Dr. McElroy
Deputy Director:
NASA-Goddard Space Flight Center

Good morning, ladies and gentlemen. I must say it is a very great pleasure on my part to be able to welcome you to this 12th PTTI conference.

This is the sixth time Goddard has hosted the PTTI and we always welcome the opportunity to do so. It is a personal pleasure because some years ago, about 10 or 15 or so, I was in the organization which housed the hydrogen maser program here at Goddard and I know the spirited discussions which came out of the previous PTTI's and related meetings. Harry Peters and Vic Reinhart and many of the others used to come back from those meetings with many interesting stories. And if this meeting is as spirited as some of those that they told me about, then I am sure it will be a very successful meeting.

I recall the subject of wall effects on hydrogen masers being a popular one for many years. I remember the vigorous arguments that went on as to whether a hydrogen maser would ever be good for anything. But we seem to have passed that stage these days.

There are a number of NASA papers that will be presented over the next three days that will discuss much of what we do here at Goddard in the Precision Frequency and Time fields, but I would like to mention just a couple of those activities and highlight them because we are, indeed, quite proud of them.

Our new hydrogen masers are now becoming available for direct support of the study of crustal movements where accuracies of less than one centimeter per year are required over distances of hundreds to thousands of kilometers. Over the next 4 years we expect to construct three to four of the NASA research or NR masers per year. These added to our existing NASA prototype, or NP masers, will give us about 15 hydrogen masers for support of various NASA programs.

These new NR masers, which have frequency stabilities of a few parts in ten to the fifteenth are under microprocessor control and will be monitored and controlled from Goddard.

The experimental work is continuing in this area with the development of variable volume masers, I am sure a subject which is of great interest to many of you, and a new field operable maser design which should be reproducible at a much lower cost than present designs, and picking up on Dr. McCoubrey's comments, hopefully with a lot higher reliability as well.

Our interferometry work continues with the use of the Mark III wide band, very long baseline interferometry systems. These systems are currently located at Westford, Massachusetts, Greenbank, West Virginia, Owens Valley, California, Fort Davis, Texas, and Onsala, Sweden.

A portable system has already been out to Germany and to England and is now presently at Goldstone, California.

The velocity measurement goals of the crustal dynamics project are accuracies of 4/10 of a centimeter per year for a 5-year measurement span and 7/10 of a centimeter per year for a 3-year measurement span.

To date we have been able to achieve an RMS value of three centimeters between Haystack and Owens Valley, a distance of 4000 kilometers over a 4-year period.

During the 1980's we are going to replace most of our worldwide ground tracking network with two large geostationary communication satellites, the Tracking and Data Relay Satellite System.

The TDRSS, as it is called, will greatly increase spacecraft communications capability, but will also be used to time synchronize the TDRSS ground terminal at White Sands, New Mexico to terminals here at Goddard and, thus, to the U.S. Naval Observatory to within some 100 nanoseconds.

In cooperation with the Naval Research Laboratory we are developing GPS timing receivers that will be used in our laser ranging network for sub-microsecond timing in support of the crustal dynamics project.

All of these activities, I think, show that Goddard is, indeed, very interested in the subject of this conference.

We have some very distinguished guests here today from other PTTI sponsoring agencies. Among them we have Rear Admiral Eustace, who is Vice Commander of the Naval Electronic Systems Command, Captain Vohden, who is the Superintendent of the Naval Observatory, and Captain Henifin, Commanding Officer, Naval Research Laboratory.

I would also like to welcome and acknowledge the attendance of our foreign guests. Many of us in our own travels are hosted and treated extremely well when we visit laboratories around the world and we are certainly delighted to have the opportunity to reciprocate at least in a small fashion.

Of the 44 papers in the program, 10 are from authors from other countries. Certainly your presence at this meeting makes for a much more meaningful discussion and you are indeed welcome.

I thank you all for coming and for the opportunity to greet you this morning and I sincerely hope that you have a very good 3 days.

OPENING COMMENTS

Rear Admiral R. J. Eustace
Vice Commander
Naval Electronic Systems Command

REAR ADMIRAL EUSTACE: Thank you, Dr. McCoubrey. Good Morning ladies and gentlemen. I want to join in welcoming all of you here today and particularly our foreign guests, as was noted.

It is a pleasure to be here as a representative of the Naval Electronic Systems Command because we are one of the cosponsors of this 12th Annual Precise Time and Time Interval Applications and Planning Meeting.

NAVELEX is the Navy's PTTI program manager. As such we are, of course, a vitally interested member of this community. We understand the problems confronting you and by sharing our problems with you we hope to achieve something from our collective efforts.

We at NAVELEX supply the Navy's fleet with electronic communications, navigation, and command and control systems. These systems have very demanding time and time interval requirements. The systems are constantly being modernized and replaced with newer systems which have even more stringent and demanding timing requirements.

It is only through your efforts to develop new, more accurate, reference standards and time dissemination and distribution systems and techniques that we in NAVELEX are able to support the demands of our fleet.

In scanning your agenda I noted that reliability is the subject of the first session. This is putting first things first. We, in the Navy, are concerned with systems that work; we have too many that don't. We need reliable support systems, including PTTI reference standards and distribution systems.

Like you, I will be interested in hearing what Mr. Willoughby and the other speakers have to say concerning the reliability requirements and capabilities.

I also note that Government PTTI planning and industry's response to that planning is high on the agenda. Again, I concur, that is the kind of dialogue which is extremely important if we in the Navy are to fulfill our increasingly demanding mission.

I encourage each of you to take full advantage of the opportunities you will have during the next three days to keep abreast of the rapidly advancing technology.

Before finishing, I would like to make two announcements which I think you will find of interest. First, in response to NAVELEX's recommendation, the Chief of Naval Operations has validated the Navy's requirement to maintain time on the Global Positioning System satellites to within 100 nanoseconds relative to Coordinated Universal Time. That requirement has been forwarded to the GPS Program Office.

Also, just last month, the Chief of Naval Operations approved the continued maintenance of time on the current TRANSIT satellites to 20 microseconds at a one Sigma relative to UTC.

It is our belief that the maintenance of time in these satellites to within these tolerances will provide the Navy, the other services, and the civilian community with an essential, valuable reference source.

I am certain you will find this planning meeting to be mutually profitable and productive. I am equally certain that the NASA people will again prove to be commendable hosts. It has been my pleasure to welcome you and to thank you for participating.

OPENING COMMENTS

Captain Raymond A. Vohden

Superintendent, U. S. Naval Observatory

CAPT VOHDEN: Mr. Chairman, Ladies and Gentlemen: This morning I have the pleasure of speaking for Admiral Williams who, regrettably, had a previous commitment as the guest speaker for the Annual Meeting of the American Institute of Aeronautics and Astronautics. Admiral Williams wears two hats, he is the Director, Naval Oceanography Division (OP-952) and the Oceanographer of the Navy, both in the Office of the Chief of Naval Operations. He is responsible for people and money resources for the Naval Observatory and he is my boss. As OP-952, he has the task of coordinating the entire Navy PTTI effort. In this capacity, he monitors precise time and time interval functions pertaining to Verdin, Communications, Navigation and the Master Clock Upgrade.

We at the Observatory are optimistic about the future of PTTI in the Navy in that Admiral Williams brings to his position a unique expertise and enthusiasm. At 12 years of age, Admiral Williams was already an accomplished navigator. A graduate from the Naval Academy in 1951, he has served as a navigator on a destroyer; he had three tours on ballistic missile submarines, once as the executive officer and twice as commanding officer. More recently, he served in the Office of the Secretary of Defense as Military Assistant to the Deputy Director, Strategic and Space Systems. At the Observatory we are convinced that, under his leadership, PTTI is on the ascendancy.

Although I have learned a great deal about "time" in the last year as the Superintendent of the Naval Observatory, I find that the more I know the more there is to learn.

The requirements for precise time continue to be more demanding, consequently the Naval Observatory continues to look for means to improve time transfers and to make the U. S. Master Clock more precise and more accessible. The upgrading of the Master Clock continues and we hope to guarantee one (1) nanosecond real-time precision. A prototype Global Positioning System (GPS) receiver has been checked out by the Naval Observatory and time transfers of 30 nanoseconds anywhere in the world are now possible. The monitor results are available on the Naval Observatory's digital information service within less than 24 hours. Of almost equal importance is the speed with which the time service information can reach the user. This year we inaugurated a new digital information service with direct access to parts of our data base and with real-time measurement capability.

While preparing my welcoming remarks, I thought it might be useful to review the proceedings from the past 11 meetings. It was interesting to discover that the original purpose of the first conference was not to duplicate the typical engineering meeting where the emphasis is on papers about new work and accomplishments but, rather, its purpose was to be a planning meeting to reveal if we were meeting all of the PTTI requirements and to determine what could be done better. The emphasis was on capabilities and user needs. Questions and discussions were indispensable to the success of those meetings. Therefore, again, I suggest to you the importance of questions and discussions as the best means to assure the optimum amount of communication among all participants. This should also lead to suggestions to PTTI users for new applications, procedures and techniques and will allow the PTTI researchers to assess fruitful directions for future research efforts.

The Naval Observatory, located on Massachusetts Avenue in Northwest Washington, is well worth a visit for those of you who may not have been there already. Besides being a place of considerable scientific interest, it is a rather pleasant place to visit. In its present location, the Observatory dates back to 1893. It was originally known as the Depot for Charts and Instruments and was founded on December 6, 1830. And for this reason, we will have the opportunity to celebrate our 150th Anniversary on December 6 of this year. A tour of the Naval Observatory is scheduled for the evening of December 2. I'm sure you will find the tour a very interesting and worthwhile experience.

You appear to have a very impressive program outlined for the next two days. I'm sure you are going to have a very productive meeting. Thank you.

OPENING COMMENTS

Captain E. E. Henifin
Commanding Officer
Naval Research Laboratory

CAPTAIN HENIFIN: Good Morning ladies and gentlemen. It is a distinct pleasure for me, on behalf of the Naval Research Laboratory, to make some brief comments at the 12th Annual Precise Time and Time Interval Applications and Planning meeting.

First a sincere thank you to Tom Young and NASA Goddard for providing the fine facilities of the Goddard Space Flight Center for the meeting. Many of you may have been expecting the meeting to be at NRL this year and I apologize if you are disappointed. However, a spurious pulse in the alternating-GSFC/NRL-hosting-circuit has caused a phase shift.

Secondly, I would like to extend to Captain Vohden, Dr. Westerhout, and to all of the employees, past and present of the Naval Observatory, a heartily happy 150th birthday and may the present lead to a bright, prosperous and timely future.

Thirdly, I would like to offer a welcome to the office of the CNO and to the National Bureau of Standards, the sixth and seventh sponsors of this meeting joining with USNO, NASA/GSFC, NAVELEX, DCA and NRL in insuring PTTI continuance.

Back in April 1969 when USNO alone sponsored the first PTTI, it's purpose was to provide a forum for discussion and coordination among Government planners. It was soon expanded to take advantage of valuable inputs from industry and foreign participants.

That original purpose remains today and it may not be the formal sessions that are of underlying importance rather it may be the informal face to face, eyeball to eyeball discussions between sessions, at coffee breaks, and at the social functions that pay the real dividends. And when the meeting is over no one will really know the value of this meeting. But exchange of ideas between planners, users, and doers is priceless. We at NRL are firm believers that meetings, small or large, are a necessity for the exchange of IDEAS.

The formal sessions and papers are the means to facilitate thinking, to generate questions, to formulate new ideas. Hence the attendees, you in the audience, need to be listeners, good listeners so that each of you can put the speakers on the spot with the hard and difficult questions that may develop new ideas. I charge you not to be passive attendees but to be active participants.

I believe the Program Committee has put together an excellent series of sessions, each with a superb group of papers and you should be on with the program.

Thank you for coming and I hope you have a rewarding three days here at Goddard.

Page Intentionally Left Blank

SESSION I

RELIABILITY

Dr. Gernot M.R. Winkler, Chairman
Naval Observatory

MANAGEMENT OF RELIABILITY AND MAINTAINABILITY;
A DISCIPLINED APPROACH TO FLEET READINESS

Willis J. Willoughby, Jr.
Deputy, Chief of Navy Material for
Reliability and Maintainability
And Quality Assurance, Navy Material Command
Washington, D.C.

It certainly is my pleasure to be here at Goddard again. It has been a number of years since I have been here. I was at NASA for a number of years in the past, but I recall a remark of my very own that came to me as I was listening to the introduction.

When Apollo was over, I said to the Administrator of NASA that I want \$10 and a new suit. I don't know whether you understand that expression or not, but when you get out of jail the first thing they give you is \$10 and a new suit.

Apollo was over. I said, I am through with reliability, we have done a job, I don't want anything more to do with it. I came from a systems engineering group and I said, I want to get back into that business and get out of this game called reliability.

Well, the \$10 and a new suit didn't last long because I was thrown into the Navy to see if we could manage to turn around a trend in the Navy which was very detrimental; the lack of operating life in Naval equipment.

Now, I use the term operating life. That is what I grew up with and the Navy calls it reliability. Whatever you want to call it, it is all the same thing.

Today you are here to learn, listen and talk a lot on the subject of precision time. I think also you should put the word precision in your mind very carefully because that is really what reliability and what the quality assurance world is all about. It is really the precision of how you do something.

What we learned in Apollo was that nothing in the terms of operating life happens by accident and that you can have reliable systems without redundancy. As a matter of fact we had many systems that were very important and that were not redundant, although we did have quite a bit of redundancy.

When you don't have redundancy, such as the military has a great lack of, then you must depend on how you design your systems and you must depend on how you manufacture your systems. So today what I would like to hold in front of you is the term "precision," because that is what it is all about. We are going to talk a little bit about the experience, what has happened in the Navy in the past years, where we have been and where we think the program is really paying off.

I think there is quite a bit of excitement in terms of our own contractors and ourselves as to what we see being introduced to the fleet, which has a primary job to do.

If you notice, in the Figure 1 we didn't put in reliability and quality assurance and that is for a very good reason. For a number of years, I think most people have become mesmerized with the word "reliability" and "quality" and there is a little story about the runner who went out to see how the war went and the runner came back and said, "the war doesn't go too well, Emperor." And the Emperor says, "shoot the runner."

That is really what I found happening, when I came to the Navy. We had reliability people standing up, answering questions that should have been properly addressed to the designer and we had people standing up in quality assurance circles trying to answer questions which really belonged to the manufacturing community. So we have decided to focus where it is important and put our hands around the throat of the guy who is really doing it to us; the designer and the manufacturer.

The reliability and quality organizations have a purpose and a point; and we are not in any way circumventing their role, but what we are trying to do is make sure that we focus on where the culprit is and that is the designer and the manufacturer. You will see very little discussion about reliability and quality itself, but you will see it more centered around the design arena and around the manufacturing arena, which is where it all takes place.

I think the thing that is important is the word "mandate", in Figure 2. On Apollo we had a mandate and that was to land three men on the moon and bring them back safely within the decade.

That mandate means a lot. The Navy decided back in the mid-'70's that the fleet was not doing well and that parts and people were not the answer to bad equipment. And they really put a mandate out and this is how I got involved.

They said, we want to change the way the Navy operates in terms of the equipment operating life and these are the three commands that are involved: the Air Command, the Elex Command and the Sea Command.

In Figure 3 is shown how the mandate carried itself out. On the slide you can see the office I now hold (06). It is a responsible role along with the logistics community and the acquisition community. The three operations report directly to the Chief of Naval Material. So that means we have recognized the mandate and the organizational structure which is, of course, very important.

A little bit in terms of motivation. I saw Figure 4 in the Patent Office on documents that I was reading not too long ago. It is a plow in combination with a gun. I am sure that the designer of this machine, back in the time period when that plow was made, was doing it for protection, but I couldn't help but think what a great motivation that would be if you were the mule who was pulling the plow.

~~Of course what we want to talk about is the management of a disciplined approach.~~ The whole secret to this business of precision is a matter of discipline (see Figure 5), how you go about it and how your understanding takes place during the course of that discipline.

Now normally speaking this is what you would find yourself dealing with in terms of reliability and what I saw the Navy dealing with back in the mid-'70's is their version of reliability. It has been charted for simple understanding, but it is what I refer to as the game of random nines.

Figure 6 is a chart that portrays how the acquisition cost (A) increases as the reliability is increased. The support cost (S) decreases as the reliability is increased.

This chart was supposed to tell you that for some Delta increase in reliability here, that there is a point on the acquisition cost curve where it would be too expensive to continue to develop the equipment in terms of placing it into a higher reliability category.

And, of course, this chart is absolutely true if you are intending to manage your reliability by a test program. If you are intending to test your reliability into your program then, of course, this is the kind of a curve you would see in terms of the acquisition costs, because you would be spending so much money for time, equipment, test chambers and it would be very late in the program, it would be a very costly kind of an operation.

And I have seen these type of curves run before on equipment and they are referred to as cost drivers. And in any program where you run into reliability as a cost driver, what you will find most times is that you are dealing with a program where the test philosophy is reigning supreme, rather than the design philosophy.

So this is the game that I got involved with when I first came to NASA back in the mid-'60's. And there was a group called PSAC that was looking over Apollo and they wanted us to do a predictive kind of analysis and to do a reliability program in what I call the game of random nines. In other words, they were trying to get us involved in the mathematical aspects of reliability rather than design and manufacturing.

Very fortunately for NASA they didn't listen to PSAC and went on and did what was right.

In Figure 7 is shown what we replaced the game of random nines with. There is nothing that we can't do in terms of acquisition fundamentals that defines the program reliability that aren't under these categories.

Actually when we were with the Apollo program there were quite a few more analytical activities than this that we could perform in order to understand reliability of our equipment while it was in the design process. But for the military application we picked these categories and said they are the ones we want to use, they are the ones that we are going to focus on and if we understand these, we are sure that we can design and build reliable devices.

There is one secret to reliability that you have to understand and it comes out very clearly in this chart and that is, reliability is a function of stress. If you understand the stress on your hardware, you understand its reliability. If you are overstressed, you are not very reliable. If your equipment is overstressed it is not reliable. These are simple analytical tools, but very powerful analytical tools that if used properly can give you as much confidence as a very complex test program.

They have the advantage of being done up front while the design is still on the paper, they have the advantage of not using a lot of capital resource and inventory and yet giving you the confidence that you need to understand whether your equipment is going to hack it or not in terms of the stress that is being put on it.

For instance, the mission profile definition is very important. You have to understand where it is going to be used, how it is going to be used and what environment it is going to be used in. Of course, that is one where we have fallen down on our swords many times because we have just inadequately defined the environment, sometimes out of ignorance and sometimes because we were just careless.

If it is something we don't know and it is perfectly understandable, we will learn what the mission really turns out to be later.

But all of these tools are designed to produce analysis and in the Navy most of our contractors have generated the necessary algorithms in the Cad and Cam work in terms of getting the analysis into the automation system such that the engineer doesn't have to do it in the long, time-consuming way.

This is a very important analysis that Apollo spent a lot of time on and as far as an analysis goes in terms of understanding stress, that is probably the most important one; the most powerful one there is, up and down the board.

The only problem was that it wasn't known outside of Apollo circles. Today it is getting the emphasis I think that it needs in industry. I think the jury is still out though as to how important it is to military systems that have not a high reliability requirement. It may come as a shock to you but in most cases military equipment doesn't demand high reliability. It demands what we call a median kind of a reliability somewhere in the 80 to 90 percent category, not like the Apollo reliability where failures were just ordained not to be, which demanded very precise design and very precise understanding of the design.

The question of sneak circuit analysis came in as whether or not it would be a type of analysis that would be valuable to the military. It turns out that it is, I think, but the jury is still out voting and the jury is really the industry. As they use it, become more familiar with it, we are finding out how cost effective it is and whether or not it is really paying its own way in terms of an analysis activity.

Next I am going to talk about design experience.

What we have here is a series of figures that show you some of the involvement of the design and what it really means in the early stages.

When I first came to the Navy we asked some very simple questions about what was the policy of say junction temperatures in the design of electronic equipment. We couldn't find any policy written.

We also went out in the fleet and did some measurements to see what typical junction temperature were in equipment and we found they were operating somewhere in the 150 to 140 degree C category.

We also know from our experience with Bell Labs that this is the temperature that they like to design in for the majority of their equipment and they have had a lot of experience with those kind of temperatures and we know what reliability we can get out of them.

If you put those numbers together what you see in Figure 8 is a difference of 900 times the reliability of the equipment depending on just simply what junction temperature you pick. We, in the Navy picked

the 100 degree standard because we couldn't afford the luxury of the weight, the extra copper that goes into designs of these very cool systems at the bottom of the chart, but we also couldn't afford the failures that we were seeing at these high temperatures. As a matter of fact, we set 100 degrees as a standard and it has turned out now that we are probably designing more in the 100 to 90 degree C region.

Our contractor has come back and told us that they really think they can probably design fairly comfortably at 110° to 120°. But we set the 110°C standard back in 1975 and we are probably going to move it very shortly into a lower temperature category since we seem to do it with a relative amount of ease.

But as you can see, even within the bandwidth of 120 to 110, we are still talking 12 times the reliability. So you can see the sensitivity of the precision of reliability requirements to just one little element, which is called junction temperature.

Also embodied in another chart, which I didn't bring today, is the electronic stress on the devices. You have two kinds of things you should look at in semi-conductors which are very important, one is junction temperature and the other is electronic stresses. I have just highlighted this one because it is very significant and easy to see.

Figure 9 is a chart that I think really portrays for people who have difficulty understanding what the relationship is between dollars, temperature and MTBF. We have collected this on a fleet of aircraft, 200 to be exact, and what we are looking at was the impact of operating temperature on MTBF and on the operating cost of the airplane. I think this is a very, very, important chart, at least it is for the Navy because it is the first time we have been able to quantify MTBF with temperature and with the dollars.

And what the chart portrays is what we did. We took a 200 fleet of airplanes and we lowered the cabinet temperatures from 110 down to 90, which is a 20 degree drop in the cabinet temperature.

And when we did that we almost doubled the MTBF. It went from about 2.7 to 4, but we found also that when we did this 20 degree drop in temperature of the box, we found that the annual operating costs decreased \$42 million for every year for those 200 airplanes. And now we find that if we can drop it another five degrees in those cabinets, we can have an annual savings of \$8.5 million a year on those 200 airplanes.

So you see, reliability has a very direct connection with the economy of how we operate, how we bill, how we buy. And in this day of inflated dollars, where we are buying less and less with the same amount of money, we have to understand more and more of these relationships and we have several other families of charts that show the economic impact of just a few degrees of temperature on the subtlety of reliability.

We have always know these numbers, like you could lower the temperature and the MTBF's would change by these amounts. Those are relatively known factors, but what we had not known is the impact of operating costs on airplanes when we just lowered it those 20 degrees.

So it shows you that for every degree you lower the temperature, you are not only dealing with MTBF, but you are dealing with operating costs.

Figure 10 is a very significant chart in terms of just the design and understanding of temperature and the design of a piece of equipment. This is a signal processor. We call it an ASP and the interesting thing about this chart is when we first looked at this program a number of years ago, the reliability it was achieving, was right around the 200 hour level, against a specified level of somewhere between 500 and 700 hours. We did a design analysis of that particular piece of equipment and we found most of the devices were running too hot. We didn't have a whole lot of money on this program, so what we told the designer of this equipment, which was IBM, that what we wanted them to do was to relocate the components on the boards and not do any new design. So essentially we went in and changed the printed circuit board only. All of the components went back on that were on there before. The electrical circuits were exactly the same. Only this time we did a sort of a regression analysis, thermal regression analysis, we put the components where they would best receive their cooling. In other words, the very hot ones were near the edge of the boards and those who needed less cooling progressively went towards the center of the boards.

We made a thermal adjustment of the parts on the board. When we put it back into service, 750 hours MTBF is the equipment reliability that we got. Now you see, to me that is very powerful. This is very inspiring for a designer to understand that the only difference between the old failure rate and the new was the fact that he relocated components.

We didn't change the design. We didn't do anything except just relocate the components on the board. Then what we noticed, when we got it out in the field was that we were still not achieving the reliability that I thought we ought to be achieving. So we took some more looks at that piece of equipment and we found that the field failures were about 50-50 parts and workmanship. In other words, the design stresses were within the limits that we wanted to be in, but parts and workmanship were a problem.

So in the next version, the initial production, we pulled that design back into the factory and changed the manufacturing process. When we fielded this piece of equipment, Figure 10 shows that the reliability went up to 1000 hours MTBF.

We looked in the field and saw that we were seeing some kind of categories that were lower than these numbers, but still a problem in the area of workmanship. We have instituted a screening program which improved the reliability prediction. We haven't fielded these units yet.

We are now putting our equipment through a vibration thermal cycle before we put it into the field and when that is completed we expect to see the reliability go up again.

I think the message of this chart is that this is a manageable process. There is nothing mystical about reliability. It has nothing to do with mathematics. I hate to tell you that, but E to the minus, Λ to the t is a dead duck in the Navy.

Figure 11 is a "show and tell" about where all of this leads if you properly follow it.

When we were getting ready to put an INS, Inertial Navigation System, into the F-18 program we found we needed five to nine times the reliability of any current system in order for the airplane to meet its design requirements.

At that time when we went into the design phase of the F-18 INS system, Litton was the primary builder of these systems and everyone of these, with the exception of the A-7 had been built by the Litton Company and, as you can notice, the best that they had in terms of MTBF on any INS they had ever built from the 1960's through the 1974 time frame, was somewhere around 90 hours MTBF. And, yet, we had to have somewhere around 500 to 700 hours MTBF on an INS system if our F-18 was going to fly the way we wanted it to fly.

So we initiated those design parameters that we talked about earlier, what we call design fundamentals, and put in the manufacturing disciplines that we wanted on the program and today that program is flying in 22 test airplanes and is demonstrating somewhere between 500 and 700 hours MTBF.

The thing that is interesting about this chart is that the same manufacturer who from 1960 to the 1972 time frame couldn't make an INS system with any more than 90 hours MTBF in it for all of those airplanes. And yet we changed the design standards, changed his manufacturing standards and today we regularly get this kind of thing out of that manufacturing operation.

So once again, I am trying to show you that it is a discipline process, it has design capability in it, it doesn't have to be mathematically driven. We simply look at our design, understand the stresses and see to it that it is built to print, which of course is a big problem.

If you look at our general industry's response to all of the initiatives that I have just talked about, in Figure 12 is shown the top 10 people who spend most of the Navy's money in terms of delivering systems to the Navy. And these are the kinds of evaluations that we have put on the industry.

As you can see, there is still some red (R) with some companies as they gradually understand the transition design and the biggest one, of course, is motivation which we are working on this year, which I think is very important.

You know, Patton once said years ago, "You can't push a wet noodle." And that is a very true statement. So what we have done is gone to the corporate people and said, we are now demanding that you ask that your equipment be reliable, that you make that first in your company.

There is no point in building equipment, no matter how well, no matter how precisioned, such as your time equipment. You know, if you build very precisioned time equipment, but it doesn't do the job, it quit on you when you want it the most, then there is really not much point in having that design. You know, let's not be infatuated with just the performance aspects of equipment.

The Japanese have shown us what happens when you become infatuated with a total equation, not only the design of the equipment, but the manufacturing and the understanding of the stress of the equipment. You know, the Japanese are just about to put us out of business electronically and that is because they have understood the equation. I think it is high time we, as Americans, understand what that equation looks like also.

So we have been working diligently in that area and it won't be long before I think that the chart is going from all red in 1975 to have it all green (G) in 1985. And I think with our top 10 contractors we will have that happen.

As I said earlier, understanding design stress is really the main part of the equation for the design aspect. But now you still have to build it to print. No matter how well the design has been carried out, no matter how well you understood the stress on the equipment and no matter how well you did your design, if the guy out there on the floor doesn't put it together the way the design is supposed to go together, then you have shot it all.

So what we are involved in Figure 13 is a heavy emphasis on the manufacturing of equipment, or what we like to refer to as build to print.

We are going to talk about today in two areas: parts and workmanship (see Figure 14). The only parts that I am going to bring up with

you today, which are occupying probably 90 percent of our problem areas, is semi-conductors. And the other thing we will talk about is workmanship. But I will first talk about the parts problem, what we see in the parts area and what I think you should be very attentive to in your precision time work in terms of semi-conductors.

Back in the late '70's we did a study, shown in Figure 15, which became very significant to us. I became aware that parts and semi-conductors were giving us an unusual amount of trouble in the fleet and we were buying mil-standard parts, high reliability parts, JANTX and JANTX-B parts, which are supposed to be the top of the line, the cream of the crop.

But we began to see equipment with these mil-standard parts in them that weren't performing the way that we thought they should. So we went out and bought a dozen part types in quantities of about 100 or 1000, I have forgotten how many were in these lots now, but we bought 12 different types of semi-conductor devices with what was referred to as a statistical quantity and then we put them in tests at one of our labs. And what you are seeing here is the summary of one part type of which the other eleven looked exactly alike.

But what I want to go into is to show you what really happens in this world that began to open our eyes.

If you go to Radio Shack to buy a given part it will cost you 59¢ for that part. If you buy the same part commercial screened, such as the FAA, or other people buy, that same part will cost you \$1.99. If you buy the part with high-rel standards, such as NASA buys, that will cost you \$3.10. If you buy the same part under what is referred to as a mil-spec the part will cost you \$12.50.

Now what we found out in this study, if you notice there is only one thing changing in this chart that you can see and that is the amount of paper you buy.

If you buy your part at Radio Shack there is no more than your receipt. You get a little more data at each higher priced part and when you get the mil-spec part you have bought a trainload full of information and it is supposed to guarantee you that you have now bought the part quality that you want.

Well, what we found in this study is that that wasn't true! What we really saw is that there was quite a difference in terms of the reliability between the first two categories. And we saw there was a lot of difference in the quality between the next two. But the significant part that came out in all 12 part types was that we could see no discernable difference between the mil-spec and commercial screened parts.

Now, why is that? We began to study it and we thought we knew the answer, and since Fairchild has blown the lid off everything we now know the answer. But at that time we were speculating.

You see, commercial screened parts is where 99 percent of the parts are sold commercially. We in government only buy three to four percent of the industry's output and what is happening is, when they run short of mil-spec parts they are just dipping in the box and getting us these commercial screened, unburned-in parts. And that is the reason we could not see the difference. They just look alike.

You know, we wrote a great mil-spec, but we just aren't able to police it or enforce it.

So that began to open our eyes. I got a couple more pieces of data here that I am going to show you. Here are six of the leading semiconductor manufacturers in Figure 16; we took their names off to protect the guilty, but I never have quite figured out why I wanted to protect them, but nevertheless every name that you know is on this list.

In one major program it became a real eye opener for us, it was a mining program where we were having trouble with some of the semiconductor devices.

We decided that we would go in and do our own pre-cap visual. The manufacturer had been doing it for us now for three years and we were having trouble with this particular device. So we said, we are going to see if anything is different. We are going to send our own people into the factory and we are going to sit down with the guy who does the pre-cap visual and we are going to do it right along with him.

When our man arrived at each one of these six plants the reject rate that showed up is shown in Figure 16. Now mind you, they had been delivering them to us all along. And, as a matter of fact, these two fellows, number three and four, came to the Navy and said that they had a 72 percent rejection when we were sitting there with them and that they previously had only a 6 to 5 percent rejection.

Those two fellows said to us, if you really want a mil-spec part we can't supply it to you and they disqualified themselves and they had been sending them to us for three years.

Now these other fellows who had still unusually high numbers, at least agreed to clean up their lines, and they began to deliver us quality semiconductor devices.

Well what we found out is there is gross cheating going on in the semiconductor world; gross cheating.

A typical example is shown in Figure 17. We screened, we took a family of them and you can see the number of parts. I won't go into it here for time reasons. But when we did the exact same test, we took mil-spec parts that had already been delivered to us and we put them through the mil-spec test again. We just sent them to an independent tester, and we said what we want you to do is submit these to a mil-spec standard test requirement just as though you were the manufacturer and do exactly the same thing he is supposed to do when he ships them to us. And that is what the column represents in Figure 17.

And when that guy was finished with testing, I think it was 20,000 parts, we found 14 percent rejection of transistors, 14 percent rejection of IC's and about 11 percent rejection of diodes.

What we are seeing consistently, in the Navy in the mil-standard world of military parts, in the semi-conductor world, is somewhere between 10 and say 17 percent rejection of mil-standard parts. Now those are parts that, you know, we are paying the \$12.00 for. They are not the Radio Shack part. They are the part that is supposed to be tested, burned-in and are supposed to be high quality devices. That has changed our whole way of doing business once we learned this.

Now here is an example of what happens. We call it the manufacturing burden.

Figure 18 is a chart I showed the industry just to show them how stupid this whole thing really is. But here is a case where a guy delivered 425 pieces of which 243 were found bad. When they were taken apart, they found they didn't even have the same die in them. Figure 18 is a picture of two different dies in the devices. What had happened is; he had just put the wrong dies into the devices. Now mind you, not only does he have the wrong quality on the die, but he also has the wrong die in the semi-conductor. Now that doesn't bother me nearly as much as the statement down on the bottom. An alert was put out, everybody was told, the manufacturer, which is National Semi-Conductor, responded to the alert in this way. And this is what was written on the alert; It says: "This situation of mixed parts does not constitute a reliability problem". It has got the wrong die in each one, but that is not a reliability problem!! They say: "All of the incorrect devices would have been detected at the users incoming, receiving testing board level checkout". In other words, "Buyers beware."

You will find that somewhere along the line at your cost and at your expense, but we don't consider that a problem. And that is the kind of thing we are dealing with in semi-conductors.

Now, of course, there was one that has really hit the street lately. I am not going to spend a lot of time on it, but as you know Schoenberg took over Fairchild in a stock option bit and when Schoenberg came into

that plant and began to do an audit of what they had bought, and my own version of this is they get what they deserve because I don't like people that do these stock option takeovers, but at any rate they now found out that they have a disaster on their hands.

You know, Schoenberg came to the Navy and came to DESEE and says, hey we don't quite understand what is happening in the Fairchild plant. We put out approximately 2 million semi-conductor devices a day -- on the military line -- and yet we don't find but 500 sockets in which we can burn them in and we don't understand how they are doing that.

Of course everybody rushed into the plant to see what it was all about and what you really found out is that they weren't burning in at all.

For the last five years Fairchild has been shipping mil-standard, high reliability devices unburned-in. And those are in all of your equipment right now. You see, what I am saying to you is you are really -- "Buyer beware."

Now the Navy has established its own programs with screening. Most all of our major vendors have bought what is referred to as "century equipment". It is a temperature screening device that we rescreen all semi-conductors. We just don't use any semi-conductor that isn't rescreened. It is just a disaster. I am sure in your precision world you should take very great note of this because I think it is very important that you recognize that just because you bought a mil-spec part doesn't mean you have got anything at all. You have got to determine what you have got yourselves.

Shown in Figure 19 is a program for which we had specified an MTBF allocation. I picked it because it was a fairly high number in terms of Navy equipment and the thing that is interesting about this curve is if you look at the JAN world, you see the mil-burned-in part is required, the thing Fairchild didn't do for us and let me just stop right here a minute.

If you think the scandal going on with Fairchild is only with Fairchild, it is just because you haven't visited the other plants yet. Don't you believe for a minute Fairchild is the only one delivering unburned-in parts. You just have to understand how semi-conductors are made, you have to understand what the volume is and having been around these plants for awhile you have to understand the term called "ship for revenue".

At the end of every month a payroll has to go out in a semi-conductor plant. And when they get near the end of the month, if they haven't sold enough devices to meet their payroll, anything that is on the shelf gets sold. That is called "shipping for revenue" and that goes on across the whole industry.

Now what this chart shows you is that there really is a break point at which the cost begins to go up, but the MTBF doesn't meet the same cost rise. And really is there sufficient reason to use the mil-burned-in part for military equipment, or should we really look at the 883 screen parts, which is where the cost cross over point is.

We are looking for cost effective reasons, does the JANTX part really pay for itself, or should we buy a couple of levels down, do our own screening and see if that isn't the most cost effective way to put the semi-conductor into military equipment.

If you think the problem is bad, Figure 20 just says you haven't seen anything yet. Because when you go to the outer circle, which is the '80's, what you are going to find out is that in the past, the outlook for the semi-conductor industry was market emphasis and then sales were sort of the thing they were interested in but in the '80's you are going to find that profitability is the only thing industrial sources are interested in.

As foreign companies come in and take over the semi-conductor houses (I will make you a prediction that within 10 years there will be no semi-conductor house in the United States that isn't owned by a foreign interest) and buy up this industry what they are going to be interested in is only word, "profitability." And you are going to have a devil of a time knowing what you have got and believing what you got unless you have some way of screening your own parts.

Figure 21 shows there is a lot going on in the semi-conductor world that I think is good. What I have said is a bad picture, but actually any place we have seen the Japanese take over the semi-conductor industry and work with the semi-conductor world, what we find immediately is the part type quality goes up.

There are all kinds of laws saying don't buy overseas, don't buy offshore, all of this kind of stuff, but it is primarily nonsense because in actual fact the Japanese build a better device. And the reason they do is because they spend more money in the design process.

You know, our manufacturers have known for years that the quality of the device would go up if they just spend more money on the masking process, just for example. They spend over twice the amount of money we do for masking their devices and, of course, they get a better device when they mask it.

So if you look into the process what you find is that the Japanese are really moving and you can look at the curve and see that. The reason is they have understood what it is that they are looking for that makes real profitability; a dependable device.

Figure 22 is a little parts story. The other part of it is workmanship. We have recognized that workmanship also is a problem, loose wires, improper manufacturing procedures, et cetera. So we instituted about a year ago, a year time frame, we instituted this screening program which is really just a matter of known literature that we put into a document. We used it on the Apollo program. It has been used in space programs and probably is nothing new to you all.

But the point is, we said, hey on all of our equipment from now on we want to see random vibration, 6G, no less than 10 minutes, no more than maybe 20 minutes, but somewhere in that time frame. And we said we also want to see thermal cycling and we want to see that thermal cycling is a function of complexity and there is a family of curves in this book that shows it. We have given this book to all of our industry and particularly the corporate people because what we want them to understand is that, it decreases corporate costs.

If you can understand what it is in your manufacturing cycle that is giving you trouble, then you can correct it and you can build the product better and better at a cheaper and cheaper cost.

So this document was sent out to the industry. It has very good response. We are now thinking about turning this into a NAVMAT publication, or maybe even a mil-standard, or I don't know what to do with it exactly. But at any rate, it has served its purpose in industry now. It has called attention to the fact that if you really want to improve your profitability of your company, as well as delivering more reliable equipment, you must do some type of manufacturing screening and that is the screen we picked that came mostly out of NASA literature and if you have seen it I am sure you are familiar with it. That is working well for us.

Between the emphasis on semi-conductors, rescreening, between doing this kind of manufacturing screening, we are seeing equipments now go out into the fleet that are sometimes two, three, and as much as five times greater MTBF then we have ever seen before and this is because we put the focus on design and manufacturing and I think that is the point I really want to make with you.

Don't play mathematical games. Don't get involved with E to the minus Λt . Those are interesting things and I am sure they have some design predictive nature, but look at the part that is really important in this whole equation and that is understanding the stress in your design and being able to build it to print.

If you can guarantee yourselves those two areas are under control, you will be building precision time equipment that just will be very dependable. And, after all, that is really what we are looking for is dependable equipment.

Figure 23 just says we haven't made quite the progress with the transition in manufacturing as we have with the transition in design, but this is because we got on it a little bit later, we got on it in the late '70 time frame recognizing these kinds of problems. There is still very little green (G) on the chart and I guess the main message in that building to print is very, very, difficult and we are working very hard to get industry standards set such that we all can have a baseline for manufacturing that we understand.

What we see is a great deal of volatility in the manufacturing process. Some companies do it one way, some companies do it another way and nobody really knows why they do it either way.

So what we are doing now is setting a family of standards for manufacturing that we are going to send out very shortly and we are going to say, now this is what we expect you to do as a minimum; if you want to do any more than that, fine. But we feel by doing that we can set a baseline in this manufacturing where we come closer to building to print within the economics of the design. So that is really what we are looking towards.

Let me just say to you in closing that, this has been a very fascinating area for me in the military. Coming from the NASA Apollo program, I really didn't think there was an achievement that I could make that could really top putting men on the moon and bringing them home.

But having been with the Navy now a number of years and working in transition with them to try to bring more reliable equipment into the fleet, try to decrease the fleet burden in terms of OMN costs, what we found is what I think is a very exciting program.

I think the Navy in the next few years will be routinely delivering reliable equipment to their fleet. It will be equipment that just like the INS system for the F-18, it will have five to nine times more reliability in it than we have ever seen in the past and we will be doing it for less dollars. That is very important. We will be doing it for less dollars.

As the inflation goes up, we just have to do more and more with less and less dollars. And by resorting more and more to the analytical understanding of reliability, rather than to the testing understanding of reliability, we find the economics that we are really looking for in this whole business.

I think the Navy is making great strides in this. As a matter of fact, I think the Air Force is moving along with it. We have spent a great deal of time with Al Slay on this matter and I think you are going to see the FSC Command begin to be very much engaged in this business. It is really quite exciting.

The thing that you will have to keep in mind is that it is very fragile. Until we can get it down to where it has some solid base under it, it is fragile. We have had programs that were doing well, we left them alone for about a year, came back and they weren't doing too well. We found that various disciplines had been dropped. The emphasis hadn't been carried through. So what we found is that right now, at least, we just can't drop any program. We have to keep them all under our visibility in order to keep them moving because they are a little fragile.

But I think as time goes by we will see it harden more and more and we will find less of this fragile business. So that is the main message I have and thank you very much.



DESIGN AND MANUFACTURING WHAT THEY MEAN TO FLEET READINESS



THE RELIABILITY MANDATE

NAVELEX

NAVAIR

NAVSEA

NAVAL MATERIAL COMMAND — NAVMAT

Figure 2



ORGANIZATIONAL STRATEGY 1980

HEADQUARTERS NAVAL MATERIAL COMMAND

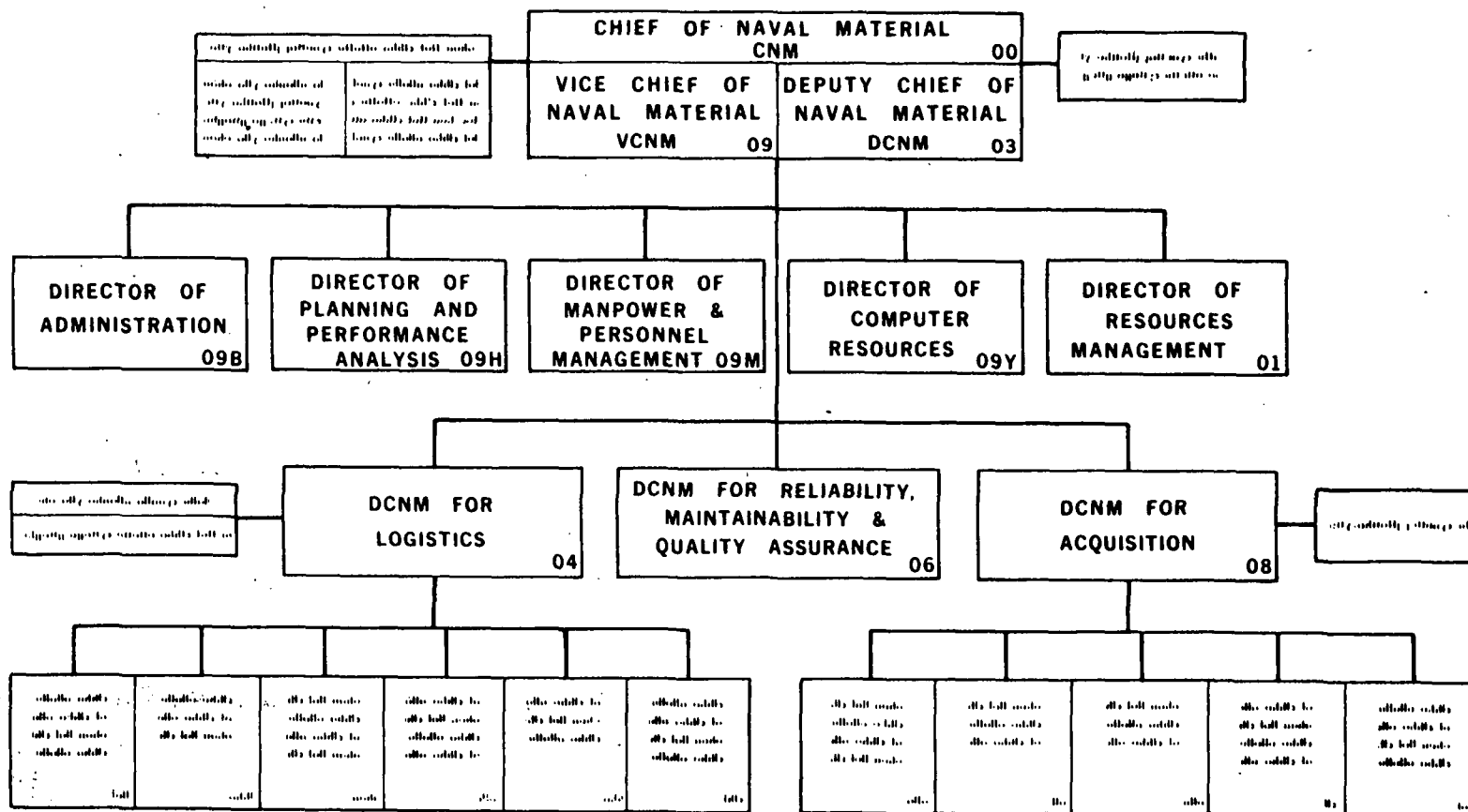
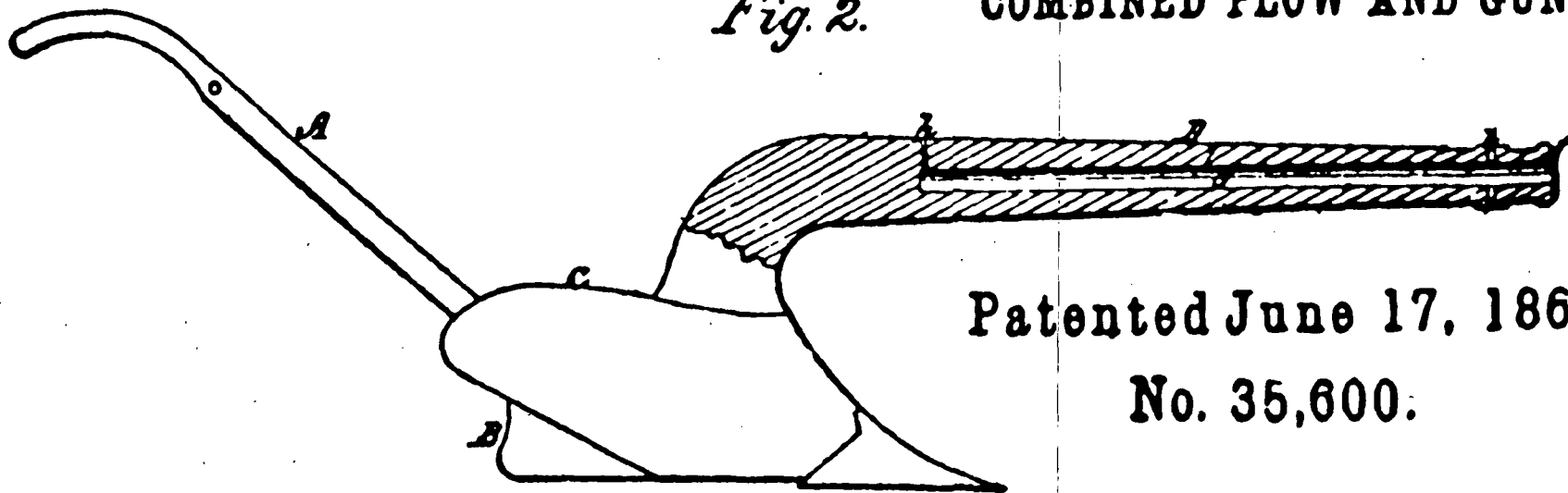


Figure 3



Fig. 2. COMBINED PLOW AND GUN.



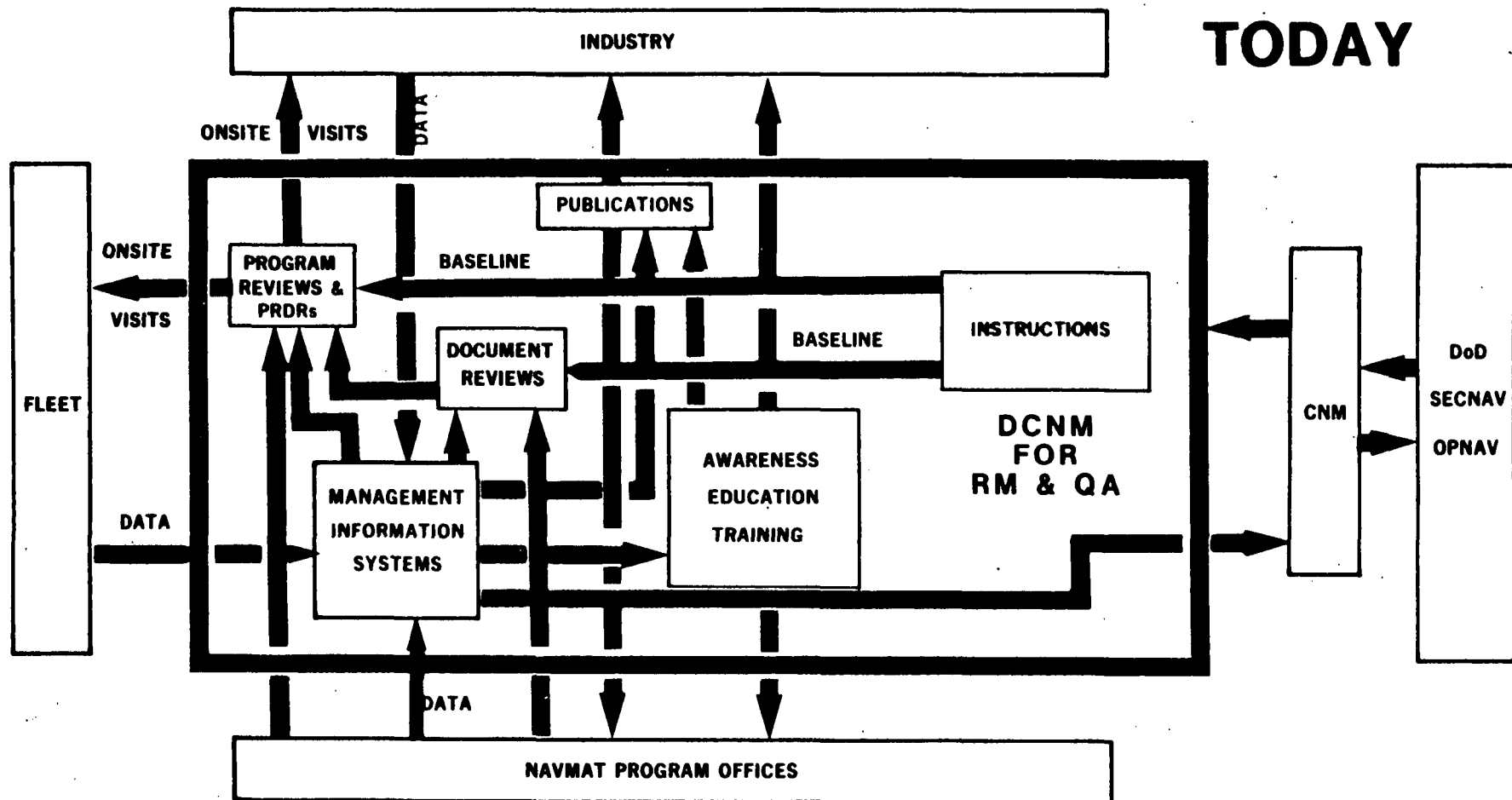
Patented June 17, 1862
No. 35,600.

MOTIVATION



MAJOR ORGANIZATION FUNCTIONS AND INTERFACES

TODAY



- NEW OBJECTIVES UNDERSTOOD - - NEED FOR POLICING DIMINISHING
- INITIATED INSTRUCTIONS, MANAGEMENT INFOSYSTEM, AWARENESS PUBLICATIONS
- INITIATED PRE-PRODUCTION RELIABILITY DESIGN REVIEWS

Figure 5



GAME OF RANDOM NINES

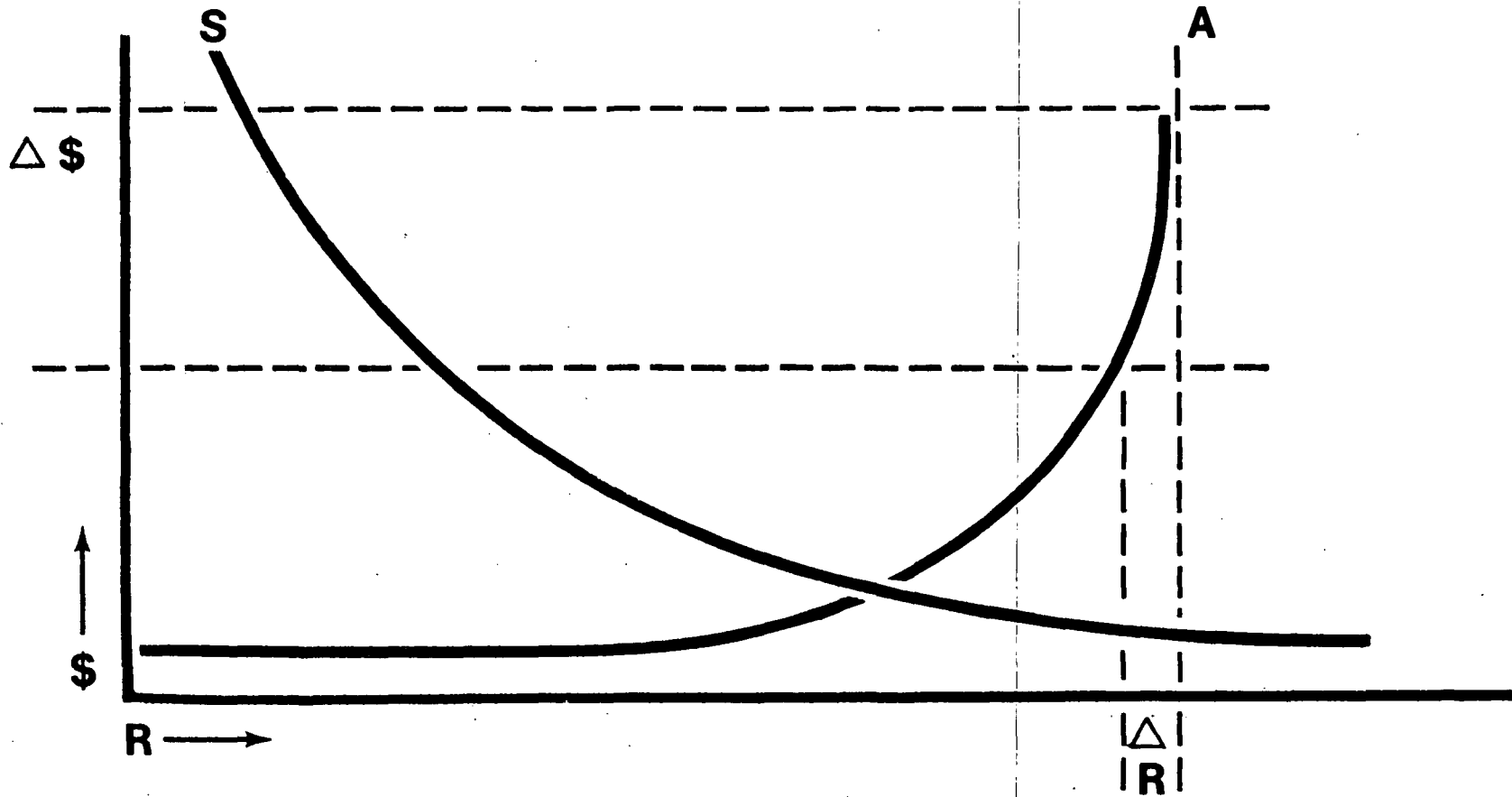


Figure 6



MATERIAL ACQUISITION FUNDAMENTALS

- **MISSION PROFILE DEFINITION**
- **STRESS ANALYSIS**
- **DERATING CRITERIA**
- **WORST CASE ANALYSIS**
- **SNEAK CIRCUIT ANALYSIS**
- **PREDICTION/ALLOCATIONS**
- **FAILURE MODES & EFFECTS ANALYSIS**
- **TEST, ANALYZE, & FIX WITH CLOSED LOOP REPORTING**
- **DESIGN REVIEWS**
- **MISSION PROFILE QUALIFICATION TEST**

Figure 7



JUNCTION TEMPERATURE IMPACT ON SEMICONDUCTOR RELIABILITY

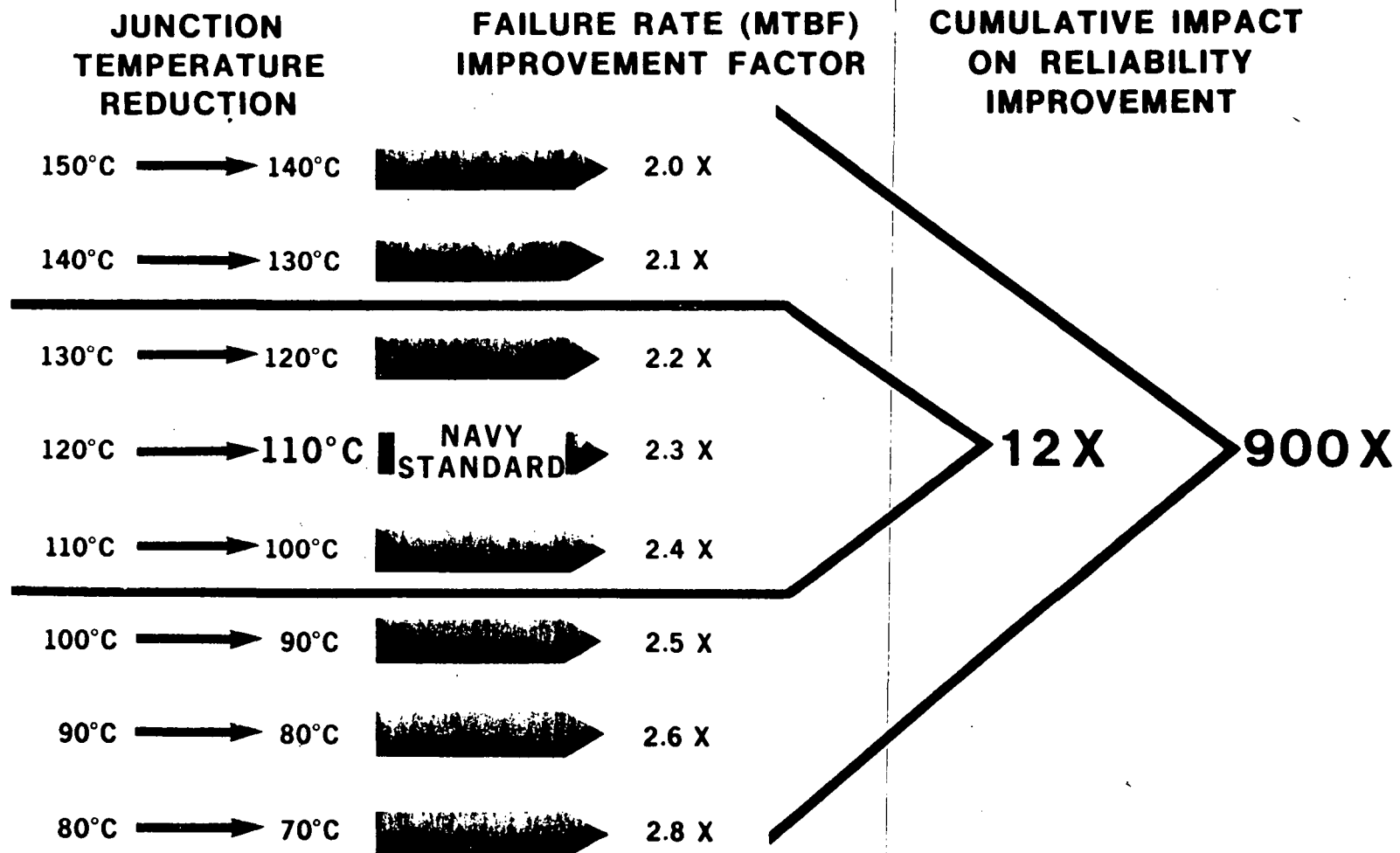


Figure 8



OPERATING TEMPERATURE IMPACT

IMPACT OF OPERATING TEMPERATURE ON ANNUAL OPERATING COST AND MTBF (BASED ON 200 AIRCRAFT)

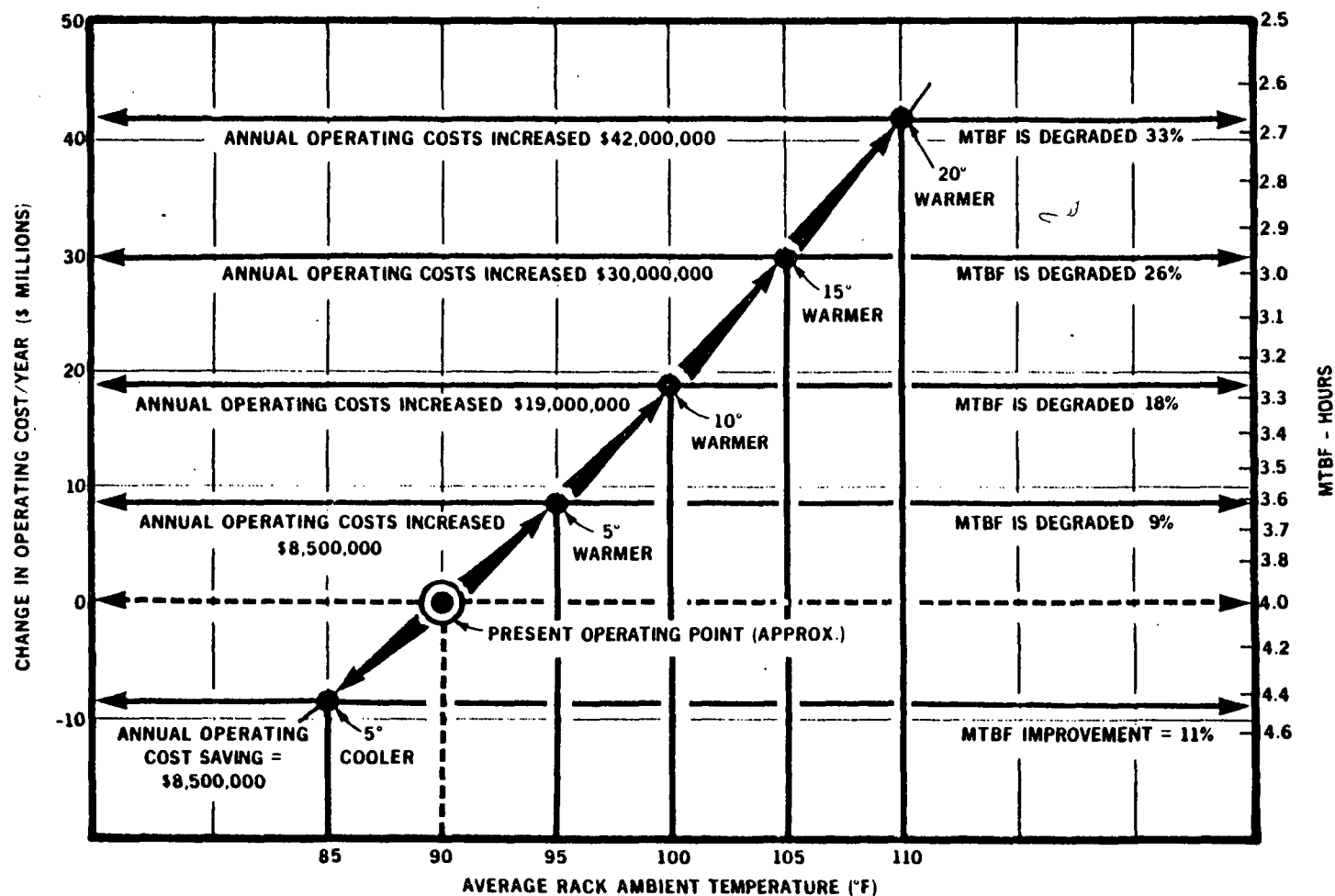


Figure 9



AN/UYS-1 ANALYZER UNIT RELIABILITY PERFORMANCE IN SERVICE USE

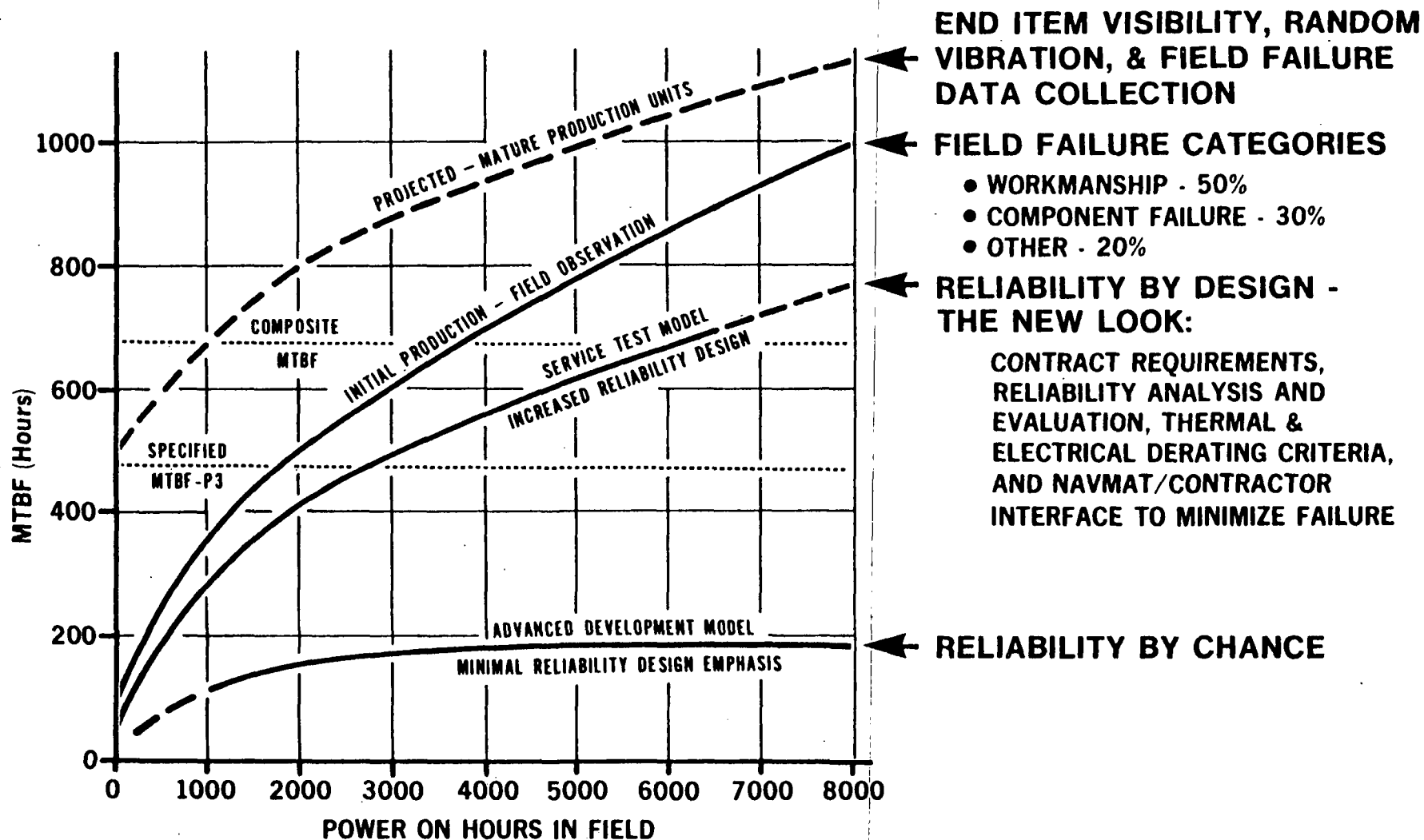


Figure 10



F-18 INS DESIGN EXPERIENCE

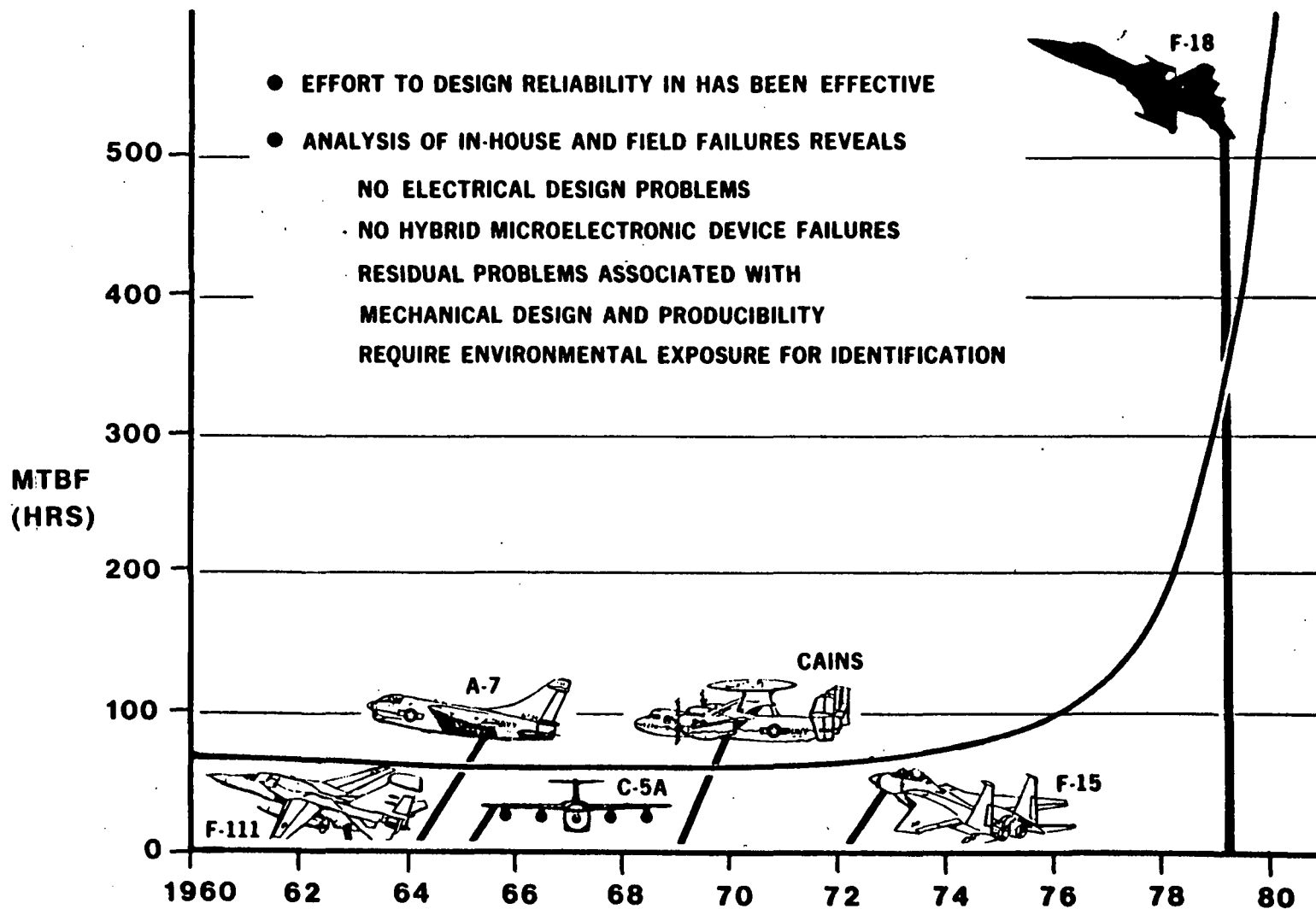


Figure 11



INDUSTRY IN TRANSITION DESIGN

R 1975 ————— 1985 **G**

REPRESENTATIVE CONTRACTORS

	1	2	3	4	5	6	7	8	9	10
POLICY IMPORTANCE OF DESIGNING RELIABLE EQUIPMENT REFLECTED IN CORPORATE STATEMENTS	Y	G	G	Y	G	G	G	G	R	G
ATTITUDES RECOGNIZES THE NEED TO IMPROVE RELIABILITY DESIGN EFFORTS	G	G	G	G	G	G	G	G	G	G
AWARENESS RECOGNIZES THE IMPORTANCE OF DESIGNING IN RELIABILITY	R	G	G	G	G	G	G	G	R	G
STANDARDS FORMAL BODY OF CONSERVATIVE AND PROVEN RELIABILITY DESIGN PRACTICES	R	G	G	G	G	G	Y	G	Y	G
MOTIVATION FORMAL PROGRAM FOR ACHIEVEMENT AND RECOGNITION	R	R	R	R	R	R	R	R	R	R

R ACTION REQUIRED

Y IN PROCESS

G ACHIEVED

Figure 12



MANUFACTURING BUILD TO PRINT



MANUFACTURING END ITEM VISIBILITY

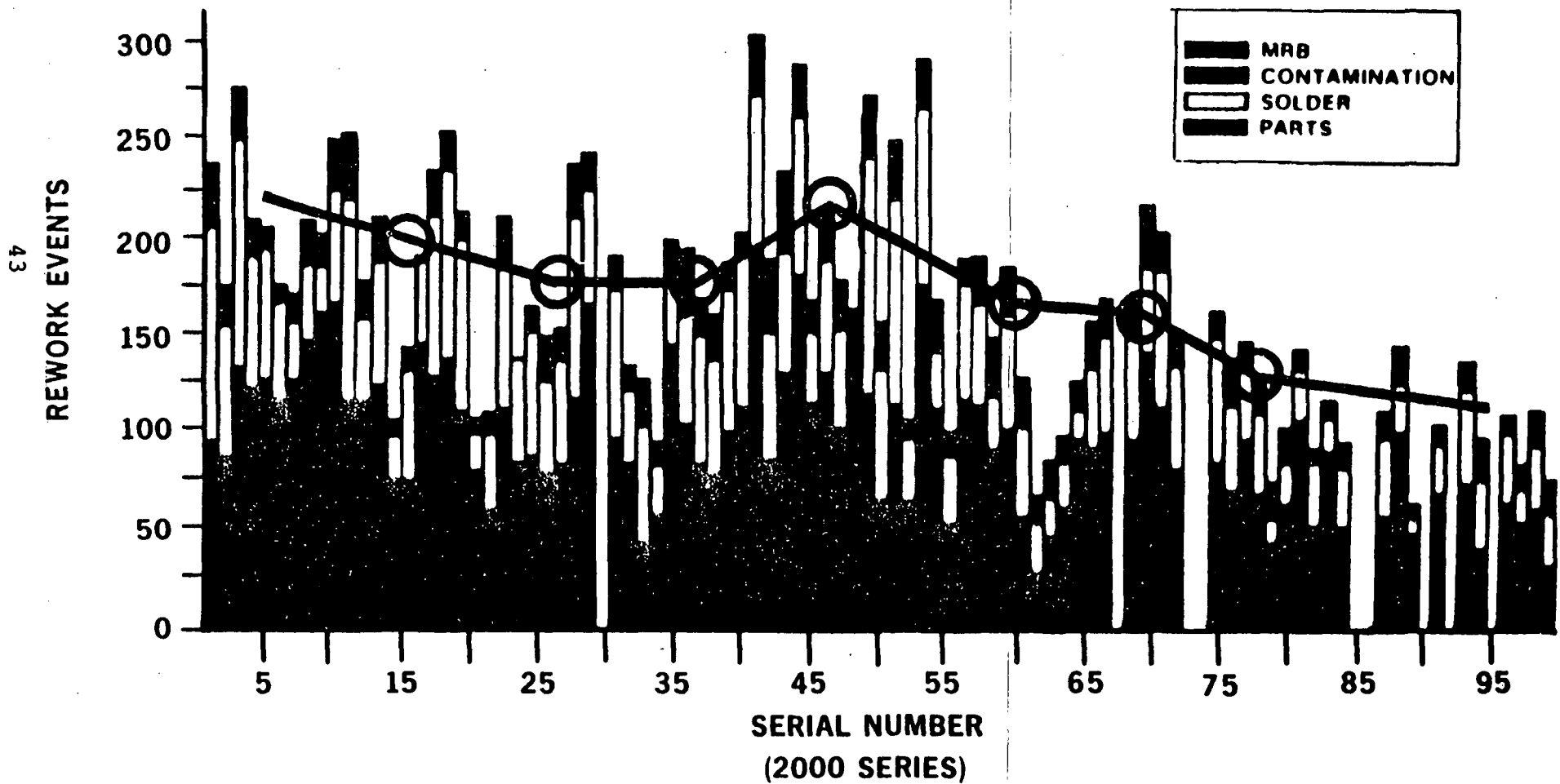
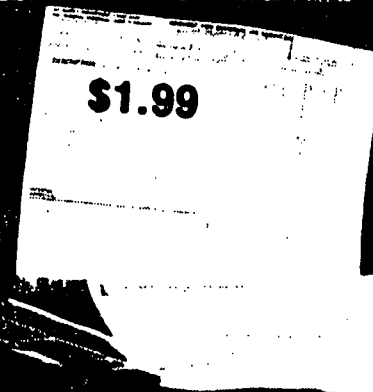
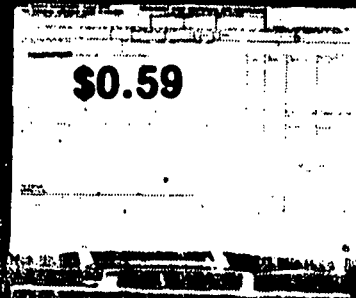


Figure 14

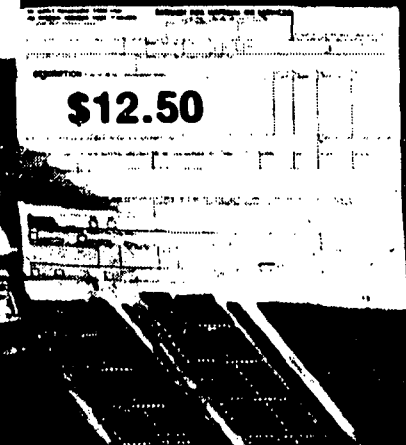
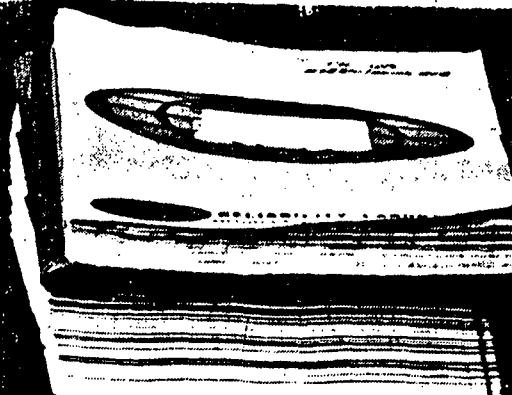
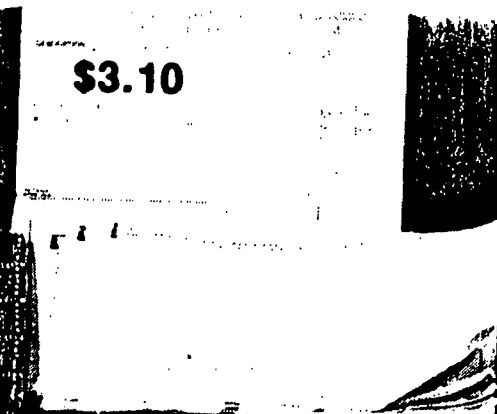


THE COST OF QUALITY



COMMERCIAL

SCREENED



HIGH-REL

MIL-SPEC

Figure 15



INTEGRATED CIRCUITS

PRE-CAP VISUAL SOURCE INSPECTION RESULTS

MFG	ACCEPTED	REJECTED	% REJECTED
1	33,000	15,200	32
2	38,000	12,700	25
3	1,389	3,597	72
4	1,219	2,268	65
5	2,804	448	14
6	446	95	18

Figure 16



PART SCREENING RESULTS

MIL-SPEC PARTS

46

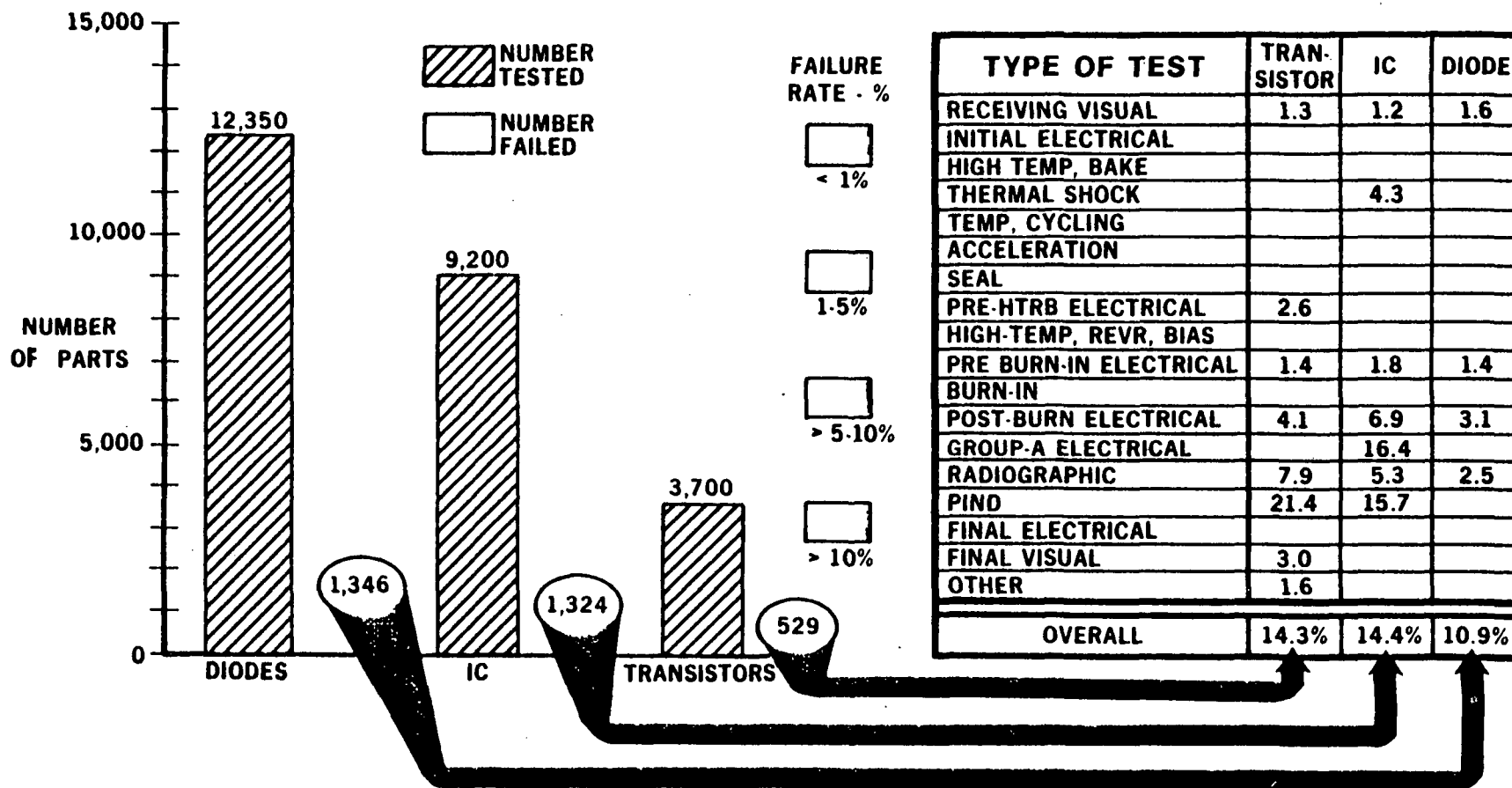


Figure 17



MANUFACTURING BURDEN

ALERT:

(T3-A-79-06)

243 DEVICES OUT OF A LOT OF 425 PIECES FAILED INCOMING INSPECTION FUNCTIONAL TEST AT ROOM AMBIENT TEMPERATURE, ON SITEK 3200 TESTER. INTERNAL VISUAL (DECAP) INSPECTION REVEALED TWO DIFFERENT DIES IN PACKAGES WITH IDENTICAL JAN MARKING. FIGURE 1 SHOWS DIE FOR UNITS THAT PASSED, AND FIGURE 2 SHOWS THE DIE FOR UNITS THAT FAILED TEST.

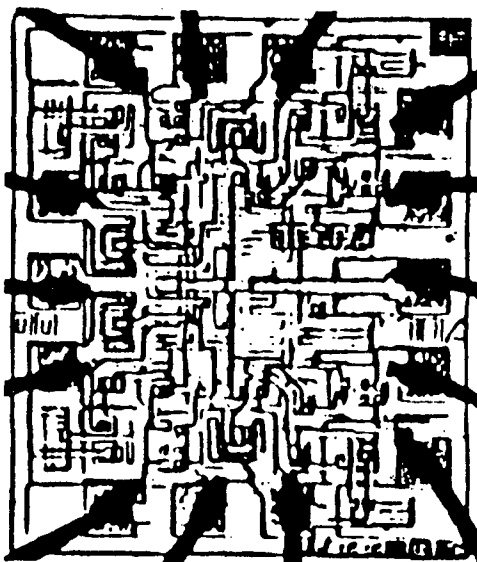


FIGURE 1 - GOOD PARTS

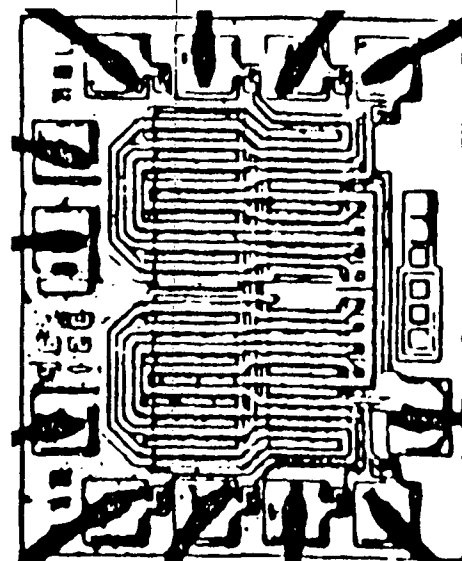


FIGURE 2 - NON-CONFORMING PARTS

MANUFACTURING RESPONSE: "THIS SITUATION OF MIXED PARTS DOES NOT CONSTITUTE A RELIABILITY PROBLEM. ALL OF THE INCORRECT DEVICES WOULD BE DETECTED AT A USER'S INCOMING TESTING OR AT BOARD LEVEL CHECKOUT."



SYSTEM RELIABILITY VS. QUALITY GRADE & TEMPERATURE

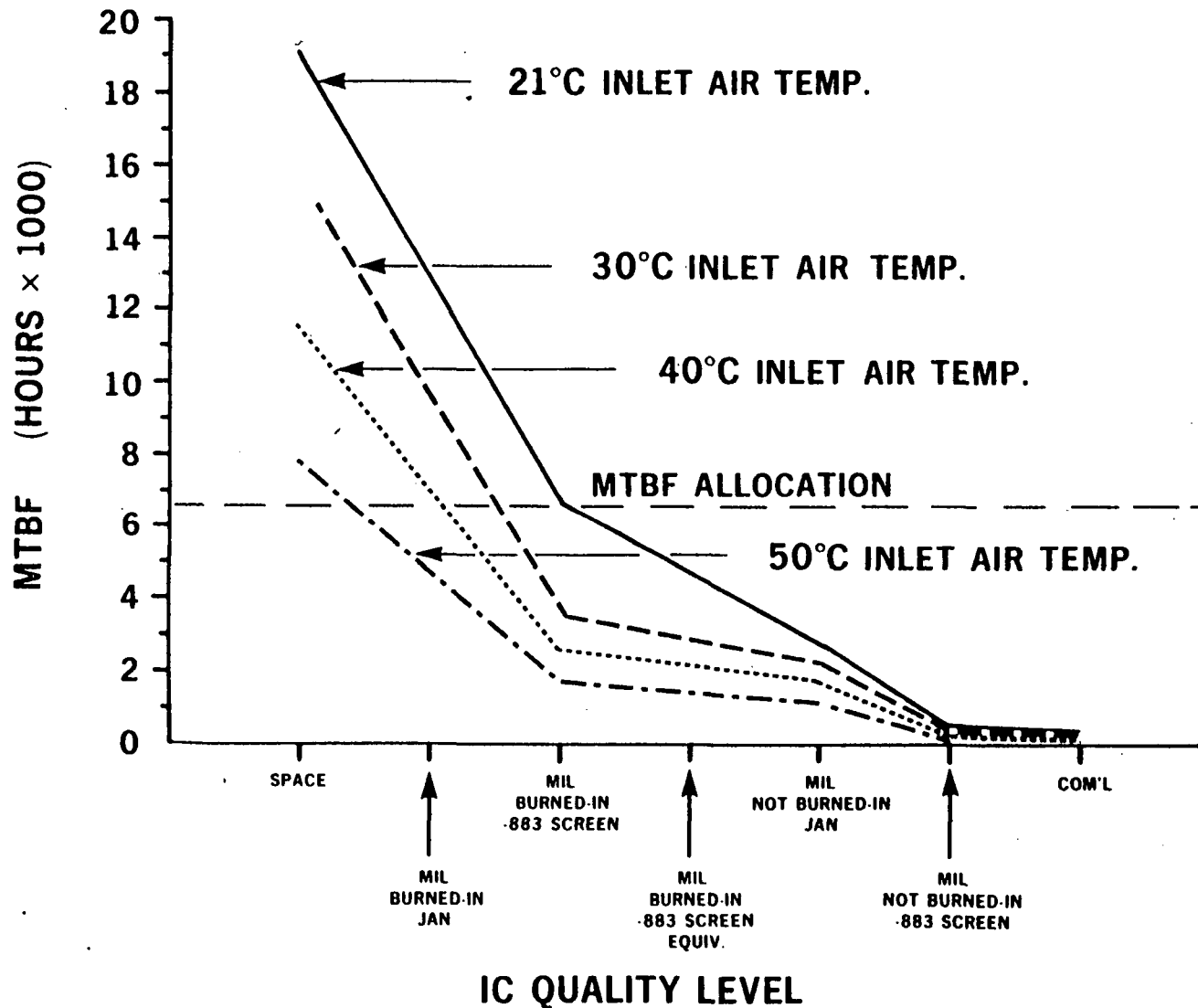


Figure 19



SEMICONDUCTOR INDUSTRY

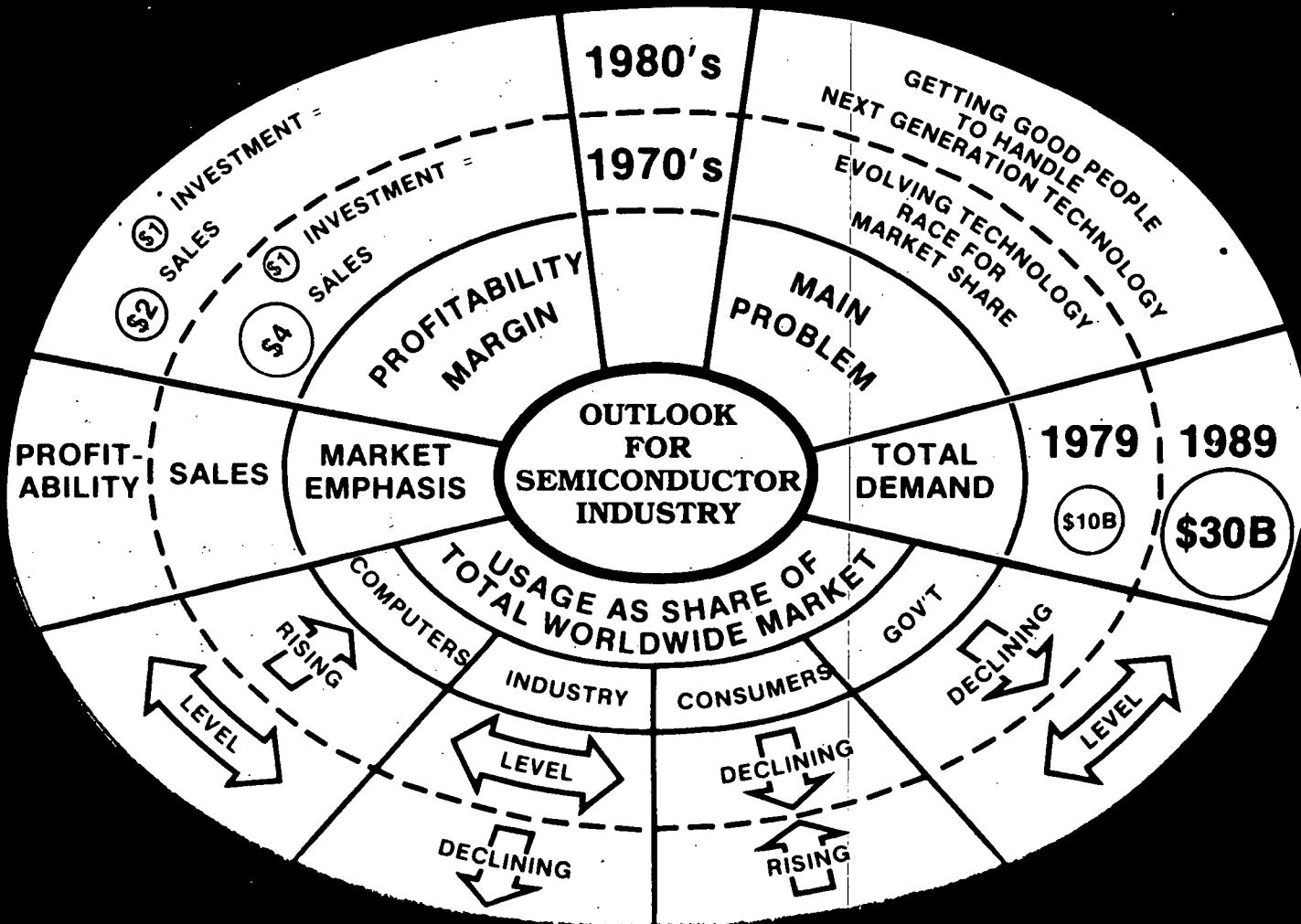


Figure 20



JAPAN'S PENCHANT FOR RELIABILITY

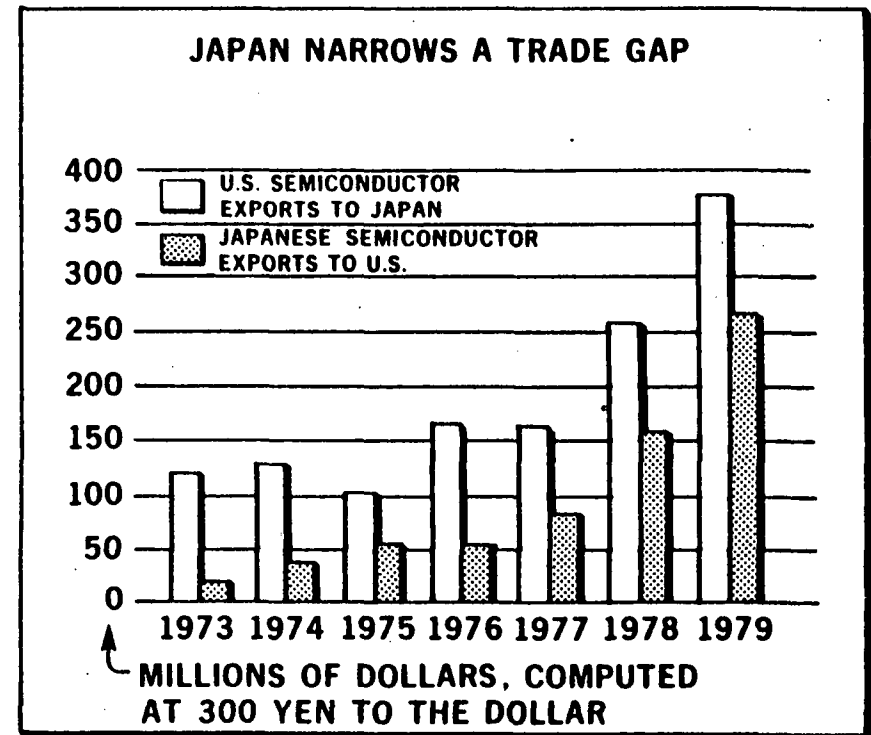
**JAPAN PRODUCES RELIABLE SEMICONDUCTORS
BY DESIGN, NOT BY CHANCE:
DEFECT PREVENTION, NOT DEFECT DETECTION**

**EXAMPLE: BETTER, MORE EXPENSIVE
PRODUCTION MASKS FOR CHIPS**

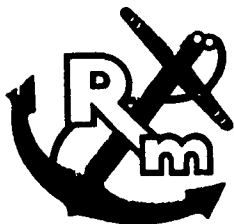
**RESULT: JAPANESE REJECTION RATES
ONE-HALF TO ONE-TENTH U.S. RATES**

**CONCLUSION: UNWILLINGNESS OF SOME
U.S. VENDORS TO PRODUCE RELIABLE
SEMICONDUCTORS IS COSTING THEM
NOT ONLY LOSS OF MILITARY BUSINESS
BUT POTENTIALLY OTHER CUSTOMERS
AS WELL**

• EVIDENCE:



• SOURCE: BUSINESS WEEK, 3 DECEMBER 1979



NAVY MANUFACTURING SCREENING PROGRAM (P-9492)

NAVMAT P-9492

NAVY MANUFACTURING SCREENING PROGRAM

DECREASE CORPORATE COSTS
INCREASE FLEET READINESS



● NAVMAT PUBLISHED P-9492 AND DISTRIBUTED TO 83 TOP CORPORATE OFFICIALS (CHAIRMEN OF BOARDS THROUGH DIVISION VICE PRESIDENTS)

● RESPONSES ENDORSE P-9492 THRUST ENTHUSIASTICALLY

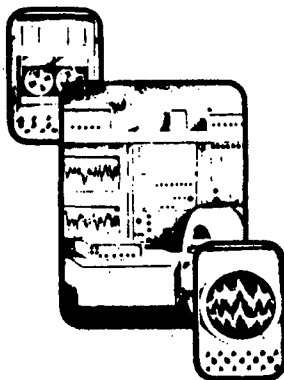
● SOME CONTRACTORS HAVE ALREADY BEEN USING P-9492 TYPE SCREENING AT THEIR OWN EXPENSE BECAUSE OF ITS OVERALL COST IMPROVEMENT

● OTHERS PROPOSE TO SCHEDULE ONTO EXISTING TEST EQUIPMENT, SINCE TEST TIME SO SHORT, IF CONTRACTS REQUIRE

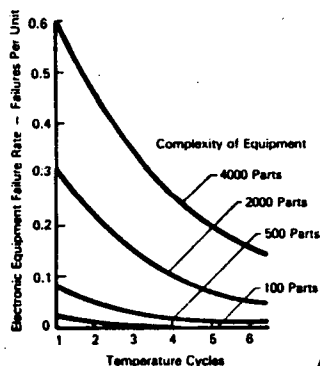
● RESPONSES INDICATE EVEN MORE STRINGENT TESTING OF LATEST COMPLEX ELECTRONIC SYSTEMS, AND TESTING AT LOWER LEVELS OF ASSEMBLY SHOULD BE REQUIRED

● GENUINELY COOPERATIVE, CONSTRUCTIVE RAPPORT DEVELOPING BETWEEN NAVMAT AND INDUSTRY WITH REGARD TO NEED FOR MANUFACTURING IMPROVEMENT

RANDOM VIBRATION



THERMAL CYCLING



DEPARTMENT OF THE NAVY

MAY 1979

Figure 22



INDUSTRY IN TRANSITION

MANUFACTURING

R 1975 ————— 1985 **G**

REPRESENTATIVE CONTRACTORS

	1	2	3	4	5	6	7	8	9	10
POLICY CORPORATE STATEMENT THAT MANUFACTURING QUALITY IS OF PRIME IMPORTANCE	R	R	R	R	R	R	R	R	R	R
ATTITUDES SELF-DISCIPLINE SHOWN IN QUALITY OF MANUFACTURING OPERATIONS	R	Y	R	Y	G	Y	Y	Y	R	G
AWARENESS RELIABILITY IN MANUFACTURING IS 'BUILDING TO PRINT'	G	G	Y	Y	Y	Y	Y	Y	Y	G
STANDARDS MANUFACTURING PRACTICES REFLECT DISCIPLINED QUALITY APPROACH	R	Y	R	Y	G	Y	R	Y	R	G
MOTIVATION FORMAL PROGRAM FOR ACHIEVEMENT AND RECOGNITION	R	R	R	R	R	R	R	R	R	R

R ACTION REQUIRED

Y IN PROCESS

G ACHIEVED

Figure 23

QUESTIONS AND ANSWERS

DR. WINKLER:

Thank you very much for a most interesting and challenging presentation. Let me add to your quote of Patton. I don't think you can put screws in the General ever.

And that is what it amounts to in some of these things. Well, if gear is to be there, then of course it is up to us to insist on quality.

There is one thing I wanted to ask you, however, and that is ~~your comment about military systems reliability in general is not~~ required to be so very great.

I would suggest that there are cases such as for instance in our case in precise timing in which we provide a commodity, precision timing, on which many operations depend. That in this case I think you have to insist on much higher reliability. The reliabilities that we are talking about in timing equipment is on the order of 20 to 50,000 hours MTBF. In this case we have an entirely different proposition. It has become uneconomical, for instance, to have maintenance people trained in some equipment because they will never see equipment fail. Or if it fails you will never have one experienced man around.

But it was certainly an extremely challenging and interesting speech. I wish we could all read it after it has become available in printed form, at least once a month on a Monday morning.

Do we have any questions?

DR. MCCOUBREY:

I wonder if values of parameters, such as junction temperature, are included in procurement specifications now?

MR. WILLOUGHBY:

You mean in ours or in yours?

DR. MCCOUBREY:

In the Navy procurement.

MR. WILLOUGHBY:

That list of what we call fundamentals up there goes into most of the Navy procurements now and we set 110 degrees as the max temperature that we will accept.

Now, I won't lie to you and say that we have accepted any temperatures with more than 110. We do, on an engineering basis, make some exceptions to that. But it is with judgement and consideration that we allow that temperature to go more than 110 degrees, which is the important point.

We know the risks we are taking and then we will let it go higher. But we are finding that we have to make less and less of those judgements.

Early in the program we had a lot of people asking for exceptions on the 110 degree. Now we find almost nobody asking for it. As a matter of fact, as I said, we are running more like 90 to 100.

It has been put into standard specs, which I think is important.

MR. RUEGER, The Johns Hopkins University, Applied Physics Laboratory

I understand that when reliability gets to a high enough number the Navy has a philosophy about not buying spare parts. Then when a failure occurs there is a long recovery cycle to get the instrument back in service.

MR. WILLOUGHBY:

Yes. You have hit on part of a problem. It has to do with mathematics once again. The Navy, in terms of sparing its equipment, uses algorithms as to certain numbers of times that the equipment has to be worked on during a years time, or during six months time. And there is a very flukey little algorithm that they use that does quantify exactly what you said.

And as the MTBF goes up, what they will do, if you follow this algorithm, you will find yourself with less and less spare parts.

See, what this has caused to happen, I will get into in just a minute. But what this has caused to happen, we have doubled, tripled and quadrupled the reliability of some equipments only to find that it is the most unavailable in the fleet in terms of availability.

The reason is from the way the sparing system is put together. We ran into an anomaly in the sparing system. That is what it amounts to. It is a logistics world. But the logistics community

is now re-looking the way they provision equipment because what they were doing was shooting themselves in the head with this particular algorithm.

And it is just simply said, significance of failure has nothing to do with it. It is only quantity. For instance, we had one piece of equipment we tripled the reliability on and the availability of the equipment went down to a mean time to repair of 13 months because they didn't even order a spare transformer for it. They had to order one at the first failure of a transformer and have it wound.

But that is a problem that is very unique to the military and let's hope nobody else does dumb things like that.

Page Intentionally Left Blank

RELIABILITY ACHIEVEMENT IN HIGH TECHNOLOGY SPACE SYSTEMS

Dean L. Lindstrom, Hughes Aircraft Company, Space
and Communications Group, El Segundo, Calif.

ABSTRACT

Long Life space systems developed from the early 1960's to the present day have demonstrated the achievement of long life and high reliability in a high technology space environment. With electronic parts improvements, decreasing failure rates are leading to greater emphasis on the elimination of design errors. The achievement of reliability is dependent on three primary factors: technical capability, good judgement, and discipline.

INTRODUCTION

My discussion will center primarily on the achievement of reliability on long life, high reliability spacecraft. These utilize a combination of proven technology and new technology. The lives of these spacecraft, for the most part, have been longer than anticipated. When we started the Intelsat IV program, for example, no one had any experience to indicate that a battery would last for the seven years required.

Several of these spacecraft have introduced new technology without compromising life or reliability. One recent development is the Compact Hydrogen Maser frequency standard for Navigational Satellites, delivered this year to NRL. It is still not space proven, but initial clock comparison data indicated performance unsurpassed for a device of its size.

DISCUSSION

Figure one (1) shows the Hughes family of satellites. This family started with the launch of Syncom (lower right corner) in 1963. This was the world's first synchronous communication satellite. It operated successfully until operation finally was discontinued in 1969. The newest member of this family in the upper left hand corner is the Leasat. This satellite, to be launched in the 1980s is our first spacecraft design optimized for a shuttle launch. Some other spacecraft are worthy of note. The ATS, launched in 1965 for Goddard Space Flight Center, is still providing useful data. The TACSAT, launched for the air force in 1969, was the first gyrostabilized or dual

DISCUSSION - Continued

spin-stabilized spacecraft. On the left hand side in Intelsat IV, which was the first large International Communication Satellite. It is capable of handling 9,000 simultaneous two-way telephone conversations. The OSO, orbiting solar observatory, with the design life of 3 years, was turned off after 4 years of successful operation.

Two spacecraft shown in this figure are shown more closely in Figure 2. Pioneer Venus Orbiter and Multiprobe spacecraft represented some very difficult technological challenges. 33 different scientific instruments for taking atmospheric measurements in Venus were integrated into these two spacecraft. For the probes that went to the surface of Venus, this meant withstanding the high temperature and acid of the Venus atmosphere plus the extremely high pressure encountered at the Venus surface.

The next two figures (Figures 3 and 4) show the operational performance of this family of satellites. Together they have accumulated over 200 spacecraft years of successful operation. More than 15 billion electronic parts hours have been accumulated with less than 30 failures attributable to electronic parts. None of these part failures has had a significant impact on spacecraft operation.

These spacecraft have demonstrated several significant things relative to reliability. First, they have demonstrated that long life in the vicinity of 7 to 10 years is achievable with complex space systems. ATS has demonstrated that, under the right conditions, a life of 15 years or more is possible. Second, they have demonstrated that the reliability of electronic parts can be extremely high and a negligible factor in overall system reliability. They have demonstrated another fact that is not apparent from these charts. When you take any element or item for granted, it will be the element that comes up and bites you. The only significant problems we have had on orbiting satellites is with travelling wave tubes. Due to oversights in the modification of existing designs, we had early life failures of travelling wave tubes on several spacecraft. Because of redundancy within the satellites, the effect of the shorter tube life was minimized. The problems have been corrected and we expect to get longer life on our tubes in the future. The second illustration is a non Hughes satellite, but it was one that caused a major investigation. The SEASAT had an early failure of slip ring power transfer assembly. In this case an existing proven design was used for a different application. The difference in the application was not recognized initially and eventually led to the failure of the satellite.

DISCUSSION - Continued

What are the keys to achieving high reliability in a high technology environment?

- Understand the Design
- Design with conservatism
- Control Parts, Materials and Processes
- Test and Analyze

Understand the Design

Generally, there is a hesitancy on the part of the design engineer to document his design and document what he understands about the design. I have two concerns about this. One is, since the full understanding of the design is in his head, what happens if someone else attempts to supply that design? And second, does he really understand the design or does he just think he does? The process of setting down on paper how the design works and interacts with other hardware systems generally leads to better understanding by the designer himself. I can refer to a recent example, where a very competent design engineer was requested to perform a hazard analysis. After the explanation by the safety engineer, the design engineer spent a day and a half fully documenting how his design works. He later acknowledged that now not only were other people able to understand how this design worked but he now understands it better himself.

Failure modes and effects analysis is an important tool in both documenting the design and identifying what can happen to cause the system to fail. Unfortunately failure modes analyses are often conducted after the design process is complete. This results in mechanically accomplishing the task to satisfy some contractual requirement. With the great reduction in part failures, design error or oversight becomes one of the principal causes of failures occurring during ground test and system operations. Therefore, it is important to identify and eliminate all failure modes as early as possible in the design process. Failure modes and effects analysis can be divided into the four areas listed below.

Functional - The functional FMEA should be initiated early. It shows the interaction of all functions of the item and the role of the individual hardware elements in the overall item operation.

Design - The design FMEA considers all hardware elements, their inputs and outputs, down to the level necessary to determine the item's failure mode and the potential of failure.

DISCUSSION - Continued

Understand the Design - Continued

Interfaces - Commonly overlooked in an FMEA is the assessment of all the interfaces and interconnections. I know of one case where the conventional failure modes and effect analysis was performed on some complex hardware. By standard considerations, it was a good FMEA. However, after some problems during system operations a reliability engineer was assigned to reassess the failure modes in that hardware. He found over 100 single point failures in that system design. In order to accomplish this analysis he had to reconstruct the interconnects and the interfaces of all the elements in that system.

Product Design - This is a new concept now being introduced in some programs. It is one which I feel will be one of the most constructive. Great attention is often paid to circuit design and system design, but product design, which can greatly affect the manufacturability and, ultimately, the reliability of hardware is often overlooked. How many of you have had a product design review?

Another element in understanding the design is testing - test to determine design limitations, safety factors, and failure modes that may have been overlooked in the failure modes and effect analysis. Development tests and qualification tests generally are aimed at proving the design capability of the hardware. While this is valuable, I maintain that testing that uncovers no failures is wasted testing. Sometime during the development process, tests should be conducted on the hardware to accelerate the failures. Failures can be accelerated through the application of environmental or performance stresses. You cannot fully understand your design until you know how it operates under extremes of temperature, thermal cycling, vibration, or performance. If a system is designed to operate for several years, it is not possible to fully evaluate that system within normal time constraints without accelerated testing. This testing must also consider the interfaces. Until all the interfaces have been tested with the adjoining equipment, a full understanding of that unit is not possible.

One other area that I think is very important in understanding the design and helping to stay out of trouble is to modularize the functions and the hardware. By this I mean divide the functions and hardware into workable independent or semi-independent elements. Design decisions are difficult under the most straightforward of circumstances. If the hardware functions are so interrelated that each decision affects all elements then you can count on overlooking some element that later causes problems.

DISCUSSION - Continued

Design with Conservatism

One of the keys to the success of our space systems has been the conservative design. From early systems, parts derating has been an important factor in achieving high reliability. The thermal environment is extremely important. We generally try to derate our parts to about 20% stress at 250 centigrade. If the temperature goes up the stress goes down. At the most, parts should not be operated over 50% of their rated values to achieve high reliability.

What have you learned from your past experience? Utilize the past experience and past problems to develop design guidelines. We have developed design guidelines aimed at preventing problems that previously have occurred or similar problems that might occur. Design check lists provide a good tool for implementation of design guidelines and for design review.

Design with Safety Factors. This is a significant factor in achievement of overall reliability. And finally, there is redundancy. I consider redundancy as a crutch to protect from what you do not know. It also protects from errors that may be introduced during the manufacturing process.

Parts, Materials and Processes Control

We establish a Parts, Materials and Processes Control Board (PMPCB) at the beginning of each program. The objective is not to prevent the introduction to the new parts and materials; rather it is to manage the introduction of new parts and materials, and to assure that proven parts and materials are used wherever possible.

Control of electronic parts through the manufacturing process, test, application, and installation in hardware is extremely important. As I said before, we have very few parts problems in Space. The driving force for the controls we place on electronic parts has been the failures on the ground. While high reliability parts may cost more initially, the savings in parts replacement, equipment repair, and test time usually more than compensate for the higher cost for the parts. Control on the materials is just as important. They should be properly specified, controlled, and analyzed so that all the materials characteristics are understood.

Probably the best term to describe the control of manufacturing process is "tender loving care". Introduction of new process specifications also is approved by the PMPCB. The associated quality controls

DISCUSSION - Continued

Parts, Materials and Processes Control - Continued

are tighter for high reliability products. Documentation is extremely important, so that when a problem does occur, you can trace its source and correct the cause.

Test and Analysis

I previously discussed the importance of the proper development and qualification testing. A technique that has been found to be very effective in producing a high reliability product, and at the same time reducing manufacturing cost, is environmental stress screening. This usually consists of thermal cycling, vibration, vacuum testing, shock, or some combination thereof, applied at various hardware levels. It may be applied as low as the card or module, or as high as the system. It is most frequently applied at the black box level. The objective of this testing is to stress the hardware sufficiently to uncover workmanship or parts defects. At the same time, it is also a good tool for finding design weaknesses. In one case, we applied thermal cycling to a spacecraft after it had completed all the acceptance tests and was ready for launch. In the process, a number of failures were uncovered, at least six of which would have caused significant spacecraft degradation during operation.

Generally tests should be conducted under conditions more severe than operational conditions. Concern is often expressed that this may cause wearout or early failures of your systems. Performed with discretion, I know of no failures in Space on Hughes systems that have been caused by over-testing. I do know of failures that have occurred because of oversight. One important aspect of testing is to test all modes of operations. This is not always possible during system testing, therefore some of that testing must take place at lower levels.

I think one of the keys to achievement of High Reliability Spacecraft has been the fact that every failure is treated as a critical failure. All failures should be reported, should be fully analyzed, and corrective action should be identified and instituted wherever possible. It sometimes takes time and costs money, but it will surely result in a more reliable system. Do not overlook the analysis of all test data. Numerous cases have occurred where failures occur in operation and subsequent analysis of test data showed that the symptoms of the failure had occurred but had been overlooked.

CONCLUSIONS

There are no simple answers for achieving high reliability in a high technology environment. Specific techniques that are applicable to one contractor, one system or one hardware element are not necessarily the same techniques that are applicable to another.

Failure-free hardware can be produced. The elements required to achieve failure-free hardware are:

- Technical expertise to design, analyze, and fully understand the design.

- Use of high reliability parts and materials control of, and tender loving care in, the manufacturing processes.

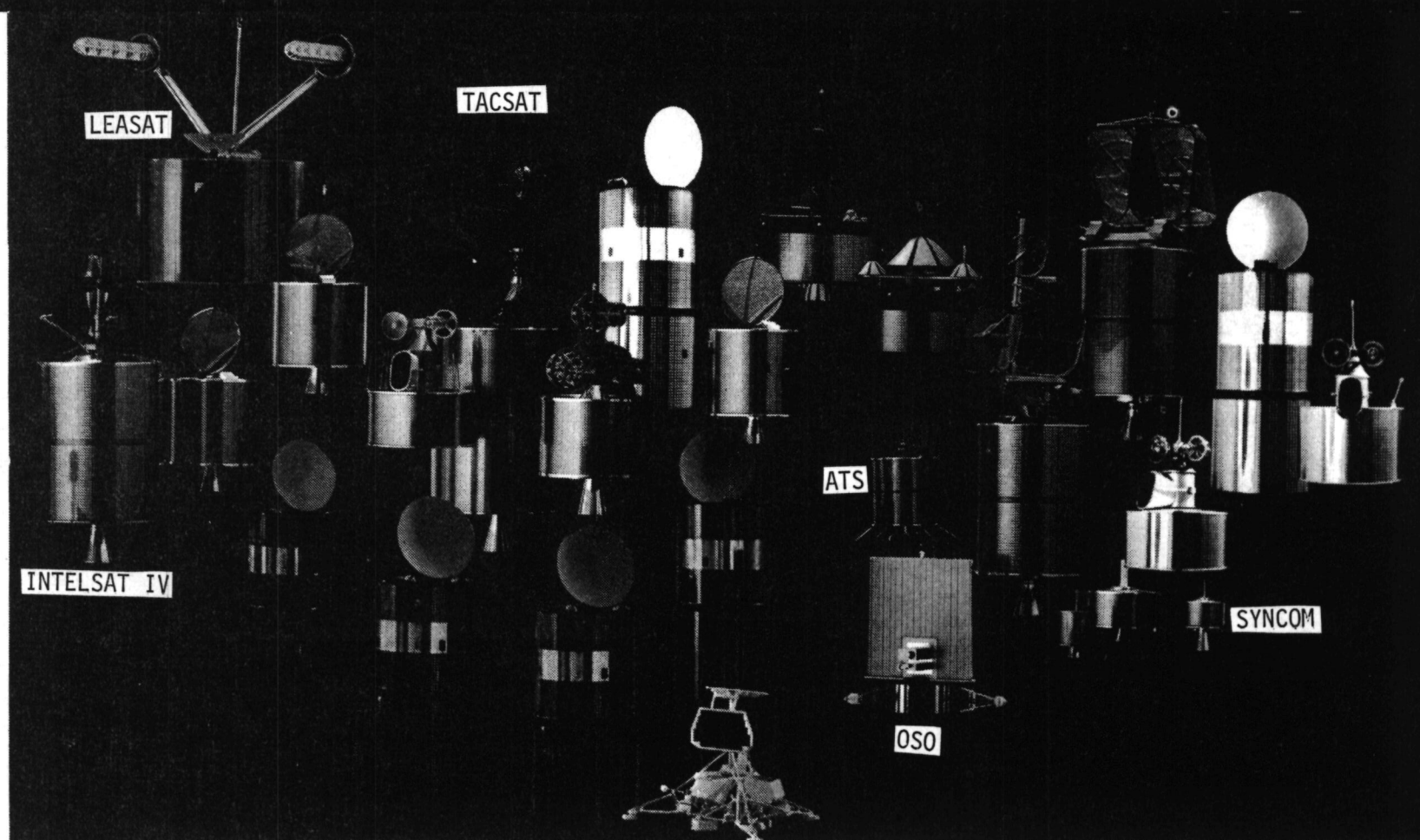
- Testing to understand the system and weed out defects.

Proper application of the above requires sound judgement in decision making and the discipline necessary to follow proven practices.

HUGHES FAMILY OF SATELLITES

HUGHES

FIGURE 1.

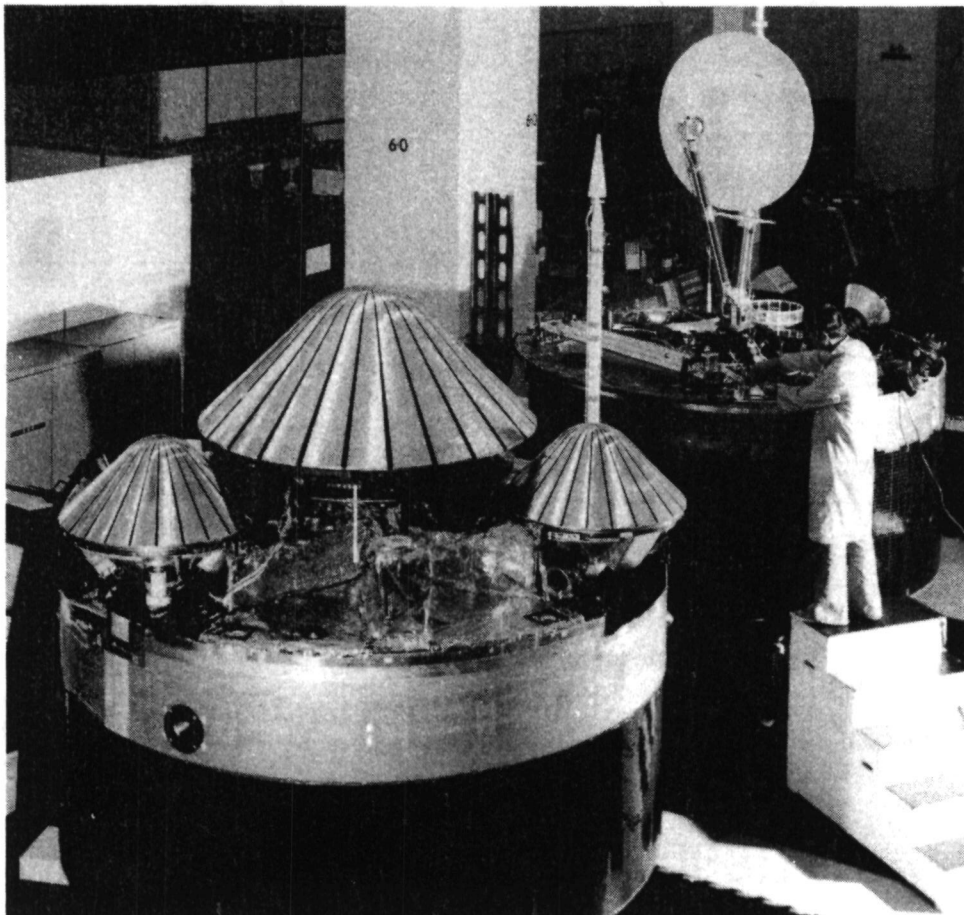


06100-86

PIONEER VENUS

HUGHES

FIGURE 2.



ORBITER

- 522 KG (1218 LB) AT LAUNCH
- S BAND
- 193 W
- LAUNCHED: 20 MAY 1978

MULTIPROBE

- 920 KG (2024 LB)
- 170 W
- LAUNCHED: 8 AUG 1978
- ENCOUNTER: 9 DEC 1978

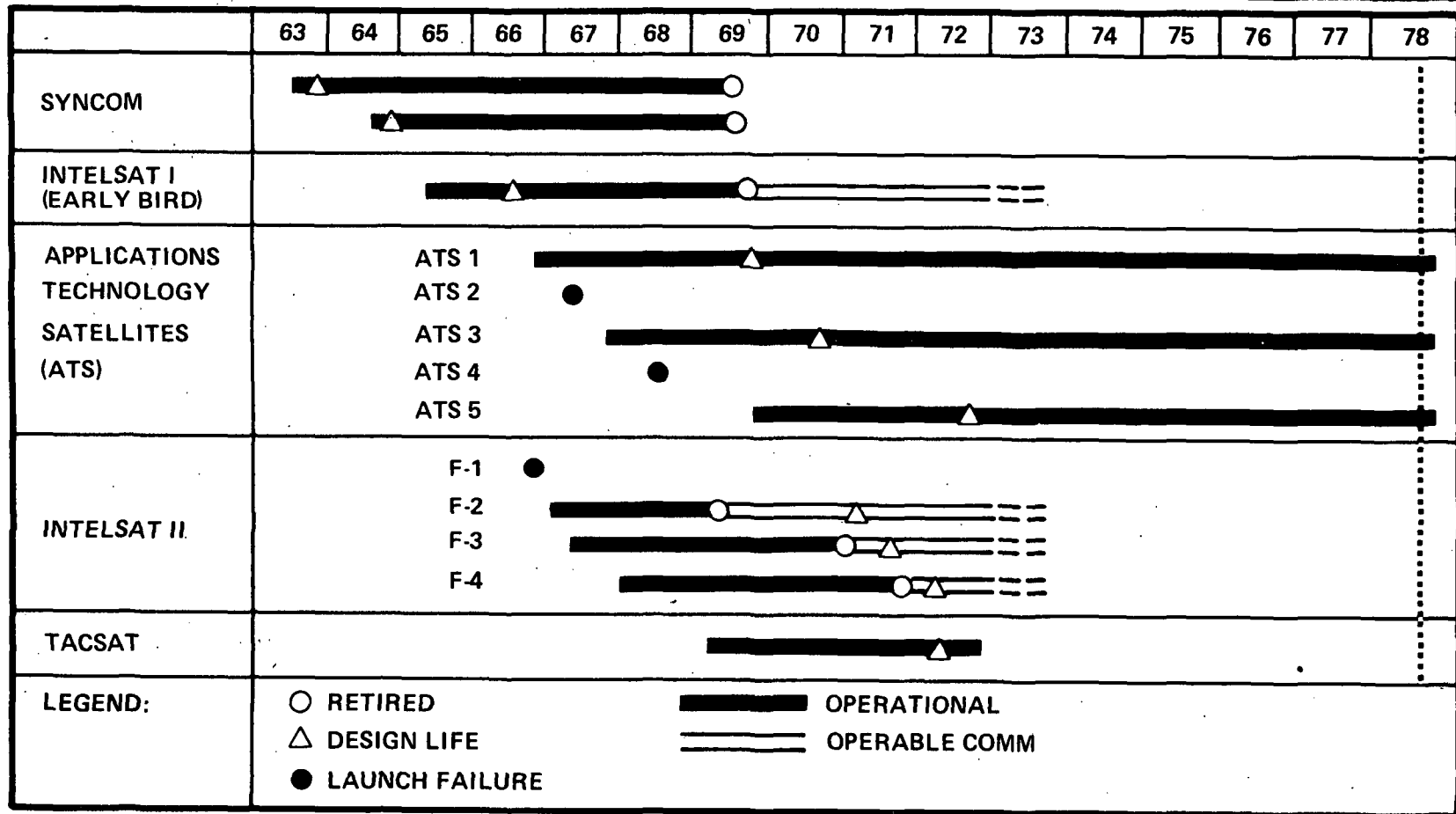
86100-49

77-61233

EARLY HUGHES SATELLITE ORBITAL PERFORMANCE

HUGHES

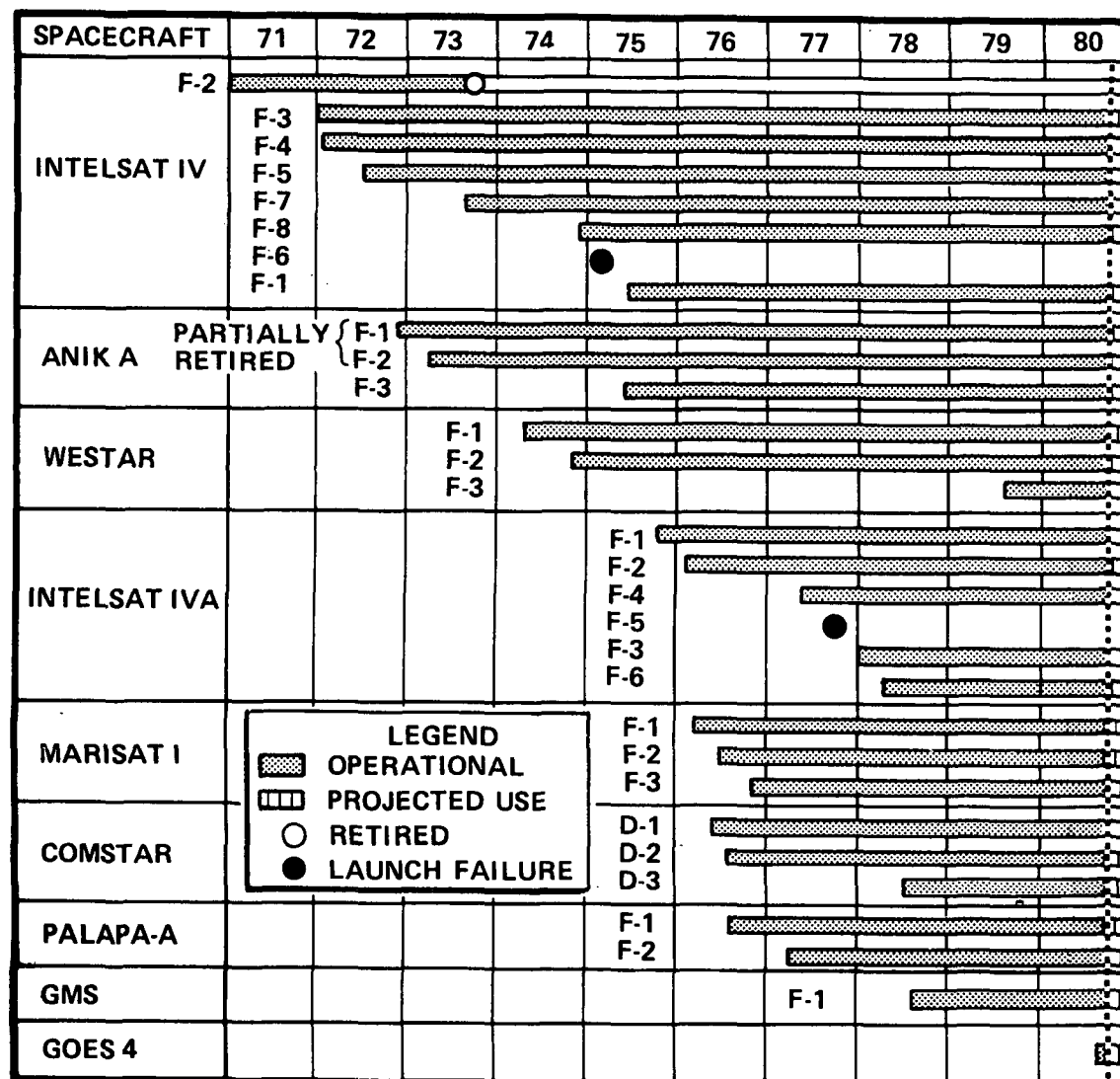
FIGURE 3.



86100-7

HUGHES

FIGURE 4.



AS OF NOVEMBER 1980 HUGHES HAD OVER 200 ORBIT YEARS EXPERIENCE

MODERN HUGHES SATELLITE PERFORMANCE

06100-8

APPROACH TO RELIABILITY
WHEN APPLYING NEW TECHNOLOGIES

John C. Bear, General Dynamics Corporation
(Pomona Division), Pomona, California

ABSTRACT

General principles derived from experience in achieving high reliability in tactical weapon systems are selectively summarized for application to new technologies in unusual environments

INTRODUCTION

The General Chairman of this meeting, in suggesting some topics for this paper, observed that much of the technology which is important in precise time and time interval applications is new and immature in the sense that it has not been fully qualified for the most demanding field applications. Tactical weapon systems, while different in many respects from PTTI applications, probably face similar risks in achieving reliability in development. A supersonic guided missile, for example, must cope with continuing modernization of its state-of-the art sensors, oscillators, and other special-purpose devices, and it must operate reliably in severe environments including high and low temperature, shock, and vibration. Perhaps some of the lessons learned in the development of tactical weapons can therefore be of value in PTTI applications.

PRINCIPLE NO. 1: START EARLY

During development the reliability of a design grows as the sources of failure are unearthed and eliminated. In this context reliability is more or less synonymous with maturity, whereas state-of-the-art technology is by definition infantile. It follows that any successful approach to the problem will require an early start and an acceleration of the normal processes for avoiding or removing the root causes of failure (Figure 1).

But many factors inhibit an early start. Cautious program managers are reluctant to transfer funds allocated to the downstream "curative" engineering into the category of upstream "preventive" engineering. After all, testing is certain to produce failures, whereas an analysis has only a probability of payoff. Then too, managers who have grown up under the heavy influence of Murphy's Law do not necessarily believe that the really big failures are preventable. Furthermore, state-of-the-art designs deal with arcane concepts that do not easily yield to analysis nor readily reveal their weaknesses. Also, the reliability experts do not come from an ancient and universally admired discipline, and their ministrations are not always trusted.

For these reasons, it is necessary to adopt a high-level, deliberate, well-focused management determination to attack unreliability at the beginning, to muster up a lot of interest and excitement in specific approaches, and to reward creative planning and successful effort. A good way to converge quickly on a plan of action is to prepare a list of the devices or design elements that are immature, and identify for each item on the list a series of tasks that will reduce the risk. What follows is a discussion of some of the more useful tasks.

PRINCIPLE NO.2: KEEP IT SIMPLE

Complexity and sophistication, obviously, are the primary obstacles to the achievement of reliability in the initial design. On the other hand, a simple design (Figure 2) is straightforward, well-balanced in its accomplishment of the essential requirements, and free of frills--one might say it is elegant in concept. But how can simplicity be achieved while striving for some new and difficult level of performance?

An effective (but often neglected) procedure for achieving a balanced design is the design trade study (Figure 3). Its value lies in forcing alternative design solutions to the surface, in clarifying the relative importance of requirements (indeed providing the basis for deleting requirements that are "costly" in one way or another), and in suggesting back-up designs in case the primary selection fails to prove out. The trade study technique adapts well to the simultaneous analysis of multiple parameters (reliability, weight, power consumption, cost, etc.) and is an excellent mechanism for bringing design features and weaknesses out of the hallowed shadows of the expert mind.

Another method for promoting simplicity, especially on larger systems, is component standardization. The benefit, of course, is reduced variability and thus fewer sources of failure. But where a design applies redundancy as a way of compensating for low reliability, one must beware of standardization in the parallel components, for under severe stress they will tend to suffer the same failure modes, thus negating the assumed independence in the probabilistic model that justifies the redundancy.

Another technique for achieving design simplicity is the FMEA (Failure Modes and Effects Analysis). There are many different ways to do an FMEA, and the scope of the analysis can be adapted to designs of different sizes. In essence, the object of the FMEA is to examine the dark side of the design. The bright side, of course, is how it works or is supposed to work, whereas the dark side is how it can fail and what will be the consequences of failure. A good way to perform the FMEA is with a team composed of the design engineer, the systems engineer, and the reliability engineer. Pooling their different viewpoints can often lead to a simplified design if they do the analysis early in the development process when changes are still relatively easy to incorporate.

PRINCIPLE NO. 3: MAKE IT STRONG

Assume now that an attempt has been made to simplify the design, with a concentration of effort on the state-of-the-art technologies that will dominate the failure rate of the operating system. The final step is to take the resulting, optimized design concept and make it strong enough to withstand its usage environment.

The general concept of conservative design (Figure 4) takes the view point that environmental stress is the ultimate cause of failure, so that failure prevention is a matter of assuring adequate separation between expected strength and expected stress.

To begin with, it is necessary to define the environments with full respect for their lethality, with regard for not only their average values, but also for their natural variability and worst-case values. The design specification must reflect these worst-case expectations.

Then the strength objective is established, either in the same specification or in formalized design guidelines. Ideally the strength requirement will take the form of a safety margin, which sets strength as a function of both its average and its variance. Or, when the variance is not known or is not a problem, the objective will take the form of a safety factor (for mechanical designs) or a derating factor (for electronic designs).

Finally, the strength-minus-stress difference is controlled by analysis. That is, a stress analysis is performed on the design before it is released so as to assure that the specifications and guidelines have been followed. Even though safety factors are as old as engineering itself, they suffer de-emphasis whenever there is pressure to squeeze extra performance out of a state-of-the-art device. The stress analysis is essential, therefore, to enforce the guidelines, to surface the risks, and to assure time for pursuing alternatives.

WHEN ALL THIS FAILS

If the foregoing approaches to preventive analysis do not materialize for one reason or another, what then? The standard fall-back position is to rely on testing, followed by diagnosis and fixing of test failures so that they can't recur. A very good technique for flushing out problems early in the test program is the overstress screen (Figure 5)). In applying this test, the high-risk devices are exposed to one or more important environments to assure that they individually exhibit an adequate strength-stress safety margin. The stress level should exceed the worst-case expected stress in actual usage. The type of environment(s) should be tailored to the suspected weaknesses of the device. The test should be performed as early as possible, ideally by the designer or supplier. Proposals for this kind of testing can evoke outspoken (and usually unwarranted) fear of damage and wearout, which can be dispelled by exploratory step-stress testing of dedicated or spare hardware.

SUMMARY

The key to achieving reliability in new technologies is to really want it--that is, to align the development team toward the essentiality of reliability right at the beginning. Given that significant attention will be devoted to

reliability early in the design phase, there are a number of analytic tools such as trade studies and failure modes analysis that will help keep the design simple, and others such as derating and stress analysis that will help make it strong. Further down stream, when hardware is available, an environmental overstress screen in selected environments will help expose remaining problems. In applying these techniques success will be directly proportional to the care with which they are tailored to fit the specific design program.

FIGURE 1

START EARLY

- **STATE-OF-THE-ART MEANS RISK**
- **CURATIVE ENGINEERING IS TOO LATE**
 - **BUT PREVENTIVE ENGINEERING CAN BE HARD TO SELL (DOESN'T GUARANTEE TO FIND ALL THE FAILURES)**
- **THEREFORE THE BOSS HAS TO GET INVOLVED AT THE START**
 - **ESTABLISH RELIABILITY AND PERFORMANCE CO-EQUAL**
 - **IDENTIFY A LIST OF RISK ELEMENTS**
 - **FUND SPECIFIC TASKS TO REDUCE RISK**

FIGURE 2
KEEP IT SIMPLE

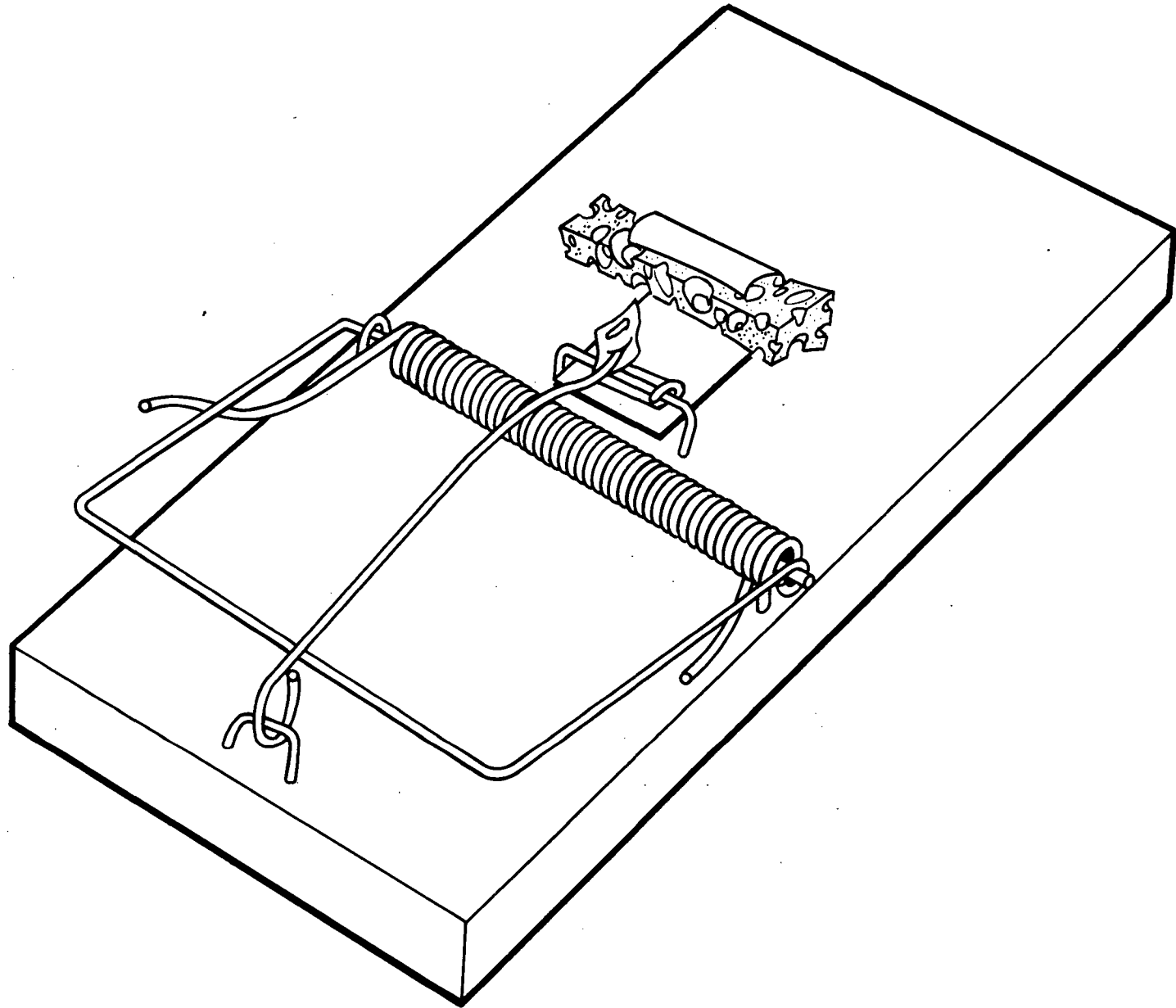


FIGURE 3
DESIGN TRADE STUDIES

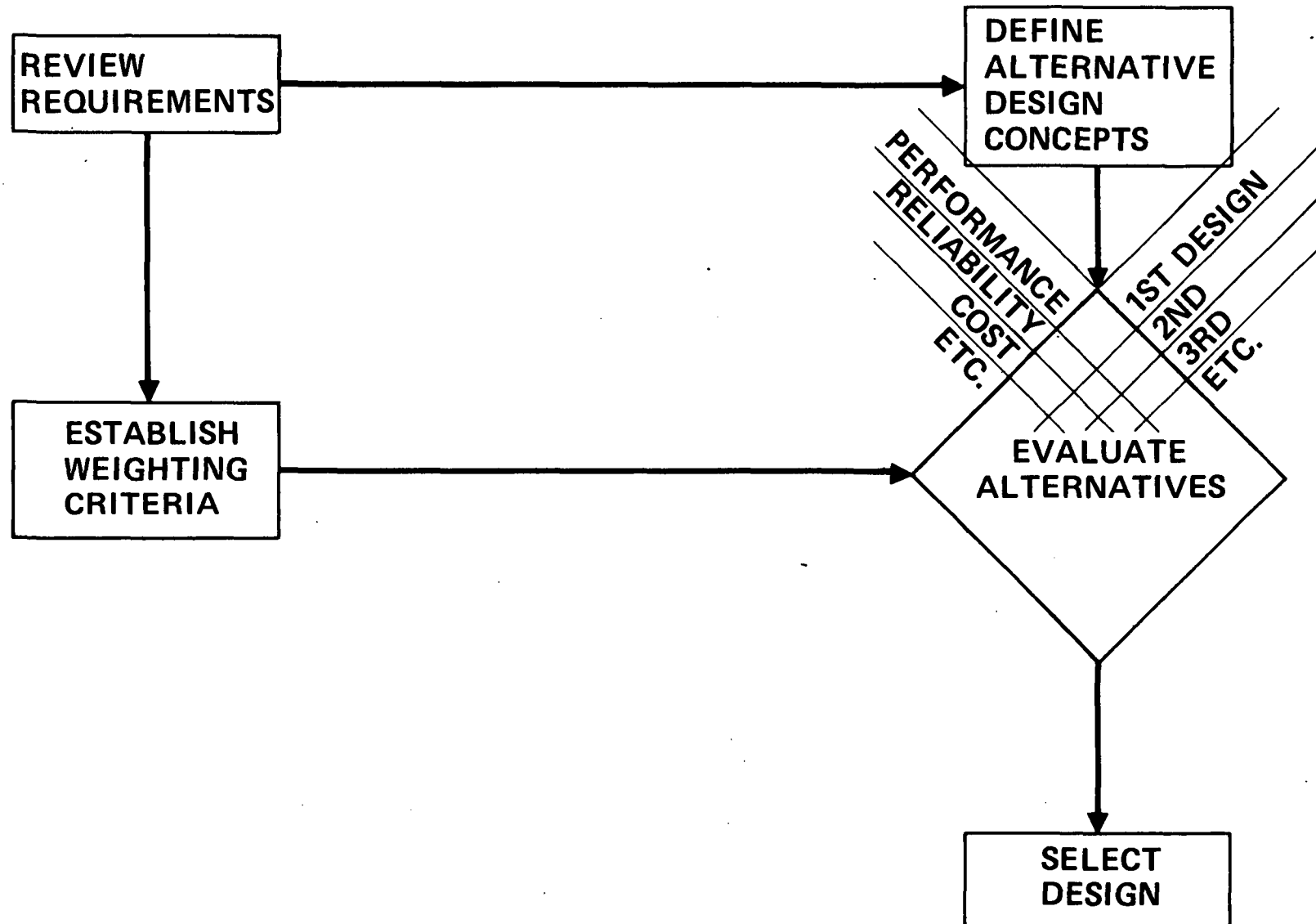


FIGURE 4 CONSERVATIVE DESIGN

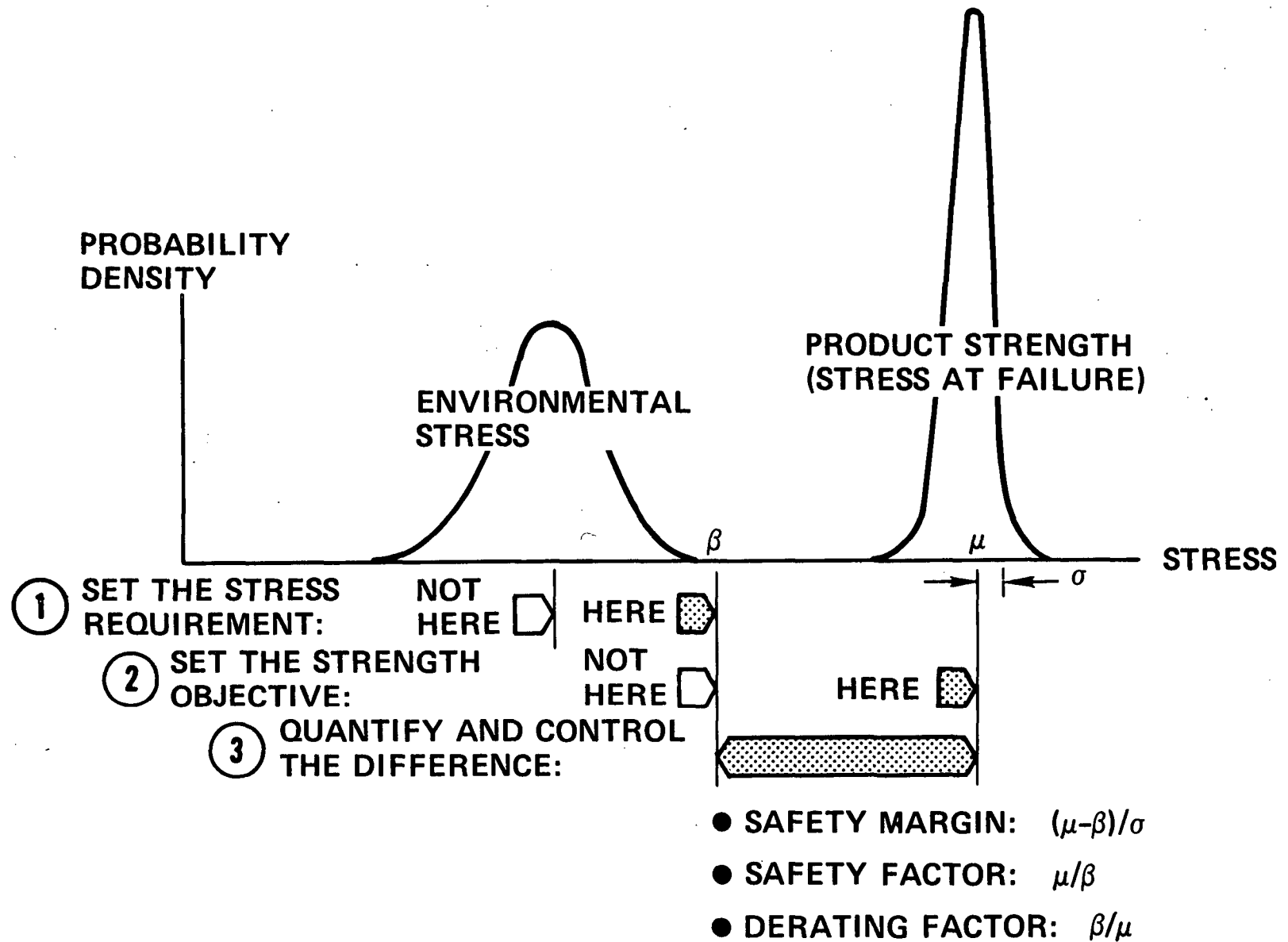
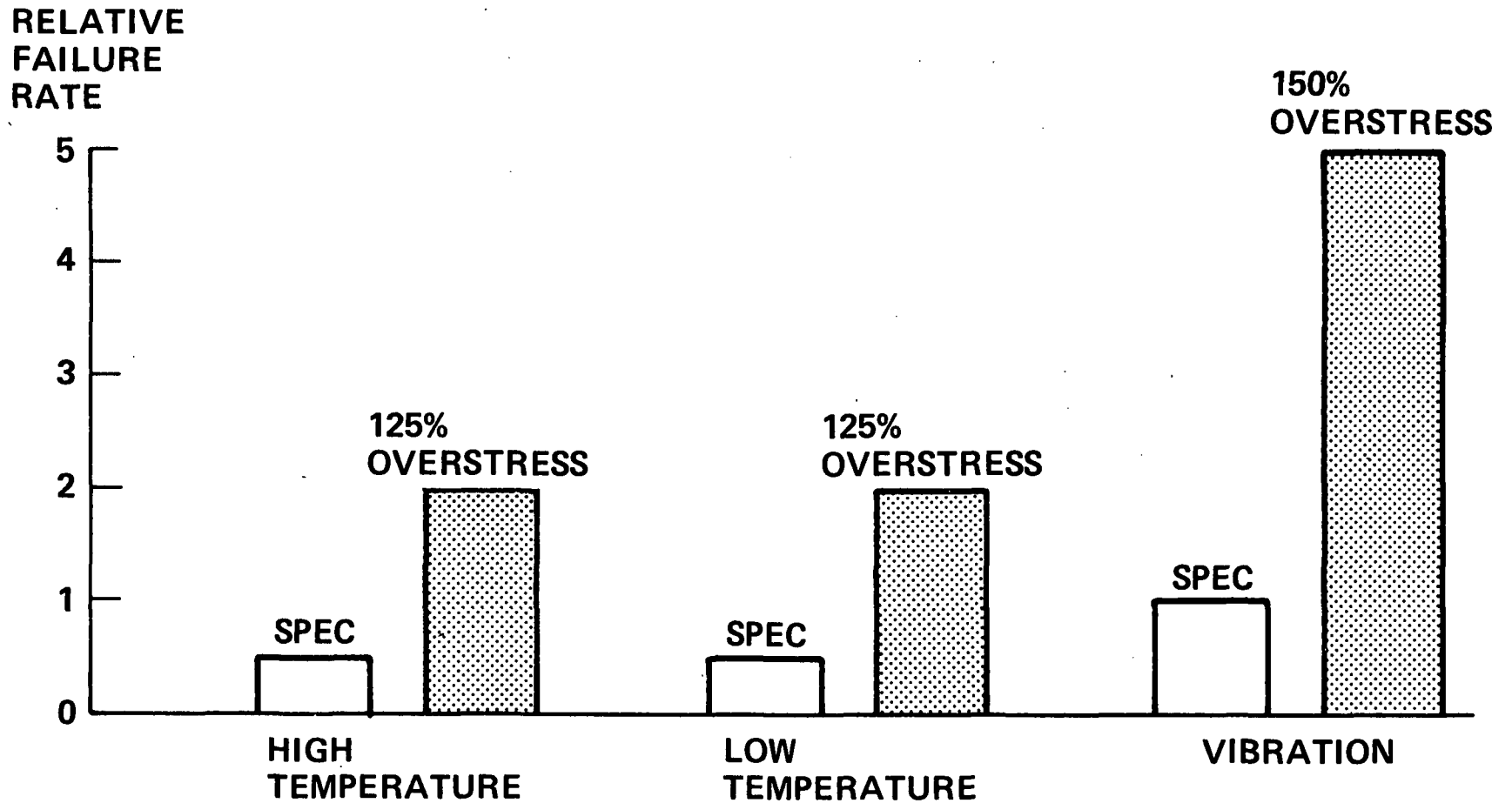


FIGURE 5
OVERSTRESS SCREENING
(DEVELOPMENT MISSILE ASSEMBLIES)



QUESTIONS AND ANSWERS

DR. STOVER:

I would like to question you about the simplest design because it seems to me that one of the most complex devices we do is the micro processing. I am convinced that using it gives us more reliable equipment than if you use the less complex method of achieving the same result that it achieves. Yet that must be by far the most complex device that we ever use in electronics.

The little tiny chip has so many parts on it, it can't be looked at as the simplest approach. But gives us the smallest, simplest project, the least soldering, the fewest connectors, they are reliable products. They are appearing in our automobiles now. I am sure the reason they are there is because they can't achieve the same result as reliably by other methods.

MR. BEAR:

I think that is a simple development.

DR. STOVER:

You do?

MR. BEAR:

Yes, I do. I think that solid state, the programs of solid state technology is moving toward simpler devices even though you count the gates, it seems more complex. Yet the reliability is going up. And the reason it is going up is that the more things are being done mechanically without human intervention and that is primarily the reason. We are doing more things in a systematic way and everytime we go to a new grade of micro processors, you are not only achieving a much higher performance, but we are also improving reliability. So I consider that to be simple.

DR. STOVER:

Well, I guess that your definition of simple needs to get around through the industry because I am sure that the design engineer who comes up with a circuit diagram that includes the circuits that are on that micro chip and then comes up with all the firms that don't use this micro chip, it is a much smaller circuit diagram, much less on it and he gives that to his manager and which one is the manager going to tell him is the least complex.

MR. BEAR:

I guess my definition would be that simplicity is eliminating sources of variability.

DR. STOVER:

How can you get the definition across to the rest of the world?

MR. BEAR:

I don't know. That is a good challenge.

DR. STOVER:

Thank you.

DR. WINKLER:

Thank you. I think we have some time to think about that and maybe return to that question of simplicity. I think it is a very interesting one since it appears to me that reliability engineering or prevention of failure has very much to do with our ability to rationalize things, to think ahead your idea of putting the best brains together into a review group and design group as early as possible. I think that would be the best way to attack that failure to be able to foresee.

RELIABILITY AND THE DESIGN PROCESS
AT
HONEYWELL AVIONICS DIVISION

Alex Bezat, Reliability Department,
Honeywell Avionics Division

ABSTRACT

This paper describes the Honeywell Avionics Division philosophy for "Designed-In" reliability, a summary of selected tasks from the Willoughby "New Look", and a comparison of reliability programs (based on electronics) for space, manned military aircraft, and commercial aircraft. The approach we have taken in this paper will cover the following items, as they relate to Honeywell AvD:

- o Reliability Philosophy and Organization
 - Reliability Interface with Design
 - Reliability Interface with Production
- o MTBF Predictions, Concept Phase through Final Proposal
 - The Laser Gyro - A New Technology
 - Electronics - An Evolutionary Technology
- o Design, Development, Test and Evaluation Phase
 - Semi-Conductor Junction Temperatures
 - Sneak Circuit Analysis
- o Production Phase
 - Production Support
 - Manufacturing Run-In (MRI)
- o Commonality Among Space, Military, and Commercial Avionics
 - Space Electronics
 - Military Avionics
 - Commercial Avionics

INTRODUCTION

This paper has been prepared in response to a request from Dr. A.O. McCoubrey, general chairman for the 1980 PTTI Meeting. As we understand the background of PTTI measurement, some of the concepts and technology are new, even unique. Reliability and Maintainability (R&M) considerations to date may, therefore, be inadequate for the projects of tomorrow. Our purpose in this paper is to present a picture of how our company--the Avionics Division (AvD) of

Honeywell, Inc.--approaches the subject of designing, building, and testing electronics equipment with controlled R&M characteristics.

The breadth of the subject is staggering in terms of a 20 minute presentation. In an attempt to avoid an overly broad-brush approach to the subject, we are making some assumptions. First (and foremost): because the Willoughby "New Look" has gained wide acceptance, we will not review all of the various tasks, tests, and analyses that it prescribes. We believe that R&M people can, in their own operations, perform or lead most or all of the salient tasks inherent in the "New Look". Therefore, this paper will dwell on efforts at AvD that are different--and in one case, unique to our operation.

We recognize that the approach we have chosen might amplify the appearance of disagreement with other people in R&M work--including, perhaps, some of you in the audience. Please, then, keep two things in mind: (1) we undoubtedly have a high degree of commonality in most of the items not discussed in detail here; and (2) the material we are covering represents a view--a series of Engineering judgments--on methods that we consider to have been effective for us.

RELIABILITY PHILOSOPHY AND ORGANIZATION

Honeywell AvD subscribes to a basic reliability philosophy that is common to most organizations where product reliability is of major importance: "Reliability is a 'designed-in' performance characteristic. Testing and inspection verify that the design meets objectives, and that the product, as built, retains the characteristics of the design." While very few people would disagree with any aspect of the philosophy as stated, the methods by which the concept is implemented by various organizations--the actual tasks and organizational responsibilities of the working reliability engineer--are diverse and, at times, seem to contradict the philosophy as expressed. At AvD, our organizational structure and our assigned charter of responsibilities are tailored to fit the accepted basic philosophy. Therefore, reliability engineers are an integral part of the Engineering Department in a service organization.

Reliability Interface With Design

Although our Engineering department is quite large--(more than 500 engineers, 400 of whom are design engineers)--we have found that a central support/services group gives flexibility to the covering of changing work loads in the various sections of the department. One section of this group is the Reliability and Design Support (R&DS) function, consisting of about 50 engineers. R&DS has responsibility for disciplines that include: reliability, maintainability, system safety, mechanical/vibrational stress analysis, thermal analysis, electromagnetic interference considerations, and electrical/electronic part standardization and specifications. There is a need for interaction within these disciplines and our organization fosters such interaction.

In the design phase of major projects, our experience has seen the assignment of one or two R&M engineers for every 10 design engineers. On recent projects, the ratio has been closer to two-to-10.

Reliability Interface with Production

There are gray areas between Engineering Department control of product performance, and those items of control that belong to the Production and/or Quality Departments. However, we believe (with Mr. Willoughby) that the prudent resolution of such gray areas is almost always in favor of making them the responsibility of the Engineering Department. Specifically, if there is any doubt about the control of the end result of a process by direct measurement of the end-product, then that process should become an engineering specification, under control of the Engineering Change Order (ECO) procedure.

Despite this effort, there are areas of overlap in which items that are not under ECO control can--and do--have an effect on reliability. Therefore, one of the tasks assigned to our reliability engineering function is to interface with engineers from the production and quality departments in order to resolve problems during product build, and for malfunctioning goods that are returned from the field. We title this task FRACA--Failure Reporting, Analysis and Corrective Action. We'll discuss this task again later, as well as some of the major differences between a quantity build (100s or 1000s of the same item) program and a space-oriented product.

Highlights of a Current Program

The remaining portions of this paper, which describe various phases of a particular program, are examples from a current commercial project that brings Honeywell AvD into a new major field of business--inertial reference/navigation for manned aircraft. It may seem strange to choose a commercial product for a discussion of "Hi-Reliability" hardware, but we believe it is applicable to the objectives of this meeting.

MTBF PREDICTIONS, CONCEPT PHASE THROUGH FINAL PROPOSAL

There are numerous R&M tasks that are significant and necessary contributors to this phase of a successful program. We have decided to discuss prediction methods because they are very important to a commercial program (warranties and guaranteed MTBFs), and because our prediction methodology (for solid-state electronics) is unique within the industry. Furthermore, we believe the concepts are also critical for space applications, and a reasonable baseline for tradeoff decisions (relative failure rates) and for projected life/redundancy considerations is needed.

The Laser Gyro - A New Technology

The Ring Laser Gyro (RLG) portion of the subsystem under consideration represents a new technology--one for which we have limited (relevant) reliability

data. As the primary motion sensor required to perform inertial navigation, the gyro's failure rate can make-or-break the ability of the system to meet its MTBF and Life Cycle Cost (LCC) goals. Because no comparable instrument exists, we projected the failure rate by the following general approach:

- o Identify failure modes as thoroughly as practical.
- o Review failure modes by (sub)function and comparable (sub)function.
- o Use failure rates for known hardware and comparable function where possible.
- o Analyze and review causes of failure in prototype gyros for compatibility with the theoretical analyses.
- o Factor-in experience during the build process.
- o Total subfunction failure rates, and review and compare those rates with known failure rates for mechanical gyros.

Although the RLG subsystem has many advantages over the gimbaled, rotating gyro mechanization, the most significant item is improved reliability at equal or lower cost. There are two considerations when comparing the new technology with the old-"random" failure rate, and mean life. However, there are no known wear-out or age oriented failure modes in the RLG during the anticipated life of the equipment. Therefore, a sum of the estimated random failure rates of the RLG is compared to the cumulative wear-out and random failure data for the mechanical gyros.

Even though the entire process tends to be better on paper than it does in practice, we have enough confidence in the procedure to use it as the basis for extended warranties and guarantees.

The RLG involved more than 15 years of research and development. The steps for reliability analysis described above, meanwhile, represent an iterative process that started almost with the original idea of a laser sensor mechanism (i.e., a motion sensor with no moving parts). The final, numerical assessment by a reliability engineer only formalizes and quantifies the accepted basic probabilities associated with the new technology.

Electronics - An Evolutionary Technology

Although MTBF projections for new technology items carry the greatest risk, electronics predictions are also critical in the reaching of good decisions at the front-end of a program. AvD has developed a unique prediction methodology for solid-state electronics hardware that is based on extensive data gathered over a period of years. Our largest, most-accurate data base is the record of failures of a digital air data computer (DADC) used in Douglas DC-10 airplanes. Considerable data is also available from AvD flight control electronics equipment on the C5-A and F-14 airplanes, as well as radar altimeters used in most of the Navy's airplanes. That data is limited in scope and accuracy, however. Specifically, the available data suggests two sources of reliability improvement in production-type solid-state electronics:

- o The universally-accepted improvement of a design, and its associated production processes through maturation
- o An aging maturity related only to operational age (average operating hours per unit).

Figure 1 shows a log-log plot of the measured failure rate of the Digital Air Data Computer (DADC) electronics vs. the average age of all equipment in the field. Each data point represents at least 35 failures. The calendar period is superimposed on the axis depicting average operating hours. Further information on this subject is available from the author.*

Based on the data cited earlier, we have developed a simple equation (Figure 2) for predicting electronic failure rates. The equation is based on the assumption that there are two components of the basic failure mechanism, such that:

$$\lambda_i = KH^\alpha + \lambda_r, \text{ where}$$

- o λ_i is the failure rate at any given instant
- o λ_r is a residual or constant λ , approached as an asymptote
- o The KH^α term is the variable λ , very large at infancy and approaching zero as an asymptote. K is a constant, H the operating hours, and α is the slope of the curve.

We recognize that failure rates will vary with temperature and could be affected by other environmental and package-design factors. For AvD purposes, the validity of our prediction is limited to equipment that operates within tight design constraints for temperature and packaging. The actual environment at the piece-part level is then controlled within these constraints. For AvD applications, we believe that the accuracy of failure data does not justify any greater precision than we get with our simple equation.

We are convinced that the data summarized in Figure 1 is a valid indication of the behavior of electronic parts. The explanation we have developed postulates that solid-state electronics have the following characteristics:

- o There are no significant wear-out modes for the operational life of the equipment involved.
- o Some electronic parts have latent defects or flaws that represent a weak link in the chain that could lead to failure.
- o All of the latent defects may still not lead to a failure during the life of the product (10,000 to 75,000 operating hours).

* "The Effect of Endless Burn-In on Reliability Growth Projections," Alex Bezat and Lyle Montague, Proceedings 1979 Annual Reliability and Maintainability Symposium.

- o Repair actions for failed parts result in the removal of the weakest part within the population at any given instant. The replacement part is, in all probability, a part that will not fail during the remaining life of the equipment.

Other investigators have arrived at conclusions similar to ours regarding both the cause and shape of the failure rate curve (there is a paper on this subject scheduled for the forthcoming R&M symposium in Philadelphia). However, the explanation must be treated as theory; the failure rate curve represents data at a high level of statistical confidence. Based on the above characteristics, the reliability prediction methods described have been used in the RLG program under discussion in this paper, as well as for all other programs where management risk/cost analyses are needed.

It should be noted, however, that MIL-HDBK-217 is still the only method that government procurement agencies can use on an "apples-for-apples" basis, so our AvD operation uses the MIL-HDBK for all such projects, as required.

Design, Development, Test and Evaluation (DDT&E)

The Willoughby "New Look" applies fundamental engineering design principles and disciplines to the design process, with the objective of attaining "designed-in" reliability at the earliest, most cost-effective phase of the program. We have adopted NAV MAT Instruction 3000.1A as a baseline for preparing a Reliability Statement of Work (SOW) for situations that are incomplete, or inadequate by contract. The checklist at the end of this paper summarizes the "New Look" tasks associated with designed-in reliability, as we applied them on the RLG program.

Semi-Conductor Junction Temperatures (T_j)

At AvD, we believe that design margin is the touchstone to cost-effective reliability. Adequate temperature margin is, in our judgment, the most important of all stress factors that impact reliability. We have found two difficulties in specifying and controlling design requirements so as to keep T_j within desired bounds. The worst of these is the paucity of data on θ_{JC} (the thermal impedance from semi-conductor case to junction). Furthermore, conflicting, often absurd values for θ_{JC} are sometimes found in both the Military Specifications and the vendor data sheets for integrated circuits. We have generated an interim solution for the item by defining θ_{JC} by measuring the forward voltage drop of the substrate isolation diode. Although we feel that our methods are far more accurate for design decisions than our previous attempts to use published data, there remains much to be desired in terms of variables other than those covered. Also, our data is incomplete, but compatible with that from other people who have taken measurements similar to ours.

The other difficulty has to do with improved dissipation of heat from medium- to high-power LSIC (Large Scale Integrated Circuits) mounted on printed-wiring boards (PWB). Thermal planes have been used extensively, but we have found no

straight-forward, reasonably-economical methods of improving the heat flow from the semiconductor case to the thermal planes. This problem is not yet fully-resolved, but we have measured significant--and highly reproducible--reductions in case temperature by the use of a silicone compound displacing the usual air gap between the case and the copper of the PWB.

Sneak Circuit Analysis (SCA)

The only item of "New Look" analysis that we by-passed on this program was SCA. We are not sure that SCA is cost effective at a level below the system or major subsystem level, and the subject was explored in detail with our customer. Our experience with SCA is that it duplicates somewhat the parts application analyses, failure mode and effects analysis, and related built-in-test (BIT) analyses for design problems within the black box. However, we believe that an SCA at the system or major subsystem level can avoid interface/interconnection problems, and simultaneously uncover design errors with optimum cost effectiveness.

Honeywell AvD experience with SCA is not comprehensive, being limited to work performed on a subcontract basis on three manned aircraft avionics items, and one manned spacecraft project. We would be highly interested in the experiences and judgments of other people with experience in this field.

PRODUCTION PHASE

Production Support

Operations at AvD are such that the engineering and production functions are in the same building as engineering. The FRACA system represents an important interface among the three departments most involved in the production phase (i.e., production, product assurance (quality), and engineering). The documentation, retention, and retrieval of anomaly (defect, failure, non-conformance, etc.) data is the responsibility of the Quality Department. The automated retrieval system is so mechanized that failure trend data is rapidly available by sorting against a variety of items (i.e., defect code, part types, part number, assembly/subassembly numbers, etc.). The FRACA system is applied either on a 100 percent basis for all anomalies, or on a selective basis by using the automated trend analysis output, working closely with production and quality engineers.

For this program, closed-loop FRACA will be used for 100 percent of all anomalies that occur during final acceptance testing, for 100 percent of manufacturing run-in on the first 50 units, and selectively for all other anomalies. The number of anomalies that are to be investigated in the detailed procedure called FRACA will be reduced with the maturity of the design and production processes. (The FRACA procedure is, of course, used extensively throughout the DDT&E phase for all failures that occur during Qual test, Rel-Development tests, etc.)

Manufacturing Run-In (MRI)

MRI (or burn-in) has been used at AvD for almost all of our avionics during the past 10 years. It is a natural outgrowth of our failure rate concept regarding the improved product reliability associated with operating age. Three factors are considered important in the MRI screening process: (1) 100 or more operating hours at elevated temperature, (2) power cycling in excess of mission requirements, and (3) 10 or more temperature cycles. Our internal standard is an MRI elapsed time of one week, four temperature cycles per day (temperature extremes beyond mission requirements, but no overstressing allowed), with power-on during the elevated-temperature portion of the cycle.

Power is cycled four times per hour during the elevated-temperature operation. A random vibration screen precedes the operational portion of the screen, and the last three temperature cycles must be failure free. The RLG program we have reviewed will use the AvD internal standard described here.

COMMONALITY AMONG SPACE, MILITARY, AND COMMERCIAL AVIONICS

Honeywell AvD has extensive experience in design and production of equipment used in military aircraft of all kinds, manned and unmanned space programs, and commercial jumbo jets of today and tomorrow. In terms of cost effectiveness, in our judgment, the essential principles of the "New Look" are just as applicable to military and commercial avionics as they are to manned space. This is particularly true for the DDT&E phase. We have found some minor differences in the production phase.

Space Electronics

The design, process, and build maturity must be nearly instantaneous for space electronics; "field" results must be at the desired reliability levels with the first unit. It is self-evident that corrective action in the field is usually impractical or impossible. Therefore, "S" level parts and extremely costly tests and screens can be cost effective for space applications. Furthermore, each failure at any level of build and assembly justifies a complete, thorough analysis for cause, as well as high-visibility decisions on corrective action (i.e., FRACA) throughout the total production build. The MRI prior to final acceptance testing should, we believe, be comprehensive to an extent that would be prohibitive for non-space applications. The AvD concept of reliability growth of electronics through operational age suggests that run-in of at least 1000 hours might be a practical requirement for space electronics. Based on our experience with APOLLO, it is reasonable to believe that little or no equipment left the ground with less than 1000 operating hours, and 3000 operating hours prior to flight was not unusual. We believe that extended testing contributes to reliability by growth-through-aging, as long as maintenance actions are not destructive.

Military Avionics

Typical military avionics can be repaired after installation. Therefore, there is a viable tradeoff between increased maintenance cost for manned aircraft avionics and the ultimate reliability built into space equipment. This factor has been misused in the past as a license for shoddiness. The AvD compromise approach has been to use FRACA extensively in the early production systems. For example, an extended MRI can be used with 100 percent failure analysis (i.e., FRACA) for the first 20 to 50 units. This type of effort is treated as an extension of "Rel-Development" testing.

Subsequent production systems can then be evaluated for trend failures or any unusual anomaly events, and the FRACA procedure is superimposed on the quality anomaly reporting system as the problem-solving vehicle. Generally, the design-and process-oriented problems can be resolved quickly and effectively with this approach. As the product matures, the proportion of failures that are analyzed declines from the 100 percent range, to as low as five percent with fully matured systems. Typically, the trend analysis becomes the "spotter" for lot-oriented part problems that sift through the inspection screens at the piece-part level, and can only be detected under the simulated operational conditions of MRI.

Electronic parts for military applications are usually specified to the MIL-STD levels (MIL-M-38510, level B for integrated circuits) where available. Non-standard parts are purchased to an AvD "Spec Control" drawing that imposes the more critical controls equivalent to the MIL-SPECS for generically similar parts. Although we have found that Government source inspection does not guarantee that parts are really tested, such MIL-STD parts appear to be generally cost effective. There is, however, one glaring exception: we believe that the added costs of MIL-M-38510 controls on standard integrated circuits cost more than they are worth. We find that reasonable specification control drawings, using mostly vendor-level requirements of MIL-STD-883B (with 100 percent hi-low temperature testing at receiving inspection) are more cost effective. The subject of parts specification and control would require a full paper of its own, so these comments will have to suffice.

Commercial Avionics

Honeywell AvD has found that R&M inputs are cost effective at essentially the same levels for commercial aviation programs as for the military. A typical three-year warranty in a commercial jet will involve 10,000 to 15,000 operating hours, which is usually equivalent to more than the full life of avionics for military fighter aircraft. A military transport (C5-A) may go as many as 1000 hours per year--or perhaps a 20,000- to 25,000- hour total life vs. 50,000 to 75,000 hours for commercial. Because we see no wear-out failure modes in solid-state electronics, the only difference between commercial and military avionics is the elapsed time to attain full maturity, which is much more rapid for the commercial.

Parts specifications and controls for commercial avionics at Honeywell AvD are the same as for the military, with one exception. Integrated circuits are usually purchased to Spec Control drawings and MIL-STD-883B, and MIL-M-38510B parts are used only when commonality and quantity-buy for the military makes them cheaper.

SUMMARY

There are a few significant points that we would like to emphasize. Most important, perhaps, is the idea that the "New Look" is just as applicable to commercial and "ordinary" military projects as it is to space hardware. The check list appended to this paper is not a shopping list--it represents the significant items associated with an effective R&M program.

Again remember that the items we have covered in detail herein were not chosen as having the highest priority--only that there are, perhaps, greater variations in how to handle them.

We mentioned that "design margin" generates a reliable product, but the importance of controlling the build process may not have been stressed adequately. It is obvious that the world's best design can be murdered by shoddy practices in the factory--or repair facility--if precautionary measures are not used.

Finally, we believe that all of the controversial items covered have a sound basis in fact. We are, however, anxious to correct our ways when better information is available; this better information often comes from people like you, with experiences in new technology. We would like to hear from you.

CHECK LIST FOR "RELIABILITY BY DESIGN"

- o Mission/environmental profile definition
- o Design alternative studies
- o Numerical allocations and reliability growth analysis
- o Conservative derating criteria
 - 110°C maximum junction temperature, worst case
 - 60°C to 85°C maximum junction temperature, normal operation
- o Part stress analysis
- o Thermal analysis
- o Thermal testing/measurement
- o Structural analysis
- o Worst case tolerance analysis
- o Failure modes and effects analysis
- o Parts and materials selection and control by technical baseline documentation
 - Screening to "hi-rel" levels: JANTX: MIL-STD-883B, etc.
 - Detailed part characteristics controlled to fit application
 - Parts teardown analyses to 883B visuals
 - 100% hi/lo/room temperature tests of key electrical characteristics
- o Design reviews
- o Reliability development test (test analyze and fix test - TAAF)
- o Design limit qualification test
- o Manufacturing run-in screening with random vibration
- o Failure free reliability verification/acceptance testing
- o Failure reporting, analysis, and corrective action
 - Design and development tests
 - Qualification tests
 - Reliability development tests
 - Production manufacturing run-in (MRI)
 - Failure free reliability verification/acceptance tests
 - Returned goods

- o Technical baseline documentation control of production processes that impact reliability and maintainability as well as the classical "form, fit, and function"
- o Adequate staffing and involvement of reliability, maintainability, and manufacturing in the design process.
- o Receiving inspection screening of electrical and electronic parts.

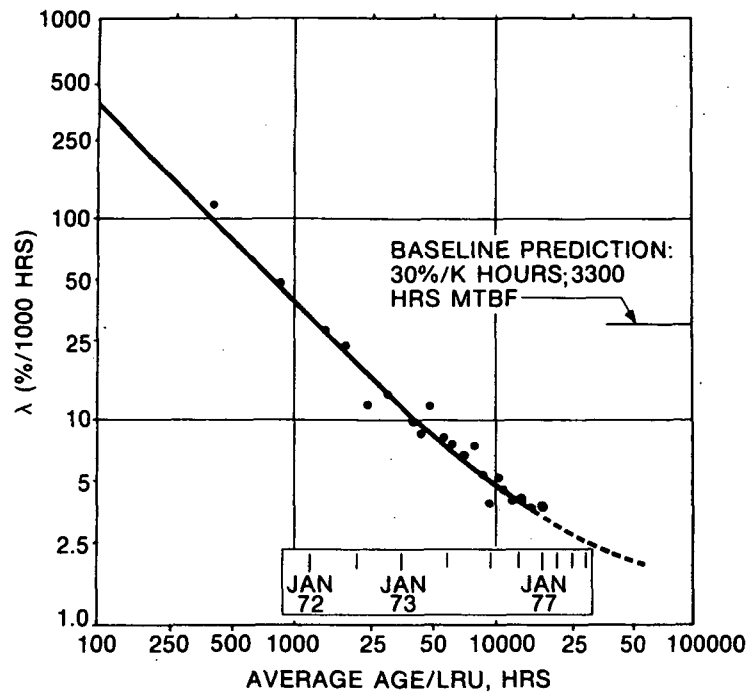


Figure 1. DADC Electronics Failure Rate

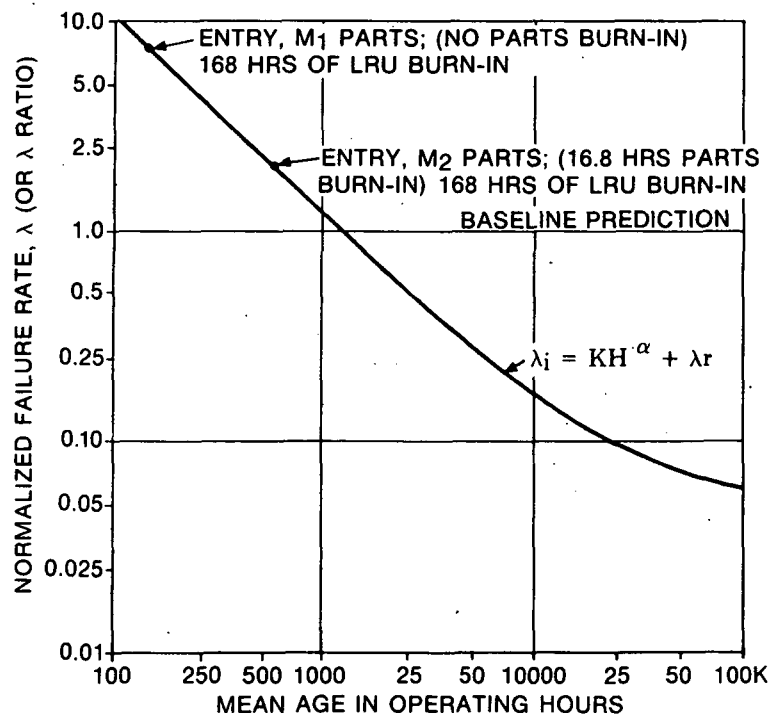


Figure 2. Honeywell Reliability Prediction Curve

QUESTIONS AND ANSWERS

DR. CARROLL ALLEY, University of Maryland

This is the first paper the term "sneak circuit analysis" was used, but I am intrigued by what that really means and it hasn't been explained.

MR. BEZAT:

Let me read it to you. I passed up discussing sneak circuit analysis. I didn't have time. I should mention that on this particular program, the ring laser gyro program for the Boeing 767-75-7 airplane, we went into considerable review of the possible application of sneak circuit analysis.

We went into it with our customer and our own analysis. We have had sneak circuit analysis done by Boeing-Houston because it is a mechanized approach and I believe General Dynamics is also doing it now.

Let me read to you what is in the work statement very quickly. "The sneak circuit analysis for hardware looks for sneak paths; that is to say energy flow on unexpected routes. It looks for sneak timing, energy flow on expected times. For sneak labels; that is to say that information and undesirable stimuli. That information is available to the pilot or what have you."

A sneak circuit for the software is virtually identical except for energy flow. You want to talk about logic flow. They also do similar things to what we would do for design margin considerations, but those are sort of an additional output.

Now, our preliminary conclusion about sneak circuit analysis in terms of its usefulness -- and I certainly don't want to talk as though we were experts on this entire subject -- our preliminary conclusion is that it is probably cost-effective at a major system or total system level because much of what would be discovered by this kind of an approach has to do with interface of equipment that is designed in different areas.

If you have a big enough subsystem, that same problem can occur. Generally we have found in our past experience, those areas where we have had sneak circuit work done -- things that were found internal to the box -- our people had found with the normal analysis. I don't know if other people agree with that approach.

DR. STOVER:

In several earlier papers, the point was made that the parts vendor couldn't really be trusted to produce reliable parts. And in your paper, you make the point about junction temperature data not being quite adequate. Does this imply that there is a place here for the independent testing organization to get involved? Some kind of organization that doesn't exist to date.

MR. BEZAT:

You need to provide an objective basis of comparison.

DR. STOVER:

Right. Where there is not the bias of being the vendor.

MR. BEZAT:

Those organizations do exist. I mentioned the Defense Electronics Center, the RADC. However, I am not sure that they are able to cover all the subjects, but particularly I believe, they could not impact the adverse that Mr. Willoughby is talking about in respect to parts and parts quality, parts reliability. We have indeed found exactly the same thing Mr. Willoughby talked about. I don't have the numbers that are anywhere near as accurate as what Mr. Willoughby indicated; we can't quantify it quite that well.

But indeed the parts are bad. I should say, though, that the data that we got from the supplier was, in general, about -- seven out of ten suppliers we contacted was much better in regard to the junction temperature coefficients than what we found from the other sources -- than any other sources including the military.

DR. STOVER:

This really applies more to previous papers than to yours, but from this standpoint of each doing their own inspection and verifying and maybe doing the same thing -- every organization doing the same thing. If some independent testing organization would do this type of failure testing and publish the results for different vendors, would not the free market -- the competitive market forces force us into more reliability?

MR. BEZAT:

I don't know that I can answer that question. I have some opinions about it from a straight economic standpoint which would say no. Simply because the total quantity of parts that are used, where we

need this relatively high reliability and where it is cost-effective to have it, is such a small proportion of the total number of parts that are used.

Therefore, it would appear that the mass production method which I think will probably move upward in quality and reliability on a competitive basis as you were pointing out, but not on a quantum jump basis. The cost of screening is ever so much lower than the cost of actually building to that high reliability at the present time. That is an opinion and I could not support it with data.

DR. STOVER:

Thank you.

CHAIRMAN WINKLER:

Thank you very much. Before we close, I would like to make just one comment concerning this section. I think, at least for me, it has been a most interesting session. Each of these papers leaves a number of suggestions behind, what to do in our specific cases. I hope you share that impression.

One thing came back very strongly to me, and that is that there is no such thing as a material failure, that all of these failures are failures of the man in one way or another; failures of our intellect to recognize the properties, to recognize the hidden problems in design, and failures, of course, in the manufacturing process. So, what we have is a much, much lower random failure level than we would have assumed until now.

The last paper has reinforced this opinion that you really are talking about weeding out the faulty components and then you have not yet reached the purely random failure rate, the Poisson distribution. For many devices you will never reach that level because in the case of cesium beam clock you end up running into the end of life phenomena, likewise the rubidium lamp problems which come up after a number of years. So, maybe it is a wrong position to take to believe that there is such a thing as a material failure. These are failures in our intelligence recognizing what is going on.

That, of course, brings me to a second point. That is, maybe a useful change in attitude, in one's own intellectual attitude, would be to remember that our ideas of characterizing a module or an atom by fixed properties may break down at the level of very complicated systems. Its actual properties change because it is exposed to a different environment which you had not foreseen.

I consider that a very general attitude and it has made me more cautious and maybe less ambitious. But again, I enjoyed that last session very much and I am sorry to see it come to an end. It is something which has been very important in precision time-keeping. Thank all of the contributors to this session.

Page Intentionally Left Blank

A SPACE SYSTEM FOR HIGH-ACCURACY GLOBAL TIME AND FREQUENCY COMPARISON OF CLOCKS

R. Decher (NASA), D. W. Allan (NBS), C. O. Alley (U. of Maryland), R. F. C. Vessot (SAO), G. M. R. Winkler (USNO)

ABSTRACT

NASA is planning a Space Shuttle experiment to demonstrate high-accuracy global time and frequency transfer. A hydrogen maser clock on board the Space Shuttle will be compared with clocks on the ground using two-way microwave and short-pulse laser signals. The accuracy goal for the experiment is 1 nsec or better for the time transfer and 10^{-14} for the frequency comparison. A direct frequency comparison of primary standards at the 10^{-14} accuracy level is a unique feature of the proposed system. Both time and frequency transfer will be accomplished by microwave transmission, while the laser signals provide calibration of the system as well as sub-nanosecond time transfer. Following the demonstration with the Space Shuttle, an operational system could be implemented in a free-flying satellite to provide permanent global time and frequency transfer.

Introduction

Plans for a spaceborne system to meet the needs for global, high-accuracy time and frequency transfer are being studied by NASA's Office of Space and Terrestrial Applications, Geodynamics Branch. The system uses a hydrogen maser clock on board a space vehicle which will be compared with clocks on the ground by one-way and two-way transmission of CW and time-code modulated microwave signals. In addition, short-pulse laser signals will be transmitted simultaneously with the microwave signals for calibration of the system and for time transfer. The unique feature of the proposed system is its capability to make direct frequency comparison of primary standards at the 10^{-14} accuracy level. No other technique or experiment in existence or planned has this capability with coverage over most of the inhabited globe. In addition, the proposed system is expected to provide time transfer with an accuracy of 1 nsec or better.

The techniques to be employed have been used successfully in earlier experiments. The microwave portion of the system is similar to a system used with the Gravitational Redshift Probe (GP-A) flown in 1976 [1]. The short-pulse laser technique was successfully used in airborne clock experiments in 1975 which

measured general relativistic effects on time [2]. Because of this experience with previous experiments, basic new technology development is not required for the Shuttle experiment.

The first step of the proposed program will be a demonstration experiment using the Space Shuttle. Following a successful demonstration, the system could be implemented with a free-flying satellite or on a space platform to provide permanent, global high-accuracy time and frequency transfer. The following discussion deals primarily with the concept of the Shuttle demonstration experiment which is the subject of a definition study in progress at Marshall Space Flight Center. The first flight is planned for 1985, pending approval of the project. Ideas similar to the concept discussed in this paper have been proposed earlier [3].

Overall Objectives

The purpose of the Shuttle experiment is to demonstrate and evaluate the techniques for a later operational global system. A variety of users would benefit from an operational system providing time transfer with accuracies of 1 nsec or better and frequency comparison with an accuracy of 10^{-14} . Potential user groups include primary standard laboratories, high-accuracy timing operations such as the computation of TAI and coordination of major BIH contributors, NASA's Deep Space Network (DSN), and various other users of precision time, e.g., radio astronomy and geodynamics research.

The stability and accuracy of precision clocks and primary frequency standards have improved far beyond present capabilities to transfer time and frequency information between widely separated standards. Further improvements in the stability and accuracy of primary standards can be expected in coming years which will result in increased requirements for high-accuracy time and frequency transfer. The most accurate time transfer method now in use is the transportable clock. This method has many logistic problems and is very expensive if high accuracies are required. The latter problem is illustrated by Figure 1, which shows estimated yearly cost for synchronization of one remote station as a function of accuracy. The operational cost becomes prohibitive if high accuracy is required. The proposed space system using an orbiting hydrogen maser clock can be viewed as an extension of the transportable clock method, providing accurate time and frequency transfer at frequent intervals with worldwide coverage and at a much lower cost for the individual user.

The current operational mode to compare primary standards in the U.S. (NBS), Canada (NRC), and West Germany (PTB) utilizes Loran C, which suffers from limited global coverage and fluctuations of the ground wave propagation delay, making the system practically incompatible with requirements of high-precision standard laboratories and time services. Other laboratories are interested in the accuracy capabilities of primary frequency standards, either directly or indirectly, but adequate means for international frequency comparison do not exist at the state-of-the-art accuracy. Other techniques of accurate time transfer have been tested experimentally or are planned for implementation in the future. A performance comparison of available and planned methods, including the proposed Shuttle experiment (Shuttle Time and Frequency Transfer Experiment, STIFT) is shown in Table 1. The following definitions apply to the table. Inaccuracy is expressed relative to a perfect portable clock. Stability is the measure of time variations over the course of the measurement (i.e., related to the phase stability of the measurement system with sampling intervals and length of data determined by the method). Cost-effectiveness is the product of inaccuracy and user cost dollars (in mega dollars), the smaller the number the better. The 24-hour frequency accuracy is derived from time stability over 24 hours which determines the accuracy of absolute remote frequency comparison. Though many of the numbers represent anticipated performance, it is believed they are within a factor of two of what will be accomplished. (Where applicable the figures in the table are rms values.) As can be seen, the STIFT experiment looks extremely attractive when compared with other techniques.

Concept of the Shuttle Experiment

The idea of the Shuttle demonstration experiment is illustrated in Figure 2. The experiment package which is mounted on a pallet in the Shuttle bay contains the hydrogen maser clock, a microwave transponder with antenna, a corner reflector array, a photodetector, an event timer, and some associated electronics. Three microwave links are transmitted between a space vehicle and a ground terminal which permits cancellation of the first-order Doppler effect and correction for ionospheric delay. Frequency comparison is accomplished by using the CW carrier frequencies. A time code modulation is applied for the time transfer function. An important feature of the proposed experiment is that the microwave system provides time and frequency transfer independent of weather conditions and that a laser system is used for calibration, providing information about time delays in the propagation path and instrumentation. In addition, the laser portion of the experiment is available for time transfer with

sub-nanosecond accuracy. Short laser pulses are transmitted from the ground station to the Shuttle and returned by the corner reflector. The arrival time of the laser pulse at the Shuttle is measured by the photodetector and event timer and is recorded in the time frame defined by the on-board hydrogen maser clock. The simultaneous transmission of laser and microwave signals should yield valuable and interesting high-accuracy data about wave propagation and related effects.

Planned Shuttle orbits have a rather low altitude (~200 n mi) which limits the time available for clock comparison during a pass over a ground station to several minutes. Otherwise, the Shuttle is rather ideal for a demonstration experiment because it provides very generous volume, weight, and power limits for the experiment package as well as return of the flight hardware with the option of reflight at minimum cost. High-inclination orbits up to 57° are planned for several Shuttle missions which give sufficient global coverage for the demonstration experiment, including all of the primary standard laboratories and many other important stations. While the Shuttle orbits are adequate to demonstrate the performance of the system, a higher orbit would be adopted for an operational time and frequency transfer satellite.

Microwave System

The key to the direct frequency comparison technique is elimination of the first-order Doppler shift. This method was successfully used with the Gravitational Probe A (GP-A) in 1976, a joint project of Smithsonian Astrophysical Observatory and Marshall Space Flight Center [1]. During this mission the frequencies of two hydrogen masers, one on the ground and one in the space probe, were compared to measure the gravitational redshift effect. For 100 sec averaging intervals, the frequency comparison was accurate to 1×10^{-14} , which was at the stability limit of the space probe maser. This mission demonstrated the capability to eliminate first-order Doppler shifts and ionospheric propagation fluctuations to achieve direct frequency comparison with an accuracy of 1×10^{-14} . Since 1976, further improvements of the hydrogen maser stability have been achieved which make 10^{-14} a safe accuracy goal for the Shuttle experiment [4].

A stability comparison of various techniques and standards including the 1976 system and the new hydrogen maser (1979) is given in Figure 3. To achieve the desired accuracy requires corrections for relativistic effects, including the second-order

Doppler shift and the gravitational redshift effect. These corrections will be calculated from orbital data of the space vehicle. Figure 3 also illustrates the relationship of time transfer accuracy and frequency stability for measurements spaced by τ seconds. The two dotted lines represent a microwave pulse system (0.6 nsec precision) and a laser pulse system (0.1 nsec precision). If time comparisons are made at 24-hour intervals (10^5 sec), a time transfer accuracy of 0.6 nsec or better is needed to compare frequencies at the 10^{-14} level.

A functional diagram of the microwave system is shown in Figure 4. Three S-band microwave frequencies are transmitted, providing one-way and two-way Doppler information in the ground station. The first-order Doppler effect is cancelled by subtracting one-half of the two-way shift from the clock down-link signal. This process also eliminates propagation effects in the ionosphere for temporal variations longer than the propagation time. The three frequencies have to be selected carefully to compensate for ionospheric dispersion. (Frequencies shown in the diagram are those used with GP-A.) A single antenna is used on the spacecraft and in the ground station to handle the three frequencies. The frequency comparison information generated in the ground terminal is contained in the beat signal of the two clock frequencies which is obtained after removal of the Doppler shift.

The frequency comparison method utilizes the phase information of the CW phase coherent carrier signals. To accomplish time transfer a PRN phase modulation is applied. The round-trip propagation delay ($2R/c$) is determined by a correlation technique applied to the two-way signals (Figure 5). The time shift between space clock and ground clock is determined from the displacement of the two corresponding time codes. The space clock time code is modulated on the clock down-link carrier. The correction for the one-way propagation delay is obtained from the two-way signal correlation process. One important objective of the proposed program is the development of a low-cost microwave ground terminal which can be afforded by a large number of users of a later operational system. The Shuttle experiment will use S-band frequencies. (The optimum frequency for an operational system is the subject of further studies.) Participation in the STIFT experiment requires a microwave ground terminal. It is anticipated that several ground terminals will be in operation for the demonstration flight(s). Most of these terminals should be located at the site of primary standard laboratories and time service operations.

Laser System

The short-pulse technique is presently the most accurate method of time transfer. This technique has been used by the University of Maryland with support from the U. S. Navy in comparing airborne clocks with clocks on the ground to measure general relativity effects with sub-nanosecond accuracy [2]. The uncertainty in the clock comparison was only a few tenths of nanoseconds. A disadvantage of the laser technique for an operational system is its dependence on weather. In the proposed time and frequency transfer system the short-pulse laser method is used primarily for calibration and performance comparison. However, the laser portion of the experiment can be used independently for time transfer experiments. Any laser ground station equipped with a stable clock and means to record epochs (event timer) can perform time transfer experiments. The Shuttle experiment will utilize existing laser ground stations.

A block diagram of the laser system, including on-board and ground station systems, is shown in Figure 6. A corner reflector array is used to return the laser signal to the ground station. Simultaneously the laser pulse is received by a fast photodetector in the Space Shuttle. The event timer measures the arrival time t_2 of the laser pulse in the time scale established by the on-board hydrogen maser clock. This information is sent by telemetry to the ground station for comparison of the space and ground clock epochs. The epochs of transmission and return of the laser pulse, t_1 and t_3 , respectively, are recorded at the ground station. Clock synchronization is accomplished by comparing t_2 (measured at the space vehicle) with the midpoint between t_1 and t_3 , including a small correction for earth rotation. Figure 7 shows the result of the 1976 short pulse laser experiments. The uncertainties of individual clock comparisons are only a few tenths of nsec. Neither the relative velocity between space vehicle and ground station nor the distance separating them enters into the comparison.

Conclusion

The proposed concept using a hydrogen maser in a space vehicle is expected to meet the future need for global high-accuracy time and frequency transfer. It has a number of advantages compared to other techniques, including high accuracy, direct frequency comparison, weather independence, global coverage (for operational system), and comparatively low cost for the user. Only a single station is needed to accomplish time and frequency transfer, namely the station which wants to synchronize

its clock or compare its frequency standard. The microwave ground terminal can be located in close proximity to the standard. In addition, the laser portion of the experiment makes time transfer available with accuracies in the sub-nanosecond region.

References

1. A test of the Equivalence Principle using a spaceborne clock, R. F. C. Vessot, M. W. Levine, General Relativity and Gravitation, 1979, Vol. 10, No. 3.
2. Relativity and Clocks, C. O. Alley, Proc. of the 33rd Annual Frequency Control Symposium, May 1979, Atlantic City, New Jersey
3. TEMPUS, A proposal for an international time transfer and precision tracking satellite, D. C. Holmes, Proceedings of the Tenth Annual Precise Time and Time Interval (PTTI) Applications and Planning Meeting, November 1978, Goddard Space Flight Center.
4. Performance evaluation of the VLG-11 atomic hydrogen masers, M. W. Levine, E. M. Mattison, R. F. C. Vessot, Proc. of the 32rd Annual Frequency Control Symposium, May 1978, Atlantic City, New Jersey

TABLE 1. INTERNATIONAL TIME TRANSFER COMPARISON ($\ll 1 \mu\text{s}$)

<u>Method</u>	<u>Inaccuracy</u>	<u>Stability</u>	<u>Cost-Effectiveness (M\$'ns)</u>	<u>24-Hour Frequency Accuracy</u>	<u>Coverage</u>	<u>When Available</u>
GPS (Common-view)	10 ns	1 ns	0.25	$\lesssim 10^{-13}$	Global	1981
Shuttle (STIFT)	1 ns	0.001 ns*	0.25	$\lesssim 10^{-14}$	To $\pm 57^\circ$ Latitude	1985
TDRSS	10 ns	1 ns	1.0	$< 10^{-13}$	All but India Long-tudes	1982
LASSO	1 ns	0.1 ns	1.0	$\sim 10^{-14}$	All but near the poles	1981
GPS	40 ns**	10 ns	2.0	$\sim 3 \times 10^{-13}$	Global	1980
2-Way (Communication Satellite)	50 ns	$\lesssim 1$ ns	5.0***	$\sim 10^{-13}$	All but near the poles	1980
Portable Clock	100 ns	N/A	6.0	$\lesssim 10^{-12}$	Global (Best accuracy within reasonable driving vicinity of Air Ports)	1980
Loran-C	500 ns	$\lesssim 40$ ns	3.0	$\lesssim 10^{-12}$	Excludes Most of Asia and Southern Hemisphere	1980

*This figure represents the time stability of the microwave Doppler cancellation system (1).

**This inaccuracy may increase if the GPS C/A code is deteriorated for strategic reasons.

***Cost includes estimate of annual rental.

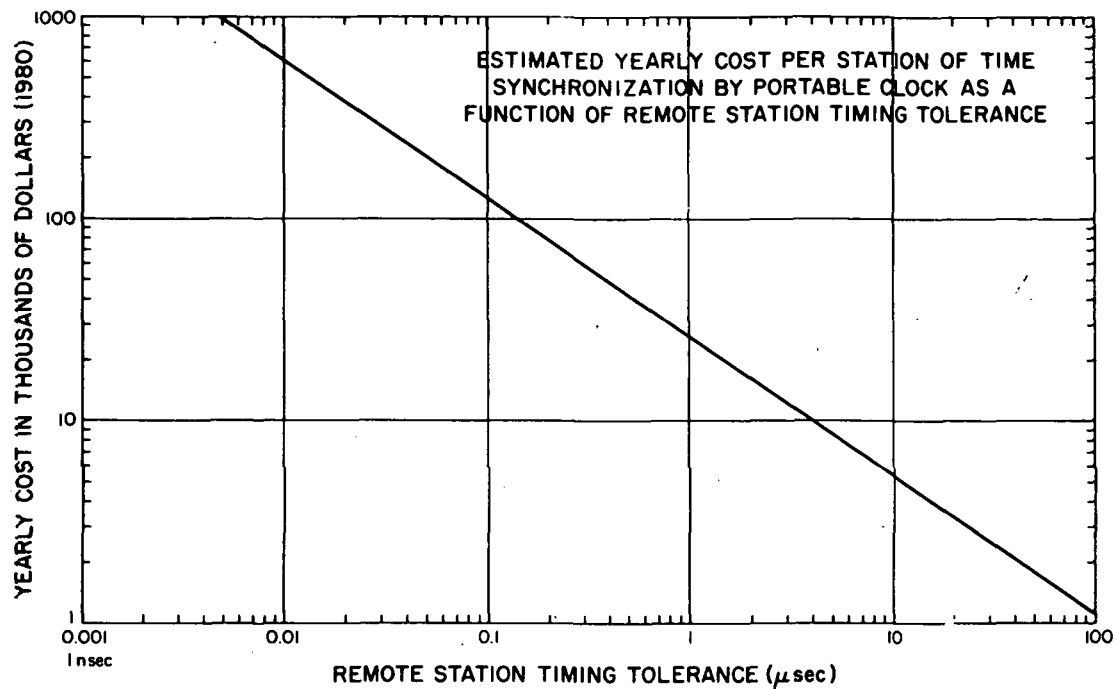


Figure 1. Cost of portable clock method.

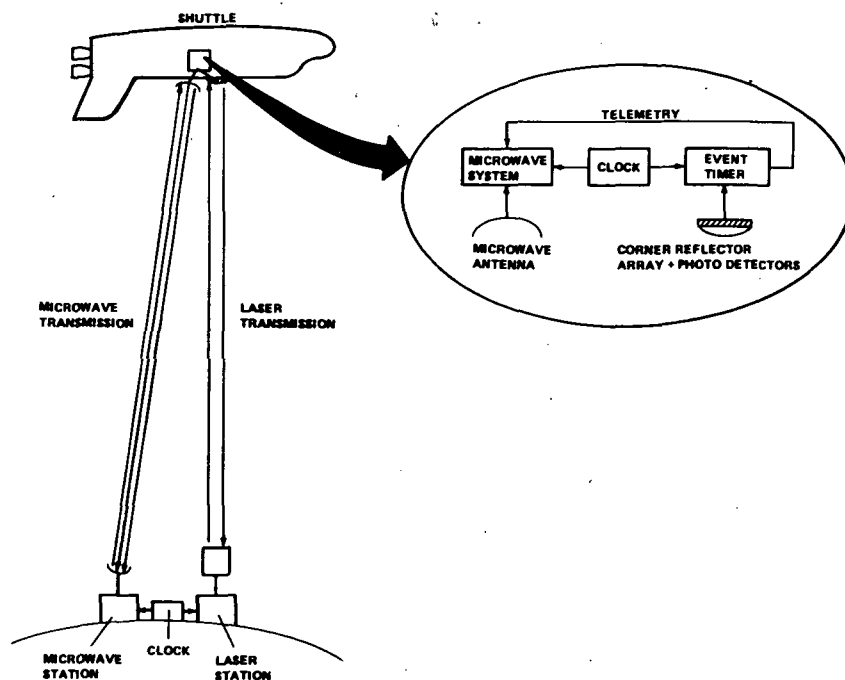


Figure 2. Shuttle time and frequency transfer experiment.

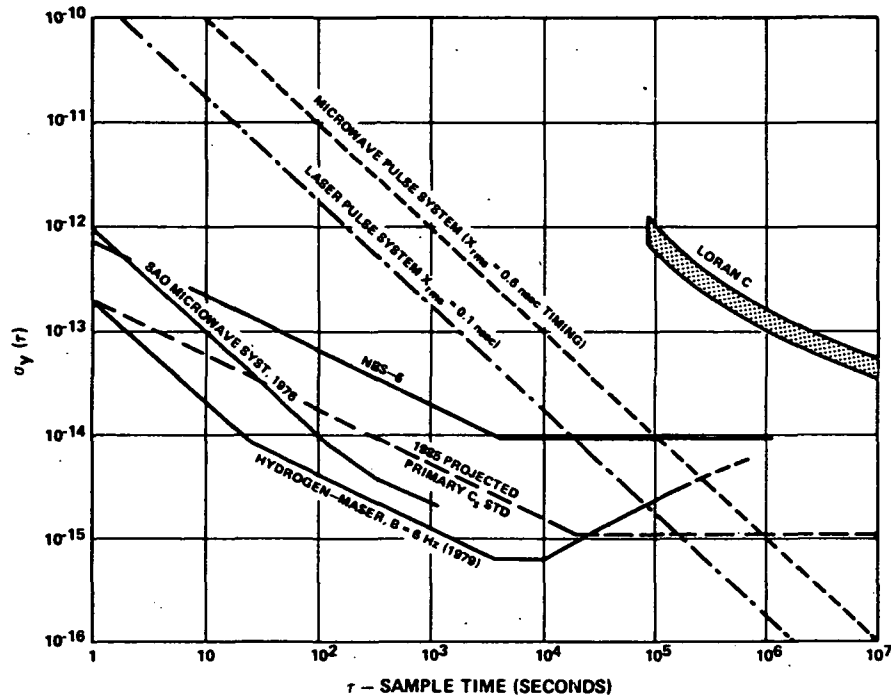


Figure 3. Stability comparison.

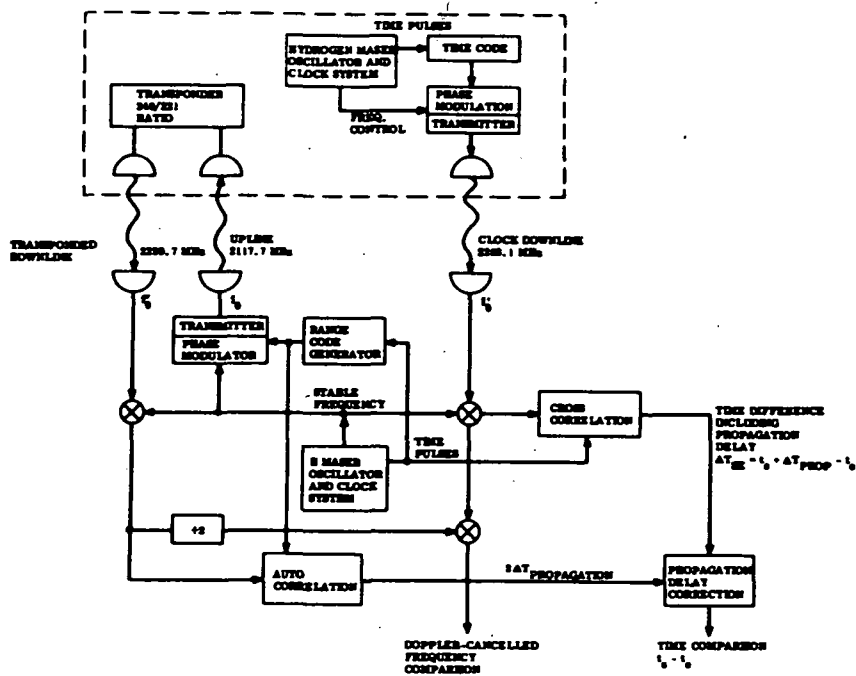


Figure 4. Microwave system block diagram.

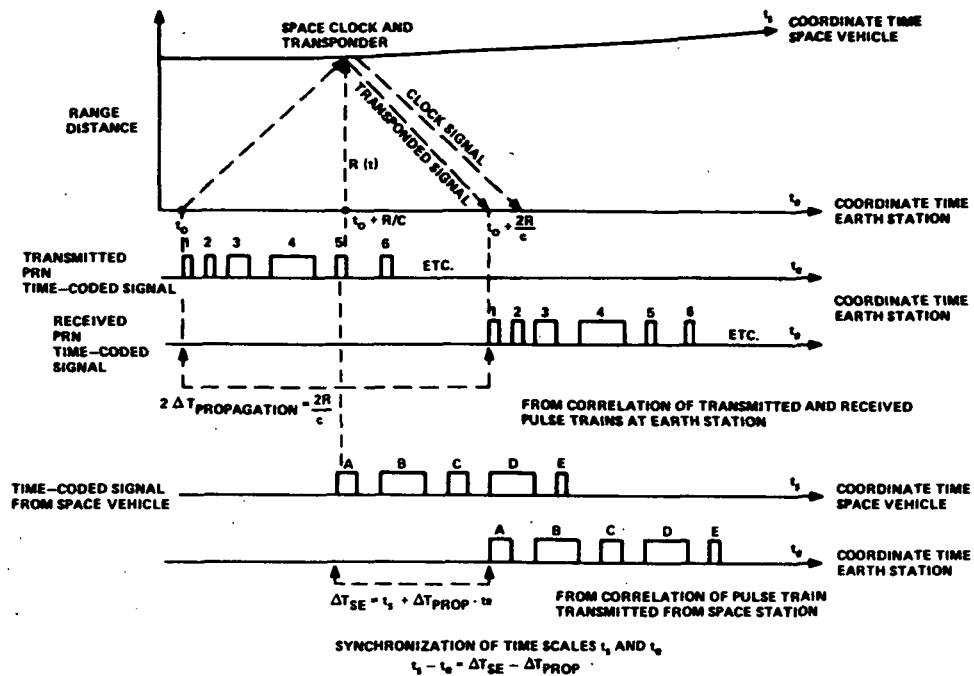


Figure 5. Microwave time transfer scheme.

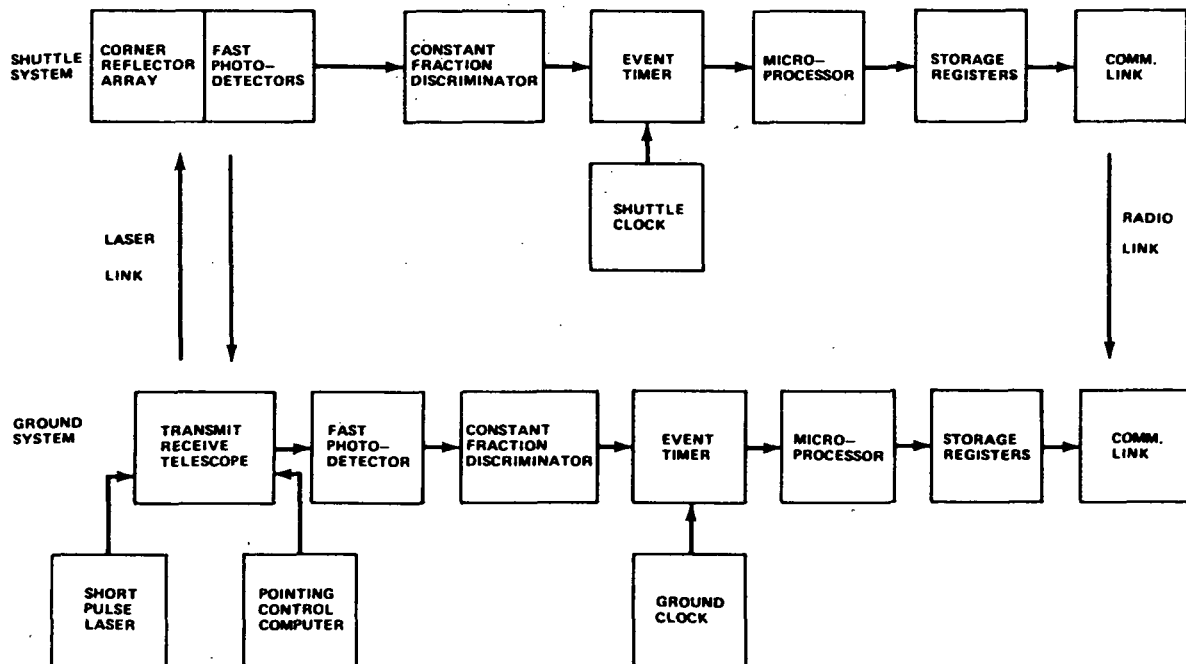


Figure 6. Laser system block diagram.

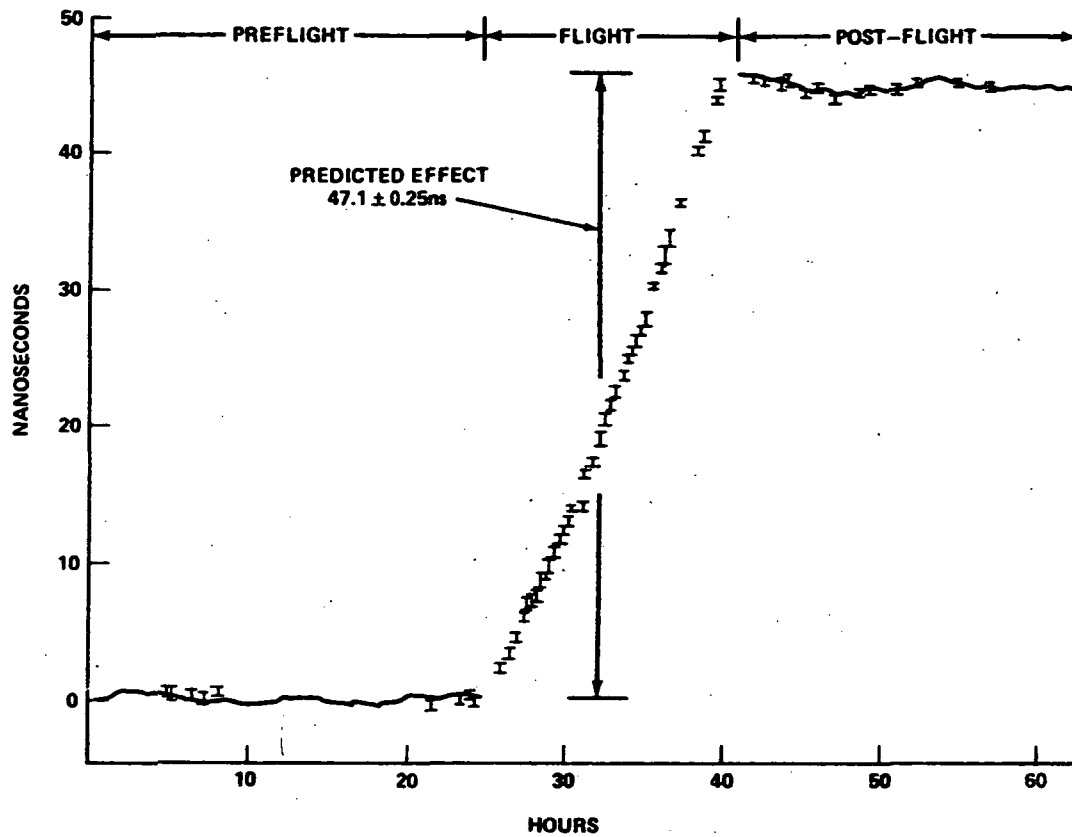


Figure 7. Results of airborne clock comparison experiments.

QUESTIONS AND ANSWERS

CAPTAIN VOHDEN:

I would like to know what the time line would be for this system becoming operational. You say the first flight would be 1985. How long after that would you envision the system being available for general usage?

DR. DECHER:

That is very difficult to answer at the present time. I think we will have several shuttle flights and then a normal lead time of such a program probably is at least two to three years.

MR. BANERJEE:

Does this experiment you have mentioned that you are expecting to do at the Maryland University provide the first calibration of the instrument that will be the elimination of the delay of that order?

DR. DECHER:

You question the accuracy of the system? Is this what you are saying?

MR. BANERJEE:

Yes.

DR. DECHER:

Well, both techniques, the laser and the microwave systems, have been demonstrated in those early experiments, and so I think we are also safe to propose this type of accuracy.

DR. ALLEY:

I would just add the comment that the limiting uncertainty of the early proposed low-altitude flight may be in the ability to measure the velocity of the spacecraft sufficiently well to include the relativistic corrections adequately.

DR. DECHER:

Yes, that is true if you want to achieve the accuracy of 10^{-14} , you have to include relativistic affects, the second-order Doppler Effect and the gravitational affect which you have to get out of the trajectory of the space vehicle. This will be no problem for a satellite system, but for the shuttle will need some doing.

Page Intentionally Left Blank

SESSION IIA

GOVERNMENT PLANNERS

**Dr. Martin Levine, Chairman
Frequency and Time System, Inc.**

Page Intentionally Left Blank

DEPARTMENT OF DEFENSE PRECISE TIME AND TIME
INTERVAL PROGRAM IMPROVEMENT PLAN

James R. Bowser, Automation Industries, Inc., Vitro Laboratories
Division, Silver Spring, Maryland

ABSTRACT

Department of Defense Directive 5160.51 assigns the United States Naval Observatory the responsibility for ensuring uniformity in precise time and time interval operations including measurements, the establishment of overall DOD requirements for time and time interval, and the accomplishment of objectives requiring precise time and time interval with minimum cost.

In support of the execution of these responsibilities, the United States Naval Observatory has embarked upon an effort to document the Department of Defense Precise Time and Time Interval's requirements and develop a master plan for overall PTTI program improvements.

This paper presents an overview of the objective, the approach to the problem, the schedule, and a status report, including significant findings relative to organizational relationships, current directives, principal PTTI users, and future requirements as currently identified by the users.

INTRODUCTION

The United States Naval Observatory is assigned the responsibility for precise time and time interval dissemination throughout the Department of Defense (DOD) components. Specifically, it is Department of Defense Directive 5160.51 titled, "Precise Time and Time Interval (PTTI) Standards and Calibration Facilities for Use by Department of Defense Components", that assigns the Naval Observatory the responsibility for insuring: (1) uniformity in precise time and time interval operations including measurements, (2) the establishment of overall DOD requirements for time and time interval, and (3) the accomplishment of objectives requiring precise time and time interval with minimum cost. The first of these responsibilities entails the technical aspects of timekeeping and time dissemination. Despite the rapidly changing systems which seek to exploit the leading edge of

technology, the Naval Observatory staff continues to keep pace in meeting this responsibility. In addition to expanded and improved means of dissemination of time and easier access to time services for the user, the basic equipments and methods of determining precise time are being upgraded. The requirement to upgrade time dissemination systems becomes self-evident through a simple comparison. DOD directive 5160.51 dated August 31, 1971, defines precise time as,---- "a time requirement to within ten milliseconds." Compare this with current user needs of time to within nanoseconds. Not only are operational requirements for time becoming more stringent with respect to accuracy, the number and variety of uses is expanding rapidly. There is a tendency for a new user, faced with a need for precise time, to approach the solution to the problem on a unilateral basis. The pitfalls to such an approach can be counter productive to achieving a fully coordinated PTTI program. Based upon the information available to the manager, a system is designed and an array of equipments is assembled that will meet the requirements. The combination of clocks, frequency dividers, time conversion modems, etc., may be totally unique to that program. This tends to result in a wide variety of non-standard systems which exacerbates the maintenance support problem and training problem. If the manager is one of foresight, he may even anticipate future requirements and design a system whose capabilities far exceed his current specifications for stability, accuracy, or other criteria. Conceivably, the full capability of the system for which the manager paid dearly, may never be fully exploited or required. The synergistic consequences of these factors is an overall PTTI program that is less than cost effective.

In recognition of the dynamic nature of the PTTI program and the influence of the aforementioned factors, the Naval Observatory has initiated an effort to ameliorate the impact of the current processes.

OBJECTIVE

The objective is to achieve improved management of the Department of Defense Precise Time and Time Interval Program in order to provide full coordination of PTTI programs and ensure economies of resources.

Although the Observatory has the lead in the endeavor within the provisions of DOD Directive 5160.51, the support of separate DOD components is engendered through the specific functional responsibilities assigned to those components in the same directive. Under paragraph VI.C., various functional responsibilities are delineated for DOD components and contractors. Of the five subparagraphs spelling out the functions, the first four deal principally with the technical aspects of timekeeping, that is; reference to the USNO master clock, use of portable clocks, etc. Paragraph VI.C.5 and paragraph VI.C.6 cover the management and planning aspects of PTTI. The separate DOD components

are directed to:

"5. Notify the U. S. Naval Observatory of:

- a. Existing and planned PTTI requirements, including information as to accuracy and stability of needs, measurement techniques planned or in operation and continuity of service required of the applicable distribution transmission.
 - b. PTTI (frequency) arrangements between DOD user components and contractors and other Federal Government agencies.
 - c. Scheduled scientific and technical meetings on PTTI (frequency).
6. Consult the Observatory prior to entering into contracts for equipment, research, studies, or services involving PTTI (frequency) in order that maximum use of existing facilities may be assured."

The degree of detail encompassed in the notification of the observatory is subject to a wide variety of interpretation. Consequently, the perception of PTTI requirements is equally subjected to a wide range of interpretation. Needless to say, a full comprehensive knowledge of the DOD requirements is essential to determining the necessary management actions to improve the overall program. The observatory's initiative can be viewed as a two-pronged approach; each inexorably entwined with the other. In support of the objective, the observatory will conduct a DOD PTTI requirements analysis and concurrently develop a DOD PTTI Improvement Plan.

APPROACH

A three-phased approach is being used for the requirements analysis portion of the task. The three phases are an identification phase, a collection phase and an analysis phase.

Identification Phase

As implied by the title, the purpose of this phase is to identify the users of precise time and time interval. The elements of information being sought to fit the definition of "identification" are somewhat more detailed than simply a name or organization. This effort will endeavor to identify the user by organization, location, points of contact by name and phone number and establish the organizational relationship of the unit with respect to higher and lower echelons of

the appropriate organizational structure. These data will serve to clarify the lines of operational control, administrative processes and logistical support. It will also provide a directory of personnel participating directly in the PTTI program and enhance the flow of information among the participants.

Collection Phase

Having identified the users of PTTI, the next step is to document essential information with respect to their participation in the program. A determination will be made as to the functional use of PTTI (e.g., navigation, communication, calibration, timing/synchronization, etc.), the essential equipment currently on hand and in use; the means whereby these equipments are timed/synchronized (traceable to USNO); and the criteria which define the users requirement in terms such as accuracy, stability, environmental specifications, or other key characteristics. Of equal interest in documenting the equipment is the maintenance policy of each organization. Information will be gained regarding the level of maintenance performed at the site (operational, intermediate or depot), and whether or not it is performed by organizational personnel or under contract support arrangements.

The full scope of information to be collected is not a fixed set at this time. Even early in the collection process, it was found that additional data elements proved most useful in revealing an overall picture of the PTTI program. As an example, the directives issued at various echelons were researched to determine the charter under which various organizations were operating. In some cases, the directives issued within the chain of command, may be useful in revealing the funding lines. Funding information will be essential if recommendations are to be developed regarding cost effective alternatives. Equally as important as documenting the current state-of-the-art is planning for future requirements. Current users will be surveyed to determine their perception of future needs or any problems they may anticipate in meeting their perceived operational requirements in the future. Developmental programs will be reviewed to determine if there may be PTTI requirements which have not yet been explicitly defined. This data on future requirements will provide a baseline for specific areas to be investigated in order to keep pace with refined requirements and broader PTTI applications.

The data collection process will consist of researching documents, interviewing personnel, either by telephone or in person, the circulation of a survey questionnaire, and on-site visits as required.

Analysis Phase

Based upon the information provided by the previous efforts, the

analysis phase will seek to delineate systems methods, systems accuracies, performance requirements, numbers of clocks, maintenance support roles, and inter/intrasystem utilization. Pertinent data elements will be reduced to graphs, charts and/or matrices to present concise, comprehensive summaries from which cogent alternative actions may be derived in support of the improvement plan.

Although it may appear that these three phases are conducted sequentially, in a series fashion, such is not the case. The process is an iterative one in which data derived in one phase may lead back to further investigations in the previous phase which may in turn lead to additional areas of investigation, data collection and analysis.

PTTI Improvement Plan

The customary approach to the development of a plan is being followed for the improvement plan. This entails the development of an outline, the development of a book plan, and finally, the development and publication of the PTTI Improvement Plan. The Book Plan development was scheduled in the early phases of the task in order to provide direction to the data collection and analysis phases. As stated earlier, the improvement plan development will be a concurrent effort which will interact on a real time basis with all three phases of the requirements analysis portion. Proposed management initiative and related recommendations will be firmly supported by clearly defined requirements.

An Executive Summary will be provided as a lead into the Improvement Plan in order to provide a concise overview of the program and recommendations. The succeeding four chapters will describe the characteristics of the PTTI program as it now exists. This will take the form of an introduction/background section; a description of the services available through the U.S. Naval Observatory; a section on users and their related requirements and a section on how those requirements are currently being met and planned improvements matched to potential needs. The next chapter will highlight the critical issues. In essence, this portion will address the shortfalls and problem areas, including cost factors, to the extent that they can be isolated and documented.

The remaining two chapters will provide alternative management actions which, if executed, should result in significant improvements in the PTTI program. Recommendations will be made as to the preferred alternative. The preferred alternative will be expanded in more specific detail with respect to responsibilities, schedule of actions, and any modifications to governing directives required to implement that alternative.

Details of the supporting rationale contained in the plan will be provided in appendices to the plan. Three levels of detail will be provided: the Executive Summary will provide an overview for decision making; the body of the plan will contain the rationale for the alternatives and recommendations. The backup data will be contained in the appendices.

SCHEDULE

Work on the project was initiated on 18 January 1980. The target date for the completed Requirements Analysis Report and the PTTI Improvement Plan is 27 December 1981. The only major interim milestone is the development of the Book Plan in June 1980. Due to the concurrent and iterative nature of the identification phase, collection phase, analysis phase and plan development, clearly delineated start-stop dates for these activities were not deemed appropriate. However, selected interim goals to be achieved have been identified in the interest of sound program management and are displayed in Figure 1.

STATUS

The identification phase commenced immediately upon initiation of the task. A two-pronged approach was used; a top-down approach and bottom-up approach. The top-down approach began at the policy level in Washington and sought to identify the individuals involved, their job title, code, location, phone numbers and the field agencies or subordinate commands under their purview. The bottom-up approach used the U.S. Naval Observatory distribution list printout for their time services bulletin. The list includes 986 domestic users and 258 foreign users. The listing was separated into categories by Service (USAF, Army, Navy, etc.) or agency. In some cases, the functional area of PTTI in which the user has primary interest may be discerned from the type of time service publications received. Such is not always the case, for there are multiple uses, as well as multiple users of the documents. Here the top-down approach seeks to clarify the functional area of interest by tracking the organizational relationship through the chain of command and the supporting directive system. DOD Directive 5160.51 required each DOD component to issue implementing directives. These, in turn, assigned responsibilities and functional areas to various commands and field activities. The directives have been researched and collected for OSD, JCS, DCA, USAF, USA and USN. To date, a preliminary directory of points of contact in the PTTI arena has been compiled, consisting of approximately sixty persons. In its current format, it lists the personnel by Service or agency, with code, address, phone numbers and any charter or directive associated with their function. Approximately thirty-five of the persons listed have been contacted in search of data. Preliminary initiatives have been made with the Federal

Aviation Administration, Defense Mapping Agency, and certain independent commercial users.

In order to accelerate the data collection process, a survey questionnaire was designed. Using the information gained in the early portion of the identification phase, a distribution list of key recipients was developed. A cover letter signed by the Superintendent of the Observatory, explaining the purpose of the effort and forwarding the questionnaire, was distributed on 7 May 1980. Responses were requested by 4 June 1980. Twenty-five completed questionnaires have been returned. A comparative analysis is now in process comparing data received from interviews and the survey questionnaires with the data required to complete the requirements analysis and fill out the element of the Book Plan. Voids in essential elements of information will be identified. Efforts to fill these voids will begin with local interviews and phone calls and finally, on-site interviews at field activities will be conducted to complete the process. In every case requiring a field visit, a point of contact will be advised in advance either by phone or by letter as to the type of information being sought.

An outline of the Improvement Plan was developed and approved on 23 April 1980. The outline was subsequently expanded into a Book Plan which was approved on 30 June 1980. The Book Plan, which defines the elements of data scheduled for incorporation into the Improvement Plan is now serving as the benchmark in guiding the collection and analysis phases.

A clearer picture of the organizational relationships has begun to evolve. Preliminary diagrams have been drafted in tiered echelons from the policy level down to field activity and users.

Although some minor difficulties have been encountered in translating stated requirements into common terms of reference for easier comparison, and ensuring that all users are identified, the program is currently on schedule with no insurmountable obstacles in view. Although not deemed insurmountable, two areas of investigation which prove more intractable than one would care to have them are those driven by security restrictions and availability of funding details. Every effort is being made to maintain the reports as unclassified in order to enhance their circulation and utility. If need be, a classified appendix may be published to provide supporting data essential to the decision making process.

PRELIMINARY FINDINGS

In the interest of brevity selected highlights of the preliminary findings are presented below in the areas of organizational

relationships, current directives, PTTI users, and future requirements.

Organizational Relationships

There are two distinct lines of staff cognizance in PTTI, the logistics side and the operational side. In most cases, the responsibilities for PTTI shift to the logistics staff at the policy level. The bulk of the documentation is written in terms of metrology and calibration responsibilities for technical laboratories or similar support units in the field. In general, these lines of responsibility through the logistic side are easily traceable. The logisticians are tasked with specific responsibilities to maintain set standards, and provide support to operational users. The operational side of the problem does not lend itself to easy traceability. It has been difficult to pinpoint the central controlling agency for operational requirements within the various organizational structures. It appears at first blush that a variety of research agencies, usually resident at the same location with a metrology/calibration facility will develop operational requirements and resolve their needs in coordination with the resident experts. As currently documented the technical or logistics side of the chain is very responsive to the users' needs and the interchange of services and information is free-flowing and continuous. However, as additional support services are required from a higher support echelon (such as the Naval Observatory), the requirement flows up through the technical chain on the logistics side of the staff. Again, the system works by virtue of the nature of the participants. However, this system places the Observatory in a reactive mode--responding to needs from the field on an "as required" basis. Ideally, the operational requirements should be centrally coordinated for each agency. The central coordinator would express these requirements to the U.S. Naval Observatory personnel who, in execution of their charter as DOD PTTI Manager, would assist in defining the system to meet the requirements. Then through the logistics side of the staff, the USNO would insure that the necessary dissemination system and proper support equipments were available to execute the PTTI support. This process would place the USNO in the requirements determination loop and insure a more cost effective, coordinated program.

PTTI requirements which transcend the bounds of single Service of single agency applications are generally addressed by committees. In some cases, the committees are formed to address specific issues and representation is established to insure that all interested parties participate. There are two standing committees which provide a forum for addressing joint requirements. The MUSIC MAN COMMITTEE and the JOINT TECHNICAL COORDINATING GROUP for METROLOGY and CALIBRATION (JTCCG-METCAL). Based upon the representation on these committees, it appears that the MUSIC MAN COMMITTEE is best suited for addressing

the operational aspects of the problem and the JTCG-METCAL is technically oriented.

There are exceptions to the general description of the interaction of operational agencies and logistic agencies as previously described. Two notable exceptions are the GPS/NAVSTAR program and the SATCOM/DCA program. These two programs have been the beneficiaries of long arduous planning and inter-agency activity. However, in spite of such coordination at the top level, the results of the survey questionnaire reveal that some participants in the PTTI program are somewhat tentative as to the precise impact the program may have on their "modus operandi".

Current Directives

Two items of interest were revealed in tracing through the directives which govern PTTI programs in the Department of Defense. First, the assignment of responsibilities in implementing directives generally substantiates the heavy influence of the technical/logistic participants in structuring the character of the program. In instances where operational staffs are tasked with responsibilities, they are usually stated in terms of verifying the compatibility of design and specifications rather than explicit responsibilities for stating and processing requirements. The second item is tracing directives to a common reference. Some implementing directives cannot be traced back to DOD Directive 5150.61, although other DOD Directives may be referenced.

PTTI Users

Preliminary findings with respect to PTTI users reveals that the laboratories, research organizations, and test ranges are best able to document their function, equipments, current operating procedures, and identify future requirements. There appears to be a significant community of beneficiaries of PTTI who tend to accept the services provided without full awareness of the impact on their program of how, by whom, and at what cost the services are made available. The investigation and full documentation of this community's PTTI programs portends to be the most difficult aspect of the task. Consequently, it will be the objective of detailed scrutiny in the iterative identification and data collection processes. Some of the PTTI users who responded to the survey questionnaires left some unanswered questions. A few indicated that they had no "next higher" echelon of command and no subordinate commands. Some provided no further time or calibration service beyond their own use, an acceptable though unlikely situation, except for a research facility. In some instances it was indicated in the survey that the time maintained on-site was not traceable to the USNO, yet the method whereby the time was maintained provides for such

traceability. Current requirements were generally implicit in the description of the users function and the capabilities of the equipments in use. Further investigation is warranted to insure the most economical and efficient use of resources.

Future Requirements

Future requirements have been expressed in a variety of characteristics desired. These include: cost, stability, accuracy, vibrational loading, G-loading, temperature sensitivity, power requirements, size, and accessibility. A number of these characteristics were described in quantified terms and others in general terms. For example, the lease cost item desired was to be less than \$100 per unit. Stability requirements have been submitted at the refined end of 4×10^{-12} /sec and $1 \times 10^{-11}/4$ hours. Accuracy statements range from "extreme" to a quantified value of 100 nanoseconds. Every effort will be made to quantify requirements to provide a common means of comparison and evaluation.

In the process of seeking answers to questions initially proposed for data collection, there appears to be a higher ratio of new questions than answers to old questions. In a program as dynamic and complex as the Precise Time and Time Interval program, one should reasonably anticipate such results in the early portion of the investigations. Hopefully, the crossover point will occur soon, wherein the number of answers neatly matches the questions at hand and no vital area which may influence the selection of viable alternatives remains unexplored. Needless to say, it is a challenging task, but one that should prove to be rewarding and beneficial to the PTTI community as a whole.

DOD PTTI SCHEDULE

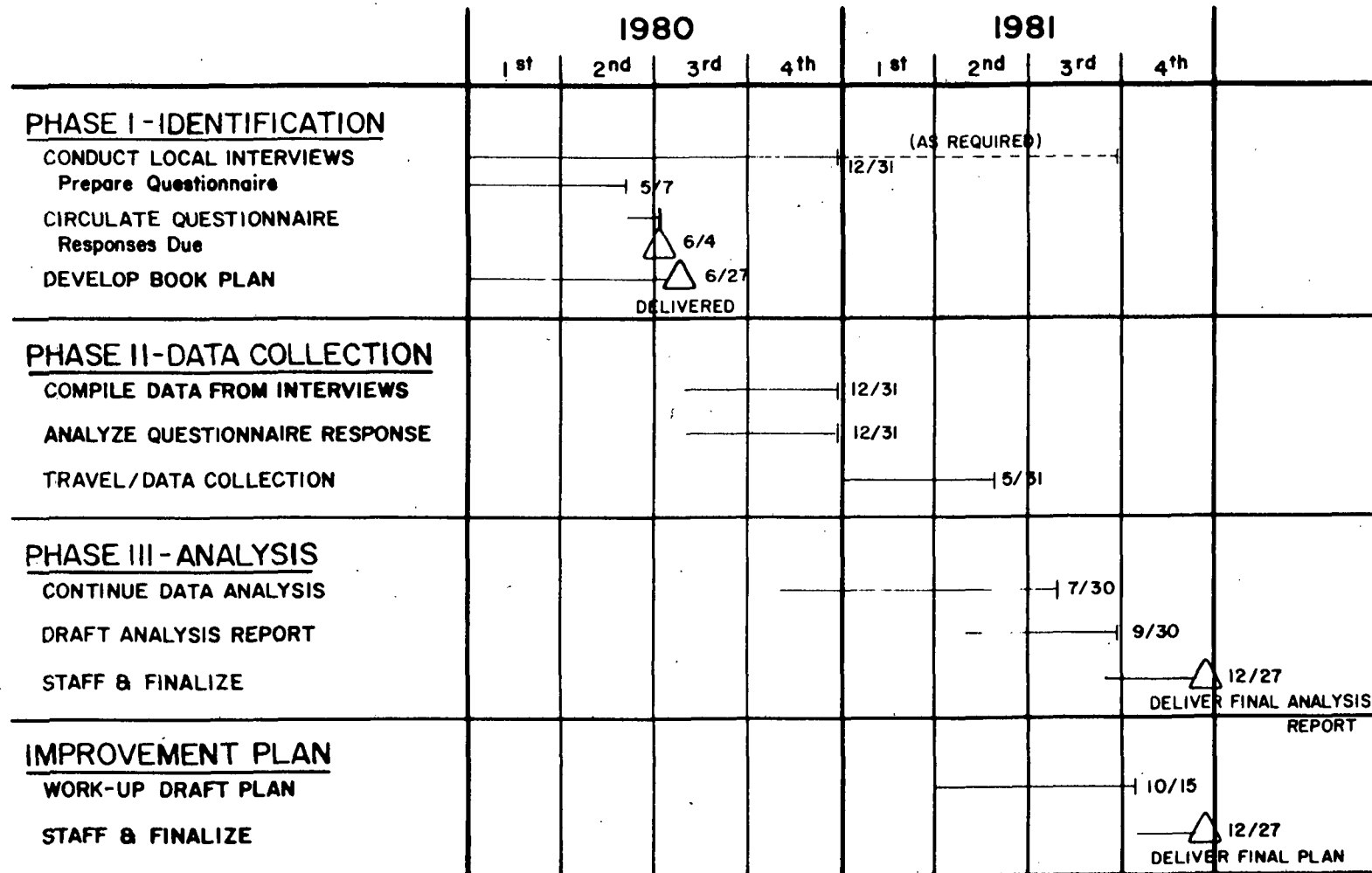


FIGURE 1

Page Intentionally Left Blank

A U.S. NAVY PRECISE TIME AND TIME

INTERVAL (PTTI) PROGRAM UPDATE

RALPH T. ALLEN

NAVAL ELECTRONIC SYSTEMS COMMAND

ABSTRACT

A review of the Navy's PTTI Program was presented at the Tenth Annual PTTI Applications and Planning Meeting. That review presented a brief history of the Navy's PTTI Program, its management organization, and current and projected requirements, capabilities and Program efforts.

This paper:

- a. Updates those previously identified Navy requirements, capabilities and Program efforts.
- b. Outlines new Program efforts.
- c. Presents overall Program growth since September 1975.
- d. Projects the Navy's areas of concern regarding future PTTI development.

A review of the U.S. Navy's Precise Time and Time Interval (PTTI) Program was presented in November 1978 at the Tenth Annual PTTI Applications and Planning Meeting (1). Since that presentation, the Program's management organization, its basic mission of providing all Navy platforms and their communications, navigation and weapon systems with PTTI information traceable to the U.S. Naval Observatory (NAVOBSY), and its PTTI System Concept, see Figure 1, have all remained essentially unchanged.

This has provided a stable base from which the Program has continued to grow and to respond to the increasing PTTI needs of the Fleet. This growth and response to Fleet needs has resulted in an increasing awareness of and support for the Program by Navy program sponsors, planners, programmers, engineers, support personnel and users.

More specifically, the review at the Tenth Annual PTTI Applications and Planning Meeting reported that the Naval Electronic Systems Command (NAVELEX) had submitted an analysis of the Navy's PTTI requirements to the Chief of Naval Operations (CNO) in November 1978. The review further reported that current, medium and long range Navy platform timing requirements were in the 100 microsecond, the one to ten microsecond, and the 10 nanosecond ranges respectively. With a few exceptions, those values are still valid.

Based on the requirements analysis findings, NAVELEX updated the Navy's PTTI Program Master Plan. CNO subsequently approved the Master Plan in January 1980.

Some of the major Navy PTTI efforts addressed in that Master Plan and reported on at the Tenth Annual PTTI Applications and Planning Meeting include the:

PTTI Maintenance and Calibration Program.

SSN-637 Class Submarine PTTI Platform Distribution System (PDS) Development.

SSN-688 and POSEIDON Class Submarine PTTI PDS Development.

NAVOBSY Master Clock System (MCS) Upgrade.

AN/URQ-23 Frequency-Time Standard.

Global Positioning System (GPS) Time Transfer Unit (TTU).

PTTI Technology Program.

O-1695 Cesium Beam Frequency Standard.

Rubidium Standard Development.

"Standardized" PTTI PDS.

The following is a brief update on each of these efforts covering the past two years.

In 1978, the Naval Electronic Systems Engineering Center (NESEC), Portsmouth was assigned the responsibility of providing maintenance and repair services for all Navy owned atomic standards and providing portable clock trips to numerous Navy installations and Army Defense Satellite Communications System (DSCS) earth terminals under the PTTI Maintenance and Calibration Program. NESEC, Portsmouth has now been formally tasked, as the Technical Manager for PTTI, with providing Field Maintenance Agent (FMA) and Depot Repair Facility services for

Navy owned PTTI equipment including the AN/URQ-23 Frequency-Time Standard and the SG-1157/U Digital Processing Clock. Future projections indicate that NESEC, Portsmouth's responsibilities as the Technical Manager for PTTI will continue to increase and expand.

The automatic, no-break SSN-637 Class Submarine PTTI PDS equipment, see Figure 2, was delivered in 1979 and completed Operational Evaluation (OPEVAL) testing in June 1980. It is currently being considered for Approval for Service Use (ASU).

A direct result of the SSN-637 Class PTTI PDS development effort has been a reduction in scope of the SSN-688 Class PTTI PDS to a manual switch, see Figure 3. Also, current planning is for the POSEIDON class submarines to use the PDS developed under the SSN-688 Class effort. While development was initiated on this PDS at the Naval Ocean Systems Center (NOSC) and the Naval Avionics Center (NAC), reversals and set-backs have necessitated reprogramming actions. A restart effort is now being scheduled.

In July 1980, CNO formally approved the Navy Decision Coordinating Paper (NDCP) for the NAVOBSY MCS Upgrade, see Figure 4. Presently, various component equipments required to upgrade the Data Acquisition System (DAS) of the MCS have been procured and installed. Also, the first of two Environmentally Controlled Monitor Stations (ECMS) have been procured and installed. The first procurement of hydrogen-masers is now scheduled for Fiscal Year (FY) 1982.

The AN/URQ-23 Frequency-Time Standard which will replace the AN/URQ-10A as the Navy's quartz crystal reference standard was granted ASU in August 1979. The first AN/URQ-23 production contract was awarded the following March and the first production units are now being delivered to the Fleet. The next procurement of AN/URQ-23's is scheduled as a competitive, multiyear procurement in FY-82.

The GPS TTU (2) feasibility model was delivered to the NAVOBSY in December 1979 where it is currently completing a one year testing program. Initial findings indicate that its performance is better than the specified 100 nanosecond time transfer capability. A production decision is scheduled for April 1981.

The PTTI Technology Program to investigate (a) time transfer via GPS using laser technology, (b) environmental effects on atomic clocks and (c) high performance standards and advanced timing has gone unfunded for the second year. NAVELEX will continue to pursue this effort by showing the potential impact of these advanced research programs on systems and equipments which are currently scheduled for installation in the Fleet.

Cognizance of the O-1695A/U Cesium Beam Frequency Standard was

scheduled for transfer to the Navy's PTTI Program in FY-79. While responsibility for the maintenance and calibration of the O-1695A/U has now been assumed by the Program, full technical cognizance of the unit has, at the request of the VERDIN Program Manager, not been transferred because of reliability problems associated with the equipment. A transition plan has been developed and will be implemented upon final resolution of those reliability problems.

The development of a rubidium standard for the Navy which was discussed in 1978 is now being held in abeyance. A Preliminary Design and Life Cycle Cost Analysis for the "Standardized" PTTI PDS, see Figure 5, was initiated in late FY-79. The Preliminary Design and Life Cycle Cost Analysis is to develop alternative designs for a modular PTTI PDS comprised of "Standardized" equipments which could be reconfigured to meet the needs of a particular platform, i.e. surface ship, submarine, aircraft or shore installation, and compare the technical, operational and economic advantages and disadvantages of those alternatives. It was decided that it would be premature to initiate the development of a rubidium standard for the Navy prior to the completion of that Preliminary Design and Life Cycle Cost Analysis.

Similarly, final approval for full scale development of the "Standardized" PTTI PDS is being held in abeyance pending the completion of the Preliminary Design and Life Cycle Cost Analysis. The "Standardized" PTTI PDS is the heart of the Navy's PTTI Program. For that reason, NAVELEX is currently attempting to recoup after the failure of the contractor to complete the Preliminary Design and Life Cycle Cost Analysis within cost and schedule constraints and to finish the effort via other alternatives. NESEC, Portsmouth again under the PTTI Technical Manager assignment has taken the lead to insure timely completion of the effort.

New Program efforts have also been kept to a minimum over the past two years for two reasons. First, the PTTI Program Manager made a conscious decision in 1975 to minimize new Fleet, operational equipment developments until the Navy's requirements had been defined and then reasserted that decision in 1978 pending the completion of the Preliminary Design and Life Cycle Cost Analysis. Secondly, there has been a lack of sufficient personnel in the Program office to manage and administer the various Program efforts. Recently, this latter reason has caused NAVELEX to notify its sponsor that it could not accept additional PTTI responsibilities.

Taking this into account, the Program has still taken on new efforts to support immediate Fleet needs. For example, in 1979, NAVELEX procured several TRANSIT Timing Receivers to support NAVOBSY requirements. More recently, NAVELEX procured a clock distribution system to meet an urgent requirement at Naval Communications Station, Japan.

These were relatively small tasks, but, as stated previously, the PTI Program has continued to grow and to support the Fleet. Figure 6 is an updated Program Milestone chart which depicts some of the preceding efforts and reflects that Program growth. Figure 7 provides a funding profile, including RDT&E, OPN and O&MN funds, of the Program from FY-75 to FY-80 which again reflects that Program growth.

Most of this is, however, history. What projections can be made regarding the future?

Broad projections indicate that there will be a continuing increase in the Fleet's need for PTI and that there will be an accompanying increase in the Navy's support for PTI.

Also, while the "Standardized" PTI PDS Preliminary Design and Life Cycle Cost Analysis has not been completed, some specific Navy projections regarding future PTI developments appear feasible.

First, it appears that currently available reference standards combined with both operational and planned PTI dissemination systems, e.g., LORAN-C, TRANSIT and GPS, will be capable of meeting the vast majority of the Navy's projected operational requirements.

Second, there is a need for a properly designed, manual switch combined with an "update and comparison" equipment capable of (a) comparing onboard reference standards with a reference signal from a dissemination system external to the platform as well as with each other, (b) providing an alarm when any one standard drifts beyond a preset limit, and (c) allowing for underway time transfers as required.

Third, there is also a need to reduce the number of reference signals being distributed on board Navy platforms. Currently there are three basic frequencies, 5MHz, 1MHz and 100KHz; two timing pulses, 1PPS and 1PPM; and an untold number of time code signals being distributed. It appears that long range planning should reduce distribution to a single reference frequency and single time code. If necessary, this might be relaxed to include a single timing pulse signal. No decisions have been reached regarding which signals should actually be "standardized" on, but this action alone would reduce the number of cables which must be run, reduce the complexity of the PTI reference signal generation and distribution equipment and notify designers of future Navy communications, navigation and weapons systems of exactly what reference signals will be available on board Navy platforms and to design their systems and equipments accordingly.

One area of greatest need is that of distribution equipment; i.e., a new frequency distribution amplifier and a "time" distribution

amplifier. The AM-2123/U Frequency Distribution Amplifier is a good, reliable amplifier, but it is an old equipment. Modern technology should be able to provide a distribution amplifier with improved reliability characteristics and capable of providing more output channels in the same space as the AM-2123/U. Additionally, the Navy currently does not have an amplifier capable of distributing multiple timing signals, i.e., both time codes and timing pulses, and the need for a "time" distribution amplifier is increasing. Both units should be capable of supplying the multiplicity of reference signals required today, but also be capable ultimately of supplying the "standardized" signals discussed previously.

A final projected need is for reliable PTTI equipment. The "Standardized" PTTI PDS will be driving virtually all of the platform communications, navigation and weapons systems. Loss of a reference standard or failure of a switch could result in system outage or downtime at a critical moment and thereby result in damage to the platform or even a loss of life. Additionally, the Navy and the Nation's taxpayers cannot afford unreliable equipment; e.g., a reference standard which requires a tube replacement in excess of \$10,000 approximately every eighteen months. Reliable equipment is a must if the concept of a "Standardized" PTTI PDS is going to or even should be accepted by the Fleet.

In summary, the Navy's PTTI Program has formed a solid base with the Requirements Analysis and the CNO approved Program Master Plan. It has experienced some setbacks because of personnel shortages, missed delivery schedules, etc. However, the Program is moving forward and providing the Fleet with needed equipment and support.

Hopefully, the next two years will see even greater growth and support both to the Fleet and from Navy sponsors, planners, programmers, engineers, etc. Hopefully, the "Standardized" PTTI PDS Preliminary Design and Life Cycle Cost Analysis will be complete and full scale development of PDS's for candidate platforms will have been initiated.

The Navy PTTI Program office is working to make these hopes become realities.

REFERENCES

1. Allen, Ralph T., "A Review of the U.S. Navy's Precise Time and Time Interval (PTTI) Program," Proceedings of the Tenth Annual Precise Time and Time Interval (PTTI) Applications and Planning Meeting, NASA Technical Memorandum 80250, November 1978.
2. Witherspoon, Jackson T. and Schuchman, Leonard, "A Time Transfer Unit for GPS," Proceedings of the Ninth Annual Precise Time and Time Interval (PTTI) Applications and Planning Meeting, NASA Technical Memorandum 78104 March 1978.

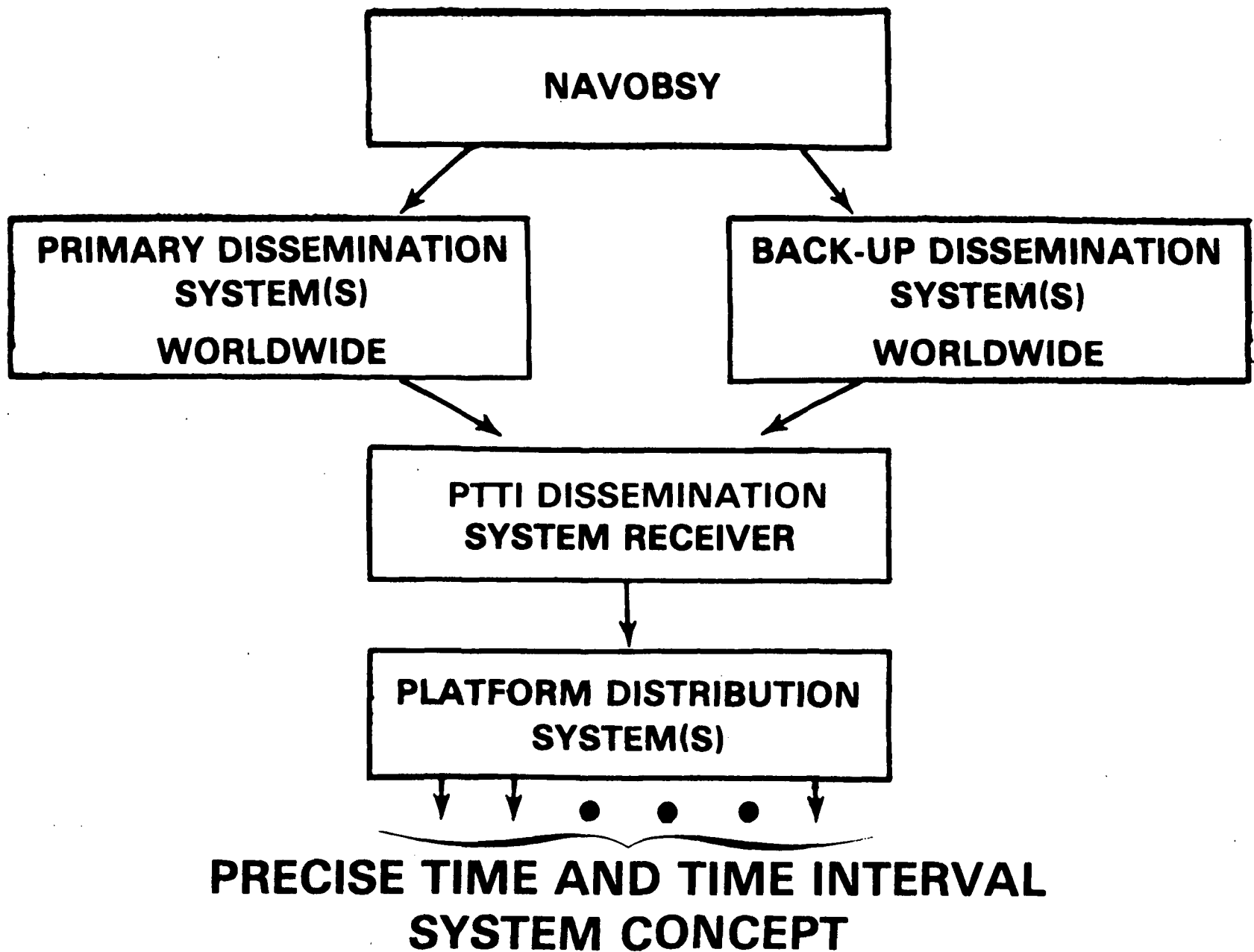


Figure 1

SIMPLIFIED DIAGRAM OF SSN-637 CLASS PTTI PDS

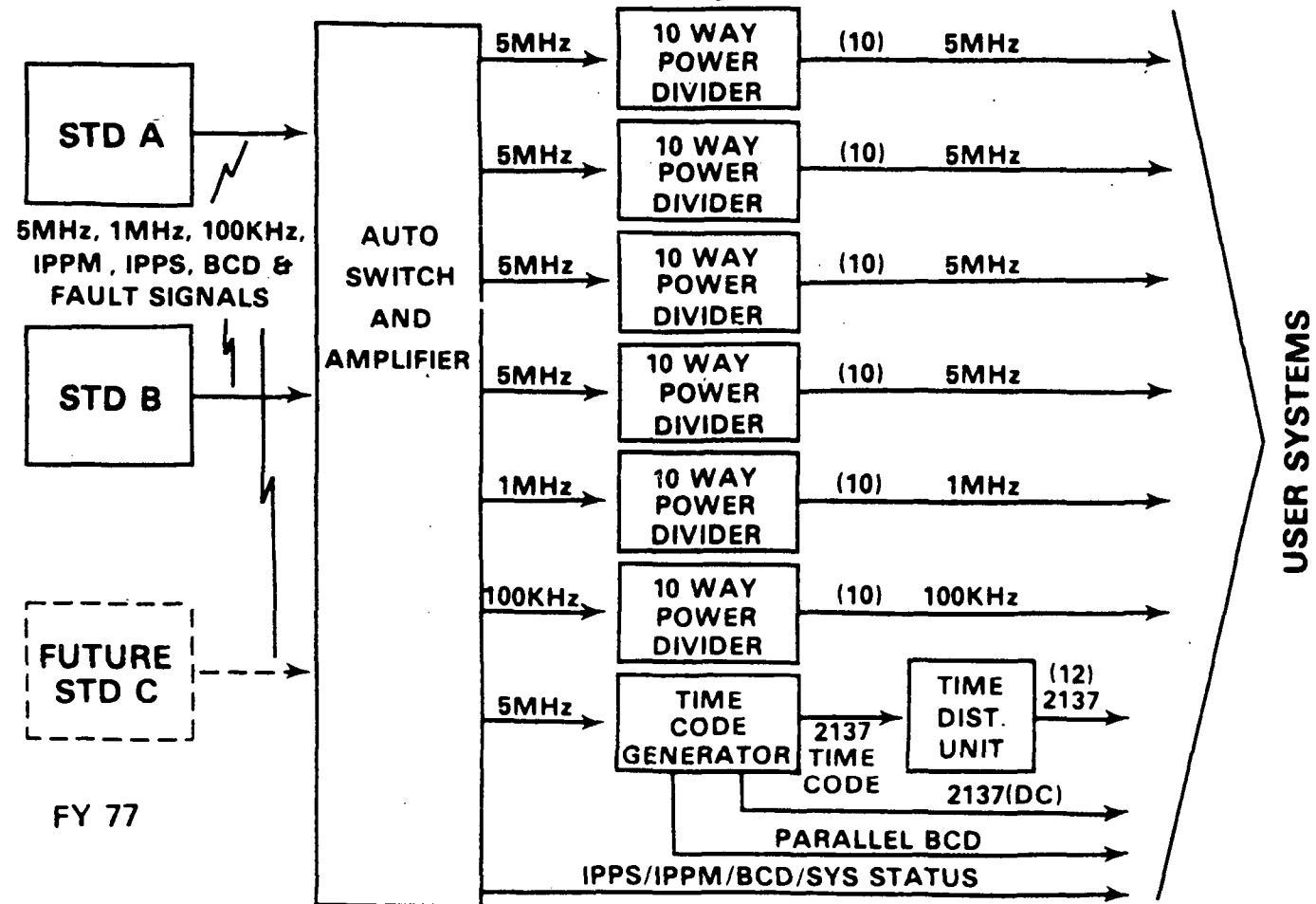
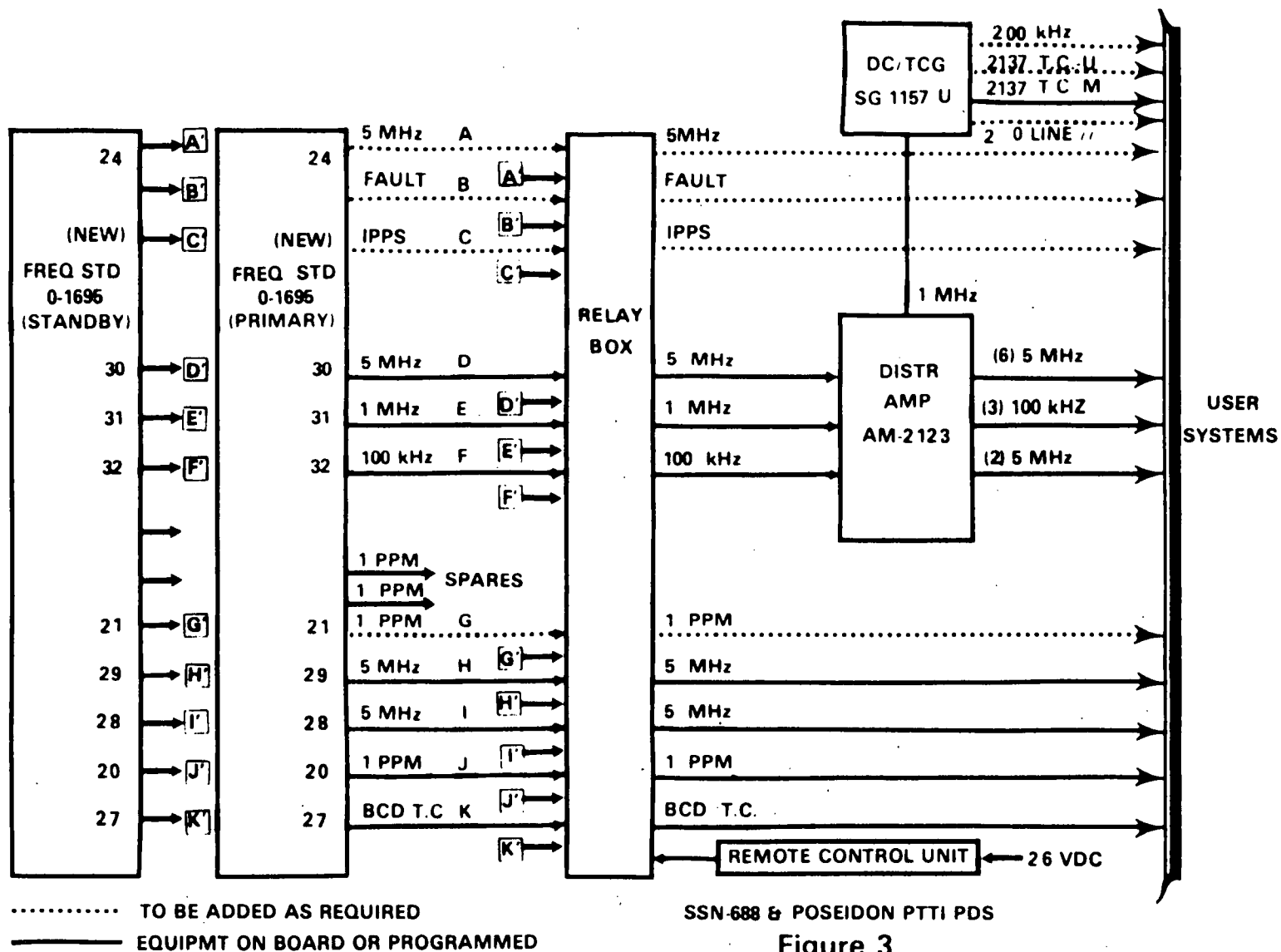


Figure 2



SSN-688 & POSEIDON PTTI PDS

Figure 3

U. S. NAVAL OBSERVATORY MASTER CLOCK SYSTEM

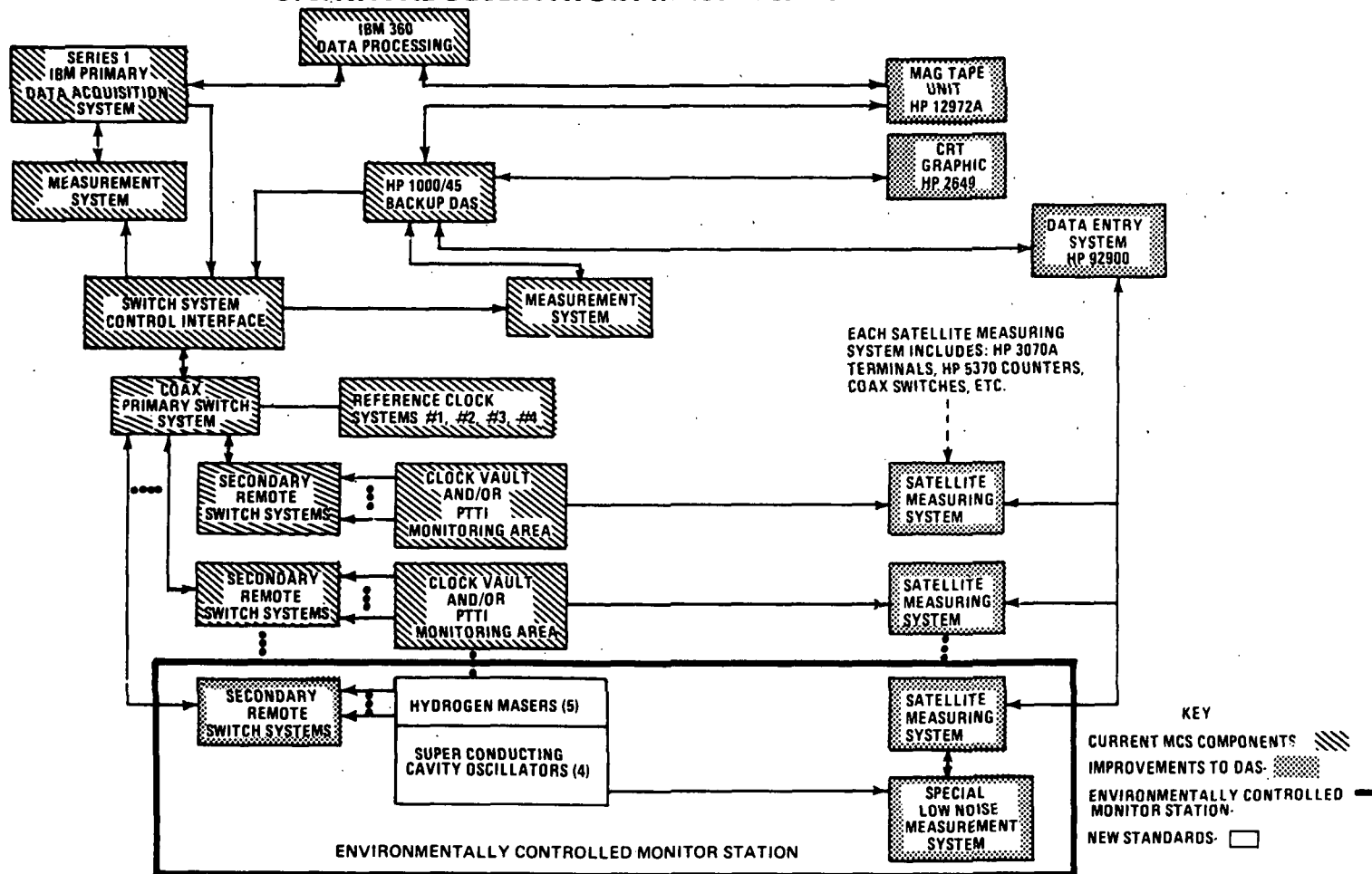
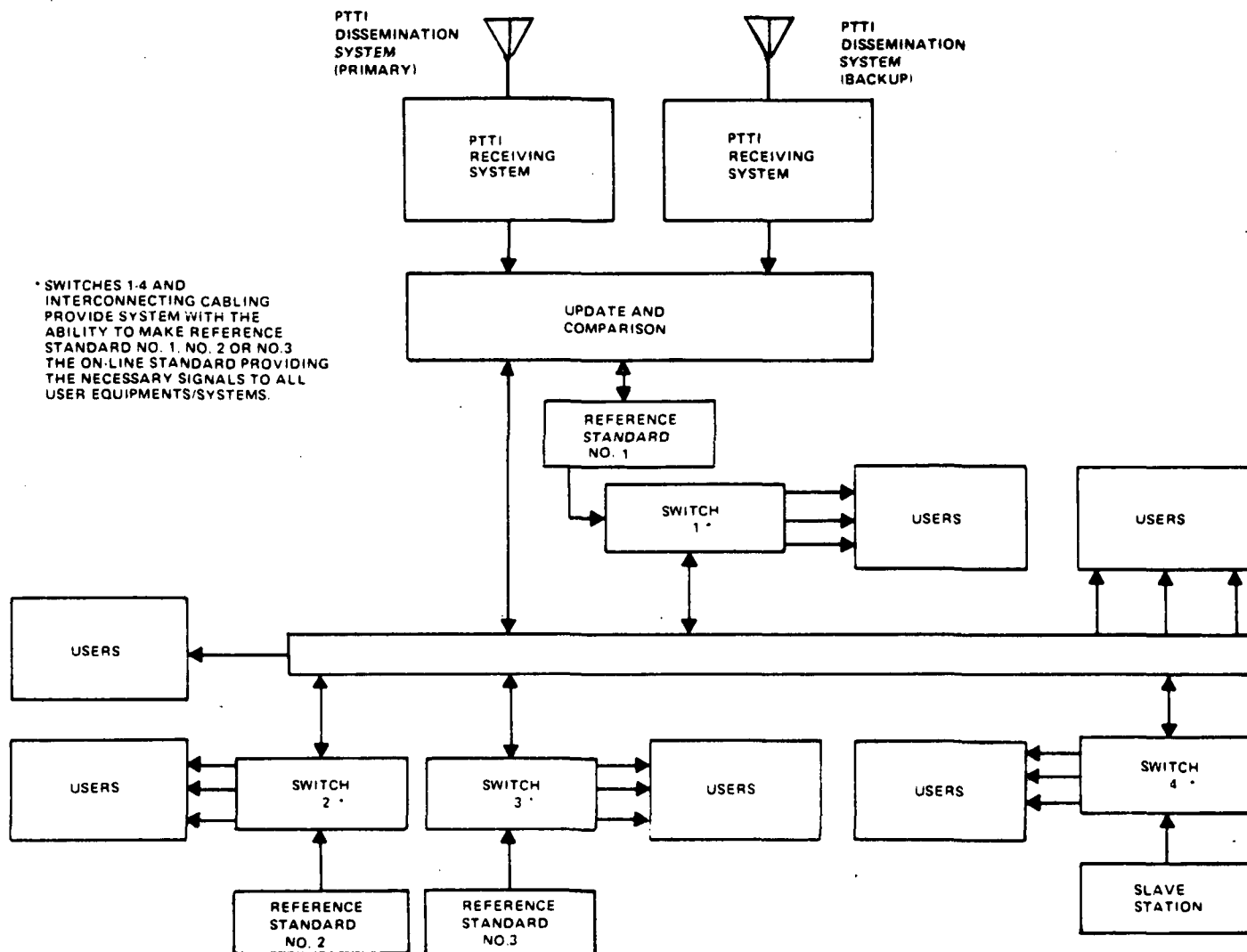


Figure 4



PTTI PLATFORM DISTRIBUTION SYSTEM CONCEPT

Figure 5

MAJOR PTTI PROGRAM MILESTONES

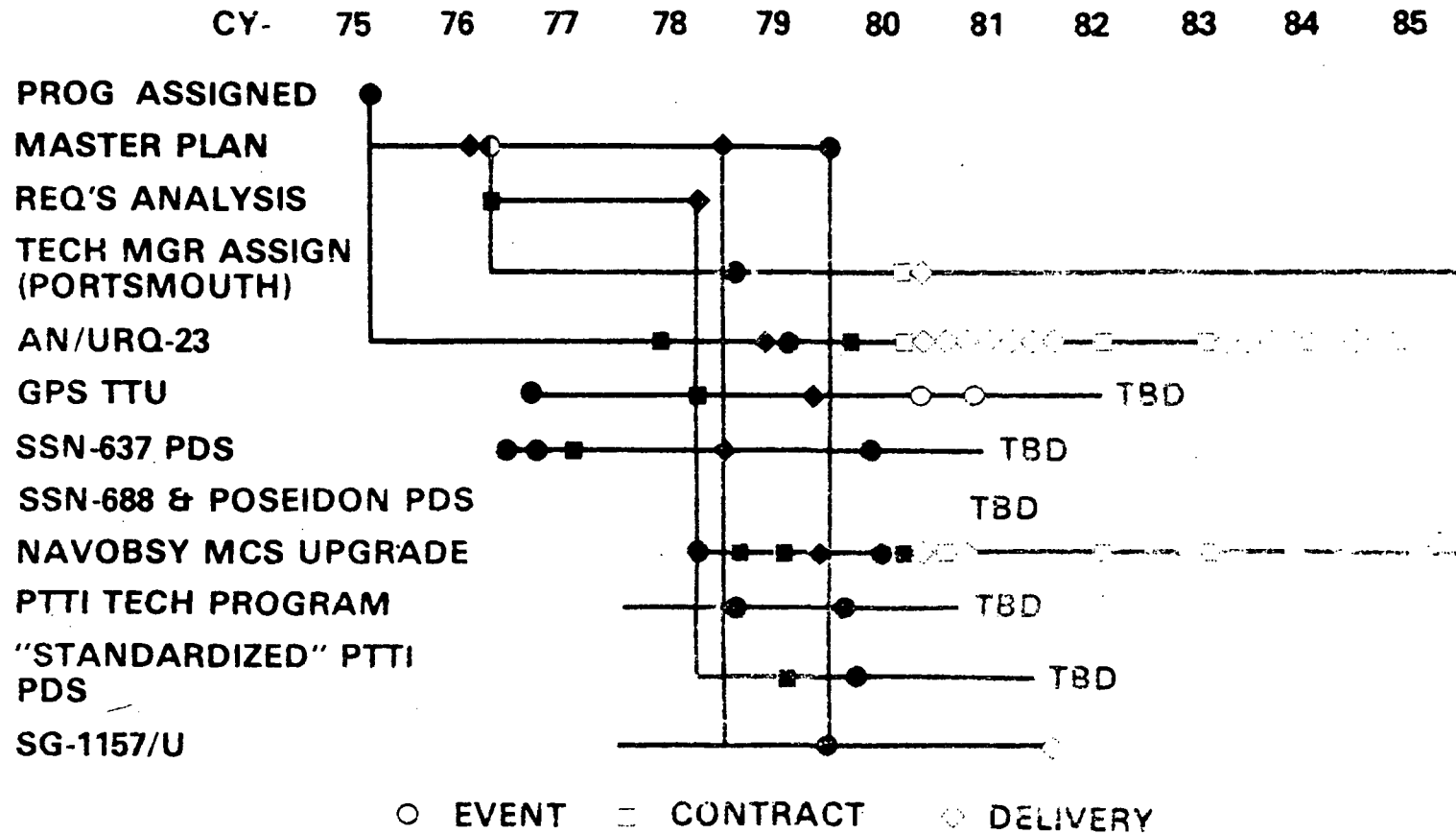


Figure 6

PTTI FUNDING PROFILE

DOLLARS IN
MILLIONS

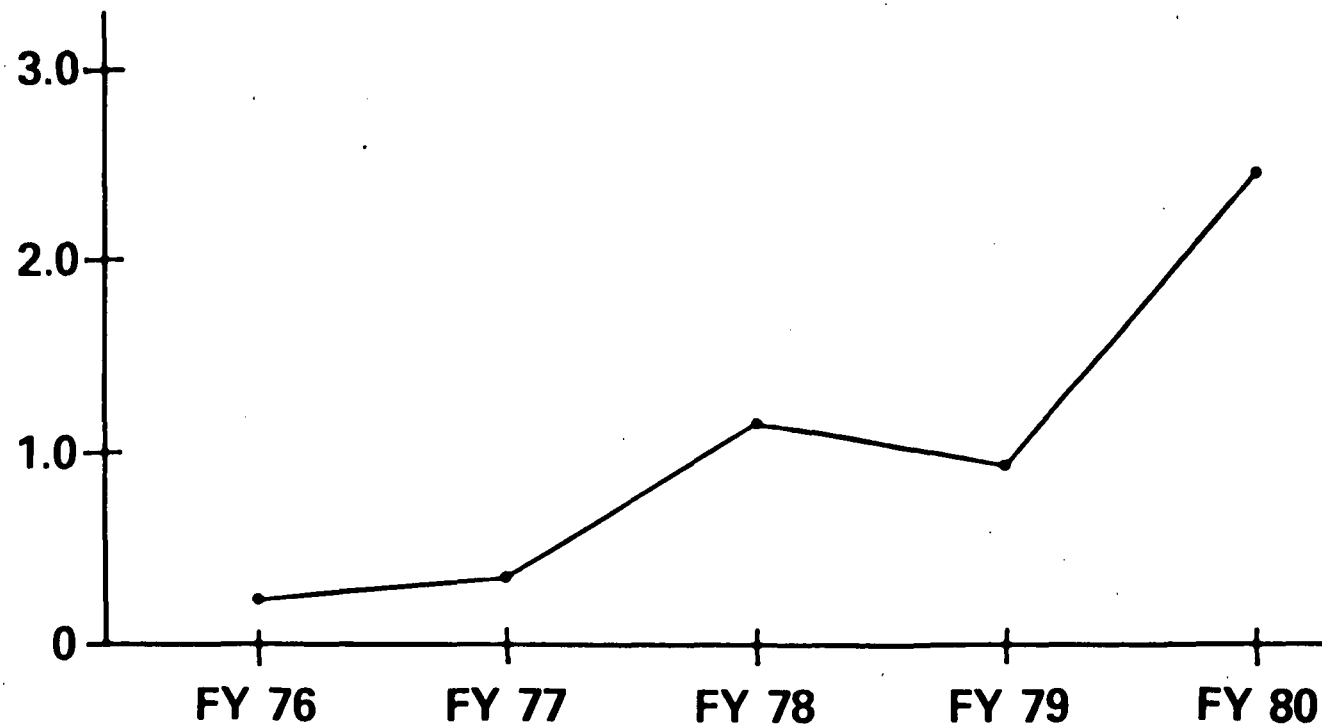


Figure 7

PRECISE TIME TECHNOLOGY FOR SELECTED
AIR FORCE SYSTEMS: PRESENT STATUS AND
FUTURE REQUIREMENTS

N. F. Yannoni
Rome Air Development Center
Deputy for Electronic Technology
Hanscom AFB, MA

ABSTRACT

Precise time and time interval (PTTI) technology is becoming increasingly significant to Air Force operations as digital techniques find expanded utility in military missions. Timing has a key role in the functions of communication and identification as well as in navigation. A survey of the PTTI needs of several Air Force systems will be presented. Current technology supporting these needs will be reviewed and new requirements will be emphasized for systems as they transfer from initial development to final operational deployment. The PTTI program activity in the Signal Processing and Timing Devices Section of the RADC Solid State Sciences Division is reviewed, and a survey is presented of areas of mutual interest to Government and industry in planning and execution of PTTI research and development programs.

INTRODUCTION

This paper reviews the status of selected systems requiring Precise Time and Time Interval (PTTI) technology: systems in which the Air Force has either sole sponsorship or participates jointly with the Army and Navy. They include PTTI applications in space, in aircraft and on ground-based platforms. Future needs in these programs are addressed in terms of generic performance improvements, the need for which has been produced by operational constraints such as the time interval for which a specific communication code key is to be used, the allowable period between resynchronization, or the logistics of the platform carrying the system of interest. The opportunity is taken to describe the evolution of the time and frequency

activity at the Solid State Sciences Division of the Rome Air Development Center (RADC) and to review the scope of the current PTTI activity from the technology-base/system-support viewpoint. Finally we address areas of common interest, and occasional concern, to the PTTI community which detail some of the factors which control our ability to provide, in a timely way, the PTTI technology required for Air Force programs.

CURRENT PROGRAMS

Several acquisition divisions of the Air Force Systems Command: - the Electronic Systems Division (ESD), Aeronautical Systems Division (ASD), and the Space Division (SD) are involved with acquisition programs requiring precision timing devices.

The space segment of the Global Positioning System (GPS) program office at SD has completed the launching of the first six satellites of the total constellation. These satellites carry redundant rubidium and/or cesium frequency standards. The clock status of the GPS space segment is to be described elsewhere⁽¹⁾ in these proceedings and therefore a detailed discussion is unnecessary in this paper. The user segment equipment is based on quartz oscillator technology which employs a common module for placement in aircraft avionics packages, in rack-mounted equipment in submarine and surface vessels, and in compact electronic units for backpack and mobile ground equipment. In comparison with the relatively benign environment of the space segment, the oscillators for the user segment will be subject to the vibration, humidity, temperature and g-force extremes of the high-performance aircraft or rough-terrain vehicle platform. Dual contractors are now involved in full scale development programs which should deliver about 100 units. Production of the user equipment will require many thousands of oscillators.⁽²⁾

The Joint Tactical Information Distribution System (JTIDS) is a secure, jam-resistant, high-capacity, flexible digital communications systems under joint development of the military services. It provides for position location, communication and identification functions via a time-division multiple access architecture. Timing requirements for this system can be satisfied with quartz technology.^(3,4) The JTIDS acquisition process is divided into three classes of terminals. The Class 1 terminal is for use in ground command and control centers and in long-

range surveillance aircraft. This terminal is now in production. Acquisition of the Class 2 terminal, which is scheduled for fighter aircraft deployment, is in the source selection process for full-scale engineering development. The Class 3 terminal, not yet initiated for acquisition, is intended for surface-based mobile users.

The United States Identification System (USIS, formerly the NATO Identification System, NIS), a tri-service effort, is in the first stages of the acquisition process. The USIS program involves both improvement of the Mark 12 IFF system now in use and the development of an entirely new IFF system designed to be secure, jam-resistant and interoperable within the NATO community.⁽⁵⁾ The system will require clocks for ground control centers and AWACS aircraft, for tactical aircraft and helicopters, and for mobile ground-based users such as tanks, trucks and surface-to-air missile crews. For the timing system, the objective is to procure the highest quality clock commensurate with system economics. The goal is to minimize the code validity interval, thus reducing the interference options available to a jammer. The frequency stability to be specified forms part of a NATO agreement scheduled for completion by the end of the year. As is the case for the GPS user segment, the number of oscillators required will run to many thousands. Therefore it is highly probable that quartz technology will play the major role in surface based and, perhaps, airborne platforms. Several studies of the clock problem for USIS have been completed and development work on several aspects of oscillator technology are planned for this fiscal year.

The 616A program is the Air Force support to the Minimum Emergency Essential Communications Network (MEECN) and is a survivable very low frequency communication system for use by the Strategic Air Command. The principal clock application is for synchronized communications between the command structure, launch control centers, and SAC aircraft. Current status of the clock is a cesium-based unit which was developed with Air Force funding. The latest design is a portable (1 hour battery capacity), radiation-hardened device which is used to carry and insert system time into the communications hardware of network participants.

The SEEK TALK program is a secure anti-jam voice communication capability for Tactical Air Force use. The system is presently in full-scale engineering development under a dual contract award. The SEEK TALK scenario includes

timing performance which requires frequency stability at the high technology end of quartz capability. Both rubidium and advanced quartz technology are considered to be candidates for the SEEK TALK oscillator. The near-term solution to the SEEK TALK requirement is vested in the HAVE QUICK program. The latter system is an ECCM modification to certain ground-based and airborne radios which gives them a frequency-hopping capability.⁽⁸⁾ A randomized channel selection sequence which is changed rapidly inhibits an enemy inteceptor or jammer from joining the communication system because of the very short residence time of the system in any one channel. The HAVE QUICK program is based on Coordinated Universal Time in order to be able to take advantage of the TRANSIT satellite system as a means of obtaining time. Reference frequency for ground-based units is supplied by rubidium oscillators and almost all of the clocks in the HAVE QUICK system are required to hold correct time to within 3 milliseconds for mission duration. An analysis⁽⁶⁾ of possible errors in initial setting accuracy coupled with ageing of the unit indicates that frequency recalibration would not be required over a period of five years in order to hold to the 3 millisecond specification.

FUTURE NEEDS

We address this topic less from the viewpoint of individual program office requirements but rather from developments which would benefit across-the-board users of PTTI technology. The importance of reviewing these topics becomes clear when we consider the 1980's as a decade when industry will be called upon to provide reliable oscillator hardware by the tens of thousands of units. When acquisition is discussed in these terms, our ability to deploy quality systems will depend to a large extent on economies of scale associated with continuing, large-quantity purchases, and the development of innovative manufacturing processes which will produce the desired equipment at prices which the acquisition divisions can afford. It is important, therefore, that substantial, serious process engineering development work be completed by the early 1980's. We believe that any plant or equipment modification plans must be finished and evaluated in pilot plant operation early enough to respond to the acquisition milestones of the programs with PTTI needs. The plant capacity topic will be addressed further in the last section of this paper.

For many systems using quartz oscillator technology, a fundamental operational choice usually emerges: whether or not to turn the unit off. If constant power is maintained, we avoid the problems associated with frequency retrace and warmup time. We pay for these benefits through providing battery backup in the case of line power failure and enough battery capacity for the stand-alone unit to maintain operation for mission lifetime. For most of the programs involving man-portable clocks, it is unlikely that continuous power will be available except for missions of rather short duration. Therefore it is important to note that improvement in the warmup time would benefit several programs which will enter the procurement phase in the 1980's. Given fast warmup, say less than 60 seconds to some narrow band around nominal frequency, the capability for tuning would complete the process of clock initialization. Without the tuning capability, the retrace of the unit must be good enough, early enough, so that the oscillator can stay within the required specification for the necessary mission period. The last few years have witnessed exciting new strides in quartz material and resonator research which are still to be fully exploited. Improved packaging and thermal controls, plus the SC-cut technology, have shown improved performance levels in terms of power consumption and warmup. Continued research and engineering effort will be needed to transfer new technologies into the small, rugged unit which will meet the military specifications of several programs.

The rubidium oscillator provides the stabilities associated with an intrinsic atomic phenomenon. Although the optical pumping system and other aspects of the physics package limit rubidium to secondary standard status, it is essentially free from the perturbations which are common with a mechanically vibrating device. We would like to see an expanded role for rubidium as a candidate in large-quantity acquisitions. This will be possible only if the price for rubidium oscillators, even in quantity procurement, is substantially reduced from current costs for military quality units. This is possibly achievable by radical design departures from state-of-the-art technology which could reduce fabrication costs. More likely to succeed are new developments in electronic configuration and physics package design which can lead to savings in the manufacturing process. Size reductions in the physics package will lead to smaller power requirements for maintaining operating temperatures: - an important factor since steady-state power requirements under temperate conditions for rubidium oscillators are five to ten times

greater than those of precision quartz oscillators. Improvements in manufacturing technology must be seriously considered as a viable avenue to substantial reductions in unit costs in large-quantity procurements.

There are now commercially available at least four, rugged, portable cesium clocks which could meet at least some of the requirements of systems needing timekeeping accuracy associated with primary standards. Given the complexity of the beam-tube design and the necessary electronics to provide a standard frequency, these devices are outstanding engineering achievements today. As with rubidium, a major driving force for broader use of cesium standards is the price factor. As demand for cesium stability becomes documented, it is in the examination and improvement of the manufacturing process where we seek the cost reductions that will permit expanded use of cesium clocks with the benefits of system performance inherent to cesium technology.

PROGRAMS

As part of this paper, we include a brief summary of program efforts conducted by the Signal Processing and Timing Devices group at RADC. The laboratory's involvement in this field began in the mid-1960's with fundamental solid state physics research programs in radiation-induced changes in the structure and properties of quartz. By the mid-1970's, RADC had been assigned as an Air Force Systems Command laboratory dedicated to support of the mission of the Electronic Systems Division (ESD). As C³I became the principal focus of the ESD program offices, it was natural that RADC take advantage of past work in quartz material research to assume an active role in quartz oscillator R&D. As the needs of system program offices diversified, the RADC activity extended into R&D on many aspects of quartz oscillators and atomic frequency standards. In 1977, RADC was designated as the lead laboratory for Air Force R&D in PTTI technology.

RADC now operates research, exploratory development, and advanced development programs both in-house and via contracts with industry, university and non-profit organizations. The in-house activity includes sophisticated research autoclave systems for quartz material improvement through advanced, closely-controlled growth processes. Complete facilities for characterization of quartz material and resonator evaluation are coupled with contract programs for material and resonator development. Advanced

quartz oscillator technology is supported at all levels from research to the development of hardware responding to specific system needs.

RADC has active programs in hydrogen, rubidium and cesium technology. Atomic clocks for use by the 616A and SEEK TALK programs are presently under development, as well as a program for fabrication of a prototype small hydrogen maser for master-station timekeeping applications. A joint in-house/NBS/University effort is evaluating several new approaches to the use of optical pumping techniques in cesium, rubidium and other potential atomic standards.

RADC operates a Frequency-Time Test Facility (FTTF) equipped to evaluate oscillator performance at standard atmosphere conditions, and at extremes of Mil-Spec parameters of temperature, humidity and aircraft altitudes. Measurements can also be made under Mil-Spec conditions of vibration and in a comprehensive radiation test facility which forms part of the RADC Solid State Sciences Division. The FTTF is being used to evaluate and qualify oscillators for several program offices and is considered an R&D test facility for Air Force-wide needs in time and frequency hardware.

The Electromagnetic Sciences Division of RADC includes a diversified program for research and development on SAW correlators/convolvers for signal processing applications and research efforts on high frequency oscillators.

AREAS OF COMMON INTEREST

In this section we address several issues which affect the ability of the Air Force to carry out the acquisition of system hardware in a timely and efficient manner. Several of these issues play a significant role in the capability of industry to respond rapidly to Air Force needs.

Program continuity is of primary importance in establishing a smooth flow of technology from the early R&D stages, through the development model sequence, to final production. Abrupt changes in fund flows, particularly at high levels in the appropriation chain, cause disruption in the work flow and interfere seriously with our ability to meet the milestones scheduled at program inception. We acknowledge that we do not have the overall view of the priorities which is available to higher organizational levels, but unexpected shifts in program support lead to deferred activity and diminished regard for program

importance. In some cases, we can blame ourselves for our inability to provide decision-makers with adequate information to allow intelligent conclusions based on complete data. Such events often lead to program deferrals and perturbations in the industrial process from which recovery is difficult and slow. It is incumbent on planners within the Government structure to ensure that adequate, significant program documentation is available both for intelligent review and to facilitate the decision-making process.

The Air Force Systems Command does not usually advocate forward-financing activity. That is, funds which are budgeted for FY80 cannot be expended in FY81. Although this is strong motivation to operate a fiscally responsive program, an unavoidable consequence is the pressure to utilize authorized funds in a rush at fiscal year end. The situation is caused frequently by the unavailability of funds for expenditure until well into the fiscal year. Even when budgeted funds are on time, the procurement process for an R&D contract can take from three to six months with the same result. The situation is frustrating to the government agency, causes serious fluctuations in flow of funds to contractual efforts, and leads to public misrepresentations in the press of what is actually taking place.

Air Force managers are keenly aware of the forces of supply and demand in the marketplace and the cost/performance benefits resulting from competition among suppliers. That is one of the reasons for multiple source development programs. HQ AFSC has exerted heavy pressure to promote competitive contracting and the fostering of multiple-sources for needed equipment. The rationale is not only to assure that more than one vendor is capable of supplying the hardware, but this policy also promotes efficiency and tight program control in the industrial community. The end result is generally a superior acquisition program for the funds expended.

The higher technology of modern C³I systems usually means higher costs per unit deployed. The impending proliferation of timing systems has been noted at the level of the Secretary of the Air Force as well as in the R&D laboratories and the acquisition divisions. RADC is involved in an attempt to consolidate program office requirements so that one or two standardized oscillators of each technology type can be used with only slight modification for a number of different programs. This activity has been stimulated by the USIS program office and participating

with RADC in this effort are the Aerospace Guidance and Metrology Center (AGMC), ERADCOM, several Navy organizations and various military program offices. We consider that an aircraft with three different systems requiring PTTI service will have higher reliability at lower costs if all the oscillators are interchangeable rather than if three independent, incompatible units are used. For those programs where many thousands of oscillators will be required, large savings can be realized by adherence to a commonality principle, and by applying extensive engineering activity to developing some entirely new and cost-efficient manufacturing processes as suggested earlier.

Finally, the US policy of government-industry-university relationships has worked somewhat adversely in the United States for certain technology areas. We consider that PTTI activity is one such area. European and far Eastern governments finance the entire birth and development of high-technology entities which finally mature enough to become stand-alone corporations in the private sector. Similarly, foreign governments have taken an active role in the sponsorship of their national academic programs and institutions devoted to precise time R&D. Such academic support provides a small but steady flow of highly-trained professionals who can enter government or industry laboratories and produce meaningful results without an extensive and time-consuming period of on-the-job training. We believe that the trend of frequency/time technology will require a formalized government effort to meet projected manpower needs efficiently. RADC, as part of its PTTI activity, is exploring the desirability and feasibility of establishing small but significant formal training programs for time and frequency R&D within the academic environment.

In closing, it is a pleasure to acknowledge helpful discussions with Lt. Col. D. Busse of ESD on the JTIDS program, with Ivan La-Garde and Gene O'Sullivan of the MITRE Corporation on the HAVE QUICK and SEEK TALK programs respectively, and with Major M. Gaydeski of ASD on the USIS program.

REFERENCES

1. D. Tennant; "Navstar Global Positioning System (GPS) Clock Program; Present and Future". 12th Annual PTTI Applications and Planning Meeting. Greenbelt, MD; December 1980.
2. Lt. Karl Kovach; Private Communication.
3. J. Sonsini; "The Joint Tactical Information System-Description of Systems Operations and Timing Requirements". 11th Annual PTTI Applications and Planning Meeting. Greenbelt, Md; November, 1979.
4. D. Neuman; "The Effects of Oscillator Characteristics on JTIDS Tactical Communication and Navigation Performance". National Bureau of Standards Workshop on Impact of Improved Clocks and Oscillators on Communications and Navigation Systems. Gaithersburg, MD; September, 1979. (To be published.)
5. Major M. Gaydeski; Private Communication.
6. I. La-Garde; Private Commuication.

NASA PTTI PROGRAMS: PRESENT AND FUTURE

Schuyler C. Wardrip

William M. Hocking

NASA-GODDARD SPACE FLIGHT CENTER

GREENBELT, MARYLAND

INTRODUCTION

With reference to Figure 1, this paper discusses the current and future PTTI programs at the Goddard Space Flight Center (GSFC) and the evolution of frequency and time requirements over past years within the various NASA satellite tracking networks. A brief history of the network development is also given.

History of the NASA Tracking Network

Today's network, called the Spaceflight Tracking and Data Network (STDN), is a global complex of tracking stations used to communicate with both the manned and scientific spacecraft. STDN is a combination of networks that have evolved (Figure 2) over the years as requirements have changed.

The first network was called Minitrack, a radio interferometry system which became operational in 1957 (Figure 3). Minitrack originally consisted of eleven stations forming a radio fence in the north-south direction. Stations in the network were added and deleted as the space program fluctuated. Some sites are part of the present network. The first internationally agreed to satellite transmitting frequency was 108 MHz which was changed to 136 MHz in 1960. This new frequency was assigned by the International Telecommunications Union for the purpose of space research, a recognition of the rapid growth of the aerospace technology. The basic function to be performed by the Minitrack system was to collect tracking data for satellite orbit determination. A second function and one which grew more important with time was to receive and record the spacecraft telemetry data, which was then sent back to the Vanguard Data Reduction Center in Washington, D.C.

Sputnik I was launched on October 4, 1957 transmitting on a "surprise" frequency of 40 MHz. Quick modifications were made to Minitrack and, in less than 24 hours, tracking data from Sputnik I were being sent to Washington, D.C. for analysis.

During the 1958-1962 period several Minitrack sites were closed and several others were established. The Minitrack Network grew in capacity and complexity and in 1967, Minitrack evolved into the Station Tracking and Data Acquisition Network (STADAN)(Figure 4). Stations in Alaska, Newfoundland and England were added to improve geographical coverage and to add a new support capability for tracking satellites in polar orbit.

Early in 1959, the major ground-rules for the man in space Mercury Project were established. An orbital inclination of 32.5 degrees became firm. The Atlantic Missile Range would be utilized for launch and recovery. The tracking network would be worldwide (Figure 5) and operate in as near real-time as communications technology would permit.

The building of the Mercury Network was an enormous task requiring government, military and industry working together. The Network became operational on June 1, 1961, ready for the first man in space launch which occurred on February 20, 1962.

There was little change in the Mercury Network for the Gemini Network (Figure 6) which became operational in 1964.

The Apollo Network or Manned Spaceflight Network (MSFN) became operational in 1967 and was developed separately from the Mercury-Gemini Network (Figure 7). The early Mercury-Gemini sites used separate systems for tracking, command, and communications. The Apollo Network combined these three functions by using the Unified S-Band (USB) system which employed 26-meter and 9-meter antenna systems. The more significant parts of the USB system were the range and range rate equipment supplied by the Jet Propulsion Laboratory and the antenna systems which were nearly identical to those used in

the STADAN. Like STADAN, the MSFN tended toward site consolidation with fewer, better instrumented, primary sites handling the complete mission support. Analog techniques gave way to digital techniques, and mission control was centralized with the field stations acting as data collection and relay points.

Finally, today's Network (Figure 8), the Spaceflight Tracking and Data Network (STDN) is a combined Network made up of the former Manned Space Flight Network (MSFN) and the former Station Tracking and Data Acquisition Network (STADAN). Administratively, this coming together was done in 1971; operationally, the merging took place over a period of several years.

During the 1970's, most of the STDN tracking facilities were fixed land sites. However, tracking ships have been used to give special support such as orbit-insertion and re-entry for the manned missions. Apollo Range Instrumentation Aircraft (ARIA), operated for NASA by the Air Force, were part of the Apollo support and later a part of the STDN supporting SKYLAB, Apollo-Soyuz, and a variety of scientific missions.

In staying abreast of the tracking technology, STDN uses a standardized data handling system to aid the NASA Communications System (NASCOM) function of efficiently transferring data from the tracking sites to Goddard Space Flight Center. Increased command and telemetry functions have necessitated the use of small on-site computer systems. Also, the STDN has had to move to higher frequencies to accommodate the greater volume of data produced by today's sophisticated spacecraft.

The Network of the 1980's will be the Tracking Data Relay Satellite System (TDRSS), the result of a conceptual study which started in 1966. In support of TDRSS a contract has been awarded to provide 50 MBS data service from the TDRSS White Sands, New Mexico ground terminal to GSFC and to Johnson Space Center, Houston, Texas. The service will use a domestic satellite system and existing earth stations to provide either 50 MBS, 4.2 MHz analog data, or television services on a switchable basis.

Chronology of Time and Frequency Requirements

Throughout all the Network growth, changes, and mergers precise time requirements have increased from tens of milliseconds to sub-microseconds. Frequency stabilities have improved from parts in ten to the eighth (1×10^{-8}) to parts in ten to fifteen (1×10^{-15}).

Figure 9 shows a chronology of precision frequency and time requirements from the late 1950's to the present and on into the year 2000, and the techniques used to achieve the needs, and some of the projects that were and will be supported over this time span.

During the Vanguard and early Mercury flights NASA relied on HF time transmissions from WWV and WWVH for millisecond timing. Figure 10 shows the first timing system that was installed in the Minitrack Network, Vantage 1958. This system was built at the Naval Research Laboratory and used a quartz crystal oscillator to develop various pulse rates and sine waves. HF receivers were used for time synchronization to within several milliseconds.

During the early to mid 1960's NASA depended on VLF phase tracking techniques to monitor the performance of station crystal clocks. This, along with HF time transmissions improved time keeping capability by about an order of magnitude to within 500 microseconds; with frequency stabilities of one part in ten to the ninth (1×10^{-9}).

Figure 11 is a picture of the second generation timing system that was installed in the Network in 1961. The systems used basically the same instrumentation as the first system. Note the Hermes Model 101 quartz crystal oscillator.

From 1966 through 1968 NASA conducted world wide time synchronization experiments using the Loran-C Navigation System and Loran-C timing receivers developed for NASA. A Loran-C capability was implemented in the Network during 1968 and 1969.

Between 1965 and 1967 the two rack timing systems in both Networks (STADAN and MSFN) were replaced with sophisticated "fail safe," redundant timing systems which used the latest state-of-the-art electronics in the frequency and time generation and distribution systems. These same systems are still in use today with the STDN. In the mid to late 1960's the crystal clocks were replaced with rubidium gas cell frequency standards, improving frequency stabilities to parts in ten to the tenth (1×10^{-10}).

Present Network Timing Systems

As a consequence of the two Network merger, the MSFN and the STADAN in 1971, the present Network (STDN) has several different timing systems and sub-systems. The two prime systems are the Collins TE-411 timing systems which are at the former MSFN sites and the Astrodats 6600 timing systems which are in the former STADAN sites. Both of these systems have been modified and updated numerous times over the past ten years to keep pace with frequency and time requirements.

The TE-411 system shown in Figure 12 provides a wide spectrum of sine waves, pulse rates and NASA/IRIG serial and parallel time codes. The frequency signals for the time systems are provided by the Precision Frequency Source (PFS) rack shown on the left in Figure 12 and utilizes three frequency standards with a high performance cesium as the on-line standard and rubidium and crystal standards as secondary. Some systems have two cesium standards with a crystal backup. Automatic switchover to a backup standard is accomplished if loss of amplitude or out-of-lock failure occurs in the primary standard. In addition, the frequency and phase of the backup standards are controlled by the master standard.

A dual 5 MHz output from the frequency combiner drives the PFS distribution amplifiers which provide outputs to the timing system at 5 MHz, 1 MHz and 100 KHz. All outputs are metered and monitored and are individually amplitude adjusted. The PFS unit has a minimum of 10 hours of battery backup in the event of a power failure. A recent addition to the timing system provides triple redundancy and majority logic to the clock generation unit.

Time synchronization is accomplished via HF, Loran-C, and portable clocks. The STDN worldwide Network is presently maintained to within 25 microseconds of the Naval Observatory Master Clock. However, stations are typically within 5 microseconds and selected sites are within 1 microsecond.

The former STADAN sites have triple redundant Astrodata 6600 timing system shown in Figure 13. The systems presently use one cesium beam frequency standard with either an additional cesium or crystal as secondary. The 1 MHz from each standard is monitored for both amplitude failure and phase difference. If the master standard fails the backup is automatically switched on-line. The master oscillator drives each of three timing units A, B, and C, the outputs of which are intercompared in majority logic, error detection circuits. Error lights indicate which standard has failed and which of the three clocks (A, B, and C) are in error and where. The systems use WWV, Loran-C and portable clocks to maintain microsecond time. Television is also used for time sync where available such as at GSFC, Hawaii and Guam.

During 1965-1967 NASA began to use crystal rubidium portable clocks to periodically calibrate the remote station clocks to within several hundred microseconds. Figure 14 shows an early Sulzer, Portable Crystal Clock. In 1968 the crystal and rubidium portable clocks were replaced with Hewlett Packard (HP) cesium beam portable clocks shown in Figure 15, thus permitting remote clock calibration to within microseconds depending on the duration of the clock trip. NASA now uses lightweight portable clocks one of which is shown in Figure 16.

Future Considerations

Future requirements for frequency and phase stability, pulse jitter and site-to-site time synchronization cannot be met with the present STDN timing systems. Recognizing this, design concepts were finalized in 1978 for a fourth generation timing system to be installed in the Network during the early 1980's in support of the GSFC Tracking and Data Relay Satellite System (TDRSS) and the NASA/JPL Consolidated Network.

Shown in Figure 17 is the new TRAK Model 8407 timing system which was designed and built to NASA specifications. This system is installed and operating at the TDRSS NASA ground terminal located at White Sands, New Mexico. The system is designed to be driven from a frequency combiner/selector with controlled 5 MHz outputs.

The purpose of the Frequency Combiner/Selector (FCS) is to provide the White Sands NASA Ground Terminal timing system with a reliable and precise source of 5 MHz. The FCS achieves reliability by using more than one precision frequency source of 5 MHz. It uses 5 MHz from two cesium standards and one from a remote source. In the normal mode, one cesium standard is selected to drive all the FCS outputs. If the FCS detects a failure in that cesium, the FCS switches all its outputs to a back up input. If the FCS detects failures in both cesium standards, the FCS will switch all its outputs to the remote 5 MHz input (input 3). The main characteristics of the White Sands timing system are as follows:

1. Fully redundant
2. Highly reliable
3. NASA-quality construction
4. Sub-microsecond precision
5. Built-in fault isolation
6. Minimum down-time
7. Multiple code and rate outputs

The basic timing system (Figure 18) contains three separate and identical time code generators which produce parallel and serial time codes with resolution and coherences of 50 to 200 nanoseconds. The outputs from the

three generators are combined in majority voters, assuring that system outputs are maintained if one or two generators fail. A distribution system provides multiple buffered outputs of the generated time codes and pulse rates. A failure sensing subsystem isolates failures to the card level. Individual power supplies are provided for each time code generator and the power supply outputs are ORed for majority voting and fault sensing circuit power.

The three time code generators accumulate time via the external 5 MHz input and distribute serial and parallel time codes and rates to the majority voters and fault sensing logic. The voted outputs from the majority voters are buffered in three types of signal distribution assemblies.

The fault sense logic isolates failures to the card level. Failure indicators are located on a control status panel. This panel also contains switches for selecting generator A, B, C or voted outputs for distribution and for output monitoring on the panel.

Millisecond time is maintained via HF receivers and sub-microsecond time is maintained via Loran-C receivers and the Tracking Data Relay Satellite (TDRSS) Time Transfer Unit (TTU). Portable clocks are also used for periodic calibration to sub-microseconds. The Global Positioning System (GPS) will also be used when it becomes operational.

Figure 19 is a block diagram of the system that will be installed in the NASA/JPL Consolidated Network sites at Madrid, Goldstone, and Canberra in the early to mid 1980's. The basic timing system on the right will be supplied by Goddard and the frequency generation source will be supplied by JPL.

Satellite Time Transfer Techniques

In the late 1960's and early 1970's NASA personnel experimented with the use of satellites for time transfer. This included the use of GEOS and ATS spacecraft. During 1973-1975 NASA conducted two-way time transfer experi-

ments using the synchronous ATS-1 satellite. This technique proved accurate to better than a microsecond between widely separated clocks. In 1974 NASA in cooperation with the Naval Research Laboratory developed timing receivers for use with the Navigation Technology Satellites (NTS). Experiments achieved less than 500 nanoseconds worldwide. In 1976 GSFC initiated studies to look at the use of the Global Positioning System (GPS) and the Tracking Data Relay Satellite System (TDRSS) for sub-microsecond timing. As a consequence of these two studies GSFC is looking to the use of both TDRSS and GPS for timing (Figure 20).

Time Synchronization Via TDRSS

Data communication via the Tracking and Data Relay Satellites is to become available to users in the 1980's. The ranging and data services provided by the Tracking and Data Relay Satellite System are to be an integral part of NASA's post-1980 Spaceflight Tracking and Data Network.

The TDRSS system will consist of two geostationary relay satellites 130 degrees apart in longitude (Figure 21) and a ground terminal at White Sands, New Mexico. The system will also include two spare satellites, one in orbit and one ready to be launched. A real-time bent-pipe concept is used in the operation of TDRSS.

Time transfer communication between the TDRSS ground station at White Sands and GSFC will be in a Multiple Access service standard mode of operation. This mode uses a combination of pseudorandom (PRN) codes and data modulation for ranging and telemetry. The capability of simultaneous ranging and data communication is directly applicable to time transfer. Ranging is accomplished by synchronized forward and return link PRN codes in a "round trip" or "two way" ranging mode (TDRSS mode 1). Forward and return telemetry data are modulated onto the respective codes allowing simultaneous two-way data transfer. The PRN code "epoch" signals or all ones "state indicators" serve as event markers for time transfer. Signal margins are such that these markers will be quite stable and code acquisition time relatively short.

To transfer time via TDRSS, the time interval between a specific event marker and the master station clock's 1 pps is measured. A similar time interval is measured by the user as his transponder receives the PRN code and, hence, event markers. The time interval measurements and other information (time of day in hours, minutes and seconds) are exchanged between master and user by forward and return telemetry. The master site makes a second time interval measurement on the return telemetry to allow estimation of the forward path delay time. A number of relatively simple calculations, using the time interval measurement data, are required for each clock error estimate. A clock error estimate would be obtained once per second. The data processing or "smoothing" would be based on a linear model of the movement of TDRSS and utilize a data span of several minutes. Microprocessor hardware/software is well suited to the synchronization and computational requirements. An important and desirable feature about TDRSS is that for time transfer, the master and user designations are interchangeable. The error in the clock difference measurement is expected to be less than 40 nanoseconds and to be available once each second. The total elapsed time required to complete a time transfer should be less than 5 minutes.

Also shown in Figure 21 is the NASA/JPL Consolidated Network of the mid 1980's and will consist of sites at Madrid, Goldstone and Canberra. All other Network sites within the present STDN are expected to be phased out over a period of years.

Time Transfer via GPS

In order to make use of the highly accurate laser ranging data, it is necessary to time tag the data from the laser stations very accurately. In applications where the data from two or more stations will be merged to determine baselines for geodetic work, polar motion determinations, etc., it is necessary that the clocks at the several stations be synchronized to within ± 1 microsecond with respect to a master clock such as that of the Naval Observatory (USNO).

GPS time transfer receivers are being developed jointly by GSFC and NRL. GSFC will use the GPS timing receivers in the Laser Ranging Network which consists of eight mobile vans and permanent installation at GSFC. The Laser Network is separate from the STDN although there may be colocations.

A typical mobile laser van installation is shown in Figure 22. Figure 23 shows an installation at Kwajalein along with the range safety radar system, and Figure 24 shows a laser system at American Samoa. Over the next several years the laser timing systems will be updated and GPS receivers installed.

Use of Shuttle for Timing

There are plans in the formative stage for a Shuttle-based laser ranging system which would transmit pulses to several hundred passive ground based targets located at points of interest. The Shuttle laser system would receive the returned reflected pulses from the various ground targets and use this information to define the Shuttle orbit in real-time, and by using trilateration, to measure the relative position of selected ground targets (Figure 25).

This technique is ideal for transferring time. A ground timing terminal may look like what is shown in Figure 26 and consists of a retroreflector, a constant fraction discriminator, an event clock and a microprocessor data recorder and analyzer.

SIRIO/LASSO Time Transfer Experiment

Other future activities include joint participation by GSFC with the USNO and NRL in the ESA SIRIO/LASSO time transfer experiment during 1981 and 1982. With reference to Figure 27, the missions of SIRIO-2 are twofold; meteorological data dissemination and synchronization of intercontinental atomic clocks.

The aim of the LASSO experiment is to provide a repeatable, near-real-time method for long-distance (intercontinental) clock synchronization with nanosecond accuracy at a reasonable cost. The pioneering aspects of this first experiment will provide the opportunity to compare the international network of atomic clocks with the internationally adopted atomic time scale (TAI) and with each other. It will also have an impact on such practical applications as the tracking of deep space missions, the calibration of other time transfer techniques such as Very Long Baseline Interferometry (VLBI), Tracking Data Relay Satellite System (TDRSS), and the Global Positioning System (GPS), and future generations of space navigation and telecommunication systems.

SIRIO-2 will be launched during October of 1981 from Kourou, French Guiana in South America into synchronous orbit at 25 degrees west longitude which is just off the West Coast of Central Africa near Liberia. The satellite, which has a 2-year lifetime design, will remain in this position for about 9 months to permit time measurements between the United States (Goddard Space Flight Center referenced to the Naval Observatory) and major observatories and time keeping facilities in Europe--principally with the Bureau International de l'Heure (BIH) in Paris, France. SIRIO-2 will then be moved over Central Africa at 20 degrees east longitude and will remain there for meteorological data dissemination until the completion of its 2-year mission. See Figure 28.

S/C Characteristics

The LASSO experiment is based on the use of laser ground stations firing monochromatic light pulses at predicted times directed toward the geosynchronous SIRIO spacecraft.

SIRIO-2 is a Spin-stabilized geostationary satellite spun around an axis vertical to its orbital plane. The spacecraft consists of a drum-shaped central body covered with solar cells. On top is mounted a mechanically

despun S-Band (1689.6 MHz) antenna for support of the meteorological and timing missions and housekeeping data. Omnidirectional antennas (VHF 136.14 MHz) serve for command, ranging and backup telemetry (Figure 29).

The LASSO payload is composed of retroreflectors, photodetectors for sensing ruby and neodyme laser pulses and a stable clock for time tagging arrival times of laser pulses.

LASSO Experiment Goals

The goals of the LASSO experiment are as follows:

1. To verify that lasers can be used to perform a two-way time transfer from a geostationary satellite to within nanoseconds or sub-nanoseconds.
2. To determine the limitations and problems of such a laser time transfer technique.
3. To verify the accuracy of other techniques such as the Global Positioning System (GPS) time transfer technique using receivers being developed for use in the Mobile Laser Network.

Description of the GSFC Laser Ranging Systems for LASSO

The GSFC laser satellite ranging system to be used for the LASSO time transfer experiment is an adaption of the laser ranging system presently used for tests and evaluation of advanced laser ranging technologies and components. There are three major systems incorporated in the system (Figure 30): the general purpose tracking telescope, the laser transmitter, and the range timing and data recording system.

The tracking telescope is a 1.2 meter aperture, F/30 Azimuth-Elevation Coudé system, controlled by a general purpose computer system. The system has a servo pointing accuracy better than 0.4 arcseconds and an open loop pointing accuracy relative to the input prediction data of better than 1.5 arcseconds. The Coudé input/outputs of the telescope is directed via a turning mirror and negative matching lens to the laser ranging system located in a clean room 15 meters from the base of the telescope.

The laser transmitter is a cw mode-locked Nd:YAG system incorporating a regenerative amplifier and three single pass amplifiers. The transmitter operates at up to 5 pulses per second with a pulse energy of 0.25 joules in less than 200 picoseconds at a wavelength of 0.53 microns. The output beam divergence is less than two times the diffraction limit. The output of the laser is coupled to the telescope through a transmit/receive switch and expanding optics. The incoming signal from the telescope is directed to the detector with a solenoid activated flip mirror and passes through conditioning optics and a narrow bandpass prediction filter. A constant fraction discriminator with a threshold of one photoelectron converts the photomultiplier detector signal to the appropriate timing signal for measurement.

The range timing system consists of a computer, multi-event range timing unit, real-time clock, and an epic timing unit. The computer controls in real-time (via inputs from the real-time clock) the operation of the laser, range gate generator, epic timer, multi-event range times, visual display unit, and data recording from each element of the ranging system.

History of Hydrogen Maser Program

Since 1961 GSFC has had a program to develop and test field operable hydrogen maser frequency and time standards. After the successful results with an experimental maser (NX-1) in 1967, the NASA Prototype or NP series of masers were developed between 1969 and 1971 providing frequency stabilities of parts in (1×10^{-14}) (Figure 31).

The four NP hydrogen masers continue to be the backbone of our frequency standard support. These masers have compiled impressive records in the field. They have accumulated a total of over 35 years of field operation and have traveled nearly 200,000 miles to 40 separate installations in support of various VLBI programs in the geodetic and astronomical work, star mapping, relativity experiments, and time transfer experiments with various worldwide observatories and laboratories.

Presently the program is directed toward the development of a new series of field operable hydrogen masers, the NASA Research, or NR series, in conjunction with the Applied Physics Laboratory. These masers, based on two new experimental masers developed at GSFC, will provide parts in ten to the fifteenth (1×10^{-15}) frequency stability for future NASA requirements.

Over the next 4 years GSFC expects to construct 3 to 4 NR masers per year for a total of about 14.

By 1985, GSFC expects to have a total of 19 to 20 masers for support of NASA programs such as the Crustal Dynamics Program.

The program is also developing primary frequency standards with parts in ten to the fourteenth (1×10^{-14}) accuracy to calibrate and improve the field operable masers. Two novel masers, the Concertina Maser and the External Bulb Zero Wall Shift Maser are being developed.

Based on discoveries made with the Concertina Maser and those at Williams College under a NASA grant, a new experimental field operable hydrogen maser with a line Q approaching ten to the tenth (1×10^{10}) is being developed. This is a factor of 3 greater than the line Q of the NR and NX masers. These masers promise to achieve parts in ten to the sixteenth (1×10^{-16}) frequency stability.

To compliment the work on improved frequency standards, an improved frequency distribution and measurement system has been developed. A modular approach was used based on the CAMAC interface standard. This allows one to combine the various modules being developed into systems tailored for various uses. This modular system is used for the frequency distribution system (frequency combiner/selector) in the next generation of Network Timing Systems and for the measurement and distribution system for the new Frequency Standards and Test Facility.

In the near future, this Frequency Standards and Test Facility will provide the frequency standards program with a controlled undisturbed environment. This will enable long term measurements to be made on the NX and NR hydrogen masers which were previously impossible. Measurements will also be made on the temperature, pressure, and magnetic field sensitivities of the NX and NR masers as well as the frequency stabilities of these masers under various conditions.

The Concertina Maser, and eventually the External Bulb Maser will be used to study the effects of the wall shift on field operable maser stability. After the two new experimental masers are constructed and operating, these tests will be repeated on them to determine their performance and to document their hoped for parts in ten to the sixteenth (1×10^{-16}) frequency stability.

Summary

In summary, Figure 32 shows the timing techniques that have been used over the years and will be used to meet NASA Project needs. Under satellite techniques, GSFC will use TDRSS and GPS for sub-microsecond timing. GSFC will continue to use Loran-C and television for localized timing and will transport portable clocks for several years to come.

GSFC PTTI PROGRAMS

CURRENT AND FUTURE

- **TIMING PROGRAM**

HISTORICAL BACKGROUND
PRESENT TIMING SYSTEMS
NETWORK CONSOLIDATION
FUTURE CONSIDERATIONS

- **HYDROGEN MASER PROGRAM**

RESEARCH & TECHNOLOGY
PROJECT SUPPORT ACTIVITIES



Figure 1. GSFC PTTI Programs Current and Future

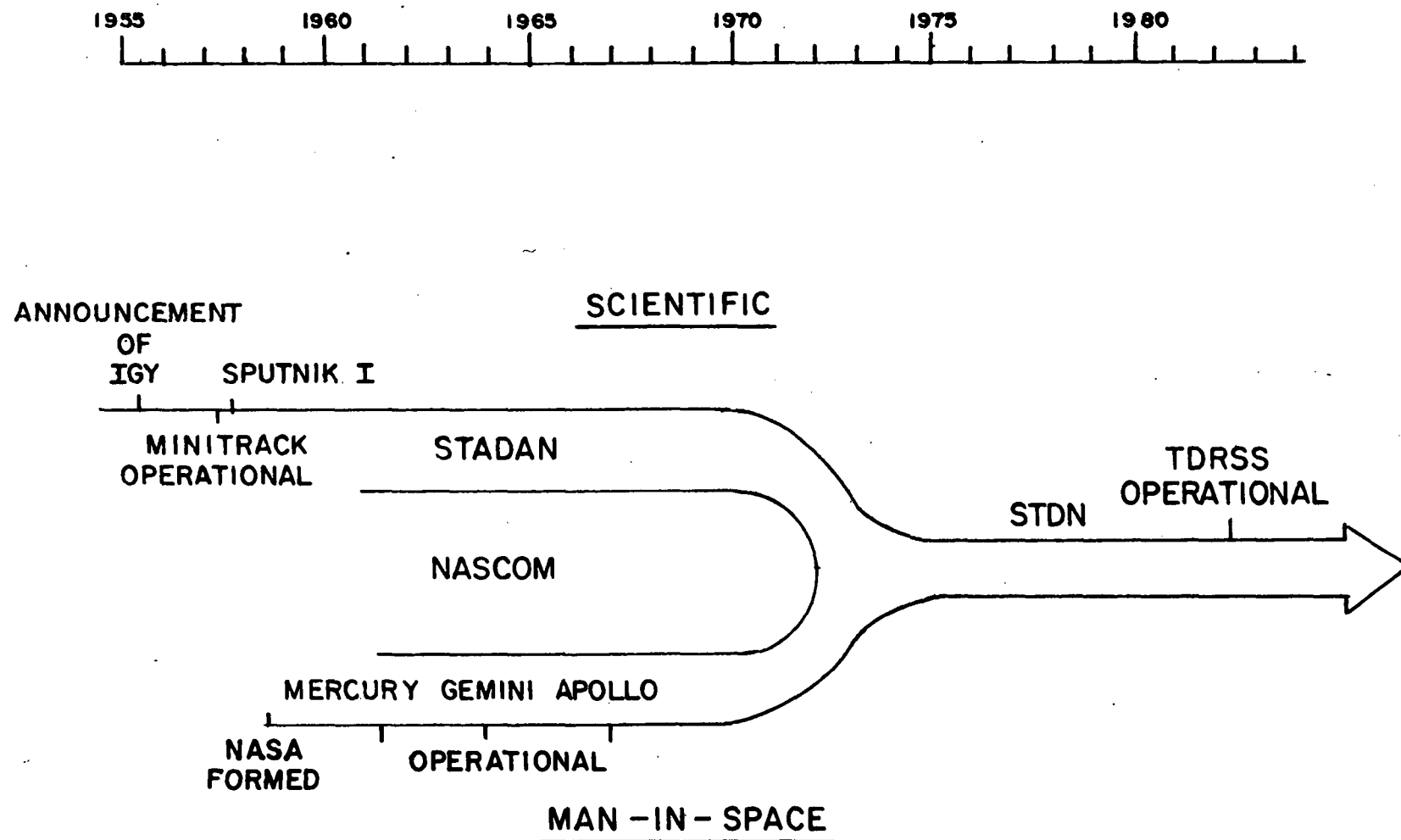


Figure 2. Evolution of the STDN Tracking and Data Acquisition Network

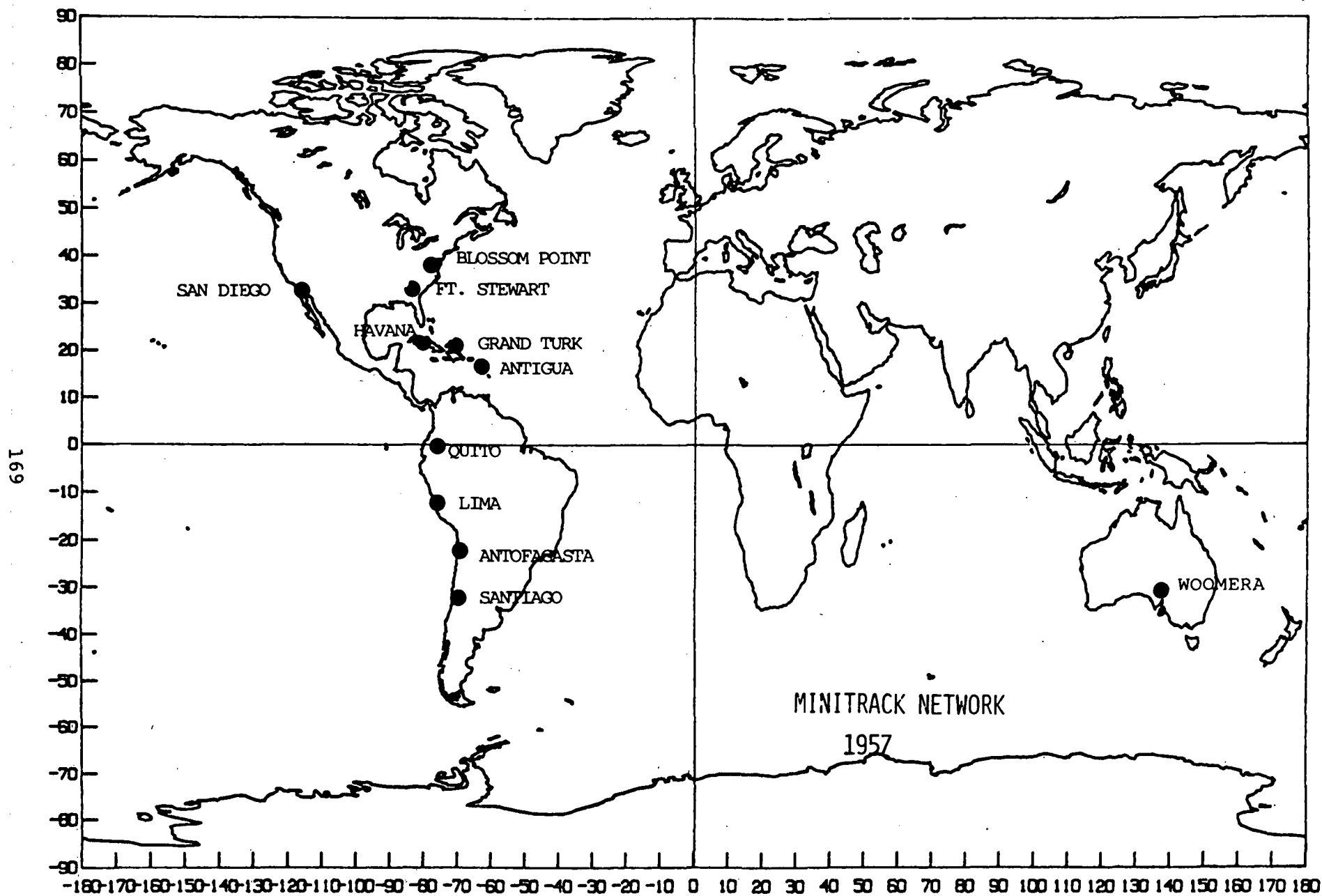


Figure 3. Minitrack Network 1957

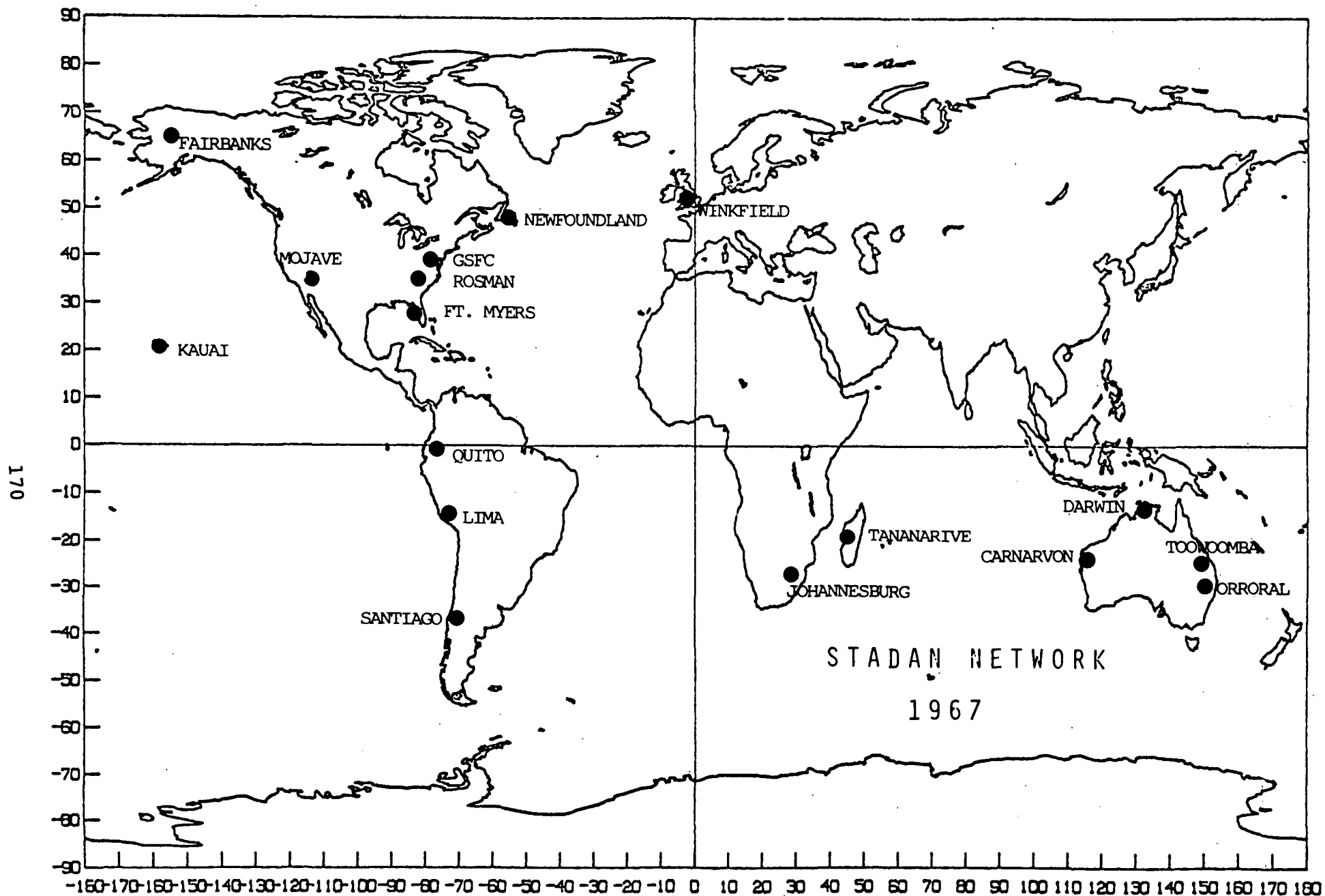


Figure 4. STADAN Network 1967

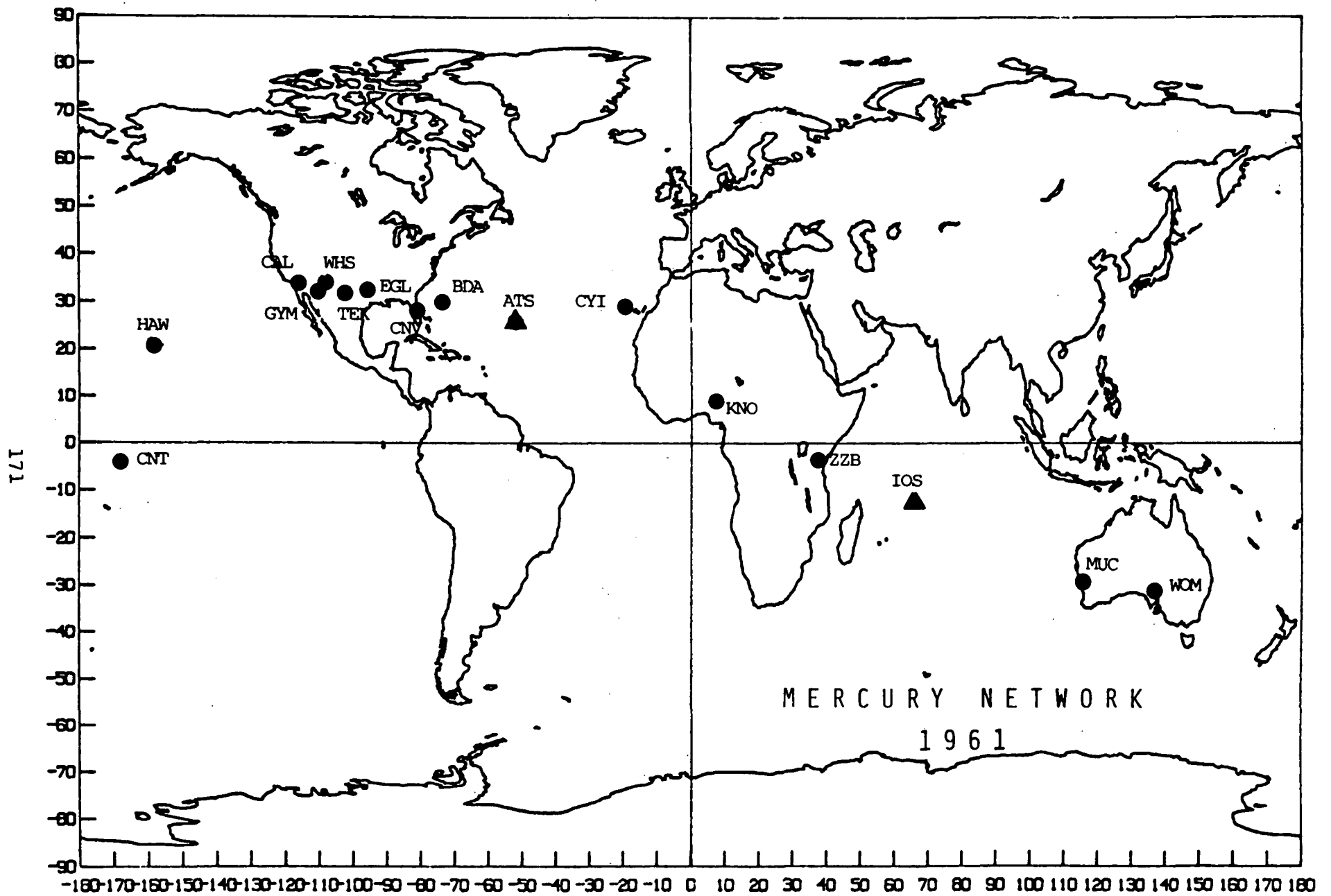


Figure 5. Mercury Network 1961

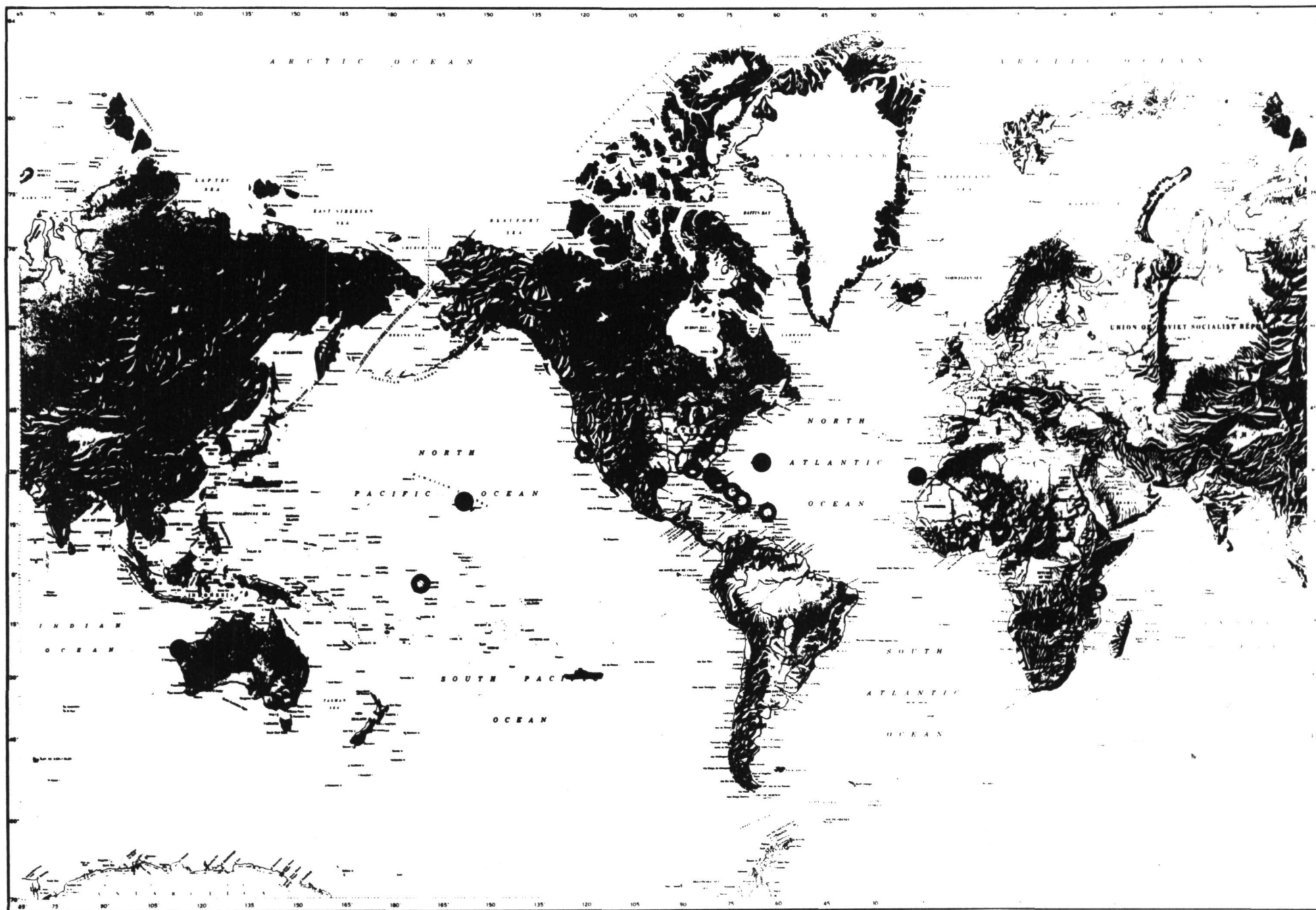


Figure 6. Gemini Network 1964

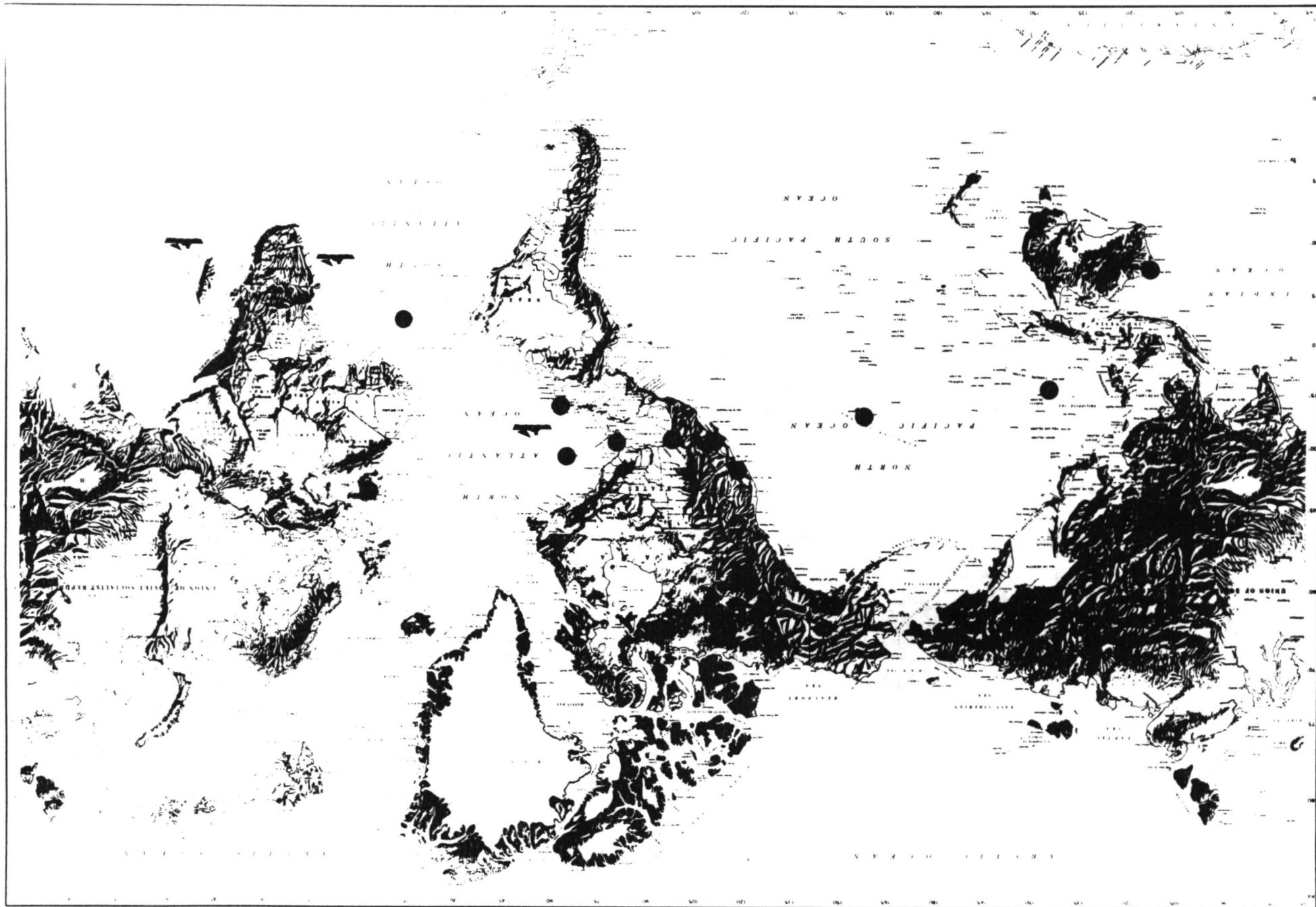


Figure 7. Apollo Network (MSFN) 1967



Figure 8. STDN Network 1978

DATE	REQUIREMENTS			TECHNIQUES	PROJECTS
	TIME SYNC	FREQUENCY STABILITY	FREQUENCY STANDARD*		
1958/61	10ms to 1ms	1×10^{-8}	XTAL	NBS, HF TIME TRANSMISSIONS (WWV & WWVH)	VANGUARD AND MERCURY
1961/63	1ms to 500 μ s	1×10^{-9}	XTAL	HF, VLF PHASE TRACKING	MERCURY, EXPLORER, OSO
1963/66	500 μ s to 100 μ s	1×10^{-10}	XTAL, Rb	HF, VLF, LORAN-C PORTABLE CLOCK (PC)	GEMINI, OGO, ATS, OAO OSO, EXPLORER, NIMBUS
1966/72	100 μ s to 50 μ s	1×10^{-11}	XTAL, Rb, Cs	VLF, LORAN-C, PC PC	APOLLO, NIMBUS, OAO, PIONEER, ATS, OSO
1972/74	50 μ s to 25 μ s	1×10^{-12}	Rb & Cs	VLF, LORAN-C, PC TELEVISION (TV) SATELLITE (ATS)	OAO, IMP, SKYLAB, RAE-B, ATS-F, SMS
1974/77	25 μ s to 1 μ s	PARTS $\times 10^{-13}$	Rb & Cs	LORAN-C, PC, TV, SATELLITE (NTS)	GEOS, ATS, ERTS, OSO, LAGEOS, SEASAT, VLBI, LASER RANGING
1977/80	1 μ s to 50ns	PART $\times 10^{-14}$	Cs & HM	LORAN-C, PC, TV, NTS	GEOS, HEAD, SEASAT, SMM, SHUTTLE, LAGEOS, VLBI, LASERS
1980/85	50ns to < 10ns	PARTS $\times 10^{-15}$	Cs, HM, Hg	TDRSS, GPS, LASER, TV, PC	TDRSS, SHUTTLE, VLBI, CRUSTAL DYNAMICS, LASER RANGING, SCIENTIFIC SATELLITES, DEEP SPACE MISSIONS
1985/2000	1 ps	PARTS $\times 10^{-16}$	ATOMIC STANDARDS		

***NOTATION**

CRYSTAL = XTAL
RUBIDIUM = Rb

CESIUM = Cs
HYDROGEN MASER = HM

MERCURY = Hg



Figure 9. Precision Frequency and Time Requirements 1958-2000

General
Description

MINITRACK
SATELLITE TRACKING UNIT

Section I
Paragraph 1.4.

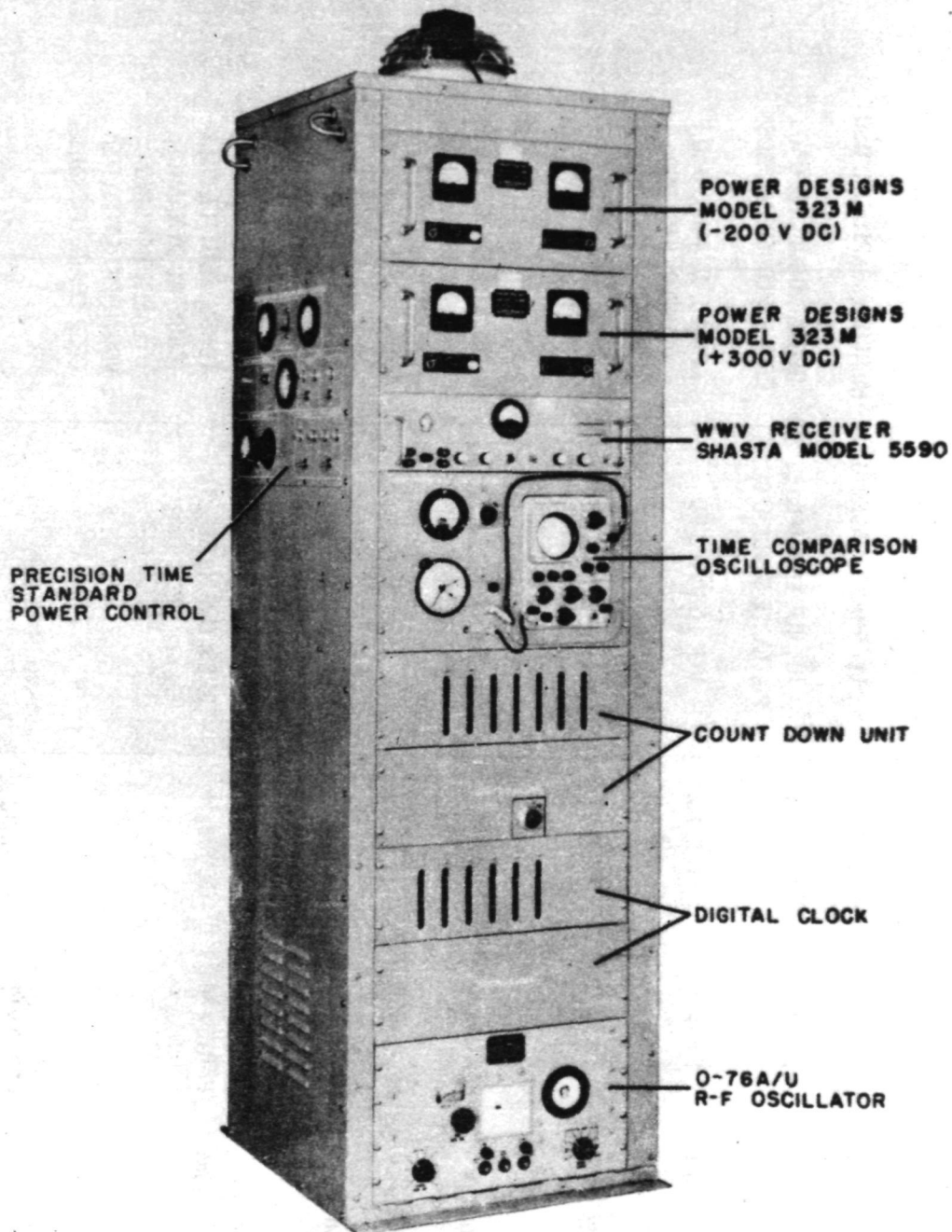


Figure 1-8. Precision Time Standard Rack, Right Oblique View

ORIGINAL

1-19

Figure 10. Minitrack Satellite Tracking Unit

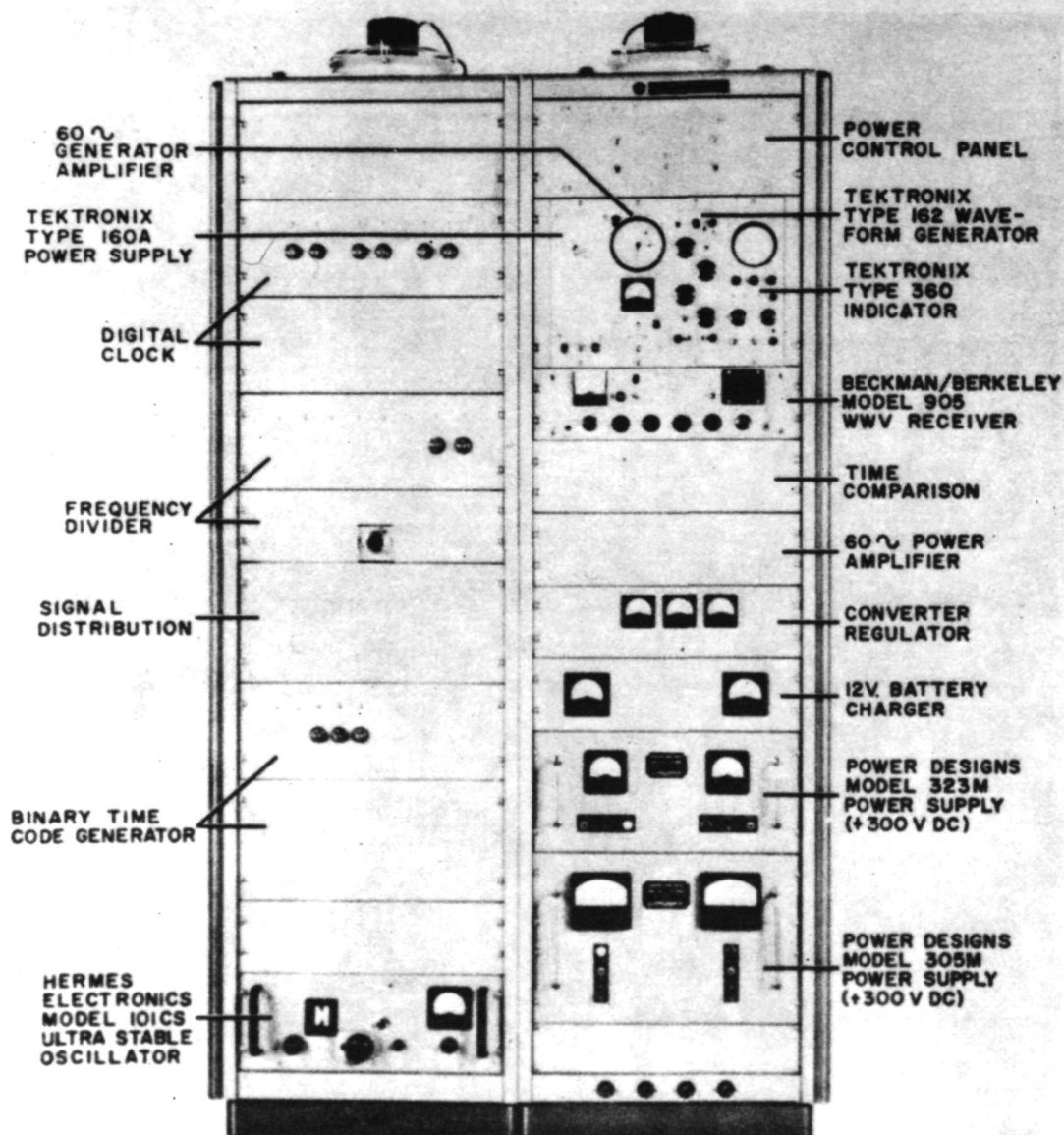


Figure 1-6. Time Standard Rack

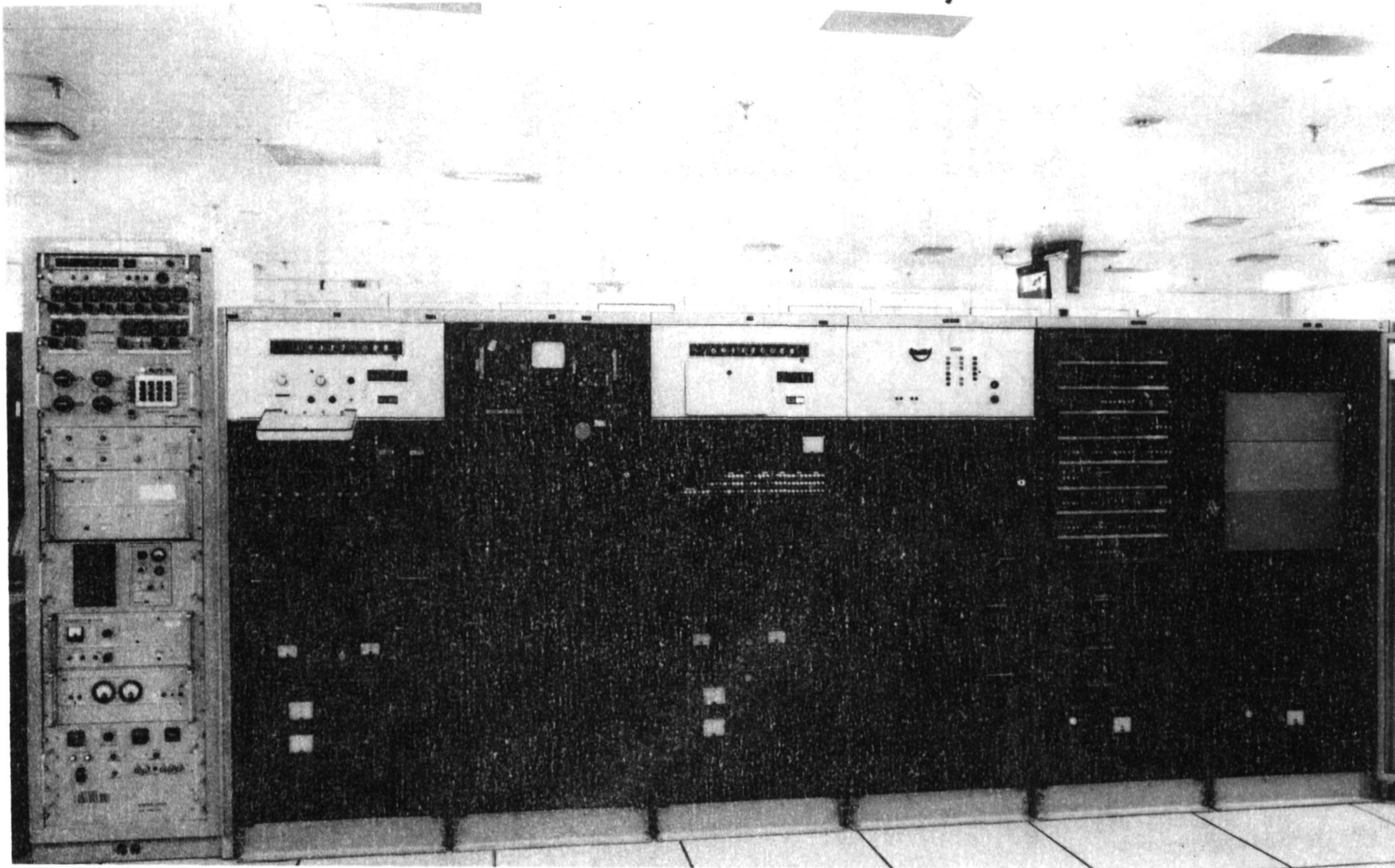


Figure 12. TE-411 System

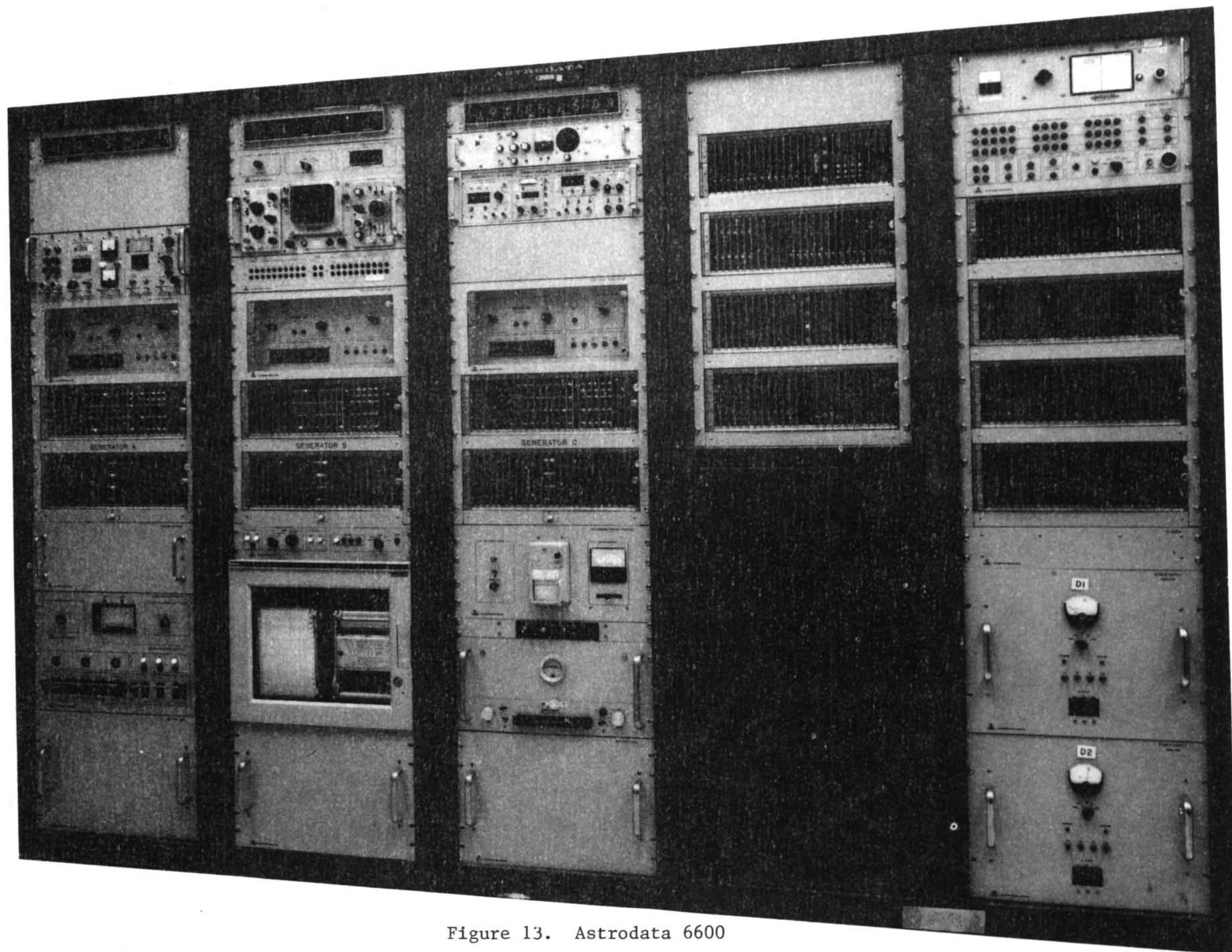


Figure 13. Astrodata 6600

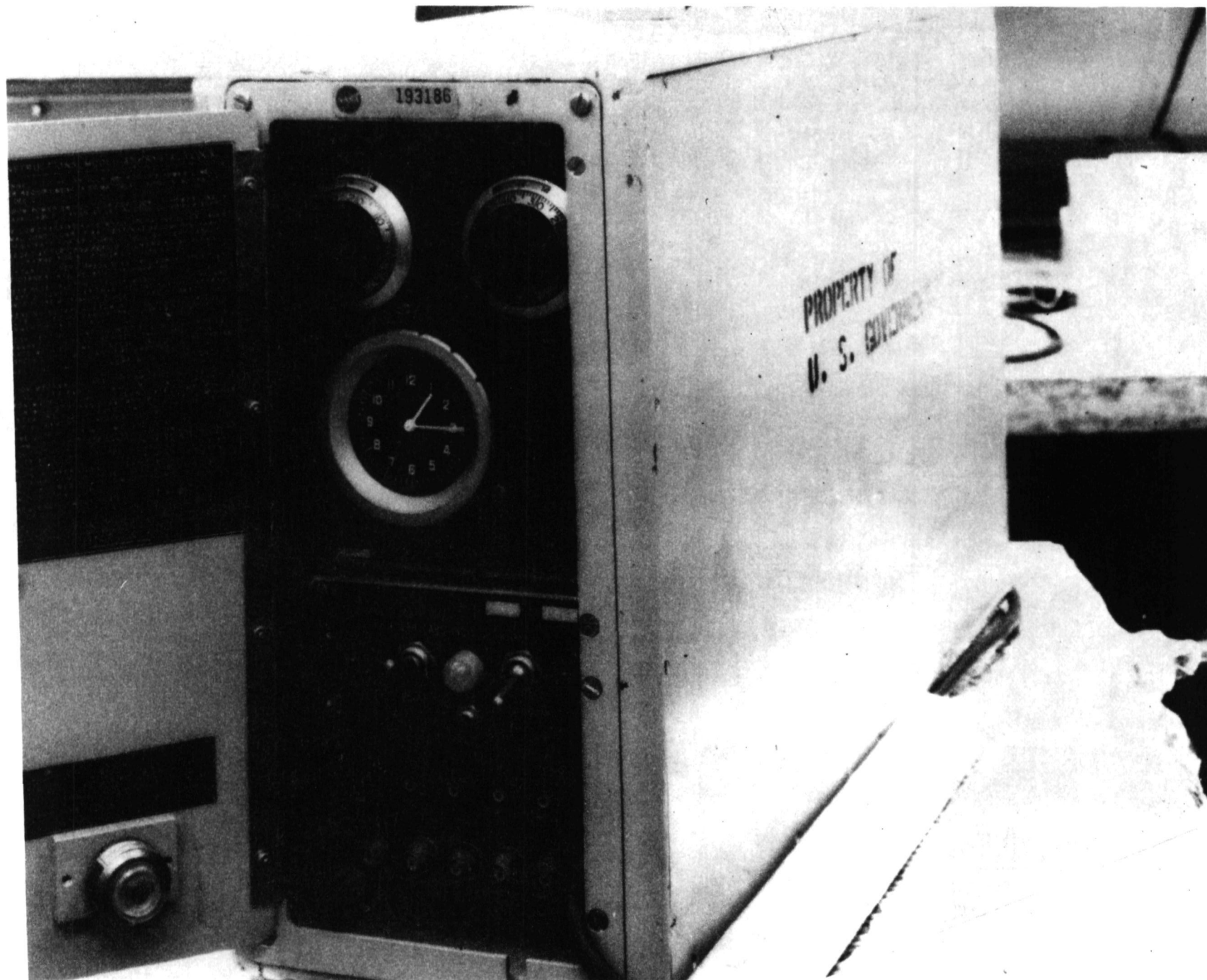


Figure 14. Sulzer Portable Crystal Clock

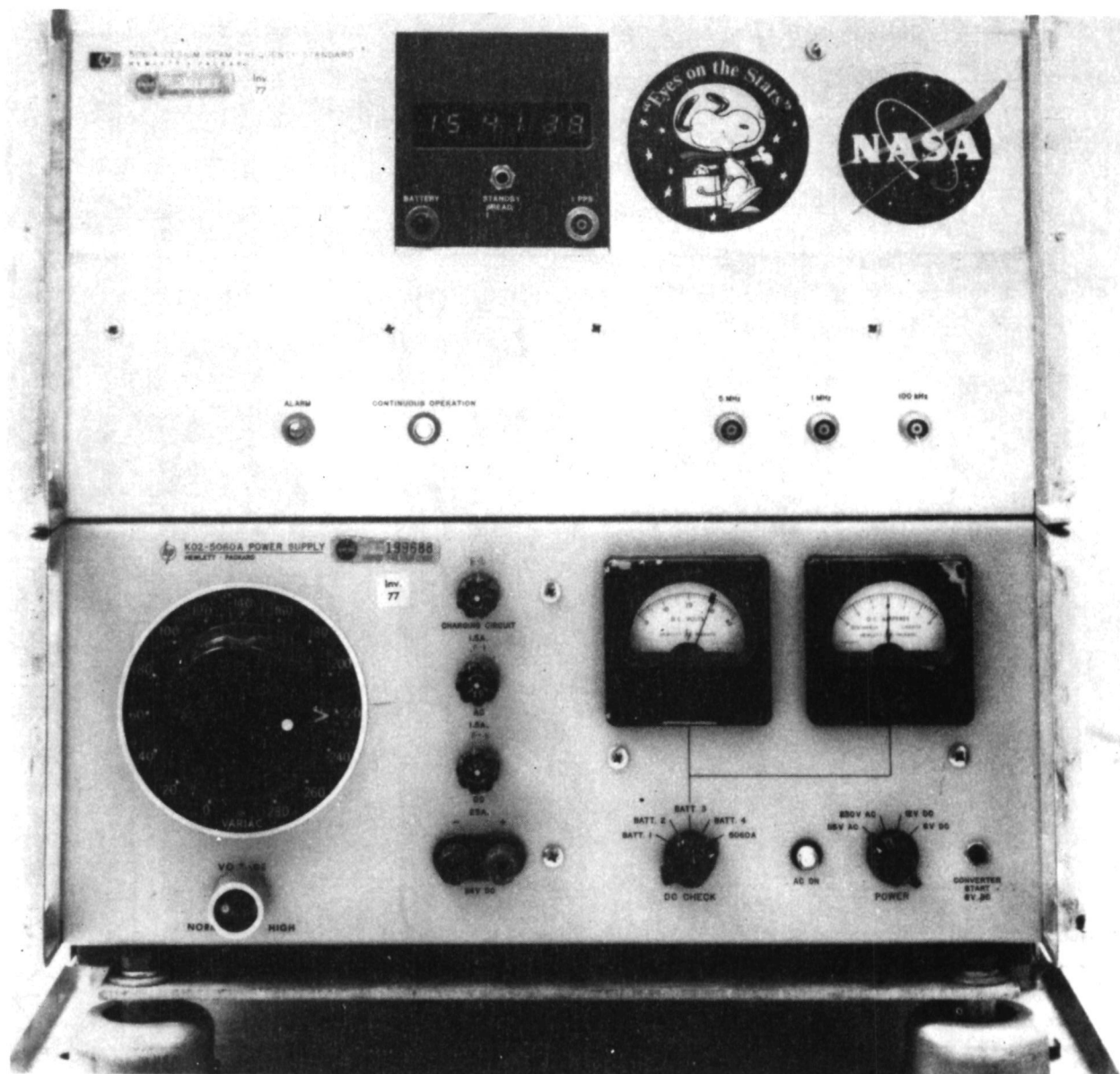


Figure 15. Hewlett Packard Cesium Beam Portable Clock

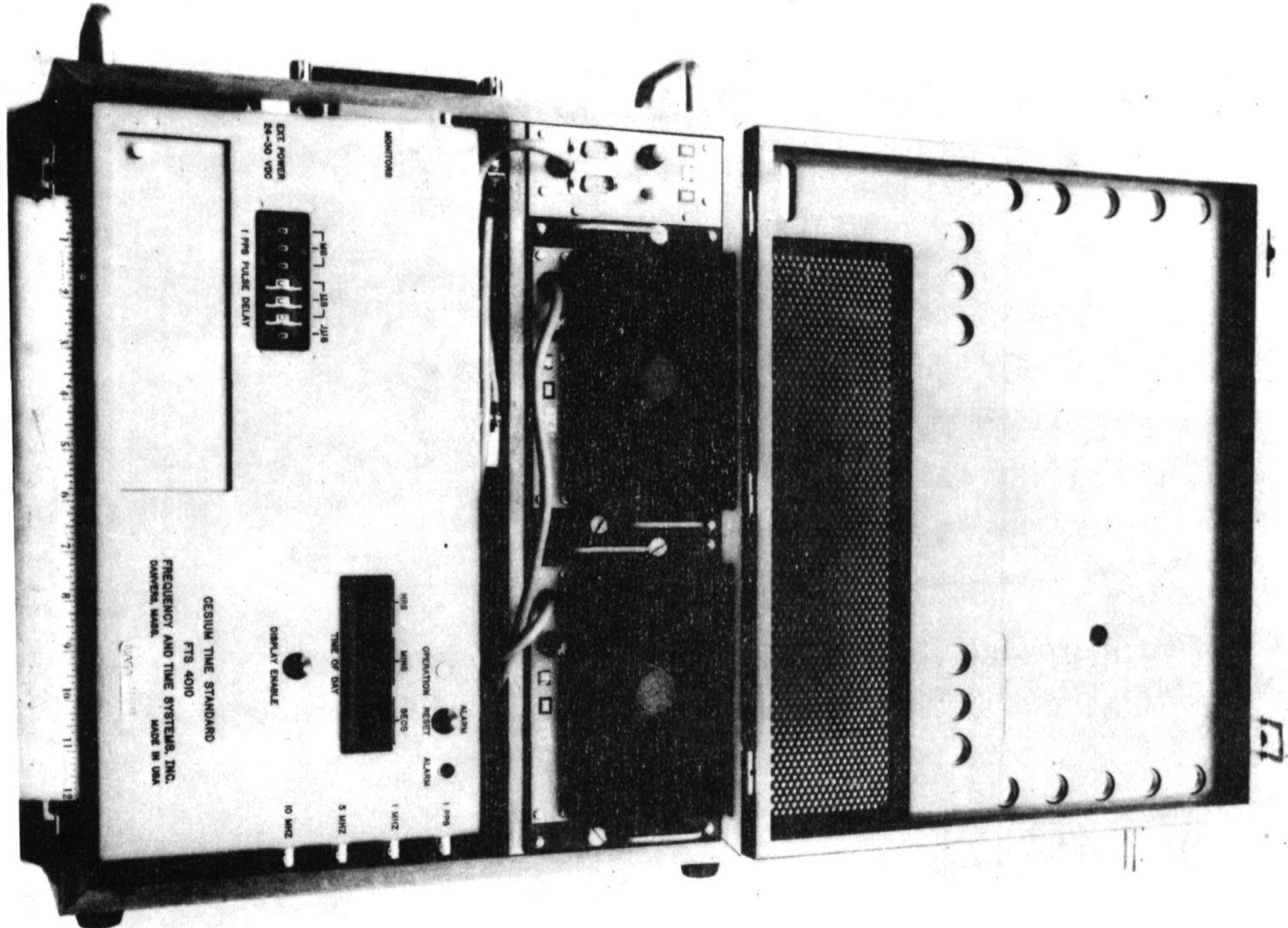


Figure 16. Currently Used Lightweight Portable Clock

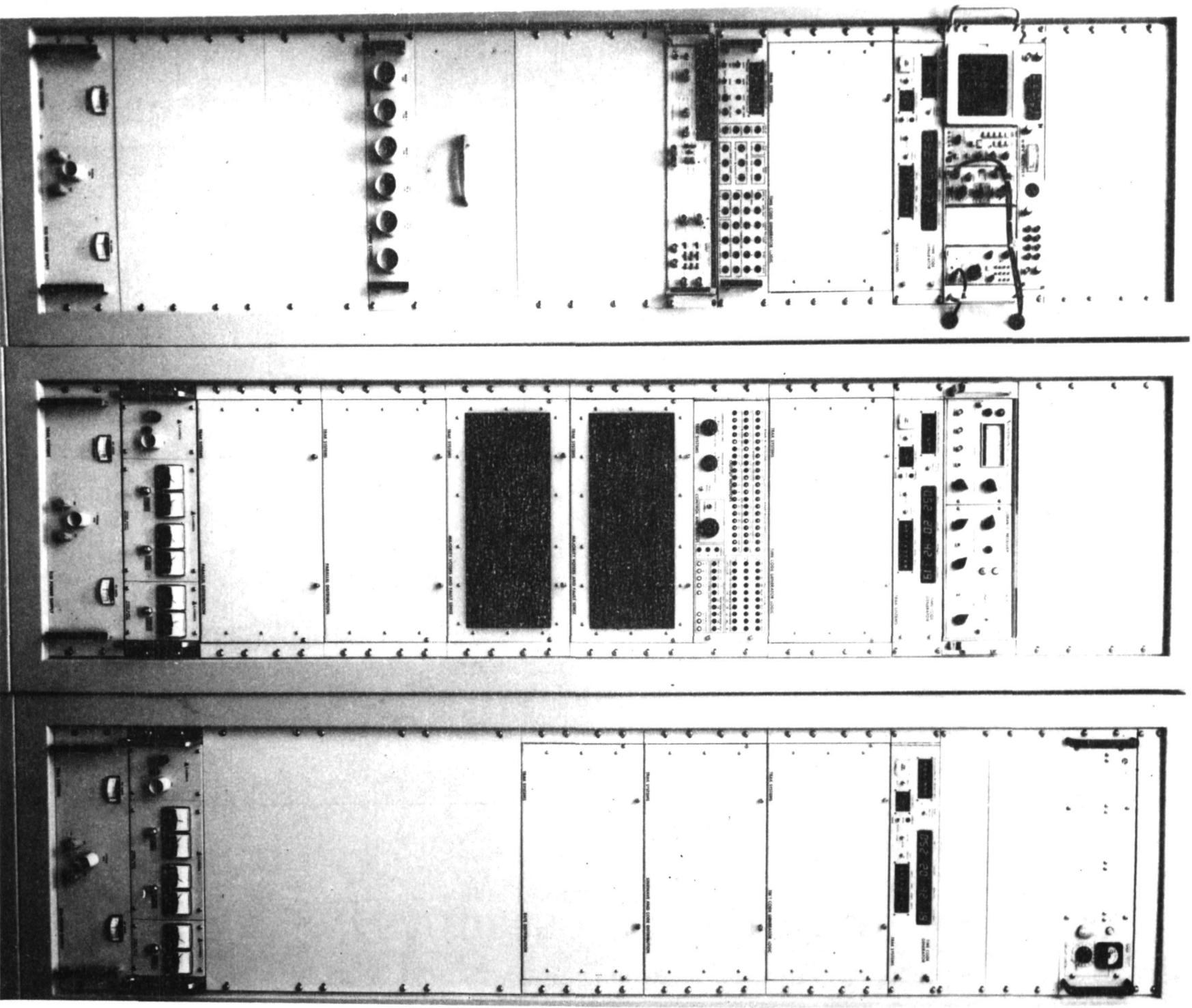


Figure 17. TRAK Model 8407

NASA/TDRSS TIMING SYSTEM WHITE SANDS

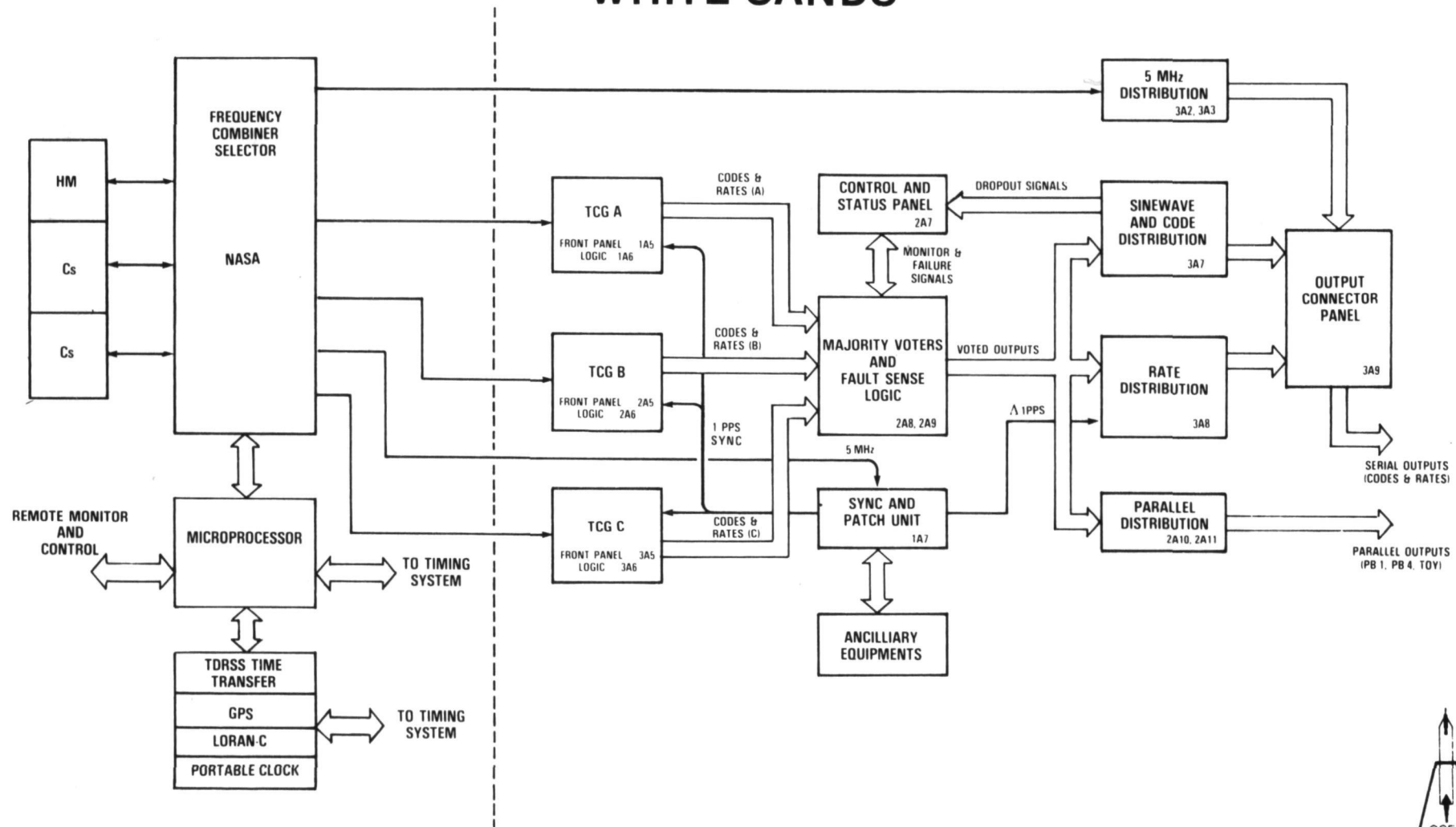


Figure 18. NASA/TDRSS Timing System
White Sands



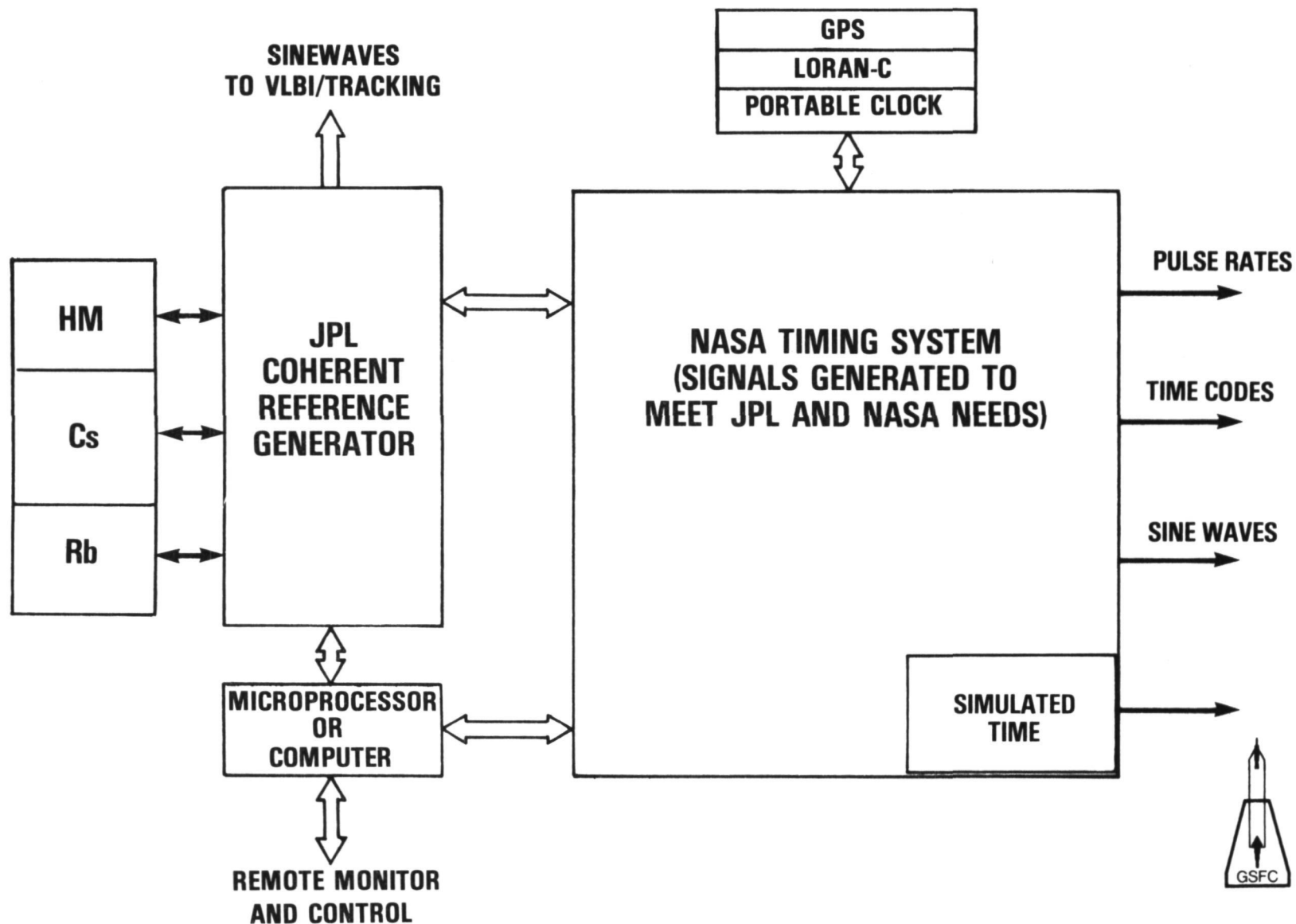


Figure 19. Consolidated Frequency/Timing System for Madrid, Goldstone, and Orroral

LESS THAN 50 NANOSECOND TIME TRANSFER

TDRSS
TRACKING DATA RELAY
SATELLITE SYSTEM
PASSIVE TECHNIQUE

GPS
GLOBAL POSITIONING SYSTEM
ACTIVE TECHNIQUE

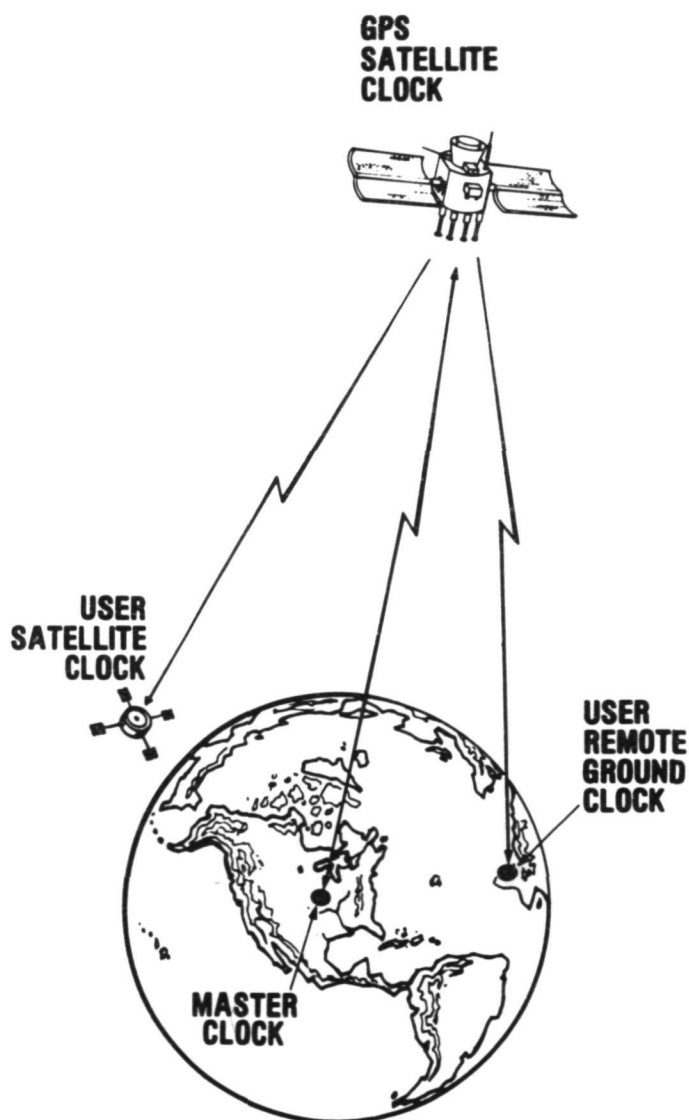
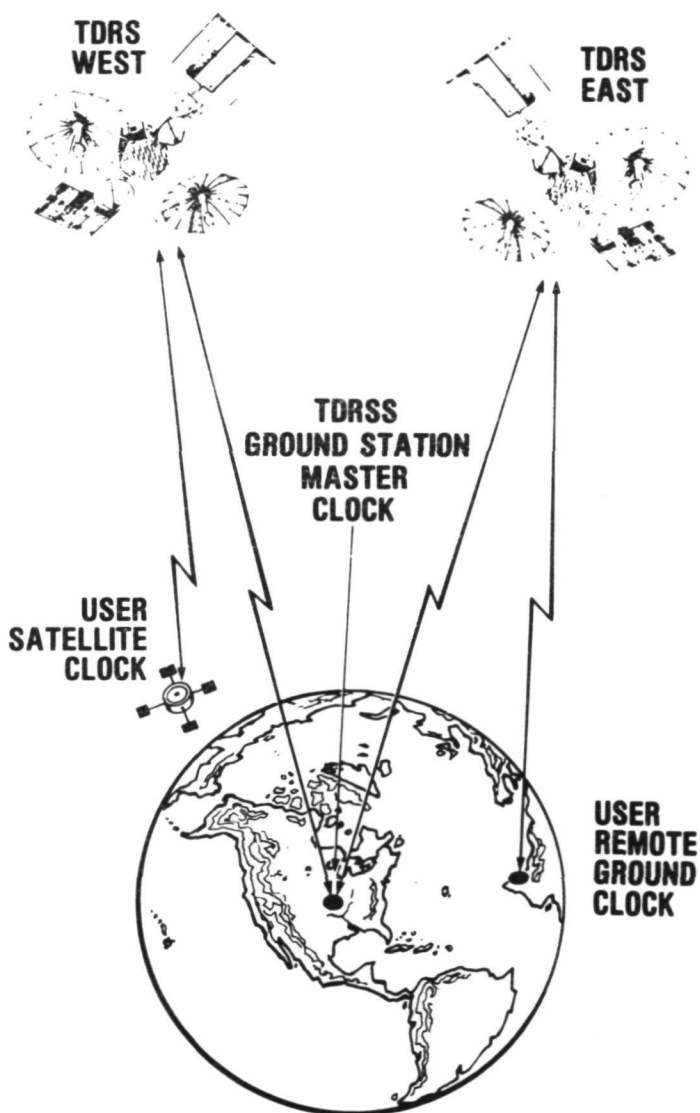


Figure 20. Future Considerations

SPACEFLIGHT TRACKING AND DATA NETWORK (STDN) PLANNED FOR THE 1980'S

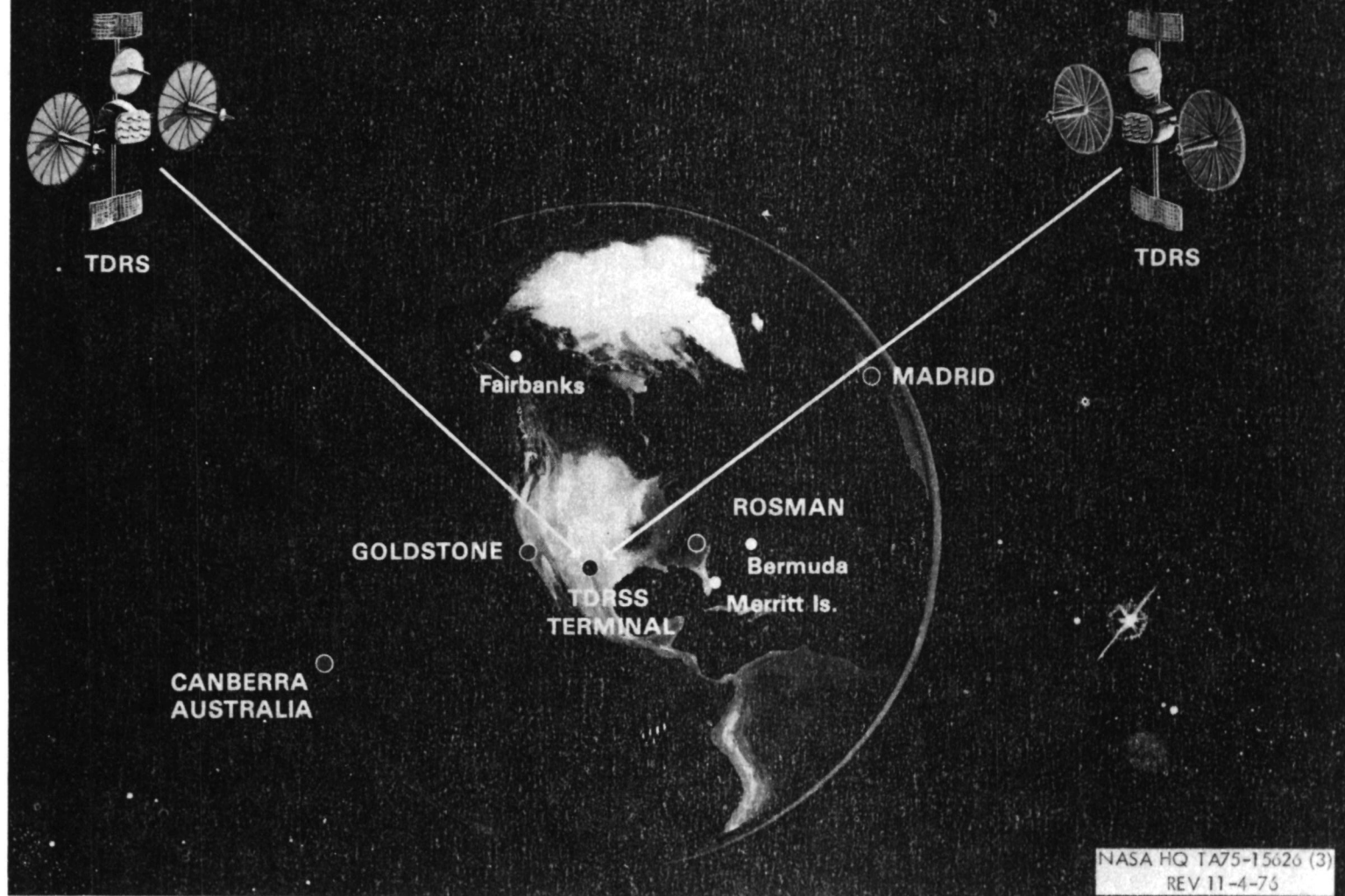


Figure 21. Spaceflight Tracking and Data Network (STDN)
Planned for the 1980's

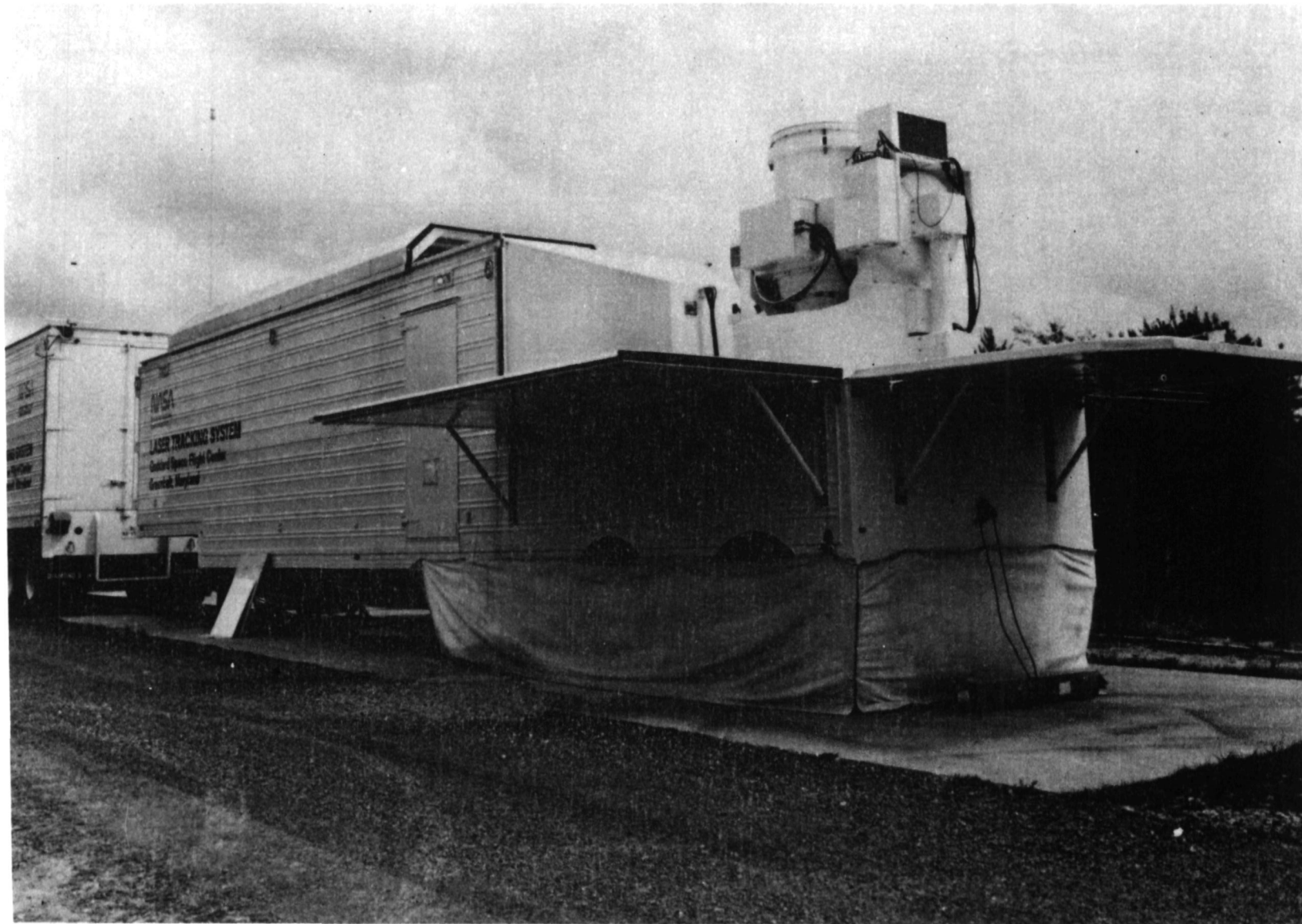


Figure 22. Mobile Laser Van



Figure 23. Kwajalein



Figure 24. American Samoa

SHUTTLE LASER TIME TRANSFER

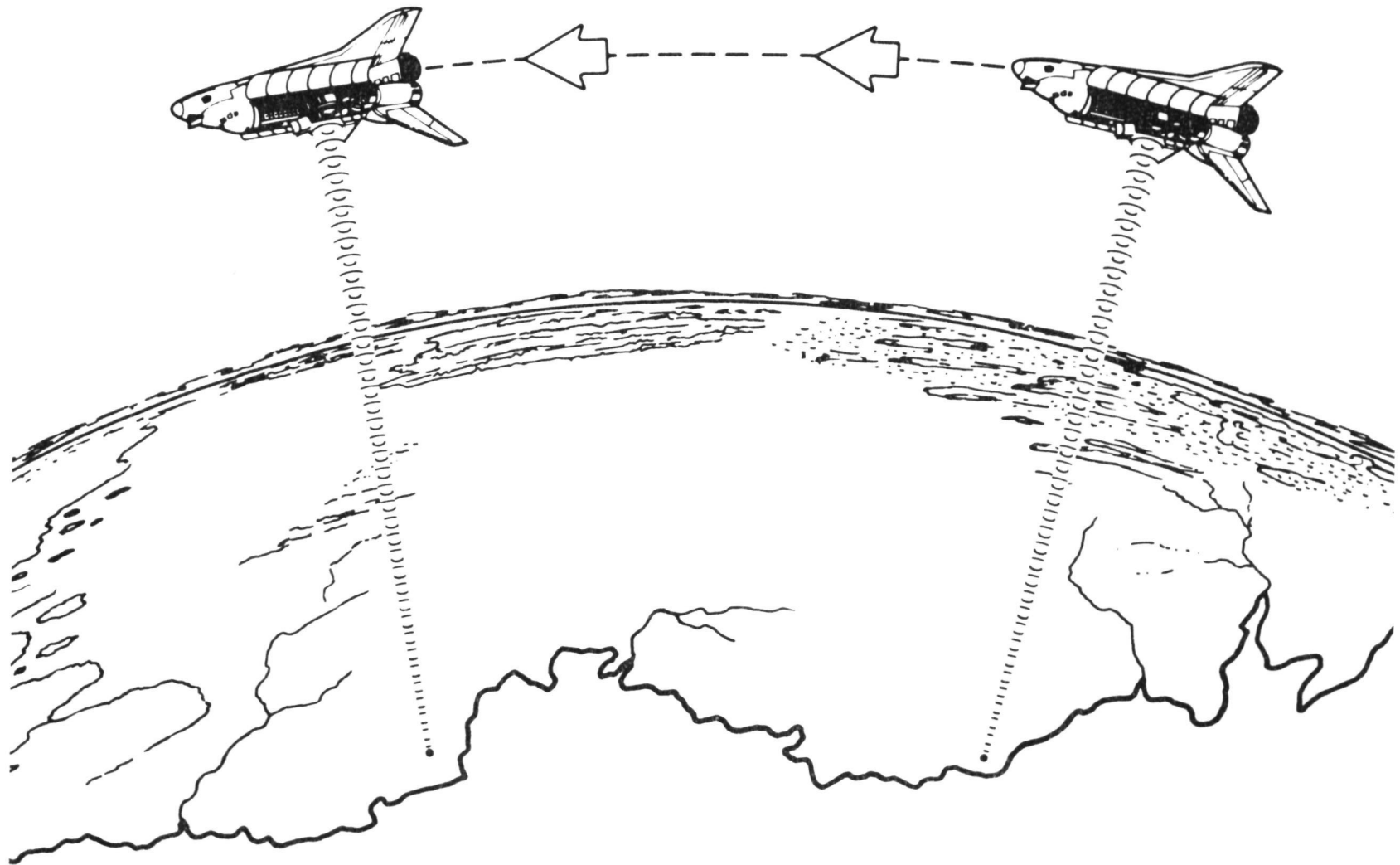


Figure 25. Shuttle Laser Time Transfer



Figure 26. Laser Time Transfer Ground System

U.S./NASA PARTICIPATION IN THE SIRIO-2/LASSO
EXPERIMENT FOR COMPARISON OF INTERCONTINENTAL/
INTERNATIONAL ATOMIC CLOCKS AT THE NANOSECOND
LEVEL VIA LASER TECHNIQUES.

SIRIO SATELLITE I TALIANO PER LA RICERCA
 ORIENTATO (ITALIAN SATELLITE ORIENTED
 RESEARCH)

LASSO LASER SYNCHRONIZATION FROM STATIONARY
 ORBIT



Figure 27. Missions of SIRIO-2

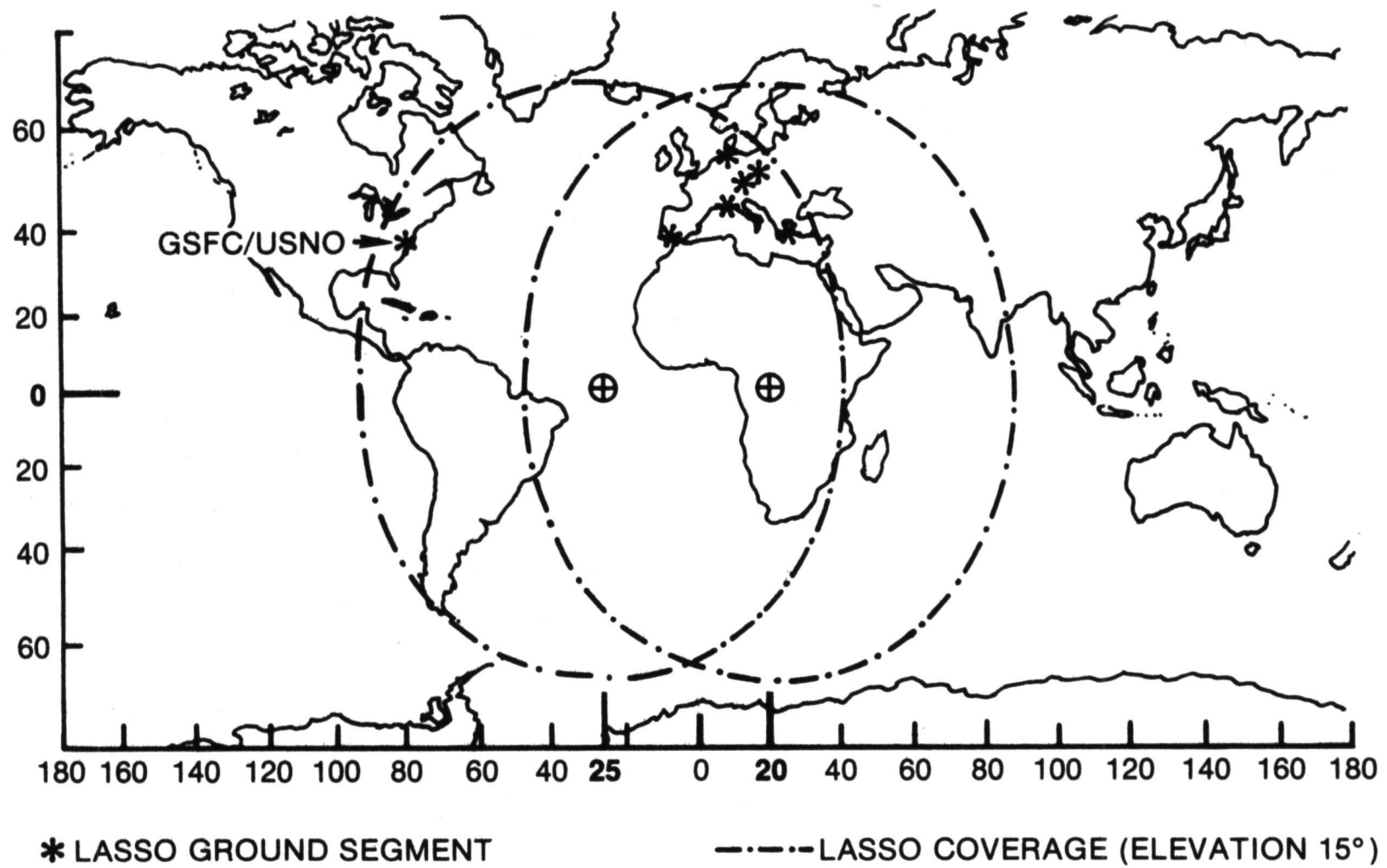


Figure 28. Provisional LASSO Coverage Zones

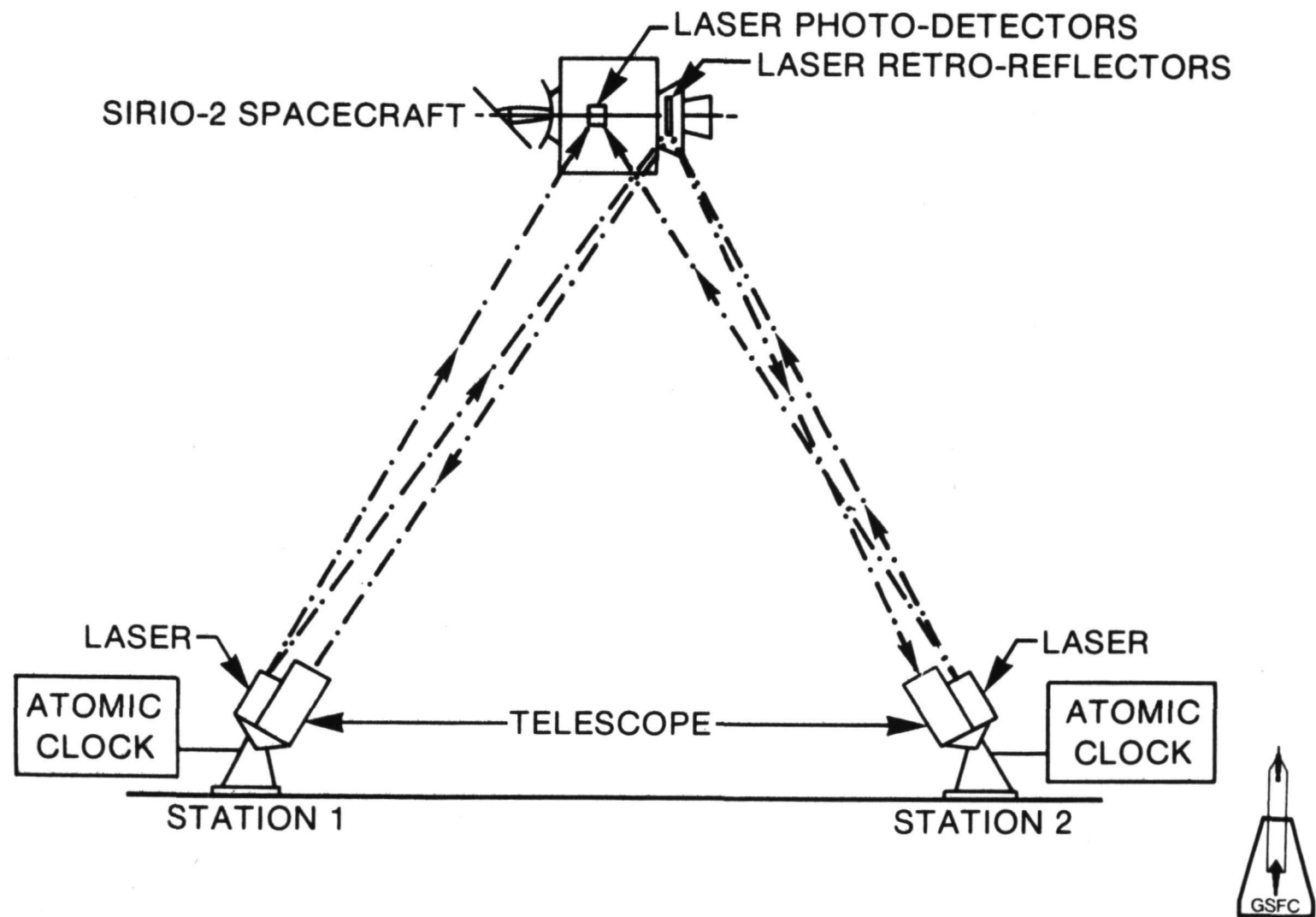


Figure 29. Schematic Diagram of LASSO Experiment

48" APERTURE PRECISION TRACKING TELESCOPE

OF THE GODDARD
OPTICAL RESEARCH FACILITY

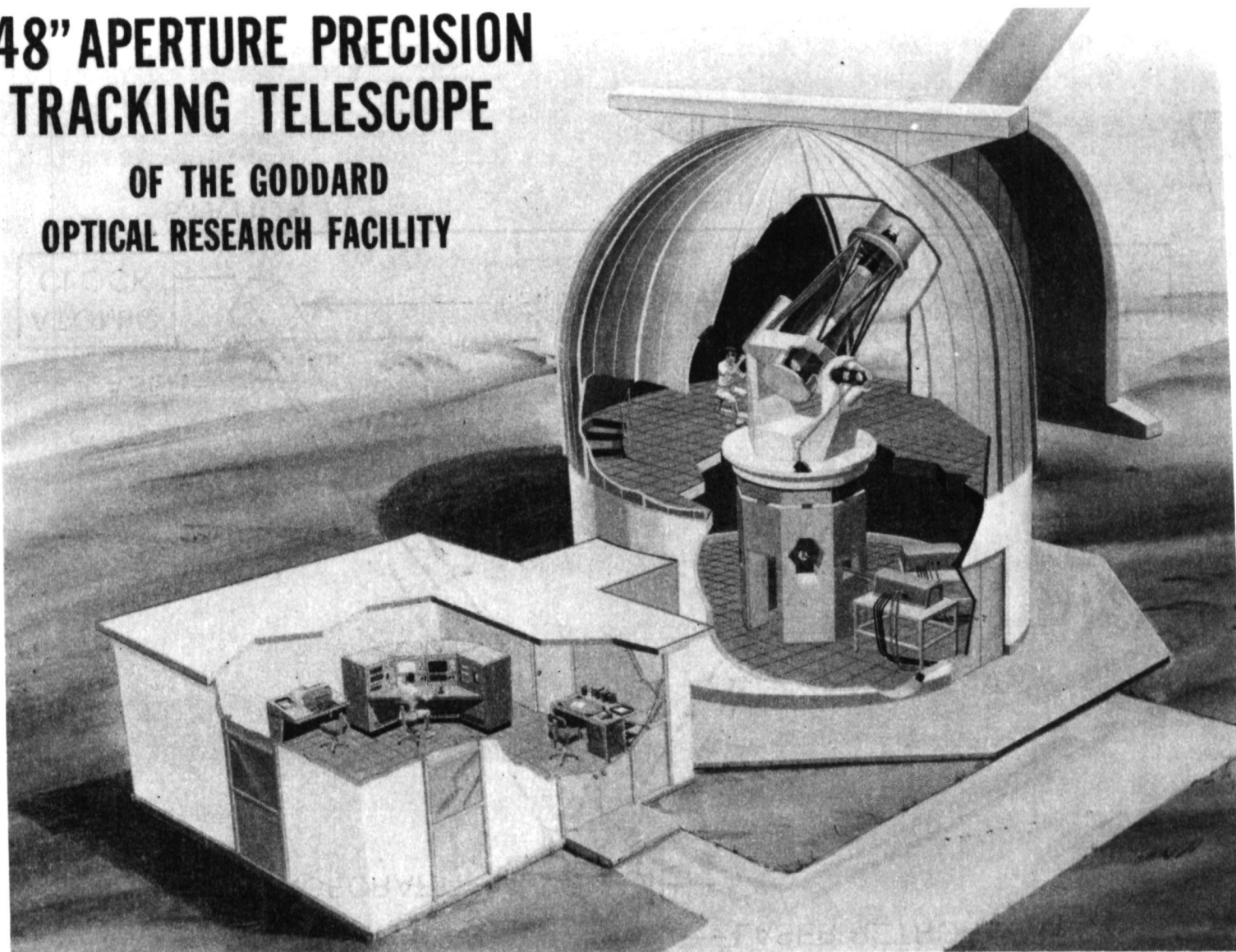


Figure 30. Artist Concept of Laser System at GSFC

HISTORY OF GSFC HYDROGEN MASERS

- 1967: NX-1, 1ST EXPERIMENTAL
- 1969: NP, FIELD OPERABLE, BASED ON NX-1
- 1973: NX-2 & NX-3, EXPERIMENTAL
- 1981: NR, FIELD OPERABLE, BASED ON NX-2 & NX-3

FUTURE PLANS

- 1983: IMPROVED NR, FIELD OPERABLE
- 1984: LOW COST MASER, FIELD OPERABLE
- 1990: SUPERCONDUCTING CAVITY LOCAL OSCILLATOR

VK02e

Figure 31. History and Future Plans of GSFC Hydrogen Masers

SATELLITE TECHNIQUES

<u>DATE</u>	<u>NAME</u>	<u>ACCURACY</u>
1965	*GEOS	40 μ s
1970	*ATS	100 ns
1977	NTS	500 ns
1981	*LASSO	1–5 ns
1980's	TDRSS	10–20 ns
1980's	GPS	10–20 ns
1980's	SHUTTLE	10–20 ns
1990's	LASERS	ps

CONVECTIONAL TECHNIQUES

<u>DATE</u>	<u>METHOD</u>	<u>ACCURACY</u>
1950	HF	10 ms
1960's	VLF	100 μ s
1965	*DUAL VLF	10 μ s
1966	*OMEGA	5 μ s
1968	LORAN-C	1 μ s–25 μ s
1970's	TELEVISION	10 ns
1965	PORTABLE CLOCKS	Sub μ s

*EXPERIMENTAL – OTHER TECHNIQUES BECAME OPERATIONAL



Figure 32. Time Transfer Techniques

CONTRACTING FOR RESEARCH AND DEVELOPMENT

DAVID H. WEBER

NAVAL ELECTRONIC SYSTEMS COMMAND

ABSTRACT

A brief and simple outline of contracting procedures and requirements for the acquisition of the Navy's needs will be presented. Examples of the roles of Engineers/Scientists in the Contracting process will be given.

The purpose of the Department of Defense's acquisition mission is to develop and supply the weapons, services and supplies required to meet the nation's defense needs. Although working under the same laws and basic regulation, the methods of achieving this goal of defense vary among the services, even among different commands within each service, and are constantly changing. Because of the variations between agencies, to explain the process in detail would almost be impossible for one person. Therefore, I propose to present a general overview of the acquisition process, particularly as it pertains to the contracting function, citing the methods used by my Command as specific examples.

The basic law governing defense contracting is Title 10, Chapter 137, of the U.S. Code known as the Procurement Act. The Act provides for two methods of contracting - formal advertising and negotiation. Formal advertising must be used except when it is impracticable and the acquisition falls within certain categories, established in the Act. The categories, or exceptions, provide the authority to negotiate. The Act also provides procedures for formal advertising and sets forth specific restrictions and qualifications as to the types of contracts that may be used. Formal advertising means acquisition by competitive bids and awards. Negotiation means acquisition made without the use of formal advertising. In negotiation, the Government asks prospective contractors to submit offers and to support them with statements of estimated cost or other evidence of reasonable price and data covering technical and management plans and capabilities to perform the required effort. Negotiation provides the flexibility to discuss the costs, technical and management effort proposed. This flexibility is not permitted under a formally advertised acquisition.

The Defense Acquisition Regulation, the DAR, is jointly issued by the Military Departments to provide uniform policies for carrying out the provisions of the Act and to establish policies for contracting areas not covered by it. In addition, the Defense Acquisition Regulation provides direction and guidance for complying with pertinent Statutes and Executive Orders. It covers policies, practices, and procedures for formal advertising and negotiation. It also covers other contracting topics such as pricing, type of contracts, contract clauses and contract cost principles.

Departmental regulations supplement the Defense Acquisition Regulation. The Army issues the Army Defense Acquisition Regulation Supplement (A DAR Sup.); the Navy, the Navy Defense Acquisition Regulation Supplement (N DAR Sup); the Air Force, the Air Force Defense Acquisition Regulation Supplement (AF DAR Sup). These regulations parallel the Defense Acquisition Regulation in outline and format providing subordinate policy and procedural guidance.

Some Department of Defense contracting policies and procedures are not suitable for inclusion in the Defense Acquisition Regulation. Others must be distributed faster than the periodic revisions of the Defense Acquisition Regulation permit. These situations are handled by issuing special instructions, directives, or circulars. The Military Departments also issue their own publications with respect to their acquisitions. Thus in the Navy, we have Secretary of the Navy (SECNAV); Navy Operations (OPNAV); Naval Material (NAVMAT); and Systems Commands (SYSCOM), in my case Naval Electronic Systems Command (NAVELEX) publications. These publications must not contradict the applicable higher level regulations.

The acquisition process may be broken down into three phases: (i) the pre-solicitation phase; (ii) the solicitation - award phase and, (iii) the post award contract administration phase.

The pre-solicitation phase begins with acquisition planning between the initiators of the acquisition request, contracting and other personnel .

(
The acquisition plan should cover such areas as:

- (i) the contracting lead-time;
- (ii) the method of contracting - formal advertising or negotiation;

- (iii) the terms and conditions - specifications, work descriptions, quantities, delivery dates and terms, contract type, reports required, data requirements, small business considerations, etc.;
- (iv) the handling of proposals - supporting information required, evaluation criteria and closing date.

The pre-solicitation stage ends with the preparation of the solicitation package, the invitation for bids in the case of formal advertising or the request for proposal in the case of negotiation. The solicitation package includes all documents and information needed to prepare a bid or proposal or refers the prospective offeror to where he can obtain the needed documents or information. The package also sets forth the terms and conditions of the proposed contract and the rules for submission of bids or proposals. Requests for proposals also include the evaluation criteria, those specific areas of the proposal that will be evaluated and their relative importance.

The solicitation-award phase of the acquisition begins with the issuance of the solicitation package and the publication of a summary of the solicitation in the Commerce Business Daily.

Firms interested in the acquisition submit bids or proposals in response to the solicitation. In advertised acquisitions the award is made to the lowest responsive, responsible bidder. A responsible bidder is one who has (i) adequate financial resources or the ability to obtain such resources for the performance of the proposed contract, (ii) be able to comply with the delivery or performance schedule, (iii) have a satisfactory record of performance, (iv) have a satisfactory record of integrity, and (v) be otherwise qualified to receive an award under applicable law and regulation.

In many ways, the negotiation process parallels formal advertising. Competition is obtained to the maximum extent practicable. Proposals are required by specified closing dates and an award may be made without discussion to a responsible offeror. In negotiation, award is made to the firm whose offer is most advantageous to the Government - price and/or other factors considered. The best price and/or pricing arrangement is often the basis for determining which of several responsible firms will receive the award. But negotiation is flexible enough so that factors other than price may be considered - to the extent of their importance. When technical competence is of prime importance for example, as in research, it and the technical proposal are the main criteria for award.

During the post-award administration phase of the acquisition process, the Government's relationship with the successful offeror is a contractual one. Therefore, the contract is the prime reference for all matters concerning performance.

Administrative responsibilities vary with the type and complexity of the acquisition. On even the simplest contract, the item to be delivered must be accepted or rejected. On a contract of any complexity, the Government acquisition team has many administrative duties. One of them is progress surveillance to make sure that the work is being carried out successfully as well as monitoring the performance for compliance with the terms and conditions of the contract.

The Government often takes an active part in contract performance. It may provide Government-furnished material or equipment, approve designs; participate in periodic program reviews, test, evaluate, inspect and accept supplies or services and provide technical information. These are some of the actions required of the Government which may condition contract performance. Delays or omissions on the part of the Government may excuse the contractor from his own related performance obligations.

The Department of Defense acquisition team is made up of specialists in many fields. It includes contracting officers, engineers, auditors, lawyers, price and cost analysts, administrative contracting officers and their technical staff and negotiators. The contracting officer has the authority and basic responsibility on all contractual matters. Many persons who do not have contracting officer authority may be delegated to act as his representative. Particularly on complex contracts, the key person delegated to act as the Contracting Officer's representative is usually the engineer. Let us briefly examine the role of the engineer in the acquisition process by following him in his capacity as acquisition manager, through a simplified version of an acquisition from planning through award of a contract in NAVELEX.

Timing is a vital part of acquisition planning. Responsibility for the timing rests with the Acquisition Engineer. Prompt coordination with interested groups within the contracting activity will surface potential problems. Upon conceiving and justifying a required need, the acquisition manager calls for an Acquisition Planning Conference (APC) to which he/she invites those parties who will constitute the Acquisition Team. At this conference, the team members plan the acquisition. The following topics are discussed:

1. The requirement and the estimated cost/price
2. Earliest required delivery date
3. Specification
 - a. type
 - b. status
4. Statement of Work
5. Approval for Service Use
6. Planned Method of Acquisition
 - a. advertised
 - b. negotiated
 - i. competitive
 - ii. sole source
 - c. type of contract
 - i. fixed price
 - ii. cost reimbursement
 - d. multi-year
 - e. options
7. Security Requirements (DD Form 254)
8. Requirement for an Acquisition Plan
9. Small and Disadvantaged Business Consideration
10. Small Business Set-Aside Consideration
11. Acquisition Schedule

For our purpose today, let us presume that the planning conference has determined that the proposed acquisition will be for research

and development and will cost in excess of \$100,000.00 and that the method of acquisition will be by negotiated, competitive, cost reimbursement contract.

At the conclusion of the Acquisition Planning Conference, the Acquisition Engineer prepares the specifications/statement of work, the integrated logistics support requirements and the data requirements and circulates them to the appropriate activities, in accordance with regulations, for review and approval. Concurrently, he/she meets with the acquisition team to prepare the formal Acquisition Plan required by DAR 1-2100. This plan sets forth the background of and justification for the requirement and the basic acquisition strategy. The Acquisition Plan and later, The Determination and Findings (D&F) and Justification for Authority to Negotiate (JAN) is forwarded to the Assistant Secretary of the Navy (Manpower, Reserve Affairs and Logistics) via Chief of Naval Material and Assistant Secretary of the Navy (Research and Systems). When the D&F is signed by the Assistant Secretary of the Navy (Manpower, Reserve Affairs and Logistics), the Contracting Officer has the needed authority to negotiate for a contract. As the activity associated with preparing the acquisition winds down, the Acquisition Engineer starts to prepare a Source Selection Plan. This plan is crucially important to the success of the acquisition effort and must be carefully prepared and strictly followed. This plan establishes specific milestones for accomplishing the acquisition and specific dates for each milestone; the Source Selection Authority (SSA); the Contract Award Review Panel (CARP) and the Technical Evaluation Board (TEB). The plan also establishes the instructions to offerors. These instructions appear verbatim in the solicitation and tell offerors which areas of a proposal most interest the Government and therefore the areas in which they should expend most of their effort. This normally results in cost savings to offerors and better proposals to the Government. The evaluation criteria is established in the plan and reproduced verbatim in the solicitation. The criteria lists in descending order of relative importance the specific elements to be evaluated and used in ranking proposals. Numerical weights are assigned to the criteria in accordance with the importance of each criterion. Criteria weights are not published by NAVELEX but are put in a sealed envelope and kept by the Contracting Officer in a secure place.

Sometime after issuing the Request for Proposal (RFP), usually thirty (30) days, a pre-proposal conference is held in which prospective offeror's ask questions, the answers to which will help them submit better proposals. Often the questions asked cannot be answered during the conference as they require research by the Acquisition Engineer. All questions and answers are reduced to writing and issued

to all recipients of the solicitation as an amendment.

On the closing date of the solicitation, the Contracting Officer removes all cost and pricing data and furnishes the balance of the proposal to the Technical Evaluation Board for technical evaluation of the proposal. The cost and pricing data is removed so as not to bias the technical evaluation by cost considerations. When the Technical Evaluation Board completes its evaluation and ranking of the offers, it prepares its report in accordance with the instructions in the source selection plan and submits it to the Contract Award Review Panel, usually chaired by the Acquisition Engineer. The Contract Award Review Panel combines the technical ranking with the cost ranking submitted by the Contracting Officer and develops a combined preliminary ranking. To this ranking, the Contract Award Review Panel applies the criteria weights furnished by the Contracting Officer and develops a final ranking. The Contract Award Review Panel prepares a report of its finding and submits it with a recommendation of a competitive range and those offers which fall within that range. The determination as to which offerors fall within the competitive range is made by the Contracting Officer. If there is doubt whether a proposal falls within the competitive range, that doubt is resolved by including it. Discussions, written or oral, are held with all offerors that are within the competitive range. They are advised of the deficiencies in their proposals and are given a reasonable opportunity to correct or resolve the deficiencies and to submit revisions to their proposals that may result from the discussions. At the conclusion of the discussions, the Technical Evaluation Board and the Contract Award Review Panel evaluate the revised proposals and rerank them. As a result, the number of proposals falling within the competitive range may be reduced. At this point, the Contracting Officer establishes a common cut-off date for discussions and so notifies the offerors still within the competitive range and offers them reasonable opportunity to submit "best-and-final" offers. Upon receipt, the "best-and-final" offers are reviewed by the Contract Award Review Panel which then recommends to the Contracting Officer a single offeror for award of the contract. The final determination for award is the responsibility of the Contracting Officer. Upon selection of a successful offeror, a contract is drafted. The drafted contract is reviewed by the Acquisition Engineer and legal counsel for technical and legal sufficiency and the Comptroller is requested to certify the availability of funds in the amount needed to finance the contract. The unsuccessful offerors are notified and the proposed contract is mailed to the successful offeror for review and signature. After signing two copies of the proposed contract, the successful offeror returns them to the Contracting Officer for execution.

After the contract is executed and issued, the Acquisition Engineer with assistance from the Contract Administration Office works with the Contracting Officer in administering the contract. He assumes the responsibility for technical performance under the contract, recommending changes to the specifications, statement of work, delivery schedules, etc.

The brief description of the acquisition process presented does not depict the time it takes to enter into a contract for a requirement. The process may take years. I know of one case where the requirement was conceived two years before contracting action was initiated. The process, once an acquisition request is received by the Contracting Officer, may take from one to seven months (see figure 1). However, on large, complex acquisitions, it may take a year to enter into a contract. Federal acquisition is no longer simply getting the right material to the right place at the right time for the right price. The federal acquisition contract is one of the most effective tools for implementing federal policy. Unlike statutory requirements which penalize for non-compliance, a contractual requirement rewards for compliance. Not only is the cost of compliance reimbursed, but profit is also paid. The Government is using federal acquisition contracts more and more to implement policy, i.e. increased EEO requirements, the small business program, the labor surplus program and requirements for compliance with the Presidential wage guidelines to name a few of the better known policies.

What does all this mean to the Acquisition Engineer? It means that each year new policies come into effect and it takes longer to get his requirements under contract. He must therefore assemble his Acquisition Team, particularly the Contracting Officer and begin his acquisition planning early in his program so as to better serve his clients.

PROCUREMENT LEAD TIME CHART

(From Time Received By The Contracting Officer To Award)

		CONTRACT TYPE							
PHASE	MILESTONE	TWO STEP			NEGOT. UNDER 10K	NEGOT. 10K - 100K	NEGOT. 100K TO 1 M	NEGOT. OVER 1 M	
		IFB TARGET IDEAL	STEP I TARGET IDEAL	STEP II TARGET IDEAL	TARGET IDEAL	TARGET IDEAL	TARGET IDEAL	TARGET IDEAL	
I PRE-SOLIC.	PRE-SOLIC. COMPLETE	3 } 3	3 } 3	- -	2 } 3	2 } 3	3 } 4	4 } 4	
	SOLIC. MAILED	2 }	2 }	2 1		1 }	2 }	2 }	
II SOLIC.	OFFER/PROPOSAL RECEIVED	5 4	5 4	3 2	3 }	3 3	4 4	5 5	
III EVAL.	ADVICE RECEIVED	3 }	8 }	3 }	1 }	3 }	4 }	5 }	
	EVAL. COMPLETE PRE-NEG. CLEARANCE COMPLETE	1 } 3 1 }	2 } 8 - }	1 } 3 1 }		1 } 3 1 }	2 } 6 3 }	2 } 7 2 }	
IV NEGOT.	NEG. COMPLETE POST NEG. CLEARANCE COMPLETE	-	- -	- -	1 }	1 } 2	2 } 3	2 } 4	
						1 }	2 }	2 }	
V AWARD	SENT TO CONTRACTOR EXECUTED	2 } 1	- -	- }	2 } 1	2 }	2 }	2 }	
	ALL ACTIONS COMPLETE		- -	2 }		1 } 3 2 }	2 } 3 2 }	2 } 3 2 }	
	WEEKS	17 11	20 15	12 7	8 5	18 14	27 20	30 23	
	DAYS	119 77	140 105	84 49	56 35	126 98	189 140	210 161	

FIGURE 1

Page Intentionally Left Blank

SESSION IIB

INDUSTRY VIEWS

**Dr. Harris A. Stover, Chairman
Defense Communications Agency**

Page Intentionally Left Blank

FREQUENCY AND TIME GENERATION AND CONTROL

Martin B. Bloch

(Frequency Electronics, Inc.), New Hyde Park, New York

ABSTRACT

FEI designs, develops and manufactures high precision quartz crystal oscillators, cesium beam atomic resonators, and cesium beam atomic standards for time and frequency generation equipment for ground, airborne, and space use. In order to utilize our resources more efficiently, the problem that we face is lack of long term visibility of DOD and NASA needs, and the enormous variety of hardware that we have to custom design for each individual program.

It is also becoming quite apparent that with the lack of significant R & D funds available from Government, advances in technology are slow, and in FEI's opinion, will not be able to meet near-future requirements such as GPS user equipment, Seektalk, and other programs. Because of the high risk factors involved, and the commercial applications of this product being too far off in the future, private capital for research and development is difficult if not impossible to obtain. More specific analysis and FEI's recommendation to overcome these difficulties will be objectively presented herein.

INTRODUCTION

FEI is a vertically integrated corporation, supplying frequency and time control components, sub-systems and systems for the military and aerospace users from the raw quartz to a finished timing system, and from the fabrication technology of the cesium resonators to the finished cesium atomic clock. It has been the Company's experience and history over the past eighteen years of its existence that the majority of its engineering talent has been applied to making modifications for each particular system of existing technologies rather than to further the state of the art and concentrate its talents on future needs and cost reduction. The Company has produced over twenty different types of distribution amplifiers; fourteen types of quartz standards; eighteen different oven controlled oscillators for the aerospace industry; and thirty-five different temperature compensated crystal oscillators, for the missile and space industry.

INSTRUMENTS AND SYSTEMS

The large variety of instruments and systems as exemplified by the equipment shown in Figures 1 thru 34, indicate the enormous amount of man hours that have been expended to hand-tailor similar functions for each particular user on pretty much of a crash basis. A careful analysis indicates that better planning and coordination between various DOD and NASA users, and the discipline to design and plan functional equipments that can be used over and over again in systems will reduce lead time costs enormously and at the same time make available the necessary engineering talent for use in the further development and the design of high reliability equipment at lower cost.

SIMILAR FUNCTIONAL MODULES

Similar functional modules that require significant redesign and repackaging in order to meet the particular specification requirements of specific systems are very expensive and time consuming to produce. There has been minimal standardization of products, which FEI feels is needed in spite of the past pitfalls of such standardization attempts which were buried in red tape and over-complications. Frequency and time generation and distribution equipment and systems need direction, standardization and long range planning in order to more effectively accomplish reliability, lower cost, and make available the desperately needed manpower to do the designs that will be required five to ten years hence.

OVEN CONTROLLED PRECISION OSCILLATORS

Oven controlled precision oscillators primarily for missile and satellite applications have been designed in hundreds of physical configurations as shown in Figures 5 thru 19. The basic functions of the oscillators, is to achieve low power (1 watt at room temperature), provide high stability ($1-5 \times 10^{-11}$ /day) and survive launch vibrations. The enormous quantity of types of oscillators could be reduced by possibly two to three times by standardization and coordination between various users. FEI has found that out of a one hundred man engineering team, approximately seventy are expended on custom redesign for a specific system application. The exact frequency is not a limitation on a manufacturer such as FEI because we build our own resonators. However, the need for accommodating the various types of input and output control signals and physical configurations and the large variation in surface finishes all impose significant cost and risk factors in meeting a timely delivery schedule. As was the case for instruments and systems, FEI would welcome closer coordination between all aerospace users so that we can better service the industry and not expend all of our engineering talents for the large variety of designs that we are presently fulfilling.

OTHER CRYSTAL COMPONENTS

Temperature compensated crystal oscillators, crystal filters, and crystal discriminators for the missile and aerospace industry is another example of the enormous variation in shapes, form factors, and input voltages that must be designed into the equipment in order to meet the particular application of each user. In spite of having over one hundred different designs available for users to pick from, we find ourselves continuously custom designing to fit each application. Coordination between various users and the investment in developing a half dozen modules would most likely meet 90% of the needs of the users in the missile and aerospace field.

While FEI, and I am sure many others in the frequency and time control field, are working sixteen hour days to fulfill various different system applications, the planning for the future, and the research required for the advancement of the art is greatly lacking. We are so busy meeting our day to day needs in terms of engineering and production in quartz resonators that there is no time left for research and development for the future. Quartz resonators, I might add, have made very little progress from the precision resonators first developed at Bell Laboratories in the early 1950's. Even the various atomic standards have progressed very slowly from the mid-1960's.

CONCLUSION

It is FEI's recommendation that the following steps be taken immediately in order to service DOD, NASA, and eventually commercial users, in the next decade.

1. Establish a well planned and coordinated program to improve the basic raw material.
2. Finance research and development with continuity of multi-year programs for the development of high performance, high reliability, quartz resonators.
3. Invest in the necessary research and development for economically manufacturing the precision quartz resonator.
4. Develop economical, high reliability, thermal controlled electronics and associated electronic circuitry to make use of the improved resonators, in order to meet the stringent future requirements of fast warmup, low g sensitivity, high stability, and high spectral purity sources of quartz oscillators and quartz standards.
5. Sponsor research in development a basic physics package to improve life and reliability, reduce manufacturing costs, and establish the capability for manufacturing the quantities of atomic standards that will be required in the next decade.
6. Coordinate and clearly outline the long range needs of ground, airborne, and space applications for frequency and time controlled components and systems in order to minimize the time and money expended by eliminating a multitude of different designs to accomplish the same function.

It is quite apparent, in FEI's view, that with the uncertainty in the production potential for DOD and NASA needs, private industry does not have the resources and the risk capital to do the basic research and development necessary to meet future needs. Therefore, it is imperative that the future specification requirements and the quantities needed be determined, and that the government sponsor basic and applied multi-year research programs if the industry is to meet the needs of the user in the next decade.

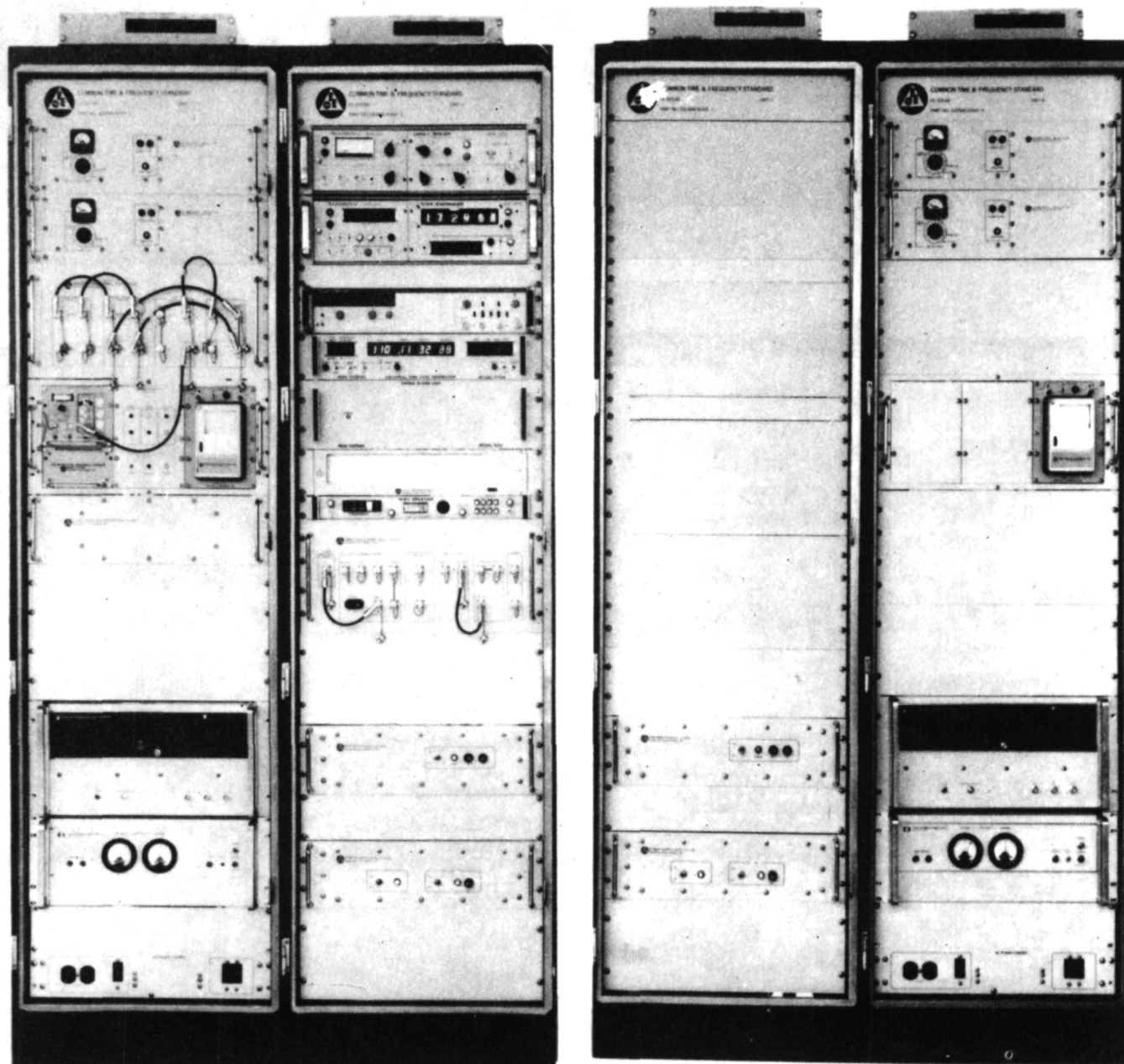


Figure 1. Common Time and Frequency Standard (CTFS)
Model FE-5054A
TDRSS Ground Station

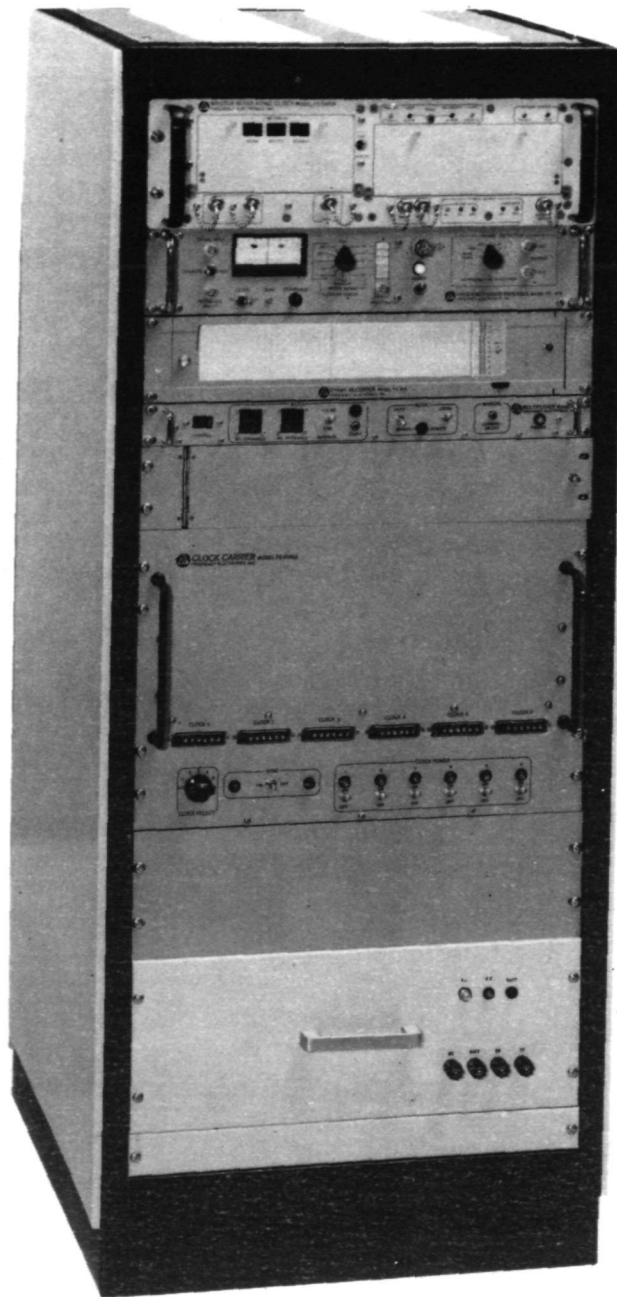


Figure 2. Frequency and Time Measuring System
Model FE-5070A
Seektalk

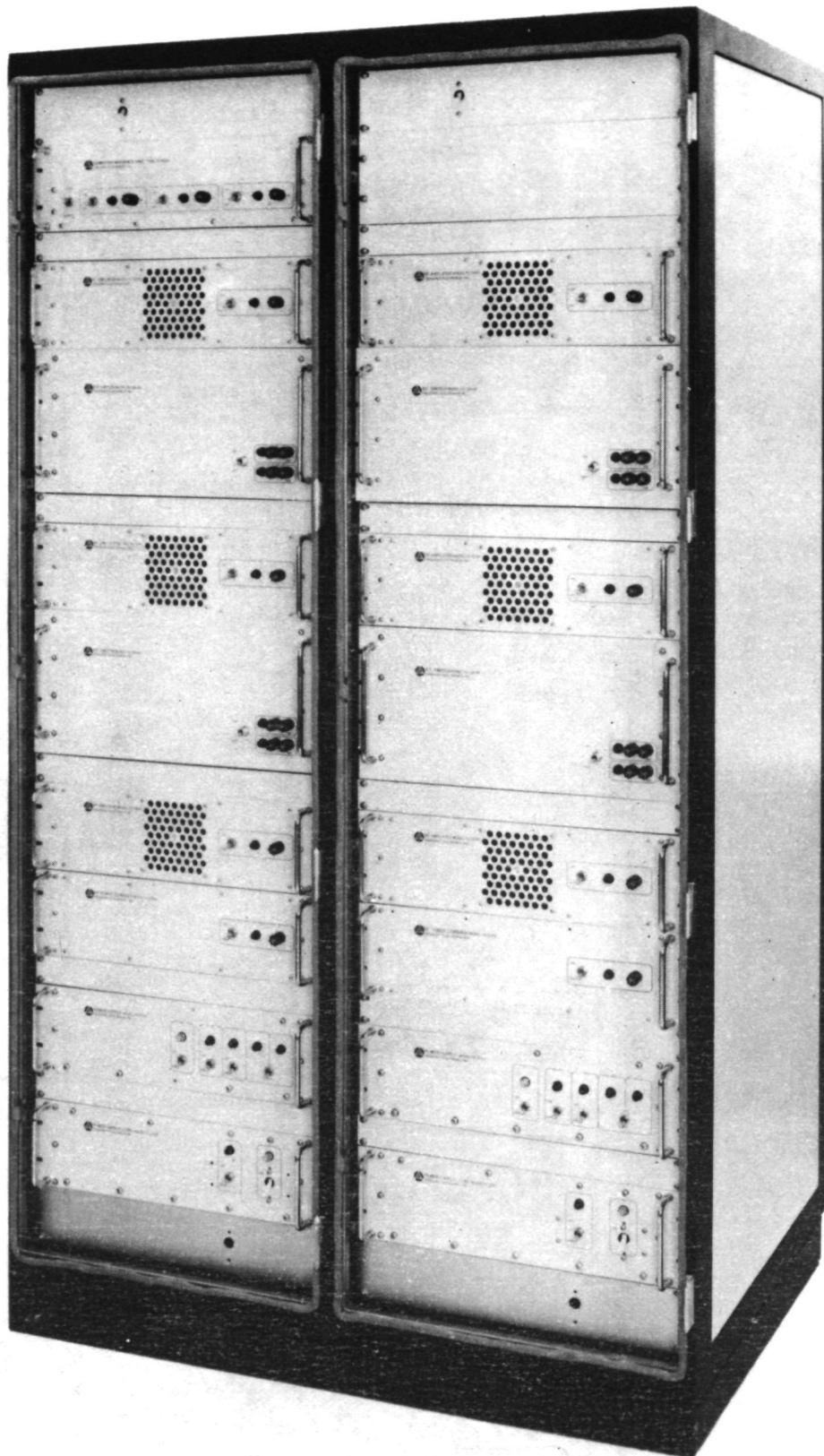


Figure 3. RF Switching Group
Model FE-7728A
HF Surveillance System

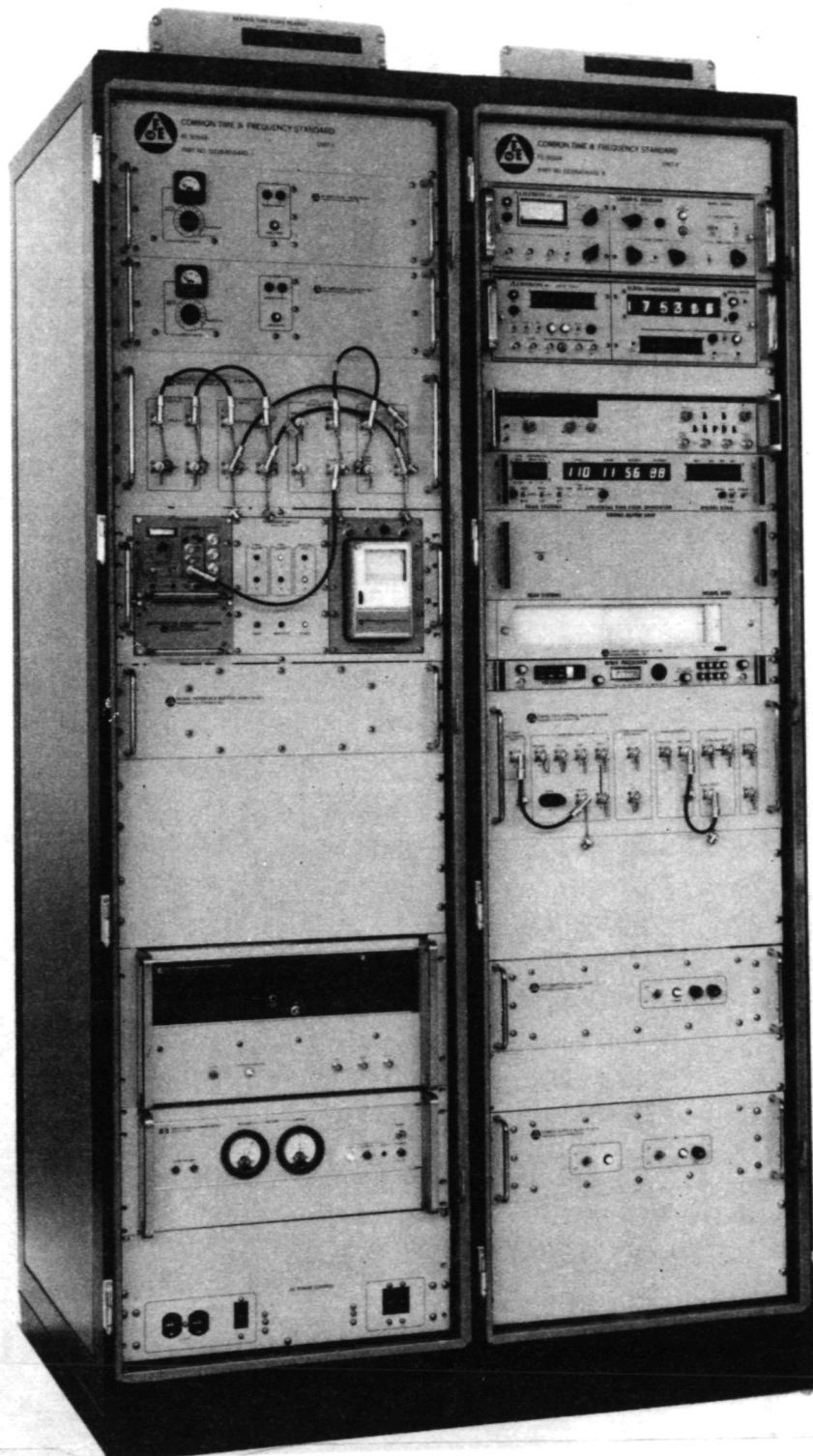


Figure 4. Common Time and Frequency Standard (CTFS)
Model FE-5054A
TDRSS Ground Station

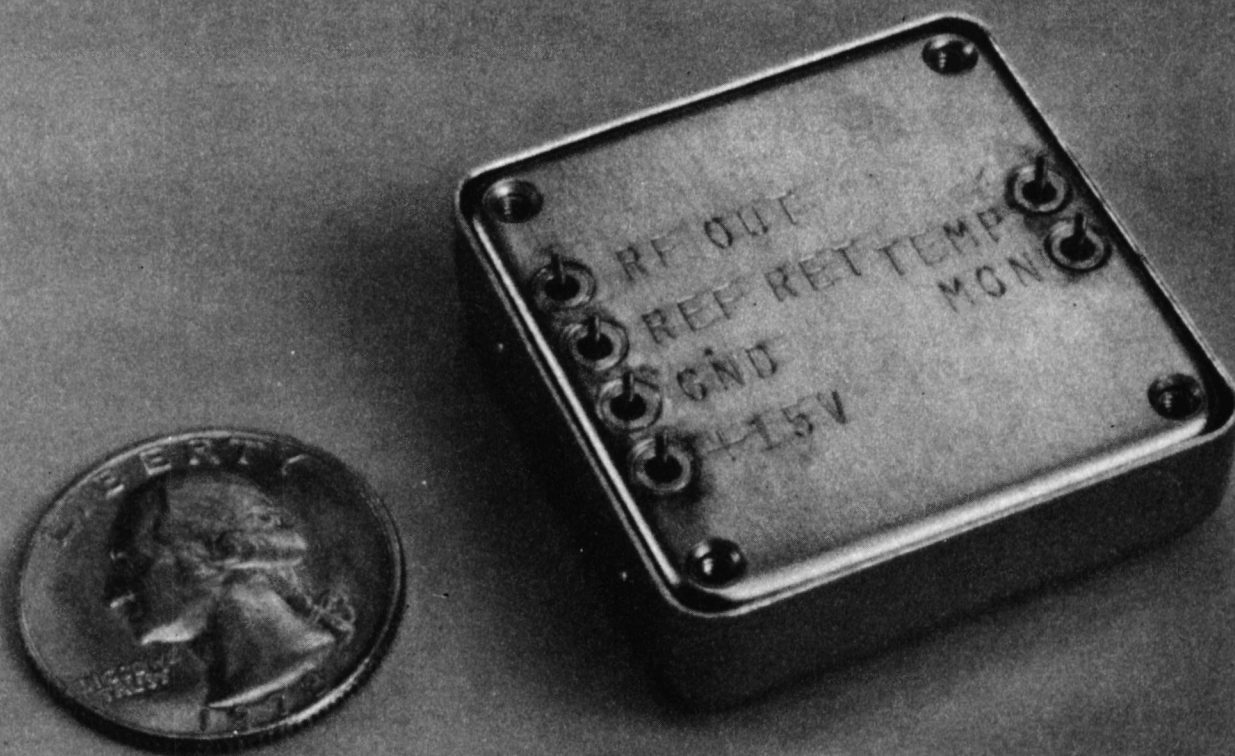


Figure 5. Temperature Controlled Crystal Oscillator (TCXO)
Model FE-8121B
Trident

220

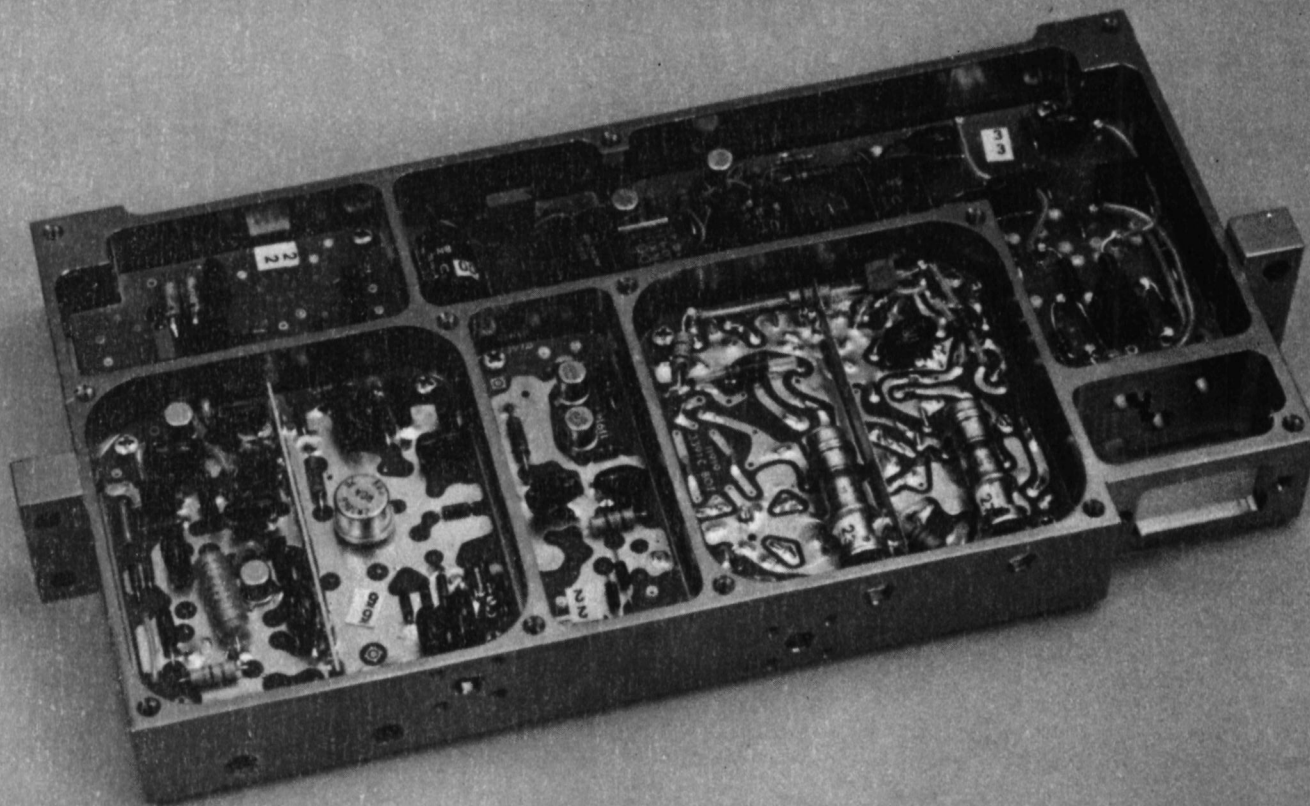


Figure 6. Double Local Oscillator
Model FE-2075A
Application Technology Satellite

221



Figure 7. Temperature Controlled Crystal Oscillator (TCXO)
Model FE-8031A
Communications Satellite (777)

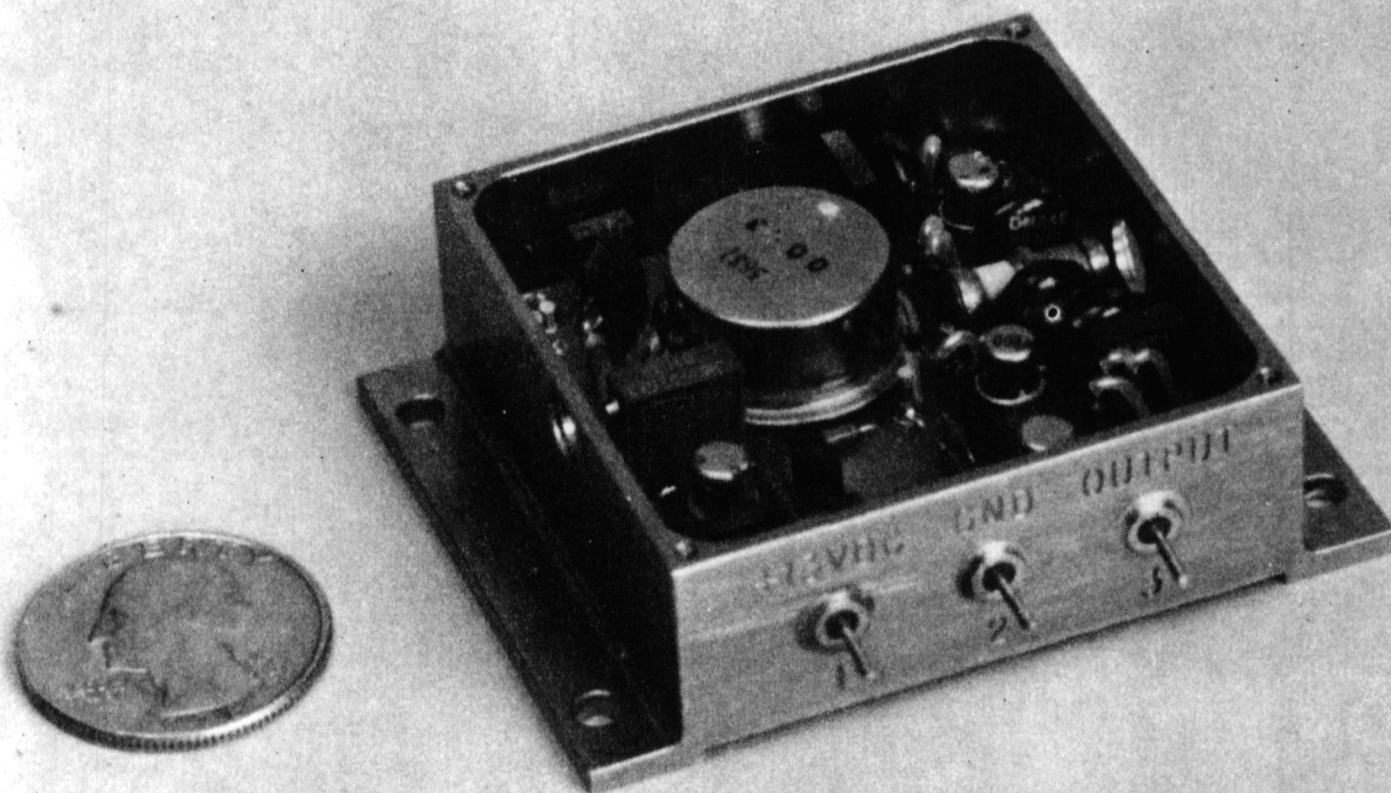


Figure 8. Temperature Controlled Crystal Oscillator (TCXO)
Top View, Model FE-8119A
Pioneer-Venus

223

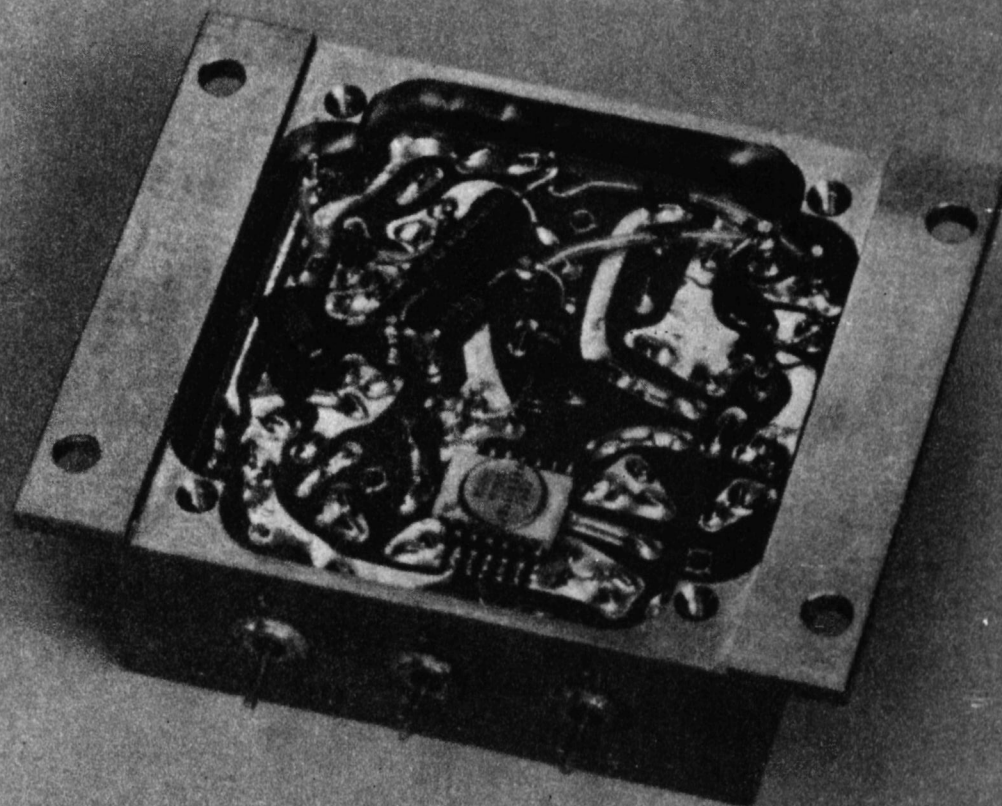


Figure 9. Temperature Controlled Crystal Oscillator (TCXO)
Bottom View, Model FE-8119A
Pioneer-Venus

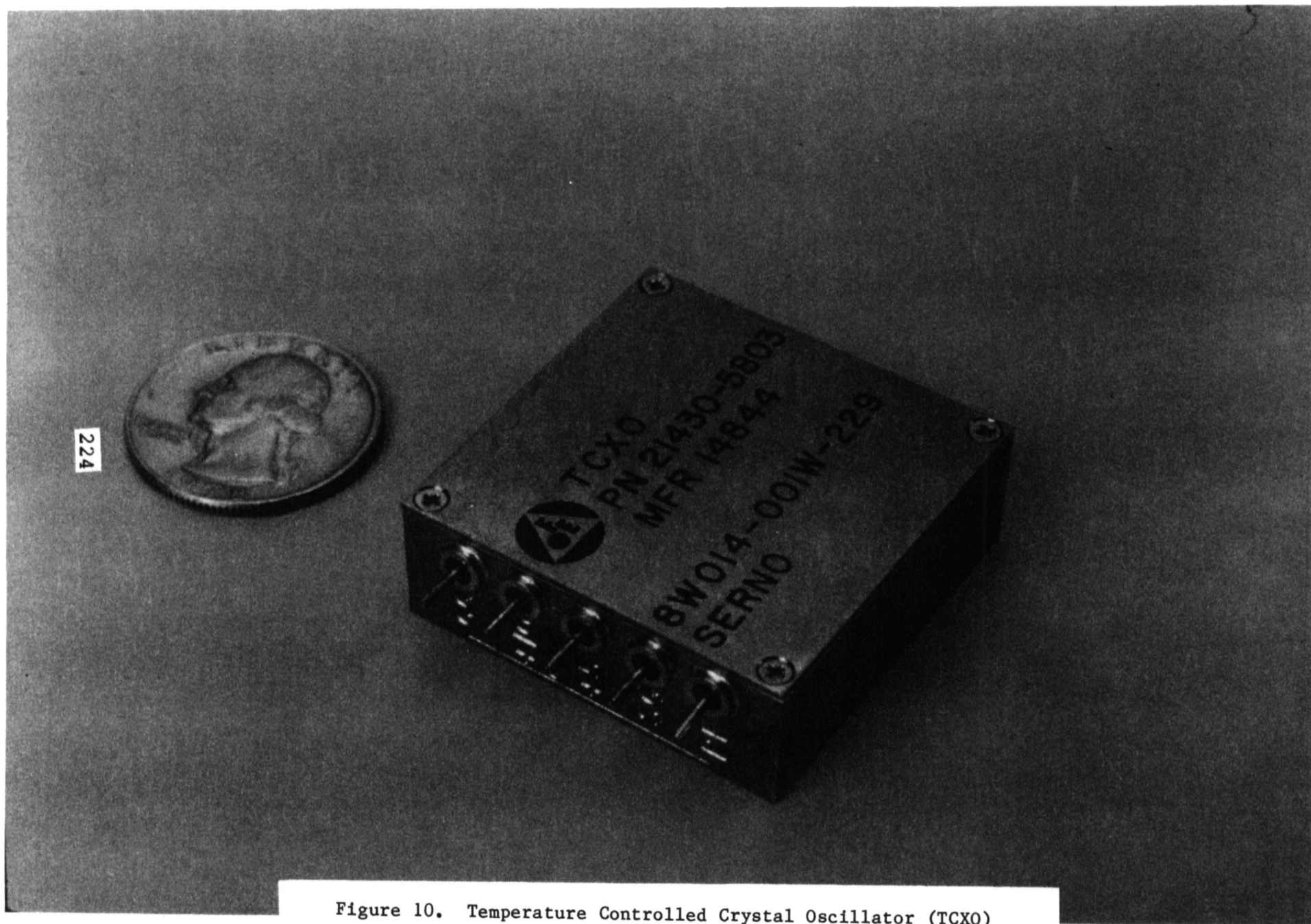


Figure 10. Temperature Controlled Crystal Oscillator (TCXO)
Model FE-8134A

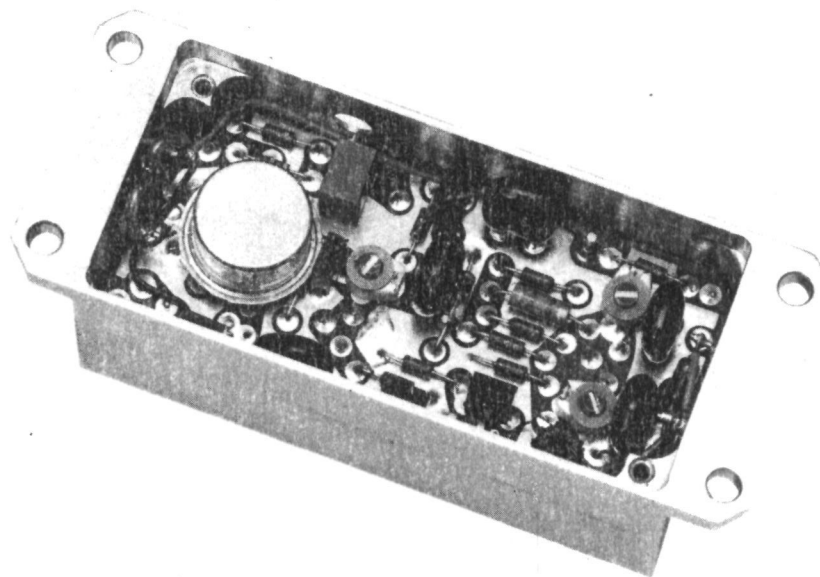


Figure 11. Temperature Controlled Crystal Oscillator (OCXO)
Model FE-8137B
Patriot Missile

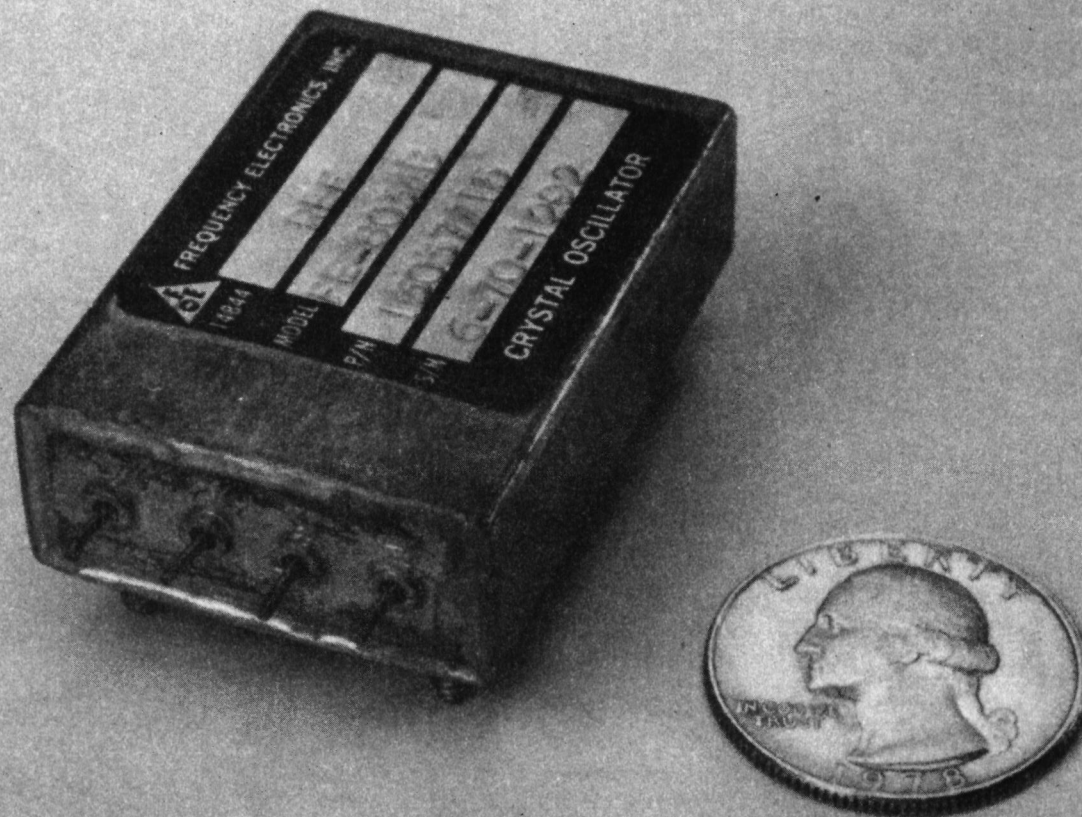


Figure 12. Temperature Controlled Crystal Oscillator (TCXO)
Model FE-8034B
Pioneer 10 and Pioneer 11

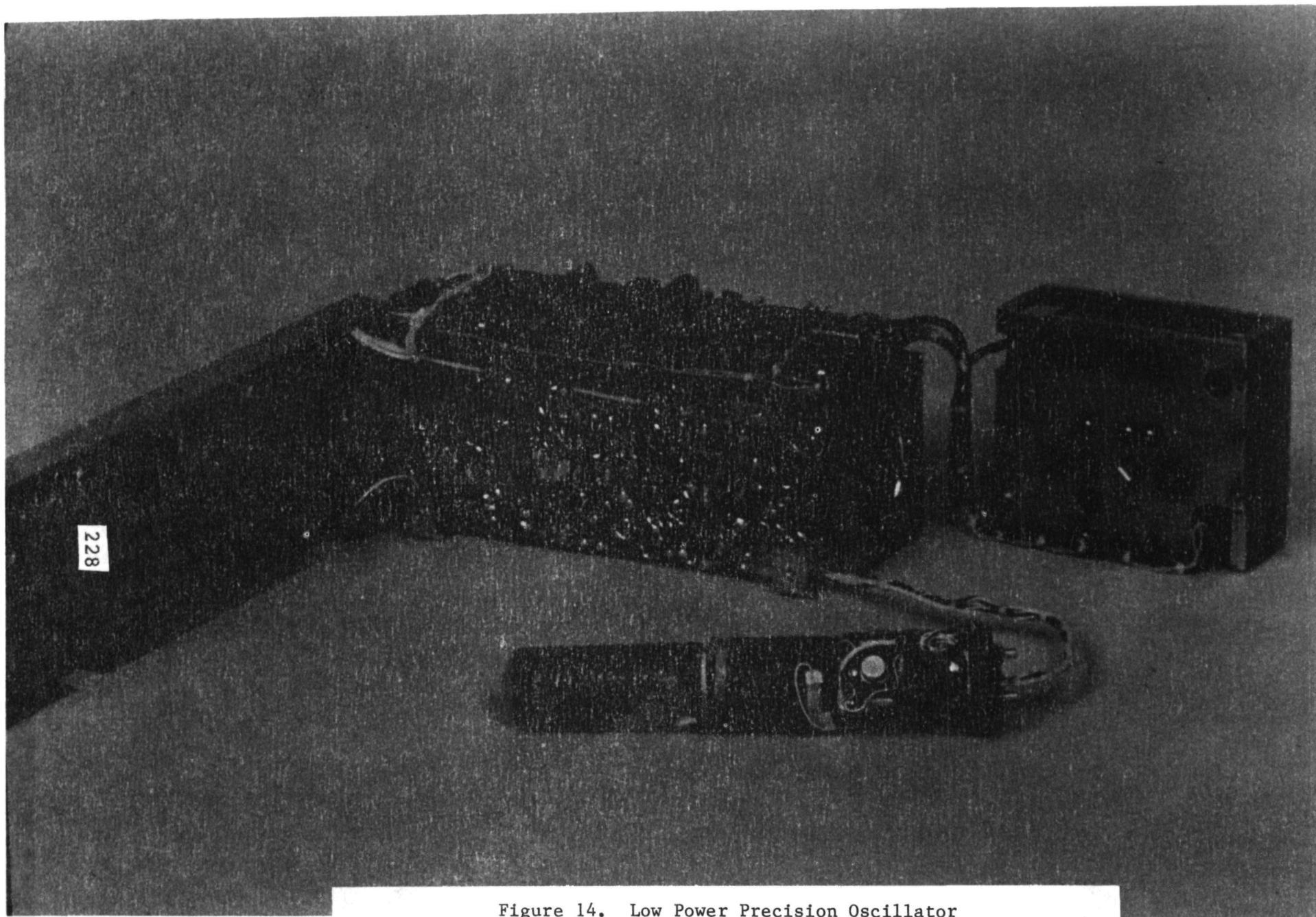


Figure 14. Low Power Precision Oscillator
Model Fe-10A-MOD-L
Timation I and Timation II

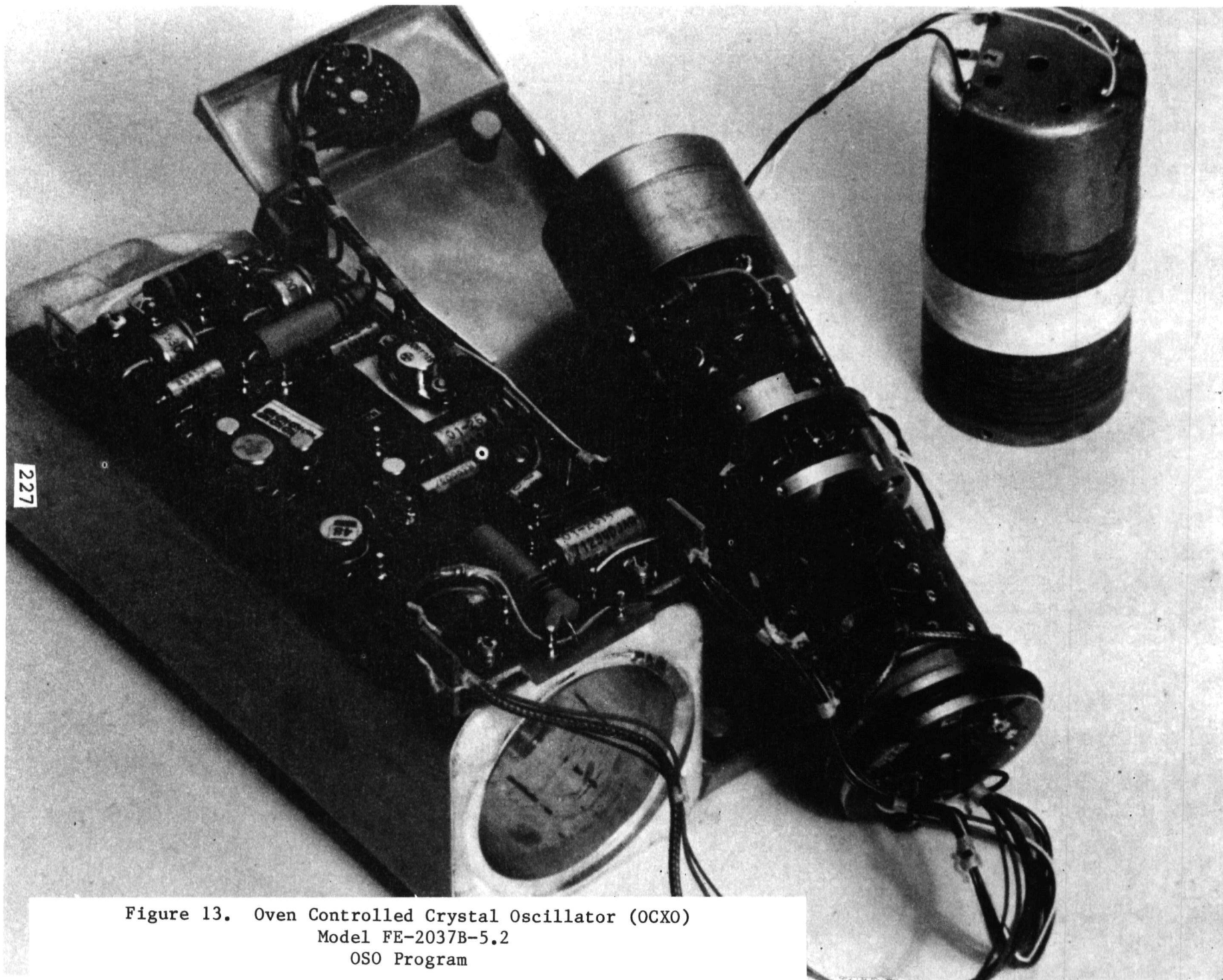
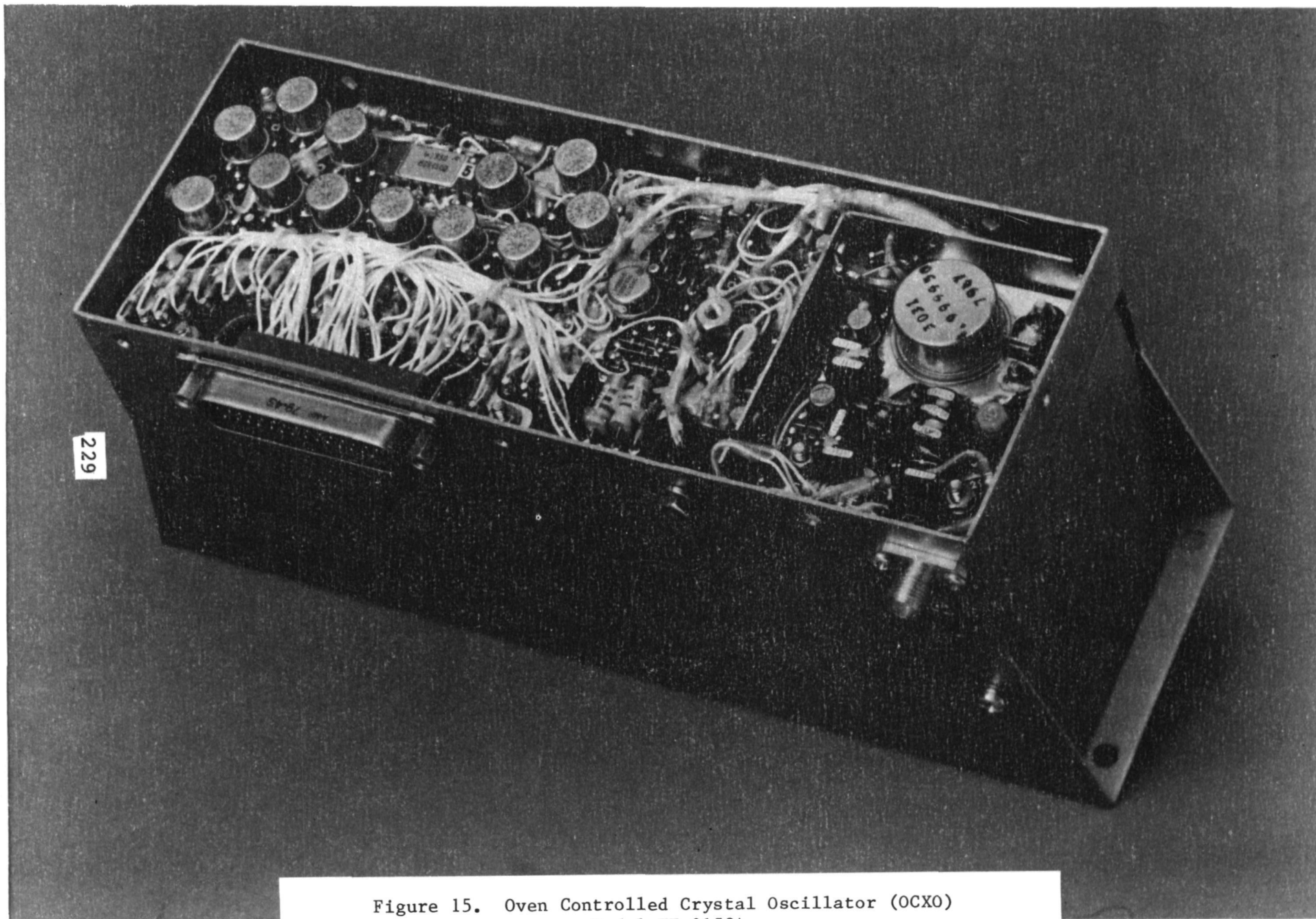


Figure 13. Oven Controlled Crystal Oscillator (OCXO)
Model FE-2037B-5.2
OSO Program



229

Figure 15. Oven Controlled Crystal Oscillator (OCXO)
Model FE-2158A
HS 350

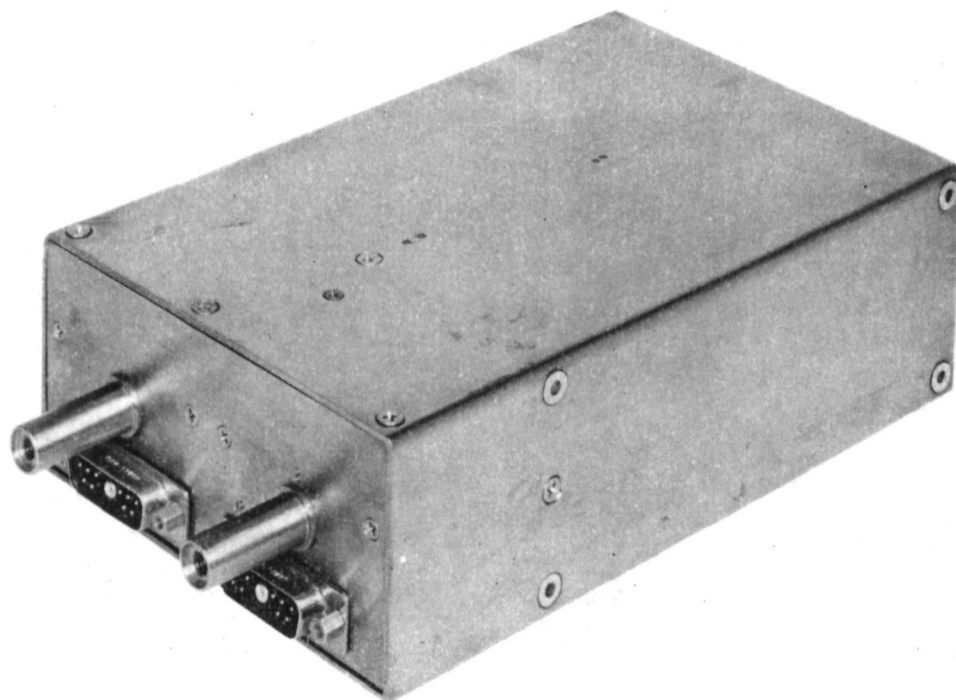


Figure 16. Ultra-Stable Oscillator (OUS)
Model FE-2108A
TIROS N

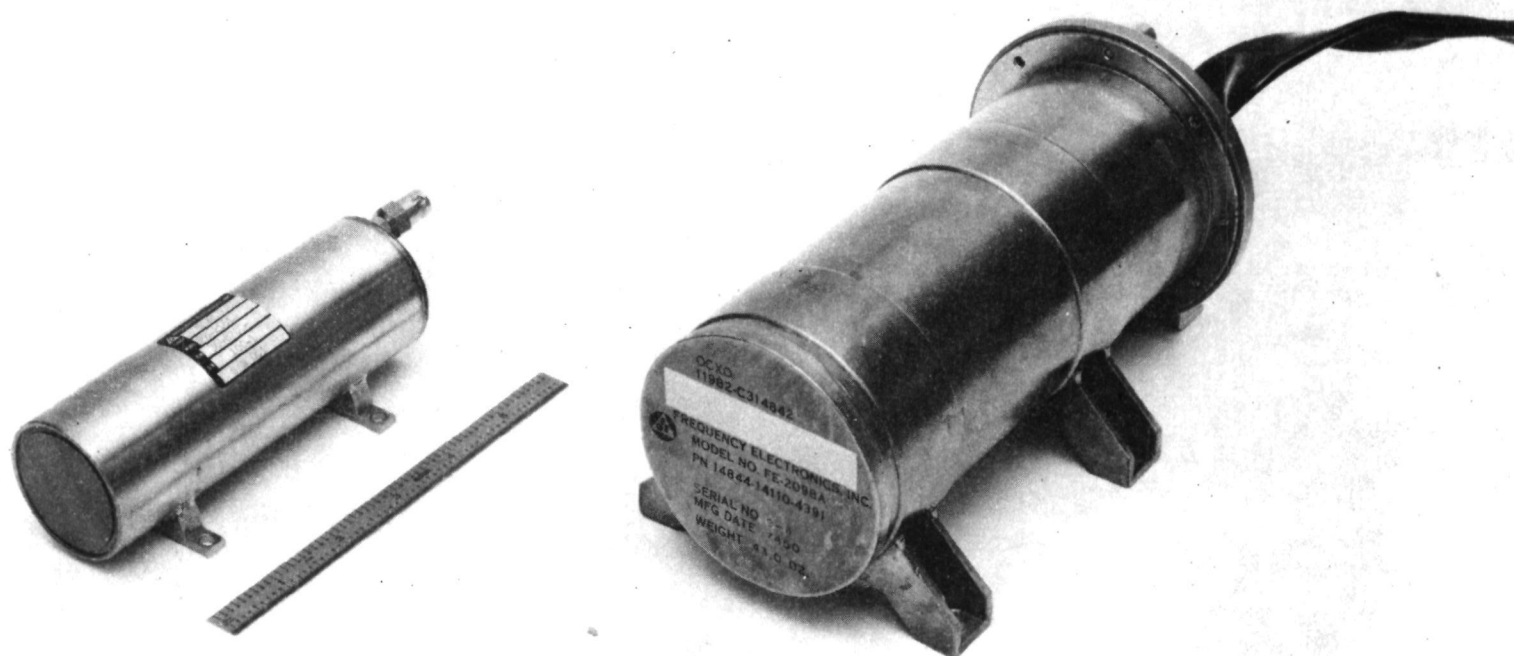


Figure 17. Stable Oscillator (OCXO) Model FE-2161A GALILEO Probe
Program vs. Oven Controlled Crystal Oscillator (OCXO)
Model FE-2098A FLTSATCOM

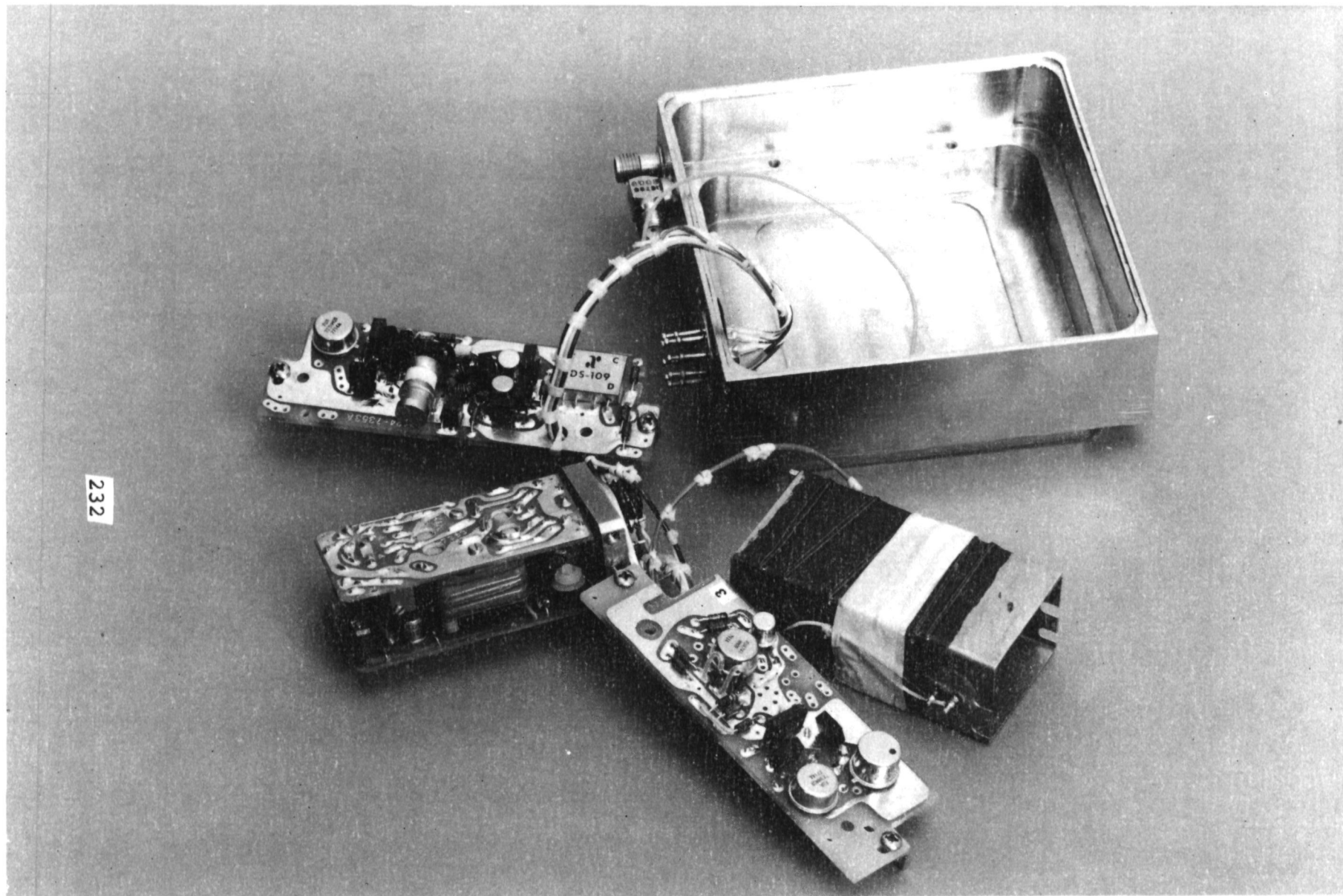


Figure 18. Fast Warmup Crystal Oscillator, SC Cut
Model FE-2163A

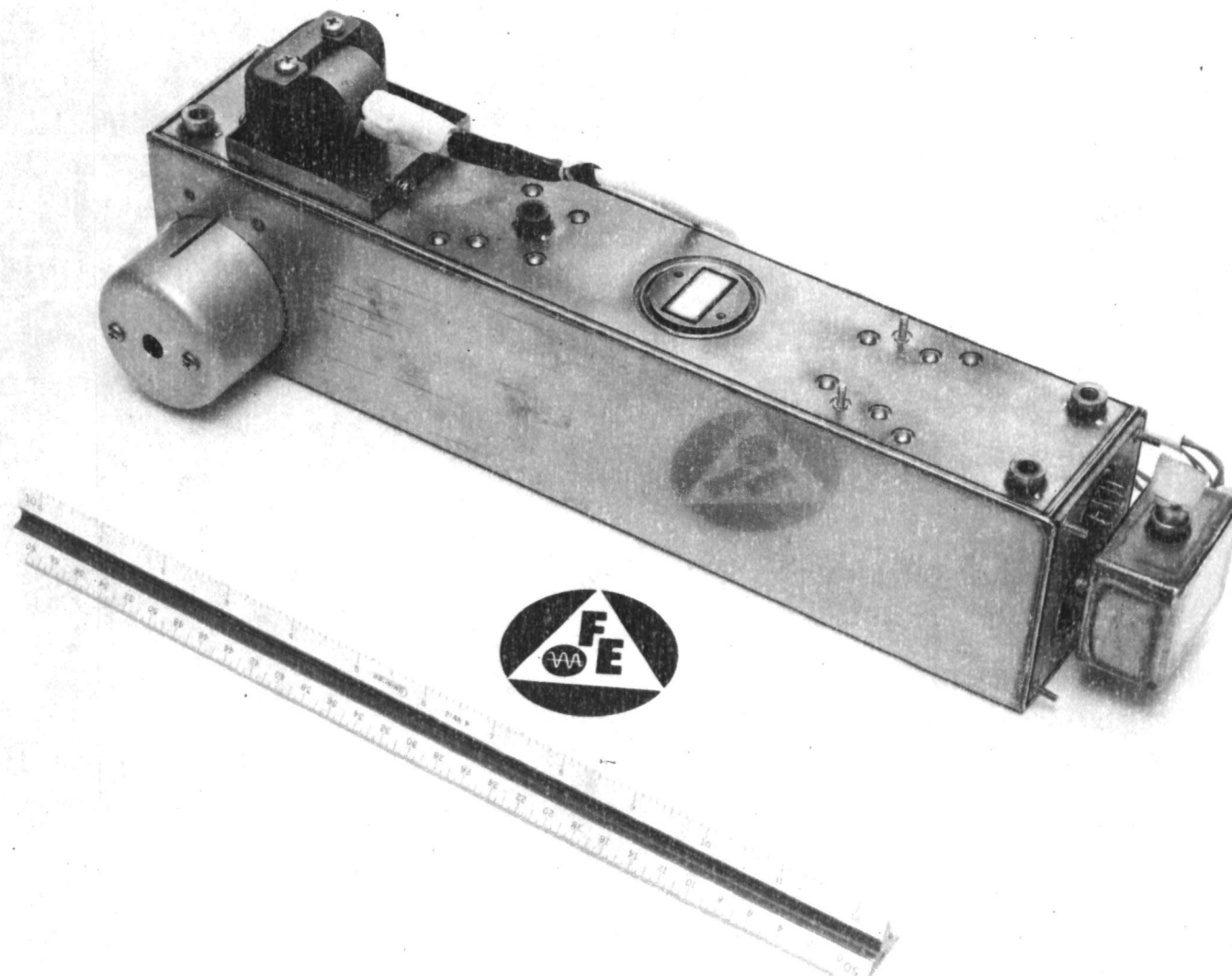
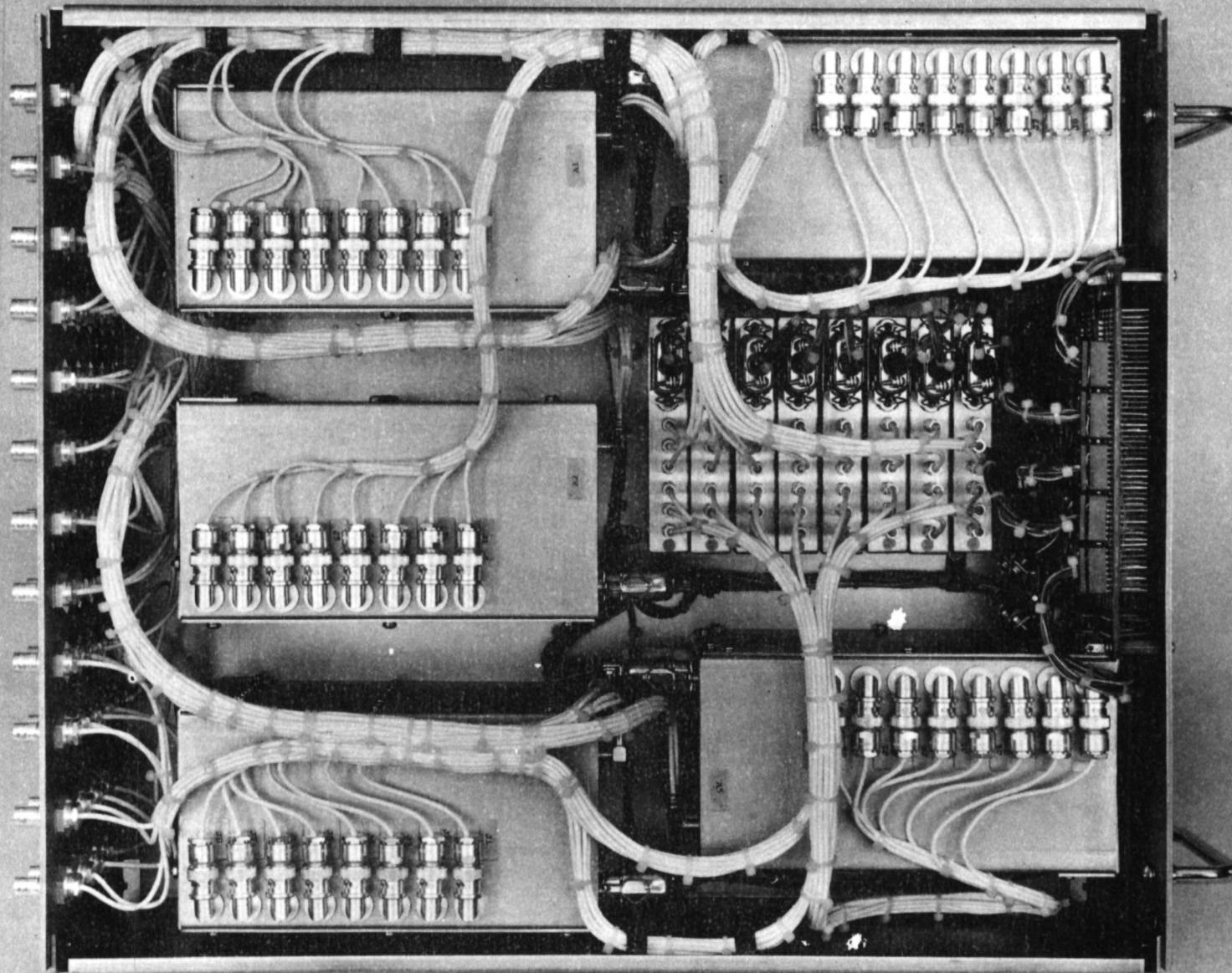


Figure 19. Lightweight Cesium Beam Tube Resonator
Model FE-6203A



234

Figure 20. Automatic Test Equipment (ATE)
Switch Matrix, Top View
Model FE-7707A

235

Figure 21. Selector Unit, Timing Standard, SA-2239/WLQ-4(V),
Precise Time and Time Interval Switch (PTTIS), Bottom View
Model FE-5055A
Cutty Sark

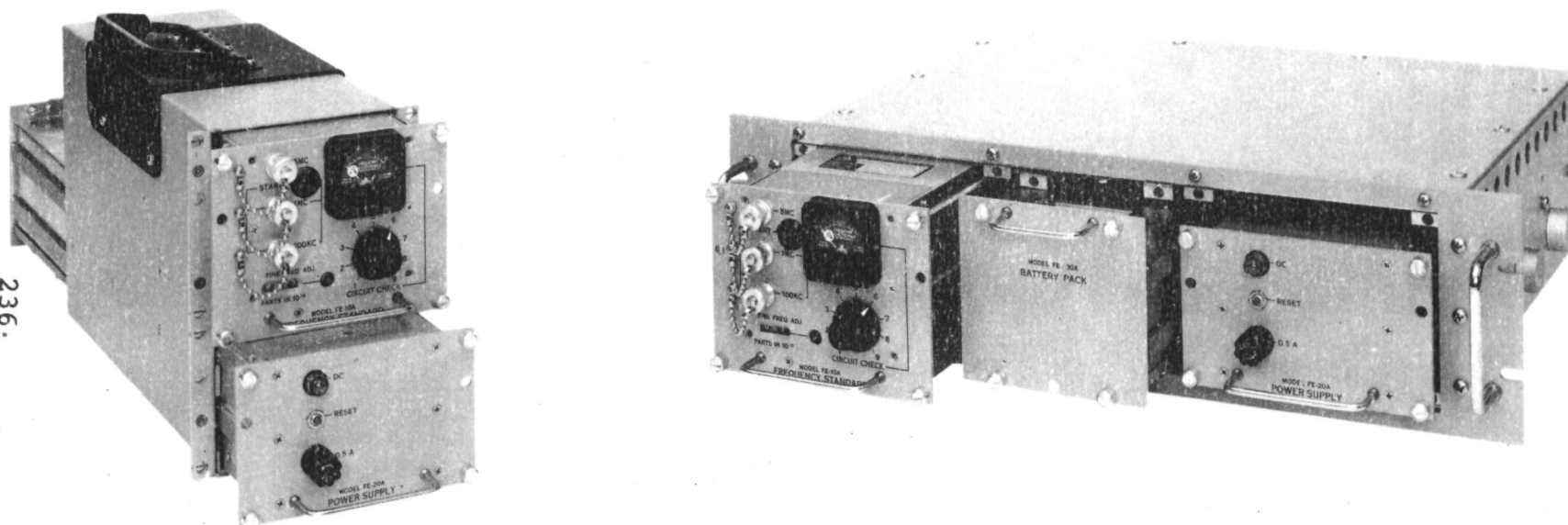


Figure 22. Frequency Standard
Model FE-1000Q
AN/URQ-10A

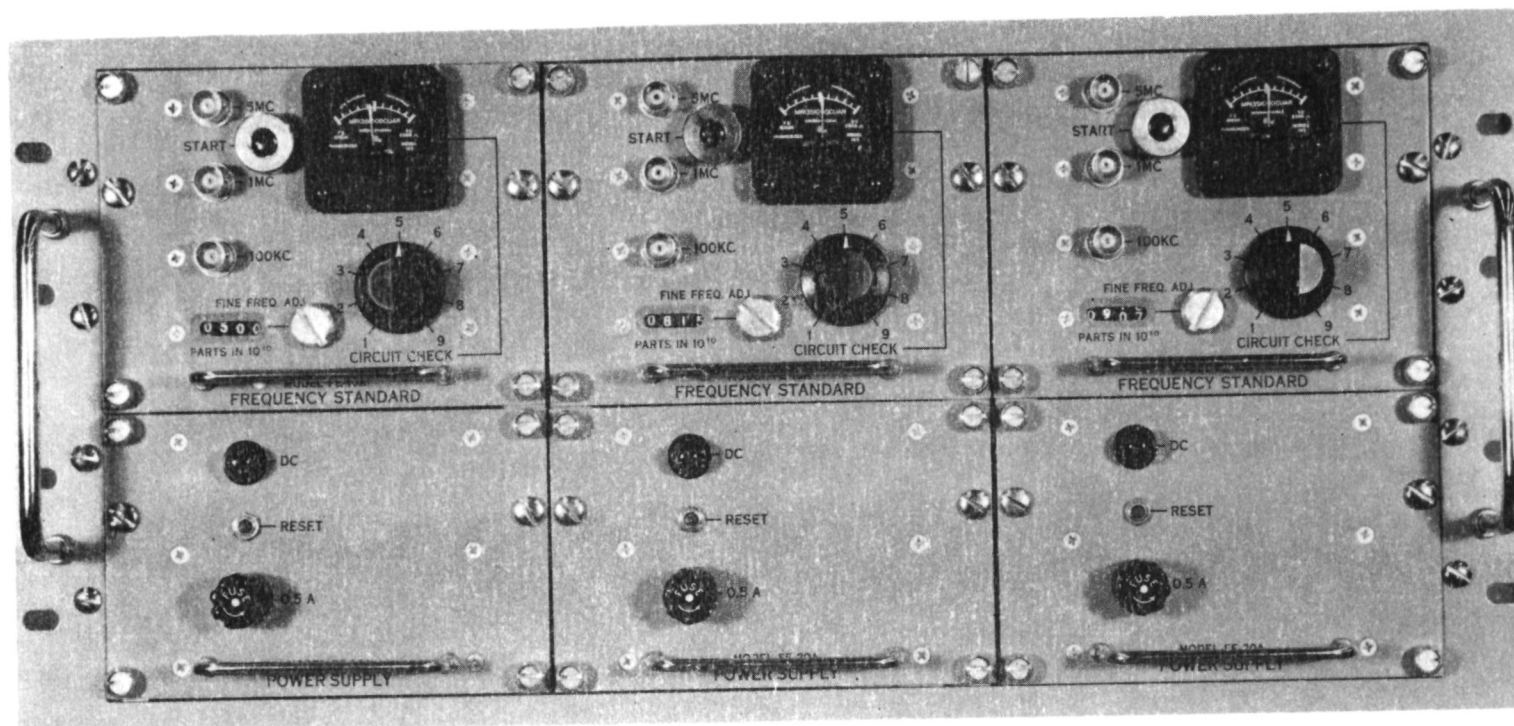


Figure 23. Three High Stability Frequency Standards
 Model FE-1000Q
 AN/URQ-10A

238

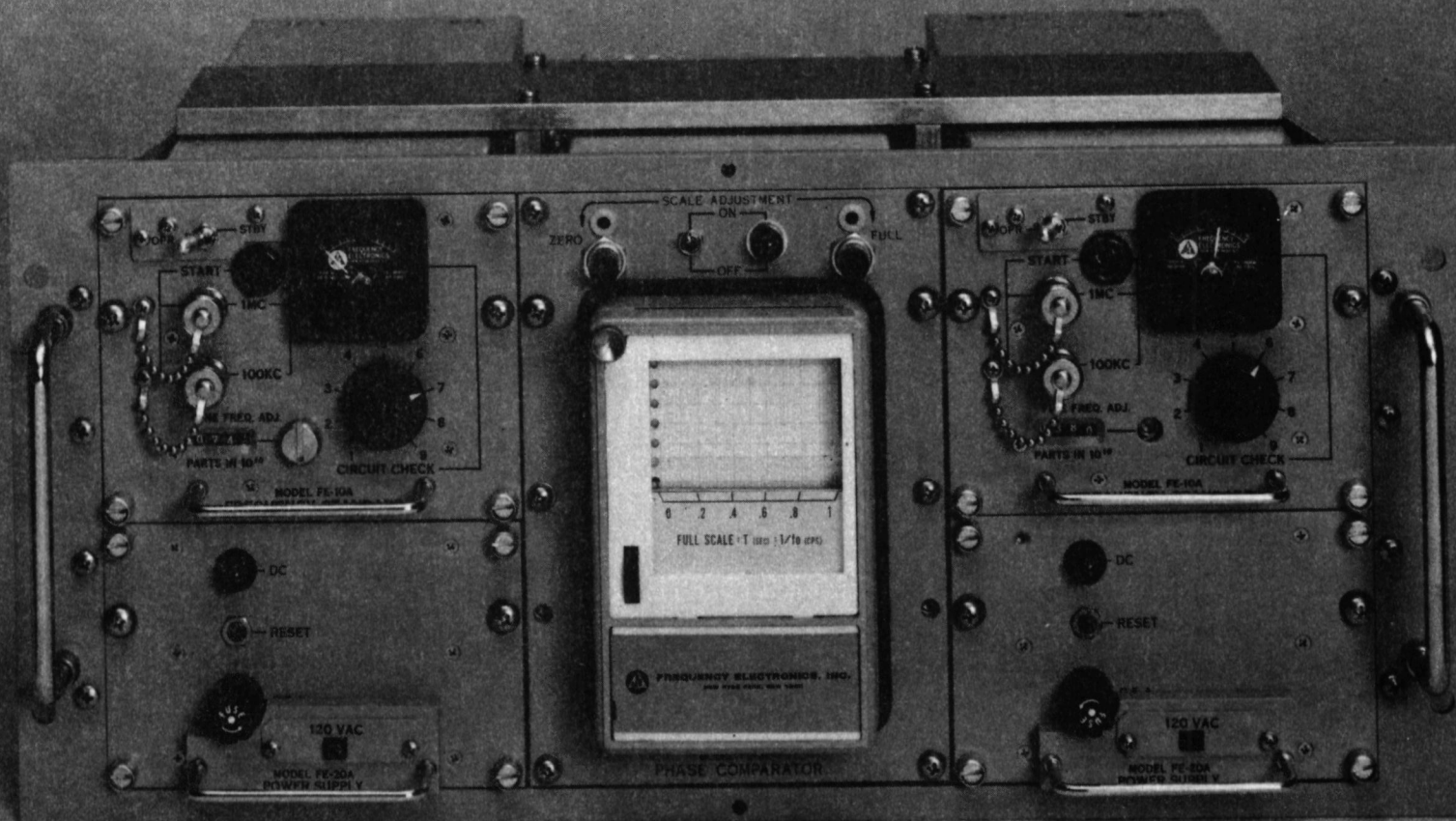


Figure 24. Frequency Generator Unit (FGU)
Model FE-5066A
NATO III



Figure 25. Disciplined Time Frequency Standard
Model FE-1050A
AN/URQ-23

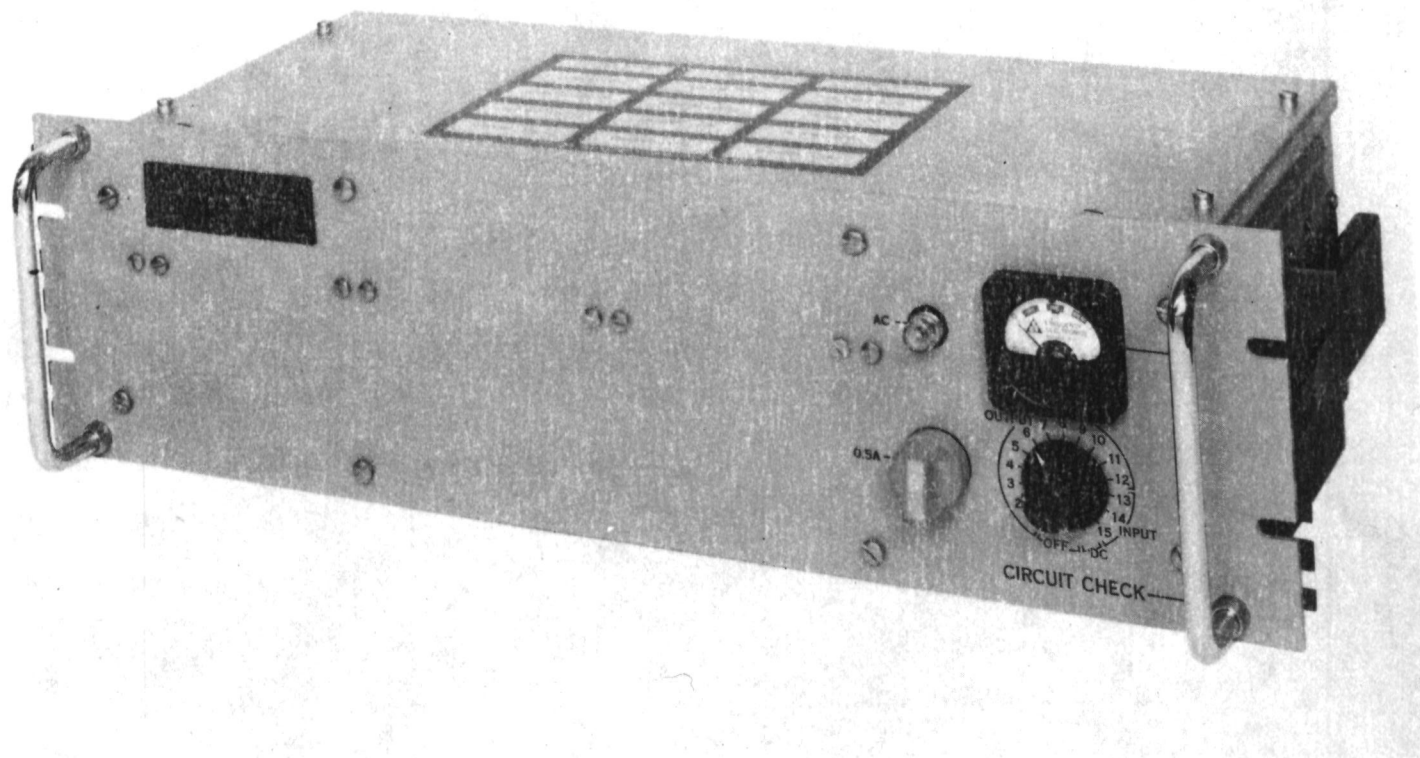


Figure 26. RF Amplifier (12 Channel)
Model FE-70Q
AM-2123A(V)/U

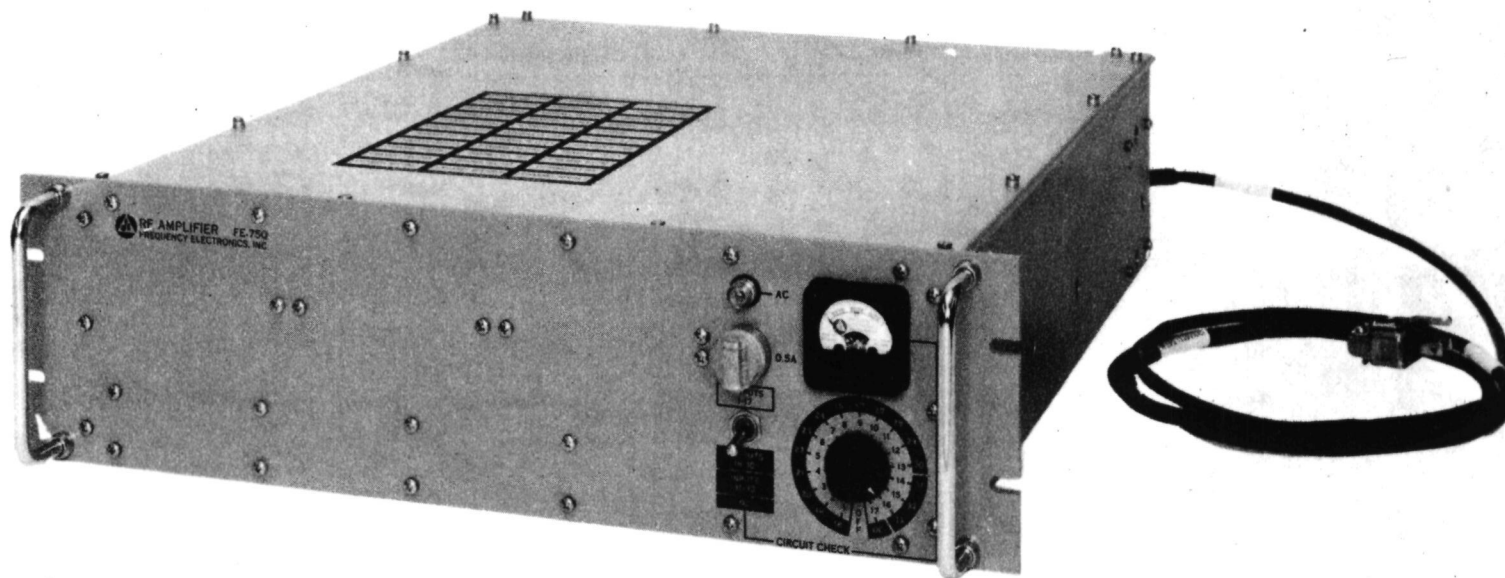


Figure 27. RF Amplifier (30 Channel)
Model FE-75Q

242

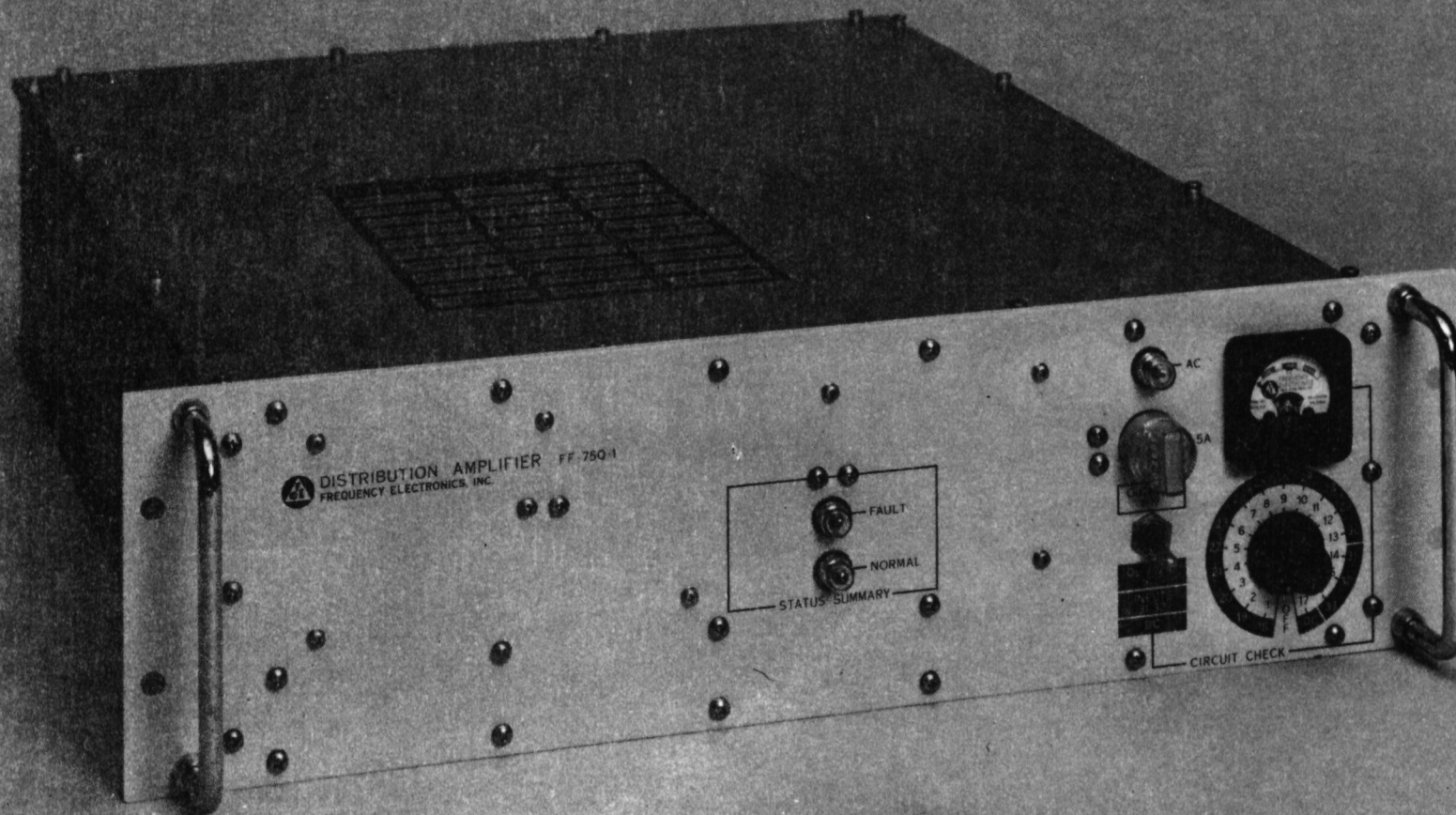


Figure 28. Distribution Amplifier (30 Channel)
Model FE-75Q-1

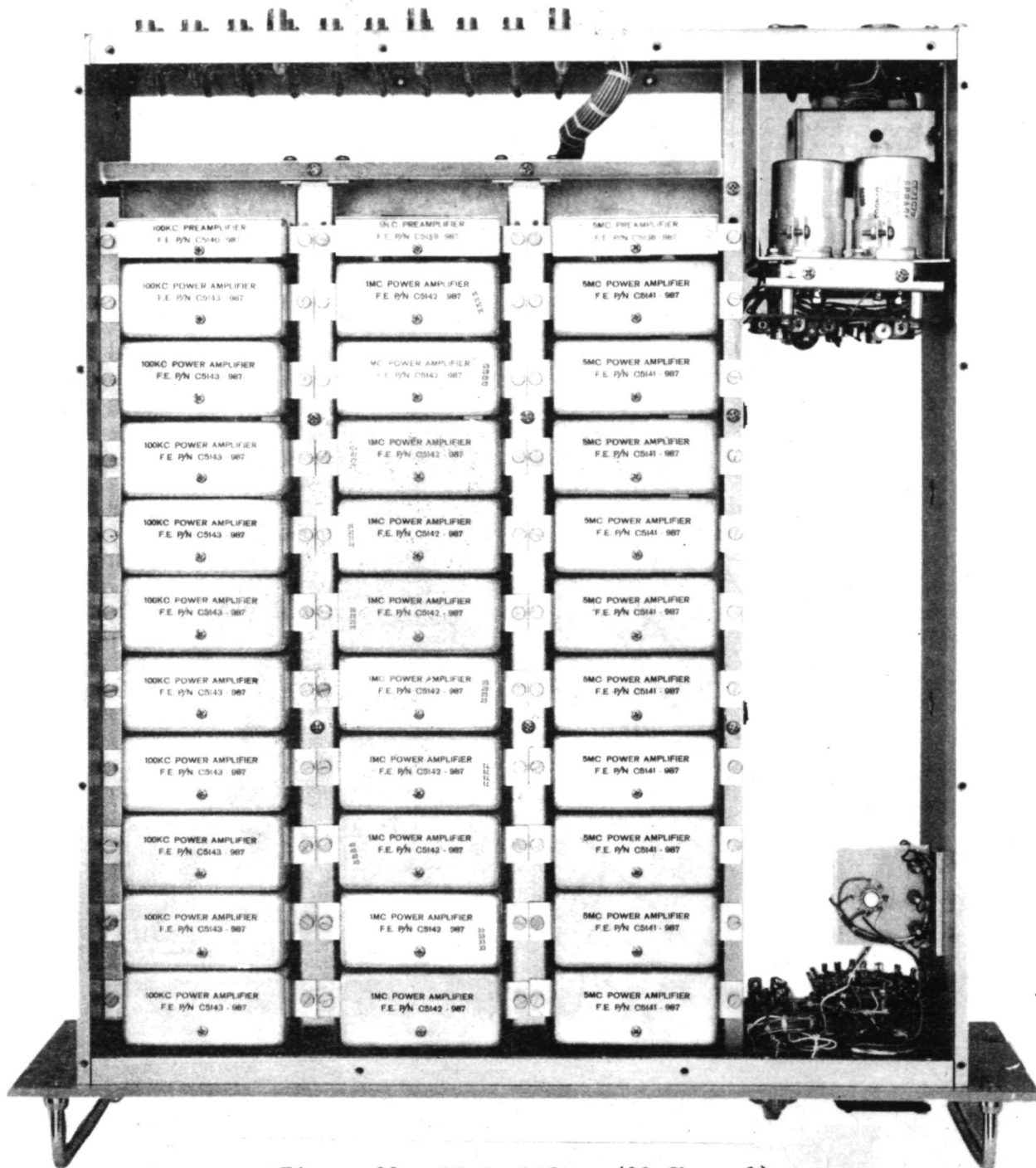


Figure 29. RF Amplifier (30 Channel)
Model FE-75Q

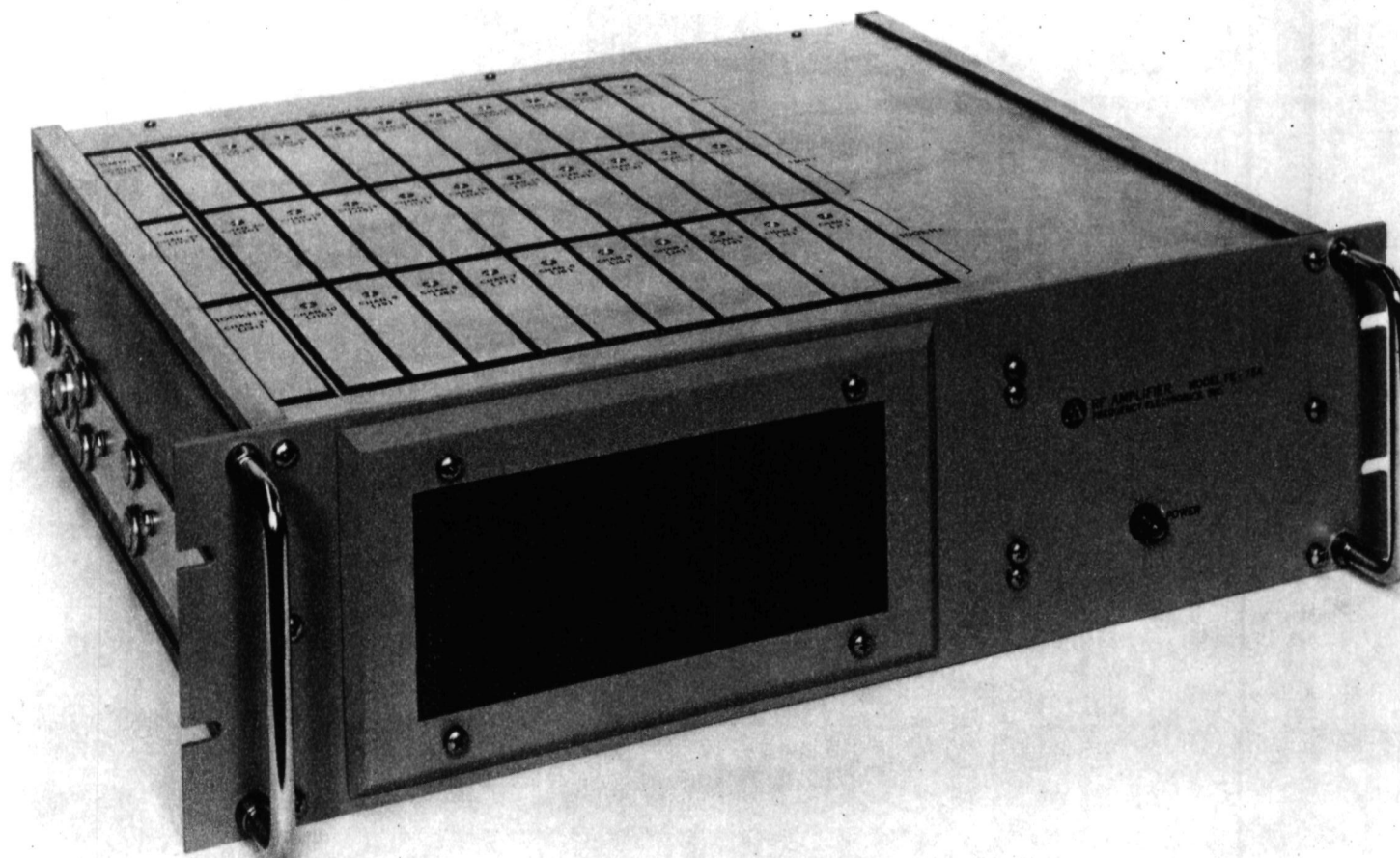


Figure 30. RF Amplifier (30 Channel)
Model FE-75A
TINKER

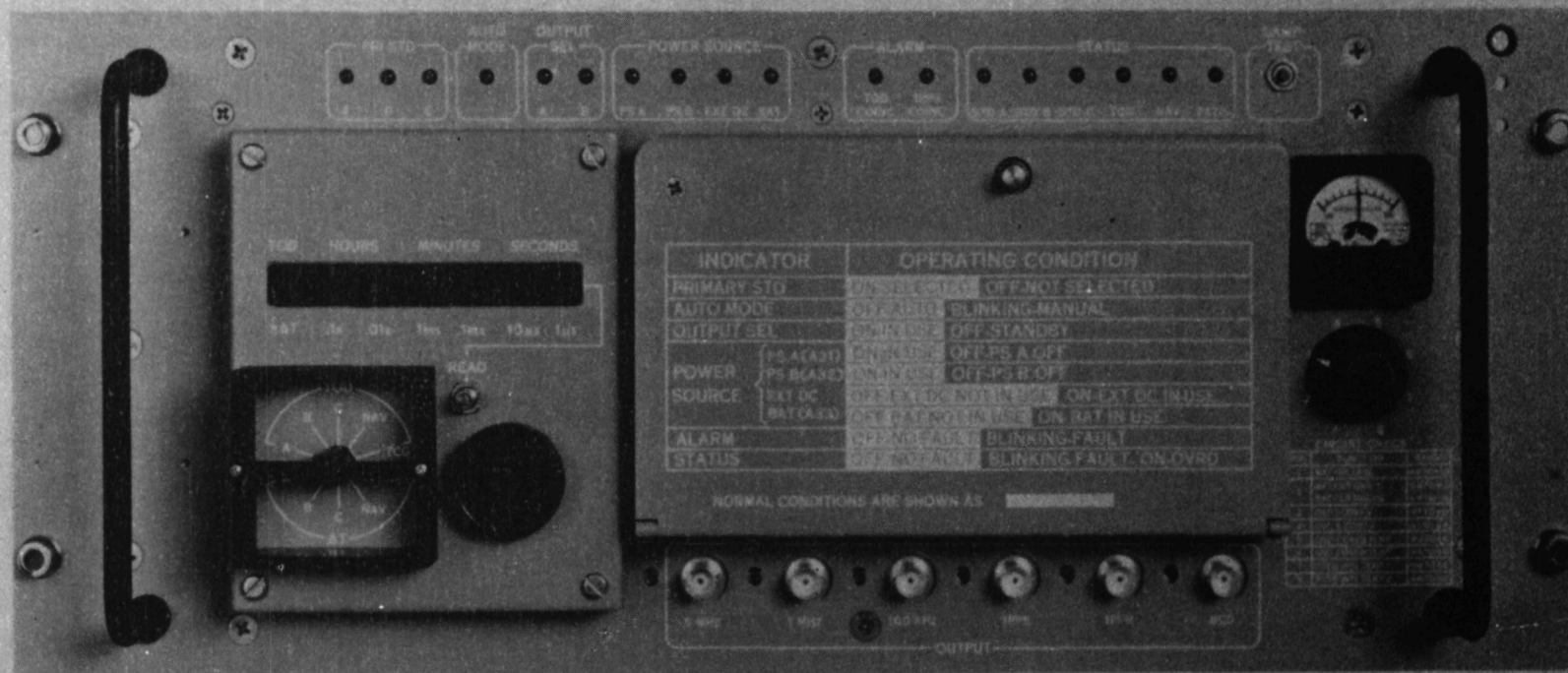


Figure 31. Selector Unit, Time Standard, SA-2239/WLQ-4(V),
Precise Time and Time Interval Switch (PTTIS), Front View
Model FE-5055A
Cutty Sark

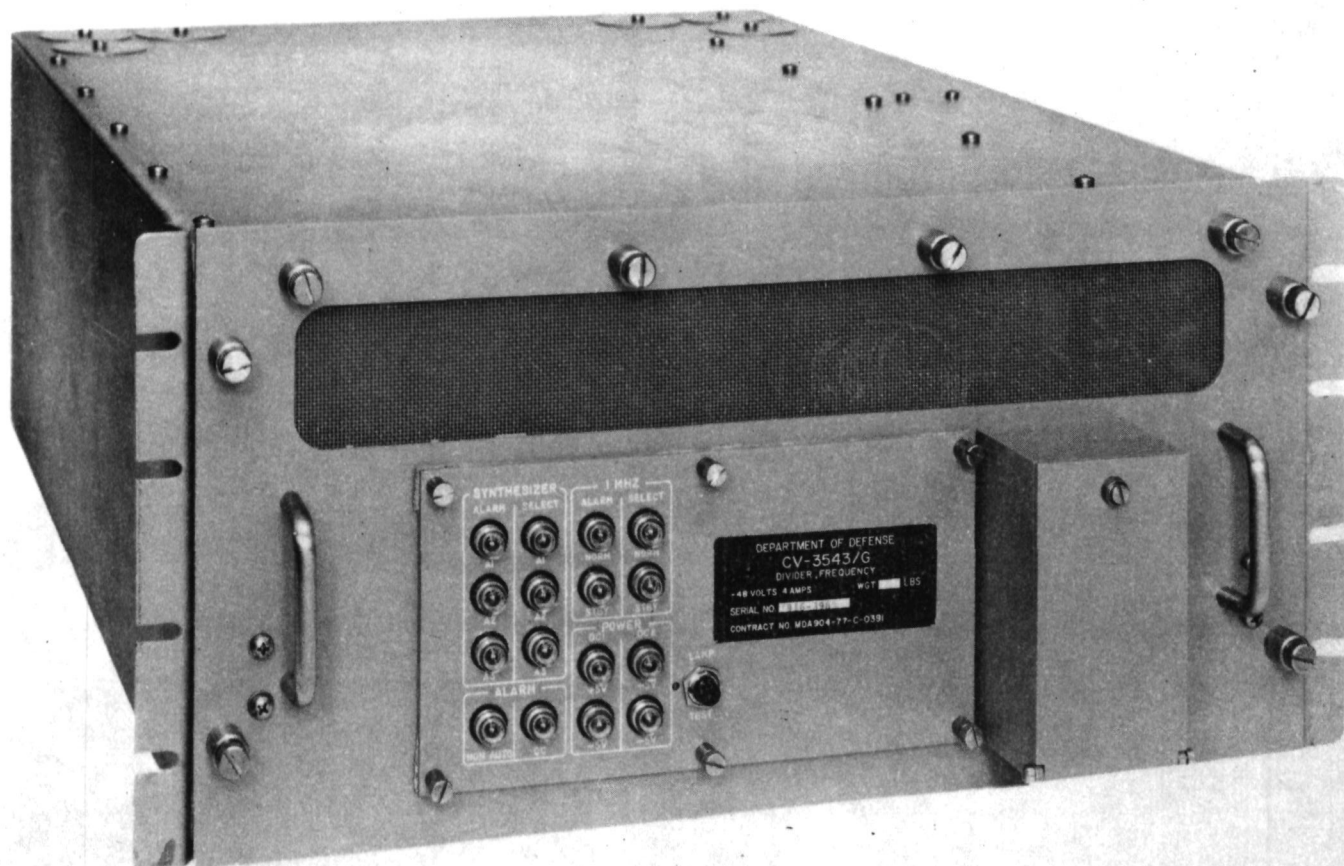


Figure 32. Frequency Divider
Model FE-7036A
CV-3543/G

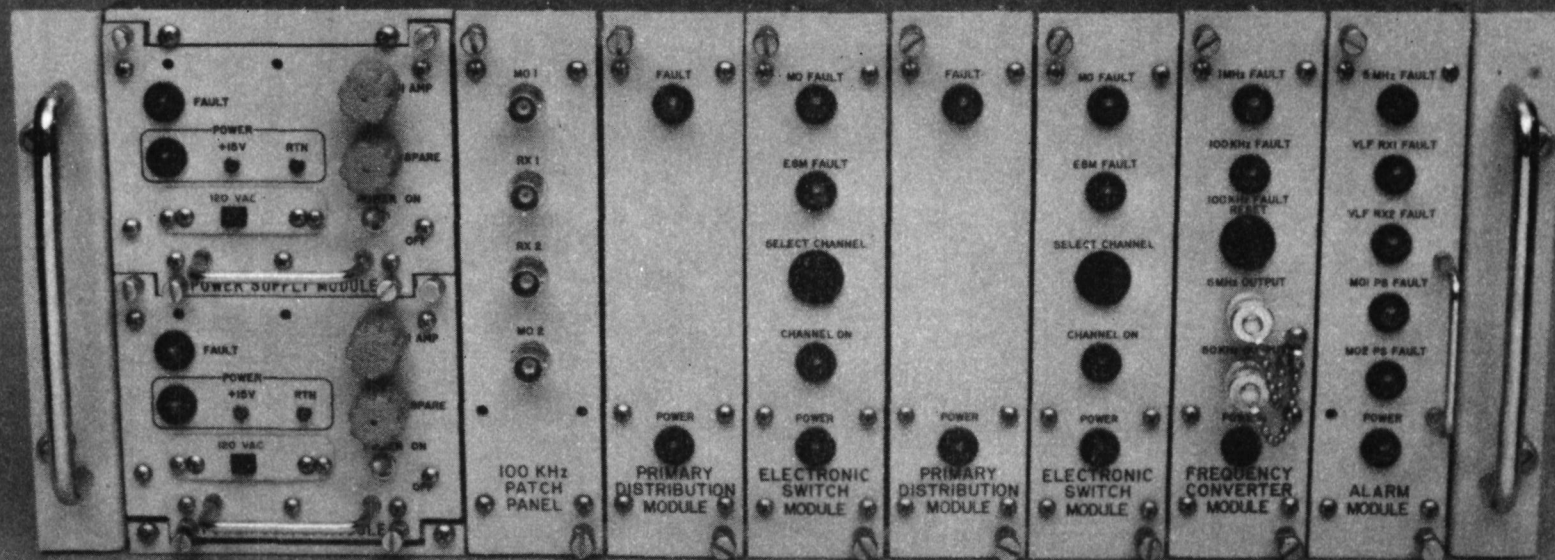


Figure 33. Primary Distribution Unit
Model FE-798A
NATO III

248

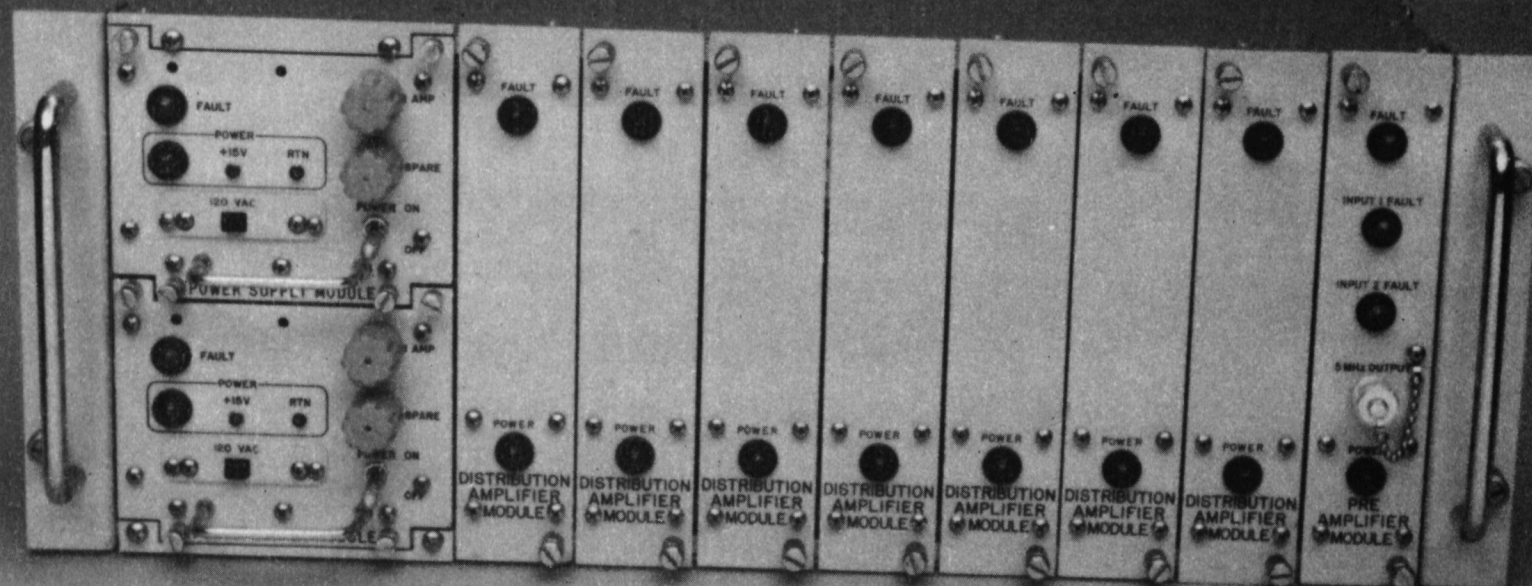


Figure 34. Secondary Distribution Unit
Model FE-799A
NATO III

QUESTIONS AND ANSWERS

CHAIRMAN STOVER:

Are there any questions?

MR. JOSEPH MURPHY, Westinghouse

Could you give us some explanation as to why the quality of the synthetic quartz has declined over the years?

MR. BLOCH:

What has happened has been an inbreeding process. You see, most of the early synthetic quartz has been grown on natural seeds that were gathered from very large pieces of quality quartz which were available in abundance. As time progressed, the seeds for the new generation of quartz material has been grown on synthetic seeds, and there has been an inbreeding process.

The inbreeding process has really destroyed the manufacturability of the crystals. We throw out one out of four bars of premium material, and then we throw out 40 percent of the resonators due to imperfections in the materials due to softness or radiation.

But it is due to inbreeding processes. I think John Vig might be able to comment on this. He has been studying it for the Army and Nick Yannoni of the Air Force.

MR. VIG:

I think you are right. The manufacturers don't have an incentive to grow this quartz because 99.999 percent of all applications are met by the currently available quartz.

For every ultra precision resonator sold, there are probably a million low quality resonators sold. For very low cost units, there are probably 10,000,000 parts sold, so they don't have the incentive to grow quartz.

MR. BLOCH:

Total needs of DOD of this precision quartz, I think, is 4,000 pounds a year and that is a very small bucket compared to about a million pounds of quartz that are now manufactured worldwide each year.

MR. MURPHY:

One more question. How many resonators would you say you have made over the past 18 years?

MR. BLOCH:

We have been manufacturing resonators since 1968 so that it is 12 years. I would estimate about 30,000.

MR. MURPHY:

Is that synthetic quartz?

MR. BLOCH:

We are primarily servicing the aerospace industry so most of our units have been premium Q swept-synthetic quartz because we are looking for radiation hardness whenever we launch into space. I would say 80 percent of the resonators that we have made are made of premium Q. For your programs under 616 A, you absolutely insist that it be premium Q-swept material for Westinghouse.

DR. WINKLER:

Mr. Bloch has been tactful enough to be silent about the real reason why the synthetic quartz degraded over the years. It is that the government has become less competent. But seriously, I think that we owe you thanks for pointing out a real serious problem. In fact, this is precisely the kind of problem which caused us to make a major effort a couple of years ago to get a requirements analysis funded.

That is precisely the direction which I think we must take in order to streamline our efforts. Government today is fragmented because of a jungle of conflicting organizations, processes, laws, regulations, what have you.

I think Dr. Yannoni has pointed to some of the difficulty that the best thought-out plans inevitably after two years become modified.

Also many of the people who write specifications and requirements, have never done designing or developing themselves. So, they do not appreciate the fact that even the slightest change can cause untold disasters. Now, you cannot blame people for adding specifications because they simply do not have enough qualified people at hand today. I think we are coming to some real limitations:

how do you organize, what can we do about planning and procurement and development, a better standardization of building blocks; that, I think, is really a big problem.

Why don't you as a bidder, when he is faced with unreasonable trivial requirements like "I want to have five more lights and seven more screws and a connector at the bottom." Why don't you say, "Look, this is my standard equipment. You can have that for \$2,499.95. Your special requirements will make the price \$6,000 per unit. Take it or leave it."

MR. BLOCH:

We do it all the time, Dr. Winkler.

DR. WINKLER:

Well, I tell you, the unfortunate part of it is that the small user doesn't give a damn. He will have his own design, independent of cost. Yesterday I had the occasion to see a new aerospace application for a classified satellite. An extended TCX0 was available which will meet all the requirements but has a height of .8 inches; but the spacecraft designer decided that all the slices are going to be .55 inches high, so we are going to spend another 100K re-designing a TCX0.

MR. BLOCH:

There is another point that this industry has faced over and over again. There was a meeting a couple of years ago where it was said, "We, the government, have the needs. Why doesn't private industry go ahead and develop reliable clocks for use that will be available?" I have explored this approach in great length. The future quantities needs are so small or so wild that it is very difficult to get private capital to commit to really meet the future needs.

When you are strictly a military supplier -- and we have tried hundreds of times with the distribution amplifiers -- saying, "Here is a standard product. Use it." No, we want the blue panel. We want an extra two lights. So, I think we need to talk with each other more to coordinate future needs.

Page Intentionally Left Blank

GOVERNMENT AND INDUSTRY INTERACTIONS
IN THE DEVELOPMENT OF CLOCK TECHNOLOGY

Helmut Hellwig
Frequency and Time Systems, Inc.

ABSTRACT

It appears likely that everyone in the time and frequency community can agree on goals to be realized through the expenditure of resources. These goals are the same as found in most fields of technology: lower cost, better performance, increased reliability, small size and lower power. This paper focuses on related aspects in the process of clock and frequency standard development which sees government and industry in a highly interactive role. These interactions include judgments on clock performance, what kind of clock, expenditure of resources, transfer of ideas or hardware concepts from government to industry, and control of production. The author believes that successful clock development and production requires a government/industry relationship which is characterized by long-term continuity, multi-disciplinary team work, focused funding and a separation of reliability and production oriented tasks from performance improvement/research-type efforts.

THE CLOCK HIERARCHY

Figure 1 shows the existing clock hierarchy, a commonly accepted ranking of clock types.¹ This ranking is not only based on the physical characteristics but also on the technology used; i.e., the crystal resonator, the rubidium gas cell, the cesium beam tube and the hydrogen storage bulb maser. We must remember that any of these concepts or atoms can be used in different combinations as we will discuss later.

This ranking of today's principal precision clocks and frequency standards is meaningful as shown in Figure 1. Listed is the typical best stability or flicker of frequency floor, σ_F , as well as the typical Q values. Figure 1 shows that increasing Q's ranging from 2 million with a crystal resonator to 1 billion with the hydrogen

storage bulb, correlate¹ to frequency stability improvements from 1×10^{-12} to 3×10^{-15} . However, we also note that size and cost correspondingly increase. Thus, we conclude that the ranking of today's frequency standards may not necessarily be based on a fundamental difference governing the crystal resonator vs. the rubidium atom vs. the cesium atom vs. the hydrogen atom but rather on particular technical realizations. They lead, on one end of the scale, to small acceptably performing devices at affordable costs and, on the other end of the spectrum, to very high performing device at substantial sacrifices in size and cost.

Historical developments have indicated² what would happen if we dropped this ranking and attempt to use these existing principles to realize either higher performance as in the case of rubidium or cesium, or lower size and cost as in the case of hydrogen storage. The basic results of these efforts are shown in Figure 2. The Q and, with it, the best frequency stability σ_F can be increased for rubidium and cesium; however, at increased cost and size. The size and cost of a hydrogen device can be decreased; however, at a sacrifice in performance. Furthermore, Figure 3 shows that nearly all of the different atoms have been subjected to the three fundamentally differing basic technologies;^{2,3,4} Beam, storage vessel, and gas cell. In addition, nearly all of the devices have operated as passive resonators serving to stabilize a crystal oscillator or as active oscillators of the maser type. Of special historical interest is the fact that the attempt to interrogate the cesium atom in a storage vessel led to the creation of the hydrogen maser;⁵ a decade later, the idea of pursuing the possibility of a cesium maser led to the passive hydrogen maser principle.^{6,7}

We may conclude from Figure 1 through 3 that there is no fundamental relationship between superior performance nor cost nor size and the particular atom or physical principle which is used, but rather that the combination of expenditure of funds in a historical chain of events is largely responsible for today's device-hierarchy.

Furthermore, it is not a foregone conclusion that very high performance in small size must be created by reducing the size of high performance devices; it may be as well to focus on performance enhancement of devices already small. Therefore, openness of mind is very much in order when judging new ideas and proposals to improve parameters ranging from stability performance to environmental insensitivity to size and cost. It just may be that a truly new idea may change an old principle of a "down-rated" atom into the best solution possible.

IDEAS AND SELECTION CRITERIA

New ideas can fall in the areas of basic research, applied research or engineering. A new idea may be basic, or it may be a solution to an existing or perceived problem, or it could be the revival of a once discontinued or discarded idea. Independent of this classification, there are four basic questions which may be asked and should be answered before resources are expended. By "resources" we mean either an approved program within a government laboratory or the funding of a program in industry or elsewhere.

The following should not lead the reader to believe that some research of an undirected nature should not be approved. Such funding, in the author's belief, is essential, but such resources must be expended in a field of technology or in a field of basic science with proposed results reasonably undefined. Resources spent in this direction have proven over the last few decades (and in fact throughout human history) to be one of the most worthwhile investments.

We now restrict ourselves to proposed ideas for proposed measurable results. They may be subjected to the four questions listed in Figure 4. These questions are aimed at a sequence of logical attack to determine whether the idea is worthwhile to pursue. One word of caution is in order; the author believes that these questions cannot always be unambiguously answered; however, if the answer is clearly a "no" for A or B, and a "yes" for C or D, no resources should be spent. An example from the mid 60's is the thallium beam.⁴ It was pursued as a cure to perceived bad aspects of cesium. As we know today, the thallium beam research was terminated a long time ago and cesium beams are still around. Figure 4 gives the scenario to questions A through D which could have been answered before any expenditure of resources in this particular case in the early 60's.

An idea which is a revival of an old idea is not necessarily bad: the old idea may have been discarded because of limitations of technology at its time, or the revival of the old idea may be worthwhile because other new ideas have created a different scenario. However, there seems to be a set of ideas which appear regularly. These are listed in Figure 5. This is not a complete list but might serve to illustrate further the questions of Figure 4. These ideas remain "new" because the questions listed in Figure 4 have seldom or never been applied to these ideas. The pretense of "new" is no reason in itself to expend resources. The author's favorite is "small size". Question C here is very appropriate; does it introduce a new problem? Using the same physical technology,

reducing the size uniformly lowers the Q . As we have seen from Figures 1 and 2, the Q is linked to the best frequency stability of atomic or crystal clocks. If the very small rubidium cell or the short cesium tube or the small hydrogen bulb lead to reduced Q , it is an illusion to believe that the stability performance of the original full size device can be retained.

Figure 6 shows the history of passive hydrogen development. This is an interesting example involving the author in a very intimate way. In 1969, at the National Bureau of Standards, D. Halford asked the author about the pro's and con's of adapting the maser principle to the cesium beam. The resulting analysis took several months of fruitful discussion and led to the idea of the passive hydrogen resonator device: the limitations of the hydrogen maser in long-term were cavity pulling; this effect was highly reduced in a passively operating device, especially if particle interrogation was used.⁷ The author then experimented with the hydrogen storage beam but ran, as did the pure beam⁹ work of H. Peters at NASA, into problems which were related to the difficulties of efficiently detecting hydrogen atoms. Thus, the future of the hydrogen storage beam is critically dependent on the availability of efficient hydrogen detectors. There still are no efficient hydrogen detectors. However, as soon as this changes, a discarded old idea may become a worthwhile new idea (Ref. Figures 4 and 5).

The author's solution to the detection problem was the concept of the passive hydrogen maser⁸ which does not fully realize the advantage one obtains in cavity pulling (or lack of it) by detecting particles but retains the advantage of a passive device over an active device in this regard. Pioneering work in the electronic design and further refinement of the concept by F. Walls at NBS then lead to experimental realizations of the low cavity- Q , small, passive hydrogen maser and the full size, passive hydrogen maser.¹⁰ These concepts now have lead to several government-funded pursuits of realizations of the passive hydrogen concept¹¹ which include the novel-cavity-mode-small-maser, the dielectric-cavity-small-maser, and the positive-feedback-small-active-maser (a combination of the small, passive maser idea with an old idea realized previously in hydrogen).¹² Thus, the time and frequency community is now dealing with a family of six, somewhat different solutions using the passive hydrogen principle and the expenditure of many millions of dollars with some of the questions previously addressed not asked or answered in full.

THE PROBLEM OF TRANSFER TO INDUSTRY

Transfer to industry for the purpose of commercial or government-need-oriented production appears to be the ultimate goal of most government funded efforts. In fact, most researchers and engineers will agree that a successful transfer to industry would be the ultimate goal of their agencies as well as an important ingredient in their personal and professional motivation. This question can be addressed from various angles. The first is depicted in Figure 7 which illustrates the role of the clock expert. The clock expert is typically an individual with privileged knowledge or background or experience in relation to what is important in clocks. Thus, the clock expert can be characterized as having special knowledge in connection with the physics package (crystal resonator, rubidium optical package, cesium beam tube or hydrogen maser) and with the problems of testing, measuring and characterizing the complete system. Frequently the clock expert also plays an important role in the interface between the physics package and the electronics system of the clock or frequency standard.

In Figure 8 we list organizational modes and probable results. Like all other technology, the making of clocks and frequency standards involves engineering, quality assurance, manufacturing and testing. If an organization has these four functions, such as they are present in most industries, we have the potential of manufacturing; however, due to the complexity of crystal and atomic clocks, the absence of a clock expert may lead to the manufacture of clocks which are beset by fundamental problems. If a clock expert is inserted into the clock making process directly contributing to the creation of hardware, the clock expert will mostly be found in either or both of the following: engineering and testing (based on the specialties of the clock expert as shown in Figure 7). In this role, the clock expert can assure that working clocks are produced but the links to quality assurance and manufacturing are not properly established; thus, there is the potential of working clocks, but only one at a time, plus potential shortcomings in reliability and serviceability. In government laboratories which are not oriented towards manufacturing, quality assurance and manufacturing as operational entities typically do not exist; thus, this example also characterizes government laboratories: They can reach out and produce prototype devices but cannot actually produce clocks. The desirable and ideal situation is approached by the third part of Figure 8 where the clock expert is placed within management or in a technical/consulting role focussing not only on the four parts of the manufacturing process but on the interfaces between these four processes. Such an organization offers the potential of making not only good working clocks, but producing these clocks in quantity with reliability.

We are now ready to answer the question: When is the best timing for transfer from government to industry? An attempt to give an answer is Figure 9. The figure depicts the sequence from the original idea to production in seven steps: The idea, the experimental verification of the idea, demonstrating feasibility in a laboratory or bread-board setting, the demonstration model which does not have size, weight or power constraints but shows all aspects of performance, the engineering development model (EDM), the pre-production model (PPM) and the production. Since industry contributes original ideas as well, we list this as an alternate idea-start. The idea is carried through experimental verification and the demonstration of feasibility. At this point the critical timing for transfer from government to industry arises. The reason for this lies in the results discussed in Figures 7 and 8. At this point, the full circle of a manufacturing operation comes into focus: Engineering, Quality Assurance, Testing and Manufacturing become a planned process, displaying a high degree of coherence which is phased in time. If government work progresses beyond this stage; i.e., through the demonstration model, or even to the EDM or PPM phase, this work becomes increasingly alien to the coherence of the industrial manufacturing process. In other words, resources spent, in a government laboratory, beyond the stage of demonstrating feasibility are probably wasted because industry will not be able to take advantage of it because aspects of quality assurance, producibility, cost, etc. are not properly accounted for.

The issue in relation to Figure 9 is not that of funding per se; we assume that funding is available and can be channelled at the right time in the right direction. The problem, rather, is that a misunderstanding may persist: As viewed from the government side, it appears that the government has spent significant resources and has come up with an almost producible clock or frequency standard; in contrast, industry must request substantial additional resources to go "back to the drawing board" for reasons of quality assurance, reliability, producibility, etc. To the government this looks like unnecessary duplication, to industry it looks like an unacceptable constraint. Therefore, we have the phenomena of reluctance to fund such work on the government side, reluctance to accept such work from the industry side in addition to issues of professionalism and recognition of contributions. Recognition of the critical timing for transfer is the more important, if one realizes that the majority of funds are expended after the demonstration of feasibility with the consequence of increased irreversibility of the process once carried too far.

CONSTRAINTS OF INDUSTRY

History has taught us that clock and frequency standard development, because of the complexity and state-of-the-art nature of the devices, may span many years or even a decade from idea to production. Industry has several concerns in the process of accepting, counter-proposing, or even rejecting government-funded work. A most serious and often overlooked aspect is the engineering content versus the manufacturing content of government-funded work. Figure 10 is an attempt to depict this predicament. Plotted is the effort level (funding level) as a function of time. The pre-EDM phase includes all stages from idea to demonstrating feasibility including the demonstration model. The effort level is comparatively low and calls almost exclusively on the research and engineering talent of the organization. The effort level is substantially increased (up to a factor of ten) but retains its largely engineering content with the engineering development model. It is important to highlight this jump in effort level because this often-overlooked fact a-priori rules out that all (even worthwhile) pre-EDM efforts can reach production maturity. There simply are not enough resources available for product realization of all good ideas. For example, the National Bureau of Standards frequency standards effort operates at about the million dollar level. If all of the ideas and concepts developed there would meet all of our criteria and lead to full scale industrial efforts, the required funding level is about ten times higher. That means we would have to have resources at approximately the 10 million dollar per year level just to execute all of the NBS ideas in industry and NBS is only one of several such laboratories.

After the EDM stage, the first significant change of effort-mix occurs: Manufacturing begins, causing a drop in the engineering content of the total effort level while the total effort level continues. The PPM stage is followed by the production stage which may be at the same level, at a higher or lower level depending on the value of the product and the rate of production. Important is the fact that the total effort level remains substantial while the engineering content is reduced to a very small level serving only as production support and trouble shooting. This fact puts industry in a predicament; as shown in Figure 10, a substantial team of engineers and scientists is needed to execute the EDM and the following PPM phase but only few basic resources are required before and after this phase.

How shall industry gear-up its engineering staff from the pre-EDM phase to the EDM and PPM phase and what should this staff do after production has started? The hard-nosed answer to this is to hire and then reduce staff again. It is the author's belief that clock efforts which are based on a quick hiring process with the potential of substantial re-orientation or loss-of-job after a relatively short time will not lead to success in the complex challenges of clock making. Thus it is incumbent upon the government to insure continuity in those efforts which exist solely because of a government mandate. Continuity can be provided by successive upgrading of the product through consecutive EDM and PPM phases time-phased with production of the previous product. Another alternative is funding of related or complementary efforts after the engineering and pre-production of the main product have been consumed.

CONCLUSIONS

In the decision making process on a new product, many thoughts and conditions have to be considered. Figure 11 depicts what may be called the decision tree for product development. This decision tree starts with an idea; this idea may come from government or from industry in the form of a proposal or a request for a proposal. Industry will first analyze this for basic validity as a solution to an existing problem or validity as a new product or capability. The first steps are the considerations on performance improvement and degradation (comp. Figure 4). If the answer to the first question is no, there will be no further consideration. If the answer to the second question is yes there still may be a valid idea if the performance degradation is acceptable. The next step is an analysis of the engineering costs; are they acceptable? With engineering costs it is not only the amount of monetary resources at stake, but also the question of human resources as discussed above; also, one must ask whether the needed engineers could produce other things of higher value than the one in question (concept of foregone benefits). If the answer is 'no', government funding must be available to offset the costs of engineering. These costs, of course, relate to the market size in the sense of return on investment. If the market size is unacceptable, the government may be the sole customer and must bear the product funding as well. Manufacturing industry will be, in general, reluctant to pursue an engineering development effort with no prospect for production. If government funding is available and/or the engineering costs are acceptable, and/or the market size is acceptable, the required capital equipment investment is analyzed. If the work is government-funded, invariably the need

for government funds for capital investment arises. Substantial capital investment needs must be offset by government furnished equipment or the funding of equipment purchases which then become property of the government.

Finally, the question whether the targeted product competes with the present product line of the company must be addressed. There will be general reluctance to develop and create a product if such a product competes within the existing market and does not serve to enlarge the market expansion. Other considerations, however, may enter here; thus the decision on this question is not clear-cut. However, a go-ahead is almost universally given if the new product opens new markets adding to sales and enhancing capabilities.

It appears proper to conclude with some thoughts about reliability. It is self-evident, that reliability is probably the most important issue in clock technology because of the very nature of the clocks principal function: time-keeping. Reliability must have proper attention in the engineering phase (reliability engineering), it must be addressed with high priority in the manufacturing process (quality control and quality assurance), but, most importantly, it must benefit from field-feedback. This latter element requires long-term continuity of the clock development, production and application scenario, which is characterized by stability of the organizations involved, by business commitments between government and industry, and by maximizing quantities of products while minimizing engineering changes outside of performance or reliability mandated actions.

REFERENCES

1. H. Hellwig, "Microwave Time and Frequency Standards", Radio Science 14, Pg. 561, 1979.
2. H. Hellwig, "Atomic Frequency Standards, A Survey", Proc. IEEE 63, Pg. 212, 1975.
3. H. Hellwig, "Areas of Promise for the Development of Future Primary Frequency Standards", Metrologia 6, Pg. 118, 1970.
4. A. O. McCoubrey, "A Survey of Atomic Frequency Standards" Proc. IEEE 54, Pg. 116, 1966.
5. D. Kleppner, N. F. Ramsey and P. Fjelstadt, Phys. Rev. Letters 1, Pg. 232, 1958 and H. M. Goldenberg, D. Kleppner and N. F. Ramsey, Phys. Rev. 123, Pg. 530, 1961.
6. D. Halford and H. Hellwig, "Private Discussions", 1969.
7. H. Hellwig, "The Hydrogen Storage Beam Tube, a Proposal for a New Frequency Standard", Metrologia 6, Pg. 56, 1970.
8. H. Hellwig and H. Bell, "Experimental results with atomic hydrogen storage beam systems", Proc. 26th Annual Frequency Control Symposium, Pg. 242, 1972.
9. H. Peters, "Hydrogen as an Atomic Standard", Proc. 26th Annual Frequency Control Symposium, Pg. 230, 1972.
10. F. L. Walls and H. Hellwig, "A New Kind of Passively Operating Hydrogen Frequency Standard", Proc. 30th Annual Frequency Control Symposium, Pg. 473, 1976.
11. Papers by Mattison et al, Howe et al, Walls et al, Wang et al, Vessot et al, Busca et al, White and Peters in the Proceedings of the 33rd and 34th Annual Frequency Control Symposia, (1979, 1980) and the Proceedings of the 11th and 12th PTTI, (1979, 1980).
12. H. Hellwig and E. Pannaci, "Maser Oscillations with External Gain", J. Appl. Phys. 39 P. 5496, 1968.

	QUARTZ CRYSTAL RESONATOR	RUBIDIUM GAS CELL	CESIUM BEAM	ATOMIC HYDROGEN STORAGE BULB
TYPICAL Q	2×10^6	2×10^7	3×10^7	1×10^9
TYPICAL σ_F	1×10^{-12}	3×10^{-13}	5×10^{-14}	3×10^{-15}
SIZE & COST (CM ³)	SMALL (10 ³)	MEDIUM (10 ³ -10 ⁴)	LARGE (10 ⁴)	ENORMOUS (10 ⁵ -10 ⁶)

THE CLOCK HIERARCHY

FIGURE 1

	QUARTZ CRYSTAL RESONATOR	RUBIDIUM GAS CELL	CESIUM BEAM	ATOMIC HYDROGEN STORAGE BULB
REALIZATION	NOT YET TRIED	MASER	PRIMARY STANDARD	SMALL PASSIVE MASER
σ_F	—	10^{-14}	10^{-14}	10^{-14}
Q	—	SOME 10^8	SOME 10^8	SOME 10^8

CLOCK HIERARCHY
(SIZE/COST EQUALIZED)

FIGURE 2

	BEAM	STORAGE VESSEL	GAS CELL	PASSIVE	ACTIVE
^1H	YES	YES	NO	YES	YES
Rb	YES	YES	YES	YES	YES
Cs	YES	(1)	YES	YES	(2)
ATOM X	YES	YES	YES	YES	YES

(1) THIS IDEA CREATED THE ACTIVE H-MASER

(2) THIS IDEA CREATED THE PASSIVE H-MASER

MATRIX OF CLOCK PRINCIPLES

FIGURE 3

- (A) DOES IT REMOVE A LIMITATION?
- (B) IS THIS LIMITATION A REAL PROBLEM?
- (C) DOES IT INTRODUCE A NEW PROBLEM?
- (D) IS THIS NEW PROBLEM A REAL LIMITATION?

EXAMPLE: THALLIUM BEAM (vs. CESIUM)

- (A) YES, MAGNETIC SENSITIVITY MUCH LESS.
- (B) NO, SINCE SHIELDING OF CESIUM IS ADEQUATE.
- (C) YES, LESS BEAM DEFLECTION; SURFACE IONIZATION NOT EFFICIENT, HIGH OVEN TEMP.
- (D) YES, TECHNICAL SIMPLICITY OF CESIUM MUST BE GIVEN UP.

NEW IDEA CHECKLIST

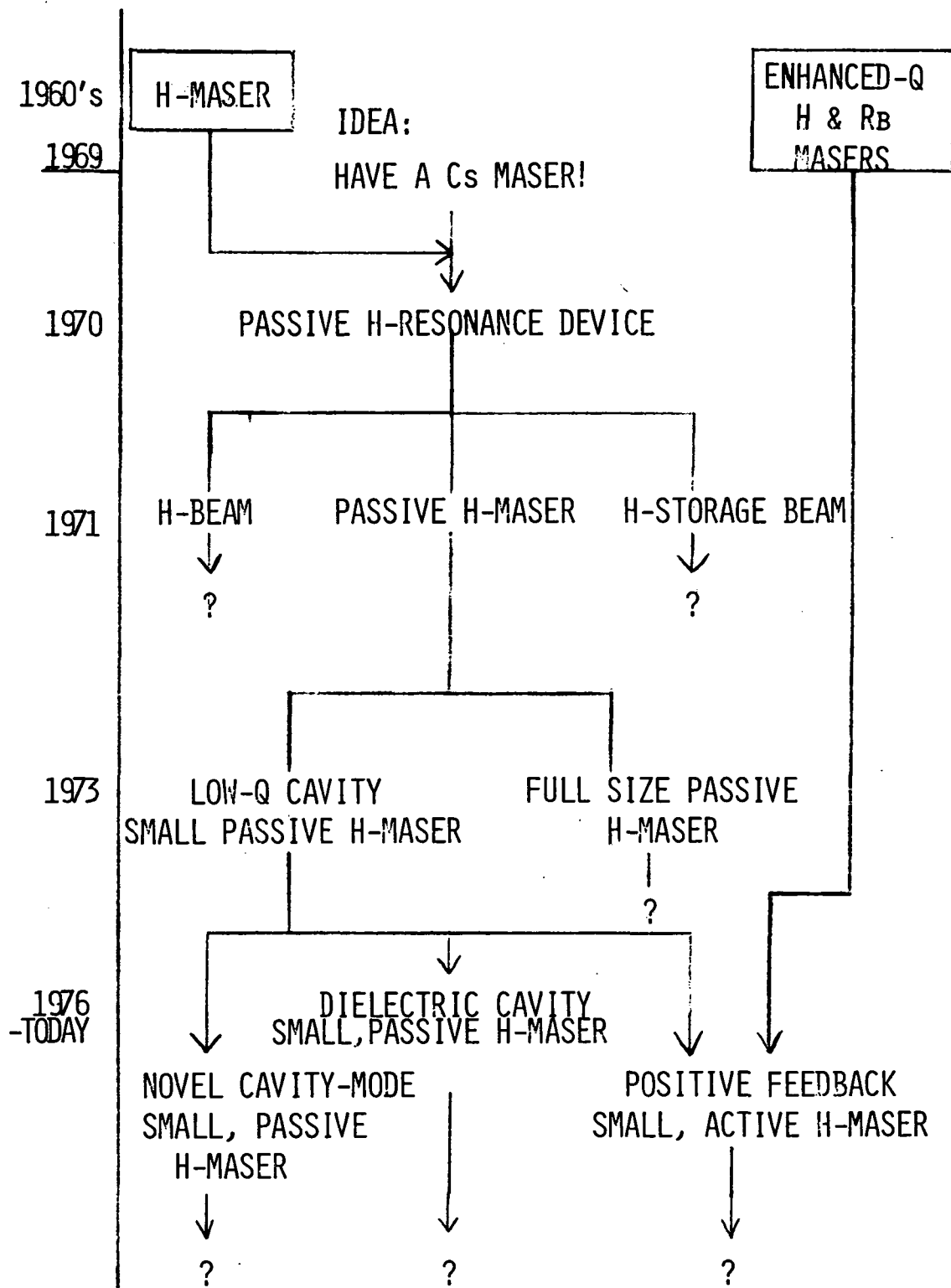
FIGURE 4

- INCREASE CAVITY - Q
- DECREASE CAVITY - Q
- RABI CAVITY
- USE A DIFFERENT ATOM
- MORE OVENS
- LESS OVENS
- MORE SERVOS
- LESS SERVOS
- SYNTHESIZERS IN THE SECONDARY LOOP
- SMALL SIZE

PLUS MANY MORE

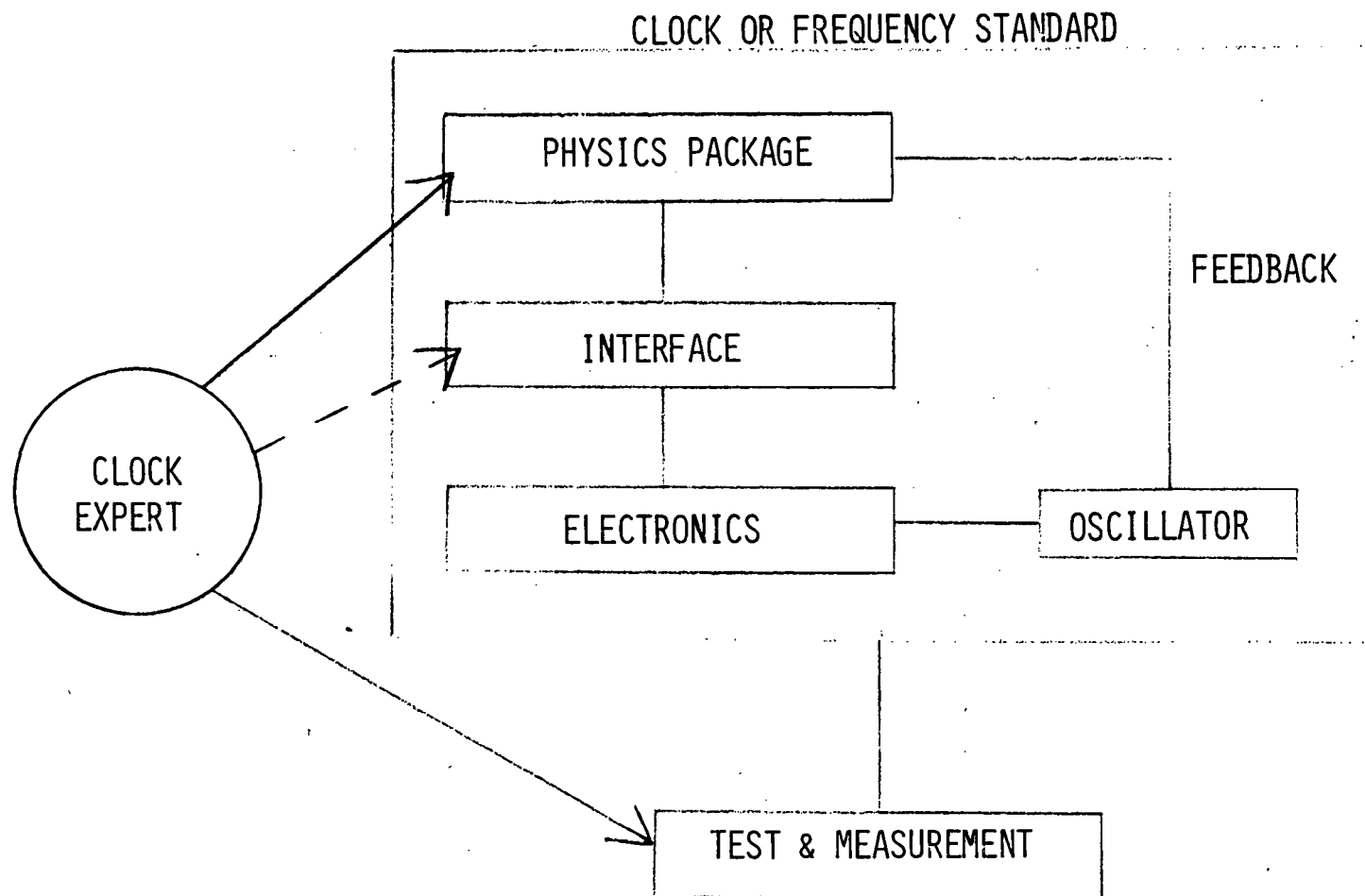
PERENNIAL "NEW" IDEAS

FIGURE 5



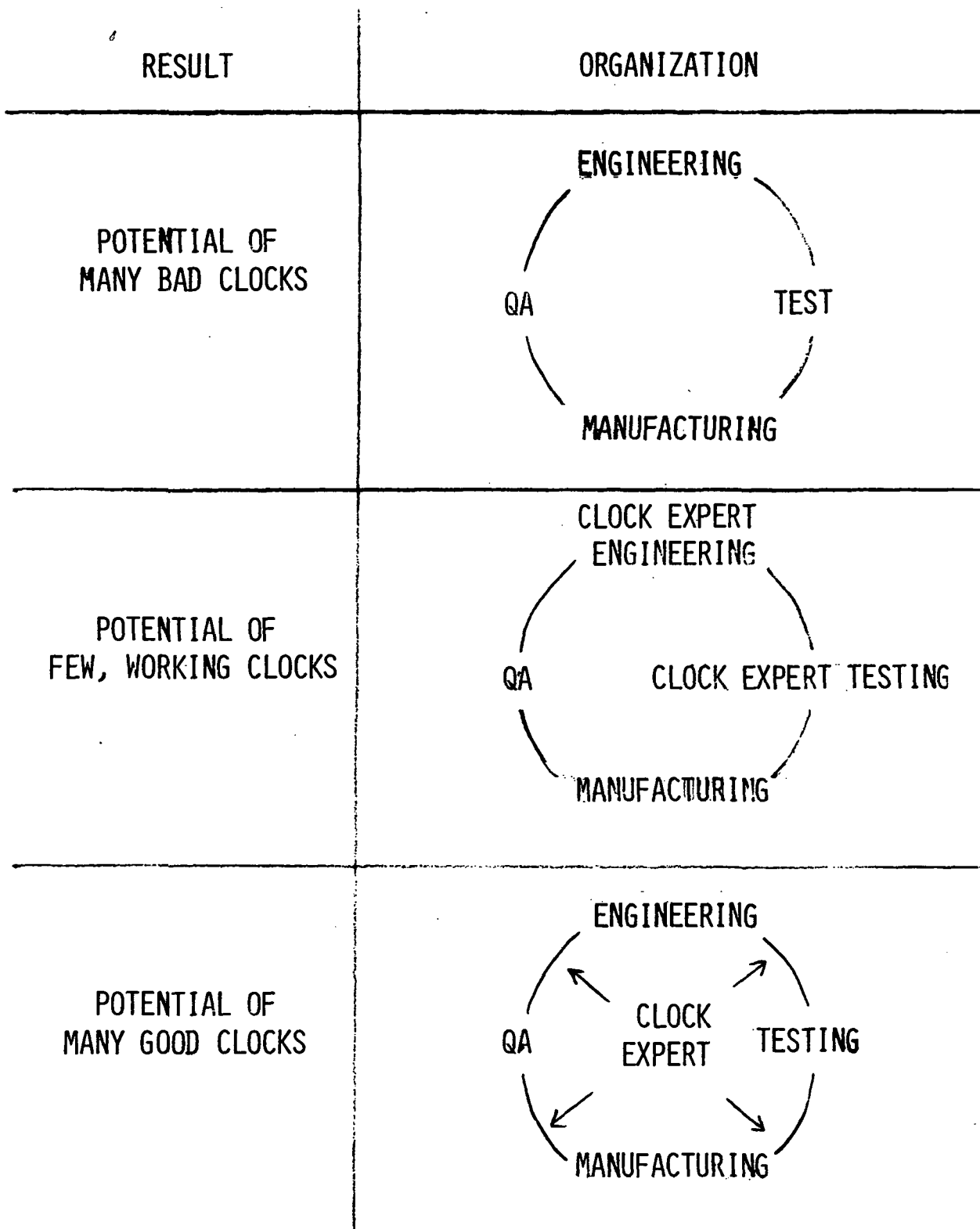
PASSIVE H-MASER FAMILY TREE

FIGURE 6



TYPICAL CLOCK-EXPERT EXPERTISE

FIGURE 7



CLOCK PRODUCTION ASPECTS

FIGURE 8

	IDEA	EXPERIMENTAL VERIFICATION	DEMONSTRATING FEASIBILITY	DEMONSTRATION MODEL	EDM	PPM	PRODUCTION
GOVERNMENT	✓	✓	✓	(✓)	(✓)	(✓)	—
INDUSTRY	(✓)	(✓)	(✓)	✓	✓	✓	✓

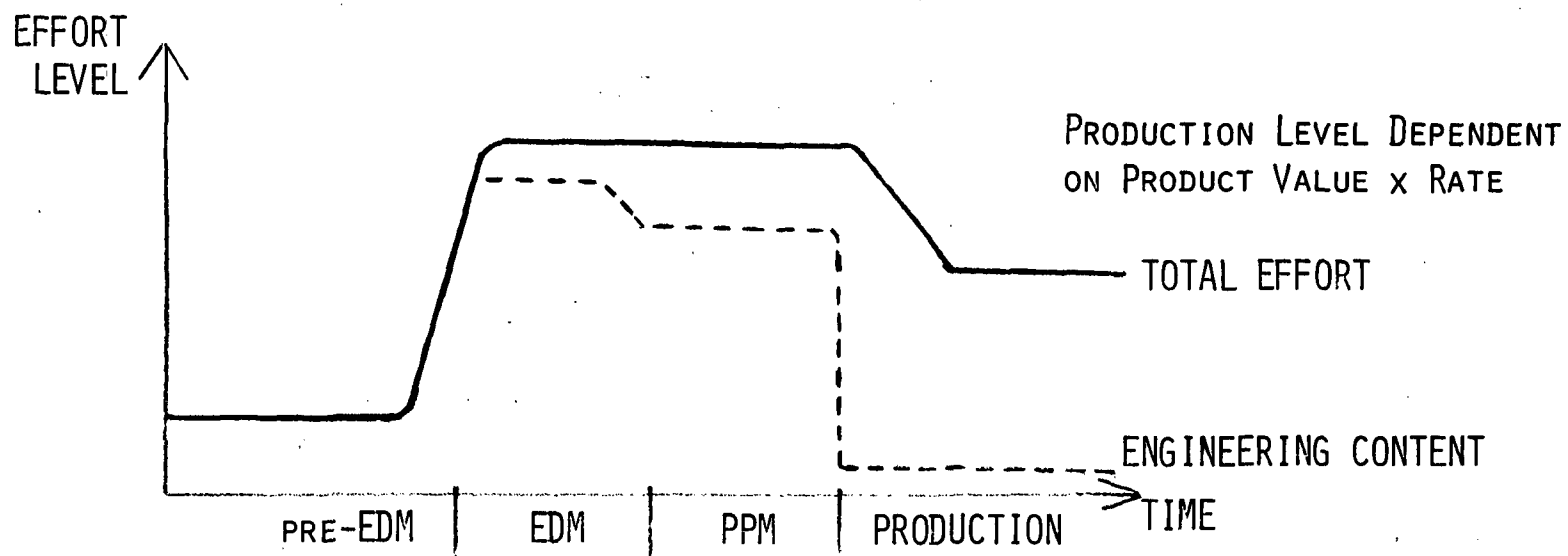
NOTE
↓

() = POSSIBLE INVOLVEMENT

NOTE: CRITICAL TIMING FOR TRANSFER

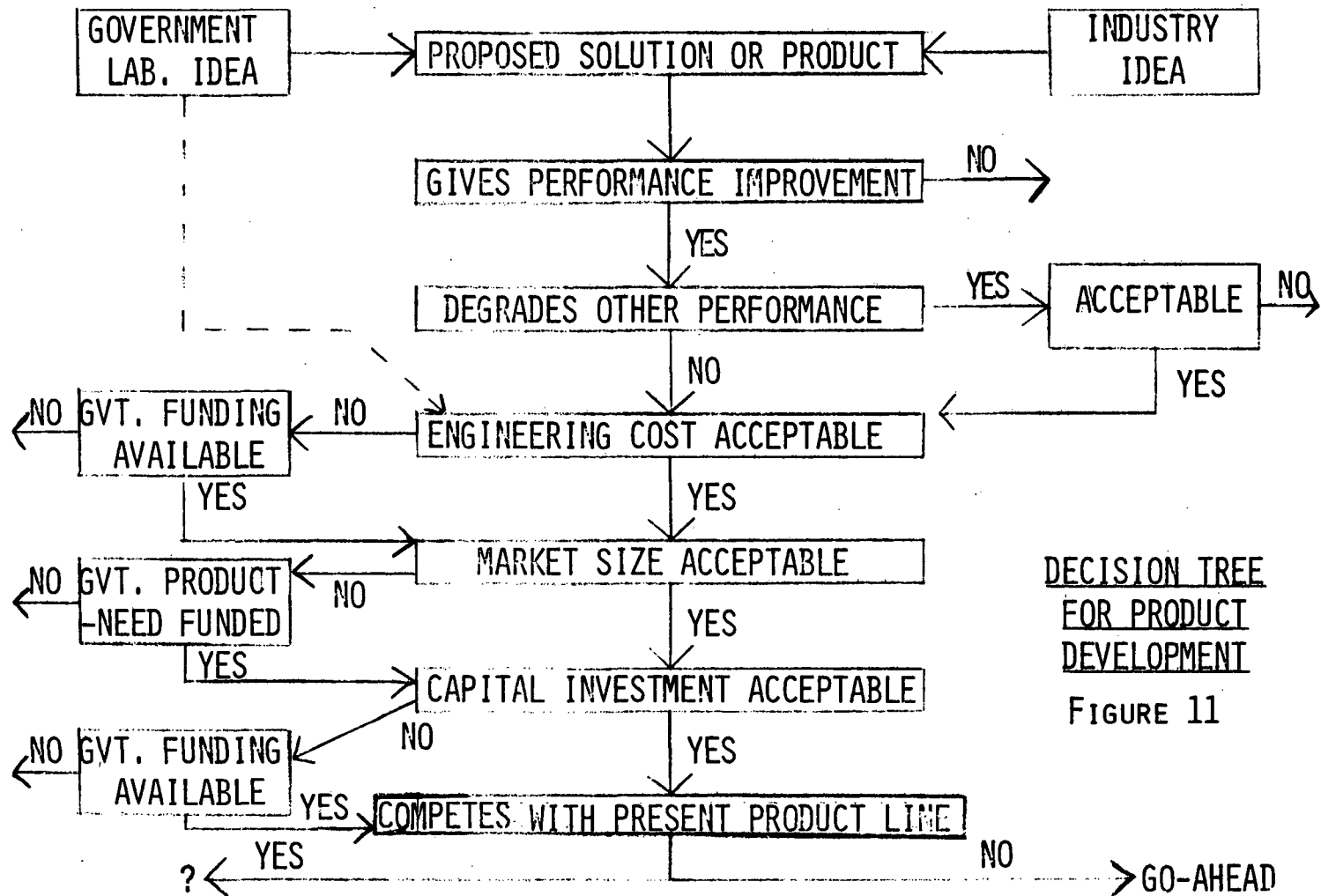
TECHNOLOGY TRANSFER

FIGURE 9



TOTAL AND ENGINEERING EFFORT-LEVEL

FIGURE 10



DECISION TREE
FOR PRODUCT
DEVELOPMENT
FIGURE 11

FIGURE 11

QUESTIONS AND ANSWERS

DR. WINKLER:

I think your excellent speech has focused on many interesting aspects; two of which are particularly important. The first one, the danger of a government laboratory trying to produce a product in mass production. I have several examples of that mistake, I am deeply concerned about it and I don't know what to do to convince the various incumbents that it is a major mistake.

It is not only contrary to our national policy to keep government out of production as much as possible (beyond the feasibility models and technology studies) but it is also a major mistake for the laboratory to absorb your creative engineering potential solving production problems. Your most precious human resource could be put much better to use on new studies, advanced concepts, and specifications, which I think are the most difficult things in the world.

Now, the second point, is that you have a bewildering array of combinations of beam lasers and active and passive and greater Q and less Q -- kind of reminds me of a very similar discussion which we had about six years ago. I hope you don't remember it.

DR. HELLWIG:

Because I will give the same example. Here in America since our major industrial achievement is the automobile, there is no better example than the automobile. There are certain engineering combinations which can be played upon. You can have the engine in front with rear-drive, engine in front with front-drive, engine in rear with rear-drive, but one that has never been tried is the engine in rear with front-drive.

In automatically controlled oscillators, all combinations have been tried, however.

INNOVATION AND RELIABILITY OF ATOMIC STANDARDS FOR
PTTI APPLICATIONS

Robert Kern
KERNCO, Inc.
Danvers, Mass.

ABSTRACT

Over the past 20 years, the U.S. Government has been the largest single customer for hyperfine frequency standards and clocks. In this same period the government directly and indirectly has provided financial support of extensive research, development and manufacturing methodology efforts in industrial and government laboratories.

The GPS/NAVSTAR Program requirements for a spaceborne clock has provided new impetus and development monies to generate multiple sources of reliable frequency standards and clocks with life expectancies of 5 to 7 years. These multiple sources will produce significant economies and performance improvements to PTTI users in the U.S.

The GPS/NAVSTAR designs should result in units with improved stability and environmental tolerance that will provide U.S. systems planners with strategic advantages in the PTTI field.

I would like to address the subject of innovation and reliability in hyperfine frequency standards and clock systems. Hyperfine standards are defined as those precision frequency sources and clocks which use a hyperfine atomic transition for frequency control and which have realized significant commercial production and acceptance. I refer to the cesium, hydrogen, and rubidium atoms and exclude references to other systems such as thallium and ammonia since these atomic standards have not been commercially exploited in this country.

In the late 50's and early 60's several companies pioneered in the development and production of atomic standards. In the mid 60's statistically significant quantities of cesium and rubidium standards were produced, sold, and put into service by PTTI user agencies. The reliable performance established by the Hewlett Packard hyperfine standards in the 1960's stimulated government interest in additional system applications and further development of the hyperfine family of standards.

In the early 70's the Department of Defense issued military specifications (MIL F 28734 & Elex F 105) which defined four types of cesium standards. Our industry saw the issuance of these MIL specifications as a clear signal by the government that there was a growing opportunity in cesium and hyperfine clocks for system applications.

Until the 1970's government support of hyperfine standards was focused on research and technology development. In the 70's the emphasis shifted and intensified toward the development of specific hardware with direct application to major systems concerned with navigation, communications, Very Long Baseline Interferometry (VLBI) and space experiments. The GPS/NAVSTAR need for development of a spaceborne clock provided great impetus for innovative activities in all three hyperfine clocks. New companies and new concepts advanced rapidly in this period producing new miniature rubidium standards, small long lived cesium standards, and prototype passive H masers. The strong levels of government funding matured these new designs and spawned a broad series of commercially available products.

In the late 70's and now into the early 80's, our industry continues to benefit and mature from both continuing government support and an active commercial marketplace for quality hyperfine standards. Contractual funding from the Department of Defense is directed toward higher system performance and multiple sources of cesium, rubidium, and hydrogen clocks.

To summarize this development activity the following table describes the companies who have been recipients of government funding and a parenthetical estimate of this funding (to date) in millions of dollars.

<u>CESIUM</u>	<u>RUBIDIUM</u>	<u>HYDROGEN MASER</u>
Atomichron, Inc.*	Autonetics - (Rockwell)	Applied Physics Lab./JHU
Freq. Control Corp.*	Collins - (Rockwell)	Hewlett Packard*
FEI	Efratom	Hughes Research Lab.
FTS	E G & G	Jet Propulsion Lab.
Hewlett Packard	General Radio*	NASA Goddard
Kernco, Inc.	General Technology*	NBS
NBS	Hewlett Packard	Sigma Tau Corporation
National Radio*	Tracor*	Smithsonian Astro .
Pickard & Burns*	Varian Associates*	U. S. Naval Res. Lab.
Varian Associates*		Varian Associates*
		Universities: Harvard
		Laval
		Williams
(20 - 25)	(15 - 20)	(25 - 30)

*No longer active in this business

The figures support public statements made that there is more support and more work available than the hyperfine companies can ingest. Many companies in this field have doubled over the past two years. Perhaps this preoccupation with growth in this period of prosperity has caused a diversion of industry attention from the issues of performance and reliability.

The U.S. Government, as a customer, has had a vested interest to develop both improved clocks and competitive sources for them. The hyperfine technologies have enjoyed strong levels of direct and indirect customer support these past ten years and must now address the question of customer payback. Current programs to qualify several suppliers for GPS/NAVSTAR clocks should favorably impact both the economics and the stability of the source(s) of supply.

The payoff to the government customer is rooted in the fact that for the first time in our business qualified competition exists in all the hyperfine standards. It is no longer adequate for the manufacturer to certify his design, build, and verify by test that the equipment initially meets all applicable acceptance specifications. In the future it should be necessary for the manufacturers both to guarantee and to demonstrate that the customer will actually realize the called for lifetime expectations. Demonstration of the lifetime cost parameter must be an integral condition for a manufacturer to receive future business.

Let me suggest a valid signal that development is truly complete when a manufacturer releases a quantity of commercial products directly spawned from the government sponsored development effort and assumes a significant commercial warranty obligations for these commercial units. It is then that the government customer, after paying for the development, has a right to expect a stable price structure, continuing product improvement and a purchase price that is less than ten times the price of the commercial unit.

The specific point I wish to make today concerns innovation and reliability in hyperfine physics packages. The intensive developments now underway would not be necessary if our industry had achieved the equipment which the government customer(s), some 90% of the market, funded to bring into being.

The technology base for hyperfine physics packages had been established and remained locked away under a "proprietary information" label by a few companies. Government scientists and engineers did not have the opportunity to participate in and evaluate the underlying design and processing philosophy of the physics packages. Nor have the manufacturers revealed the details of factory and field failure history of the design. Only by customer-supplier discussion and analysis of such data can specific problems be quantified and user insights applied to yield simple environment compatible solutions to engineering or processing weaknesses.

This lack of physics package 'know-how' and the lack in the visibility of data make it difficult for a user to evaluate whether a given supplier can consistently meet his lifetime and performance requirements. Usually the customer can provide verification that the electronic components are procured, screened and assembled to a specified practice. When it comes to the physics package used in the equipment, the PTTI user must accept company assurance that the 'proprietary unit' was built according to strict process specifi-

cations and in facilities unique to the system requirements. Then, screening and in-house unit testing will do the rest of the reliability and performance job.

Until recently the development sponsoring agency could not purchase cesium or rubidium physics packages without buying the whole standard or clock. In my opinion what remains to be done is for the Department of Defense customer to conduct specific in-house testing and make design appraisals of the hyperfine physics package. By establishing end user data concerning the reliability and lifetime performance of a given design, in a government laboratory, the customer could compare results with data provided by the manufacturer.

The tests to be performed by the government laboratory can include several tests usually conducted by the manufacturers and can be expanded to include tests which reveal the design limits of the device.

PHYSICS PACKAGE TESTS FOR DESIGN CHARACTERIZATION

- o Accelerated Life Testing
- o High/Low Ambient Temperature Runs
- o Irradiation
- o Over Voltage Testing
- o Temperature Gradient Induction
- o R.F. Power Shift Stimulation
- o Spectral Sensitivity

The appearance of multiple manufacturers in the GPS/NAVSTAR hyperfine marketplace will provide economic and performance benefits to the whole of the PTTI community. It now remains for the U.S. Government to establish an in-service capability for the assessment, evaluation and lifetime testing of the physics units utilized by these manufacturers. With data and the institution of manufacturing controls and safeguards the government's support can finally produce an economic and performance return on investment.

QUESTIONS AND ANSWERS

DR. HELLWIG:

Maybe just a comment on the availability of physics packages for testing. If I remember right, Varian was willing and able to sell tubes in the '60's. I think Hewlett-Packard did so in the early days -- 1970's -- and FTS has sold tubes over the past years to the U.S. government. That is not a question of lack of availability.

It is a lack of focus on this problem which I totally agree with you, Bob. I think this is one of the major problems.

CHAIRMAN STOVER:

Well, there seems to be a common thread through the papers we have heard so far of need for more cooperation between industry and government. We will see if that continues with our other two papers.

R & D: TO FUND OR NOT TO FUND

Terry N. Osterdock
Hewlett-Packard Company
Santa Clara, California

ABSTRACT

The U.S. Government spends vast sums of money each year to fund the research and development of electronics for a variety of applications. Commercial enterprises also spend large sums on R & D of electronics and other areas of interest to the U.S. Government and its agencies. The government can take advantage of industrial R & D and thereby maximize the utilization of their own R & D funds.

INTRODUCTION

In accomplishing any task, we are faced with limited resources such as: manpower, materials, time, and funds. Faced with a given task we must both conserve and make maximum use of ALL our resources. One drop of oil spilled will never be recovered. One second wasted is lost forever. The watchword everywhere should be the maximum utilization of available resources. If we are to conserve, we must not waste one drop of oil, one second of time, or one dollar of funds. As taxpayers we want the government to take less of our income for taxes. More importantly, however, we want the government to spend each dollar they do take as wisely and effectively as possible. This spending efficiency should be applied to the area of Research and Development (R & D) as well as all other areas of government spending.

RESEARCH AND DEVELOPMENT

Before discussing the funding of R & D let us define and characterize R & D so that we have a common base from which to build.

Definition of Research and Development

Research and Development can be defined in a number of ways. However, for our purposes I will define it as the process of finding a solution to a problem. The most difficult part of R & D is defining the problem. The professors in my freshman engineering courses (many years ago) stressed that once you had defined the problem, you had it half-solved.

Types of Research and Development

There are three types of R & D which are pertinent to our discussion: 1. Basic Research, 2. Development and 3. Modification or redesign.

Basic research is the investigation of specific phenomena to further our understanding of the sciences, the world we live on, and the worlds around us.

Development on the other hand, is the application of known or SEMI-KNOWN Technology to solve a specific need or problem. I say SEMI-KNOWN technology because we can generally produce one of anything in the laboratory but producing one hundred or one thousand is a much more difficult task to accomplish.

Redesign or modification allows us to use a currently available off-the-shelf product to solve a new need or problem. The older product doesn't fit the solution exactly, but with a little modification it will do just great.

SOURCES OF PRODUCTS AND TECHNOLOGY

If we were to determine how many dollars were spent each year on R & D by both the government and private industry we probably would be astonished. Each year thousands of new products are introduced into the marketplace and scores of new technological breakthroughs are realized.

Have you ever wondered how mankind manages to come up with all of these fantastic products and ideas? Both products and technologies come from three sources.

Problems

Problems are the manifestation of needs. The customer has a specific need or problem which must be solved. Someone thinks he can fill that need and hence, the R & D process is initiated. As a result, a product is created which solves the problem or fills the need.

An example of problem solving is when our customers told us they would like to be able to have Cesium beam frequency standard performance at several locations within their plant or system. However, they could not afford to purchase a multitude of Cesium standards. As a result the 5087A Distribution Amplifier was developed, thereby filling the need and solving the customer's problem.

Solutions

Here we find the R & D Engineer, Physicist, Chemist or researcher that has discovered or developed a fantastic product or process. The question we all would ask is "Does anyone need it?" The solution, therefore, is looking for a problem to be solved. In the early days of Cesium standards it was mainly a laboratory curiosity. Later it became apparent that the Cesium standard was the solution to a number of communications and navigation problems.

Accidents

In Research and Development, the researcher is looking at technologies, processes, needs, and a myriad of other things. Someday, with a little bit of luck, he may discover something that will be useful to someone, somewhere. More than likely if he finds it, it won't be what he thought it would be, nor will it be the solution to the problem he had originally set out to solve. Instead it will be the byproduct of his efforts. Totally by accident he will find something useful to mankind.

Some years ago we had an engineer working on the design of a frequency counter. He became totally frustrated with trying to determine the state of a logic gate. Because of this frustration he designed a device to determine whether the Logic gate had a "1" or a "0" on its output or input. From this first logic probe came a whole series of logic test equipment. Totally by accident was this product concept discovered.

R & D PROCESS

The R & D process starts with either a need or an idea. In the case of starting the process with the needs, (figure 1) the company attempts, first, to determine what the customers need. Once we have determined that something is needed, we look at the limited resources available in terms of people, materials, funds, and even in terms of ideas to develop.

If the company thinks it can solve a problem and fulfill the need, then it proceeds to develop the solution.

The product is designed and tested and if everything works, it is put into production. The customers now have a solution to their problem.

If instead we start with an idea (figure 2), i.e. a possible solution searching for a problem, then the process is similar. The R & D Team comes up with an idea. The company then looks to the marketplace to see if there is a need for a product using that idea. If so then the design and development begins and the product developed.

To determine what the customers need, a company will simply ask their customers (including the government) what they think they will be needing sometime in the future, say 5 to 10 years (figure 3). The customers typically respond with a not so simple answer, e.g., "I don't know, what will be available in 5 to 10 years?" This circular questioning continues back and forth. Sometimes we arrive at an answer, sometimes the process continues without resolution.

ROLE OF INDUSTRY

Industry has specific responsibilities in the R & D process:

Query Customers for Needs

They must ask customers what they need. Industry needs to know what people will be doing in 5 to 10 years. Companies have to be wizards of fortune telling and be able to forecast the future. They need to watch trends in government, military, and private sector activities.

Analyze Technology

Industry must also analyze technology. Somehow we need to determine a prognosis for the state-of-the-art. We might examine technologies and ask which hold promise for solutions to problems which may exist in 5 to 10 years. We need to look at what technologies are currently available and which need to be developed before they can be utilized in specific solutions to problems.

Develop Solutions

Finally, industry must take existing technologies and design products which can be solutions to problems in the near future. And if possible, they need to develop promising technologies to the point of being useful.

ROLE OF GOVERNMENT

If industry does all that, what is left for the government to do?

Determine User Needs

First, the government should determine user needs. Requirements for communications, navigation, space exploration, air traffic control need to be examined. The government should look at Military needs for the next 5 to 10 years as well as examine needs of other agencies such as the FAA. The government might even go so far as to look at forecasting the commercial needs for similar products. This would provide a real service for industry.

Disseminate Information

These needs must then be communicated to industry. In sharing what the government agencies know about their future requirements, industry will be better able to design products which the government can use.

Look at Available Products

The government's system designers need to look at currently available, proven, off-the-shelf hardware to satisfy as many needs as possible. To ignore off-the-shelf hardware might be related to the NIH or Not Invented Here Syndrome. Nothing is more wasteful than reinventing the same product when an off-the-shelf piece of hardware will do.

Buy Solutions

A solution may simply be the purchase of off-the-shelf hardware. Or it may be slightly modified hardware integrated into specially designed systems. Or the solution might be to fund the basic research in an area which looks promising, but the need is too tenuous to convince an industrial company to invest its own R & D funds.

ADVANTAGES OF OFF-THE-SHELF HARDWARE

Why buy off-the-shelf hardware, you might ask. First of all, because its reliability is known; it is not simply computed, but based on real experience. Its early problems probably have been worked out.

Second, it is more serviceable. The bugs have been worked out, people have learned how to repair it, and it is more thoroughly documented. Service information, operating instructions, and test procedures are generally available.

Lastly, you will generally buy the item for less money than a specific design for only one application. The R & D costs are shared by all the buyers, in essence, not just one. Ergo, you don't have to pay ALL of the R & D costs.

FUNDING OF R & D

Both government and industry commit vast sums of money each year to develop solutions to problems. But because our resources are limited, it is important to utilize the resources we do use to get the maximum benefit. The government can greatly improve the impact of the taxpayer's dollars by trying to identify its own needs and by letting industry know what it needs, even to the extent of letting industry know if there is any commercial benefit. If the government can assist in the forecasting effort by letting industry know what lies ahead for future requirements, industry might be able to respond. In this way the government could impact the commercial design efforts to the extent of being able to buy off-the-shelf hardware and not having to fund the effort.

Of course the government has a problem when it tries to provide industry with information. They would like some information in return. They would like to know what the companies are developing and if they will commit to development of a specific solution. However, the government will encounter resistance on the part of industry to commit to a specific project. Companies, in all areas not just PTTI, are not likely to disclose what they are developing or when it will be available in the marketplace. Generally, a company doesn't want its competition to know what it is doing; this allows the company that invents a new product to be first in the marketplace with that product. A company needs to be able to protect its investment on each product and thereby maximize its return on that investment as its shareholders expect.

GOVERNMENT FUNDING

So what should the government fund? Primarily, they should fund the purchase of off-the-shelf hardware. After what I have said earlier you would be disappointed if I didn't list this one first. Secondly, they should fund minor modifications to off-the-shelf hardware. Thirdly, they should fund elementary R & D only if the product is not currently available. And, of course, they should fund basic research in unknown but promising areas. The results of these efforts should be made available to all potential industrial users to maximize spread of technology funded by taxpayer dollars. This will result in more technical solutions being available at an earlier time than if all associated funding was left to the government.

BENEFITS

Definite benefits can be obtained by government participation in the R & D process. Because the government will have provided information and shared in the forecasting process, industrial firms will be able to better consider incorporating the needs of the services and agencies in their future product developments. This will result in the government being able to purchase off-the-shelf equipments to satisfy more of its needs. R & D funds will be used more efficiently in the few most critical areas, and fewer taxpayer dollars will be wasted.

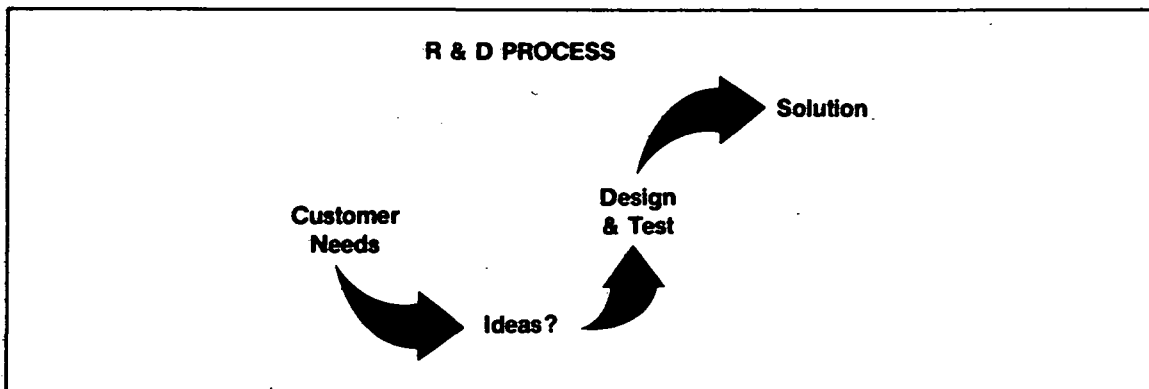


Fig. 1 - R & D Process (Needs)

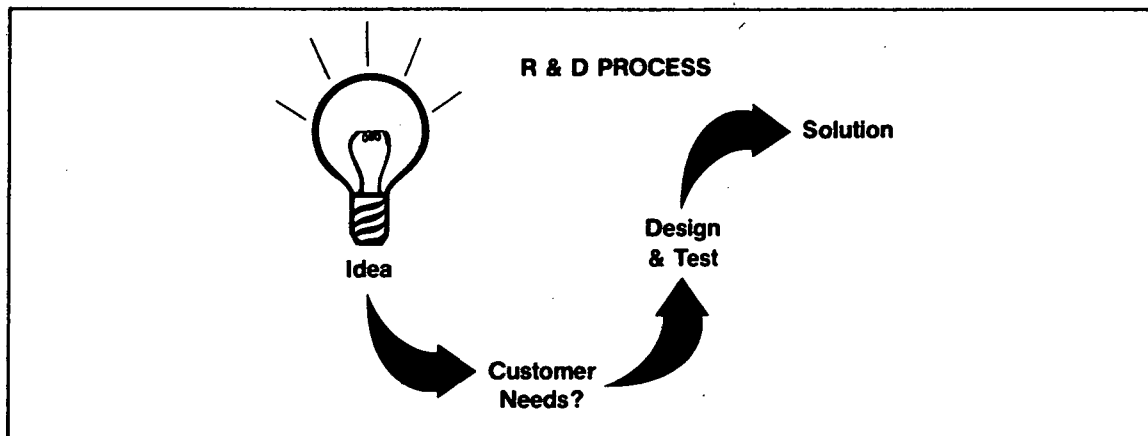


Fig. 2 - R & D Process (Ideas)

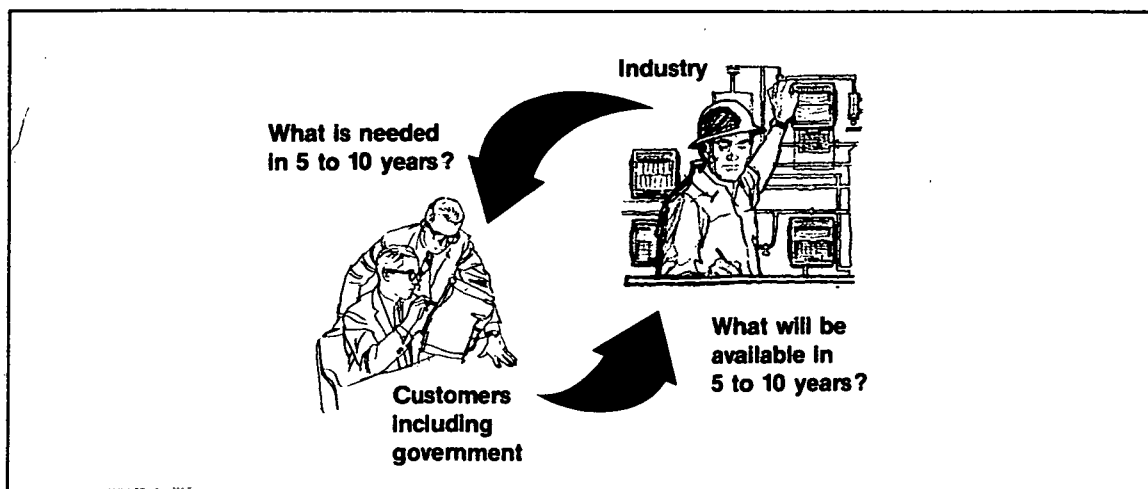


Fig. 3 - Forecasting the Future

QUESTIONS AND ANSWERS

CHAIRMAN STOVER:

Your request that the government tell you what they need may be, in many cases, unreasonable. The government is no different from other people, and many times they don't even know they need it until they have used it. I think that is even more true in the government than it is in the public in general. If you haven't used it, you don't really know you need it yet.

I think the government has a great deal of that problem: not knowing what they need because they don't know what it will do for them. How do you propose to solve that problem?

MR. OSTERDOCK:

I think that is part of that circular questioning that I describe; basically trying to figure out what happens, and by all of us continuing to communicate that way, maybe we will get some answers. I don't have a specific solution for that part of it.

Forecasting is the most difficult part of the process. I don't think that anybody can really say what technology is going to be like in 10 years any more than we could have back in the '60's.

CHAIRMAN STOVER:

If you go to a Field Commander and ask him what new technology he needs next year, what is he going to tell you? He has to have a shopping list of some kind, right?

Page Intentionally Left Blank

CONTRACTOR POINT OF VIEW
FOR
SYSTEM DEVELOPMENT & TEST PROGRAM

F. K. Koide
Defense Electronics Operations
Rockwell International
Anaheim, California

D. E. Ringer
North American Space Operations
Rockwell International
Seal Beach, California

C. E. Earl
Defense Electronics Operations
Rockwell International
Anaheim, California

ABSTRACT

This paper will present industry's practice of testing space qualified hardware. An overview of the GPS Test Program will be discussed from the component level to the sub-system compatibility tests with the space vehicle and finally to the launch site tests at Vandenberg AFB, California, all related to the Rubidium clock.

INTRODUCTION

Rockwell International has been involved in the development and production of space qualified Rubidium Frequency Standards for the GPS Program since the initial inception of the program in 1974. To date, we have produced a total of 29 Rubidium clocks consisting of prototypes, engineering models, and production units.

The first series of six satellites are in orbit and have been declared operational, with each carrying three redundant Rubidium clocks. Initial test results demonstrated navigation accuracies of a few meters in three dimensions. Rockwell is currently in the process of developing Rubidium clocks on the Phase II/III Program for the GPS Satellites 9 through 12.

The Rubidium clock test cycle covers two major phases, the pre-production and the acceptance level testing. The pre-production covers the board, system assembly, and assembly tests. The acceptance level testing includes the environmental and certification tests. All Rubidium clock tests are performed in different test facilities of Rockwell's Defense Electronics Operations in Anaheim, California.

The space vehicle undergoes integrated acceptance testing through test conditions simulating and exceeding the environments which it will encounter from launch through on-orbit operation. The acceptance test of the space vehicle is performed at Rockwell's Space Operations and Satellite Systems Division at Seal Beach/Downey, California, and the North American Aircraft Division located in Los Angeles, California.

SPACE QUALIFIED TEST PROGRAM

Rubidium Clock Automated Test Station

Rockwell's Rubidium clock has been developed from a commercial Efratom Rubidium Frequency Standard. Extensive modification and repackaging have been performed to meet spacecraft requirements and to improve reliability and stability. Acceptance testing of production clocks are required to assure compliance with the design goals and conformity to the procurement specification.

Computer automation of the Rubidium clock testing is utilized because of the large amount of data to be gathered over an extended time period and the need to extensively process this data.

A central or a time share computer concept was selected to allow for greater versatility of utilization and to allow implementation of additional test stations. The computer system utilizes a sophisticated version of BASIC as the programming language available to users and can be extended to service up to 16 terminals. The time share computer is a pdp-11/35 micro-computer which includes 256K, 16 bit word fixed head disc, 1.2 mega bit word movable head disc, dual dectape storage and 28K words of core memory. It is essentially a minimum system requirement to support the data storage and processing requirements.

In the existing configuration, four terminals or test stations are supported by the pdp-11/35 minicomputer. Three of the four test stations are equipped with micro-computer systems that provide redundant data collection and storage capabilities if the time shared computer should fail. At the end of the test, these data would then be transferred to the pdp-11/35 for analysis. System redundancy prevents the loss of test time without interruption. A functional block diagram of the Rubidium clock test station and a photo of three of the four test stations are shown in Figures 1 and 2 respectively.

A valuable feature of the RSTS time share concept utilized is the ability to access data being stored on disc from one program using one I/O port by executing an independent program from a

second port. This feature allows data analysis without interrupting data collection program while using a number of different programs.

Failsafe features are incorporated into all test stations to protect against loss of data in the micro-computer due to transient in the power line voltage, clock supply over-voltage and current, over and under base-plate temperatures, and water flow rate restriction in the vacuum pumps.

Rubidium Clock Test

The testing of Rockwell's Rubidium clock is controlled by two specifications, one an assembly and alignment procedure and the second an Acceptance Test Procedure (ATP). These test procedures have been witnessed and certified by Quality Engineering. There are approximately 76 inspection points where a Quality Assurance Inspector must approve and stamp off the work before additional testing can proceed. All these steps are planned and recorded in a FAIR book system. FAIR is an acronym for Fabrication-Assembly-Inspection-Record.

This system also keeps track of all parts installed into the Rubidium clock. If a failure occurs during assembly, the retest must start over per the retest matrix listed in the assembly procedure. If a failure occurs during the ATP, the failure must be documented by Reliability Engineering, who also notifies the prime contractor, and generates a failure analysis report.

At the completion of a successful ATP the test data is assembled into a data package by Quality Engineering and a formal data review is conducted with the prime contractor, Air Force (SAMSO) and the technical consultants for the Air Force.

After the data review, the Rubidium clock is packaged and shipped to the prime contractor. The data is impounded in the Data Submittal department where it is available for review at a later date. This data includes all acceptance test record cards, "FAIR" books, computer printouts and strip charts.

Figure 3 shows the Product Acceptance test flow for the Rubidium clock from the Module Assembly level to the point of shipment, the space vehicle factory test. A typical calendar time for product acceptance test is approximately three months.

Space Vehicle Factory and Launch Site Tests

As prime contractor for the GPS Space Vehicle, installation of sub-systems and integration tests are initiated at Rockwell's

Seal Beach Operation Factory Test Clean Room Facility. Figure 4 shows the test flow and the type of tests performed at these levels on the space vehicle. The Rubidium clock is primarily tested for interface compatibility with the different sub-systems. The performance of the individual sub-system is tested at each phase of buildup to assure reliable operation during the five year mission life. The test criteria are structured to verify that each sub-system performance is within specified limits, and the performance is monitored for stability and continuity from test phase-to-test phase. Departures from expected performance, even well within specification limits, are evaluated in detail and corrective actions are implemented.

Two mobile vans equipped with test systems to perform factory tests follows the space vehicle to Rockwell's acoustics and thermal vacuum chamber environmental test facilities located in the Los Angeles area.

At Rockwell's Los Angeles Operation Acoustic Chamber, the space vehicle is subjected to a broad spectrum of acoustic frequencies to simulate the lift-off, boost, and separation environment. The thermal vacuum chamber at Rockwell's Downey, California, operation simulates the heat, cold, and vacuum of space to verify assembly, workmanship of space vehicle components.

Figure 5 shows the qualification space vehicle in a thermal vacuum chamber. Each individual sub-system component is mounted on the Space Vehicle thermal control plates and driven to temperatures exceeding on-orbit temperatures by 21°C for qualification testing and 11°C for acceptance testing. The thermal design of the entire spacecraft is thus validated by thermal-vacuum testing in a large vacuum chamber with a typical test time of about 3 months. Each Rubidium clock is turned on in a programmed sequence to test stability at the temperature extremes with the four different sub-systems during the thermal vacuum tests. These four sub-systems include navigation; electrical power (Ni-Cd batteries); attitude and velocity control; and the telemetry, tracking, and command (Figure 6).

After the completion of the Thermal Vacuum Test, the space vehicle is shipped to Rockwell's Seal Beach Clean Room Facility for a series of final tests. These tests include the mission profile, space vehicle's static and dynamic balance and functional tests. One of the key tests is the spin balance which is designed to make precision determinations of the Space Vehicle Mass Properties.

At Vandenberg AFB, the space vehicle is prepared for launch by performing satellite and master control L&S band RF link com-

atibility tests and a simulated flight and mission dress rehearsal (Figure 7). Normally, one of three redundant Rubidium clocks is turned-on as a master clock for the L-Band RF link compatibility tests. The S-Band links with the Satellite Control Facility located in Sunnyvale, California, and is used as a down-link to receive the telemetry and other information from the satellite.

SUMMARY

It has been shown that the role of automation is essential in the development of a Space Qualified Test Program. Use of automation has been a key factor in the success of the test program to date. Because of the accelerated schedules and heavy demand on test systems, it is highly unlikely that the present state of development could have been achieved without automation techniques. Expertise in the field of precision frequency and time measurements as well as the capability to interface special test equipment with computer technology are essential in meeting test requirements for the space-qualified clocks. Automatic test systems have essentially provided unattended operation 24 hours a day, thus reducing cost and increasing productivity.

The test program plays a major role in producing Rockwell International products for Government contracts. By employing a regimented type test program, it has been shown that tests uncover latent faults which otherwise may have gone undetected. The program has also demonstrated interface compatibility among sub-systems. The use of well documented test procedures has provided uniform testing from location-to-location; test personnel-to-test personnel; and inspector-to-inspector.

In conclusion, when involved in a major program such as GPS, a considerable amount of effort is expended in tests and as such is a key element in the success of the program.

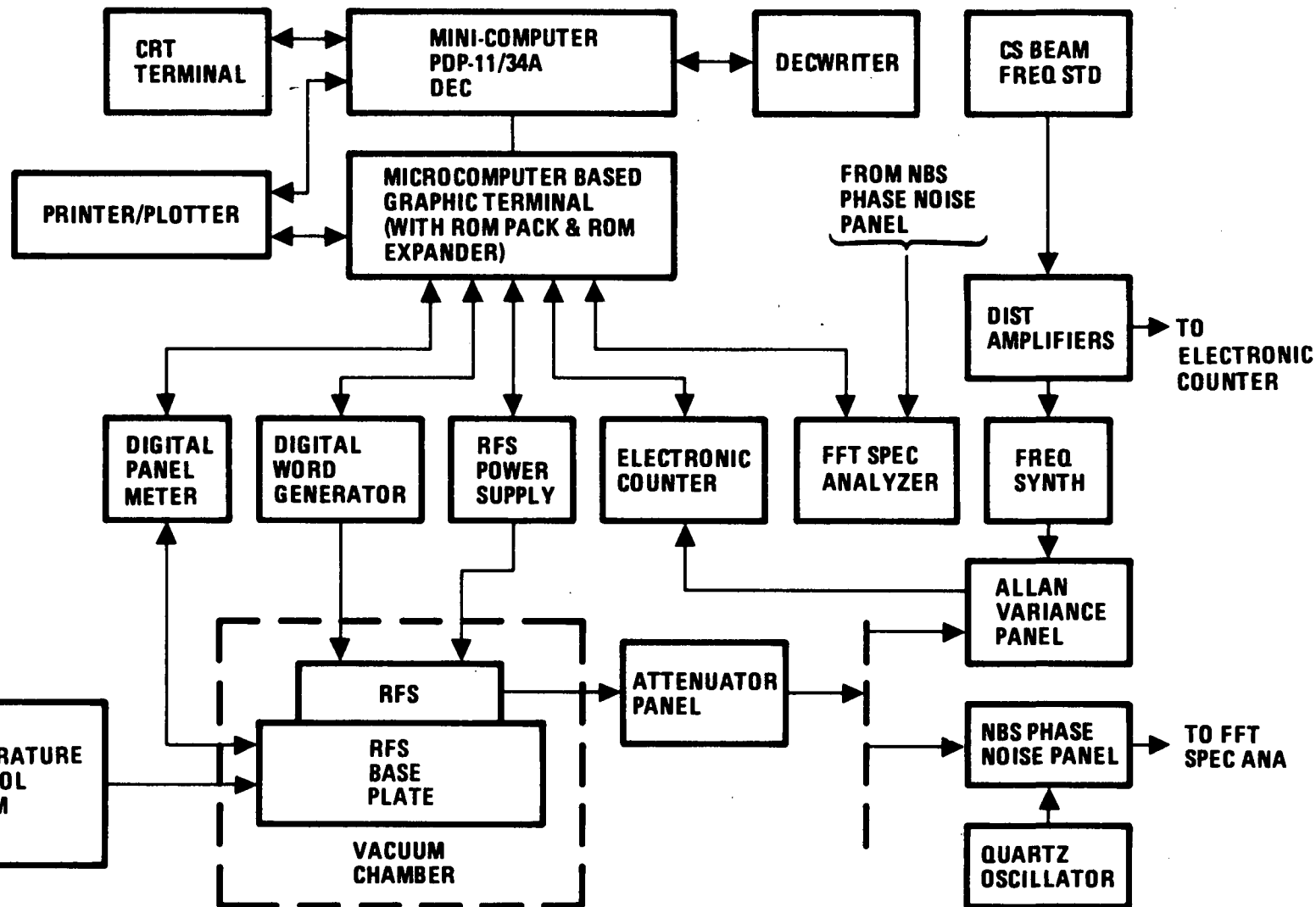


Figure 1. Functional Block Diagram of Automated Rubidium Clock Test Station

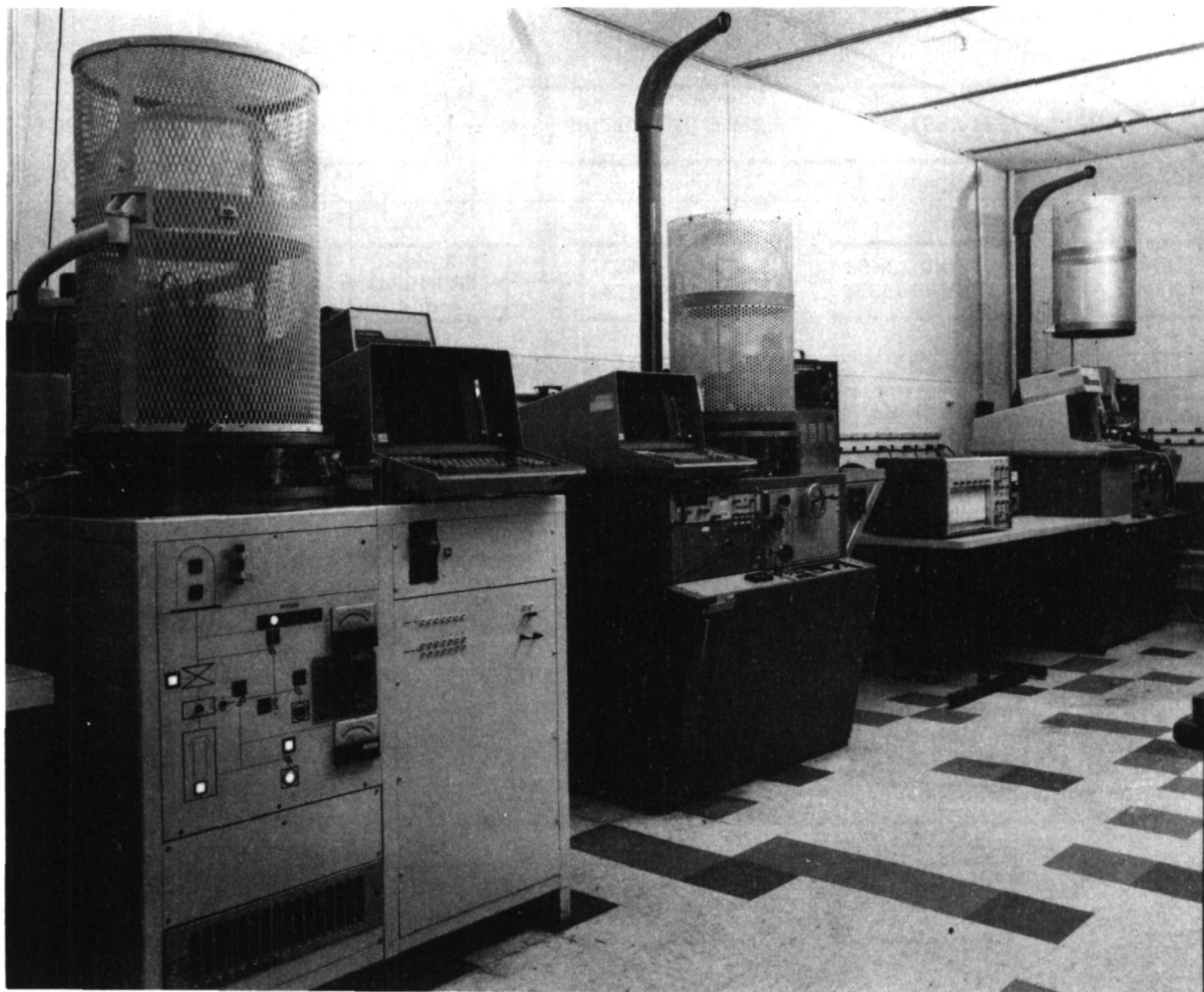


Figure 2. Automated Rubidium Clock Test Stations

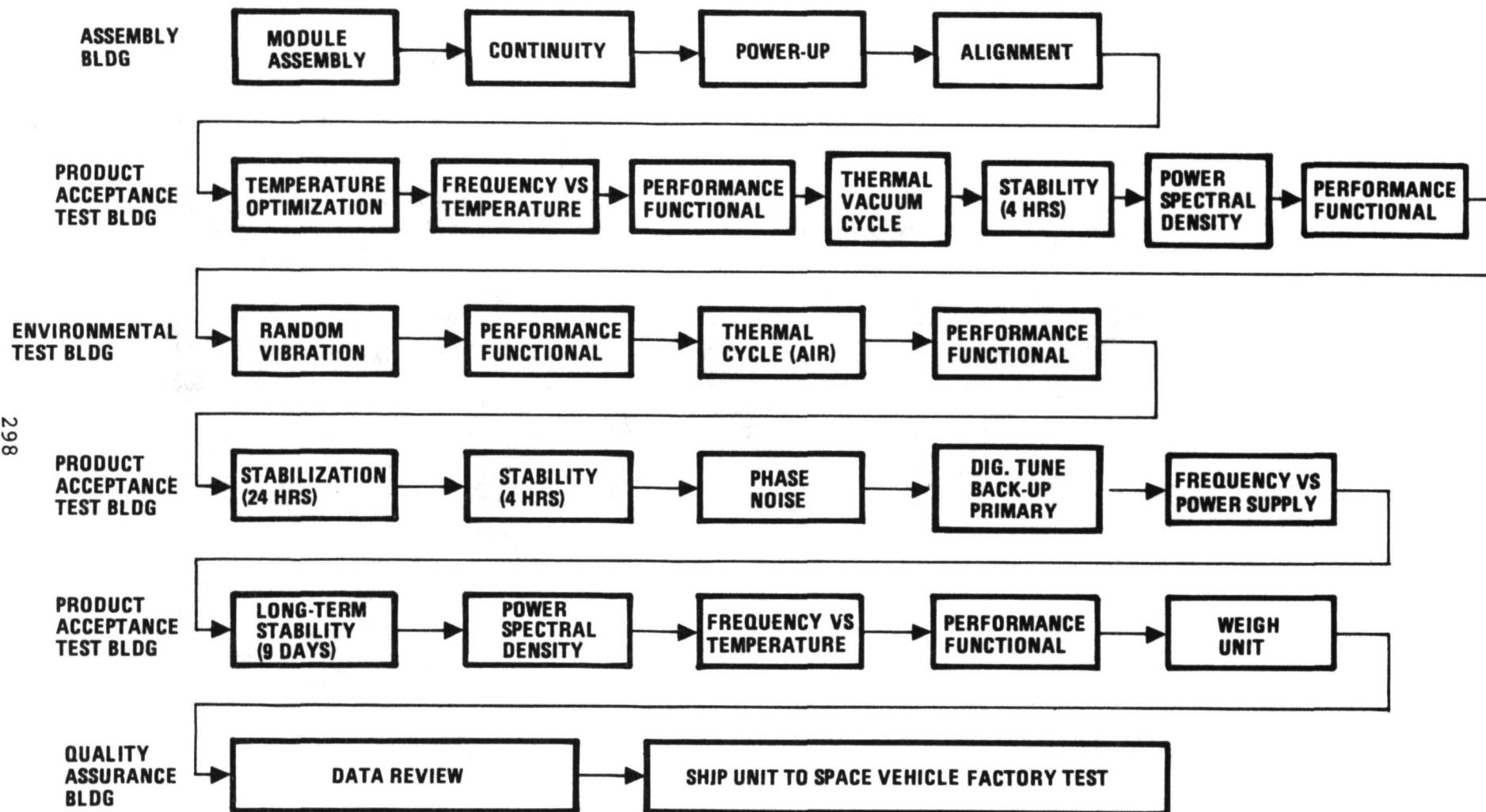


Figure 3. Rubidium Clock Test Flow

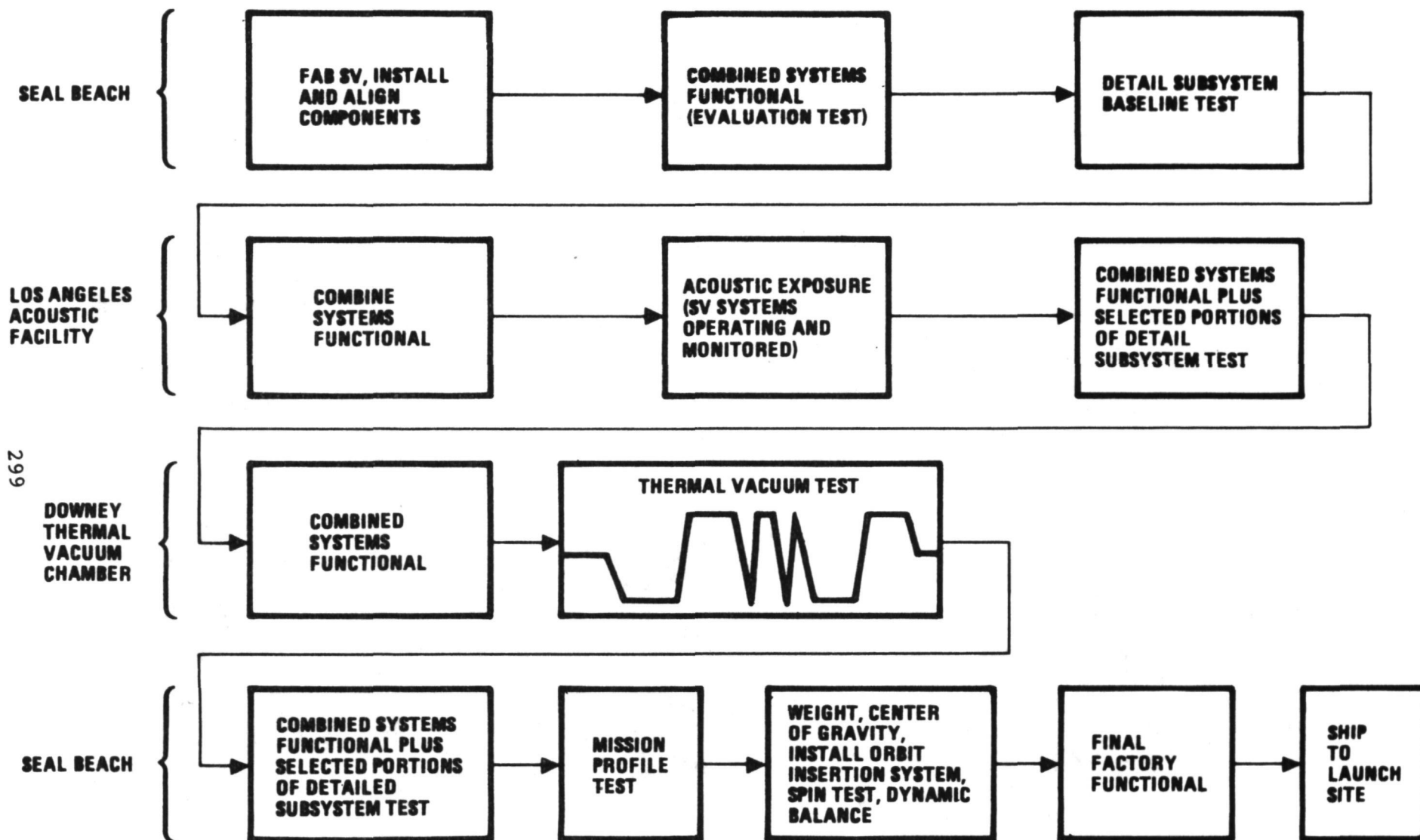


Figure 4. Space Vehicle Factory Test Flow

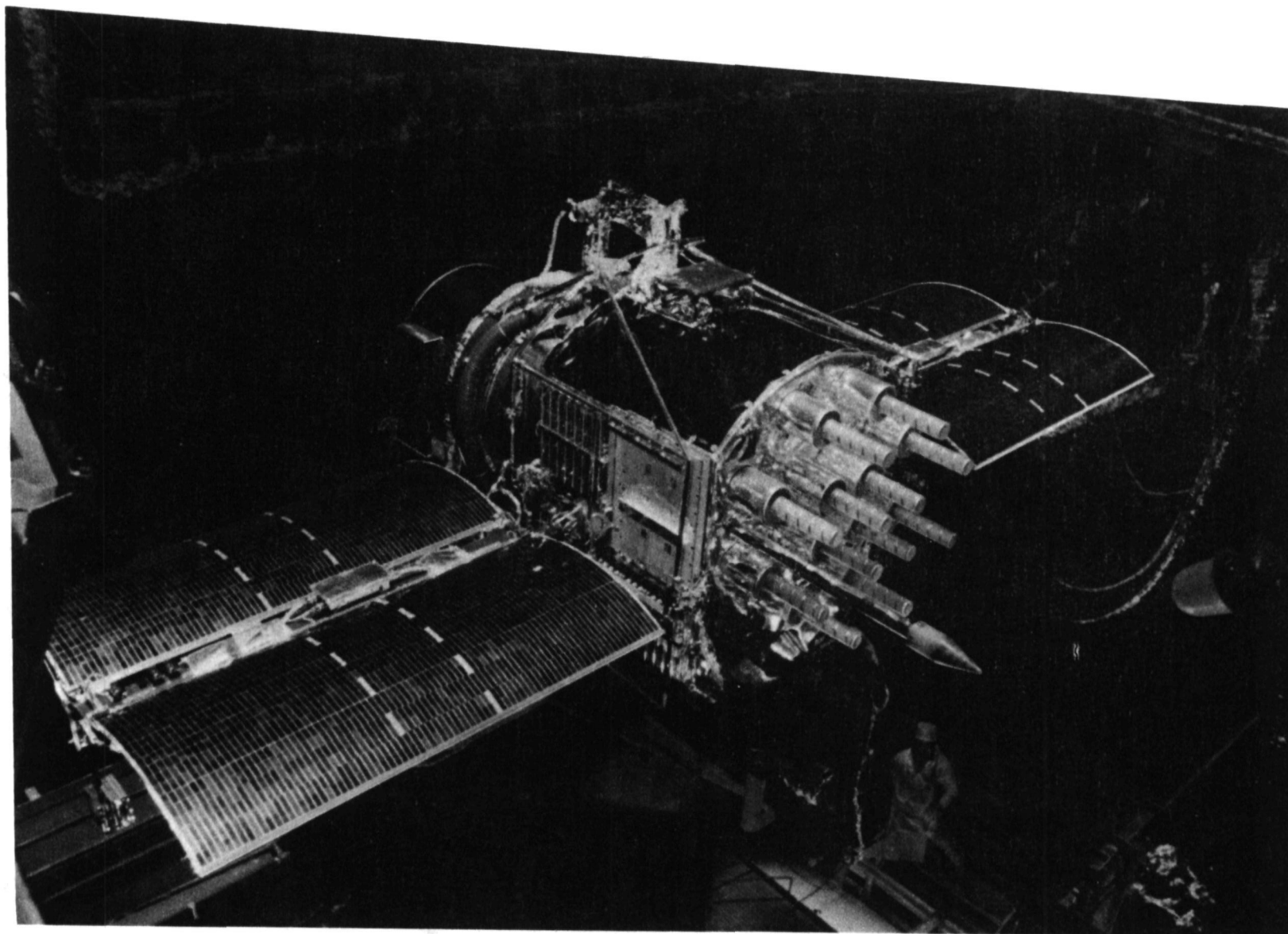


Figure 5. Thermal Vacuum Testing of Space Vehicle

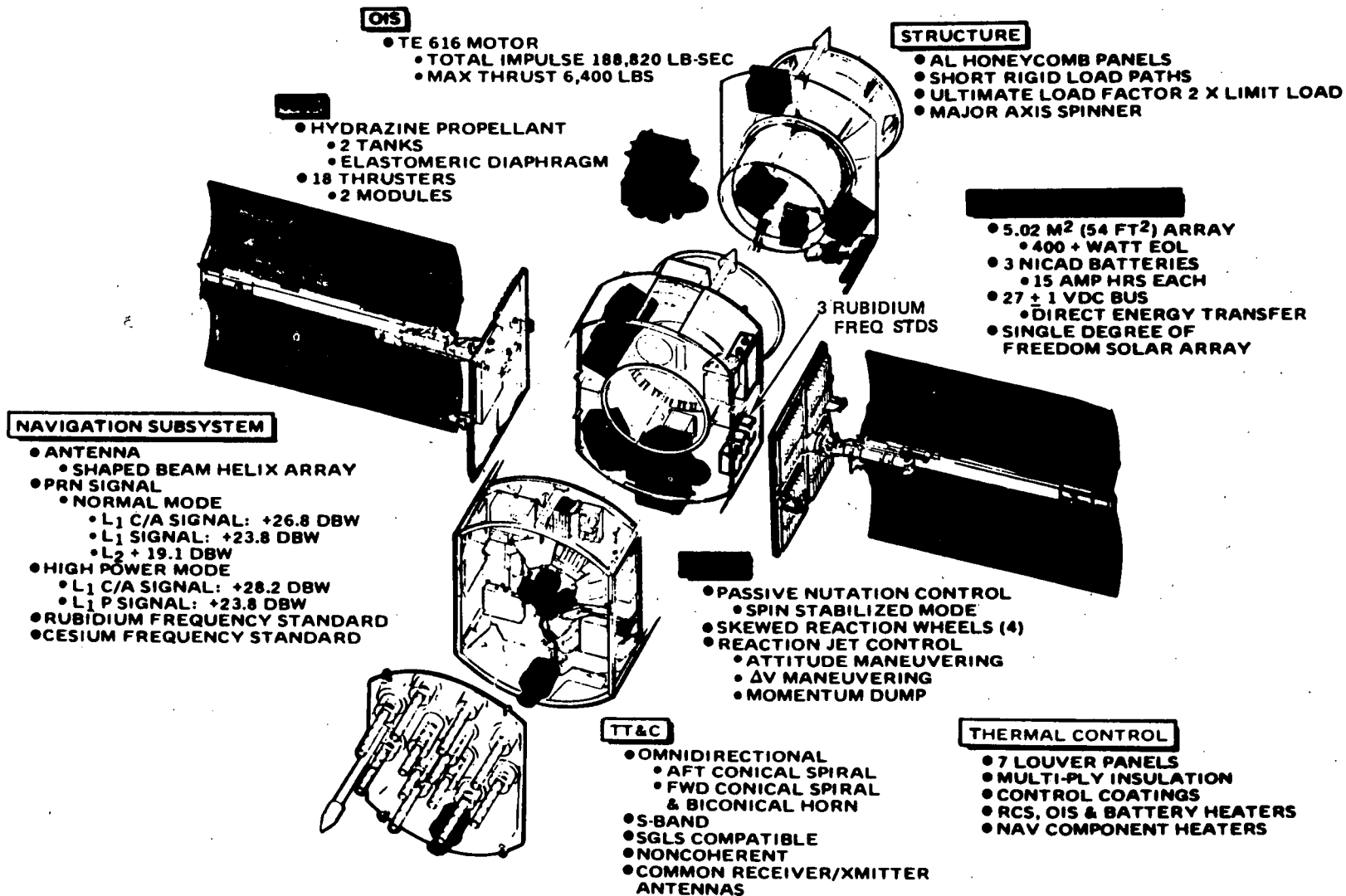


Figure 6. Satellite Subsystems

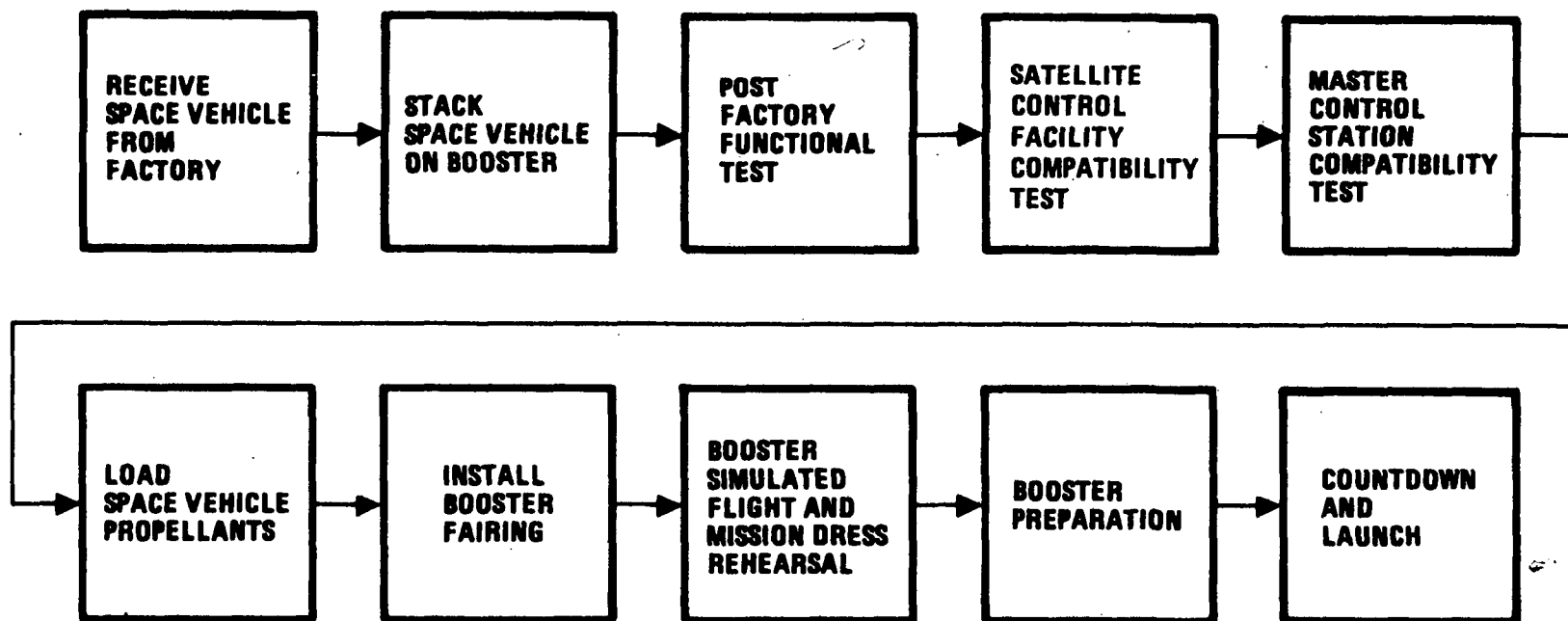


Figure 7. Launch Site Test Flow (Vandenberg AFB, California)

QUESTIONS AND ANSWERS

DR. VESSOT:

If you could explain a little more about what I consider to be the most important test -- and that is the on-going operation of the clock and the monitoring of its operation for very, very long periods of time. Even though these are extreme stages of testing, in my opinion, you do not observe the clock operating for as long as you possibly can while it is in your possession before it goes into space.

A lot of those long-term tests I feel are very minor.

MR. KOIDE:

The long-term tests uses trade-off schedules -- production schedule trade-offs. So, we felt that the long-term type testing will be the Allan variance test which will get out to 100,000 seconds. We get our data points up to about seven data points to give us some assurance of confidence that it has maintained this particular level of task.

DR. VESSOT:

This is not the kind of test I had in mind -- which is the test wherein you prove that this device is going to work for a period of several months while you still have it on the ground. At no time while it is in your possession, I feel, should you fail to take data from the clock in the operating condition.

This is the clean shake, shock, vibration, thermal vac, and all the rest of it -- keep it running and monitor it.

MR. KOIDE:

Yes, we do have the acceptance level testing for the rubidium frequency standard. Once the rubidium frequency standard gets over to the factory test level and integrated into the space vehicle, you are primarily concerned with the interface compatibility between systems.

So, you do monitor all the time -- you do the test while you are testing or monitoring the telemetry lines. You do a lot of other types of tests, but is mainly for the interface compatibility of other systems.

DR. VESSOT:

But does that interfere with the frequency or the stability testing?

MR. KOIDE:

No, that is not the prime function when we get into the vehicle testing.

DR. VESSOT:

I suggest that is a mistake; that you can't avoid that issue of keeping an eye on the piece while you still have it as long as you possibly can.

MR. KOIDE:

Well, we try to do that. We are trying to set up a long-term test, a life test for the RFS and that is another issue.

Page Intentionally Left Blank

SESSION III

TIME TRANSFER

James A. Buisson, Chairman
Naval Research Laboratory

Page Intentionally Left Blank

PROGRESS OF THE LASSO EXPERIMENT

Dr. B.E.H. SERENE

European Space Agency, Toulouse, France

ABSTRACT

The LASSO (Laser Synchronisation from Stationary Orbit) experiment has been designed to demonstrate the feasibility of achieving time synchronisation between remote atomic clocks with an accuracy of one nanosecond or better by using laser techniques for the first time. The experiment uses ground-based laser stations and the SIRIO-2 geostationary satellite, to be launched by ESA towards the end of 1981.

The first part of the paper is dedicated to the qualification of the LASSO on-board equipment, with a brief description of the electrical and optical test equipment used.

The second part gives the progress of the operational organisation since the last PTTI meeting, including the provisional list of participants.

1. INTRODUCTION

Since the last PTTI meeting an important number of activities have taken place in the framework of the SIRIO-2 programme and more specifically for the LASSO experiment :

- the units of the mechanical model have been integrated and successfully tested with the complete satellite,
- a design review has been held to examine breadboard results with a view of authorising the manufacture of the qualification units,

- the units of the qualification model have been delivered to the Centre National d'Etudes Spatiales (CNES) for integration and performance evaluation at subsystem level,
- after acceptance of the principal investigators by ESA, two LASSO Experimenters and Users Team (LEUT) meetings were held in Geneva and Paris respectively,
- the LASSO Coordination Centre (LCC) was subcontracted to the Italian firm TELESPIAZIO which is already in charge of the SIRIO-2 Operations Control Centre (SIOCC).

2. QUALIFICATION OF THE LASSO PAYLOAD

2.1. LASSO On-Board Equipment

The specifications and the design concept were largely presented at the last PTTI meeting (1). It is recalled that the LASSO payload consists of :

- the retro-reflectors,
- the photo-detectors for sensing ruby and neodyme laser pulses,
- the ultra-stable oscillator,
- the counter to time-tag the arrival of the pulses.

These time-tags are to be encoded in time division multiplex with satellite housekeeping before transmission to the ground.

An overall block diagram is shown in Figure 1.

2.2. LASSO Test Equipment

The test equipment has been designed and built for easy transportation and operation with a maximum of automatic test sequences. It is used at :

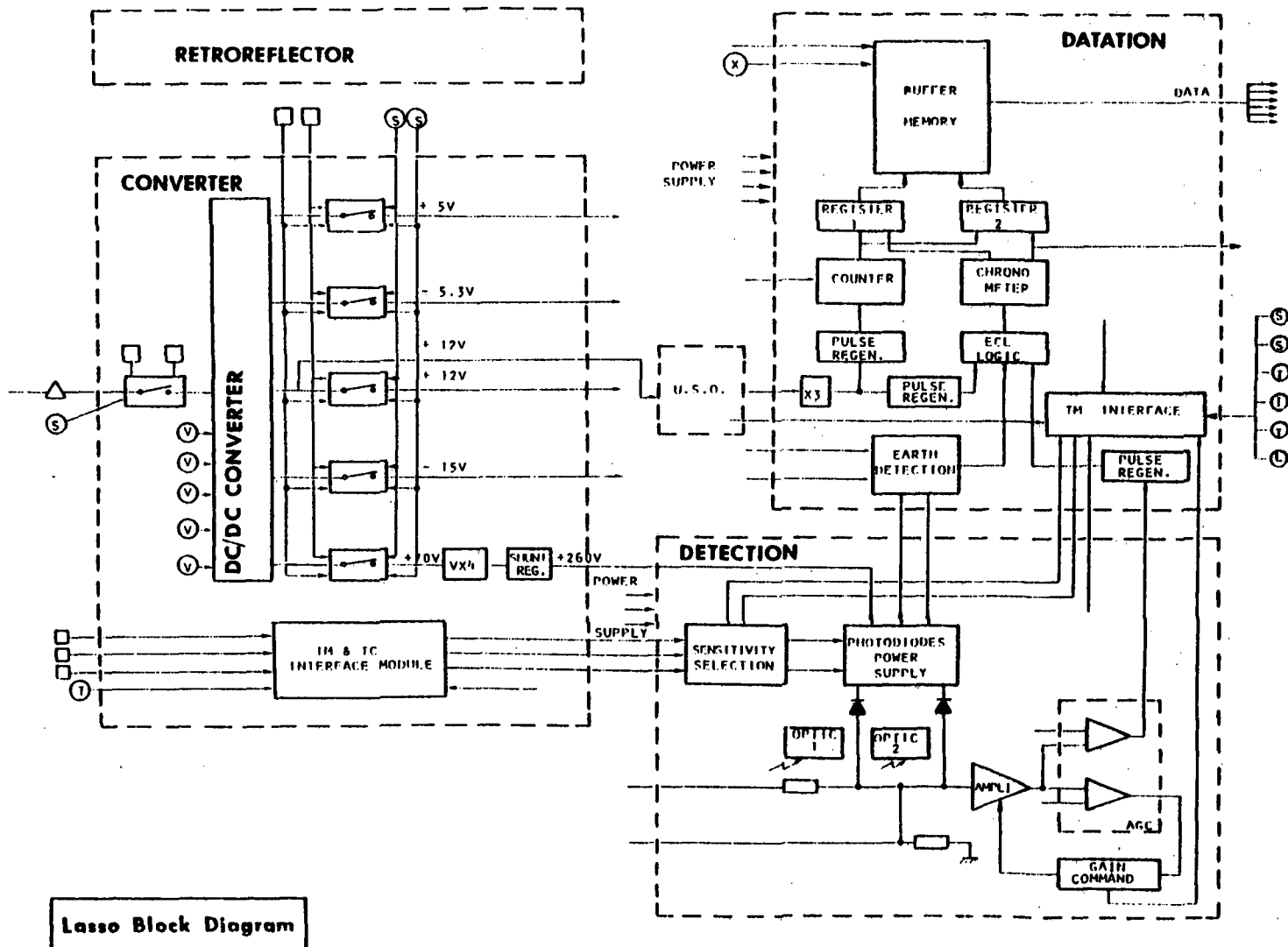
- subsystem level for qualification and acceptance tests,
- system level for integration and pre-launch tests,

and consists of two inter-connected parts : the electrical test equipment (ETE) and the optical test equipment (OTE).

(1) SERENE B. and ALBERTINOLI P.,

"The LASSO Experiment on the SIRIO-2 Spacecraft", ESA Journal, Vol. 4, pages 59 to 72, 1980

FIGURE 1



2.2.1. Electrical test equipment

In order to allow a complete check of the LASSO payload, the ETE must perform the following functions :

- (a) satellite interface simulation concerning power supply, telecommand transmission, telemetry acquisition and synchronisation with satellite rotation.
- (b) laser pulse simulation by means of an electrical pulse generator which is used directly behind the photo-detectors or indirectly to trigger the OTE. In both cases, stimuli pulses are time-tagged by the ETE; these measures are used as references to verify those carried out by the LASSO equipment.
- (c) LASSO housekeeping monitoring; this function concerns temperatures, voltages, currents and status recognition.
- (d) interface with the satellite check-out equipment after integration of the LASSO payload in the satellite.

Overall control of the ETE is performed by a desk-top computer running automatic and semi-automatic test sequences and providing finally statistical treatment of the measurements performed.

An overall block diagram is shown in Figure 2.

2.2.2. Optical test equipment

The OTE, under ETE software control, sends laser pulses towards LASSO detectors and simulates the light generated by the earth albedo inside a time window corresponding to earth visibility.

The departure of the laser pulses are detected in the OTE by fast photo-diodes which provide an electrical feed-back signal time-tagged by the ETE.

The block diagram of the OTE is given in Figure 3, and the main characteristics of the different parts are listed below :

LESSO SUBSYSTEM TEST CONFIGURATION

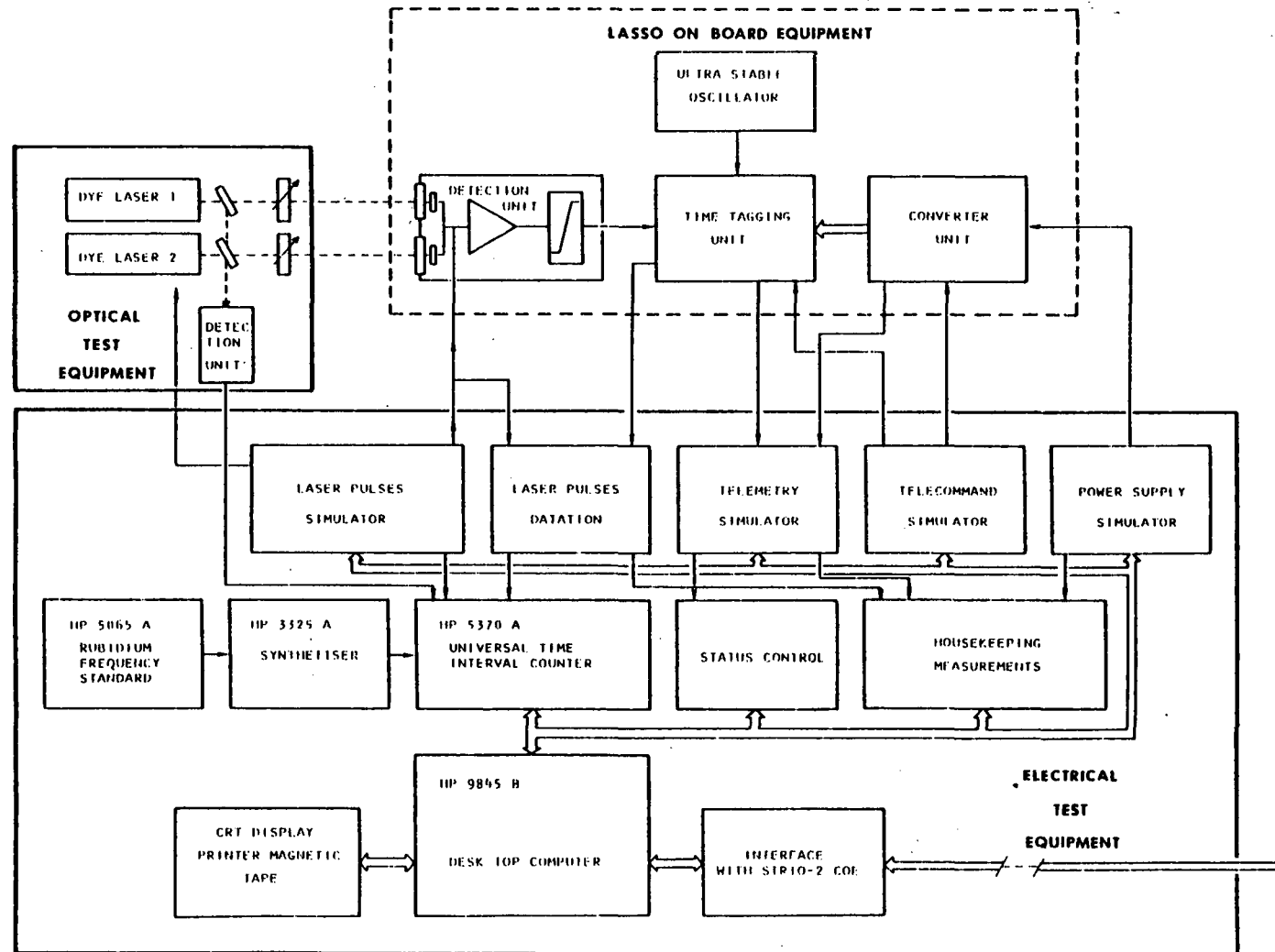
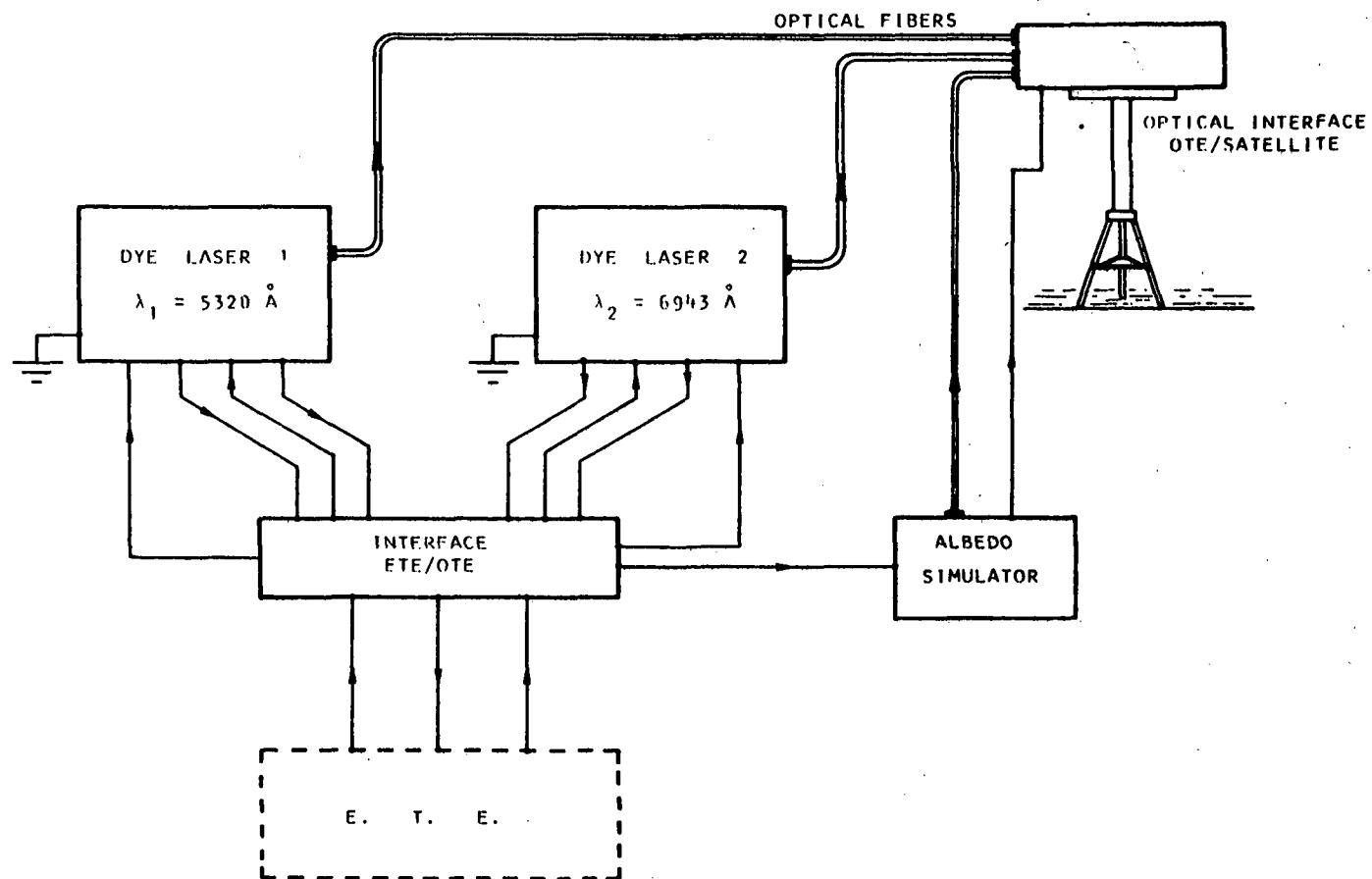


FIGURE 2



Lasso Optical Test Equipment

FIGURE 3

(a) dye laser for neodyme simulation

$$\lambda_1 = 532.0 \text{ nm}$$

$$1 < \text{PWHA}^* < 3 \text{ nsec.}$$

$$0.1 < E < 30 \text{ mW/cm}^2$$

maximum repetition rate : 20 Hz

(b) dye laser for ruby simulation

$$\lambda_2 = 694.3 \text{ nm}$$

$$1 < \text{PWHA}^* < 3 \text{ nsec.}$$

$$0.05 < E < 20 \text{ mW/cm}^2$$

maximum repetition rate : 13 Hz

(c) earth albedo simulator where a quartz-iodine lamp provides the illumination :

$$22 \text{ } \mu\text{W/cm}^2 \text{ for } \lambda_1 \pm 6 \text{ nm}$$

$$16 \text{ } \mu\text{W/cm}^2 \text{ for } \lambda_2 \pm 6 \text{ nm}$$

(d) optical interface which collects, by means of optical fibers, the light generated by the three simulators above; after being mixed and merged into a parallel beam, the light is chopped by a mechanical shutter driven by the earth appearance signal.

(e) electrical interface between the OTE and the ETE.

* Pulse width half amplitude

2.3. LASSO Units Test

2.3.1. Retro-reflectors

The qualification programme was run by AEROSPATIALE on a test sample made of 94 dummy glass corner cubes and 4 flight-worthy quartz corner cubes. The diffraction figures of the 4 quartz corner cubes were measured before and after each test :

- vibration (sinusoidal and random)
- thermal cycle under vacuum (+50°C, -60°C)

The measured efficiency for normal incidence is in fact 20 for 694.3 nm and 17.5 for 532 nm;

2.3.2. Optics

The qualification programme on the two sets of optics was conducted by MATRA and EMD.

For the neodyme optics the results are :

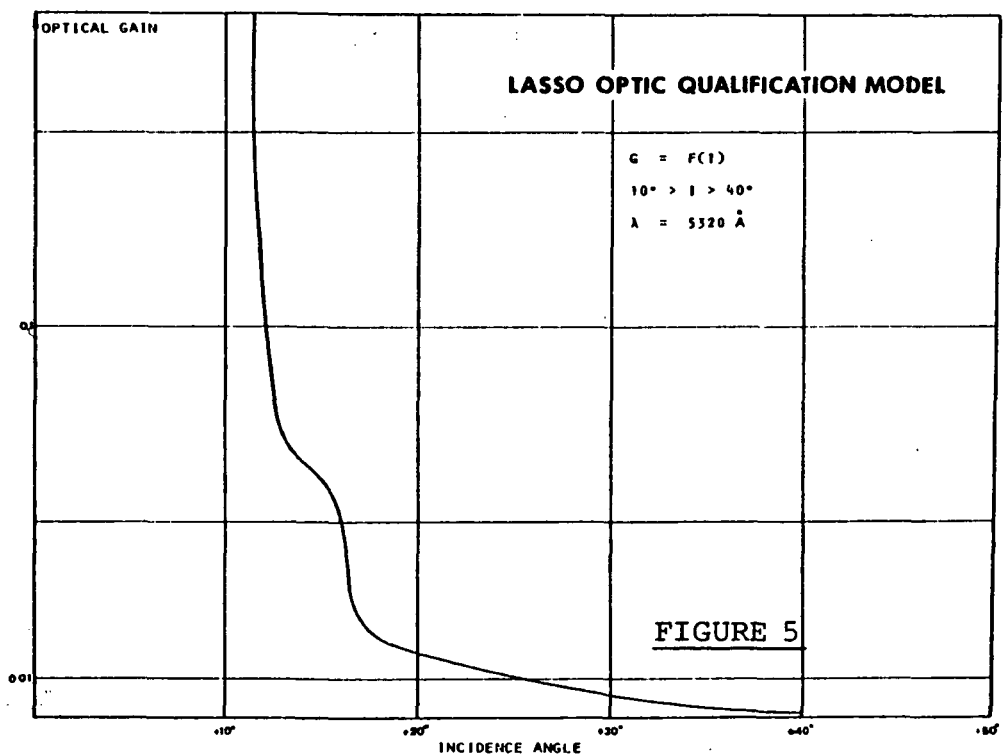
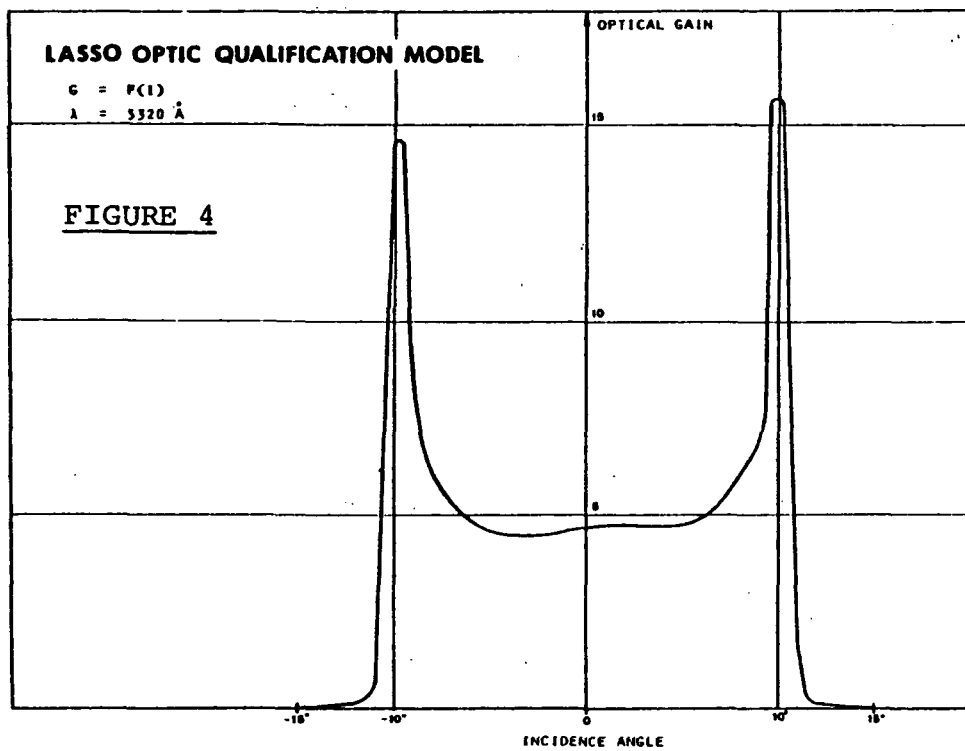
- normal incidence $\lambda_c = 534.3$ nm with a bandwidth (half amplitude) of 11.8 nm;
- 10 degrees incidence introduce a shift of the central wavelength of -2.3 nm; the bandwidth remains the same;
- the optical gain versus incidence angle was measured and the results are given in Figure 4 and 5;

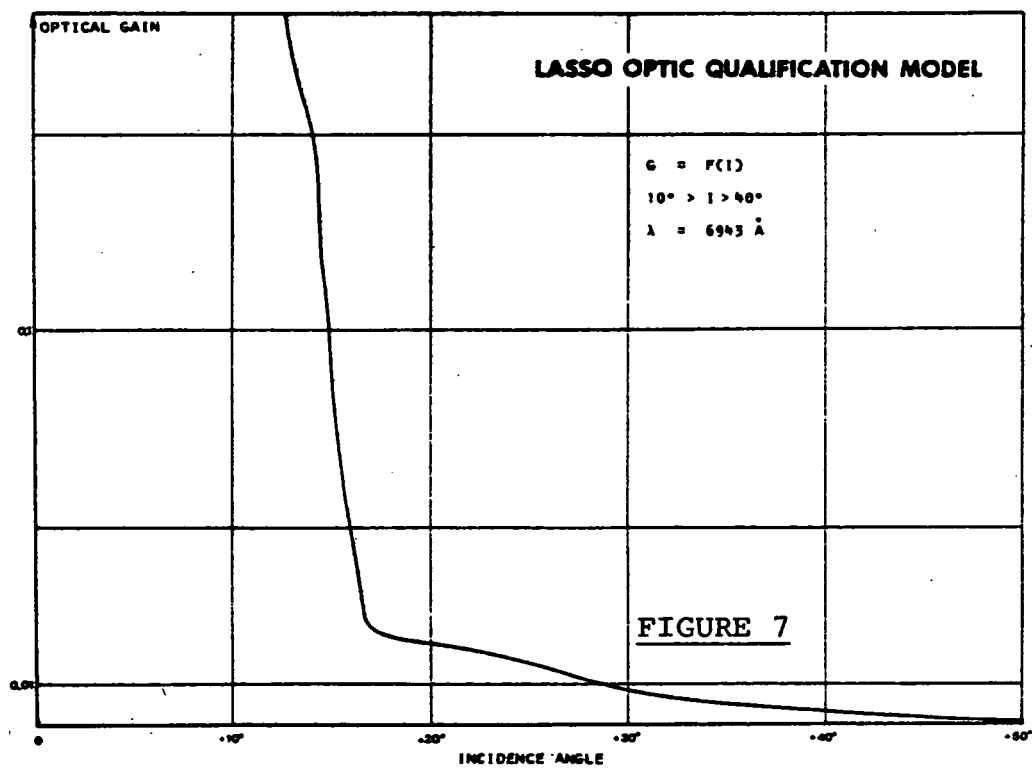
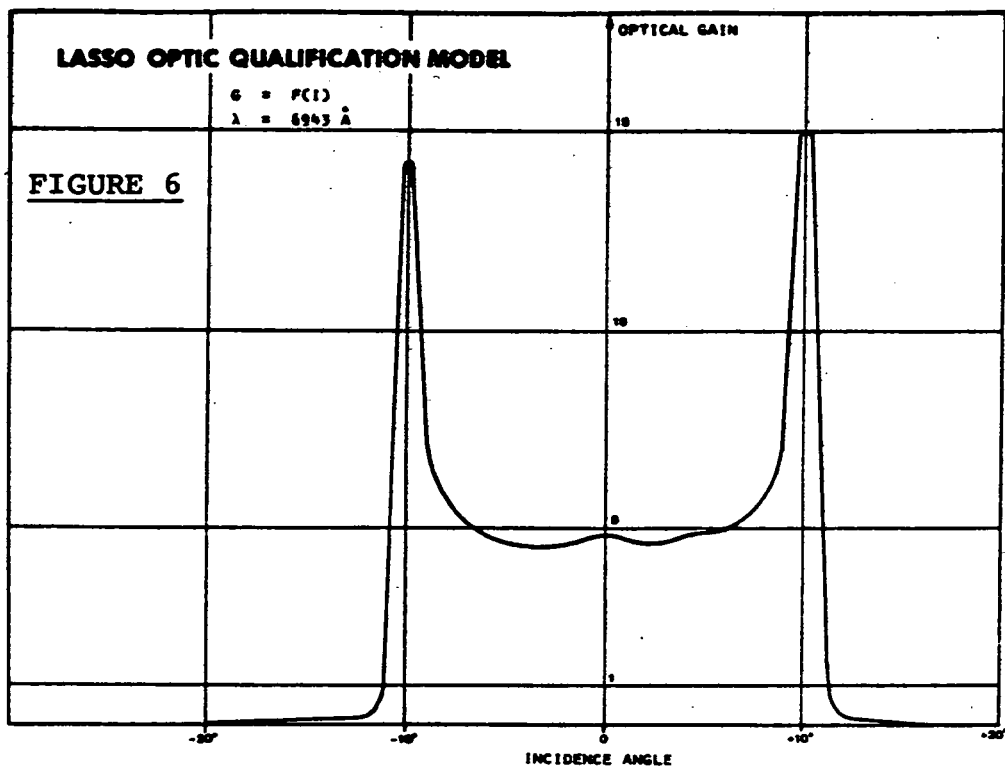
For the ruby optics the results are :

- normal incidence $\lambda_c = 696.9$ nm with a bandwidth (half amplitude) of 12.1 nm;
- 10 degrees incidence introduce a shift of the central wavelength of -2.5 nm, the bandwidth remaining the same;
- the optical gain versus incidence angle was measured and the results are given in Figures 6 and 7.

2.3.3. Ultra-Stable Oscillator (U.S.O.)

This unit, manufactured by F.E.I. (USA), was delivered fully qualified.





2.3.4. Converter

The qualification programme was conducted by LABEN and the following test sequence was applied :

- electrical performance,
- vibration (sinusoidal and random),
- electrical performance,
- thermal cycles under vacuum (+60°C, -20°C)
- final electrical performance.

2.3.5. Detection and datation

The qualification programme was conducted by EMD on both units, using only the ETE. The following test sequence was applied :

- electrical performance,
- vibration (sinusoidal and random),
- electrical performance (repeated),
- thermal cycles (+50°C, -10°C),
- electrical performance (repeated).

The electrical performance was controlled for six different configurations which are listed below :

Configu- ration	Pulse width (half amplitude) (nsec)	Time Sep- aration between 2 pulses of a same pair (msec)	Time Sep- aration between 2 pairs (msec)	Pulse amplitude (mV)	Time Sep- aration between 2 se- quences (msec)
1	2	0.284	1164	200	70
2		72.7			
3	20	0.284		8 000	
4		72.7			

A 5th configuration is used for false detection evaluation, with and without the presence of the earth albedo, during a period of five minutes.

Yet another configuration, No. 6, is used for the chronometer dead-time evaluation, i.e. time tagging pulses far apart of 200 μ sec.

The results obtained for the different configurations are summarised in the Table 1.

Confi- guration	sensitivity	albedo	Standard deviation (psec)	False detection
1	normal	no	148	-
2	"	"	377	-
3	"	"	137	-
4	"	"	456	-
1	maximal	yes	159	-
2	"	"	280	-
3	"	"	141	-
4	"	"	296	-
5	"	"	-	0
5	"	no	-	0
1	normal	yes	185	-
2	"	"	286	-
3	"	"	145	-
4	"	"	240	-
5	"	"	-	0
6	Operating properly			

TABLE 1

2.4. LASSO Subsystem Test

For this purpose a satellite mock-up was manufactured, enabling the units to be mounted in their exact position.

After delivery to CNES, the detection, the datation and the ultra-stable oscillator were integrated on the mock-up and inter-connected with the qualification model harness. This partial subsystem was submitted to thermal cycle under vacuum (+50°C, -10°C) during which the electrical performance was extensively controlled using the OTE and ETE.

The main results are :

- for 1900 pairs of pulses generated by the neodyme and the ruby laser simulators, in all the configurations, the standard deviation is 341 psec with a bias of 68 psec due to the fact that two different time references are used.
- the number of false detections is always less than one per hour.

After delivery to CNES, the converter was integrated in the partial subsystem. The test programme for the qualification of the complete subsystem is at present ongoing with the following activities :

- electrical performance,
- electromagnetic compatibility, including electrostatic test,
- thermal cycles,
- final electrical performance.

3. OPERATIONAL ORGANISATION

The overall SIRIO-2/LASSO organisation is shown in Figure 8.

The industrial consortium is led by the Compagnia Nazionale Satelliti per Telecomunicazioni (CNS) with two co-contractors, CNES and SELENIA, in charge of the LASSO and MDD payloads respectively, while for the operational activities the company TELESPAZIO has been entrusted, under ESA contract, to run the SIOCC and the LCC.

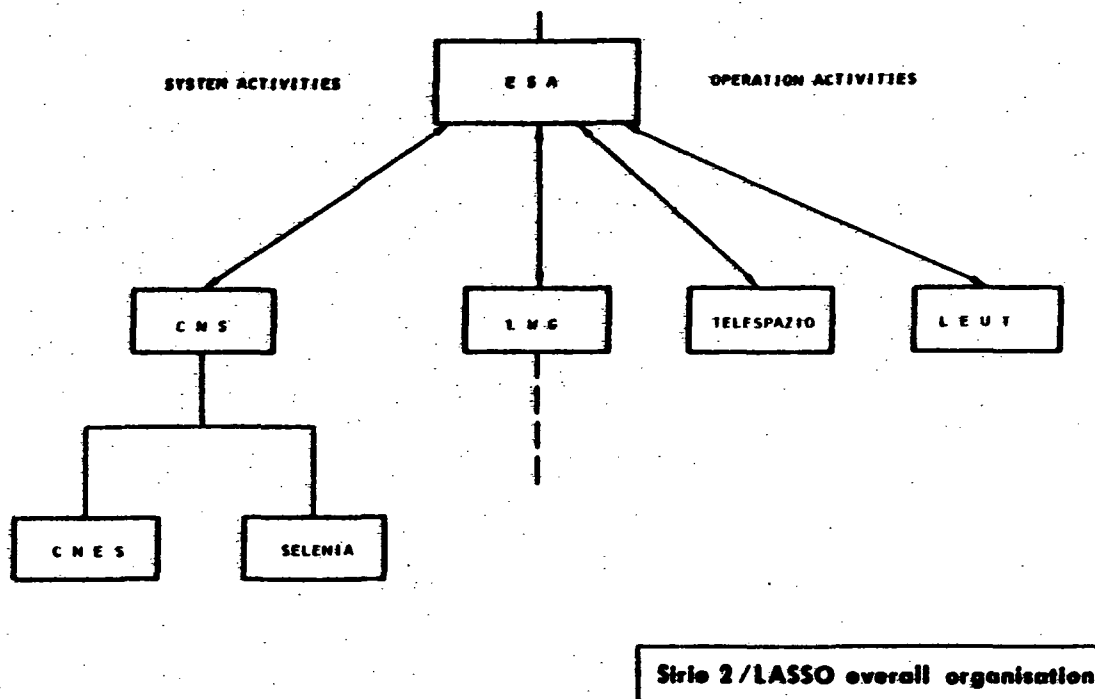


FIGURE 8

The LASSO Working Group (LWG), which is composed of seven European scientists, has been created to advise ESA on the validity of the proposed participation, the capabilities of existing and envisaged laser stations, and potential LASSO applications (time and frequency, geodesy, geophysics).

The LASSO Experimenters and Users Team (LEUT) is composed of the principal investigators of the admitted experiments. The purpose of the group is to clear the technical and operational interfaces between the ESA-provided services and the users intentions. It also enables the users themselves to be involved at the very beginning of the experiment coordination process.

The SIRIO-2/LASSO operational organisation is given in Figure 9.

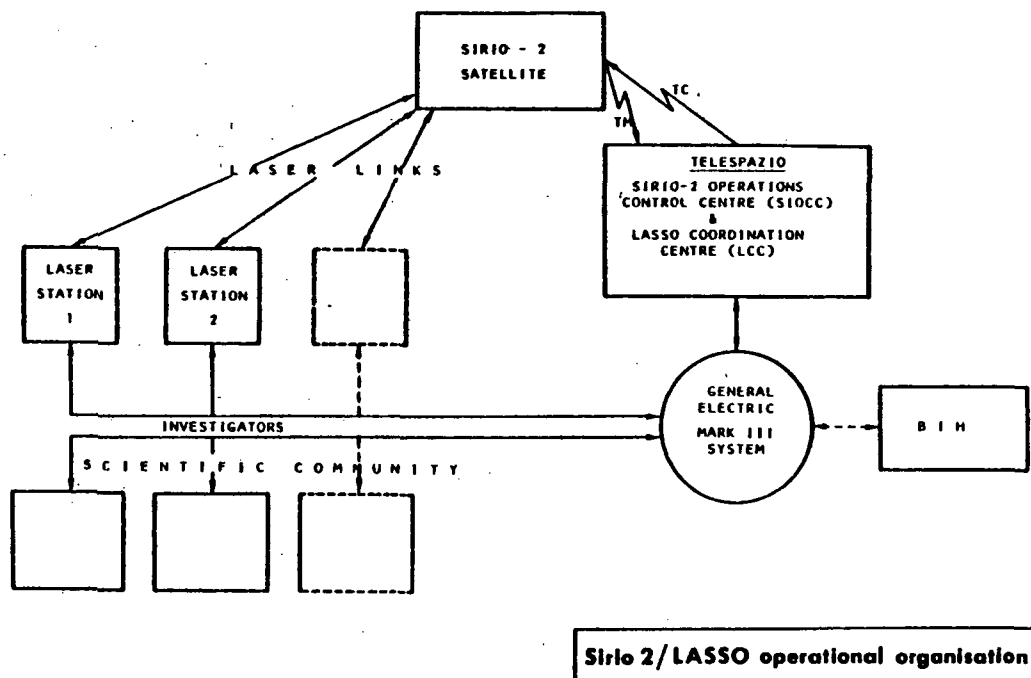


FIGURE 9

3.1. The Scientific Community

The Announcement of Opportunity was issued by ESA in September 1979 and distributed worldwide. Replies were received and analysed with the support of the LWG during the first quarter 1980. Provisional admittances were notified to the principal investigators, and two LEUT meetings were held in June and September 1980.

The provisional list of participants in the LASSO mission is given in Table 2.

Country	Entrusted Laboratory	Principal Investigator	Laser Station	Status
Austria	U.T. Graz	Prof. W. Riedler	Lustbühel	Purchase in progress
Brazil	CNPq	P. Mourilhe Silva	Information not available	
France	GRGS BIH LPTF	Dr. F. Barlier	Grasse	Operational
E.Germany	Academie der Wissenschaften	Dr. G. Hemmleb	Potsdam	Operational
W.Germany	PTB IFAG	Dr. G. Becker	Wettzell	Operational
India	NPL STARS	Dr. B.S. Mathur Dr. P.S. Dixit	Kavalur	Under refurbishment
Italy	Cagliari Obs. OAT IEN Univ. Pavia	Prof. E. Proverbio Prof. M.G. Fracastoro Prof. B. Bertotti	Cagliari Turino n.a.	" " Purchase in progress off-line
Netherlands	Van Swinden U.T. Delft	Dr. R. Kaarls	Kootwijk	Operational
Spain	Instituto y Obs. de Marina	J. Benavente	San Fernando	Under refurbishment
U.S.A.	USNO NASA GSFC NBS Univ. Maryland Dept. of Navy	Dr. G.M.R. Winkler Dr. R.J. Anderle	NASA GSFC n.a.	Operational off-line
ESA	ESOC	W. Flury & J.M. Dow	n.a.	off-line

TABLE 2

The LASSO Principal Investigators are undertaking preparatory work for LASSO participation in the following typical areas :

- adaptation of laser station equipment (e.g. acquisition of datation timers, modification of laser beam width, intensity, pulse length);
- preparation of computer software for time synchronisation calculation and geophysical or orbitographical analysis;
- affiliation to the General Electric Mark III System for data exchange;
- attendance at the LASSO Experimenters and Users Team (LEUT) meetings organised by ESA.

3.2. The L.C.C.

Telespazio has been requested to prepare for the set-up, operation and maintenance of the LCC for the purpose of :

- (i) experiment preparation (hours, minutes before daily laser transmission session), including :
 - orbit determination,
 - S/C spin phase prediction,
 - laser firing times,
 - telescope pointing angles,
 - dissemination and acknowledgment;
- (ii) experiment monitoring (during daily session) :
 - LASSO telemetry real-time analysis,
 - operational feedback to/from laser stations,
 - updating of operational modes (e.g. phasing of transmissions);
- (iii) compilation and annotation of data (after daily sessions) :
 - LASSO telemetry preprocessing to correlate timing with stations,
 - laser station timing data,
 - orbital ranging data,

- S/C spin phase information,
- session narrative summary;

(iv) dissemination and archiving of results.

3.3. Communication System

Data exchange between LCC, laser stations, time institutes and research laboratories will, as far as practicable, take place using the worldwide General Electric Mark III System.

Specialised or validative data processing will be performed by various user institutes primarily to satisfy their own needs, but the results will be made available to the user community as a whole by way of the G.E. Mark III file interrogation feature.

The LCC data output will consist of laser transmission and reception times at the participating laser stations, along with the datation extracted from the satellite telemetry. The data will be distributed to principal investigators via the G.E. Mark III System.

3.4. Cooperation with the "Bureau International de l'Heure" (BIH)

The BIH has offered its cooperation with ESA in the LASSO mission in three areas :

- time comparison over long periods, by statistical treatment, for atomic clocks attached to laser stations;
- special processing allowing the participation of one-way laser stations;
- data exchange via the G.E. Mark III System.

3.5. ESA Responsibility

The LASSO principal tasks to be carried out by ESA under the SIRIO-2 Exploitation Phase during 24 months after geosynchronous orbit acquisition are :

- (a) schedule and prepare the overall LASSO mission in terms of monthly, weekly and daily activities, in liaison with participating principal investigators and laser station operators;

- (b) build, operate and maintain a LASSO Coordination Centre (LCC);
- (c) collaborate with LASSO Principal Investigators in the calculation of time asynchronisms among participating atomic clocks with the aim of demonstrating the feasibility of achieving a precision of one nanosecond or better;
- (d) transport and maintain a transportable calibration device in order to monitor secular drift phenomena in the laser transmission and reception equipment at participating laser stations;
- (e) evaluate and report on the performances of the LASSO mission in comparison with other space and ground methods for time transfer.

4. CONCLUSION

The testing of the LASSO qualification model and the manufacturing of the flight model hardware is progressing in a satisfactory manner.

The LASSO mission implementation is facilitated by the overwhelming support of users, consisting mainly of laser station operators, time and frequency institutes, and researchers in the field of geodesy and geophysics.

The LASSO exploitation is benefitting from the fact that the users have developed, over the years, an informal but well-established scientific and operational relationship as a result of earlier land and space programmes.

Accordingly, users in Europe, America and Asia are undertaking procurement or adaptation of ground hardware, along with software development, in order to render the LASSO mission and their own participation as fruitful and rewarding as possible.

- o0o -

QUESTIONS AND ANSWERS

PROFESSOR CARROLL ALLEY, University of Maryland

Could you give us more details on the results of the testing, particularly as to the minimum detectable signal in the presence of maximum Albedo and in the presence of minimum Albedo?

DR. SERENE:

Well, I am surprised you have any questions, Professor, but no I don't have this information here. Have you any problem concerning the detection level? Because as far as I understand you plan to use a quite powerful laser and you have more problem to avoid destroying the equipment on-board than to know the threshold.

PROFESSOR ALLEY:

We need to know both. Let me go a bit further. You reported that the false alarm turns out to be at a rate of less than one per hour, whereas the specifications call for one per minute. This suggests to me that perhaps the threshold levels for detection is set higher than it might be necessary and that one might have a better sensitivity if one adjusted that.

DR. SERENE:

Well, the threshold detection is just to avoid filling the memory with any stray lights, but actually that is not involved in the threshold for the detection of the laser pulse because we have two modes. The normal mode and the sensitive mode on-board, and I don't see the point, because the spec for one false detection per minute is more to limit electronic noise than light noise.

PROFESSOR ALLEY:

Well, I would think that they would get mixed up at the final level. Perhaps we should continue this discussion elsewhere.

DR. SERENE:

Yes, no problem. But, we can have electronic noise and passive light. That is where the false detection comes from, because if you have something recorded in the memory perhaps not coming from the detection, but coming by electromagnetic coupling that is a false detection. It has nothing to do with the threshold.

PROFESSOR ALLEY:

Well, I think this is not the forum to continue this detail but let us continue it later.

Page Intentionally Left Blank

TWO-WAY SEQUENTIAL TIME SYNCHRONIZATION:
PRELIMINARY RESULTS FROM THE SIRIO-1 EXPERIMENT(*)

E. Detoma, S. Leschiutta
Istituto Elettrotecnico Nazionale "Galileo Ferraris"
Torino - Italy

ABSTRACT

A two-way time synchronization experiment was performed in the spring of 1979 and 1980 via the Italian SIRIO-1 experimental telecommunications satellite.

The experiment was designed and implemented by the Istituto Elettrotecnico Nazionale, Torino (Italy), to precisely monitor the satellite motion and to evaluate the possibility of performing a high-precision, two-way time synchronization using a single communication channel, time-shared between the participating sites.

The results of the experiment show that the precision of the time synchronization is between 1 and 5 ns, while the evaluation and correction of the satellite motion effect has been performed with an accuracy of a few nanoseconds or better over a time interval from 1 up to 20 seconds

INTRODUCTION

The principal features of the SIRIO-1 time synchronization experiment can be briefly summarized as follows:

- the experiment was designed to precisely monitor the satellite motion and the effects of this motion on the time synchronization accuracy;

(*) Work supported by the Italian National Research Council.

- the time synchronization is performed using the two-way time synchronization technique and a single communication channel, time-shared between the two sites;
- the experiment tests a new technique that has been proposed to correct for the satellite motion effect while performing the time synchronization;
- by using a single communication channel, no effects affecting the accuracy of the time synchronization at the 1 ns level are due to the space segment (from one ground antenna to the other), thanks to the high frequencies used for the RF carriers;
- the time signals used allow the independent determination of the uncertainties of the time-of-arrival measurements at the two stations, to separate the contribution of each station to the total precision.

This last feature can be important to understand the contribution of local phenomena (ground equipment, atmospheric conditions affecting the signal attenuation, especially rain, etc.) to the synchronization precision.

ORGANIZATION OF THE EXPERIMENT

A detailed description is given in ref. 1. Only a few remarks are given here, mainly for reference purposes.

Two ground stations, Fucino and Lario (fig. 1), participate to the experiment. Both sites are in Italy, in the northern (Lario) and in the central part (Fucino) of the country; one IEN Cesium clock was installed at each site.

Fucino (fig. 2) transmits its time signal at 0 seconds of the synchronization frame (Fucino time), acting as station 'A', while Lario transmits its own signal at 0.5 s (Lario time), acting as station 'B'.

Two times-of-reception are then measured at each site; with reference to fig. 3, these are T_4 and T_3 at Fucino and T_1 and T_5 at Lario (we have no need to measure T_0 and T_2 since these are known).

To simplify the notation and for a better understanding, we may note that $T_4 - T_0$ is the time of propagation of the time signal from Fucino to Fucino, $T_1 - T_0$ is (neglecting for now ϵ) the time of propagation from Fucino to Lario, etc., so we can write:

$$(1) \quad \begin{aligned} T(\text{FF}) &= T_4 - T_1 = T_4 \\ T(\text{FL}) &\approx T_1 - T_0^* \approx T_1 \\ T(\text{LF}) &\approx T_3 - T_2^* \approx T_3 - 0.5 \\ T(\text{LL}) &= T_5 - T_2 = T_5 - 0.5 \end{aligned}$$

(*) local time reference

$T(\text{FF})$, $T(\text{FL})$, $T(\text{LF})$ and $T(\text{LL})$ are the actual results of the time measurements at the two sites [except for the subtraction of 0.1 s, resulting from the hardware implementation, see ref. 1] and will be used in any following computation.

Two data types are considered: pseudo-range data, such as $T(\text{FF})$ and $T(\text{LL})$, that are the time intervals measured against the same time reference, and synchronization data, such as $T(\text{LF})$ and $T(\text{FL})$; the starting and ending times of the latter intervals are measured with reference to different clocks.

Data format

Actually, each one of the values listed in (1) results from the measurement process as the mean over ten independent measurements: a rough data file is shown in fig. 5. Each time of arrival is then evaluated as the arithmetic mean of the measured data. The data is rejected if the associated standard deviation is larger than 100 ns; however, less than 0.5% of the data was rejected because their standard deviation was exceedingly large. On the average, the standard deviation for each of the time-of-arrival evaluations, based on ten data values, is in the range 10 to 50 ns.

The basic synchronization frame lasts 1 s and is repeated every 10 s; during the 1979 series of measurements, small groups of data (10 to 15 measurement frames) were recorded sequentially, to characterize the performance of this technique over time intervals of 100 to 150 seconds: this was actually performed also to verify the assumption of a linear motion of the satellite and the validity of the correction used (see eq. (7) to (15), ref. 1) over this time interval.

During 1980 a second series of measurements were performed over longer time intervals (up to 16 minutes); the comparison between the results obtained via the satellite, the TV method and portable clock trips are shown in fig. 6, where ϵ_t is the difference between the two atomic clocks located at the ground sites. An expanded view over four consecutive days of satellite measurements is given in fig. 7.

The overall accuracy of the clocks comparison was estimated to be between 50 and 100 ns, with reference to some portable clock comparisons.

Synchronization estimate ($\tau = 1$ s)

The clocks difference ϵ_t at the time t , defined as:

$$(2) \quad \epsilon_t = t(B) - t(A) = t(LAR) - t(FUC)$$

is given (see ref. 3), over the basic synchronization frame time interval τ ($\tau = 1$ s), by the equation:

$$(3) \quad \epsilon_t(\tau = 1 \text{ s}) = \frac{T_t^{(FL)} - T_t^{(LF)}}{2} + (0.5) \cdot C$$

since $(t_2 - t_1)$ is 0.5 s (see fig. 3).

The range-rate correction C to ϵ_t , as defined in ref. 1, is computed as:

$$(4) \quad C = + \frac{1}{2} \frac{[T_{t+10}^{(FF)} - T_t^{(FF)}] + [T_{t+10}^{(LL)} - T_t^{(LL)}]}{20}$$

The magnitude of C was usually found to be in the range 2-4 ns/s, yielding a range rate correction of 1 to 2 ns over the basic frame.

An estimate of $\bar{\epsilon}$ is obtained by taking the arithmetic mean of a number of successive data (from 100 s up to 16 minutes). If ϵ would be constant over this measurement interval, then the standard deviation $\sigma(\epsilon)$ of the data would be related to the precision of the method.

The evaluation of $\bar{\epsilon}$ and $\sigma(\epsilon)$ is carried on by applying a 3-sigma width filter; that is, the ϵ_t value is rejected if the residual $|\bar{\epsilon} - \epsilon_t| > 3\sigma$; if any ϵ_t has been rejected, a new

$\bar{\epsilon}$ and $\sigma(\epsilon)$ are evaluated using the remaining data. This procedure is repeated until no more data are rejected; usually this filter rejects less than the 5% of the available data.

Assuming a normal distribution of the data, the one-sided estimated error $|\delta\epsilon|$ in the determination of $\bar{\epsilon}$ is given, with the 99.5% confidence, as:

$$(5) \quad |\delta\epsilon| = \frac{\sigma \cdot t_{0.995}^{(n-1)}}{\sqrt{n}}$$

The magnitude of $\delta\epsilon$, when $\bar{\epsilon}$ is computed over 50 to 100 data ϵ_t , ranges usually between 1 and 5 ns (see fig. 7 and fig. 8).

The capability to look at the precision of the method over short time intervals is demonstrated by fig. 8 and fig. 9, where two-hours data are plotted, together with an unweighted least-squares fit of the available data.

As it can be seen, the average error of the fit is quite small, less than 1.5 ns.

Expanded time synchronization frame ($\tau = 10$ s and $\tau = 20$ s)

As explained in ref. 1, the time synchronization frame can be lengthened by simply rearranging the data.

This shows the capability of the method to synchronize two clocks by using a single communication channel even if a fast switching of the RF carrier at the two sites is not possible and a large effect due to the satellite motion is then expected; however, the amount of the correction due to this motion can be computed very accurately by using the pseudo-range data available.

In this case, the clocks difference ϵ_t can be computed as:

$$(6) \quad \epsilon_t(\tau = 10 \text{ s}) = \frac{T_t^{(FL)} - T_{t+10}^{(LF)}}{2} + (10.5) \cdot C$$

(since now $(t_2 - t_1) \approx 10.5$ s) where C is given by eq. (4).

This is equivalent to have a station transmitting its time signal at t_0 and the other site transmitting at $(t_0 + 10.5)$ s.

Accordingly, to simulate a longer time interval ($\tau = 20$ s) we can write:

$$(7) \quad \epsilon_t(\tau = 20 \text{ s}) = \frac{T_t(\text{FL}) - T_{t+20}(\text{LF})}{2} + (20.5) \cdot C$$

where now C is computed as:

$$(8) \quad C = + \frac{1}{2} \frac{[T_{t+20}(\text{FF}) - T_t(\text{FF})] + [T_{t+20}(\text{LL}) - T_t(\text{LL})]}{40}$$

A comparison of single measurements of ϵ_t , evaluated by using eq. (3), (6) and (7) is presented in fig. 10, over a 200 s time interval. The agreement between the values of ϵ_t for different τ 's is remarkable, if we note that the correction to be applied to eq. (6) and (7) amounts respectively to about 48 and 95 ns in most cases.

Further analysis on the experimental data

Instead of using the differences between the measurement data $T(\text{FL})$ and $T(\text{LF})$ to compute ϵ_t , it is possible to use a polynomial fit of the data and then evaluate ϵ_t over the coefficients of the fitted polynomial.

This procedure has the advantage that less data are exchanged between the two sites (the fit coefficients only) and that also missing data points at one site can be recovered from the fitted curve.

By writing:

$$(9) \quad \begin{aligned} T(\text{FF}) &= \sum_{i=0}^n a_i (t-t_0)^i \\ T(\text{LL}) &= \sum_{i=0}^n b_i (t-t_0)^i \\ T(\text{FL}) &= \sum_{i=0}^n c_i (t-t_0)^i \\ T(\text{LF}) &= \sum_{i=0}^n d_i (t-t_0)^i \end{aligned}$$

eq. (3) can be written as:

$$(10) \quad \epsilon_t(\tau = 1 \text{ s}) = \frac{1}{2} \sum_{i=0}^n (c_i - d_i) (t-t_0)^i + (0.5) \cdot C$$

where:

$$\begin{aligned}
 (11) \quad C &= + \frac{1}{2} \frac{\sum_{i=0}^n (a_i + b_i) (t - t_{0+10})^i - \sum_{i=0}^n (a_i + b_i) (t - t_0)^i}{20} = \\
 &= + \frac{1}{2} \frac{\sum_{i=1}^n (a_i + b_i) \cdot 10^i}{20}
 \end{aligned}$$

If ϵ_t is constant over the measurement interval, then $\epsilon_t = \epsilon_{t_0}$ and eq. (10) becomes:

$$(12) \quad \epsilon_t = \frac{1}{2} (d_0 - c_0) + (0.5) \cdot C$$

If only the linear (velocity) terms are significant and any higher order term (acceleration) of the satellite motion is neglected, then C is given by

$$(13) \quad C = + \frac{a_i + b_i}{4}$$

This procedure was actually carried on over measurements intervals up to 600 s; over time intervals up to 200 s it was found that a linear (first order) fit (as given by eq. (12) and (13)) was usually good enough to evaluate ϵ_t and any further increase in the degree of the polynomial does not improve the fit; obviously this result depends mainly on the clocks and the synchronization process behaviour.

This was also a further check of the correctness of the linear motion assumption as given by eq. (4).

The test of statistical significance (see ref. 2) of the computed coefficients of the polynomials (9) was carried on by computing the standard deviation of the estimated coefficients.

This was done in the following way: the least squares fit is expressed by the normal equations that, in matrix form, are:

$$(14) \quad (X'X)\psi = (X'Y)$$

where: $(X'X)$ is the normal equations matrix (or x-products matrix);

$(X'Y)$ is the cross-products matrix;
 ψ is the vector of the coefficients.

An estimated value of the standard deviation of the fit is computed as:

$$(15) \quad \sigma^2 = \frac{1}{(n-k)} \cdot \sum_i r_i^2$$

where n is the number of data, k is the number of estimated coefficients and r_i is the i -th residual. The estimated standard deviation (ref. 2) of the k -th coefficient is given by:

$$(16) \quad \sigma_k = \sigma \sqrt{c_{kk}}$$

where c_{kk} is the k -th diagonal element of the matrix $(X'X)^{-1}$. Actually the computation of the $(X'X)^{-1}$ matrix was performed with Gauss-Jordan reduction and pivot search to minimize the numerical computation errors. Then an estimated confidence interval for the coefficient can be computed, by using the Student t -distribution at $(n-k)$ degrees of freedom.

Ground-equipment delays measurements

Two types of measurements were performed: test-loop-translator (TLT) measurements and transmitting-chain delay measurements (LARIO site only).

Test-loop-translator measurements

The experimental set-up is shown in fig. 11. The measurements performed showed a precision around 1 ns and a long term (1 month) stability of the delay in the order of 1 to 3 ns, if the ground equipment is operated at the same power level. The measurements were performed in the same operating conditions as during the synchronization sessions.

The loop-delay was found to be 3.776 μ s (LARIO) and 4.618 μ s (FUCINO) on the average.

Transmitter delay measurements (LARIO site only)

The proposed use of a microwave cavity as a frequency discriminator was tested. The cavity was characterized by a Q of 1500 at the transmission frequency. Unfortunately, the only

way to couple the cavity near the TLT was via an existing directional coupler, that attenuates the signal more than 40 dB.

The rectified signal consequently was very small, since the cavity contributed an additional attenuation of about 12 dB, and, under these conditions, the measurement was impossible.

In order to increase the rectified signal, it was necessary to increase the frequency deviation: in these conditions the communication equipment was working outside the range of normal operation and the overall system response degraded noticeably. The measurement jitter, for instance, increased up to 50 ns (1 sigma), as compared to the 1 ns found in the TLT measurements; this was verified by performing the same TLT measurement, but with the larger frequency deviation.

The reproducibility of the measurements, mainly related to the critical setting of the microwave cavity (the cavity resonance was adjusted at the RF carrier frequency when no modulation was applied), was better than 100 ns, even when working in these very critical conditions.

ACKNOWLEDGMENTS

The authors would like to thank the Telespazio personnel at the two ground stations for their assistance in performing the experiment.

We wish also to acknowledge the work of the IEN personnel that actually carried on the measurements; we are especially grateful to V. Pettiti, E. Angelotti, L. Canarelli, F. Cordara, V. Marchisio, G. Moro and L. Pietrelli, to Mr. G. Galloppa for the drawings and to Mrs. M. Castello for the typewriting.

One of the authors (E. Detoma) wishes to dedicate his work to Mrs. Marina Castello, for her constant cooperation, encouragement and sincere friendship: to acknowledge that friendship and loyalty towards the friends are always more important than scientific and personal achievements.

REFERENCES AND NOTES

1. E. Detoma, S. Leschiutta - The SIRIO-1 timing experiment, Proc. of the 11th Precise Time and Time Interval Meeting (PTTI), Nov. 1979 (Washington, D.C.)
2. M.G. Natrella - Experimental statistics, NBS Handbook 91 (1963).
3. The actual computations were carried on by computing ϵ as:

$$\epsilon = t(\text{FUC}) - t(\text{LAR})$$

However, while the data plotted result from these computations, in the text of this paper the same notation is used as in ref. 1.

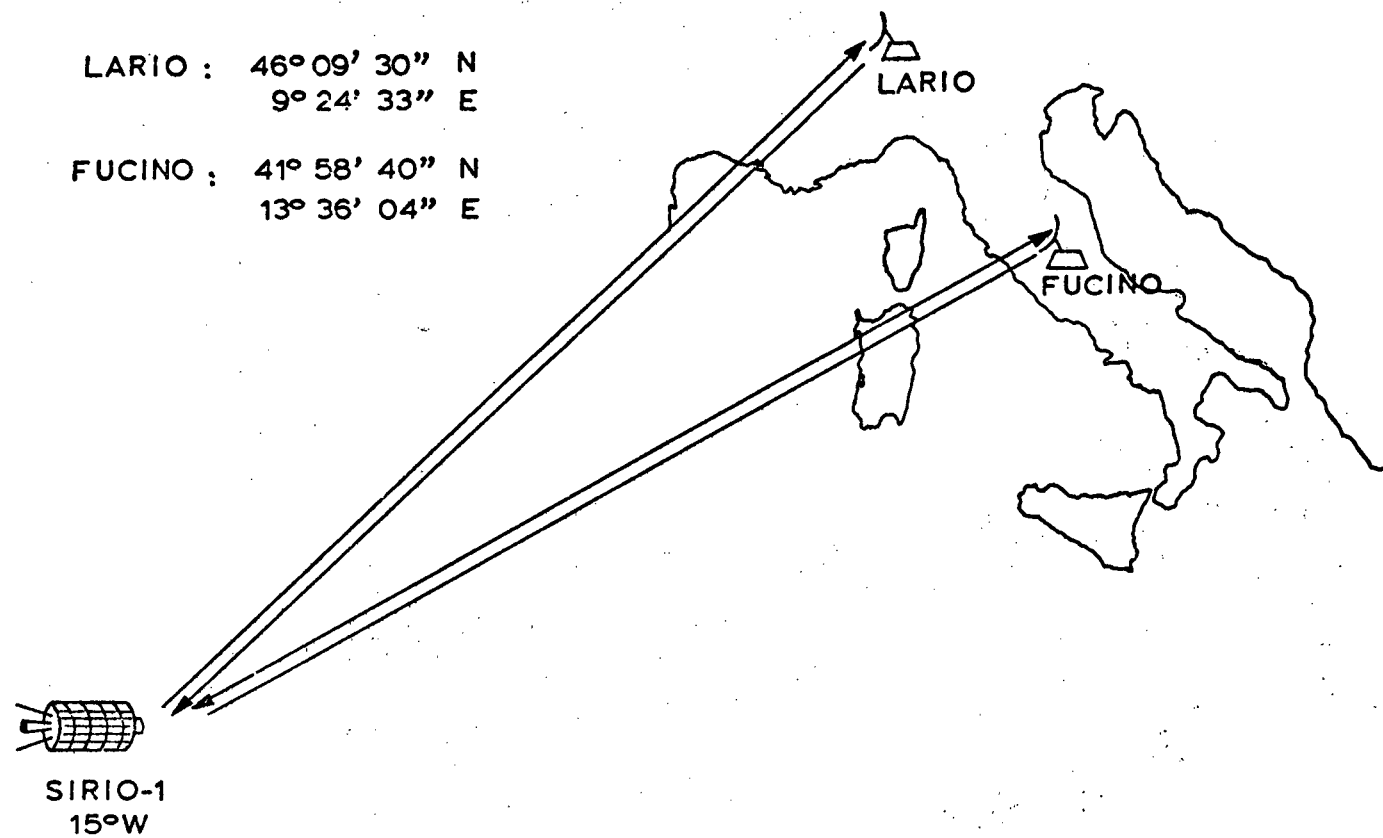


Fig. 1 - Sites geometry

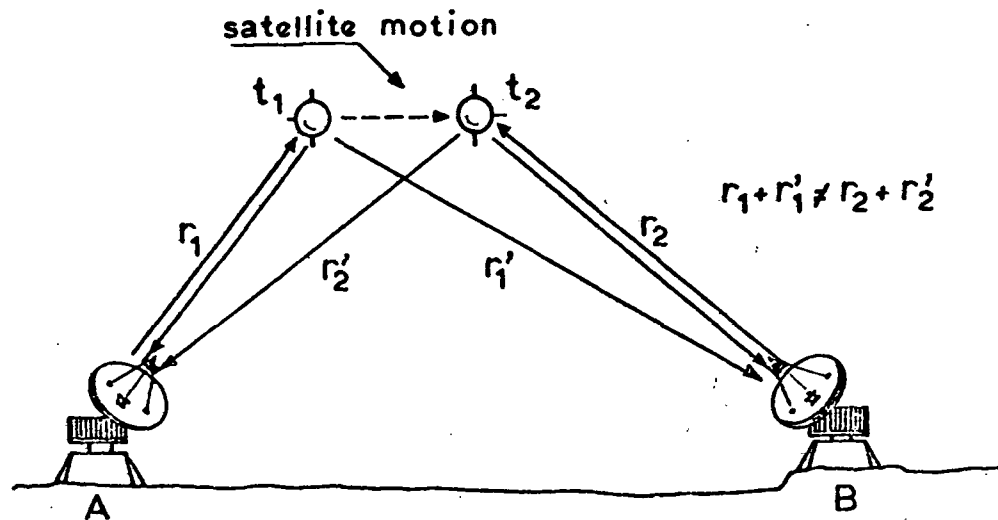


Fig. 2 - Two-way sequential time synchronization

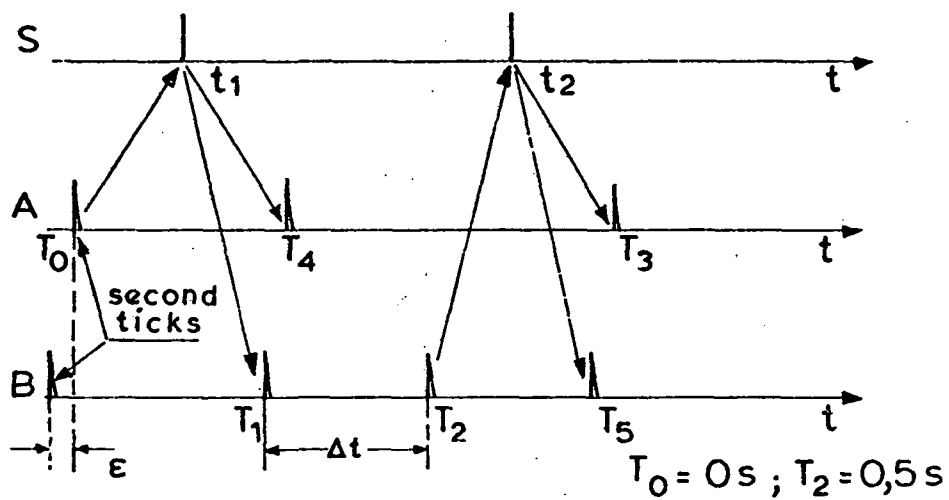


Fig. 3 - Timing diagram



Fig. 4 - The LARIO station antenna

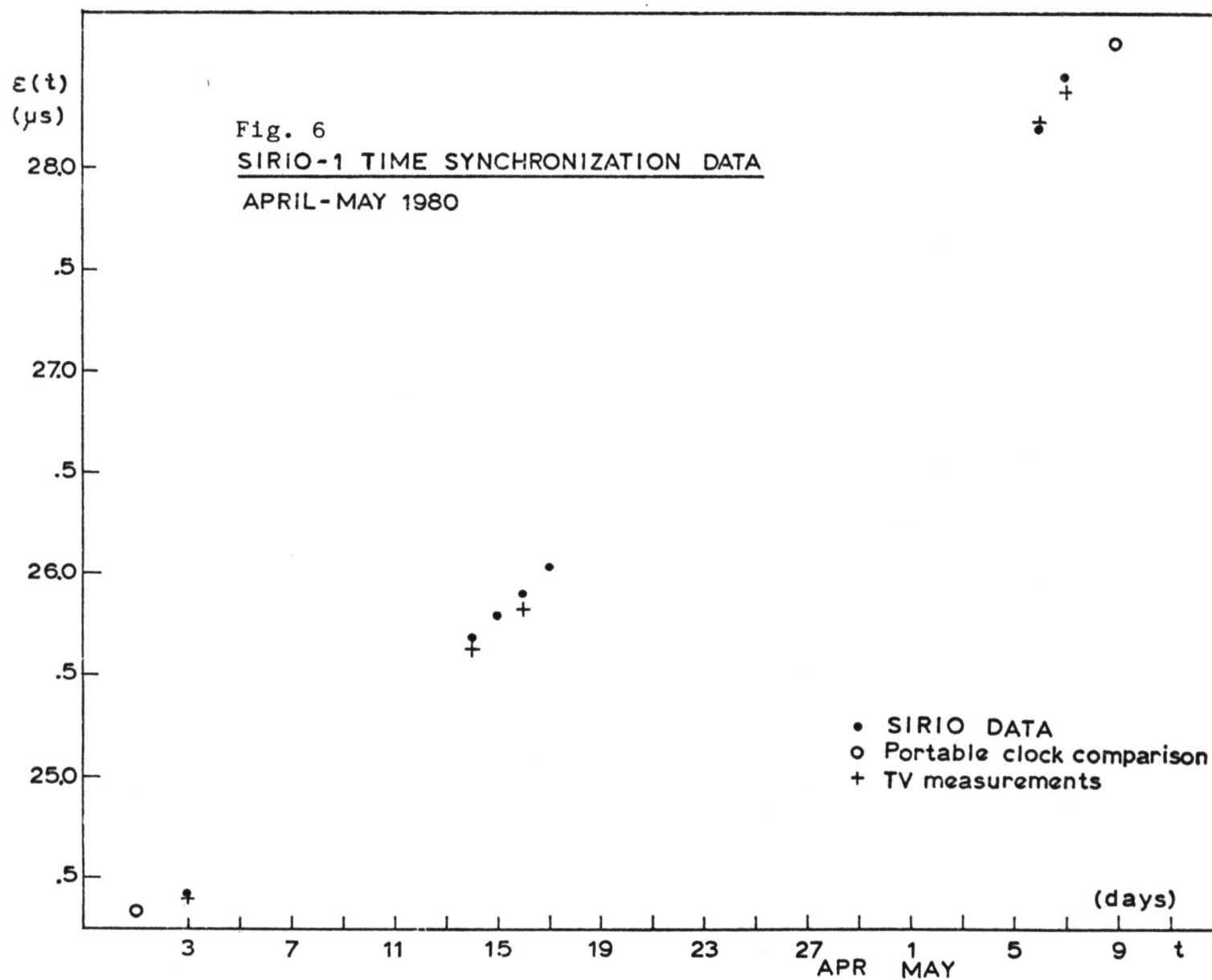
```

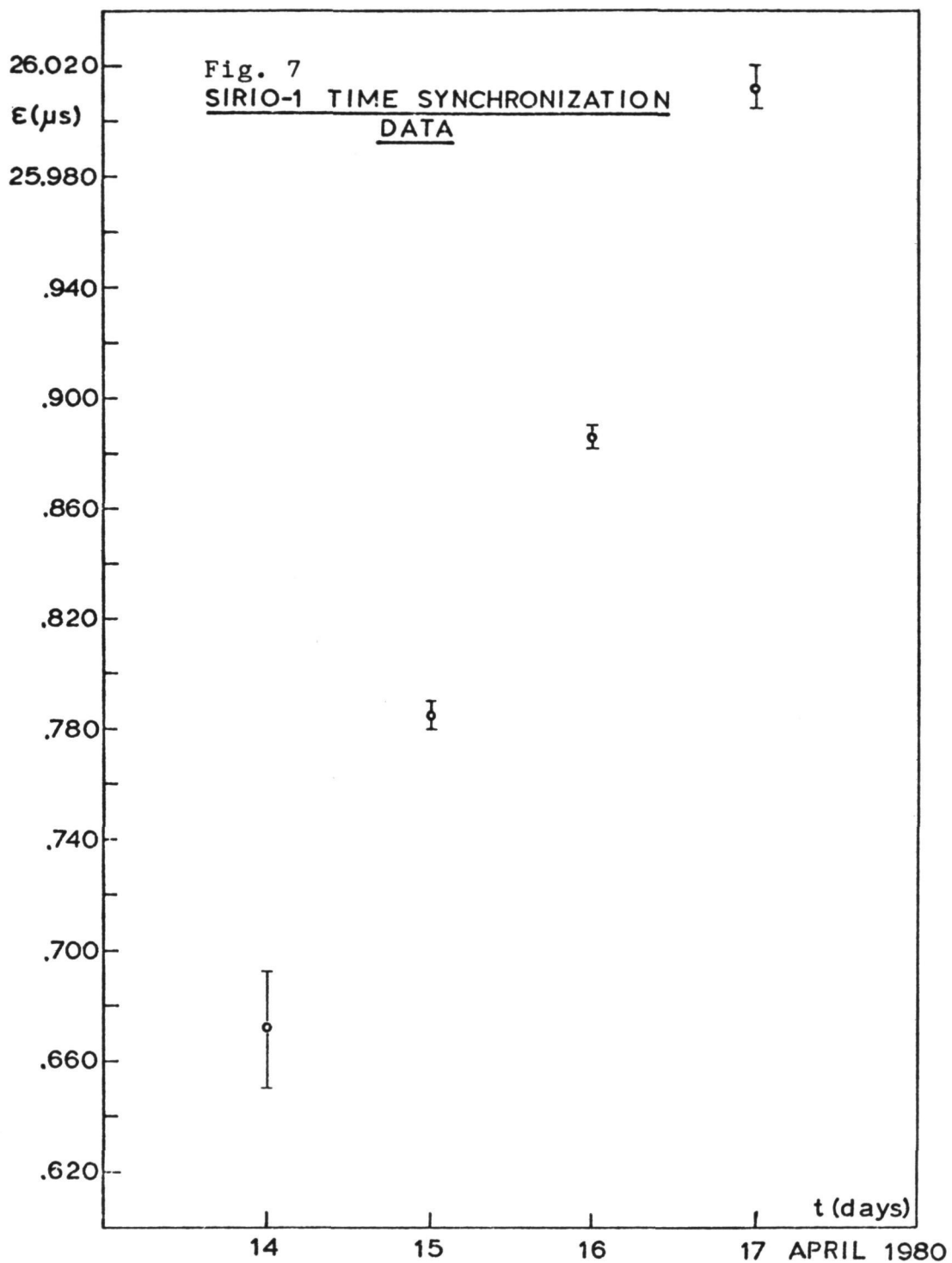
FILE N.      21

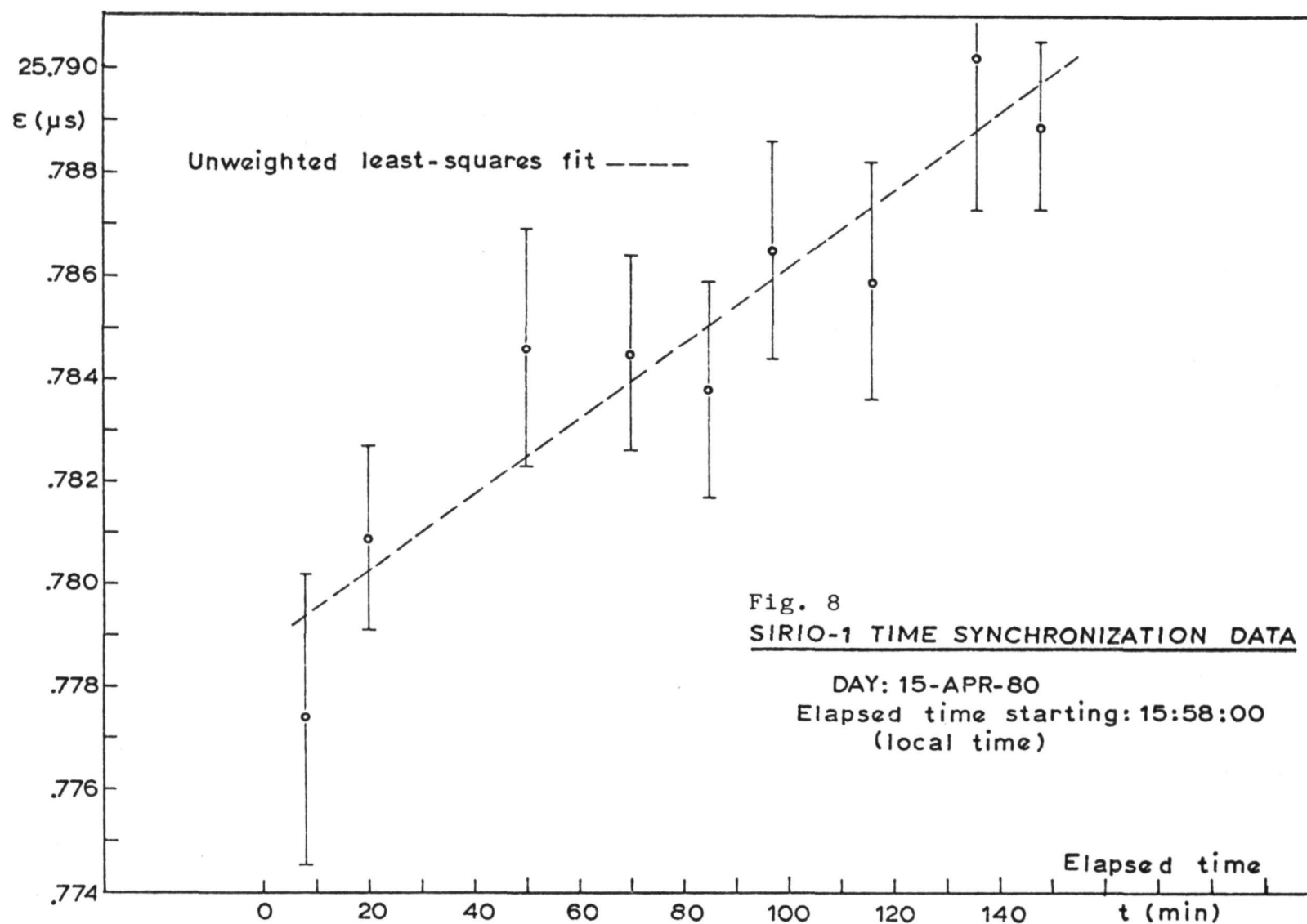
9.205060000 -04 — Time tag
1.560251000 -01 —  $T_1$  - Time of reception-(- 0.1 s)
6.025154000 -03 —
6.025144000 -03 —
6.025124000 -03 — Time measurements
6.025188000 -03 — modulo the repetition
6.025142000 -03 — period
6.025154000 -03 —
6.025242000 -03 —
6.025144000 -03 —
6.025162000 -03 —
1.565590840 -01 —  $T_5$  - Time of reception-(- 0.1 s)
6.559078000 -03 —
6.559078000 -03 —
6.559088000 -03 — Time measurements
6.559100000 -03 — modulo the repetition
6.559080000 -03 — period
6.559188000 -03 —
6.559106000 -03 —
6.559094000 -03 —
6.559094000 -03 —

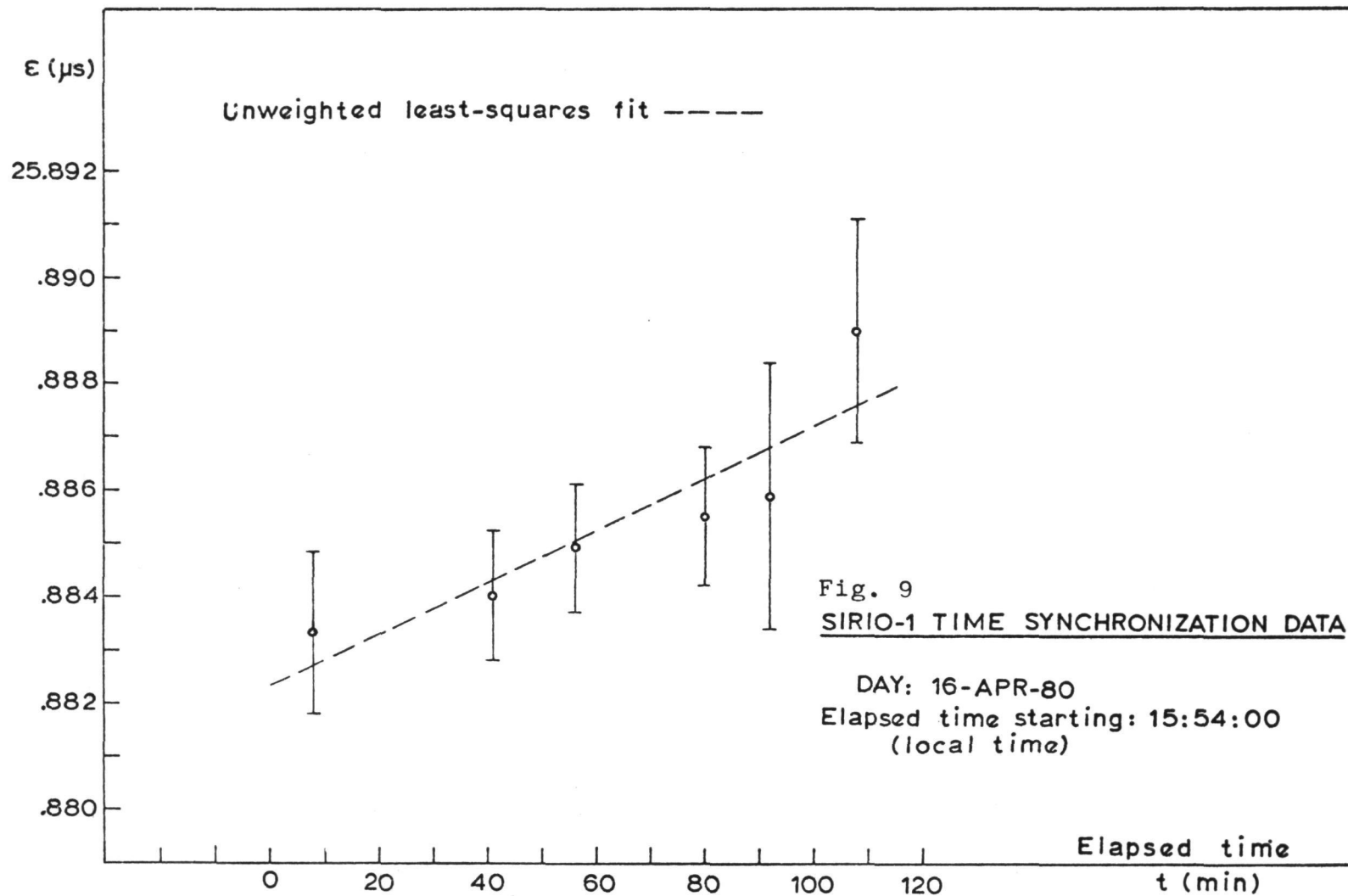
```

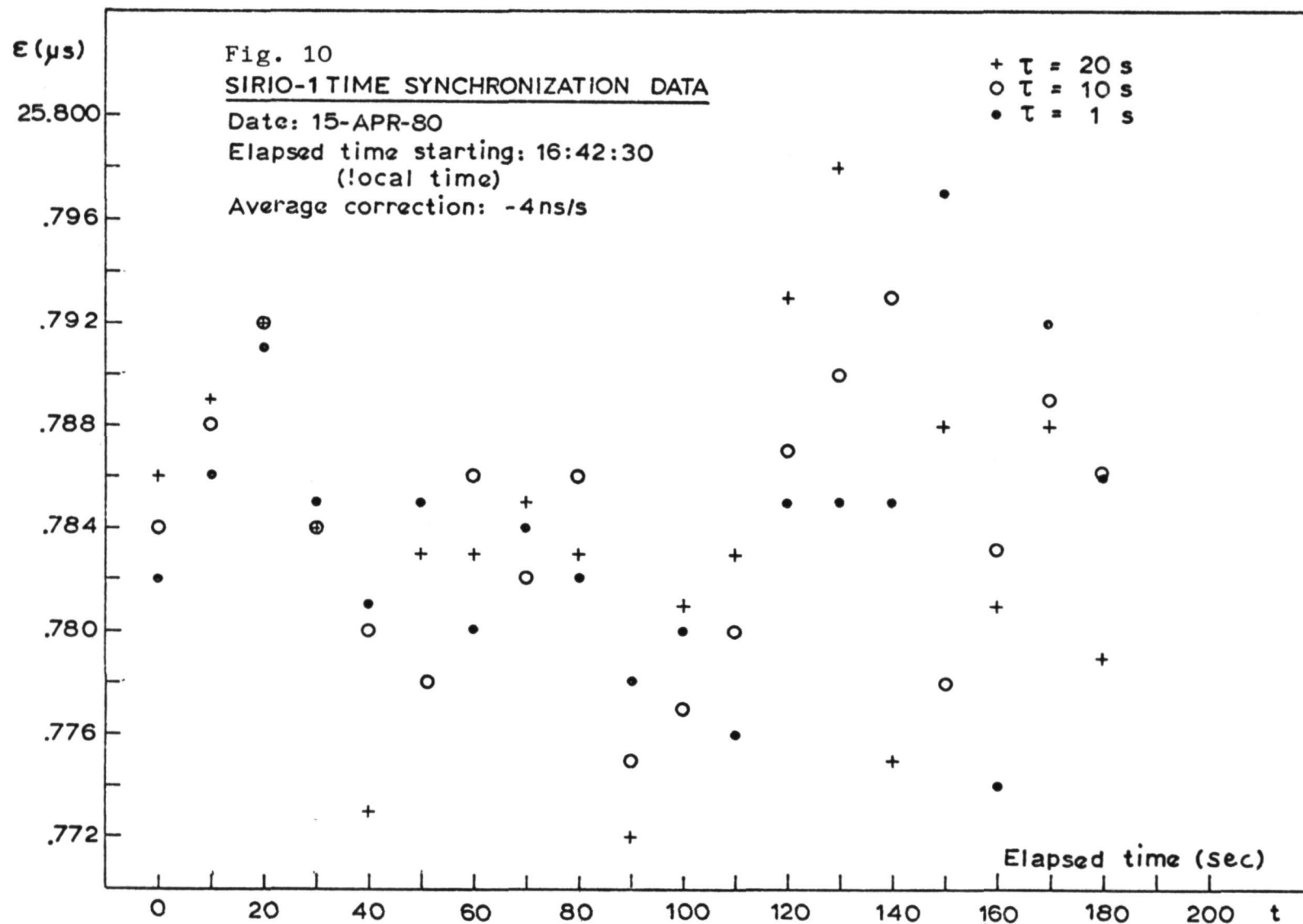
Fig. 5 - Sample data file











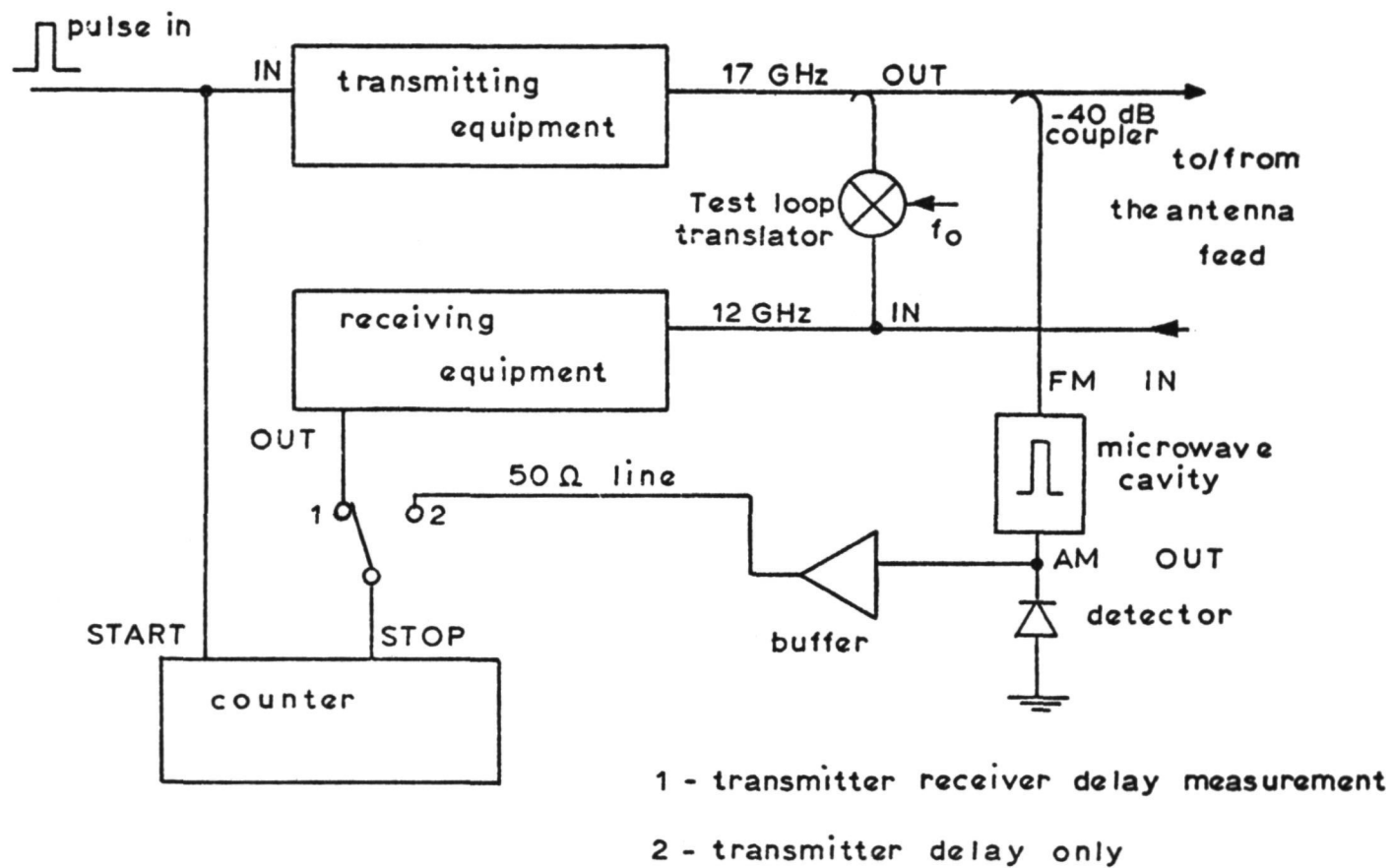


Fig. 11 - Ground equipment delay measurement set-up

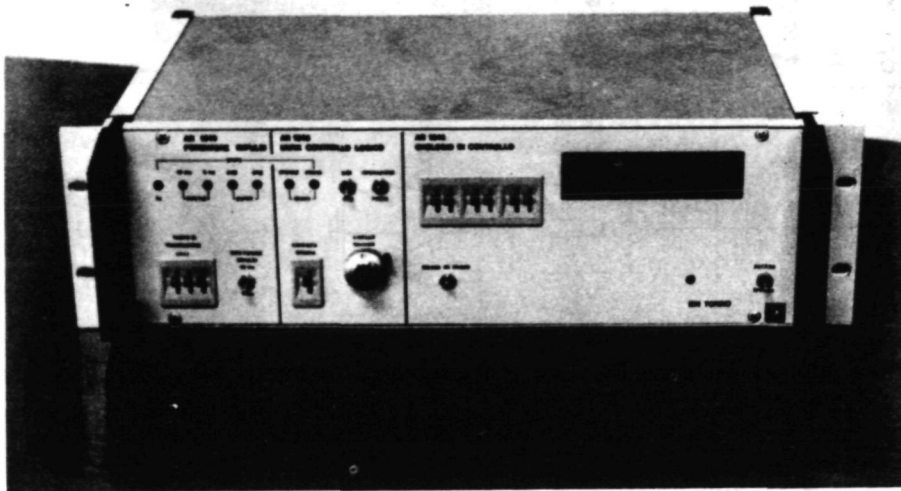


Fig. 12 - The time transfer unit (TTU)

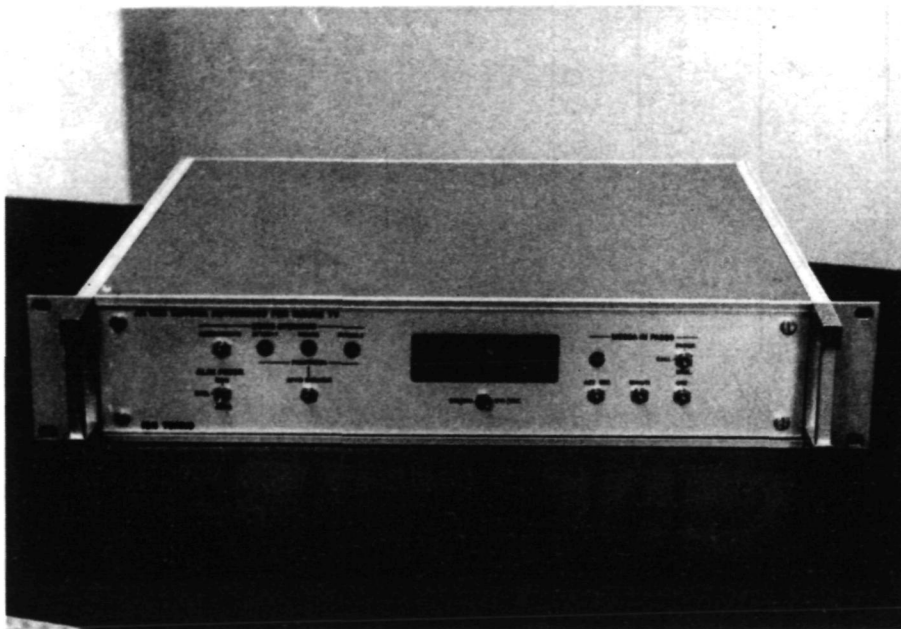


Fig. 13 - Automatic TV measurements subsystem

QUESTIONS AND ANSWERS

MR. DAVID ALLEN, National Bureau of Standards

Two questions; one what is the size of the antenna involved?

PROFESSOR LESCHICUTTA:

Yes, please. In the ground station the size is 17 meters with a true bandwidth -- RF bandwidth of 34 megahertz. Also, in the repeater satellite in the real bandwidth of base band bandwidth of 6 megahertz.

As regards the experiment on the ship, the diameter of the dish is on the order of 2 1/2 meters but the bandwidth is just 1.5 megahertz. So, obviously the precision should be deteriorated.

MR. ALLEN:

I thought it was a very excellent result that you received. I have one question in regard to the equation. Because the stations are basically north/south you would not see any effect due to the SANYAC correction.

PROFESSOR LESCHIUTTA:

Yes, the SANYAC correction is 13.5 nanoseconds, in our case because the area of the path is very small in the equatorial plan.

MR. ALLEN:

The correction was not in the equation?

PROFESSOR LESCHIUTTA:

No, no, it was not included but is in the order of 14 nanoseconds.

MR. ALLEN:

Thank you.

PROFESSOR LESCHIUTTA:

13 foot.

MR. ALLEN:

Very good.

CHAIRMAN BUISSON:

Any other questions?

MR. LAUREN RUEGER, The Johns Hopkins University/Applied Physics Laboratory

Do you ever take advantage of planning your experiments on the satellite motion when the relative changes to the stations are minimized?

PROFESSOR LESCHIUTTA:

There, again, we are not in a position to do so. We just receive for some hours during the day, but we are planning periods of experiments to make all day measurements in order to follow the satellite.

In previous experiments we have seen the maximum relative speed of the satellite is of the order of 3.5, 4 meter per second.

FLIGHT AND GROUND TESTS OF A GOES SATELLITE TIME RECEIVER FOR SATELLITE COMMUNICATIONS APPLICATIONS

Roger L. Swanson, Air Force Wright Aeronautical Laboratories,
Wright-Patterson Air Force Base, Ohio and Stephen A. Nichols,
Naval Research Laboratory, Washington, DC

ABSTRACT

A satellite time receiver has been tested by the Air Force Wright Aeronautical Laboratories in various environmental conditions during the past year. The commercial receiver which was designed to work with the National Oceanic and Atmospheric Administration's (NOAA) Geostationary Operational Environmental Satellites (GOES) was purchased from Arbiter Systems, Inc. The test program included operation at low elevation angles (less than five degrees), operation during flight in a military cargo aircraft and long term comparison with laboratory standards.

Modern military spread spectrum communications systems require accurate timing to achieve synchronization. These systems will be deployed on various mobile platforms with attendant start-up problems at remote locations. The GOES satellite time receiver offers an opportunity to provide easy wide area coverage synchronization at low cost.

Two receivers were delivered in December 1979. One was carried to Thule, Greenland in March 1980 where the elevation angle was less than five degrees. Comparisons were made at Thule, Greenland and Goose Bay, Labrador with a Hewlett Packard Rubidium Traveling Clock. Test results from this trip will be presented. The results of long term testing which has been performed at Wright-Patterson Air Force Base to determine the reliability and accuracy for use in testing of potential military communication systems will be presented. The test phase which involves integration into the test aircraft and related test results will be described.

INTRODUCTION

Modern military spread spectrum communications systems require accurate timing to achieve synchronization. These systems will be deployed on various mobile platforms with attendant start-up problems at remote locations. In many spread spectrum communication systems,^{1,2,3,4} time is used as a parameter to start or to be a part of the pseudo-random sequence. In the evaluation of prototypes, time accuracy one to two orders greater than required by the prototype, is an aid to the test effort.

Typically, aboard the Avionics Laboratory satellite communications (SATCOM) C135B test aircraft or other flight test aircraft (such as those used to track Apollo or other space launches), a crystal clock, Rubidium or Cesium time/frequency standard has been used. Accuracies experienced in using the Rubidium standard have been excellent (1 to 3 microseconds drift/day). However, as all power is removed from an unattended aircraft, the clock equipped with multiple input AC/DC power supplies and battery pack, are moved to ground power in order to keep time. The threat of power loss, dropping the clock during movement to ground power, the simple hassle of moving 100 pounds of equipment often by hand over good to snowy/ice-covered surfaces leaves much to be desired.

Broadcast time would provide a convenient source if: (1) sufficiently accurate with or without range correction, (2) sufficiently quick to acquire and to produce reliable time, (3) available to the user at his geographical location, and (4) it is a cheap alternative to the portable clock. In addition, a broadcast time might provide a confidence check on a portable clock.

In 1980-83 the Avionics Laboratory's SATCOM test program requires a source of time common both to the flight test aircraft (Figure 1) and the Avionics Laboratory's Rooftop Satellite Facility (Figure 2). HF transmissions do not have the required accuracy; LORAN C and Global Positioning System equipments are not available. The National Bureau of Standard Time (NBS) which the National Oceanic and Atmospheric Administration (NOAA) broadcasts over the Geostationary Operational Environmental Satellite (GOES), should provide an adequate turn on/turn off time source.⁵ An accuracy of ± 100 microseconds would suffice for the test program.

Two GOES Time System Receivers, Arbiter Systems Model 1060A (Figure 3) and two Model 1036 Broad Coverage Plate Antennas with Preamplifier were bought. One system was installed at the Rooftop Facility and one on the test aircraft.

This satellite time receiver was tested by the Avionics Laboratory at various locations in various environmental conditions during the past

year. The results of this testing are presented in this paper.

TEST PROGRAM DESCRIPTION

NBS time signals are transmitted by NOAA from NASA's facility at Wallops Island, Virginia to the GOES satellite at 75 degrees West and 135 degrees West. The downlink signal is a Code Phase Shift Keyed modulation of ± 60 degrees on a 468.8375 MHz or a 468.8250 MHz RF carrier respectively. This signal is received by the Arbiter GOES time receiver which derives the satellite's ephemeris and a one second time tick from the signal. The time tick is corrected for range delay through front panel entry of the receiver's latitude and longitude. The receiver delay correction is entered internally and once set correctly should not need to be reset. Figure 4 shows the test concept.

The antenna used was an omni-directional plate antenna with a 20 dB preamplifier mounted directly behind the antenna. The antenna fed 20 feet of RG 214 coaxial cable which connected to the receiver.

The test compared the one second time tick of the GOES receiver and the tick of a Rubidium or Cesium clock, which had been synchronized to the 4950th Test Wing's time shop standard. The time standard accuracy is maintained within ± 2 microseconds and is traceable to the Naval Observatory.

The Arbiter GOES receiver contains a digital time interval counter which measures the time difference between the receiver time tick and an external time tick. This difference, up to ± 999 microseconds, is converted to an analog equivalent voltage. The convention is that a positive voltage means the external time tick is earlier than the GOES receiver time tick. The Arbiter receiver's time interval counter accuracy was verified before use.

Any time difference was plotted on a strip chart or printed out from a time interval counter. When feasible, receiver AGC voltage and loss of synchronization indications along with UTC were also recorded on the strip chart which was recording the time difference. The test configuration is shown in Figure 5.

LONG TERM TESTING AT WRIGHT-PATTERSON AFB

Ground tests at Wright-Patterson AFB were begun 3 June 1980. Initially, the Hewlett Packard (HP) 5060A Computing Counter was programmed to measure and print out the maximum peak to peak time difference over each 10 minute period. While some data was gathered, this technique proved susceptible to unknown "glitches" which required the program to be reinitiated. This technique was abandoned. By mid-July a strip chart recorder was obtained and the time difference was recorded on

the strip chart. Definitive data was not available until 29 July 1980.

From 29 July to 29 August 1980, the strip chart displayed a daily variation of about 160 microseconds peak to peak increasing up to 450 microseconds peak to peak. For a period from 4 August to 14 August 1980 the data was invalid. Figure 6 is a plot of this daily variation. This daily variation was traced to incorrect satellite ephemeris data, which resulted in the wrong range correction. As a result, long term statistics are not available.

The variation stopped at 1430Z, 29 August 1980. Figure 7 is the record of the change. Note the abrupt decrease to the time drift. The step change every two to four minutes is typical of the well behaved range calculation. From 1430Z, 29 August 1980 to 1820Z, 4 September 1980, the peak to peak time variation of the time receiver was 30 microseconds (135 microseconds earlier to 165 microseconds earlier than the Rubidium clock time). The average fixed offset of 150 microseconds was discovered to be an incorrect receiver delay setting. Later calibration of the receiver delay at the 4950th Test Wing's time shop changed the receiver delay from 4265 to 4420 microseconds, moving the receiver time tick 155 microseconds later. This emphasized the necessity of assuring that the correct receiver delay is properly entered into the delay calculation.

The peak to peak variation when the receiver was locked was not more than 30 microseconds for a one week period after removal of the incorrect receiver delay setting. However, there were outages.

Outages during this trial were variable. From 1200Z, 29 July 1980 to 0400Z, 1 August 1980, outage was 53 percent of the 40 hours. From 0400Z, 1 August 1980 to 2359Z, 3 August 1980, outage was 8 percent of the 94 hours. From 2400Z, 3 August 1980 to 1400Z, 14 August 1980, the data is questionable and no results could be gathered. While not certain, many of the outages appear to be caused by local line of sight UHF transmissions. Indeed, the better performance over the weekend, 2-3 August 1980, points to other testings at Wright-Patterson AFB, Ohio as a possible cause of the outages.

However, beginning at 1400Z, 14 August 1980 to 0400Z, 28 August 1980, outages almost disappeared. During the 14 days, individual outages of 40, 10, 30, 10 and 15 seconds occurred. The total outages were 105 seconds, giving an outage rate of .0089 percent.

Beginning 0400Z, 28 August 1980 through 1800Z, 5 September 1980, solar eclipse type outages began, running 26, 33, 41, 50, 56, 60, 143, 125 and 86 minutes for the succeeding days. Total outages were 1920 minutes or 15.5 percent for the eight day period. Figure 8 depicts the availability and the outages experienced at Wright-Patterson AFB.

WORLDWIDE TESTING

From March 1980 through November 1980 the SATCOM test aircraft flew missions to numerous locations in North and South America, the North and South Atlantic, Africa and Europe. This created an opportunity to test the GOES time receiver at these locations. The eastern GOES (75 degrees West) satellite was used for all tests but one. Figure 9 shows the flight test routes.

Two types of tests, time sync and time comparison, were run. At some locations, before takeoff the receiver was turned on, the antenna set out on a wing and the receiver time output was used to synchronize the aircraft instrumentation clock. The instrumentation clock was then set to free run and a time comparison was made. Synchronization was judged successful if over the next five minutes the time comparison remained less than ± 100 microseconds and appeared "well behaved."

At other locations the time comparison measurements were recorded for the length of the stay. Table I lists the locations, the elevation angle to the East (75 degrees West) satellite, and the type of test.

Receiver latitude and longitude at these locations was determined from the appropriate Instrument Flight Approach/airport charts and other surveyed maps as required. Receiver location was determined to within 30 seconds.

REMOTE LOCATION TIME SYNC

Time synchronization was successful in 26 out of 26 attempts. Twenty-five used the East (75 degrees West) GOES satellite; one synchronization at Omaha, Nebraska used the West (135 degrees West) satellite. The time syncs obtained were then used for each of the missions.

Within the United States, time syncs were obtained at Dayton, Ohio; Omaha, Nebraska; Dallas, Texas; Langley AFB, Virginia; Homestead AFB, Florida. Overseas time syncs were obtained in Greenland, Iceland, Labrador, Canada, England, Senegal, Ascension, Brazil and Peru.

REMOTE LOCATION TIME COMPARISONS

Time comparison measurements were made on three overseas trips: a March 1980 polar trip, a September 1980 equatorial trip and a November 1980 polar trip. Table II is a summary of the time comparisons.

March 1980 Polar Trip

The March 1980 polar trip stopped at Sondrestrom, Greenland; Thule AB, Greenland; Iceland; and Goose Bay, Labrador.

TABLE I
Short Term Testing at Various Locations

<u>Date</u>	<u>Location</u>	<u>Test Type</u>	<u>Elevation Angle to East Satellite</u>
11-14 Mar 80	Offutt AFB, Omaha NE	Time Syncs (3)	36 degrees
24-27 Mar 80	Sondrestrom AB, Greenland	Time Comparison Time Sync (1)	13 degrees
29 Mar 80	Thule AB, Greenland	Time Comparison Time Sync (1)	5 degrees
30 Mar 80	Keflavik NAS, Iceland	Time Sync (1)	5 degrees
3 Apr 80	Goose Bay, Labrador, Canada	Time Comparison Time Sync (1)	27 degrees
5 Jun 80	Dallas Love Field, Texas	Time Sync (1)	44 degrees
27 Jun 80	Langley AFB, Virginia	Time Sync (1)	45 degrees
14-16 Jul 80	Homestead AFB, Florida	Time Syncs (2)	65 degrees
8-9 Sep 80	Lima, Peru	Time Sync (1)	75 degrees
11 Sep 80	Rio de Janeiro, Brazil	Time Sync (1)	45 degrees
12-16 Sep 80	Ascension Island, South Atlantic	Time Comparison Time Sync (1)	20 degrees
17 Sep 80	Dakar, Senegal	Time Sync (1)	21 degrees
18-19 Sep 80	Ramstein AB, Germany	Out of Coverage	Below Horizon
20 Sep 80	Mildenhall AB, England	Time Sync (1)	0 degrees
4-7 Nov 80	Goose Bay, Labrador, Canada	Time Comparison Time Sync (1)	27 degrees
8-11 Nov 80	Sondrestrom AB, Greenland	Time Comparison Time Sync (1)	13 degrees
12-14 Nov 80	Thule AB, Greenland	Time Comparison Time Sync (1)	5 degrees
11 Mar 80 to 14 Nov 80	Wright-Patterson AFB, Ohio	Time Syncs (7)	44 degrees

TABLE II

<u>Location</u>	<u>Time</u>	<u>Event</u>	<u>Hours of Adequate Reception</u>	<u>GOES TIME Variation (μsecs)</u>
Thule, Greenland	27 Mar 2016	Start test, in lock		
	2335	Lost Lock	3:19	26 to 35 early
	28 Mar 1440	Lockup		
	29 Mar 0427	Lost lock	11:47	43 late to 45 early
	29 Mar 1604	Still out, end test	14:66	
Total Test Hours: 43:23				
Availability: 34.8%				
Goose Bay, Labrador	2 Apr 0143	Start test, in lock		
	0432	Solar eclipse	2:49	27 to 37 early
	0536	Lockup		5 to 25 early
	1109	Antenna fell down	5:33	
	1120	(time removed from test hours)		
	3 Apr 0432	Solar eclipse	17:12	10 to 34 early
	0530	Lockup		0 to 12 early
	1003	End test	4:27	
Total Test Hours: 33:09				
Availability: 90.5%				
Ascension Island, South Atlantic	13 Sep 0927	Acquired GOES, synced reference Rubidium to GOES		15 to 35 early
	14 Sep 0424	Solar eclipse, lost lock	18:53	
	0548	Lockup		
	15 Sep 0424	Solar eclipse, lost lock	22:36	
	0550	Lockup		
	16 Sep 0424	Solar eclipse, lost lock	22:35	
	0550	Lockup		
	1600	Rubidium Time Check		
Total Test Hours: 108.27		Other outages during test	4:19	
Availability: 92.1%		End test	16:04	

Table II (continued)

<u>Location</u>	<u>Time</u>	<u>Event</u>	<u>Hours of Adequate Reception</u>	<u>GOES TIME Variation (μsecs)</u>
Sondrestrom, Greenland	9 Nov 0300	Start test, lockup		2 to 18 early
	0737	Out of lock, scintillation	4:37	
	0932	In lock again	23:25	
	10 Nov 0857	Out of lock (antenna blew over)		5 late to 20 early
	2258	Antenna reset		
	2400	In lock	3:19	12 early to 15 late
	11 Nov 0217	Out of lock, scintillation		
	0250	In lock		
	0335	Out of lock, scintillation	0:45	15 late to 44 early
	0557	In lock		10 late to 7 early
	0611	Out of lock, scintillation	0:14	
	1215	In lock		
	1230	End test	0:15	40 to 10 late
Total Test Hours:		57:30 less 16:01 (antenna blew over) = 41:29		
Availability:		78.7%		
Thule, Greenland	11 Nov 2200	Start test, locked up		50 early to 50 late
		Scintillation occurred more than 90% of the test time. Twenty-two outages occurred, ranging from four minutes to 6 hours 22 minutes, totaling 34 hours 24 minutes.		
	14 Nov 1228	End test		
Total Test Hours:		64:28		
Availability:		46.7%		

Thule, Greenland

Time comparison began at 2016Z, 27 March 1980 at Thule, Greenland (elevation angle 4-5 degrees). The antenna was propped up outside the dormitory window and pointed towards the east satellite. After correcting for a 15 microsecond late offset in the Rubidium standard, and a 1.25 microsecond position offset (actual position and Rubidium offset were determined after the data was taken), the time error upon receiver acquisition was 30 microseconds early.

Time reception continued until loss of lock at 2335Z, 27 March 1980, about the time of the solar eclipse. While locked during this 3 hour 19 minute period, the GOES receiver time variation was 21 to 36 microseconds early.

GOES time was reacquired 1530Z, 28 March 1980, retaining lock until 0427Z, 29 March 1980. Peak to peak variation was from 43 microseconds late to 45 microseconds early. This larger spread was due to abnormal step correction (Figure 10) of 23 microseconds early to 42 microseconds late. At the next range correction time the offset returned, stepping from 43 microseconds late to 15 microseconds early. The cause of such an abnormal step is not known.

Total test time was 43 hours 23 minutes. Adequate reception occurred for 15 hours 6 minutes. Availability was 34.8 percent.

Goose Bay, Labrador

Testing at Goose Bay began on 0143Z, 2 April 1980. Outages due to solar eclipse existed from 0432Z and ended 0536Z on 2 April 1980. The peak to peak error during reception was 0 to 37 microseconds early. Total test time was 33 hours 9 minutes with adequate reception occurring 30 hours 1 minute. Availability was 90.5 percent, with outages due to solar eclipses and a nine minute loss of antenna pointing.

During this test a UHF transmission at 235.5 MHz degraded the time accuracy. A 15 microsecond advance of the GOES receiver time was observed to correlate with the transmission (Figure 11). Loss of lock did not occur.

For this trip the receiver (S/N 61) delay was factory set at a nominal 4400 microseconds. The data taken tends to indicate the receiver delay was about 15 microseconds less than it should have been. Calibration at the time shop of the 4950th Test Wing resulted in a delay setting of 4420 microseconds.

September 1980 Equatorial Trip

This trip departed Wright-Patterson AFB, 8 September 1980, for Peru, Brazil, Ascension Island, Senegal, Germany and England. Time syncs were accomplished at all stops but Germany which was out of satellite coverage. Only on Ascension Island were time comparison measurements made.

Ascension Island

GOES Time Receiver S/N 62, which had been on the Rooftop Facility was used for this trip. Its delay setting was 4334 microseconds (nominal 4400 microseconds) which had been set during the August period when the ephemeris was in error. This had the effect of creating a fixed offset in the GOES data of about 65 microseconds early.

In this test, the reference Rubidium standard after 10 hours warm-up was synced to the GOES receiver at the beginning of the test on 0927Z, 13 September 1980. A time check, 1600Z, 16 September 1980, showed the Rubidium to be 81.4 ± 2 microseconds early compared to the USAF Eastern Test Range Cesium Time Standard. The peak to peak variation presented in Table II is corrected for 66 microseconds of receiver delay (4400 microseconds nominal - 4334 microseconds receiver setting), and the Rubidium error of 81 microseconds.

GOES receiver time variation during this test was 15 to 35 microseconds early. Solar eclipses occurred for each day, total outage was 4 hours 15 minutes. Other outages totaled 4 hours 19 minutes. Availability was 92.1 percent.

November 1980 Polar Trip

On 4 November 1980 the test aircraft departed for Goose Bay, Labrador, Canada; Sondrestrom AB, Greenland; and Thule AB, Greenland. GOES time receiver trials were run at Sondrestrom AB and Thule AB. Receiver S/N 61 was used. The receiver was calibrated before departure.

To ensure that the receiver delay was correct, the receiver was set up in the time shop of the 4950th Test Wing. Receiver delay was adjusted so that the received time agreed with the shop time standard. Final delay setting was 4420 microseconds.

Sondrestrom, Greenland

Testing began at 0300Z, 9 November 1980 and ended at 1230Z, 11 November 1980. Total hours of testing were 57 hours 30 minutes. Sixteen hours were lost when the antenna blew over, giving a net test time of 41 hours 29 minutes.

Ionospheric scintillation caused 8 hours 51 minutes of outages. Scintillation also caused an unusual drifting of the time tick. Figure 12 shows a normal well behaved time trace and matching receiver AGC. Figure 13 shows the drifting time trace and the AGC during the scintillation.

Signal availability at Sondrestrom was 78.7 percent.

Thule, Greenland

At Thule, Greenland testing began at 2000Z, 11 November 1980 and ended on 1228Z, 14 November 1980. The data was not well behaved with the time variation often ± 50 microseconds. The degradation is believed to be due to scintillation. The abnormalities were large step changes (Figure 14), rapid drift (Figure 15) and a random walking of the time trace. This random walk occurred during both heavy scintillation (Figure 16) and mild scintillation (Figure 17). Nine periods of this walking occurred, for a total time of 1 hour 14 minutes.

Scintillation was present for more than 90 percent of the test time. This took its toll in the form of 22 outages, ranging from 0 hours 4 minutes to 6 hours 22 minutes. Variation during lock was ± 50 microseconds.

The total outages were 34 hours 24 minutes during a test time of 64 hours 28 minutes.

Signal availability at Thule was 46.7 percent.

FUTURE PLANS

Testing During Flight

For inflight testing, the antenna was to be installed beneath the radome located between the wings (Figure 1). Latitude and longitude would be manually entered from a Litton LTN-51 Inertial Navigation System. Later, automatic entry would be provided.

However, this modification to the aircraft has been delayed until March 1981. Inflight testing will not occur until the Summer of 1981.

Shipboard Testing

One receiver and antenna will be located on the USS Texan during December 1980. Performance while at sea will be evaluated. Particular attention will be given to periods of large rolling or pitching of the ship.

CONCLUSIONS

The GOES Time Transfer System and the Arbiter GOES Time Receiver can satisfy the ± 100 microseconds accuracy. When all was working well, accuracy was usually within ± 30 microseconds. Good performance was achieved for elevation angles from 2-3 degrees to 75 degrees in temperatures from -20 degrees Fahrenheit (Thule, Greenland) to 95-100 degrees Fahrenheit (Homestead AFB, Florida).

The turn on/turn off feature of this type of system won rapid acceptance among the flight test crew. GOES time syncs were used for 26 flights following a preflight checkout.

However, caution must be observed in the following areas:

(1) The ephemeris data must be correct. The system needs a feedback loop/monitor loop to provide an alarm for discrepancies. For roughly one month the ephemeris which was transmitted was in error.

(2) Receiver delay must be verified and correctly entered before use. To do this using the satellites and an external Rubidium/Cesium quality source is feasible, assuming the ephemeris is good. A minimum of one day of recording the time difference is recommended.

(3) If using the receiver alone, or to set other clocks, a signal quality monitor is recommended. Viewing the demodulated data stream and recording the receiver AGC worked well.

(4) During the trials, ionospheric scintillation did cause outages in the polar regions. Although no outages due to scintillation were experienced in the equatorial regions, other data suggests such outages should occur.⁶

(5) The effects of local interference was readily apparent in the AGC record. Use of this record would increase confidence in a time transfer.

REFERENCES

1. S. A. Nichols, et al, "Interim Test Report of the SEACOM Modem/ Radio," NRL Memo Report 4138, 1979.
2. D. G. Woodring, S. A. Nichols, R. L. Swanson, "Timing and Frequency Considerations in the Worldwide Testing of a Spread Spectrum Communication System," 11th Precise Time & Time Interval Planning Meeting, 1979.
3. R. V. Groves, Capt, USAF, "Flight Evaluation of the AN/USC-28 ADM PN Modem," AFAL-TR-75-185, Wright-Patterson AFB OH.

4. A. Johnson, "LES 8/9 Communication System Test Report," AIAA Symposium, April 1978.
5. D. W. Hanson, et al, "Time from NBS by Satellite," Proceedings of the Ninth Annual Precise Time and Time Interval Planning Conference, March 1978, pp. 139-152.
6. A. Johnson, "The Effects of Ionospheric Scintillation Fading on Aircraft-to-Satellite Communications," Air Force Avionics Laboratory Report, AFAL-TR-78-171, 1978.



Figure 1 C135B SATCOM Test Aircraft

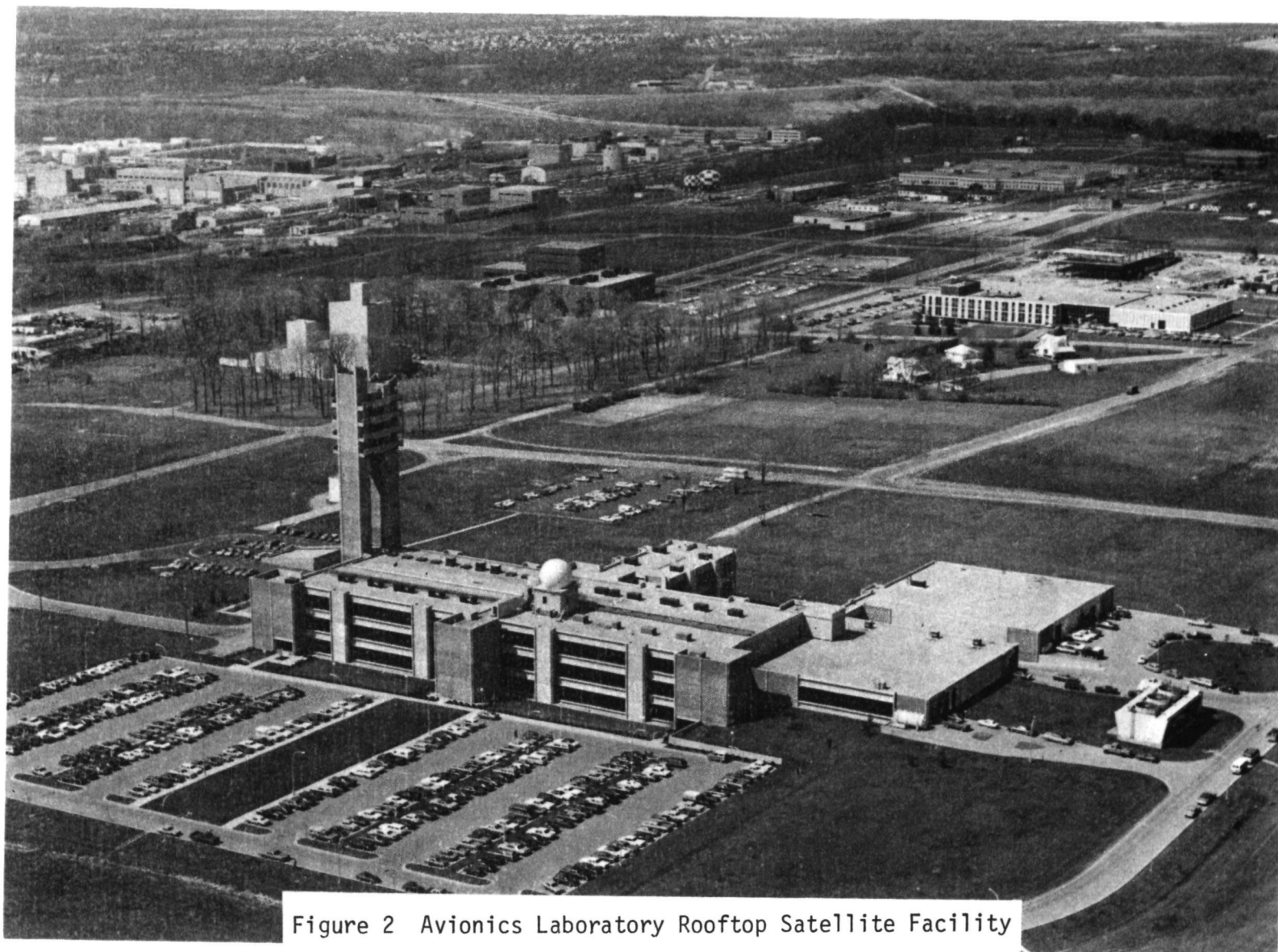
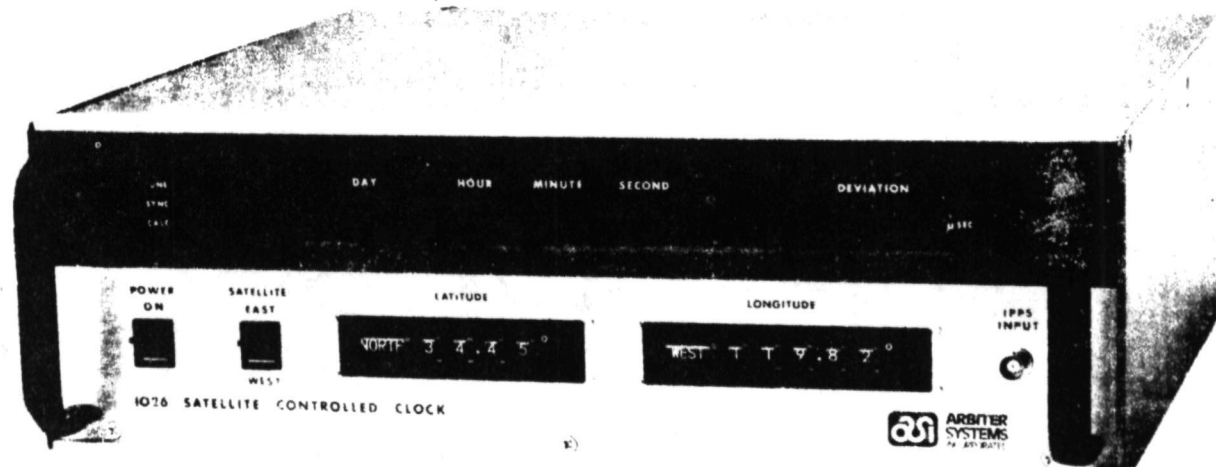


Figure 2 Avionics Laboratory Rooftop Satellite Facility



The Arbiter Systems 1026 Satellite Controlled Clock receives and decodes time signals relayed by the National Oceanic and Atmospheric Administration (NOAA) Geostationary Operational Environmental Satellite (GOES).

These signals, which are continuously available in the covered area and are in synchronism with Coordinated Universal Time (UTC) generated by the National Bureau of Standards, are fully corrected by internal processing circuitry for transmission path delays. The received time



in days, hours, minutes and seconds is displayed and is available as multiplexed and IRIG-B formatted data outputs at a rear panel connector. A time corrected one PPS output derived from the satellite signal is provided for user applications. The 1026 incorporates a time interval meter with a 3 digit display that indicates the time difference in microseconds between a user supplied 1 PPS input and the UTC 1 PPS signal. The instrument is designed to operate with a modest antenna in the satellite coverage area that presently includes the North and South American Continents, the Atlantic and Pacific ocean basins and parts of Europe and Africa.

Figure 3 GOES Satellite Time Receiver

367

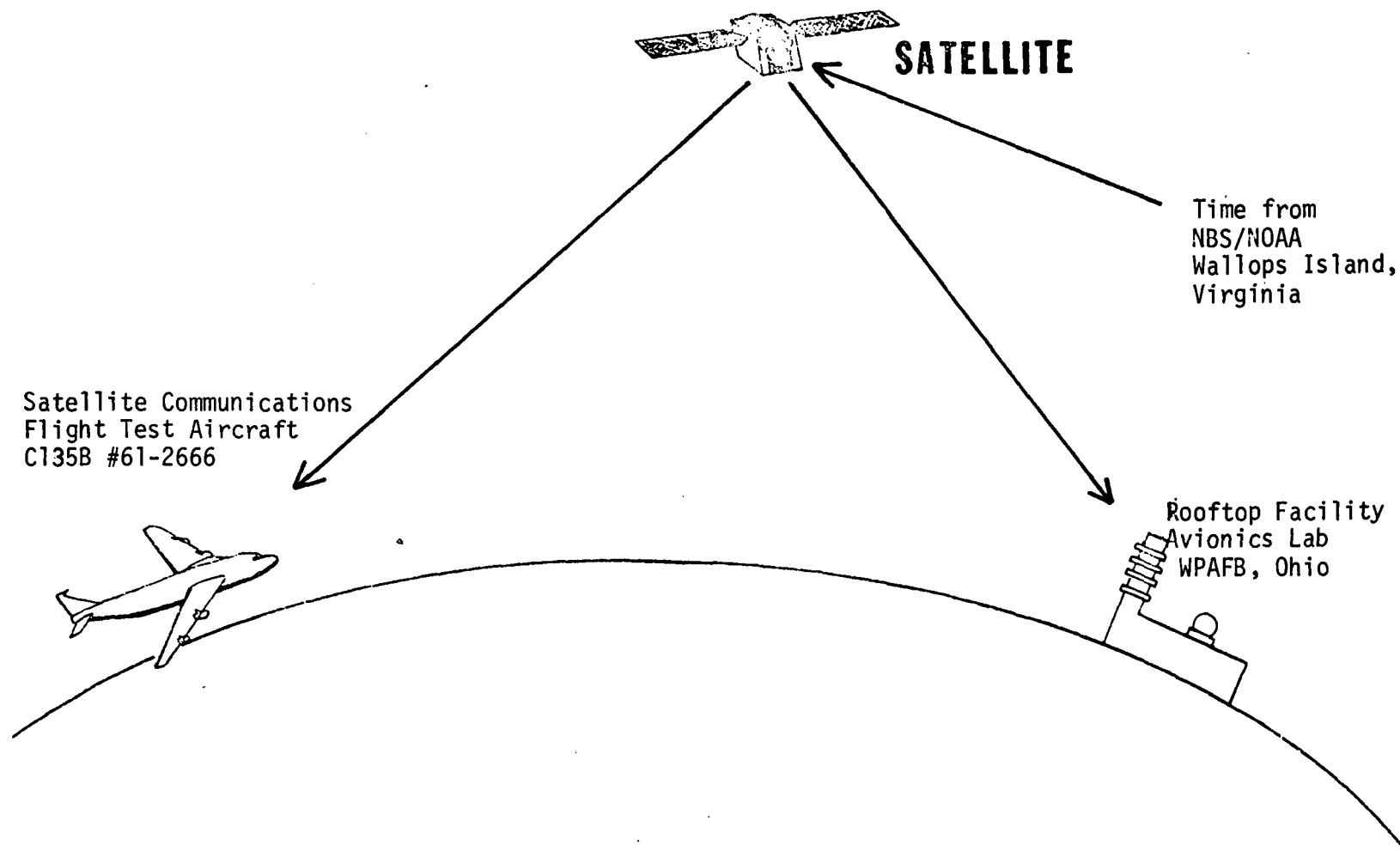


Figure 4 Test Concept for GOES Time Receiver

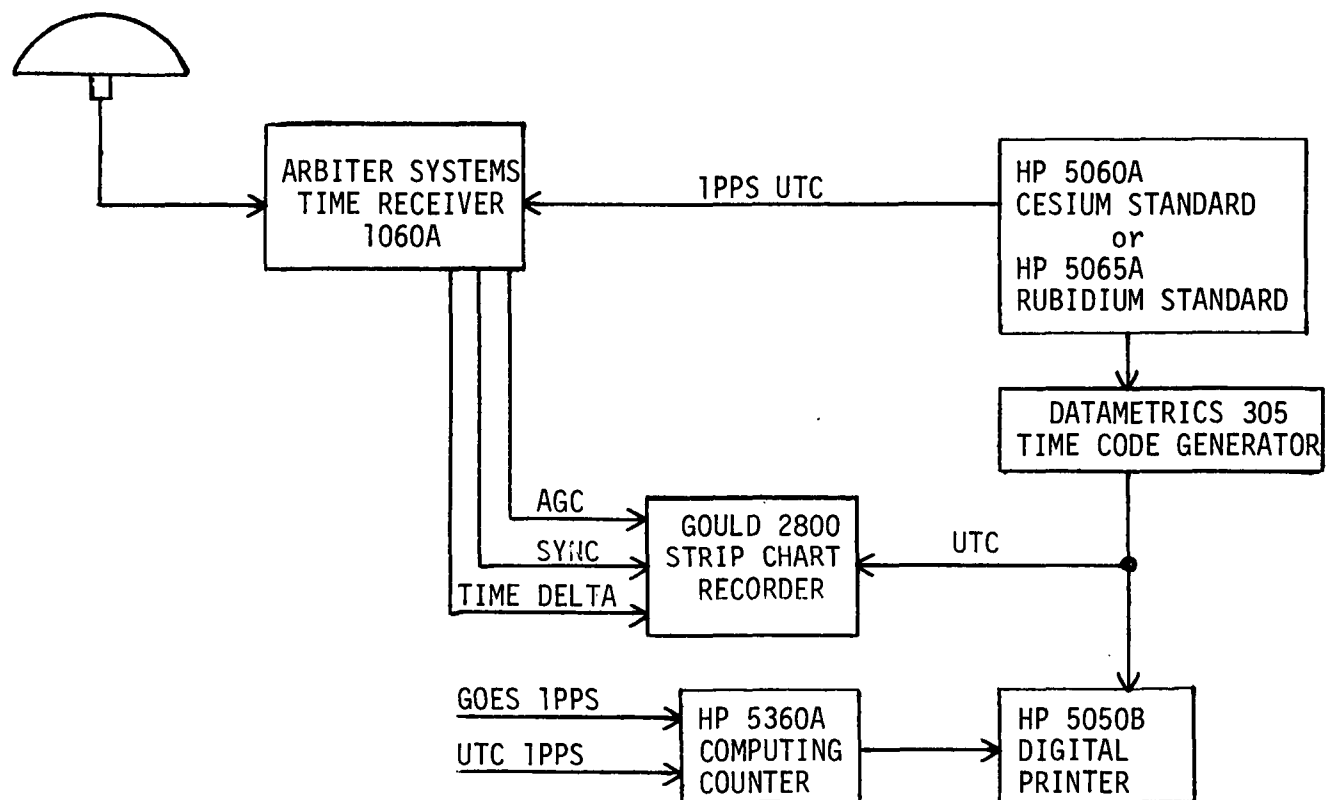


Figure 5 Test Configuration for Time Comparison

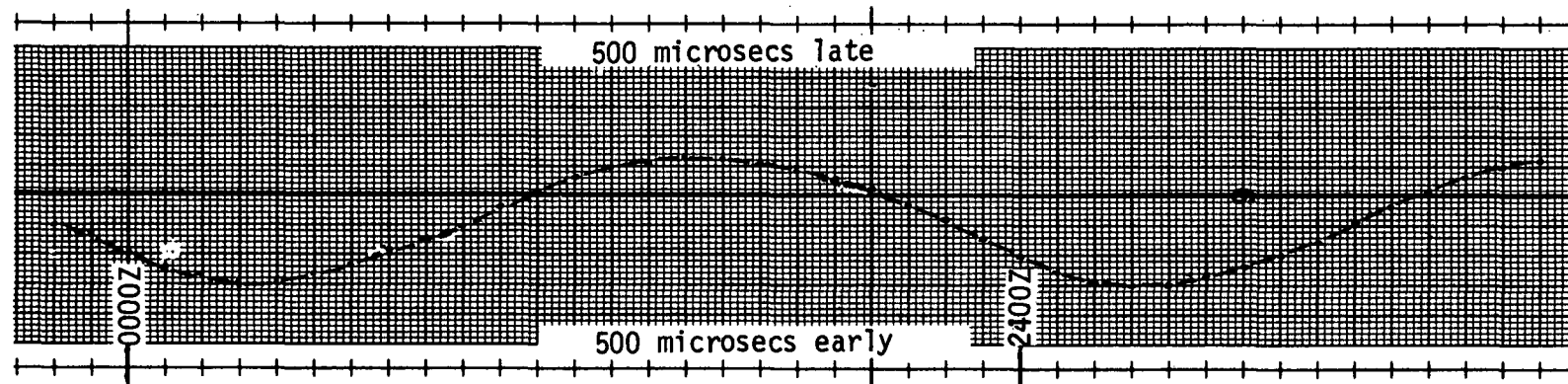


Figure 6 Daily Variation During Incorrect Ephemeris

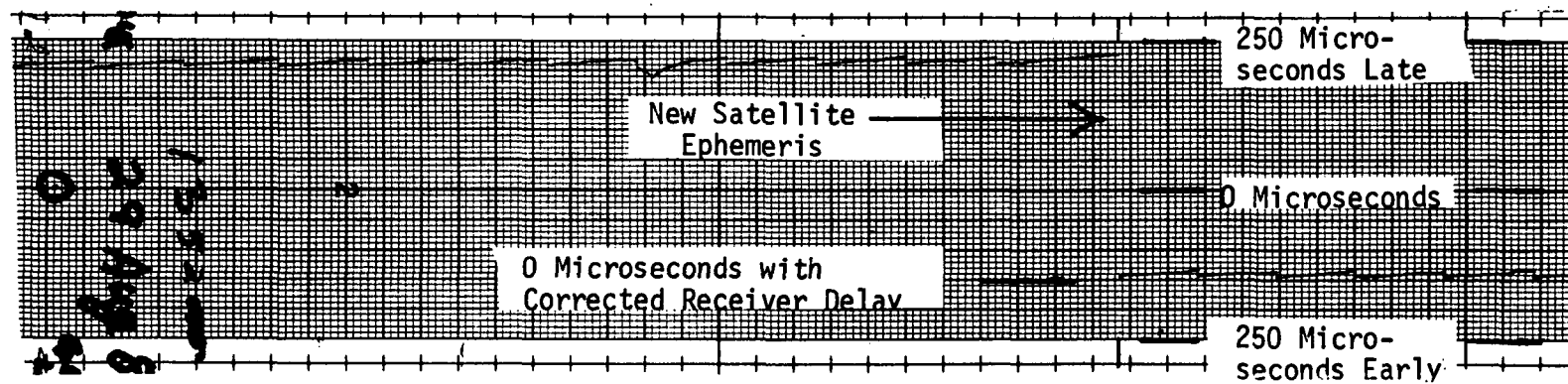


Figure 7 End of Large Daily Variation Due to New Ephemeris Data

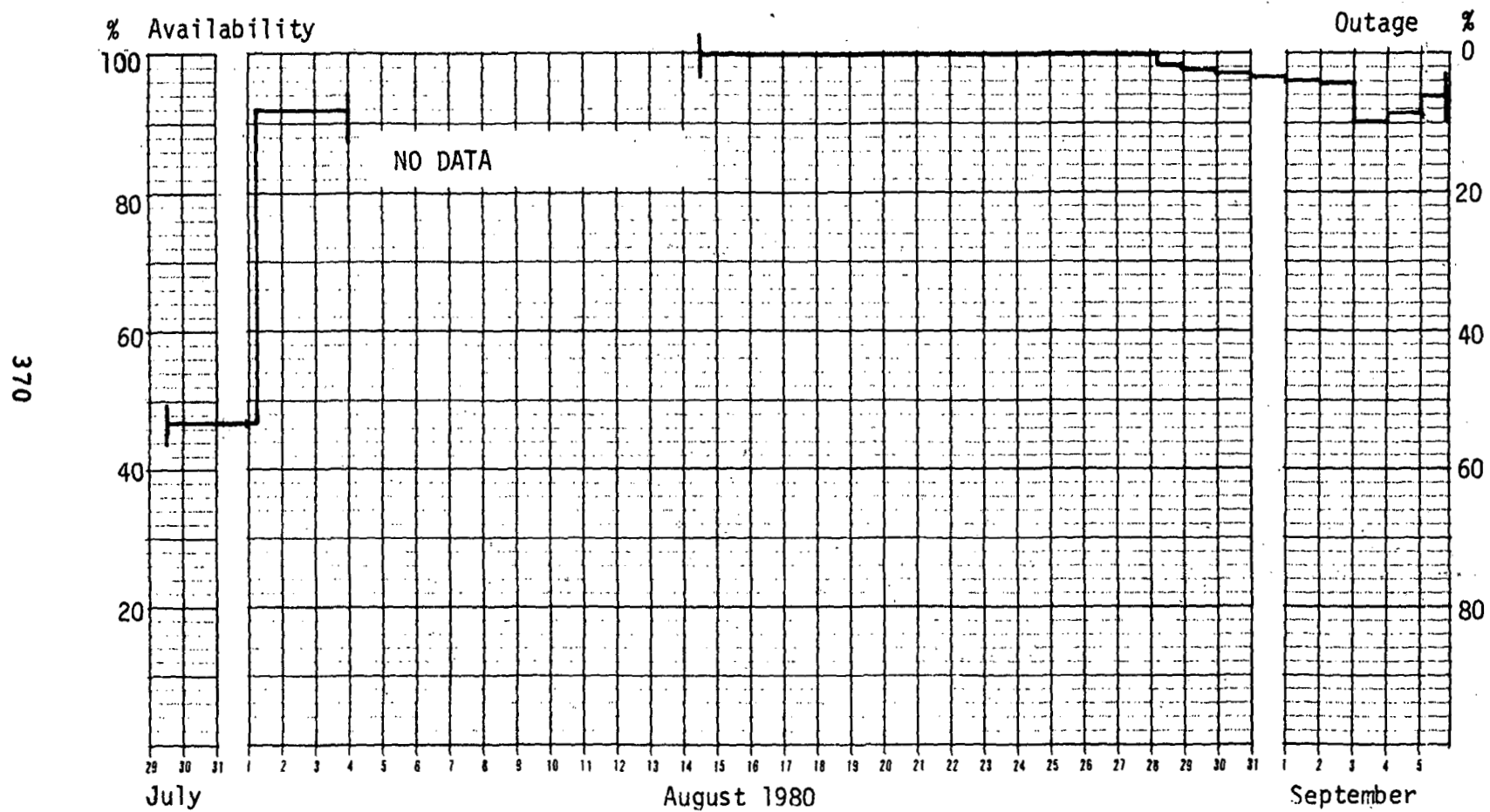


Figure 8 Availability/Outage of GOES Receiver Time at Wright-Patterson Air Force Base

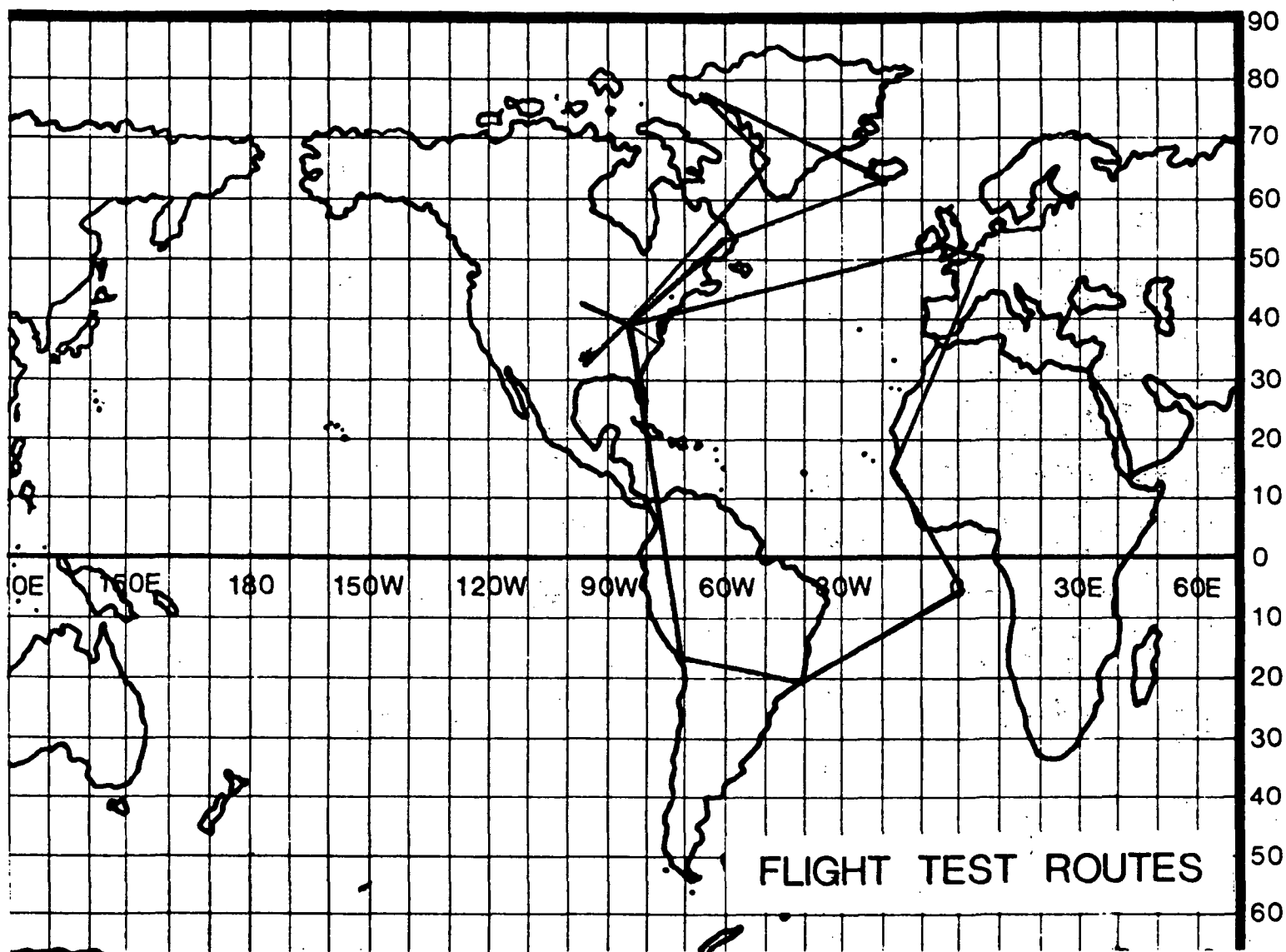


Figure 9 Flight Routes During GOES Time Receiver Testing

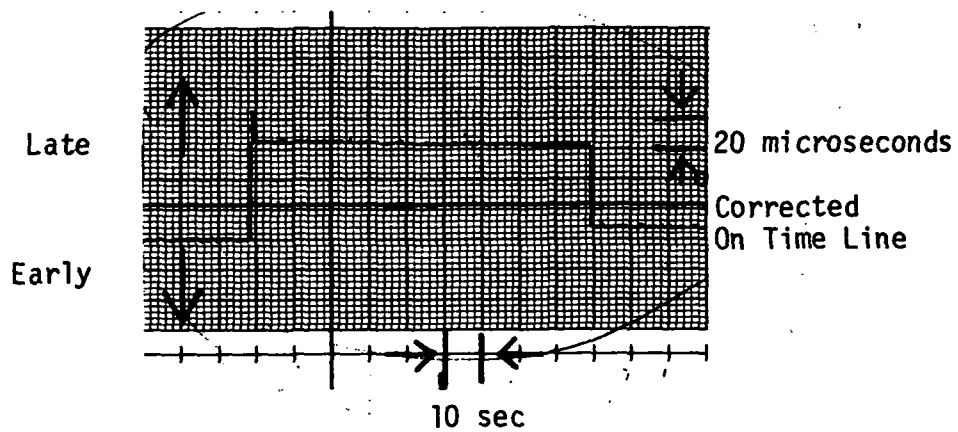


Figure 10 Abnormal Step Change at Thule, Greenland

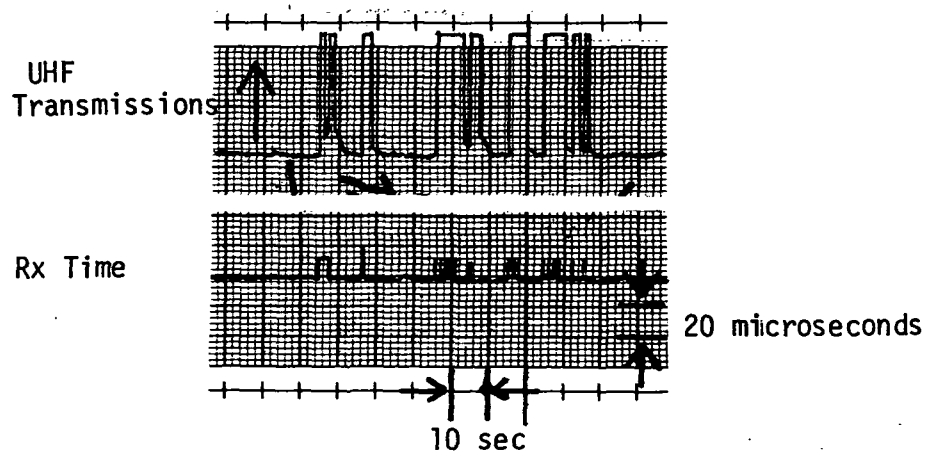


Figure 11 UHF Transmission Effects Upon GOES Receiver Time

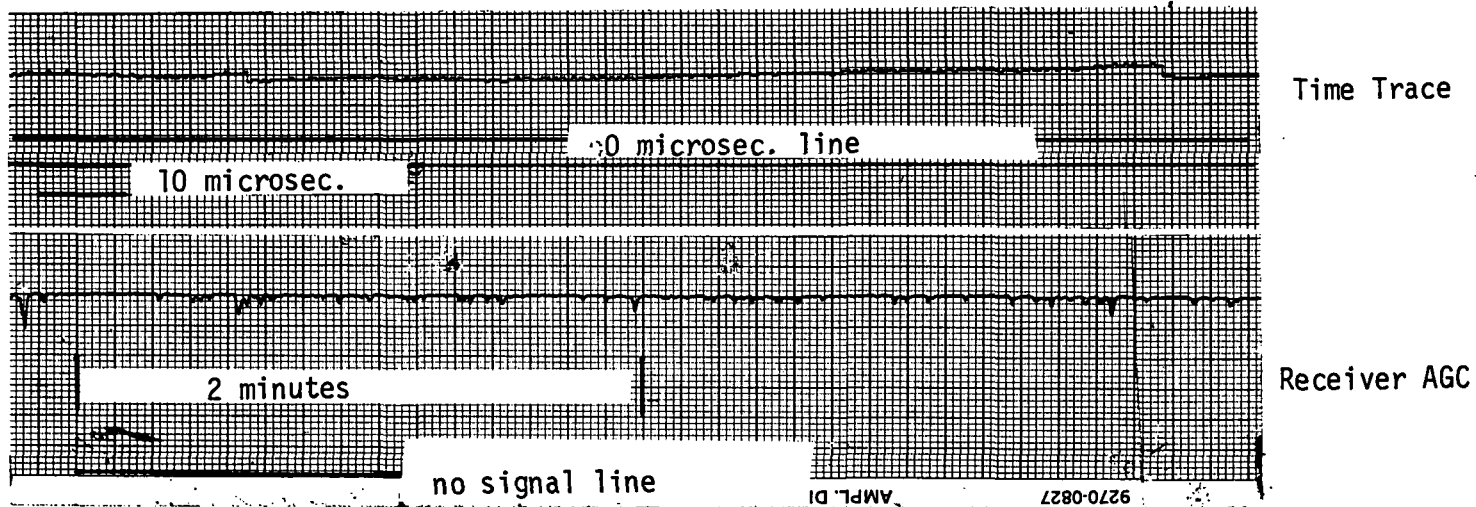


Figure 12 Normal Well Behaved Signal at Sondrestrom AB, Greenland

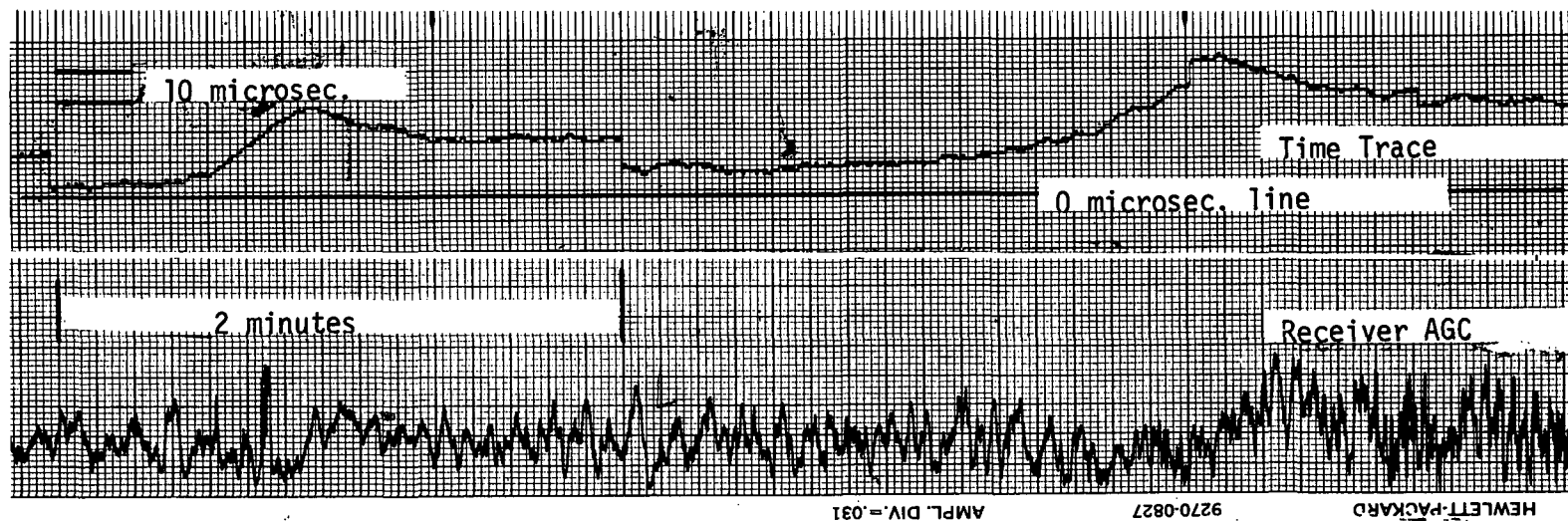


Figure 13 Time Shift during Ionospheric Scintillation

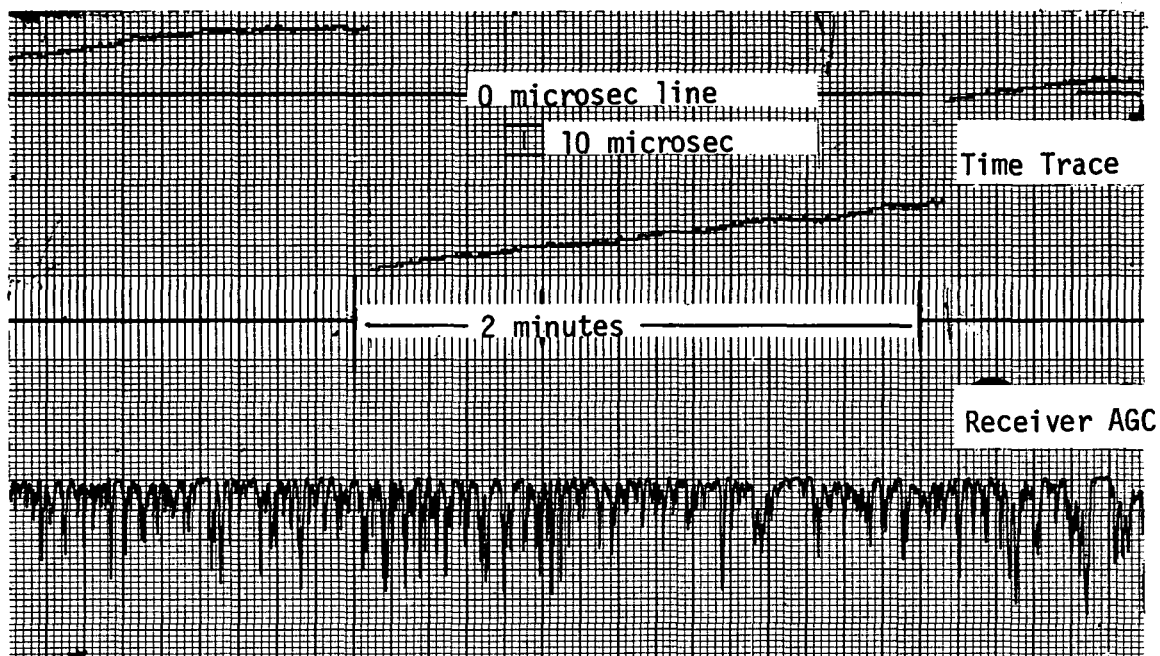


Figure 14 Large Step Change of Time Trace, Thule, Greenland

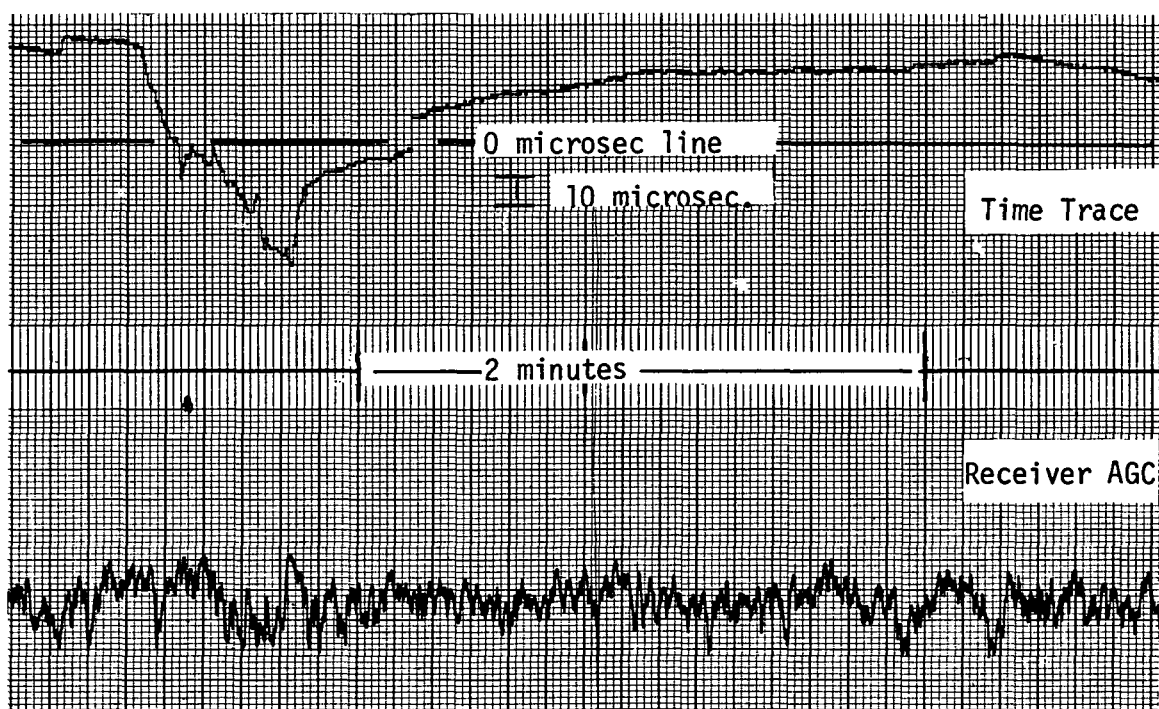


Figure 15 Time Trace Drift During Scintillation, Thule, Greenland

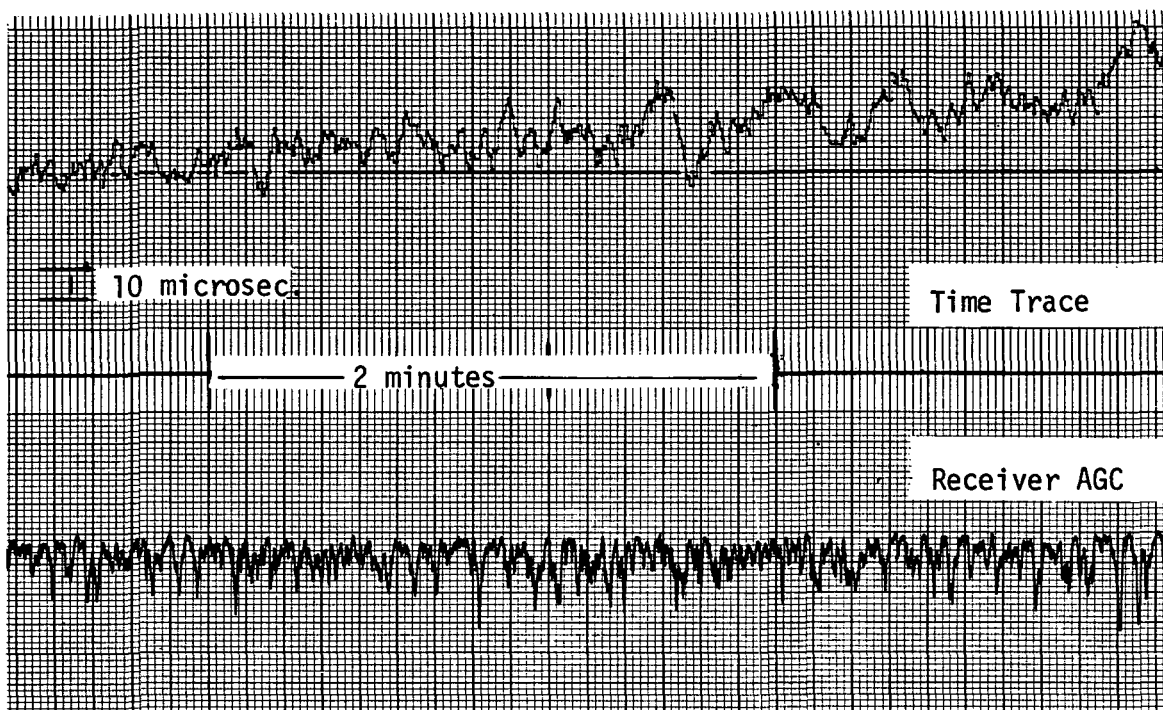


Figure 16 Random Walk of Time Trace During Heavy Scintillation

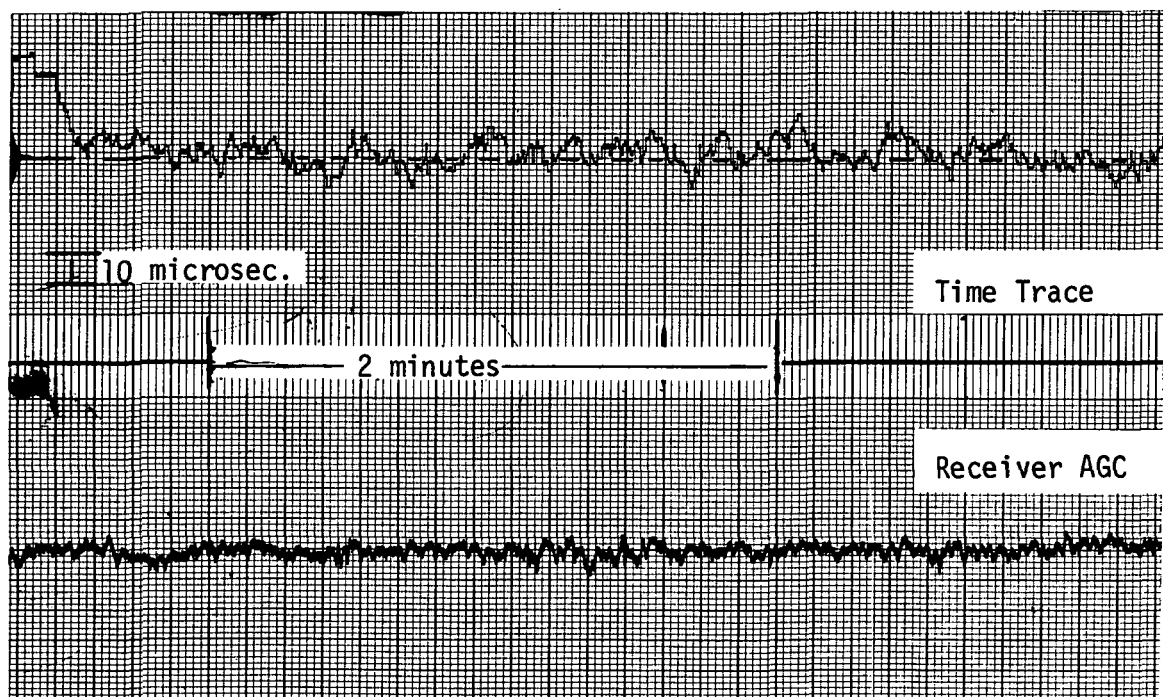


Figure 17 Random Walk of Time Trace During Mild Scintillation

QUESTIONS AND ANSWERS

MR. GEORGE PRICE, Austron

As an operational experiment, or an operational procedure on-board an aircraft to get time to 30 microseconds are you able to use it with a commercially available piece of equipment, and if so then what do you have to add to it to make those measurements?

MR. SWANSON:

Yes, we use the Arbitors System Model 1060 receiver which cost about \$5,000 and the plate antenna that went with it. For our time comparison measurements we carried a HP 5065 rubidium and battery pack, which was synchronized at the time shop at Wright-Patterson.

We used two techniques. One being the Hewitt-Packard computing counter, with its time interval device and print out. We used that to verify the digital comparator that is inside the Arbitors receiver which creates an analog voltage with the resolution of plus or minus a microsecond.

We confirmed that that did work and then relied upon a strip chart as the recording device running the pulse from the rubidium into the Arbitor time comparer circuit and taking the analog equivalent and voltage out onto the strip chart.

At the same time then we also recorded one minute time hacks from the UTC time from the rubidium or from the Arbitor, just to keep track of where we were in the strip chart.

MR. PRICE:

But, to make an operation -- a day to day type of experiment a day to day type of measurement, on-board an aircraft could you do it with just the Arbitor receiver and the antenna and nothing else?

MR. SWANSON:

I would not want to do that with any great confidence, no. The restriction being that you don't know whether you have had local interference or not. I would feel much more comfortable having just a nice crystal running along side of it. Such that I could plot a small, very slow trace and say, obviously I am 500 microseconds off from what I was a minute ago and therefore, I won't accept the time off the GOES receiver now.

PTTI APPLICATIONS AT HYDRO-QUÉBEC

by G. Missout, J. Béland, G. Bédard
IREQ, Québec, Canada

ABSTRACT

As a power utility, Hydro-Québec used the PTTI techniques. The time dissemination system in the Hydro-Québec Network (11th PTTI) is now installed in several points.

We have since built a portable clock using a rubidium standard and associated circuitry (a microprocessor IRIG B reader-generator, time interval counter, time accumulator etc.) which are necessary for our measurement. The article describes the apparatus and the experimental results obtained.

We have also used GOES synchronized clocks for making precise voltage angle measurement on the Hydro-Québec Network. Some modifications have been made on a commercial unit. Applications and results will be presented.

I INTRODUCTION

As a Power Utility, Hydro-Québec should use all facilities available to reduce outage probabilities. We are presently working on two main PTTI applications: time dissemination for event recording purposes and angle measurement of a 60 Hz voltage.

The first one was described in more detail at the last PTTI (1). We show here the development and construction of a portable clock to make time delay calibrations. The second one is an application of a GOES synchronized clock. We present the whys, hows and problems encountered in this case.

II TIME DISSEMINATION

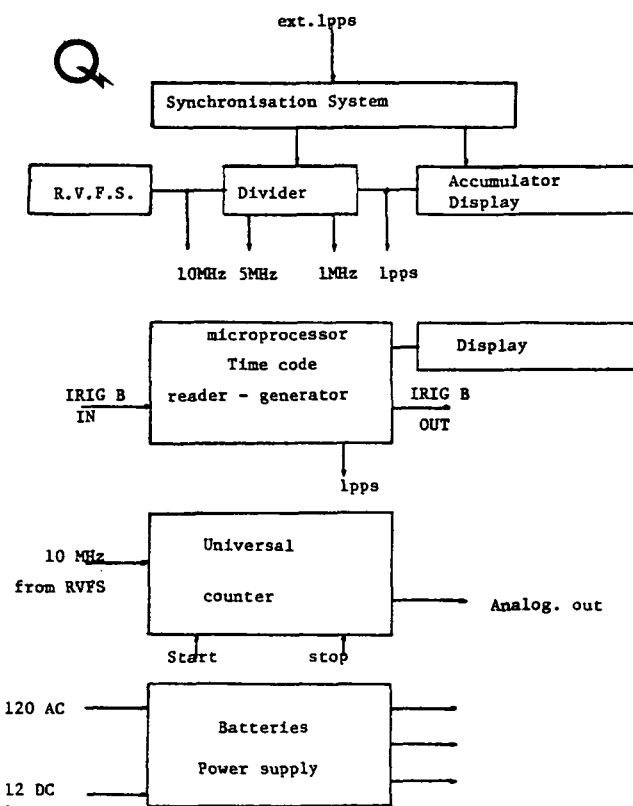
Actually, from a master clock, we disseminate time code to most of the main power stations of the Hydro-Québec network. The code is used in each place to put a date on each event's recording. The precision required is 1 ms. To calibrate the propagation delays between the master clock and the remote ones we have built a portable clock called HM2.

The characteristics of the clock are:

- Weight 32 kg
- Dimensions: 9" x 16" x 20"
- Rubidium vapor frequency standard
- IRIG B decoder-generator
- Universal counter (frequency-time delay) with analog output
- 24 hours autonomy on batteries
- 110 VAC and 12 VDC input.

The block diagram is shown in Figure 1. Only the clock part (excluding the display) runs on battery during travel. The divider is synchronized by an external 1 pps source.

The time code reader has an 1 pps output, so an operator can receive a time code in a power station, check the value of the transmitted date and measure the delay between the internal 1 pps of the clock and the one decoded from the time code using the universal counter. Figure 2 gives a typical recording.

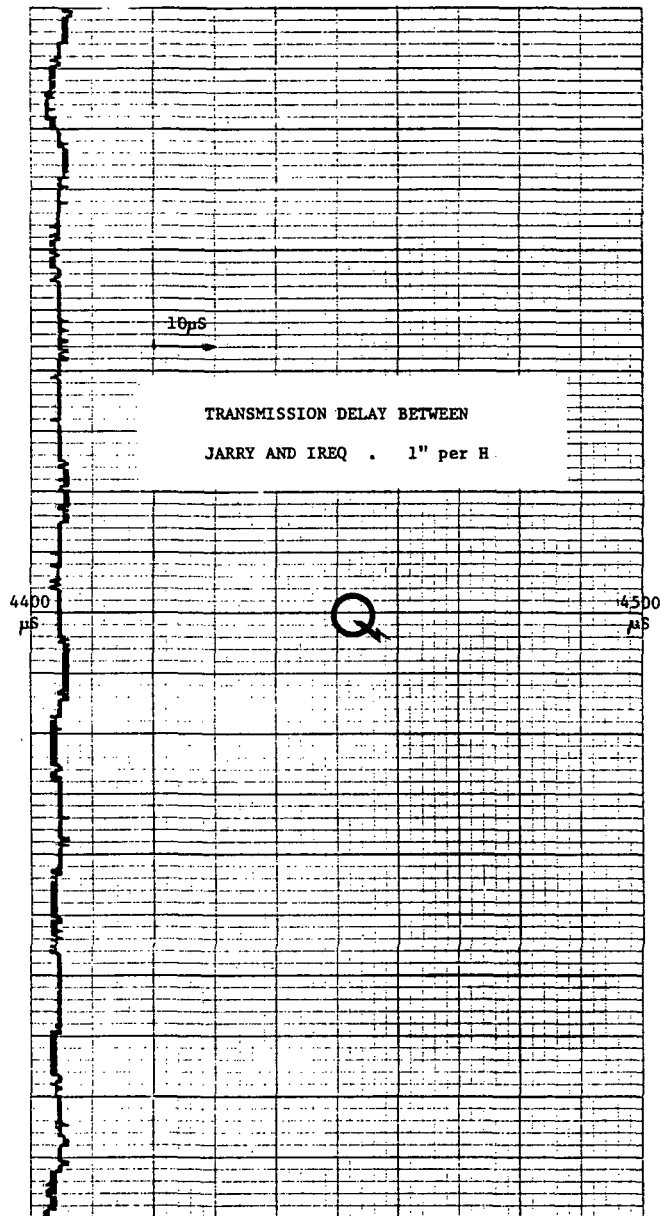


HM2 BLOC DIAGRAM

FIG. 1

One could use HM2 as code generator to send a time code to other apparatus in order to check them.

The portable clock will also be used to calibrate in the field Xtal oscillators with the help of a frequency comparator. This is useful for stationary apparatus or for precise setting of running oscillators. We



Transmission time delay record using HM2

FIG. 2

also plan to use the portable clock as backup of the main frequency standard at the master station because in case of failure it can take some months to repair it.

III 60 Hz VOLTAGE ANGLE OF A TRANSMISSION LINE

3.1 Definition-interest

The 60 Hz voltage angle is the phase angle between the two voltages which exist at the ends of a transmission line. Roughly the angle depends on the load of the line, the length of the line, and the number of lines used in parallel between two points.

Voltage angle is the most important parameter of a power system network. Until now, it was only calculated. Its direct measurement gives a lot of information on the behavior of the power system network. Its recordings during fault can be used in postmortem studies of the network, or used to adjust or correct the theoretical model.

3.2 Measurement procedures

Points of measurement are far away from each other (hundreds of km) and most of the attempts to code and send voltage waveforms from one point to the other failed due to transmission time delay variations of the same order of the thing to be measured (1° at 60 Hz equals $40 \mu s$).

So we (2) and others (3) in the past have done some experiments using two (or more) local references at 60,000 Hz synchronized together. Then one can measure and code the local (or absolute) voltage angle and send those values to a central station which now may calculate the voltage angle by subtraction. Figure 3 illustrates this method.

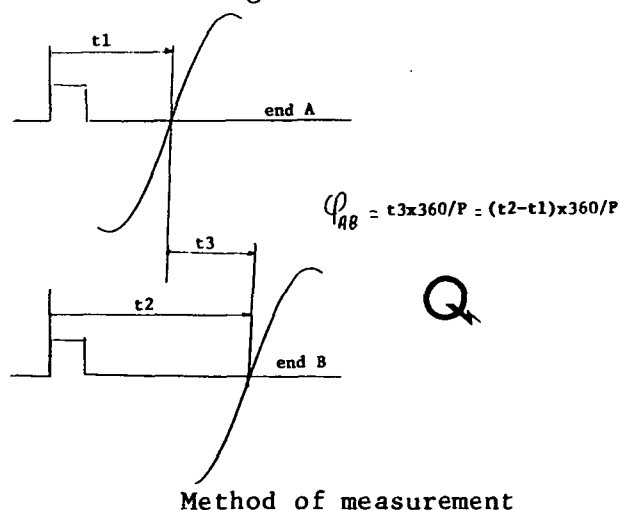


FIG. 3

Using this concept we built a system with the following objectives in mind:

- fully automatic system
- 24 hour operation every day of the year
- accuracy of measurement better than 1° at 60 Hz ($\approx 40 \mu\text{s}$)
- 30 measurements per second.

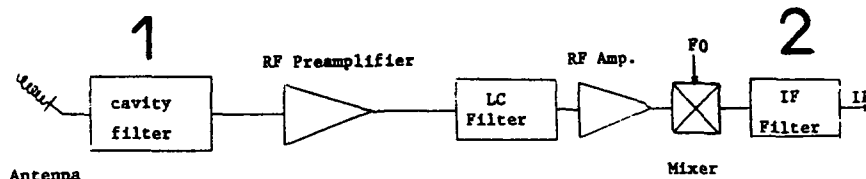
Using the GOES time code to synchronize the 60,000 Hz reference has created some problems.

3.3 Problems in using GOES time code-Hydro-Québec's improvements

GOES time code is in an experimental phase. From time to time data are wrong or absent. Or there is a change in the satellite used, so the helix antennas are in the wrong direction.

GOES frequency is not exclusive: so there are several radio interferences due to mobile radio and the only commercial clock available with automatic correction of time delay propagation has a lack of selectivity which perturbs its operation during RFI.

We made two modifications of the clock (Figure 4)



Hydro-Québec's improvement of the GOES synchronized clock

FIG. 4

- 1) We added a cavity filter to limit RF band pass and possible saturation of the RF preamplifiers
- 2) We changed the IF quartz filter. The original one gives 40 to 45 dB of ultimate rejection, the new one gives 75 to 80 dB of rejection limited mainly by the printed circuit on which it is installed.

By comparison a typical mobile radio has over 90 dB of rejection.

In severe environment the unmodified clock synchronized only during the night (no or few users of mobile radio) but remains totally unsynchronized during the day (except on weekends). The modified model remains synchronized during the day. In other environments (few mobile radio) the improved model makes less errors than the unmodified one. Figure 5 shows typical results of the modified one (in favorable environments) and Figure 6 typical errors when we remove the cavity (but improved filter in place). We don't have recordings of the original clock, but, errors are more numerous.

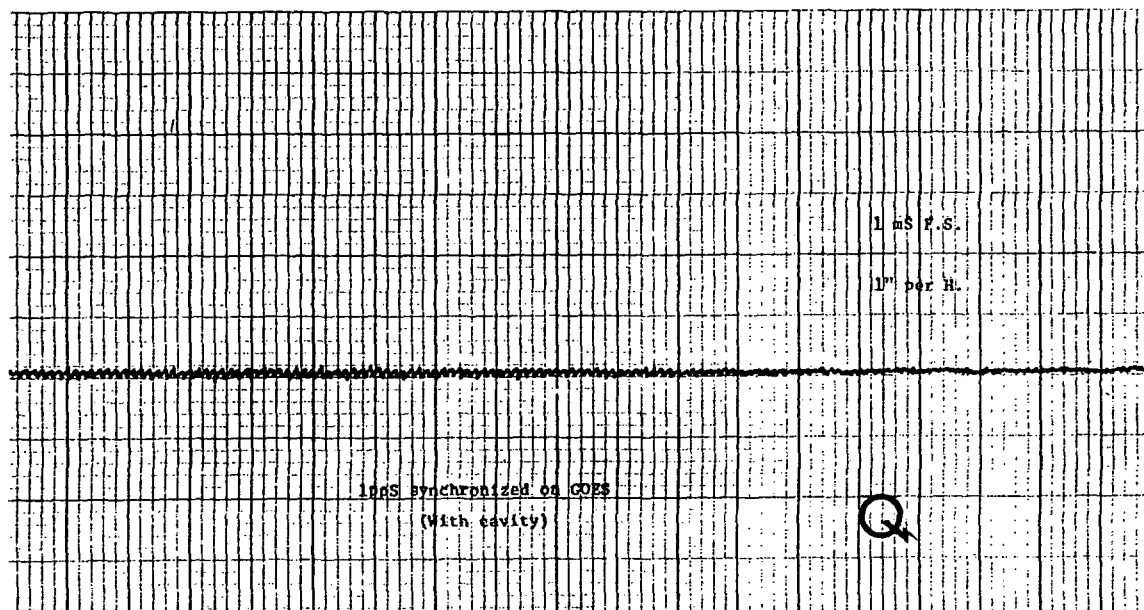


FIG. 5

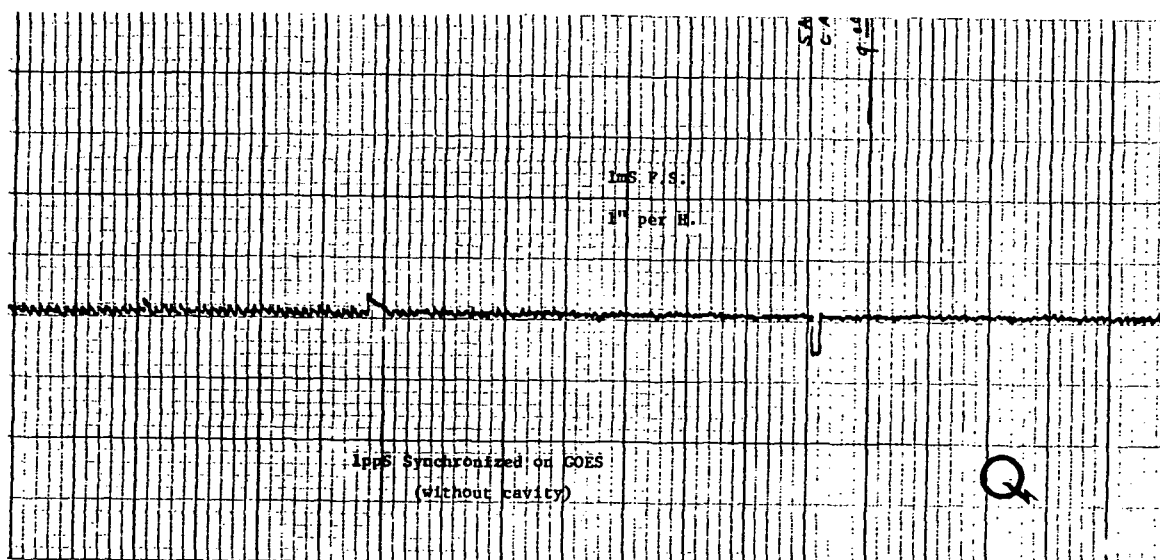
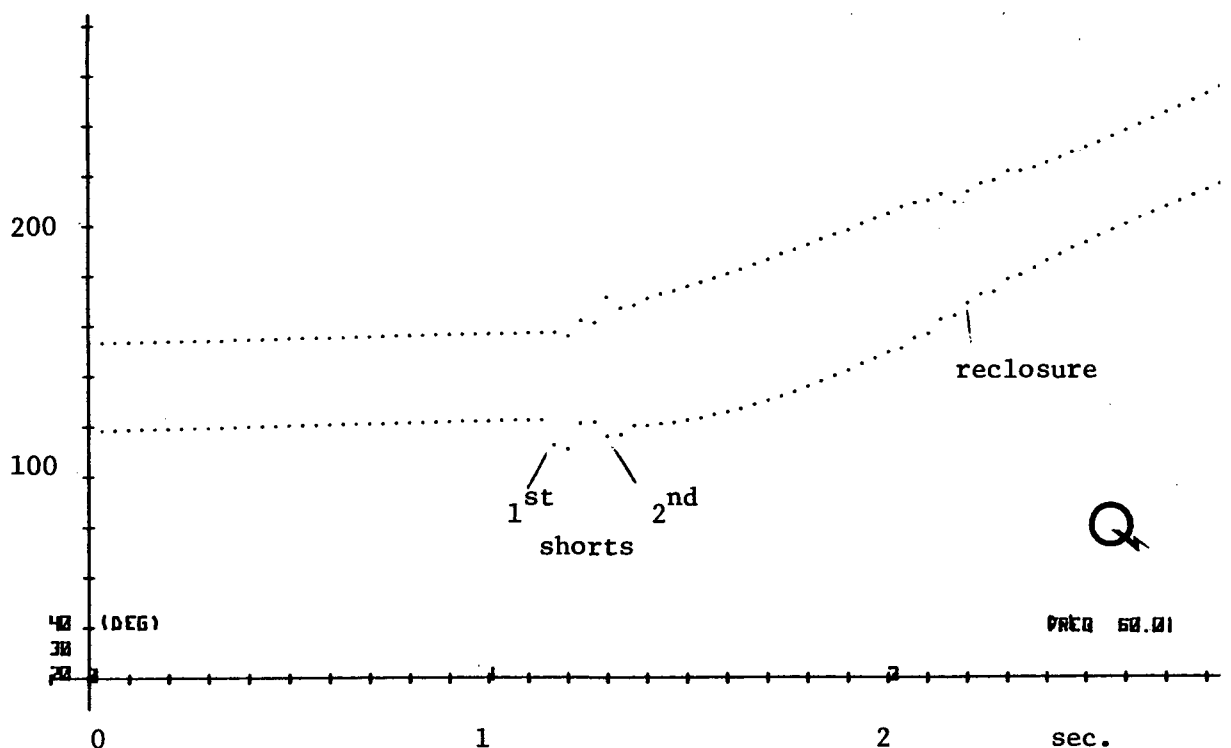


FIG. 6

3.4 Results

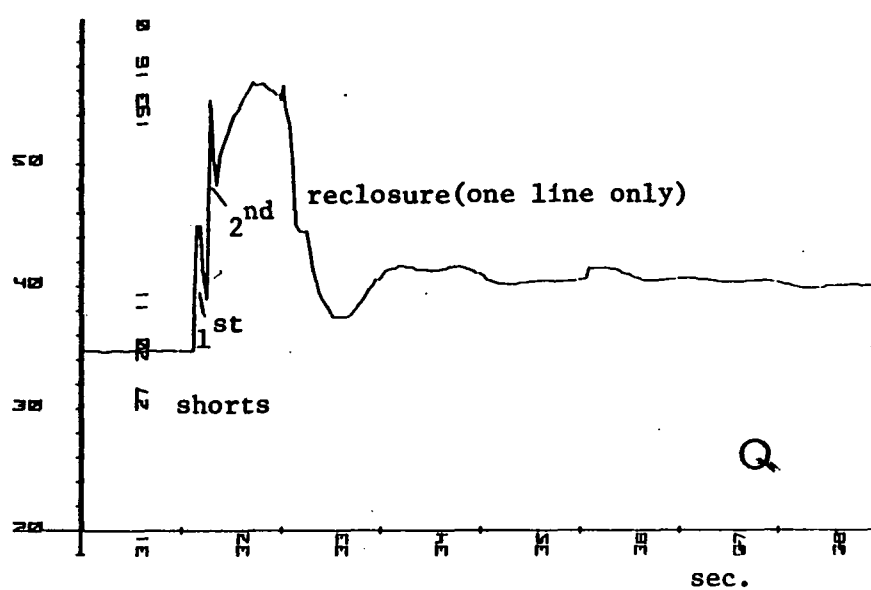
Figures 7, 8, 9 show a typical recordings of local angle, voltage angle and frequency during short-circuits on two parallel lines, with automatic opening and reclosure.



Local phase record

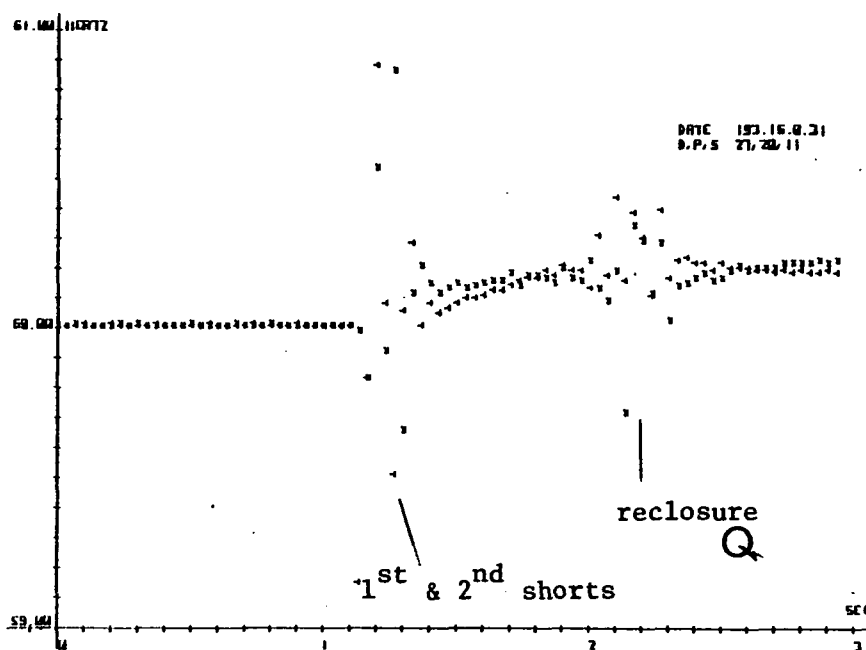
FIG. 7

- [1] G. Misout, W. LeFrançois, L. LaRoche, "Time dissemination in the Hydro-Québec Network," 11th PTTI, P. 343.
- [2] G. Missout, P. Girard, "Measurement of bus voltage angle between Montreal and Sept Iles," IEEE Trans. on PAS-99, No. 2, pp.536, March/April 1980.
- [3] G. Rovera, A. Schiavi, "La misura a distanza dell angolo de fase dei vettori tensione nelle retielecttriche," Instuto Ellectro-technico Nazionale Galileo Ferrarir, Vol. LVII, No. 1418-1421, 15-21, Sept. 74.



60 Hz voltage angle

FIG. 8



Frequencies of both extremities of the line

FIG. 9

QUESTIONS AND ANSWERS

MR. DAVID HOWE, National Bureau of Standards

I am delighted that you are using the GOES experiment time code and it represents an important application of such dedication. However, you pointed out, it is an experimental system. What are your plans in the future for that system? Have you got any?

MR. MISSOUT:

There are some possible plans. First of all, we will try to find a new system of dissemination on the Hydro-Quebec microwave network to find the same accuracy as we have now.

Secondly, if this fails we may wait for a system like GPS which gives us more than one satellite. Because, actually, we use phase angle measurement for postmortem. But, it is possible to use automation. If you use the phase angle measurement for automatic control of the system, you have to be sure that it works.

So, actually each time we lose the satellite for whatever reason, the system doesn't work properly, and in fact, gives false measurements. So, we try to operate independently in our system; and secondly if it doesn't work we try your other system.

Page Intentionally Left Blank

USNO GPS PROGRAM

Kenneth Putkovich
U. S. Naval Observatory, Washington, D. C.

Abstract

The U. S. Naval Observatory (USNO) has historically been and continues to be at the forefront in the development of new concepts, techniques and equipment for the generation and dissemination of Precise Time and Time Interval (PTTI). With the advent of the Global Positioning System (GPS) and its predicted capability of time transfers on a worldwide basis to a precision of ten nanoseconds or better, the USNO secured funding to develop a GPS Time Transfer Unit (GPS/TTU) and is currently engaged in a program to validate and disseminate PTTI data from GPS.

Initial test results indicated that the GPS/TTU performed well within the ± 100 nanosecond range required by the original system specification. Subsequent testing involved the verification of GPS time at the Master Control Site (MCS) via portable clocks and the acquisition and tracking of as many passes of the space vehicles currently in operation as possible. A description and discussion of the testing, system modifications, test results obtained, and an evaluation of both GPS and the GPS/TTU are presented. Finally, the content of USNO GPS reports is discussed and current work and future program plans outlined.

INTRODUCTION

This paper deals specifically with the description, testing, and evaluation of GPS as a means of time transfer at the present time. A brief description of the GPS system is provided as background to aid in achieving some understanding of the overall system. More detailed information is available in the literature.¹

The GPS, as originally planned, was to consist of a space segment of twenty-four satellites and a ground segment of a Master Control Site (MCS) and five or more Monitor Sites (MS), one of which was to be located at the USNO. At present, the MCS is located at Vandenberg AFB in California and MS are located in California, Hawaii, Alaska, and Guam. The function of the Monitor Sites is to receive transmissions from each of the satellites, referred to a local clock, and to re-transmit this information to the MCS over secure data communication links. The function of the MCS is to correlate this information with

other information, perform the calculations necessary to determine current satellite performance characteristics and upload these parameters to the spacecraft on a daily basis, or as needed. This upload provides current information on clock performance, satellite locations, required clock corrections and all other information necessary to allow an accurate extrapolation of performance over the ensuing twenty-four hours.

The satellites were to be equally distributed in three planes inclined to the equatorial plane of the earth by 63° and intersecting the equatorial plane at 120° intervals. Due to funding cutbacks, present plans call for a space segment of eighteen satellites. The elimination of six satellites from the constellation has little adverse affect on PTTI, since at least one satellite will be in view at any time anywhere on earth and only one is necessary for time recovery. Studies are presently underway to determine the best orbital configuration for navigation.²

As a further result of funding cuts, the configuration of ground stations has also changed several times and the USNO Monitor Site was apparently eliminated from the plan.

GPS SATELLITE SIGNAL³

Information is transmitted from the satellites on two carrier frequencies, the primary (L_1) at 1575.42 MHz and the secondary (L_2) at 1227.6 MHz. The L_1 or primary transmission is modulated by both a precision code (P) code and a coarse/acquisition (C/A) code simultaneously. The L_2 or secondary transmission is modulated by either a P or C/A code. The data stream is transmitted at 50 bits per second and is common to both the P and C/A codes on both the L_1 and L_2 bands. All signals are derived from the same onboard clock. A complete data message is a frame of 1500 bits repeated every six seconds. Each frame is divided into five 300-bit subframes which are further subdivided into ten 30-bit words. The first two words of each subframe contain telemetry and code handover information. The last eight words of Subframe 1 contain clock corrections, an age of data word, and ionospheric delay model coefficients. The last eight words of Subframes 2 and 3 contain the space vehicle's ephemeris and the associated age of data words. The last eight words of Subframe 4 contain an alphanumeric message of interest to users. The last eight words of Subframe 5 contain an almanac (an abbreviated version of information in Subframes 2 and 3) for each of the satellites in the constellation. Each Subframe 5 contains information on a single satellite. Thus the complete almanac for the entire satellite constellation requires the reception of a sequence of frames. The length of the sequence is dependent on the number of satellites in orbit with twenty-four being the maximum.

In order to recover time relative to GPS, a user must be able to receive reliably the satellite signal and demodulate and decode the data

stream. Utilizing this information, one can calculate a corrected pseudo-range, compare it to a pseudo-range measured against a reference clock, and from the difference, determine the clock difference.

TIME TRANSFER SYSTEM

The GPS/TTU (Figure 1) consists of four major components - the receiver, the processor, the pseudo-range counter and the system software. As the processor (Hewlett-Packard 1000/45) and the counter (Hewlett-Packard 5328A) are off-the-shelf equipment, no description of them will be provided. A detailed description of the GPS/TTU and the Time Transfer Technique is provided in Reference (4); therefore only a brief description of the receiver and software are provided here.

The receiver is a single channel, spread spectrum Doppler tracking receiver capable of tracking and decoding the C/A code on the L_1 frequency. It receives the signal (from an antenna with a nearly hemispherical coverage pattern) through a low noise preamplifier. Preselective filtering in the preamplifier and further filtering at the receiver limit the effect of out-of-band noise. The signal is then down-converted to an IF frequency and fed to a code loop and correlator which track the C/A code and despread the spread spectrum signal. A carrier tracking loop then demodulates the signal and provides both C/A code epochs and navigation data to detection and synchronization circuits which provide the satellite information to both the measurement and computer systems.

The software system consists of an HP RTE-M operating system, two major application programs, and approximately forty-five subroutines for the acquisition, reduction, and recording of GPS data. Three major operational modes - full automatic, semiautomatic, and manual - are supplemented by auxiliary modes which provide access to satellite visibility and Doppler information and allow initialization and updating of data base and almanac files.

Initial operation requires loading the operating system, setting the system clock on time, initializing the data base with the geodetic coordinates of the antenna, receiver delays, satellite constellation, etc., and manually acquiring one satellite. Once successfully completed, the procedure need be repeated only if parameters change or a system malfunction occurs.

Calling up the full automatic mode of operation (after initialization) results in the generation and implementation of a daily tracking schedule based on current satellite constellation visibility as determined from the almanac recovered during the previous satellite pass. The schedule is regenerated daily thereafter until tracking operations are manually terminated. The only constraint imposed on the automatic mode design was that of requiring that each satellite identified in the data

base be tracked at least once per day. A system generated schedule is shown in Figure 2.

Operation in the semiautomatic mode requires the development of a tracking schedule by the system operator. Satellite visibility is determined by utilizing the visibility subroutine, which results in an information display identical to Figure 2. The selected tracking schedule for a twenty-four hour period is entered (utilizing an interactive dialogue between the computer terminal and the operator) as shown in Figure 3. The completed schedule (Figure 4) is presented for verification and is then implemented by a negative response to the "CHANGE (YES/NO)?" query. Daily tracking continues on this schedule until the operator intervenes or the satellite constellation precesses to the point where specified satellites are no longer visible during the scheduled viewing time.

Operation in the manual mode requires the operator to enter a satellite identification number and an estimate of the carrier Doppler frequency. The receiver then goes into an acquisition loop based on this information and continues in this loop until the chosen satellite comes into view. At the point where the Doppler frequency of the satellite signal falls within a window centered on the original estimate, the receiver locks onto the received signal and continues tracking until the satellite sets or the operator intervenes. Daily tracking of the satellite continues indefinitely until the operator intervenes.

In all modes of operation, data in both raw and processed forms are available for viewing on the system console CRT and can be written onto magnetic tape mini-cartridges and an IEEE-488-1975 general purpose instrumentation bus.

USNO GPS DATA

Initial test results showed the GPS and GPS/TTU capable of time transfers with a precision of better than 100 nanoseconds (Figure 5).⁵ Subsequent tests resulted in the same level of performance but revealed what appeared to be several discontinuities in GPS time (Figure 6). An investigation showed the cause of these steps to be clock changes and failures at the Monitor Sites. The GPS system software as presently implemented can apparently absorb these time discontinuities with little or no degradation of navigational capabilities. However, discontinuities of this type reduce the system's usefulness in the PTTI area to an unacceptable level. This point has been brought to the attention of the GPS Program Office in order to emphasize the importance of a coordinated effort in the timekeeping aspects of the program.

Figures 7 and 8 show GPS performance that has been observed over the past several months. A comparison of these data with Figure 6 shows

some apparent improvement in that the magnitude and frequency of discontinuities appear to be less in the more recent data. These data also show that the GPS clock is ahead of the USNO Master Clock by over thirty-six microseconds and that it is high in frequency by 1.2 parts in 10^{12} at present. The data in Figure 7 show excellent performance capability over the long term if one ignores the outliers due to a poorly performing satellite. The disturbance recorded between day 44572 and 44578 is ill-defined due a combination of a lack of data during that period and an apparent discontinuity in the little data that was recovered during that time. Examination of Figure 8, which is essentially a plot of the residuals to a linear fit of the data, shows a pattern of variation around the linear fit which appears again in later data from individual satellites. The two extremely large outliers between day 44575 and 44577 appear inverted in Figure 8 due to an aberration in the plotting subroutine used.

Figures 9 through 13 provide a comparison of clock performance for each satellite relative to the USNO Master Clock. Linear fits were applied to the data to remove a large part of the offset that exists between the USNO Master Clock and GPS clocks. The data plotted in these graphs are average values of the measured pseudo-range or time of arrival corrected by subtracting a calculated pseudo-range or time of arrival, ionospheric corrections, tropospheric corrections, and receiver system delays. This is analagous to other one-way, synchronized time transmissions (Loran-C, HF, etc.), where a measured time of arrival is corrected by applying corrections for calcualted or measured propagation and system delays. In both cases, the result consists of the relative clock difference or offset between the local and remote clock, and the uncertainties and instabilities of both clocks, the measurement systems, and the corrections applied. Since in this case the local clock is the USNO Master Clock, all the offset and uncertainties can be attributed to the satellite clock and the measurement process and system. The cause of the large excursions shown in the SV#4, SV#5, and SV#8 plots has yet to be determined - although it is likely that they are due to system adjustments made to these satellites. The more important point illustrated by these plots is that, with the exception of SV#4, the clocks are well-behaved and perform exceptionally well. SV#4's poor performance is due to unpredictable behaviour in the upload or control mechanism rather than in the clock itself. Were it not for the two large perturbations in the SV#5 and SV#8 plots, it is likely that they would be comparable to that of SV#6. This clock exhibits a characteristic signature for a Rubidium frequency standard with uncharacteristically high performance, staying within ± 3 microseconds of a fixed linear offset for nearly a one hundred day period. SV#9 is the only satellite presently operating from a cesium oscillator. As expected, its transmissions are exceptional in that it has an offset of only 1.5 parts in 10^{-13} and has stayed within 125 nanoseconds of this offset for nearly one hundred days.

Figures 14 through 18 provide a comparison of the performance of the individual satellites and an indication of how well the GPS system is performing from the standpoint of utilizing the full capabilities of the satellite clocks. In these plots an additional correction factor is applied to the clock differences shown in the previous five figures. The message transmitted by each satellite contains a parameter which gives a continuous, real time estimate of the difference between the GPS clock and the satellite clock. This parameter is determined by the MCS using clock differences (between ground clocks and satellite clocks) measured at the monitor sites. Imbedded in this factor are the combined offsets, instabilities, and uncertainties of both clocks. Thus GPS system performance is equally dependent on ground clock and satellite clock performance, the individual contributions of which cannot be separated without reference to a third clock system. As before, the data from SV#4 are poor. Data from the other four satellites show a high degree of correlation which can be directly attributed to the performance of the ground clock. Furthermore, a comparison of Figures 13 and 18 shows that the data from SV#9 suffers considerable degradation due to the application of the GPS clock - satellite clock correction factor.

USNO GPS DATA REPORTS

Data from the satellites are recovered daily and made available at present through the USNO Time Service Automated Data Service (ADS). At present, the data are recorded on magnetic mini-cartridge tape cassettes, reduced and entered into the Time Service Data Base daily during the regular workweek (Monday through Friday). Weekend values are entered on Monday. Figure 19 is a typical example of several days of reduced data as available from the ADS. The first line gives the date/time when data collection began for the immediately following listing. The second line gives the date/time when the data were processed. An explanation of the column headings and data is presented in Table 1. Access to the ADS is available to any user over a standard dial-up telephone line, using a modem and terminal combination able to communicate at 300 or 1200 baud in a full duplex mode with even parity. The commercial telephone number is (202) 254-4080 and the AUTOVON number is 294-4080.

PROGRAM IMPROVEMENTS

Although the GPS program is in the middle stages of development, it is felt that the potential for time dissemination can be realized much earlier than the full navigational capability. The USNO and the GPS Joint Program Office and Master Control Site are in the early stages of a program to develop the means of linking the GPS clock with the USNO Master Clock with the objective of establishing a high degree of coordination between the two until the system becomes fully operational in the late 1980's. At that time the system should have the inherent

capability to accomplish this coordination since the operational phase specification requires coordination with UTC and USNO. The goal of the present effort is to synchronize the GPS clock in time and frequency with the USNO Master Clock, to eliminate frequency shifts and time jumps in the GPS ground clock system, to maintain the GPS clock in synchronism with the USNO Master Clock, and to disseminate the resultant data to the timekeeping community in a timely and useful manner. Present plans call for the investigation of the time jumps and frequency shifts that have been observed on GPS, the establishment of a link between the ground clocks at the Master Control Site and the USNO, and the establishment of procedures to permit the synchronization of the two. Recent modifications to the USNO/TTU will allow its integration into an automated data acquisition system and provide automated satellite tracking on a programmed basis. This will provide users continuous access, in near real time, to GPS data collected by the USNO.

CONCLUSION

The USNO is currently engaged in a program to provide PTTI users on a worldwide basis to an accuracy of 100 nanoseconds or less on a real time basis. In addition to affording all users a worldwide capability heretofore unavailable, successful completion of these programs will mean significant improvements to international efforts in coordinated timekeeping.

REFERENCES

1. Global Positioning System, The Institute of Navigation, Washington, D.C., 1980.
2. Book, S. A., Brady, W. F., and Mazaika, P. K., "The Nonuniform GPS Constellation", IEEE Position Location and Navigation Symposium Record, December, 1980.
3. System Specification for the NAVSTAR Global Positioning System, USAF Space and Missile Systems Organization, 31 January 1979.
4. Hua, Q. D. and Bustamante, H. A., "A GPS Time Transfer System", Standord Communications, Inc., 1980.
5. Putkovich, K., "Initial Test Results of USNO GPS Time Transfer Unit", Thirty-Fourth Annual Frequency Control Symposium, May 1980.

TABLE 1

Explanation of Columnar Headings and Data on USNO GPS ADS Message

SV#	- Satellite identifier transmitted in satellite message.
BEG.TRK DDD.ddd	- Beginning of tracking period. Given as a Modified Julian Date minus 44,000 in hundreds of days (DDD) and decimal fractions of a day (ddd) with .500 being 1200 UTC.
BEG TRK D HHMMSS	- Beginning of tracking period. Given in GPS day of week (D) and UTC (HHMMSS). Sunday is day zero.
TRK TIME SSSS	- Length of tracking period in seconds.
MC-GPS US	- Time difference between USNO Master Clock and GPS as determined from satellite transmission. It is referred to BEG TRK time and is given in microseconds. A negative value means GPS is ahead of UTC.
SLOPE PS/S	- Slope of linear fit through all data collected during TRK TIME. Line originates at MC - GPS at BEG TRK.
RMS NS	- Standard deviation of data collected during TRK TIME.
ELV	- Elevation angle of satellite at USNO at BEG TRK.
AZMT	- Azimuth angle at USNO at BEG TRK.
D.AGE DHHMM	- Age of data is the time elapsed since last upload of information to the satellite. It serves as a confidence level value for the time dependent parameters transmitted by the satellite.
MC-SAT NS	- Satellite clock difference in nanoseconds uncorrected for GPS - SV clock difference.

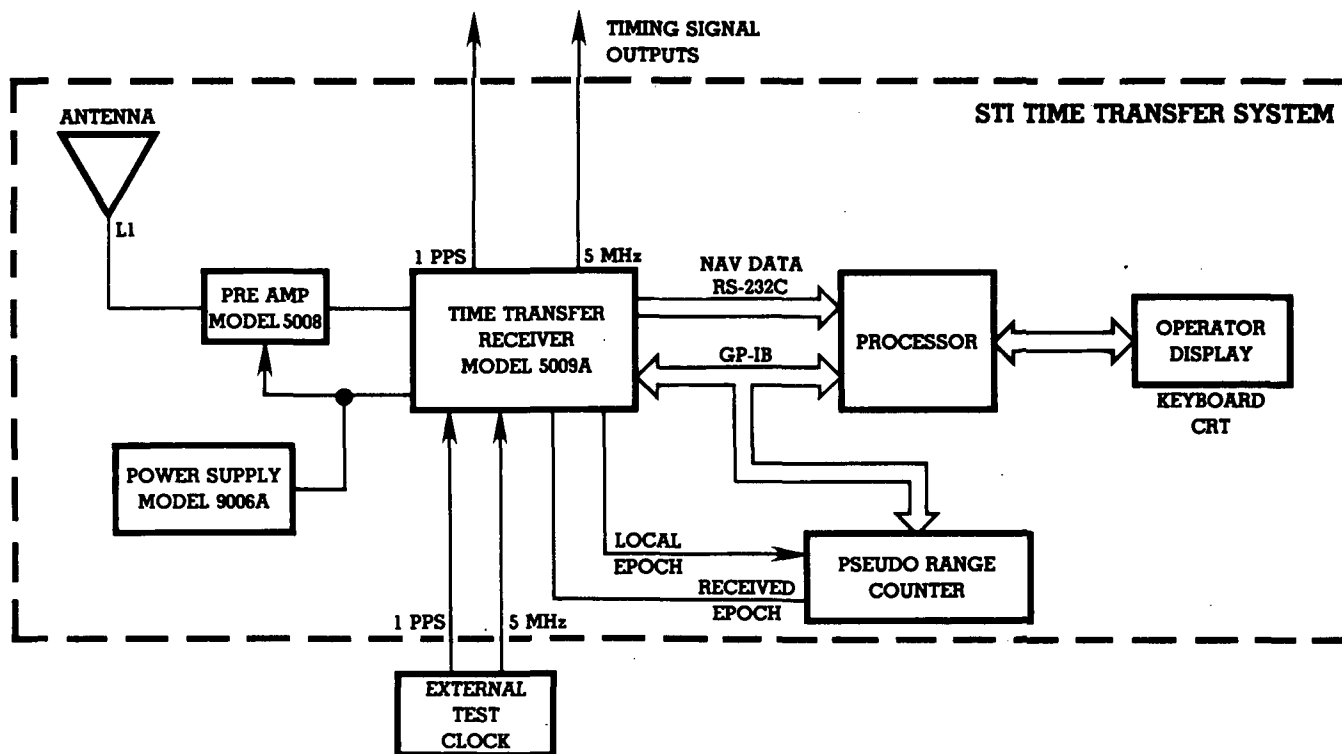


Figure 1. GPS/TTU Block Diagram

VISIBILITY ON MJD : 44610 DAY : 6 YEAR : 1981

SV: 4 RISE 13: 0 SET 19:45

SV: 5 RISE 14:45 SET 21:30

SV: 6 RISE 0: 0 SET 1:30 RISE 12:30 SET 17:15 RISE 23: 0 SET 24: 0

SV: -7 RISE 1:15 SET 6: 0 RISE 17: 0 SET 19:30

SV: 8 RISE 11:15 SET 17:15

SV: 9 RISE 0: 0 SET 3:15 RISE 14:30 SET 18:30 RISE 23:30 SET 24: 0

COMPUTED 24-HOUR SCHEDULE

START TIME	STOP TIME	SV
0: 0	1:30	6
1:30	3:15	9
11:15	16:45	8
16:45	17:15	6
17:15	18:30	9
18:30	19:45	4
19:45	21:30	5
23: 0	24: 0	6

GPSTT : STOP 0000

Figure 2. Visibility Subroutine Output Display

```
24-HR SCHEDULE SETUP
--> START TIME 0: 0
    ENTER STOP TIME(HR,MIN),SVID ? 00:06,6
--> START TIME 0: 6
    ENTER STOP TIME(HR,MIN),SVID ? 01:05,0
--> START TIME 1: 5
    ENTER STOP TIME(HR,MIN),SVID ? 01:11,9
--> START TIME 1:11
    ENTER STOP TIME(HR,MIN),SVID ? 13:50,0
--> START TIME 13:50
    ENTER STOP TIME(HR,MIN),SVID ? 14:02,8
--> START TIME 14: 2
    ENTER STOP TIME(HR,MIN),SVID ? 14:15,6
--> START TIME 14:15
    ENTER STOP TIME(HR,MIN),SVID ? 14:27,4
--> START TIME 14:27
    ENTER STOP TIME(HR,MIN),SVID ? 14:39,9
--> START TIME 14:39
    ENTER STOP TIME(HR,MIN),SVID ? 14:51,5
--> START TIME 14:51
    ENTER STOP TIME(HR,MIN),SVID ? 24:00
```

Figure 3. Interactive Semi-automatic Mode Scheduling Display

24-HOUR SCHEDULE

START TIME	STOP TIME	SV
0: 0	0: 6	6
1: 5	1:11	9
13:50	14: 2	8
14: 2	14:15	6
14:15	14:27	4
14:27	14:39	9
14:39	14:51	5

CHANGE DATA (YES/NO) ?

Figure 4. Semi-automatic Mode Schedule

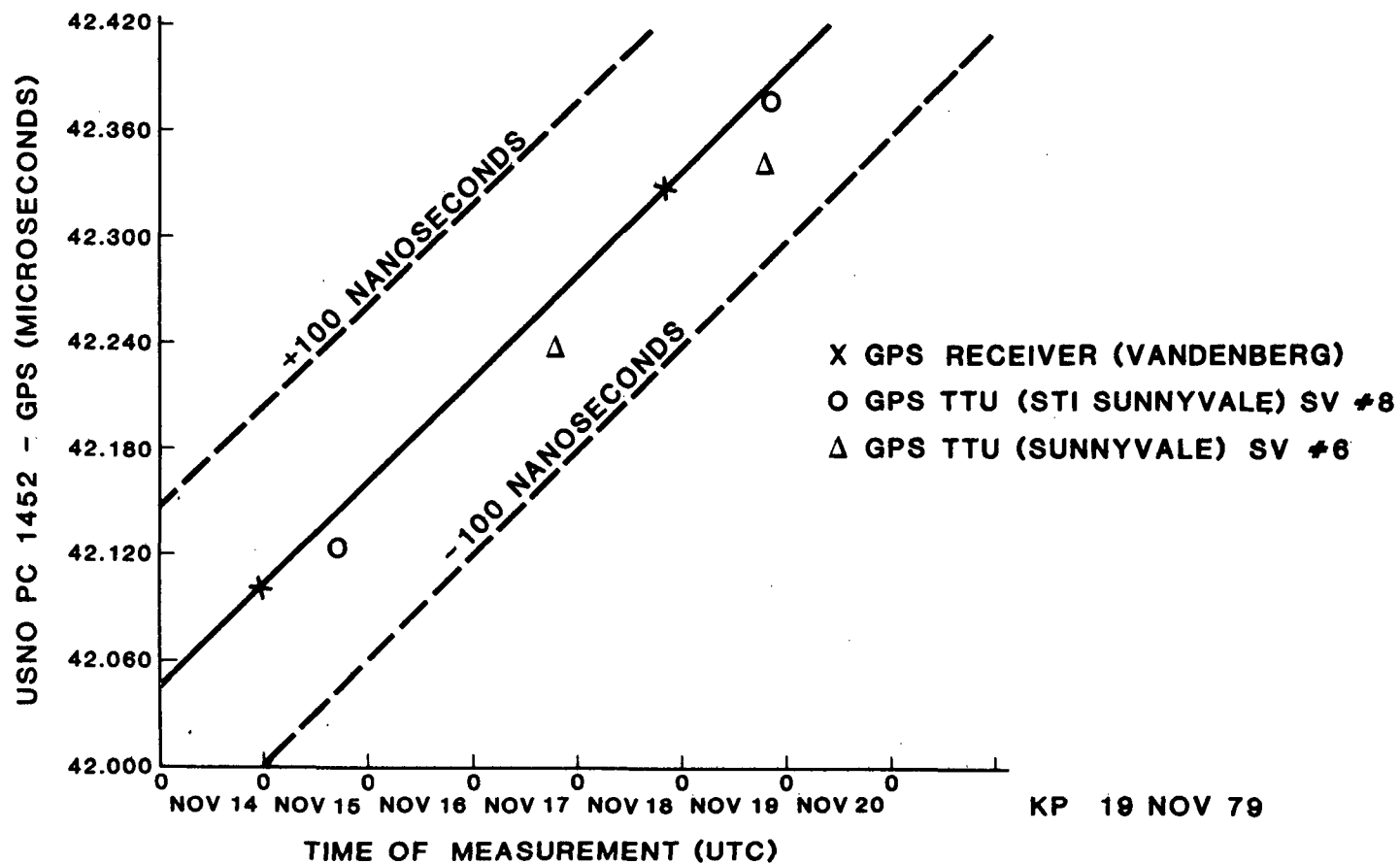


Figure 5. Initial Test Results

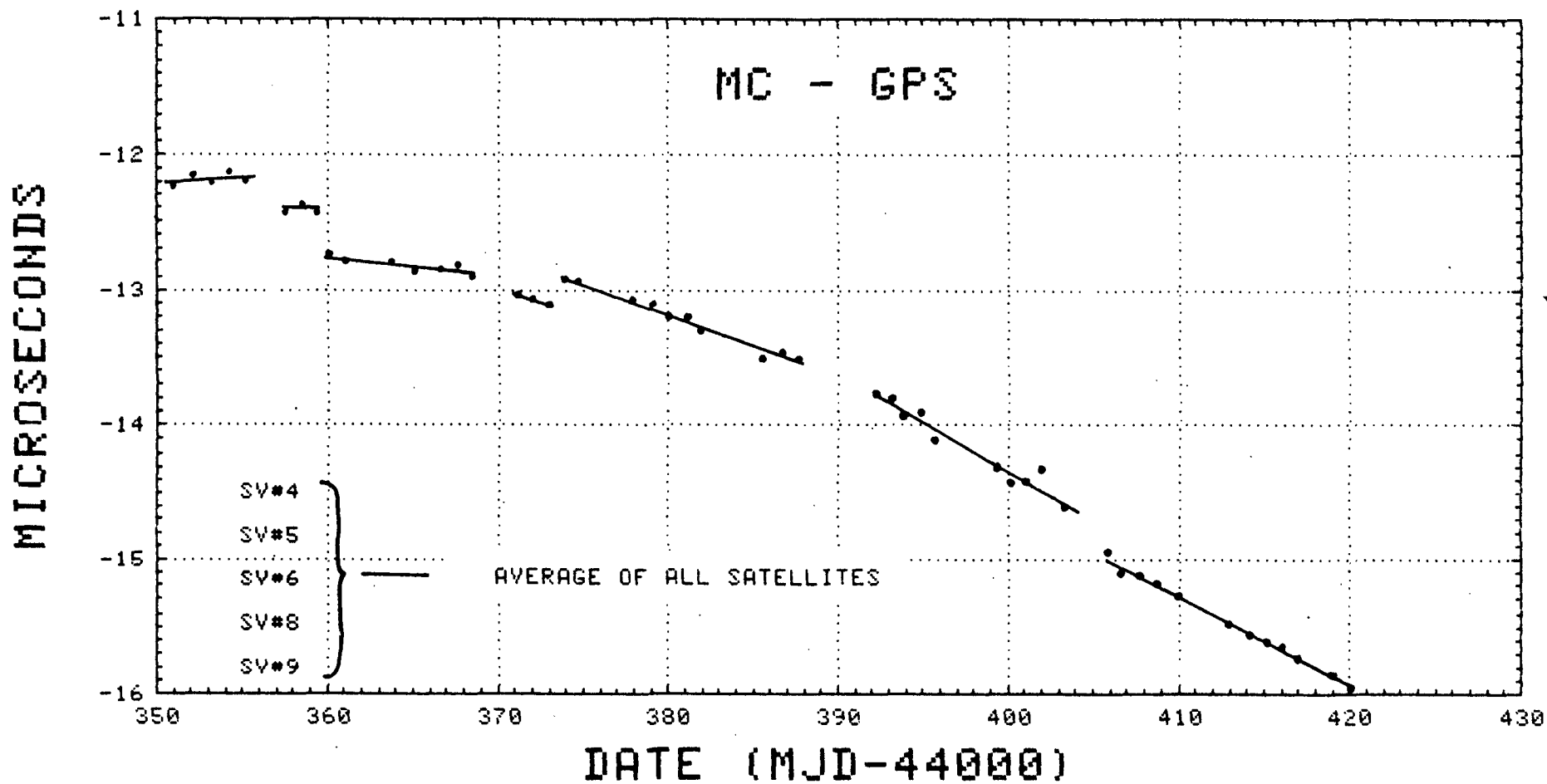


Figure 6. Early Test Results

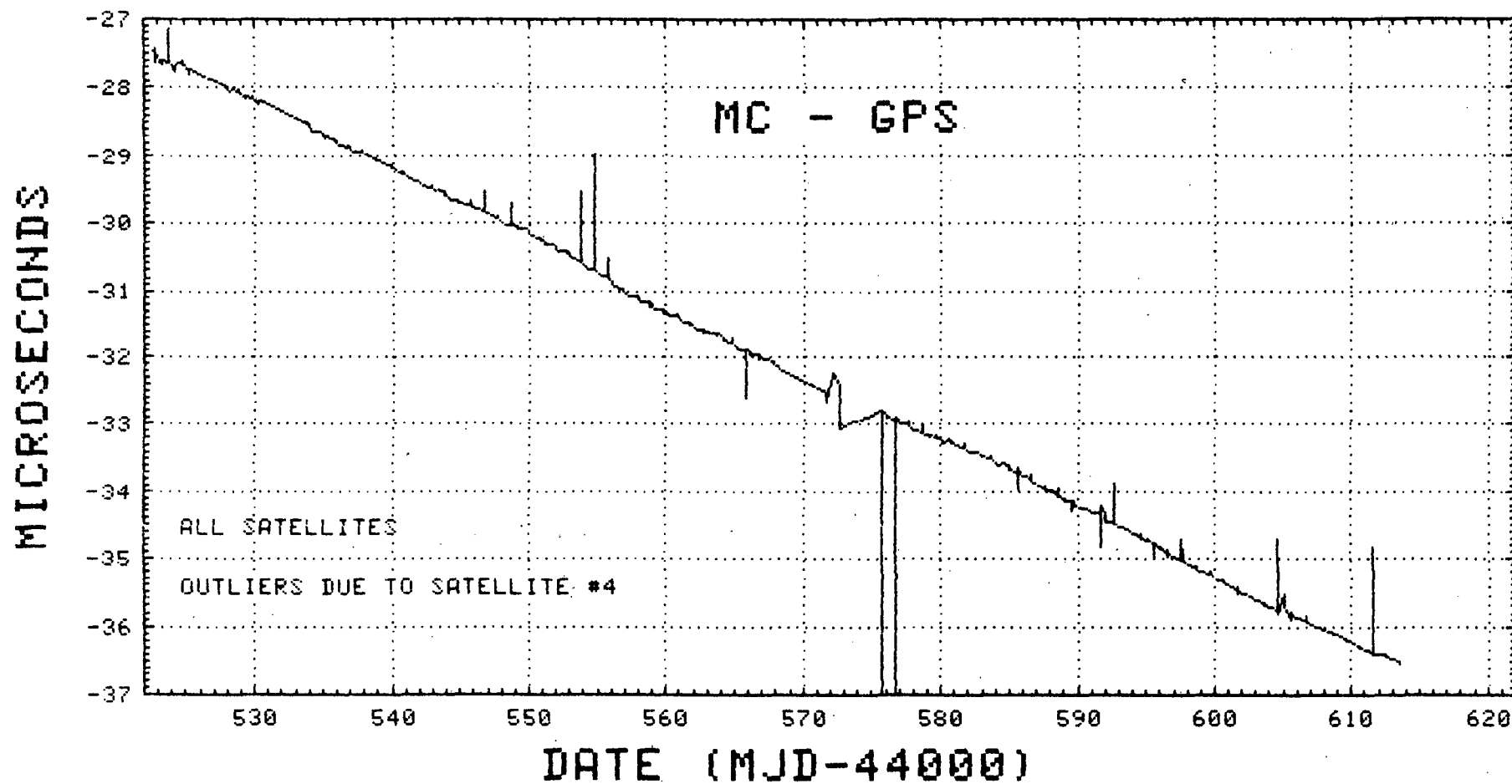


Figure 7. USNO Master Clock (MC) - GPS Utilizing All Satellites

NANOSECONDS

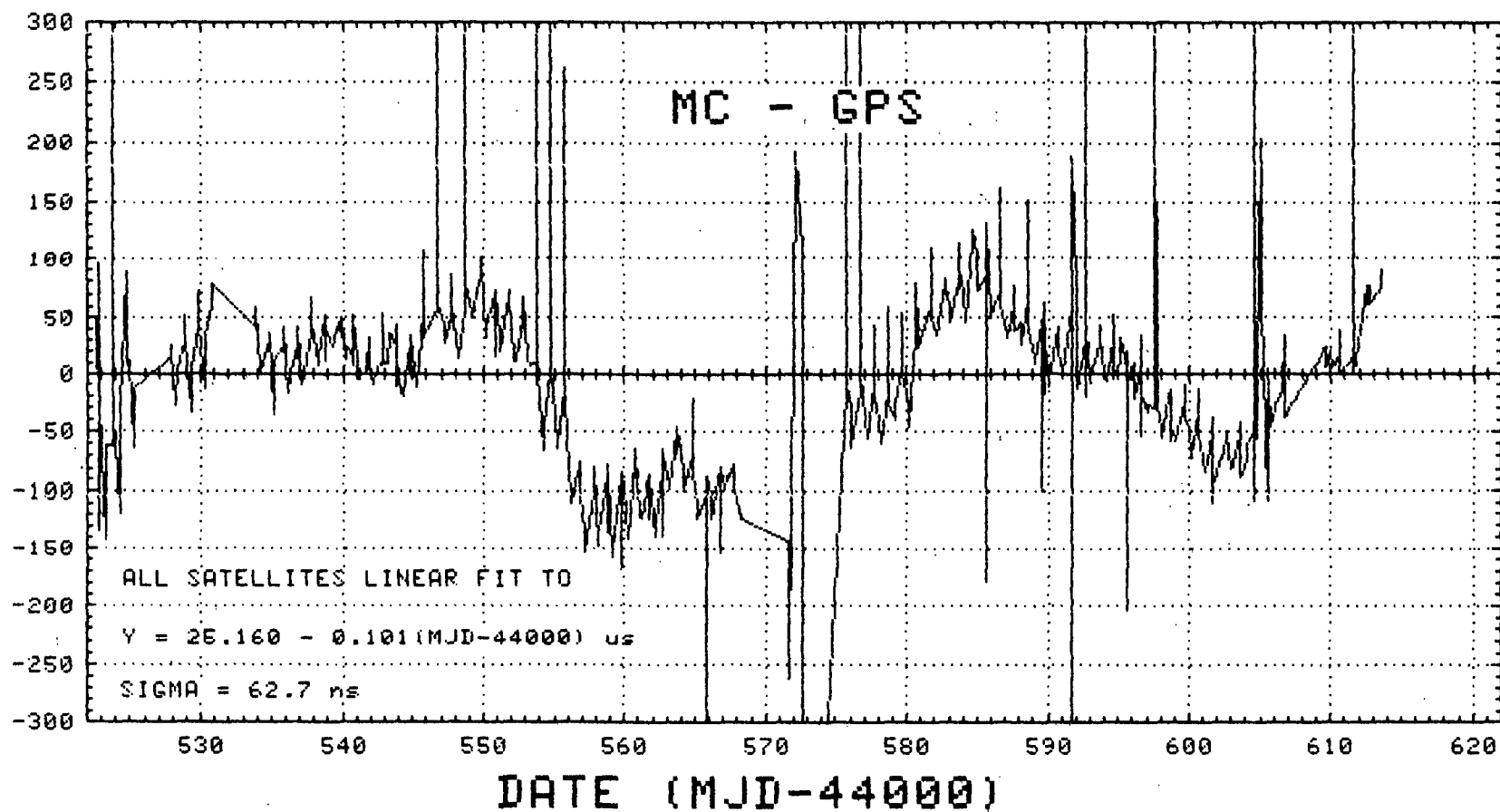


Figure 8. USNO MC - GPS Linear Fit and Residuals Utilizing All Satellites

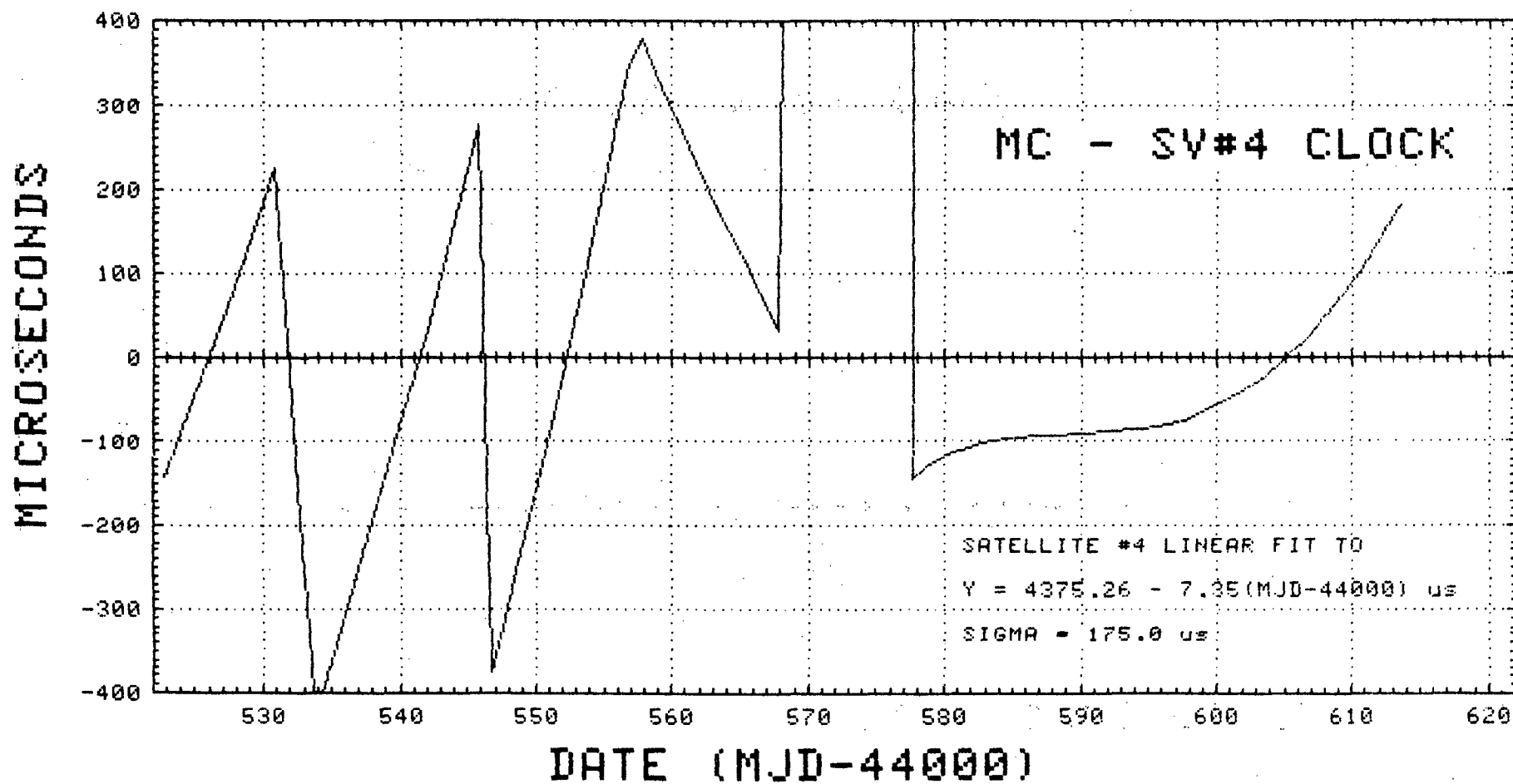


Figure 9. USNO MC - GPS SV#4 Clock Linear Fit and Residuals

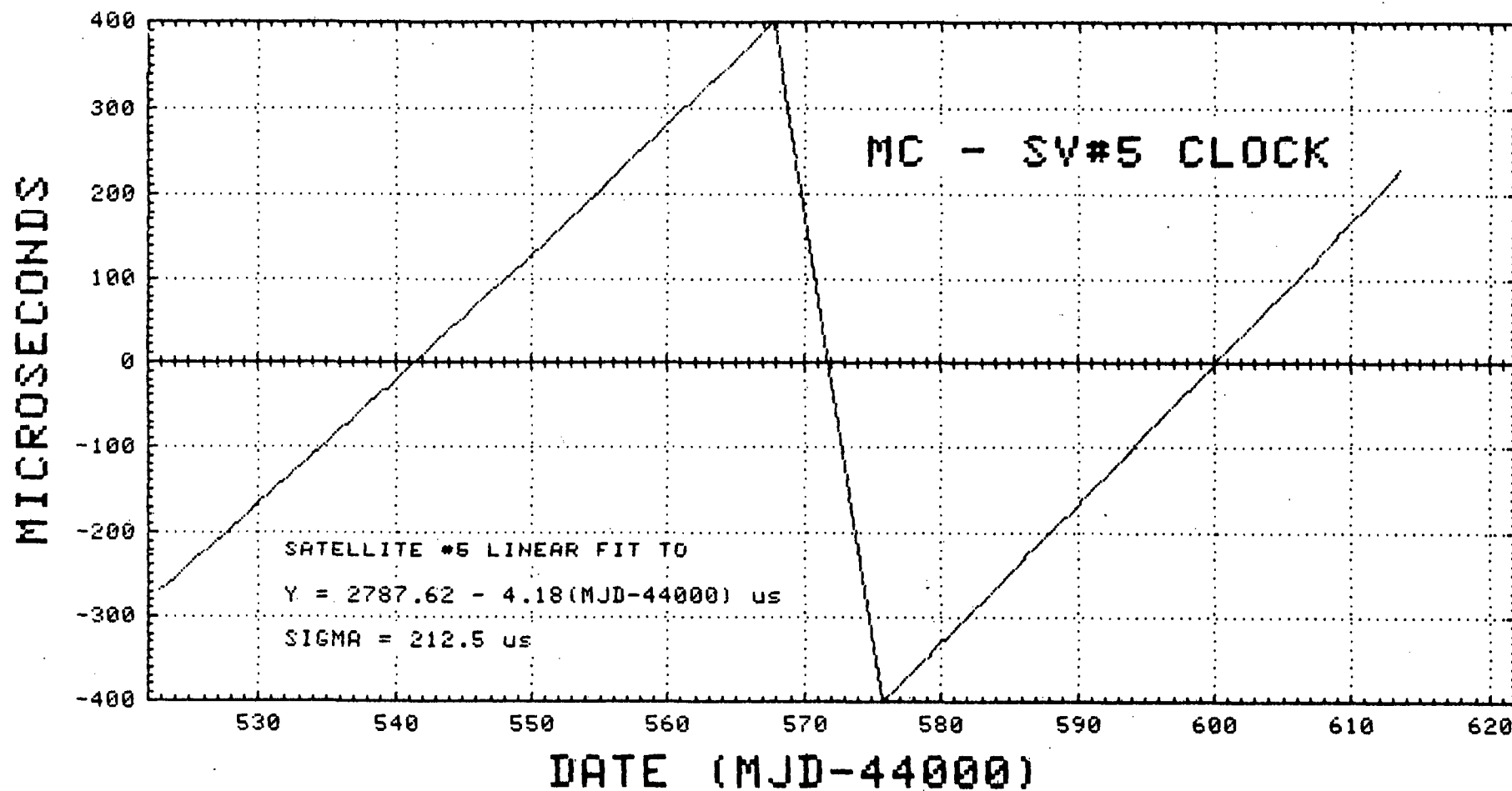


Figure 10. USNO MC - GPS SV#5 Clock Linear Fit and Residuals

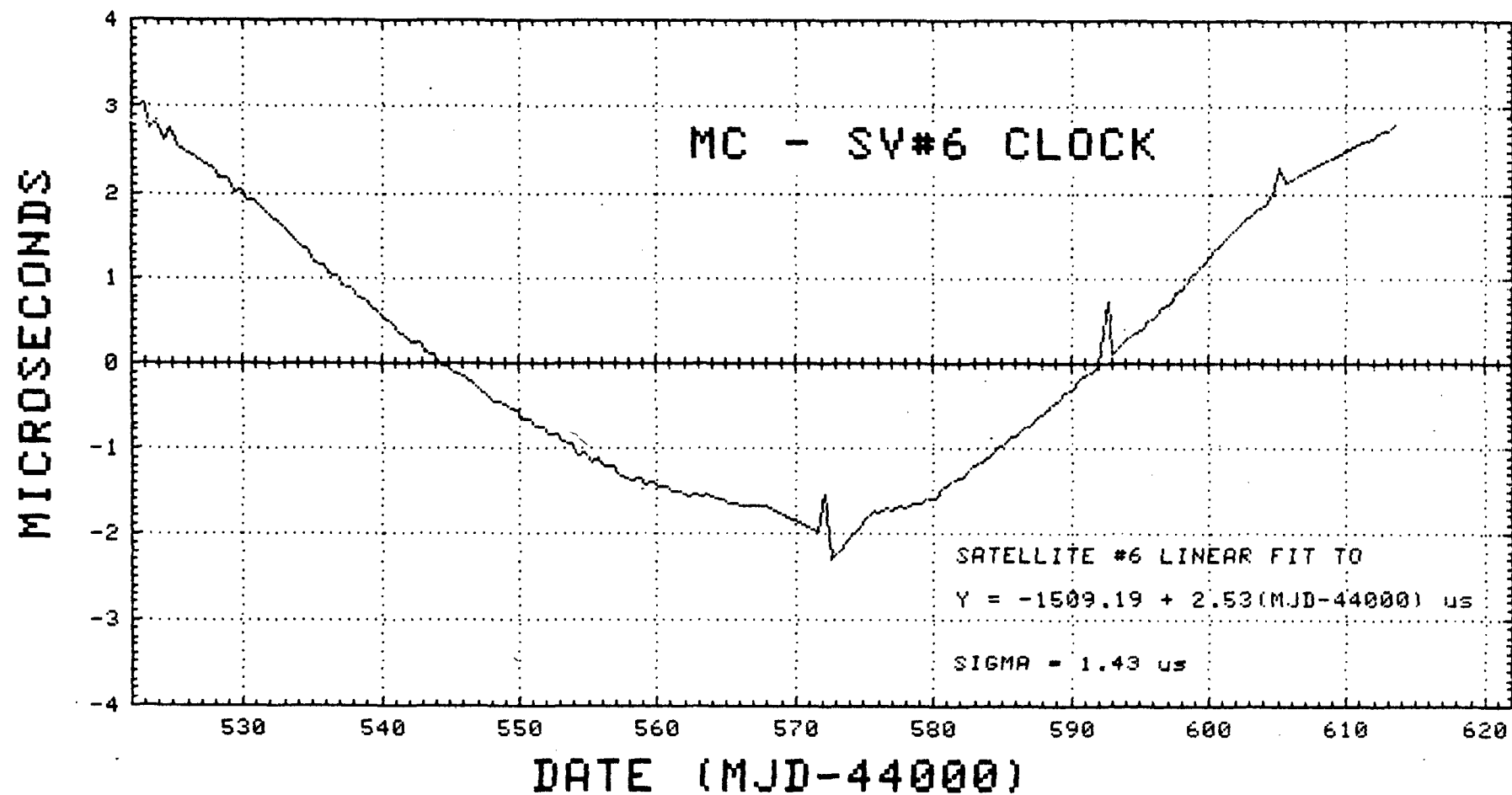


Figure 11. USNO MC - GPS SV#6 Clock Linear Fit and Residuals

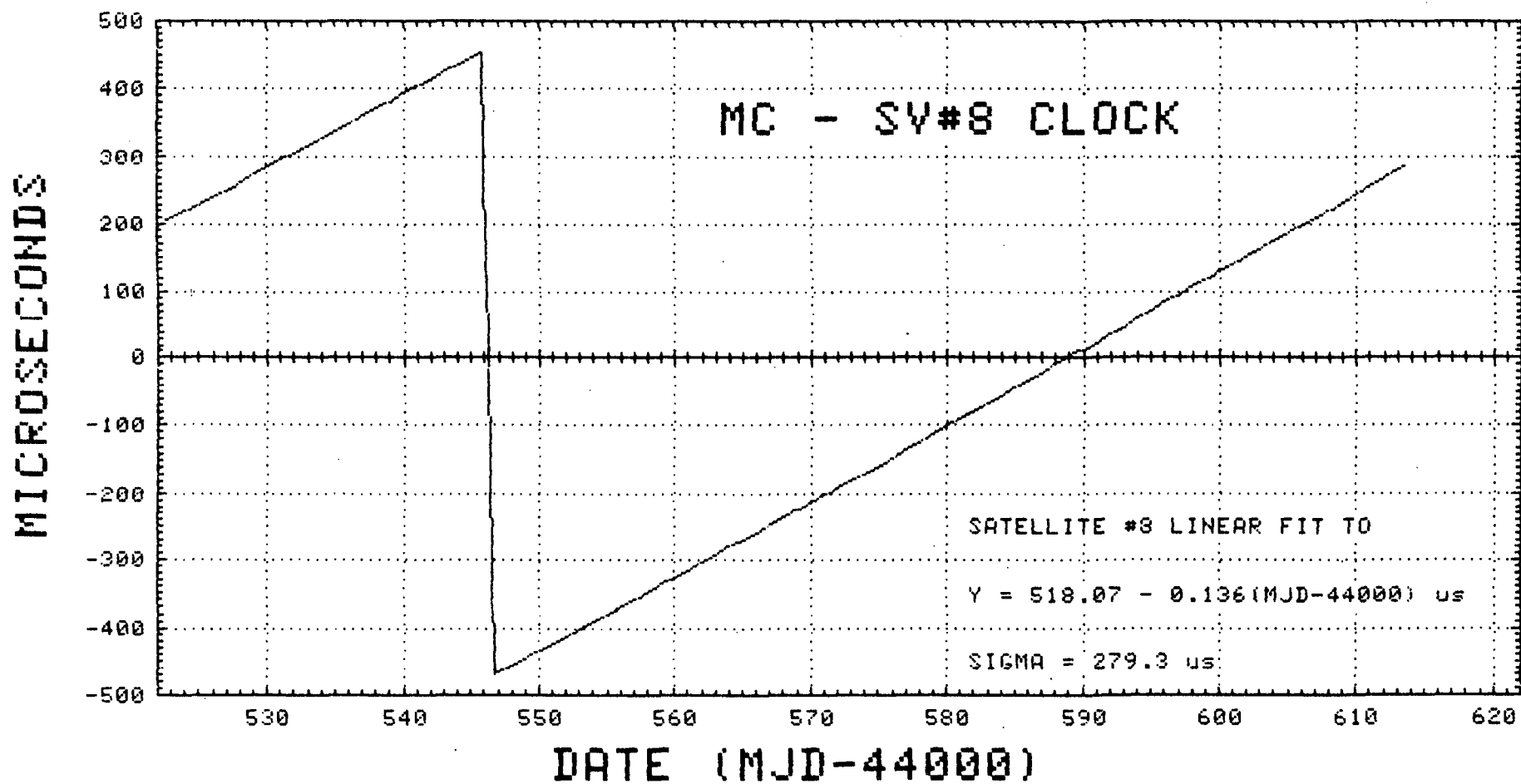


Figure 12. USNO MC - GPS SV#8 Clock Linear Fit and Residuals

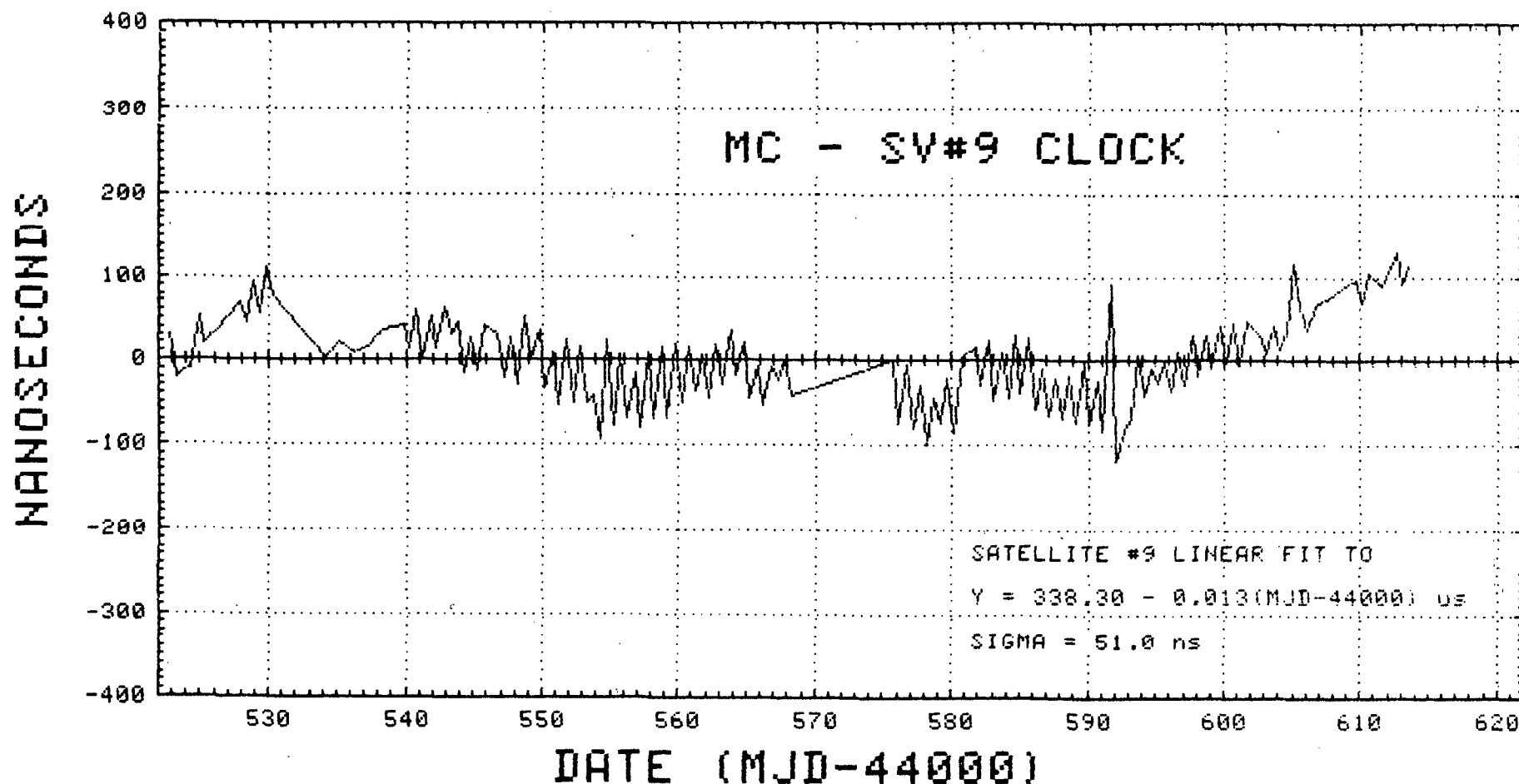


Figure 13. USNO MC - GPS SV#9 Clock Linear Fit and Residuals

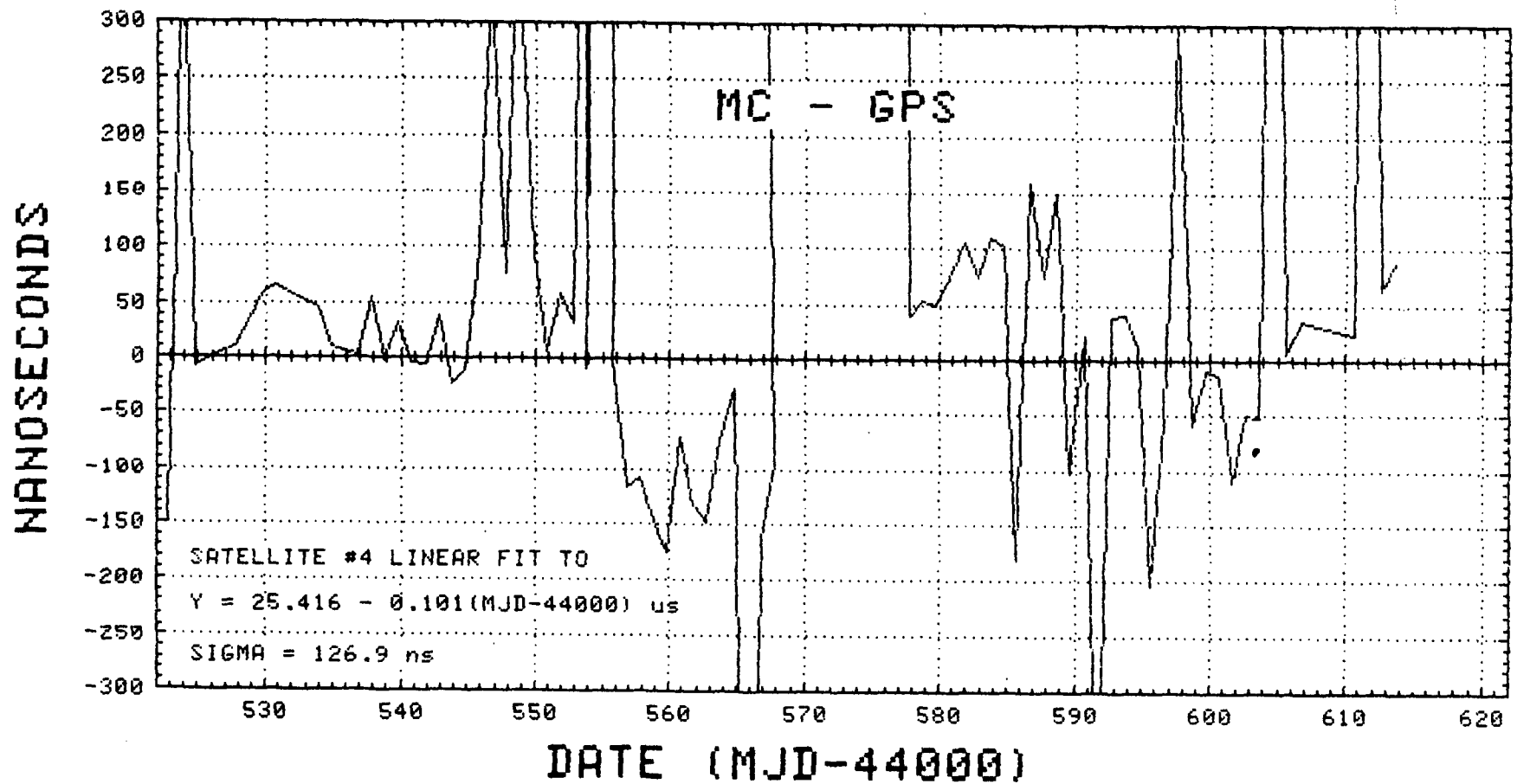


Figure 14. USNO MC - GPS Linear Fit and Residuals for SV#4

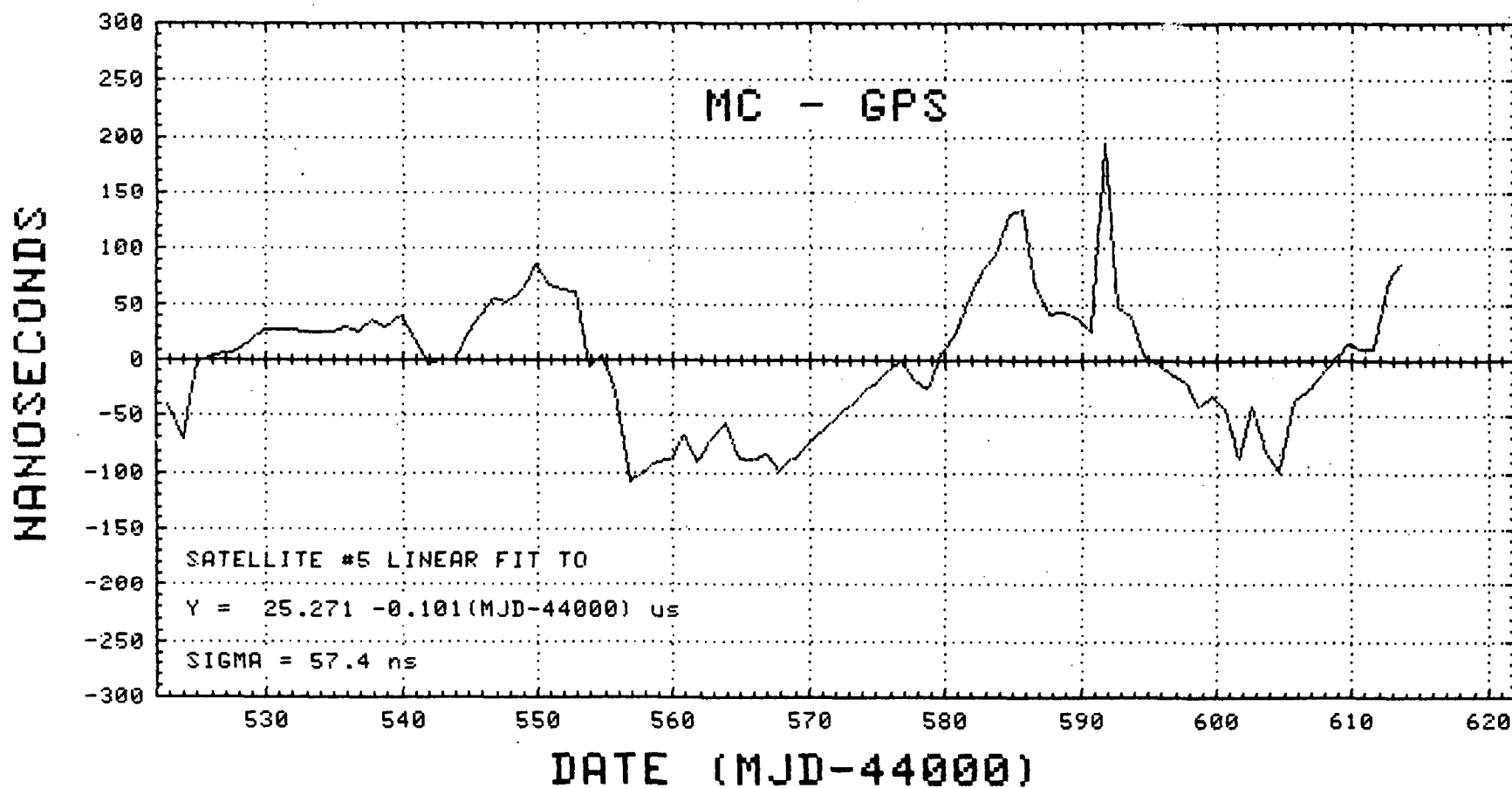


Figure 15. USNO MC - GPS Linear Fit and Residuals for SV#5

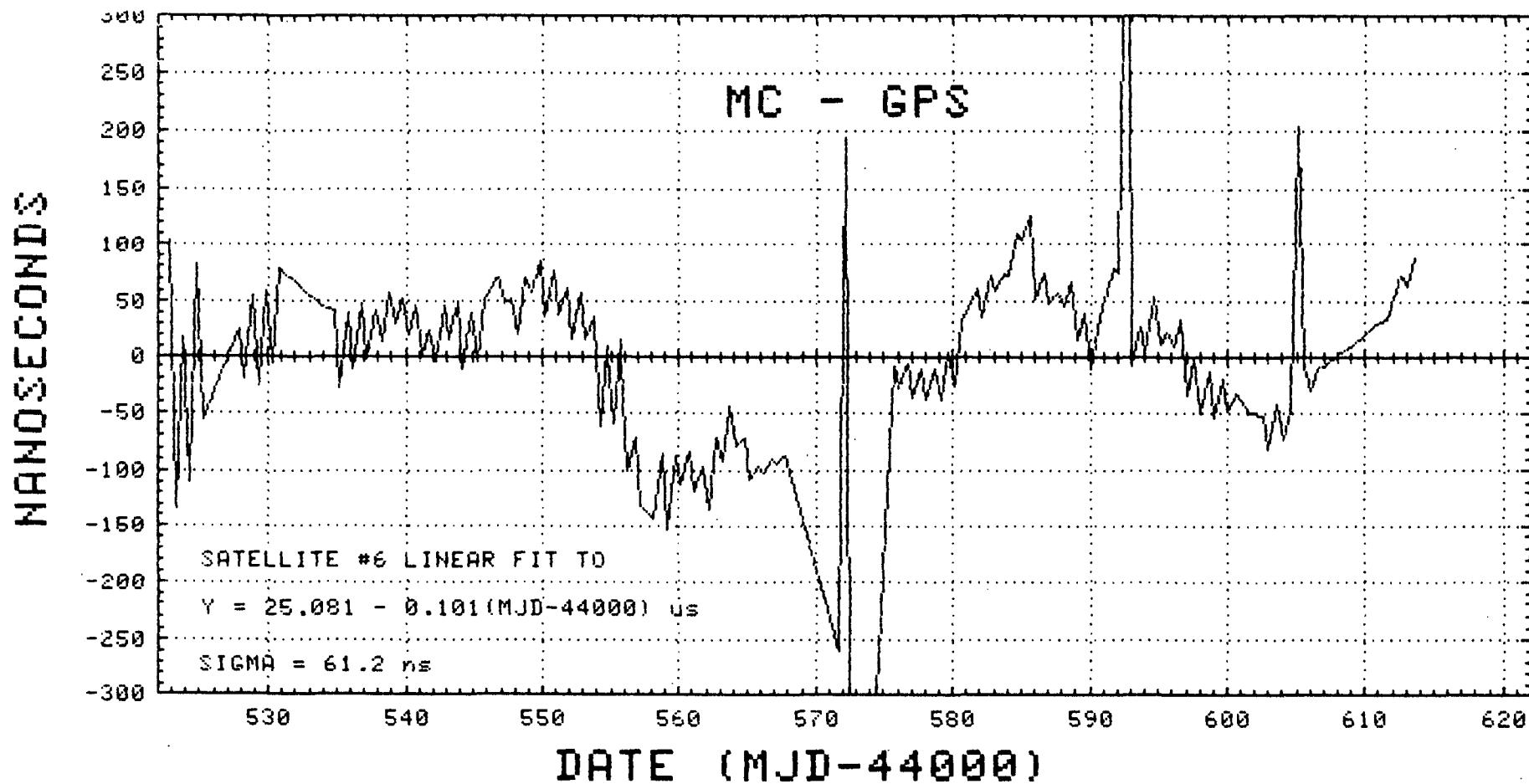


Figure 16. USNO MC - GPS Linear Fit and Residuals for SV#6

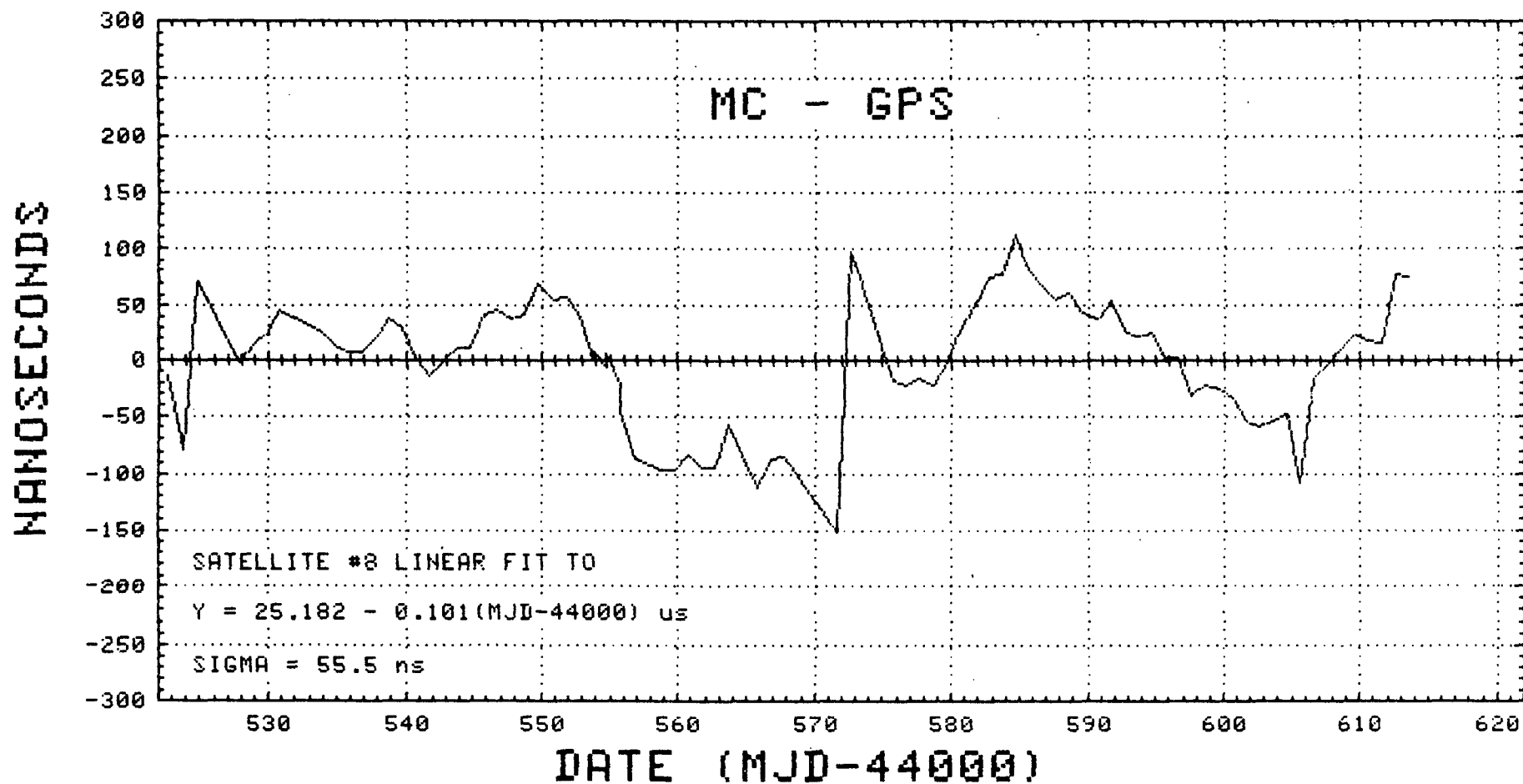


Figure 17. USNO MC - GPS Linear Fit and Residuals for SV#8

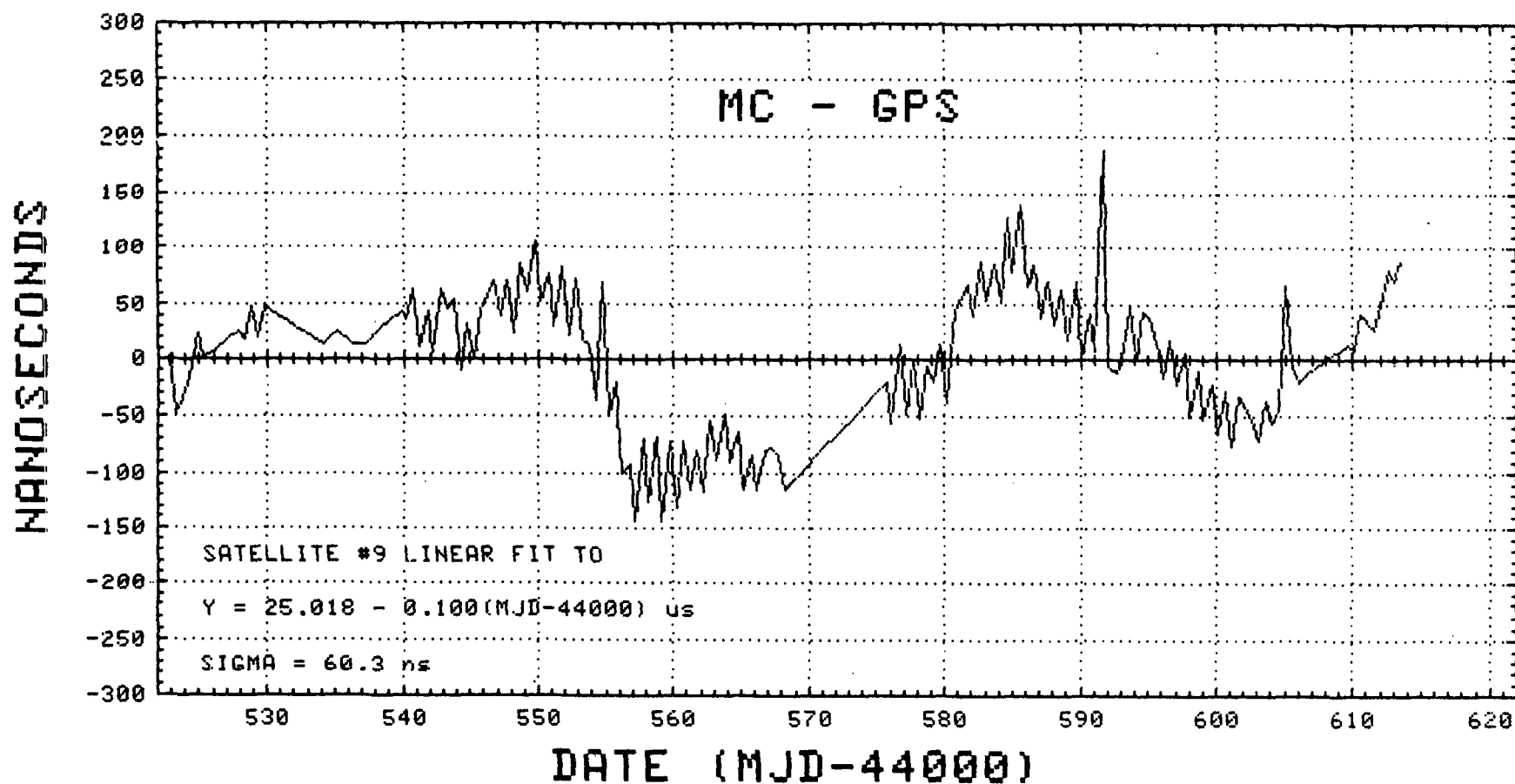


Figure 18. USNO MC - GPS Linear Fit and Residuals for SV#9

DATA COLL. START MJD 44613
DATA PROCESSED MJD:44616

WKDAY 5 FR DAY/UT: 9 23 46 11
(UT) 8:15 PM MON., 12 JAN., 1981

SV#	BEG. TRK DDD.ddd	BEGTRK D HHMMSS	TRKTIME SSSS	MC-GPS US	SLOPE PS/S	RMS NS	SAMP N	ELV	AZMT	D. AGE DHHMM	MC-SAT NS
6	613.990	5 234612	354	-36.553	10	19	60	23	59	01019	-34519
9	614.036	6 05148	258	-36.551	-79	13	44	40	84	0 626	346540
8	614.564	6 1332 0	606	-36.612	-7	13	102	77	320	0 2 7	733234
6	614.572	6 134330	816	-36.591	-8	14	137	53	320	0 219	-33003
4	614.583	6 135854	672	-36.896	-15	14	112	42	249	0 048	91072
5	614.601	6 142554	492	-36.622	-19	22	83	12	245	020 5	465293
6	614.991	6 234630	330	-36.613	50	16	56	23	57	712 2	-31905
7	615.036	0 05154	252	-36.651	18	14	43	40	81	0 641	346556
8	615.563	0 133118	642	-36.709	-12	11	108	77	327	0 2 7	744864
6	615.572	0 1344 0	786	-36.687	-2	14	131	55	318	0 219	-30374
4	615.583	0 1359 0	666	-36.738	-7	12	110	43	251	0 048	117036
9	615.592	0 1412 0	606	-36.701	-1	12	102	15	328	020 6	346580
5	615.600	0 142430	570	-36.692	-48	21	95	13	246	01953	478366
6	615.991	0 234630	330	-36.726	-24	16	56	23	55	012 2	-29282
9	616.036	1 05130	276	-36.762	-11	9	46	40	79	0 641	346575
8	616.563	1 133048	672	-36.795	-3	12	111	76	333	0 039	756512
6	616.572	1 134330	810	-36.779	-6	16	134	57	317	0 051	-27749
4	616.583	1 135854	666	-36.774	35	13	111	44	253	0 1 7	144822
9	616.592	1 141242	558	-36.787	-16	14	93	17	328	0 016	346605
5	616.600	1 142354	276	-36.805	-45	22	46	14	247	0 028	491453

Figure 19. USNO Automated Data Service Message for GPS

QUESTIONS AND ANSWERS

MR. VAN WECHEL:

I have three questions. The first is: Did you use the data block information on the ionospheric area to make your corrections, or did you get data externally?

MR. PUTKOVICH:

No, all the data that was taken here was with information derived from the satellite. The only thing that we put into the system is our position location and our time.

MR. VAN WECHEL:

The next question was: Did you have to do anything special as far as eliminating the one millisecond ambiguity, or is the signal-to-noise ratio in the bit detector enough to get rid of that?

MR. PUTKOVICH:

No, we didn't do anything.

MR. VAN WECHEL:

In other words that is automatic, you don't have a one millisecond ambiguity problem?

MR. PUTKOVICH:

I don't understand what the one millisecond ambiguity is that you are talking about.

MR. VAN WECHEL:

Well, the CA code repeats every millisecond and I was wondering if you could be one millisecond off or is that just a problem of the bit sync being reliable?

MR. PUTKOVICH:

We haven't answered that yet. I can't answer that question.

DR. WINKLER:

Each one millisecond is identified by the time code which comes down. So that is taken care of automatically.

MR. VAN WECHEL:

I thought there was a time code only every six seconds.

DR. WINKLER:

Yes, that is true too but you are counting the millisecond segments from that standard moment. Please identify yourself.

MR. VAN WECHEL:

Oh, I am sorry. I am Bob Van Wechel from Interstate.

The last question I had was relative to the intentional degradation of accessibility or denial of access I guess they call it. Do you think that it is likely in the future that a CA code will be degraded so you couldn't get 100 nanoseconds performance anymore?

MR. PUTKOVICH:

I really don't know. The whole GPS program seems to be in such -- I don't want to say disarray, but I don't know what is happening in the program.

One would hope that there is somebody around that knows what is happening, but I don't, and in that particular question I don't know what they will do. That has been kicked around the same way many of the other things have.

CHAIRMAN BUISSON:

Let me just say something about that. I think there is a paper tomorrow on GPS by people from the GPS office.

GPS is not an operational system yet, and I think that some of these points will be discussed in that paper.

Page Intentionally Left Blank

DESIGN CONSIDERATIONS FOR A LORAN-C TIMING RECEIVER
IN A HOSTILE SIGNAL TO NOISE ENVIRONMENT

J. W. Porter, J. R. Bowell, G. E. Price

AUSTRON, INC.
Austin, Texas 78758

ABSTRACT

The environment in which a Loran-C Timing Receiver may function effectively depends to a large extent on the techniques utilized to insure that interfering signals within the pass band of the unit are neutralized. This paper discusses the baseline performance of the present generation manually operated timing receivers and establishes the basic design considerations and necessary parameters for an automatic unit utilizing today's technology. Actual performance data is presented comparing the results obtained from a present generation timing receiver against a new generation, microprocessor controlled, automatic acquisition receiver. The achievements possible in a wide range of signal to noise situations are demonstrated.

INTRODUCTION

The effectiveness of a Loran-C Timing Receiver to operator in a hostile signal to noise environment, at present, uses many devices to apply as tools to aid the operator. These are tunable notch filter rejection, long time averaging coherent detection, envelope recognition schemes, time of coincidence procedures, time of arrival establishment, and special antenna orientation.

The success of making the time measurement, to the accuracy that is present in the Loran-C transmission, depends a great deal on the skill of the operator to employ the tools available as well as his understanding of the particular signal to noise environment in which the measurement must be made.

BASELINE PERFORMANCE

As an initial step to evaluate the performance of a new generation automatic acquisition timing receiver, it is necessary to formalize a baseline of performance. A current generation manual receiver was employed to establish a baseline for Loran-C signal reception in the Austin, Texas area. Key performance indicators of Loran-C reception that pertain to a receiving system are signal to noise ratio, time constant of averaging, equipment gain, and directivity of the antenna. The signal to noise environment depends directly on the transmitter power radiated, conditions prevalent over the path of propagation, and the local noise features. Fortunately,

Austin, Texas and in particular the plant site at Austron, Inc., offers an ideal low local noise situation. Therefore the signal to noise is mainly influenced by propagation path and transmitter power. See following chart for transmitters monitored. (Chart #1.)

The antenna system used for Loran-C reception employed alternately a 3 foot loop antenna and a 9 foot whip antenna. The loop antenna was considered as basic to eliminate the effects of local interference but since the site of observation did not experience much local interference, it was not a major contributor. The 9 foot whip antenna, because of its larger effective height, was very helpful in insuring that adequate signal level was delivered to the input of the receiver. The data collected indicated that measurements taken with the loop antenna were degraded some 19 dB from the signal level received using the whip antenna. These results reinforce our application concept that when local noise is not of paramount consideration, a whip antenna is more advantageous because of the greater effective height. A further consequence of antenna selection is the radiation pattern discrimination of the loop antenna. The loop's figure eight type of radiation pattern would discriminate against long range noise sources that occur at the null points but would also discriminate against a desirable signal arriving from that direction.

Two major operating parameters of the Loran-C receiver are its gain (front end attenuation) and effective time constant (bandwidth). The settings for receiver performance for a manual acquisition receiver normally would range from 5 dB attenuation in a low signal level

MONITORED LORAN-C STATIONS

MANUAL VS AUTOMATIC LORAN-C RECEIVER TECHNOLOGY

STATION	TRANSMITTED POWER	DISTANCE (Km)	RECEIVER LOCATIONS
MALONE	800kW	1215	AUSTIN
GRANGEVILLE	800kW	680	AUSTIN
RAYMONDVILLE	400kW	438	AUSTIN
CAROLINE BEACH	550kW	1915	AUSTIN
SENECA FALLS	800kW	2335	AUSTIN
NANTUCKET	275kW	2775	AUSTIN
DANA	400kW	1410	AUSTIN
BAUDETTE	520kW	2060	AUSTIN
FALLON	400kW	2168	AUSTIN
GEORGE	1.6mW	2665	AUSTIN
MIDDLETON	400kW	2460	AUSTIN
SEARCHLIGHT	500kW	1710	AUSTIN
CAPE RACE	1.8m	2129	WASH., DC (USNO)
CAPE RACE	1.8m	3135	PATRICK AFB, FL

Chart #1

performance for a manual acquisition receiver normally would range from 5dB attenuation in a low signal level situation to as much as 99dB in a strong Loran-C source environment such as in the near field of a radiating transmitter. The approximate setting for the averaging time constant in a manual receiver directly determines the effective bandwidth of performance. A longer period of averaging will allow the receiver to capture more energy coherent with the Loran-C source and reject sources that do not contribute to making the time measurement.

The equipment used to collect the baseline data is shown in Figure 1. The set up consists of both an automatic and manual Loran-C timing receiver; as well as all the ancillary equipment required to provide a comparison. Please also refer to Figure 2 for the geographical features of paths to Austin.

The propagation paths into Austin, Texas that were used to collect data ranged from a 2665 kilometers path with a radiated power of 1.6 megawatt over a stressful total land path to a 438 kilometer path from a nearby transmitter radiating 400kW. In addition, observations were made at receiving sites in Washington, D.C., and at Patrick AFB to get additional path-type observations over various conditions. The two extremes for long path measurements dealt with a path length of 2700 kilometers over mountain and rocky terrain. Total attenuation expected over this path is well over 100 dB. Please refer to Chart 2 for received signal levels and identification of propagation path properties.

LORAN-C CONDUCTIVITY CHART

STATION	TRANSMITTED POWER	DISTANCE (km)	CONDUCTIVITY/TYPE OF PATH	RECEIVED POWER μ WATT/METER
RAYMONDVILLE	400kW	438	GOOD/Sandy Loam Soil	1368.5
GRANGEVILLE	800kW	680	GOOD/Sandy Loam Soil	1697.0
MALONE	800kW	1215	GOOD/Sandy Loam Soil	354.6
JUPITER	275kW	1785	EXCELLENT/ 44% Seawater, 56% Sandy Loam	55.7
CAROLINE BEACH	550kW	1915	POOR/Mountains, Rocky Terrain	98.0
SENECA FALLS	800kW	2335	POOR/Mountains, Rocky Terrain	96.0
DANA	400kW	1410	FAIR/Hilly Terrain	134.6
BAUDETTE	520kW	2060	POOR/Rockey and Hilly Terrain	80.1
FALLON	400kW	2168	POOR/Mountains And Rocky Terrain, Salt Flat	56.9
GEORGE	1.6MW	2665	POOR/Mountains, Rocky Terrain	150.7
MIDDLETON	400kW	2460	POOR/Mountains, Rocky Terrain	44.1
SEARCHLIGHT	500kW	1710	POOR/Hills and Rocky Terrain	114.4
NANTUCKET	275kW	2775	POOR/Mountains, Rocky Terrain	24.0

Chart #2

A long total sea water path of 3153km was used to provide a test for receiver performance. A shorter path having a mixture of attenuation characteristics is the one from Cape Race, Newfoundland to Washington, D.C., 2129 km, and about half is over sea water. Attenuation over this type of path would be expected to be under 90 dB. Please refer to Figure 3 for geographical features. The resultant performance of these paths is shown in Chart 3.

The accuracy of the Loran-C timing measurement is traceable to the synchronization of the Loran-C transmitter to the U.S. Naval Observatory null second pulse and thus UTC can be derived from the received pulse. The determination of accuracy is best when a solid groundwave signal is present. Under these conditions, a local 1PPS can be developed to better than 1 microsecond with respect to UTC. As the distance from the transmitter to the observation point is increased, the potential for skywave contamination exists. As the distance becomes too large to sustain any groundwave measurement, the Loran-C skywave can be used to determine time but with degraded accuracy. The task of an operator of a Loran-C receiver is to maximize his potential to receive unambiguous groundwave and derive a 1PPS synchronization from it. By virtue of the pulse-type of transmission from Loran-C and the accurate synchronization of transmissions, it is practical to distinguish the groundwave propagated signal clearly from the skywave. The distance from the

PERFORMANCE OVER SEAWATER

○ Automatic Loran-C Receiver

STATION	RECEIVER LOCATION	DISTANCE (Km)	TRANSMITTED POWER	ESTIMATED RECEIVED POWER	GROUNDWAVE ACQUISITION TIME
CAPE RACE, NEWFOUNDLAND	PATRICK A.F.B., FLORIDA	3153.4	1.8MW	180 μ W	30 minutes
CAPE RACE, NEWFOUNDLAND	U.S.N.O. WASHINGTON, D.C.	2129.1	1.8MW	400 μ W	30 minutes

424

Chart #3

transmitter for unambiguous groundwave reception is 1000km. Skywave presence can become a significant influence at distances greater than 1500km. The technique for distinguishing groundwave reception has to do with the precise timing synchronization of the pulse transmission. Please review Figure 4 to obtain a better appreciation of the actual observations recorded using a path length over which significant skywave signals are present.

The operator of the manual Loran-C timing receiver must have a basic knowledge of electronic test equipment and an understanding of radio propagation. The test equipment required consists of a time interval counter, an oscilloscope and a strip chart recorder. The ancillary instruments required are a time-of-day clock, frequency source and possibly at long distances in noisy areas, a synchronous filter and/or notch filter. The operator must first obtain a coarse clock synchronization to within 10 milliseconds of UTC by a reference timing signal such as WWV or WWVB. The operator then sets the time-of-day clock to the reference, selects a Loran-C station and accomplishes acquisition. The most difficult step of Loran-C time recovery is to recognize and lock onto the correct tracking point. This is complicated by low signal to noise conditions.

The degree of operator skill required to operate the manual Loran-C timing receiver is inversely proportional to the received Loran-C signal strength, the amount of radio-frequency-interference (RFI), and the noise level. These factors also determine the amount and type of

ancillary instruments to achieve proper identification and tracking of the received pulse. The manual operator with minimum skill, within 1000km of the transmitter of interest and in a relative low noise area will achieve desired results in a short period of time with minimum ancillary instruments. A hostile radio-frequency environment, where the pulse strength is below that of the noise and/or RFI levels, requires the operator to be a very experienced user of Loran-C timing reception techniques and proficient in the use of various ancillary instruments. An automatic receiver that will provide the desired results in both environments reduces the operator skill level required, the operator time involved, and makes a significant decrease in the quantity and type of ancillary instruments required to achieve the acquisition and final tracking of the desired Loran-C pulse.

DESIGN GOALS

The first goal to address in the design of an automatic acquisition receiver is sensitivity. The receiver must adequately amplify a minimum usable signal level of .01 microvolts RMS to the level required by the acquisition and tracking hardware. An additional consideration is band pass filtering. The requirement is to exclude RF energy outside the required information bandwidth of the Loran-C signal. Since any band pass filter limits the faithful reproduction of the input signal while improving the noise performance, the design task is to select the proper bandwidth to optimize performance and obtain the best noise rejection. A

narrow BW for acquisition and a wider BW for precise phase tracking are needed and identified as objectives for the design activity.

Gain must be automatically adjustable over the entire dynamic range of operation. This allows automatic selection of the optimum level. In view of the wide variation of propagation conditions, normally observed in long path monitoring of Loran-C transmissions, a decision was made to use an automatic adjustment by a microprocessor system. This concept allows for optimum tracking of the incoming signal in dynamic signal to noise situations. An additional design feature is the use of numerical averaging of the Loran-C signal received to reduce the effects of non-coherent noise and CW interference. The goal for numerical processing of the signal is to improve performance over a manual receiver by 15 dB or more.

The operation of an automatic acquisition Loran-C timing receiver should not require special skills or training of the operator. Ancillary equipment should not be required other than to provide a IPPS coarse time source to within 10 ms of UTC for initial synchronization programmable operations from a remote location are desirable. A standard reference frequency to at least an accuracy of 1×10^{-8} is required.

A very important design goal of the automatic system is to identify all acquirable Loran-C signals at the selected transmission rate and to establish the most acquirable one. Design decisions were made to use correlation techniques with a narrow band pass filter

(4 kHz bandwidth) and hard limit the RF sampled at a period of 100 microseconds over one transmission frame. The process allows for all usable signals to be identified and graded as to their signal to noise property and represented by quantitative correlation numbers. Subsequent sampling at a wider bandwidth operates on the most desirable stations to identify the proper cycle upon which to make the measurement of coincidence with respect to the Loran-C transmissions.

Much care has been taken in the selection of the time constants that control the digital servo loops and which establish the effective bandwidth of the receiving system. The design approach here is to provide an adaptive time constant which is automatically controlled by the signal to noise ratio. Once the loop error is sufficiently small the receiver goes into a track mode. At this time, the servo system is ready for synchronization with a null second from the Loran-C transmitter.

Additional factors to be considered in the design of an automatic acquisition Loran-C receiver are size, weight, power, cost, reliability, and maintainability. The size selected was the smallest rack-mountable size consistent with proper attention to human factors; such as push button size, observable display and legend readability. The weight and power were minimized by use of large scale integrated circuits and a switching power supply. Reliability was enhanced through use of LSI parts and long lifetime components. The maintainability of the unit is insured by the use of plug in cards with universal bus structure where possible, built in test routines with

signature analysis, and flip open front panel for easy access to components. Replaceable software allows for future improvements and additions to the capabilities. Optional remote control capability through the IEEE-488 interface is available for installations requiring remote or fully automated operation.

MEASURED PARAMETERS

Chart #4 summarizes differences between automatic and manual receivers. The key features which permit successful operation in a hostile signal to noise environment are automatic gain control and adaptive signal to noise control.

The comparison test of the automatic Loran-C receiver with the manual one was conducted through the use of a relatively inexperienced University of Texas electrical engineering student who was hired specifically to operate the equipment. He had no previous operational experience with low frequency radio propagation or with precise time determination equipment using Loran-C transmission. The key items for making this comparison are acquisition time, operator attention, need to employ a synchronous filter, variation of measured delay, and a relative signal to noise indication. See Chart #5 for data summary.

The significance of operator attention and acquisition time for the different receivers may be too subtle to be clearly obvious. The major point in recording the time data here is to emphasize the lack of constant operator attention needed by the automatic receiver. In the case of

MANUAL vs AUTOMATIC PARAMETERS

RECEIVER SPECIFICATIONS

MANUAL

AUTOMATIC

SENSITIVITY

.01 μ VRMS

.01 μ VRMS

GAIN RANGE

0-99 dB

0-128 dB

AUTOMATIC GAIN CONTROL

No

Yes

BANDWIDTH

Acquisition: 5 kHz
Tracking: 20/50 kHz

4 kHz
40 kHz

AVERAGING TIME CONSTANT

Selectable

Adaptive

TRACKING POINT

Slewable-.1 μ s Res.

Automatic-8nsec

TIME OF COINCIDENCE SYNCHRONIZATION

Manual

Automatic

OPERATOR SKILL AND ATTENTION REQUIRED

High

Low

ANCILLARY EQUIPMENT REQUIRED

Oscilloscope

N/A

Time Interval Counter

N/A

Coarse Time Source (UTC)

Coarse Time Source (UTC)

1 MHz Freq. Ref.

1, 5, or 10 MHz Ref.

Strip Chart Recorder

N/A

Synchronous Filter

Included

. Time of Day Clock

Included

REMOTE CONTROL OPTION

None

IEEE-488

MANUAL vs AUTOMATIC LORAN-C DATA COLLECTION (WHIP ANTENNA)

STATION	SYSTEM	RECEIVED SIGNAL			MEASURED DELAYS μSEC	AUXILIARY EQUIPMENT	ACQUISITION TIME	OPERATOR ATTENTION
		RAW RF mVp-p	NOISE mVp-p	SIGNAL NOISE				
RAYMONDVILLE	Manual	820	70	21dB	28908.3	no	10 min.	10 min.
	Automatic	820	70	21dB	28907.8	no	5 min.	3 min.
GRANGEVILLE	Manual	700	70	20dB	15066.6	no	15 min.	5 min.
	Automatic	700	70	20dB	15065.8	no	8 min.	5 min.
MALONE	Manual	500	80	16dB	4064.7	no	17 min.	17 min.
	Automatic	500	80	16dB	4064.0	no	6 min.	4 min.
JUPITER	Manual	76.1	60	2dB	51112.7	no	20 min.	20 min.
	Automatic	76.1	60	2dB	51112.2	no	10 min.	5 min.
CARLOLINE BEACH	Manual	48.5	75	-3.8dB	42801.7	yes	50 min.	50 min.
	Automatic	48.5	75	-3.8dB	42801.4	no	20 min.	5 min.
DANA	Manual	210.4	80	8.4dB	4728.4	no	45 min.	45 min.
	Automatic	210.4	80	8.4dB	4727.5	no	15 min.	5 min.
SENECA FALLS	Manual	.271	80	-50dB	38942.7	yes	45 min.	45 min.
	Automatic	.271	80	-50dB	38942.9	no	20 min.	8 min.
BAUDETTE	Manual	.394	80	-46dB	54625.0	yes	1 hr. 30 min.	1 hr. 30 min.
	Automatic	.394	80	-46dB	54624.8	no	30 min.	15 min.
NANTUCKET	Manual	.211	75	-50dB	35383.9	yes	1 hr. 30 min.	1 hr. 30 min.
	Automatic	.211	75	-50dB	35383.2	no	45 min.	15 min.
GEORGE	Manual	.674	80	-42dB	22655.6	yes	1 hr. 45 min.	1 hr. 45 min.
	Automatic	.674	80	-42dB	22654.7	no	45 min.	15 min.
FALLON	Manual	.43	80	-45dB	7282.1	yes	2 hrs.	2 hrs.
	Automatic	.43	80	-45dB	7281.3	no	45 min.	15 min.
SEARCHLIGHT	Manual	52	80	-3.7dB	47640.7	yes	45 min.	45 min.
	Automatic	52	80	-3.7dB	47640.1	no	25 min.	10 min.
MIDDLETON	Manual	.199	80	-50dB	36280.1	yes	1 hr. 45 min.	1 hr. 45 min.
	Automatic	.199	80	-50dB	36279.2	no	40 min.	15 min.

NOTE: OPERATOR SKILL - Four hours of training on each receiver system just prior to start of test.

Chart #5

Seneca Falls, the time to acquire for an automatic receiver was 20 minutes as compared to 45 minutes for the manual receiver. On the other hand, the operator attention time was reduced from 45 minutes to 8 minutes.

The data collected from Raymondville, Texas indicated a very strong signal of 820 millivolts. Either technique required a minimum amount of acquisition time and similar operator attention spans. The worst case condition for time to acquire was noted in the signal from Fallon, Nevada which, at the peak cycle, measured only 430 microvolts, showing a signal difference of 66 dB. In this situation, the manual receiver required the use of the synchronous filter and took 2 hours of acquisition time and constant operator attention. The automatic receiver made the measurement in 45 minutes and took 15 minutes of operator attention. The best performance using the manual receiver unaided by the synchronous filter was monitoring Jupiter, Florida. The acquisition and operator attention required using the manual receiver was 20 minutes. The automatic receiver performed the task in 10 minutes and required only 5 minutes of operator attention.

The variation of measured delay between the automatic receiver and the manual one was never any greater than 0.9 microsecond in the range of data collected. The difference between the two measurements had a standard deviation of 0.22 microseconds and a mean value of 0.66 microseconds. In addition, it should be noted that the synchronous filter was necessary to complete the time measurement using the

manual receiver in eight out of the 13 transmitters monitored and that operator attention in these situations using the automatic receiver was never longer than 15 minutes.

SUMMARY AND CONCLUSIONS

The present manual system of precise time determination uses a number of ancillary items and operator assist devices to accomplish a time measurement to an accuracy of one microsecond. Please refer to Figure 5 for a view of the total manual system. The large variety of propagation conditions, noise environment and long range potential possible with Loran-C make an automatic microprocessor controlled receiver a very desirable instrument.

We have attempted to show clear evidence of reception success over a wide range of conditions using an automatic Loran-C timing receiver. Please see Figure 6 for a comparison of the relative complexity of automatic instrumentation versus manual.

A key factor demonstrated in the measurements is the reduction in operator attention. Demonstrated differences show a reduction of operator attention from 2 hours to 15 minutes for the worst case situation.

A good ground wave time measurement was made to better than one microsecond of UTC over a sea water path of length of 3153 kilometers from a 1.8 megawatt transmitter and over a land path of length of 2665 kilometers from a 1.6 megawatt transmitter using the automatic receiver.

One of the most serious operational complications that arises in establishing an accurate time using Loran-C is the ability to deal with the skywave presence at long ranges from the transmitter. The automatic receiver has successfully detected and made an accurate time measurement in the presence of skywave signals more than 20 dB greater than ground wave.



Figure #1

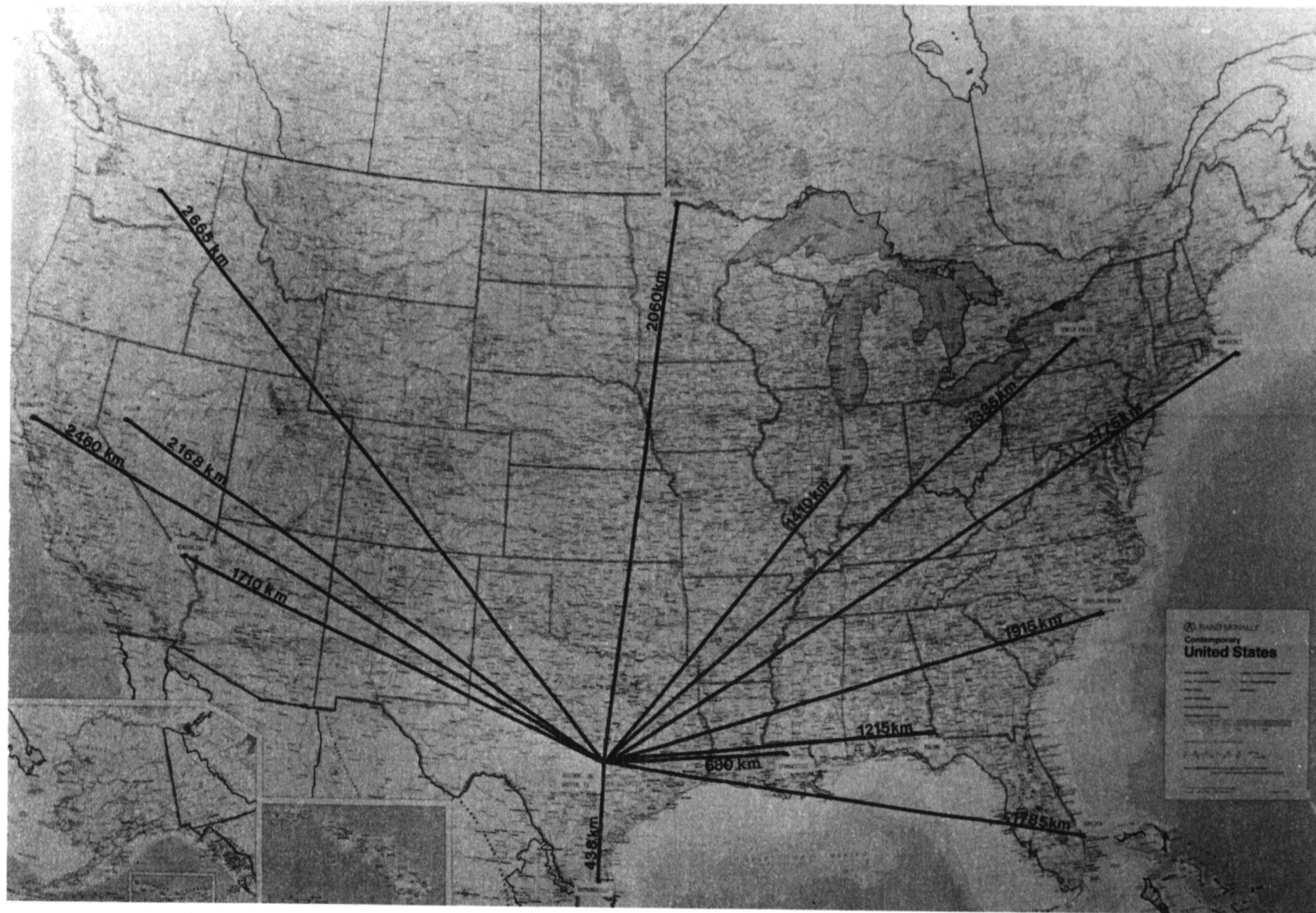
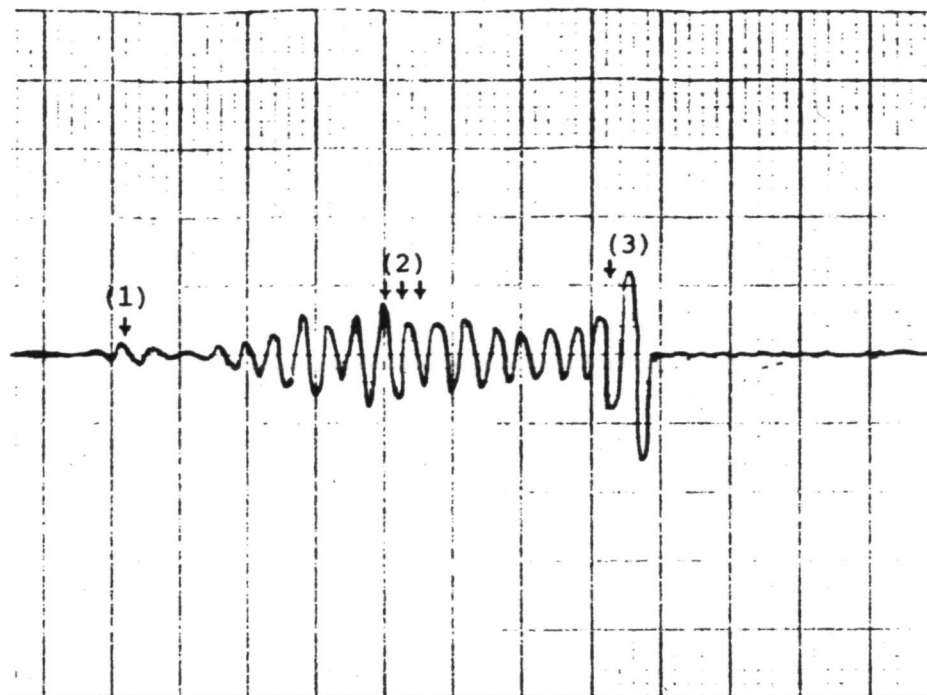


Figure #2



Figure #3



RECORDING OF RECEIVED LORAN-C SIGNAL

TRANSMITTER: George, Washington

TRANSMITTER POWER: 1.6 MW

PATH DISTANCE: 2665 KM

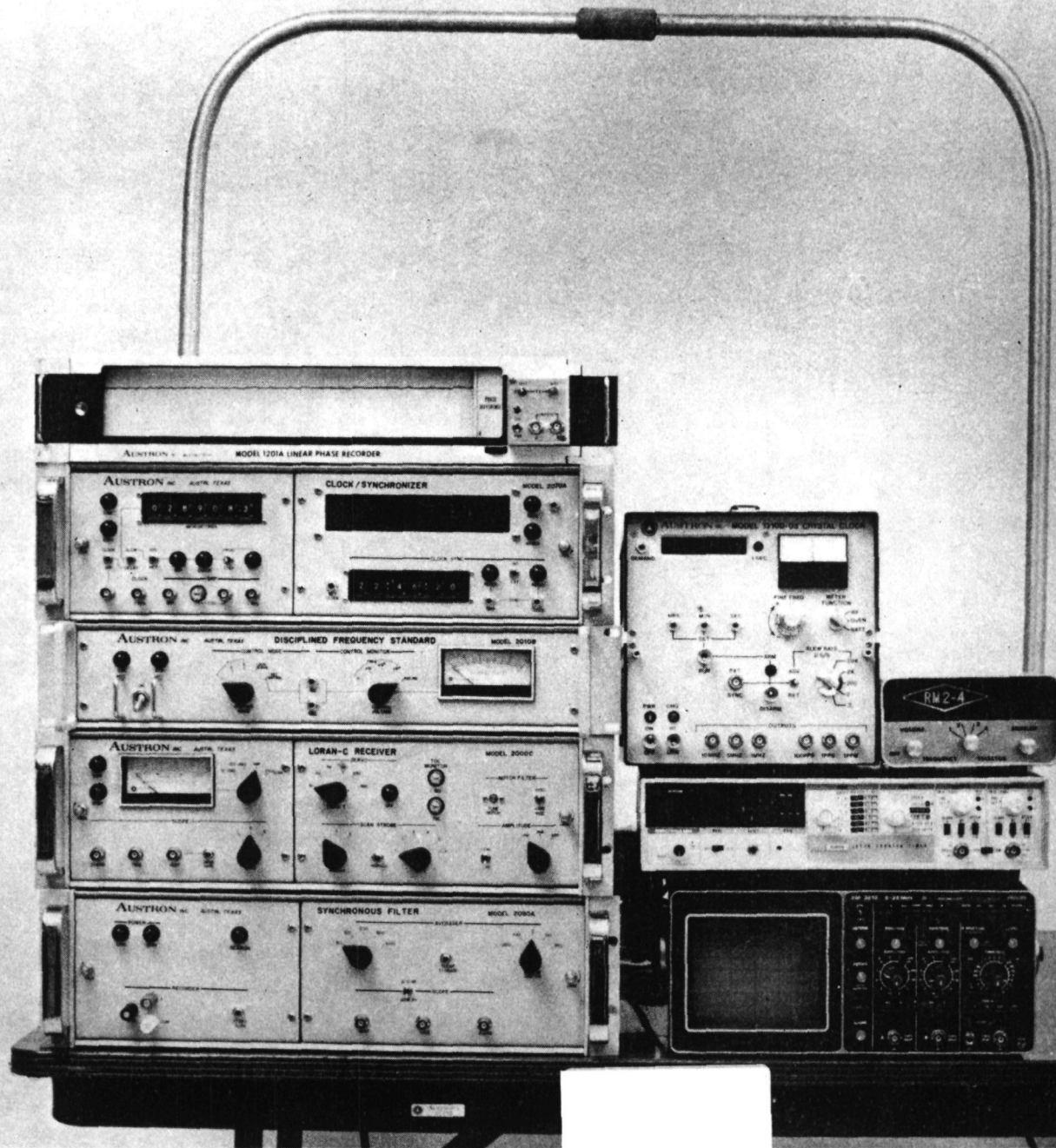
TIME OF RECORDING: 0300 Hours UTC
9:00 PM Local

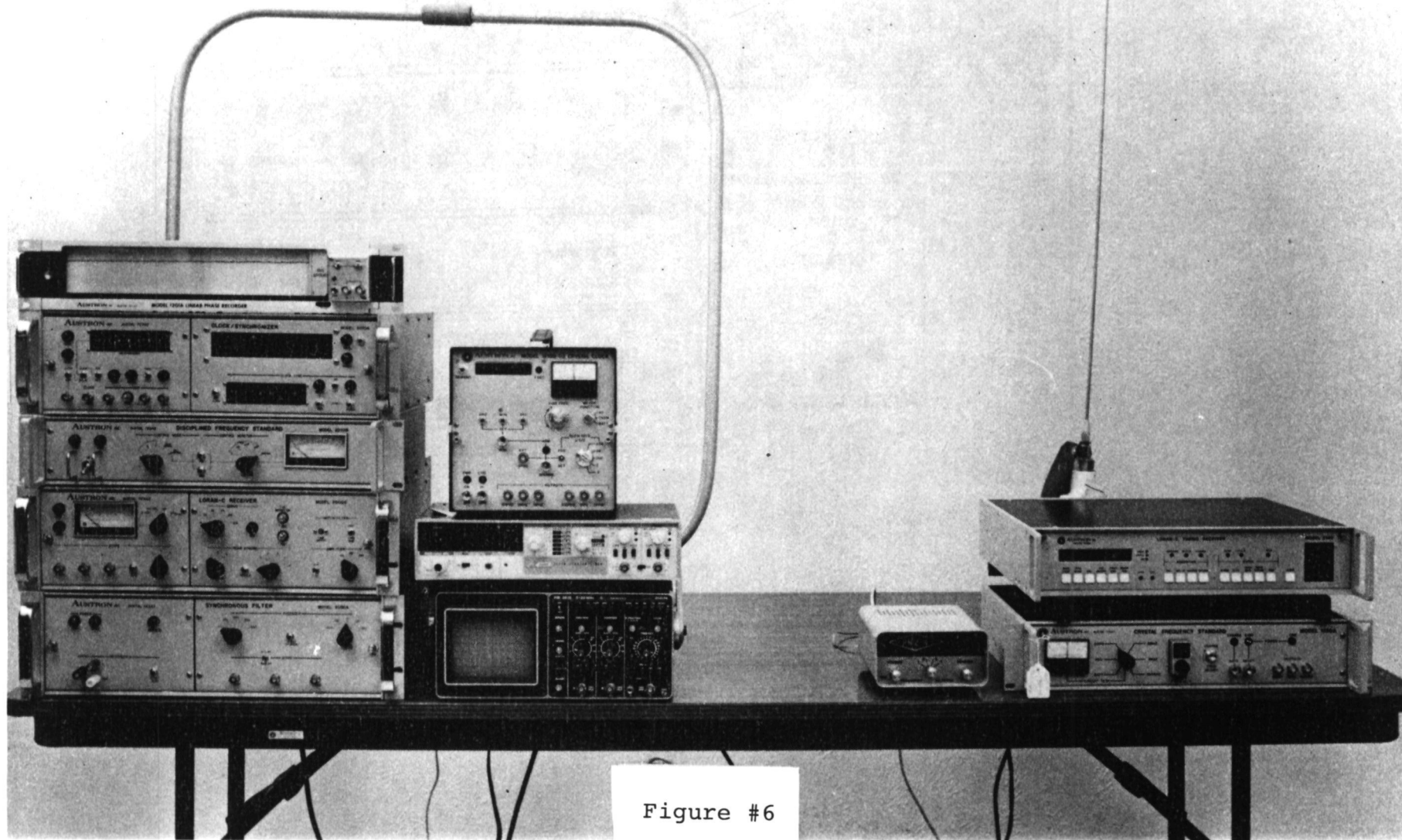
RECEIVER SITE: AUSTIN, TEXAS

TYPE RECEIVER SYSTEM: Manual Receiver with Ancillary
instruments.

NOTES: (1) Groundwave
(2) First Hop
(3) Second Hop

Figure #4





QUESTIONS AND ANSWERS

DR. WINKLER:

You mentioned that your receiver has the IEEE 488 bus capability. I just wonder whether you can increase that time that you have listed of eight minutes, or so by simply connecting it to a controller.

MR. PRICE:

That is right. If it is remotely programmable and can be controlled from a mobile location, you can replace the person sitting there watching it.

Yes?

MR. BANERGEE:

How is this table system going to improve the performance?

MR. PRICE:

I think your question is will this receiver improve the performance of capturing the ground wave in the face of the sky wave?

Is that the question?

MR. BANERGEE:

The question is that we can't receive the ground wave because we are out of the range.

MR. PRICE:

Well, how far out is your distance? Are you like 1,500 kilometers, are you like 2,000 kilometers?

MR. BANERGEE:

More than 1,500 kilometers.

MR. PRICE:

More than 1,500 kilometers?

MR. BANERGEE:

Much more than 1,500 kilometers.

MR. PRICE:

I think probably in that case you might just have too much attenuation to get a significant ground wave and you may need to make a sky wave measurement. What is your accuracy requirements for time?

MR. BANERGEE:

I would like to know how we could receive these with this type of receiver?

MR. PRICE:

Okay, if we were using a sky wave signal which we didn't talk about using a measurement because I would rather use a ground wave, we can probably get about 50 microseconds accuracy. UTC, within 50 microseconds, if you are using the ground wave you might expect to get within a microsecond.

MR. BANERJEE:

Thank you.

MR. JERRY PUNT, Interstate Electronics

What is the difference between the 15 minutes of operator time and the 8 minutes of operator time in this function?

MR. PRICE:

Jerry, either the signal-to-noise environment is tougher where you take a little longer period of time, or it might just be it has some trouble sorting out the sky wave from the ground wave because of the particular distance that you are from the transmitter.

We haven't really analyzed exactly why those figure differences are there, but I think that all of those factors bear on the amount of time a receiver takes to make a measurement.

MR. PUNT:

I understand the receiver time, but what about the operator time, what does the operator have to do that this requires 15 minutes in certain cases and only 8 minutes in another case?

MR. PRICE:

Sometimes he has to just wait for another TOC, because there is 15 minutes separation between TOC on some of the chains. Time of Coincidence is what the Naval Observatory calls it.

PROFESSOR LESCHIUTTA:

Just for my information I would like to know if using the IEEE bus, could we possibly give instruction to the receiver in order to study at one time the ground wave and at some other time the sky way; or perhaps the instruction to the receiver that always tries to get the first signal, the ground signal?

MR. PRICE:

My answer is that that is not normally the way we would expect it to be programmed. With the flexibility that we have we could work with you and hopefully we could make some arrangements to do some of those things.

Page Intentionally Left Blank

SHORT TURN-AROUND INTERCONTINENTAL CLOCK SYNCHRONIZATION USING
VERY-LONG-BASELINE INTERFEROMETRY--A PROGRESS REPORT*

G. A. Madrid, T. P. Yunck, R. B. Henderson

Jet Propulsion Laboratory
4800 Oak Grove Drive
Pasadena, CA 91109

ABSTRACT

During the past year we have been working to bring into regular operation a new VLBI system for making intercontinental clock comparisons (as well as UT1 and polar motion measurements) with a turn-around of a few days from the time of data taking. Earlier R&D VLBI systems have required several weeks to produce results. The new system, which is not yet complete, incorporates a number of refinements not available to us in earlier systems, such as dual frequency ionospheric delay cancellation and wider synthesized bandwidths with instrumental phase calibration. In this paper we report on the state of the new system and give examples of its current performance.

INTRODUCTION

In order to meet the increasingly higher accuracy demands of spacecraft navigation to the outer planets, the Deep Space Network (DSN) is in the process of implementing a short turnaround clock synchronization technique utilizing Very Long Baseline Interferometry (VLBI) [1-5]. This technique has already been demonstrated to be an effective method of measuring relative clock offsets and offset rates at intercontinental distances [6, 7]. A review of the utility of VLBI for timekeeping and geodesy was presented by Fanselow in 1977 [8]. The system being developed at JPL for this purpose differs from those used in previous demonstrations in that it is designed as an "operational" system to provide clock offsets as well as earth rotation and polar motion measurements on a weekly basis from approximately three hours of observing. This paper reports our progress in implementing this system and gives typical results.

* This paper represents one phase of research carried out at the Jet Propulsion Laboratory under NASA Contract NAS7-100.

OBJECTIVES

The development of a short turnaround clock monitoring system using VLBI has progressed from the prototype system reported in 1979 [9] to an early version of the operational system. This new system utilizes bandwidth synthesis [10], S- and X-band ionospheric delay cancellation, and instrumental phase calibration. The Deep Space Network intends to operate the three-station interferometer on a weekly basis. Each week's observations will include an east-west and a north-south baseline to permit the estimation of earth rotation and polar motion as well as clock synchronization parameters.

An average of 20 extragalactic radio sources will be observed during three hours each week. Based on the precision expected from a VLBI system [8] we expect to determine:

- o UT1 to ± 0.7 msec
- o Polar Motion (X and Y) to ± 0.3 m
- o Clock epoch offset to ± 10 nsec
- o Clock frequency offset to ± 3 parts in 10^{13}

From the collected weekly observations we will be able to measure long-term clock stability to a few parts in 10^{14} . Although we are currently performing our processing on the general purpose computer facilities at Caltech, we are in the process of converting the post-correlation software to a JPL computer system which will be dedicated specifically to VLBI. Once all the elements of the new system are in place we expect to be able to produce results within 48 hours of receipt of data. A simplified diagram of the system is shown in figure 1.

* DSS 14 at Goldstone, California; DSS 43 at Tidbinbilla, Australia, and DSS 63 at Madrid, Spain.

SYSTEM OVERVIEW

Our application is essentially a classical VLBI technique [10-13] wherein each pair of stations is independently scheduled to observe a specified set of extragalactic radio sources. The data from each observation are recorded at both S- and X-bands on eight time-multiplexed channels, each 250 KHz wide, spanning a 40 MHz receiver bandwidth. As soon as possible after the observing session the recorded data are transmitted over a 56K bit per second communication channel to JPL where they are recorded on magnetic tape for processing. In the final implementation, mass disk storage will be employed for recording.

In the present interim processing mode, prior to the activation of the new hardware correlator and dedicated processing computer, the magnetic tapes from both stations are read and correlated in software on an IBM 3032 computer. Then a Fast Fourier Transform (FFT) is performed on the correlation sums from each channel, with the resulting values of fringe frequency and amplitude inserted as a priori estimates to a more precise fringe-fitting processing which compensates more exactly for the troposphere and geometric delays. This produces estimates of fringe amplitude, frequency, phase and delay for each channel as well as synthesized delays for all channel pairs up to a spanned bandwidth of approximately 30 MHz. (The final system will have a 40 MHz spanned bandwidth.)

Additional software takes the estimates for each source and produces a maximum likelihood estimate for clock offset and clock rate over the observing time span. These values and BIH UT1 and polar motion values are then used as the a priori for the final step where the data from both baselines are brought together for simultaneous estimation of clock, UT1 and Polar Motion parameters.

Calibration of the data for instrumentation delays [14, 15] and charged particles takes place prior to the final estimation step. It is performed only if phase calibration tones have been injected into the RF amplifier so that the instrumental delays can be determined. Dual frequency cancellation of charged particle effects cannot be properly performed if the instrumental delays have not been removed.

DEVELOPMENT PLAN

An exposition of the development steps involved is presented to demonstrate the progress that has been made to date. Figure 2 illustrates the development steps, where we were in that progression last year, and where we are now. The transition from the prototype system includes an interval where the level of precision on measured clock offsets drops from 50 ns to 150 ns. We are currently in this interval as is evident by the results reported.

The main reason for this loss of precision is that we have transferred from a 4 Mb/s system to a 500 Kb/s system. By the time of our report last year [9], the 4 Mb/s system had been upgraded from 64-26 meter antenna pairs to all 64 meter pairs and had been provided a more precise source catalog. Those measures were to help compensate for the signal to noise loss in going to 500 Kb/s this year.

To obtain 10 ns clock offset accuracy with the 500 Kb/s system we must use bandwidth synthesis to span the 40 MHz receiver bandpass. This capability cannot be realized until instrumental and charged particle effects can be calibrated. Thus figure 2 places the dual frequency and instrumental delay capabilities as steps that must be implemented prior to our being able to enter the 10 ns precision regime. At this time the dual frequency capability is functional but is not being used pending the installation of instrumental delay calibrators. Consequently clock offsets are now measured by averaging the bit stream alignment delays obtained on four 250 KHz channels, which results in the reduced precision of approximately 150 ns.

Once the instrumental delay calibration is available, further enhancements will refine the instrument's precision and improve turnaround. The transferral of data processing to a dedicated system will introduce a hardware correlator unit and a computer system which can receive the data directly from the communication lines without recourse to the intermediate magnetic tapes now being produced. This will permit us to achieve 48 hour turnaround, possibly in the summer of 1982. After this, installation of water vapor radiometers and modification of the software to utilize these measurements will conclude our development.

CURRENT RESULTS AND COMMENTS

Typical results from our weekly observing sessions are shown in figures 3 and 4; the results are tabulated in tables 1 and 2. No useful trend analysis of the data can be performed because of frequent clock resets and frequency standard changes producing epoch jumps. Individual results, however, are useful for the purpose of measuring the relative offsets and offset rates at particular points in time.

The results are sparse because of scheduling conflicts with Voyager Project operations and the usual problems of breaking in a new system. The variability of the reference standards as well as our operational readiness have improved considerably since the interval reported and problems in this area are expected to diminish measurably as we enter into the latter phase of development. Our objective for next year's report will be the presentation of preliminary results involving the use of dual frequency charged particle cancellation and instrumental delay calibrations.

ACKNOWLEDGEMENTS

We wish to express our gratitude to all the men and women of the Deep Space Network who contributed to the data acquisition, data processing and system engineering aspects of this development. We are especially thankful for the help and cooperation received from Marshall Eubanks, Rick Shaffer, John LuValle, Pam Wolkins, Dolly Gibbs, and Jeannine Gunckel.

REFERENCES

1. B. F. Burke, "Long Baseline Interferometry," Phys. Today, Vol. 22, pp. 54-63, July 1969.
2. M. H. Cohen, "Introduction to Very-Long-Baseline Interferometry," Proc. IEEE, vol. 61, pp. 1192-1197, September 1973.
3. C. C. Counselman, III, "Very-Long-Baseline Interferometry Techniques Applied to Problems of Geodesy, Geophysics, Planetary Science, Astronomy, and General Relativity," Proc. IEEE, Vol. 61, pp. 1225-1230, September 1973.
4. J. B. Thomas, et al., "A Demonstration of an Independent-Station Radio Interferometry System with 4-CM Precision on a 16-KM Baseline," J. Geophys. Res., Vol. 81, pp. 995-1005, February 1976.
5. I. I. Shapiro, "Principles of Very-Long-Baseline Interferometry," in Proc. of the 9th GEOP Conference, Applications of Geodesy to Geodynamics, October 2-5, 1978, Dept. of Geodetic Science Rept. No. 280, The Ohio State University, Columbus, Ohio, pp. 29-33.
6. C. C. Counselman, III et al., "VLBI Clock Synchronization," Proc. IEEE, Vol. 65, pp. 1622-1623, November 1977.
7. T. A. Clark et al., "Synchronization of Clocks by Very-Long-Baseline Interferometry," IEEE Trans. Instr. Meas., Vol. IM-28, pp. 184-187, September 1979.
8. J. L. Fanelow, "VLBI and Its Current Application within the Solar System," Proceedings of the Ninth Annual Precise Time and Time Interval Applications and Planning Meeting, Goddard Space Flight Center, Greenbelt Maryland, November 29-December 1, 1977.
9. T. P. Yunck and G. A. Madrid, "Early Results from a Prototype VLBI Clock Monitoring System," Proceedings of the 11th Annual Precise Time and Time Interval Applications and Planning Meeting, Goddard Space Flight Center, Greenbelt, Maryland, November 27-29, 1979.
10. A. E. E. Rogers, "Very-Long-Baseline Interferometry with Large Effective Bandwidth for Phase-Delay Measurements," Radio Sci., Vol. 5, pp. 1239-1248, October 1970.

11. J. B. Thomas, "An Analysis of Long Baseline Radio Interferometry," in The Deep Space Network Progress Report, Technical Report 32-1526, Vol. VIII, p. 37, Jet Propulsion Laboratory, Pasadena, California, February 1972.
12. J. B. Thomas, "An Analysis of Long Baseline Radio Interferometry, Part II," in The Deep Space Network Progress Report. Technical Report 32-1526, Vol. VIII, p. 29, Jet Propulsion Laboratory, Pasadena, California, May 1972.
13. J. B. Thomas, "An Analysis of Long Baseline Radio Interferometry, Part III," in The Deep Space Network Progress Report, Technical Report 32-1526, Vol. XVI, p. 47, Jet Propulsion Laboratory, Pasadena, California, August 15, 1973.
14. A. E. E. Rogers, "A Receiver Phase and Group Delay Calibration System for Use in Very-Long-Baseline Interferometry," NEROC Haystack Observatory, Westford, Massachusetts, Haystack Technical Note 1975-6, 1975.
15. J. B. Thomas, "The Tone Generator and Phase Calibration in VLBI Measurements," DSN Progress Report 42-44, pp. 63-74, January-February 1978.

TABLE 1

Block 1 Clock Offset Data for California-Australia Baseline
8 June 1980 - 23 October 1980

<u>Date</u>	<u>Epoch</u>	<u>Measured Offset, μ sec</u>	<u>Residual to Fit, ns</u>	<u>Square Root Allan Variance, $\times 10^{-13}$</u>
24 June	15.20404	45.72	251	
15 July	16.99444	47.30	381	
31 July	18.374500	47.28*	-	
24 Aug.	20.43114	52.06	131	1.6
				(BREAK)
30 Sept.	23.61826	-5.30*	-	-
16 Oct.	24.9983888	-5.42*	-	-

* not included in fit

TABLE 2

Block 1 Clock Offset Data for California-Spain Baseline
8 June 1980 - 23 October 1980

Date	Epoch	Measured Offset μ sec	Residual to Fit, ns	Square Root Allan Variance, $\times 10^{-13}$
7 June	13.68634	-3.82*	-	-
17 June	14.51530	-6.16	62	
14 July	16.90876	-7.84	-242	
19 July	17.35684	-7.78	74	
25 July	18.15724	-8.21	102	2.88
				(BREAK)
24 Aug.	20.41996	-4.88	25	
15 Sept.	22.32136	-4.45	-43	
17 Oct.	25.06342	-3.67	17	0.11
RMS = 108 ns				

* not included in fit.

CURRENT AND PLANNED IMPLEMENTATIONS

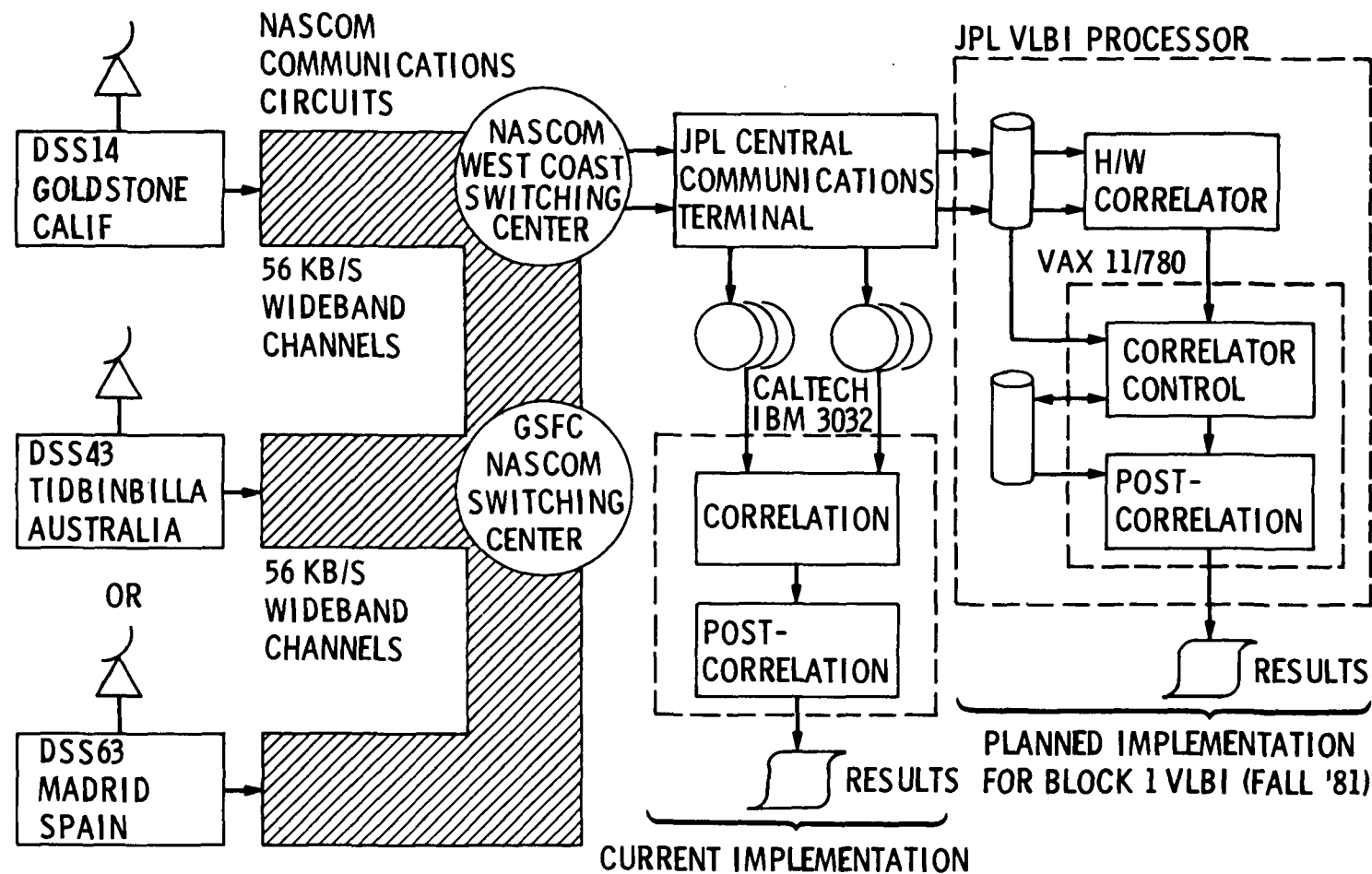


Figure 1. JPL-DSN Short Turnaround VLBI System Configuration Showing Current and Planned Implementations

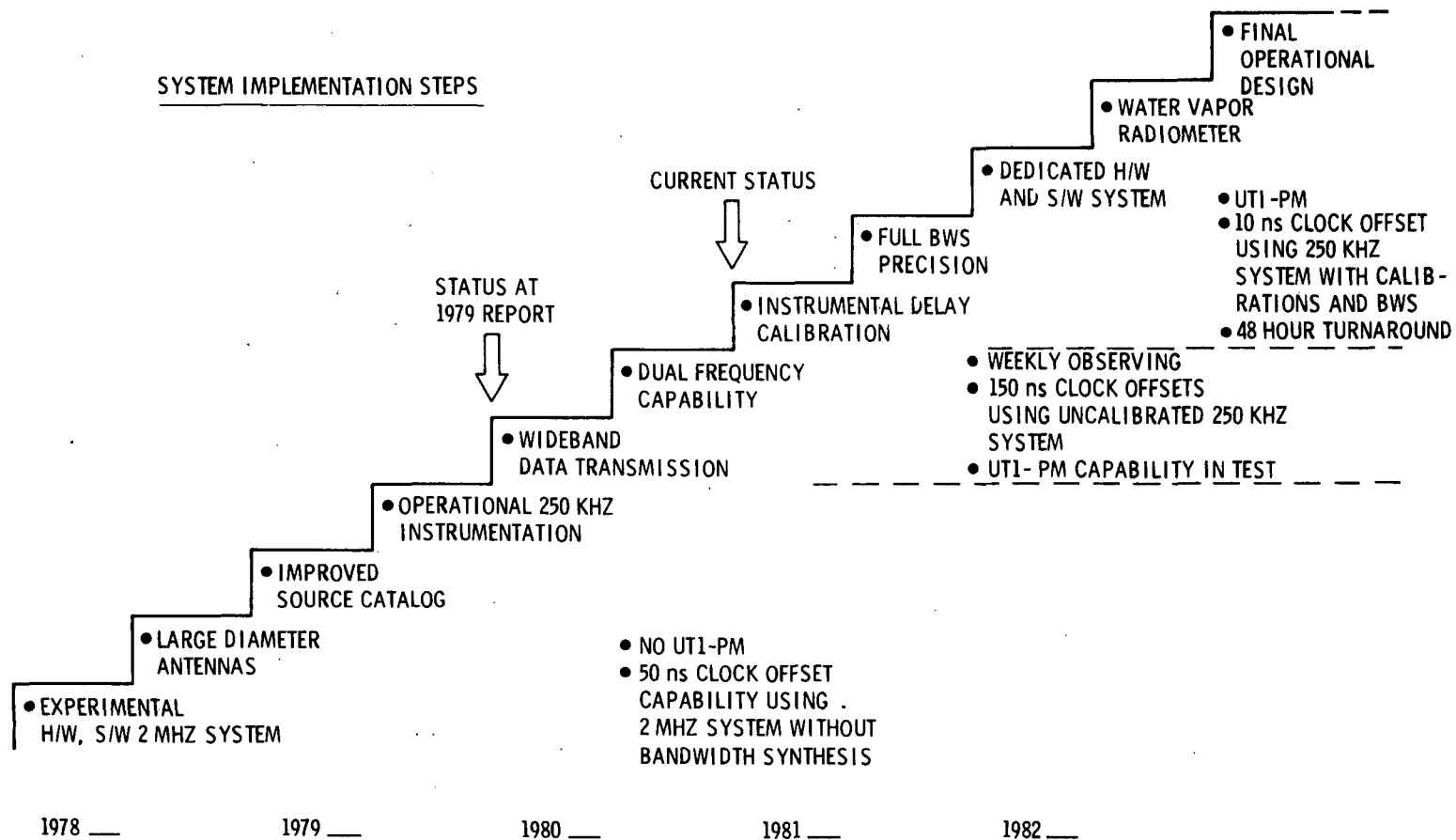


Figure 2. JPL-DSN Short Turnaround VLBI System Implementation Steps

• TYPICAL CALIFORNIA - SPAIN CLOCK MEASUREMENTS
WITH UNCALIBRATED 500 KB/S VLBI SYSTEM

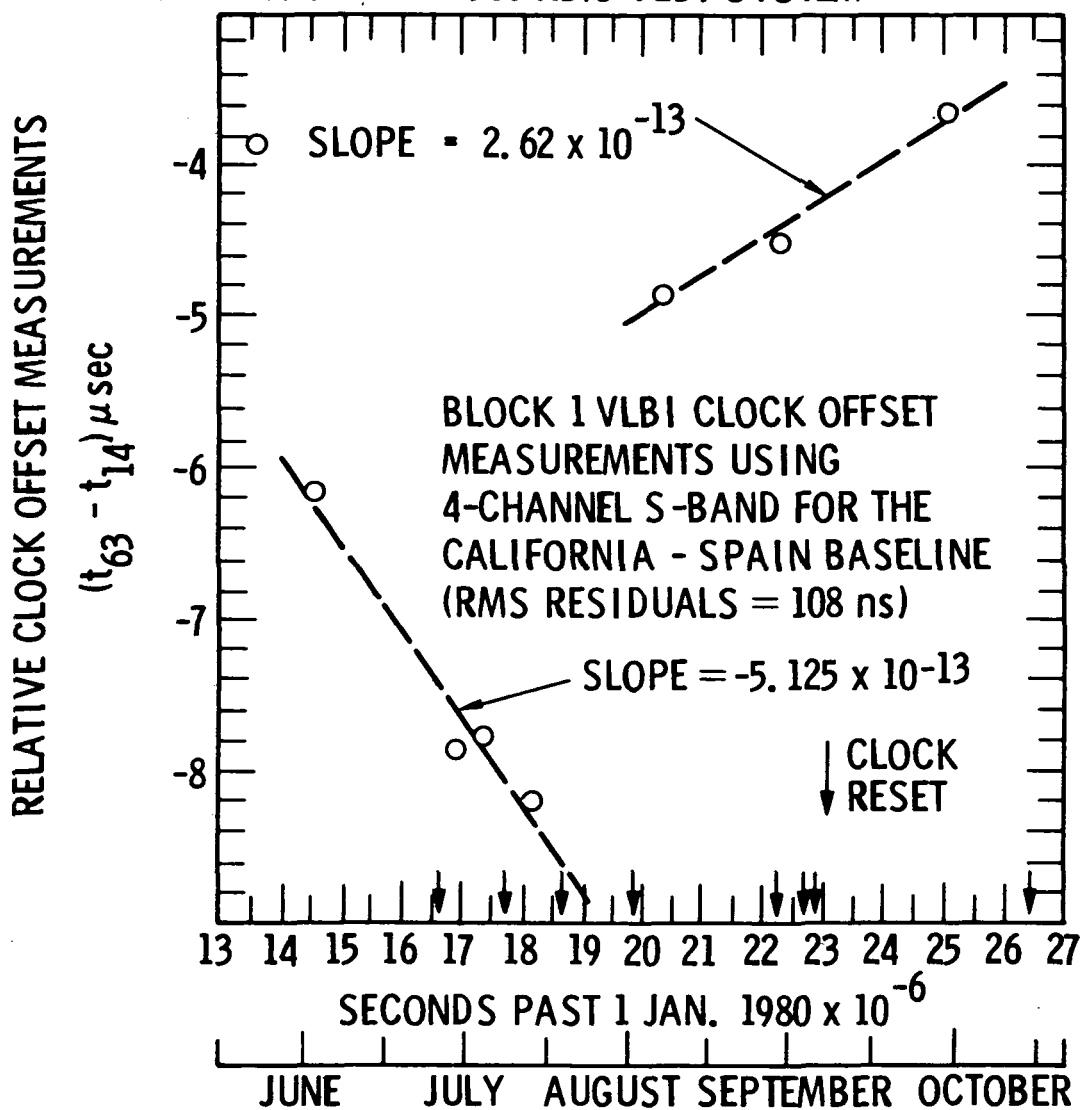


Figure 3. Typical VLBI Relative Clock Offset Results for the California-Spain Baseline Using the Uncalibrated 500 KB/s System

TYPICAL CALIFORNIA-AUSTRALIA CLOCK MEASUREMENTS
USING UNCALIBRATED 500 KB/S VLBI SYSTEM

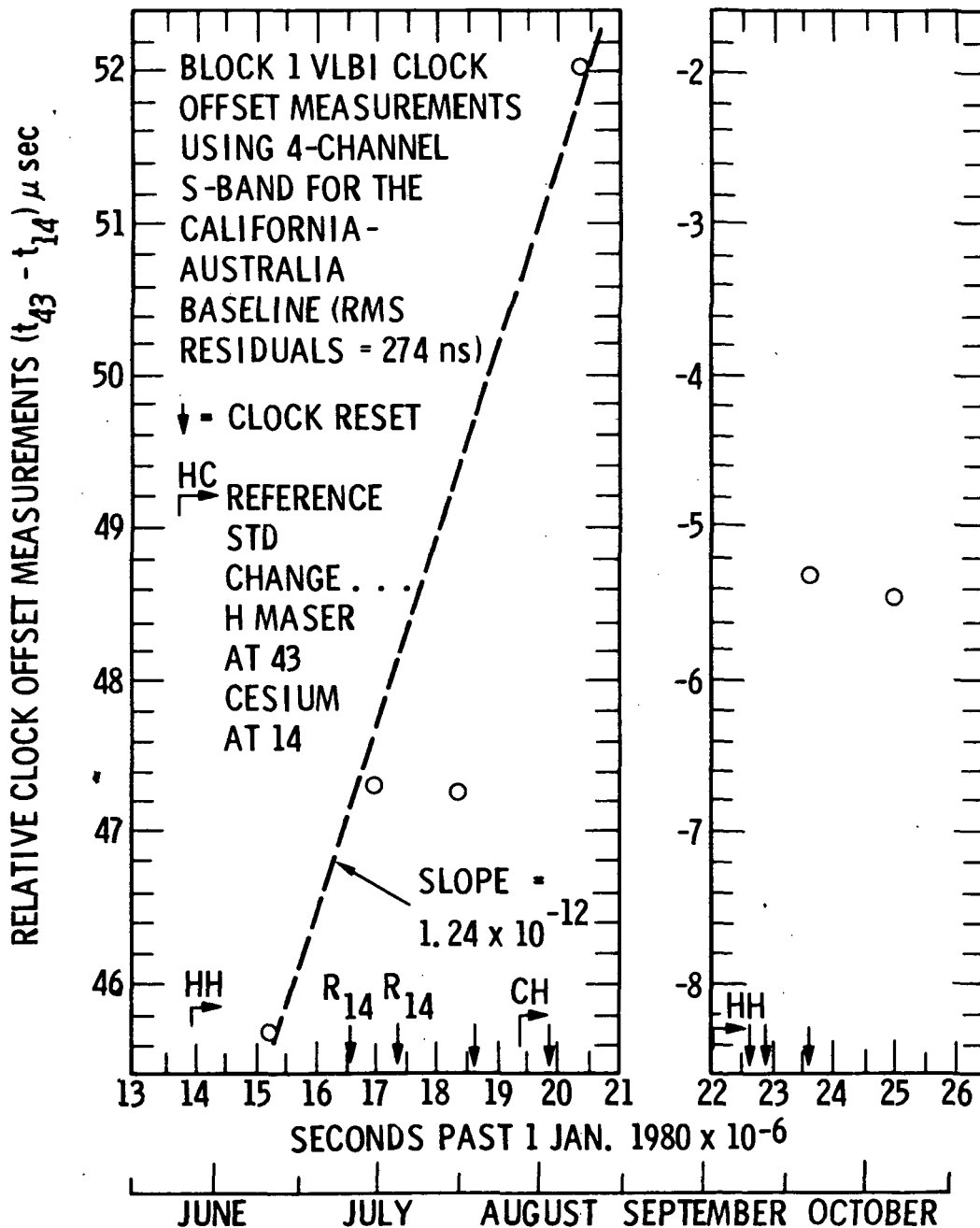


Figure 4. Typical VLBI Relative Clock Offset Results for the California-Australia Baseline Using the Uncalibrated 500 KB/s System

QUESTIONS AND ANSWERS

DR. WILLIAM WOODEN, DMA

Do you have any preliminary results for the polar motion studies that you talked about. You said that you had done some studies but you didn't give any numbers, how well do your results seem to compare with say the Naval Observatory results?

MR. MADRID:

Well, we do have some preliminary results but we haven't issued them because we have not fully understood their significance yet. We have compared them with BIH polar motion results and there seems to be a bias in our results which we cannot fully explain at this time. We are undergoing an analysis of our software and our modeling to understand what the nature of the problem is.

We do feel that it is probably due to a modeling problem which can, once we understand what the situation is, there is no reason to feel that we will not be in line with the BIH results.

MR. PAT FELL, Naval Surface Weapons Center

You use a bias to correct the linear model to model the clock synchronization between your two stations.

MR. MADRID:

Yes.

MR. FELL:

What are you observing? What time interval? What length of time do you apply that model load with?

MR. MADRID:

That was over a two month period at the longest.

MR. FELL:

Do you use one linear model over two months?

MR. MADRID:

That is right, essentially we have hydrogen masers most of the time, except for one case where we had a cesium at one station,

and we expected that most of our drifts would be of that order, although I think our reason for using a linear model is this; that we fit initially to a linear case and we find that if the linear does not produce the right residuals than we would consider using non-linear models to try to determine the functioning of the standards.

MR. DAVID ALLEN, National Bureau of Standards

In regard to the driving force during this experiment, do you have a stronger need to determine UT-1 than you do the clock synchronization? For example, if you could obtain synchronization via GPS an alternate route, perhaps, would you still need to do it to get UT-1, or could you obtain adequate accuracy in the results from the BIH for the UT-1 values for deep space tracking?

MR. MADRID:

Yes, I believe that there are alternate systems that we could use. In fact, we have been using BIH for our space navigation up to now. And, there are two driving factors here.

One of the reasons that we are in the UT-1 polar motion business is that we have seen at the laboratory that there is going to be a need for a change in the next 10 years. That BIH is still operating with optical instruments essentially, and that there is going to be a period of change and a need to review all of the instruments that are being used to obtain UT-1 polar motion and we want to cooperate and be part of that cooperative effort to determine if laser ranging or VLBI or what other technique is available. The best way to do this is to be producers of UT-1 polar motion and have an inter-comparison of different techniques that will be useful to the scientific community to determine what instruments, in the future, can be used for UT-1 polar motion determination.

Now, as far as clock sync, there are alternative systems and we have considered GPS as an alternative. However, the fact that we have the REA telescopes operable there and they are busy and there are crews there, makes it sort of a natural thing for us to try to achieve clock sync using these REA telescopes at times when they are not occupied in supporting a mission.

MR. ALLEN:

I understood that the demands on the telescope were such that if you wouldn't have to use them then that would be a definite advantage.

MR. MADRID:

Well, that all depends on the load. I think right around Saturn encounter and Jupiter encounter, that was the case, however, our loading in the future is going to be rather different, and I think we are looking toward the future in that regard in the sense that we are not going to be supporting as many space missions within the next few years and we are trying to use the equipment and the facilities that we have for other cooperative ventures including time sync in UT-1 polar motion.

Page Intentionally Left Blank

SESSION IV

FREQUENCY STANDARDS AND CLOCKS

**Dr. James Barnes, Chairman
National Bureau of Standards**

RECENT PROGRESS
IN THE
NASA-GODDARD SPACE FLIGHT CENTER
ATOMIC HYDROGEN STANDARDS PROGRAM

Victor S. Reinhardt
NASA-Goddard Space Flight Center
Greenbelt, Maryland

ABSTRACT

At NASA-Goddard Space Flight Center, and through associated contractors, a broad spectrum of work is being carried out to develop improved hydrogen maser frequency standards for field use, improved experimental hydrogen maser frequency standards, and improved frequency and time distribution and measurement systems for hydrogen maser use. The Applied Physics Laboratory of Johns Hopkins University under the technical direction of NASA-Goddard Space Flight Center, has been developing a new generation of field operational hydrogen maser frequency standard called the NASA Research or NR hydrogen maser. Recent data has shown the NR maser to have a frequency stability floor of 1×10^{-15} , a magnetic sensitivity of less than 3×10^{-14} per gauss, a pressure sensitivity of 5×10^{-15} per inch of mercury, and a temperature sensitivity of 4.5×10^{-14} per degree celsius with about a one day time constant. At Goddard Space Flight Center, a new low cost, high performance field operable hydrogen maser is being designed. The new design is presented. Novel and unique features are stressed. At Goddard Space Flight Center, extensive theoretical and experimental work has been performed on the use of digital phase locked loops to average the phases of several atomic standards. More recently, this work is being continued at the Applied Physics Laboratory. A brief presentation of the principles of these loops and recent experimental results on the performance of these loops is given.

INTRODUCTION

At NASA-Goddard Space Flight Center and through associated contractors, a broad spectrum of work is being carried out to develop improved hydrogen maser frequency standards for field use, improved experimental hydrogen maser frequency standards, and improved frequency and time distribution and measurement systems for hydrogen maser use. This paper will report on recent progress in these areas. The paper is broken into three more or less independent sections: recent results on the NR masers being built by the Applied Physics Laboratory (APL) of Johns Hopkins University, the development of a new low cost hydrogen maser at Goddard Space Flight Center (GSFC), and work on a low noise phase comparison system and digitally phase locked crystal oscillator called the Distribution and Measurement System.

NR MASERS

The Applied Physics Laboratory of Johns Hopkins University under the technical direction of NASA-Goddard Space Flight Center, has been developing a new generation of field operational hydrogen maser frequency standards called the NASA Research or NR hydrogen maser. The NR maser is shown in Figure 1. The maser is a completely self-contained field instrument, capable of running off 120 VAC or 28 VDC, and containing its own emergency battery supply capable of running the maser for about 12 hours. The maser also contains a microprocessor based diagnostic and control system which gives diagnostic information on more than 64 monitoring points in the maser and allows maser operation to be controlled remotely. Communication with the maser is via any one of three RS-232 I/O ports. A typical diagnostic output on one of these ports is shown in Figure 2.

The NR maser is designed to be easily field serviceable. It is shown opened for servicing in Figure 3. One servicing feature unique to this design is field serviceable vacuum pumps. There are two 60 l/s Vacion pumps in the unit which can be valved off so they can be replaced without letting the maser up to air. The whole replacement process takes about 2 hours.

The performance parameters of the NR masers measured to date are as follows:

Magnetic Sensitivity

1×10^{-14} to 3×10^{-14}

Pressure Sensitivity

5×10^{-15} per inch of mercury

Temperature Sensitivity

4.5×10^{-14} per degree celsius with about a one day time constant.

Stability

The fractional frequency stability of NR-1 versus NX-2 is shown in Figure 4. The stability statistic is the Allan deviate divided by the square root of 2 to normalize the data to a one maser error. The data shows the stability with and without the NR autotuner on. Notice that, in the NR masers, there is essentially no degradation in short term stability with autotuning.

Figure 5 shows the Allan deviate of NR-1 versus the Jet Propulsion Laboratory's (JPL) DSN-2. The data was taken by JPL. In this plot, the NR-1 vs DSN-2 data is not divided by the square root of two, but the DSN-2 stability is removed with the three corner hat method by using DSN-1 vs DSN-2 data taken simultaneously with the NR-1 vs DSN-2 data.

NEW MASER DEVELOPMENT

At Goddard Space Flight Center, a new low cost, high performance field operable hydrogen maser is being designed. A block diagram of what it will look like is shown in Figure 6. Our goal is to reduce the cost of producing

a hydrogen maser by \$100,000.00. We are attempting to achieve this cost reduction by using commercial electronics and packaging in the maser wherever possible.

The maser, hopefully, will also have improved long term stability over previous designs. We hope to achieve this by using the cavity and storage bulb design shown in Figure 7. The basis of the improved long term stability will be the improved mechanical stability achieved by fusing a quartz microwave cavity and quartz storage bulb into one piece. After fusing, the storage bulb will be coated with teflon and the outside of the cavity will be coated with silver or aluminum. The cavity will be coarse tuned by grinding it successively after measuring its frequency in vacuum.

DISTRIBUTION AND MEASUREMENT SYSTEM

At Goddard Space Flight Center, a low noise phase comparison system and frequency distribution system called the Distribution and Measurement System (DMS) is being developed. The purposes of this system are: to inter-compare the phases of 5 MHz supplied by several atomic frequency standards, to digitally phase lock a 5 MHz crystal oscillator to the average phase of these standards, and to distribute this phase locked 5 MHz in a low noise manner.

Figure 8 shows a simplified block diagram of the DMS. A digitally controlled crystal oscillator (DXCO) is used to provide the 5 MHz output of the DMS under normal conditions. A phase comparison system is used to monitor the difference in phase between the 5 MHz output of the DXCO with a resolution of 0.4 ps. This information is used by an LSI-11 microprocessor to phase lock the DXCO to the average phase of the atomic standards. In this phase lock mode, the frequency of the DXCO can be arbitrarily offset with respect to the average frequency of the atomic standards with a range of $\pm 1 \times 10^{-7}$ (fractional frequency). This effectively turns the DXCO into a low noise synthesizer.

In practice, the frequency resolution of this synthesizer is virtually infinite. The processor controls the DXCO frequency with a resolution of 8×10^{-13} per bit. But the phase lock loop allows the processor to change the frequency of the DXCO ten times a second so that the loop can adjust the phase of the DXCO in 0.08 ps steps. The 0.4 ps phase comparison system resolution is larger than this by a factor of 5, and so is the real limiting factor in the phase tracking loop. The system, thus, has a frequency tracking resolution of:

$$\frac{\delta f}{f} = \frac{0.4 \text{ ps}}{t}$$

where t is the averaging time in seconds.

The frequency offsetability of the phase lock loop is used to keep the DXCO output on time with UTC (Universal Coordinated Time) regardless of the frequencies of the input standards. An event clock monitors the difference in time between the local timing system lpps output driven by the DMS and UTC information provided via LORAN-C or some other time source. The proper frequency offset to keep this time difference zero is maintained either manually or in a secondary loop.

The DMS also performs error detection and monitoring functions. The health of the input standards, the DXCO, and other system elements are constantly monitored. If a standard fails, it is thrown out of the phase lock loop. Errors that will cause loop failure, including processor failure, cause the 5 MHz output to be switched from the DXCO to the first standard. A teletype and digitally controlled multichannel strip chart recorder constantly provides hard copy documentation of system operation. This information can also be sent to remote locations via several RS-232 interfaces in the DMS.

Control of the DMS is accomplished locally through the teletype and can be accomplished from remote locations via the RS-232 interfaces.

HARDWARE DESCRIPTION

A more detailed block diagram of the FCS is shown in Figure 9. The system contains the following hardware which performs the functions listed:

- A. Offset Crystal Oscillator (LO): Provides 4.999990 MHz to the Buffer/Mixer Section.
- B. Buffer/Mixers (B/M): Uses the 4.999990 MHz from the LO to down convert the 5 MHz inputs to 10 Hz beats. In the buffer/mixers, zero crossing detectors turn the low level signals from the mixers into TTL square waves.
- C. Multichannel Event Clock (CL): Records the epoch of the 10 Hz beats and 1 pps inputs to 200 ns. Because the B/M conserves phase angles in down converting the 5 MHz inputs to 10 Hz, the CL effectively measures the phases of the 5 MHz inputs relative to the LO with 0.4 ps resolution. When the processor takes the difference in epoch between any two 10 Hz channels, the phase of the LO is subtracted out.
- D. Interpolator (INT): Used in conjunction with CL to measure the epoch of the 1 pps inputs to 10 ns. Used to keep the timing system 1 pps on time with respect to UTC.
- E. Digitally Controlled Crystal Oscillator (DXCO): Provides the main 5 MHz output in normal operation. The output frequency is controlled by the processor with better than part in ten to the twelfth resolution.
- F. RF Switch (SW): Switches the main output to the 5 MHz input designated CS1 when the processor fails to send a check pulse once every 120 ms or when the DXCO output fails.
- G. RF Filter (FL): Removes glitches when SW switches the main output.

- H. Strip Chart Recorder (REC): A 16-channel, digitally controlled strip chart recorder which is used to provide a visual record of the phase and 1 pps data.
- I. RS232 Interfaces (RS232): 4 RS232 interfaces are provided to interface to the teletype and remote devices.
- J. Teletype (TTY): Controls and communicates with the microprocessor and provides an alphanumeric record of phase and 1 pps data.
- K. Microprocessor (UP): An LSI-11 microprocessor is used to perform system control functions.
- L. Buffer Amplifiers and X2 Multiplier: Provides 6-5 MHz and 2-10 MHz outputs for the main output.
- M. Multichannel A/D Converter (A/D): Monitors voltages in the atomic standards for error detection.
- N. TOC Output (TOC): Provides a pulse output and a 1 second TTL gate controlled by UP for providing a TOC pulse for setting up the timing system.
- O. CAMAC: CAMAC is an IEEE digital instrumentation standard used to house the digital portion of the DMS (CAMAC Crate), provide a data bus for communication between the UP and most digital subsystems (CAMAC data-way), and the module structure for digital subsystems (CAMAC modules).

Phase Comparison System

Before describing the theory of the phase comparison system, it is helpful to review some pertinent frequency standard theory. The output of a frequency standard can be described by:

$$V = A \sin [2 \pi f_0 + \phi(t)] \quad (1)$$

where f is its nominal or ideal frequency and $\phi(t)$ describes all the phase deviations from ideal behavior. One can show that if this signal source is used to drive a counter used as a clock, that at any instant, the error in this clock's reading is given by:

$$x(t) = \frac{\phi(t)}{2\pi f_0} \quad (2)$$

x is called the normalized phase error or clock reading error. For simplicity, in this document, x will be called the phase or phase error.

By taking the time derivative of ϕ , one obtains the instantaneous angular frequency offset from $2\pi f_0$:

$$\frac{d\phi}{dt} = \dot{\phi} = 2\pi \delta f(t).$$

Dividing this by $2\pi f_0$ yields the instantaneous fractional frequency error:

$$y = \frac{\delta f}{f_0} = \frac{\dot{\phi}}{2\pi f_0} = \frac{dx}{dt} = \dot{x}. \quad (3)$$

That is, the instantaneous fractional frequency offset, y , is the time derivative of the clock error, x . Averaging y over some time τ :

$$\bar{y}(t + \tau, t) = \frac{1}{\tau} \int_t^{t+\tau} y(t') dt', \quad (4)$$

yields the important relation:

$$\bar{y}(t + \tau, t) = \frac{x(t+\tau) - x(t)}{\tau}. \quad (5)$$

Now, within this framework, the phase comparison system can be described.

The phase comparison system is a generalization of the dual mixer phase comparison technique.¹ To understand the detailed operation of the phase comparison system, consider an input on channel i of the form:

$$V_i = A_i \sin (2 \pi f_0 t + \phi_i(t)),$$

and a signal from the local oscillator of the form:

$$V_L = A_L \sin (2 f_0 t + \phi_L(t)),$$

where $f_0 = 5$ MHz. Notice that all the phase deviations in these signals from that of an ideal 5 MHz oscillator have been put into ϕ_i and ϕ_L respectively (included in ϕ_L is the 10 Hz offset from 5 MHz). The mixer for channel i outputs the beat frequency between the local oscillator and the channel i input. Since the local oscillator is lower in frequency than all the channel i inputs, the i th mixer output is of the form:

$$V_M = A_M g(\phi_L(t) - \phi_i(t)),$$

where g is some sine-like function whose only important properties for this discussion are that:

$$g(m\pi) = 0,$$

and that the slope of g is positive for:

$$\phi_L - \phi_i = 2m\pi.$$

Zero crossing detectors in the buffer/mixers turn the function, g , into a square wave whose positive edge occurs at:

$$\phi_L(t_{ni}) - \phi_i(t_{ni}) = 2n\pi,$$

where the phases ϕ_L and ϕ_t have been defined to make $\phi_L - \phi_i$ zero at the time (epoch) of the first positive edge under consideration, t_{0i} . Using (2), this becomes:

$$x_L(t_{ni}) - x_i(t_{ni}) = \frac{n}{f_0}$$

Taking the difference between two channels, gives:

$$x_i(t_{ni}) - x_j(t_{mj}) = x_L(t_{ni}) - x_L(t_{mj}) - \frac{n-m}{f_0}$$

Using (5), for \bar{y}_L and \bar{y}_j , the fractional frequency offset of the LO and

CSj respectively, this becomes:

$$x_i(t_{ni}) - x_j(t_{mj}) + \frac{n-m}{f_0} = [\bar{y}_L(t_{ni}, t_{mj}) - \bar{y}_j(t_{ni}, t_{mj})] (t_{ni} - t_{mj}). \quad (6)$$

This is the equation we are after since it relates the phase difference between two inputs to the t_{ni} which are measured by the multichannel event clock.

To use (6), \bar{y}_L and \bar{y}_j must be known. In practice, some estimates of \bar{y}_L and \bar{y}_j are used. The error this will introduce is:

$$\delta x = \delta \bar{y} (t_{ni} - t_{mj}).$$

Typically $t_{ni} - t_{mj} \leq 100$ ms. If \bar{y} is measured to 10^{-12} , δx will be less than 10^{-13} s. So, in practice, since the LO is a low noise crystal oscillator whose stability from 1 s to 100 s is 1×10^{-12} , one can use any input whose accuracy is 10^{-12} to estimate \bar{y} and one can take up to 100 s or so to make the measurement and have an accuracy of 10^{-13} s for differential phase measurements. Since the noise floor of the LO is 10^{-12} , this also means that the system noise is 10^{-13} s or better if limited by the LO.

If the multichannel event clock has a resolution, R , the smallest phase change that can be measured is:

$$\delta x \approx \bar{y}_L R$$

For $\bar{y}_L = 2 \times 10^{-6}$ (10 Hz offset), and $R = 2 \times 10^{-7}$ s, $\delta x = 0.4$ ps.

Digital Phase Lock Loop

Consider first, locking the DXCO to a single reference input. Let y be the fractional frequency output of the DXCO. If the digital control has a sensitivity of S ($\delta f/f$ per bit) and the control register value is Y :

$$y = S Y + y_f,$$

where y_f describes the free running behavior of the DXCO. Let x_{ni} be the phase difference between the DXCO and the reference oscillator:

$$x_{ni} = x_0(t_{n0}) - x_i(t_{ni}).$$

Using (6):

$$x_{ni} = R (T_{n0} - T_{ni})(\bar{y}_L - \bar{y}_i),$$

where channel 0 is the DXCO channel, R is the resolution of the event clock, and T_{ni} is the time of the n^{th} beat zero crossing for channel i in bits. Since we are locking on only one reference, we can assume it is on frequency, that is, $\bar{y}_i = 0$.

A first order phase lock loop is given by the equation:

$$Y_n = - (B/S) x_{ni},$$

which for times long compared with the best period, τ_0 , is equivalent to:

$$\frac{dx}{dt} = -Bx + y_f.$$

This has the solution:

$$x = x_0 e^{-Bt} + y_f/B,$$

where B^{-1} is the time constant of the phase lock loop.

Because the DXCO is less noisy than a cesium frequency standard up to about a 100 s averaging time, B^{-1} should be about 100 s for use with cesium standards. This causes problems, however, due to y_f . The DXCO has a rated frequency drift of less than 10^{-10} per day or:

$$\frac{dy_f}{dt} \approx 10^{-15} \text{ s}^{-1}$$

Since this is a slow drift:

$$\frac{dx}{dt} \approx B^{-1} \frac{dy_f}{dt}$$

$$\frac{dx}{dt} \approx 10^{-13}$$

Thus, this drift rate in the free running DXCO would cause a frequency offset of 10^{-13} in the phase locked DXCO, an unacceptable error.

To overcome this problem, a second order loop is used. The DXCO register is incremented at each beat period, τ_0 , by:

$$\Delta Y_n = - (B/S) \Delta x_{n1} - (C\tau_0/S) x_{n1},$$

where Δa_n is defined as:

$$\Delta a_n \equiv a_n - a_{n-1}.$$

This is equivalent to:

$$\frac{\Delta Y_n}{\tau_0} = - (B/S) \frac{\Delta x_{ni}}{\tau_0} (C/S) x_{ni},$$

or for times long compared to τ_0 :

$$\frac{d^2 x}{dt^2} = - B \frac{dx}{dt} - Cx + D,$$

where D is the drift rate of the DXCO. This equation, in general, has the solution

$$x(t) = \frac{1}{\sqrt{B^2 - 4C}} [(\dot{x}(0) + r_1 x(0))e^{-r_1 t} + \dot{x}(0) + r_2 x(0))e^{-r_2 t}] + \frac{D}{C}, \quad (7a)$$

where

$$r_1 = B/2 + \frac{1}{2}\sqrt{B^2 - 4C},$$

$$r_2 = B/2 - \frac{1}{2}\sqrt{B^2 - 4C},$$

and $x(0)$ and $\dot{x}(0)$ are the phase and frequency at $t = 0$, respectively. For the phase lock loop to be stable.

$$B^2 \geq 4C.$$

At $B^2 = 4C$, we have critical damping, in which case the solution is:

$$x(t) = t (\dot{x}(0) + r_c x(0))e^{-r_c t} + x(0)e^{-r_c t} + \frac{D}{C} \quad (7b)$$

where

$$r_c = B/2 \text{ and } C = \frac{B^2}{4}.$$

In this case, a frequency drift will only produce a phase offset:

$$x = D/C$$

For critical damping, $r_c^{-1} = 100$ s, and $D = 10^{-10}$ /day, $x = 10$ ps. This is below the phase jitter of the average phase of even 10 cesium standards, and so, should not cause problems even if there are daily changes in the drift rate of the DXCO when used with cesium standards.

Consider, now a second order phase lock loop tracking the DXCO to the average phase of several atomic standards (CS_i) offset by an adjustable fractional frequency offset, y_0 . Again, the phase difference between the DXCO and CS_i is:

$$x_{ni} = R(T_{n0} - T_{ni})(\bar{y}_L - \bar{y}_i)$$

where again R is the resolution of the clock, and T_{ni} is the i^{th} channel beat zero crossing epoch. But in a practical phase lock loop, a problem in computing x_{ni} occurs. Since the frequency of the DXCO is not the same as that of CS_i , even if $y_0 = 0$, $T_{n0} - T_{ni}$ will diverge in time.

This means that an infinite memory would be required to store all the values of T_{ni} required to compute $T_{n0} - T_{ni}$ at any given instant. To avoid this problem, using (6) again, we can rewrite x_{ni} as:

$$x_{ni} = R(T_{n0} - T_{mi})(\bar{y}_L - \bar{y}_i) - \frac{n - m}{f_0}. \quad (8)$$

This allows us to use the closest T_{mi} to T_{n0} and not have to store past values. From (8), we can obtain the difference between the DXCO phase and the average phase of N cesiums.

$$x_n = \frac{1}{N} \sum_{i=1}^N \left[R(T_{n0} - T_{mi})(\bar{y}_L - \bar{y}_i) - \frac{n - m(i)}{f_0} \right] \quad (9)$$

where the fact that m is a function of i is explicitly indicated.

To lock the DXCO to the average phase of the cesiums with a fractional frequency offset y_0 , we can define a variable:

$$X_n = y_0 (T_{n0} - T_{00}) - \frac{x_n}{R}$$

where the units of X_n are in bits. Using (9) and the fact that the event clock is driven by 5 MHz from the DXCO, so that when the DXCO is locked:

$$R = \frac{1}{f_0},$$

we obtain:

$$X_n = \frac{1}{N} \sum_{i=1}^N [(T_{ni} - T_{n0})(\bar{y}_L - \bar{y}_i) + J_{ni}] \quad (10)$$

$$+ y_0 (T_{n0} - T_{00}),$$

where

$$J_{ni} = n - m(i).$$

With this variable, a second order loop is defined by:

$$\Delta Y_n = \left(\frac{B}{Sf_0}\right) \Delta X_n + \left(\frac{C\tau_0}{Sf_0}\right) X_n, \quad (11)$$

where, again, ΔY_n is the amount the DXCO control register is incremented. In practice, ΔY_n should be limited to:

$$-L \leq \Delta Y_n \leq L,$$

in order to keep the Y register from being changed drastically by a bad data point.

Because the CS_i have different frequencies, the J_{ni} and $y_0 (T_{n0} - T_{00})$ will be unbounded as n goes to infinity. This will cause computational problems. But the other terms in X_n are bounded and X_n itself is bounded because of the phase lock loop. Therefore:

$$K_n = \frac{1}{N} \sum_{i=1}^N J_{ni} + y_0 (T_{n0} - T_{00}),$$

is bounded as n goes to infinity. So to avoid computational problems, (10) can be rewritten as:

$$X_n = \frac{1}{N} \sum_{i=1}^N (T_{mi} - T_{n0})(\bar{y}_L - \bar{y}_i) + K_n, \quad (10a)$$

where K_n is computed incrementally by computing:

$$\Delta K_n = \frac{1}{N} \sum_{i=1}^N \Delta J_{ni} + y_0 \Delta T_{n0}. \quad (12)$$

The ΔJ_{ni} can be computed by two methods. The simplest method is to use the definition of the J_{ni} and increment ΔJ_{ni} for each DXCO zero crossing and decrement ΔJ_{ni} for each CS_i zero crossing. The disadvantages of this is that should a noise pulse cause a false T_{ni} or should a zero crossing be skipped, the DXCO will shift in phase by 200 ns/N.

To avoid such permanent phase shifts in the DXCO, another method for calculating the ΔJ_{ni} can be used. With the convention that T_{mi} is the first channel i event after T_{n0} occurs:

$$D T_{ni} = T_{mi} - T_{n0}$$

will range between zero and approximately τ_0 . If the \bar{y}_i and y_0 are not too large, DT_{ni} will change slowly with n until 0 or τ_0 is reached. Then, the value of DT_{ni} will suddenly change. Thus, to compute ΔJ_{ni} , one can use the algorithm:

$$\text{If: } D T_{ni} - D T_{n-1,i} > \frac{\tau_0}{2R}$$

$$\text{then: } \Delta J_{ni} = -1.$$

If: $D T_{ni} - D T_{n-1}, i < - \frac{T_0}{2R}$,

then: $\Delta J_{ni} = +1$.

Otherwise: $\Delta J_{ni} = 0$.

The advantage of this method is that if there is a bad J_{ni} or a skipped zero crossing, ΔJ_{ni} will switch between +1 and -1 or vice versa on successive calculations leaving no permanent phase shift.

\bar{y}_L and the \bar{y}_i can be calculated from the event clock data. Once the DXCO is locked, it defines local time, and by definition is at frequency f_0 . Therefore, \bar{y}_L and the \bar{y}_i can be estimated by:

$$\bar{y}_{nL} = \frac{\bar{f}_{nL} - f_0}{f_0} = \frac{m}{T_{n+m,0} - T_{n0}}, \quad (13)$$

and

$$\bar{y}_{nL} - \bar{y}_{ni} = \frac{\bar{f}_{nL} - \bar{f}_{ni}}{f_0} = \frac{m}{T_{n+m,i} - T_{ni}}. \quad (14)$$

Because the LO is a free running crystal oscillator, \bar{y}_L must be constantly updated to correct for crystal drift. Since only $\bar{y}_L - \bar{y}_i$ must be known, to calculate X_n , (14) is all that is needed for loop operation. To make the estimate error on the order of 10^{-12} or less, but often enough to correct for LO changes, m should be about 1000 (100 second averages). (13) is used to determine \bar{y}_i from (14) for diagnostic purposes.

DMS Performance

The performance of the phase comparison system and the 5 MHz distribution amplifiers used in the DMS have been presented elsewhere² so this data will not be presented here. Figures 10, 11, and 12 show the critically damped second order phase lock loop performance for 1 s, 10 s, 100 s time

constants respectively using two Hewlett Packard high performance cesium frequency standards as input standards. Besides showing the parameters discussed in the previous sections, the figures also show the 1 pps from one of the cesiums monitored by the clock. This shows whether the loop jumps cycles of 5 MHz. In the figures, X_e is X_n and VXCO is Y_n from the theory section. In the boxes are listed the top of scale (TOF) and bottom of scale (BOF) values for each variable. Notice that in the 10 s loop there is brunching of the VXCO (Y variable) noise distribution and that in the 100 s loop there is a sudden jump in X_e accompanied by a jump in VXCO representing about a 4×10^{-12} jump in the DXCO crystal. (Notice also that in the 100 s loop the 1 pps did not jump. This shows that the loop does not jump cycles even under a severe disturbance.) We think both of these phenomena are due to vibration of the AT cut crystals used in the DXCO (FTS-1000) by fans in the rack holding the DMS. Currently we are trying to cure this problem by vibrationally isolating the DXCO.

ACKNOWLEDGMENTS

The author would like to acknowledge Al Bates, Lauren Rueger, Charles M. Blackburn, Lee Stillman, Jerry Norton, Ed Mengel, Don Stover, Paul Underwood, Henry Smigocki, and Phil Zerkle of the Applied Physics Laboratory for the design and construction of the NR maser. The author would also like to acknowledge Al Kirk and Paul Kuhnle of the Jet Propulsion Laboratory for taking and allowing the author to publish the NR-1 vs DSN-2 stability data. For designing and building several of the digital modules in the DMS, the author would like to acknowledge Bob Bush and Harry Smith of Bendix Field Engineering Corporation. Finally, for writing the software used in the DMS and taking the data presented, the author would like to acknowledge Raymond Costelow of the Applied Physics Laboratory.

REFERENCES

1. D. W. Allan and H. Daams, "Picosecond Time Difference Measurement System," 29th Annual Symposium on Frequency Control (Atlantic City, New Jersey, 1975).
2. V. Reinhardt et. al., "A Modular Multiple Use System for Precise Time and Frequency Measurement Distribution," Proceedings of the Tenth Annual Precise Time and Time Interval Planning Meeting (Washington, D.C., 1978).

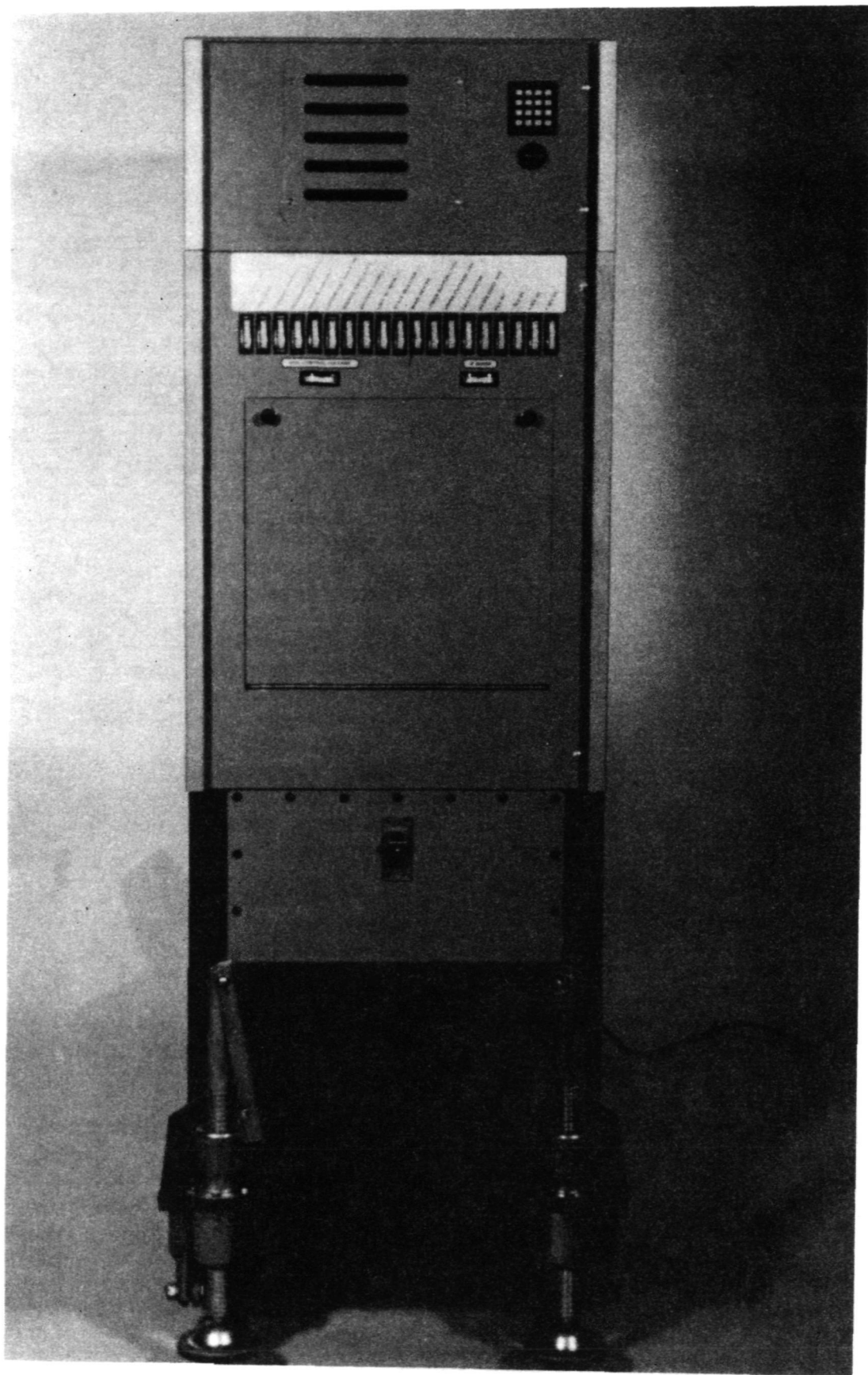


Figure 1. NR Maser

MASER 04 80 239 19 41 33 FH M-001600L025065 11 14 113740 SYN M 0588 1224 858
 015 0050 DGSW 100111101011 DACWDS 50 08 65 12 010204 020110 031105

1	VOLTAGES V	28.029	17.329	05.044	17.344	03.640	14.010	20.665	01.941
2	BUFFERS V	00.161	00.166	00.083	00.148	00.569	00.528	00.577	00.215
3	MULT SEN V	00.019	00.427	00.344	00.119	00.440	00.225	00.143	09.627
4	CURRENTS A	05.843	00.210	00.042	00.021	00.477	00.004	00.007	00.007
5	HEATERS A	00.552	00.878	00.351	00.066	00.083	00.062	00.217	00.220
6	CONTROL MA	00.038	00.004	00.019	00.000	00.000	00.000	00.225	00.005
7	MISC	02.583	02.307	115.248	00.222	00.217	00.489	03.187	07.507
8	THERM. C	47.438	35.500	46.563	29.062	29.688	34.000	72.313	71.939

Figure 2. Microprocessor Output

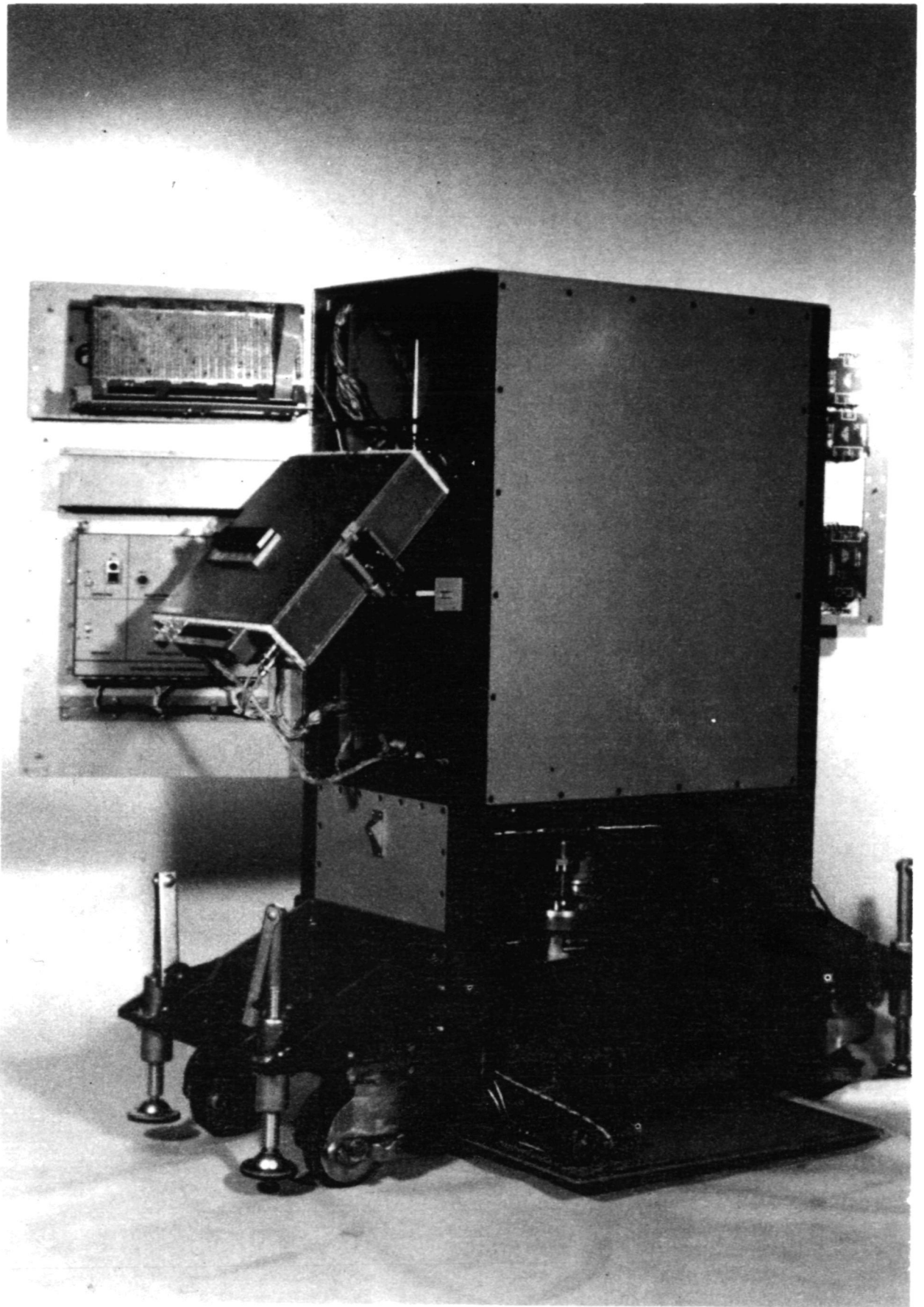


Figure 3. NR Maser Opened For Servicing

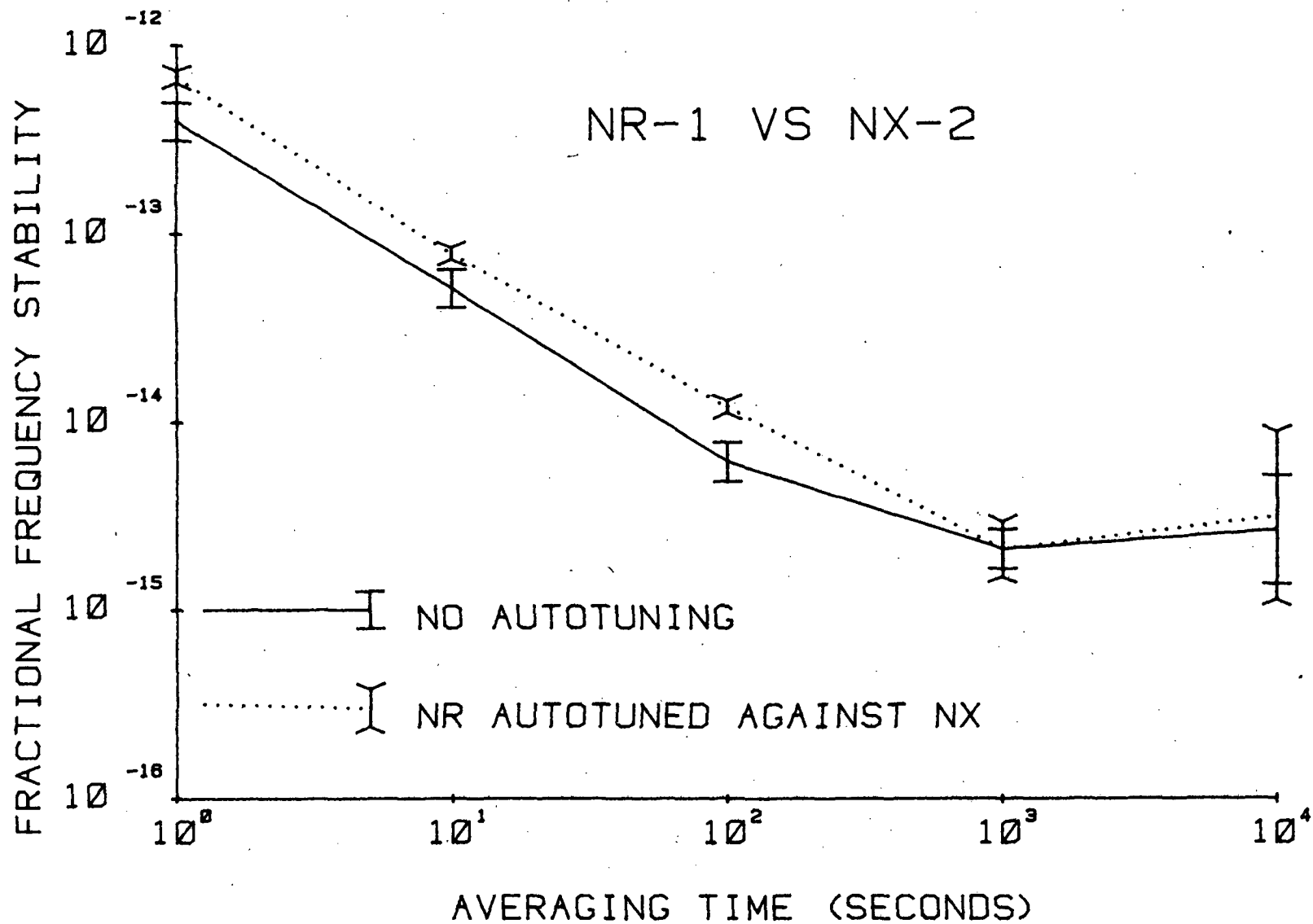


Figure 4. Stability of NR-1 vs NX-2

FRACTIONAL FREQUENCY STABILITY

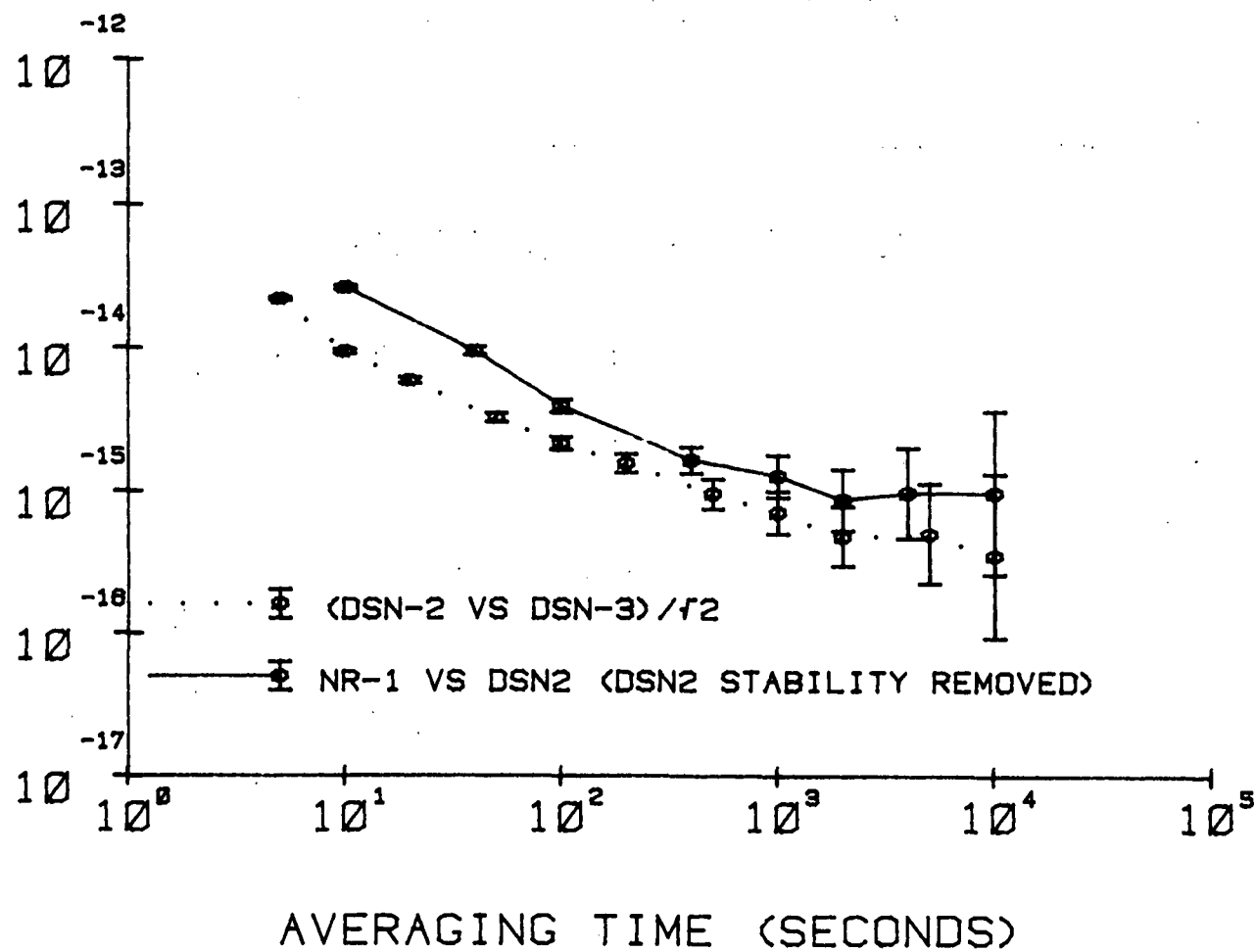


Figure 5. Stability of NR-1 vs DSN-2

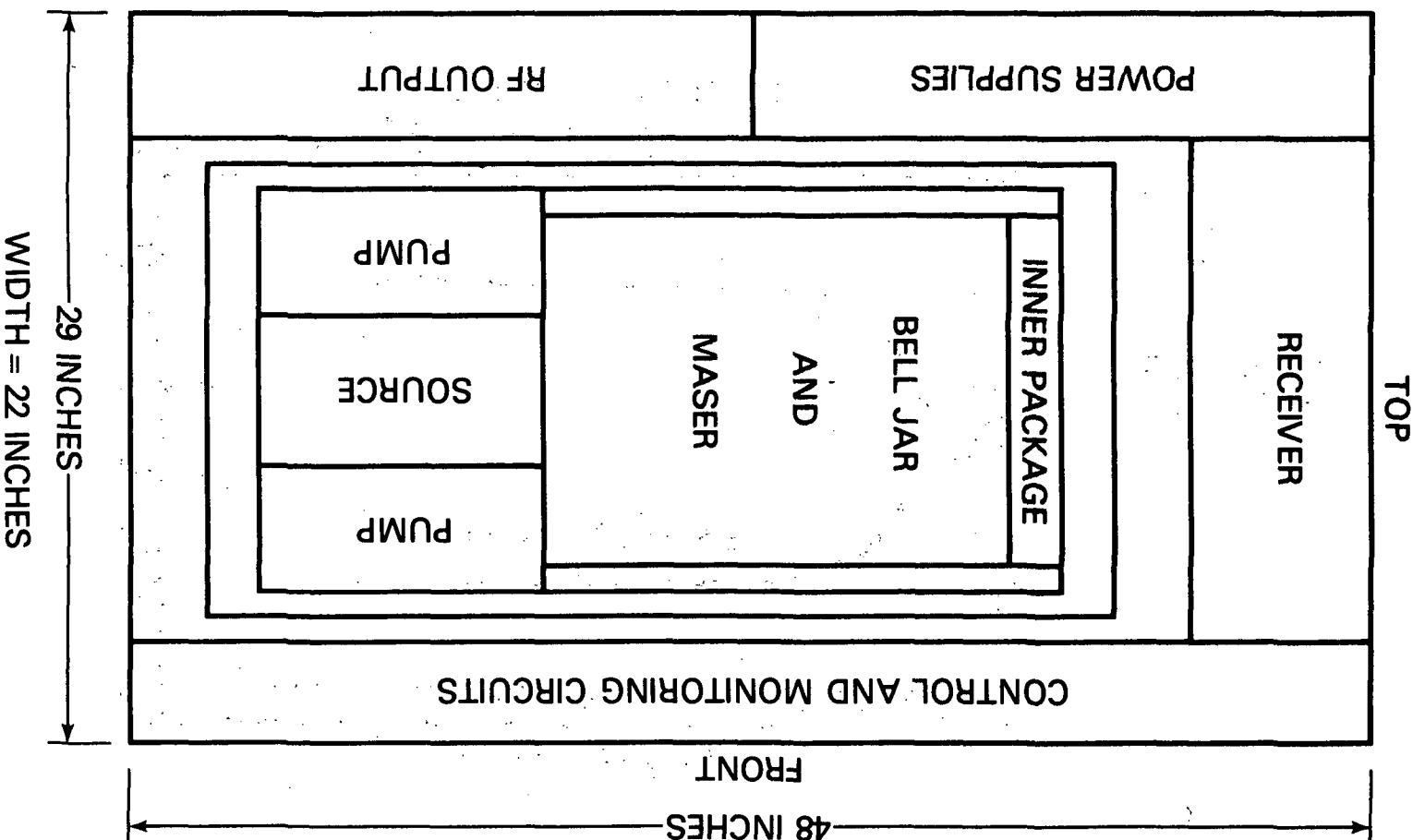


Figure 6. Low Cost Hydrogen Maser

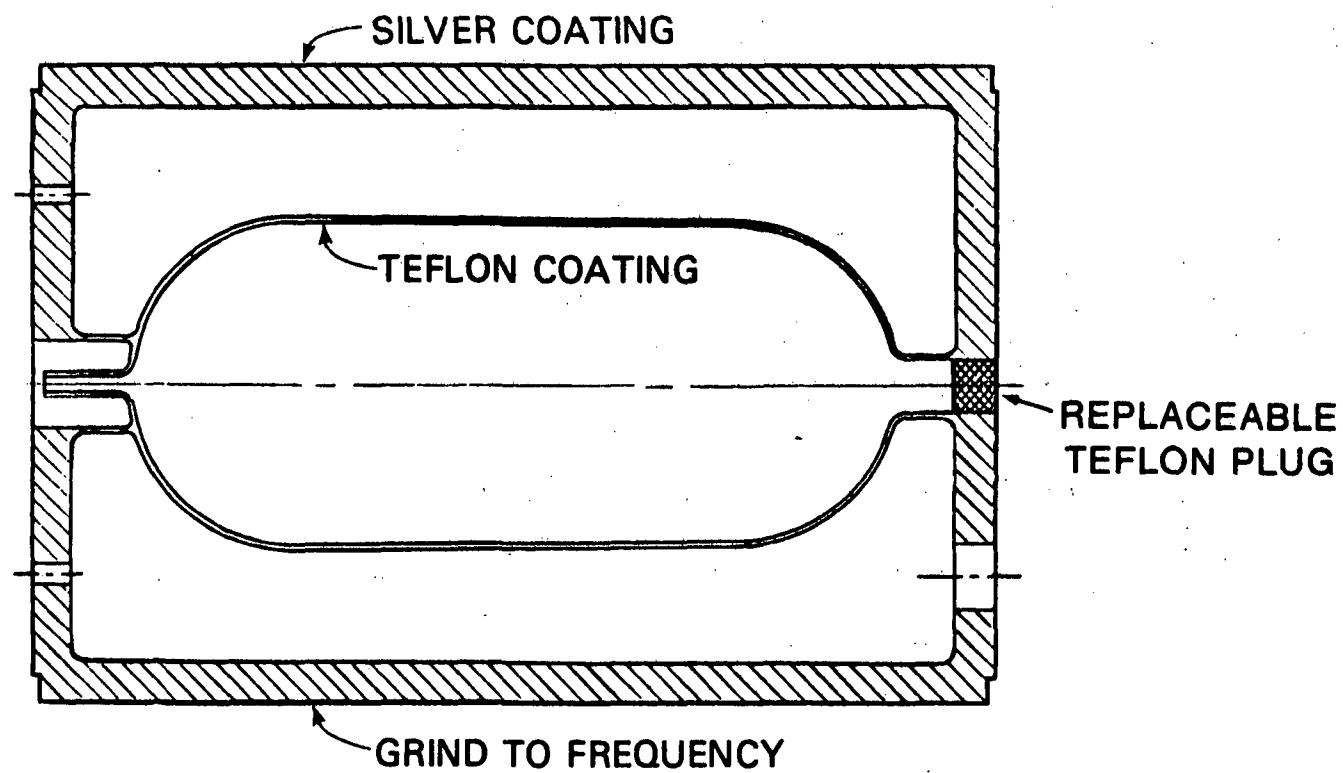


Figure 7. Integral Cavity and Storage Bulb

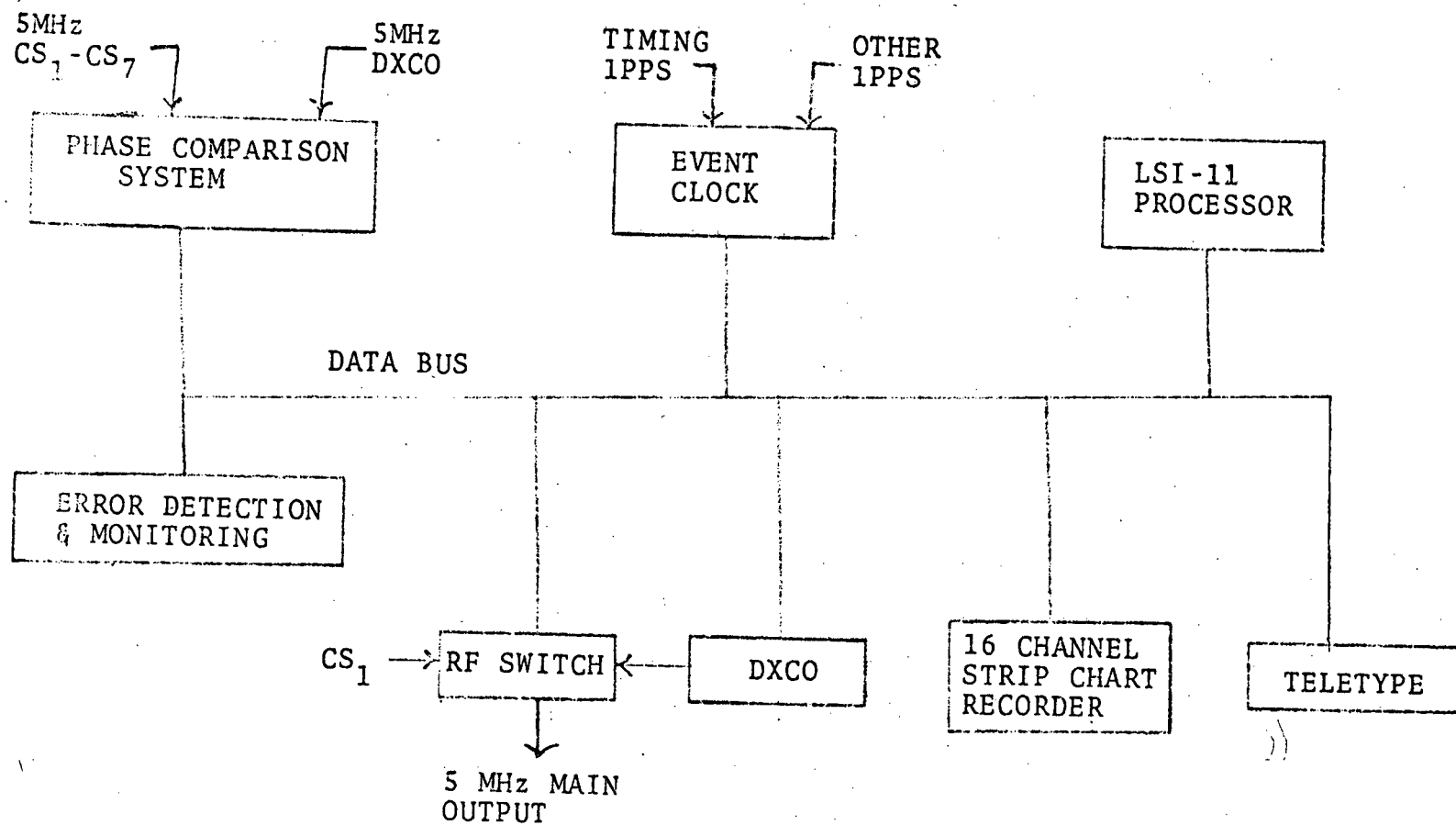


Figure 8. Simplified Block Diagram of the Distribution and Measurement System

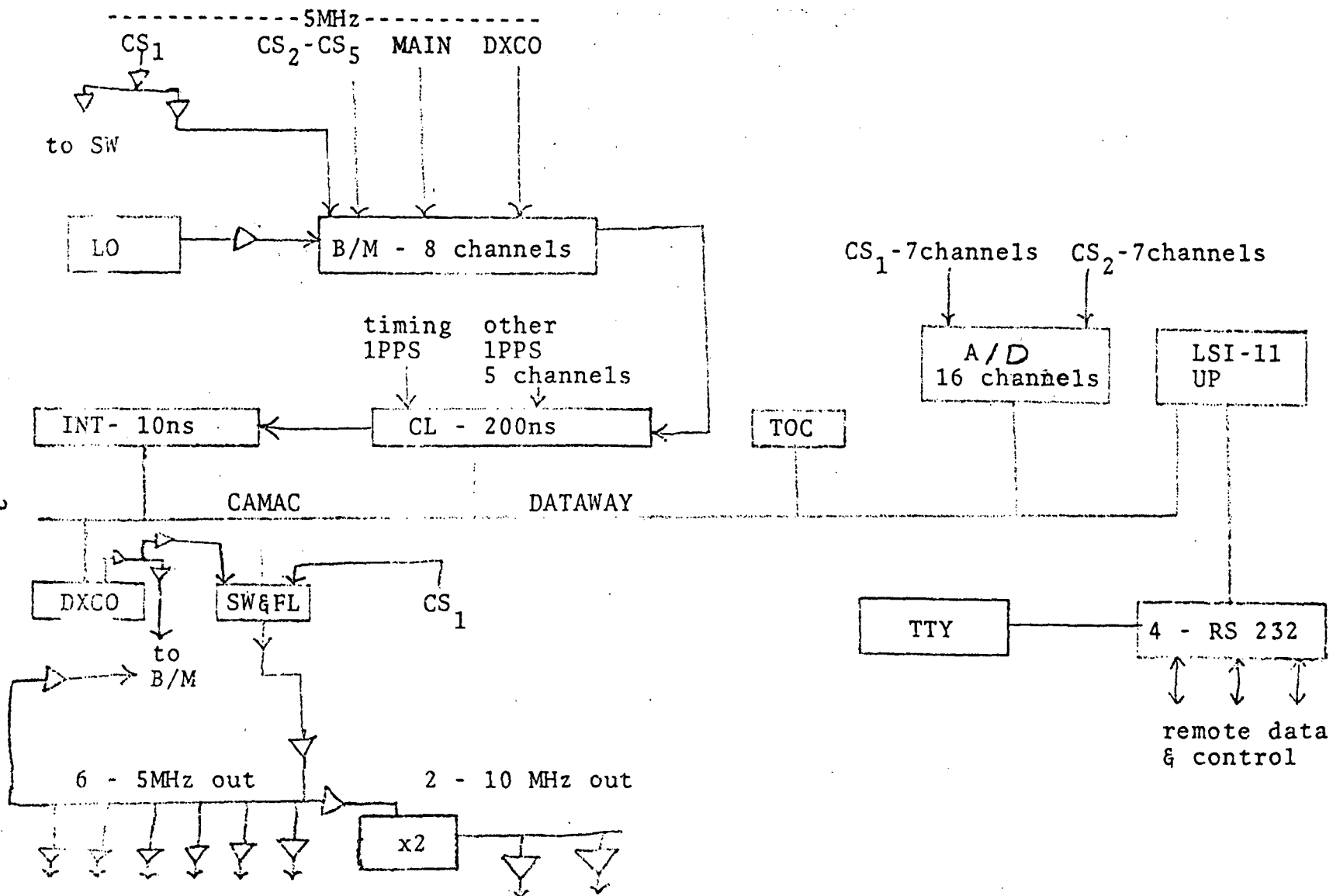


Figure 9. Detailed Block Diagram of the Distribution and Measurement System

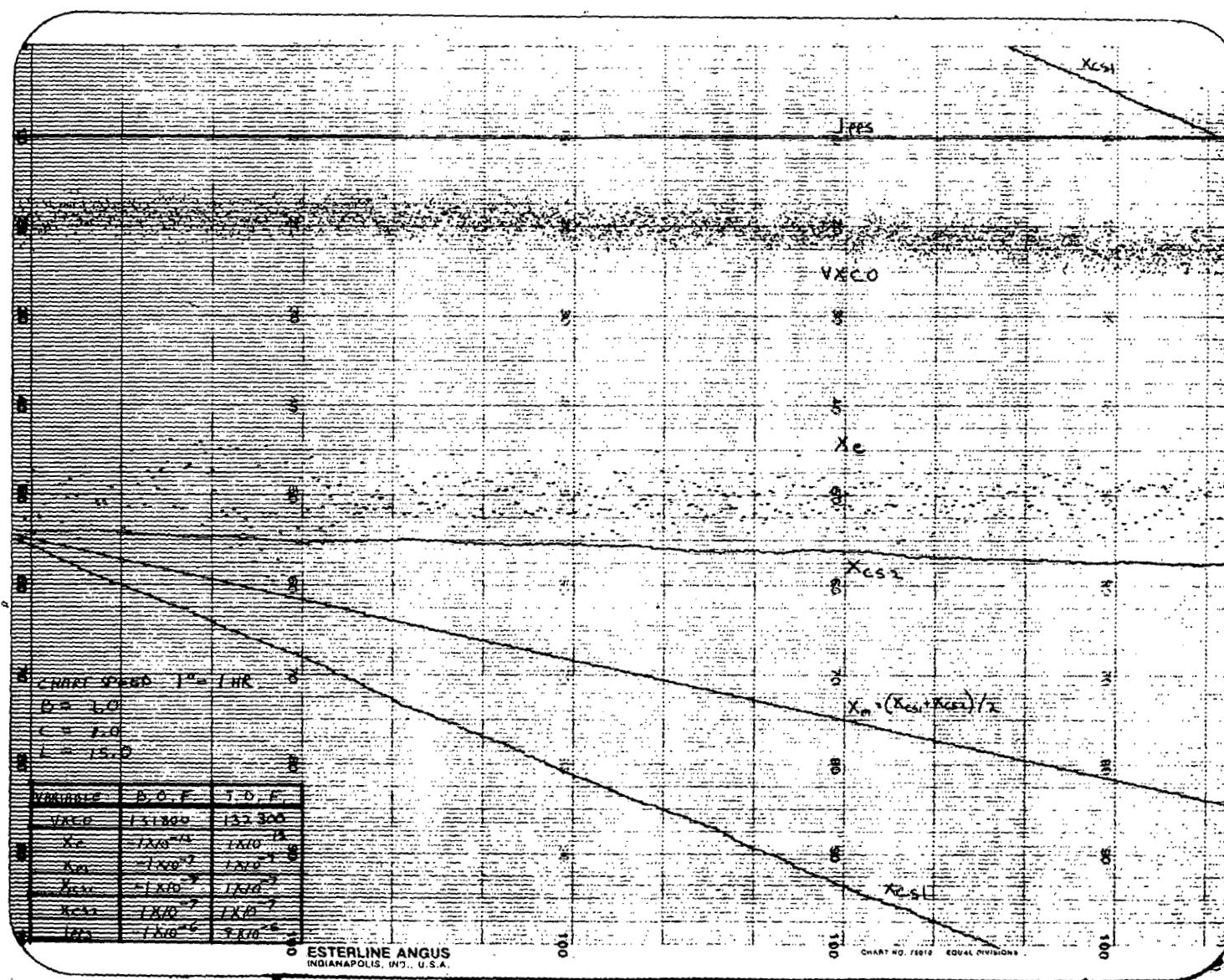


Figure 10. DMS Phase Lock Loop for 1-Second Time Constant



Figure 11. DMS Phase Lock Loop For 10-Second Time Constant

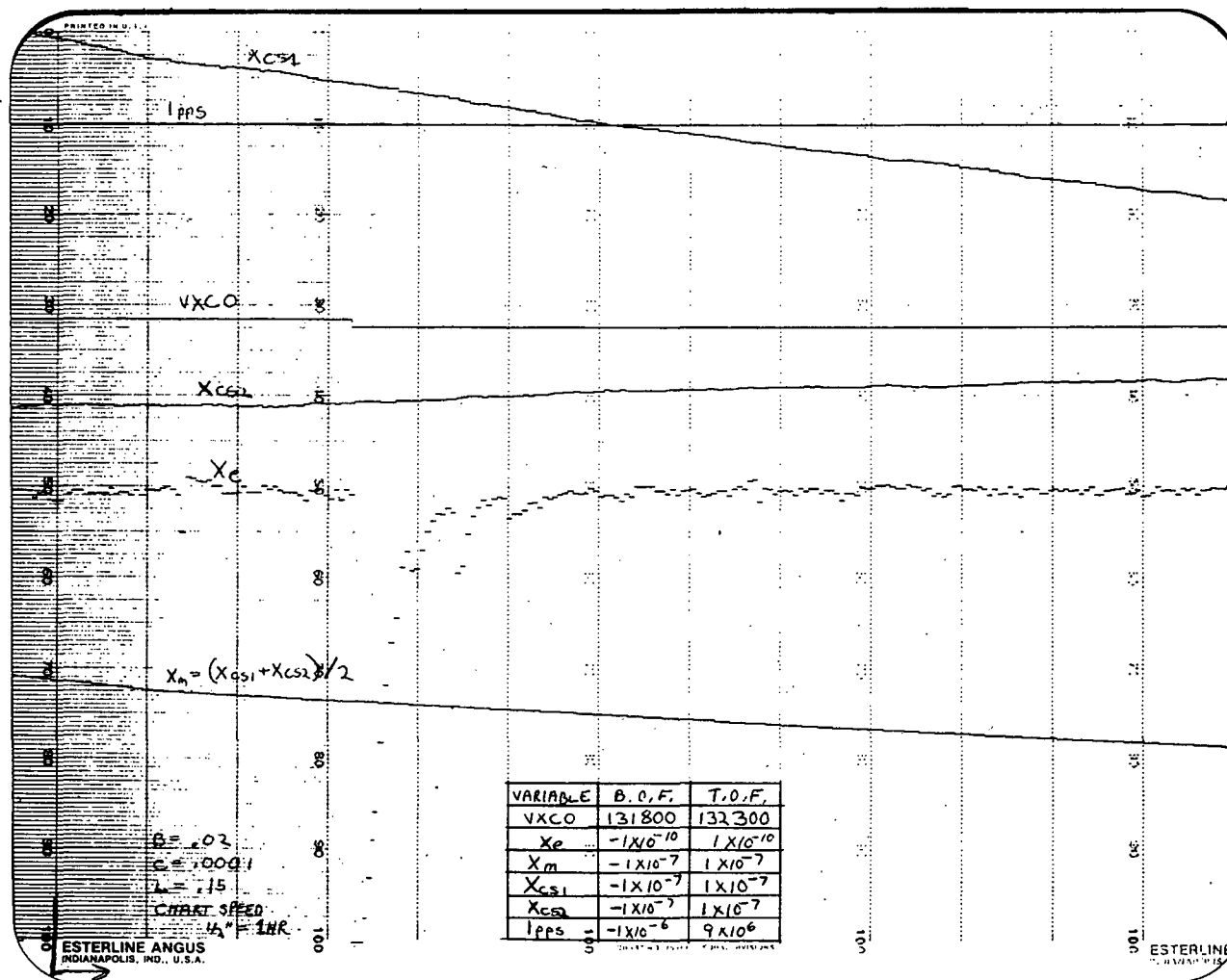


Figure 12. DMS Phase Lock Loop For 100 Seconds Time Constant

PASSIVE MASER DEVELOPMENT AT NRL

J. White, A. Frank and V. Folen
Naval Research Laboratory
Washington, D.C.

ABSTRACT

The Naval Research Laboratory has been investigating the application of passive hydrogen masers to satellites. This effort has included development of a working small maser at NRL and contractual support of work at Hughes Research Laboratory and the National Bureau of Standards.

The NRL maser is of compact design suitable for the space environment. It is based on a dielectrically loaded sapphire cavity and uses a computer optimized set of four shields. The mechanical structure was developed in a cooperative effort with the Smithsonian Astrophysical Observatory. The servo design is a novel phase sensitive method which directly measures the phase dispersion of the interrogating signal as it passes through the cavity. Test results will be presented.

A brief synopsis of the results of the contractual work will also be presented.

INTRODUCTION

The Naval Research Laboratory is involved in development of passive maser technology for applications both in spacecraft and in ground stations. This represents a continuation of the work done previously in the TIMATION and GPS programs. The goal of this effort is to provide a clock for GPS and other potential users which is more stable at periods of several days and which is also capable of operating reliably in military environments. This project includes in-house development and also relies on outside technology development by other government and industry laboratories.

This program began in the early 1970's with the work by the Smithsonian Astrophysical Observatory (SAO) in the building of the first VLG-10 maser¹. NRL also supported development of the first

VLG-11 masers at SAO² and directed the contractual program at Frequency and Time Systems which produced the first space qualified cesium clocks³. We are currently engaged in efforts to develop additional sources of space qualified cesium standards.

The space hydrogen maser program began several years ago with preliminary work to locate qualified aerospace industry sources to develop and manufacture a space qualified active maser. This work was taken on by Hughes Research Laboratory (HRL) and RCA in a competitive effort. Both contractors delivered operating, prototype masers^{4,5}. HRL was selected to do additional work. It was at this point that the National Bureau of Standards (NBS) produced their passive maser⁶. The passive concept gave two distinct advantages over active masers. The first was the option of using a smaller, lower Q RF cavity. That meant a large reduction in weight and volume along with some simplification in pumping and magnetic shielding requirements. The second advantage was the possibility of achieving better long term performance due to the application of a cavity control servo.

The work on passive masers has since been in these areas. NRL and SAO have worked cooperatively to build a small passive maser. HRL has been contracted to follow other promising approaches to small masers while developing technology which might be used in other parts of the program. As originally defined HRL remains the link to major aerospace capabilities. NBS has been funded to continue their development of passive maser technology.

NRL Passive Maser

In 1978 the decision was made to build a small passive maser at NRL. This effort not only includes NRL but also support from other laboratories. This maser is viewed as a means of assembling the most promising parts of the existing technology and also as a way of extending knowledge in the areas where the existing work falls short of the goals. Like the NBS maser the basic approach is passive with separate servo controls for the hydrogen line and the cavity. As will be discussed in the section on the electronics, there are some differences in the application of these controls. The desired product is summarized as follows:

1. Suitable for military/space operating environment
2. Highly reliable
3. Long term stability of 1×10^{-14} at 10 days

4. Compact size
5. Low weight
6. Low power

To approach these goals the clock is examined in terms of its subassemblies.

1. Cavity and shields
2. Mechanical and thermal
3. Vacuum
4. Electronics

Cavity and Shields

The physics unit of the NRL maser consists of the hydrogen beam source and optics, magnetic shields, cavity thermal control, vacuum system and mechanical support for the microwave cavity. In the present configuration, this cavity operates in the TE_{011} mode and is loaded with single crystal (low loss) sapphire, figure 1. Three slots in the cavity cover plate provide the necessary coupling. The volume available in the cavity for the hydrogen atoms is 217 cm^3 and the surface of this volume is coated with FEP 120 teflon in order to minimize hydrogen-wall interactions. The hydrogen atom source consists of an rf dissociator from which the atoms emerge into a hexapole state selector magnet.

The magnetic shield set, consisting of 4 nested molypermalloy shields, was designed for a lightweight small-volume configuration (figure 2) with a substantial shielding safety factor to provide a frequency stability of 1 part in 10^{14} for any orientation in a 1 gauss field⁷.

Mechanical and Thermal Design

The importance of the mechanical and thermal control designs is especially great when operation outside the laboratory is required. NRL has chosen to make use of the extensive experience available in this area at SAO. SAO's probe maser launch for the red shift experiment has given them a unique understanding of the requirements for spaceflight as applied to the Hydrogen maser. SAO has, under contract to NRL, designed, fabricated and delivered two units of a developmental model maser⁸. As input SAO was given the environmental requirements, the cavity/shield system, the

vacuum system and hydrogen source system. The first design, the Exploratory Development Model (XDM), was delivered in 1979. A refined version of the XDM, the Advanced Development Model (ADM) is scheduled for delivery in late 1980.

Figure 3 shows the XDM design. The cavity is mounted to a Belleville spring to provide essentially constant force on the end plates. The cavity is enclosed in a separate vacuum can rather than using the cavity as the vacuum envelope. This adds weight and volume but allows greater isolation of the cavity from its environment. The entire assembly is designed to meet the GPS vibration (~ 19 g rms) requirement.

The thermal design is similar to that of the VLG series active masers using a multi-zone, double oven approach. The vacuum tank is the primary temperature control surface. A second oven is used to isolate the tank from external heat paths. The XDM masers used a conventional foam insulation between the shields. As an enhancement, the ADM masers use a vacuum type insulation which takes advantage of the vacuum environment of space to reduce heat loss and weight. The nominal oven power of XDM-1 is about 7.4 watts. For ADM-1, in vacuum, the measured power is 2 watts. While this superinsulation scheme is best applied in vacuum, it has been found also to provide excellent thermal stability in air at increased input power. The oven system was designed to provide a temperature stability of better than 5 millidegrees at the cavity. It may be argued that the cavity control servo reduces the need for such excellent thermal stability but for non laboratory applications this conservative design can greatly reduce system problems.

Pumping System-Hydrogen Supply

The design life of a space borne maser is five years of operation. Historically vacuum systems have been a weak area in maser reliability. The ion pumps themselves do not thrive on pumping hydrogen and the required high voltage power supplies are also troublesome, particularly if vacuum operation is desired. The dissociator is likewise a sensitive area in masers⁹. While most contemporary masers show good dissociator life, they do tend to run hot and thus require forced air cooling. Fortunately, solutions are available for both problems.

Recently a very effective, high capacity hydrogen getter pump has become available. Both HRL and NRL have investigated these pumps for maser use ^{4,10}. Since the getter pump is a passive device it requires no external power after activation and is also inherently reliable. For the NRL maser, a combination pumping system using getters and multiple small ion pumps has been built. This system, more fully described elsewhere in these proceedings ¹⁰, pumps the primary hydrogen gas load with the getter and requires only a small ion pumping capacity to maintain the desired vacuum. Redundant ion pumps with isolated supplies further increase reliability.

There are several approaches to the problem of operating the dissociator in vacuum. A simple pyrex bulb design from HRL operates at under 50°C. Other designs are also being investigated. One obvious method to obtain cooling is to conduct heat away through the walls of the bulb. Pyrex, which is the most popular material in dissociators, has relatively poor thermal conductivity. HRL and RCA both experimented with quartz bulbs but to date there is little assurance that these will have long life. SAO has designed a pyrex bulb which runs cool by virtue of thick walls and short paths to heat sinks. A radical departure in design is being pursued at NBS. They propose a small dc discharge. Since there is no longer a requirement to pass RF energy through a wall, the choice of materials and configuration broadens. Such a design, if successful, would also have the advantage of reduced RF interference to the electronics.

ELECTRONICS

The servo subsystem consists of the electronic control to lock a voltage controlled crystal oscillator (VCXO) to the hydrogen hyperfine transition and the electronic control to tune the cavity symmetrically about the hydrogen line. NRL has devised a scheme to compare the phases of a set of coherent microwave frequencies, which are coupled through the dielectric loaded cavity, versus the VCXO.

The phase comparison technique uses a high percentage of digital circuits in the synthesis of the microwave frequencies and in the phase detection networks. The digital circuits reduce the necessity for analog adjustments, and offer low operating power consumption, reduced weight, compactness, and a broad environmental operating range. These features are ideal for space applications.

Figure 4 is a block diagram of the SERVO electronics.

The hydrogen line servo employs three microwave signals that are synthesized from the VCXO. These signals are time shared, coupled through the cavity, phase detected, and used to control the VCXO. One synthesizer frequency is at the hydrogen resonance. The others are symmetrical about the hydrogen resonance but well outside the hydrogen line width and still near the center of the cavity resonance width. This method is used to establish a phase reference for the hydrogen line.

The output of the set of frequencies coupled through the cavity is amplified, translated, phase detected, averaged in an up-down counter, transferred to a digital analog converter (DAC), and used to control the VCXO. These frequencies are all passed through the same broadband receiver and are translated with an offset set of frequencies from the synthesizer. The resulting signal frequency with plus or minus the phase of the hydrogen line or cavity line is narrowband filtered. The filtered signal is shaped in a zero crossing detector and phase compared with a signal divided down from the VCXO.

The output of the phase comparator is used to control an updown counter. Phase comparator output corresponding to the hydrogen resonance frequency is averaged for a period of time in an up count direction after a settling time. Phase comparator output corresponding to the symmetrical frequencies is averaged over one-half the period of the hydrogen resonance frequency each after a settling time in a down count direction. Transfer of the up-down counter contents to the DAC which controls the VCXO frequency is executed after completion of the up-down counter cycle.

The cavity line servo consists of three microwave signals which are synthesized from the VCXO. These signals are time shared with the hydrogen line signals during a period when the hydrogen servo is quiescent. One of the frequencies is the hydrogen transition frequency used with the hydrogen servo and the other two frequencies are symmetrical about this transition frequency and fall within the passband of the cavity resonance. The symmetrical frequencies are time shared and simultaneously coupled through the cavity with the hydrogen transition frequency.

The signals coupled out of the cavity are amplified and translated to an intermediate frequency (IF) with the same broadband circuits used with the hydrogen servo. This IF is detected, narrowband filtered, shaped with a zero crossing detector, and phase compared versus a signal divided from the VCXO. The phase comparator controls an up-down counter which averages the time shared signals after a

settling time. Controls allow an up count corresponding to the composite lower symmetrical frequency and hydrogen transition frequency and a down count corresponding to the composite upper symmetrical frequency and hydrogen transition frequency. Transfer of the up-down counter contents to a DAC is executed upon completion of the up-down counter cycle. Tuning of the cavity is accomplished by controlling a varactor with this DAC output voltage. The varactor is coupled to the cavity and reactively tunes the cavity proportional to the DAC control voltage.

System Performance

The XDM masers from SAO have been used to experimentally verify system performance. The width of the hydrogen line under optimum pressure and magnetic field is 2.0Hz thus giving a line Q of 7×10^8 . The phase slope at center frequency is about 6° per Hz. The stability of this maser measured at the output of the electronics is $7 \times 10^{-12}/\sqrt{\tau}$ for the range $\tau = 10$ to 3000 seconds (figure 5). Work is currently underway to optimize the cavity servo and extend this stability level to better than 1×10^{-14} .

Outside Work

In addition to the work done with SAO, NRL has also contracted with Hughes Research Laboratory (HRL) and the National Bureau of Standards at Boulder (NBS).

The current contractual relationship with HRL has grown from the original competition efforts on the active maser. Following the shift in emphasis from the active to passive mode, HRL was directed toward small maser concepts and development of technologies applicable to small masers. Dr. Wang has previously reported on HRL maser development 11, 12. HRL is presently working on Q-multiplier type servo using a small, slot loaded cavity. This maser was tested at NRL (figure 6). It had a stability of $2 \times 10^{-12}/\sqrt{\tau}$ for $\tau = 10$ to 10000 seconds. HRL has also done investigations of getter pumping systems, free induction servo techniques and dissociator design.

NRL has been providing funding support to NBS for passive maser development. NBS has delivered one of the first small passive masers (figure 7) to NRL. This maser uses a ceramic loaded cavity.

It is a laboratory model which has relatively stringent requirements on its environment and operation. Tests at NRL show a stability of $2 \times 10^{12} / \tau$ for $\tau = 1$ to 10,000 seconds. This is virtually identical to that of the Hughes maser, both are shown in figure 8.

NRL has also continued support of the VLG-11 maser program with the purchase of a third VLG-11 last year. Our tests on the VLG-11 confirm the published SAO data on performance in the 1 to 3000 second region. We have, however, observed that a new maser has a significant cavity tuning drift rate in the first 6 months to 1 year of its life. A brief series of tests have just been completed on two masers over a year old. In this case instead of finding a decrease in stability beyond 3000 seconds, there still is a gradual improvement as far out as 10000 seconds.

REFERENCES

1. Vessot, R.F.C.; Levine, M.W., "Performance Data of Space and Ground Hydrogen Masers...", Proc 28th Annual Symposium on Frequency Control, 1974, 408-414.
2. Levine, M.W.; Vessot, R.F.C.; Mattison, E.M., "Performance Evaluation of the SAO VLG-11 Atomic Hydrogen Masers", Proc 32nd Annual Symposium on Frequency Control, 1978, 477-85.
3. White, J.O.; "NTS-2 Cesium Beam Frequency Standard for GPS", Proc PTTI, 1976, 637-664.
4. Wang, H.T.M.; Lewis, J.B.; Crampton, S.B.; "Compact Cavity For Hydrogen Frequency Standard", Proc 31st Annual Symposium on Frequency Control, 1977, 543-548.
5. Sabisky, E. S.; Weakliem, H.A., "An Operating Development Model Spacecraft Hydrogen Maser", Proc 32nd Annual Symposium on Frequency Control, 1978, 499-500.
6. Walls, F.L.; Howe, D.A., "A Passive Hydrogen Maser Frequency Standard", Proc 32 Annual Symposium on Frequency Control, 1978, 492-8.
7. Wolf, S.A., et al, "Shielding of Longitudinal Magnetic Fields with Thin, Closely Spaced, Concentric Cylindrical Shells with Applications to Atomic Clocks", Proc 32nd Annual Symposium on Frequency Control, 1978, 131-146.
8. Mattison, Em et al, "Design, Construction and Testing of a Small Passive Hydrogen Maser", Proc 33rd Annual Symposium on Frequency Control, 1979, 549-553.
9. Ritz, V.H. et al, "Characterization of Degraded Hydrogen Dissociator Envelopes by AES", Journal of Applied Physics, 48, 5, 1977, 2096-2098.
10. Wolf, S.A.; Gubser, D.U.; Jones, L.D., "Vacuum Pumping Systems for Spaceborne Passive Hydrogen Masers", Proc 12th Annual PTTI, 1980.
11. Wang, H.T.M., "Hydrogen Frequency Standard Using Free Induction Technique," Proc 31st Annual Symposium on Frequency Control, 1977, 536-542.

12. Wang, H.T.M., "An Oscillating Compact Hydrogen Maser",
Proc 34th Annual Symposium of Frequency Control, 1980,
364-369.

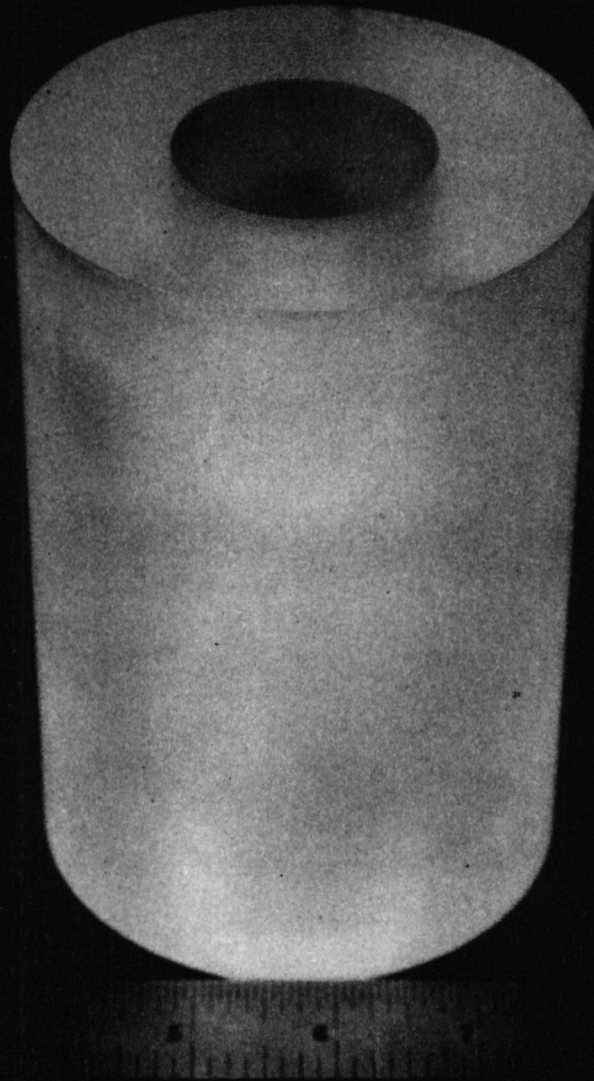


Figure 1 Sapphire Cavity

506

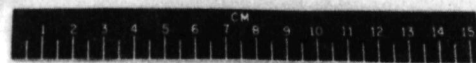
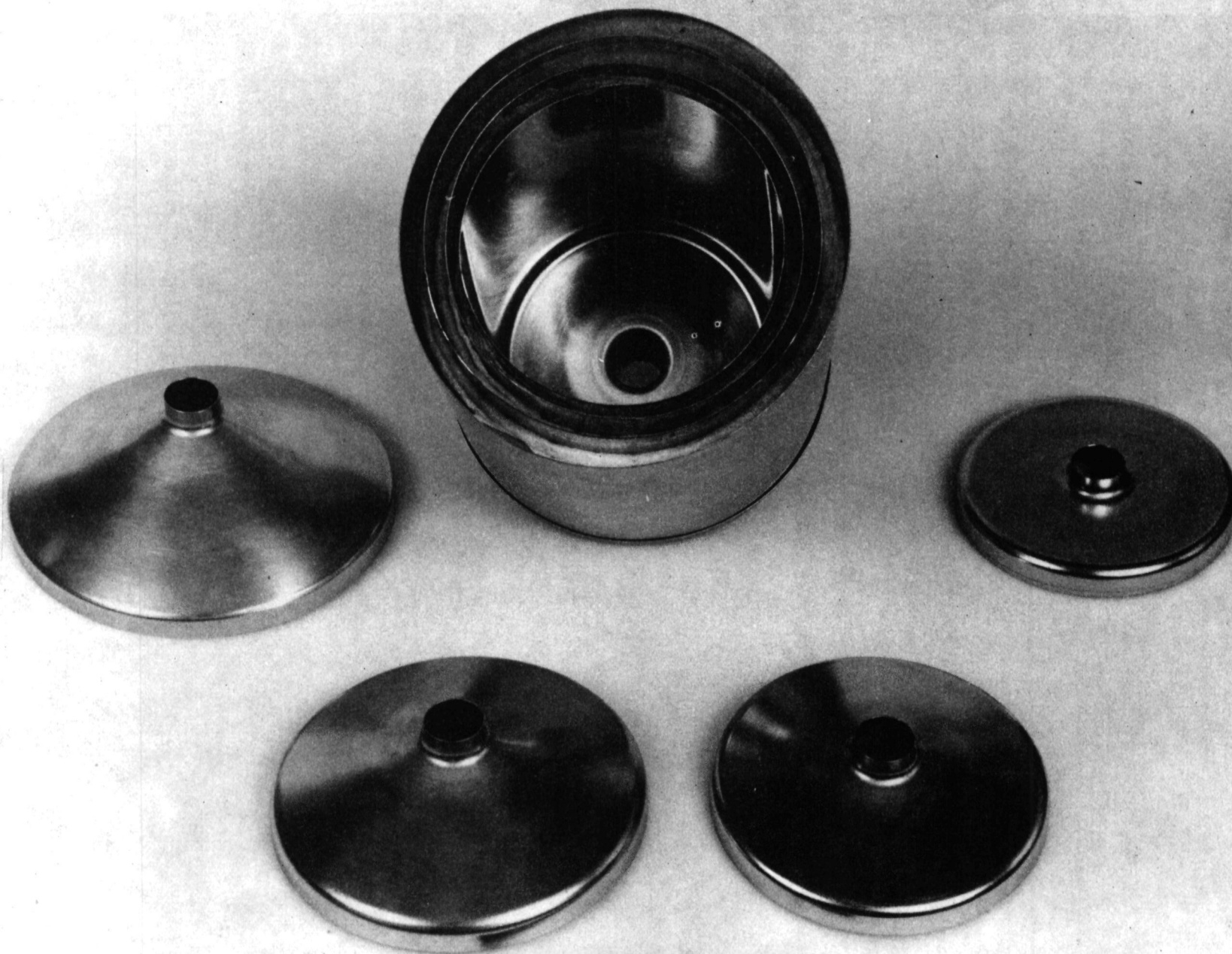
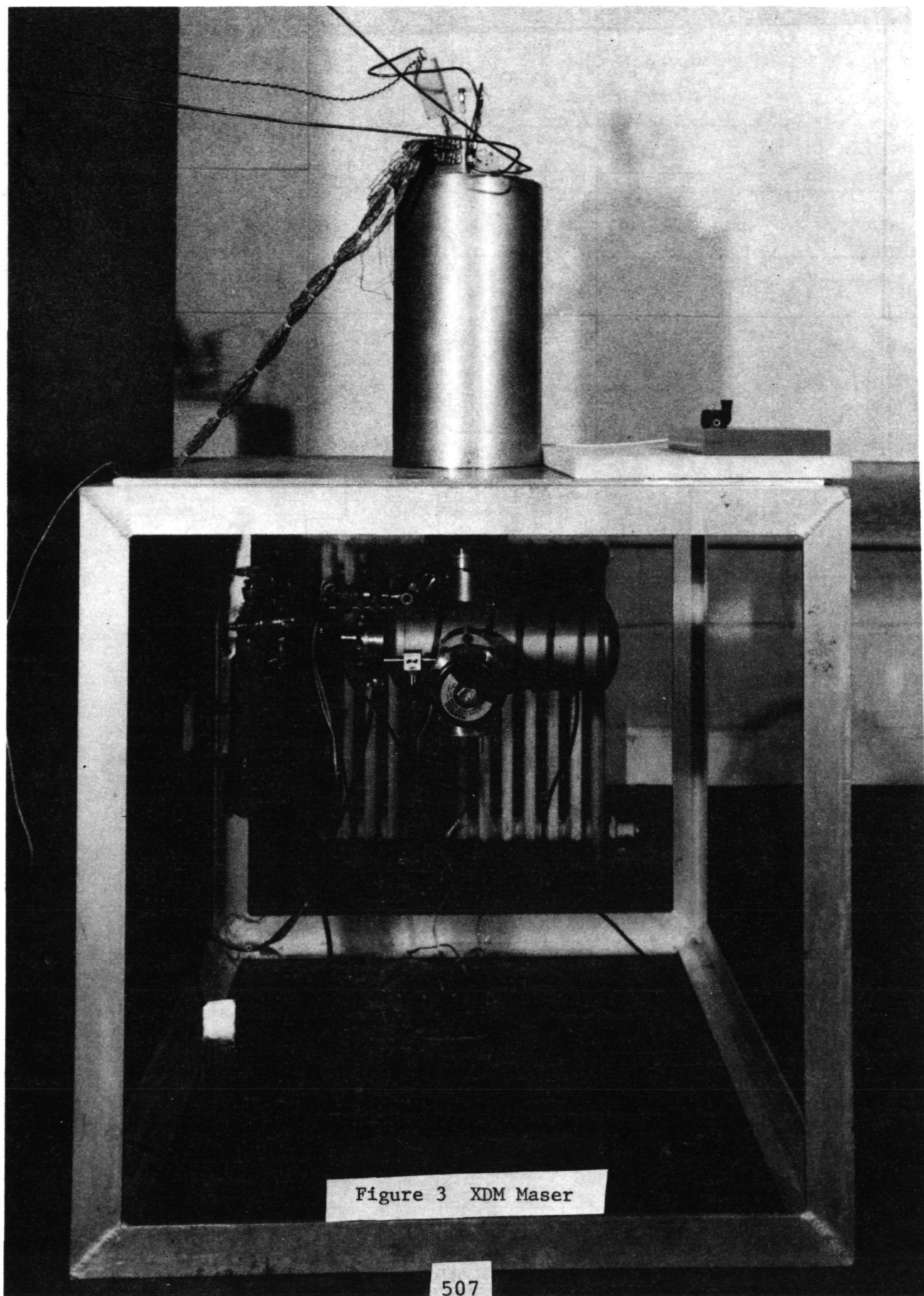


Figure 2. Shell A-11



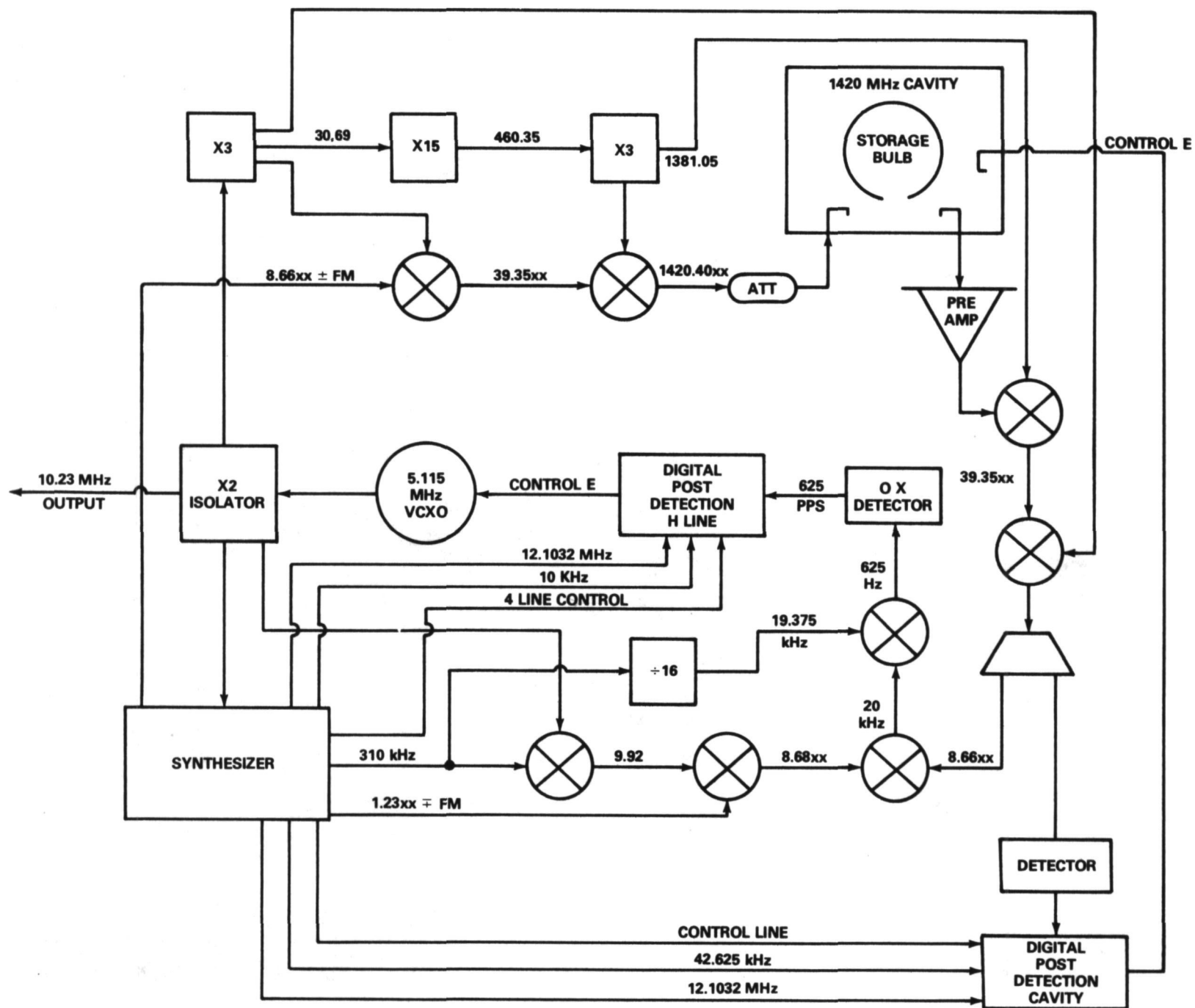


Figure 4 Block Diagram of Servo

NRL PASSIVE MASER

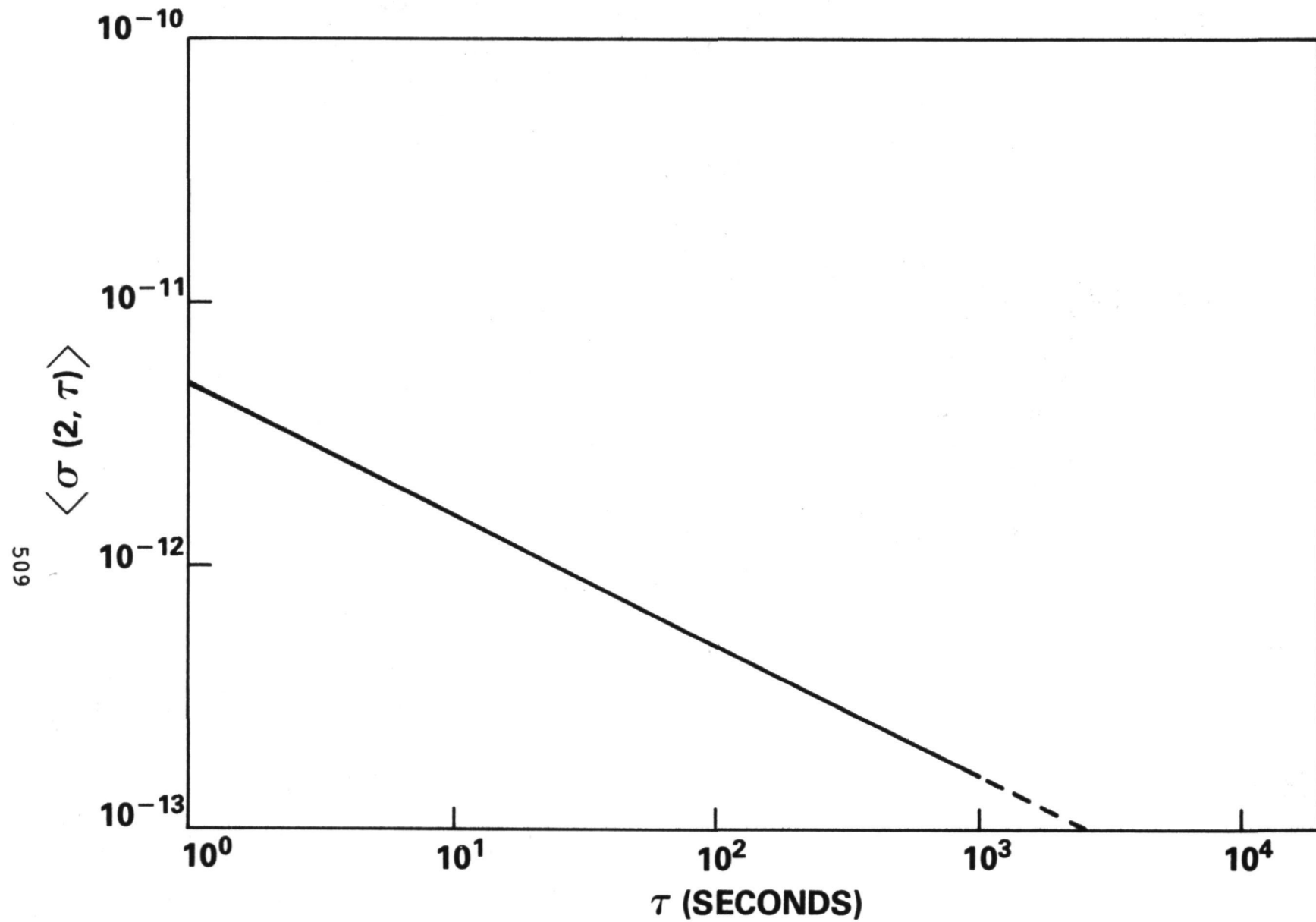


Figure 5 XDM Performance

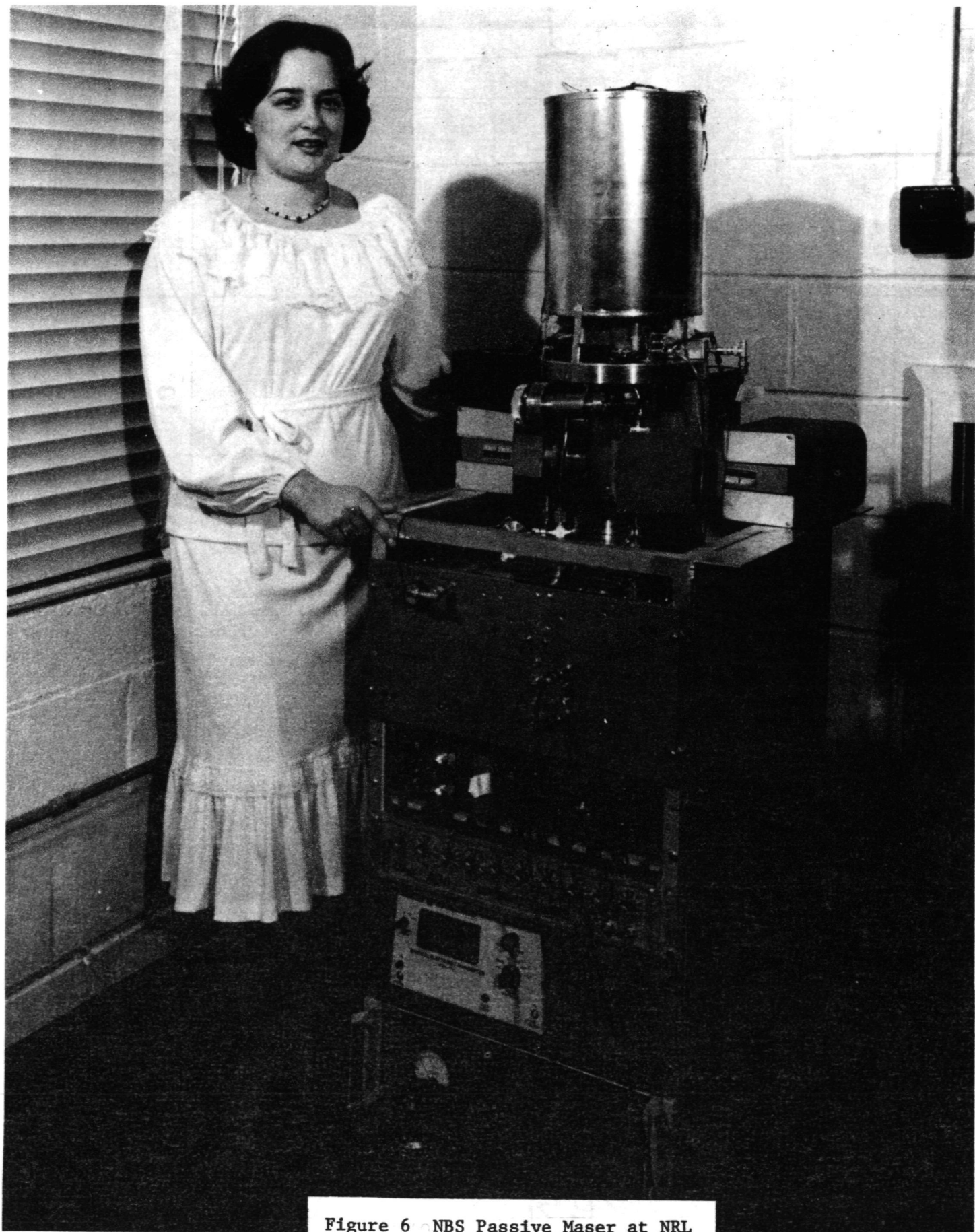


Figure 6 NBS Passive Maser at NRL
510

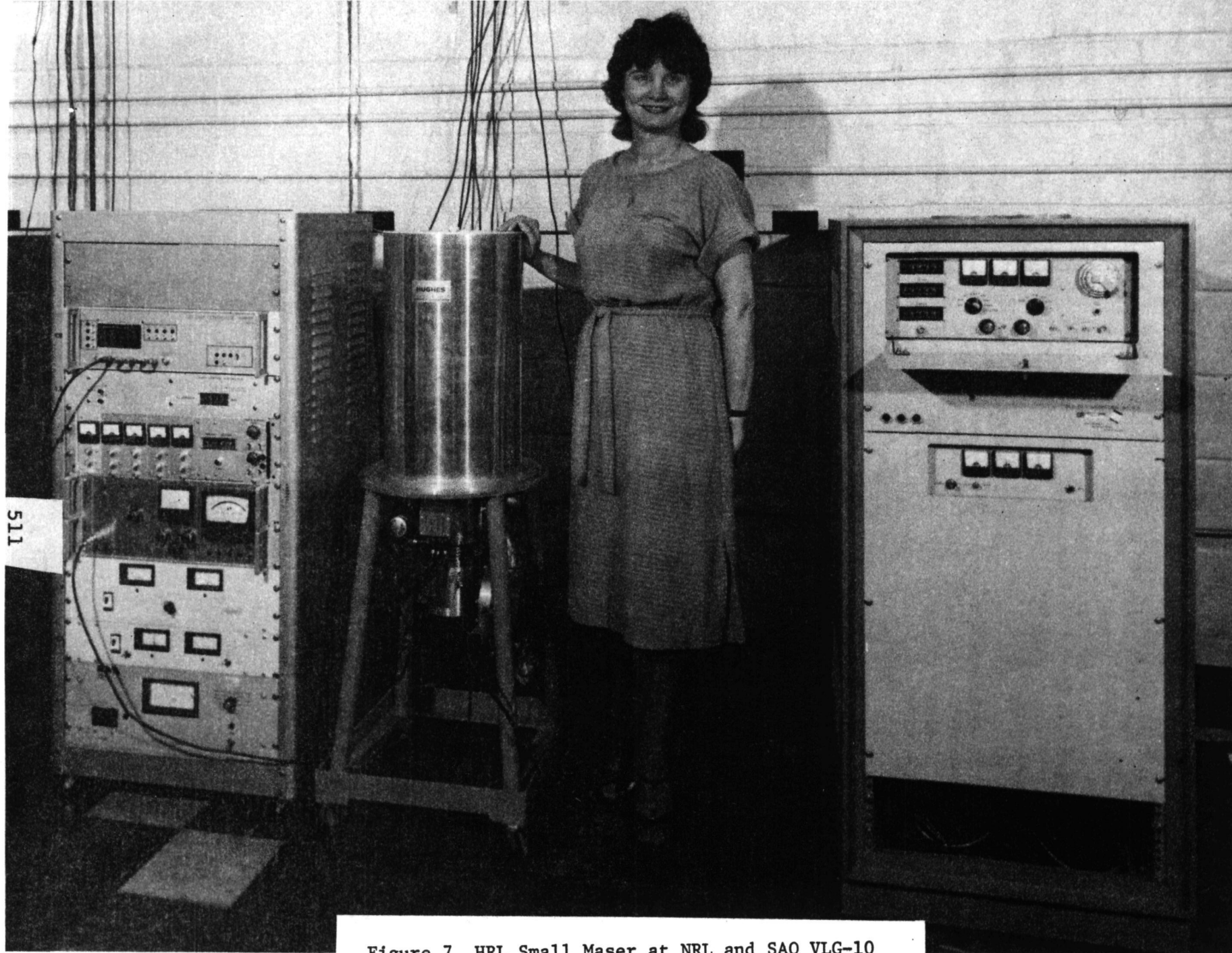


Figure 7 HRL Small Maser at NRL and SAO VLG-10

PASSIVE MASER PERFORMANCE

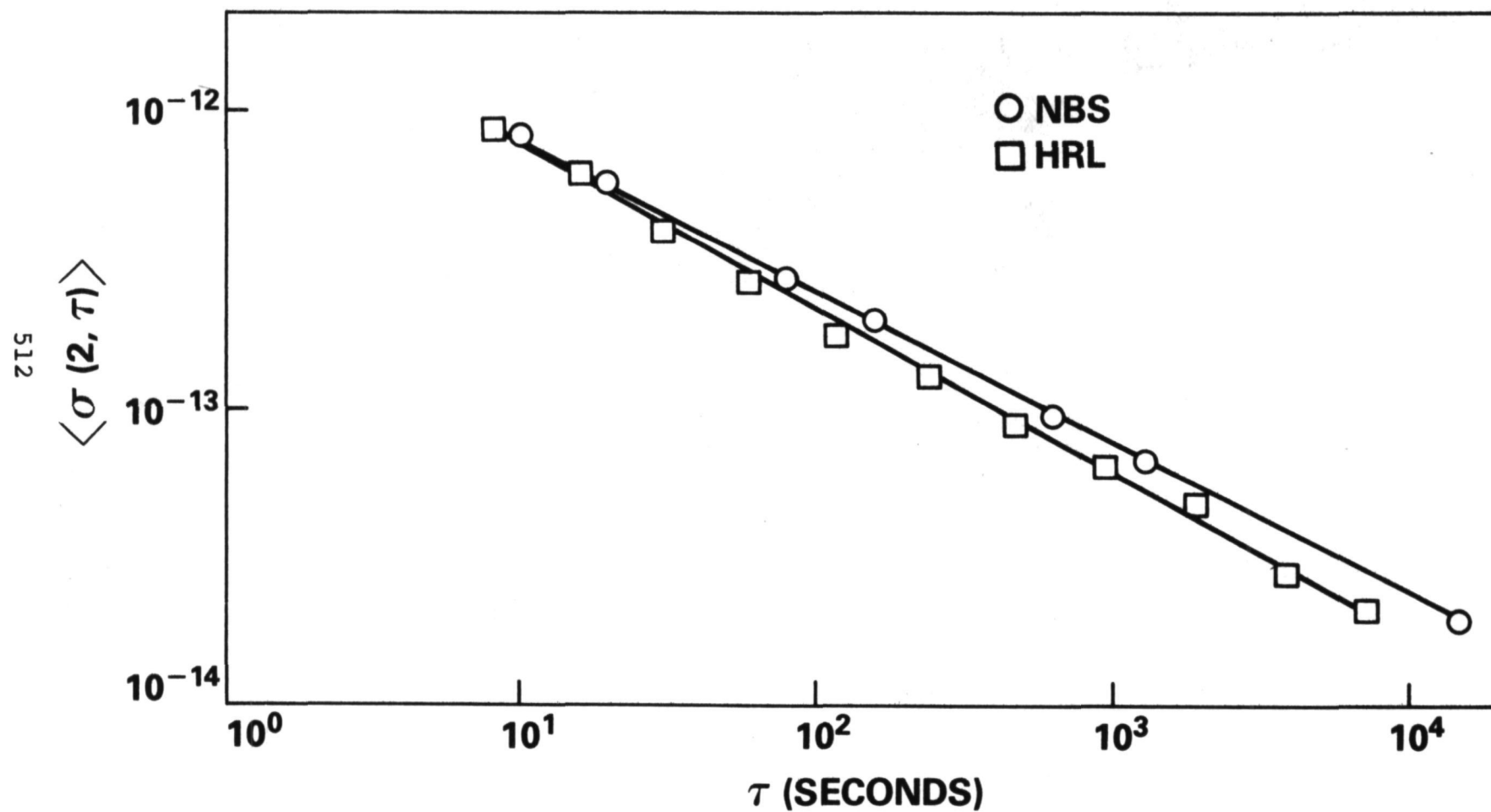


Figure 8 NBS/HRL Performance

QUESTIONS AND ANSWERS

MR. PETERS:

I just wanted to say that the maser that you showed us in Philadelphia was built by Harry Wang, Hughes Research.

MR. WHITE:

Oh, I am sorry, Harry. I got the wrong Harry indeed.

Page Intentionally Left Blank

REFERENCE CLOCK PARAMETERS FOR DIGITAL COMMUNICATIONS SYSTEMS APPLICATIONS

Peter Kartaschoff

Swiss Post Office Research and Development Division
Berne, Switzerland

ABSTRACT

The choice of correctly defined and useful parameters for characterizing the performance of reference clocks used in digital communications systems is a subject of efforts in the CCITT and the CCIR, the consultative technical bodies of the ITU. The operation of the systems depends on timing. Thus the CCITT has chosen in its Recommendation G811, to specify the clock performance requirement by starting a maximum allowable time interval error, i.e. a clocks time departure after initial synchronization.

On the other hand the commonly used characterization of clock performance is based on frequency instability as the basic phenomenon. CCIR Recommendation 538 therefore states the well known polynomial form of the spectral density of random frequency departures. It is now possible to estimate a probable time interval error if the model parameters of the clock are known. This error depends on the initial synchronization error, the frequency drift, the initial frequency setting error and the random frequency instability.

With established relations between the frequency instability of clocks and the timing properties required for the system, the relevant parameters determining the timing properties can be identified.

In a network these parameters are a) the characteristics of the clocks located at the nodes and b) the spectral densities of the delay variations of the links. One important optimization problem is the design of remote control systems for clocks from a master clock over links affected by delay variations and noise. The result depends on the bandwidth of the control loop and the free running stability of the controlled clock.

1. INTRODUCTION

The purpose of this paper is to present some definitions, relations and practical data for the planning and design of network timing in digital communications systems. It is based on information which in most cases has already been published in various forms and also provides an update on the current work on recommended performance standards which is going on in the International Telephone and Telegraph Consultative Committee (CCITT) and the International Consultative Committee on Radiocommunications (CCIR) of the International Telecommunications Union (ITU).

There is a need for clarification of concepts and unification of language among the people working on new devices and systems related to the field of PTTI Applications.

The system planner and designer needs well established theoretical concepts. In addition, he needs a good feeling for the orders of magnitude for the relevant parameters. The data presented in this paper are mainly illustrative and not intended to promote a particular design or product.

In section 2 clock parameters are summarized. Section 3 deals with the concept of Time Interval Error and section 4 with transmission delay variations i.e. the degradation of timing information occurring on communication links. In section 5 the performance of a remote controlled clock is discussed by means of numerical examples.

2. CLOCK PARAMETERS

The performance of clocks is described by the following set of parameters.

- Environmental influences: - temperature
 - shock
 - acceleration
 - humidity
- Frequency drift or aging
- Random frequency instability

Environmental influences limit the performance of free running clocks. In the case of frequency controlled clocks, the control range will have to be large enough in order to compensate for these effects. Environmental specifications therefore constitute an important set of design parameters which often determine the choice of a system configuration and the requirements on the devices used. The values given in the numerical examples are for a mild environment typical for civi-

lian applications (Temperature +10 to +50°C, Humidity 30 to 80 percent relative, negligible shock and acceleration). Military or civilian mobile and aeronautical applications require other sets of parameters.

Assuming thus that we have environment under control, we can concentrate on the other two parameters, whereby these specifications include some residual environmental effects (e.g. the flicker frequency instability in most operational clocks).

Table 1 contains stability data on the following types of clocks

cesium
rubidium
crystal, oven controlled, high stability types

The aging coefficients are upper limits derived either from manufacturer's specifications or from operational experience. Four different types of crystal oscillators have been considered.

No. 1 is a 5 MHz commercial type in wide use today
No. 2 is a less expensive small oven controlled VCXO
No. 3 is a low noise 10 MHz VCXO
No. 4 is a projection of new designs

The random instability coefficients are those of the well known theoretical model [1-6] recommended by the CCIR [7] and based on the spectral density of normalized random frequency departures:

$$S_Y(f) = h_{-2}f^{-2} + h_{-1}f^{-1} + h_0f^0 + h_1f^1 + h_2f^2 \quad (1)$$

$$\text{with } y(t) = \frac{v-v_0}{v_0}$$

v being the actual "instantaneous" value of the frequency, v_0 the nominal value and f the "Fourier"-frequency. The values in the table are computed from the time-domain data given by the manufacturers as the square root $\sigma_Y(\tau)$ of the two-sample Allan-variance, using the relation:

$$\begin{aligned} \sigma_Y^2(\tau) = & h_{-2} \frac{4\pi^2\tau}{6} + h_{-1} 2\ln 2 + h_0 \frac{1}{2\tau} \\ & + h_1 \frac{1}{4\pi^2\tau^2} (4.5 + 3\ln(2\pi f_H \tau) - \ln 2) + h_2 \frac{3f_H^2}{4\pi^2\tau^2} \end{aligned} \quad (2)$$

where f_H is the upper cutoff frequency of the measurement system used to measure $\sigma_Y(\tau)$, and τ the sampling time.

The figures given are all conservative upper limits, usually guaranteed by the manufacturers and not so-called "typical" values which often tend to be optimistic. Only the crystal oscillator example No. 4 constitutes a projection not yet confirmed by large scale operational experience, but prototype results are available [8].

The values missing from the table have not been included because they are either not significant for the applications discussed in this paper (short term, high f fluctuations for Cesium and Rubidium) or small compared to the other terms (h_0 for crystal oscillators).

3. TIME INTERVAL ERROR

Timing is an essential function in any digital communications system. Therefore, international standards defining the minimum performance of the clocks used for network timing are required in order to achieve world-wide digital communication. The CCITT Study Group XVIII working on standardization of digital networks has issued a Recommendation G811 in 1976 (9). A revised edition will be published in 1981 after the recent 6th General Assembly (Geneva 10-24 November 1980). This document specifies the minimum performance of clocks suitable for plesiochronous operation of international, i.e. border-crossing digital links. Plesiochronous operation between networks means that each network is controlled by a master or reference clock which is free-running with respect to that of the neighbouring network. This requires close tolerance frequency adjustment and high stability in order to keep the rate of occurrence of slips below one in 70 days in any 64 kbit/s channel.

The long term normalized frequency departure must therefore be less than 1 part in 10^{11} in normal operation. The probability of degradation to 1 part in 10^9 shall be less than 10^{-5} and that of unavailability less than 10^{-6} .

The clock performance limits are defined as a maximum allowable Time Interval Error (TIE):

$$\text{TIE}(t) = \Delta T(t+\tau) - \Delta T(t) \quad (3)$$

where ΔT is the time difference between the actual timing signal and an ideal timing signal. Using a more familiar notation [2, 3, 4, 6, 7] we have for any time interval τ :

$$\text{TIE}(t_0) = x(t_0+\tau) - x(t_0) = \int_{t_0}^{t_0+\tau} y(t)dt \quad (4)$$

For a clock which has been adjusted to the nominal frequency and synchronized at $t=0$, the probable time interval error $\sigma_x(t)$ can be estimated. $\sigma_x(t)$ is the standard deviation of the time departures of an ensemble of identical clocks having random instabilities described by the model of equation 1. The following relation has been demonstrated by means of computer simulations [10];

$$\sigma_x(t) = t \left(\sigma_{y0}^2 + \sigma_y^2 (\tau=t) \right)^{1/2} \quad (5)$$

σ_{y0} is the standard deviation of the initial frequency adjustment and $\sigma_y(\tau)$ the two sample standard deviation (square root of equation 2) describing the random frequency instability. It is assumed that the parameters characterizing the clock do not change with time and that the initial adjustment error and the subsequent random frequency fluctuations are statistically independent. In addition to the random instability and the initial adjustment error, frequency drift has to be considered and this leads to a combined systematic and random estimate of the TIE

$$\text{TIE}_{\text{est.}} = \frac{a}{2} t^2 + t \left(\sigma_{y0}^2 + \sigma_y^2 (\tau=t) \right)^{1/2} \quad (6)$$

Eventually, significant cyclic environmental effects will have to be included, too. The method of estimating the TIE using equation 6 has been discussed in the CCIR Study Group 7 and included in a draft Report [11].

The allowed limit of the TIE recommended in CCITT G811 is shown in Fig. 1.

On the short term we see different curves which depend on the bit rate of the communications channel considered. This is due to the fact that the limit defined in this range is $100 \tau + 1/8$ unit interval, expressed in nanoseconds where the unit interval is the inverse of the bit rate.

In a real situation the random component of the time departure determines a finite probability of violation which can be computed for the model described above. A recommended value will have to be defined after further study.

4. TRANSMISSION DELAY VARIATIONS

The systematic and random departures of the timing instants from the ideal periodic timing waveform are designated by the terms of "jitter" and "wander". In the literature we find these departures referenced either to the signal period (phase jitter) or to a reference time

scale (timing jitter). The latter form is to be preferred since it does not depend on the particular bit rate.

The distinction between jitter and wander is at present not very precisely defined. One could treat it as a matter of Fourier Frequency since most specifications of jitter spectral density and jitter transfer functions stop at the low end around about 20 Hz.

In a recent update on synchronization [12] one finds some examples extending the frequency domain to quite lower values for spectral densities having the character of white phase (or timing) noise.

The word "wander" appears in some CCITT documents as a designation for slow systematic and random phase or time fluctuations.

The time fluctuations observed at the receiving end of a transmission link are the sum of the fluctuations originating in the clock at the transmitting end and the path delay fluctuations [13]. The planning and design of a network timing system requires quantitative knowledge of both phenomena. As summarized in sections 2 and 3 we have a fairly complete picture on the modeling of clock performance. Reliable data on path delay variations are more difficult to obtain. This may be due to the large variety of transmission systems in use or under development and to the fact that long term path delay measurements on operational transmission systems are much more difficult to organize than laboratory measurements on oscillators. Therefore, the data given below are neither complete nor definitive but rather an illustration of orders of magnitude to be expected and subject to some revision.

The best known example of jitter accumulation on long transmission links is that occurring on the lowest hierarchy PCM links with a bitrate of 1544 kBit/s (USA and Japan) or 2048 kbit/s (Europe). The basic theory has been established many years ago [14] and recent measurements known to the author [15, 16, 18] appear to confirm the theoretical predictions. The spectral density of the timing jitter has the general approximate form shown in Fig. 2. This figure represents an envelope drawn above the spectrum which is more complex and has maxima and minima depending on the digital word structure or pattern of the signal. Using the envelope for design purposes is a conservative approach. The timing jitter spectral density envelope can be described by

$$S_x(f) = h_{200} \left(1 + \frac{f}{f_B} \right)^{-1} \quad (7)$$

where h_{200} and f_B are functions of the number N of cascaded regenerators and the bandwidth or Q of the regenerator timing circuit.

Fig. 3 shows this dependence on N for two examples: passive LC circuit regenerators with $Q = 80$ and PLL-type regenerators with $Q = 500$.

We see that for Fourier frequencies below f_B , the PCM-line jitter has the character of white timing (or phase) noise.

For random, zero mean normally distributed test signals this property appears to be true for arbitrarily low Fourier frequencies. For real voice and data traffic the statistics can be different. However, modern coding techniques tend to approach random or pseudo-random signal statistics. Similar descriptions of transmission delay statistics can be developed for all kinds of digital transmission systems. A complete review is beyond the scope of this paper.

Systematic slow delay variations are mainly caused by environmental influences on the transmission medium. In the case of satellite systems, the dynamics of the system configuration [orbit parameters] play a major role.

Temperature coefficients of metallic and optical fibre cables are summarized in Table 2. These figures are orders of magnitude and may vary depending on the cable type and manufacturer. A published reference [17] has been found only for the optical fibers, the other data have been gathered from various unpublished reports. The temperature variations show a daily and yearly cycle which depends on the climatic conditions. In temperate regions such as Europe an average temperature of $+10^\circ\text{C}$, a peak-to-peak range of 20°C (year) and 2°C (day) can be expected.

For transmission over a geostationary satellite, a 24 hour cyclic variation of the transmission delay is due to imperfect orbital parameters (eccentricity, inclination). Taking into account the necessity of improved stationkeeping due to the increasing population on the geostationary orbit, a peak-to-peak daily delay variation of 600 microseconds should not be exceeded. Long term drift and orbit repositioning will cause additional variations [20]. Terrestrial microwave links over line of sight paths are known to be very stable, probably less than 5 nanoseconds variation due to the radio path itself.

A mostly unknown parameter is the delay variation due to environmental conditions acting on the equipments used in the various transmission systems. Much work remains to be done and it is surprising to note that J.R. Pierce's plea for information on this matter in 1969 [19, p. 629] went almost unnoticed. Whereas theoretical work is abundant and sometimes elaborate in the published literature [12], reliable experimental data on transmission delay variations still remains scarce. It is therefore difficult to see which and what part of the many theoretical approaches are really relevant for operating system design.

For a given transmission system, the quantitative description of delay variations must comprise both random and cyclical components. The random component is conveniently represented in the form of a timing fluctuation spectral density $S_x(f)$. It is at present not known if low frequency divergent terms (flicker or random walk) are significant at very low Fourier Frequencies. If such effects exist, they are probably small compared to the effects caused by temperature cycles. Accumulated statistics on extended systems subject to many temperature cycles with different amplitudes and phases could result in a flicker-like spectrum having significant density down to frequencies of one cycle per year. There is however a fundamental difference between transmission delay and clock time variations: The electrical length of the transmission path is always finite and its variations remain within physically limited bounds, whereas the time departure of any real clock grows without bounds.

5. REMOTE CONTROLLED CLOCK

The problem of remote control of the timing properties of a clock over a transmission link arises whatever the type of system organization chosen in practice, i.e. mutual synchronization, hierarchical master-slave (HMS) or any of possible combinations, refinements and self-organization schemes [21, 22]. The basic system elements are always a reference clock, a transmission link and another clock the time and frequency of which is to be controlled by some means in order to obtain the fulfillment of a specification such as CCITT Rec. G811. The reference might be itself a controlled clock or a free running master. The examples discussed in this section are on a quite elementary level compared to those discussed in recent publications [23-26], but include spectral density models of the transmission time jitter and of oscillator instability based on real data.

In most systems currently in operation and under development, the hierarchical master-slave (HMS) type of operation is applied. HMS is straightforward and fits well into the structure of existing public networks at the local and regional level. Compliance with CCITT Recommendation G811 requires that master clocks are accurate in frequency with an uncertainty of less than ± 1 part in 10^{11} and this implies reference to the frequency of UTC. Cesium clocks operated in a reasonable environment are accurate and stable enough to satisfy the requirements with only a minimum of surveillance and very few, if any readjustments. Rubidium and crystal clocks require initial frequency setting and subsequent frequency control from an external reference to compensate for the inherent frequency drift (aging).

Figures 4 and 5 show the time-domain frequency instability $\sigma_y(\tau)$ of typical cesium, rubidium and crystal clocks based on the data of Table 1.

Fig. 6 shows the estimated time interval error for some clocks (see table 1) operated in the free running mode. It is thereby assumed that each of these clocks has been adjusted in frequency and synchronized at $t=0$.

The uncertainty σ_{y0} of the initial frequency adjustment for each type of clock is assumed to be minimized, i.e. the averaging time for the measurement used for the readjustment is chosen so that the uncertainty corresponds to the minimum, flat portion ("flicker-floor") of the $\sigma_y(\tau)$ diagram of Fig. 4 and 5 respectively. In some cases, noise in the process of measurement through a transmission link may lead to a higher value of σ_{y0} and this must be taken into account in such situations. Figure 6 gives an idea of the possibilities of manual readjustment based on measurements. It allows to determine how long a lower hierarchy clock can be operated in the free-running mode within the specified limits of G811 after interruption of the link to the master clock. It is assumed that the frequency control system memorizes the last valid setting of the oscillator control before the interruption [27, 28]. It turns out that a cesium clock can be operated indefinitely, a rubidium clock ($a = 1 \cdot 10^{-11}$ per month) for 52 days and crystal oscillators No. 1 ($a = 3 \cdot 10^{-11}$ per day) for 1.6 days and No. 4 ($a = 5 \cdot 10^{-12}$ per day) for 5.2 days.

To illustrate further the operation of a remote controlled clock, Figure 7 shows a block diagram comprising a cesium master clock, a PCM link as mentioned in section 4 and a crystal oscillator controlled by the most elementary form of a phase-locked-loop, i.e. a first order PLL having a single pole RC loop filter. The jitter transfer analysis of the PLL is made using the phase-time formalism described in [4, p. 188 ff].

Table 3 shows the formulas used in the computations of $\sigma_{y4}(\tau)$ describing the random frequency instability of the slave oscillator. Then the estimated time interval error of the slave oscillator is computed using the relation:

$$TIE_4(t) = t \sigma_{y4}(\tau=t) + \frac{at}{K_x} \quad (8)$$

The first term is similar to equation 5 and the second term is due to the fact that we use a first order PLL, a is the aging coefficient of the slave oscillator. If the slave oscillator is to be controlled over a noisy link, a low value of K_x ("loose control") is desired but then the second term shows the possible limit of improvement obtainable for a slave oscillator having a given aging coefficient.

The input data for the numerical examples are given in the Tables 4 and 1. The figures which follow show a selection of some typical cases.

Figure 8 shows the spectral density $S_{y_4}(f)$ of the controlled oscillator output for the 4 slave oscillators considered, both values of K_x shown in Table 4 and with and without the PCM line jitter.

Figure 9 shows the corresponding time domain stability $\sigma_{y_4}(\tau)$.

Figure 10 shows the TIE estimate obtained by means of equation 8.

It is to be emphasized that these results do not constitute a design proposal. They are shown to illustrate the relation between reference instability, line timing jitter, control loop parameters and slave oscillator instability using a simple PLL-Control System.

In a practical design, step frequency control with a memory and provided with a fast acquisition mode as described in [27, 28] or perhaps higher order or microprocessor controlled adaptive systems are or will be used. There is not much difference between the loop transfer function H_x in our illustrative example and those used in [27, 28], except for the larger computation effort required for the analysis of these more sophisticated designs.

The difference between the computed TIE estimate and the design limit imposed by Rec. G811 constitutes a margin in which the systematic cyclic delay variations remain to be included. The allowed amplitude of these variations depends on the probability of violation allowed in the design.

In the case of directed control HMS, the type of transmission medium limits the allowable distance between master and slave clocks. Double-ended timing [22] can in principle reduce the effect of slow delay variations but the delays involved in the back and forth transmission of timing information may change the transient response of the control system and careful analysis is required in order to ascertain the stability of the control.

6. CONCLUSIONS

The basic parameters relevant to the design of network timing systems describe the random and systematic time departures of the system elements, i.e. master (or reference) clocks, transmission links and other clocks controlled over the links. Using the definitions and notations recommended in CCIR and CCITT texts, the quantitative relations between these parameters have been established and illustrated by means of numerical examples based on available measured data. The examples have been limited to a simple PLL-control system but the analysis can eventually be applied to more sophisticated systems at the cost of increased computational effort.

The author gratefully acknowledges the contribution of Kurt Hilty who did the programming for the computations of the numerical examples.

REFERENCES

- [1] Proc. IEEE, vol. 54, no. 2, Feb. 1966. Special Issue on Frequency Stability.
- [2] J.A. Barnes et al., "Characterization of Frequency Stability", IEEE Trans. Instrum. Meas., vol. IM-20, pp. 105-120, May 1971.
- [3] B.E. Blair, Ed., "Time and frequency - Theory and fundamentals", NBS Monograph 140 U.S. Gov. Print. Off. SD Catalog C 13:44:140, May 1974.
- [4] P. Kartaschoff, Frequency and Time. London, England: Academic Press, 1978.
- [5] W.C. Lindsey and C.M. Chie, "Theory of oscillator instability based upon structure functions", Proc. IEEE, vol. 64, no. 12, pp. 1652-1666, Dec. 1976.
- [6] J. Rutman, "Characterization of phase and frequency instabilities in precision frequency sources: Fifteen years of progress", Proc. IEEE, vol. 66, no. 9, pp. 1048-1075 Sept. 1978.
- [7] CCIR Report 580-1 and Recommendation 538, Kyoto 1978, ITU Geneva.
- [8] R.J. Besson and D.A. Emmons, "Initial Results on 5 MHz Quartz Oscillators equipped with BVA-Resonators", Proc. 11th PTTI Conference, pp. 457-468, NASA Conference Publication 2129 (1979)
- [9] CCITT 6th Plenary Assembly, "Orange Book", Rec. G811, Vol. III-2, pp. 485-468, ITU, Geneva 1977.
- [10] P. Kartaschoff, Computer Simulation of the Conventional Clock Model, IEEE Trans. on Instrumentation and Measurement, Vol. IM-28, No. 3, pp. 193-197 (September 1979).
- [11] Draft Report AC/7, CCIR Study Group 7 Interim Meeting, Doc. 7/77, ITU Geneva (27 June 1980).
- [12] IEEE Transactions on Communications, Special Issue on Synchronization, Vol. COM-28, Nr. 8 (August 1980).
- [13] P. Kartaschoff, Frequency Control and Timing Requirements for Communications Systems, Proc. 31st Frequency Control Symposium, U.S. Army Electronics Command Ft. Monmouth, N.J. (1977), pp. 478-482.
- [14] C.J. Byrne, B.J. Karafin and D.B. Robinson, "Systematic jitter in a chain of digital regenerators", Bell Syst. Tech. J., vol. 42, No. 6, pp. 2679-2714 (November 1963).
- [15] A. Kaeser, "Quelques mesures de taux d'erreur et de gigue en ligne sur les systèmes à 2 Mbit/s sur câbles", Bull. Tech. PTT (Suisse), Vol. 54, No. 11, pp. 428-430 (November 1976).
- [16] A. Kaeser, private communication.
- [17] L.G. Cohen and J.W. Fleming, Bell Syst. Tech. J., Vol. 58, No. 4, pp. 945-951 (April 1979).
- [18] E.P. Graf, private communication.
- [19] J.R. Pierce, "Synchronizing Digital Networks" Bell Syst. Tech. J., Vol. 48, No. 3, pp. 615-636 (March 1969).
- [20] CCIR Reports 214 and 383, CCIR Vol. IV, ITU Geneva 1978 (revisions to be published).

- [21] H.A. Stover, "Suggested attributes for timing in a digital DCS", Proc. 11th PTTI Conference, pp. 15-26, NASA CP-2129 (1979).
- [22] H.A. Stover, "Network Timing/Synchronization for Defense Communications", see [12], pp. 1234-1244.
- [23] D. Mitra, "Network Synchronization": An Analysis of a Hybrid of Master-Slave and Mutual Synchronization, see [12], pp. 1245-1259.
- [24] W.C. Lindsey and A.V. Kantak, "Network Synchronization of Random Signals", see [12], pp. 1260-1266.
- [25] A. Kajackas, "On Synchronization of Communication Networks with Varying Channel Delays", see [12], pp. 1267-1268.
- [26] W.R. Braun, "Short Term Frequency Instability Effects in Networks of Coupled Oscillators", see [12], pp. 1269-1275.
- [27] E.A. Munter "Synchronized Clock for DMS-100 Family", see [12] pp. 1276-1284.
- [28] E.P. Graf and B. Walther, "Generation of Base-Band Frequencies for FDM and TDM Telecommunications, Proc. 31st Annual Frequency Control Symposium, pp. 484-488, USAEC. Ft. Monmouth, N.J. 1977.

TABLE 1

Type of clock	Aging	Random instability coefficients			
		$h_{-1}(s)$	h_0	$h_1(s^{-1})$	$h_2(s^{-2})$
Cesium	$<5 \cdot 10^{-13}/\text{year}$	$2,885 \cdot 10^{-26}$	$8 \cdot 10^{-21}$	-	-
Rubidium	$<1 \cdot 10^{-11}/\text{month}$	$1,803 \cdot 10^{-25}$	$5 \cdot 10^{-23}$	-	-
Crystal 1	$<3 \cdot 10^{-11}/\text{day}$	$7,2 \cdot 10^{-25}$	-	$9,4 \cdot 10^{-25}$	$3,13 \cdot 10^{-26}$
" 2	$<5 \cdot 10^{-10}/\text{day}$	$2,89 \cdot 10^{-22}$	-	-	$8,42 \cdot 10^{-25}$
" 3	$<5 \cdot 10^{-10}/\text{day}$	$7,23 \cdot 10^{-23}$	-	$7,88 \cdot 10^{-25}$	$7,88 \cdot 10^{-27}$
" 4	$<5 \cdot 10^{-12}/\text{day}$	$2,89 \cdot 10^{-26}$	-	$9,4 \cdot 10^{-26}$	$3,13 \cdot 10^{-27}$

TABLE 2

Type of cable	Temperature coefficient of delay in ns/km x °C
Symmetrical pair, wire diameter 0.8 mm paper insulation	3...5
Symmetrical pair, wire diameter 0.8 mm polyethylene insulation	0.3...0.75
Coaxial cable polyethylene/air insulation 1,2/4,4 mm 2,6/9,5 mm	0.03...0.075
Optical fibre SiO ₂ core [17]	0.035

TABLE 3

Input data:

Source:	(1)	(2)	(3)	(4)
	S_{y_1}	$S_{x_{\text{Line}}}$	$H_x(jw)$	$S_{y_{40}}$

Derivations: S_{x_1} $S_{x_{\text{Line}}}$ $S_{x_{40}}$

$$S_{x_2} = S_{x_1} + S_{x_{\text{Line}}}$$

Output:

$$S_{x_4} = S_{x_2} |H_x|^2 + S_{x_{40}} |1 - H_x|^2$$

Transformations:

$$S_{y_4} = 4\pi^2 f^2 S_{x_4}$$

$$\sigma_{y_4} = \frac{2}{\pi\tau} \int_0^u S_{y_4} \left(\frac{u}{\pi\tau}\right) \frac{\sin^4 u}{u^2} du$$

with $u = \pi f\tau$

General Relations used:

$$S_{y_i} = 4\pi^2 f^2 S_{x_i}$$

TABLE 3 (CONTINUED)

PLL-Data:	DC Loop Gain K_x $[s^{-1}]$
	Single pole RC Filter
	Time Constant T_1 $[s]$
	Damping ratio: $\zeta = \frac{1}{2\sqrt{K_x T_1}}$
	natural frequency $f_n = \frac{1}{2\pi} \sqrt{\frac{K_x}{T_1}}$

Loop transfer
function:

$$|H_x|^2 = \frac{1}{(1-\Omega^2)^2 + 4\Omega^2\zeta^2}$$

$$|1 - H_x|^2 = \Omega^2(2\zeta + \Omega)^2 |H_x|^2$$

$$\text{with } \Omega = \frac{f}{f_n}$$

TABLE 4

$$S_{y_1} = 2.885 \times 10^{-26} f^{-1} + 8.0 \times 10^{-21}$$

$$S_{x_{\text{Line}}} = 2.49 \cdot 10^{-16} \cdot \text{max. Jitter} \quad \begin{array}{l} N = 552 \\ Q = 80 \end{array}$$

PLL parameters

$$1) K_x = 10^{-3} s^{-1} \quad \zeta = \frac{1}{\sqrt{2}} \quad f_n = 2.3 \times 10^{-4} \text{ Hz}$$

$$2) K_x = 0.1 s^{-1} \quad \zeta = \frac{1}{\sqrt{2}} \quad f_n = 2.3 \times 10^{-2} \text{ Hz}$$

(Crystal Oscillator Parameters see Table 1)

Measurement system cutoff frequency

for time-domain instability $\sigma_y(\tau)$

$f_H = 1000 \text{ Hz}$ for all cases.

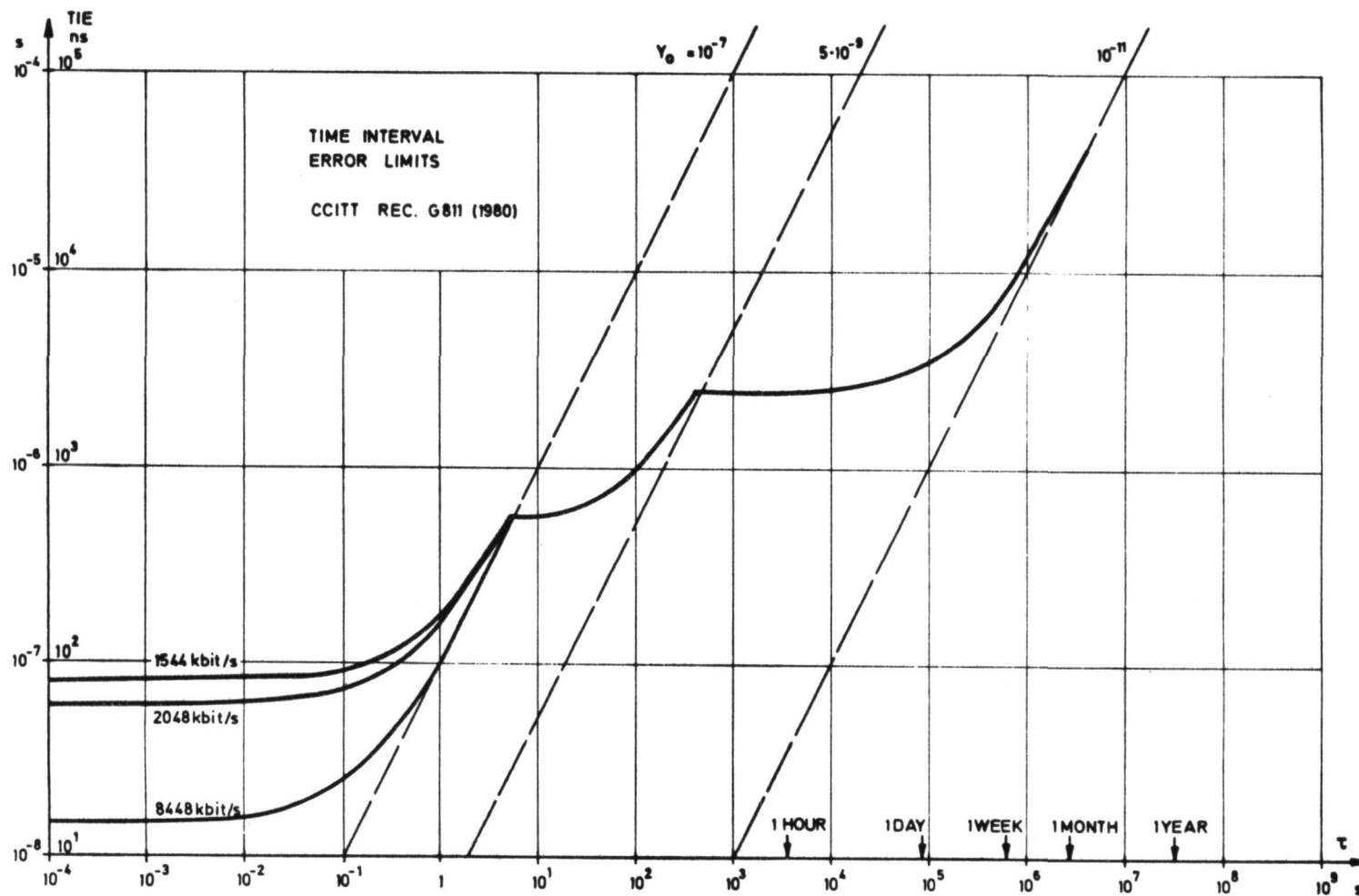


Fig. 1 Time Interval Error Limits, CCITT Rec. G811 (Draft Revision 1980)

Fig. 2 PCM Timing Jitter Spectral Density

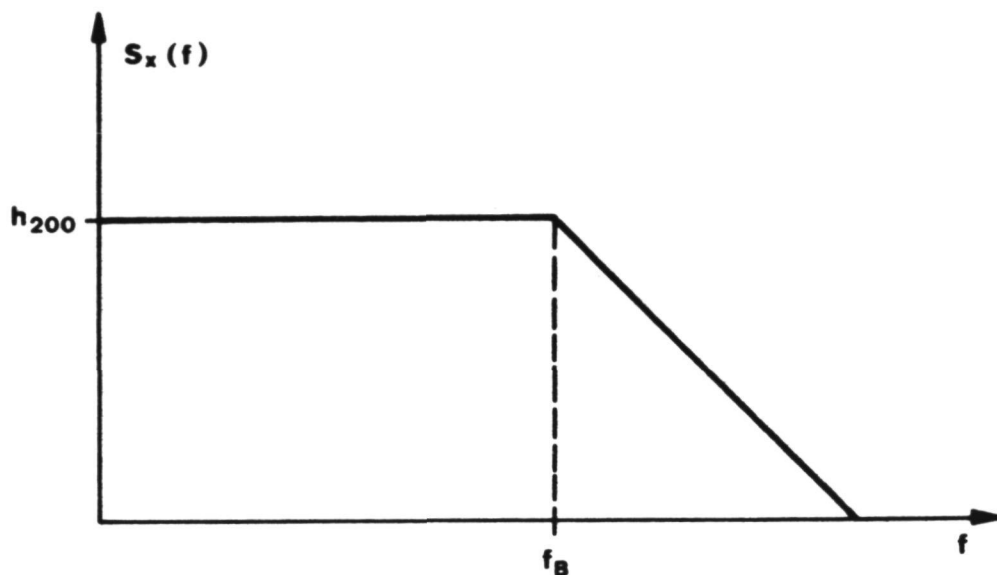


Fig. 3 PCM Timing Jitter Parameters

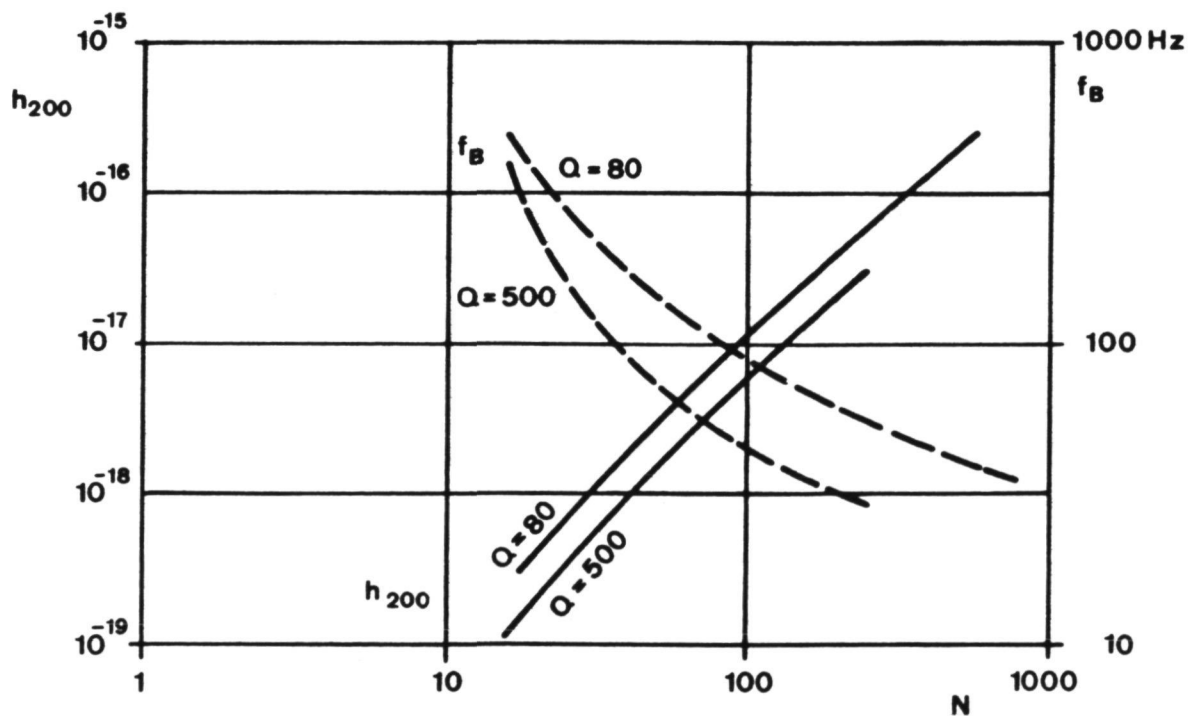


Fig. 4

Cesium and Rubidium clock instability

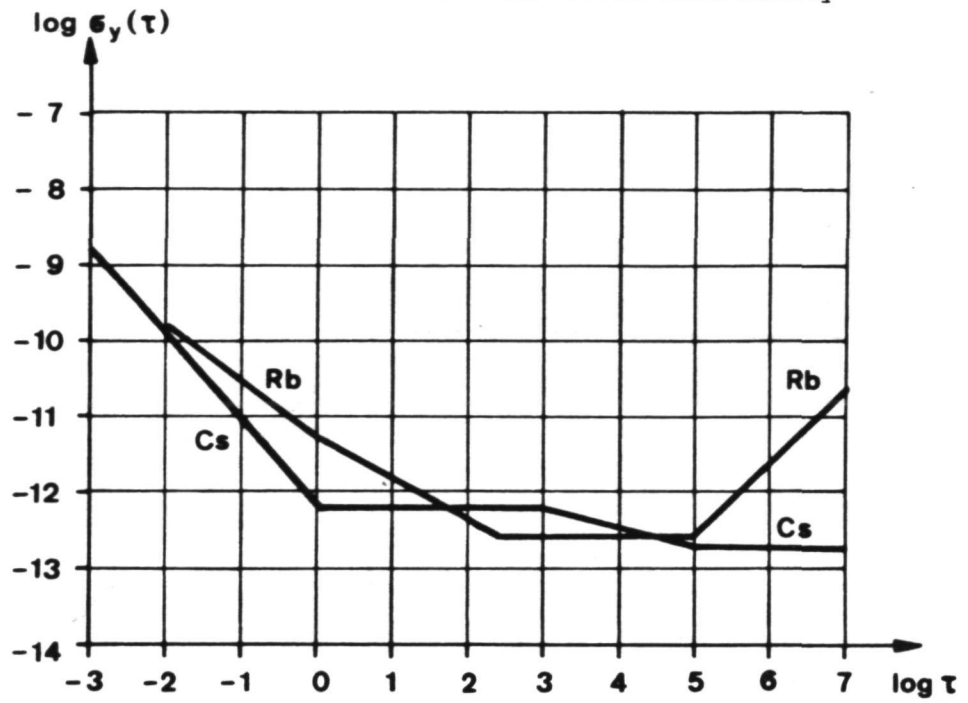
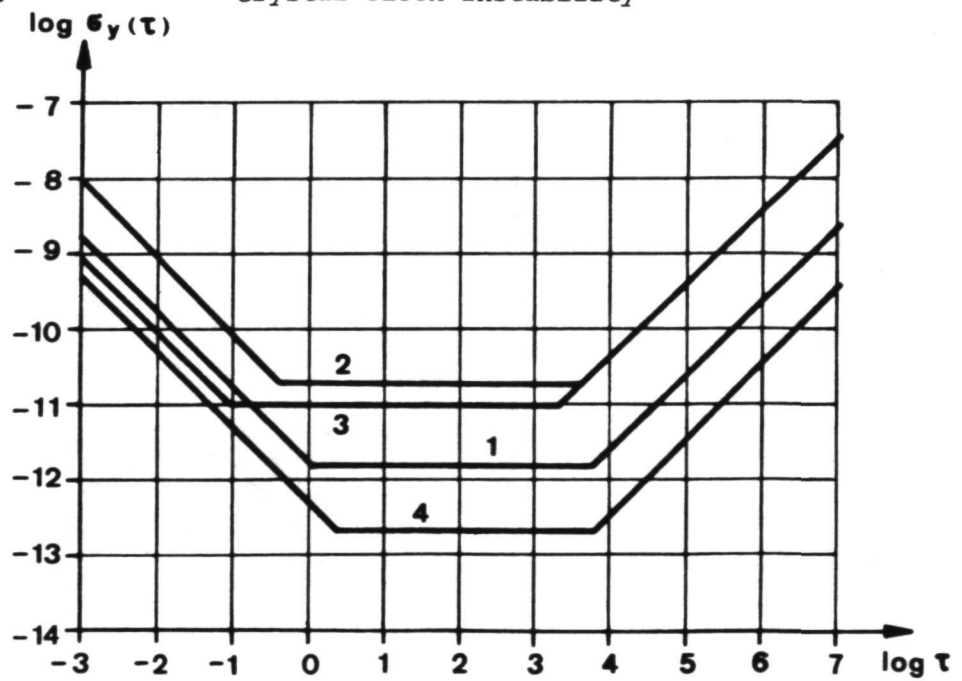


Fig. 5

Crystal clock instability



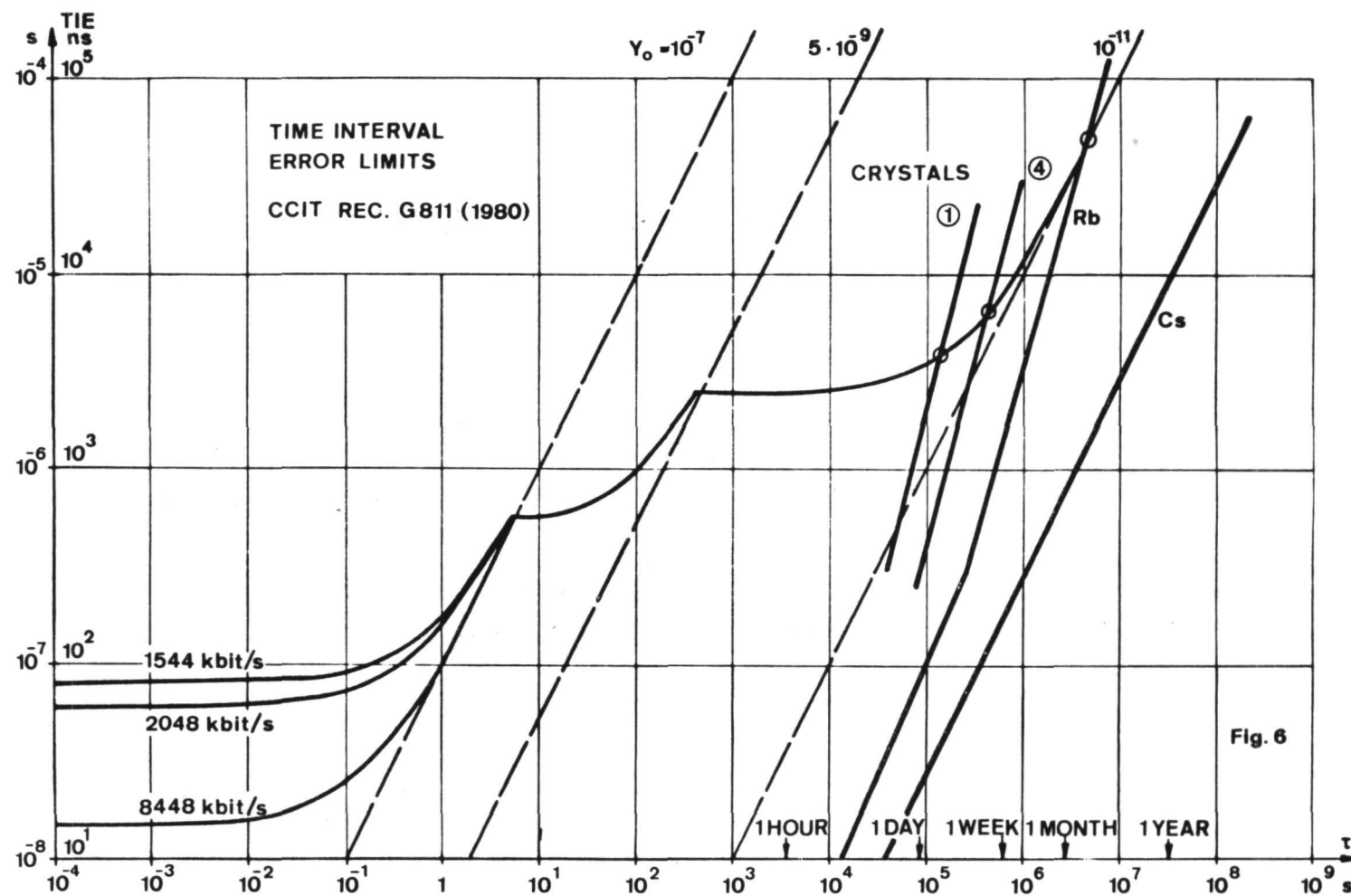


Fig. 6 TIE for free running clocks

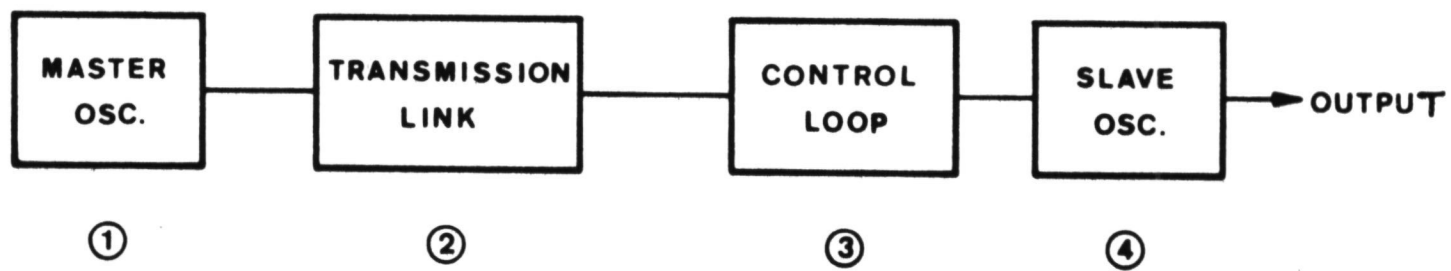


Fig. 7

REMOTE CONTROLLED CLOCK

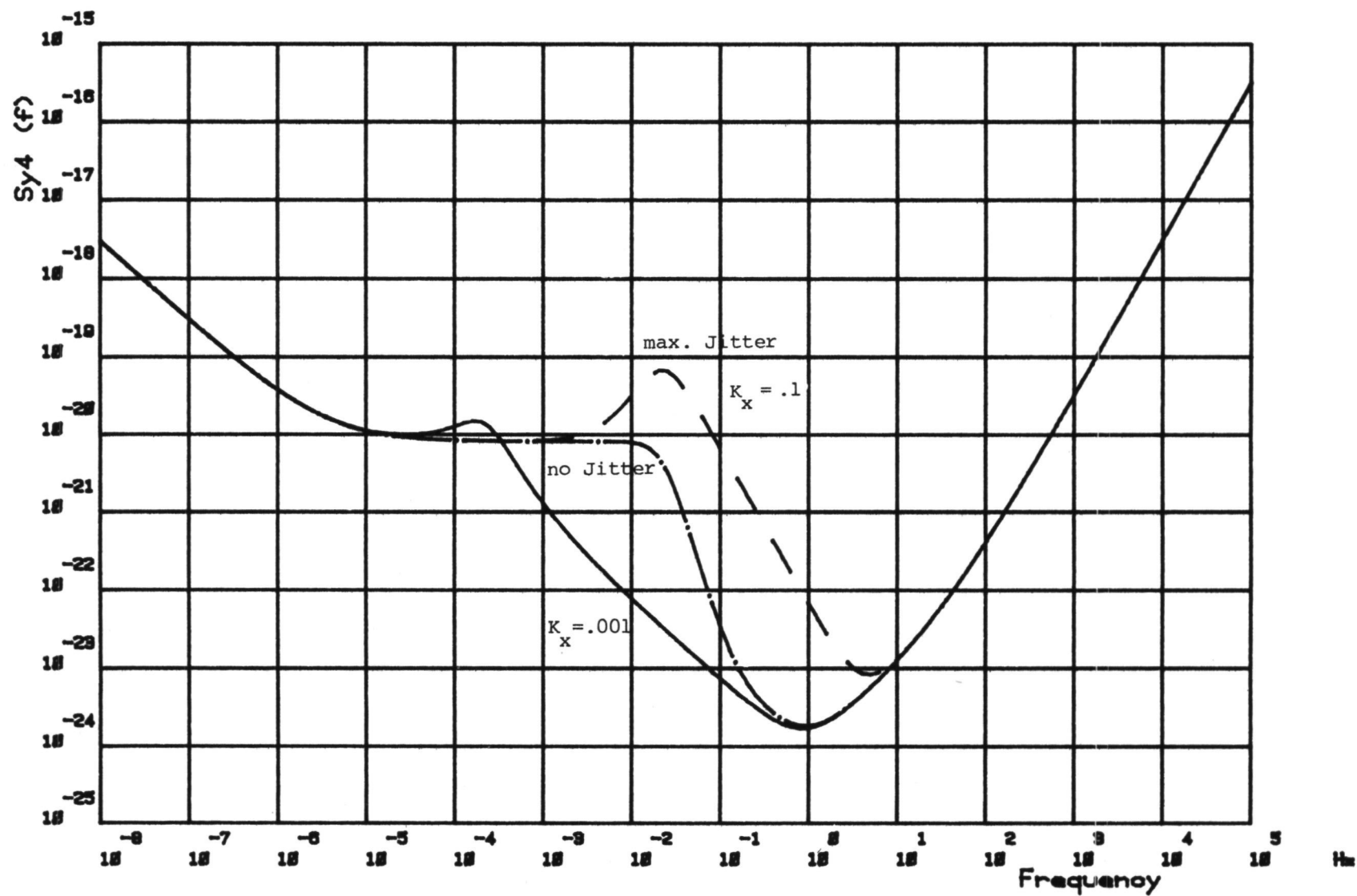


Fig. 8 a) Controlled oscillator frequency domain instability, slave oscillator No. 1

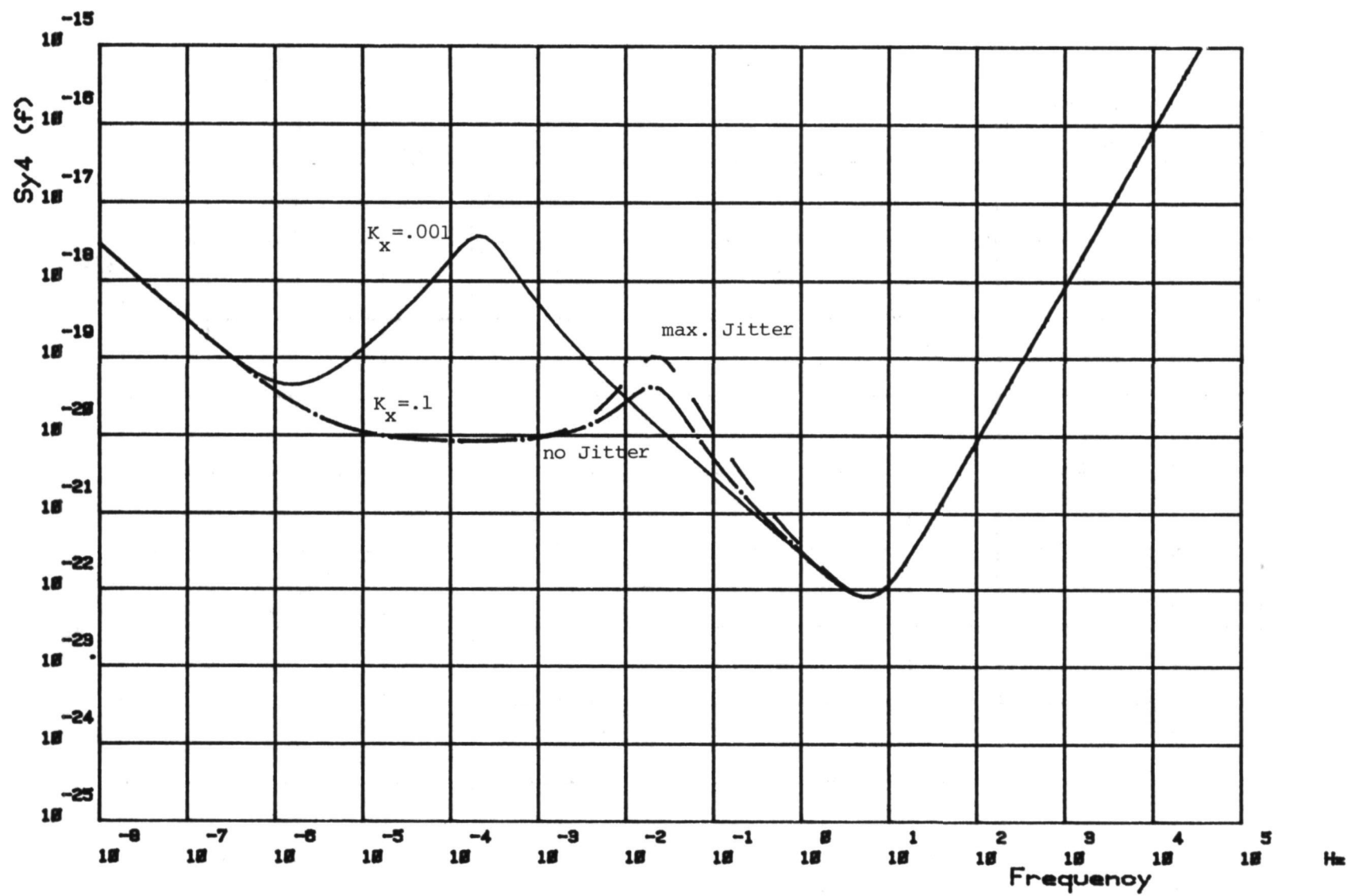


Fig. 8 b) Controlled oscillator frequency domain instability, slave oscillator No. 2

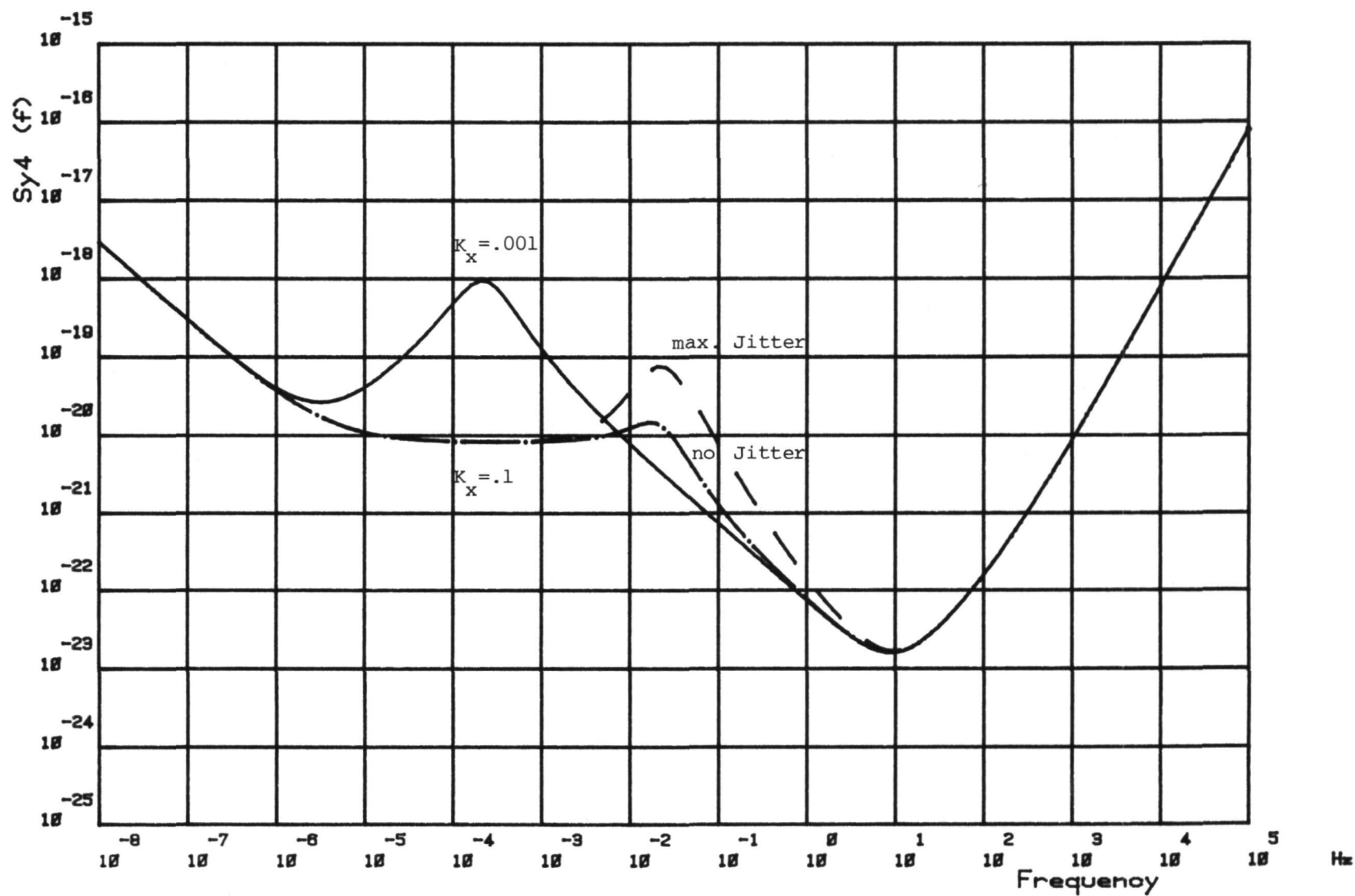


Fig. 8 c) Controlled oscillator frequency domain instability, slave oscillator No. 3

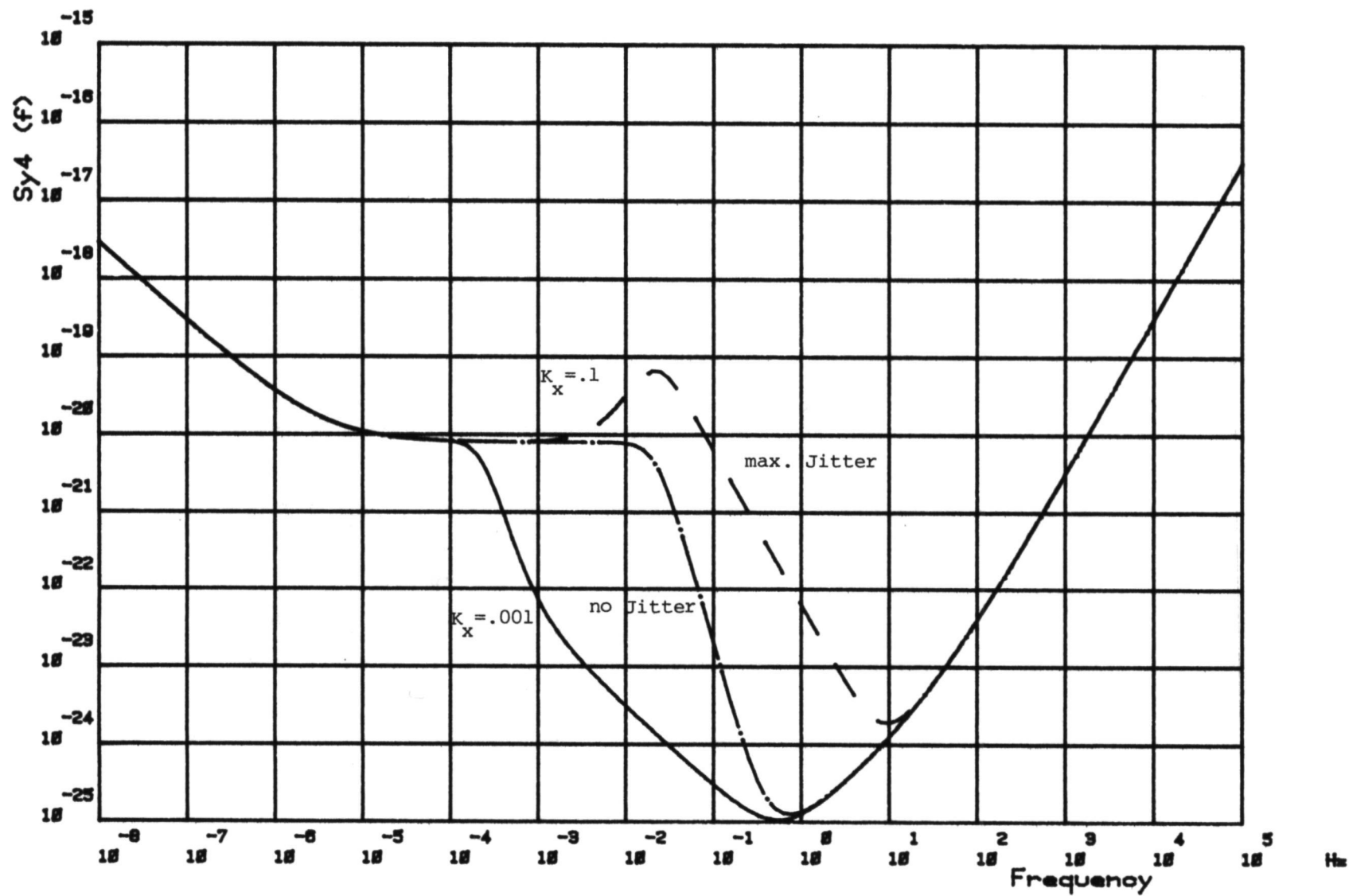


Fig. 8 d) Controlled oscillator frequency domain instability, slave oscillator No. 4

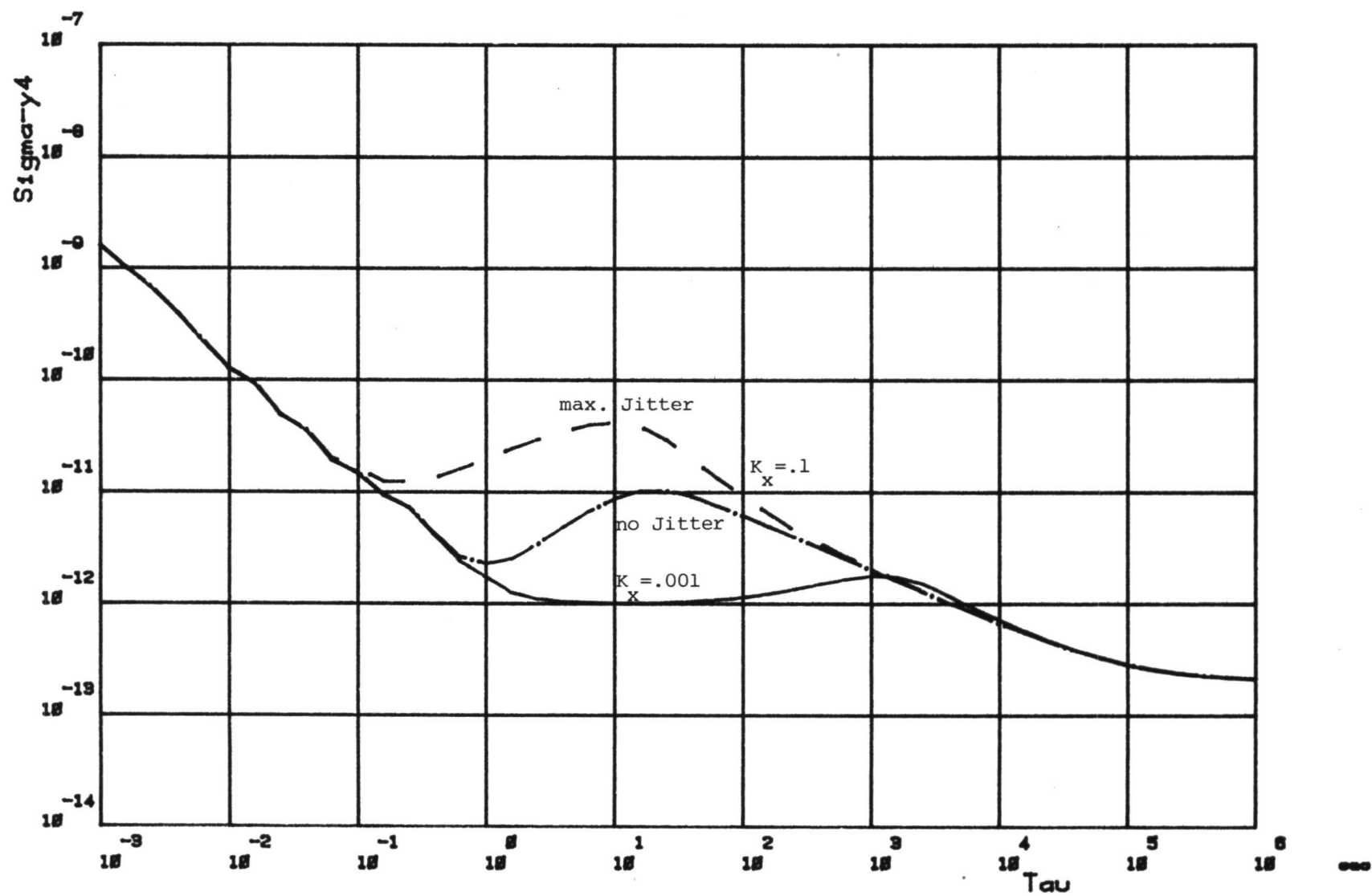


Fig. 9 a) Controlled oscillator time-domain instability, slave oscillator No. 1

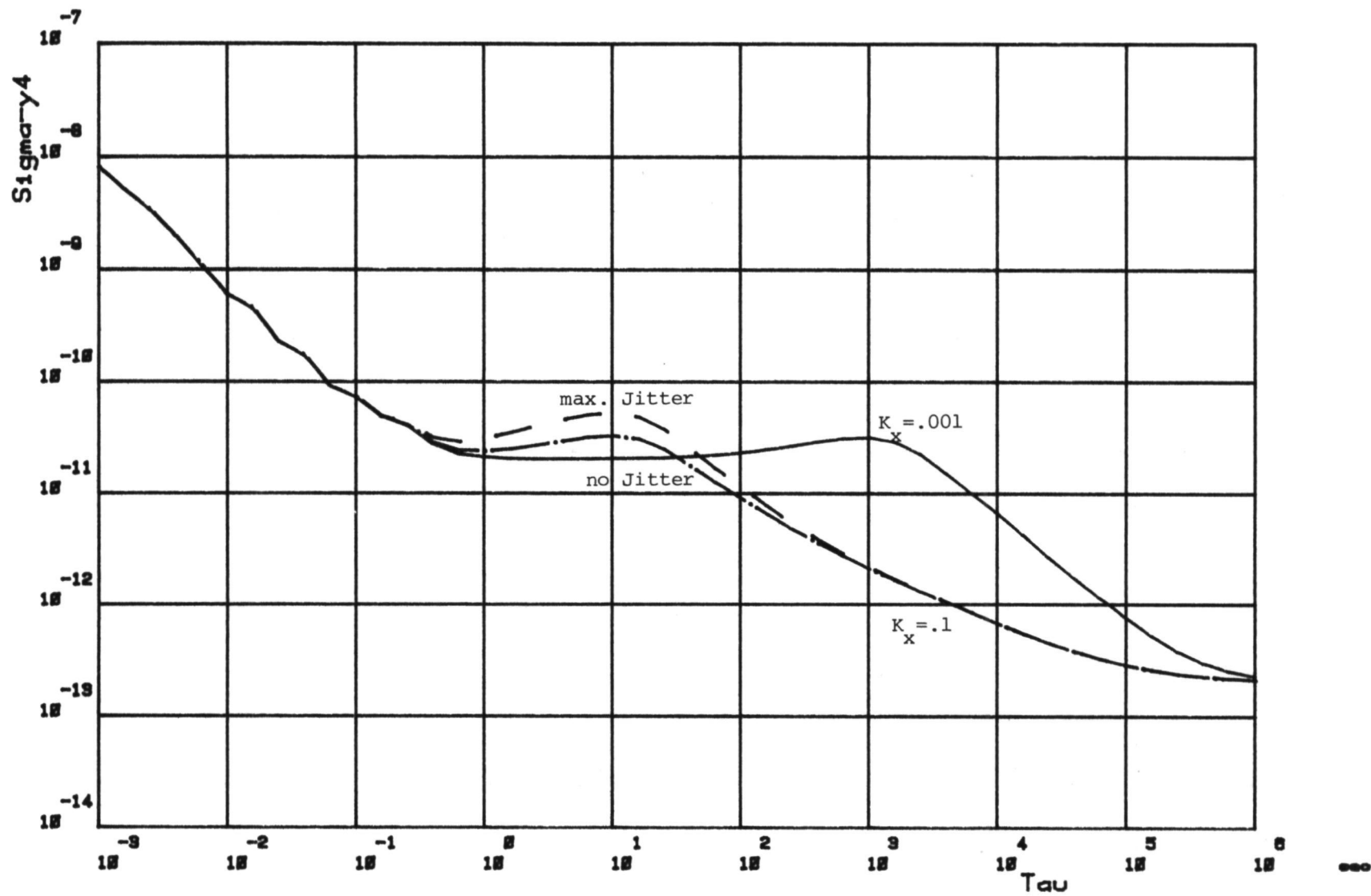


Fig. 9 b) Controlled oscillator time-domain instability, slave oscillator No. 2

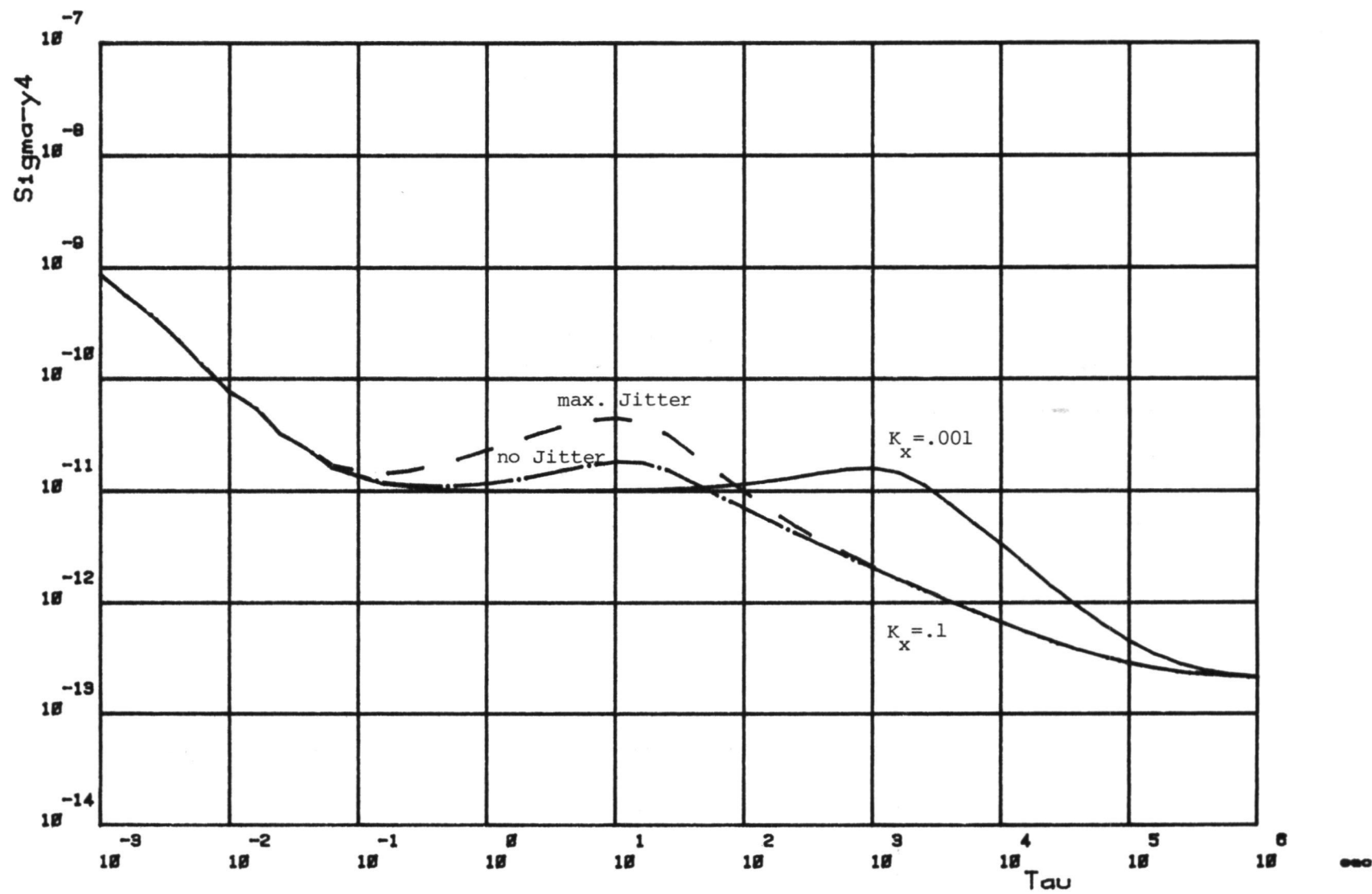


Fig. 9 c) Controlled oscillator time-domain instability, slave oscillator No. 3

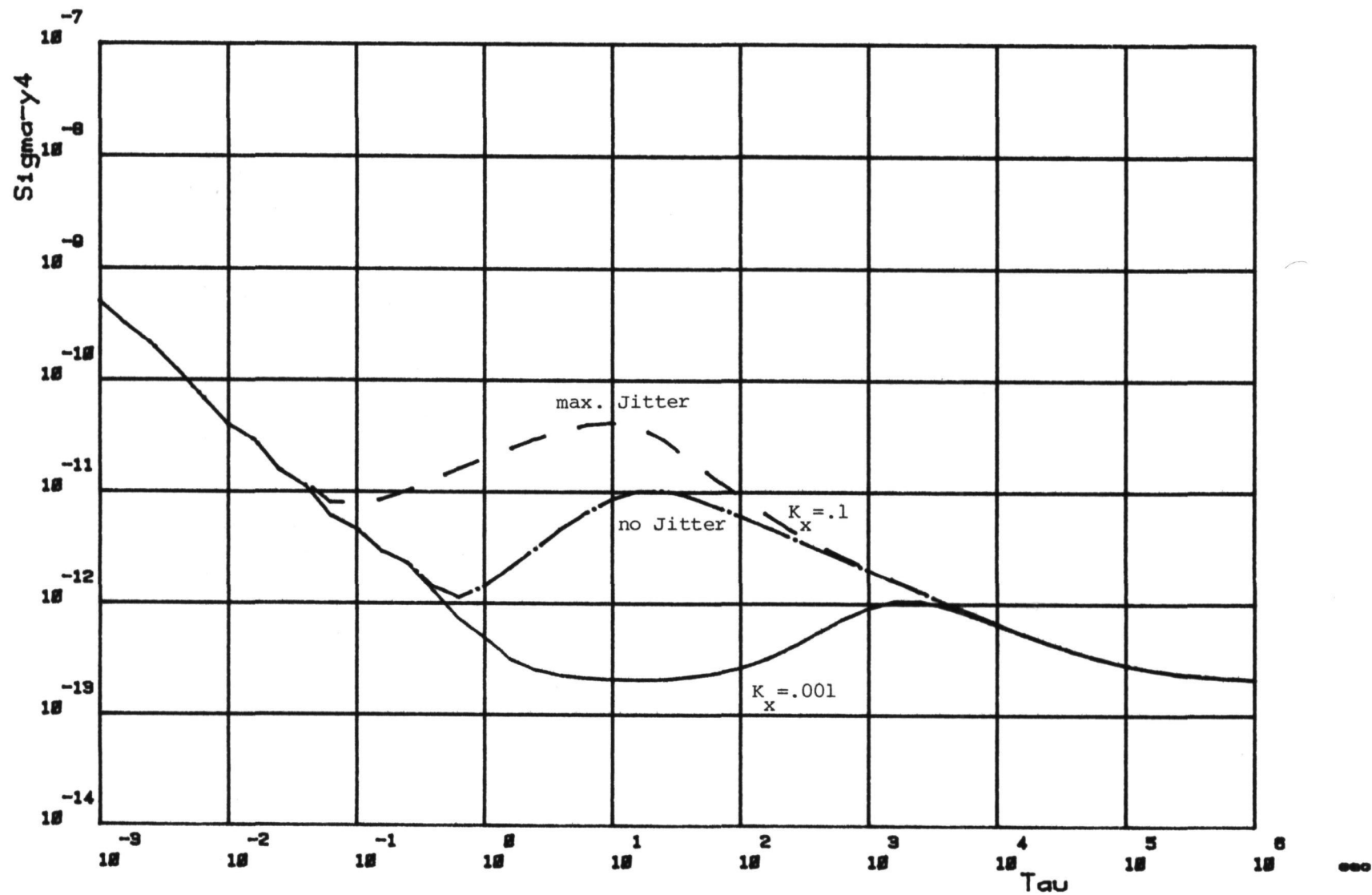


Fig. 9 d) Controlled oscillator time-domain instability, slave oscillator No. 4

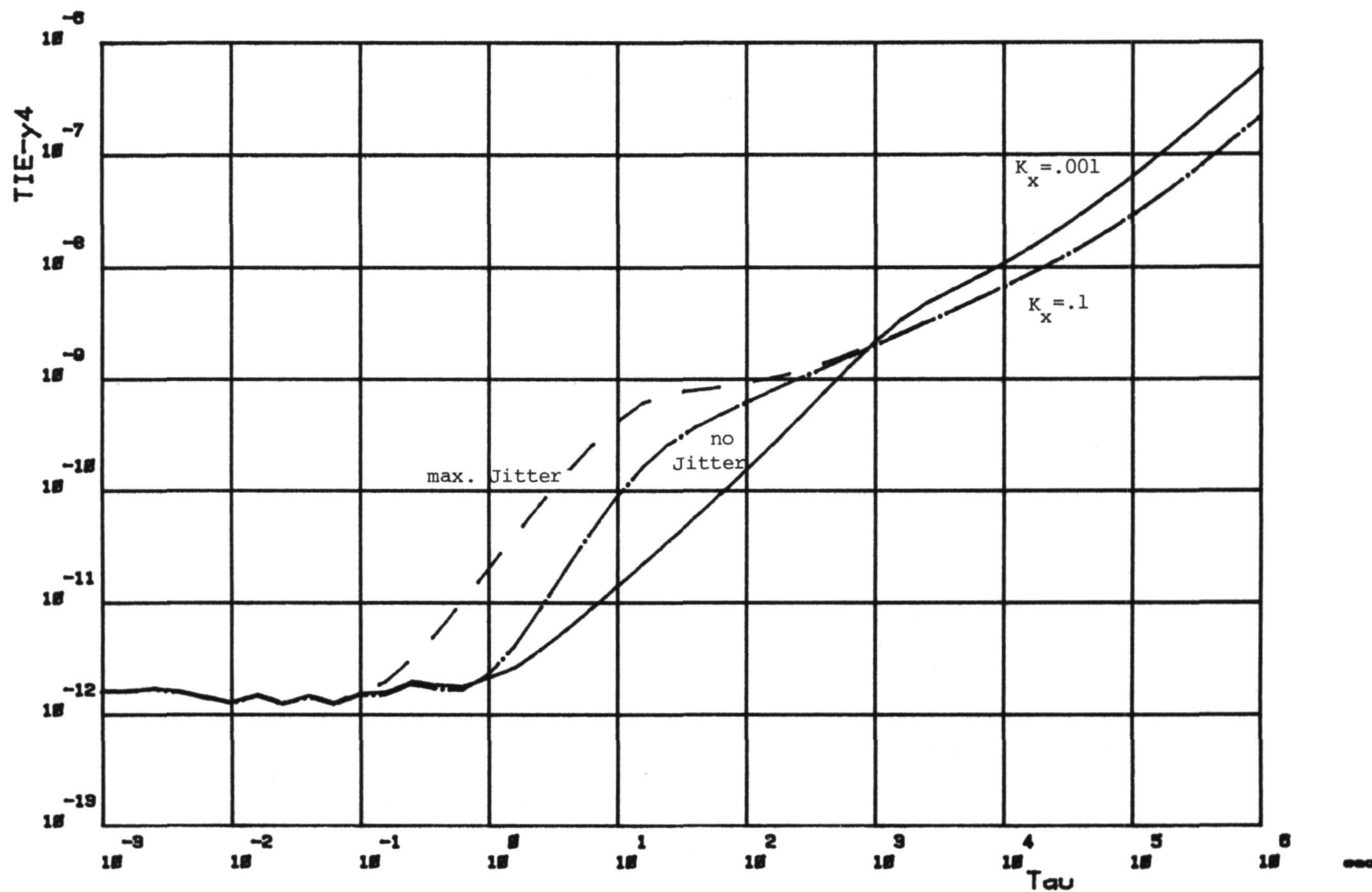


Fig. 10 a) Controlled oscillator time interval error, slave oscillator No. 1

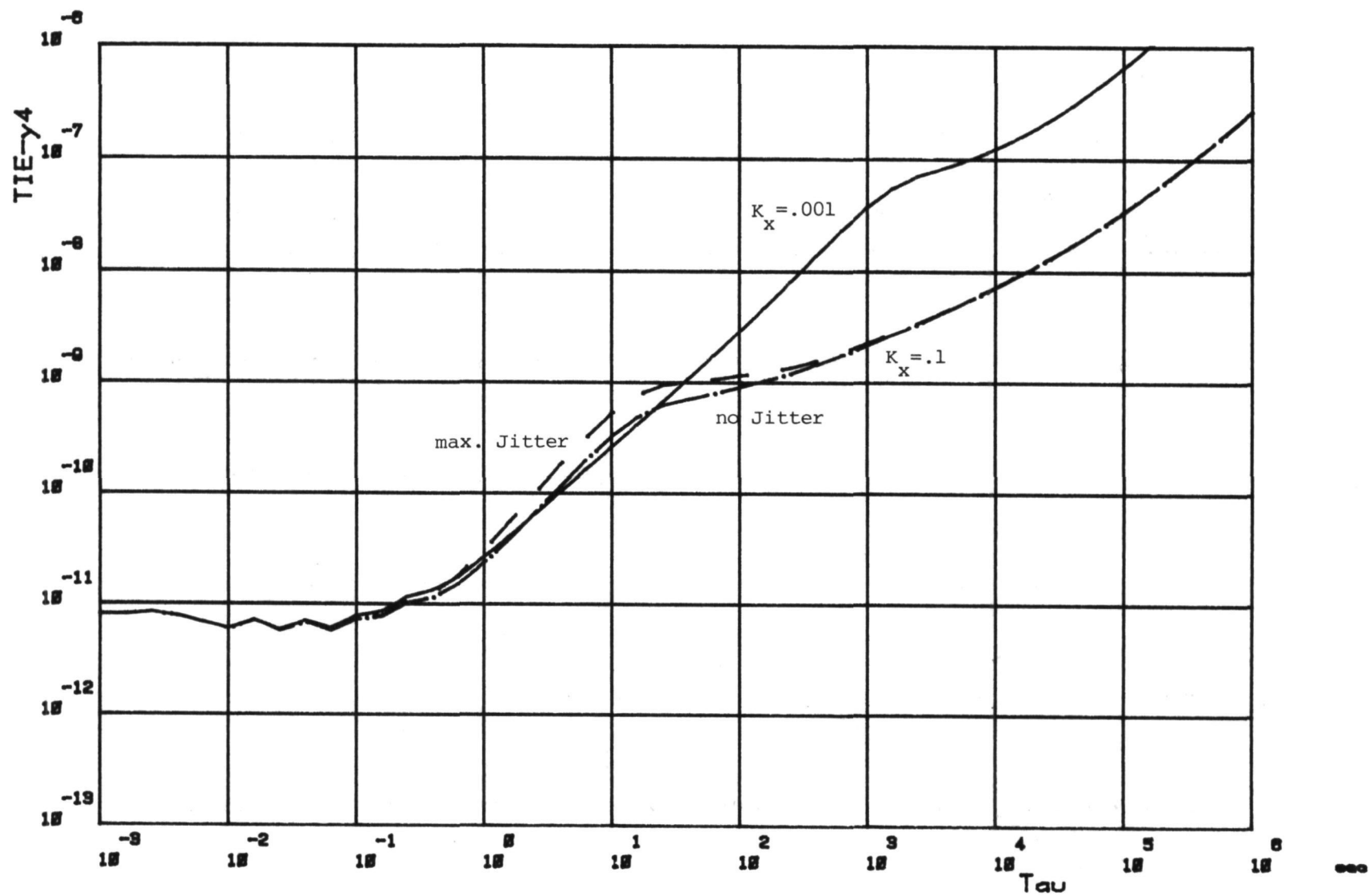


Fig. 10 b) Controlled oscillator time interval error, slave oscillator No. 2

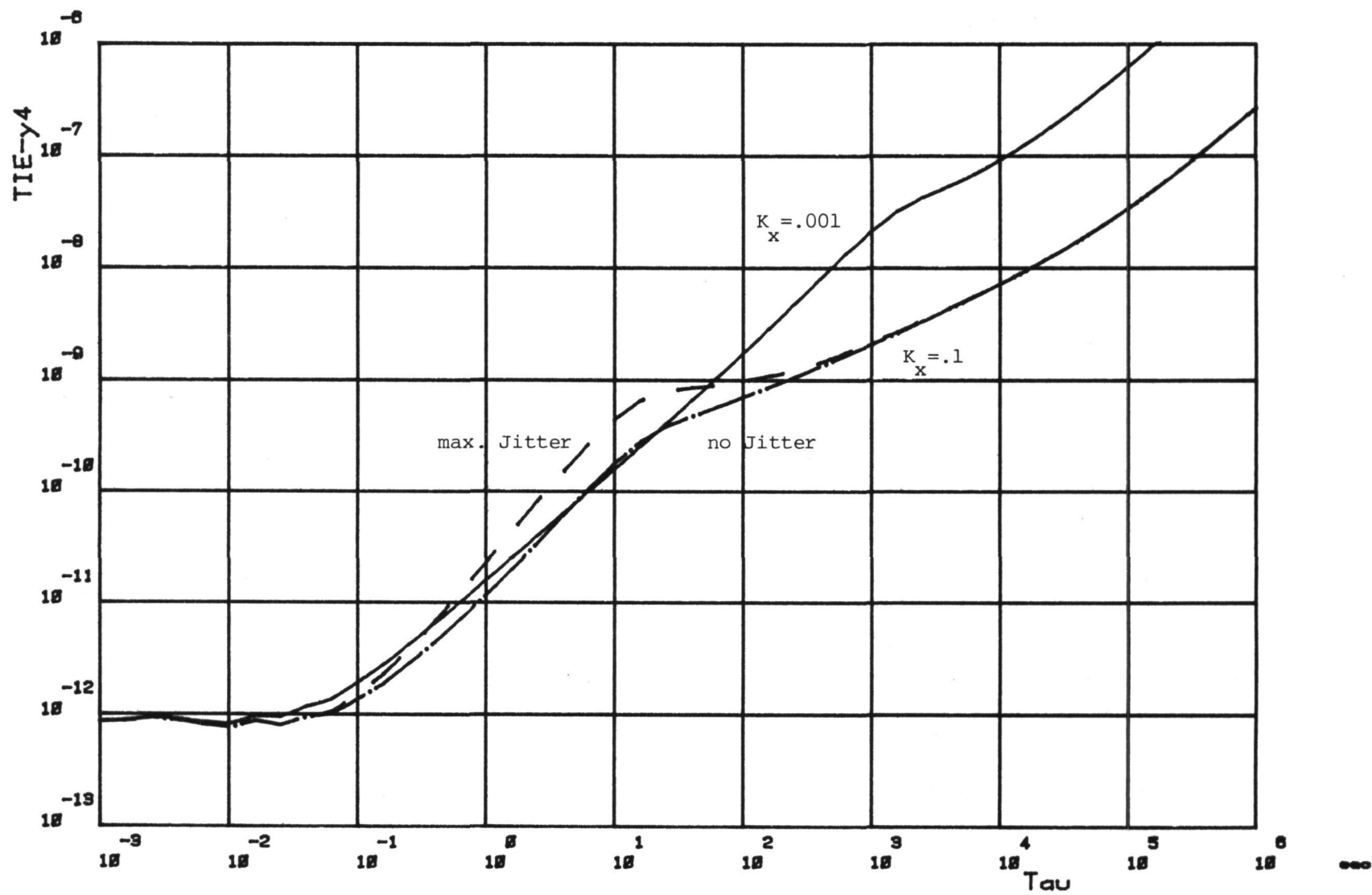


Fig. 10 c) Controlled oscillator time interval error, slave oscillator No. 3

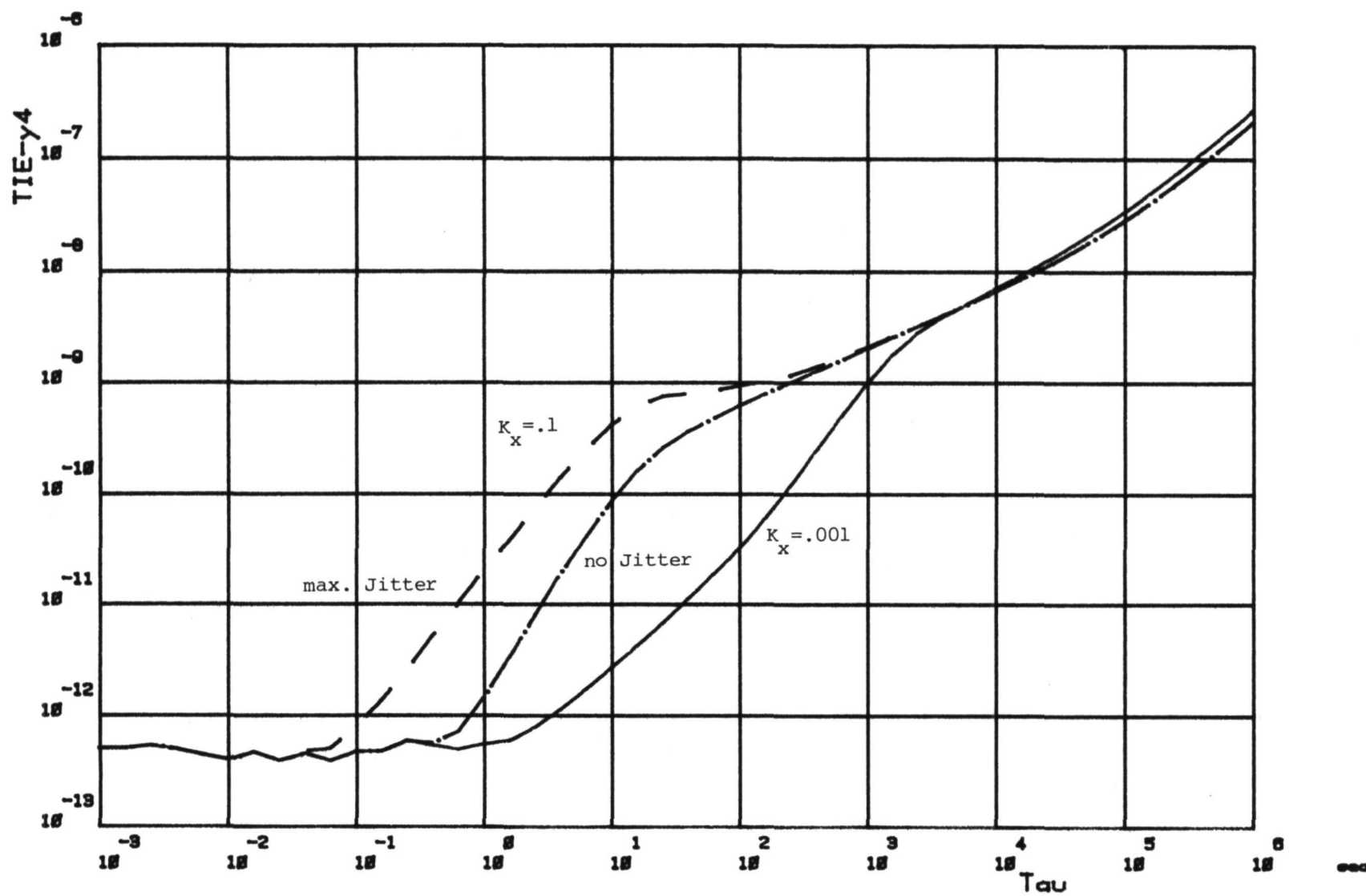


Fig. 10 d) Controlled oscillator time interval error, slave oscillator No. 4

QUESTIONS AND ANSWERS

MR. GEORGE PRICE:

I have drawn the conclusion that one ought to spend a lot of money to get a very, very good high stability crystal oscillator for a digital communications system, because the requirements of CCIR or CCITT are such that we need that. Is that a wrong conclusion?

DR. KARTASCHOFF:

It is a right conclusion. You can use crystal, or rubidium, or cesium, you can also use very clean links and a lot of crystals.

There are many, many possible solutions. Of course, we would welcome having a little bit better crystals.

MR. PRICE:

I could get by with a very cheap oscillator or I could get by with a real expensive one, and whether I spent the money to get a very expensive one would probably depend upon what? -- accuracy requirements, or slip requirements for the communications? I just don't know why I would spend the money to get a more expensive oscillator, is what I am saying. Is there a communication efficiency advantage in going to a very, very highly stabilized BVA type resonator that you recommended here a bit ago?

DR. KARTASCHOFF:

Well, I do not recommend it, I just have seen that it is a possibility that probably will come on the market, and of course it makes things easier, but the communications system will also work with the present oscillators.

Page Intentionally Left Blank

AN ANALYTIC TECHNIQUE FOR STATISTICALLY MODELING RANDOM ATOMIC CLOCK ERRORS IN ESTIMATION

Patrick J. Fell
Naval Surface Weapons Center, Dahlgren, Virginia

ABSTRACT

Minimum variance estimation requires that the statistics of random observation errors be modeled properly. If measurements are derived through the use of atomic frequency standards, then one source of error affecting the observable is random fluctuation in frequency. This is the case, for example, with range and integrated Doppler measurements from satellites of the Global Positioning System used for precise geodetic point positioning and baseline determination for geodynamic applications. In this paper an analytic method is presented which approximates the statistics of this random process. The procedure starts with a model of the Allan variance for a particular oscillator and develops the statistics of range and integrated Doppler measurements. A series of five first order Markov processes is used to approximate the power spectral density obtained from the Allan variance. Range and Doppler error statistics are obtained from the integration of the corresponding autocorrelation function. Statistics for residuals to polynomial clock models are then obtained by linear transformation. Examples are given for rubidium and cesium clocks.

ATOMIC CLOCK ERRORS AND FREQUENCY STABILITY

A clock is any device which counts the cycles of a periodic phenomenon and among the most stable clocks in use are the atomic clocks which form the basis for atomic time scales such as International Atomic Time (TAI). Atomic time is used primarily as a measure of time interval and is based on the electromagnetic oscillations produced by quantum transitions within the atom. The precise definition of stability is found in Blair (1974). Basically it is a measure, usually given statistically, of the random fluctuations in frequency which can occur in a clock's oscillator over specified periods of time. For a given time interval a particular oscillator is considered best if the expected level of frequency fluctuation is a minimum in terms of the Allan variance defined below.

Equation (1) is the model used to describe the types of error present in atomic time scales

$$T_i(t) = \frac{1}{2} D_i(t - t_0)^2 + R_i(t - t_0) + T_i(t_0) + \tilde{x}(t) \quad (1)$$

The deterministic errors consist of bias, drift, and ageing terms modeled as a quadratic polynomial in time. The ageing term is less observable for clocks whose long-term stability is good such as cesium. The term $\tilde{x}(t)$ in equation (1) represents the random time error due to the integration of random fluctuations in frequency:

$$\tilde{x}(t) = \frac{1}{f_I} \int_{t_0}^t \tilde{f}(\tau) d\tau = \int_{t_0}^t y(\tau) d\tau \quad (2)$$

The magnitude of this term depends on the stability of the clock and on the interval of time which has passed since the scale was reset or calibrated.

Hellwig (1977) points out that "the characterization of the stability of a frequency standard is usually the most important information to the user especially to those interested in scientific measurements and in the evaluation and intercomparison of the most advanced devices (clocks)." Since the frequency stability of a standard depends on a variety of physical and electronic influences both internal and external to the standard, measurement and characterization of frequency stability are always given subject to constraints on environmental and operating conditions. In addition frequency stability depends on the exact measurement procedure used to determine stability.

Frequency stability characterization is done in both the frequency and time domain. In the time domain a frequently used measure of stability is the Allan variance or its square root. In the frequency domain it is the power spectral density.

The Allan variance as a time domain measure of frequency stability is found especially useful in practice since it is obtainable directly from experimental measurements and contains all information on the second moments of the statistical distribution of fractional frequency error. The Allan variance is defined as follows: let $y_0, y_1, y_2, \dots, y_k, y_{k+1}, y_{k+2}, \dots$ be observed fractional frequency errors separated by a repetition interval of T seconds. For each integer N greater than or equal to 2, calculate \bar{y}_m from

$$\bar{y}_m = \frac{1}{N} \sum_{k=mN}^{(m+1)N-1} y_k \quad m = 0, 1, 2, \dots, M. \quad (3)$$

This is an average over N consecutive values of y_k . The Allan variance, $\sigma_y^2(N)$, is then obtained from the averages \bar{y}_m by

$$\sigma_y^2(N) = \frac{1}{2M} \sum_{m=0}^{M-1} (\bar{y}_{m+1} - \bar{y}_m)^2. \quad (4)$$

An examination of this equation reveals that the Allan variance for a particular sampling interval NT is the average two-sample variance of the $\bar{y}_m(N)$.

For frequency standards the square root of the Allan variance is usually given in graphical form on a log-log scale. For individual classes of frequency standards models for the Allan variance are used which portray general frequency stability characteristics. Hellwig (1975) gives examples of such models for many oscillator types. Figure 1 shows the typical form. In this form, $\sigma_y(\tau)$ is the square root of the Allan variance for the sample interval τ . The quantity σ_f is called the flicker floor and τ_1, τ_2, τ_3 are the break points of the plot. The constants associated with this figure are usually specified for each type of frequency standard. A comparison of such information can facilitate the selection of a frequency standard for a specific application.

The stability characteristics shown in the three regions of Figure 1 are typically present in many Allan variance plots of specified oscillator performance. The first part, region I, reflects the fundamental noise properties of the standard. This behavior continues with increased sampling time until a floor is reached corresponding to region II. After τ_2 the performance deteriorates with increased sampling time. Hellwig (1977) outlines the error sources corresponding to each portion of the graph. The magnitude and slope of each segment will depend on the particular category of standard.

An alternative procedure for specifying the stability of a frequency standard, in the frequency domain, is the use of the power spectral density (PSD) of instantaneous fractional frequency fluctuations $y(t)$. Allan et al. (1974) have given a useful model to represent the PSD for various categories of frequency standards. This model is in the form of a power law spectral density having the form

$$s_{yy}(\omega) = \begin{cases} h_\alpha \left(\frac{\omega}{2\pi}\right)^\alpha & 0 \leq \omega \leq \omega_h \\ 0 & \omega > \omega_h \end{cases} \quad (5)$$

where α takes on the integer powers between -2 and 2 inclusive depending on how the interval $(0, \omega_h)$ is to be divided into subintervals, one for each α to be used. The quantity h_α is a scaling constant, and the PSD is assumed to be negligible beyond the frequency range $(0, \omega_h)$.

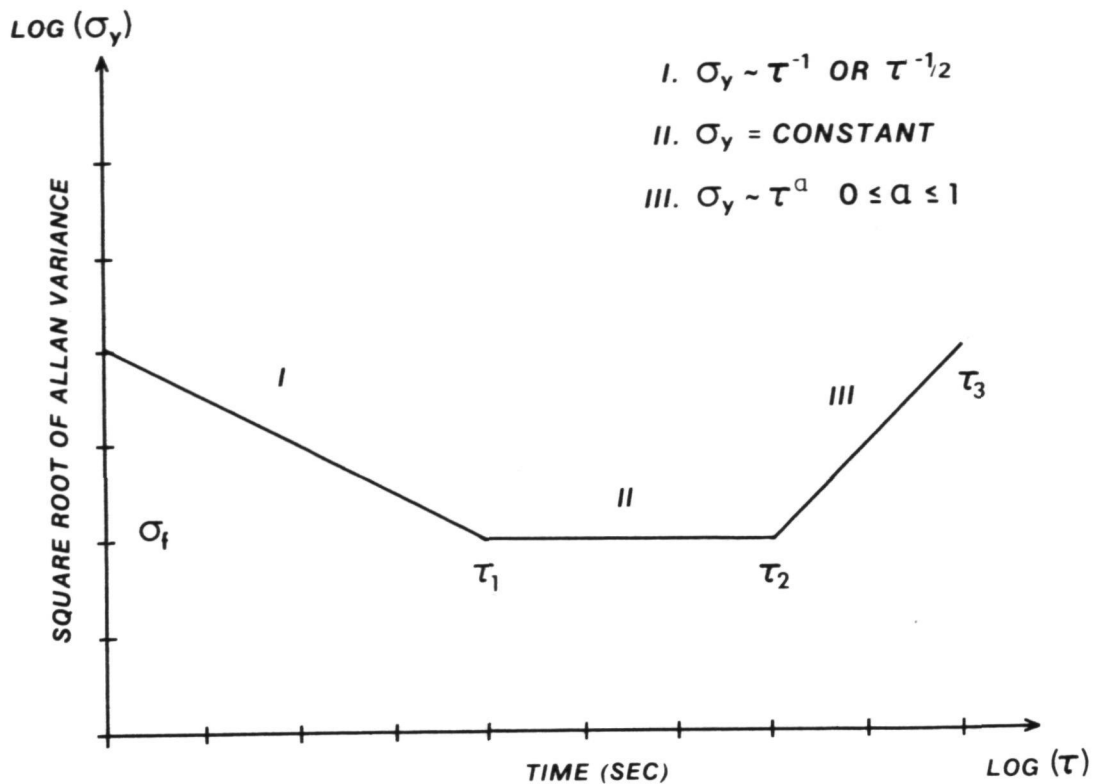


Fig. 1-General frequency stability characteristics

Barnes et al (1971) and Meditch (1975) give the transformations between the time domain measures of frequency stability in the form of the Allan variance and the power law spectral densities. Table 1 taken from Meditch gives these conversions for three types of fractional frequency error sources.

Table 1-Allan variance and power spectral density for common error sources

ERROR SOURCE $y(t)$	ALLAN VARIANCE $\sigma_y^2(\tau)$	TWO SIDED SPECTRAL DENSITY $S_{yy}(\omega)$
WHITE NOISE	$\frac{N_0}{\tau}$	N_0
FLICKER NOISE	$\frac{2N_1 \ln 2}{\pi}$	$\frac{N_1}{ \omega }$
INTEGRAL OF WHITE NOISE (RANDOM WALK)	$\frac{N_2 \tau}{3}$	$\frac{N_2}{\omega^2}$

RANGE AND DOPPLER OBSERVATION ERRORS DUE TO RANDOM ATOMIC CLOCK ERROR

As previously discussed, an atomic clock's time scale can be expected to differ from ideal time due to both deterministic and random errors. The random component is due to integration of fractional frequency errors. A range observation determined from radio signals broadcast by a satellite is subject to the random errors of the frequency standards in both the satellite and the tracking receivers. The effective range error at time t due to the timing error in one of the time scale is

$$\delta R_i(t) = cT_i(t) \quad (6)$$

with the random component being the random walk

$$\eta_i(t) = c \int_{t_s}^t y(\tau) d\tau \quad (7)$$

where c is the velocity of light. The random component is due to the accumulated effect of fractional frequency error since the clock's start or reset at t_s .

The random error $\eta_i(t)$ is correlated in time. Consider two measurements of range $R(t_j)$ and $R(t_k)$ based on the use of the oscillator in the satellite, and assume momentarily that the receiver's oscillator is free from random error. The covariance between these measured ranges due to correlated fractional frequency error in the satellite oscillator is

$$\begin{aligned} E[R(t_j)R(t_k)] &= E[\eta(t_j)\eta(t_k)] \\ &= c^2 E\left[\int_{t_s}^{t_j} y(\tau) d\tau \int_{t_s}^{t_k} y(\tau') d\tau'\right] \\ &= c^2 \int_{t_s}^{t_j} \int_{t_s}^{t_k} E[y(\tau)y(\tau')] d\tau d\tau' \\ &= c^2 \int_{t_s}^{t_j} \int_{t_s}^{t_k} \phi_{yy}(\tau - \tau') d\tau d\tau' \end{aligned} \quad (8)$$

where $\phi_{yy}(\tau - \tau')$ is the autocorrelation function for fractional frequency error $y(t)$ defined by

$$\begin{aligned}\phi_{yy}(\tau - \tau') &= E[y(\tau)y(\tau')] \\ &= \int_{-\infty}^{\infty} \int_{-\infty}^{\infty} yy' f(y, y', \tau, \tau') dy dy'.\end{aligned}\quad (9)$$

The function $f(y, y', \tau, \tau')$ is the joint probability density function for fractional frequency error. Here it is assumed that $y(t)$ is a mean zero stationary random process. The function $\phi_{yy}(\tau - \tau')$ could be obtained by the inverse Fourier transform of the given power spectral density $S_{yy}(\omega)$:

$$\phi_{yy}(t) = \frac{1}{2\pi} \int_{-\infty}^{\infty} S_{yy}(\omega) e^{i\omega t} d\omega \quad (10)$$

where

$$t = \tau - \tau'.$$

An alternate procedure for obtaining the autocorrelation function $\phi_{yy}(t)$ from the Allan variance is given below.

The variance of a range observation is obtained from equation (8) by setting t_j equal to t_k :

$$\sigma_{R_j}^2 = c^2 \int_{t_s}^{t_j} \int_{t_s}^{t_j} \phi_{yy}(\tau - \tau') d\tau d\tau'. \quad (11)$$

The presence of random frequency error in the receiver oscillator introduces additional, but similar, terms into equations (8) and (11) which must be considered when assessing the range uncertainty due to all random clock errors effecting the measurement.

For integrated Doppler or range difference observations the random measurement error associated with system clocks is the integral of fractional frequency error over the Doppler integration interval. The random error in range difference due to one oscillator is

$$\begin{aligned}\eta_{ij} &= \eta(t_j) - \eta(t_k) \\ &= c \int_{t_i}^{t_j} y(\tau) d\tau.\end{aligned}\quad (12)$$

Notice in equation (12) that the random error η_{ij} is a function of t_i , t_j , and $y(t)$. The error does not depend on t_s . Range difference measurements have the following correlation for each oscillator

$$\begin{aligned} E[\Delta R_{ij} \Delta R_{kl}] &= E[\eta_{ij} \eta_{kl}] \\ &= c^2 \int_{t_i}^{t_j} \int_{t_k}^{t_l} \phi_{yy}(\tau - \tau') d\tau d\tau' \end{aligned} \quad (13)$$

with the variance

$$\sigma_{\Delta R_{ij}}^2 = c^2 \int_{t_i}^{t_j} \int_{t_i}^{t_j} \phi_{yy}(\tau - \tau') d\tau d\tau'. \quad (14)$$

Observe that the random range difference errors, whose statistics are given by equations (13) and (14), are stationary; however, random range errors, whose statistics are given by equations (8) and (11), are not. A stationary random process is one whose statistics are invariant in time.

For the oscillator performance specifications shown in Figure 2 examples of the contribution to the range error are given for both oscillators in Figures 3 and 4 over a five-day span. The clocks are assumed to be perfect initially. Also included is the standard error for the random walk $\eta(t)$ obtained using equation (11). The procedure used in simulating the random range error is discussed in Meditch (1975).

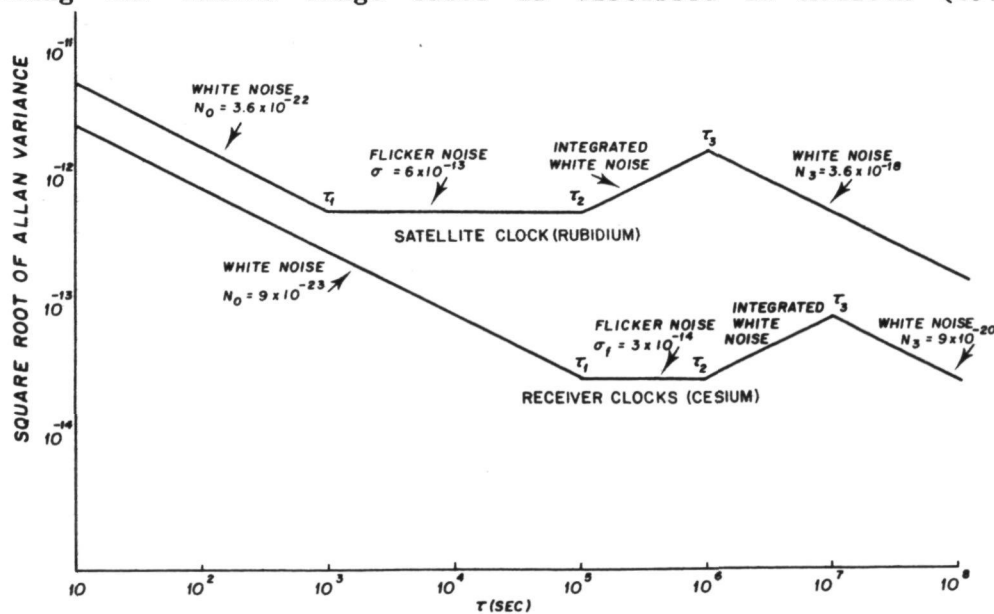


Fig. 2-Allan variance for satellite and receiver oscillators

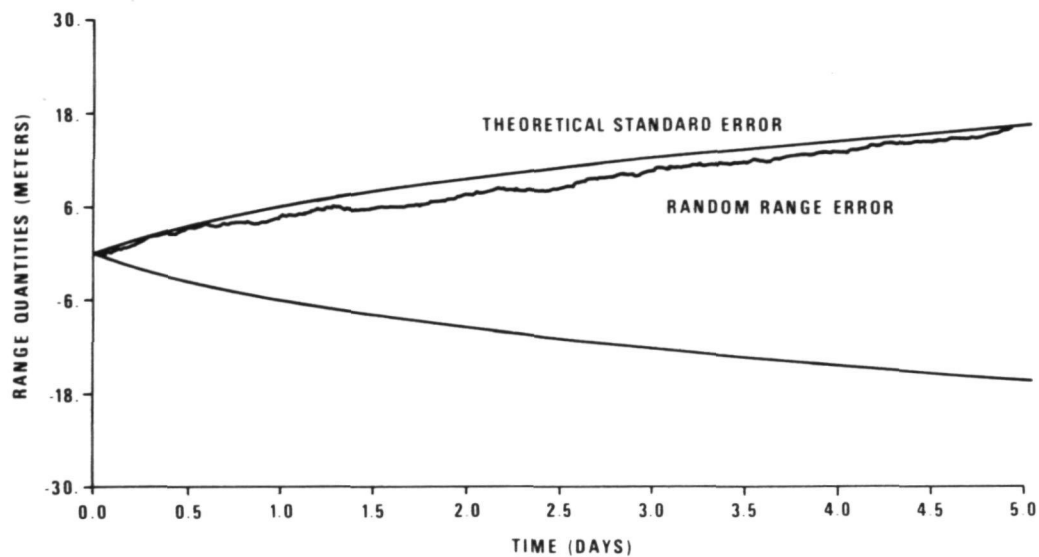


Fig. 3-Standard error and random range error based on receiver cesium specifications

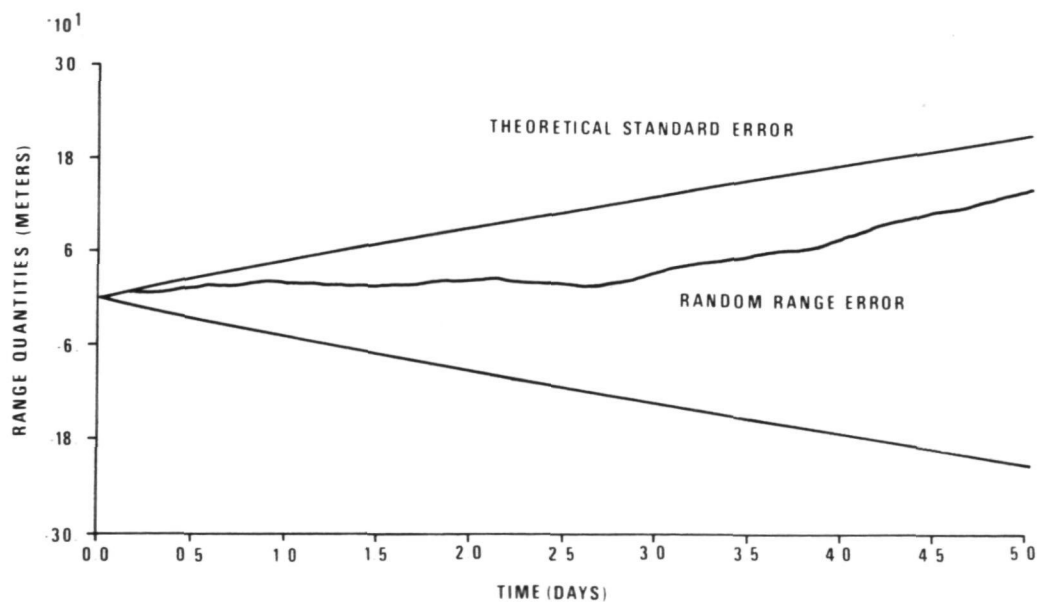


Fig. 4-Standard error and random range error based on satellite rubidium specifications

RANGE AND DOPPLER OBSERVATION ERROR STATISTICS

Fractional Frequency Autocorrelation from the Allan Variance

The equations giving the second order statistics of random range and integrated Doppler observation errors due to random fractional frequency errors were presented in the last section. Those equations require that the fractional frequency autocorrelation function be known. In this section discussion of a procedure for obtaining an analytic approximation to this function from the Allan variance is given. This method yields a simple analytic autocorrelation function and avoids numerical difficulties that may arise when the inverse Fourier transform of the power spectral density is evaluated.

The Allan variance models shown in Figure 2 for the satellite rubidium and receiver cesium oscillators are a function of the sampling time τ having the form

$$\sigma_y^2(\tau) = \begin{cases} \frac{N_0}{\tau} & \tau_0 < \tau < \tau_1 \\ \sigma_f^2 & \tau_1 < \tau < \tau_2 \\ \frac{N_2 \tau}{3} & \tau_2 < \tau < \tau_3 \\ \frac{N_3}{\tau} & \tau_3 < \tau < \infty. \end{cases} \quad (15)$$

Using the transformations in Table 1 the power spectral density for fractional frequency may be developed from equation (15):

$$S_{yy}(\omega) = \begin{cases} N_3 & 0 < \omega < \omega_0 \\ \frac{N_2}{\omega^2} & \omega_0 < \omega < \omega_1 \\ \frac{N_1}{\omega} & \omega_1 < \omega < \omega_2 \\ N_0 & \omega_2 < \omega < \omega_h. \end{cases} \quad (16)$$

The square roots of the power spectral densities corresponding to the Allan variance specifications of Figure 2 are given in Figure 5. The constants associated with the two functions and the formulas for computing the constants associated with the power spectral density

function based on the Allan variance are given in Table 2. These formulas are developed from the transformations of Table 1.

The autocorrelation function $\phi_{yy}(t)$ can be obtained from the power spectral density using equation (10)

$$\phi_{yy}(t) = \frac{1}{2\pi} \int_{-\infty}^{\infty} S_{yy}(\omega) e^{i\omega t} d\omega.$$

However, as a result of transforming the band limited white noise portion of the spectrum, this form for the autocorrelation function has an oscillatory behavior for small t . This is an artificiality of the model.

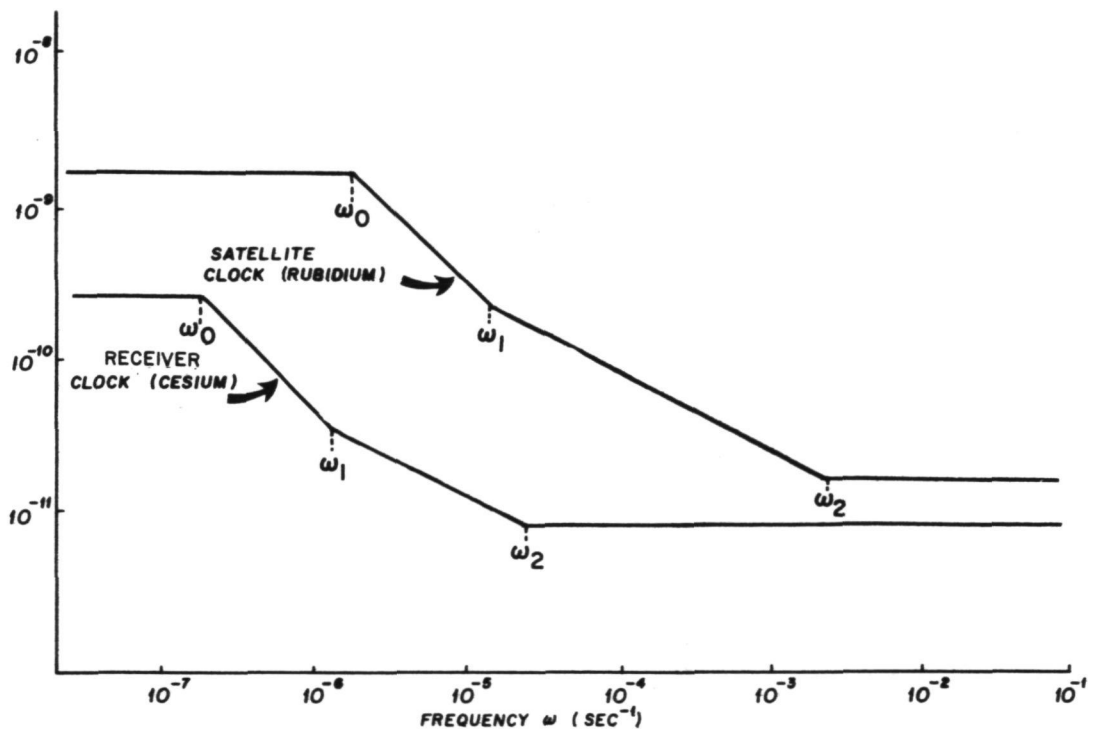


Fig. 5-Square root of PSD

An alternate approach for obtaining an autocorrelation function is to approximate the power spectral density model with a smooth function whose autocorrelation is expressible in simple analytic form. The first step in this development is to approximate the flicker noise

Table 2-Oscillator parameters

QUANTITY	UNITS	FORMULA	SATELLITE CLOCKS (RUBIDIUM)	RECEIVER CLOCK (CESIUM)
τ_1	sec		1.00×10^3	1.00×10^5
τ_2	sec		1.00×10^5	1.00×10^6
τ_3	sec		1.00×10^6	1.00×10^7
ω_0	sec ⁻¹	$\sqrt{3}/\tau_3$	1.73×10^{-6}	1.73×10^{-7}
ω_1	sec ⁻¹	$6 \ln 2 / (\pi \tau_2)$	1.32×10^{-5}	1.32×10^{-6}
ω_2	sec ⁻¹	$\pi / (2 \tau_1 \ln 2)$	2.27×10^{-3}	2.27×10^{-5}
σ_f			6.00×10^{-13}	3.00×10^{-14}
N_0	sec	$\tau_1 \sigma_f^2$	3.60×10^{-22}	9.00×10^{-23}
N_1		$\pi \sigma_f^2 / 2 \ln 2$	8.16×10^{-25}	2.04×10^{-27}
N_2	sec ⁻¹	$3 \sigma_f^2 / \tau_2$	1.08×10^{-29}	2.70×10^{-33}
N_3	sec	$\sigma_f^2 \tau_3^2 / \tau_2$	3.60×10^{-18}	9.00×10^{-20}
α		$(\omega_2 / \omega_1)^{1/6}$	2.36×10^0	1.61×10^0
ω_a	sec ⁻¹	$\omega_1 \sqrt{\alpha}$	2.03×10^{-5}	1.67×10^{-6}

segment of the spectrum by a series of cascading functions whose values alternate between being constant and being inversely proportional to the square of the frequency. This type of procedure is described by Meditch (1975) in constructing a linear system which simulates flicker noise using a white noise input. Figure 6 shows the transfer function for flicker noise. A three stage cascading transfer function is superimposed consisting of the functions F_A , F_B , and F_C which are defined in Table 3. These functions are defined to have the required properties and give a continuous although not smooth approximation to the flicker noise power spectral density.

The constants of this approximation are now derived over frequency intervals as given in Meditch (1975). The general form of the function F_A is

$$F_A(\omega) = \frac{N_A}{\omega_a^2} \quad (17)$$

between the frequencies ω_a and $\alpha \omega_a$. At frequency ω_a , defined in Table 2, the function F_A takes on the value

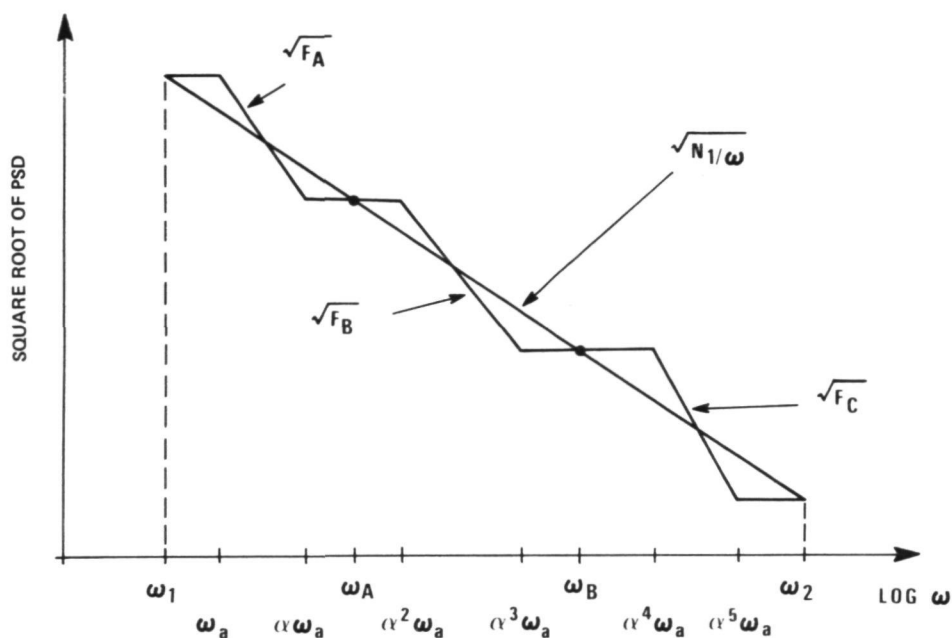


Fig. 6-Three stage transfer function approximation of flicker noise spectrum

Table 3-Definition of three stage transfer function approximation

FUNCTION	INTERVAL	DEFINITION (PSD)
F_A	$\omega_1 \leq \omega \leq \omega_a$	N_1/ω_1
	$\omega_a \leq \omega \leq \alpha\omega_a$	N_A/ω^2
	$\alpha\omega_a \leq \omega \leq \omega_A$	$N_A/\alpha^2\omega_a^2$
F_B	$\omega_A \leq \omega \leq \alpha^2\omega_a$	$N_A/\alpha^2\omega_a^2$
	$\alpha^2\omega_a \leq \omega \leq \alpha^3\omega_a$	N_B/ω^2
	$\alpha^3\omega_a \leq \omega \leq \omega_B$	$N_B/\alpha^6\omega_a^2$
F_C	$\omega_B \leq \omega \leq \alpha^4\omega_a$	$N_B/\alpha^6\omega_a^2$
	$\alpha^4\omega_a \leq \omega \leq \alpha^5\omega_a$	N_C/ω^2
	$\alpha^5\omega_a \leq \omega \leq \omega_2$	N_o

WHERE

$$N_A = \alpha\omega_1 N_1$$

$$N_B = \alpha^3\omega_1 N_1$$

$$N_C = \alpha^5\omega_1 N_1$$

$$a = \left(\frac{\omega_2}{\omega_1} \right)^{\frac{1}{2n}}$$

$$\omega_a = \omega_1 \sqrt[n]{a}$$

$$n = 3$$

$$F_A(\omega_a) = \frac{N_A}{\omega_a^2} = \frac{N_1}{\omega_1} \quad (18)$$

since the flicker noise power spectral density has the same function value at frequency ω_1 . Solving equation (18) gives

$$N_A = \frac{N_1 \omega_a^2}{\omega_1} = \alpha \omega_1 N_1. \quad (19)$$

A similar analysis gives the constant N_B . The function F_B has the form

$$F_B(\omega) = \frac{N_B}{\omega^2}. \quad (20)$$

At frequency $\alpha^2 \omega_a$, F_B has the function value

$$F_B(\alpha^2 \omega_a) = \frac{N_B}{\alpha^4 \omega_a^2} = \frac{N_A}{\alpha^2 \omega_a^2} \quad (21)$$

since at $\alpha^2 \omega_a$ the function F_B has the same value as function F_A at frequency $\alpha \omega_a$ (see Figure 6). Solving equation (21) and using equation (19)

$$N_B = \alpha^2 N_A = \alpha^3 \omega_1 N_1. \quad (22)$$

For the function F_C ,

$$F_C(\omega) = \frac{N_C}{\omega^2} \quad (23)$$

its function value at frequency $\alpha^4 \omega_a$ equals the value of F_B at frequency $\alpha^3 \omega_a$ giving

$$F_C(\alpha^4 \omega_a) = \frac{N_C}{\alpha^8 \omega_a^2} = \frac{N_B}{\alpha^6 \omega_a^2}. \quad (24)$$

Using equation (22) gives the solution

$$N_C = \alpha^2 N_B = \alpha^5 \omega_1 N_1. \quad (25)$$

Numerical values for α and ω are given in Table 2. The power spectral density consisting of the three cascading functions and the remainder of the original function will be denoted as the second power spectral density model for each oscillator.

The next step in the development of a simple analytic autocorrelation function is to approximate various segments of this second model with a first order Markov process power spectral density function, a function of the form

$$S(\omega) = \frac{2\sigma^2\beta}{\omega^2 + \beta^2} \quad (26)$$

where β is the inverse of the correlation time (see Gelb (1974)). The autocorrelation function for a first order Markov process is

$$\Phi(t) = \sigma^2 e^{-\beta t} \quad (27)$$

Notice in equation (26) that the power spectral density decreases as the inverse of the square of the frequency. This is the type of functional behavior seen in the interior of the cascading functions F_A through F_C . It is also the behavior of the original power spectral density in the interval (ω_0, ω_1) . In addition the power spectral density of the Markov process remains virtually flat until the frequency reaches a point at which the function decreases rapidly. These properties make this function an excellent choice for approximating the second power spectral density model piecewise.

The second model is then divided into five segments defined in Table 4. The high frequency cut off ω_h , shown as 10^{-1} in Figure 5, will be increased so that the band limited white noise component of the power spectral density may be approximated better by the first order Markov power spectral density.

Table 4-Division of second PSD model for Markov process approximation

<u>NOTATION</u>	<u>INTERVAL</u>
I_1	$[0, \omega_1]$
I_2	$[\omega_1, \alpha\omega_a]$
I_3	$[\alpha\omega_a, \alpha^3\omega_a]$
I_4	$[\alpha^3\omega_a, \alpha^5\omega_a]$
I_5	$[\alpha^5\omega_a, \omega_h]$

The approximation consists then of fitting a function in the form of equation (26) to each subdivision of the second model $S'_{yy}(\omega)$ given in Table 4. There are two parameters σ and β to be determined for each segment giving a total of ten parameters.

The procedure which was adopted was an asymptotic approximation whereby two constraints were imposed on the Markov power spectral density function giving σ and β directly. This procedure was implemented because of simplicity and because the results compared favorably with a least squares approach. The asymptotic approach develops an approximation on the interval I_j ,

$$I_j \sim [\omega_k, \omega_\ell]$$

using the following constraints:

(i) at zero frequency the approximating Markov power spectral density equals the second model at frequency ω_k :

$$S_j(0) = S'_{yy}(\omega_k) \quad (28)$$

(ii) in the limit as ω increases the value of the function $S_j(\omega)$ converges to the following function

$$\lim_{\omega \rightarrow \infty} S_j(\omega) = \frac{2\sigma^2\beta}{\omega^2} \quad (29)$$

and at ω_ℓ this limiting value is set equal to the value of $S'_{yy}(\omega)$:

$$\frac{2\sigma^2\beta}{\omega_\ell^2} = S'_{yy}(\omega_\ell). \quad (30)$$

Equations (28) and (30) are a system of two equations in two unknowns. Their solution yields the parameters σ_j and β_j for the approximating Markov power spectral density function $S_j(\omega)$. The nature of the second constraint, equation (30), is to force the function $S_j(\omega)$ to asymptotically approach $S'_{yy}(\omega)$ at ω_ℓ . The first constraint is necessary to approximate the white noise or flat component of $S'_{yy}(\omega)$ at the beginning of each subinterval.

Finally a comment concerning the approximation in the last subdivision I_5 is necessary. In order to obtain a good approximation to $S'_{yy}(\omega)$ in that interval it is necessary to choose ω_h large enough to allow the

flat portion of the Markov process spectral density to fit the white noise component which dominates this interval (see Figure 5). Choosing ω_h three or four orders of magnitude larger than 0.1 and $S'_{yy}(\omega_h)$ two or three orders of magnitude smaller than N_0 , enables a good approximation to be made but adds power at these higher frequencies. The result is an autocorrelation function which tends to a delta function as ω_h goes to infinity and whose variance increases as ω_h is chosen larger (see Figure 7). However, this will have negligible effect on range and range difference statistics.

The smooth fractional frequency autocorrelation function $\phi_{yy}(t)$ is given by the inverse Fourier transform of the five Markov process power spectral densities $S_j(\omega)$. The result of each transformation is an analytic function whose form is given by equation (27). The final result is the sum of these functions

$$\phi_{yy}(t) = \sum_{j=1}^5 \sigma_j^2 e^{-\beta_j |t|}. \quad (31)$$

For range and integrated Doppler observations the statistical contribution due to random oscillator error is obtained using equation (31) in equation (8) through (14).

Figures 8 and 9 show the original transfer functions and the asymptotic approximations. The parameters obtained using this approximation procedure are given in Table 5.

Observation Error Statistics Based on Markov Process Approximations

The first order Markov autocorrelation function, equation (31), and equations (8) through (14) give the second order statistics for random range and integrated Doppler observation errors due to each oscillator used in the measurement process. These integrals may be evaluated giving analytical expressions for the variance and covariance of range and Doppler observations.

Let $R(t_i)$ and $R(t_k)$ be range observations subject to one random clock error only. The covariance between the observations is given by equation (8). Using the first order Markov approximations, the integration of equation (8) gives the covariance as

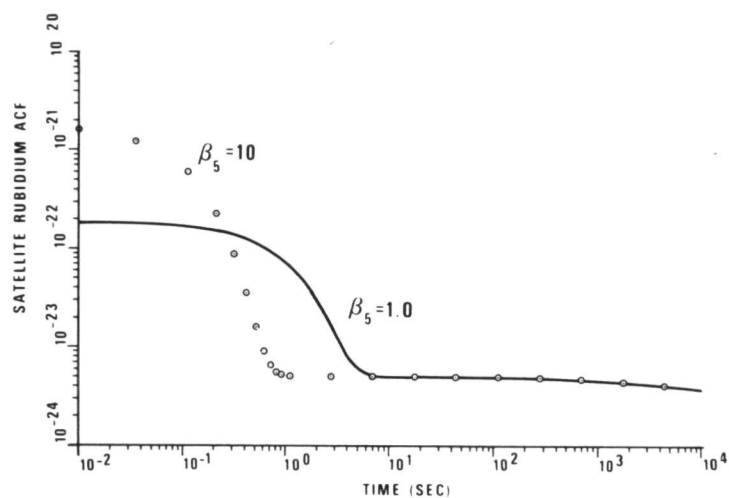


Fig. 7-Asymptotic fractional frequency autocorrelation functions based on Markov process approximations

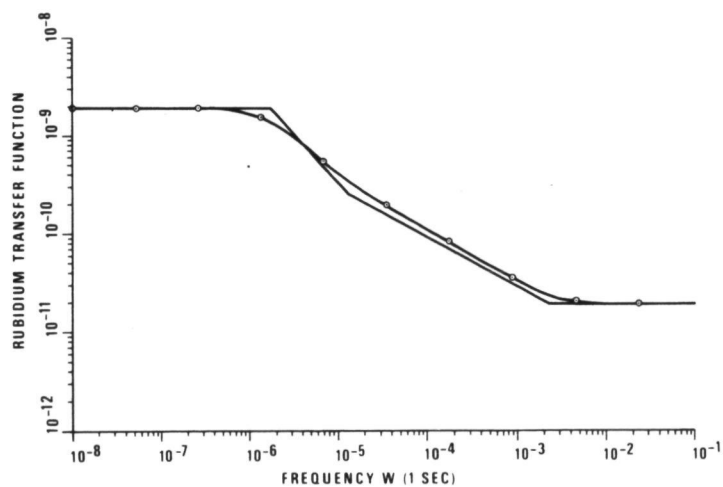


Fig. 8-Satellite oscillator transfer function and sum of asymptotic approximations

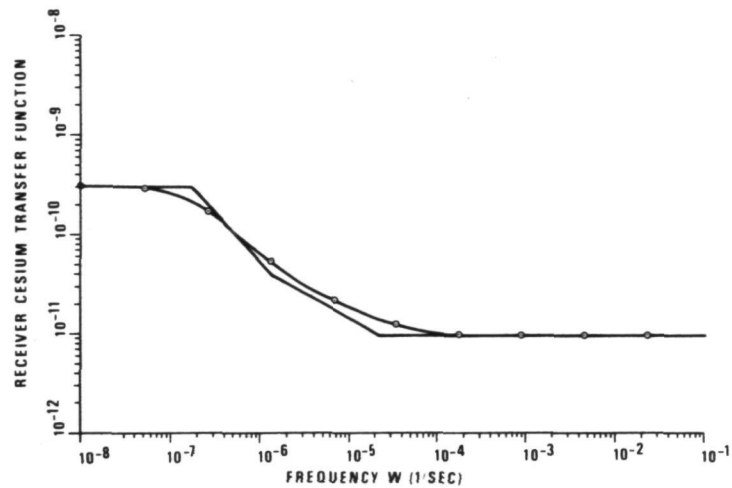


Fig. 9-Receiver cesium transfer function and sum of asymptotic approximations

Table 5-Fractional frequency autocorrelation function parameters for Markov process approximations

OSCILLATOR TYPE	INTERVAL	ASYMPTOTIC		LEAST SQUARES	
		(ALPHA) ²	BETA	(ALPHA) ²	BETA
RUBIDIUM (SPEC)	I ₁	3.1177×10 ⁻²⁴	1.732×10 ⁻⁶	3.3719×10 ⁻²⁴	1.681×10 ⁻⁶
	I ₂	6.2625×10 ⁻²⁵	2.032×10 ⁻⁵	7.6238×10 ⁻²⁵	2.255×10 ⁻⁵
	I ₃	6.2625×10 ⁻²⁵	1.128×10 ⁻⁴	7.6245×10 ⁻²⁵	1.252×10 ⁻⁴
	I ₄	6.2625×10 ⁻²⁵	6.262×10 ⁻⁴	7.6245×10 ⁻²⁵	6.947×10 ⁻⁴
	I ₅	1.8000×10 ⁻¹⁹	1.000×10 ^{3*}	1.9343×10 ⁻¹⁹	9.631×10 ^{2*}
CESIUM (SPEC)	I ₁	7.7942×10 ⁻²⁷	1.732×10 ⁻⁷		
	I ₂	1.2922×10 ⁻²⁷	1.677×10 ⁻⁶		
	I ₃	1.2922×10 ⁻²⁷	4.321×10 ⁻⁵		
	I ₄	1.2922×10 ⁻²⁷	1.113×10 ⁻⁵		
	I ₅	4.5000×10 ⁻²⁰	1.000×10 ^{3*}		

* $\omega_h = 1.0 \times 10^4$ $S'_{YY}(\omega_h) = N_0 / 1.0 \times 10^2$

$$\begin{aligned}
E[R(t_i)R(t_k)] &= E[\eta(t_i)\eta(t_k)] \\
&= c^2 \sum_{j=1}^5 \frac{\sigma_j^2}{\beta_j} \left[2(t_i - t_s) + \frac{1}{\beta_j} \left(e^{-\beta_j(t_j - t_s)} \right. \right. \\
&\quad \left. \left. + e^{-\beta_j(t_k - t_s)} - e^{-\beta_j(t_k - t_i)} - 1 \right) \right] \quad (32)
\end{aligned}$$

for t_k greater than t_i , where t_s is the start or reset time of the clock. The variance of the random range error is obtained by setting t_k equal to t_i in equation (32)

$$\begin{aligned}
E[R(t_i)R(t_i)] &= E[\eta(t_i)\eta(t_i)] \\
&= c^2 \sum_{j=1}^5 \frac{2\sigma_j^2}{\beta_j} \left[(t_i - t_s) \right. \\
&\quad \left. + \frac{1}{\beta_j} \left(e^{-\beta_j(t_i - t_s)} - 1 \right) \right]. \quad (33)
\end{aligned}$$

The range error $\eta(t)$ resulting from the integration of fractional frequency error $y(t)$ is a statistically nonstationary process. An examination of equations (32) and (33) reveals terms which are functions of t_i , or t_k , minus t_s . Thus, for instance, the variance increases with time. This is illustrated in Figure 10 for the rubidium clock. The standard error of a range measurement based on the use of this clock is given for 20 range observations spaced at 15-minute intervals starting five minutes, one hour, and five hours after the start of the clock. The increase in variance is almost linear. An examination of the autocorrelation function shows that this function, dominantly flat, is similar to a random bias having a constant autocorrelation and whose integral is a random ramp which increases exactly linearly. Hence a linear growth in variance is expected as seen in Figure 10. The correlation coefficients ρ_{li} between the first and the i 'th range observation in each of these sequences are given in Figure 11. As the starting time of the sequence increases from t_s , so does the correlation among the random errors. This again is expected, since the variance increases with time and the errors are correlated.

Figure 12 gives the autocorrelation function for the cesium clock based on the Markov process approximation and Figures 13 and 14 give the standard error and correlations of range errors based on this clock. A comparison of Figures 10 and 13 reveals the greater stability of the cesium clock. After ten hours of operation the standard error of the cesium clock output is approximately 3.5 nanoseconds compared to 63

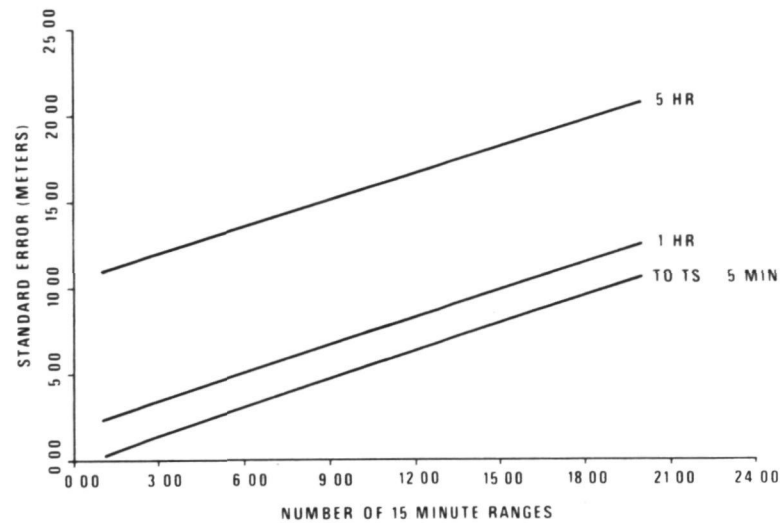


Fig. 10-Standard error of range observations based on satellite rubidium oscillator

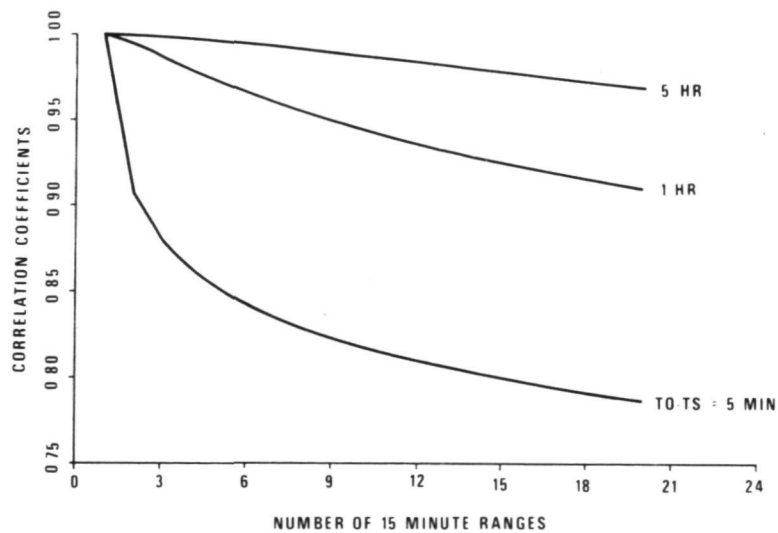


Fig. 11-Correlation coefficients between range 1 and range i (rubidium clock)

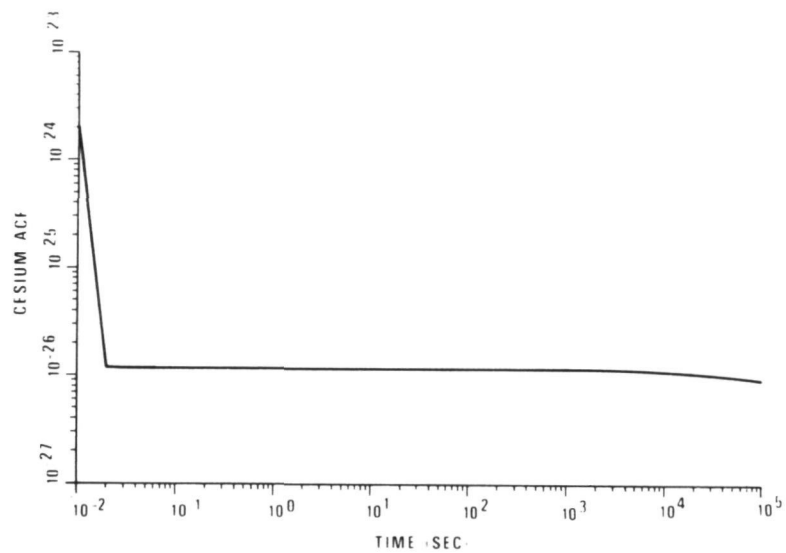


Fig. 12-Asymptotic fractional frequency autocorrelation function for cesium standard

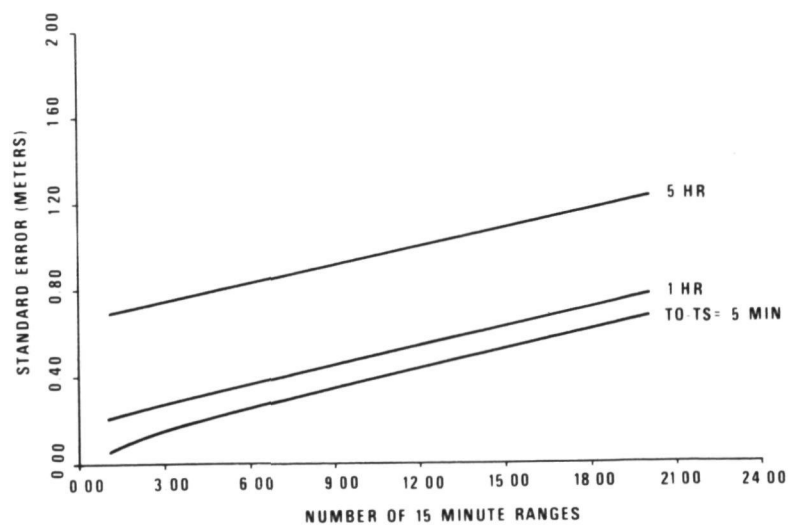


Fig. 13-Standard error of range observations based on cesium oscillator

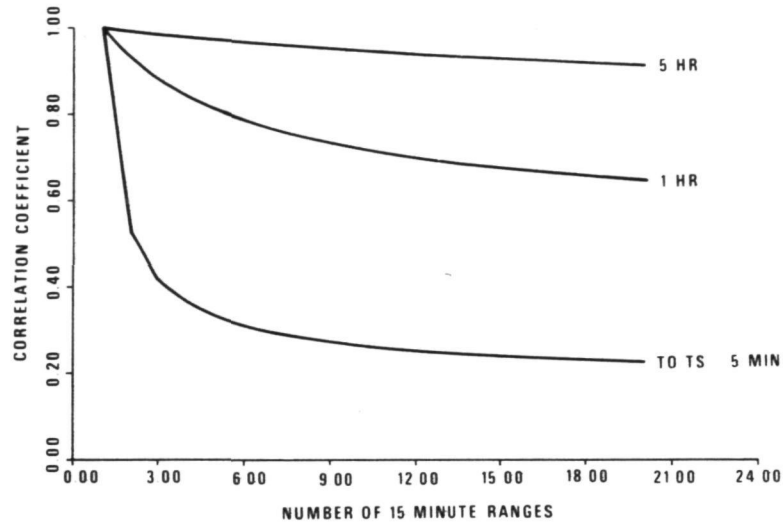


Fig. 14-Correlation coefficients between range 1 and range i (cesium clock)

nanoseconds for the rubidium standard. In addition, the correlations among the cesium clock errors decrease more rapidly than the rubidium clock errors. Considering both random clock error sources the total variance and correlation of range observations $R_k(t_i)$ and $R_k(t_j)$ measured by receiver k are given by the equations

$$E[R_k(t_i)R_k(t_i)] = E[\eta_s(t_i)\eta_s(t_i)] + E[\eta_k(t_i)\eta_k(t_i)] \quad (34)$$

$$E[R_k(t_i)R_k(t_j)] = E[\eta_s(t_i)\eta_s(t_j)] + E[\eta_k(t_i)\eta_k(t_j)] \quad (35)$$

where the variances and correlations of the random error η are given by equations (32) and (33). The subscript "s" refers to the satellite rubidium clock.

For simultaneous observations of range by two receivers the covariance of the observations $R_k(t_i)$ and $R_\ell(t_j)$ is given by

$$E[R_k(t_i)R_\ell(t_j)] = E[\eta_s(t_i)\eta_s(t_j)]. \quad (36)$$

In the above equations the random errors η have zero mean which is a consequence of fractional frequency error being zero mean.

Let $\Delta R(t_n)$ be an integrated Doppler or range difference measurement over the interval (t_i, t_n) and $\Delta R(t_\ell)$ a similar measurement from the

same receiver over the interval (t_k, t_ℓ) . The covariance of the observations is

$$\begin{aligned}
 E[\Delta R(t_n), \Delta R(t_\ell)] &= E[\eta(t_n) - \eta(t_i), \eta(t_\ell) - \eta(t_k)] \\
 &= E[\eta(t_n)\eta(t_\ell)] - E[\eta(t_n)\eta(t_k)] - E[\eta(t_i)\eta(t_\ell)] \\
 &\quad + E[\eta(t_i)\eta(t_k)] \\
 &= c^2 \sum_{j=1}^5 \frac{\sigma_j^2}{\beta_j^2} \left[e^{-\beta_j(t_\ell - t_n)} - e^{-\beta_j(t_k - t_n)} \right. \\
 &\quad \left. - e^{-\beta_j(t_\ell - t_i)} + e^{-\beta_j(t_k - t_i)} \right]. \quad (37)
 \end{aligned}$$

The variance of a range difference observation is given by

$$E[\Delta R(t_n)\Delta R(t_n)] = c^2 \sum_{j=1}^5 \frac{2\sigma_j^2}{\beta_j} \left[(t_n - t_i) + \frac{1}{\beta_j} \left(e^{-\beta_j(t_n - t_i)} - 1 \right) \right]. \quad (38)$$

Equations (37) and (38) are independent of the clock epoch t_s . The statistics of the range difference error depend only on the Doppler integration interval or the time difference between observations. Thus the random range difference error is stationary. Expressions analogous to equations (34) through (36) express the complete statistics of range difference observation errors for individual or simultaneous observations due to clock error.

STATISTICS OF RESIDUALS TO POLYNOMIAL CLOCK MODELS

The statistical characteristics of fractional frequency error and its integrated effect on range and Doppler observations have been discussed in detail. For range observations assume that the total random error is due to three sources, two of which are correlated noise processes. Then the total random range error is expressed as

$$\eta(t) = \eta_s(t) + \eta_k(t) + \xi(t) \quad (39)$$

where η_s and η_k are the correlated random range errors due to satellite and receiver random clock errors respectively. The quantity ξ represents receiver white noise. The total integrated Doppler random error over the integration interval $[t_j, t_\ell]$ is

$$\Delta\eta(t_\ell) = \eta_s(t_\ell) - \eta_s(t_j) + \eta_k(t_\ell) - \eta_k(t_j) + \xi_\ell \quad (40)$$

where ξ_ℓ is the white noise associated with the Doppler measurement procedure.

Depending on the stability of the clock, the random range or Doppler error components, $\eta_s(t)$ and $\eta_k(t)$, may appear quite systematic over fixed time intervals and may be represented by polynomial models of varying degree. For short time intervals the models for clock error were taken to be a bias and drift for range observations and a frequency bias for Doppler observations. However, these models and even higher order polynomial models are not sufficient to entirely represent this correlated error. Thus knowledge of the statistical properties of the deviations of the error from such a model becomes important, as these residuals represent an unmodeled part of the observation equation after the inclusion of the polynomial model.

Proceeding, equation (39) is expressed as follows

$$\eta(t) = P_{ms}(t) + P_{nk}(t) + r_s(t) + r_k(t) + \xi(t) \quad (41)$$

where $P_{ms}(t)$ is an m 'th degree polynomial chosen to model the correlated random error $\eta_s(t)$ and $P_{nk}(t)$ is an n 'th degree polynomial modeling the random process $\eta_k(t)$. The statistics of the range residuals $r(t)$ may be developed from the covariance of the random clock errors. The second order statistics of the range residuals $r(t)$ to a polynomial model are obtained as

$$E[r(t)r^T(t)] = GE[R(t)R^T(t)]G^T \quad (42)$$

where

$$G = [I - A(A^T A)^{-1} A^T] \quad (43)$$

and A is the least squares design matrix for the polynomial model selected. The $E[R(t)R^T(t)]$ is the covariance matrix of the random clock error being modeled. This covariance is given by equations (32) and (33).

For integrated Doppler observations the statistics of the residuals to a given degree polynomial model are similarly obtained from equations (42) and (43), using the covariance matrix for integrated Doppler random error due to each system clock, equations (37) and (38). The equation may be written as

$$E[\Delta r(t)\Delta r^T(t)] = HE[\Delta R(t)\Delta R^T(t)]H^T \quad (44)$$

where the matrix H is similar to the matrix G of equation (43) with changes due to the choice of the model adopted for clock-induced random Doppler errors

$$H = [I - A'(A'A')^{-1}A']^T. \quad (45)$$

After the selection of the polynomial model, equation (40) has the form

$$\Delta\eta(t_\ell) = P_{is}(t_\ell) + P_{jk}(t_\ell) + \Delta r_s(t_\ell) + \Delta r_k(t_\ell) + \xi_\ell. \quad (46)$$

If the statistics of these residuals were ignored in an estimation problem, then the resulting parameter covariance matrix would be optimistic. An increase in the degrees of the polynomial clock models would offset this optimism to some extent since the level of unmodeled error would be decreased. However, if a rigorous estimation is to be performed, then these residual statistics must be included in the weight matrix to account for the unmodeled error $r(t)$ or $\Delta r(t)$ in a statistical rather than parametric fashion. The estimation algorithm should then produce a valid parameter covariance matrix regardless of the order of the polynomial models used provided numerical problems are not encountered and the parameters are independent and well observed.

Finally, the theoretical standard errors for range residuals to a linear fit were determined using equation (42) for the rubidium and cesium clocks. The results are given in Figures 15 and 16. These figures graphically demonstrate that the statistics of the residuals to the clock modeling polynomial are not stationary. The variance of a residual depends on the order of the polynomial, the interval length and the location within the sample. However, the statistics of the residuals will be constant from interval to interval of the same length provided the sampling is performed equivalently and the same order polynomial is used.

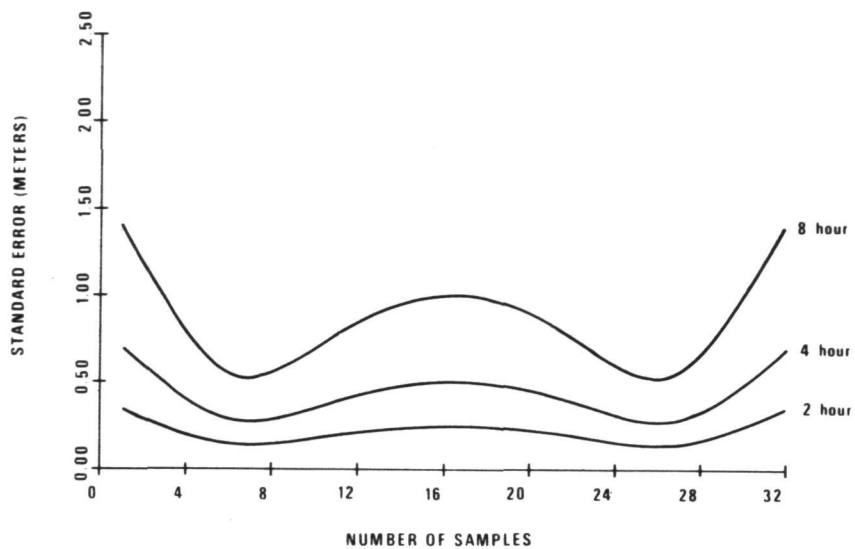


Fig. 15-Standard error of satellite rubidium clock residuals based on a linear fit

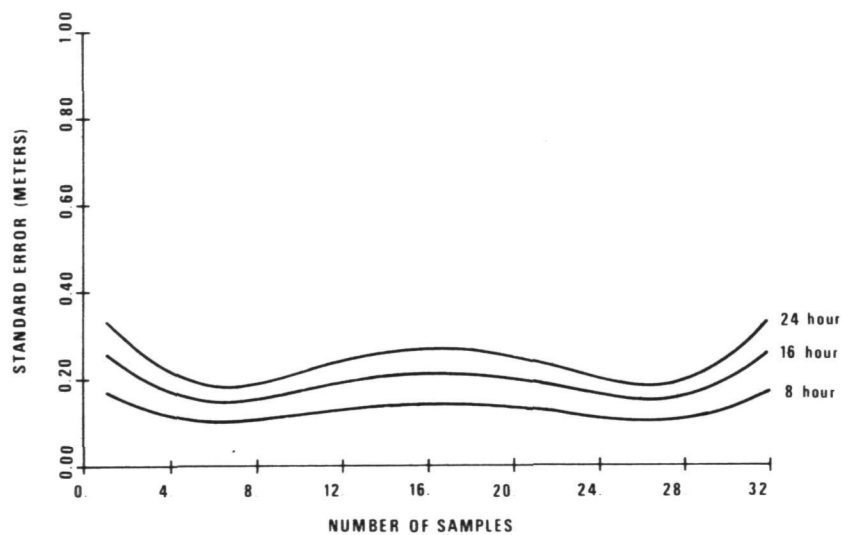


Fig. 16-Standard error of cesium clock residuals based on a linear fit

REFERENCES

- Allan, D. W., J. H. Shoaf, and D. Halford, 1974. "Statistics of Time and Frequency Data Analysis," Time and Frequency: Theory and Fundamentals, National Bureau of Standards Monograph 140, Blair (Editor).
- Anderle, R. J., 1978. "Clock Performance as a Critical Parameter in Navigation Satellite Systems," Proceedings of the Tenth Annual Precise Time and Time Interval (PTTI) Applications and Planning Meeting, National Aeronautics and Space Administration Technical Memorandum 80250, Greenbelt, Maryland.
- Barnes, J. A. and S. Jarvis, 1971. "Efficient Numerical and Analog Modeling of Flicker Noise Processes," National Bureau of Standards Technical Note 604, Boulder, Colorado.
- Barnes, J. A., A. R. Chi, L. S. Cutler, D. J. Healey, D. B. Leeson, T. E. McGunigal, J. A. Mullen, Jr., W. L. Smith, R. L. Sydnor, R. F. C. Vessot, and G. M. R. Winkler, 1971. "Characterization of Frequency Stability," IEEE Transactions on Instrument and Measurements, Vol. 20, No. 2.
- Bartholomew, C. A., 1978. "Satellite Frequency Standards," Navigation, Vol. 25, No. 2.
- Blair, B. E. (Editor), 1974. Time and Frequency: Theory and Fundamentals, U. S. Department of Commerce/National Bureau of Standards Monograph 140, U. S. Government Printing Office, Washington, D.C.
- Fell, P. J. and B. R. Hermann, 1979. "An Empirical Evaluation of the Effect of Oscillator Errors on Dynamic Point Positioning Based on the NAVSTAR GPS System," Proceedings of the Second International Geodetic Symposium on Satellite Doppler Positioning, Applied Research Laboratories, The University of Texas at Austin.
- Fell, P. J., 1980. "Geodetic Positioning Using a Global Positioning System of Satellites," Department of Geodetic Science Report No. 299, The Ohio State University, Columbus.
- Gelb, A., (Editor), 1974. Applied Optimal Estimation, MIT Press, Cambridge, Massachusetts.
- Hellwig, H. W., 1975. "Atomic Frequency Standards: A Survey," Proceedings of the IEEE, Vol. 63, No. 2.

Hellwig, H. W., 1977. "Frequency Standards and Clocks: A Tutorial Introduction," National Bureau of Standards Technical Note 616, U. S. Government Printing Office, Washington, D.C.

Meditch, J. S., 1975. "Clock Error Models for Simulation and Estimation," The Aerospace Corporation, Report No. TOR-0076 (6474-01)-2, El Segundo, California.

QUESTIONS AND ANSWERS

DR. KARTASCHOFF:

I have just one question that you have been remodeling the flicker noise level with these five processes, and I was asking myself now when I hear it what do you think about if one just could use directly the time interval error estimation, as I had shown just before, also for estimating the range error?

Furthermore, one could try to estimate the uncertainty of that estimation by using the uncertainty of the Allan variance using the theory of Audoin-Lesage that limited the sample that we always, for a given time, τ , on the flicker level, and we always have an uncertainty that is given as the number of samples. For the last point you measured, you have only two samples; so you have 2000 percent error as the uncertainty.

I think it would be an interesting exercise to repeat the calculation using these estimations and using your process. Very probably both will give very similar results and both can be used. That would be interesting, I think.

MR. FELL:

I think you are right. This is just one way that you could do this approximate method, those Allan variances. They are specified for a clock and are only an approximation of actual performance, but for a long time people have ignored this type of residual error which is left in the estimation problem. And I think that because we are now trying to get down to such small errors, namely baseline errors of less than 10 centimeters, that we are going to have to take a second look at our modeling and make sure that it is sufficient for the problems that we are addressing.

Otherwise the parameter of statistics which we get out of the estimation algorithm are going to be too optimistic.

DR. VICTOR REINHARDT, NASA/Goddard

You also, if you do your conversions to your range statistics, or range rate statistics, up front you will find that your range rate estimator is one of the weighted Allan variances, and you can just use the tables that are published from converting to the zero dead time Allan variance to the Allan variance with dead times to get your range statistics. That all combined with some factor like C or $\frac{C}{\sqrt{2}}$.

And you can do this not even with a hand calculator on the back of an envelope, do the same thing just by looking up the NBS publications on the various weighings for the various models since all of the frequency standards that we use breakup into well defined regimes we have, you know, a well defined parallel.

Vacuum Pumping System for Spaceborne Passive Hydrogen Masers

S.A. Wolf, D.U. Gubser and L.D. Jones
Naval Research Laboratory
Washington, DC 20375

ABSTRACT

The ultimate utility of hydrogen masers as highly accurate clocks aboard navigation satellites depends on the feasibility of making the maser lightweight, compact, and capable of a 5-7 year unattended operation. We have designed and fabricated a vacuum pumping system for the SAO-NRL Advanced Development Model (ADM) maser that we believe meets these criteria.

The pumping system was fabricated almost completely from 6AL-4V Titanium alloy and incorporates two (three years minimum) or four (six years minimum) sintered zirconium carbon getter pumps with integral activation heaters. These pumps were designed in collaboration with SAES getters and fabricated by them for these systems. In addition to these pumps, small getter ion pumps ($\sim 1\ell/\text{sec}$) are also appended to the system to pump the inert gases.

In this paper we will illustrate the manner in which the getter pumps were mounted to insure that they will stand both the activation (900°C for 10 minutes) and the shock of launch.

Data on the total hydrogen capacity and pumping speed of this system will also be presented.

INTRODUCTION

To fully utilize hydrogen masers as clocks aboard navigation satellites, they must be lightweight, compact and capable of 5-7 years of unattended operation. We have designed and fabricated a vacuum system for the SAO-NRL Advanced Development Model (ADM) maser that we believe meets these requirements.

The design was based on three main criteria; to utilize light weight yet strong materials, minimize the number and size of flanges and most importantly, to find the

optimum combination of getter and ion pumps to match the system requirements for pumping speed and total hydrogen capacity. The remainder of this paper will discuss the details of the system specifications and the design we believe satisfies them.

SYSTEM SPECIFICATIONS

The vacuum system must be light weight, compact, and strong. To minimize the weight without sacrificing structural strength a material had to be found which was lighter than stainless steel but comparable in strength, yet which could be fabricated by machining, forming and welding in our laboratory. The material and the weld joints also had to be compatible with a stress anneal so that any hydrogen embrittlement would be minimized.

The design also had to minimize the number and size of flanges which add considerable weight and complexity to the system, yet be flexible enough for pump, and dissociator replacement. The system needed to be as compact as possible minimizing the overall dimensions. The pumps needed to be capable of 5-7 year unattended operation with a minimum of electrical power.

The load on the pumps depends on the hydrogen flow rate required to maintain the desired signal strength. For the expected flow rate of 2.3×10^{-5} torr liters/sec,¹ this translates to a total hydrogen capacity of 3600 torr-liters for a 5 year lifetime. The hydrogen pumping speed needs to be $5 \frac{1}{6}$ /sec or better to maintain the system pressure below 5×10^{-6} torr. In addition all residual gases must be pumped by the pumping system and kept at a background level considerably below the hydrogen partial pressure. The pumps must be mounted to withstand both the shock of a launch and the activation of the getter material. Finally, the design had to mate with the cavity chamber manufactured by SAO and maintain a rather precise alignment.

SYSTEM DESIGN

We believe we have designed and built a pumping system that meets all the specifications elucidated above.

The material chosen was a titanium alloy 6AL4V which has proven itself in aerospace applications. It is about (60%) the weight of stainless steel yet is at least as strong. It can be formed into cylinders, machined into flanges, and welded in an inert atmosphere. Procedures

for stress annealing are well documented and minimize the diffusion of hydrogen into the bulk of the alloy thus minimizing the possibility of hydrogen embrittlement and consequent failure of the pumping system. A sketch of one of two vacuum system designs is shown in Fig. 1.

This design incorporates two getter pump chambers with gold O-ring flanges, a port for connection to small ion pumps, a Viton-O-ring flange for connection to the dissociator and state selection magnet system, a port for welding to the cavity chamber and a pumpout port. A picture of this system is shown in Fig. 2. A second design, similar to Fig. 1 has four getter pump chambers located symmetrically around the main chamber. The rationale for the second design will be explained below.

The getter pumps which handle the hydrogen and all other active gases were built by SAES getters. The design of the getter pumps themselves was a collaborative effort and were a compromise based on what SAES Getters thought they could achieve and what we desired. A pump of the size we needed had not been built previously from their Zr-C interred alloy, ST171 which pumps hydrogen and other active gases at 25°C. In addition we required an internal heater for the specified activation of the material which is 900°C for a minimum of 10 minutes. Since pumps as large as these had not been previously built, we had to rely on estimates of their pumping speed and hydrogen capacity based on their experience pumping with smaller pumps. The expected pumping speed and capacity of these pumping elements are listed along with their other specifications in Table I. Note that the capacity per pump was estimated to be ~ 2000 torr liters for an end of life pumping speed of approximately 10 ℓ /sec. Our two pump design was based on these estimates with a safety margin of having the total pumping speed (for 2 pumps) of 20 ℓ /sec at 4000 torr liters consumed. Unfortunately, the first tests of these pumps which performed by SAES after a 10 minute activation at 900°C were discouraging. Their initial pumping speed was about 120 ℓ /sec and their capacity at a final pumping speed of about 1.5 ℓ /sec was less than 1000 torr liters. Thus to provide a 5 year lifetime, four pumps instead of two seemed necessary. A four pump design was conceived based on the initial test and is almost completely fabricated. Very recently, however Hughes Research Labs¹ have taken similar pumps [100 gms vs 150 with no internal heater] and have activated them at 925°-950° for two hours using inductive heating techniques. To date, their pump has pumped over 1000 torr liters and is expected to have an end of life (pumping speed $\leq 10 \ell$ /sec)

capacity of 1200 torr liters. This translates to a capacity of ~ 1800 torr liters for our 150 gm pumps and means that our two pumps design may be adequate provided we activate our pumps at $\sim 925^{\circ}\text{C}$ for two hours.

The mounting for our pumps to provide both shock mounting and thermal isolation is shown in Fig. 3. The pumps are supported around a molybdenum rod by two molybdenum washers. The washers are held in place by two stainless steel Belleville Springs and the whole assembly is rigidly clamped by a large stainless steel nut which also acts as a thermal baffle. The pump assembly is attached rigidly to the flange which mates to the pump chamber via a gold O-ring seal. We believe the gold O-ring design can withstand the shock of launch and the thermal extremes of activation. The electrical feed times for the activating current were specially fabricated by Ceramaseal, and incorporate a ceramic to titanium seal. They are capable of passing 30 amps of current, more than is required for a 925°C activation. The pump assembly mates into a combination support flange and thermal baffle which is welded to the far end of the pump chamber. When inserted the pump is rigidly supported inside the chamber. The nut, baffle, and support baffle together eliminate any optical path from the pump to the magnet chamber thus shielding the large chamber from thermal radiation. A removable water cooled shroud for the pump chambers will keep the outside of the chamber and the pump flange cool during activation.

The pumps described above will effectively pump the hydrogen that is introduced as well as the nitrogen, residual oxygen, CO , H_2O , and CO_2 that is in the chamber and leaks off the walls. However, these pumps will not pump the helium, argon, and other inert gases that are present in the chamber or leak off the walls. A small ion pump or pumps are required to pump these gases. However, small ion pumps become readily saturated with hydrogen so a means must be found to prevent them from pumping much hydrogen. There are several options. One is to have the ion pump located backstream from the getters in such a place that it is exposed only to those gases not pumped by the getter pumps, or secondly one can adjust the voltage to the ion pumps so that they are very inefficient for hydrogen pumping relative to their speed for argon and other inert gases. It is this second option which we have incorporated into our design. Two small Varian appendage ion pumps, are located just outside the main chamber on a stainless steel swagelock coupled port. Their voltages will be set so that they will not pump hydrogen efficiently (≤ 2000 volts). If one does

Table I

Properties of Zr-C ST 171 Pumps

	<u>Projected</u>	<u>Measured by SAES</u>	<u>Expected from Hughes Results</u>
Size	42x45 mm	42x45 mm	--
Weight	171 gms	171 gms	
Activation	900°C-10 min	900°C-10 min	925-950°C-2 hours
Initial Pumping Speed	450 ℓ/sec	120 ℓ/sec	> 100 ℓ/sec
Hydrogen Capacity	2000 torr liters	900 torr liters	1800 torr liters
at	at	at	at
Final Speed	10 ℓ/sec	1.5 ℓ/sec	10 ℓ/sec

Table II

Properties of Two Getter Pump Vacuum System

Material:	Ti - 6AL4V
Overall Size:	< 36 cm (14 in)
Weight:	1.93 kg (4.25 lbs)
Pumps:	2 SAES Getters ST171/H1/45-40/1500C 2 Varian Miniature Appendage Ion Pumps
Lifetime:	~ 5 years at $(2.3 \times 10^{-5} \text{ torr } \ell/\text{sec H}_2)$
Power Consumption:	< 1 watt

become saturated, the other pump can be activated. These pumps will consume about a watt of power.

The final port is a pump out port which will be attached to a Turbomolecular pump during activation of the getter pumps. After activation of the getters this port will be sealed off with a copper nipple. The specifications of the overall system are summarized in Table II.

SUMMARY

This paper has illustrated the requirements for a spaceborne passive hydrogen maser vacuum system and our particular solution. We have designed and fabricated a titanium alloy chamber with ports for either two or four Zr-C getter pumps and for two small ion pumps. These pumps should be capable of providing 5-7 years of unattended pumping for a passive maser with a hydrogen flow requirement of 2.3×10^{-5} torr liters/sec. The system should be capable of withstanding both the getter activation and the shock and vibration of launch. Both activation and shock and vibration tests will be performed in the near future.

ACKNOWLEDGMENTS

We greatly appreciate the support and assistance of V. Folen, J. White, and C.A. Bartholomew in this program. We also thank D. Bratz of SAES Getters for his invaluable technical assistance. This work is sponsored by NAVELIX PME106-2.

REFERENCE

1. Hughes Research Lab. - private communication.

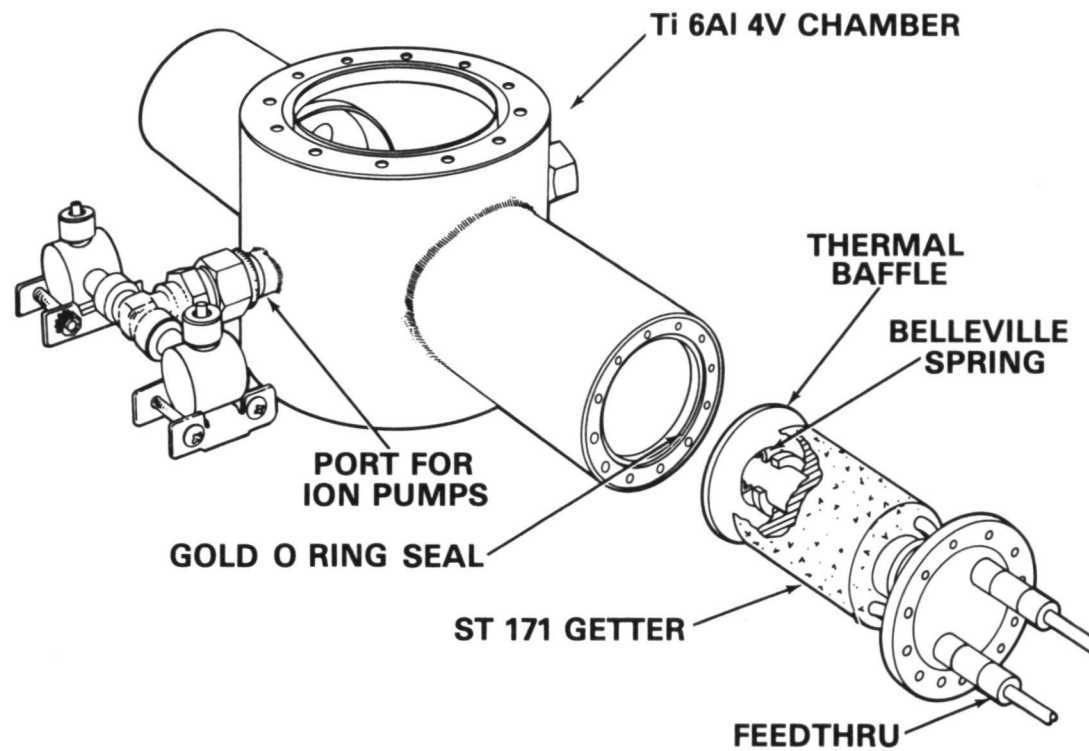


Fig. 1-Sketch of vacuum system design.

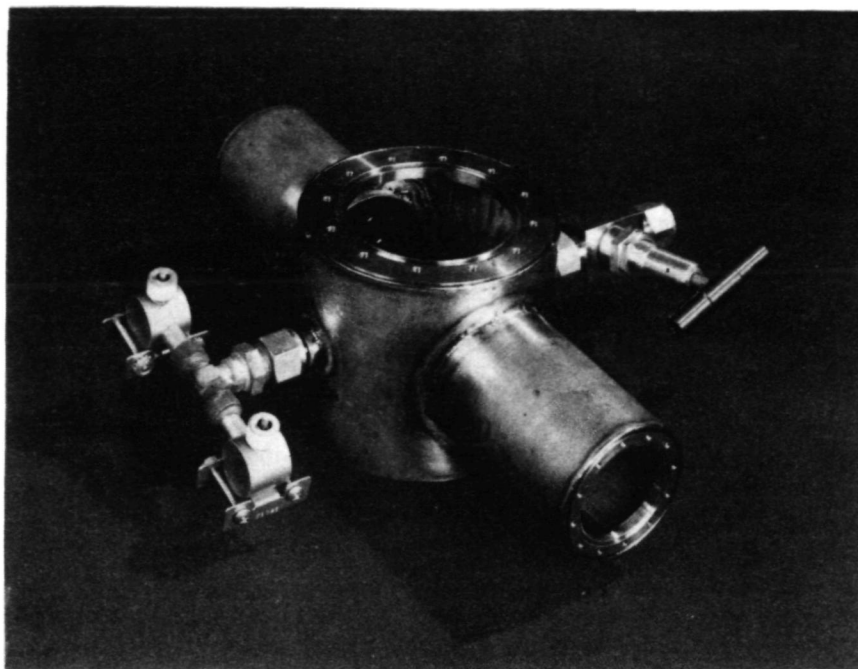


Fig. 2-Photograph of vacuum chamber.

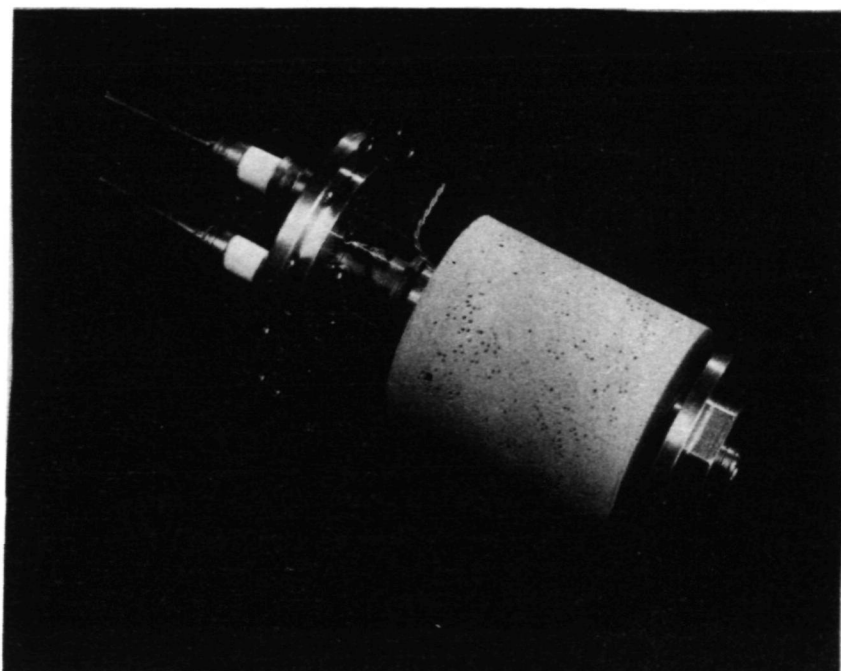


Fig. 3-Photograph of getter pump and mounting.

QUESTIONS AND ANSWERS

MR. JOHN DEAN, U.S. Army

I am sure that you have considered the use of cryo pumps as many satellites already contain refrigerators, I wanted you to comment on why you chose to go this way instead of using a cryo pump?

MR. WOLF:

Well for the main reason of reliability and power consumption. This pumping system would work fine with only one watt of power and the cryo pumps actually take a significant amount of power.

We also considered the possibility of a miniature turbo pump, turbo molecular pump. Again I think that the power requirement is what ruled it out. If this works it has no moving parts. Just one activation on the ground which can be checked. So I think from the standpoint of simplicity if it works it will be much better.

DR. VESSOT:

I don't think that there is any question that it will work. We know these things are remarkably hungry for hydrogen. The comment I would like to make though is that in the case of those four, and should you activate them together, especially with prolonged cycle of two hours, the whole thing is going to get hotter than blazes.

And I strongly recommend that you put a small water coil at the hex magnet. We found that even with absorption cartridge that we flew in '76 that that damn thing would have died if we hadn't used the water cooler.

MR. WOLF:

I am sorry that I forgot to mention that we have fabricated a water cooling shroud for the whole thing, and when it is activated the whole chamber will be water cooled, but this chamber will be removable after activation so it will not be launched. But I thank Bob for pointing out the fact that yes we do certainly intend to water cool it during activation.

Page Intentionally Left Blank

FREQUENCY AND TIMING SYSTEM FOR THE
CONSOLIDATED DSN AND STDN TRACKING NETWORK

R. C. Coffin, D. E. Johnson, and P. F. Kuhnle

Jet Propulsion Laboratory*
California Institute of Technology
Pasadena, California

ABSTRACT

For NASA, JPL is presently in the planning phase of consolidating the existing Deep Space Network (DSN) and colocated Goddard Spaceflight Tracking and Data Network (STDN) stations into a multiple antenna array.

Each site will include a Signal Processing Center (SPC) centered in an array of four or five antennas each located within approximately 300 to 800 meters of the SPC. A central Frequency and Timing System (FTS) located in the SPC will contain reference frequency, timing and time code generation, and distribution equipment for both the SPC and each antenna with its associated front end antenna control building.

The reference frequency distribution and clock equipment will be driven by a Hydrogen Maser as the prime frequency standard with Cesium Beam Frequency Standard as the secondary.

This paper will present the proposed equipment configuration and preliminary performance specifications for the above Frequency and Timing System.

INTRODUCTION

The advent of the Tracking Data Relay Satellite System (TDRSS) will herald major changes to NASA's ground-based tracking networks. An offshoot of these changes, which will be discussed in more detail below, is

*This paper presents the results of one phase of research carried out at the Jet Propulsion Laboratory, California Institute of Technology, under Contract No. NAS 7-100, sponsored by the National Aeronautics and Space Administration.

the consolidation of JPL's globally-distributed Deep Space Network with colocated elements of GSFC's Ground Spaceflight Tracking Data Network (GSTDN). In conjunction with these modifications to the ground tracking networks, there will be requisite changes to the Frequency and Timing Subsystem (FTS) which provides references for the telemetry, command, and tracking applications of these stations.

The schedule of modification to the Ground Tracking Networks is driven primarily by spacecraft events such as launches and planetary encounters, and by funding availability. Present planning indicates that major implementation activities will occur in the 1983-1985 time period. Consequently the state of the design is still functional at this time. Early assessments of the Frequency and Timing System requirements have been made and a high-level system functional design has evolved. Additionally, the subsystem functional requirements have been tentatively established and are currently being revised. The purpose of this paper is to introduce the Consolidated Space Communication Network to the frequency and timing community and to show the present thinking at Goddard and JPL about the design of the Frequency and Timing System to support that network.

NETWORKS CONSOLIDATION PROGRAM OVERVIEW

Decisions were made by NASA in 1979 which will, by 1985, result in the merger of the colocated tracking facilities of the Ground Spaceflight Tracking and Data Network (GSTDN) and the Deep Space Network (DSN). This Consolidated Space Communication Network, to be operated by JPL, will be responsible for all ground tracking support for Deep Space Missions including high earth-orbital missions. It will NOT support low earth-orbital spacecraft which will be supported exclusively by the TDRSS. The decision to consolidate resulted from a study performed by the Networks Planning Working Group, which was established by the NASA Office of Space Tracking and Data Systems (OSTDS) in 1979. The working group membership consisted of representatives from OSTDS, the Goddard Space Flight Center (GSFC), the Jet Propulsion Laboratory (JPL), the Spanish Instituto Nacional de Tecnica Aeroespacial (INTA), and the Australian Department of Science and Environment (DSE). This study is concentrated on the capabilities, requirements and costs of the ground segment of the NASA Tracking Networks.

There were three basic drivers for the study effort. First, the early-to-mid eighties will be a period of lowered tracking activity for all space missions. Second, the early eighties will see the advent of the TDRSS which will carry the majority of the tracking load for earth-orbital spacecraft, including the low-altitude spacecraft. Third, the

increased activity in space during the second half of the eighties. To prepare for this increased load, it is appropriate to modify and reconfigure the Ground Tracking Network(s) now, for more cost-effective operation later. Figure 1 shows the present day (1980) locations of the antennas to be colocated. All other GSTDN sites will be closed after the TDRSS becomes operational.

Both the 64-meter and 34-meter antennas at each DSN complex will be used to track planetary and interplanetary spacecraft. The colocated GSTDN 9-meter antennas will be converted into a subnet to support future high earth-orbital spacecraft. Signal Processing Center (SPC) equipment should be interchangeable between planetary and high earth-orbital links. Figure 2 is an overview of the Consolidated Space Communication Network. The antennas and their associated front-end area operate in an unattended mode for all normal tracking.

The SPC will contain the centralized monitor and control equipment, telemetry demodulation, command processing equipment, frequency and timing, receiver, exciter, radio science, and communication equipment.

All manual control points for the communication complex will reside in the monitor and control equipment in the SPC. Each communication link will be supervised through a dedicated control console with all consoles centrally located in the SPC. Equipment configurations are to be such that signal combining, telemetry signal detection, and telemetry and command processing will be normally dedicated to a specific link, but can be switched for mutual backup. All antennas and front-end area subsystems which are arrayed together for a communications link will be supervised through the control console for that link. Figure 3 shows a view of a typical complex after reconfiguration.

The frequency and timing requirements are being driven by two factors. First, the impending consolidation of DSN with the colocated GSTDN is placing new requirements on the existing FTS. These requirements fall primarily into the areas of increased distribution capacity and capability, the need for centralized monitor and control of the frequency and timing equipment, and finally the need to provide time offsets (under operator control) to selected users for the purpose of simulating upcoming tracking events for training purposes. The second factor driving the requirements to develop new frequency and timing equipment is the need to replace aging equipment. The present complement of equipment at both GSTDN and DSN stations are antiquated, much of it having been implemented in the nineteen sixties.

The approach that has been followed is to take the best equipment available in either network and to design the remainder. In general, the FTS can be thought of as a series arrangement of functions as shown in Figure 4.

Sinusoidal reference generation and distribution functions will be supported by existing equipment. GSTDN equipment will be used to generate and distribute epoch time and timing pulses. The distribution capacity function, the monitor and control function, and simulation time will require new equipment.

Consolidation of the network will have a significant impact on FTS requirements. Distribution of sinusoidal reference frequency is presently made to all users in the control room and antenna. However, timing signals are a different matter. Present distribution capability of timing signals only extends to users in the control room where computers are located. With the implementation of the NCP configuration, the distribution requirements change in two ways; first, there will be more users in the SPC than currently served by the 64-meter control room FTS. Secondly, there will now be a need to provide signals to remote front-end area locations.

Coincident with implementation, the DSN will replace the monitor processors which do not have the capacity to accommodate the increased load. Implementation of monitor and control equipment will provide centralized operator capability. Additionally, the design is based upon unattended front-end areas. The ramifications of these monitor and control changes to frequency and timing is that (1) the new equipment planned for the front-end area must be unattended, and (2) the frequency and timing equipment in the SPC must have a single, digital, monitor, and control interface for the central monitor and control processor.

Simulation time code generation and distribution is another major area of change being imposed upon the frequency and timing equipment. For testing prior to critical tracking events such as encounters or spacecraft maneuvers, and for training of personnel, the FTS generates and distributes a time code that is offset (by operator command) from real time. Traditionally, the DSN has been able to offset time for all users at a station. With a Consolidated Network, that will not be possible. It will be necessary to provide selectable time (real or simulated) separately to each user. The central link operator will select, for each assembly, which time epoch to use.

FREQUENCY AND TIMING FUNCTIONAL REQUIREMENTS

In order to support the frequency and timing functions of the Consolidated Network, certain complex and network level functions must be satisfied. These functions arise out of the globally distributed nature of the FTS, the requirement for complex time synchronization, complex frequency and timing distribution, and the discipline required for maintenance of time and frequency performance records. Figure 5 is a hierarchical input-output chart depicting the FTS interfaces and the functions that serve the DSN.

Knowledge of the time offset of the DSN relative to the national standards at the National Bureau of Standards (NBS) is presently obtained by traveling clock visits from DSS-14 (Goldstone 64-meter antenna). DSS-14 serves as the DSN master frequency standard and clock and the other stations are synchronized to it. Future plans assume that this function will be performed via a Global Positioning Satellite (GPS) System with GPS time synchronization ground based receivers at both DSS-14 and NBS in Boulder, Colorado. The time offset of the DSN master frequency standard relative to USNO/NBS is maintained within 50 microseconds. Knowledge of this offset is maintained within 5 microseconds. This requirement is based upon navigation accuracy needs and stems from the need to couple ranging, doppler and VLBI measurements to the earth platform.

The measurement of frequency and time offset of each complex master standard relative to the Network Master Standard at Goldstone is achieved by a variety of techniques. Typical techniques are Very Long Baseline Interferometer (VLBI), traveling clock visits, LORAN-C time synchronization (Spain), and TV pulse time synchronization (Australia). With the inception of the Global Positioning Satellite (GPS) System and the implementation of DSN GPS time sync receivers, all but the VLBI technique will be severely curtailed. VLBI plus LORAN-C and TV sync methods are used, along with time service bulletins to provide an independent correlation of the measurements. The time offset at each complex is maintained to within 50 microseconds of the Goldstone complex and knowledge of time offset is required to be within 10 microseconds. Knowledge of the frequency offset of the frequency standard at one complex relative to the other complexes is to be within 3 parts in 10^{13} . Frequency standard errors translate into apparent spacecraft positional errors when making navigational measurements using two-station techniques such as VLBI or downlink one-way ranging. Time offset is critical to the planetary ranging methods used by the DSN.

Within each complex, there are several physically separated frequency standards and clocks. In the Network Consolidation era, most of these will be relocated to the central SPC. However, at Goldstone one

station, a 34-meter transmit-receive facility will remain physically remote from the SPC and will, therefore, still retain its stand alone frequency standard and clock. For synchronization of that station, a one pulse per second signal will be transmitted from the complex master via the area microwave system. The transmission modes are of a known and stable time delay. Time synchronization will be maintained within 50 microseconds of the complex master and knowledge of time offset will be within 3 microseconds. Knowledge of frequency offset is not as critical as for complex-to-complex offset since this station is not involved in dual station navigation measurements. Therefore, the knowledge of the frequency offset will be within 1 part in 10^{11} .

Generation and distribution of reference frequencies, timing pulses, and epoch time codes to system users in each SPC, FEA, Antenna Area and Network Operations Control Center (NOCC) is the primary purpose of the frequency and timing equipment. The sinusoidal reference frequencies, timing pulses, and epoch time codes that are generated at the complex master FTS for distribution to frequency and timing users are shown in Figure 6. Table 1 depicts the Allan variance stability requirements for reference frequencies within a complex.

The NOCC, located at JPL, Pasadena, California, requires timing pulses and epoch time codes (1 p/s, 10 p/s; 30-bit parallel BCD, 30-bit parallel binary and 36-bit serial NASA time code). The FTS presently installed at NOCC will continue to be utilized. Time synchronization is traceable to NBS/USNO through the JPL standards laboratory.

Reliability of 99.9 percent at the three complexes will be achieved with the implementation of a second Hydrogen Maser frequency standard and an upgraded Triple Redundant Timing System (TRTS) at each Network Consolidation complex. This level of reliability is based upon the reliability requirements for telemetry and tracking data and an understanding of system design in which frequency and timing references are a prerequisite to valid data.

Validation, recording, and publishing of the performance of frequency and time parameters including configuration and synchronization is an extremely important aspect of any timing system. Performance recording of reference and epoch time signals are often used as a yardstick for DSN measurements. In some applications, uncertainties in reference frequency or epoch time can be translated into measurement errors. Consequently, the stability requirements of the references and the calibration of epoch time requires accurate measurements (validation) and rigorous record maintenance. To accomplish these functions, a performance measuring capability, sufficient to ascertain functional operability, will be required. It is planned that the measurements of time and frequency stability (Allan variance) will be an automated function implemented within the Frequency and Timing Monitor and Control

System at each station. The time-variant configuration as well as alarm status will also be monitored and recorded at each station.

Network level monitoring and performance analysis will be accomplished in a semi-automated mode by the Network Operations and Analysis (NOA) Section at JPL. This NOA Section will receive reports from each station tabulating stability performance, configuration, and the results of station level offset measurements such as LORAN-C, TV sync pulse, and traveling clock visits. Additionally, the analysts will receive measurement results from VLBI data. An analysis of these data will then culminate in a periodic (monthly) report on station stability performance, complex-to-complex time and frequency offset and an analysis of any anomalous behavior.

Figure 7 is a simplified flow chart showing the data gathering process for frequency and timing performance analysis. VLBI time synchronization measurements are performed approximately on seven day centers. Upon receipt of the VLBI measurement data at a complex, the data is converted to digital form and transmitted to the VLBI Processor Subsystem at the NOCC. After processing, the data is made available for analysis at the Network Operations and Analysis (NOA) Section. Complex FTS performance parameters are data linked to the NOCC Monitor and Control (NMC) Subsystem from the Complex Monitor and Control Console (CMC). The NMC provides complex FTS monitor and status reports to the NOA. FTS monitor and status reports and the VLBI correlated data are compiled and analyzed as to time and frequency offsets between complexes and for complex master frequency standards and clock behavior.

FREQUENCY AND TIMING FUNCTIONAL DESIGN

Reference Distribution

The frequency and timing functional design is still evolving and it will continue to change as the NCP design solidifies. Complicating the process is the fact that frequency and timing signals are required to be one of the first elements of the system to become operational. The present high level block diagram for frequency and timing in the Network Consolidated era is shown in Figure 8.

The frequency and timing design is based upon the existing DSN complex master frequency standards and sinusoidal reference generators. Located at each SPC, the complex master frequency standard will consist of two Hydrogen Masers backed by two Cesium Beam Frequency Standards. These standards, which are located in an environmentally controlled area, are provided with an uninterruptible power source for possible emergencies. Switching provided in the sinusoidal reference generator allows selection of any of the four standards as the input for the complex. Switching from standard-to-standard may be

by manual operator command but, in the event of frequency standard failure, the standards are switched automatically.

Sinusoidal signals not available from the frequency standards are synthesized and distribution amplifiers provided in sufficient quantities to meet all users needs in the SPC. The amount of equipment resident in the SPC will be greater than now supported by the DSN reference generators. One reference generator will have to meet the needs of equipment that is now supported by individual reference generators at standalone stations. The extent of the needed expansion in capability is being determined, however, it is anticipated that the quantity of new distribution amplifiers will perhaps double.

Reference frequency distribution is not the only capability that will have to expand in the NCP area. Timing signal (pulses) and epoch time code distribution capability is also not adequate for a Consolidated Space Communication Network. The present planning assumes the availability of Goddard Triple Redundant Timing Systems at each complex for generation and distribution of clock signals. These timing systems are functionally identical to the timing system presently installed at the White Sands TDRSS Tracking Station.

Sinusoidal reference signals for users at the antenna areas will be distributed to the antennas either directly by uncompensated but buried cables, or by actively stabilized cables. The actively stabilized cables are used, today, only for VLBI which requires reference signals on the antenna having essentially the same stability as that of the Hydrogen Maser reference frequency standard.

Simulation Time

This function, which is not easily conveyed by a block diagram, will be achieved by a system design utilizing serial time code distribution and users individually mounted time code translators that can be individually time offset upon command. This design avoids central switching and multiple clocks while simplifying distribution. In conjunction with this effort, there will be a restriction of the types of codes available to users.

Monitor and Control

At the SPC, FTS performance parameters from the FTS master will be routed to the Complex Monitor and Control (CMC) Console via an FTS controller. The FTS performance parameters will then be data linked from the CMC to the NOCC Monitor and Control (NMC) Subsystem at JPL via the GCF, GSFC NASCOM Switch, and the JPL Central Communications terminal. Monitoring of FTS parameters via the CMC and the NMC is new for the Consolidated Space Communication Network.

Within the NOCC at JPL, the VLBI Processor Subsystem and the NOCC Monitor and Control (NMC) Subsystem perform functions for the DSN Frequency and Timing System. At the VLBI Processor Subsystem, complex VLBI time synchronization data is received over a 56 kb/s NASCOM circuit. The VLBI correlator will process the VLBI data and make it available for the Network Operations and Analysis Section (NOA).

The NMC will receive FTS parameters data linked from the complexes and will provide Monitor FTS Displays for use by the Network Operations Control Team. The NMC will also provide FTS monitor and status reports to the Network Operations and Analysis Section (NOA).

The Network Operations and Analysis Section (NOA), as a DSN supporting element, will receive complex-to-complex time and frequency offset compiled data from the VLBI correlator and FTS monitor and status reports from the NMC. The data will be analyzed as to time and frequency offsets between complexes and for complex master frequency standard and clock behavior. The NOA will advise the complexes of the results by TWX and/or written reports. The reports will also be available to the FTS Cognizant Operations Engineer (COE), Cognizant Design Engineer (CDE) and the FTS Systems Engineer (SE). The FTS services performed by the NAO are not unique to the consolidated network.

Time Synchronization

Figure 9 further illustrates in more detail, the interfacing and data flow for time synchronizing the network. Complex-to-complex time synchronization, referenced to the National Bureau of Standards, will be accomplished via Global Positioning Satellite (GPS), System and a GPS Receiving System at each complex. It is anticipated that the GPS, with its planned 18 satellites, will provide a means of synchronizing the three complexes to an accuracy of better than 50 nsec and with a time stability day-to-day of better than 10 nsec allowing an absolute frequency difference between any of the three complexes to better than 1 part in 10^{13} .

The high accuracy calibrations are achievable because of the bandwidth and signal strength the GPS offers and use of state-of-the-art atomic oscillators on-board each of the satellites. The clear access (CA) code on the L1 carrier from the GPS satellite clocks will be used. Completed procurement and implementation of GPS receivers for time synchronization at the three complexes is expected in 1984.

Complex FTS master to DSN FTS master (Goldstone) synchronization measurements are accomplished using the Very Long Baseline Interferometer (VLBI) time synchronization technique. In this technique, real-time data is sent to JPL for reduction and computation of time offset and frequency rate. The data obtained is also used for navigational

purposes. The VLBI requirements are not new to the Consolidated Space Communication Network.

COMPLEX DESIGN

The following areas within the FTS will be new for the Consolidated Space Communication Network:

- (1) Expanded distribution of reference frequencies, timing pulses, and epoch time code to support additional FEAs.
- (2) Upgraded clocks (Triple Redundant Timing System - TRTS).
- (3) Monitoring functions of FTS performance parameters.

The new TRTS will provide timing pulses and epoch time codes and a function for simulation time. The capabilities that the new clocks will have and that do not presently exist at the complexes are:

- (1) Year End: Automatic reset
- (2) Leap Year: Automatic extra day addition
- (3) Leap Second: Simple addition or subtraction of leap second
- (4) Resettability: Simple clock adjustments

Monitoring of FTS performance parameters will incorporate FTS controller equipment implemented within the FTS at the SPC. Monitor outputs of the FTS master will be routed to the controller. The controller at Goldstone will have additional inputs for monitoring of the FTS performance parameters from the standalone FTS at DSS-12. The FTS controller will route the FTS performance parameters to the DMC where measurements of time and frequency offset will be accomplished by automatic functions within the Monitor and Control System. The DSS-12 will have a monitor microprocessor which will perform the transfer functions for routing the FTS parameters to the FTS controller via the Ground Communications Facility (GCF 10).

STATUS AND SCHEDULE

The design and implementation of reference frequency and timing equipment (FTS) is paced by the first-scheduled installation completion coincident with the relocation of DSS-44 in the spring of 1983. All Signal Processing Centers, 64-meter and 34-meter Deep Space Network (DSN) antennas must be completed prior to the Voyager 2 spacecraft encounter at the planet Uranus during November 1985. The three GSTDN 26-meter antennas will be released for relocation after the TDRSS satellite is operational, currently scheduled for December 1983. The three

GSTDN 9-meter antennas are scheduled for relocation during 1986. A schedule depicting programmatic milestones, FTS equipment design and implementation and station conversion is shown in Figure 10.

CONCLUSIONS AND SUMMARY

The Consolidated Space Communication Network has been described with particular emphasis on the frequency and timing aspects of the network. System requirements have also been presented with the identification of the requirements that are different from those existing today as follows;

- (1) Increased distribution capability
- (2) Centralized monitor and control
- (3) Generation and distribution of simulated time to individual users when required.

Finally, a functional design has been presented that will meet the existing and new requirements. This design involves selection of the most modern equipment from both the DSN and the GSTDN. As the architectural design of the Consolidated Space Communications Network evolves, the FTS design will, of necessity, also change.

Table 1. Reference Frequency Stability

σ	Allan Variance $\sigma(\tau)$	
	Signal Processing Center	VLBI Antenna-Mounted Equipment
1 sec	1×10^{-12}	1×10^{-12}
10^4 sec	1×10^{-14}	1×10^{-14}
12 hours	1×10^{-14}	1×10^{-14}
10 days	2×10^{-14}	2×10^{-14}

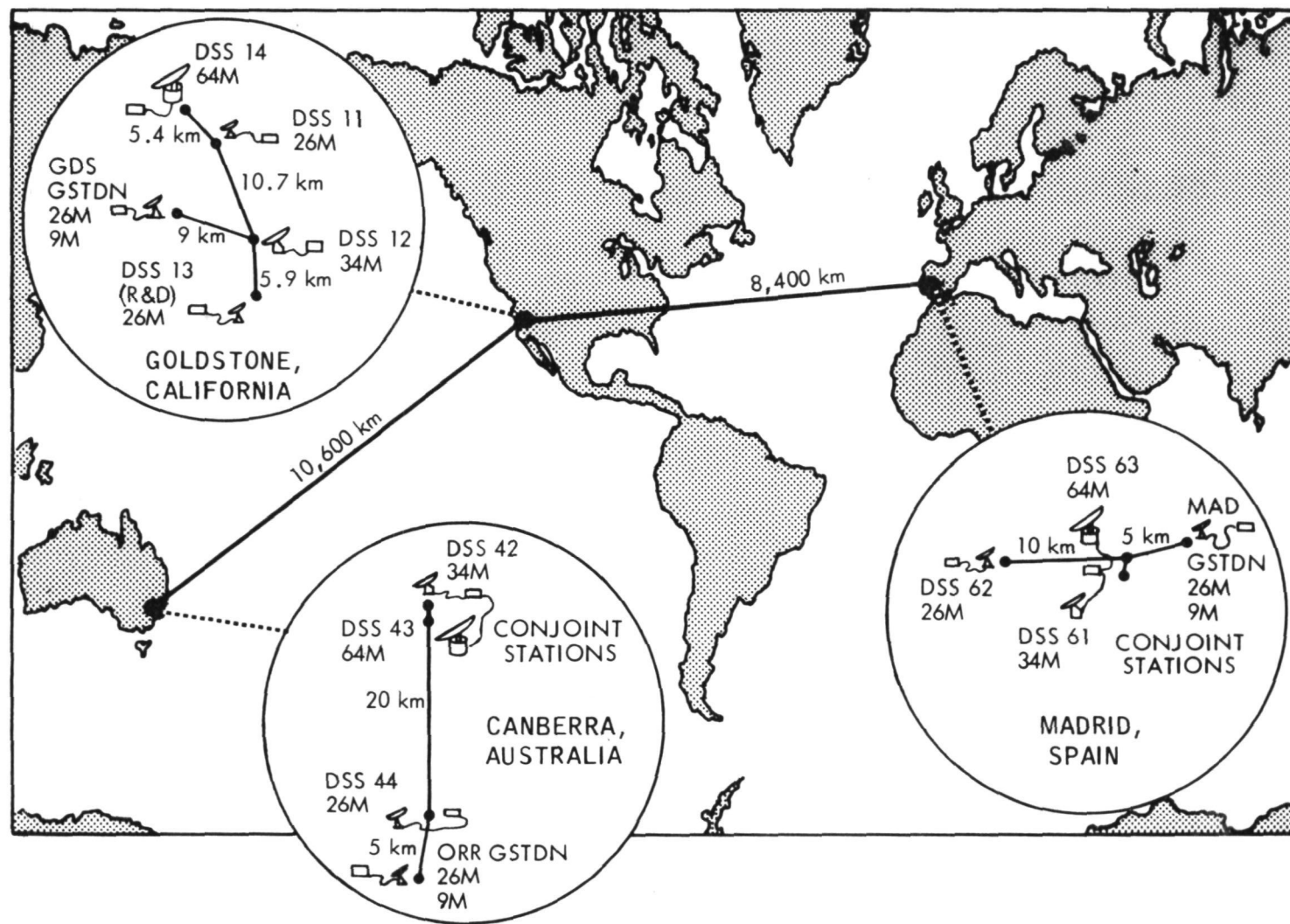


Fig. 1—Space Communication Network Complexes - 1980

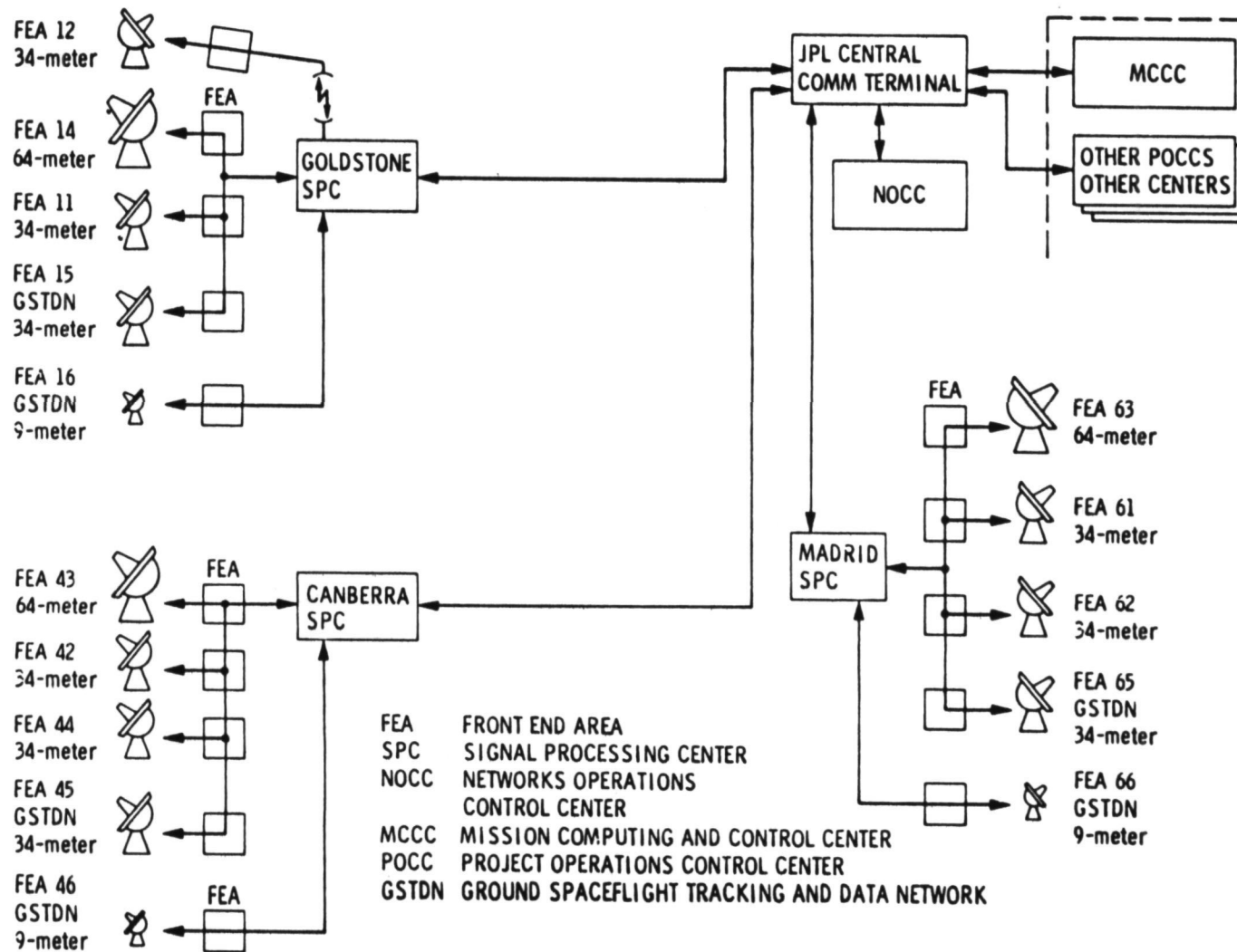


Fig. 2-Consolidated Network Configuration - 1986

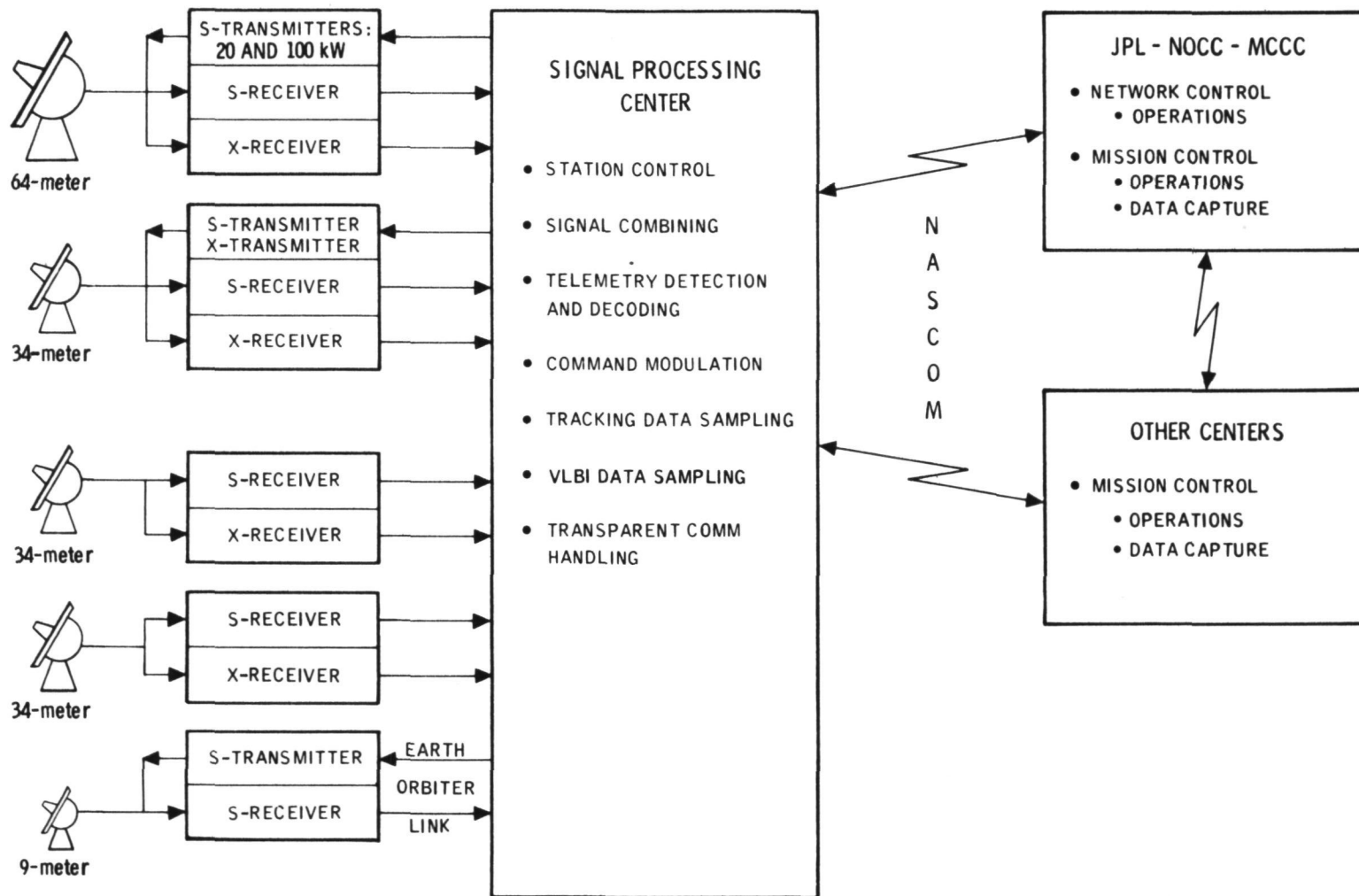


Fig. 3—Typical Complex Configuration

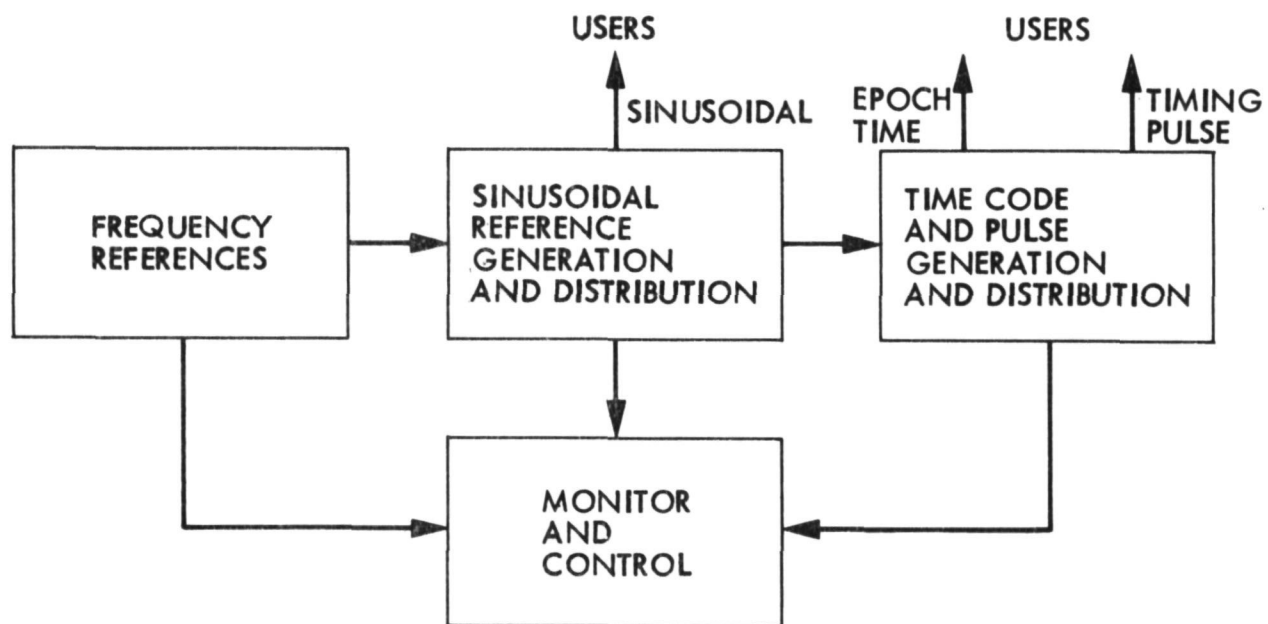


Fig. 4—Frequency and Timing System Conceptual Block Diagram

INTERFACES

USNO AND/OR NBS
UTC AND GMT

FUNCTIONS:

- MEASURE TIME OFFSETS BETWEEN DSN AND USNO AND/OR NBS
- MEASURE FREQUENCY AND TIME OFFSETS BETWEEN COMPLEXES
- PROVIDE SYNCHRONIZED TIME AND MEASURE FREQUENCY OFFSETS WITHIN EACH COMPLEX
- GENERATE AND DISTRIBUTE REFERENCE FREQUENCIES, TIMING PULSES AND EPOCH TIME CODES TO SYSTEM USERS IN EACH SPC, FEA AND NOCC WITH 99.9% AVAILABILITY
- VALIDATE, RECORD AND PUBLISH MONTHLY THE PERFORMANCE OF FREQUENCY AND TIME PARAMETERS INCLUDING CONFIGURATION AND SYNCHRONIZATION

INTERFACES

DSN FREQUENCY STABILITY
AND TIME OFFSETS
FREQUENCY AND TIMING
CORRELATED DATA

VLBI SYSTEM

REFERENCE FREQUENCIES
TIME PULSES
EPOCH TIME CODES

ALL DSN SYSTEMS

FREQUENCY AND TIMING
CORRELATED DATA AND
DSS FTS RPT (M&C)

FREQUENCY AND TIMING
DATA ANALYSIS REPORTS
AND DSS FTS REPORTS

DSN SUPPORTING ELEMENTS:
DSN NETWORK
OPERATIONS
AND ANALYSIS (NOA)

FREQUENCY AND TIMING
DATA ANALYSIS REPORTS

USERS

MONITOR
PARAMETERS

MONITOR AND
CONTROL PARAMETERS

MONITOR AND
CONTROL SYSTEM

Fig. 5—Functions and Interfaces Frequency and Timing System

- **SINUSOIDAL REFERENCE FREQUENCIES**

- 0.1 MHz (SPC ONLY)
- 1.0 MHz
- 5.0 MHz
- 10.0 MHz
- 10.1 MHz (SPC ONLY)
- 45.0 MHz
- 50.0 MHz
- 55.0 MHz (SPC ONLY)
- 100.0 MHz (VLBI ONLY)

- **TIMING PULSES**

- 1 p/s
- 10 p/s
- 100 p/s
- 1k p/s (SPC ONLY)

- **EPOCH TIME CODES**

- 36-BIT SERIAL
- 36-BIT PARALLEL BINARY

Fig. 6—Reference Signal Types

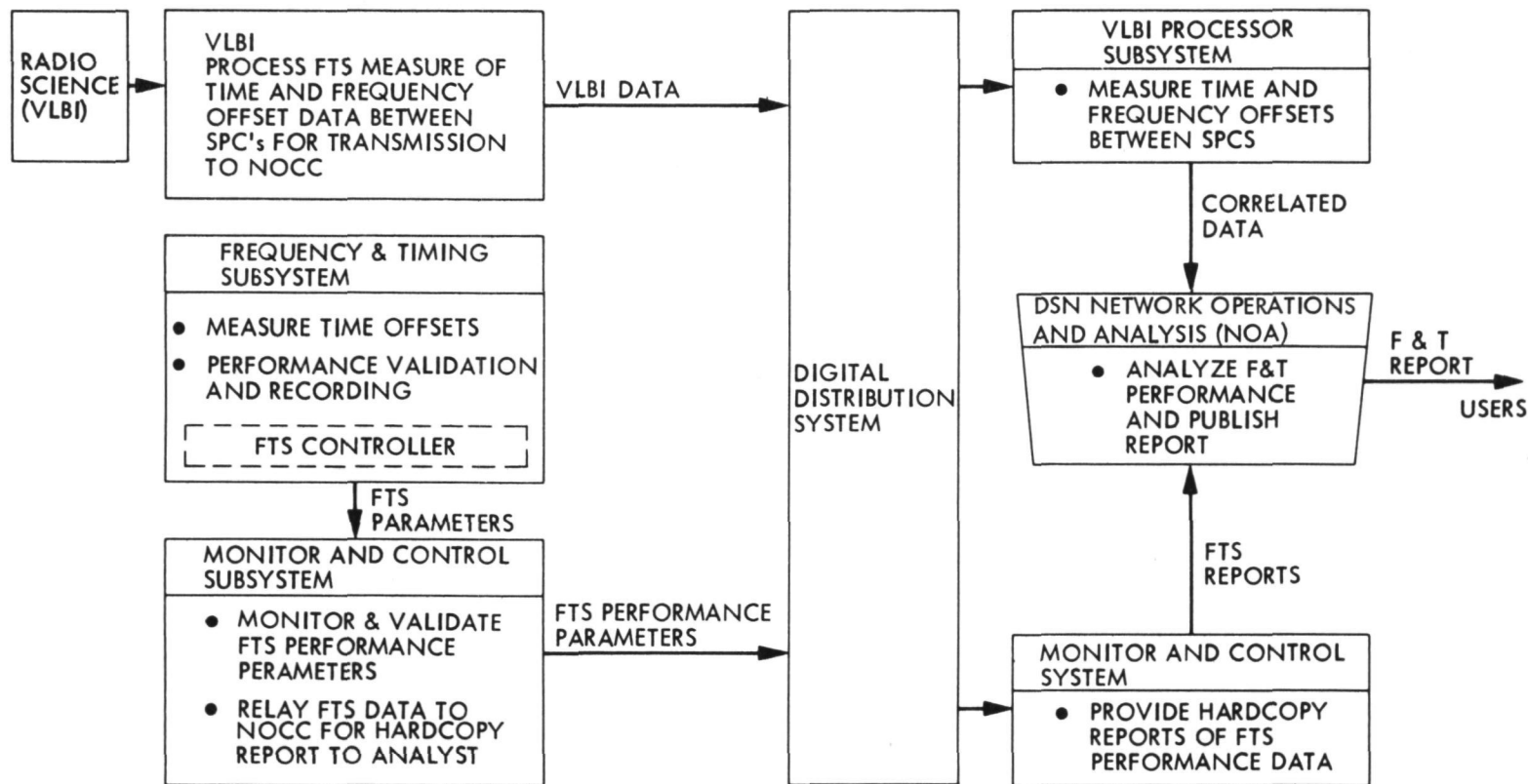


Fig. 7—Performance Analysis and Reporting

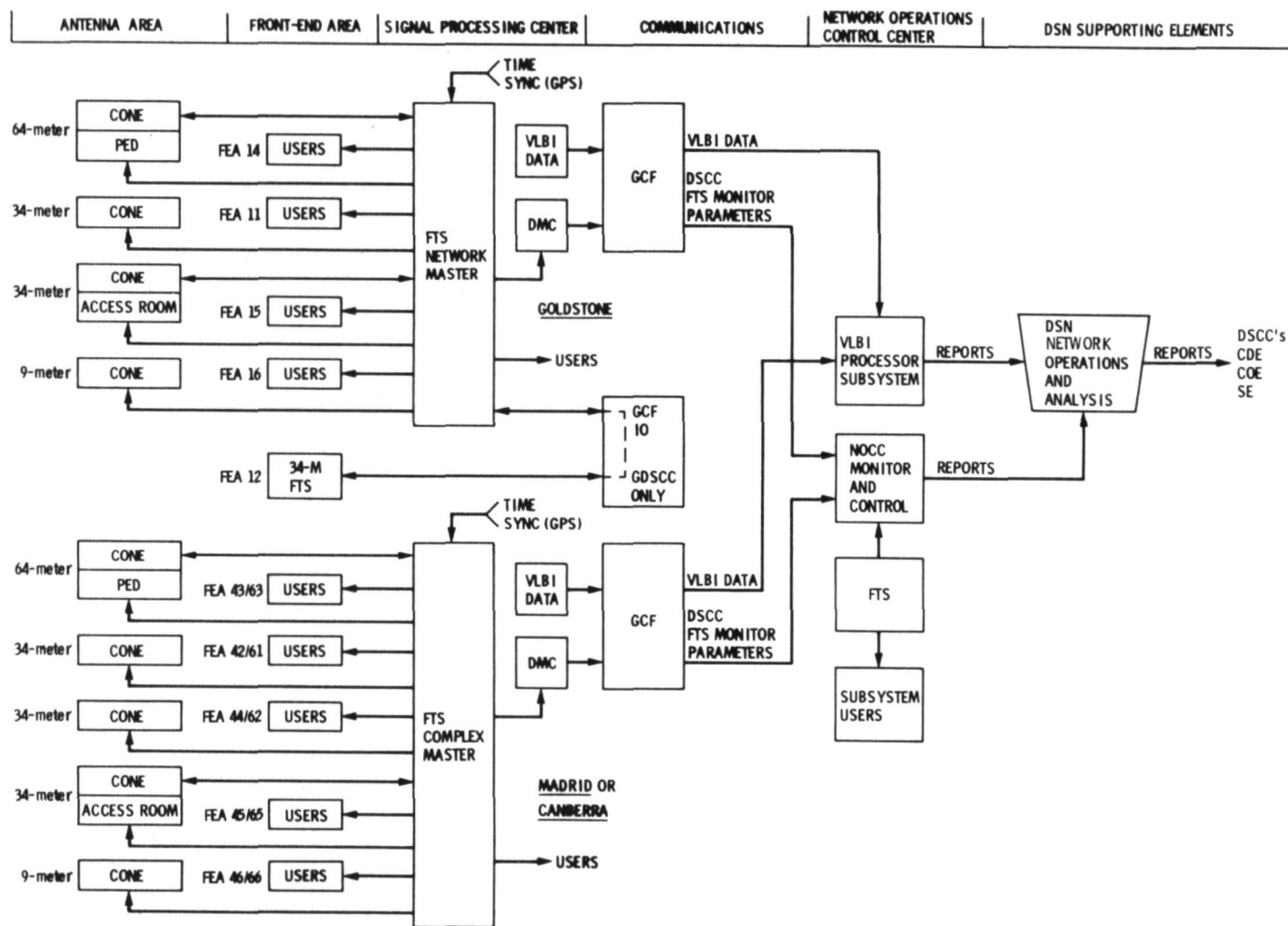


Fig. 8-Frequency and Timing System Network Level Block Diagram

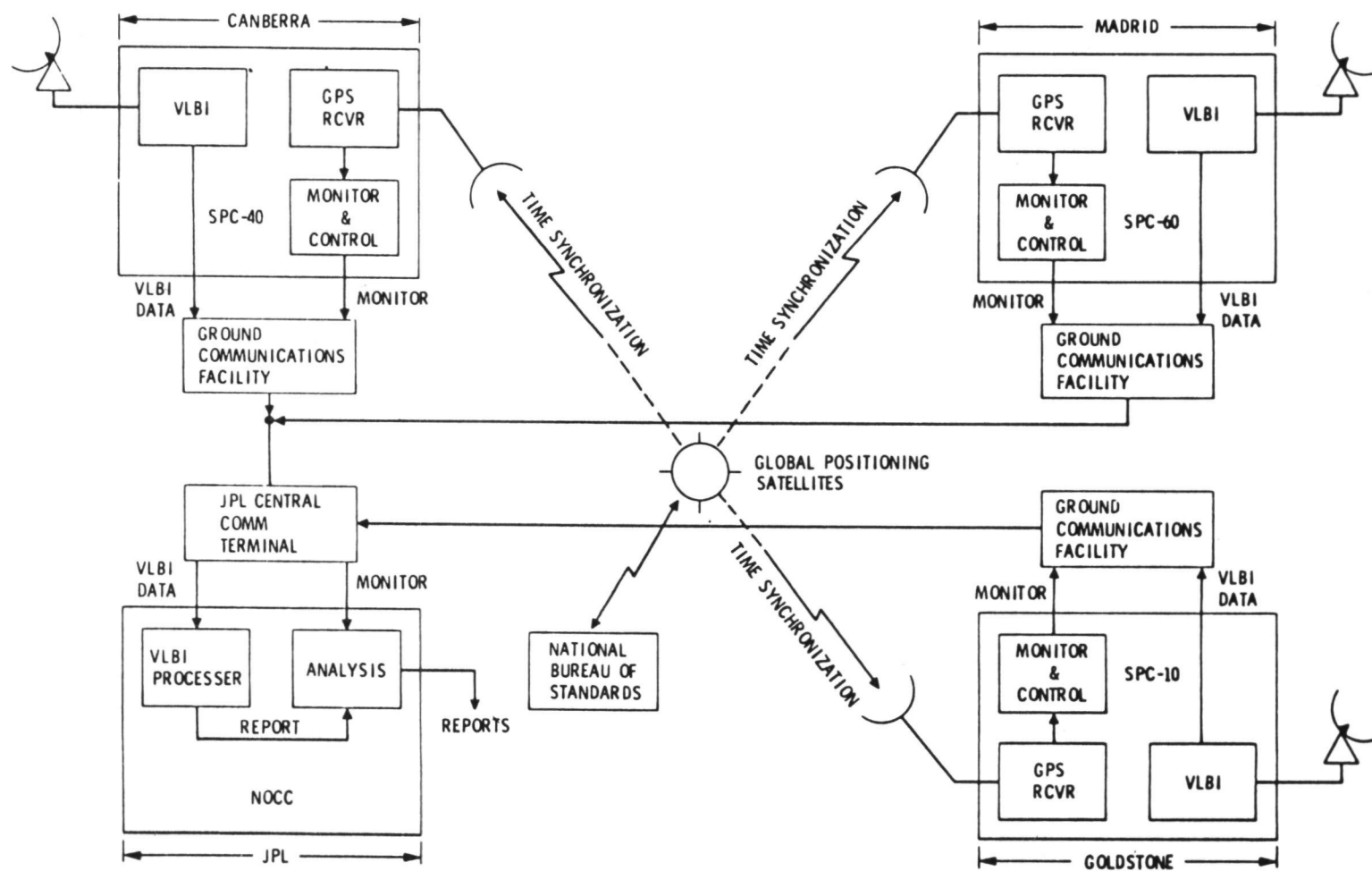


Fig. 9-Time Synchronization

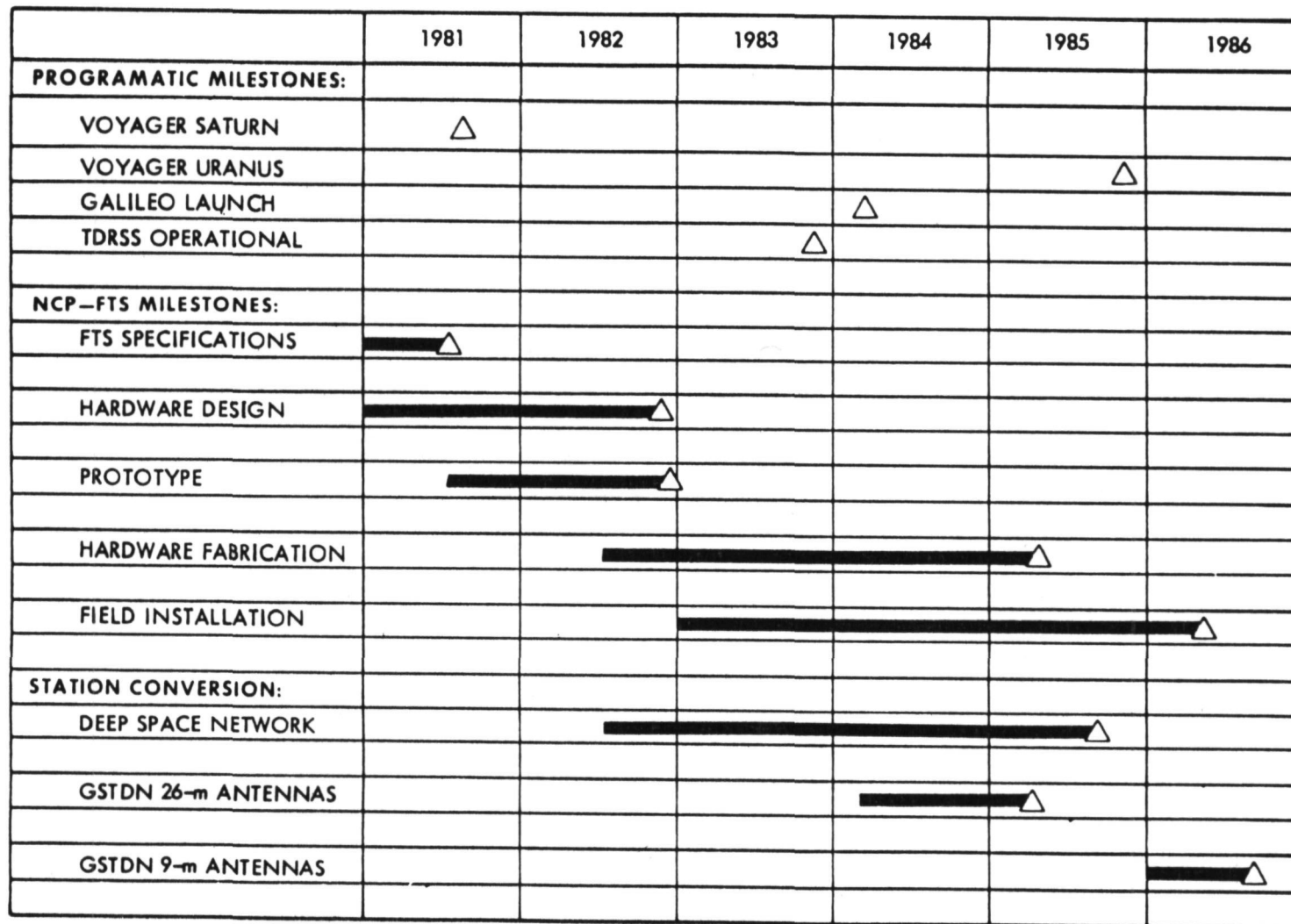


Fig. 10-Implementation Schedule

QUESTIONS AND ANSWERS

MR. SAM WARD, The Jet Propulsion Laboratory

Dick could perhaps the synchronization to the southern hemisphere region be improved by supplying defense department mapping for the GPS receiver?

MR. COFFIN:

Well, that might be. It sounds like an interesting idea. That hadn't occurred to me Sam. It might be a good idea. Of course, you are going to ask the question after that, what about the Spanish equivalent of the Department of National Mapping I would expect.

MR. WARD:

Not necessarily.

MR. COFFIN:

Okay.

PROFESSOR LESCHIUTTA:

Yes, thank you. You mentioned the active stabilized connection between the data processing center and the antenna mount area. Would you be so kind as to explain about this? Thank you.

MR. COFFIN:

This is a stabilized link which I think, if you will see me afterwards I can put you on to a paper that will describe it in more detail but basically what it amounts to is that there is an inactive phase shifter which is part of a servo loop in which a signal is sent up to the antenna and modulates the down link. It is divided and somehow modulates the down link back down that same cable, and the signal is phase compared at the bottom and an error signal generated for this phase shifter. If you want to see me afterwards I will put you with one of the designers of that who happens to be in this room.

PROFESSOR LESCHIUTTA:

Thank you.

DR. WILLIAM WOODEN, DMAHTC

I wonder if you have given any thought to what type of receiver you were planning to install, have you given any thought to this?

MR. COFFIN:

Well I happen to know that there is work in several areas going on in GPS receivers. I think that there is some work here at Goddard and at several other locations. I believe that the National Bureau of Standards is also working on that and we have provided some funds to the National Bureau of Standards to support them in that work. And I don't know whether that will be the receiver we will finally implement, but that is certainly one possibility.

THE OPERATIONAL PERFORMANCE OF
HYDROGEN MASERS IN THE DEEP SPACE NETWORK
(The Performance of Laboratory Reference
Frequency Standards in an Operational Environment)

Samuel C. Ward

Frequency and Time System Cognizant Operations Engineer
Jet Propulsion Laboratory, Pasadena, California

ABSTRACT

Spacecraft navigation to the outer planets (Jupiter and beyond) places very stringent demands upon the performance of frequency and time (F&T) reference standards. The Deep Space Network (DSN) makes use of hydrogen masers as an aid in meeting the routine F&T operational requirements within the 64-m antenna network (one antenna each in Goldstone, California; Madrid, Spain; and Canberra, Australia).

The operational syntonization (frequency synchronization) requirement is a $\pm 3 \times 10^{-13}$ between any two 64-m Deep Space Stations (DSS) and a $\pm 1 \times 10^{-12}$ between any 64-m DSS to UTC(NBS). The clock (epoch) synchronization requirement is $\pm 20 \mu\text{s}$ 64-m DSS between any two 64-m DSS, and $\pm 20 \mu\text{s}$ offset between any 64-m DSS to the UTC(NBS) epoch.

Both the sync and the synt were established through use of a specially calibrated H-P E21-5061A Flying Clock. The sync/synt to UTC is being maintained using LORAN and TV in the simultaneous reception mode. The sync/synt within the 64-m net is maintained through the use of Very Long Base Interferometry (VLBI).

Results as of October, 1980 indicate the hydrogen masers are performing within the required specifications. However two problem areas remain that affect operations performance: (1) there is insufficient control over the environment in which the reference standards reside and, (2) frequency drift makes it very difficult to maintain the 64-m DSS to 64-m DSS synt over the 130-day period required by the flight project.

INTRODUCTION

The "laboratory standards" are three hydrogen masers, Smithsonian Astrophysical Observatory (SAO) model VLG10B, and six cesium oscillators, Hewlett-Packard model 5061A-004 option. The "operational environment" is an isolated temperature controlled room at each of three NASA/JPL Deep Space Network (DSN) complexes.

This Precision Time and Time Interval (PTTI) application is in support of refined spacecraft navigation to the outer planets (Jupiter and beyond) and to provide wideband (>100 kilobits) telecommunications channels at S and X band. The Voyager project Navigation team guides the spacecraft to Jupiter, Saturn, Uranus, and perhaps Neptune. The Telemetry and Image Processing teams have brought us the beautiful full color pictures of the planets and their satellites. Last, the Radio Science team uses spectral analysis to detect and measure the constituents of planetary atmosphere, orbital rings, and gravimetrics.

REQUIREMENTS AND SPECIFICATIONS

Because the Voyager project requirements are currently the most stringent, they have been the dominant force in the design of the Frequency and Time System (FTS). The requirements are: (1) the fine-spectral performance of and longterm stability of the hydrogen maser, (2) the accuracy and reliability of the cesium, and (3) some means of synchronizing the intercontinental network of tracking stations.

The specifications relating to a typical frequency and timing system using H-masers and Cs are listed in the PTTI literature, manufacturers specifications, etc. and will not be dealt with further in this paper. I will instead address the very stringent requirements for syntonization and synchronization.

Syntonization Requirements

1. The frequency offset between any pair of 64-m Deep Space Stations (DSS) shall be known to within less than $\pm 3 \times 10^{-13}$, such as DSS 63 (Madrid, Spain) vs. DSS 43 (Canberra, ACT) = $< \pm 3 \times 10^{-13}$, or DSS 63 vs. DSS 14 (Goldstone, California) = $< \pm 3 \times 10^{-13}$, or DSS 63 vs. DSS 14 = $< \pm 3 \times 10^{-13}$.
2. The frequency offset of the DSN master (DSS 14) shall be maintained within $\pm 3 \times 10^{-13}$ of UTC(NBS).

Synchronization Requirements

1. The time offset between any pair of 64-m DSS shall be known within $\pm 20 \mu\text{s}$.
2. The time offset of any 64-m DSS from UTC shall be known within $\pm 20 \mu\text{s}$ and further, it shall actually be maintained to within $\pm 50 \mu\text{s}$ over the 130-day period August 4 through December 12, 1980.

METHODOLOGY

Both the synchronization and syntonization were established through use of a specially calibrated 5061A-001-004 portable unit¹. For purposes of maintaining the individual DSS synchronization to UTC, the portable unit was carried to the host country frequency and time metrology agency. The San Fernando Observatory in Spain where the sync/synt tool used is Mediterranean chain LORAN-C. In Australia the responsible agency is the Department of National Mapping and the F&T maintenance resource is ABC television (see Figure 1). In America, at Goldstone, regular 60-day flights to and daily VLF transmissions from National Bureau of Standards are used, in addition to LORAN-C and traveling clocks from other agencies (Goddard Space Flight Center and the USNO). The DSS to DSS synchronization and syntonization is being maintained through the use of Very Long Base Interferometry (VLBI). Some of the results are reported in paper No. 21 of this session (12th PTTI). Figure 2 illustrates how the DSS to DSS and the DSN to UTC synchronization is maintained.

Each 64-m DSS has been delegated the responsibility of maintaining its own internal synchronization. Figure 3 illustrates the hardware configuration and data flow paths that achieve this. In addition it is responsible for establishing and maintaining the synchronism of other DSS within the complex (see the detail in upper and lower right hand segments of Figure 2).

¹After allowing 24 hours for the portable 5061A to stabilize to its temperature and magnetic environment, the unit was degaussed and a measurement was made of the zeeman frequency vs. frequency offset of the unit references to the DSN master. Using a digital frequency synthesizer and a differential voltmeter, the zeeman frequency readings were reproducible within 0.7 Hz. The portable unit was then carried to the remote DSS to be syntonized. Here again the unit was given 24 hours to stabilize, was degaussed and the zeeman frequency was measured. If the zeeman changed by more than 1.4 Hz it was reset. Otherwise a correction factor of $8.3 \times 10^{-15}/\text{Hz}$ and $1 \times 10^{-13}/\Delta^{\circ}\text{C}$ was applied to the syntonization.

TEST RESULTS

Environmental Tests

Table 1 lists the results of environmental tests performed on five of the six 5061A cesiums presently deployed within the DSN. These tests were performed at the Reference Standards Test Facility in Pasadena. Note that serial No. 1718 in its response to temperature variations differed from the others. When this unit was sent to the Goldstone Reference Standards Laboratory for zeeman calibration, it exhibited phase glitches. It was returned to Pasadena for further environmental testing.

Table 2 lists the results of environmental tests performed on the three hydrogen masers presently deployed within the DSN. Figure 4 illustrates the behavior of H-maser SAO serial No. 6 in a changing pressure environment. Note the improvement (8.2 dB) in its performance after being refurbished (Table 2, column 6).

Figure 5 illustrates the performance of SAO serial No. 7 in a changing magnetic environment. Having been given erroneous information on how far the 26-m antenna was from the planned site for the frequency standards room, it was decided that no further magnetic shielding would be required. SAO serial No. 6 failed in spring 1980 and was returned to the manufacturer for refurbishment. Table 2, column 5 indicates a 2.7 dB degradation to its performance in a changing magnetic environment.

Figure 6 illustrates the performance typical of a H-maser in a high temperature environment. The H-maser is JPL serial No. 1 and the environment was an unventilated room in the cellar of DSS 43. The high temperatures caused the unit to fail in late summer (southern hemisphere). An air conditioner with 0.1°C temperature control was installed early September 1980.

Stability Tests

Figure 7 illustrates the short term stability (spectral performance) of a typical 5061A-004 cesium and a typical H-maser. These measurements were made in Spain at DSS 63 where the Complex Maintenance Facility (CMF) was close enough to permit use of a coaxial cable from the H-maser. Cesium serial No. 1511 was the portable unit and it was carried to the CMF facility.

Table 1. Cesium Environmental Parameters Test Data

PARAMETER	HEWLETT-PACKARD 5061-A 004				
	#1694	#1695	#1717	#1718	#1719
TEMPERATURE $\frac{\Delta F}{F} / ^\circ\text{C}$	4.3×10^{-14}	6.25×10^{-14}	5.4×10^{-14}	1.2×10^{-13} TO -2×10^{-13}	5.6×10^{-14}
BAROMETRIC PRESSURE $\frac{\Delta F}{F} / \text{"Hg}$	1×10^{-13}	1×10^{-13}	1×10^{-13}	1×10^{-13}	1×10^{-13}
MAGNETIC FIELD $\frac{\Delta F}{F} / \text{GAUSS}$	1×10^{-13}	1×10^{-13}	1×10^{-13}	1×10^{-13}	1×10^{-13}

Table 2. H-Maser Environmental Parameters Test Data

PARAMETER	(AFTER REFURBISH BY MFR)				
	SAO 5	SAO 6	SAO 7	SAO 5	SAO 6
TEMPERATURE $\frac{\Delta F}{F} / ^\circ\text{C}$	-1.6×10^{-14}	-1×10^{-13}	7.0×10^{-14}	-1.2×10^{-13}	7.2×10^{-14}
BAROMETRIC PRESSURE $\frac{\Delta F}{F} / \text{"Hg}$	2.6×10^{-14}	-3.4×10^{-13}	2.3×10^{-14}	2.5×10^{-14}	-5.1×10^{-14}
MAGNETIC FIELD $\frac{\Delta F}{F} / \text{GAUSS}$	1.6×10^{-12}	5.0×10^{-12}	2.8×10^{-12}	3.0×10^{-12}	3.4×10^{-12}

Figures 8a and 8b give the stability performance characteristics of the three H-masers presently deployed². Figure 9 illustrates the stability characteristics of a recent series (serial Nos. 1718 and 1719) of 5061A-004 cesium.

SYNCHRONIZATION AND SYNTONIZATION DATA

Epoch Synchronization

Prior to departure for the trip to Spain the portable clock designated RSL-2 was used to synchronize itself and the DSN master clock at DSS 14 to within $0.2 \mu\text{s}$ of the NBS and USNO epoch. It was then transported to DSS 63 at Robledo, Spain then on to the San Fernando Observatory (SFO) at San Fernando, Spain. One day prior to leaving Spain the clock was transported to DSS 62 at Cebreos and the Madrid STDN station. Thus the three stations in the Madrid complex were synchronized to SFO and the DSN master to less than one μs .

Upon returning to America the clock was immediately taken to Goldstone for closure against the DSN master. It then was taken to Australia where it was used to synchronize DSS 43 at Tidbinbilla to the Dept. of National Mapping (DNM) installation in the Orroral Valley. On the day prior to leaving Australia the portable clock was used to synchronize DSS 44 (Honeysuckle Creek) and Orroral (the STDN station) to the DNM, DSS 43, and the DSN.

The portable, RSL2, was then returned to America where closure was refined against both NBS and USNO. All the elements and agencies synchronized on these trips remain synchronized to within less than one μs and are being maintained within $10 \mu\text{s}$ peak to peak.

Syntonization

Each time the calibration process was performed, 24 hours was allowed for thermal stabilization and then 80 hours (10 8-hour samples) of comparative phase data was collected. This was performed with instrumentation configured as in Figure 3 except that a 4th phase comparator was added to permit the intercomparison of the H-maser, Cs No. 1, Cs No. 2 and the portable (RSL2).

At DSS 63 after settling from the trauma of the trip and after thermal stabilization the zeeman frequency of RSL2 had shifted but 1.7 Hz. A C-field adjustment removed approximately $1/2$ the zeeman offset and the

²Figures 8a and 8b have been reprinted from a paper presented by Paul Kuhnle at the 11th Annual PTI.

calibration process of the H-maser began. At the end of the 88-hour calibration period the H-maser frequency offset from the DSN master was found to be zero \pm the instrumentation noise of $\pm 5 \times 10^{-14}$. It was thus unnecessary to make any adjustment to the H-maser. It was however necessary to adjust both Cs No. 1 and Cs No. 2. Data collected via LORAN-C indicates the frequency offset of the H-maser and Cs No. 2 remain at zero $\pm 4.8 \times 10^{-13}$ as of November 8, 1980.

At DSS 43 the thermal stabilization period was extended to allow for the lack of good circulation (the air handler installation was still in process). Also the H-maser had been installed just a few weeks and was still drifting. At the end of an 80-hour calibration period the offset of the maser from the DSN master was 4.73×10^{-13} . Since this was beyond the Voyager specification and, since the drift was in a positive direction, the H-maser synthesizer was reset to reduce its frequency by 6.345×10^{-13} . Frequency offset data of this maser vs. UTC(AUS) collected using simultaneous TV with the DNM indicate its drift has cancelled the value reset on September 30. Close examination of recent data indicate the 2nd order drift term has dropped from 4.6×10^{-14} /day to 2.1×10^{-14} to 0.7×10^{-14} /day.

All indications are that the frequency drift of SAO No. 5, the DSN master, has dropped well below its former value of 1×10^{-14} /day as observed between departure for Spain and return for closure. At present SAO No. 5 vs. UTC(NBS) = $-2.84 \times 10^{-13} \pm 0.3$ as verified by two closures against UTC(NBS) within a 21-day period. Figure 10 gives time offset data vs. UTC(DSN) and associated frequency offset data for each of 3 64-m DSS. Figure 11 gives time offset data vs. UTC(NBS&USNO) and the associated frequency offset data vs. UTC(NBS) of the DSN master reference.

SUMMARY

- (1) Hydrogen masers require 4 to 6 weeks thermal stabilization time before their long-term stability can be fully utilized.
- (2) To fully utilize the full potential of present day H-masers and cesium reference frequency standards, care must be exercised in providing a thermally stabilized and magnetically isolated environment.
- (3) Syntonization to UTC can be accurately and economically maintained within a part in 10^{13} (after 1 week of daily observations) through use of the simultaneous reception of LORAN-C or TV transmissions by the DSS and the host country frequency and time metrology agency.

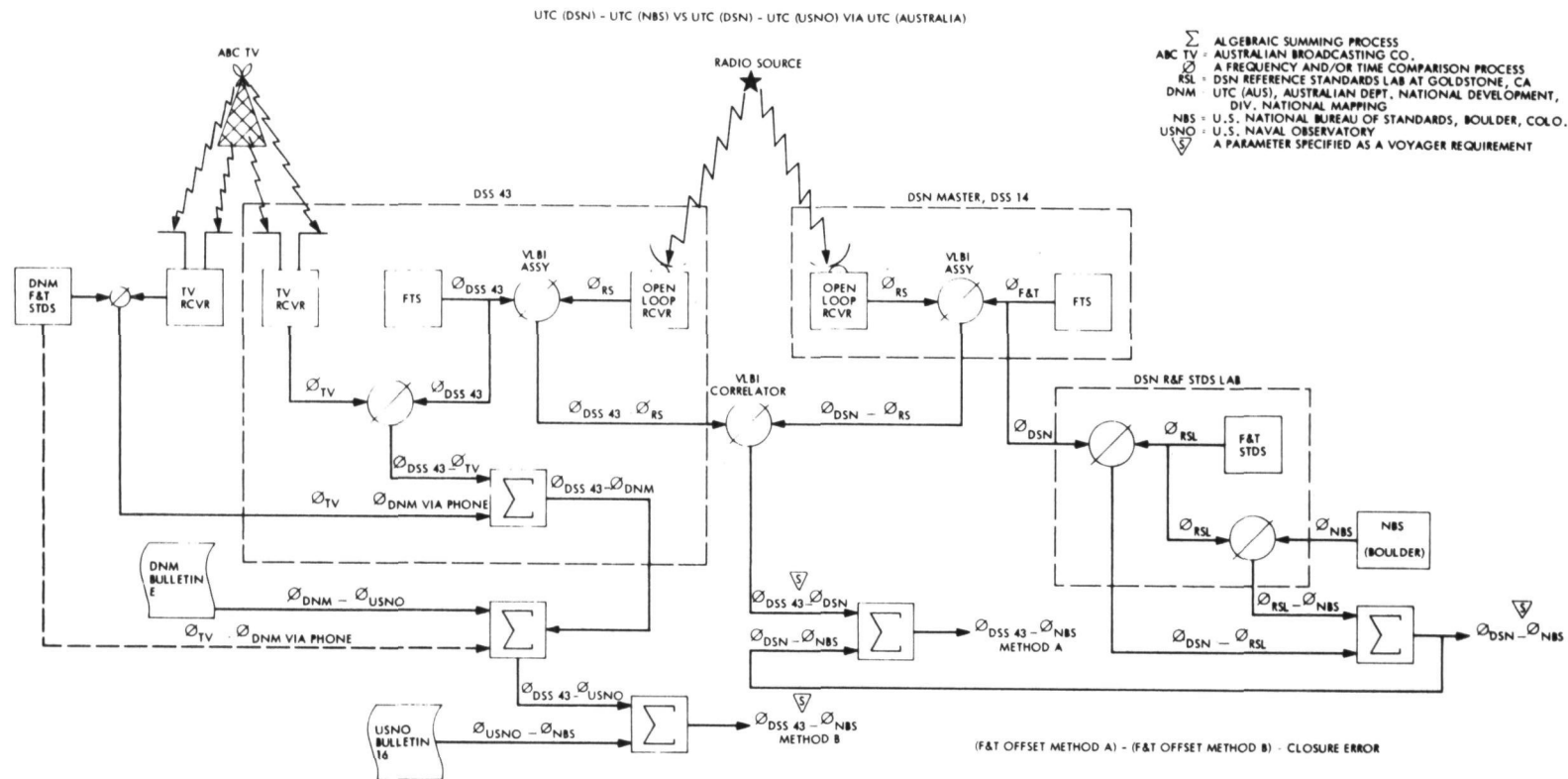


Figure 1. UTC(DSN) - UTC(NBS) vs. UTC(DSN) - UTC(USNO) via UTC (Australia)

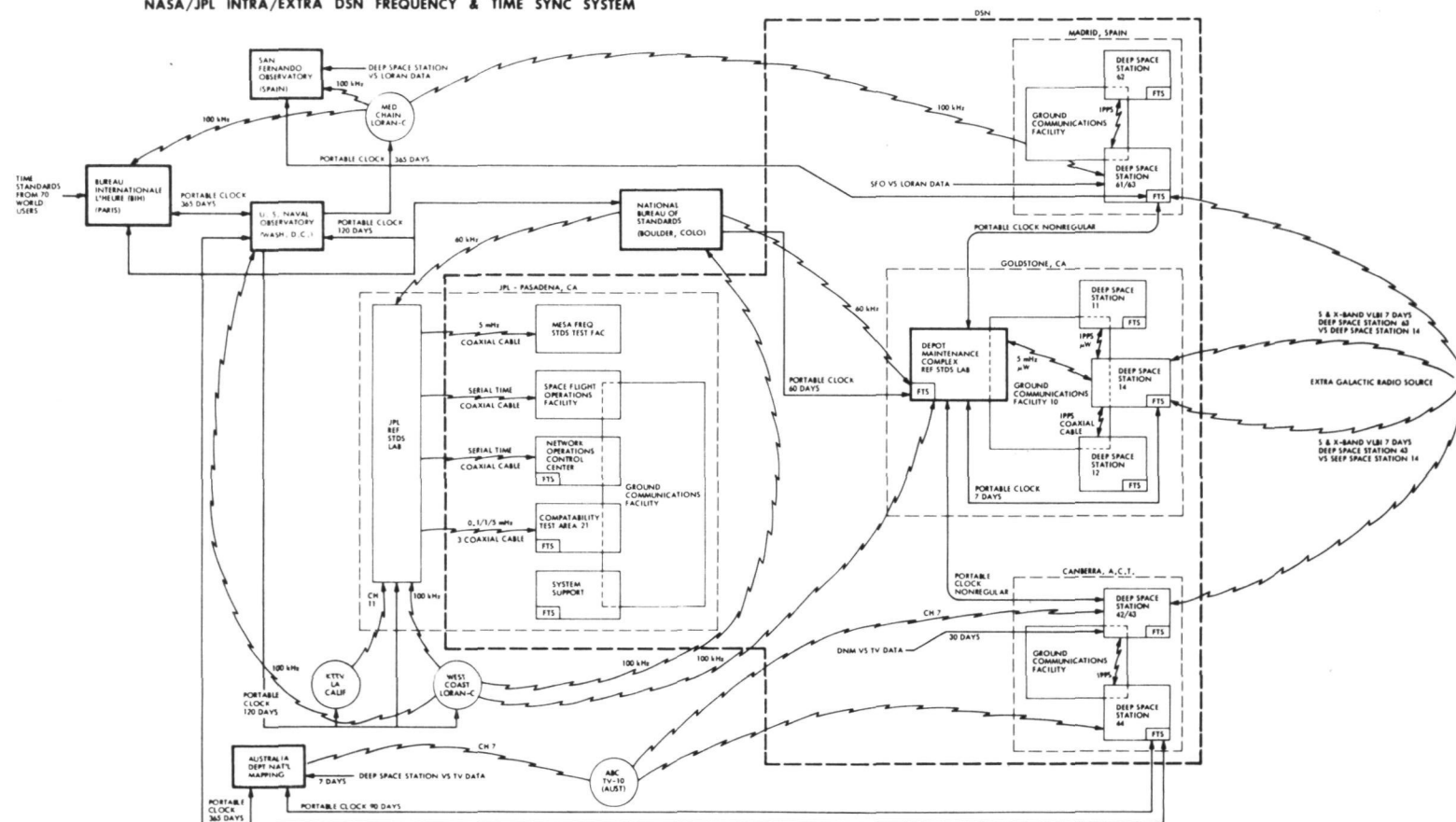


Figure 2. NASA/JPL Intra/Extra DSN Frequency and Time Sync System

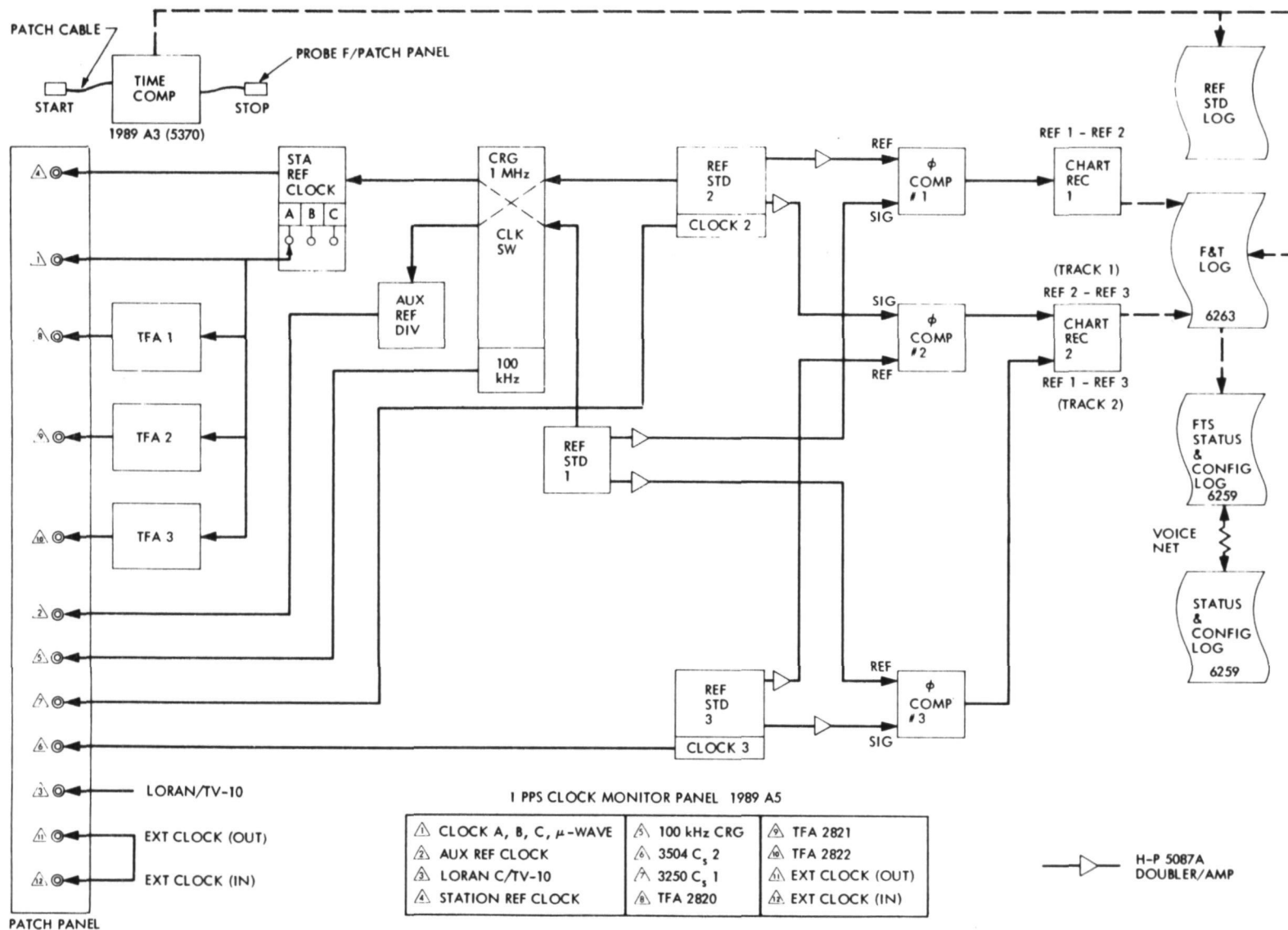


Figure 3. Frequency and Time Monitoring at 64-m DSS

DSS 14 vs UTC (NBS) via MICROWAVE AND PORTABLE CLOCKS

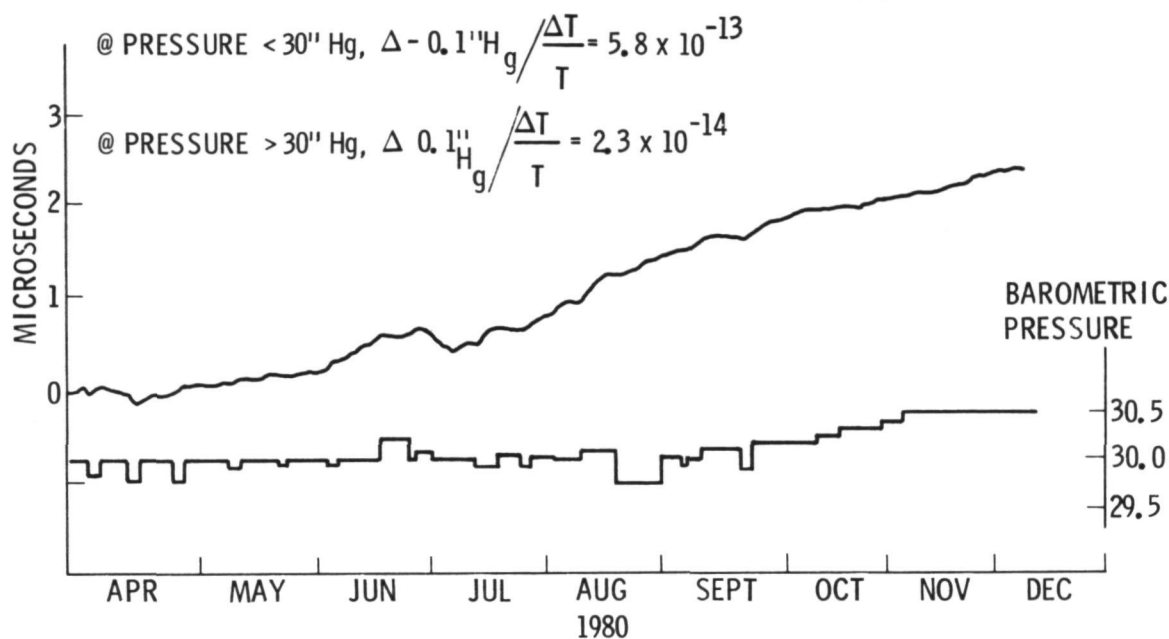


Figure 4. H-Maser Performance in a Changing Barometric Pressure Environment

DSS 63 vs UTC (USNO) via LORAN-C, MED. CHAIN

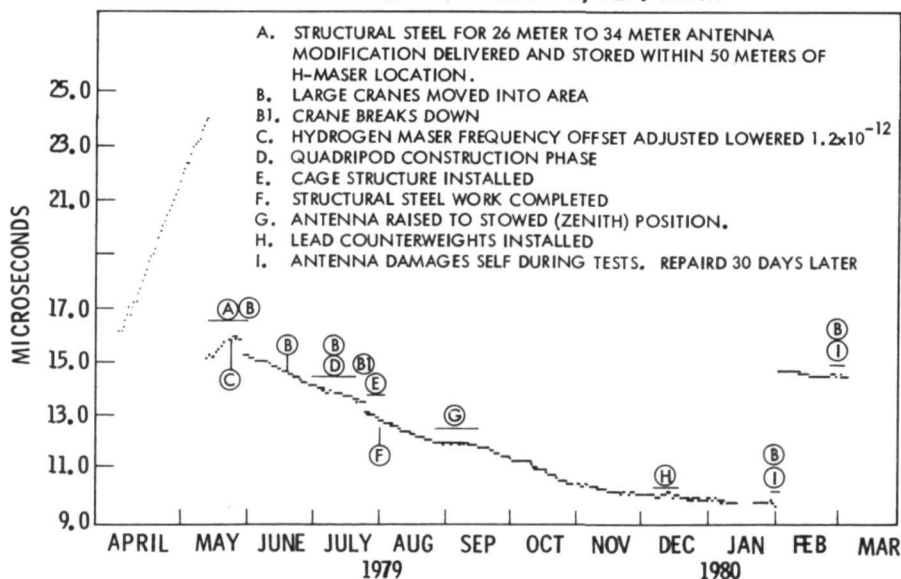


Figure 5. H-Maser Performance in a Changing Magnetic Environment

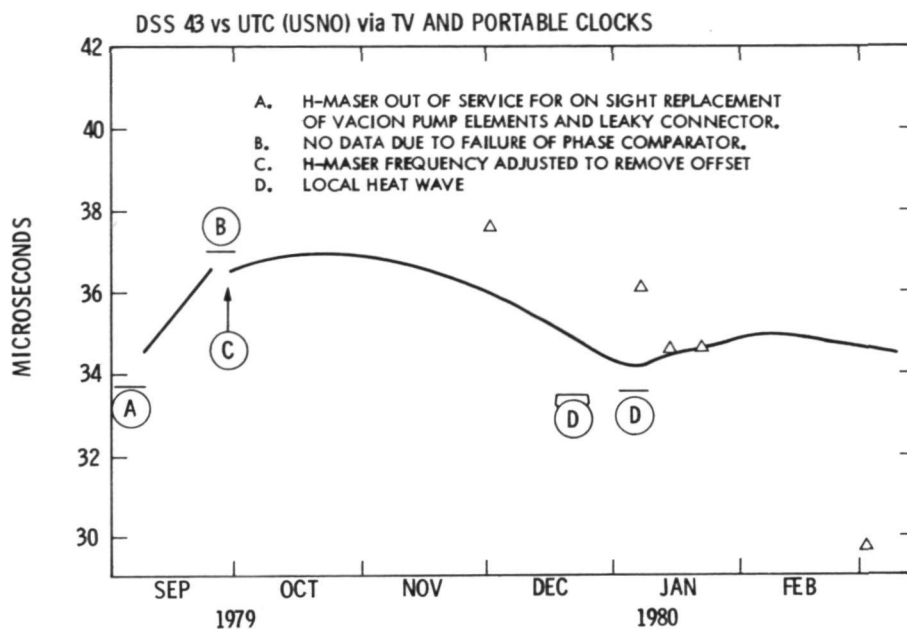


Figure 6. Maser Performance in a Changing Temperature Environment

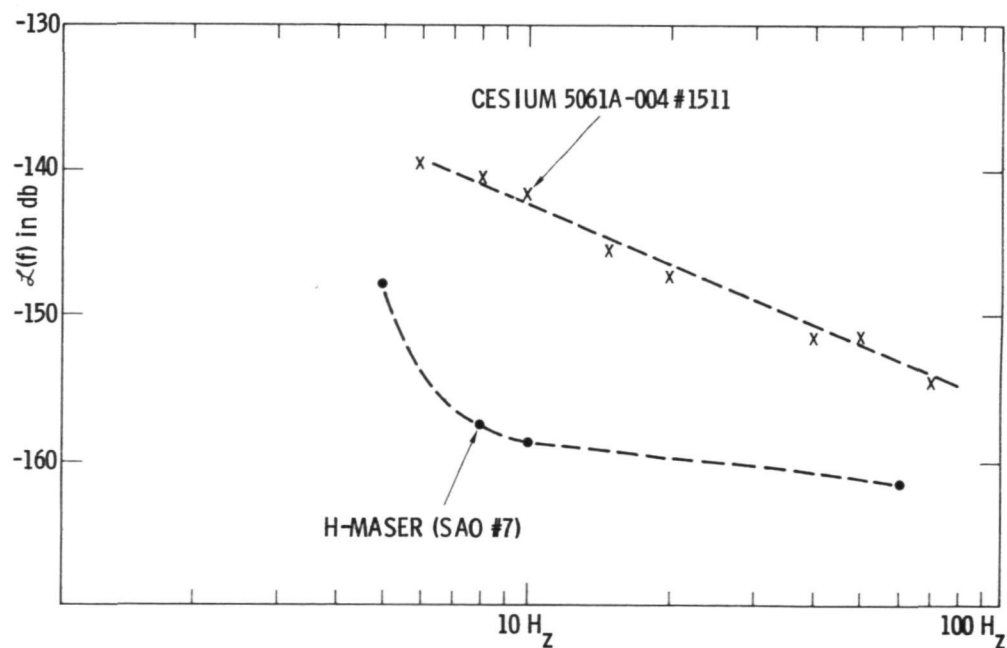


Figure 7. Reference Standards Spectral Performance, $L(f)$ vs. Frequency

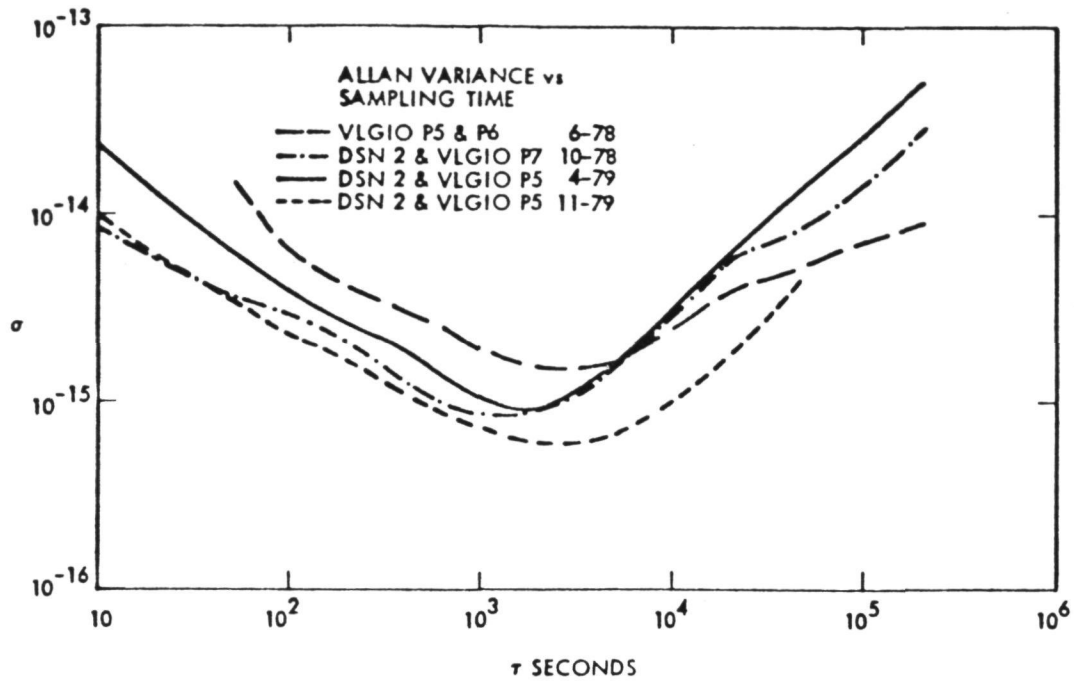


Figure 8a. Allan Variance vs. Sampling Time

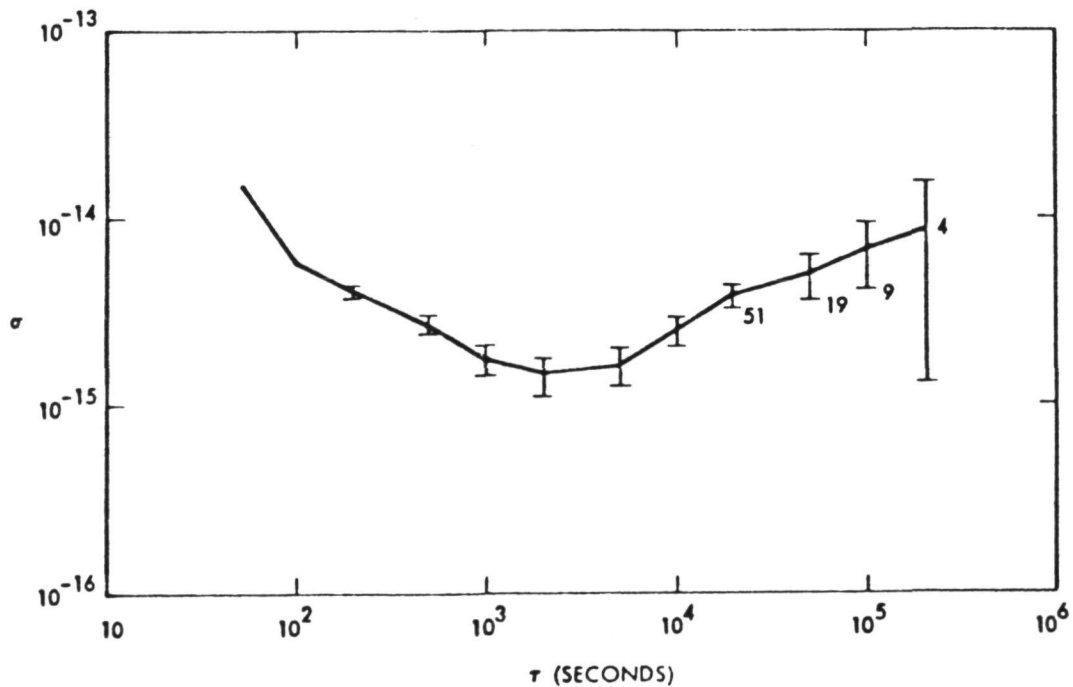


Figure 8b. Allan Variance vs. Sampling Time, with Error Bars

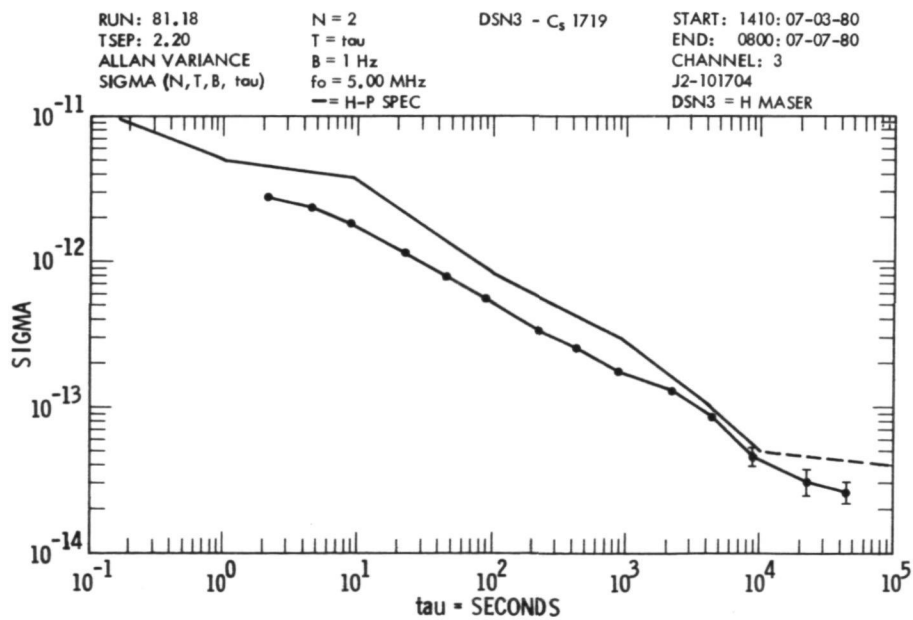
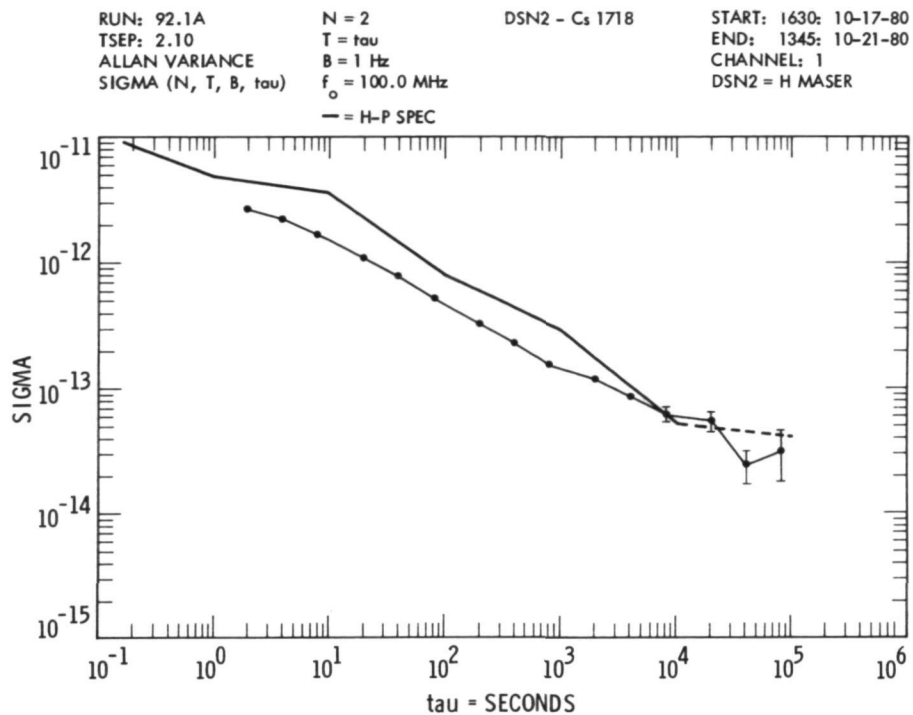


Figure 9. Stability Test Data

FTS Quicklook Data

DSS-14			DSS-42/43		DSS-61/63	
DOY	T.O. (μ s)	Rel.Rate (μ s/ μ s)	T.O. (μ s)	Rel.Rate (μ s/ μ s)	T.O. (μ s)	Rel.Rate (μ s/ μ s)
286	0.00	-----	-2.70	-----	2.3	-----
287	0.00	0.0	-2.70	0.0	2.3	0.0
288	---	-----	-2.67	3.47 (-13)	2.2	-1.16 (-12)
289	0.00	-----	-2.63	4.63 (-13)	2.3	1.16 (-12)
290	0.80	9.26 (-12)	-2.60	3.47 (-13)	2.3	0.0
291	0.80	0.0	-2.56	4.63 (-13)	2.2	-1.16 (-12)
292	0.80	0.0	-2.52	4.63 (-13)	2.2	0.0
293	1.00	2.31 (-12)	-2.49	3.47 (-13)	2.3	1.16 (-12)
294	0.80	-2.31 (-12)	-2.44	5.79 (-13)	2.4	1.16 (-12)
295	1.20	4.62 (-12)	-2.41	3.47 (-13)	2.4	0.0
296	0.80	-4.62 (-12)	-2.38	3.47 (-13)	2.3	-1.16 (-12)
297	0.80	0.0	-2.34	4.63 (-13)	2.3	0.0
298	-0.30	-1.27 (-11)	-2.31	3.47 (-13)	2.4	1.16 (-12)
299	-0.30	0.0	-2.27	4.63 (-13)	2.4	0.0
300	-0.20	1.16 (-12)	-2.24	3.47 (-13)	2.5	1.16 (-12)
301	-0.30	1.16 (-12)	-2.20	4.63 (-13)	2.4	1.16 (-12)
302	-0.28	2.31 (-13)	-2.17	3.47 (-13)	2.4	0.0
303	-0.30	-2.31 (-13)	-2.13	4.63 (-13)	2.4	0.0
304	-0.30	0.0	-2.10	3.47 (-13)	2.3	1.16 (-12)
305	-0.35	-5.79 (-13)	-2.06	4.63 (-13)	2.3	0.0
306	-0.40	-5.79 (-13)	-2.03	3.47 (-13)	2.3	0.0
307	-0.30	1.16 (-12)	-2.00	3.47 (-13)	2.3	0.0

Considering weekly segments:

Over	$T_e - T_s$	Rel.Rate	$T_e - T_s$	Rel.Rate	$T_e - T_s$	Rel.Rate
286-293	1.00	1.45 (-12)	0.21	3.04 (-13)	0.0	0.0
293-300	-1.20	1.74 (-12)	0.25	3.62 (-13)	0.20	2.89 (-13)
300-307	-0.10	1.45 (-13)	0.24	3.47 (-13)	-0.20	-2.89 (-13)

Figure 10. 64-Meter DSS F&T Offset Report

jjl →

INCOMING MESSAGE

GJP053A
RR JJPL JHIL JZED
DE JGLD 014
12/1714Z
FM W WOOD/J W MYERS
TO JJPL/S WARD/J LUVALLE/J MANKINS
INFO JJPL/R COFFIN/R LATHAM/T TAYLOR
JHIL/K BEUTLER/J C LAW
JZED/NET ANALYSIS
DLD/R RUXLOW/B MCPARTLAND/J MCCOY

SUBJECT: UTC(RSL) - UTC(NBS) EPOCH TIME SYNCRONIZATION.

TWO PORTABLE CLOCK TRIPS TO BOULDER, COLO. IN OCTOBER ALLOWED US TO REFINING THE ESTIMATE OF OUR TIME AND FREQUENCY OFFSETS TO NBS, USNO, AND B.I.H.

1. PUBLISHED DATA, AND DERIVATIONS BASED ON PUBLISHED DATA:

(NBS TIME & FREQUENCY BULLETIN 274, USNO SERIES 7-669)

UTC(USNO) - BIH = -0.694×10^{-13}

UTC(USNO) - UTC(NBS) = -0.9513×10^{-13}

TA NBS - UTC(NBS) = -0.0143×10^{-13}

TA NBS - BIH = $+0.243 \times 10^{-13}$ (+/- 0.279×10^{-13})

2. RESULTS OF MEASURED DATA:

	DAY 281	DAY 302	$\Delta F/F \text{ } \eta s/\text{DAY}$
RSL2-UTC(RSL) =	-0.244US	+0/182US	
RSL2-UTC(NBS) =	+0.103US	+0.349US	
UTC(RSL)-UTC(NBS) =	+0.347US	+0.166US	-8.658
UTC(RSL)-UTC(USNO) =	+0.788US	+0.799US	-0.431
CS1 14-UTC(NBS) =	+0.487US	+0.374US	-5.2546
CS1 14-UTC(USNO) =	+0.928US	+0.987US	+2.7656
CLOCK 'A' 14-UTC(NBS) =	+2.168US	+1.641US	-24.574
CLOCK 'S' 14-UTC(USNO) =	+2.609US	+1.995US	-16.326
H2M14-UTC(NBS) =	NA	NA	-26.604
H2M14-UTC(USNO) =	NA	NA	-18.394

NOTE: THE H2M(14) FREQUENCY OFFSET IS TAKEN FROM THE PHASE RECORDER COMPARISON TO CS1 14, AND IS OVER THE SAME PERIOD AS THE CLOCK CLOSURES TO NBS. NOTE ALSO THAT CLOCK 'A' 14 (DRIVEN BY THE H2M) IS PROBABLY A MORE PRECISE ESTIMATE OF THE H2M POSITION.

REGARDS

Figure 11. DSN Master Frequency and Time Report

QUESTIONS AND ANSWERS

DR. VICTOR REINHARDT, NASA/Goddard

What kind of R mass errors were you getting with that difference in technique for Loran-C?

MR. WARD:

Loran-C is down in units of nanoseconds around seven or eight.

DR. REINHARDT:

Okay, that is just by the two stations hearing the same trend alert?

MR. WARD:

What they do at noon local solar noon, they both observe the same station, and take the raw offset and they exchange the data. And then 24 hours later do the same thing. And when you take that second difference all that is left is the difference in your rates in your clocks.

DR. REINHARDT:

Thank you.

CHAIRMAN BARNES:

Other questions?

MR. WARD:

Oh incidently what I didn't say we have been using the new Hewlett-Packard counter and one of the other things that is exchanged with the data is a sigma on the measurement.

Page Intentionally Left Blank

SESSION V

ADVANCED TECHNOLOGY

**David Howe, Chairman
National Bureau of Standards**

Page Intentionally Left Blank

SOURCE STRUCTURE ERRORS IN
RADIO-INTERFEROMETRIC CLOCK SYNCHRONIZATION
FOR TEN MEASURED DISTRIBUTIONS

J. B. Thomas
Jet Propulsion Laboratory
Pasadena, California

ABSTRACT

Source structure can introduce errors in radio interferometry measurements whenever natural radio sources are used. To increase our understanding of this problem, an analysis previously applied to analytical cases has been extended to the brightness distributions measured for ten extragalactic sources. The results of this analysis are presented along with an approach for avoiding the largest structure errors.

INTRODUCTION

As the accuracy of the radio interferometry technique improves, the extended structure of natural radio sources will become an increasingly important source of error. To further increase our understanding of structure effects, this paper extends an analysis that was presented at last year's PTTI conference (1). That earlier presentation included a brief introduction to the theory of structure corrections and applied the theory to the analytical cases of a double-point source and a triple-point source. Although analytical examples are instructive, only a thorough study of many actual source distributions can give a complete picture of source structure effects. To begin such an investigation, ten brightness distributions measured by the Caltech VLBI group (2, 3) have been analyzed. This paper includes a summary of the results of this more recent analysis and presents a visibility-dependent limit formula that, if verified, would be valuable in both estimating and reducing the overall structure effect in bandwidth-synthesis (BWS) delay. Since BWS delay is currently the primary observable in geophysical and clock-synchronization applications, the analysis will focus on that observable.

STRUCTURE THEORY

In order to tie in with the earlier presentation, the theory of structure corrections will be briefly discussed before proceeding to the results. The effect of structure on the cross-correlation signal, the interferometer fringes, can be obtained by evaluating the Fourier transform of the brightness distribution:

$$R(u, v) = \iint D(\beta, \gamma) e^{-2\pi i [u(\beta - \beta_0) + v(\gamma - \gamma_0)]} d\beta d\gamma$$

in which

$$(u, v) = \left(\frac{x_s}{\lambda}, \frac{y_s}{\lambda} \right)$$

where (β, γ) are plane-of-the-sky coordinates, (β_0, γ_0) is an assigned reference position, $D(\beta, \gamma)$ is the brightness distribution, (x_s, y_s) is the sky-projected baseline vector and λ is the observing wavelength. The modulus of this complex quantity gives the effect of structure on the amplitude of the fringes while its phase gives the shift in fringe phase. As one can see, the transform is generally a complicated function of the instantaneous baseline vector between the two antennas. The dependence on baseline enters as the "sky-projected" vector (x_s, y_s) , the two-dimensional vector obtained by projecting the baseline vector onto the plane perpendicular to the source direction. Thus, to obtain a general picture of the effect of a given brightness distribution, one must compute and plot structure effects as a function of (x_s, y_s) . As suggested by the transform, it is convenient to express the two baseline components in units of λ , the observing wavelength at RF. When expressed in this form, the two components are usually designated (u, v) . To obtain the effect of structure on amplitude and BWS delay, rewrite the brightness transform in the form

$$R(u, v) = |R(u, v)| e^{i2\pi\phi_B(u,v)}$$

where $|R|$ is fringe amplitude, and ϕ_B is structure phase. The effect of structure on BWS delay, which will be referred to as structure delay, is approximately computed by taking the partial of structure phase with respect to frequency:

$$\Delta\tau \approx \frac{\partial\phi_B}{\partial f}$$

(The computation of structure delay is actually carried out through an intermediate calculation of effective position (4). For brevity, that procedure will not be discussed here.) For the amplitude effect, it is convenient to define a quantity called fringe visibility that gives fringe amplitude relative to maximum amplitude:

$$v_s \equiv \left| \frac{R(u, v)}{R(o, o)} \right|$$

Thus, once the brightness distribution for a source has been supplied, one can compute visibility, structure phase and structure delay as a function of the sky-projected baseline vector (u, v).

RESULTS FOR MEASURED BRIGHTNESS DISTRIBUTIONS

Table 1 summarizes the 10 brightness distributions measured by the Caltech group (2, 3) and lists the source name, date of measurement, observing wavelength, interferometer stations, and the maximum values of (u,v) present in each measurement. In all, there are seven separate sources observed on continental baselines at wavelengths of 2.8 to 18 cm. Figure 1 displays the brightness distribution for one of the sources (Distribution #9, 3C345) and shows contours of constant brightness on the plane of the sky, with east to the left and north along the vertical.

The measured distributions can be passed through the structure equations to obtain for each distribution plots of fringe visibility, structure phase, and structure delay. Figure 2 gives the results for visibility for the particular distribution in Figure 1. Contours of constant visibility are plotted as a function of (u, v), the components of the sky-projected baseline vector. A similar contour plot for structure delay is given in Figure 3. In the plots, u is defined to be positive to the east and v positive to the north. Since the u-v coverage associated with a given distribution should not extend beyond the maximum values allowed by baseline length considerations, the contour plots are marked with an approximate boundary outside of which the output has been discarded. One important point concerning the current analysis is that all of the structure delays have been computed on the basis of an "artificial" frequency of 8.3 GHz ($\lambda = 3.6$ cm). In effect, this assignment of f pretends that, for structure

delay computation, all distributions were measured for the specified u - v values at 8.3 GHz even though they were not. The reason for this assignment is that most of our work will be carried out at X-band and it is therefore important to compare all structure delay results at one frequency. To obtain the structure delay at the actual frequency, one can easily scale the results by f^{-1} (or by λ). To use the delay plot for a given observation, one would compute the sky-projected baseline vector for that observation and obtain the structure delay for that point on the plot. For this particular source, the structure delay reaches about 150 psec at its worst point but usually falls in the range 0 to 50 psec.

Even though the results for the other nine distributions were just as complex, some general descriptive statements can be made. The magnitudes of the structure delays (computed for X-band relative to the centroid) were as large as a nanosecond but typically fell between 0 and 150 psec. The largest delays (~ 1 nsec) occurred in very localized regions in the u - v plane where very small fringe visibilities (~ 0.03) occurred. On average, structure delay increased as fringe visibility decreased, as one would expect (4).

A LIMIT APPROACH TO STRUCTURE DELAYS

These results indicate that, if subnanosecond clock synchronization becomes a goal, some method must be devised for reducing or calibrating structure effects. In geophysical applications, there is already a need for delay accuracies better than 0.1 nsec. A possible method for removing structure delays is the aforementioned calibration scheme based on measured brightness distributions. The primary difficulty with this approach is that an individual VLBI structure measurement is currently a fairly expensive and time-consuming process. The prospect of working with very large catalogues, possibly containing many time-varying members, makes the calibration approach even less inviting. It is therefore worthwhile to investigate alternate methods for overcoming structure problems.

Another approach is suggested by the general tendency of structure delay to increase with decreasing fringe visibility. Suppose a general formula could be established that, purely on the basis of the value of fringe visibility, places an upper limit on structure delay. Then, if the limit turned out to be sufficiently small for some upper range of visibility values, the larger, unacceptable structure delays could be eliminated by merely deleting observations with the smaller visibility values. Such an approach is attractive since fringe visibility can

often be obtained along with each VLBI observation. If the visibility determinations were accurate enough, the experiment would not depend on supplementary measurements of brightness distributions. One important point that should be made is that the proposed upper limit would not have to be an absolute limit, valid for every source. For example, it would be useful to establish, if possible, an approximate 3σ statistical limit so that structure errors could be treated like other errors. Another example would be a limit that was valid for all sources except for infrequent pathological cases. In fits with redundant observations, such pathological cases could be discovered and deleted through residual analysis.

To begin an assessment of the limit approach, a particular formula associated with a double-point source has been tested. The candidate limit equation is given by

$$\Delta\tau \lesssim \frac{1}{4f} \frac{1-v_s^2}{v_s}$$

which can be rewritten in units of length in the form

$$c\Delta\tau \lesssim \frac{\lambda}{4} \frac{1-v_s^2}{v_s}$$

where f and λ are the observing frequency and wavelength respectively; where v_s is the fringe visibility for the observation at hand; and where $\Delta\tau$ is the structure delay relative to the ordinary centroid. A plot of the function is shown in Figure 4 for X-band. Several arguments can be advanced to support this formula as a general upper limit. First, for small (u , v), one can prove analytically that the formula sets a valid (but loose) upper limit for any source. Second, for a number of special cases, one can prove that no greater structure delay can be obtained for a given visibility (4). Finally, with regard to form, one would expect structure delay to increase, on average, in inverse proportion to visibility for small visibilities (4). Although there are these supporting arguments, one cannot prove analytically that the equation sets a valid upper limit for any arbitrary distribution. Thus, the next step would be comparisons with a large number of measured distributions. When the limit was tested with the ten measured distributions, it was found that, for those cases, the limit was approximately valid for all v_s .

If the same result is obtained for nearly all real sources, then the limit equation would be of great value in both reducing and estimating structure effects in BWS delays. For example, if one set of a lower limit of 0.2 on fringe visibility, then the maximum structure delay predicted by the limit formula would be about 150 psec at X-band (8.3 GHz). Many observations would have visibilities larger than 0.2 and therefore would have smaller limits on structure delay. Further, for the cases analyzed here, actual structure delays were almost always much less than the limit, with the RMS value being about $1/3$ of the limit or less at a given value of visibility. If we hypothesize on the basis of this information that the aforementioned maximum delay of 150 psec is an approximate estimate of the 3σ delay for all observations, then the 1σ error in delay for all observations would be about 50 psec. This calculation suggests one might be able to reduce the 1σ structure delay to about 50 psec simply by deleting observations with fringe visibilities less than 0.2.

SUMMARY AND CONCLUSIONS

To begin a study of structure effects for natural sources, 10 brightness distributions measured by the Caltech group have been analyzed. The magnitude of structure delay (the BWS delay effect computed for X-band relative to the ordinary centroid) was as large as a nanosecond but typically fell between 0 and 150 psec. On average, structure delay tended to increase as fringe visibility decreased. These features suggest the possibility of a limit approach to structure delay. To begin an investigation of this approach, a visibility-dependent limit formula has been suggested that appears to correctly set an approximate upper limit on structure delay for 10 particular brightness distributions. The results for these sources suggest that source structure effects in BWS delay might be reduced to about 50 psec (1σ) simply by deleting observations with fringe visibilities less than 0.2. If this technique or some refinement proves successful in reducing the 1σ structure delay to 50 psec or below, then it would not be necessary to make supplementary brightness distribution measurements for the purpose of calibrating a source catalogue until the goal for total delay error (1σ) falls below about 100-150 psec. In the near future, these high accuracies will probably be in greater demand in geophysical and astrometric applications than in clock-synchronization applications.

A final word of caution would be that the limit approach in its present form has not yet been verified. It may turn out that, at the large u-v values associated with intercontinental baselines, too few natural sources possess sufficiently large fringe visibilities in the required u-v regions. Further, the measured distributions considered here are too few in number and too limited in u-v coverage and observing frequency to provide a general verification. The u-v coverage is too limited because (a) the absence of short baselines (≤ 300 km) can allow important large scale structure to be resolved out and missed and (b) the absence of intercontinental baselines can allow important small scale structure to remain unresolved. One example of a source distribution that would violate the limit formula would be a large, strong diffuse component displaced by a considerable distance from a weaker compact component. In this case, the effective position would move from the centroid of both components to the center of the compact component as baseline length increased. If the separation of components were great enough, large changes in structure delay could occur. More survey data is required to determine whether the percentage of sources that fall in this category, or other disallowed categories, is too large for the limit equation in its present form to be valid. Even if the present form is unsuitable, it should be possible to construct another visibility-dependent limit that is valid for nearly all sources. How useful the the final form will be in overcoming source structure problems remains to be determined.

In future work, we plan to investigate more sources with more detailed analysis with the hope that the present limit approach, or some refined version, can be generally established.

ACKNOWLEDGEMENTS

The author wishes to thank S. G. Finley for her enthusiastic and skillful support in generating the software for the contour plots. This paper presents results from one phase of research carried out at the Jet Propulsion Laboratory, California Institute of Technology, under contract number NAS7-100, sponsored by the National Aeronautics and Space Administration.

REFERENCES

- (1) J. B. Thomas, "Source Structure Errors in the Synchronization of Clocks by Radio Interferometry", Proceedings of Eleventh Annual PTTI Meeting, NASA Conference Publication 2129, p. 599, November 1979 .
- (2) T. J. Pearson, A. C. S. Readhead, and P. N. Wilkinson, "Maps of the Quasars 3C119, 3C286, 3C345, 3C454.3 and CTA102 with a Resolution of 5 milliarcseconds at 1.67 GHz", Astrophysical Journal 236, 714, March 1980.
- (3) A. C. S. Readhead, T. J. Pearson, M. H. Cohen, M. S. Ewing and T. A. Moffet, "Hybrid Maps of the Milliarcsecond Structure of 3C120, 3C273 and 3C345", Astrophysical Journal 231, 299, July 1979.
- (4) J. B. Thomas, "An Analysis of Source Structure Effects in Radio Interferometry Measurements", A JPL report to be published.

SUMMARY OF BRIGHTNESS DISTRIBUTION MEASUREMENTS

TABLE 1

DISTRIBUTION NUMBER	SOURCE	MEASUREMENT DATE	OBSERVING WAVELENGTH (cm)	TOTAL FLUX (Jy)	INTERFEROMETER STATIONS	U _{MAX} / V _{MAX} (10 ⁶ λ)
1	3C119	MAY, 1976	18	7.5	1, 2, 3, 4	19 / 12
2	3C286	MAY, 1976	18	13.5	1, 2, 3, 4	19 / 10
3	3C345	MAY, 1976	18	6.5	1, 2, 3, 4	19 / 12
4	3C454.3	MAY, 1976	18	12.0	1, 2, 3, 4	19 / 8
5	CTA102	MAY, 1976	18	6.4	1, 2, 3, 4	19 / 7
6	3C273	JULY, 1977	2.8	41.0	1, 2, 3, 5	135 / 40
7	3C345	JULY, 1977	2.8	7.5	1, 2, 3, 5	140 / 80
8	3C273	DECEMBER, 1977	6	46.2	1, 2, 3, 4	60 / 15
9	3C345	DECEMBER, 1977	6	7.8	1, 2, 3, 4	60 / 40
10	3C120	DECEMBER, 1977	6	6.6	1, 2, 3, 4	60 / 20

STATION CODE: 1 = NRAO; 2 = FDVS; 3 = OVRO; 4 = HCRK; 5 = HSTK

AN EXAMPLE BRIGHTNESS DISTRIBUTION

3C 345

DISTRIBUTION 9

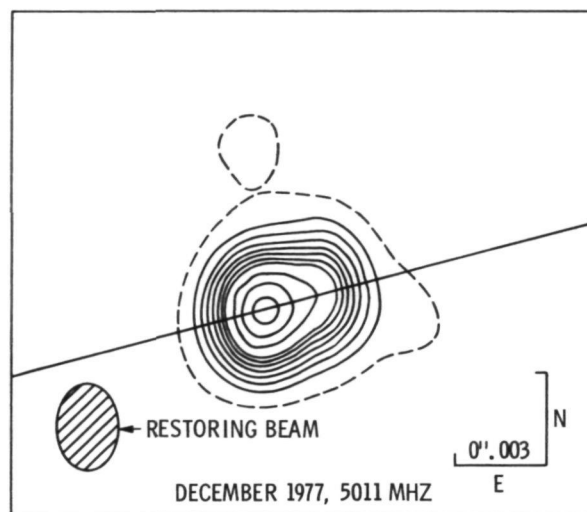


FIGURE 1

FRINGE VISIBILITY

3C 345

DISTRIBUTION 9

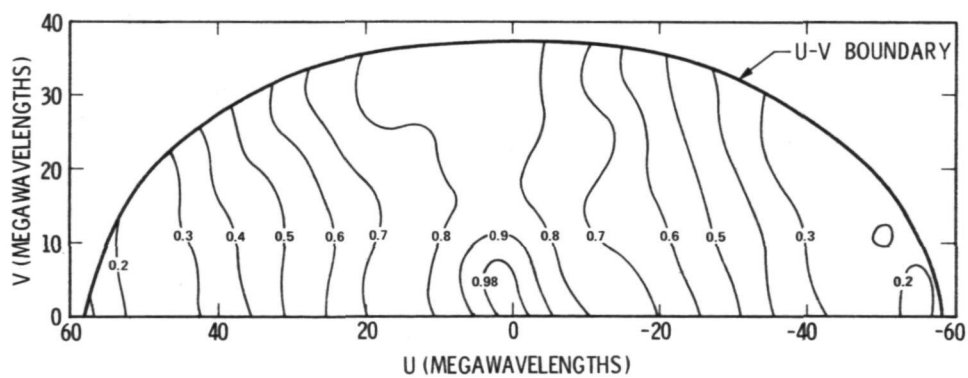
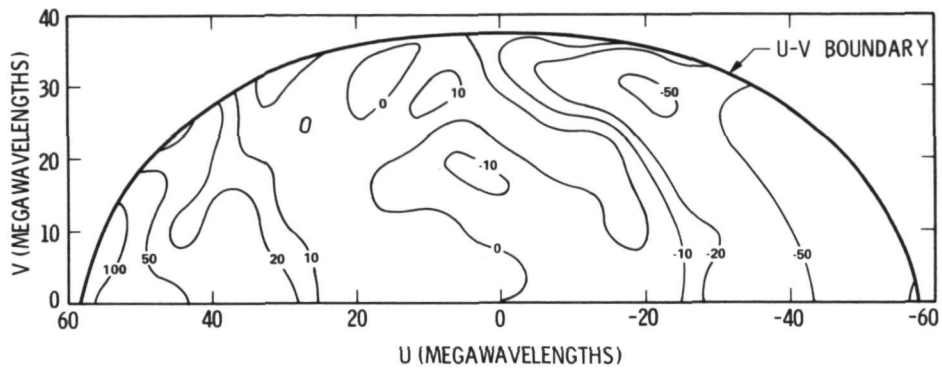


FIGURE 2

**STRUCTURE DELAY* RELATIVE TO
BRIGHTNESS CENTROID
3C 345 DISTRIBUTION 9**



* FOR X-BAND IN PSEC

FIGURE 3

**A LIMIT FORMULA FOR
STRUCTURE EFFECTS* IN BWS DELAY**

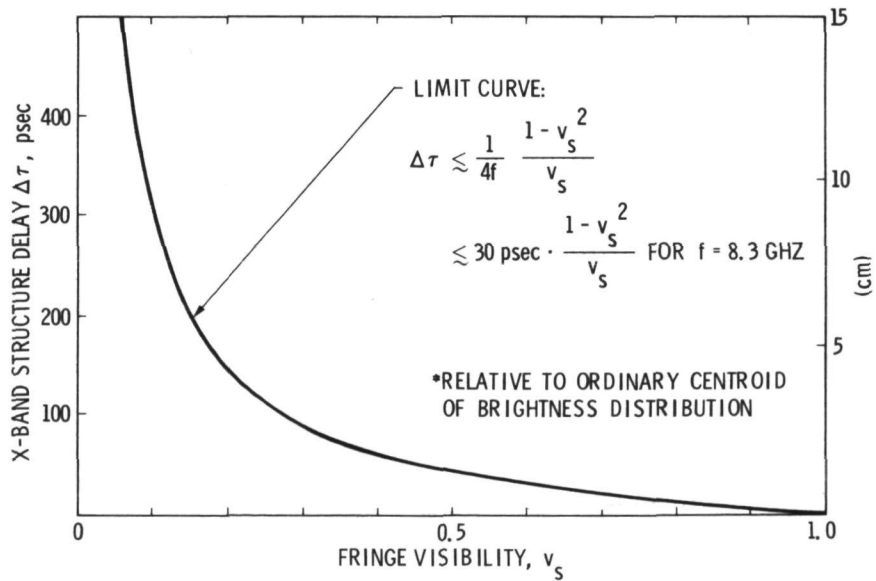


FIGURE 4

Page Intentionally Left Blank

GEODYNAMICS FREQUENCY AND PHASE

F. O. Vonbun and V. S. Reinhardt
NASA Goddard Space Flight Center
Greenbelt, Maryland

ABSTRACT

The objective of this paper is to discuss NASA's geodynamics experiments in relation to precise time and time interval requirements. In particular we are focusing on two specific experiments, namely the Apollo-ATS-6 gravity anomaly experiment which took place during the 1975 US-USSR Apollo-Soyuz test project and a dedicated earth gravity field mission called GRAVSAT which is planned to take place during the 1986-88 time frame. In these experiments, the earth's gravity field and in particular its spatial variation is determined by measuring extremely small changes in the range rate between two spacecraft.

The ATS-6-Apollo experiment, satellite to satellite range rate errors of about 300 $\mu\text{m/s}$ were realized. It will be shown that errors of this magnitude are to be expected from the known phase noise of the Cs-standards used.

For the GRAVSAT mission range rate tracking errors of about 1 $\mu\text{m/s}$ are needed. This in turn dictates extremely high engineering requirements in frequency and phase. A fractional frequency stability of 1 part in 11 over 4 second averaging time is required of the reference oscillator. In addition a time interval stability of about 10^{-15} sec over the same averaging time is needed for GRAVSAT range rate tracking system.

(Paper not Submitted)

Page Intentionally Left Blank

TIME AND FREQUENCY STABILITY FOR THE CRUSTAL DYNAMICS PROJECT

R. Coates, J. Ryan (Goddard Space Flight Center, Greenbelt, MD),
T. Herring (Massachusetts Institute of Technology, Cambridge, MA)

ABSTRACT

The Crustal Dynamics Project utilizes very long baseline interferometry (VLBI) and laser ranging to artificial satellites and the moon to determine vector baselines between stations with precisions of about one part in 10^8 . Both laser ranging and VLBI require initial relative epoch timing of about one microsecond for stations distributed over the globe. Very stable frequency standards are the key to VLBI because they are used to maintain frequency coherence between stations. In order to have less than one radian rms X-band phase perturbation accumulated in a 1000 second integration period, the frequency standard must have a stability of 1×10^{-14} . In the VLBI data analysis to determine accurate baselines, the clock offsets and variations must be solved for in order to fit the data with less than 0.1 nsec (3 cm) rms deviation over 24 hours. This is a fit to 1×10^{-15} . Over the next six years the Crustal Dynamics Project plans to improve the accuracy of the VLBI technique by about an order of magnitude. This will require a frequency stability of about 1×10^{-15} for periods of hours to days and solutions for frequency variations to about 1×10^{-16} .

The NASA Crustal Dynamics Project was formed last year to apply the NASA-developed techniques of satellite laser ranging (SLR) and very long baseline interferometry (VLBI) for the measurement of crustal motions of the earth. Both of these techniques have the virtues that measurements with an accuracy of 1 part in 10^8 can be made over baselines of several thousand kilometers, and these baseline measurements can be made across any terrain, sea or land. The Crustal Dynamics Project is determining regional deformations and strain accumulations in active earthquake regions by making frequent measurements of baselines between many stations in the active areas near plate boundaries. By making regular measurements of baselines

between a global set of stations on the different tectonic plates, the Project is determining the tectonic plate motions and the internal stability of the plates. Quite frequent measurements with a global set of fixed stations are being used to determine very accurately the motion of the pole of the earth and variations in earth rotation.

Both SLR and VLBI require initial relative epoch timing of about one microsecond for stations distributed over the globe. In addition, the VLBI system has a very stringent requirement for frequency standard stability because frequency coherence must be maintained between the VLBI stations. Figure 1 is a diagram of a pair of stations used for a VLBI measurement. The figure shows two antennas at remote distances on the surface of the earth receiving signals from the same radio source, a quasar. The signal received at both stations is translated to base band using a very stable hydrogen maser frequency standard. The base band signal is digitized and recorded. The recorded data from the two stations are then processed in a correlator which determines the time delay between the arrival of the quasar signal at the two stations. Since the two antennas are located on a rotating earth, the delay has a diurnal sinusoidal signature which is a function of the quasar position and the baseline length and orientation. By measuring the delay and delay rate signatures of a number of quasar sources, one can calculate very accurately the vector baseline between the two stations.

The hydrogen maser clocks at the two stations are independent; thus they will have neither the same epoch time nor the same frequency behavior. In the VLBI solutions for the baselines, it is necessary to solve for the clock offset and the rate difference between the clocks, and in some cases even clock frequency drift.

The use of very stable hydrogen masers as frequency standards is the key to the success of VLBI. In order to have less than one radian rms X-band phase perturbation accumulated in a 1000 second integration period, the frequency standard must have a stability of better than 10^{-14} for periods of up to a few minutes. In the VLBI data analysis to determine accurate baselines, the clock offsets and variations must be solved for in order to fit the data with less than 0.1 nanoseconds (3 centimeters) rms deviations over 24 hours. This implies modelling behavior to about 1 part in 10^{-15} . Figure 2 shows a rather typical example of a plot of delay residuals after the clock offsets and the linear rate difference between the clock have been solved for and removed. This data is from stations at Haystack Observatory,

Massachusetts, and Owens Valley Radio Observatory, California. The rms fit of this data is approximately 0.1 nanoseconds. Typically, from data like this we are able to determine the baseline from Haystack Observatory to Owens Valley Observatory to a precision of a few centimeters. Repeated measurements of that baseline over the past four years have shown an rms deviation of 4 centimeters for this 4,000 kilometer baseline. This is a precision of 1 part in 10^{-8} in the determination of the baseline.

The Project has acquired data that has higher quality than that shown in Figure 2, and also worse. Sometimes there have been malfunctions which degraded the measurement precision. The purpose of this paper is to show how well we can recover accurate baselines when there are problems with the frequency standard and distribution system at the VLBI station. One such malfunction is a sudden change in rate of the frequency standard. An example of this is shown in Figure 3 which is a plot of delay residuals in which only the clock offset has been removed so that the rate difference between the two clocks are shown. There are two rate changes evident in Figure 3. The first change in rate between the two clocks occurred at approximately 4.4 days and was a rate change of 4×10^{-14} . The second rate change at about 6.4 days was a rate change of 7×10^{-13} . In this experiment, there were three stations involved--Haystack Observatory, Owens Valley Radio Observatory and the Harvard Radio Astronomy Station in Texas. With the data from the three stations we were able to determine that the changes in the rate of the clocks occurred at Haystack Observatory. With a clock change like this, the VLBI solution's clock model can be broken up into segments corresponding to the time periods during which the clock was behaving in a normal manner. In the example in Figure 3 there were three segments used in the solution, the first segment from 0 to 4.4 days, the second segment from 4.4 to 6.4 days, and the third segment from 6.4 to 8 days. In the solution, three clock rates were determined, one corresponding to each time segment. As long as there is enough observing time to permit an accurate determination of the clock epoch and rate for each segment, the precision of determination of the baselines is still a few centimeters.

The data set just shown in Figure 3 was selected because it was a particularly bad set which contained three different malfunctions of the frequency and distribution system. The other two malfunctions become more apparent when the data is plotted with the three clock rates removed, as shown in Figure 4. With the greatly amplified delay residual scale (± 5 nanoseconds), diurnal signatures are quite

apparent in the data. Since the viewing of the radio sources with the interferometer produces a delay which is a diurnal signature, a diurnal signature produced in the frequency standard and distribution system is of great concern because it can alias directly into the baseline results and create a significant error. In this particular case, the diurnal sinusoid showing in Figure 4 was caused by two different failures at the Harvard Radio Astronomy Station. The first failure, which caused most of the diurnal sinusoid, was a component failure in the frequency distribution and calibration system. This extended over the entire period of the observation. The second problem was caused by the failure of the temperature control system for the hydrogen maser room which occurred on October 19. This is illustrated in Figure 5 which is a plot of the hydrogen maser temperature as a function of time. Normally the temperature is controlled to a small fraction of a degree. After the failure, the hydrogen maser room varied in temperature about one degree with a diurnal signature. Hydrogen masers have a temperature coefficient of a few parts in 10^{-14} per degree C, so a diurnal temperature variation does produce a diurnal frequency change in the output of the hydrogen maser. Fortunately, the time constant of the frequency change with temperature change is longer than the diurnal period, and the amplitude of the diurnal frequency variation is attenuated considerably. Consequently, the diurnal sinusoid due to the temperature control failure was significantly smaller than the diurnal sinusoid due to the frequency and calibration system failure.

In order to determine the effects of such a diurnal signature on the accuracy of the baselines determined from this data, an analytical simulation of this problem was conducted. For this simulation, theoretical observables were used for data for the three stations, a one nanosecond diurnal sinusoid was added to one clock, and the baseline lengths were solved for using standard procedures to determine the errors caused by the diurnal clock variation. Next the simulation was repeated using real observed data from other sessions where there were no clock failures. The simulations were performed with a solution for one day. One day was chosen because that would produce the worst case result. Figure 6 shows the simulation results for three different variations in analysis strategy. In the first case, linear clock terms were used in the solution for determining the relative clock rate, and the resulting error in baseline length with this simple clock parameterization was almost 20 centimeters. Such a simple parameterization ignores the fact that there are terms other than linear variations present in the residuals. In the normal process

of analyzing the data, we also have the capability of putting in higher order polynomial clock terms. The second case utilized a quadratic clock parameterization for the malfunctioning station and linear clock terms at the other stations. The worst error in baseline length for this second case was only 2.2 centimeters. The simulations with real VLBI data gave similar results.

In these first two solutions, the source positions were used as a priori positions and the solutions were done with those source positions fixed. In the third case these source positions were solved for in order to see what the effects would be if one solved for the source positions at the same time one was solving for clocks and baselines. The result was that large errors occurred when source positions were solved for even when the quadratic clock terms were used in the solutions. The reason for this is quite understandable. Since the delay of the signal from a source has a diurnal signature, the diurnal clock error will cause an error in the determination of the position of the source which in turn produces an error in the baseline solution. The result of this third case indicates that one should not solve for both baselines and source positions in a single experiment solution. Accurate positions of radio sources can be determined from solutions with large batches of data which cover several years of time. With such a large span of data, the clock effects will tend to cancel themselves out, and the resulting positions determined for the sources will be quite accurate. These accurately determined source positions can then be used in the individual measurement solutions using the quadratic clock terms as in case 2 to produce accurate baseline results. By following this type of strategy one can produce baseline determinations with a few centimeters precision even with malfunctions of the type described above. This result is consistent with the history of baseline measurements with a precision of 4 centimeters that have been obtained over the past four years.

Good geophysics can be done with 4 centimeters baseline precision, and the Crustal Dynamics Project has deployed both VLBI and laser systems around the globe for measurements of plate motions and stability, and has initiated campaigns in California for measuring regional deformation. However, higher measurement accuracy will result in better geodetic results. Thus, the Project goal is to achieve a 1 centimeter measurement precision. Actions are underway now in the frequency standard area that are aimed at improving the performance of the VLBI system. It was mentioned earlier that there is a temperature controlled room for the hydrogen maser at the Harvard Radio Astronomy Station. That is the first installation of

temperature controlled rooms for hydrogen masers. The Project is in the process of installing such temperature enclosures for all of the hydrogen masers that are being used in the Project. The goal is an order of magnitude improvement in the stability of the frequency of the hydrogen masers operating in the field. In addition, the new hydrogen masers are equipped with extensive monitoring capability for recording the environmental parameters that affect maser operation. It is our plan to determine the relationship between the environmental parameters (temperature for example) and the maser frequency in order to determine the actual frequency performance from the measurements of the environmental parameters. By determining the fine frequency variations due to environmental changes, we expect to be able to know the frequency of the masers to an order of magnitude better accuracy than we do today. This should reduce clock errors in our solutions by an order of magnitude. There are other error sources, such as atmospheric propagation, which contribute errors to the overall baseline solution at the centimeter level. The Project has efforts underway to reduce all of the known error sources to the millimeter level in order to reach the goal of one centimeter baseline accuracies.

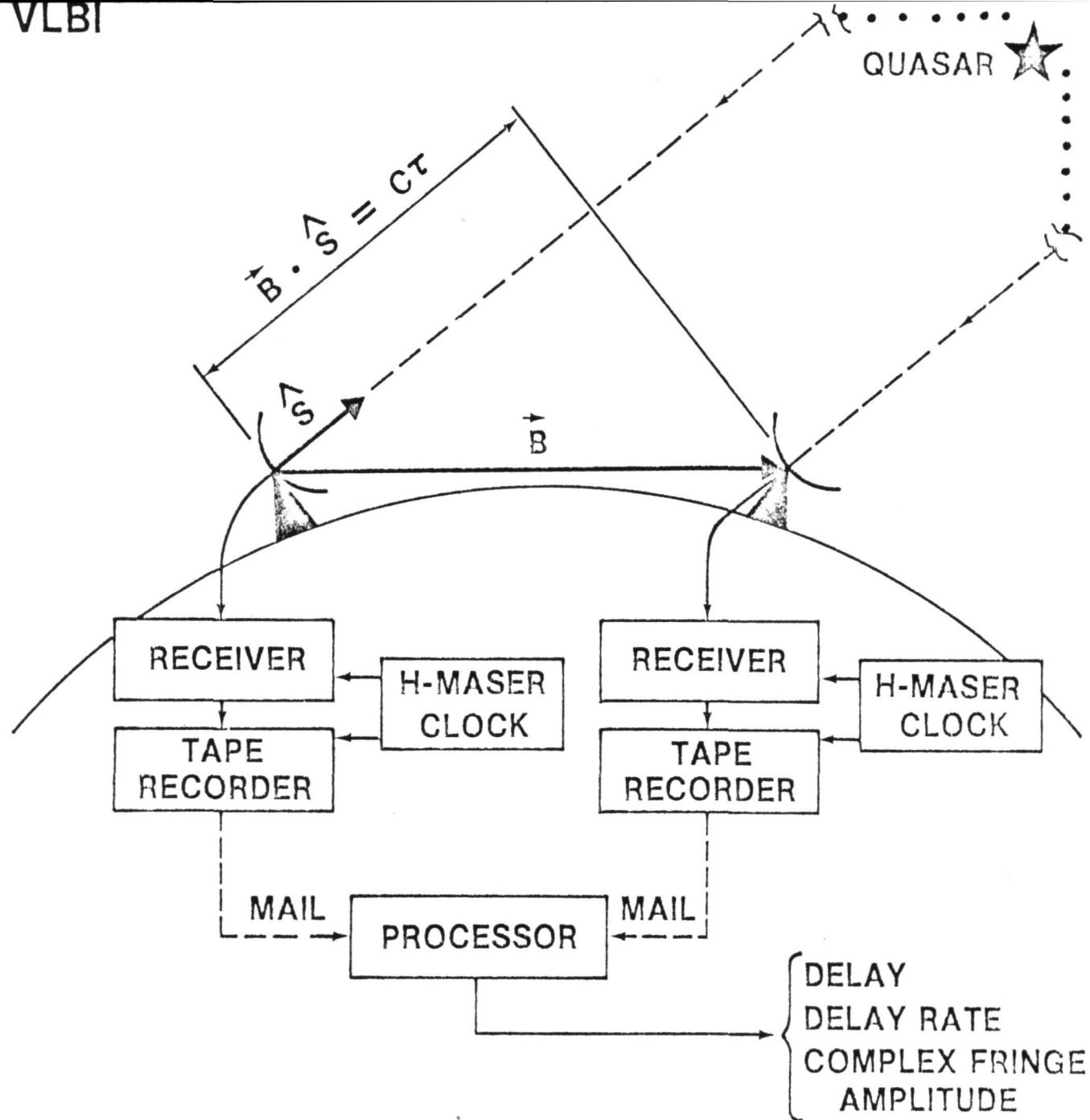


FIGURE 1



HAYSTACK-OVRO 130 8/ 4/79. RUN CODE 10330-2052

656

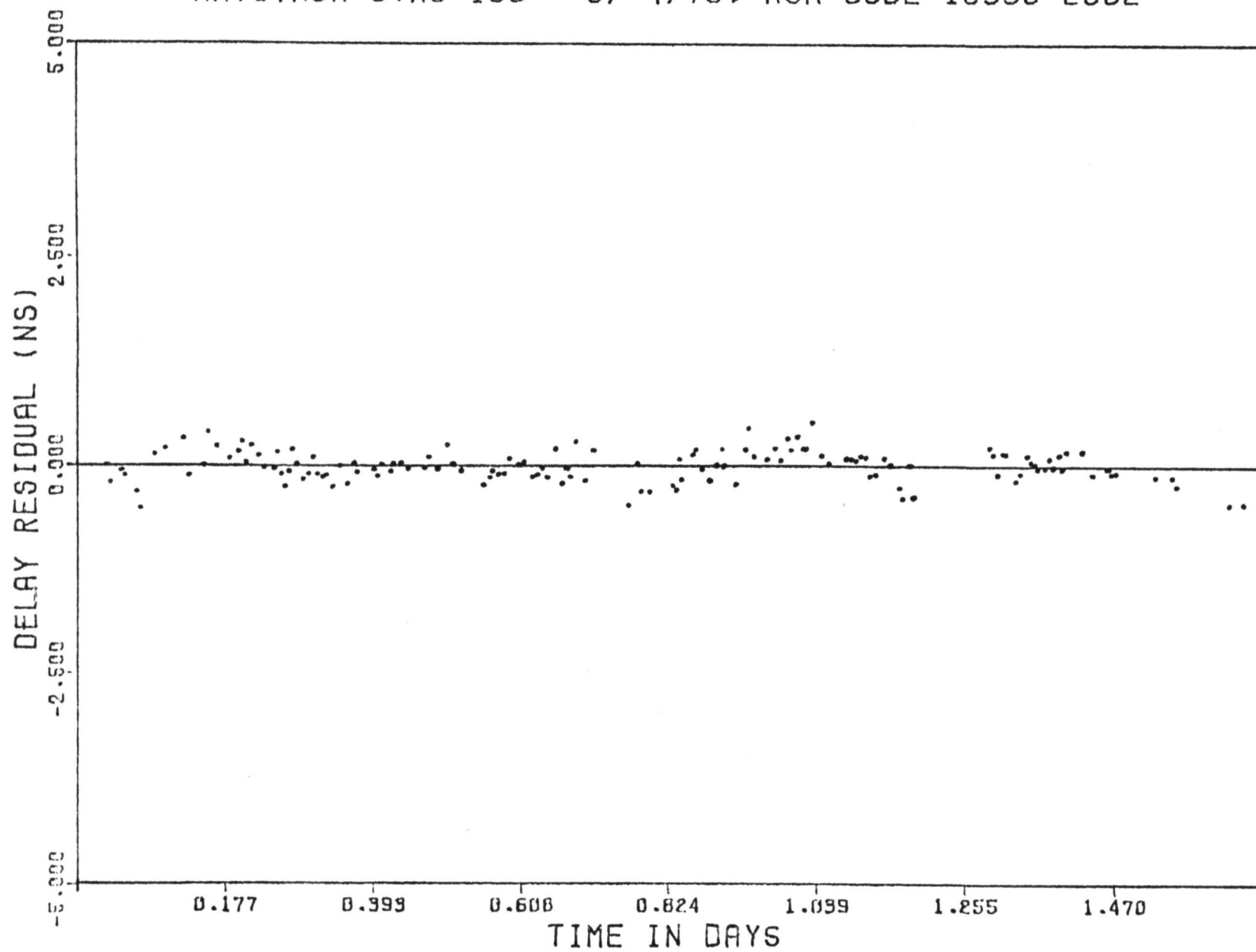


FIGURE 2



657
DELAY RESIDUAL (NS)

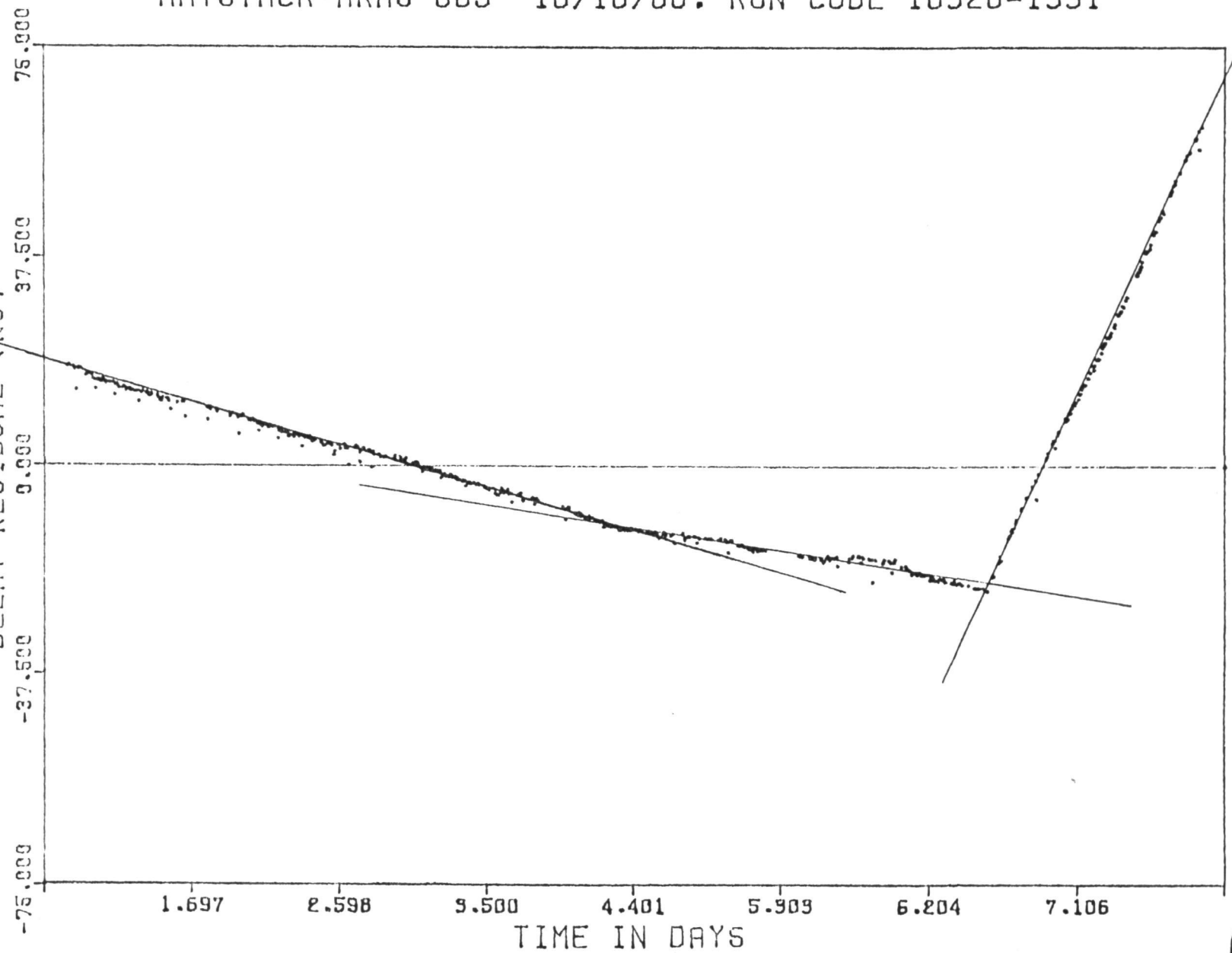


FIGURE 3

HAYSTACK-HRAS 085 10/16/80. RUN CODE 10326-1245

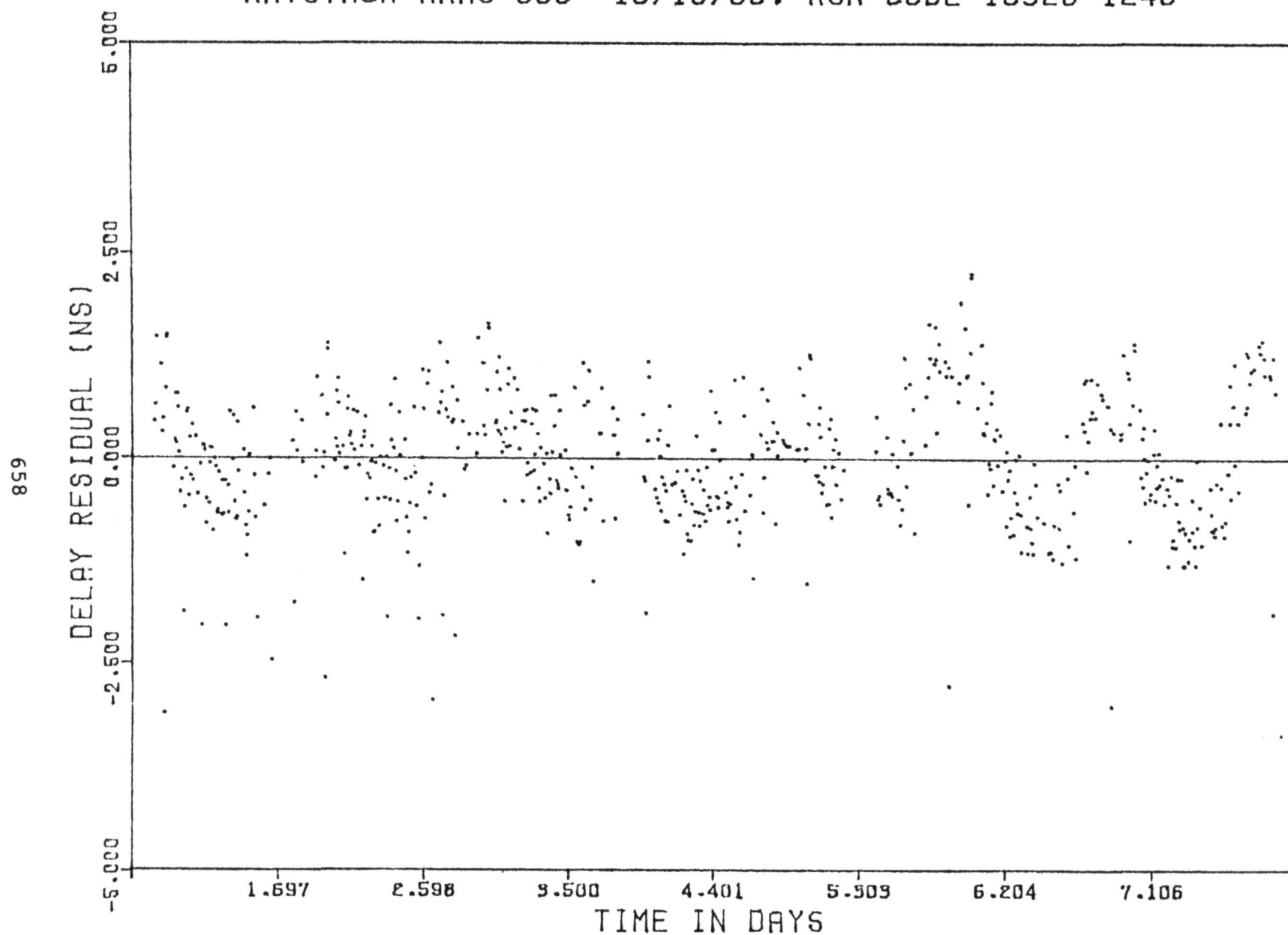


FIGURE 4

NR-2 TOP CABINET TEMPERATURE (FT. DAVIS)

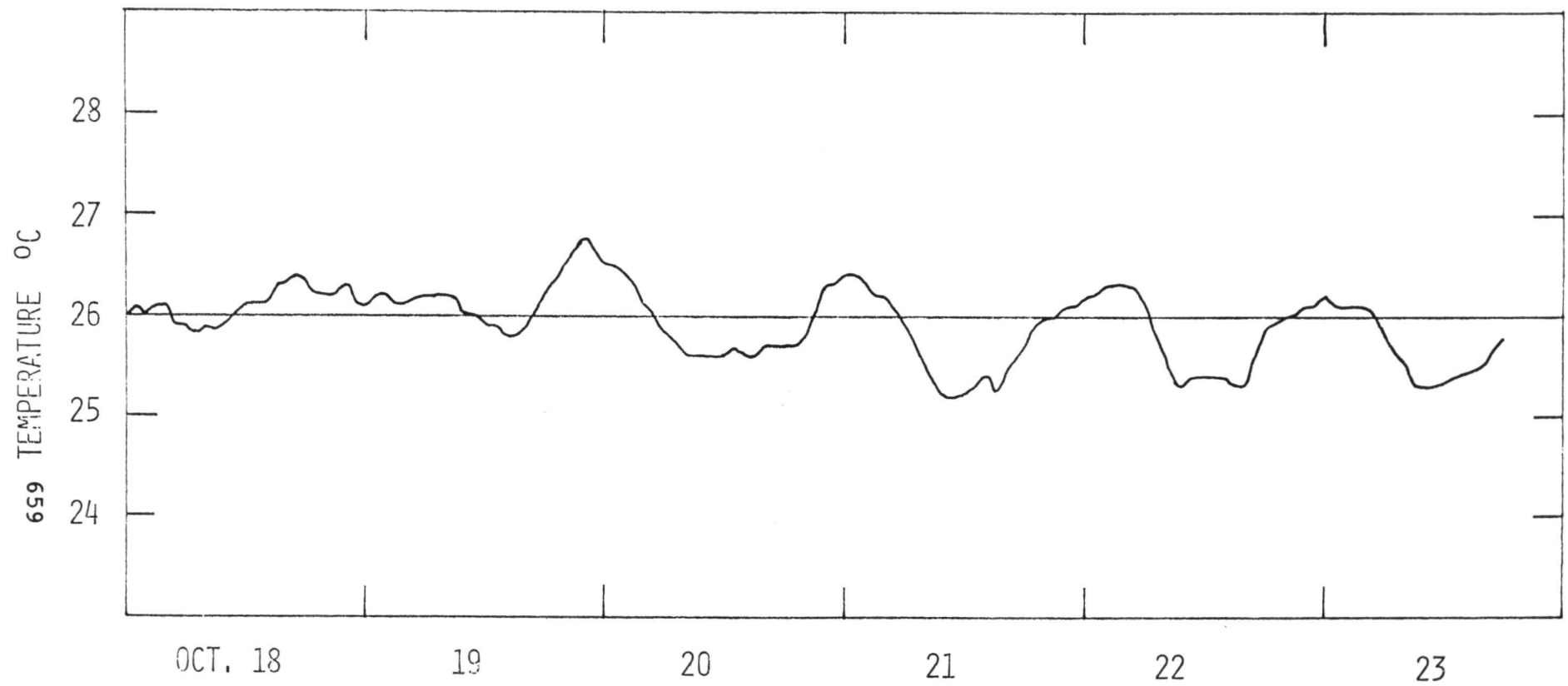


FIGURE 5



SIMULATION RESULTS FOR THE
HAYSTACK-FT. DAVIS-OWENS VALLEY BASELINE LENGTH ERRORS
CAUSED BY 1 NS DIURNAL SINUSOID TIME ERROR AT HAYSTACK

<u>SOLUTION PARAMETERIZATION</u>	<u>WORST ERRORS (CM)</u>		
	<u>HA-OV</u>	<u>HA-FD</u>	<u>FD-OV</u>
o LINEAR CLOCKS AT HAYSTACK & OVRO	-12.1	-19.9	-4.7
o QUADRATIC CLOCK AT HAYSTACK, LINEAR CLOCK AT OVRO	- 2.4	- 0.3	-1.8
o QUADRATIC CLOCK AT HAYSTACK, LINEAR CLOCK AT OVRO, SOURCE POSITIONS	-18.7	-18.6	-9.5



FIGURE 6

QUESTIONS AND ANSWERS

CHAIRMAN HOWE:

You have gone to some length to attempt to look or take out the one nanosecond diurnal sinusoid term. I might suggest that you also look at perhaps other effects since you can monitor temperature, but you might look at humidity, temperature gradients, and even power line fluctuations.

You can make certain assumptions about unit correlation with these long-term effects, but you will see them definitely on the relatively inexpensive data logger.

DR. COATES:

We do monitor the environment; we monitor the temperature, the pressure, and the humidity, I didn't mention pressure. Some masers are pressure-sensitive; the ones that we have been using in these experiments are not contributing a pressure effect that is significant, but we do monitor all of these parameters.

The new masers that we have are almost independent of power lines variations. We have gone to great extents to eliminate that as a factor. When we are after extreme stabilities that we are talking about here, we need to really go all out. You are quite right.

DR. VICTOR REINHARDT, NASA/Goddard

I think this shows pretty conclusively that the effects due to temperature and pressure, humidity, are well-modelable, and I think for the JPL tests as well as the JPL, DSN, VLBI uses and other uses, there is no reason that these things can be just modeled out very easily in the least squares fit, especially since with Paul Kuhnle's new test facility, each of the masers is very well characterized for each of these things when we go out into the field.

So, I really, for the long-term, don't see this is a problem; just as something that is getting into the system. So, the VLBI people, now that they are aware of the problem, can just easily put that into their programs because a few more parameters of fit really doesn't make a significant difference in terms of computing time in this case.

DR. THOMAS, The Jet Propulsion Laboratory

I wonder how you isolated the diurnal sinusoid to the clock and not to other possible effects like other instruments, the ionosphere, and so forth.

DR. COATES:

There are other effects that you can see that are systematic. We do SX determination of the ionosphere. However, in the particular example I gave, you could see that the difference between two sets of data is quite large. The effect was determined very precisely by looking at three stations' data that shows there was something at one station. It was something like an extensive active ionosphere which would show up at all the stations.

There was a diurnal sinusoid at the beginning of the observing period. In the middle of the observing period, there was an increase in that diurnal sinusoid. That increase in the diurnal sinusoid matches with the change in the temperature control on the maser enclosure.

OPTICAL FIBERS FOR THE DISTRIBUTION OF
FREQUENCY AND TIMING REFERENCES *

George F. Lutes

Jet Propulsion Laboratory
California Institute of Technology
4800 Oak Grove Drive
Pasadena, California 91109
(213) 354-6210

ABSTRACT

An optical fiber communications link was installed for the purpose of evaluating the applicability of optical fiber technology to the distribution of frequency and timing reference signals. It incorporates a 1.5km length of optical fiber cable containing two multi-mode optical fibers. The two fibers were welded together at one end of the cable to attain a path length of 3km.

This paper reports preliminary measurements made on this link, including Allan Variance and power spectral density of phase noise.

INTRODUCTION

A three kilometer stabilized optical fiber distribution link for the dissemination of ultrastable reference frequencies has been demonstrated. The fractional frequency stability ($\Delta f/f$) of this link as a function of the sampling interval (τ) is compared to the stability of a Hydrogen maser in Figure 1.

The effective stability and accuracy of a frequency and/or timing standard is no better than the stability of the distribution system that delivers its output signal to the user. Therefore it is important to improve distribution systems simultaneously with improvements in the stability of frequency and timing standards.

This paper will begin with a discussion of three basic stabilized frequency distribution systems with variations and a description of a coaxial system that has been implemented. This will be followed by an

*This paper presents the results of one phase of research carried out at the Jet Propulsion Laboratory, California Institute of Technology, under Contract No. NAS7-100, sponsored by the National Aeronautics and Space Administration.

examination of error sources encountered in the implementation of these systems. Then the applicability of optical fiber technology to frequency and timing dissemination will be discussed. Finally the details of the stabilized optical fiber frequency distribution system which has been implemented, will be discussed, followed by possible future improvements.

Basic Systems

The three basic kinds of stabilized frequency distribution systems of the two way transmission type are shown in Figure 2(a), (b) and (c).

In each of these figures the forward and return signal paths are drawn separately but in practice the signals are transmitted both ways in the same signal path (coaxial cable, optical fiber, etc.). This is done to assure that the delay (τ) plus the change in delay ($\Delta\tau$) is the same in both directions. The change in delay, $\Delta\tau$, is caused by the effect of temperature variations, pressure changes and mechanical disturbances on the signal path.

In the feed-forward system shown in Figure 2(a), the phase difference between the input signal and the return signal is measured. This difference is divided by two and subtracted from the phase of the output signal. This can be done in a phase shifting device in series with the output signal as shown or in the users software.

In the feed-back system in Figure 2(b), the phase difference between the input signal and the return signal is held constant by controlling the phase shifter such that any change in delay ($2\Delta\tau$) is cancelled.

The phase of the input signal is changed, in the conjugation system shown in Figure 2(c), such that it is always the conjugate of the return signal relative to the zero phase of the reference signal. This forces the output phase to remain at zero.

There are four variations in the way the return signal is generated and each of them is applicable to any of the three basic systems.

The first way, shown in Figure 3(a), is to terminate the transmission line with a mismatch at the far end so that some of the signal is reflected back down the line.

A system was implemented by P. Clements, reference 1, in 1974 using this variation with the feedback system. The phase shift was accomplished by changing air pressure in an air dielectric coaxial cable.

In the second variation, shown in Figure 3b, the terminating impedance at the far end of the line is not only mismatched to the line, but is also varied (modulated) sinusoidally at a low frequency.

This causes the power of the reflected signal to vary with the modulating frequency, generating two sidebands on the return signal which are evenly spaced about the input frequency. This is done so the return signal can be separated, with filters, from the input reference signal. A more complicated form of detector is required, with this variation, to compare the return signal to the reference.

This variation was developed by A. Rogers, Reference 2, in the early 1970's, and was used first in the feed-forward system (Figure 2(a)) and later in the feed-back system (Figure 2(b)).

The last two variations, shown in Figure 3(c) and (d), are similar to the two variations previously discussed, except that the signals are received at the far end of the line and then filtered and amplified, and in the final variation, modulated and retransmitted back down the line. This results in a higher signal to noise ratio at the error detector and may in some cases result in better short term stability of the output signal.

A stabilized microwave distribution system using the modulated turn-around return signal variation with a conjugation system (Figure 2(c)) was developed by J. MacConnell and R. Sydnor in 1976-1977, Reference 3. Two such links were installed at the NASA Deep Space Network (DSN) Complex at Goldstone, California. They were connected end to end in opposite directions so that a signal could be transmitted over a 9 km distance by one link and returned to the origin over the other link. The return signal was compared to the reference to determine the stability. This data is shown in Figure 5.

Coaxial Cable System

The modulated turn-around variation was used in a negative feedback system that was implemented by the author in 1975 (reference 4). A block diagram of this system is shown in figure 4. It was used to stabilize a 300 meter length of coaxial cable and reduced a 10 cm length change on the cable to approximately 2 mm.

A 5 MHz reference frequency was transmitted through a directional coupler and a phase shifter down the coaxial cable to the far end where it was received and divided by 1000. The 5 KHz signal out of the frequency divider was used to modulate the received 5 MHz signal. The modulation resulted in a double sideband suppressed carrier signal that was transmitted back down the coaxial cable through the phase shifter to the directional coupler where it was separated from the forward signal and was directed to the detector. The phase of the return signal was compared, in the detector, to the phase of the reference signal and an error signal was generated that controlled the phase shifter to reduce the error.

Error Sources

One of the most difficult error sources to eliminate is the leakage of the input signal (reference) into the return signal path. This leakage can be due to inadequate isolation in the directional couplers or from the input signal being reflected back toward the source by intermediate reflections in the signal path. This reflection problem is particularly bad in a microwave transmission system, such as the one previously discussed, and makes it necessary to use gated detector techniques to reduce it.

In the case of the modulated return signal type of system, inadequate suppression of the carrier (reference signal) at the return port of the detector can be a source of error.

Drift in the error detector will not be reduced. Any change in the one way signal path will only be reduced by a factor of 2. Error detectors are generally sensitive to amplitude changes. These changes can have several causes and are most likely to occur on the return signal. If a standing wave exists on a transmission line, for example, small changes in the length of the line can cause relatively large changes in amplitude.

When the modulated return signal type of system is used, dispersion in the transmission medium, filters or phase shifter may cause an error by upsetting the phase relationship between the two sidebands and the carrier. This effect gets worse as the sidebands get further apart in frequency and as the distance increases.

Another problem that occurs in a modulated return signal type of system is the problem of eliminating the modulation frequency from the output signal.

Applicability of Optical Fiber Technology

Several characteristics associated with optical fibers can be used to advantage in the dissemination of frequency and timing references.

The change in propagation delay versus temperature is approximately 10 parts per million per degree centigrade. This is comparable to the most stable coaxial cables which are more expensive than fiber optic cable.

Multi-mode optical fibers with 1 GHz-km bandwidth are readily available. This is much greater than any practical coaxial cable.

A wide bandwidth provides the capability of disseminating a wide range of frequencies, possibly several simultaneously on the same fiber.

Wideband optical fibers exhibit low dispersion of 1 ns/km or less. Because of this there is much less spreading of timing pulses than is possible with coaxial cables. In stabilized frequency dissemination systems utilizing modulated return signals, the relationship between the generated sidebands and the carrier is affected much less than it would be in most other propagation media.

Optical fibers are available with optical losses of <3 dB/km at 850 nm wavelength. At 1,300 nm wavelength the loss can be <0.5 dB/km. Laser diodes that operate at this wavelength will soon be available as will diodes capable of much more output power than the typical 1 to 5 milliwatts of C.W. optical power generated with presently available devices.

Solid state laser diode transmitters are available that have modulation bandwidths greater than 1 GHz, and can be linearly or digitally modulated. Receivers are available with a bandwidth from D.C. to 3 GHz.

Optical fibers do not radiate or pick up RFI or EMI. This can be a major source of noise in other propagation mediums.

Electrical isolation can be maintained between an optical transmitter and receiver, thereby eliminating ground loops.

Optical fiber cables are small, lightweight and corrosion resistant.

The installation of optical fiber cables is comparable to coaxial cables; discontinuities can readily be located using an optical time domain reflectometer; and they can be repaired by welding, even in an adverse field environment. Repairs can be made with no more difficulty than repairing coaxial cables.

Directional couplers are available with isolation greater than 80 dB and signals can be transmitted in both directions in an optical link at the same frequency with extremely high isolation between them.

Optical Fiber System

The subject optical fiber link consists of a commercial optical transmitter and receiver and a 1.5 km length of two conductor optical fiber cable.

About 1.5 mW of optical power is emitted, by the optical transmitter, at a wavelength of ≈ 830 nm. The output can be linearly amplitude modulated from 20 Hz to 1.2 GHz.

The modulation frequency response of the receiver is from D.C. to 3 GHz and the gain can be controlled over a 40 dB range.

The cable contains two optical fibers of the multimode graded index type with a bandwidth of 400 MHz-km and 6 dB/km loss. The outside diameter of the fibers is 125 μm with a 62.5 μm core diameter.

The two fibers are welded together at the far end of the cable to attain a round trip signal path length of 3 km.

A directional coupler has been welded to each of the fibers at the near end. This provides an input and an output for each fiber to which a receiver and transmitter has been connected. In this configuration there are two separate links, operating in opposite directions, sharing the same fiber. If the output of one link is connected to the input of the second link a path length of 6 km is attained. The separation between these links is >60 dB. There are 15 welded splices and two connectors in the fiber in this configuration.

The instantaneous bandwidth of each 3 km link is limited by the fiber to 130 MHz. One way (3 km) signal loss in the fiber is 24 dB. The power spectral density of phase noise (reference 4) is ≈ 120 dBc in a 1 Hz bandwidth, 10 Hz from a 100 MHz signal.

Intermodulation distortion products are down more than 40 dBc for two signals separated by 1 kHz around 25 MHz and with a modulation depth of 70%.

A stabilized optical fiber frequency distribution system could be implemented by merely inserting an optical fiber two way link, as described above, between the ends of the stabilized coaxial system shown in figure 4. The result of this would be the system shown in figure 6. However, for most applications, the simpler system shown in figure 7 may be used.

This simplification is made possible by the high degree of isolation between the forward and reverse signals and the relative freedom from reflections in the optical portion of the system.

The stabilizer is of the conjugation type using the nonmodulated turn-around method to generate the return signal. It was breadboarded with individually packaged building blocks such as amplifiers, mixers, low pass filters and operational amplifiers, and no attempt was made to protect them from normal variations in room temperature.

It has been determined that further improvement in the stability of the distribution system is limited by the noise of the optical transmitters and/or the optical receivers being used. Significant improvements in the stability of these devices should be possible.

If the input frequency is changed by some Δf and the resultant phase change $\Delta\phi$ across the phase shifter is carefully measured, the absolute

time delay of the line can be determined, thus eliminating the modulo uncertainty. Once this is done the input frequency can be fixed and the phase across the phase shifter will be a precise indication of the time delay down the link. The link can then be used to transfer very accurate timing signals.

Future Plans

Several problems will be given immediate attention. An effort must be undertaken to reduce the noise of the optical transmitters and/or receivers. Of equal importance is the need to better understand the problem of propagation delay versus bending in optical fibers (reference 6).

Single-mode optical fibers appear to be better in nearly every respect to multimode optical fibers for this application, but the problem of coupling light into the $\approx 10 \mu\text{m}$ core must be resolved. An effort is being started in this area at JPL/CIT.

Work will be continued on the development of optical components such as an R.F. optical phase shifter (reference 5) which shifts the phase of the R.F. modulation on the optical carrier. This will further simplify the stabilized distribution link.

Conclusion

The present capability is adequate for many applications but several refinements are needed to achieve our goal of distributing reference frequencies with a stability of 3 parts in 10^{16} , at averaging times greater than 100 seconds, over a distance of 20 km without appreciably degrading them.

- Reference 1 - A personal discussion with P. Clements at JPL, Nov. 1980.
- Reference 2 - A. Rogers, "A Receiver Phase and Group Delay Calibrator for Use in Very Long Baseline Interferometry," Haystack Observatory Technical Note 1975-6.
- Reference 3 - J.W. MacConnell, R.L. Sydnor, "A Microwave Frequency Distribution Technique for Ultrastable Standard Frequencies," The JPL Deep Space Network Progress Report, 42-28, pp. 34-41, Jet Propulsion Laboratory, Pasadena, Ca., Aug. 15, 1975.
- Reference 4 - G. Lutes, "A Transmission Line Stabilizer," The Deep Space Network Progress Report, 42-51, pp. 67-74, Jet Propulsion Laboratory, Pasadena, Ca., June 15, 1979.
- Reference 5 - K.Y. Lau, "A Voltage-Controlled Optical Radio Frequency-Phase Shifter," The Deep Space Network Progress Report 42-53, pp. 24-32, Jet Propulsion Laboratory, Pasadena, Ca., Oct. 15, 1979.
- Reference 6 - K.Y. Lau, "Propagation Path Length Variations Due to Bending of Optical Fibers," to be published.

RUN: 82. 2A
TSP: 3. 16
ALLAN VARIANCE
SIGMA (N, T, B, TAU)

N = 2
T = TAU
B = 1 Hz
fo = 100.0 MHz

SA014 - SA06

START: 1720: 07-13-80
END: 0710: 07-14-80
CHANNEL: 1

670

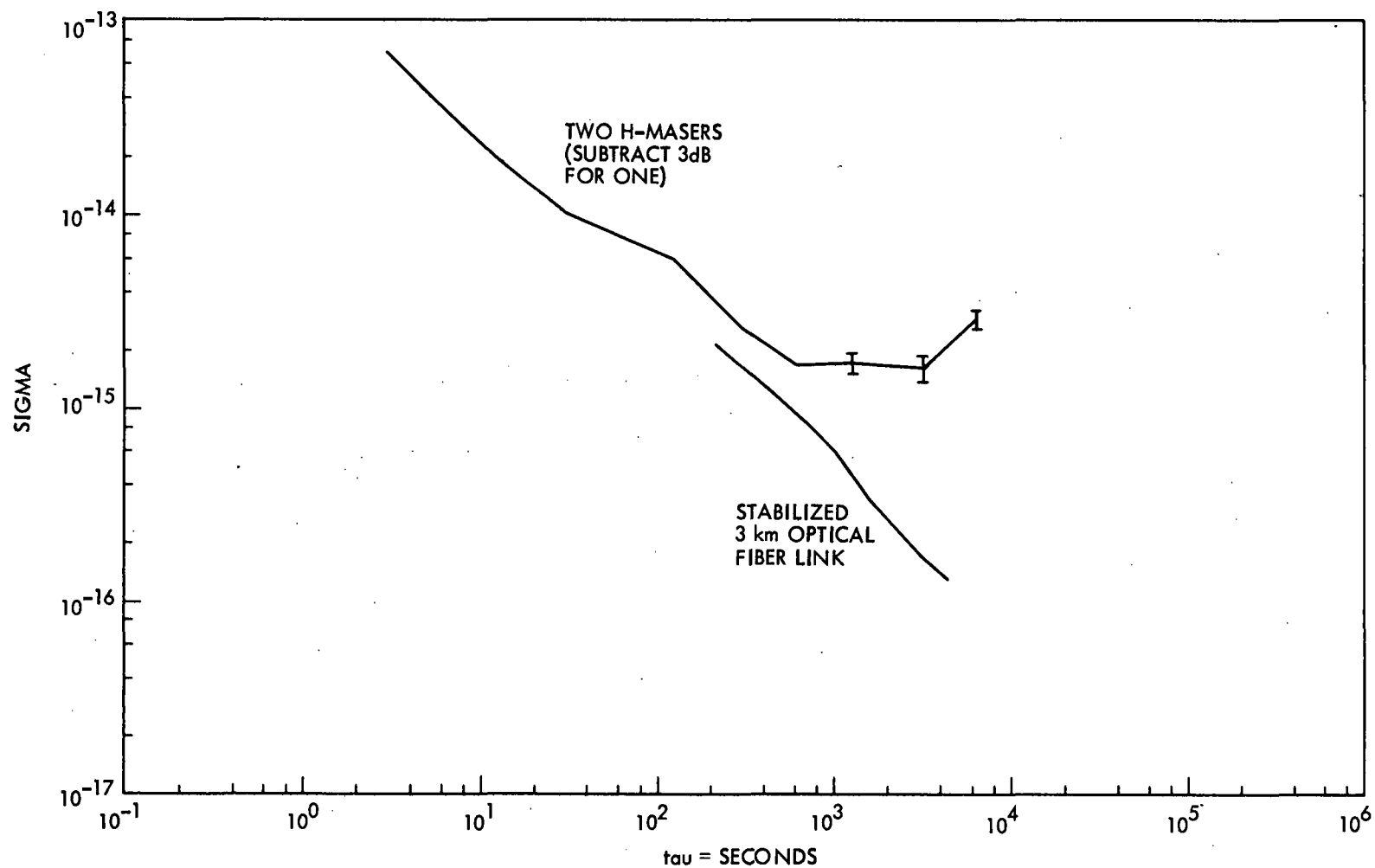


Figure 1. Stabilized Optical Fiber Link Compared to a H-Maser

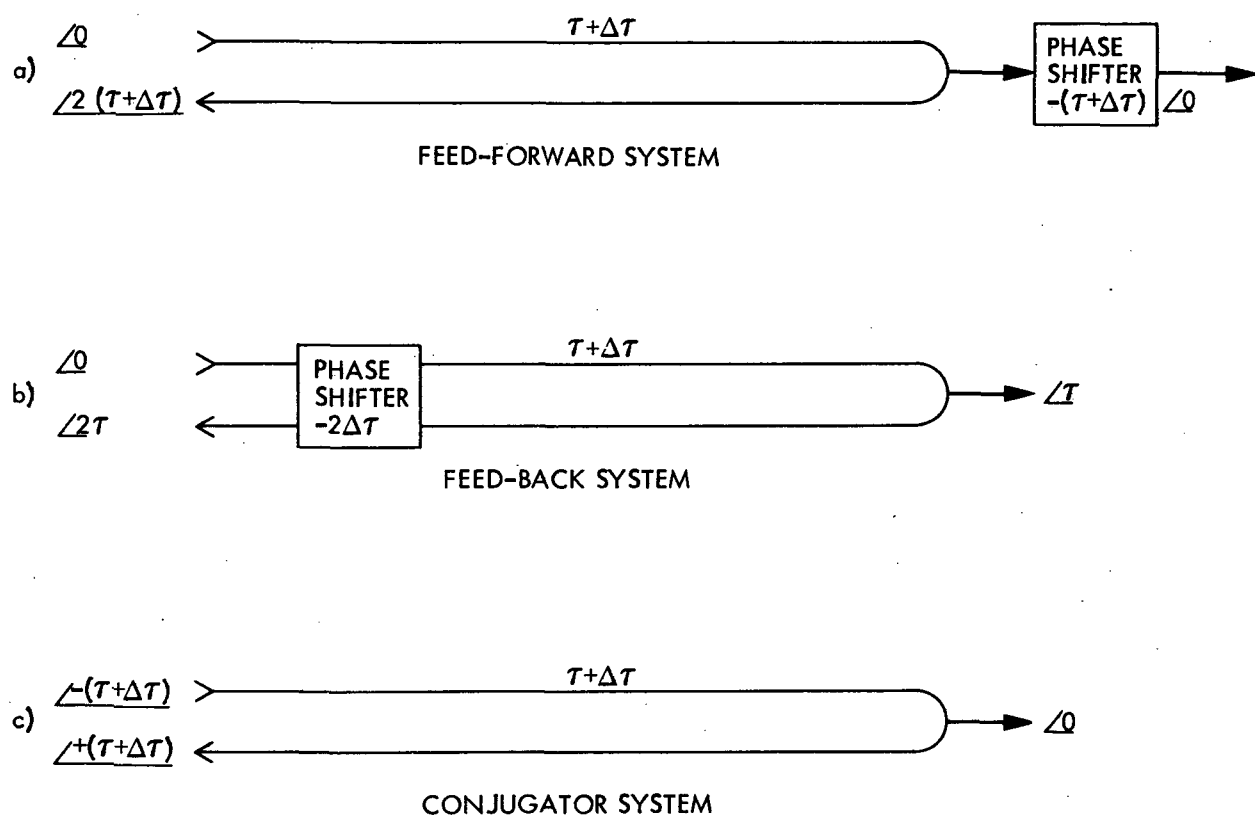


Figure 2. Basic Two Way Transmission Stabilization Systems

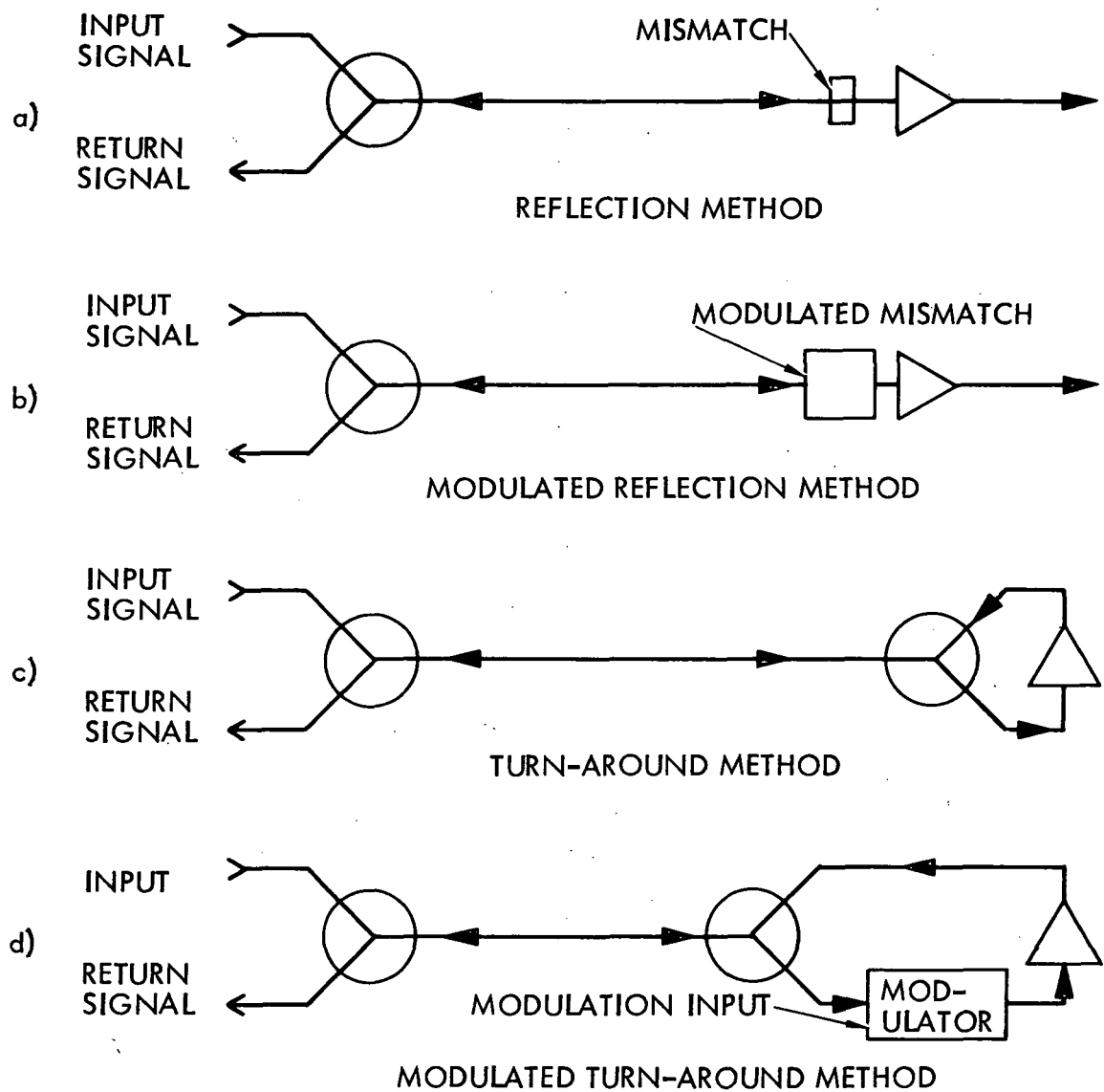


Figure 3. Return Signal Generation Variations

STABILIZED COAXIAL CABLE SYSTEM

673

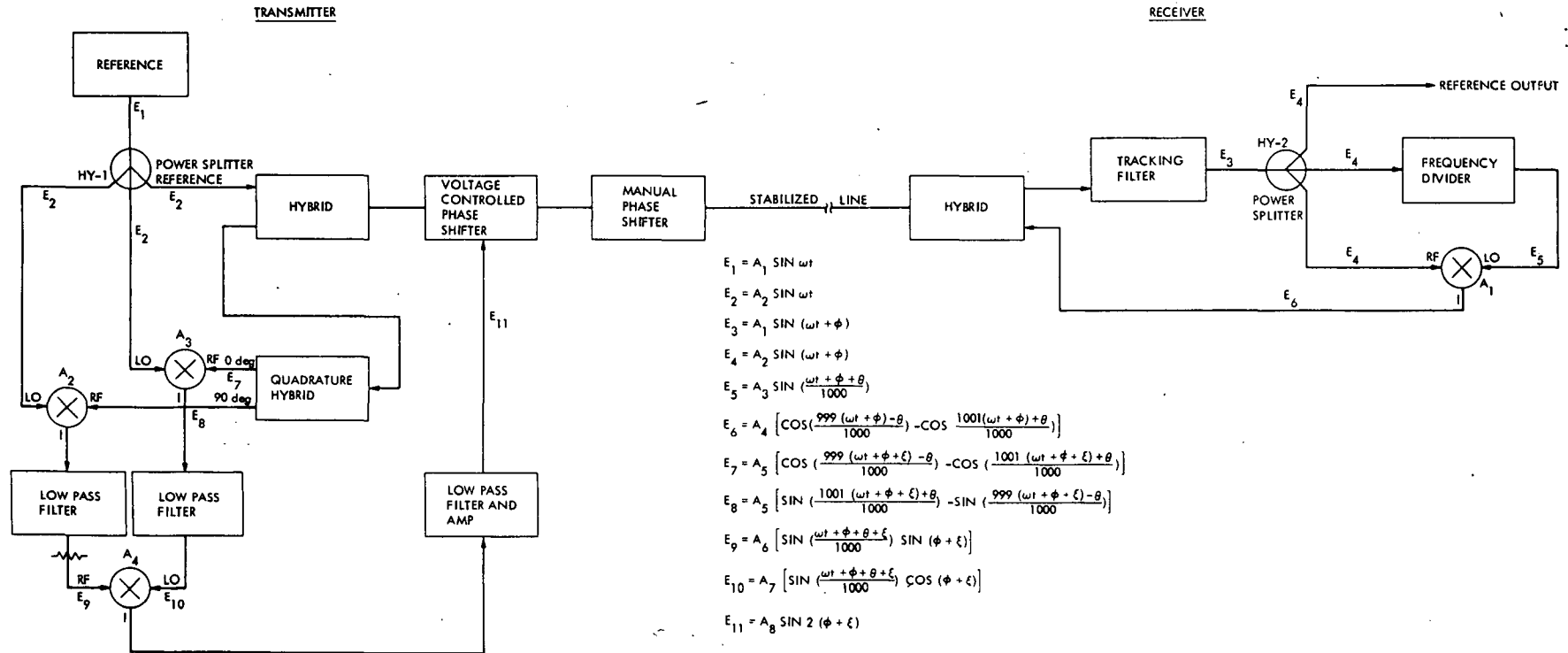


Figure 4. Stabilized Coaxial System

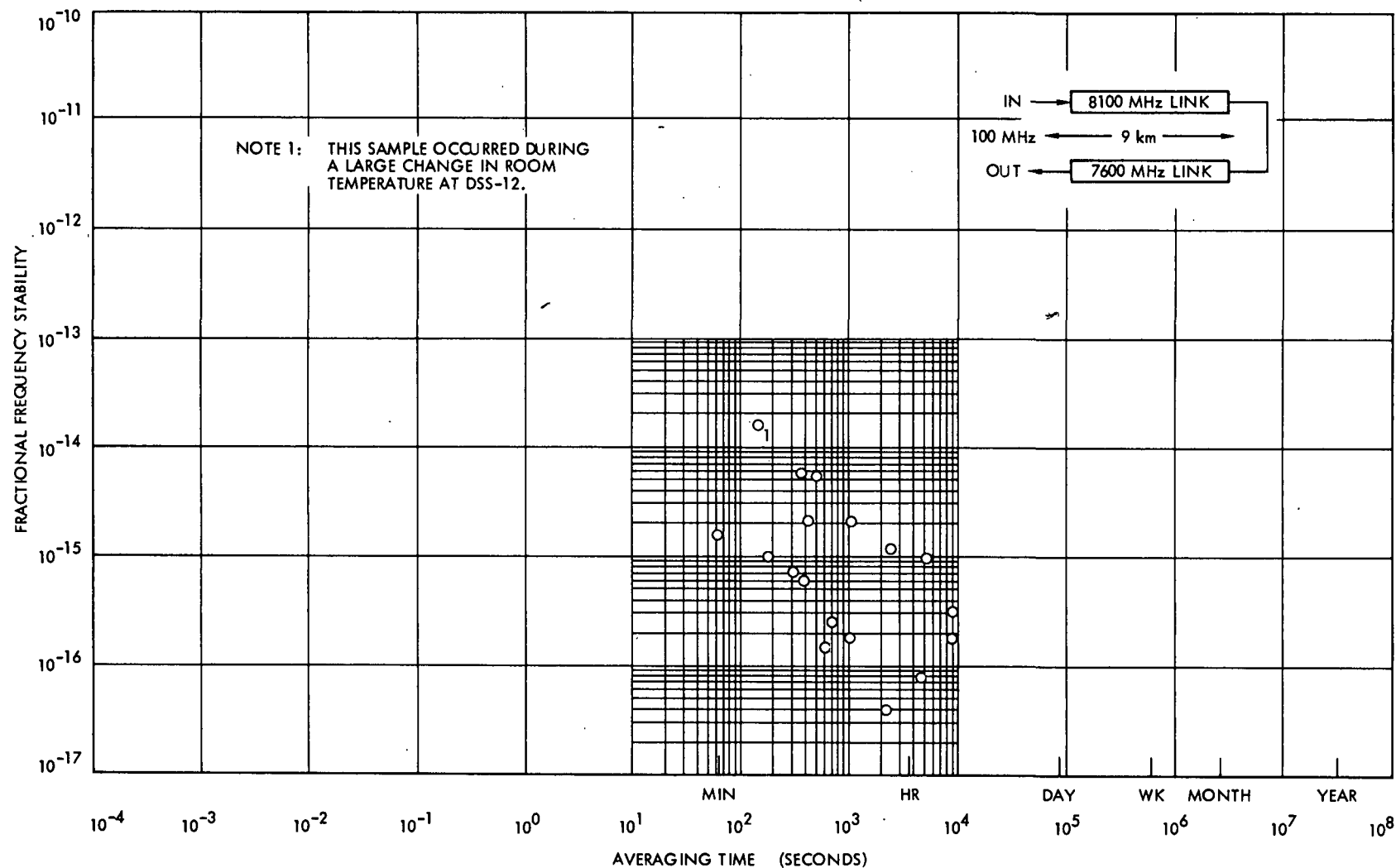


Figure 5. Worst Case Samples of the Fractional Frequency Stability for Two Phase Stabilized Microwave Links Connected in Series Over a Total Distance of 18 km

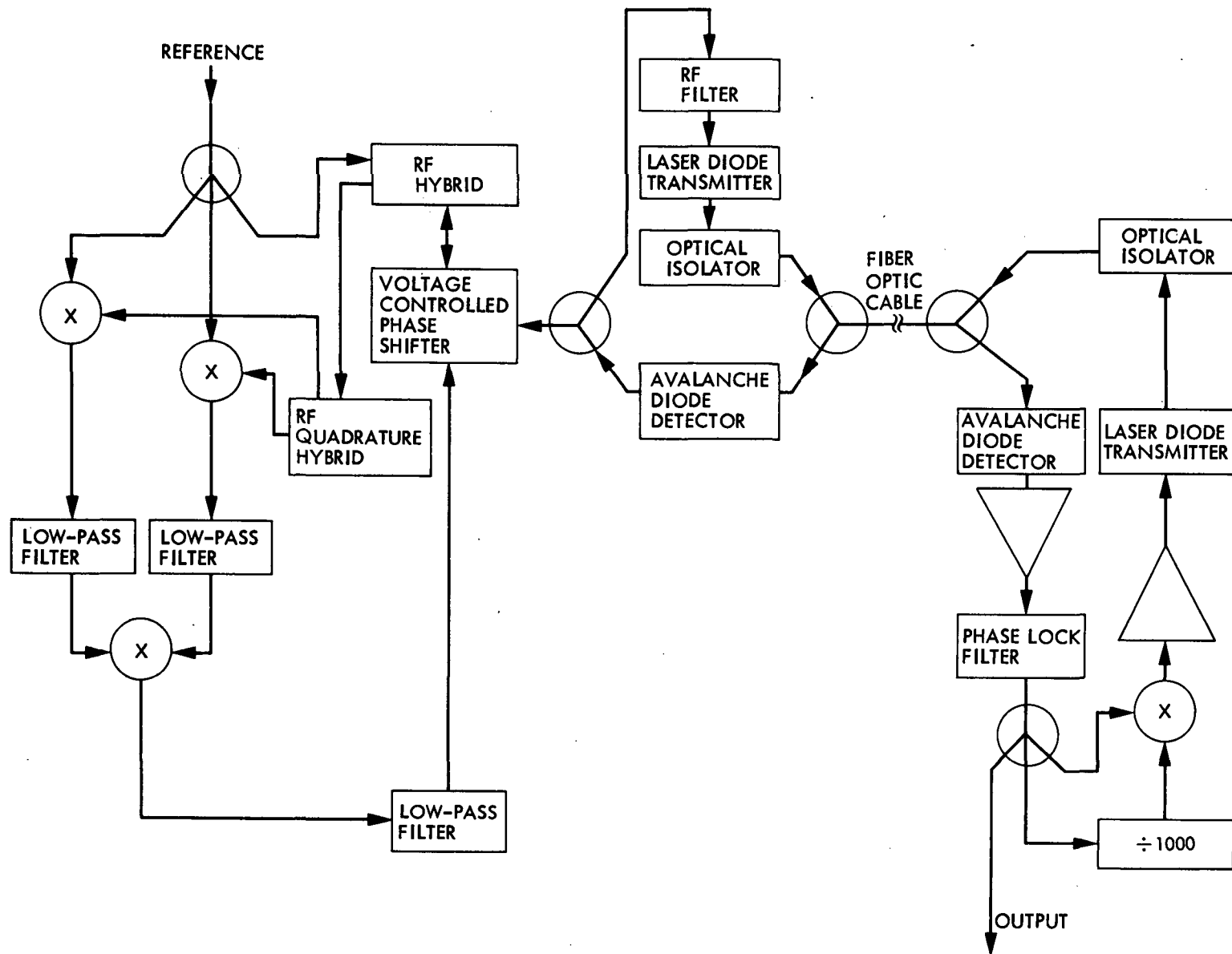


Figure 6. Optical Fiber Implementation of a Stabilized Frequency Dissemination System

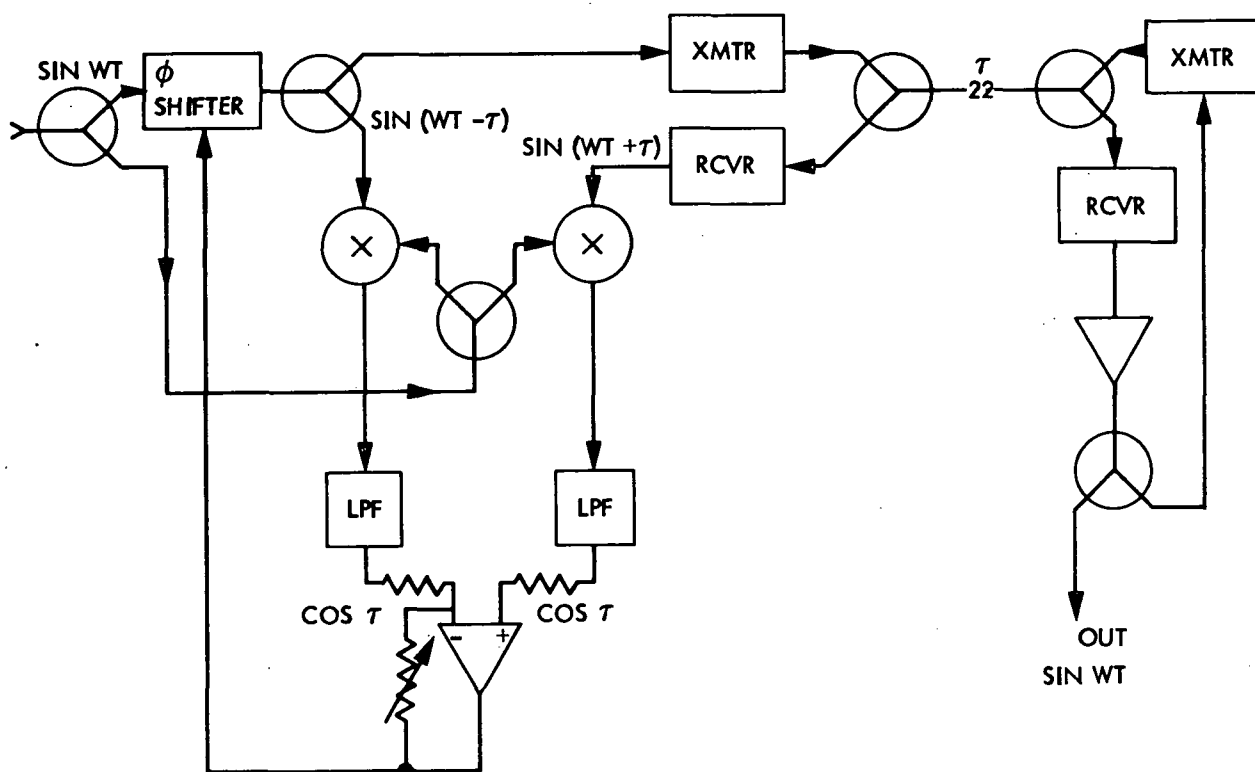


Figure 7. Present 3 km Optical Fiber Stabilized Distribution Link

QUESTIONS AND ANSWERS

DR. VICTOR REINHARDT, NASA/Goddard

What are you achieving with the optical fibers?

DR. LUTES:

We are achieving the curve shown in the second viewgraph. Why don't we show that again?

This curve is the stability we are achieving at the present time. That stability is limited right now since changes in the one-way signal path due to the optical transmitter and/or receivers are compensated by a factor of two. They are causing the limit at the present time.

Improvements in those devices should improve this considerably.

DR. REINHARDT:

What is that about?

DR. LUTES:

This is 225 seconds sampling interval, which is about four parts in 10^{15} . Down here is 4,000 seconds, somewhere around a part in 10^{16} .

PROFESSOR LESCHIUTTA:

We have established a more simple system in my laboratory but we are plagued with the problem of reliability of transmitting diodes. What is your experience of the useful life of the transmitting diodes? Thank you very much.

DR. LUTES:

We have had no failures in transmitting diodes. We had some failures in the receivers which are state-of-the-art receivers as far as bandwidth goes, probably not as far as noise goes though. The laser diodes are guaranteed for 10,000 hours mean time between failure. They are expected to last much longer than that. The projected life is well over 50,000 hours mean time between failures.

PROFESSOR CARROLL ALLEY, University of Maryland

Have you had any experience in transmitting ultra short pulses of light over these optical fibers for strictly timing comparisons?

DR. LUTES:

Yes, we have run some experiments where we transmitted pulses that were about 30 picoseconds in width over short distances, but not over this particular length. That is as short a pulse as we can resolve with our receiver.

PROFESSOR ALLEY:

What kind of spreading did you observe? You mentioned one nanosecond dispersion over a kilometer. Is that an observed quantity?

DR. LUTES:

We haven't transmitted these over a line length of that distance so we don't know. We would expect from the experience we have that it is somewhere very close to one nanosecond or better for a kilometer. Actually, for very long lines it gets better than that. Most of the dispersion takes place in the first kilometer. Then, after that, it gets somewhat better.

PROFESSOR ALLEY:

I might comment for the possible interest of the group that we have recently been transmitting 100 picosecond pulses over a 25 kilometer distance without fibers using a mirror upon the Washington Cathedral and one on a water tower near Goddard in order to compare times between the Goddard Optical Research site and the Naval Observatory.

We are hoping for a 100 picosecond resolution in this system once it is completely worked out. Thank you.

DR. LUTES:

Yes, we have done some work in the area determining how long the propagation delay on these lines are. One way of getting rid of the module ambiguity is to change the frequency slightly and measure the phase. This we can do very well with the measuring techniques that have been developed.

Once we get rid of the module of ambiguity, then we can just look at the phase of the error and further resolve the length of the line. We can resolve the length of the line in this case to about a picosecond for a three kilometer system.

DR. BOB COATES, NASA/Goddard

I am interested in the performance of optical connectors in such a fiber length. Did your link have connectors in it and what are their stability?

DR. LUTES:

For the link that we showed here, most of the connections were welded connections. We have 11 welded connections and two connectors. The only place that we use connectors in this link are at the receivers. The reason that we can get away with it there is that the detector area is fairly large compared to the core diameter of the optical fiber so that the alignment is not very critical. Everywhere else we use welded connections, and the average loss (we haven't measured the actual loss at the connectors because there is some difficulties involved in doing it on short pieces of fiber) is less than half a dB per splice.

It is probably more like a tenth of a dB or less.

DR. TOM CLARK, NASA/Goddard

You alluded to information on the performance of these fibers under bending and that one is our concern, too, because many of the applications do require you to be able to bend cables. Could you comment on that?

DR. LUTES:

With multi-mode fibers, there appears to be a problem with bending and this problem can result in the phase propagation in the two directions on the line not being reciprocal. Therefore, these systems will not cancel that kind of a difference.

We suspect this is not true for single mode fibers, although we haven't actually made measurements to validate this. We are somewhat worried about this problem, also.

VOICE:

At what frequencies?

DR. LUTES:

You can see about two degrees at 100 megahertz for short-bending radiuses of three or four centimeters. It is very obvious when you do bend the fiber; it is more sensitive toward the receivers

of the fiber than it is further away. This is because of the way that this effect occurs. It is a moding effect and once the moding stabilizes, the effect is no longer there and the line becomes reciprocal. So any bends within one kilometer from the transmitter of multi-mode fiber is a problem.

However, we suspect it is not with single mode fiber because there are no other modes to add to the phase or subtract from phase.

ON ESTIMATING THE EFFECTS OF CLOCK INSTABILITY
WITH FLICKER NOISE CHARACTERISTICS*

Sien-Chong Wu
Jet Propulsion Laboratory
California Institute of Technology
Pasadena, CA 91109

ABSTRACT

Clock instability is an error source to high-precision radio metric and radio interferometric observations. Under most circumstances, such observations take place over a period of time within which modern precision clocks reveal a fluctuation characterized by a flicker noise. An undesirable property of flicker noise is the correlation among all observations, with hopelessly complicated correlation coefficients. This complication prohibits one from treating flicker noise as random noise in covariance analysis estimating its effects. This paper introduces two alternative approaches. The first is that of generating a sequence of number simulating the flicker noise and then treating it as a systematic error. A scheme for flicker noise generation is given. The second approach is that of successive segmentation: A clock fluctuation is represented by 2^N piecewise linear segments and then converted into a summation of $N+1$ triangular pulse train functions (TPTF). The statistics of the clock instability are then formulated in terms of two-sample variances at $N+1$ specified averaging times. The summation converges very rapidly that a value of $N > 6$ is seldom necessary. An application to radio interferometric geodesy shows excellent agreement between the two approaches. Limitations to and the relative merits of the two approaches are discussed.

*This paper presents the results of one phase of research carried out at the Jet Propulsion Laboratory, California Institute of Technology, under Contract No. NAS7-100, sponsored by the National Aeronautics and Space Administration.

INTRODUCTION

The developments of advanced technology in radio metric observations for space navigation (Refs. 1, 2) and in radio interferometric observations (Refs. 3, 4) have been in a high gear during the last decade. Among the error sources limiting the precision of these observations is the instability in time and frequency standards. The estimation of the effects of such clock instability is becoming a vital part in system designs.

For a short averaging time, τ , most precision atomic clocks possess a two-sample variance (Allan variance) of frequency fluctuation, σ_y^2 , which decreases as τ^{-2} or τ^{-1} . In other words, the fluctuation behaves either as a white phase noise or as a white frequency noise. When one estimates the effects of such clock instability via a covariance analysis with phase (or delay) observables, a white phase noise can be treated as a random process with no correlation among observations. A white frequency noise can be treated in the same way except that all observations are correlated, with simple correlation coefficients. Hence such clock instabilities can be handled without difficulties.

However, most radio metric and radio interferometric observations take place over a longer period of time within which a clock fluctuation reaches its "flicker floor", having a constant two-sample variance over all averaging times of interest. Such flicker noise has the undesirable characteristic of complicated correlation among all observations, especially when observations are taken at uneven intervals of time. Direct covariance analysis is generally impractical.

This paper introduces two alternative approaches. In the first approach, a sequence of numbers simulating flicker noise is generated over the time period of interest. Its effects can then be treated as that of a systematic error, with the error sensitivity defined by the sequence of numbers. The second approach is that of a successive segmentation: The statistics of a clock fluctuation are represented by the amplitudes of a number of triangular pulse train functions (TPTF). These amplitudes are, in turn, related to the two-sample variances at successively halved averaging times. The problem is thus reduced to that of estimating the effects of a number of (usually not more than 7) TPTF with specific RMS amplitudes.

Examples are given for an application to baseline vector determination by radio interferometry. The numerical results show excellent agreement between the two approaches. Limitations to and the relative merits of these two approaches are discussed.

CLOCK INSTABILITY CHARACTERIZED BY $\sigma_y^2 \propto \tau^{-2}$ and $\sigma_y^2 \propto \tau^{-1}$

For convenience in investigating the effects of clock instability, we shall briefly review the basis of covariance analysis. Let there be M independent phase observations from which N_p parameters are to be estimated. The "computed covariance matrix" is given by

$$P_x = (A^T W A)^{-1} \quad (1)$$

where A is an $M \times N_p$ sensitivity matrix with the $(m,n)^{th}$ element being the partial derivative of the m^{th} observation with respect to the n^{th} estimated parameter; W is usually a diagonal weighting matrix with elements ϵ_m^{-2} where ϵ_m is the assumed RMS random error of the m^{th} observation. The diagonal elements of P_x in (1) are the variances of the estimated parameters due to the assumed random error in observations.

The effects of an error source different from the assumed random errors can be calculated by the following "consider covariance matrix" (Ref. 5)

$$P'_x = (P_x A^T W) P_c (P_x A^T W)^T \quad (2)$$

where P_c is the error covariance matrix of the M observations.

For a clock instability characterized by a two-sample variance $\sigma_y^2(\tau) \propto \tau^{-2}$, its effects on the M observations are the same as that of an uncorrelated random error with a standard deviation $\tau\sigma_y(\tau)$. Thus P_c in (2) becomes a unity matrix multiplied by a constant $\tau^2\sigma_y^2(\tau)$. The effects on the estimated parameters are given by the square roots of the diagonal elements of P'_x .

For a clock instability characterized by a two-sample variance $\sigma_y^2(\tau) \propto \tau^{-1}$, its effects on the m^{th} phase observation is the accumulation of phase, from the beginning of the experiment, due to a white frequency noise. That is, the error covariance matrix P_c will have elements

$$p_{m,n} = \tau\sigma_y^2(\tau) \sum_{i=1}^{\min(m,n)} (t_i - t_{i-1}) \quad (3)$$

$$= \tau\sigma_y^2(\tau) [t_{\min(m,n)} - t_0]$$

where

$$\min(m,n) = \begin{cases} m, & \text{if } m \leq n \\ n, & \text{if } n \leq m \end{cases} \quad (4)$$

t_0 is the epoch of the experiment and t_i is the mean time at which the i^{th} observation is taken. With P_c calculated by (3) and (4), the effects of such clock instability on the estimated parameters are again given by the square roots of the diagonal elements of P'_x in (2).

SIMULATION OF CLOCK INSTABILITY CHARACTERIZED BY $\sigma_y^2 \propto \tau^0$

A clock fluctuation characterized by a constant two-sample variance independent of averaging time is said to behave as a flicker noise. It has strong correlation among observations. To the knowledge of the author no exact expression exists for the error covariance of observations due to such noise. A close approximation can be derived from the following flicker noise model of Barnes and Allan (Ref. 6):

$$\phi_m = \sum_{i=1}^m (m+1-i)^{2/3} g_i \quad (5)$$

This model simulates equally spaced (in time), discrete flicker noise from a sequence of independent, random numbers g_i (or discrete white phase noise) of unity variance. For observations taken at even time intervals Δt , the error covariance matrix P_c will have elements

$$\begin{aligned} p_{m,n} &= (\Delta t)^2 \sigma_y^2 \langle \phi_m \phi_n \rangle \\ &= (\Delta t)^2 \sigma_y^2 \sum_{i=1}^{\min(m,n)} (m+1-i)^{2/3} (n+1-i)^{2/3} \end{aligned} \quad (6)$$

where $\langle \rangle$ denotes the ensemble average and $\min(m,n)$ is defined in (4). For observations taken at uneven time intervals $I_m \Delta t$, the elements of matrix P_c become

$$p_{m,n} = (\Delta t)^2 \sigma_y^2 \sum_{i=1}^{\min(k_m, k_n)} (k_m+1-i)^{2/3} (k_n+1-i)^{2/3} \quad (7)$$

$$\text{with } k_m = \sum_{j=1}^m I_j \quad (7a)$$

Therefore, the calculation of the elements of P_c becomes complicated and impractical.

An alternative approach is to simulate the clock instability in the time period of interest by a flicker noise model, such as that given in (5), and then treat it as if it were a systematic error. (However, statistical results can be obtained only through averaging an ensemble of such errors. This will be further discussed later). In other words, the P_c in (2) is decomposed into CC^T where C is a column matrix with its M elements given by

$$\epsilon_m = \Delta t \sigma_y \phi_{k_m} \quad (8)$$

for observations at uneven time intervals $I_m \Delta t$. Here ϕ_{k_m} is defined in (5) and (7a).

Equation (8) suffers from the disadvantage of having to record a very large number of random samples g_i and to perform a very large number of summations. A computationally more efficient flicker noise model can be generated by the following empirical recurrence formula (for $\sigma_y = 1$):

$$\begin{aligned} \phi_m &= 1.95 \phi_{m-1} - 0.95 \phi_{m-2} \\ &+ \sum_{i=1}^{100} i^{0.6} g_{m+1-i} - 1.95 \sum_{i=1}^{99} i^{0.6} g_{m-1-i} \\ &+ 0.95 \sum_{i=1}^{98} i^{0.6} g_{m-1-i} \end{aligned} \quad (9)$$

where g_i are now random numbers of standard deviation 1.35.

To compare the two flicker noise models, eq. (5) and eq. (9), 4001 samples are computed from each model. Two-sample variances are calculated and plotted in Fig. 1. The $\sigma_y^2 \propto \tau^\alpha$ behavior is verified for both models with the recurrence formula of (9) being slightly better. Note that for larger τ the number of samples in the calculation of σ_y is smaller and the uncertainty of σ_y is larger. With the flicker noise model given in (9), the solution covariance matrix P'_x can be calculated from (2) with $P_c = CC^T$; the elements of the column matrix C are

$$\epsilon_m = \Delta t \sigma_y \phi_{k_m} \quad (10)$$

with k_m defined by (7a).

SEGMENTATION OF CLOCK INSTABILITY

In this section, the effect of clock instability is studied by an alternative approach. It is clear that a clock instability characterized by $\sigma_y^2(\tau) \propto \tau^\alpha$ with $\alpha \geq -1$ will have a cumulative effect. Hence, a clock with instability behaving differently from a white phase noise will appear as clock drift. Such clock drift in the time period of interest, say $0 < t < T$, can be approximated by a piecewise linear representation as shown in Fig. 2 (a) and (b). The number of segments can be arbitrary; however, for the convenience of the following study, it is selected to be 2^N . Fig. 2 (b) is a special case of $N = 4$.

The piecewise linear representation of a clock drift can further be decomposed into the summation of a sequence of $N + 1$ triangular pulse train functions (TPTF), F_n :

$$\text{Drift}(t) = \sum_{n=0}^N F_n(b_{n,1}, b_{n,2}, \dots, b_{n,2^{n-1}}; t) \quad (11)$$

where F_n contains 2^{n-1} triangular pulses of widths $T/2^{n-1}$ and of heights $b_{n,1}, b_{n,2}, \dots$, and $b_{n,2^{n-1}}$ (for $n = 0$, F_n contains half a triangular pulse of height b_0). Fig. 2 (c) displays the component terms of (11). Therefore, a given clock drift functions which is

approximated by 2^N piecewise linear segments is uniquely defined by 2^N heights of triangular pulses. Since these TPTF are independent of and uncorrelated with one another their total effect is the quadratic sum of individual effects. That is,

$$\text{Effect of Drift } (t) = \left[\sum_{n=0}^N F_n^2 (b_{n,1}, \dots, b_{n,2^{n-1}}; t) \right]^{1/2} \quad (12)$$

The RMS values of $b_{n,m}$ are related to the two-sample variances σ_y^2 by the definition of σ_y^2 :

$$\sigma_y^2 (T/2^n) = \frac{1}{2} \left\{ \frac{2b_{n,i}}{T/2^n} \right\}^2, \quad n \neq 0 \quad (13)$$

where $\{\}$ denotes the RMS value. Hence all triangular pulses in the same TPTF have the same RMS height which is directly related to σ_y^2 at a specified averaging time:

$$\{b_{n,i}\} = \{b_n\} = (\sqrt{2}/2) (T/2^n) \sigma_y (T/2^n), \quad n \neq 0 \quad (14)$$

$$\text{For } n = 0, \{b_0\} = T \sigma_y (T) \quad (14a)$$

Therefore, the RMS effect of clock instability with known $\sigma_y(\tau)$ for $T/2^N < \tau < T$ can be represented by the superposition of TPTF of specific RMS heights. Only terms with $T/2^n$ longer than the shortest time interval between observations need be included in (12). For instance, a 12-hour experiment with a minimum time interval of 10 minutes between observations requires only 7 TPTF, with the last term containing $T/2^6$. Furthermore, for $\sigma_y^2 \propto \tau^0$ (flicker noise), eq. (12) converges very rapidly; neglecting all but the first three terms will result in an error of less than 1%.

In most radio metric observations for space navigation, the estimated parameters are the amplitudes of diurnal sinusoidal functions (Ref. 2). Hence, over a view period of 8 hours or shorter, the error signature can be divided into three categories: A bias error (approximating $\cos x$ with small x), a ramp error (approximating $\sin x$ with small x) and a random error. On the other hand, radio interferometric observations for clock synchronization, baseline vector determination, polar motion/UT1 determination, etc. are taken "randomly" on many different radio sources. It is such randomness that loosens the coupling between systematic error sources and estimated parameters. However, for such "random" observations, the error sources can also be divided into bias, ramp and random errors.

The RMS values of bias, ramp and random components of TPTF are calculated in the appendix. The values for the first 7 TPTF are summarized in Table I. Since these components are independent and uncorrelated the quadratic sum of their effects yields the effects of the TPTF. Also, as mentioned earlier, the TPTF are independent of and uncorrelated with one another. Hence, the magnitudes of errors of the same categories (bias, ramp and random) from all TPTF can be quadratically summed together, the effects of which are then individually estimated. Therefore, the estimation of clock instability effects is reduced to the estimations of the effects of a bias error, a ramp error and a random error (white phase noise) which are trivial.

NUMERICAL EXAMPLES

To illustrate and compare the two approaches introduced above, they are applied to a problem of baseline vector determination by radio interferometry. The baseline chosen is 300 km in length with its center at a latitude of 35° North. Both 6-hour (33-observation) and 8-hour (44-observation) experiments are studied. The observation sequences are parts of a 30-hour sequence observing 14 extragalactic radio sources. To reduce the effects of observation sequence, each of the 6-hour and 8-hour time periods scans through the 30-hour sequence and the mean error is calculated from all possible 6-hour or 8-hour periods. The error source considered is a clock instability with $\Delta f/f = 10^{-14}$ for all τ on each end of the baseline, thus $\sigma(\tau) = \sqrt{2} \times 10^{-14}$. A unity matrix is chosen as the weighting matrix, W . The quadratic sum of the baseline component errors is to be examined.

In practice, one or more clock parameters can be included in the estimated parameter list to reduce the effects of clock instability (Ref. 7). In the following, we shall study the problem under different circumstances: Estimating 3 baseline components alone, 3 baseline components and a clock offset, and all the preceding plus up to 8 equal segments of clock rate offset. It should be noted that when 2^m segments of clock rate offset are to be estimated, the effects of F_n for $n \leq m$ are to be excluded.

Table II summarizes the baseline solution sensitivities to a bias error, a ramp error and a white phase noise. These sensitivities are to be used in the segmentation approach: The effects of clock instability are to be determined by (i) calculating the RSS values of bias, ramp and random components, according to (14) and Table I, from all TPTF of concern, (ii) multiplying by the corresponding baseline error sensitivities in Table II, and (iii) quadratically summing these three error components.

Fig. 3 compares the effects of the clock instability on baseline solutions as estimated by simulation approach and by segmentation approach, for both the 6-hour and 8-hour experiments. Excellent agreement between the two approaches is seen.

DISCUSSION AND SUMMARY

Two different approaches have been introduced for the estimation of clock instability effects on radio metric and radio interferometric observations. The simulation approach is straightforward and can be applied to any type of problems; but it requires the simulation of a flicker noise. The statistical characteristics of a flicker noise can be attained only when a large number of samples are included. In the above examples, the 33 and 44 consecutive observations scan through a 30-hour sequence, resulting in, respectively, 128 and 117 different clock instability samples. Hence the mean values of the solution errors approach to their statistical values. Without such averaging the results fluctuate a good deal. Fig. 4 shows such fluctuation of a solution error from the 128 individual samples of 33-observation sequence.

The segmentation approach requires the estimation of the effects of a bias, a ramp and a random noise. The RSS magnitudes of these components from a few TPTF need to be calculated. However, this approach results in statistical values of clock instability effects without the need of averaging over many samples. Also, the segmentation approach is so versatile that clock instability with any shape of $\sigma_y(\tau)$ can be treated since the variation of σ_y is explicitly accounted for (cf. equation 14) in the error estimation procedure.

When a problem with a diurnal variation has a view period exceeding 8 hours, bias and ramp together can no longer represent the systematic error signature. An additional error component, a single triangular pulse, F_1 , with its mean value removed, needs to be considered. This is equivalent to adding a quadratic term into the small-argument approximation of a cosine function. With this modification, the RMS value of the random component for $n=1$ in Table I is to be transferred to the new component. Of course, the random component from F_n with $n > 1$ will still be needed.

APPENDIX

Calculation of RMS values of Bias, Ramp and Random Components of TPTF of Unit RMS Heights

Bias Component:

A sequence of triangular pulses of height +1 has a bias value of +1/2. Since F_0 and F_1 contain no more than one pulse their bias values are simply $\pm 1/2$. For $n > 1$, each pulse in F_n may have an independent sign (+ or -). Since F_n contains 2^{n-1} triangular pulses, each of them has an RMS bias value of $(1/2)(1/2^{n-1}) = 1/2^n$. The RMS value of bias for all pulses in F_n is the quadratic sum of those of all 2^{n-1} pulses. Hence

$$\begin{aligned} \{\text{bias}\} &= [(2^{n-1}) (1/2^n)^2]^{1/2} \\ &= 2^{-(n+1)/2} \end{aligned} \quad (\text{A.1})$$

Ramp Component:

It is readily shown that F_0 , containing one half of a triangular pulse, has a ramp component of RMS value $1/2\sqrt{3}$ and that F_1 , containing one pulse, has no ramp component. For F_n with $n > 1$, the triangular pulses can be grouped into symmetrical pairs (with respect to the center of the time period). A pair of pulses with the same signs (++ or --) does not contribute to ramp component. A pair with opposite signs (+- or -+) has a ramp component of heights $\pm 3m/2^{2n-2}$ where m is the separation between the two pulses of the pair ($m = 1, 3, \dots, 2^{n-1} - 1$). The RMS value of such ramp component is $1/\sqrt{3}$ its height, i.e., $(3m/2^{2n-2})(1/\sqrt{3})$. The probability of forming a pair of pulses with opposite signs is 1/2 (the other 1/2 for pulses with the same signs). Hence the RMS value of the ramp component of all 2^{n-2} pairs of pulses in F_n is given by

$$\begin{aligned} \text{ramp} &= \left[\sum_{m=1,3,\dots}^{2^{n-1}-1} \left(\frac{1}{2} \right) (3m/2^{2n-2})^2 (1/\sqrt{3})^2 \right]^{1/2} \\ &= \left[\left(\frac{1}{2} \right) (3/2^{4n-4}) \sum_{m=1,3,\dots}^{2^{n-1}-1} m^2 \right]^{1/2} \end{aligned}$$

$$\begin{aligned}
&= [(3/2)^{4n-3} (2^{3n-4} - 2^{n-2}) / 3]^{1/2} \\
&= [2^{-(n+1)} - 2^{-(3n-1)}]^{1/2}
\end{aligned}
\tag{A.2}$$

Random Component:

The total RMS value of F_n is the same as that of a single triangular pulse, $1/\sqrt{3}$. With the bias and ramp component given by (A.1) and (A.2) the RMS value of the random component of F_n is simply

$$\{\text{Random}\} = (1/3 - \{\text{bias}\}^2 - \{\text{ramp}\}^2)^{1/2}
\tag{A.3}$$

References:

1. D.W. Curkendall, "Radio Metric Technology for Deep Space Navigation: A Development Overview", paper presented at the AIAA/AAS Astrodynamics Conference, Palo Alto, Calif, August 7-9, 1978.
2. W.G. Melbourne and D.W. Curkendall, "Radio Metric Direction Finding: A New Approach to Deep Space Navigation", paper presented at the AAS/AIAA Astrodynamics Specialist Conference. Jackson Hole, Wyoming, September 7-9, 1977.
3. C.C. Councilman, III, "Very-Long Baseline Interferometry Techniques Applied to Problems of Geodesy, Geophysics, Planetary Science, Astronomy, and general Relativity", Proc. IEEE. vol. 61. No. 9. September 1973. pp. 1225 - 1230.
4. K.M. Ong, et. al., "A Demonstration of a Transportable Radio Interferometric Surveying System with 3-cm Accuracy on a 307-m Baseline", J. Geophy. Res., vol. 81, Nov. 20, July 1976. pp. 3587 - 3593.
5. G.J. Bierman, Factorization Methods for Discrete Sequential Estimation, Academic Press. 1977. Chapter 8.
6. J.A. Barnes and D.W. Allan, "A Statistical Model of Flicker Noise", Proc. IEEE, vol. 54, No. 2, February 1966. pp. 176 - 178.
7. P.F. MacDoran, et. al., "Radio Interferometric Geodesy Using a Rubidium Frequency System", Proc. 7th Annual PTTI Applications and Planning Meeting, Greenbelt, Md., December 1975, pp. 439-454.

TABLE 1

RMS Values of Bias, Ramp and Random Components
of TPTF of Unit RMS Heights*

n	{Bias}	{Ramp}	{Random}
0	0.500	0.289	0
1	0.500	0	0.289
2	0.354	0.306	0.339
3	0.250	0.242	0.461
4	0.177	0.175	0.521
5	0.125	0.125	0.550
6	0.088	0.088	0.564

* A triangular pulse of unit height has a total RMS value of $1/\sqrt{3}$.

TABLE II: Baseline Solution Sensitivity to Observation Errors of Unit RMS Values

T	M	Error Type	$N_p = 3$	$N_p = 4$	$N_p = 5$	$N_p = 6$	$N_p = 8$	$N_p = 12$
6	33	Bias	1.32	0	0	0	0	0
6	33	Ramp	0.55	0.91	0	0	0	0
6	33	Random	0.60	1.05	1.07	1.09	1.11	1.18
8	44	Bias	1.33	0	0	0	0	0
8	44	Ramp	0.48	0.76	0	0	0	0
8	44	Random	0.50	0.89	0.90	0.91	0.93	0.96

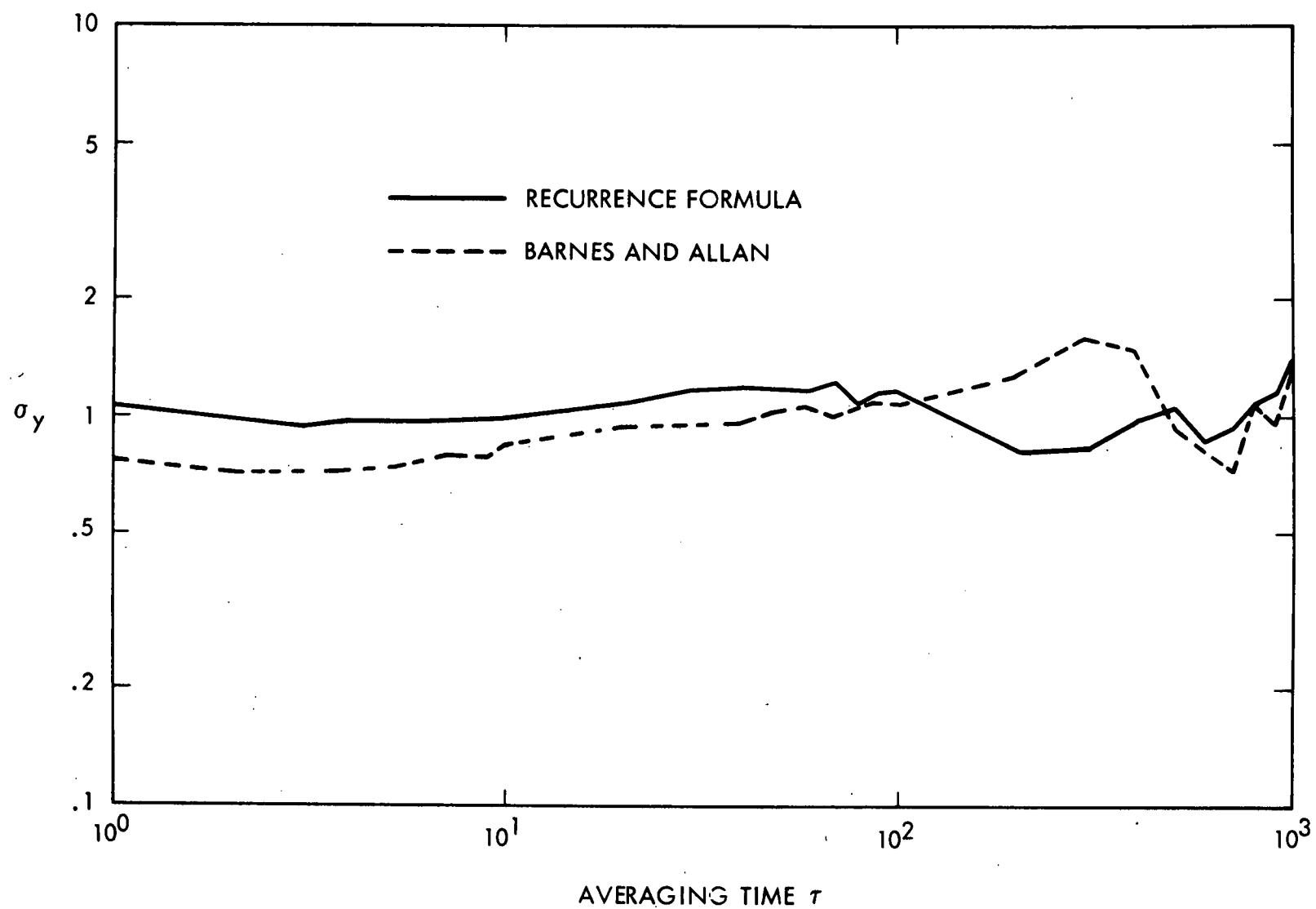
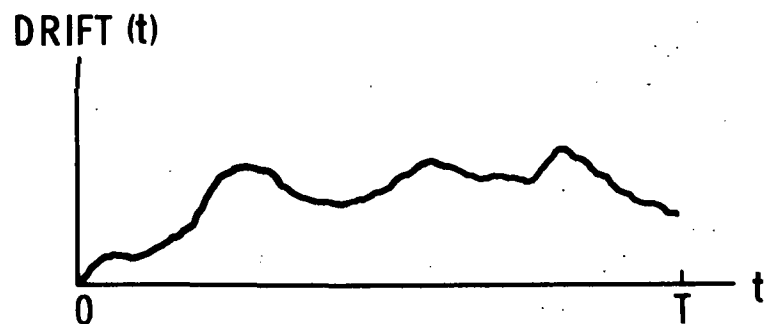
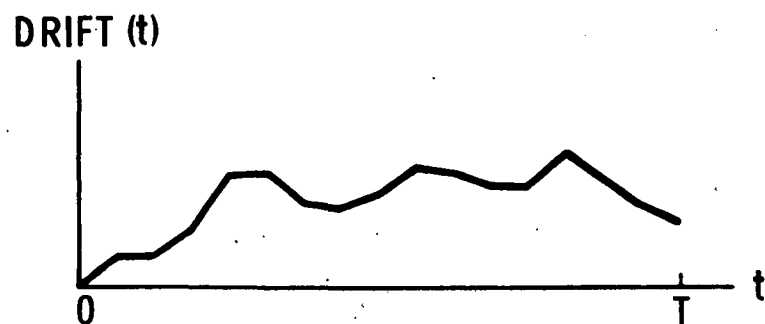


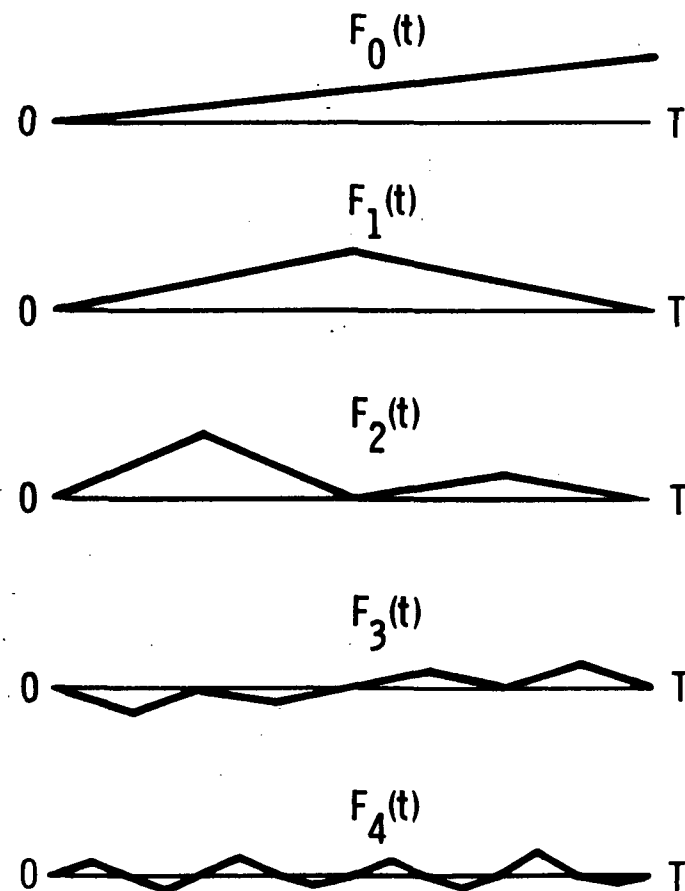
FIGURE 1. TWO-SAMPLE DEVIATIONS OF TWO FLICKER NOISE MODELS



(a) CLOCK DRIFT FUNCTION



(b) PIECEWISE LINEAR REPRESENTATION
OF (a)



(c) COMPONENT TERMS OF (b)

FIGURE 2. SEGMENTATION OF CLOCK INSTABILITY

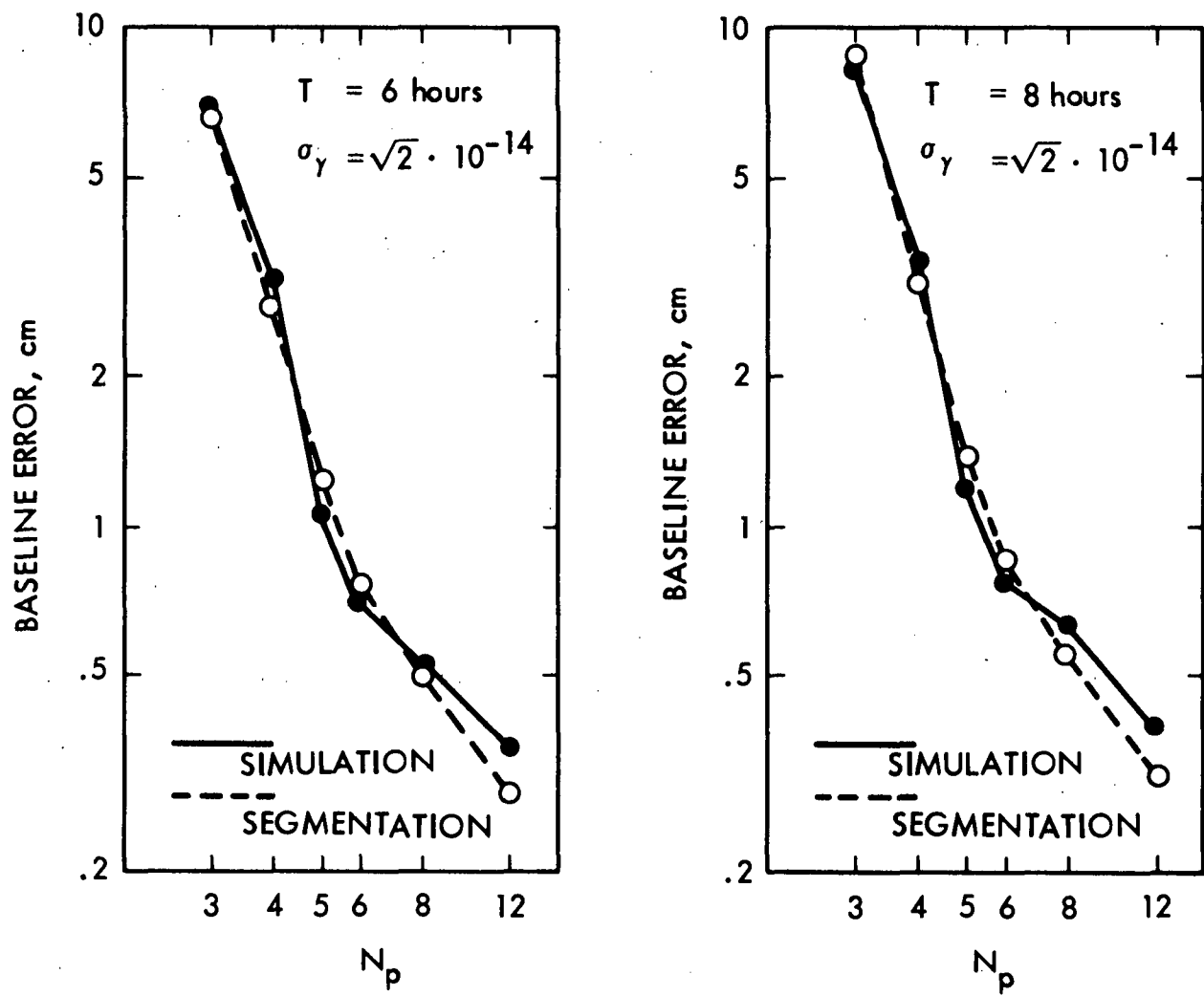


FIGURE 3. INTERFEROMETRIC BASELINE DETERMINATION ERRORS DUE TO CLOCK INSTABILITY

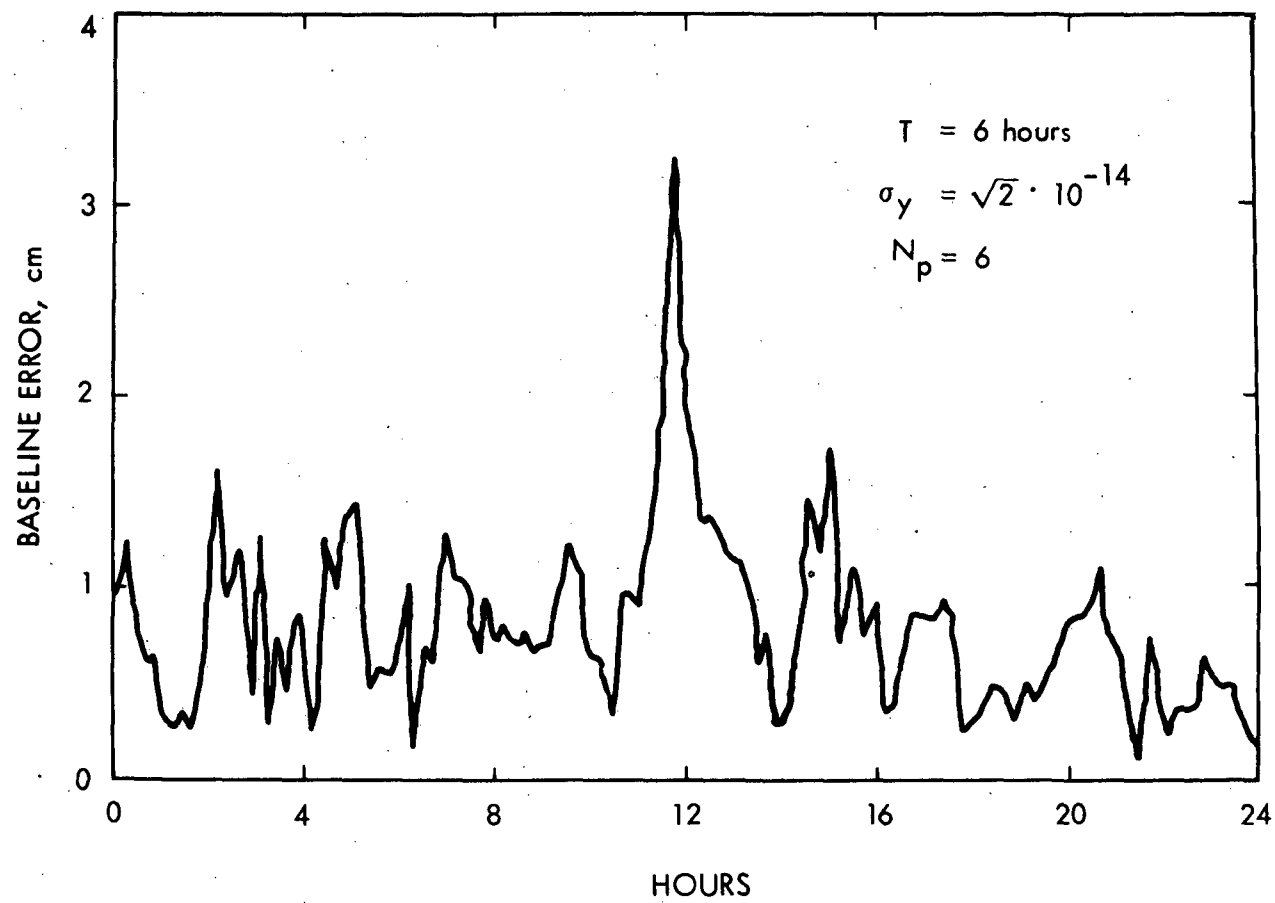


FIGURE 4. FLUCTUATION OF BASELINE ERROR ESTIMATED BY SIMULATION APPROACH

QUESTIONS AND ANSWERS

DR. REINHARDT:

Recent data have indicated over the past couple years that the problem with hydrogen masers or with cesiums too is not really flicker noise. It is a combination of environmental effects and random walk which can be analytically treated much more easily than flicker noise. Have you looked into using those approaches to handling problems of correlation noise in frequency standards?

DR. WU:

Well, of course, flicker noise is just an assumption of clock instability. It is an approximation, but the segmentation approach I was just introducing here can be applied to any sigma versus tau shift. That means it doesn't necessarily have to be a flicker frequency noise.

DR. REINHARDT:

If you use other noise models which are really applicable like random walk of frequency or an environmental effect, they are analytically solvable, while flicker noise presents a lot of computational problems; they do not. And you might get a more fruitful result by using the real models for behavior.

DR. WU:

If the characteristic is purely white phase noise or white frequency noise, you can easily do it with conventional covariance analysis, but whenever there is some combination of these noises or you have some variations in the sigma versus tau shape, then you have difficulty.

DR. PETER KARTASCHOFF, Swiss Post Office

I wonder if in the segmentation approach you used here, what is the statistical uncertainty on these ramp and drift and random components in this approach, because I am asking myself if you just have a statistical uncertainty, if you repeat this process which will be of the same order of magnitude, then the uncertainty you get with the simulation process is mainly according to the theory of Audoin and Lesage?

Whereas, that there might be a danger that the segmentation approach used on limited data would give a too optimistic result, and then if you repeat the same experiment more and more, and

finally you get this very slow convergence to the flicker noise process, and there I would recommend what Victor Reinhardt said, that actually there have been for ten or more years, efforts to turn around the flicker process.

And the combinations of white and random walk rates and so on, but I think we have to live with the fact that the flicker process is here and nature doesn't care about mathematical difficulties; nature is there and the flicker process is there, and for many years we had no physical models on flicker process, but three years ago there was a conference in Tokyo only on flicker phenomenon.

Now, we have about ten models of flicker noise, ten physical models. We just do not yet know which is the good one, but I think we will have to live many years with the problem of flicker. I just would like to make these comments. One should look in this approach you made because it is very interesting in its computational simplicity, but I would say a little bit of warning. What is the real uncertainty? I would bet it will fall back on Audoin's and Lesage's prediction on uncertainty of the estimates. Thank you.

DR. WU:

Of course, what I am introducing here is just a technique to estimate clock instability with a given shape of sigma versus tau shift. So, whether the actual clocks will be right on flicker frequency noise or not is another story.

Page Intentionally Left Blank

NAVSTAR GLOBAL POSITIONING SYSTEM (GPS) CLOCK PROGRAM: PRESENT AND FUTURE

**Capt Douglas M. Tennant
Air Force Systems Command
Space Division/YEZ
Los Angeles, California**

ABSTRACT

The Global Positioning System (GPS), well into its developmental phase, provides the most salient example today of both Rubidium and Cesium Atomic Frequency Standards being applied in a space environment. Indeed, the whole success of the GPS program rides on the performance and reliability of space-qualified atomic clocks. Program status is provided by this paper and plans for ensuring the long-term continuation of the program are presented as well. Performance of GPS clocks is presented in terms of on-orbit data as portrayed by GPS Master Control Station Kalman Filter processing. The GPS Clock Reliability Program is reviewed in depth and future plans for the overall clock program are published.

Introduction

The Navstar Global Positioning System (GPS) was first conceived by Department of Defense planners as the ultimate answer to the question of how to provide precise, continuous, real-time navigation data to friendly military forces deployed world-wide. With passive equipment, the user, it was planned, would merely "dial-up" the several satellites in his view and know directly, with practically "pin-point" accuracy, where in the world he was, as well as the correct time.

Data gathered since Navstar 1 first became operational in March 1978, later to be joined by Navstar's 2 through 6, provide conclusive and persuasive evidence that the system works extremely well, for all the different potential operational users, under all ordinarily-encountered circumstances of ambient environment.

Clock performance, then has not recently been a GPS issue; the really significant question facing GPS has long been the reliability of the atomic clock. Reliability has, in the past, been given mainly "short-shrift" insofar as GPS clocks have been concerned. Schedule imperatives have demanded that satellites be committed to launch containing clocks using designs not thoroughly proven by ground test. Failures occurred, and it was necessary to implement design, material, and process changes in the same real-time as space vehicles were being prepared for launch. We bent some of the rules of good engineering practice, but enough good luck and extremely good people were with us, so that we got the job done. Now the situation is different and has improved. We have the "breathing room" to reassess and change our tactics. Our firm intention, and the plan, is to develop a good ground-test baseline for space-reliable clocks, and then to allow only a minimum perturbation of our proven design.

Navstar makes use of the state-of-the-art in both the rubidium (Rb) and cesium (Cs) atomic frequency standard technologies. Six years ago, when the Air Force first began to procure atomic clock hardware for GPS, neither type of clock had been space-qualified, to levels specified by military standards. Today, with relatively minor exception, Navstar flies fully space-qualified clock hardware of both varieties, and Rb clocks are performing head-to-head with the Cs standard on Navstar 6. The Rb standard was intended originally to be employed as an interim device, against the time when Cs standards, with their known superior long-term stability, would be ready. Rb's performance has been excellent and with some improvements aimed at decreasing temperature sensitivity, may be the right answer for the operational satellite. The Navstar 6 Cs standard, on the other hand, has also been performing in an excellent fashion and while it has exhibited behavior (to be discussed in detail later) which requires further examination and understanding, it has shown that it fits well into the Navstar navigation system and is, therefore, a completely viable candidate for use in the operational satellite. The above states then, the quandry and trilemma of the GPS program office: Should GPS proceed with Rb clocks, Cs clocks, or a combination of both? The right answer to this question, provided in a timely fashion, could save the government a considerable sum and practically guarantee the long-term existence of GPS.

GPS Navigation System Tutorial

As shown in figure 1, the GPS navigation system consists of three segments: Space, Control, and Users. The Space Segment is the set of orbiting satellites, each one containing redundant atomic clocks which, running one-at-a-time, provide precise timing to that satellite's Navigation Subsystem (Nav). Within the Nav, several functions are performed as follows: two L-band carriers are synthesized from the 10.23 MHz clock output; a pseudo-random

noise code (PRNC) is generated based upon the clock's timing; ephemerides and clock data for the whole GPS constellation are impressed on the PRNC and used to modulate the L-band carriers for transmission to the users and to the Control Segment.

Periodic updates of each satellite's ephemeris and clock data are performed by the Control Segment, which also continuously predicts the major parameters of total GPS system performance using a Kalman filter. The Control Segment consists of monitor stations, located in Guam, Hawaii, Alaska, and Vandenberg AFS, CA., with primary and secondary upload stations located at Vandenberg AFB, CA., and Sunnyvale AFS, CA., respectively, and a Master Control Station (MCS) at Vandenberg. Put in basic terms, the monitor stations receive the satellites' L-band Nav signals and pass them to the MCS for processing. The MCS, using a Kalman filter, takes the raw satellite data, makes the known, systematic corrections, weighs it statistically in the context of previous data, compares it with the best available reference, and then outputs its "best guess" as to the behavior of the several major Space and Control Segment operating parameters for the next 24 hours. The model thus generated is uploaded to each satellite daily or as necessary to keep the satellites, individually and collectively, operating in a useable fashion. The reference is periodically refreshed by passing data from Kalman to the Naval Surface Weapons Center for generation of a new reference.

The several space vehicles transmit the clock and ephemeris information, pertinent to all the satellites, by impressing it upon the two L-band carriers, as described above. Special equipment of the User Segment receive and process this data and develop a navigation solution, in the four dimensions of space and time, for the specific user. To date, users have successfully employed the GPS Navigation System to determine their position accurately on land, at sea, and in the air. Air Force has used it convincingly in exercise bombing runs, as has the Navy for instrumentation of test firing missiles at sea.

Clock Program Status

It has been said that the atomic clock is the heart of the satellite. Perhaps the idea needs to be expressed more strongly. Without reliable clocks on board each space vehicle, of high stability and modellability, the GPS navigation program cannot reasonably proceed.

The GPS Program Office is firmly of the view that there is a bright future for GPS. This very positive perspective has not come easily or without much effort and agony on the part of the government and its several clock vendors alike. Numerous problems, some of them potentially catastrophic to the program, have been worked over the past two years and two are now discussed.

a. Transformers: The power converter board of the Rb clock contains a power transformer and a timing transformer. There have been two iterations of redesign in terms of the materials and processes used to construct the transformers. The basic problem is that, because of constraints introduced by the total clock design, the power transformer runs at about 100°C and is a significant source of heat for the rest of the clock. Materials originally chosen for this device were not intended for compatible operation at elevated temperature and numerous clock failures, on the ground, and on-orbit, resulted. A program to redesign and retrofit clock transformers was instituted at Rockwell, Anaheim and the present transformers have operated without failure in Navstar 3 and subsequent vehicles since then.

b. Lamps: The lamps included in the Rb clocks have been, naturally, a subject of great interest and controversy, industry-wide, in the light of the GPS lamp failures on Navstars 1-4. Because of these several failures, reliability improvement and lamp study programs were set in motion by the program office. Outputs from these programs, to date, include lamps of known, adequate Rb fill which are flying in Navstar 5 and subsequent vehicles. Increased perception into the mechanism of lamp failure is being pursued by the Aerospace Corporation in conjunction with EFRATOM, Inc., the lamp maker. EFRATOM is also hard at work on an improved process for building and filling lamps which shows great promise for follow-on GPS satellites.

At present GPS has six satellites on-orbit, five of which are considered operational for contractual purposes. Navstar 2, whose three Rb standards have all failed in the atomic mode, still produces a navigation signal but this satellite is not regularly uploaded so the information it provides is of relatively little value to present users. Status of the 5 operational satellites is shown in Table A. Of special interest and note are that Navstar 1 has functioned reasonably well on a crystal clock since 25 Jan 1980.

Recent Kalman filter data from this clock is shown in figure 2. Navstar 3 is on a Rb clock which is the longevity leader, now running nominally and continuously for 22 months as of 20 Nov 80. Typical Kalman data is in figure 3. Navstar's 4 and 5 are also working well on Rb clocks with data shown in figures 4 and 5 respectively. Navstar 5 deserves special mention because it contains the first Rb lamps of known, adequate fill. In fairly large measure, the long-term viability of the GPS program may depend upon whether a lamp failure occurs in Navstar 5 in the near future. A lamp failure would send us back to the drawing board.

Navstar 6, with Kalman data in figure 6, contains the first successfully operating space-qualified pre-production model (PPM) Cs standard. Its performance has been excellent overall for its approximately seven months of on-orbit operation. It has shown, however, some anomalous behavior as graphed in

figure 7. The combination of decreasing Cs beam current, intermittent changes in beam current coupled with output frequency shifts, and rising ion pump current has, to say the least, been of interest and concern to the program office. This matter has been discussed, in detail, on several occasions, with the technical staff of the vendor, Frequency and Time Systems Inc., (FTS). Some diagnostics (thermal cycling in vacuum of the PPM qualification (qual) unit at NRL) have been done and added little perception to the problem. Further testing, with the qual unit at FTS, and on-orbit, are planned in the near future.

Navstar 7 is planned for launch in the Spring of 1981, and like Navstars 4-6 contains three Rb clocks and one Cs standard. Present plan is to make use of the Cs standard first but a firm decision has not yet been made. Navstar 8 will be launched in late summer next year with the same complement of clocks.

Navstar GPS Clock Plan

Given as first principle that GPS intends to fly, on each satellite, the best clock hardware available at that time, the clock plan is multifaceted and involves many corporate entities. The intelligent evolution of the overall clock design and testing to ensure the long-term reliability of that design are, *prima facie*, conflicting efforts but the program office intends to pursue them both, making good engineering trade-offs as clock development proceeds.

As part of the former effort, the GPS program office is funding relatively small design improvements to the Rockwell-built Rb clock. Further, automatic thermal control, which will hold clock baseplate temperature steady to 0.1°C , while its environment changes by $3^{\circ}\text{--}5^{\circ}\text{C}$ diurnally, will be added to at least one Rb clock on Navstar 8. Offline, in addition, the program office is funding a second-source Rb clock using EG&G Inc., in Salem, MA. This clock uses a physics package different from that of the Rockwell clock, as well as numerous state-of-the-art circuit advances not known at the time that GPS first entered the clock business.

In the Cs arena, the Naval Research Laboratory (NRL) is funding the offline improvement of the FTS PPM with an immediate eye to eliminating the several qual deficiencies of that clock; an incremental improvement in the clock's performance should be derived. NRL is also funding two alternate sources of Cs clocks, on a head-to-head basis, using KERNCO in Danvers, MA., and FEI in Long Island, N.Y., respectively. Both of these clocks are being designed with a view to supporting the needs of the GPS operational phase.

Relative to the reliability issue, the GPS program office is sensitive to criticisms arising from the paucity of good long-term stability and reliability data for both the Cs and the Rb clock. It is not that long-term tests haven't been done under the banner of this program office. Both Rockwell, Anaheim.,

and NBS, Boulder., have generated bodies of long-term stability data for the Rb clock over periods as long as 100 days. NRL, in its turn, has run the PPM qual unit for a total of about four months. The results have been positive and encouraging but not really enough of the right kind of data to prove the reliability for the design. The program office is taking action to free-up, as soon as possible, at least one Rb clock, of flight configuration, to operate in long-term thermal vacuum, at NRL. Coincidentally, NRL is buying a separate flight PPM Cs clock for the same kind of very purposeful testing. It is planned to have both a Rb and a Cs clock, into long-term testing by early Spring, 1981. Further planned is the purchase of critical subassemblies, for example Cs beam tube and power supply combinations for the same kind of long-term test.

The Future of GPS

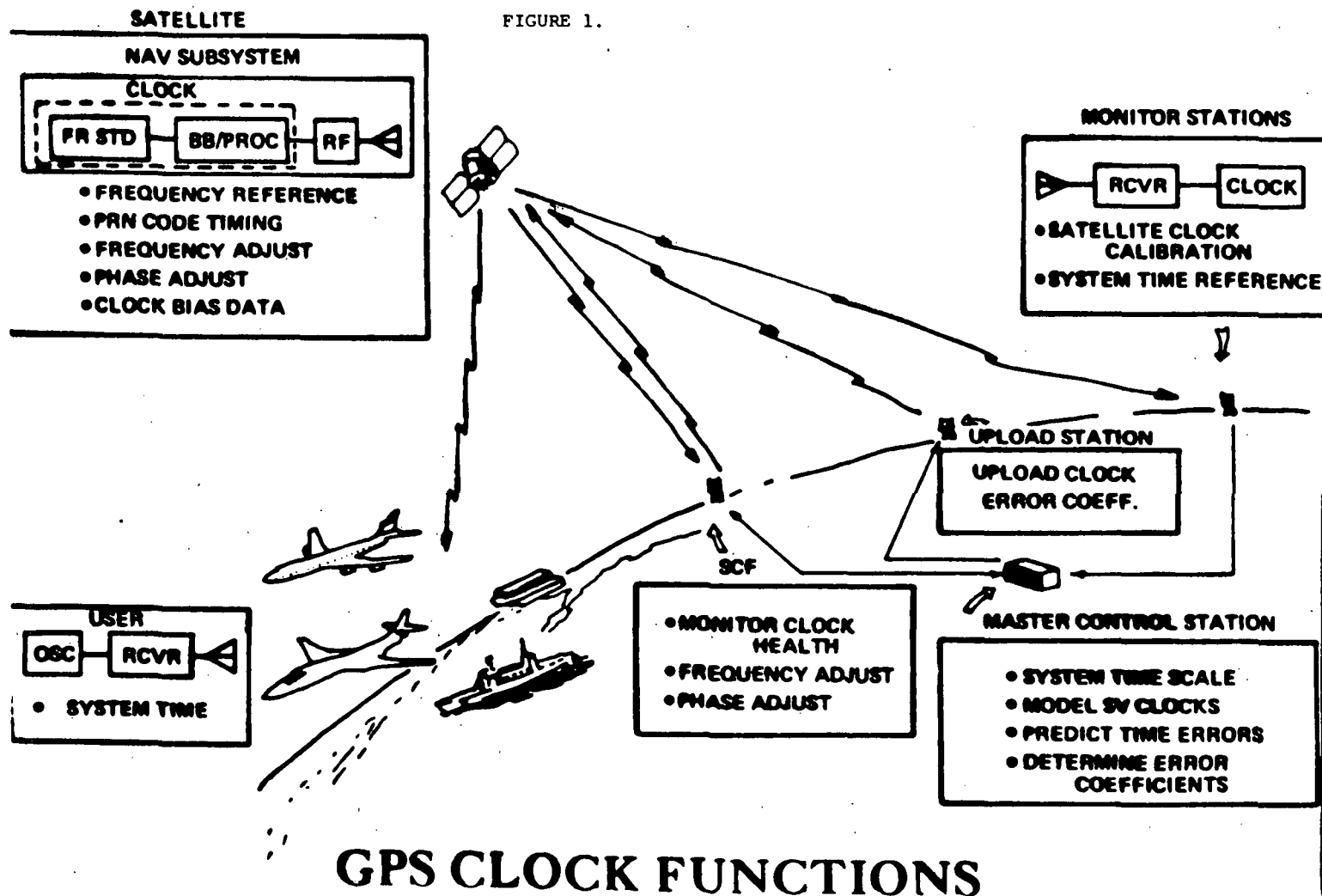
To paraphrase Peter F. Drucker, "Where is the GPS Clock Program going, and where should it go?" We who are concerned about the future of GPS Clocks see the Hydrogen Maser looming brightly on the horizon. NRL is funding some excellent exploration in this area and the program office is watching that effort with tremendous interest. As the future slowly unfolds with new data and experience daily, the same issues come to mind in different forms, again and again. Do we really need the unquestionably superior long-term stability of the maser or even the Cs beam standard, in the satellite, to make the system perform to the desired minimum level of navigation accuracy over time? Maybe we are unnecessarily diluting our effort and especially our resources by pursuing the several atomic clock technologies. Rubidium, we've seen, has better short-term noise and stability than Cs but drifts far more. Given the differences between Rb and Cs, can one or the other be considered "better" for our application? Available data, to date, suggest that whereas Cs scarcely drifts, its higher noise level, in the short-term, renders it neither more modellable nor more predictable than Rb. For our purposes, Rb may well be just as good as Cs with no space-borne need for Hydrogen Masers. Time and additional data, perhaps, will tell us with certainty.

Table A — GPS Clock Status

	Rb #1	Rb #2	Rb #3	Cs #4
Navstar 1	(10) L	(7) T	(2) (11/X)	
Navstar 2	(4) T	(10) L (3/X)	(11) L	
Navstar 3	22	(3) ?	U	
Navstar 4	10	(13) L	U	P
Navstar 5	U	9	U	U
Navstar 6	U	U	U	7

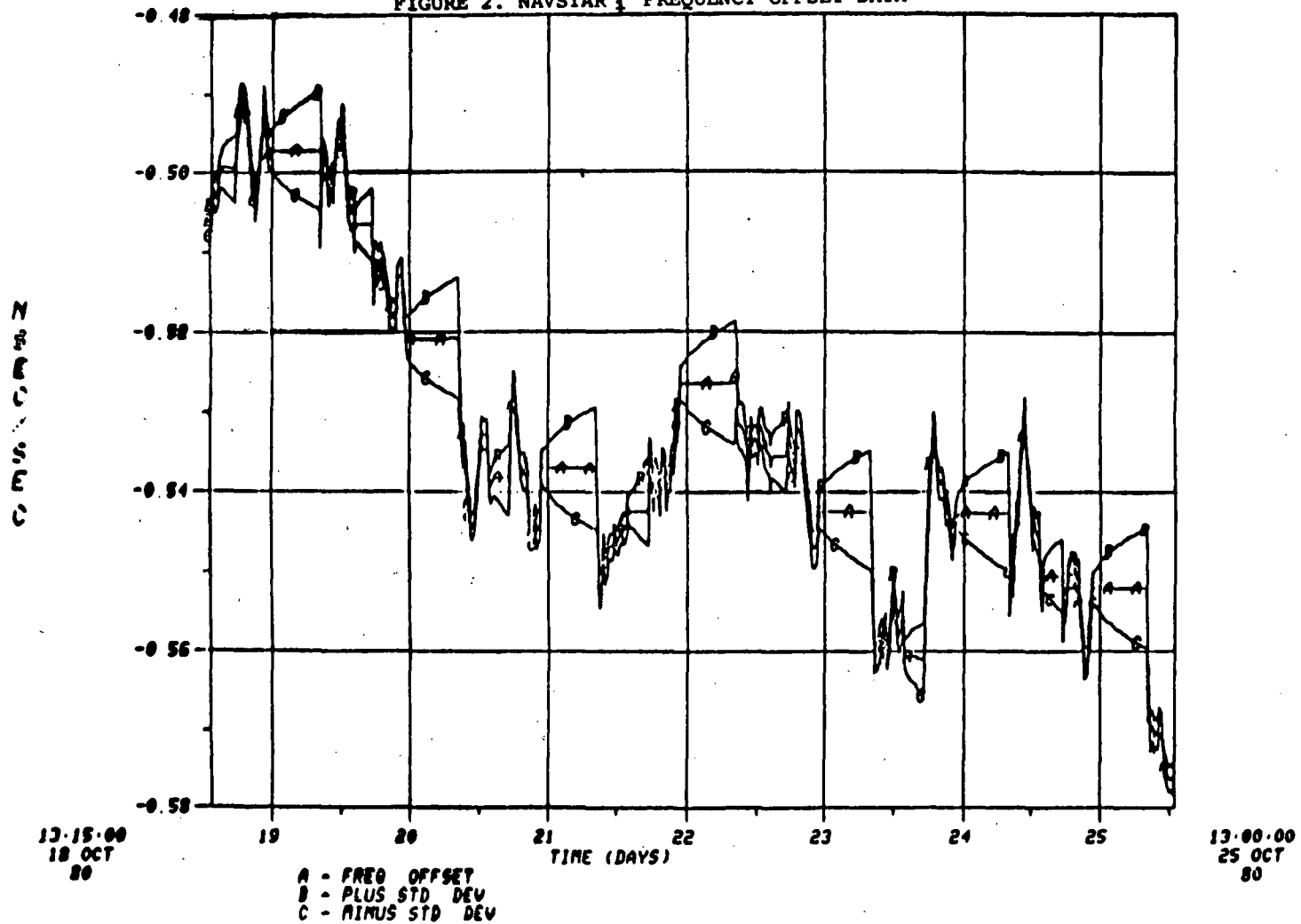
LEGEND:

- n = n months of nominal atomic mode operation
- (n) = n months of nominal operation before failure
- (n/X) = n months of crystal-mode operation
- U = Clock untried on orbit
- L = Lamp failure
- T = Transformer failure
- P = Power supply failure
- ? = Unexplained anomaly

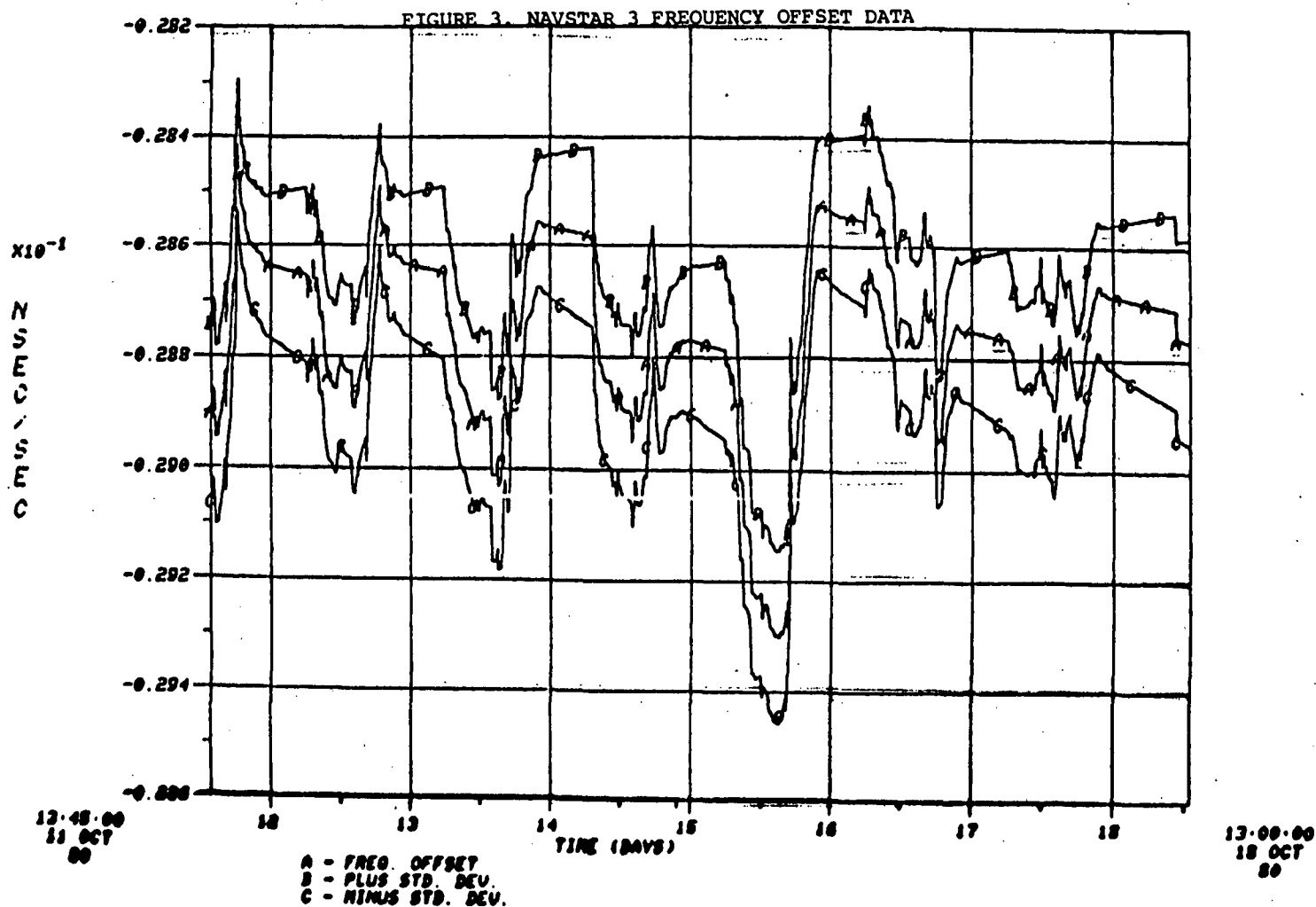


CURRENT KALMAN SV CLOCK ESTIMATE RESIDUAL AND
STANDARD DEVIATION FOR SV NO. 4
18:22:38 25 OCT 80/299

FIGURE 2. NAVSTAR 1 FREQUENCY OFFSET DATA

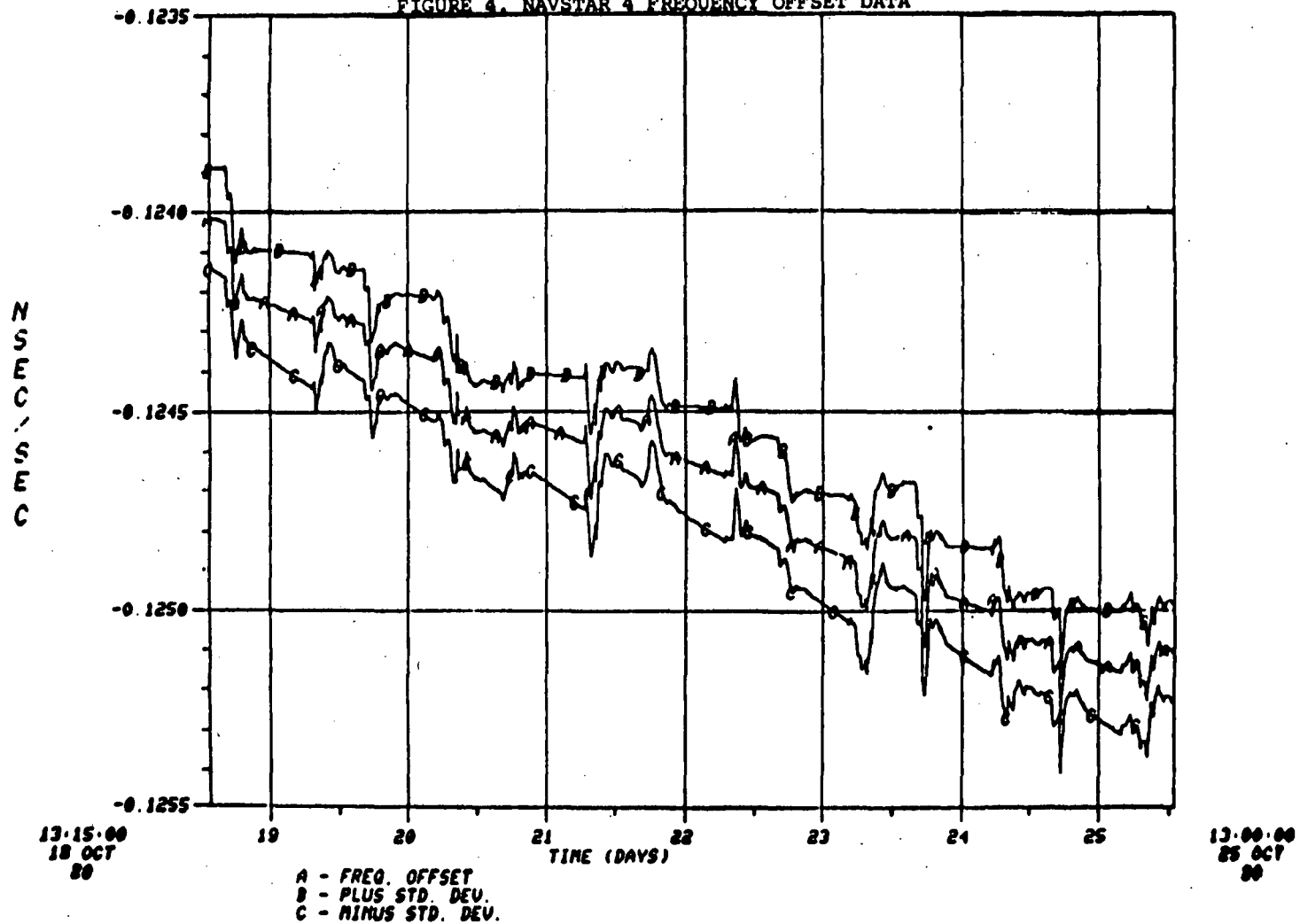


CURRENT KALMAN SV CLOCK ESTIMATE RESIDUAL AND
STANDARD DEVIATION FOR SV NO. 6
16:56:36 18 OCT 80/292



CURRENT KALMAN SU CLOCK ESTIMATE RESIDUAL AND
STANDARD DEVIATION FOR SU NO. 8
21:42:44 25 OCT 80/299

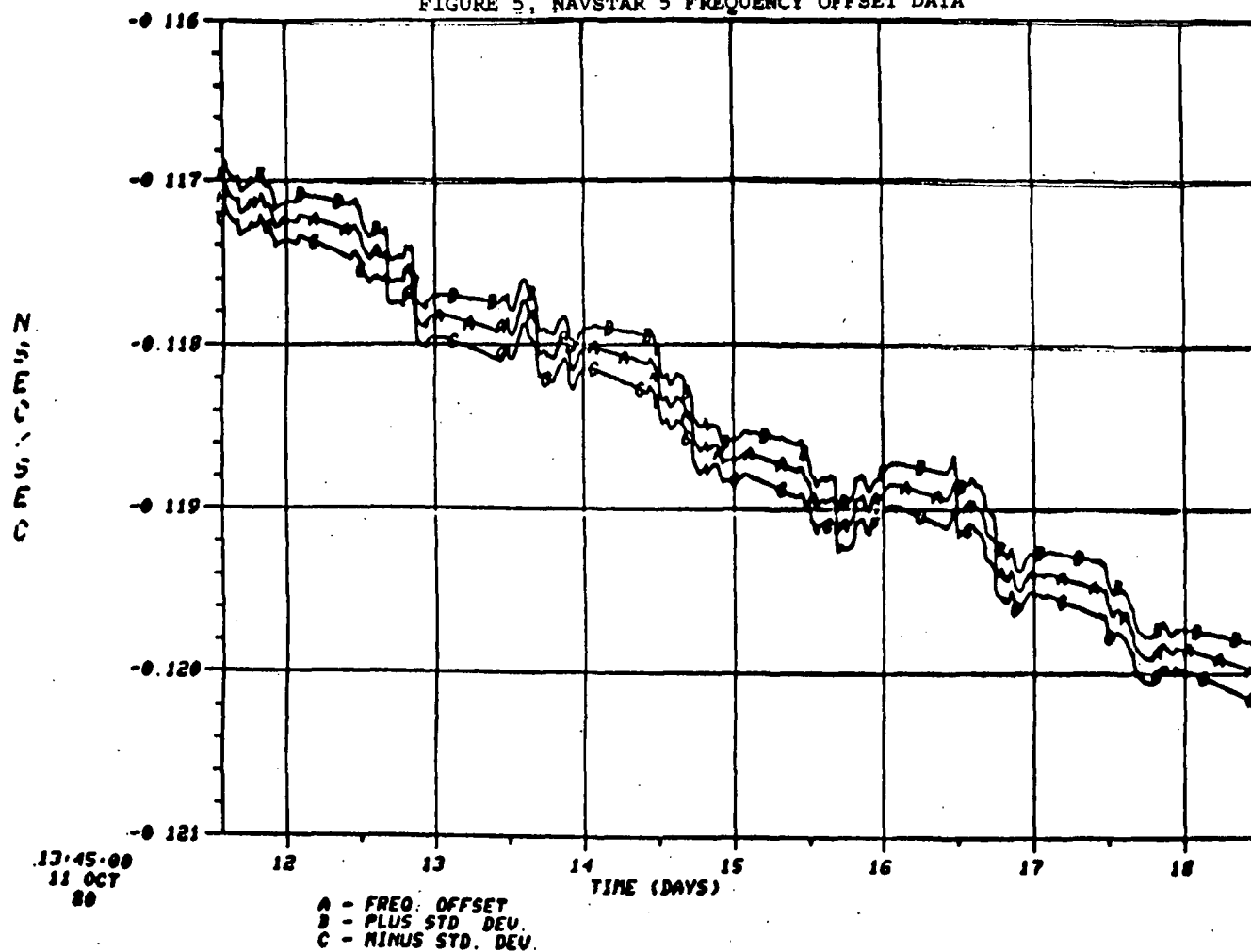
FIGURE 4. NAVSTAR 4 FREQUENCY OFFSET DATA



CURRENT KALMAN SU CLOCK ESTIMATE RESIDUAL AND
STANDARD DEVIATION FOR SU NO 5

18.38.29 18 OCT 80/292

FIGURE 5, NAVSTAR 5 FREQUENCY OFFSET DATA



CURRENT KALMAN SU CLOCK ESTIMATE RESIDUAL AND
STANDARD DEVIATION FOR SU NO 9
20:41:46 15 OCT 80/292

FIGURE 6. NAVSTAR 6 FREQUENCY OFFSET DATA

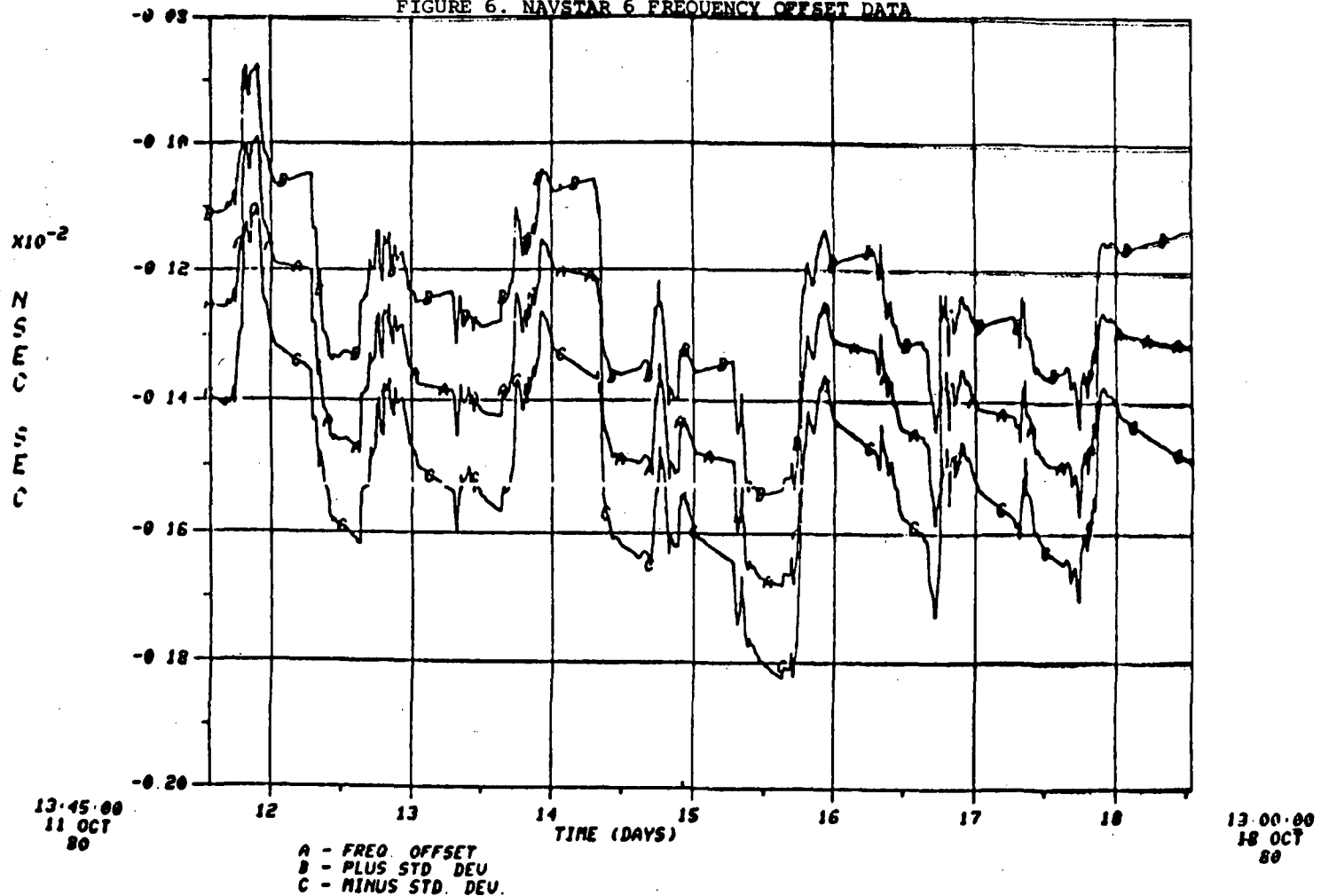
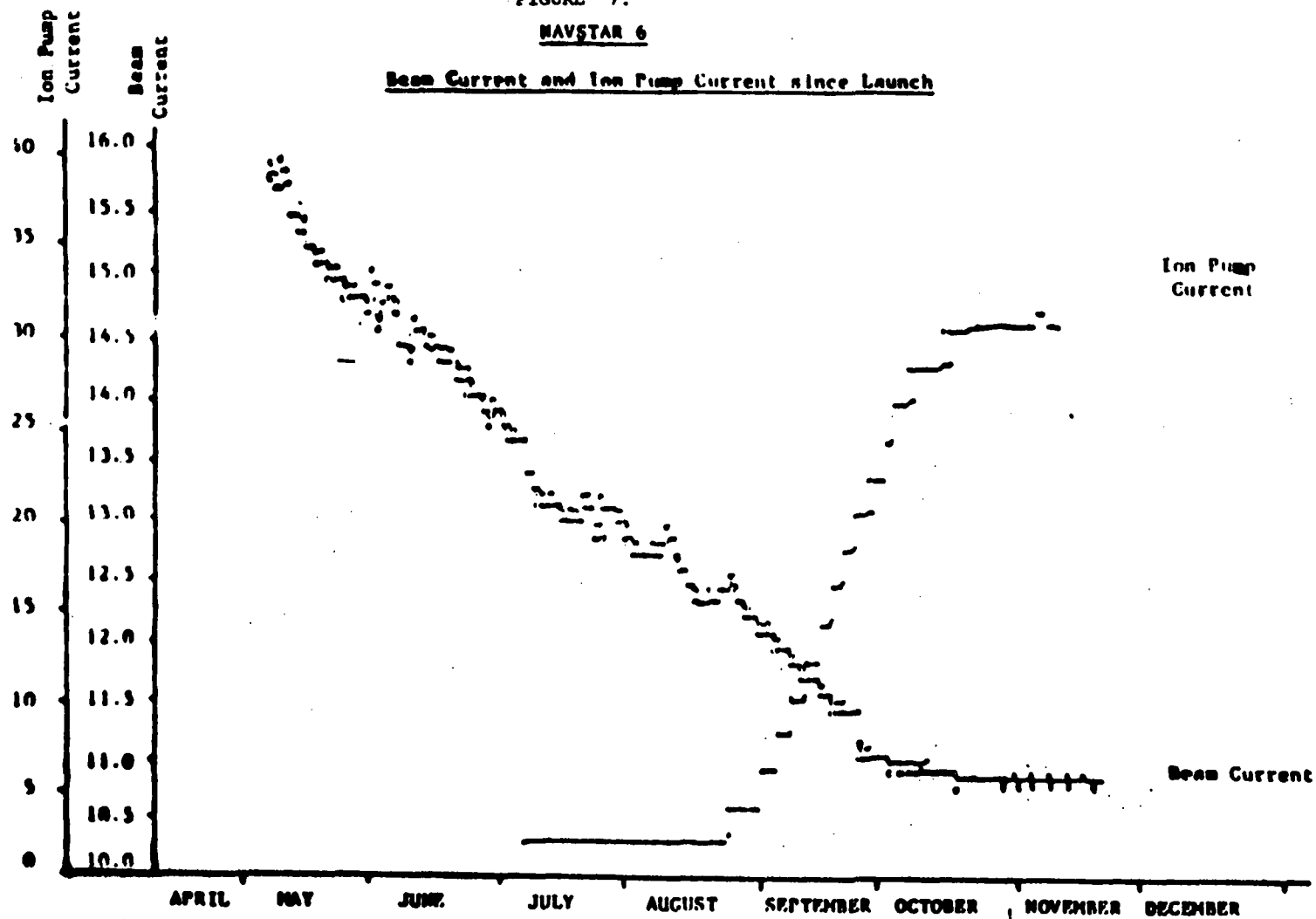


FIGURE 7.

NAVSTAR 6Beam Current and Ion Pump Current since Launch

QUESTIONS AND ANSWERS

CAPTAIN TENNANT:

I believe the question was asked yesterday, relative to the potential for encryption of the CA codes emanating from the satellite. The fact of the matter is the CA code, like the P code, is probably going to be encrypted, by way of making the accuracy of those signals collectively available. If you don't have the decryption gear, your accuracy is going to be fairly limited to like 300 to 1,000 meters. Don't know how bad that would hurt you, compared to what you are getting now.

I expect right much. The availability of the decrypting apparatus is going to be a function of your ability to satisfy the program office and especially the National Security Agency that you need to be able to decrypt the signal and that you can protect the decryption gear if you have it. Other questions, comments?

PROFESSOR CARROLL ALLEY, University of Maryland

I would like to compliment Captain Tennant on his very enlightening and forthright talk about the clock development program. I remember when the RFP went out a number of years ago. It was several feet high, and the amount devoted to clocks was about one page. So that the statement that the whole success of the GPS rides on the performance and reliability of space clocks has at long last been adequately recognized. Thank you.

DR. REINHARDT:

The GPS program is a classic example of the problems that were brought up in the first meeting. You say that reliability and performance were primary concerns, but in fact, what has happened is that non-critical elements, such as size, have been the real drivers. What I see is a lot of research going into areas, unknown areas like new passive masers, shrinking down masers in size, and even cesiums, when that is not necessary if you just make the satellite 50 percent bigger. This is precisely the kind of thing we are talking about -- of designers arbitrarily saying that your box must fit in this little cube and a lot of money and a lot of effort and a lot of loss of reliability is being wasted because of that. Can you comment on that? Is there anything intrinsically that keeps the satellite from being a little bigger or even 50 percent bigger?

Or is it just that the satellite now is too far down the line for anybody to make changes?

CAPTAIN TENNANT:

I am not really qualified to fully answer that question. I know that in terms of the cost; the availability of the hardware to put the satellite we are talking about into orbit; given where we were six years ago; and given the priority associated with putting the satellites up, getting the program moving; we had to go with what we had at the time.

DR. REINHARDT:

A specific example of what I mean is that NASA had just spent \$2,000,000 developing a red shift probe maser to be a flyable maser which would have taken a very small step to turn into a very reliable long-term maser, and it was only 70 pounds. You know it was obviously flyable because it flew on a Redstone.

CAPTAIN TENNANT:

Only 70 pounds? All my clocks weigh less than that.

DR. REINHARDT:

Is there any intrinsic reason that they have to weigh 70 pounds? This is something that is known. People know how to launch heavier satellites and control them. What you are asking the frequency standard people is to go into completely unknown areas and then yet meet scheduled reliability in very short time.

CAPTAIN TENNANT:

The question is too big for me. I am a clock man, not a space vehicle man.

MR. HUGO FRUHAUF, Efratom

To answer the question of satellite weight and resulting clock weight; it was primarily a function of the launch vehicle that was available at the time. The whole program and cost was keyed to a cheap launch vehicle which was the Atlas. So, therefore, the space satellite size and the 11,000 mile nautical orbit was primarily a function of that problem.

At the present time, future launches are planned with the shuttle, and your question and comment at that point should be re-considered.

DEVELOPMENT OF A SUB-MINIATURE RUBIDIUM OSCILLATOR FOR SEEKTALK APPLICATION

H. Fruehauf, W. Weidemann, E. Jechart
Efratom
Irvine, California

ABSTRACT

For some time now the Efratom 4-inch cubed Rubidium Oscillator has been used in numerous navigation and secure communication systems. The SEEKTALK program, however, and other programs of similar nature, present new challenges to oscillator makers in terms of warm-up time, size, power, operating environment, and unit cost in large quantities.

This paper will present our approach to these new warm-up and size challenges as well as the problems involved in these tasks. In order to define the improvements needed, a comparison will be made between the performance of the present off-the-shelf M-100 Military Rubidium Oscillator and that expected for the Sub-Miniature Rubidium Oscillator that is currently in development (called M-1000). Methods of achieving 1.5 minute warm-up will be discussed as well as improvements in performance under adverse environmental conditions, including temperature, vibration, and magnetics. Expected performance curves of the new oscillator as well as our microelectronics approach will be presented.

An attempt will be made to construct an oscillator error budget under a set of arbitrary mission conditions.

GENERAL

In order to clearly indicate the improvements that will be realized for this new M-1000 Oscillator development, Table 1 is provided to compare the off-the-shelf M-100 Oscillator with the M-1000. The SEEKTALK program spec requirements are shown as tentative design goals, pending a final Air Force spec release in early 1981. The most challenging performance requirements are (a) ultra fast warm-up, (b) MIL-E-5400 Class II temperature environment, (c) operation in a severe vibration environment and (d) our attempt to make the M-1000 less than one half the volume of

the present M-100 Oscillator. Figure 1 depicts the subject oscillators. The M-100 measures approximately 4" x 4" x 4.8" (or $\sim 77 \text{ in}^3$) and the M-1000 approximately 2.3" x 3.5" x 4" (or $\sim 33 \text{ in}^3$) with future goals toward further reduction in size.

Figure 2 is a functional block diagram of the present off-the-shelf M-100 oscillator. The highly stable output of the M-100 is obtained from a 10 MHz voltage-controlled crystal oscillator (VCXO), whose frequency is locked to an atomic frequency reference. The atomic reference is provided by the 6.834...GHz ground-state hyperfine transition of ^{87}Rb . The VCXO is locked to the rubidium resonant frequency f_{Rb} , at approximately 6.8 GHz, in the following manner: A microwave signal, having a frequency in the vicinity of f_{Rb} , is synthesized from the 10 MHz VCXO output. This microwave signal is used to excite rubidium atoms that are contained within a microwave cavity. The frequency synthesis scheme is designed so that the VCXO frequency is exactly 10 MHz when the microwave frequency is exactly equal to f_{Rb} . The frequency of the signal applied to the microwave cavity can be maintained equal to f_{Rb} by generating an error signal when the microwave frequency differs from f_{Rb} and using this error signal to servo the VCXO via its control voltage.

TABLE -1- SPEC COMPARISON (Sheet 1 of 7) 11-4-80				
DESCRIPTION	ANTICIPATED SEEK TALK SPEC	OFF-THE-SHELF M-100 OSC.	IN DEVELOPMENT M-1000 OSC.	REMARKS
Output	10 MHz sine wave 0.5 Vrms \pm 10% 50 Ohms \pm 10%	10 MHz sine wave 0.5 Vrms \pm 30,-10% 50 Ohms \pm 10%	Same as M-100	
Input Power	<13W @ 25°C (Amb) 22-32 VDC (28 VDC Nom)	17W @ 25°C 22.5-32 VDC	Same as SEEK TALK	
		Separate Heater power avail- able.	Separate heater power available	
Transient Protection	MIL-STD-704 Category A	MIL-STD-704 Category C	Same as M-100 (Working on a compromise 704A Spec)	704C Should be adequate for program. Pushing AF Spec change from A to C.
Warm-up Characteristics	≤ 1.5 minutes to reach 5×10^{-10} @ 25°C (Amb); <4 min. from -55°C (Amb).	< 10 minutes to reach 2×10^{-10} @ 25°C (Amb.) < 25 minutes from -55°C (Amb.)	Same as SEEK TALK	
Warm-up Power	Power available not specified with engines running.	4 min. option, ~ 100 watts.	< 100 watts; * $\sim 80\text{W}$ typical for less than 1 minute.	* Max peak current at 32 VDC <6A

TABLE -1- SPEC COMPARISON (Sheet 2 of 7) 11-4-80				
DESCRIPTION	ANTICIPATED SEEK TALK SPEC	OFF-THE-SHELF M-100 OSC.	IN DEVELOPMENT M-1000 OSC.	REMARKS
Power On/Off Cycling (Retrace)	$\leq 1 \times 10^{-5}$ with off times < 1 hr.	Retrace within few parts in 10^{11}	Same as M-100	
Operating Temperature	< 5×10^{-10} from -55°C to +55°C Amb 71°C Amb. for 30 min Prefer Class II -55°C to +71°C Amb. 95°C Amb. for 30 min	< 4×10^{-10} from -55°C to ~+60°C Amb; (+68°C Baseplate). Parts in 10^9 offset at 71°C Amb. Ops	< 3×10^{-10} from -55°C to +71°C Amb; (~80°C Baseplate) parts in 10^9 offset at 95°C Amb	
Long Term Drift	5×10^{-10} /year	< 3×10^{-11} /month < 3×10^{-10} /year 1×10^{-11} /month option available	< 6×10^{-11} /month 5×10^{-10} /year	
Short Term Stability	< 4×10^{-11} , $\tau = 1s$ < 1×10^{-11} , $\tau = 10s$ < 4×10^{-12} , $\tau = 100s$	Same	Same	
Trim Range / Adjustment	3×10^{-9}	Same	Same	

TABLE -1- SPEC COMPARISON (Sheet 3 of 7) 11-4-80				
DESCRIPTION	ANTICIPATED SEEK TALK SPEC	OFF-THE-SHELF M-100 OSC.	IN DEVELOPMENT M-1000 OSC.	REMARKS
Voltage Variation	Not specified.	< 1×10^{-11} for $\pm 10\%$ input voltage change.	Same as M-100	
Magnetic Field	Meets spec under 1×10^{-11} /Gauss	< 8×10^{-11} /gauss (worst case orientation)	< 1×10^{-11} /Gauss	Note: 1 Gauss = 79.59 AM^{-1}
Signal to Noise (SSB 1Hz BW)	> 120 dB @ 100 Hz > 130 dB @ 1 KHz	> 120 dB @ 100 Hz > 135 dB @ 1 KHz	Same as M-100	
Harmonic / Non Harmonic	30 dB down 80 dB down	Same	Same	
Sinusoidal Vibration (operational)	< 1×10^{-10} 5-14Hz-0.10" D.A. 15-23Hz- $\pm 1g$ pk 24-52Hz-0.036" D.A. 54-500Hz- $\pm 5g$ pk	Tested to ~ 1g 20-500 Hz; parts in 10^9 at narrow critical freq.	Goal is to im- prove M-100 performance significantly	More testing needed to evaluate performance

TABLE -1- SPEC COMPARISON (Sheet 4 of 7) 11-4-80				
DESCRIPTION	ANTICIPATED SEEK TALK SPEC	OFF-THE-SHELF M-100 OSC.	IN DEVELOPMENT M-1000 OSC.	REMARKS
Random Vibration (operational)	$< 1 \times 10^{-10}$ 15-50Hz-0.02g ² /Hz 51-300Hz-+4dB/oct. 301-1KHz-0.1g ² /Hz 1001-2KHz-6dB/oct.	Tested to .02g ² /Hz 20-50Hz falling to .001g ² /Hz at 500Hz parts in 10 ⁶ for an Allen Vari- ance of $\tau = 1$ sec.	Goal is to im- prove M-100 performance sign.	More testing needed to evaluate performance (major design problem)
Acoustical Noise	$< 1 \times 10^{-10}$ MIL-STD-810 Method 515.2 Procedure I Category A	TBD - Not tested	TBD	
Storage Temp. (non-operational)	-62°C to +80 C Prefer Class II: -62°C to +95°C	-62°C to +85°C	-62°C to +95°C	
Acceleration (operational)	$< 1 \times 10^{-8}$ for 10g's in any axis.	-4×10^{-12} /g (Worst case orientation)	$< -4 \times 10^{-12}$ /g (worst case orientation)	
Temperature Altitude	MIL-E-5400 Class II $< 5 \times 10^{-10}$ S.L. to 70K ft 71°C to 10°C Amb.	$< 1 \times 10^{13}$ /mbar; with temp change $< 5 \times 10^{-10}$ total *	$< 1 \times 10^{-13}$ /mbar with temp change $< 2 \times 10^{-10}$ total **	* M-100 has not been tested to 70K ft; but expect no problems ** Vacuum Ops is goal.

TABLE -1- SPEC COMPARISON (Sheet 5 of 7) 11-4-80				
DESCRIPTION	ANTICIPATED SEEK TALK SPEC	OFF-THE-SHELF M-100 OSC.	IN DEVELOPMENT M-1000 OSC.	REMARKS
Temperature Shock	MIL-STD-810 Method 503.1 Procedure	OK	OK	
Transient Temp.	Meet Spec @ 2°C/ sec from -55°C to +85°C, 71° Amb.	OK	OK	
EMI	MIL-STD-461A Notice 3 CE 01, 02, 03, 04 CS 01, 02, 06 RE 02, 04 RS 01, 02, 03	MIL-STD-461A Notice 3 CE 01, 02, 03, 04 CS 01, 02, 06 RE 02 RS 01, 02, 03	Same as M-100	RE04 not applicable.
Radiation Hardening	Not specified.	Hard to ground tactical environ- ment of a major program.	Hardness level to be assessed.	
Reliability	MTBF>20,000 hrs. 60% DR @ 55°C Amb. Airborne uninhab- ited fighter envi- ronment. MIL-HDBK- 217C, Not.1, Sec 2	MTBF>19,000 hrs. 60% @ 68°C base- plate Airborne inhabited transport environment MIL-HDBK-217C	MTBF>20,000 hrs. 60% @ 71°C Amb. Airborne uninhab- ited fighter MIL- HDBK-217C	Reliability level for unit largely controlled by hybrid screening level and can be im- proved accordingly.

TABLE -1- SPEC COMPARISON (Sheet 6 of 7)				11-4-80
DESCRIPTION	ANTICIPATED SEEK TALK SPEC	OFF-THE-SHELF M-100 OSC.	IN DEVELOPMENT M-1000 OSC.	REMARKS
Humidity	MIL-STD-810 Method 507.1 Procedure III	95%	100%	
Shock (Bench Handling)	MIL-STD-810 Method 516.2 Procedure V	OK	OK	
Size	5 x 5 x 5½" max 2¼ x 2¼ x 4" Goal	<80 in ³ (3.94 x 3.90 x 4.8)	<30 in ³ (2.5 x 3.0 x 4")	
Weight	TBD	4.5 lbs. max	< 2 lbs.	
Salt Fog	MIL-STD-810 Method 509.1 Procedure 1	TBD - not tested	OK	

TABLE -1- SPEC COMPARISON (Sheet 7 of 7)				11-4-80
DESCRIPTION	ANTICIPATED SEEK TALK SPEC	OFF-THE-SHELF M-100 OSC.	IN DEVELOPMENT M-1000 OSC.	REMARKS
Fungus Resistance	MIL-STD-454 Requirement 4	OK	OK	No test data available.
Explosive Atmosphere	MIL-STD-810 Method 511.1 Procedure 1	OK	OK	
Sand and Dust	MIL-STD-810 Method 510.1 Procedure 1	TBD - Not tested	OK	
Maintainability Requirements	~ 90% Fault Det- ection with a BITE	OK	OK	Use of lock monitor.
Shop Level Maintenance	Required	NO	NO	An atomic standard does not lend itself to de- tailed AF field level maintenance.

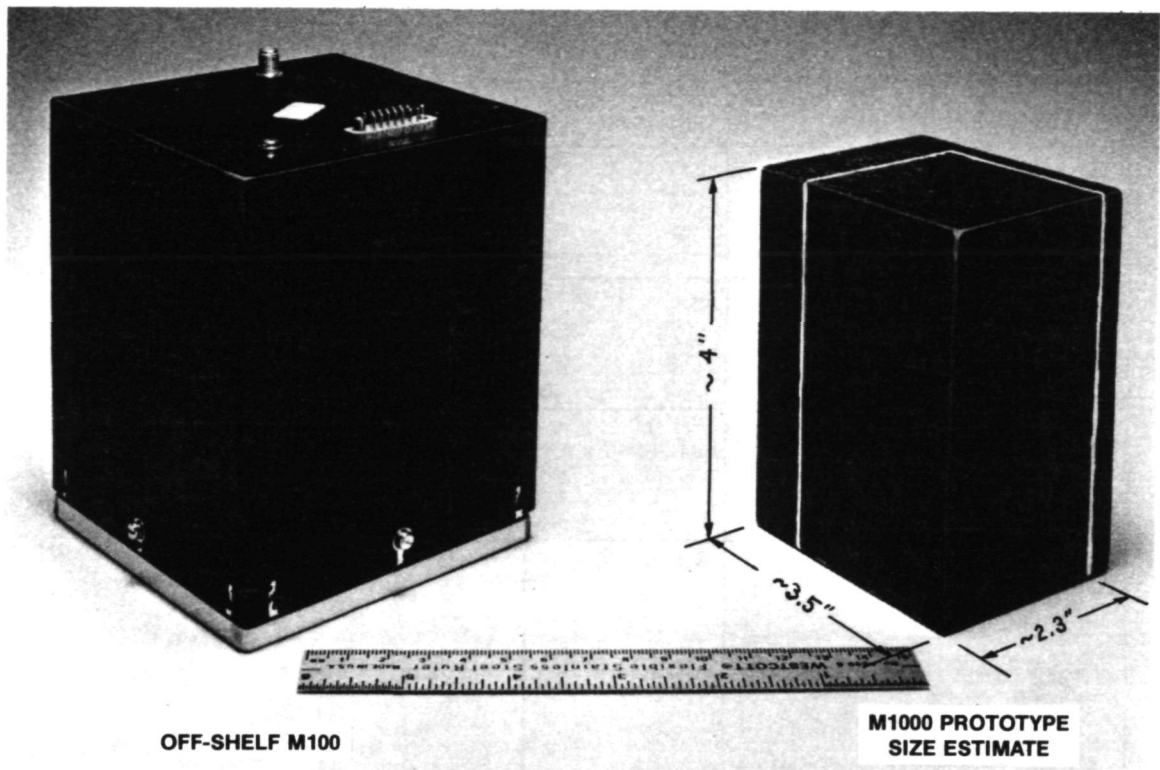


Figure 1. M-100/M-1000 Size Comparison

The error signal is generated by the Physics Package using the method of optical pumping (not discussed here) and appears as a current from the photocell in the Physics Package. When the applied microwave frequency is equal to f_{Rb} , the Rb atoms resonate with the microwave field in the cavity resulting in a decrease (minimum) of the photocell output current. Conventional modulation techniques are used to locate the minimum in the photocell current characteristic (Figure 3). In the M-100, the applied microwave frequency is sine-wave modulated at 127 Hz. This modulation results in an a.c. component of output current from the photocell. When the microwave frequency is different than f_{Rb} , there is a 127 Hz component present whose phase (positive or inverted) depends on whether the microwave frequency lies above or below f_{Rb} . This phase information is used to steer the VCXO in the proper direction to bring the microwave frequency into coincidence with f_{Rb} (at which point the 127 Hz signal is zero). From a practical point of view, the M-100 is considered locked to the atomic resonance when its output frequency is within 1×10^{-9} of exactly 10 MHz.

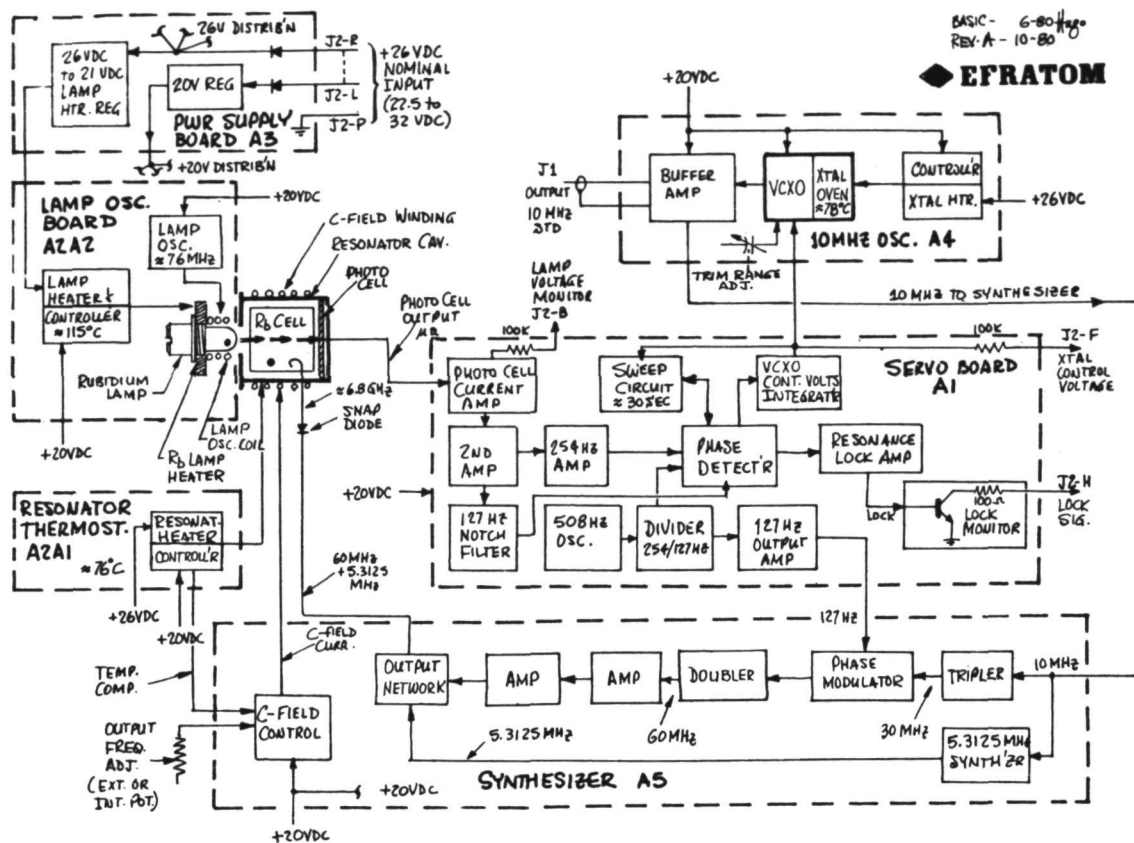


Figure 2. M-100 Functional Block Diagram

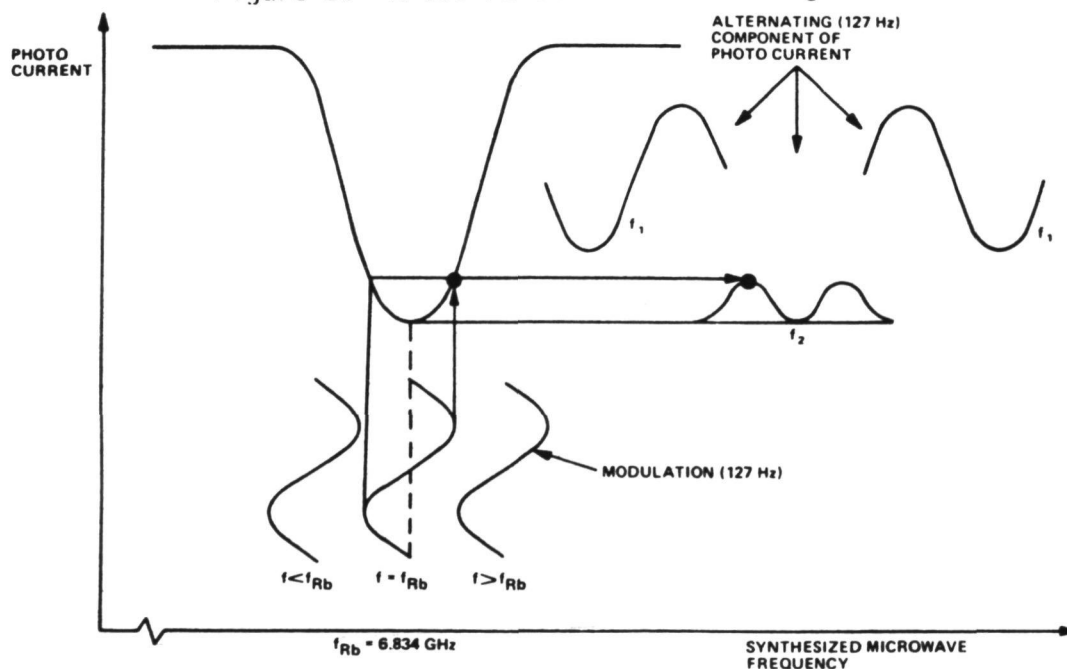


Figure 3. M-100 Modulation Scheme

The M-1000 differs from the M-100 Oscillator in the area of the Physics Package, form-factors and some electronic changes. These changes are summarized below but will be discussed in detail later. As noted on the M-1000 Block Diagram of Figure 4, (a) the modulation frequency has been changed from 127 Hz to 254 Hz to reduce sensitivity to the vibration spectrum below 250 Hz, (b) the 40 second sweep during warm-up has been reduced to 6 seconds including a new resonance detection scheme which is among the several things necessary to achieve to 1.5 minute warm-up requirement, (c) a special lamp ignition system to prevent operation in undesired lamp modes which could result from power on-off cycling or external power supply transients, (d) physics changes to allow for MIL-E5400 Class II temperature operation (71° Amb. continuous) including size reduction, (e) an integrated SC Cut VCXO/Rb resonator package with overall lower mass to facilitate the fast warm-up requirement, (f) a Hybrid electronics circuits approach to reduce the overall size of the oscillator.

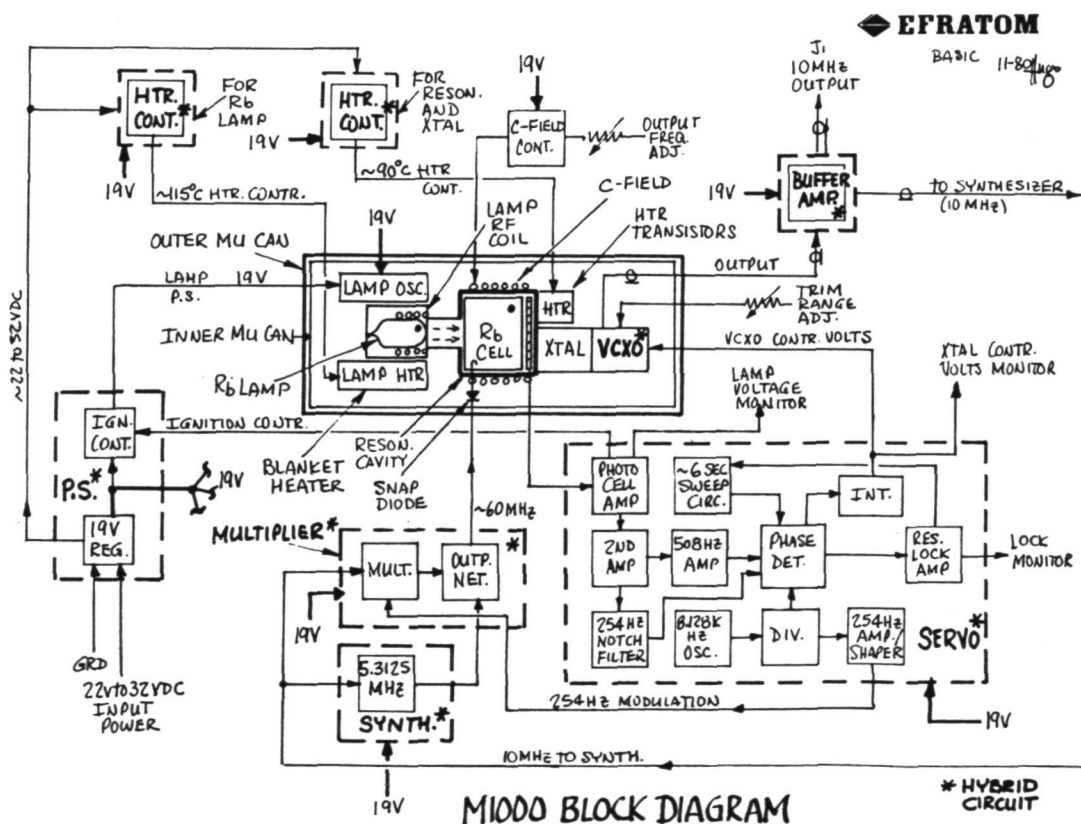


Figure 4. M-1000 Functional Block Diagram

OVERALL MECHANICAL DESIGN

The present design approach will allow for a reduction to half the M-100 volume. The presently planned form-factors are shown in Figure 5. The resonator portion of the Physics Package has been reduced in both size and mass proportions, housing a smaller Rubidium Vapor Cell decreased in length from $1\frac{1}{2}$ in. to $\frac{7}{8}$ in. This has reduced the size of the resonant cavity as illustrated in Figure 6.

The lamp oscillator, Figure 7, does not readily lend itself to Hybridization and thus has been repackaged to make the overall assembly smaller. The major size and mass reduction comes from the use of blanket heaters in place of heating transistors. Since the lamp is not sensitive to varying magnetic fields, the blanket heater approach presents no problem.

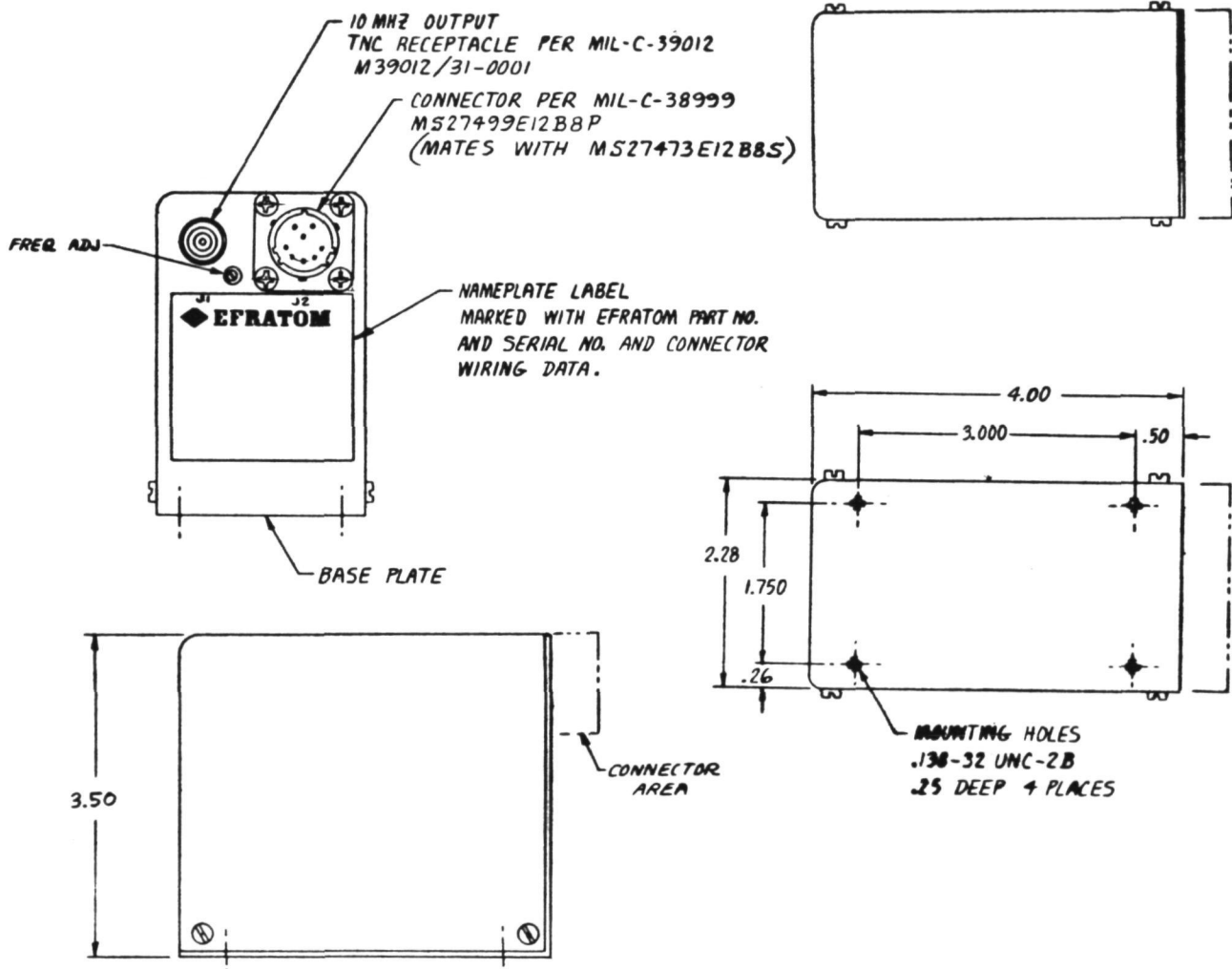


Figure 5. M-1000 Form-Factors

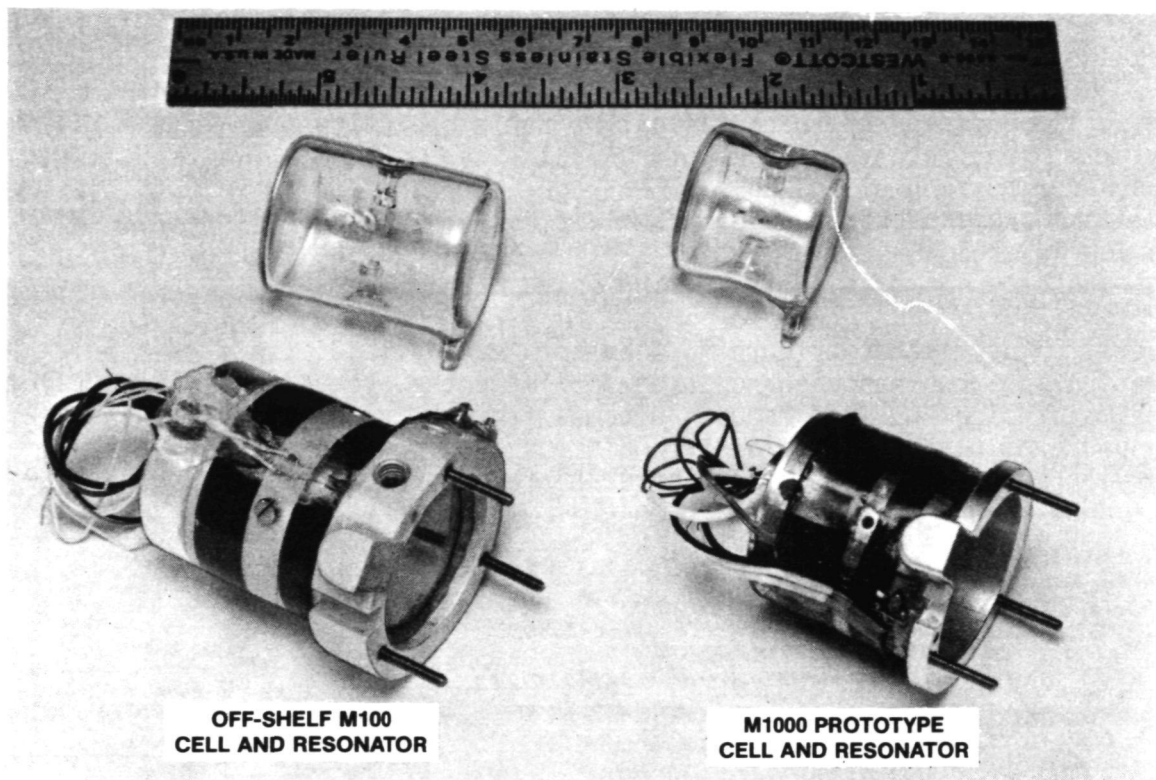


Figure 6. Resonator Comparison

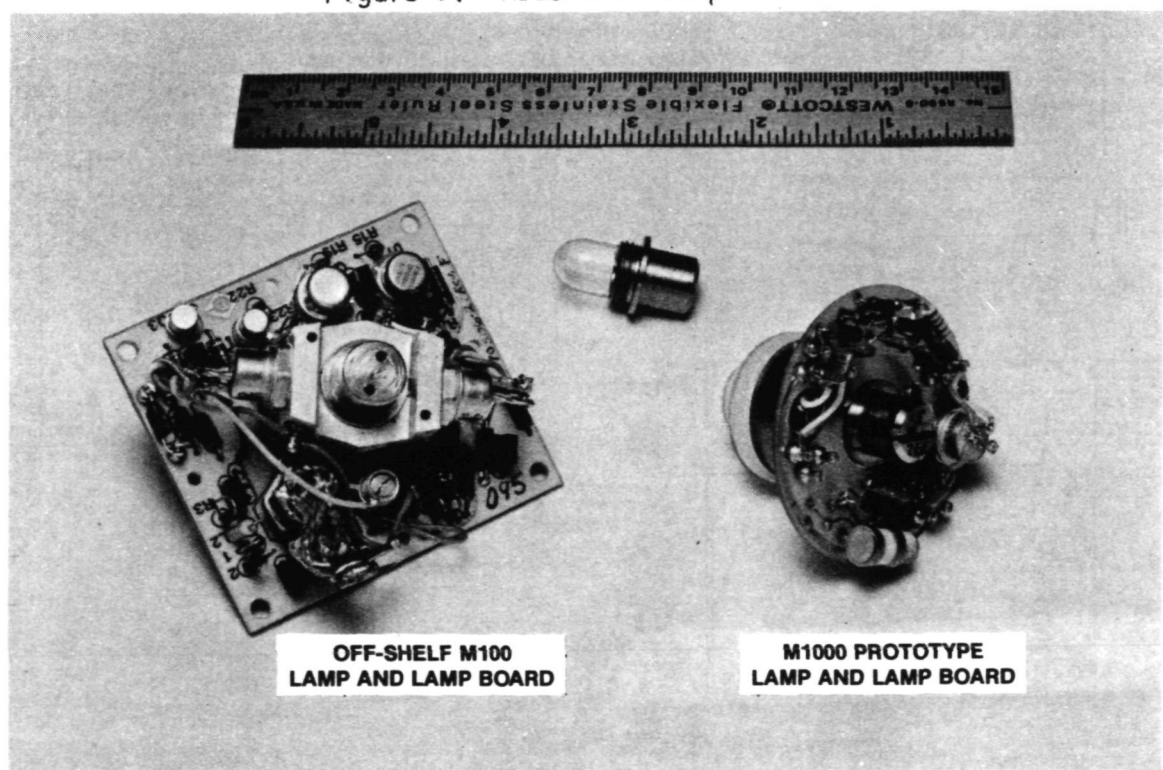


Figure 7. Lamp Board Comparison

These sub-modules integrated into an overall assembly, will resemble the M-1000 Physics Package shown in Figure 8. This integrated assembly will be foamed into an inner Mu-metal housing for reduction of vibration sensitivity with a second outer Mu-metal case again at the Physics Package. This eliminates the need for the outer Mu-metal cover which has been the M-100 design approach and allows for a standard cover which can be sealed to meet salt spray, sand and dust specs. The M-1000 unit thermal design will allow for operation from sea level to hard vacuum space craft applications. All heat will be conducted to the M-1000 mounting baseplate.

The major size reduction comes from our hybrid electronics approach. The Servo Hybrid, before lid-closure, is shown in Figure 9. More than 95% of the electronic parts count will be contained in Hybrid circuits. As shown in Figure 4, the Hybrid circuits are as follows: (a) Servo Hybrid, (b) Power Supply Hybrid, (c) two identical Heater Control Hybrids, (d) the M-100 synthesizer approach has been split into two sections; Multiplier and Synthesizer Hybrids: this allows for more flexibility for future changes in synthesizer approach which may be necessary when mass production quantities are required (2000 or more per year).

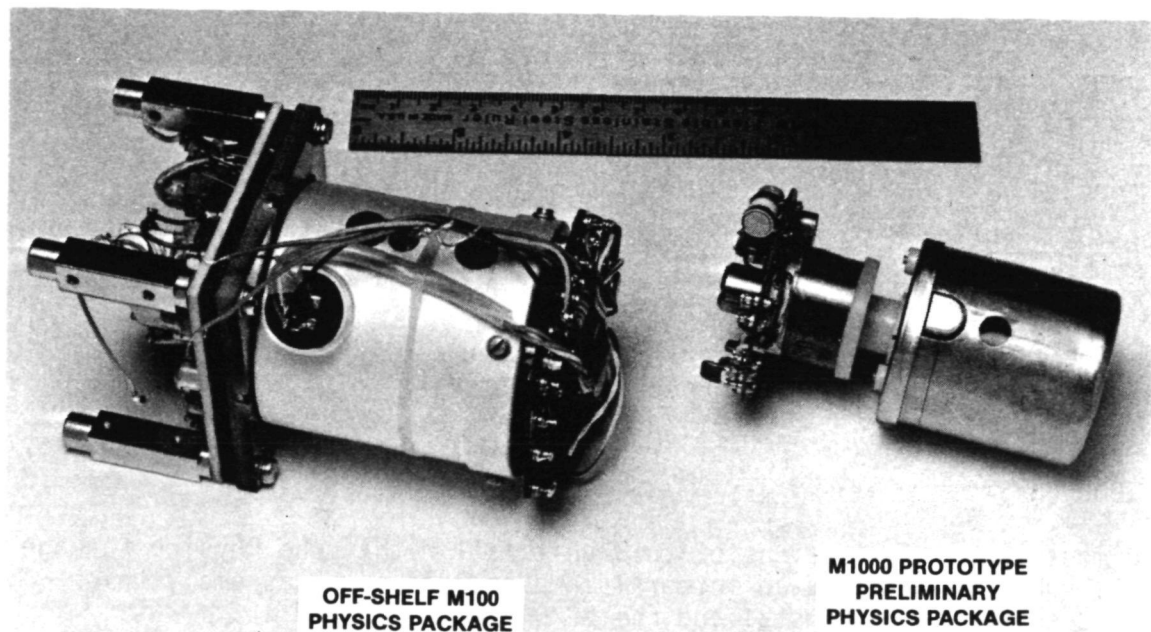


Figure 8. Physics Package Comparison

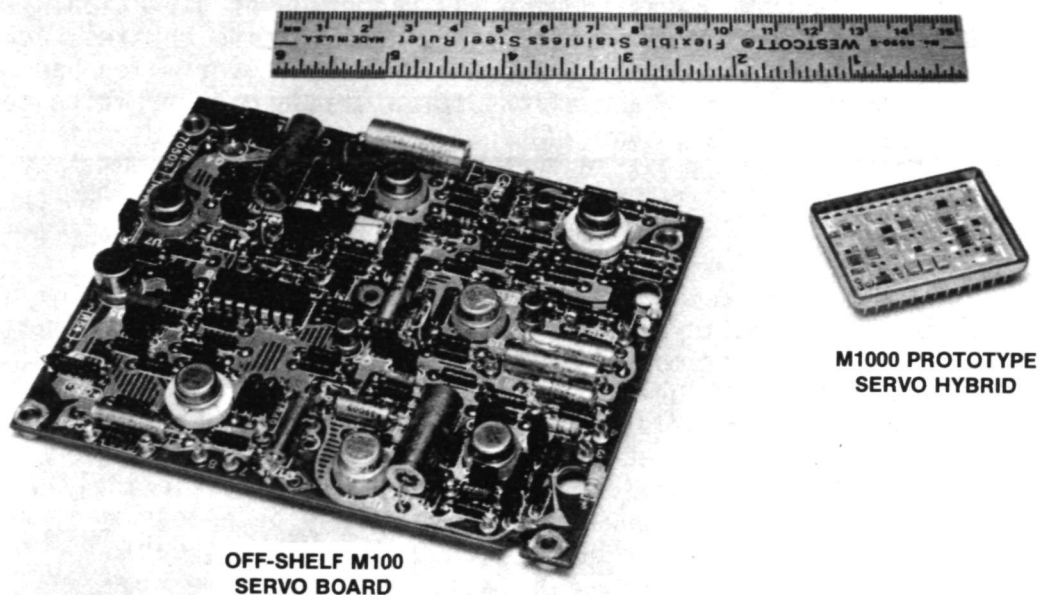


Figure 9. Servo Board Comparison

(e) VCXO Hybrid which will be an integral part of crystal and resonator assembly, and (f) the Buffer Amp Hybrid mounted outside the Physics Package to provide isolation and output drive.

Including eight (8) Hybrids, the M-1000 is expected to have approximately 80 electronic piece parts.

M-1000 PHYSICS

The most innovative designs of this unit fall within the Physics Package area. We have designed an integral lamp and resonator assembly which includes the SC-Cut Crystal and the VCXO Hybrid.

The lamp is our conventional unit but without the usual brass holder. This allows a size reduction. The blanket heater approach allows for rapid heating to the nominal 115°C. The overall temperature of the resonator, which houses a smaller cell, has been raised to approximately 85°C to allow 71° Amb. continuous operation (approximately 80°C base-plate) which meet MIL-E-5400, Class II temperature requirements.

The assembled package will be foamed into the inner Mu-metal can as discussed earlier. VCXO Control Voltage trim range adjustment is accomplished with a varactor diode so that a control pot can be mounted external to the Physics Package.

M-1000 PERFORMANCE CHARACTERISTICS

The most challenging design requirement is the ultra fast warm-up. This task is accomplished by a combination of several concepts discussed earlier. They are: (a) smaller cell/lower mass Physics Package, (b) use of SC-Cut Crystal, (c) use of blanket heater on lamp and cell, (d) special constant power heater control using pulse width modulation, and (e) a fast sweep circuit in the Servo Hybrid.

These factors contribute to the M-1000 warm-up time shown in Figure 10. The off-the-shelf M-100 standard warm-up and fast warm-up options are illustrated for reference. The approximate output frequency that can be expected during warm-up is shown in Figure 11. The frequency will be in the range of $\sim \pm 3 \times 10^{-6}$ until atomic lock. 15 to 20 seconds after the sweep circuit stops, the frequency will be $\sim 5 \times 10^{-10}$. Shortly thereafter, parts in 10^{11} can be expected.

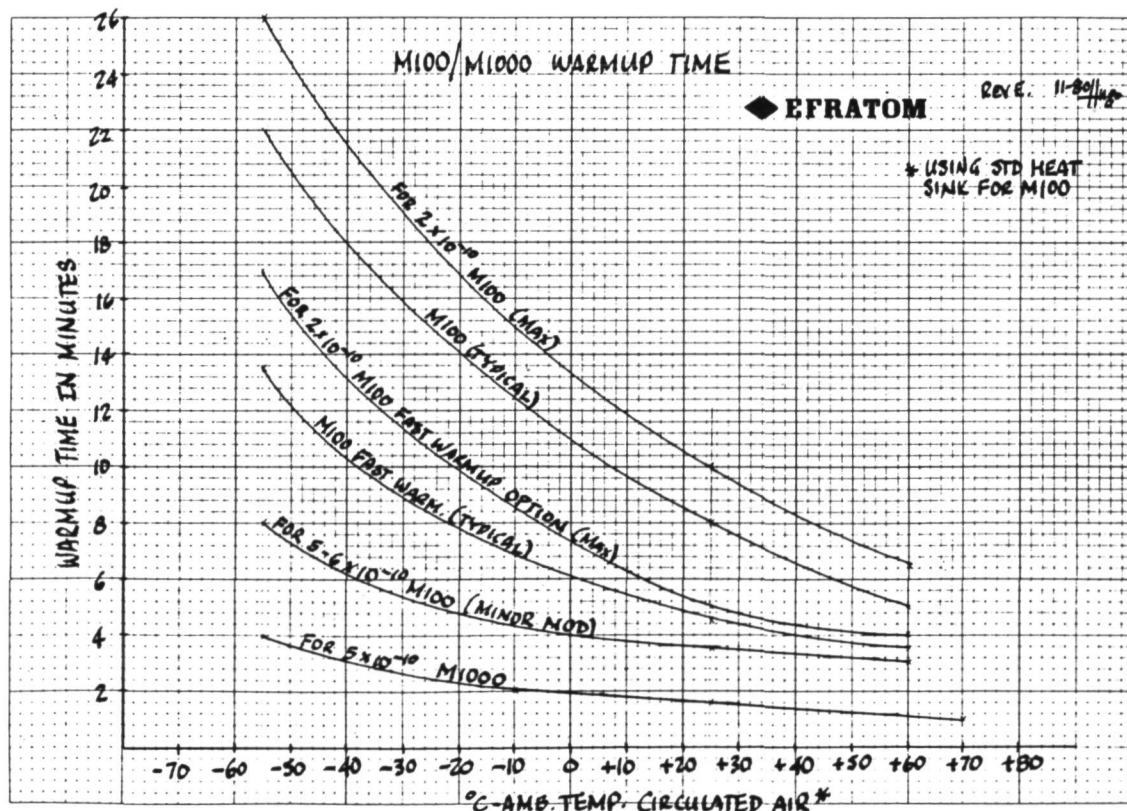


Figure 10. Warm-up Time

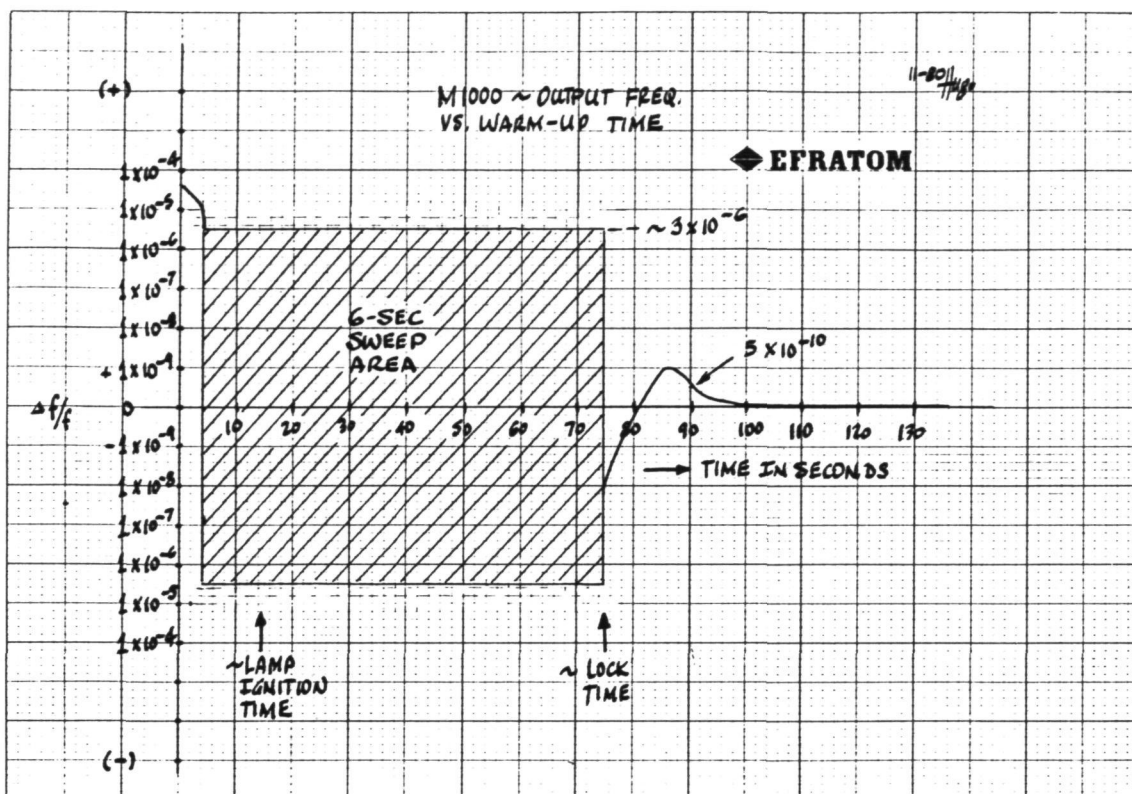


Figure 11. Output Frequency During Warm-up

The M-1000 power dissipation is expected to be 12 watts or less (steady state at 25°C) see Figure 12. A goal of 8 to 10 watts is set for second and third generation units. VCX0 performance is expected to be similar to the M-100 spec. The short-term stability is shown in Figure 13 and phase noise in Figure 14. Magnetic field susceptibility is expected to be a factor of 8 to 10 better than M-100 spec and is illustrated in Figure 15.

At present satisfying solutions have been found for all SEEKTALK requirements and environmental specs with the exception of sine and random vibration performance. These specs are most challenging and extremely difficult to meet. Typical performance under a 1 g sine environment for an M-100 style Physics Package is illustrated in Figure 16. These data are exaggerated, however, since the sweep is extremely slow and tends to amplify the response of the unit at the modulation frequency and it's harmonics.

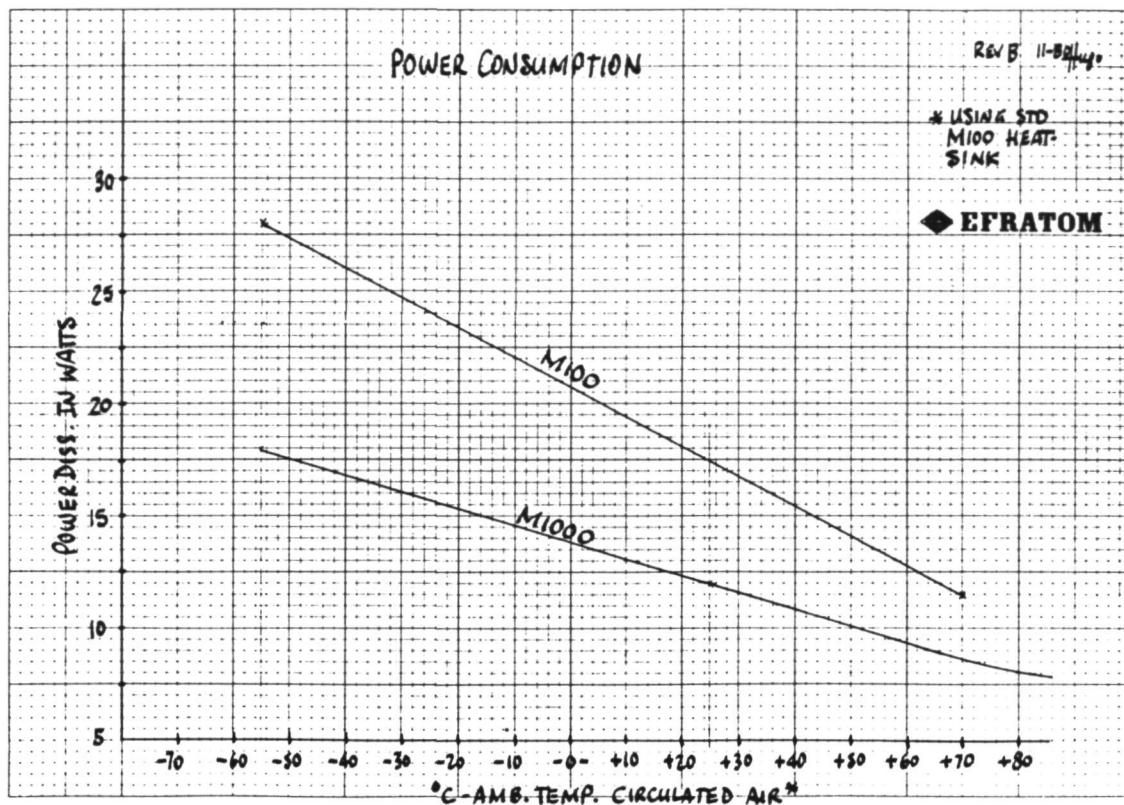


Figure 12. Power Dissipation

Figure 17 shows considerable improvement when the M-100 is modified with the 254 Hz M-1000 servo scheme. This scheme, plus the new M-1000 mechanical approach to the Physics Package should provide a significant improvement over the M-100 data and will certainly make vibration frequencies below 250 Hz less influential. Present M-100 performance at 1 g is parts in 10^8 peak to peak at the modulation frequency; M-1000 performance is expected to be in parts in 10^{10} . Under random vibration, M-100 performance is $< 1 \times 10^{-10}$ at $0.02 \text{ g}^2/\text{Hz}$ at $\tau = 1$ second. This is still considerably higher than the $< 1 \times 10^{-10}$ requirement which is the present SEKTALK spec in a $0.04 \text{ g}^2/\text{Hz}$ environment.

Rb OSCILLATOR "LIFE" CONSIDERATIONS

Useful field life of any electronic equipment or system is generally evaluated in light of hardware peculiarities which will in time render the equipment at a life-limit. This analysis usually excludes random parts failures but is oriented toward wear-out mechanisms.

The M-100/M-1000 oscillator "life" limit revolves around the aging characteristics of the Rubidium Vapor Cell; assuming the Rb lamp has no

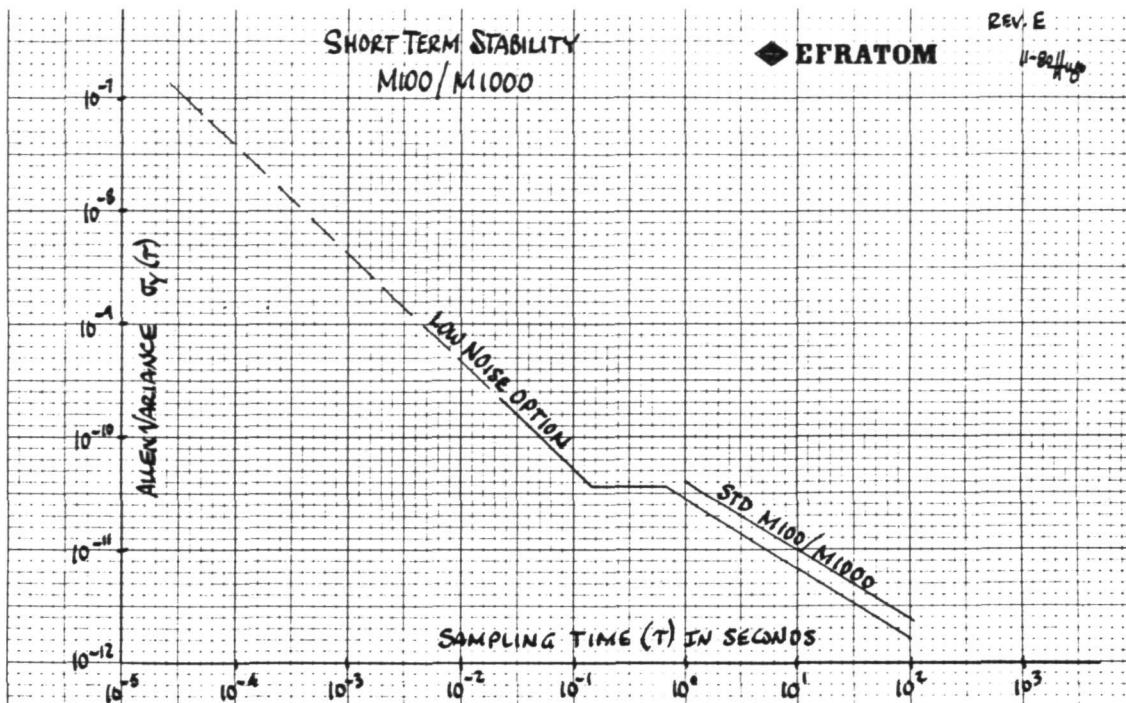


Figure 13. Short Term Stability

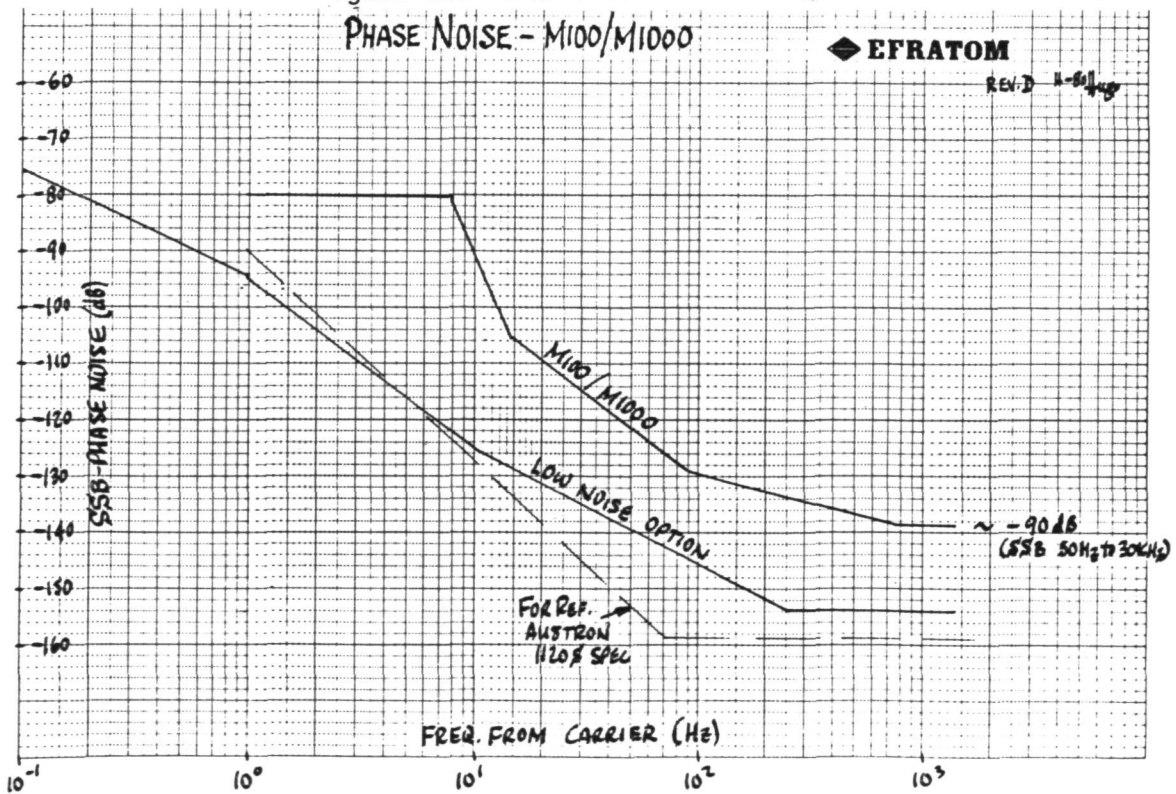
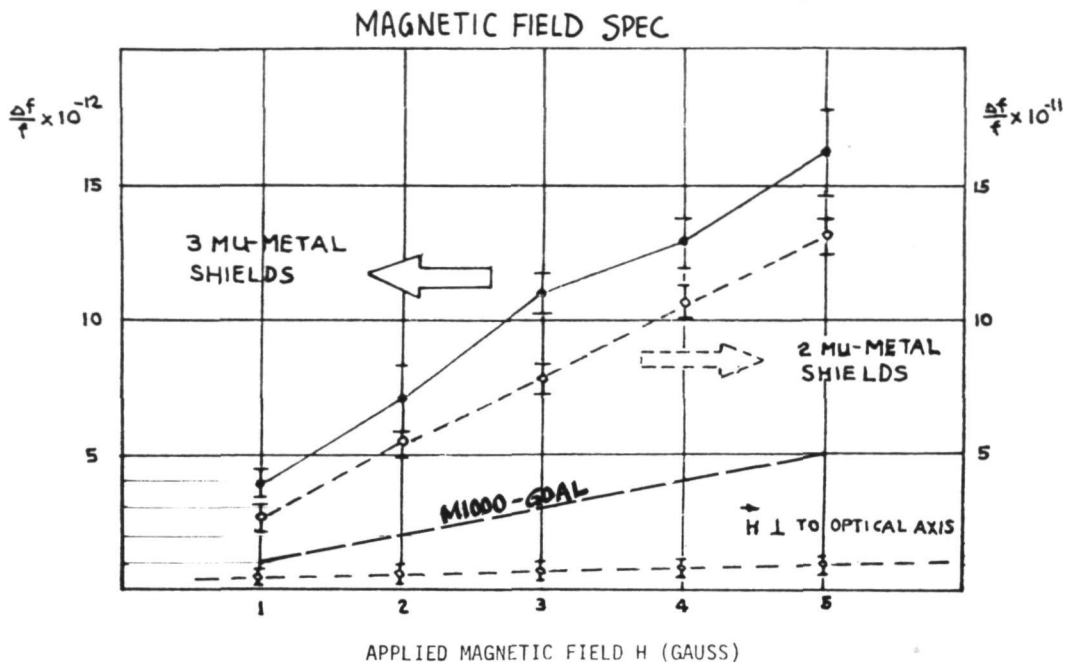


Figure 14. Phase Noise



FRACTIONAL FREQUENCY CHANGE OF THE MODEL FRK-H DUE TO A
STATIC MAGNETIC FIELD APPLIED PARALLEL TO THE OPTICAL AXIS

Figure 15. Magnetic Field Susceptibility

systematic wear-out mechanisms, which it does not, if everything is done properly. When the cell is manufactured, it is made with a deliberate negative off-set of approximately $\geq 4 \times 10^{-9}$ which is zeroed by the addition of a magnetic field (C-field). With a C-field trim range of $\pm 1.5 \times 10^{-9}$, the oscillator will allow normal adjustments as long as the frequency of the cell has not aged past the $\Delta f/f$ equivalent of (+) 1.5×10^{-9} of 10 MHz.

As can be seen in Figure 18, the typical oscillator will begin to age at a rate of (-) $3 \times 10^{-11}/\text{mo}$ for about 5 to 6 months while steadily improving to $\leq 1 \times 10^{-11}/\text{mo}$. After the initial (-) aging, the oscillator may drift (+) or continue (-). Long-term aging data show that the oscillator will not always drift in the same direction. The data also show, however, that the typical oscillator, while operating, continues to improve, with the monthly drift tending to decrease in magnitude. Aging improvements have also been observed for stored units with the extent of the improvement depending on the storage temperature. For illustration purposes, Figure 18 shows three curves. Curve (a) is for a typical oscillator that, after 5 to 6 months, continues to age always negative (best case). In this case, the frequency off-set that accumulates can be cancelled by increasing the magnetic field (C-field current). Under these conditions, the normal C-field trim range of $\pm 1.5 \times 10^{-9}$ will have been reached in

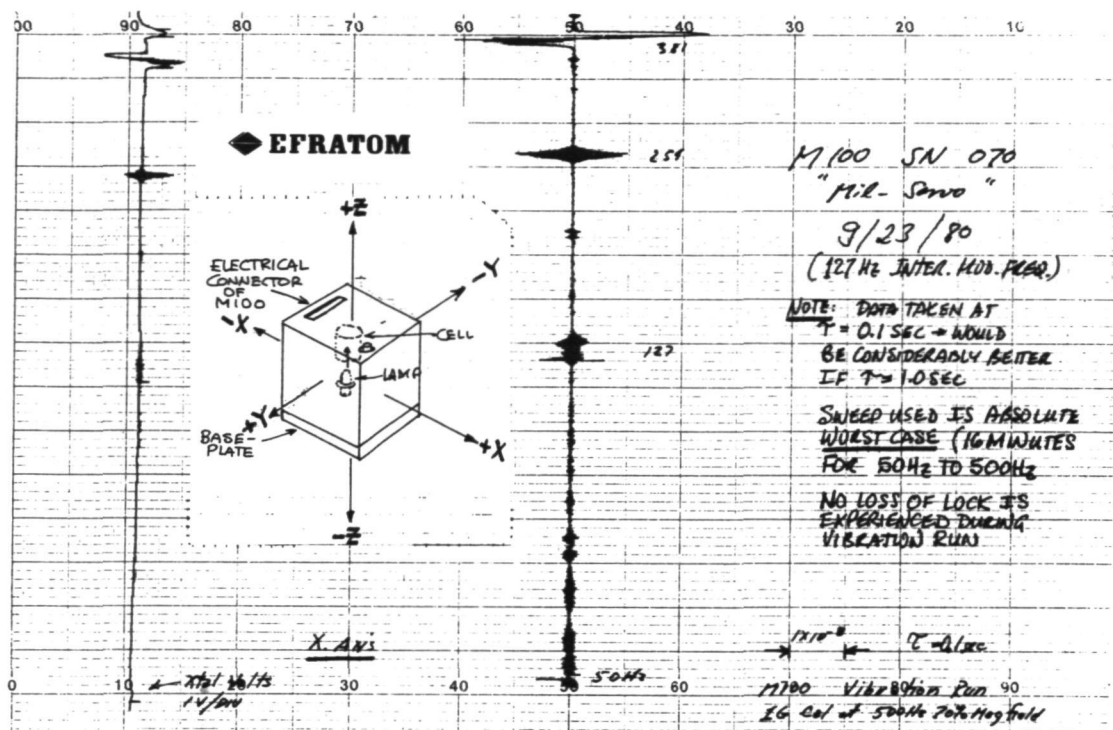


Figure 16. Sine Vibration Data - 1 g
(127 Hz Modulation)

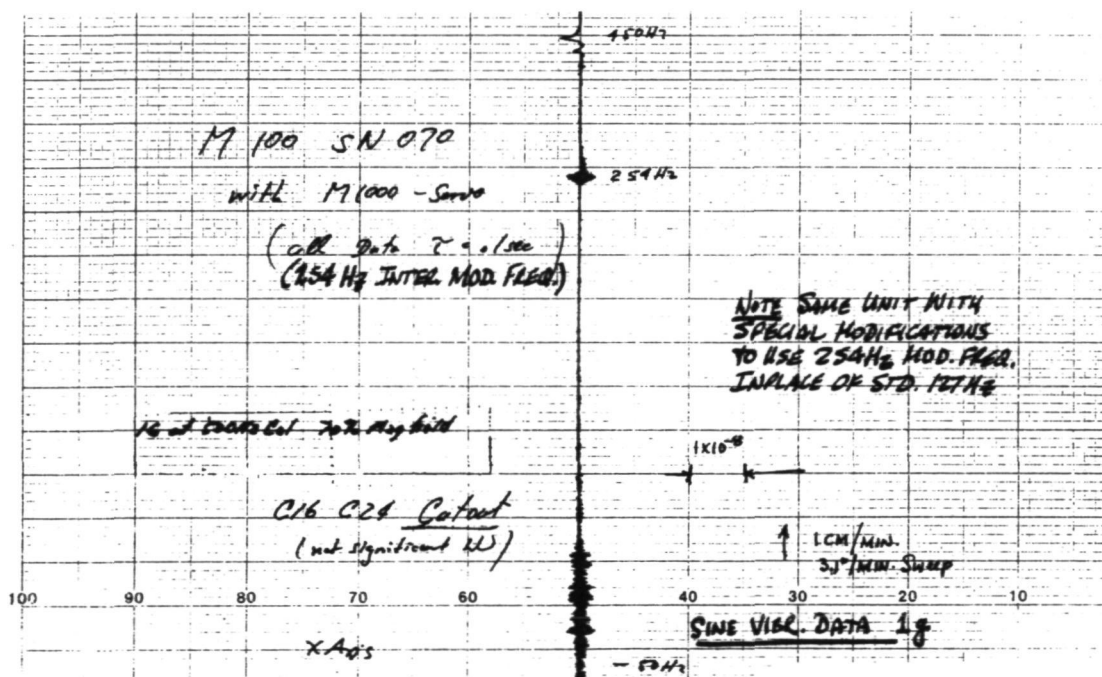


Figure 17. Sine Vibration Data - 1 g
(254 Hz Modulation)

~ 11 years. In practice, magnetic field can be added at that time but at a degradation of unit magnetic field spec; doubling the C-field current approximately doubles the external field sensitivity. For example, if we allow a degradation of the shielding factor of $\sim 50\%$, the end of the useful life will be reached after ~ 80 years.

Curve (b) applies for the case of an oscillator that, after the first 5 to 6 months, ages continually positive. Here the $\sim 3 \times 10^{-9}$ point is reached in approximately 35 years. Since the positive aging cell requires a reduction in magnetic field, the cell at this point is for practical purposes at zero magnetic field. As aging continues past this point, the oscillator will still operate in a completely stable fashion (according to spec), but it will no longer be possible to zero the offset that will gradually accumulate.

The third case, curve (c), is absolutely the worst case and as far as we know, has never occurred. In this phase, the oscillator ages continuously positive at the constant rate of $3 \times 10^{-11}/\text{mo}$, reaching zero frequency off-set at zero magnetic field after approximately 11 years.

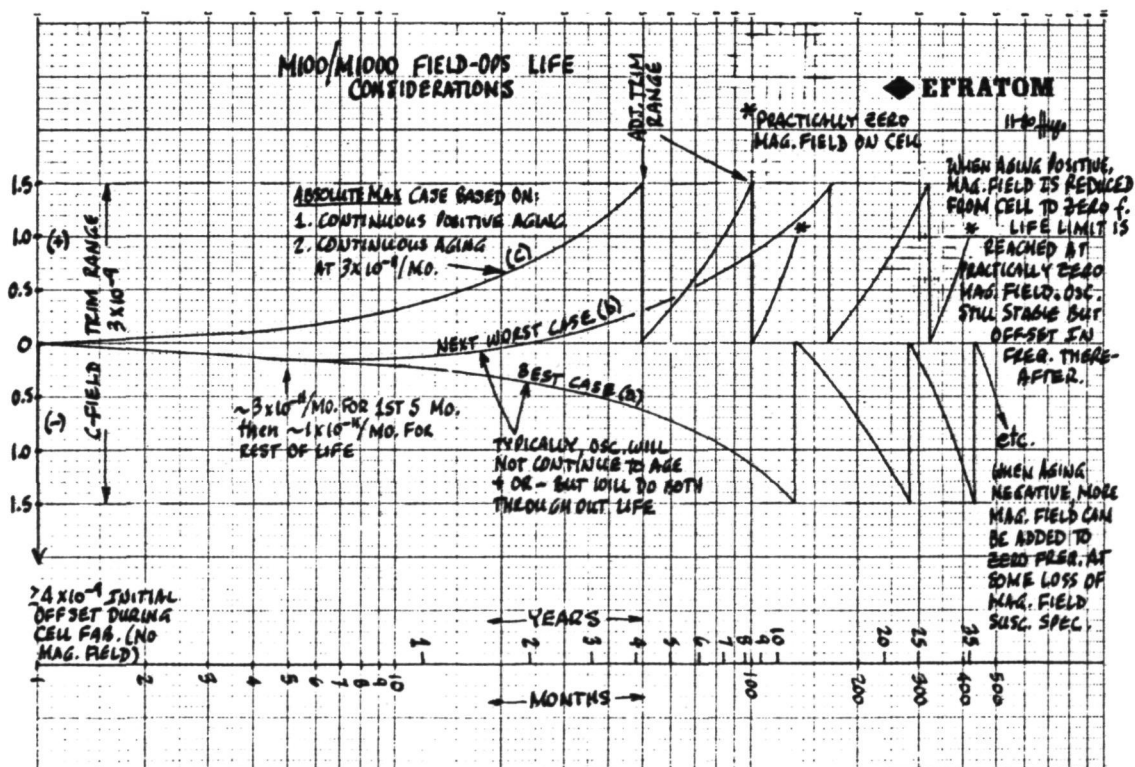


Figure 18. Oscillator Life

MISSION PROFILE

Figure 19 illustrates an arbitrary mission profile and resultant oscillator performance. The concept for a precision timing system for tactical aircraft, revolves around the ability to have an oscillator within parts in 10^{10} , 1.5 minutes after engine start (assuming no battery power is available prior to that time). This ability provides ample time for a timing-sync (possibly RF linked) before aircraft is very far from its origin, minimizing RF link propagation delay errors. Due to the accuracy and retrace ability of the Rb oscillator, frequency sync would not be necessary prior to a mission as long as a periodic calibration plan is in effect. The 1.5 minute warm-up capability would appear to greatly simplify the tactical system. No battery power is required on the aircraft and no external warm-up scheme is needed.

Factors which have the most significant effect on oscillator time error are temperature changes and vibration. The least impact are voltage variations, magnetic field changes, and acceleration. Oscillator aging

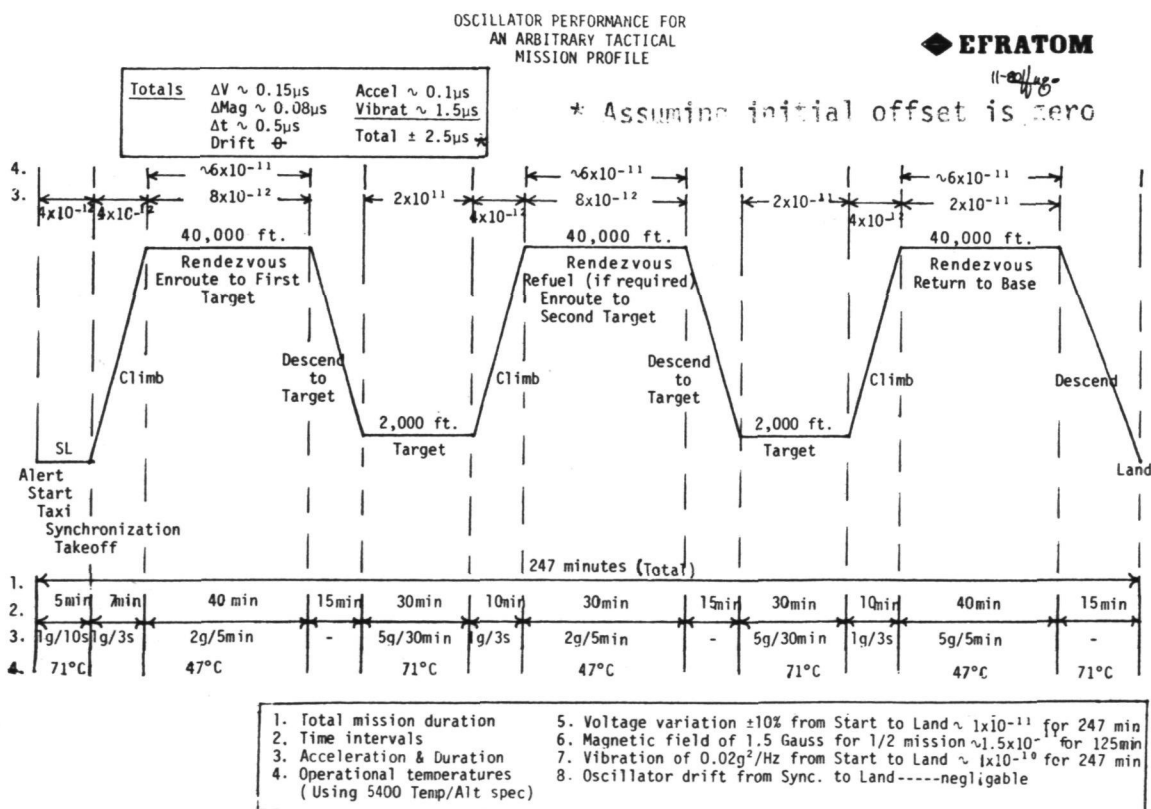


Figure 19. Typical Mission Profile

or drift is negligible. Since the oscillator is used as a clock, many of the environments such as magnetics and vibration should have a somewhat cancelling effect with only residuals influencing the time error.

Preliminary data has been received from Edwards Air Force Base for flight tests of similar mission profiles using shock-mounted EFRATOM commercial FRK-L units. The data indicates an accumulated time error scatter of ~ 1.3 to $12.1 \mu\text{s}$. Flight duration of these tests varied between ~ 7 to 11 hours.

CONCLUSION

We are proceeding with full speed to complete this new M-1000 development in mid 1981 to meet the SEEKTALK schedule. Several prototype units will be delivered to RADC at that time for test and evaluation. We believe that the 1.5 minute warm-up atomic oscillator will revolutionize the tactical warfare theater and will greatly improve the present-day military communication and navigation system capabilities.

The major portion of the Hybrid vendor costs for the initial prototype units is being funded by RADC.

SUMMARY OF ENVIRONMENTAL PERFORMANCE

0 VIBRATION^Δ

M100

M1000

(REALISTIC) - 0.02g²/Hz, 20-50Hz, SLOPING
to 0.001g²/Hz at 500 Hz
(~ 1.6g rms)

1×10^{-10} , $\tau = 1 \text{ sec}^*$
AT-CUT XTAL
0.2 $\mu\text{sec}/\text{HR}^*$

BETTER; WILL USE
SC-CUT XTAL
< 0.2 $\mu\text{sec}/\text{HR}$

(SEEKTALK) - 0.04g²/Hz ~ FLAT 1.5 - 500Hz
(~ 4.4g rms)

PARTS 10^9 , $\tau = 1 \text{ sec}$
AT-CUT XTAL

SHOULD BE MUCH
BETTER:
(SEEK-TALK SPEC IS
 1×10^{-10})

5 $\mu\text{sec}/\text{HR}$

*

0 MAGNETICS - 180° TURN (MAX EARTH FIELD)

SPEC 3 to 5×10^{-11}
ACTUAL ~ 1×10^{-11}

PARTS IN 10^{12}

0 ALTITUDE - S.L. to 40K ft
(NEGLECTING TEMP Δ)

(-) ~ 7×10^{-11}

SAME; POSSIBLY
BETTER

0 TEMPERATURE - (RAISING Δ +25°C)

(+) ~ 1×10^{-10}

(+) ~ 6×10^{-11}

0 ACCELERATION - (WORST AXIS)

(-) ~ $4 \times 10^{-12}/g$

BETTER

^ΔNOTE: Edwards AFB - Modified Thunderbird Tests
- Shock Mounted Commercial FRK
~ 1.3 μs to ~ 12.1 μs for Test Durations
~ 7 to 11 HRS.

*12-2-80 TEST DATA ON
#018, #111 M100 UNIT

QUESTIONS AND ANSWERS

MR. SAMUAL WARD, Jet Propulsion Laboratory

Have you considered whether or not the so-called vibration or gravitational effects on the unit may be induced currents that are getting into the XVCO loop?

MR. FRUHAUF:

You mean, on the vibration table?

MR. WARD:

Correct.

MR. FRAUHAUF:

Yes, we have checked very carefully the magnetic fields that are set up on the vibration head, and we have got that pretty well nailed down.

MR. WARD:

Was the power supply -- how much of the unit was being shaken?

MR. FRUHAUF:

In these particular tests?

MR. WARD:

Yes.

MR. FRAUHAUF:

The entire unit.

MR. WARD:

Shielding and all.

MR. FRUHAUF:

Right. We have been sensitive to that area, so we characterized the table very carefully before we draw a lot of conclusions from the data.

MR. WARD:

It looks suspicious because the power goes up as the vibration frequency goes up.

MR. FRUHAUF:

What goes up, please?

MR. WARD:

The power -- the effect -- how much it is being pulled off frequency, which appears to me power related.

Normally, as you shake it faster, that should go down.

MR. FRAUHAUF:

It is primarily related to resonances in the system. It is definitely not the magnetic field from the shake table.

THE NATO III 5 MHZ DISTRIBUTION SYSTEM

A. Vulcan and M. Bloch
(Frequency Electronics, Inc.), New Hyde Park, New York

ABSTRACT

This paper describes a high performance 5 MHz distribution system having extremely low phase noise and jitter characteristics and providing multiple buffered outputs. The system is completely redundant with automatic switchover and is self-testing. Faults can be isolated to a modular level by observing front panel status indicators. Since the 5 MHz reference signals distributed by the NATO III distribution system are used for up-conversion and multiplicative functions, a high degree of phase stability and isolation between outputs is necessary. Unique circuit design and packaging concepts are utilized to insure that the isolation between outputs is sufficient to guarantee a phase perturbation of less than 0.0016° when other outputs are open circuited, short circuited or terminated in 50 ohms. The circuit design techniques include high isolation cascode amplifiers, the use of negative feedback to stabilize system gain and minimize circuit phase noise contributions, the use of balanced lines in lieu of single ended coaxial transmission media to minimize pickup and degradation of noise floor and the development of simplified fault detection and switchover circuitry to insure continuous operation.

The distribution system is fed by redundant high stability quartz frequency standards which use special crystals with low phase noise and jitter and a daily aging rate better than 5×10^{-11} .

INTRODUCTION

A 5 MHz signal generation and distribution system is described which provides the basic reference frequencies for both a transportable and fixed satellite ground station. The system has extremely low vibration induced phase jitter and high isolation between outputs. Both of these characteristics are required for the NATO III satellite terminal mission. The system is modular and self-testing and any modules can be replaced without disturbing system operation.

SYSTEM DESCRIPTION

The block diagram of Figure 1 shows how a dual frequency standard, Primary Distribution Unit (PDU) and Secondary Distribution Unit (SDU), are interconnected to provide a failsafe system having fifty-six 5 MHz outputs, four 1 MHz outputs and four 100 kHz outputs. Two frequency standards in the Frequency Generation Unit (FGU) provide redundant, stable, low noise signals for the system input. The Electronic Switch Module (ESM) in the PDU accepts the 5 MHz input and feeds it to two Primary Distribution Modules (PDM). The dual electronic switches provide redundancy in the event of failure of either frequency standard, interconnecting cable, or ESM. The Primary Distribution Module receives the redundant 5 MHz inputs and provides seven balanced outputs which feed various Secondary Distribution Units which can be located up to 500 feet from the PDU. Although the PDU, SDU and dual frequency standards comprise the NATO III station distribution system, the SDU can stand alone as a totally independent fifty-six channel low noise distribution system. Interconnection between the PDU and SDU is accomplished on a redundant basis such that the failure of either balanced interconnecting cable or PDM will not effect the final output signal. The requirement for low spurious signals and phase noise necessitates the use of double shielded RG-22B/U twinaxial 95 ohm balanced cable. The entire signal transmission system is isolated from the environmental ground reducing the pickup of unwanted signals due to ground loops and non-common mode noise. Table 1 lists the performance characteristics of the system and Figures 2 and 3 are the detailed block diagrams for the PDU and SDU, respectively.

An amplitude limiting circuit in the SDU Preamplifier Module (PAM) maintains a constant output level of +5 dBm from the SDU over a wide range of input signal levels. This is important so as not to affect the operation of user equipment when interconnecting cables are disconnected or a PDM module in the PDU is removed. Seven independent modules each having eight outputs comprise the balance of the SDU.

The equipment is designed to operate from American or European ac main voltages and frequencies. Dual power regulators ensure that 60 Hz and 120 Hz line related phase modulations are reduced to negligible levels. A high current regulator in each of the dual power supplies and an additional three-terminal device in each module provides 0.01% line regulation with 150 microvolts of noise. An additional benefit of this system is that radiated susceptibility of the equipment from pickup of extraneous signals from colocated high power RF devices is minimized since the module regulators have the ability to reject interfering input signals by at least 80 dB from 30 Hz to 10 kHz and 40 dB up to 300 kHz. Additional RF filtering is used to meet the EMC requirements up to 18 GHz.

Each active circuit which is critical to system operation is failure-detected. Diode detectors are used for RF alarm generation and micrologic comparators sense the degradation of signal level below a preset value. The alarm signals are summed in each particular subsystem and fed to a common point where an output is provided to external monitoring equipment. Additionally, front panel indicators on the various modules visually indicate the occurrence of a failure or out of spec condition.

The system is designed such that removal or replacement of any module can be effected without causing intolerable phase or amplitude perturbations on other active outputs. This design insures that 5 MHz perturbations which can be multiplied 1000 to 2000 times in subsequent chains of frequency multiplications do not cause system outages. Minimal phase perturbations are insured by the use of high isolation amplifiers and a high degree of shielding between active circuitry.

CIRCUIT DESIGN

The following paragraphs describe two important functional blocks of the the distribution system.

RF Amplifiers

The amplifier stages used for 5 MHz processing in various parts of the system are cascode circuits with high isolation, low noise, and high dynamic range. This circuit is shown schematically in Figure 4. To meet the isolation requirement of 100 dB, special layout and packaging techniques were utilized. Circuit gain is controlled by the unbypassed emitter resistor which provides ac and dc stabilization of the circuit. Output transformation circuitry converts the collector impedance to 50 ohms with a source VSWR of 1.2 to 1. Good grounding techniques with minimization of base lead inductance and parasitic reactances are necessary to insure optimal performance of the circuit. In the case where a balanced 95 ohm output impedance is required, a small toroidal transformer is utilized to effect the impedance transformation.

Diode CR1 provides bias temperature compensation and CR2 is an RF detector. Capacitor C10 is selected for a detected output voltage of 0.25 volts at the nominal RF level. The dc voltage feeds a voltage comparator whose reference voltage is set to provide an alarm signal at a point approximately 1-1/2 to 2 dB below the minimum acceptable RF level. Thus, temperature effects and other drift parameters will not cause a false alarm.

The various alarm signals are fed into the alarm module in the PDU and preamplifier module in the SDU to generate a composite alarm. These alarm signals which are TTL compatible, are summed with externally generated alarms which are translated to the proper levels and

impedances before summation. In the case where the external alarm signals are fed from long twisted shielded pairs or are generated from relay contacts and/or noisy sources which may have high ac ground loop currents, optical couplers are used to isolate the noisy environment from the systems.

Limiting

The SDU must be capable of accepting an input dynamic range of 10 dB and maintain a constant output of $+5 \text{ dBm} \pm 1 \text{ dB}$. Hence, a limiting circuit is necessary which has low noise characteristics and a constant input and output impedance to properly terminate the power splitters and maintain high isolation. Figure 5 shows the limiter used to achieve these objectives. Closely matched back-to-back RF signal diodes limit the RF amplitude to ± 0.7 volts and the reflected power is absorbed in the hybrid terminations. The quadrature hybrids are implemented with lumped elements as shown in the figure.

PHASE PERTURBATION MEASUREMENT

Figure 6 is a block diagram showing how the 0.0016 degree 5 MHz phase perturbation requirement is verified. The 5 MHz input signal feeds two high isolation amplifiers. One amplifier output feeds a X1000 multiplier chain and is used as the unperturbed reference. The other amplifier output feeds the unit under test which then drives an identical multiplier. The 5000 MHz outputs are mixed to yield a dc signal where amplitude is proportional to the phase difference at the mixer inputs. The mixer output is amplified and fed to a high sensitivity oscilloscope. Prior to making a measurement, the variable phase shifter is adjusted for maximum outputs from the FE-6093A Microwave Test Set. This condition determines E_0 in the relationship $\Delta\phi = \sin^{-1}(\Delta e/E_0) \times 10^{-3}$ where $\Delta\phi$ is the 5 MHz phase perturbation and Δe is the change in dc output voltage. The phase shifter is then adjusted for zero volts at the oscilloscope input (point of maximum mixer sensitivity), and the system is perturbed. The value of Δe is noted and $\Delta\phi$ is calculated. For example, if E_0 is 1.50 volts and a Δe of 50 millivolts is recorded, $\Delta\phi$ equals 0.0015 degrees. This measurement technique is quite versatile and is used for measuring both steady state and transient phase shifts that occur from shock and vibration events, removing and replacing modules, changing load impedances, and varying ac voltage inputs.

MECHANICAL PACKAGING

A modular concept has been used for the frequency distribution subsystem in order to enhance maintainability, simplify logistics, and permit economic manufacturing. Figure 7 is a photograph of the FGU showing both quartz frequency standards and a phase comparator. Internal batteries are provided for 24 hours of operation without ac power.

Figures 8 and 9 show the PDU which consists of five different module types. Each module is totally enclosed and has an RFI filter compartment in order to preserve shielding integrity. The modules can be inserted or removed directly from the front panel without disturbing other modules. Each module has a power indicator and various status and fault lights. Front panel test points are provided for monitoring the redundant dc voltages. Figures 10 and 11 shows the mechanical construction of the SDU. This drawer consists of three different module types, preamplifier, distribution amplifier and power supply. Seven distribution amplifiers are used to provide the fifty-six outputs. Figure 12 shows the internal construction of a preamplifier module. Each amplifier section is shielded to maintain an isolation of 100 dB between outputs. The RFI filtering compartment is totally isolated and the input connector directly addresses this compartment. Power, command and alarm signals are RFI filtered at this interface.

ENVIRONMENTAL CONSIDERATIONS

The frequency distribution subsystem has been designed to meet the environmental specification shown in Table 1. Conservative component derating ensures that the equipment has a service life of 15 years. Performance specifications are met during high G inputs specifically encountered in transportable vans. Care has been taken to insure that microphonically induced phase and amplitude modulations are reduced to negligible levels. Critical circuit elements are staked in place using resilient adhesives and all RF interconnection cables are likewise encapsulated. The PC Boards are coated with a humidity resistant material. The circuitry has been designed to be essentially broadband in nature to minimize the effect of temperature variations on output levels. Over a range of 0 to +50°C, the level variation is less than +0.2 dB.

CONCLUSION

This paper describes a low noise frequency distribution system which is designed for continuous use in severe environments. The design stresses both long term reliability and electrical performance which emphasizes low spurious signals, low cross talk and low phase perturbations. The system consisting of a Frequency Generation Unit, a Primary Distribution Unit and a Secondary Distribution Unit has been qualified to MIL-E-16400 for environment and MIL-STD-461 for electromagnetic compatibility.

TABLE 1
PERFORMANCE CHARACTERISTICS
FREQUENCY DISTRIBUTION SUBSYSTEM

1. OUTPUTS:	FIFTY-SIX 5 MHz AT + 5 dBm FOUR 1 MHz AT + 13 dBm FOUR 100 KHz AT + 13 dBm ONE 50 KHz AT - 100 dBm
2. IMPEDANCE:	50Ω UNBALANCED, 95Ω BALANCED
3. VSWR:	1.2:1
4. PHASE PERTURBATIONS:	0.0016°
5. AMPLITUDE PERTURBATIONS:	0.01 dB
6. SPECTRAL PURITY:	- 120 dBc FROM 50 Hz TO 2 MHz OFFSET FROM CARRIER
7. PHASE NOISE:	2 dB ADDITIVE COMPONENT, - 165 dBc/Hz FLOOR
8. HARMONICS:	40 dB
9. FREQUENCY STABILITY:	1×10^{-9} /MONTH, 2×10^{-12} /SECOND
10. MICROPHONICS:	1×10^{-9} /G
11. MTBF:	30,000 HOURS
12. EMC:	MIL-STD-461
13. VIBRATION:	2.5G FROM 2 Hz TO 500 Hz
14. SHOCK:	15G FOR 11 mSECOND
15. HUMIDITY:	95% RELATIVE
16. TEMPERATURE:	- 20°C TO + 65°C

ASSOCIATED BLOCK DIAGRAMS

1. PDU D31104-7591

2. SDU D31204-7592

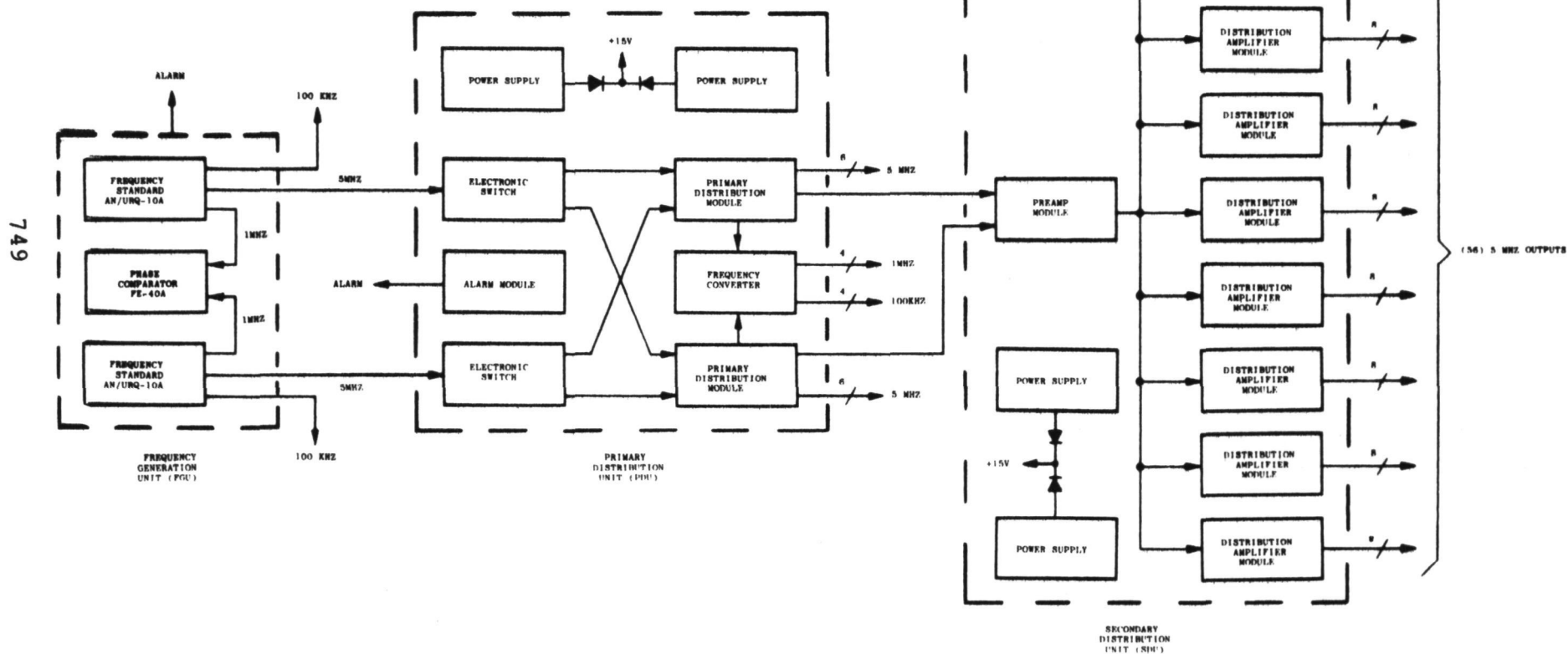


Figure 1. Frequency Distribution Sub-System Block Diagram

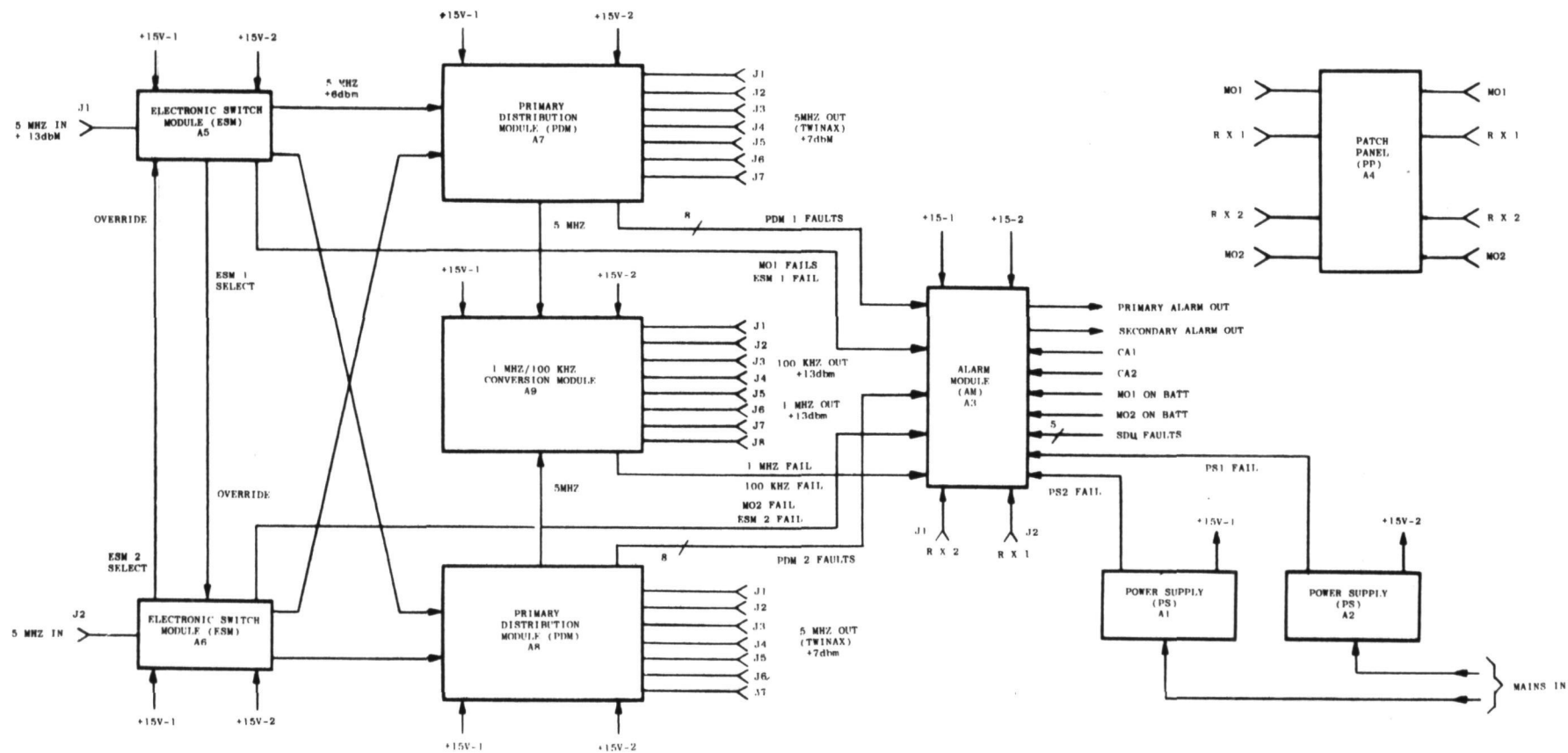


Figure 2. Primary Distribution Unit (PDU), Model FE-798A,
Block Diagram

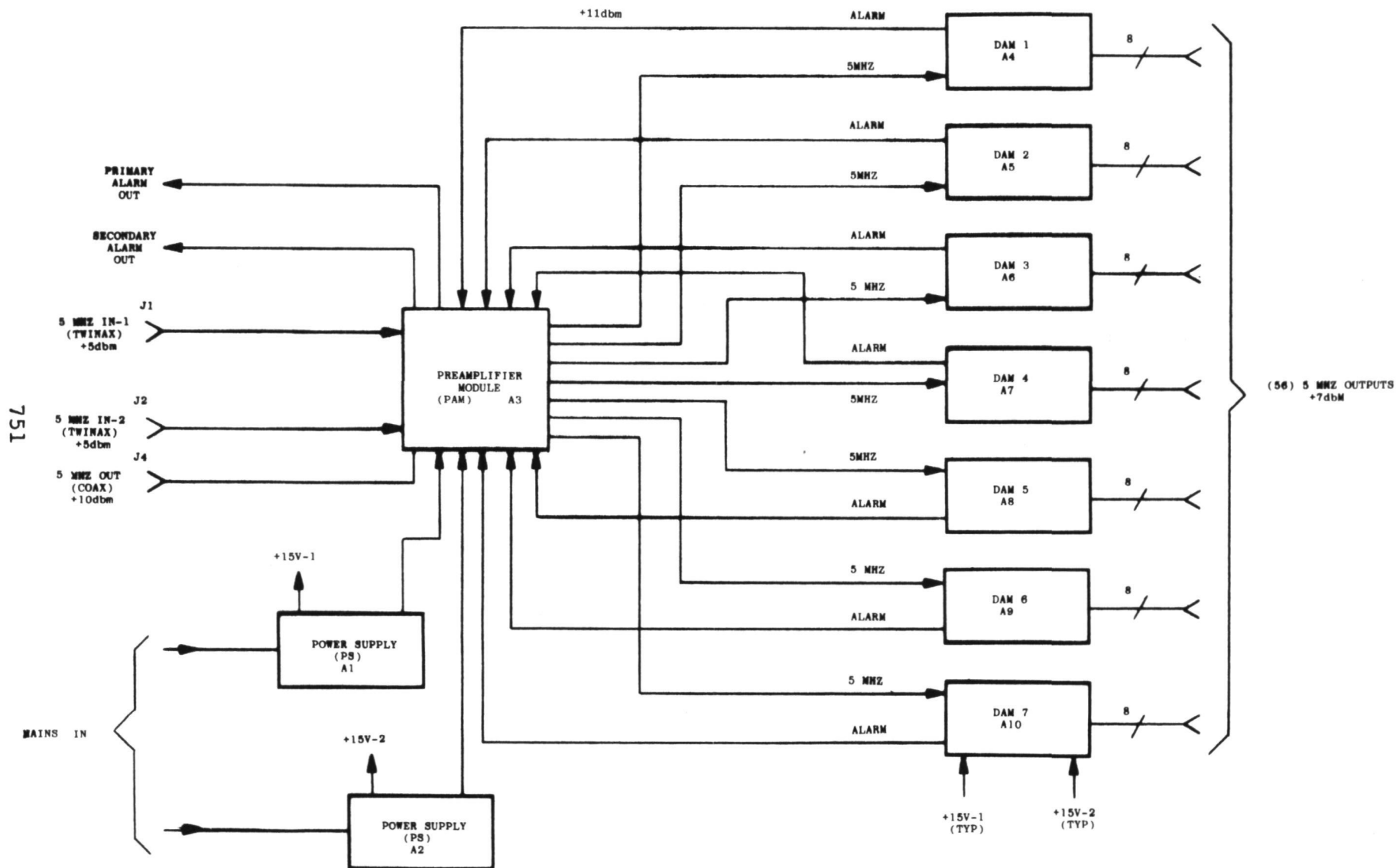


Figure 3. Secondary Distribution Unit (SDU), Model FE-799A

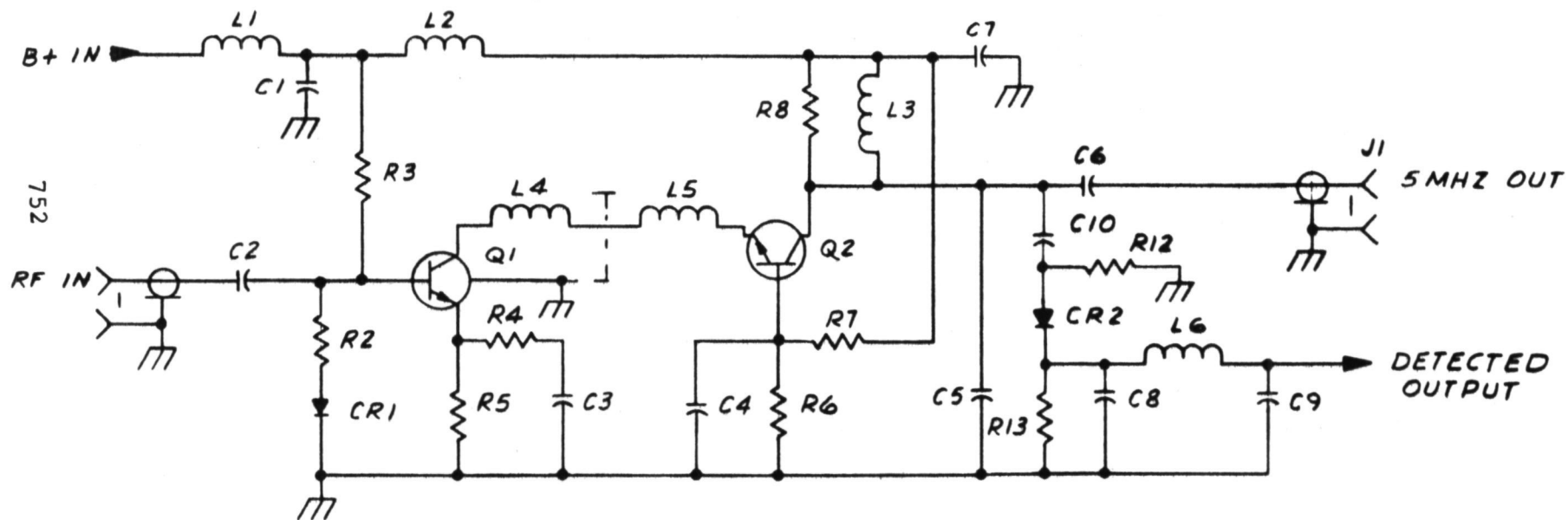


Figure 4. Cascode Amplifier, Schematic Diagram

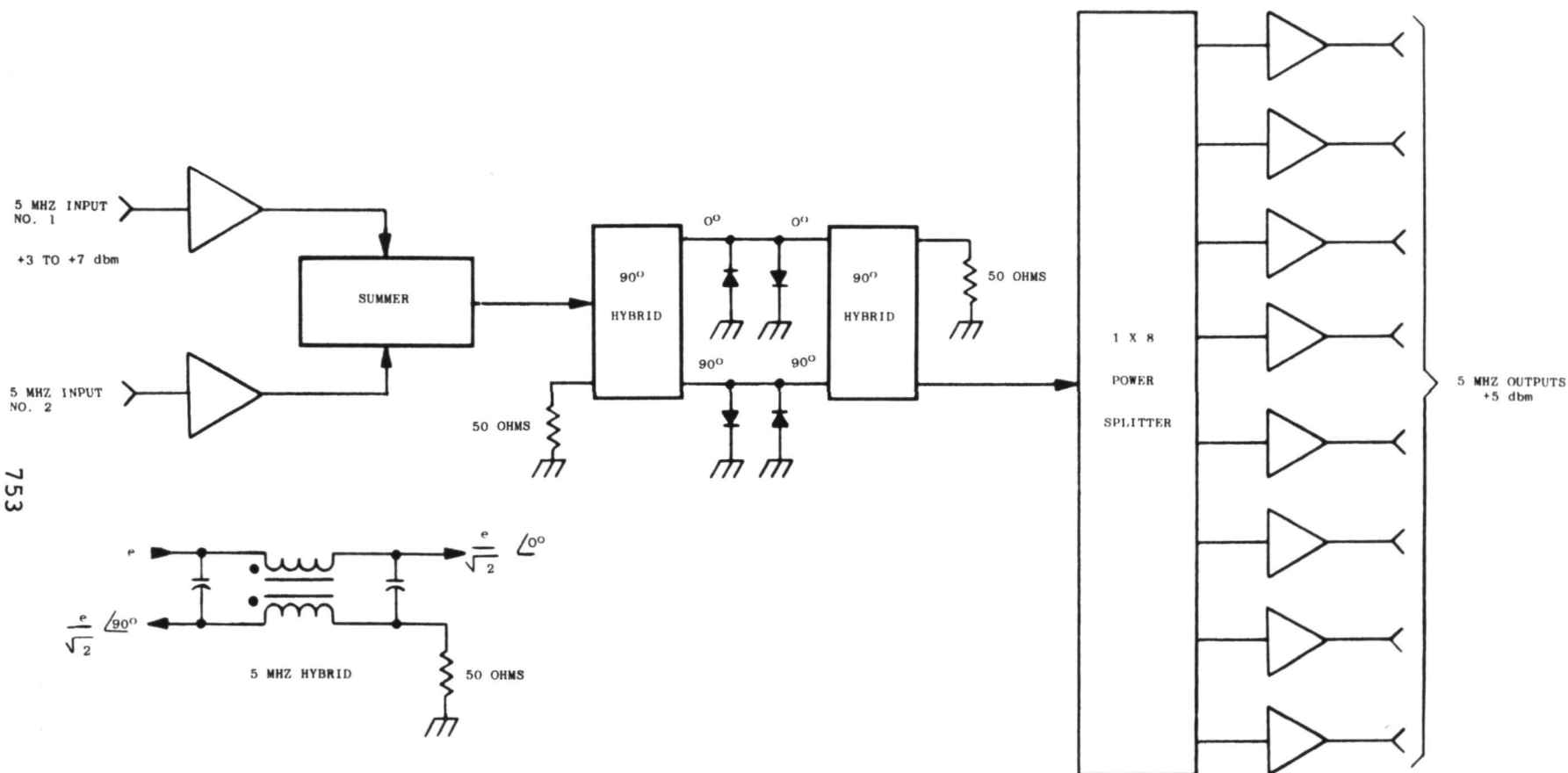


Figure 5. Block Diagram, Constant Impedance Limiter

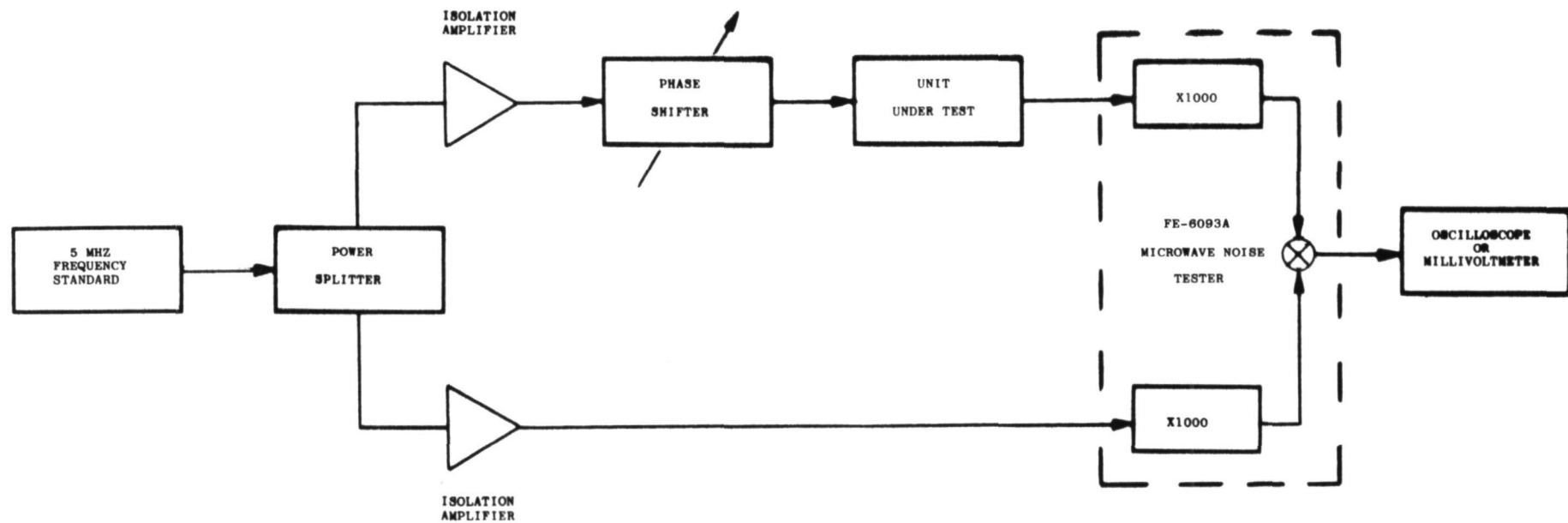


Figure 6. Test Set-Up, Phase Perturbations, Block Diagram

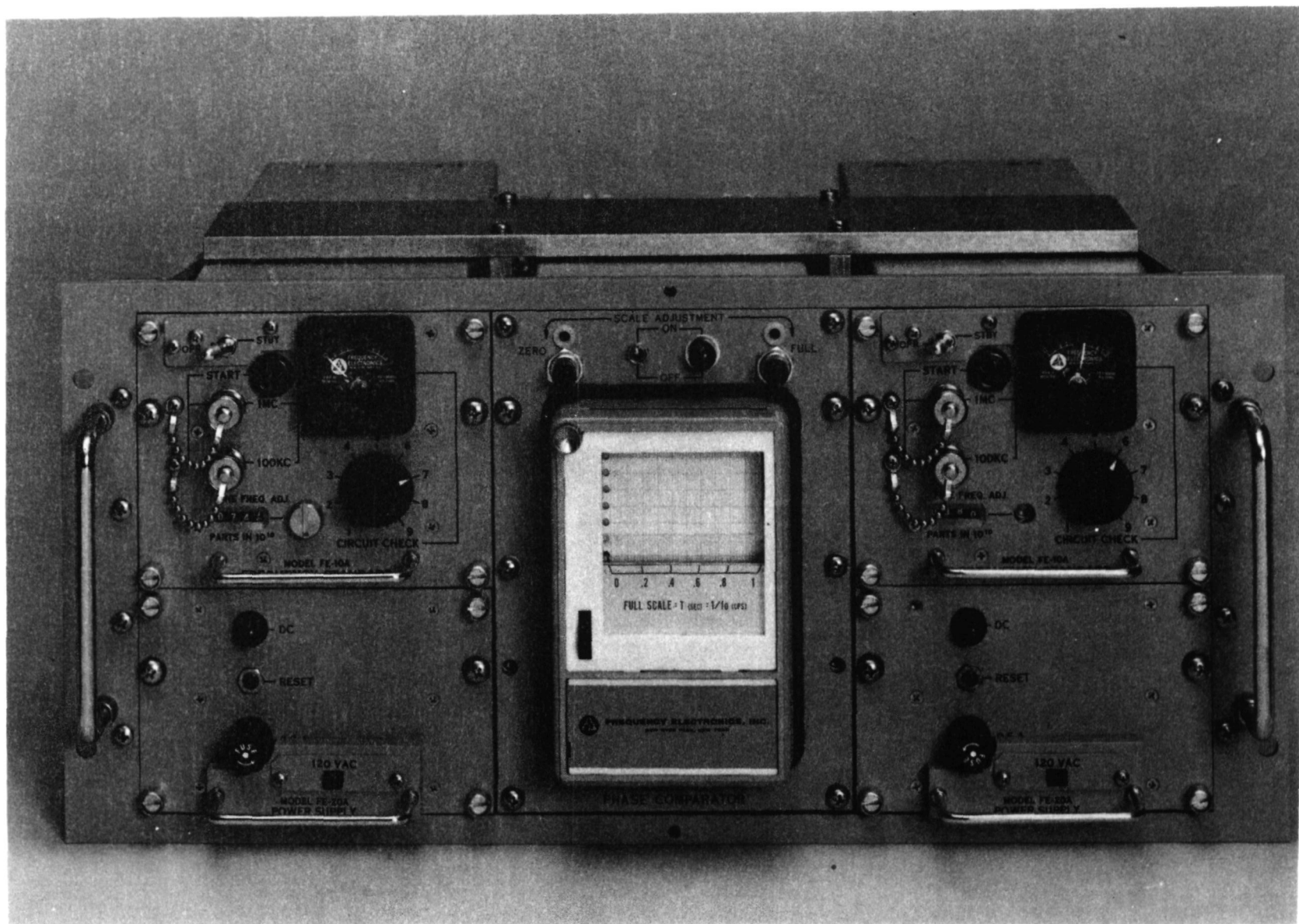


Figure 7. Frequency Generation Unit (FGU), Model FE-5066A,

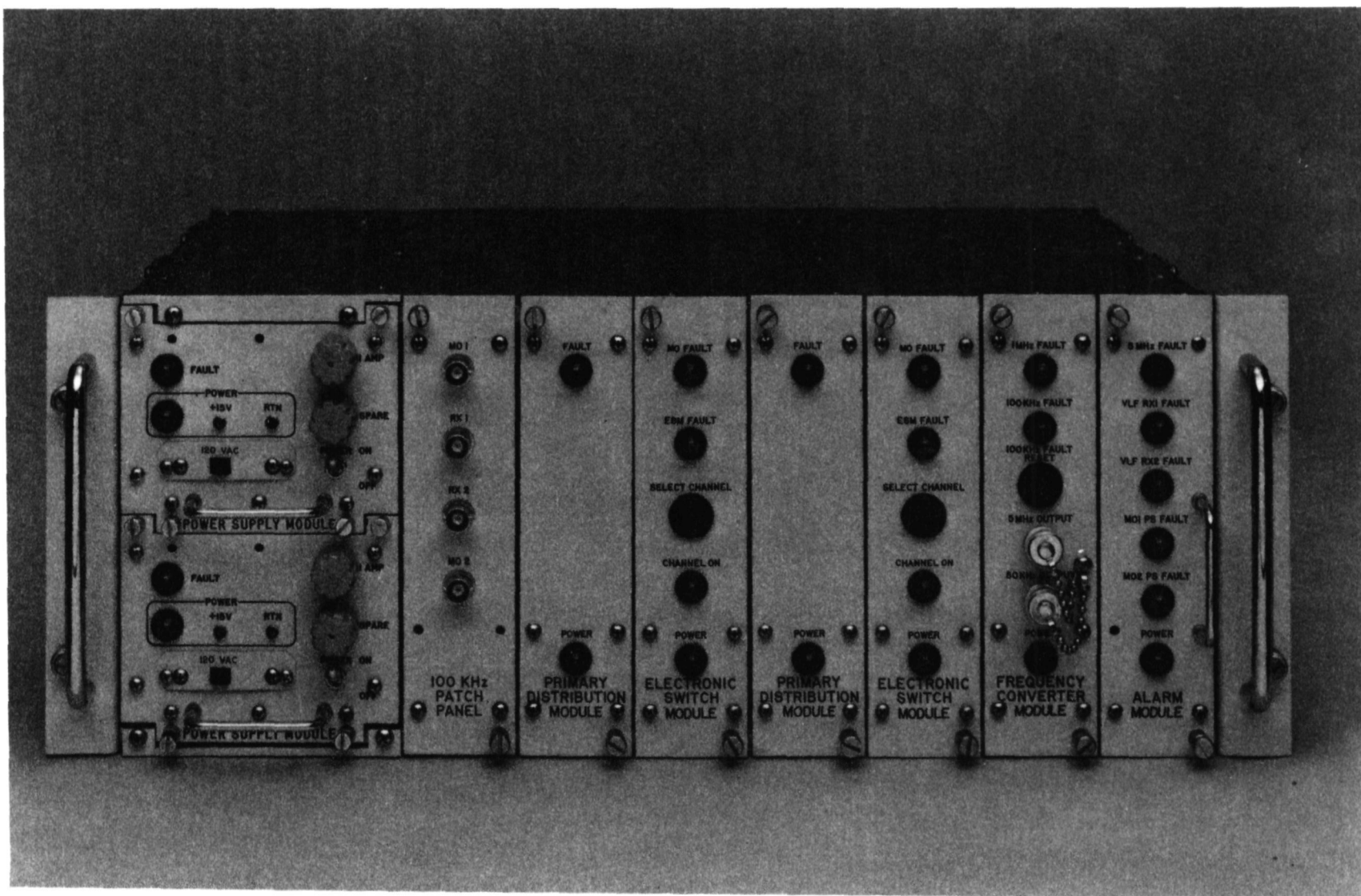


Figure 8. Primary Distribution Unit (PDU), Front View
Model FE-798A,

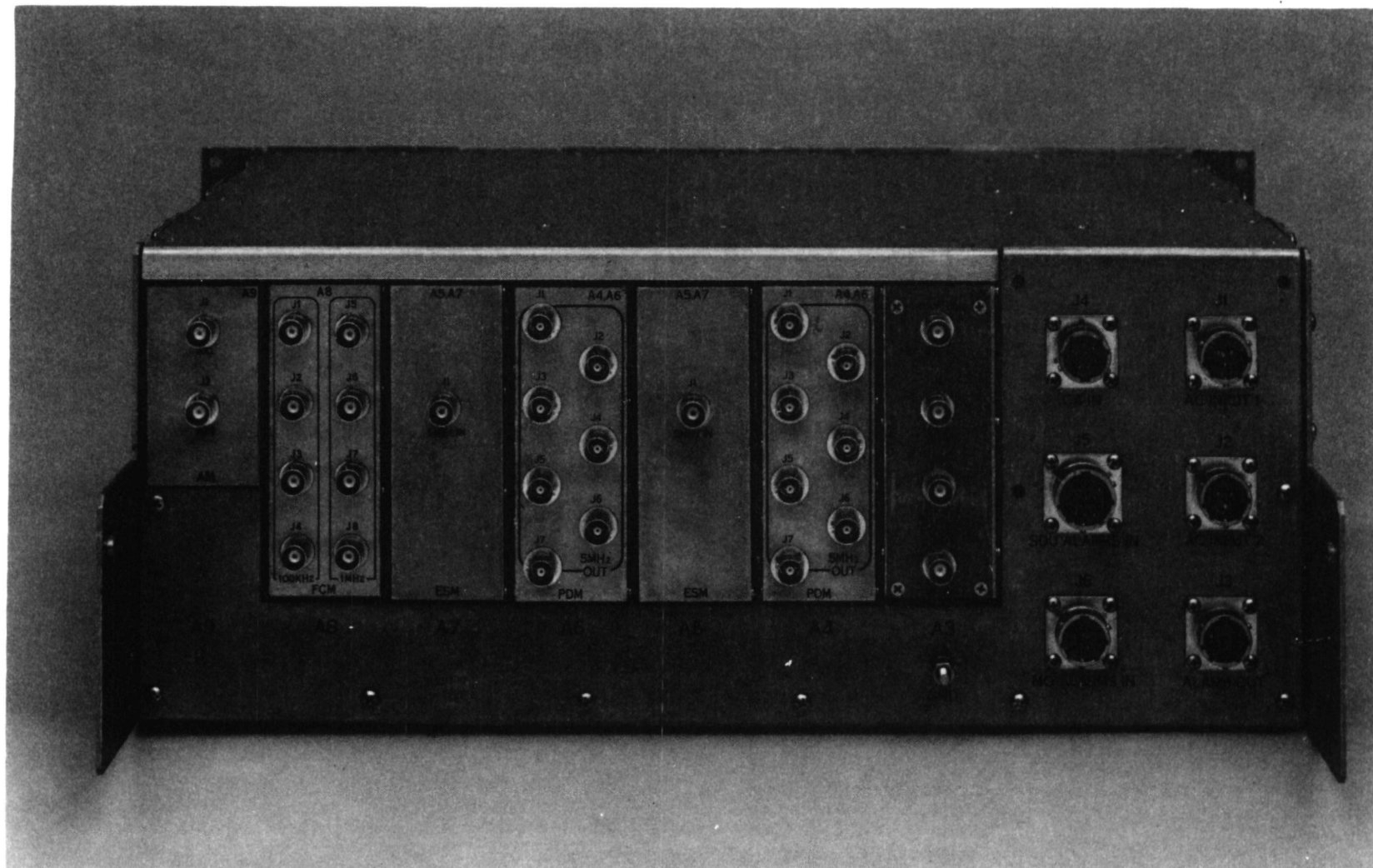


Figure 9. Primary Distribution Unit (PDU), Rear View
Model FE-798A

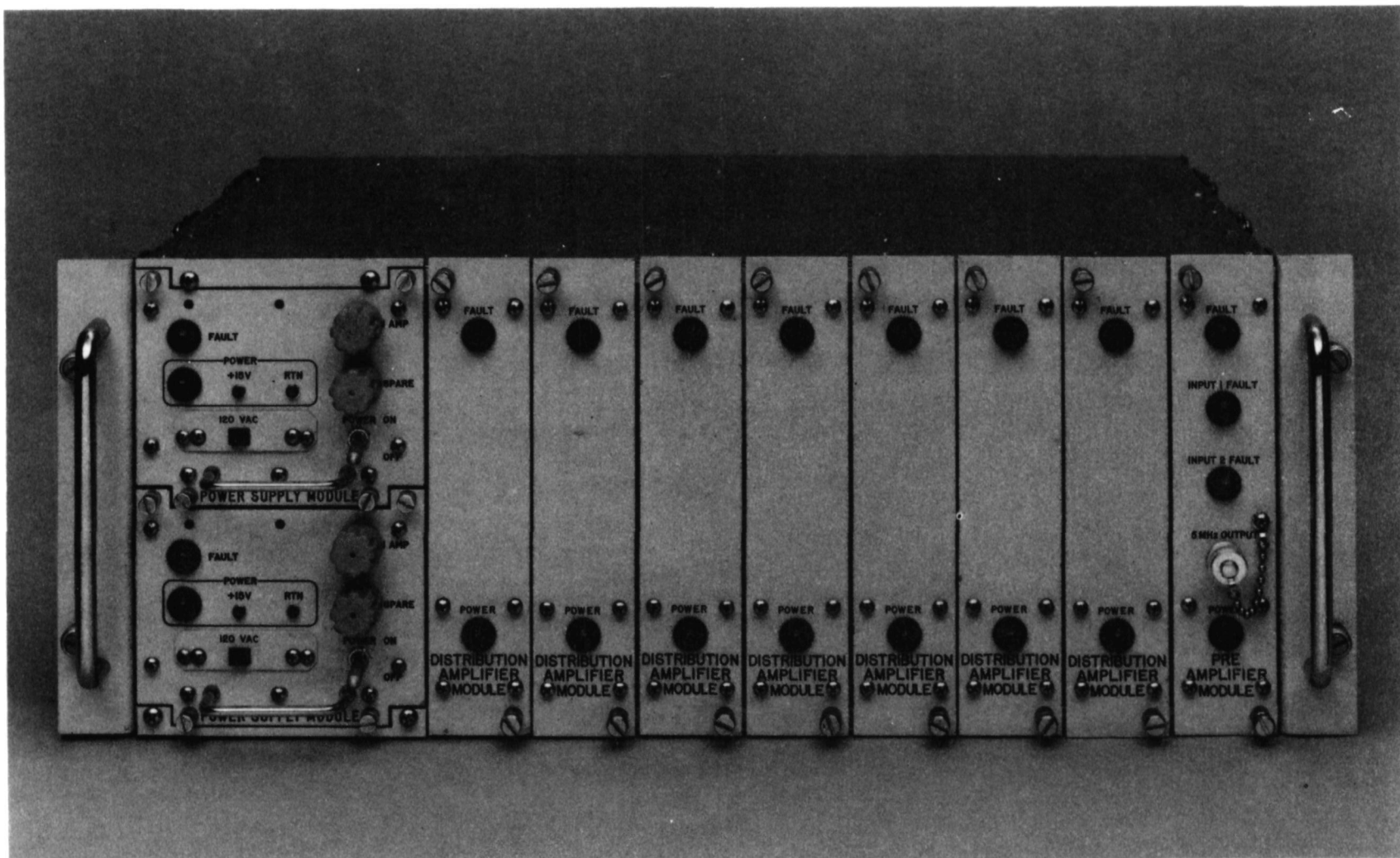


Figure 10. Secondary Distribution Unit (SDU), Front View
Model FE-799A

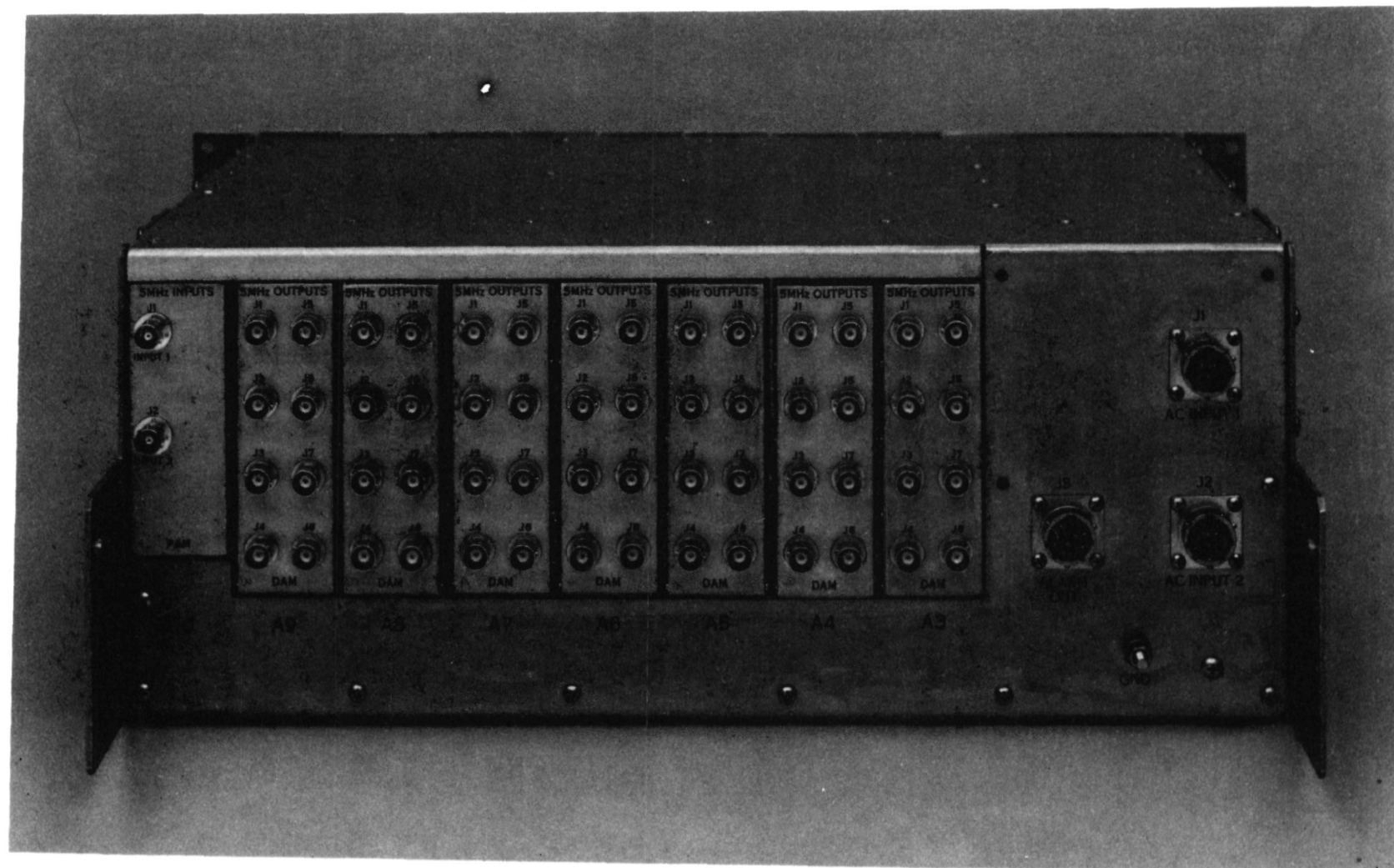


Figure 11. Secondary Distribution Unit (SDU), Rear View
Model FE-799A

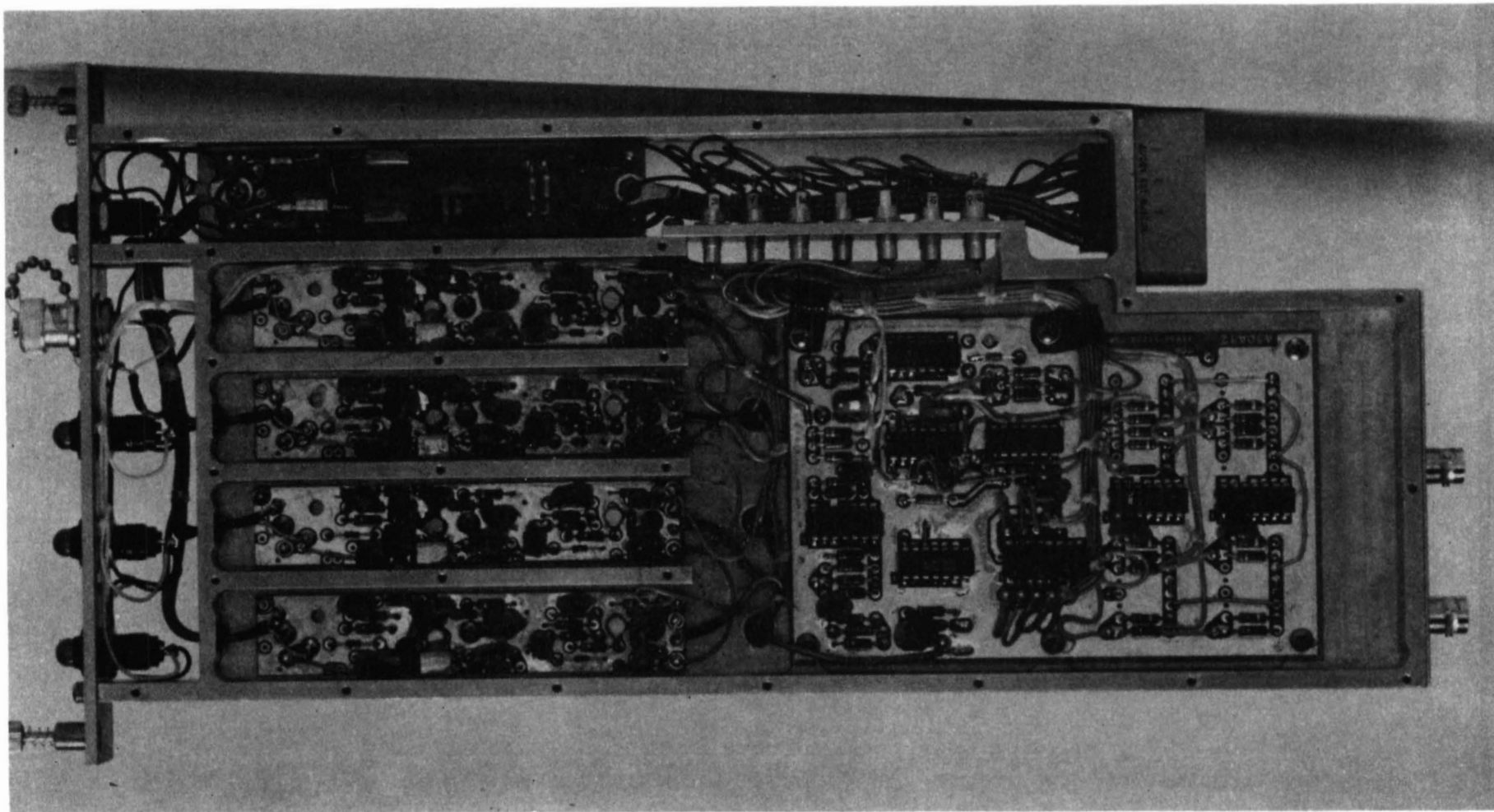


Figure 12. Distribution Amplifier Module, Top View

QUESTIONS AND ANSWERS

MR. GEORGE PRICE, Austron

Marty, you said the frequency was being controlled by Loran-C? Is that true? Or was it VLF? I remember earlier that a NATO III was going to use VLF for frequency control.

MR. BLOCH:

It is LORAN. As a matter of fact, it is your receiver. Is that what you wanted to let me tell you, George?

MR. PRICE:

No, I thought the original plan was VLF, and I am surprised to see that it is LORAN-C.

MR. BLOCH:

We talked them out of it.

MR. PRICE:

Good.

MR. BLOCK:

But George, the basic concept involved is that LORAN is monitoring rather than driving, so in case there is any problem in an interruption, the system is still operational on the frequency standard. So that is a manual correction system that they chose.

MR. GEORGE LUTES, The Jet Propulsion Laboratory.

What is the magnitude of the amplitude to phase conversion? Did you say?

MR. BLOCH:

Are you taking in a limiter?

MR. LUTES:

Yes.

MR. BLOCH:

It is a very good question. I can only give you a guesstimate. I would estimate that it adds to the noise floor about 4 dB. So for optimum use, you are better off not using the limiter. There is no question about it; however, you can get 170 dBc, because the typical outputs over here are +5 dBm with the limiter, so anywhere from about 2 to 4 dB is added by the limiter -- if you had a ideal source driving it.

MR. LUTES:

If the amplitude of the signal changes by 10 dB, for instance, how much phase change would that be in your system?

MR. BLOCH:

Al, did we measure that?

MR. VLUCAN:

It is one to two degrees.

MR. BLOCH:

It is a couple degrees at X-band over the whole dynamic range. The basic idea is that if you have a very good impedance match and the better your match the diode, you can theoretically have no phase shift at all. The phase shift is just a measure on the mismatch in the limiting diodes.

MR. LUTES:

Do you have any data on the phase change versus temperature?

MR. VULCAN:

No, but they are pretty broadband circuits.

MR. BLOCH:

What Al is saying is that they are broadband circuits and he wouldn't expect much of a change over temperature. We will be testing them over the temperature range. Most of the requirements are short-term changes rather than long-term changes with temperature, because they don't want to unlock their up and down converters.

Taking a look at similar type of circuitry, my guesstimate would be that at X-band, it would probably be the equivalent of about two or three degrees over 0 to 50°C change. Or about two or three millidegrees at 5 megahertz.

MR. LUTES:

Thank you.

DR. STOVER, Defense Communications Engineering Center

In the first part of your talk where you are talking about all the redundancy so that failures can occur without losing the signal, if you have a failure, can you detect and replace the failed part while you are still in service?

MR. BLOCH:

Absolutely. That was one of the major driving forces in this design: that you should be able to replace any and all modules and keep the equipment on line without disturbing the ones that have not failed. So when you pull in and out the power supply, there is less than a one millidegree shift in output phase and less than .01 dB in amplitude. And if you have a 8-channel module that has failed, you can take that one out (again without disturbing the rest of the system) or one part of the electronic switch. That is why the electronic switch is not in one module. It is in two modules in order to have that type of feature.

You can take out the failed module without disturbing the rest of the system and put another tested module in, and you are back on line. And the faults are shown on the front panel as well as indicated remotely to a central monitoring point.

MR. P. BANERJEE, National Physical Laboratory, India

Actually, in India we are facing a very peculiar problem, because there is often power failure. And with the power failure on and off, you will find some high frequency surge which disturbs the system phase and all those things. I really want to know with your power supply, how much protection can it give against all these frequency surges?

MR. BLOCH:

Could you repeat the question?

MR. HOWE:

He wants to know about protection and transients, I believe, on the power supply.

MR. BLOCH:

Are you talking about transients on the AC line?

MR. BANERJEE:

Yes.

MR. BLOCH:

This power supply has filtering and double regulations where large transients will (short-term transients in the millisecond range) have zero effect on the phase. There is no phase perturbation with fairly large short-term transient. And the input level can go from about 95 to 140 volts AC without affecting the output.

We are basically maintaining the voltage regulations of each module to about a millivolt. So it can take very large AC transients, because that is part of the problem that NATO III application has. They are normally on one power source and then they have a diesel backup and as soon as the power source fails it takes over to the diesel and there is a large transient that happens in this transition. So they have built in lots of transient and yet they must work through those transients.

THE SA-2239/WLQ-4(V) CUTTY SARK DISTRIBUTION SYSTEM

Alfred Vulcan and John Ho
(Frequency Electronics, Inc.), New Hyde Park, New York

ABSTRACT

This paper describes a redundant frequency and time distribution system providing a multiplicity of isolated outputs, all of which are derived from three atomic frequency standards. The distribution system monitors input parameters of the signals coming from the Cesium Standards and selects one to be the primary standard, phase locks an internal oscillator which has excellent aging characteristics in the open loop mode and acts as a filter to provide phase noise improvement, and generates 1 megahertz and 100 kHz by direct synthesis.

Additionally, the system distributes RF and timing signals consisting of 5 MHz, 1 MHz, 100 kHz, BCD Time-of-Day, 1 pps and 1 ppm.

INTRODUCTION

Modern submarines use a multitude of frequency standards for navigation, missile guidance, communications and time-keeping purposes. It has become necessary to develop a signal processing and distribution unit which accepts the input signals from the primary standards, provides readouts of signal integrity, improves signal characteristics, and distributes the signals to various users on the boat. The SA-2239/WLQ-4(V) Time Standard Selector Unit performs these functions utilizing redundant hardware with automatic switchover to maximize reliability and eliminate single point failures. The system is qualified to operate in a submarine environment and has battery backup providing thirty minutes of operation during ac mains failure.

SYSTEM DESCRIPTION

The Cutty Sark system can be split into three major subsystems. The first is the RF processing and distribution system, the second is the timekeeping, test and distribution system, and the third is power generation and distribution. Table 1 itemizes the various interface signals of the SA-2239/WLQ-4(V). The three Cesium Standards supply 5 MHz, 1 PPS, 1 PPM, BCD Time-Of-Day (TOD), and a Standard fault signal.

Additional 1 PPS and TOD inputs are fed from the Navigation Center and Time Code Generator (TCG). Twenty-four sinewave signals, twelve timing pulses, and six TOD outputs are generated.

RF Distribution

Figure 1 is a block diagram of the RF distribution system. Three 5 MHz signals are accepted from the Cesium Standards and feed fast fault-detector circuits which detect a dropout of a signal and switch over to a standby input without introducing a phase shift in the system output signal exceeding 90° . The phase perturbation is relatively slow so as not to upset user equipment. The 5 MHz input is multiplied to 30 MHz and fault detected. The detection circuitry senses a failure within one cycle at 30 MHz. The 30 MHz signal then passes through a high speed, high isolation diode switch. The outputs from the three Input Modules are combined at the input to the two phase locked oscillators. A 30 MHz narrow band filter provides a flywheel effect eliminating signal dropout and a high speed comparator converts the sinewave to a TTL level. A divide-by-six circuit provides 5 MHz which phase locks a low noise VCXO. The oscillator provides rejection to spurious signals, improves the phase noise floor and acts as a redundant signal source in the event of failure or removal of the primary inputs. The oscillator output feeds a frequency divider subassembly generating 1 MHz and 100 kHz. These signals are filtered to provide sinewaves and are fed to a three channel driver amplifier which boosts the signal level for driving the output amplifiers. Since there are twenty-four RF outputs each at a level of +27 dBm, it is necessary to design the output amplifiers with high efficiency to minimize power drain and permit cooler system operation. Thus a Class C configuration is chosen with hybrid coupled amplifiers used to provide improved operating parameters.

Time Distribution System

The Digital System, shown in Figure 2, accepts three 1 PPS and 1 PPM inputs from the Cesium Standards. These signals are fault detected, selected, and amplified. Redundant output amplifiers are selected automatically or manually. An additional function of the SA-2239/WLQ-4(V) is to check and compare 1 PPS and TOD which is inputted from the Cesium Standards, Time Code Generator, and the Navigation Center. Once a particular source is selected as the primary source, all other inputs are compared to that signal and the information is presented on the front panel. Time coincidence errors in the leading edge of the 1 PPS or 1 PPM signals of greater than 200 microseconds trigger an alarm condition.

Power Management

The Cutty Sark requirements present a unique set of operating constraints regarding the generation and distribution of dc power internal to the chassis. Power source priorities are external ac;

external dc; and internal battery. When operating on battery, non-critical circuits are disabled but front panel displays can be manually enabled. Due to the tight packaging density and internal power dissipation of 120 watts, a low-noise (RF and acoustical) fan circulates air throughout the chassis. The system is designed to operate without external cooling although rack cooling is normally provided in the submarine environment. To minimize power dissipation, redundant dc to dc switching regulators and power supplies are utilized. On board linear regulation is provided for those circuits which cannot tolerate 25 kHz switching transients. Each module is RFI filtered with low pass filters having a 5 kHz bandwidth. Coaxial line filters are used at the ac and dc input interface. The entire package is RFI shielded to meet the requirements of MIL-STD-461A. Internal temperature is monitored for presentation on the front panel test meter.

CIRCUIT DESCRIPTION

The Cutty Sark mission requirements of non-dropout input switchover, multiple +27 dBm RF outputs with low source VSWR, and continuous comparison of multiple timing inputs required the development of several unique circuits. The following paragraphs discuss specific circuits developed to meet these goals.

Input Processing

The input module senses the integrity of the Cesium Standard output signals and switches over to standby inputs in the event of failure. Three input modules are utilized, one for each atomic standard. As shown schematically in Figure 3 the 5 MHz input is amplified by Q1 and then multiplied by six with Q2. The 30 megacycle signal passes through a high isolation switch which has an on to off ratio of 120 dB and a switching speed of 30 nanoseconds. Faults are detected both at 5 MHz and 30 MHz. These detectors provide a switchover command in less than 20 nanoseconds if the input signal amplitude falls below +10 dBm. The three module outputs are combined after selection by the high isolation switch. Only one of the three inputs is selected at a given time. Failure is detected and switchover occurs in less than one cycle at 30 megahertz which corresponds to 60° at 5 MHz. The selected 30 MHz signal passes through a narrow band LC filter and is divided by six in the phase locked oscillator to restore 5 MHz. The purpose of the multiplier, filter, high speed sensing circuit, and high isolation switch is to enable selection of the standby pass without interruption of the output signal and with a phase perturbation of less than 90 degrees.

Figure 4 is the schematic diagram of the 1 PPM timing fault detection circuit in the input module. The +10V input pulse is attenuated by a factor of two and feeds one-shot multivibrator U1 whose output is a 3 millisecond wide pulse at a rate of 1 PPM. This signal feeds timer U2

which is configured as a retriggerable one-shot with a time constant of sixty-five seconds. A pulse dropout causes an alarm signal which is summed with the other module alarms. A composite alarm signal is thus generated which selects the appropriate cesium standard input. Fault detection of the 1 PPS and BCD inputs is accomplished in a similar manner with the retriggerable one-shot time constant set to be 10% greater than the input signal period in each case. This system is relatively straightforward but a failure occurrence may not be detected for approximately one pulse repetition period if the failure occurs immediately after a triggering pulse sets the one shot. This, however, is sufficient since other alarm signals will generally flag a particular failure condition before the digital detectors. Each module has an independent LED indicator showing module status. These indicators are illuminated when a module failure occurs. Additionally, a front panel summary fault indicator alerts the operator to a particular alarm condition.

Figure 5 shows the mechanical construction of the input module. Independently shielded compartments are used for the different functions and dc power is RFI filtered at section interfaces to maintain a high degree of isolation between RF sections and RF to power carrying lines.

RF Amplification

The four channel, 5 MHz amplifier shown in Figure 6 was developed specifically for the Cutty Sark distribution system. The two major design characteristics are a collector efficiency of 72%, and a constant low output VSWR over a broad range of frequencies. The first goal is accomplished through Class C operation. The resultant high level of harmonics are reduced to -40 dB to below the carrier with LC output filtering. Each amplifier uses two quadrature hybrid coupled transistors to minimize transistor power dissipation and provide a constant input and output VSWR. Since the transistors are essentially operating in a switching mode during Class C operation, they present identical impedances to the isolated ports of the hybrids and any reflected power is absorbed in the hybrid 50 ohm terminating loads. Hence the overall amplifier input and output impedances is 50 ohms \pm 10% over a 10% bandwidth. The hybrid is implemented as two 90 degree phase shift low pass sections which are capacitively coupled. The basic design of the 1 MHz and 100 kHz amplifiers is identical to the 5 MHz unit. A sample of each RF output is fed to a diode detector and low level sensing comparator circuit. The comparator outputs are wire-or'd to present a single logical zero in the event of failure of any amplifier. High current PIN diodes at each amplifier output enable the appropriate amplifier outputs upon command from the fault logic priority circuit. Figure 7 shows the 5 MHz amplifier package. Since a high degree of isolation is not required between the active stages a single non-enclosed double-sided PC board with a continuous ground plane is utilized for the structure.

Time-of-Day and 1 PPS Comparison

The system accepts five independent time-of-day (TOD) inputs. Four are 24 bit BCD codes from the three Cesium Standards and the Navigation Center and the fifth is a 2137 code from a time code generator. The 2137 code is an amplitude modulated 1 kHz sinewave consisting of 20 bits of TOD at a 25 PPS pulse rate. Four of the TOD inputs are compared to the fifth which is manually or automatically selected as the primary TOD input. The 2137 input is normalized to 24 bits by a pulse injection technique and the amplitude is shifted for compatibility with the BCD signals. The four TOD pulse trains are then compared on a bit by bit basis with the primary. Any deviation of more than 2 milliseconds generates a front panel alarm and remote alarm output. The operator can then sequentially display the five TOD's to determine the error location and magnitude.

The 1 PPS inputs from the five sources are similarly compared to determine leading edge coincidence. An offset of more than 200 microseconds triggers an alarm. Time coincidence is measured by counting pulses generated from a 1 MHz signal derived from the selected primary input.

The display section uses a six digit numeric LED indicator which indicates TOD or 1 PPS coincidence with a resolution of 50 nanoseconds. A serial to parallel converter and storage register drives the display. Information is updated every second.

Power Splitters

The 5 MHz, 1 MHz and 100 kHz outputs from the SA-2239/WLQ-4(V) feed power splitters which provide ten isolated outputs from one output. The splitters have 12 dB of insertion loss, isolation in excess of 40 dB from dc to 500 megahertz, and a VSWR of 1.3 to 1 maximum. As was discussed in the section RF Amplification, the output VSWR of the system is held to 1.10:1 over a ten percent bandwidth in order to provide a proper source impedance for the power splitters. This is necessary to insure that the isolation requirement is met. Outside of 10% band extremes, the isolation between outputs is maintained by two-pole LC filters on each output port. These filters have 60 dB of attenuation at the frequencies where the inherent power splitter isolation properties are no longer effective. Figure 8 is a view of the power splitter showing the filtering components and Figure 9 shows the overall power splitter enclosure. In conjunction with the power splitters, a single Cutty Sark switch is capable of supplying 150 5 MHz outputs, 30 1 MHz outputs, and 30 100 kHz outputs at a level of +13 dBm. Physically identical power splitters are used for distribution of 1 MHz and 100 kHz. As shown in the figures the modules are potted to reduce vibration induced noise and sidebands.

MECHANICAL PACKAGING

Figures 10, 11 and 12 show various external views of the Cutty Sark Distribution System. As seen in Figure 12, the top view, high density packaging is necessary to provide the required functions in a single rack panel assembly. Since the unit dissipates 120 watts in the AC mode of operation, the subassemblies are heatsunk to the main chassis and air flow is provided by a high volume fan. Each module and subassembly is directly removable from the top without disturbing others. The modules have alarm override switches which enable the module to be turned off to conserve power when certain outputs are not needed and yet not create an alarm condition. A visual LED indicator on the top of each module indicates module failure. The three redundant input modules are seen in this Figure as are the two VCXO's and various amplifier boards. With the exception of the battery and time display circuitry, every module is redundant and switchover to a standby module is accomplished automatically. The entire chassis is of milled construction to meet the stringent naval shock and vibration requirements. The entire assembly weight 68 pounds.

CONCLUSION

This paper describes the main features of the Cutty Sark Distributions System. The RF and timing distribution system are discussed and a detailed description of three unique functional blocks is presented. The mechanical package is photographically shown and the design of the auxiliary CU-2253/U 1 x 10 power splitter is described.

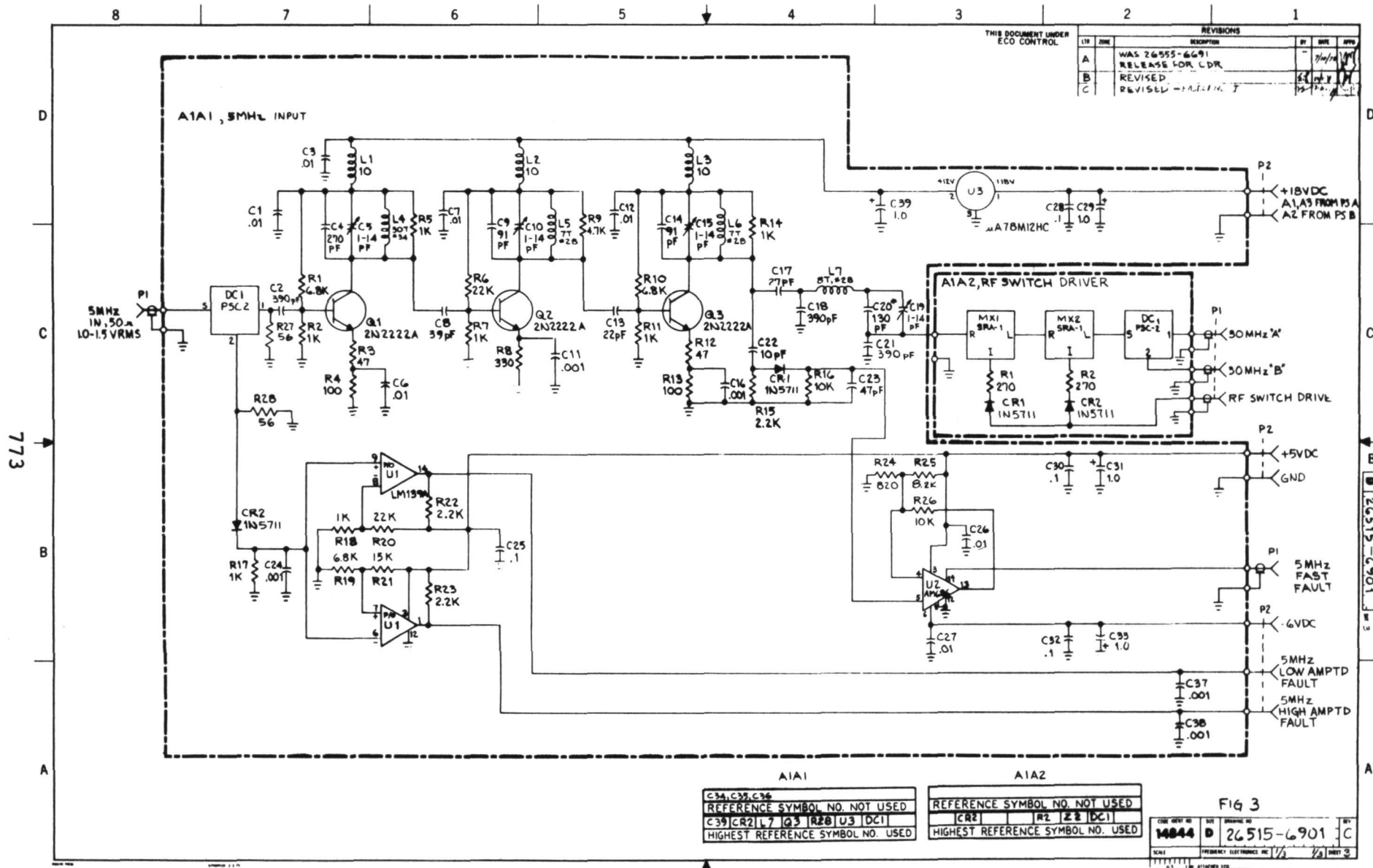


Figure 3. Digital System, Block Diagram (Sheet 2 of 3)

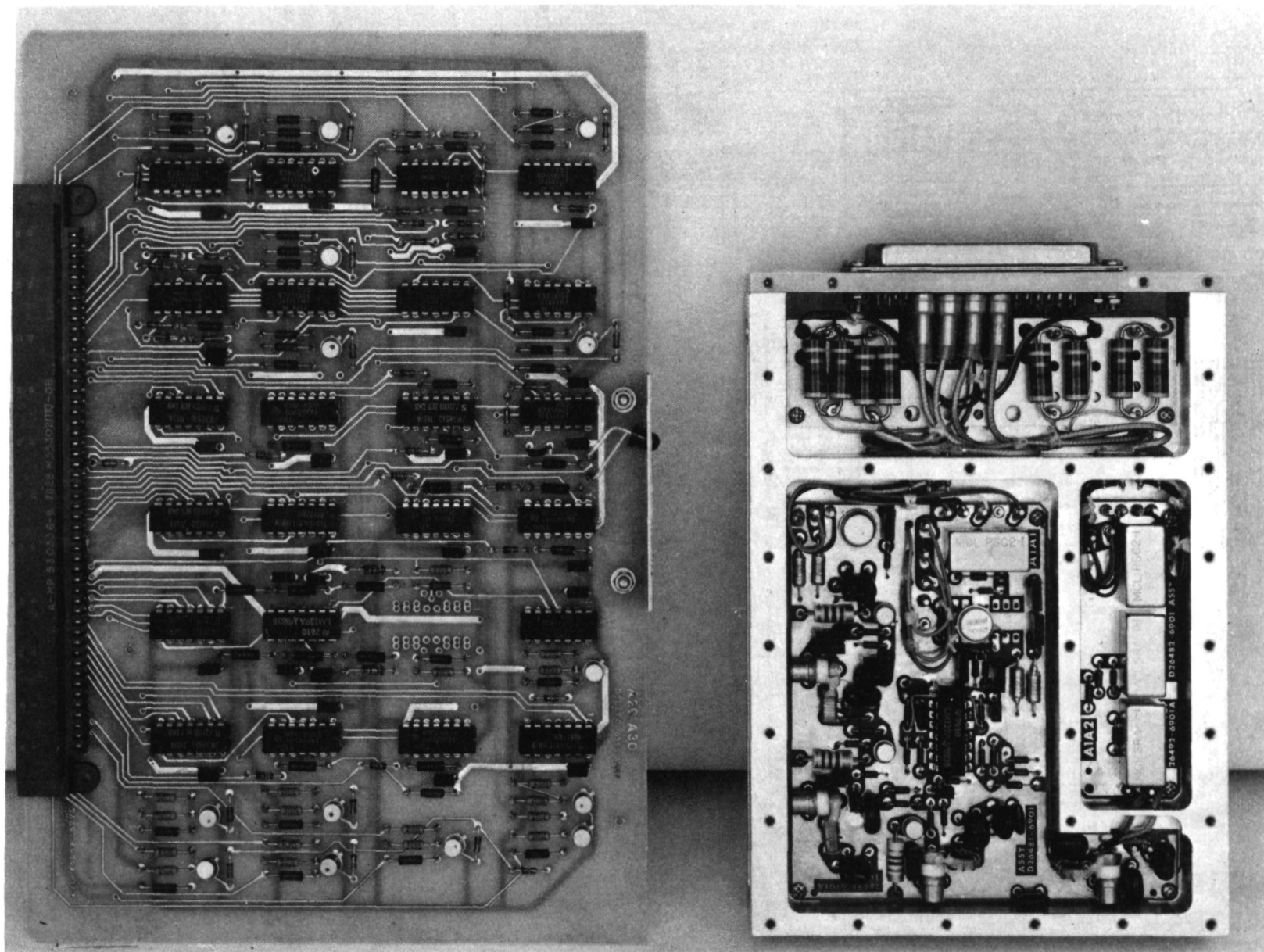


Figure 5. Input Module

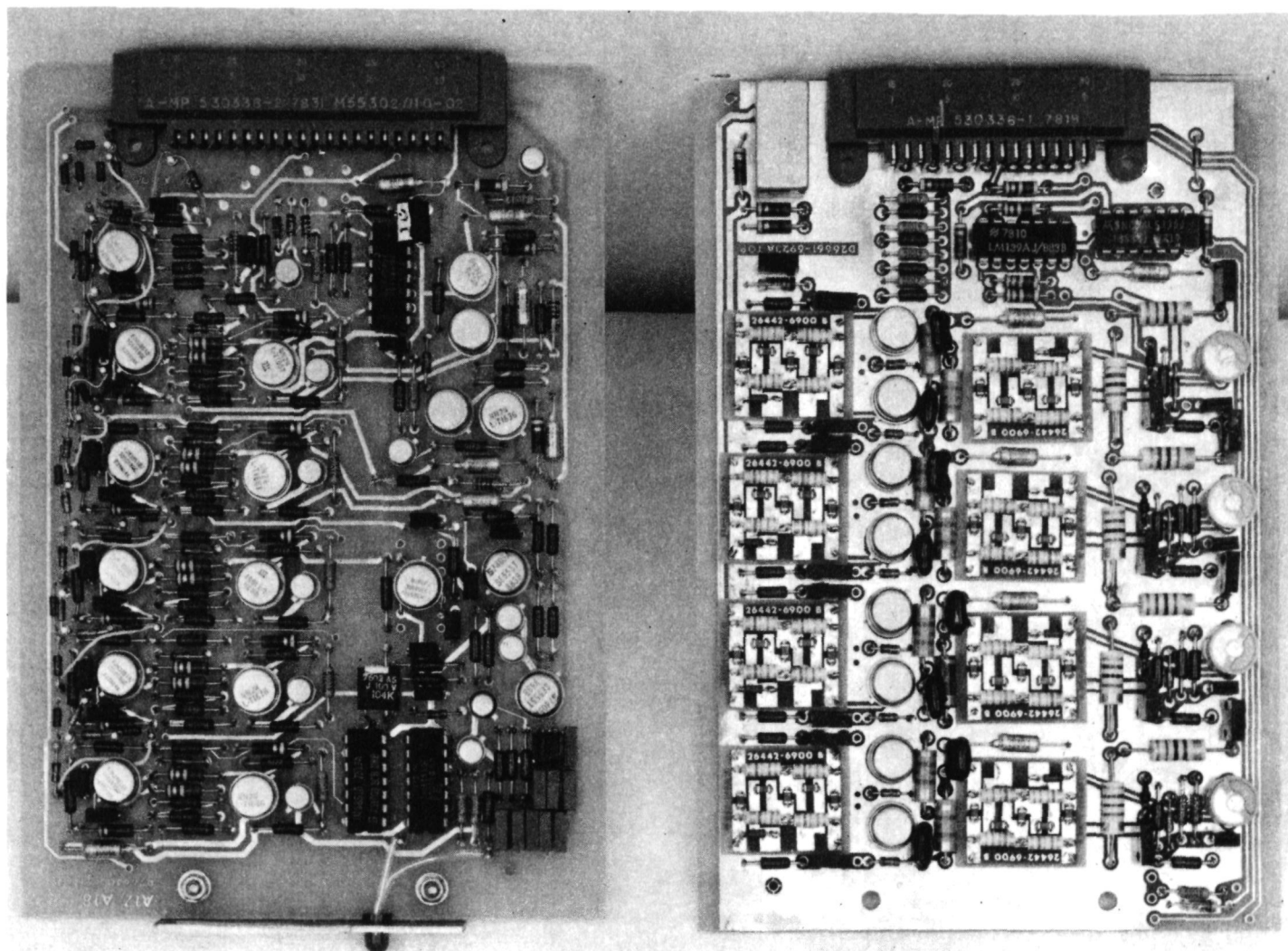


Figure 7. 5 MHz Amplifier

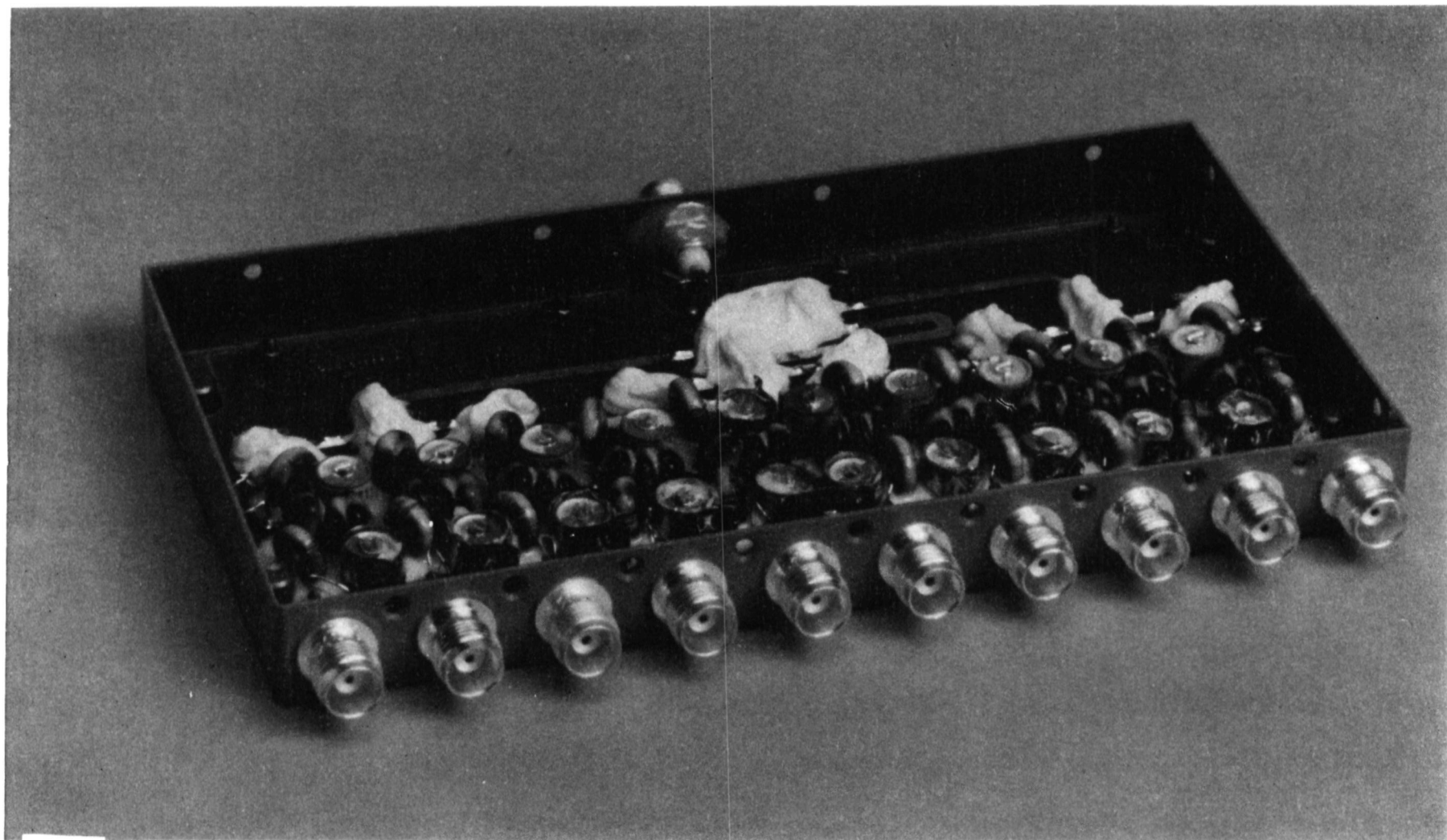


Figure 8. Power Splitter (1 X 10), Inside

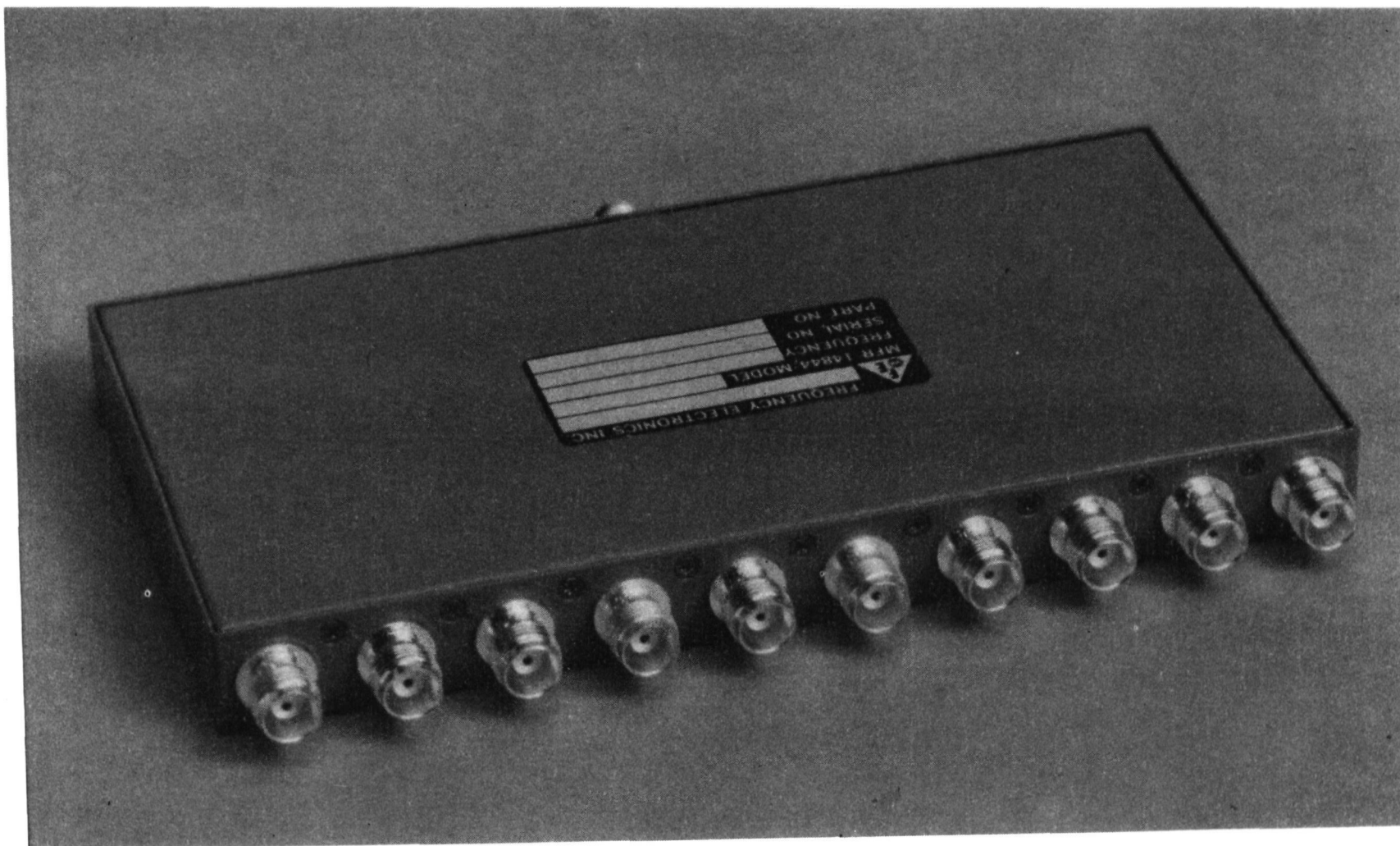


Figure 9. Power Splitter (1 X 10), Outside

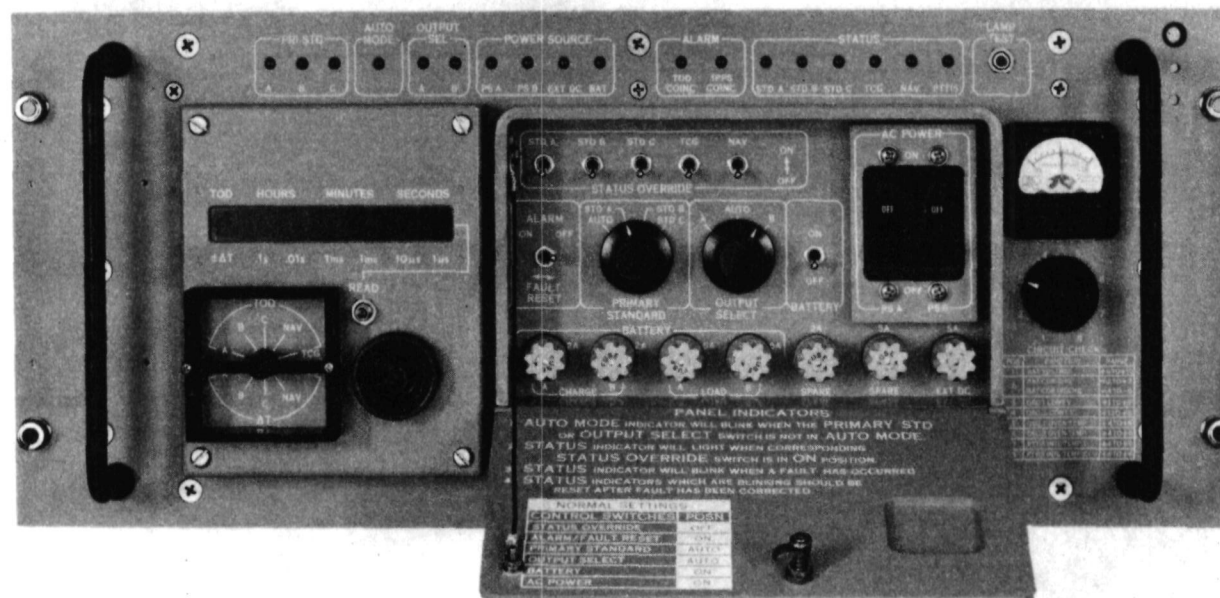


Figure 10. PTTI Switch, Front Door Open

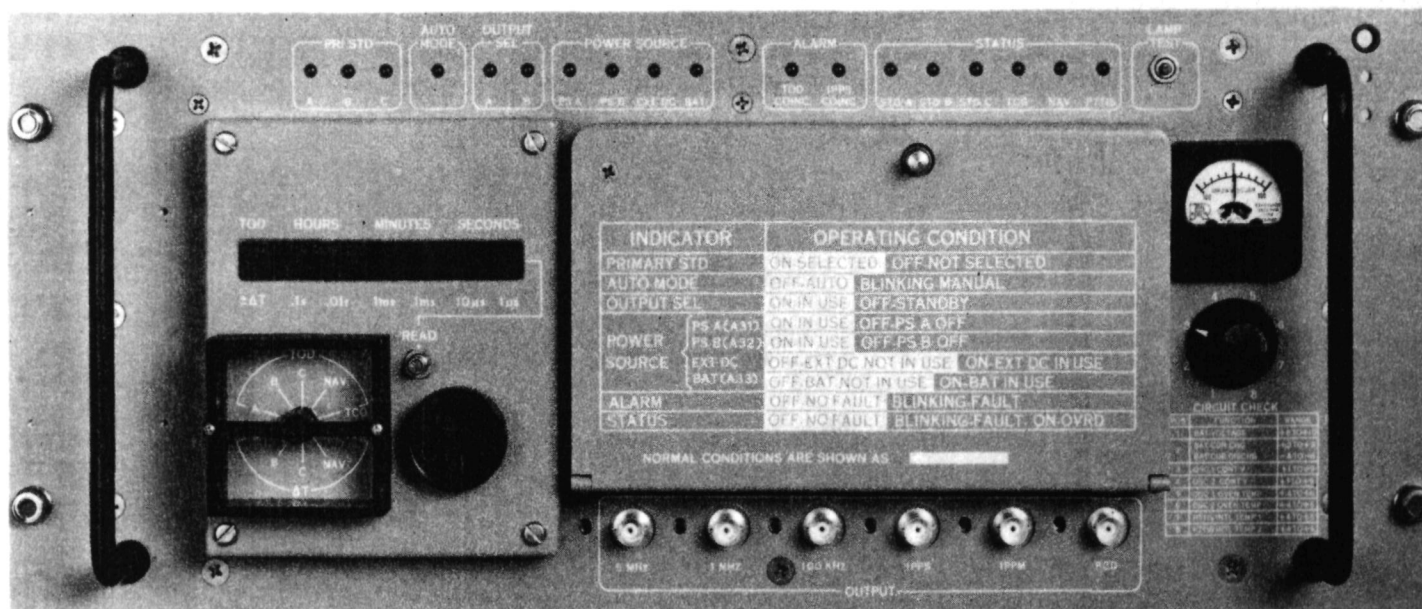


Figure 11. PTTI Switch, Front Door Closed

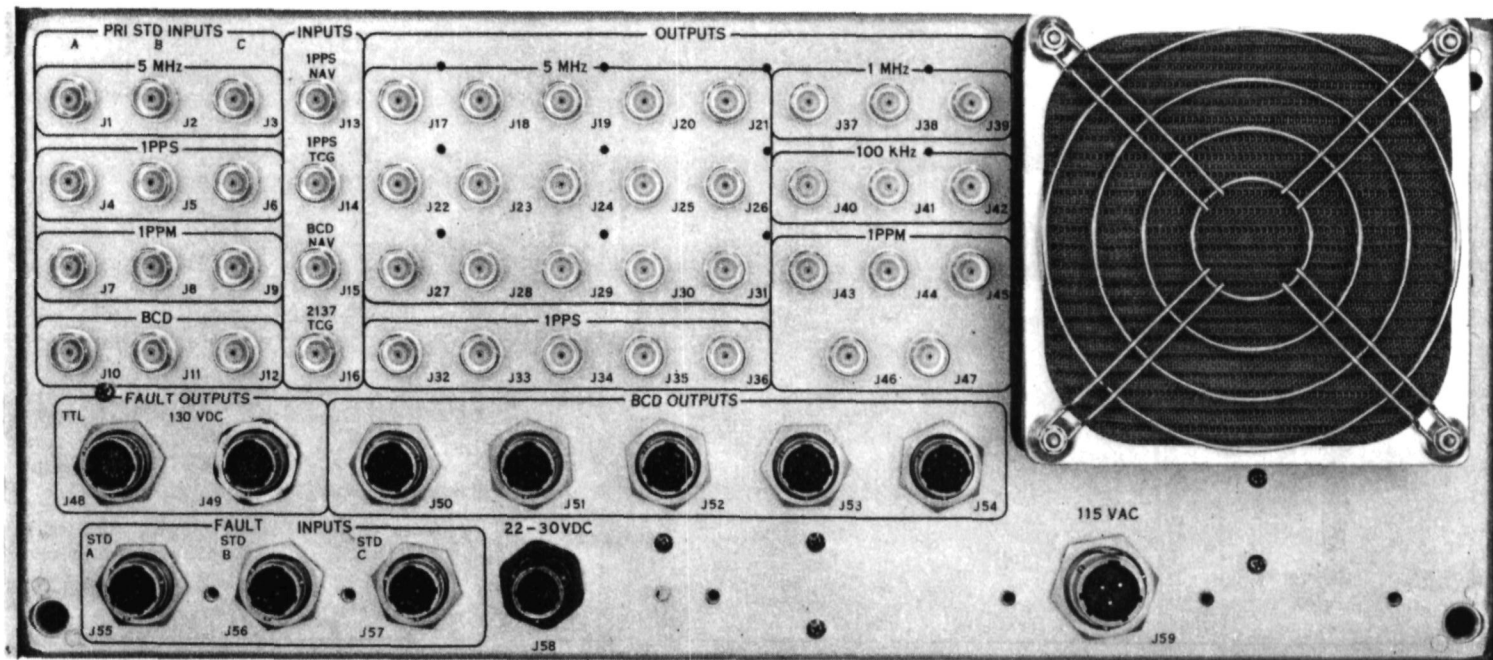


Figure 12. PTTI Switch, Rear View

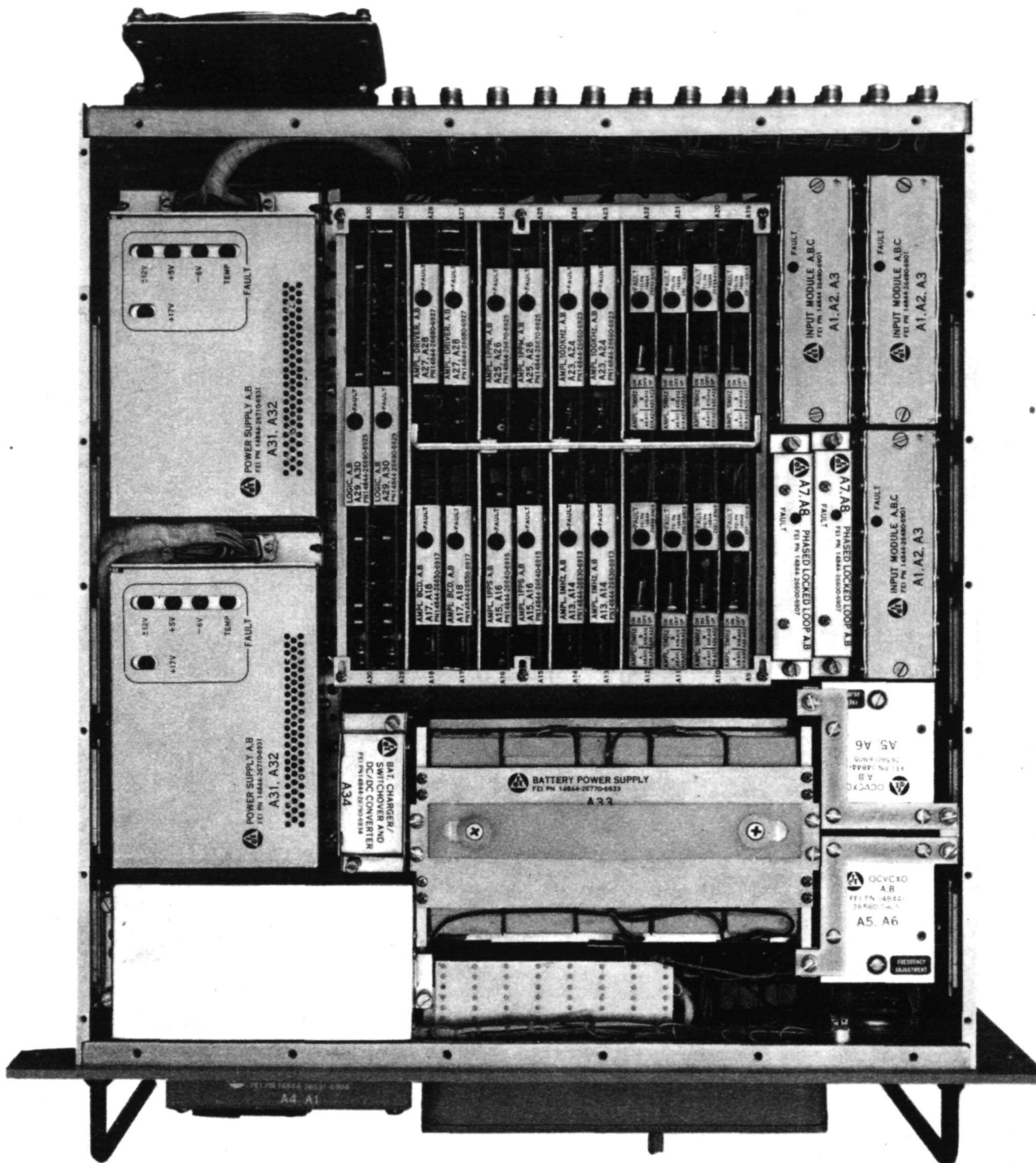


Figure 13. PTTI Switch, Top View

Page Intentionally Left Blank

PRECISION TIMEKEEPING USING A SMALL PASSIVE HYDROGEN MASER*

F. L. Walls and D. A. Howe
Frequency and Time Standards Group
National Bureau of Standards
Boulder, CO 80303

ABSTRACT

The timekeeping ability of a prototype small passive hydrogen maser developed at NBS was recently compared to UTC(NBS) based on 10 cesium frequency standards including a large primary standard, NBS-4. The frequency of the passive maser was monitored as a function of source pressure, cavity temperature, microwave power, modulation width, and magnetic field. Based on these measurements one would expect a frequency stability of better than 6×10^{-15} over many days, implying a timekeeping ability of order 0.5 ns/day. Measurements vs. UTC(NBS) indicate a joint timekeeping stability of order 1.2 ns/day. In order to obtain a better estimate of the maser performance, simultaneous time measurements were made between NBS-4, UTC(6600), and the small passive maser. UTC(6600) is a time scale composed of nine commercial cesium standards. The estimates for the time stability of each were:

Small passive maser	0.99 ± 0.4 ns/day
NBS-4	0.74 ± 0.3 ns/day
UTC(6600)	0.74 ± 0.3 ns/day

Peak to peak time variations of the small passive maser vs UTC(6600) was 10 ns for the full 32 days if the average rate and drift are taken into account.

The frequency stability of the small passive maser vs UTC(NBS) was $\sigma_y(\tau) = 1.1 \times 10^{-14}$ for $\tau = 1$ to 8 days based on 32 consecutive days of data.

*Contribution of the National Bureau of Standards; not subject to copyright in the United States.

INTRODUCTION

The NBS passive hydrogen maser program has been directed toward the achievement of exceptional long-term frequency stability in order to provide a state-of-the-art frequency reference and basis for improvements in the stability of UTC(NBS), our official time scale. Two major advances have been made. The first demonstrated virtually unequalled frequency stability from 1 to 4 days using a passive full-sized hydrogen maser cavity design [1,2]. The second milestone, which is described in detail here, demonstrates that similar performance can be attained in a more rugged passive design that is about a factor of 5 smaller in size, weight, and cost than any previous design. Such a design is eminently suitable for use in precision time scales as well as space and field use.

SMALL PASSIVE MASER

Many of the features of the small passive maser were described earlier. Briefly, the passive maser allows for lower cavity

Q's, which permits different approaches to the cavity design (see Fig. 1). The type used here ultimately leads to a smaller cavity package [3]. Other small cavity designs have been proposed [4,5,6]. The cavity is a conventional TE_{011} mode with the addition of low loss alumina dielectric material on the inside of the electrical wall. The cavity design is a right circular cylinder with a bore down the central axis. The ends of the bore are capped with the same alumina dielectric material. The closed central bore then is the hydrogen storage volume. It is therefore possible to achieve good filling factor with this geometry, since the instantaneous rf magnetic field reverses sign in the dielectric and not in the open bore, which has the volume of hydrogen being interrogated. This geometry also has the benefit of good symmetry about all axes of the rf magnetic field in the storage volume (see Fig. 2).

Most masers use a conventional TE_{011} mode microwave cavity with a diameter of about 21 cm and length of about 50 cm. The lumped constant equivalent circuit for such a cavity consists of an inductance L in series with a capacitance C in series with a resistance R . The insertion of the low-loss dielectric affects the propagation constant ϵ thus increasing C and decreasing the frequency of the cavity. The overall dimension of the cavity can then be reduced to compensate for the effect of the dielectric. Symmetry, dielectric constant, overall dimension, and filling factor are then considered in order to achieve an optimum geometry. The effect of the frequency of the TE_{011} mode is taken into account at this stage. The dielectric loading of the cavity affects the electric field. The rf magnetic field (which excites the atoms) is pinned to the defined orientation of the electric fields within the cavity. It is possible to choose a cavity open diameter so that the oscillating axial H field does not reverse sign within this volume. Consequently, the inside bore can substitute for the

storage bulb used in a conventional maser with little compromise in the filling factor (see Fig. 3) [3]. A picture of the completed small maser cavity and shield assembly is shown in Fig. 4.

MEASUREMENTS OF PERFORMANCE

Identical designs were used for two small passive hydrogen masers (H3 and H4) which have the same linewidths (about 1Hz) and the same S/N ratios. Other clocks used in the comparisons are the cesium standard NBS-4 and the UTC(6600), a time scale consisting of nine commercial cesium clocks.

The first set of data was compiled based on a 32 day uninterrupted comparison between H3, NBS-4, and UTC(6600). These three sources were treated as independent clocks. By simultaneously comparing three independent clocks, it is possible to deduce the stability of each individual clock. The points shown in figure 5, which extend beyond averaging times of 10,000 seconds, represent the individual performance of H3 in a three-way intercomparison. The relations for determining the stability of an individual clock in a three-way comparison is [7]

$$\sigma_i^2 = \frac{1}{2} [\sigma_{ij}^2 + \sigma_{ik}^2 - \sigma_{jk}^2] \quad \text{Eq. 1}$$

The slight rise in σ_y of H3 at averaging times of about $\frac{1}{2}$ day and 1 day are most likely attributable to environmental effects (a diurnal). Day-to-day temperature and pressure changes appear to enter at about the 1×10^{-14} level. Although there is some degradation of stability for times around 1 day, the longer term stability is on an improving trend as shown by the last σ_y point at an averaging time of eight days (4 data samples). The eight-day value of σ_y is 8.1×10^{-15} ($\pm 5.6 \times 10^{-15}$).

Figure 6 and figure 7 show the frequency fluctuations as a function of time for H3. Figure 6 shows a comparison between H3 and NBS-4 and figure 7 is the comparison between H3 and UTC(6600). A more graphic comparative measure is the residual time fluctuations indicated in figure 8 and figure 9. Over the 32 day data run, figure 8 shows the time residual (taken from day-to-day epoch data) between H3 versus NBS-4. The time residuals are the integrated fractional frequency fluctuations. Figure 9 shows the same plot of time residuals between H3 and UTC(6600). To a large extent, the measurements of long-term stability are limited by the stabilities of NBS-4 and UTC(6600). The peak-to-peak time difference of H3 versus NBS-4 is 14 nanoseconds and the peak-to-peak difference of H3 versus UTC(6600) is 10 nanoseconds. For these long term data, the fluctuations are noticeably smoother in the comparison to the UTC ensemble of nine Cs clocks. The end points for these runs of data are deliberately set to return to zero time difference, thus removing an average frequency offset. In this 32 day data set, there appears to be correlated frequency changes of parts in 10^{15} with period of order 7 days. This possible effect is under further study.

Shorter term stability measurements (from 1 second to 10,000 seconds) on H3 and H4 consistently produced the straight solid line shown on the stability plot of figure 5. This is the white frequency behavior of the masers at $1.7 \times 10^{-12} \tau^{-1/2}$ and is the stability referred to each individual hydrogen maser. This individual stability was based on the three-way comparison among each: H3, H4, and NBS-4. NBS-4 has an individual stability of about $2.7 \times 10^{-12} \tau^{-1/2}$.

First attempts to compare H3 with H4 in a stability measurement uncovered a number of problems. These problems were evidently

associated with a cross-talk signal which affected the phase of the output of a maser when the other nearby maser was in operation and being compared. Virtually identical hardware exists in the generation of 1.420 GHz in each maser. This is accomplished in each by multiplying a quartz crystal oscillator at 4.93 MHz by 288. Non-linear amplification at various stages in the multiplication chain generates a spectrum of lines extending from 4.93 MHz to 1.420 GHz. Two such multiplier chains, located within close proximity of one another, present an opportunity for both to have a preferred common phase, if the two oscillators are very close in frequency. In the case of the masers here, the frequency difference between the two hydrogen masers is 5×10^{-12} or less. Stray rf coupling between oscillators/multipliers created a type of injection locking which was very troublesome. The multipliers were subsequently repackaged and additional shields applied around the input amplifiers. This has eliminated the problem.

CORRELATION STUDY

Long term measurements of environmental temperature and barometric pressure were made coincident with frequency in order to determine the level of sensitivity to these environmental effects. Interestingly, there is no perceivable barometric pressure effect to the 1×10^{-14} level limited by the length of the data set. The barometric pressure changed by 7% (maximum) during this 32 day comparison. Other parameters were adjusted and their effects on the maser frequency are summarized in Table 1.

SUMMARY OF SMALL PASSIVE MASER PERFORMANCE

<u>EFFECT</u>	<u>OFFSET</u>	<u>INSTABILITY</u>
1. Spin Exchange	2×10^{-13}	2×10^{-15}
2. Resonator Temperature Sensitivity	$< 3 \times 10^{-14}/K$	$2 \times 10^{-15}/K$
3. Magnetic Field	3×10^{-13} for $\pm 0.3G$	10^{-15}
4. Power Dependence	$< 10^{-13}/dB$	10^{-15}
5. Phase Modulator Drive	$< 10^{-13}/dB$	10^{-15}

Frequency Stability: $\cong 1.7 \times 10^{-12} \tau^{\frac{1}{2}}, 1 < \tau < 10^5$

Drift vs. UTC(NBS): $7 \pm 20 \times 10^{-16}/\text{day}$
17 day measurement
for H3 and also H4

TABLE 1

DRIFT

The long-term stability measurements presented in figure 5 represent a 32 day accumulation of data. In this data, a linear drift term of $4 \times 10^{-15}/\text{day}$ was removed. After degaussing, another measurement of 17 days was made which exhibited a drift vs UTC(NBS) of $7 \pm 20 \times 10^{-16}/\text{day}$ for both H3 and H4.

Based on separate long-term stability measurements made in a three-way comparison, the drift of the passive hydrogen masers is at most the same level as UTC(NBS) over several weeks against which it was compared. The uncertainty in this level is about 2×10^{-15} per day over several weeks limited by the day to day fluctuations of UTC(NBS).

The largest contributor to the originally observed drift of the H3 maser was due to the drift in the magnetic shields after moving the maser from one lab to another without degaussing. Degaussing in position apparently removed the drift. Environmental changes of temperature and pressure appear to affect the maser stability at the 1×10^{-14} level.

CONCLUSION

We have taken, and are continuing to take, intercomparative frequency stability measurements among four clocks; passive H3 and H4 hydrogen masers and NBS-4 and UTC(NBS). No appreciable drift above 2×10^{-15} per day has been detected. Some environmental sensitivity (pressure and temperature) affects frequency stability at about the 1×10^{-14} level. We have made considerable improvements in the original small passive maser design in the area of increased maser-to-maser isolation and increased environmental insensitivity. The preliminary long-term stability measurements presented here indicate great potential for the passive maser design as clocks. For the first time, small passive hydrogen masers will be contributors to the NBS time scale. In the future, we plan to deploy a full-size hydrogen maser (of passive design) also into the time scale. The large maser has the potential to perform with a stability of:

$$\sigma_y(\tau) = 1.3 \times 10^{-13} \tau^{-1/2} + 1 \times 10^{-15}, \quad 0 < \tau < 10^5 \text{ sec.}$$

ACKNOWLEDGEMENTS

The authors thank D. W. Allan and J. Levine for help in processing of clock comparison data. This work is partially supported by Jet Propulsion Laboratories, Pasadena, CA and Naval Research Laboratories, Washington, DC.

REFERENCES

1. F. L. Walls and H. Hellwig, "A New Kind of Passively Operating Hydrogen Frequency Standard," Proc. 30th Ann. Symp. on Freq. Control, 473, 1976.
2. F. L. Walls, "Design and Results from a Prototype Passive Hydrogen Maser Frequency Standard," Proc. 8th Ann. Precise Time and Time Interval (PTTI) Planning Meeting, 369, 1976.
3. D. A. Howe, F. L. Walls, Howard E. Bell, and Helmut Hellwig, "A Small, Passively Operated Hydrogen Maser," Proc. 33rd Ann. Symp. on Freq. Control, 554, 1979.
4. H. T. M. Wang, J. B. Lewis, and S. B. Crampton, "Compact Cavity for Hydrogen Frequency Standard," Proc. 33rd Ann. Symp. on Freq. Control, 543, 1979.
5. E. M. Mattison, E. L. Blomberg, G. U. Nystrom, and R. F. C. Vessot, "Design, Construction, and Testing of a Small Passive Hydrogen Maser," Proc. 33rd Ann. Symp. on Freq. Control, 549, 1979.
6. Harry E. Peters, Sigma Tau Corporation, "Small, Very Small, and Extremely Small Hydrogen Masers," Proc. 32nd Ann. Symp. on Freq. Control, 469, 1978.
7. James A. Barnes, et al., "Characterization of Frequency Stability," IEEE Trans on Instr. and Meas. IM-20, 105, 1971.

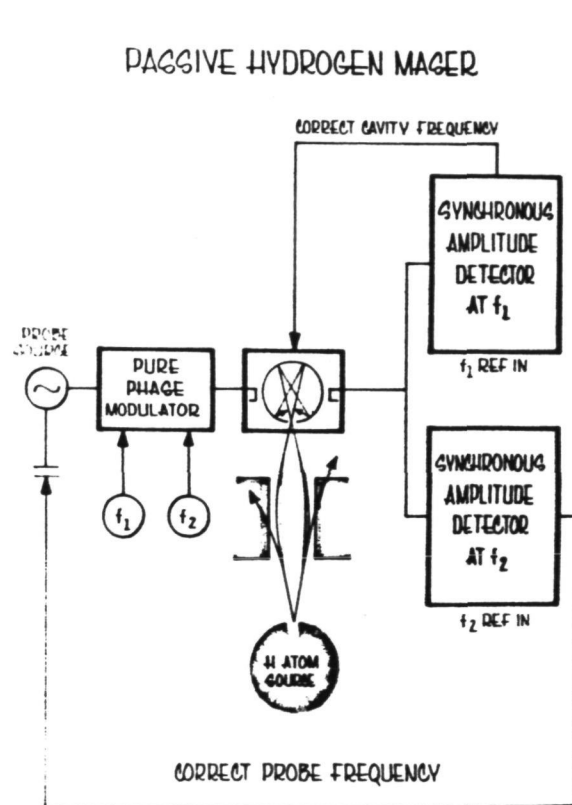


Fig. 1. In the passive mode, the H-maser is not oscillating. The NBS H3 and H4 electronics use two servo systems involving the narrow H-line and the cavity separately.

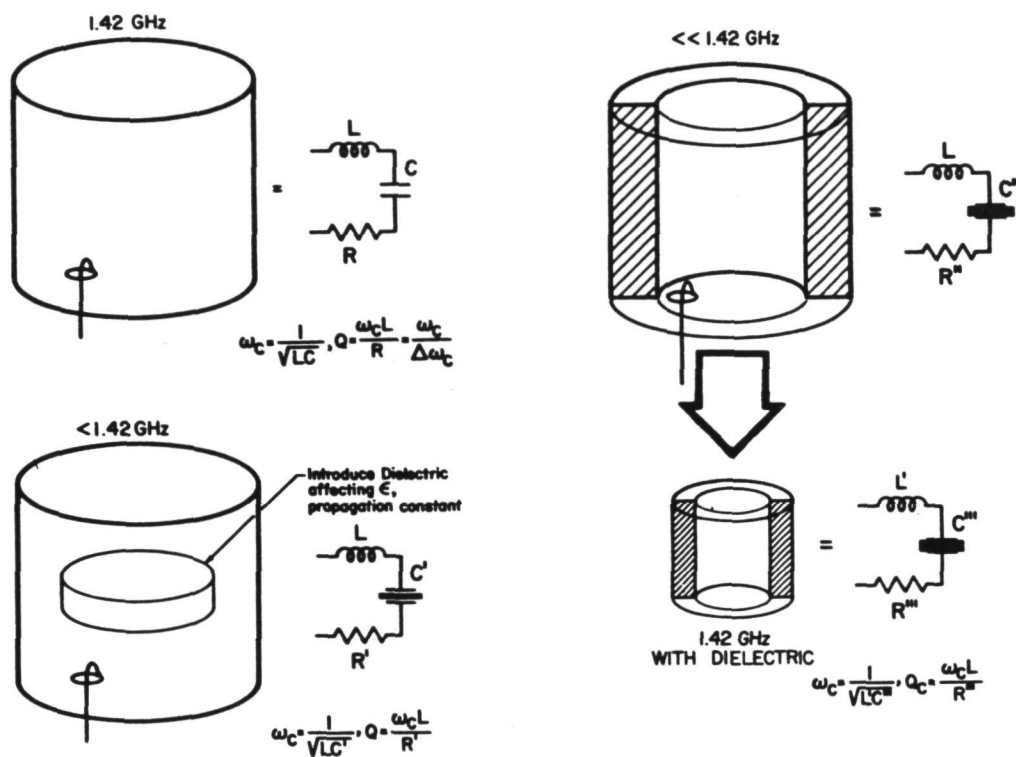
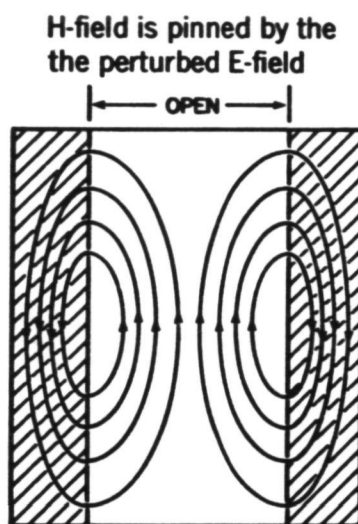


Fig. 2. A small cavity is realized by the addition of a low-loss alumina dielectric.



A geometry is chosen so that
the oscillating H-field
does not reverse sign in the
open bore.

No bulb is needed to confine
the interrogated atoms to a
volume of non-reversing H-field,

Fig. 3. The conventional H-maser storage bulb is eliminated and
the wall of the open center is coated with Teflon.

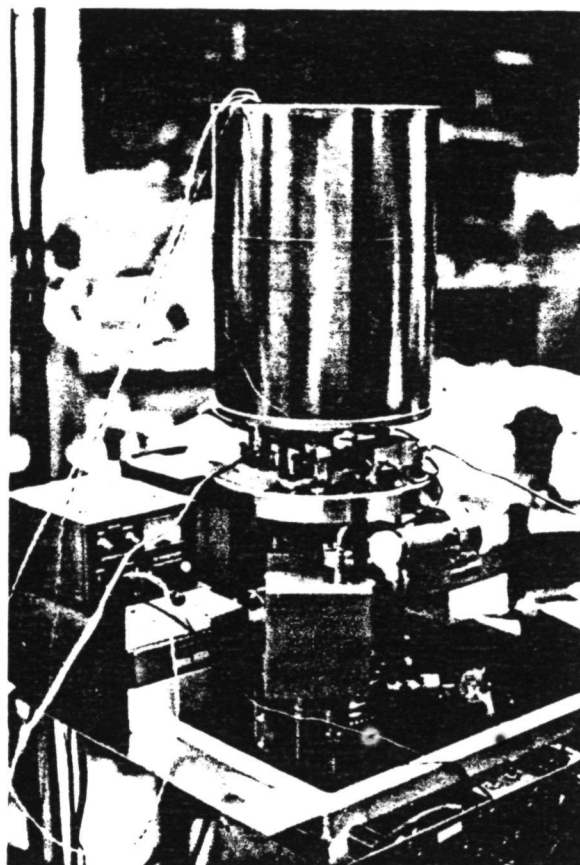


Fig. 4. Completed prototype cavity assembly with four nested magnetic shields.

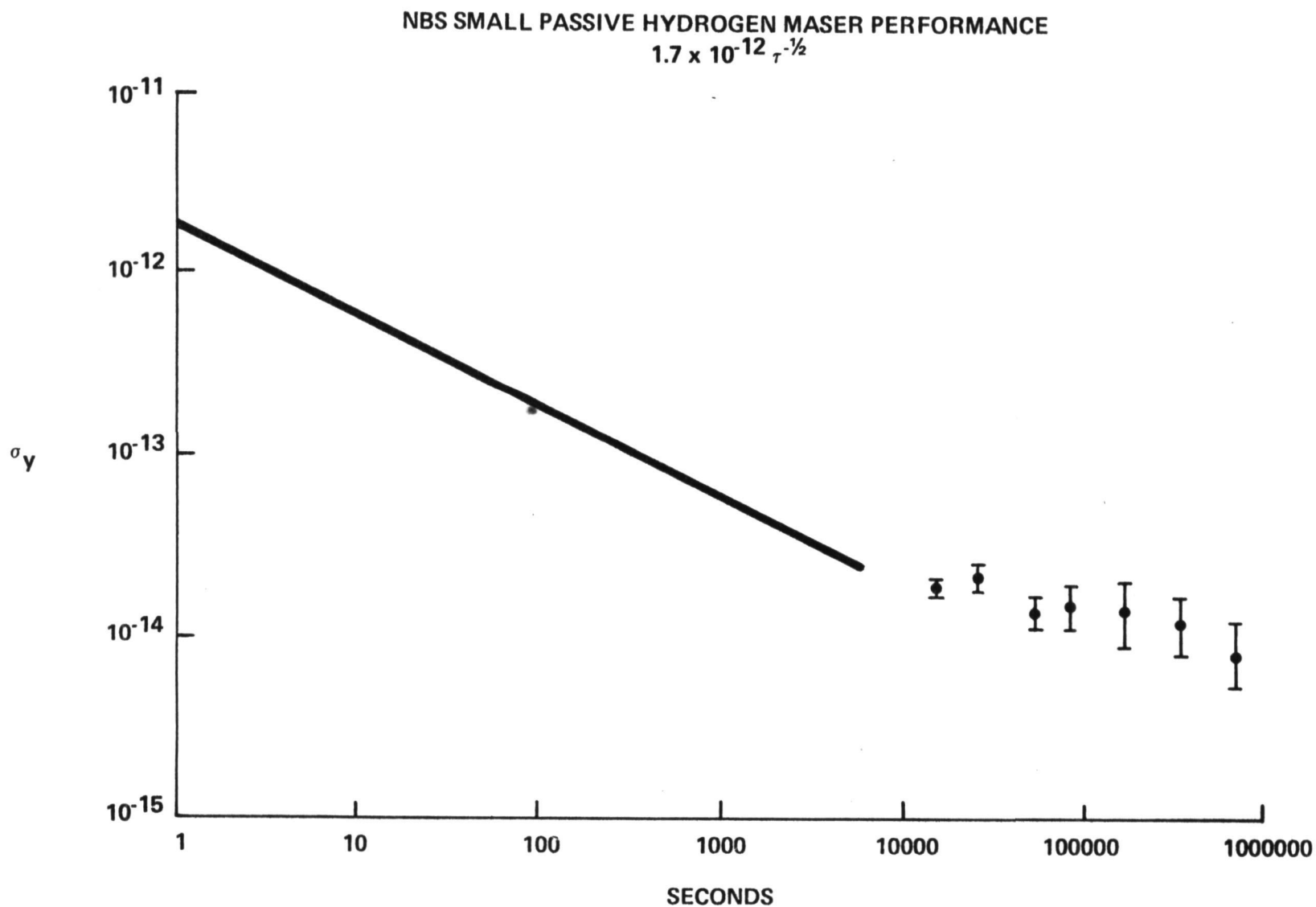


Fig. 5. Frequency stability of small H-maser based on 32 day comparison simultaneously against UTC(6600) and cesium standard NBS-4.

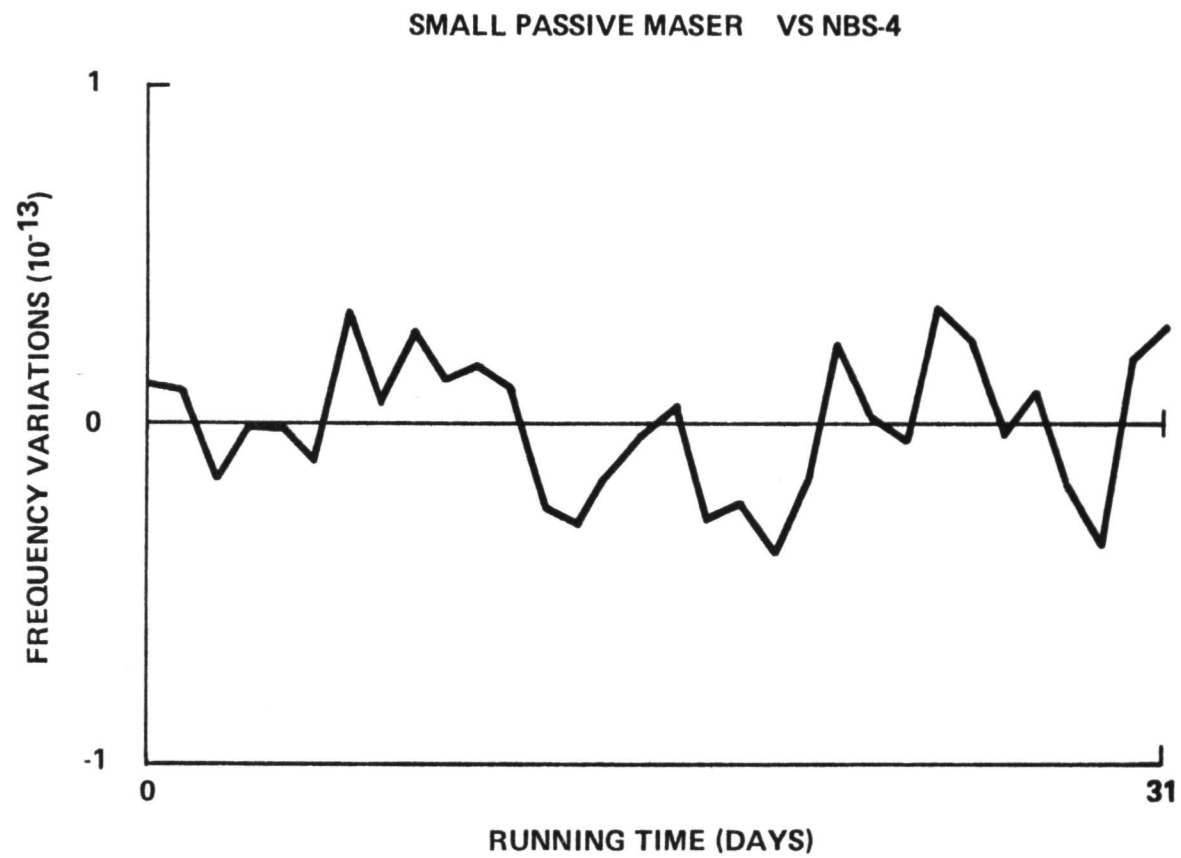


Fig. 6. Daily frequency of H3 vs. NBS-4 (average frequency offset removed).

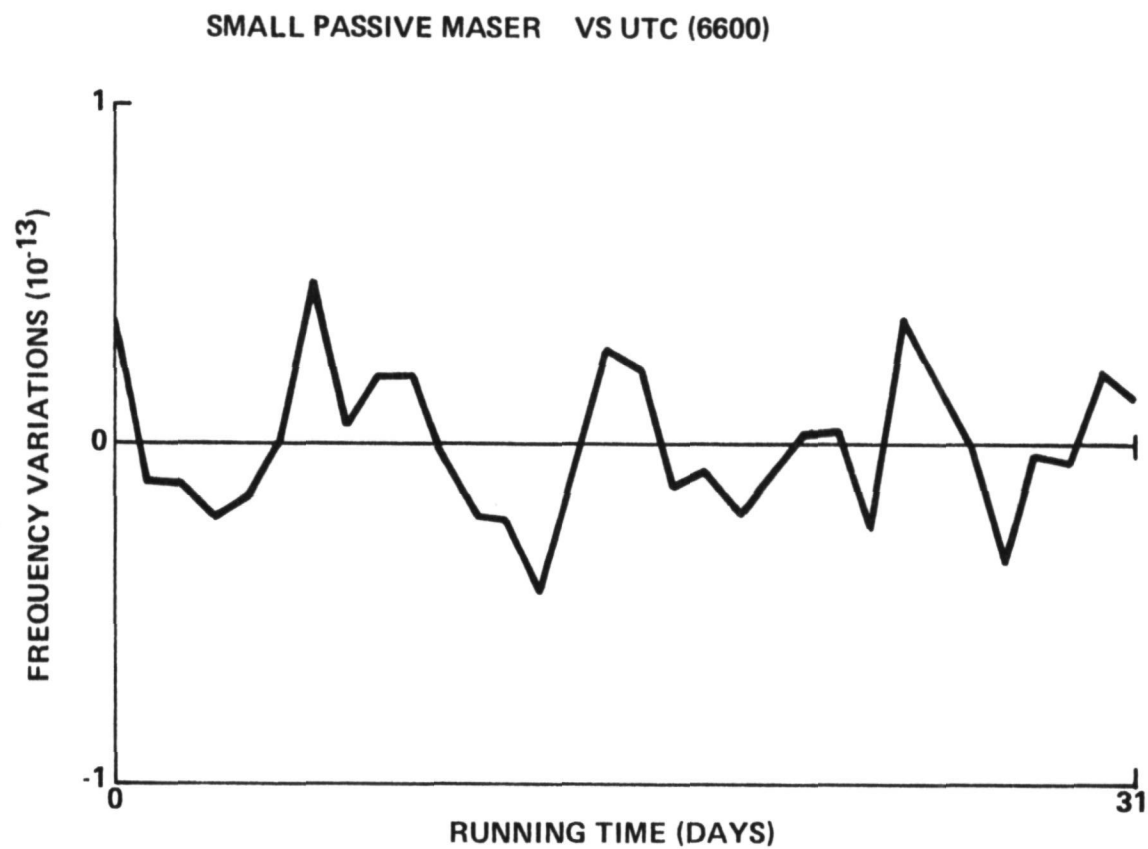


Fig. 7. Daily frequency of H3 vs UTC(6600) (average frequency offset removed).

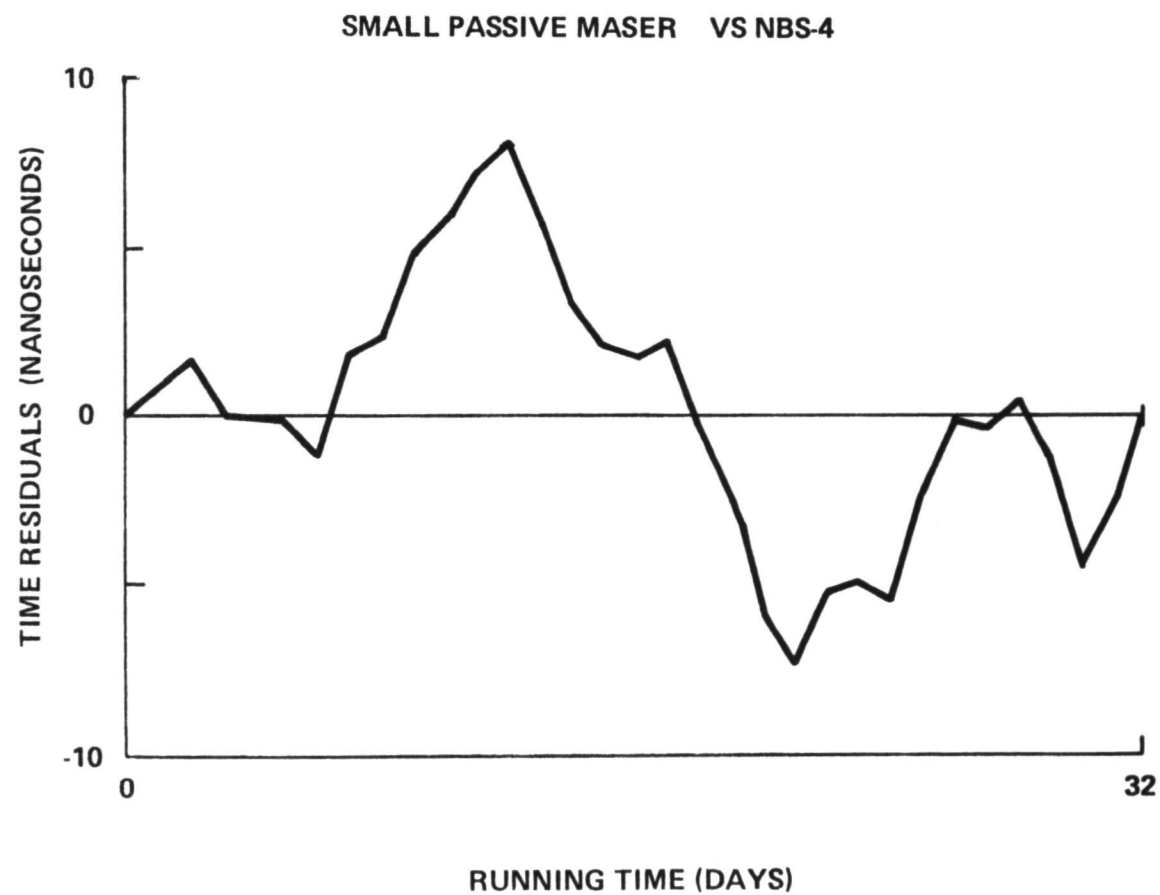


Fig. 8. Daily time of H3 vs. NBS-4 (average frequency offset removed).

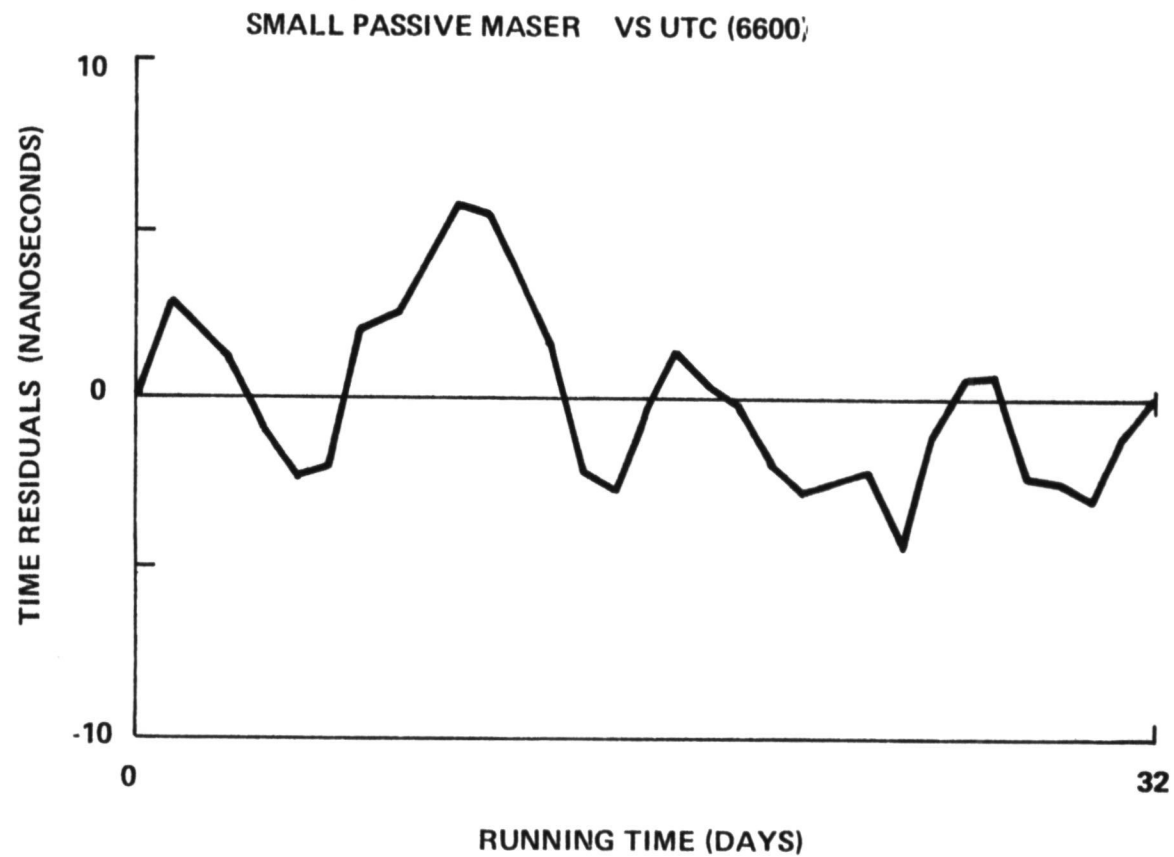


Fig. 9. Daily time of H3 vs. UTC(6600) (average frequency offset removed).

QUESTIONS AND ANSWERS

MR. SAM WARD:

Is it artifact, my imagination or what? It appears to be a 14-day periodicity in your data.

MR. HOWE:

I won't attempt to comment on the periodicity at 14 days. We have not been able to uncover any appreciable correlations with other effects. We have looked at correlation with such things as pressure and temperature as well as other parameters, operating parameters, within the masers. You must consider too that this data is the best data we have seen on our cesium standard NBS-4. We have not been in a good position to measure these long-term effects, and those sorts of fluctuations are not unusual in long-term for cesium devices.

MR. WARD:

How was that 31 or 32 day period selected?

MR. HOWE:

Simply selected because we had an inspiration and stopped the data. The 33-day segment was the longest segment. We had taken about five 2-week segments. One of the factors which have to be borne in mind here is that it takes so long to see some of these subtle effects.

DR. BONNIER:

In view of the fact that you are not compensating in the maser here for spin exchange, interaction, and shift, what is the arrangement you have to keep the pressure constant over such periods of time?

MR. HOWE:

Our total spin exchange shift is 1×10^{-13} , which is roughly a factor of 10 lower than in an active maser. That was derived from an empirical measurement of doing a flux density modulation and looking then at the fractional frequency fluctuation. At 1×10^{-13} for the absolute shift, we need to resolve that to one percent to start looking for effects at the 1×10^{-15} level. We are

using the best manometer we can find; it has an accuracy spec of at the one percent level and a stability spec at the 0.1 percent level. You are right, we have to expend a great deal of attention on that problem since we are not compensating for spin exchange.

STATISTICAL ANALYSIS ON THREE TV-BASED TIME SCALES
IN ITALY: ACCURACY AND PERFORMANCES

L. Mureddu
Stazione Astronomica Internazionale di Latitudine
Cagliari, Italy

(Paper not Presented)

(Paper not Submitted)

Page Intentionally Left Blank

PROGRESS REPORT ON HYDROGEN MASER DEVELOPMENT
AT LAVAL UNIVERSITY

Jacques Vanier, Guy Racine, Ryszard Kanski and Marcel Picard

Laboratoire d'Electronique Quantique
Département de Génie Electrique
Université Laval
Québec G1K 7P4
Canada

ABSTRACT

The paper describes the physical construction of two hydrogen masers which have been under development at Laval University for a few years. Results of measurements made on one of the two masers are given. These include: cavity Q, thermal time constant, line Q, signal power output, magnetic shielding factor.

INTRODUCTION

In the hydrogen maser [1,2], the wall shift remains one of the major perturbations [3]. In the determination of the size of that perturbation one is faced with the problem of cavity tuning accuracy. In the standard or classical technique of tuning by means of spin-exchange broadening [4], one requires, first, a good medium term stability in the range of averaging times from 10 seconds to 1000 seconds. Secondly, one requires the possibility of changing the line quality factor, Q_L , by a large amount. Those two requirements are much more stringent if the final aim is a measurement of the stability of the wall shift with time. There are reasons to believe that such an effect may exist, and reports on the long term stability of the wall shift, for a given maser design, have been given [5]. That effect, if common to all masers, would have important consequences when the maser is used in precision time and time interval applications. Our intent is to measure accurately the wall shift over long periods of time and to determine its actual stability. For that reason we have started the development of two new hydrogen masers which 1) should have the required stability over the averaging times needed and 2) should be tunable easily by means of the spin exchange interaction.

The present paper is a progress report on this development. It describes briefly: a) the main features of the physical construction of the masers, b) the electronic control systems, c) the phase-locked-loop system for locking a 100 MHz crystal oscillator to the maser signal. The paper gives also results of measurements of the actual characteristics of one of the two masers.

THE MASERS PHYSICAL CONSTRUCTION

A schematic drawing of the masers is given in Figure 1. A photograph of an actual maser is shown in Figure 2. The design follows from logical conclusions derived from a study of the various types of masers made by other researchers working in that field, and from an analysis of the results published. An intercomparison of the performance of several of the best masers fabricated up to now has been reported earlier [6]. From the results published, it is concluded that the main limiting factors of the frequency stability of the hydrogen maser are in general:

- 1) sensitivity to temperature fluctuations in the environment,
- 2) sensitivity to barometric pressure fluctuations,
- 3) sensitivity to external magnetic field fluctuations.

The masers were thus designed in such a way as to try to minimize their sensitivity to those perturbations.

1) It is believed that the main cause of instability of a temperature-compensated-cavity is due to temperature gradients in the cavity structure itself. A perfectly compensated cavity by definition will have a zero temperature coefficient. However, the temperature compensation usually done at one end of the cavity coupled to the temperature sensitive dielectric constant of the storage bulb makes the cavity rather unsymmetrical. As a consequence gradients play a very important role. The present design tries to avoid these gradients by means of two heavy "*thermal barriers*" made of aluminum and placed inside a heavy vacuum enclosure. These barriers are held together by means of ceramic insulators for rigidity. The cavity itself is made of quartz. It is thermally compensated by means of a re-entrant OFHC copper disk attached with three OFHC copper rods to one of the quartz end plates. The quartz cavity cylinder and bottom plate are coated with pure silver, by chemical deposition. The loaded quality factor is 35 000 with a coupling coefficient $\beta = 0.2$. The cavity is held inside the inner thermal barrier by means of Be-Cu springs. Furthermore the whole assembly is held at constant temperature by means of 10 independent temperature regulators placed symmetrically around the structure. Such a structure has a very long time constant. Figure 3 is a preliminary result showing the variation of the cavity resonance frequency as a function of time after a step function of temperature has been applied to the vacuum enclosure. The long settling time is essentially a measure of the decoupling between the cavity and the outside world. The temperature coefficient in that case is of the order of 200 Hz/°C. If the cavity can be held to $\pm .001$ °C we expect a frequency stability of $\pm 2 \times 10^{-15}$.

2) That same structure design has also the advantage of decoupling the cavity from external barometric pressure fluctuations. In practice it is observed, that the barometric pressure affects the resonance frequency of the cavity through a mechanical distortion. The importance

of this distortion is a function of the nature of the bottom plate of the vacuum envelope and of the type of attachment of the cavity to that bottom plate. In the present design, the mechanical decoupling created by the thermal shields and the spring mounting of the cavity should make this effect negligible. Conclusions on the performance of the design will be drawn from actual measurements.

3) The sensitivity to magnetic field is expressed through the following equation:

$$\nu = \nu_0 + 2752 < B^2 >$$

Normally the maser operates in an induction of 1 mgauss. The sensitivity to magnetic field fluctuations is then given by the expression:

$$\delta\nu_B = 5.5 \Delta B$$

In order to achieve frequency fluctuations less than 1×10^{-15} , one requires that the magnetic fluctuations be less than $0.25 \mu\text{gauss}$. We have chosen a magnetic shielding system consisting of 5 moly-permalloy cylindrical enclosures with end caps [7]. The bottom caps have a 2 inch hole for the pumping duct. The dimensions of these shields are respectively:

Shield N°	1	2	3	4	5
Radius R (inch)	12	11	10	9	8
Length L (inch)	30	28	26	24	22
Thickness (inch)	0.050	0.025	0.025	0.025	0.025

Table 1 - Dimensions of the magnetic shields

The shielding factor is defined as follows:

$$S = \frac{\text{External field}}{\text{Internal field}} = \frac{H_{ext}}{H_{int}} = \text{Shielding factor}$$

or

$$S_{dB} = 20 \log \frac{H_{ext}}{H_{int}}$$

For a single cylindrical shield with end caps, the shielding factors are given by the expressions [8]:

$$S_t = \frac{1}{2} \mu t'$$

$$S_l = 2 D \mu t' \left[1 + \frac{R}{L} \right]^{-1}$$

where subscript t refers to transverse while subscript l refers to longitudinal. In these expressions t' is the ratio of the material thickness to the shield radius R , L is the length of the shield, μ

is the permeability of the material at the actual level of magnetic induction B_m inside the material. The value of B_m is obtained from the relation:

$$B_m = 2 \gamma H_{ext} / t'$$

where γ is a geometrical factor close to 1. The symbol D stands for demagnetisation factor. In our case it has a value between 0.26 and 0.28 for the 5 shields considered. The calculated values of S_t and S_l for the five shields are given in Table 2. The measured values of S_t are also given.

Shield N°	1	2	3	4	5
$S_i(H_{ext})$					
S_l (1 oersted) calculated	165	145	145	145	148
S_t (1 oersted) calculated	181	147	150	153	164
S_t (1 oersted) measured	125	118	140	130	125
S_l (Low field limit) calculated	50	27	30	33	35
S_t (Low field limit) calculated	62	34	38	42	47

Table 2 - Calculated and measured shielding factor of the five individual shields

The measured values are slightly lower than the calculated ones. This may be due to the fact that the actual μ of the material used varies slightly from shield to shield and does not have exactly the tabulated value.

In the case of two concentric shields with end caps the transverse shielding factor is given by:

$$S_t = S_{t_1} \times S_{t_i} \left(1 - \frac{R_i^2}{R_1^2}\right) + S_{t_1} + S_{t_i}$$

where i refers to the inner shield and 1 refers to the outer shield. The value of S_{t_i} has to be taken as the low field value. We have made measurements with the four smaller shields placed one at a time inside shield #1. The results for the transverse shielding factor are given in Table 3. This table gives also the calculated values for the combinations in question, using the calculated values shown in Table 2. These results are also shown in Figure 4. The agreement between the calculated and the measured values is relatively good. Finally, the shielding factors S_t and S_l were measured for the cumulative effect of the five shields. The results are shown in Figure 5 and illustrate

Shields Combination	N° 1 + 2	N° 1 + 3	N° 1 + 4	N° 1 + 5
S_t calculated [dB]	61.6	67.2	71.0	73.9
S_t measured [dB]	61.1	67.7	70.5	72.0

Table 3 - Calculated and measured values of the transverse shielding factor for various combinations of two shields.

the increase in shielding factor with the number of shields used. The maximum shielding factor of the five shields is thus:

$$S_t (1 \text{ oersted}) = 128 \text{ dB ; measured}$$

$$S_\ell (1 \text{ oersted}) = 100 \text{ dB ; measured}$$

The longitudinal shielding factor is lower than the transverse shielding factor as expected. The value obtained means that external longitudinal fluctuations are attenuated by a factor of 10^5 . This also means that, for a frequency stability better than 10^{-15} , a fluctuation of the external field larger than 25 mgauss cannot be tolerated. Although the measurements reported here were done in a field 1 gauss, they are expected to apply approximately in the earth's field. This is due to the fact that only the outside shield changes its state of magnetization and that it is not saturated. Consequently, the overall shielding factor is not much affected. We expect that, with the present arrangement, we can tolerate a fluctuation of the earth's field of 10%, and still meet the requirement on stability set above.

Two other important items in the hydrogen maser construction are the source and the storage bulb.

1) In the hydrogen source, we have paid attention specially to the plasma-glass interaction. To minimize this effect we have used a large glass envelope as the dissociator. It is essentially a glass cylinder 2 inches long and two inches in diameter. The plasma is excited by a transistorized oscillator (100 MHz, 3 watts) whose tank circuit surrounds the discharge bulb.

The hydrogen pressure is stabilized with the help of a servo system controlling the temperature of a "Ag - Pd" hydrogen leak. The temperature is measured with a thermistor bead. The hydrogen leak is made of a fine finger glove, 4 cm long, 1 mm in diameter, and 0.1 mm thick [9]. The heating current passes directly through the finger glove. Approximately 1.5 A is required in normal operation. The source is completely assembled with Cajon fittings and copper gaskets. A block diagram of the system is shown in Figure 6. The dynamic response of the whole servo was tested with a step function command. The results are shown in Figure 7. It is observed that the time for equilibrium to be

achieved is about 5 seconds. This fast response is extremely important in regards to cavity tuning by means of spin exchange broadening.

2) The storage bulb: the storage bulb of the maser is made of quartz. In one of the masers it is a sphere 15 cm in diameter and coated with FEP 120 Teflon. The bulb collimator is made of 12 small tubings of commercial Teflon clustered at the entrance of the bulb. That approach has the advantage of presenting a large opening to the incoming beam, while holding the bulb escape time constant long. The arrangement works extremely well in the sense that the bulb line Q is very high and the maser oscillates at very low hydrogen fluxes. A typical result is shown in Figure 8. In that figure the signal output in arbitrary units and the line Q are plotted as a function of the pressure read on the servo control. In Figure 9, the inverse of the line Q is plotted as a function of pressure. This graph permits an extrapolation to zero pressure and gives the value of the line Q without spin exchange interaction. In the present case it is observed that the low pressure limit line Q is 3.2×10^9 while the high pressure limit is 9.6×10^8 . This corresponds to a variation greater than 10 in flux between the low pressure and the high pressure flux thresholds. The quality factor q of the maser is evaluated to be approximately 0.10. This is calculated from the theory developed in Reference [2].

The accuracy to which the maser can be tuned is given by [10]:

$$\frac{\delta_{\text{offset}}}{\nu_0} (\text{LP}) = \frac{(\nu_m (\text{LP}) - \nu_m (\text{HP}))}{\nu_0} \left[1 - \frac{Q_\ell (\text{LP})}{Q_\ell (\text{HP})} \right]^{-1}$$

where $(\nu_m (\text{LP}) - \nu_m (\text{HP}))$ is the difference in frequency of the maser between low and high pressure of hydrogen in the storage bulb and, $Q_\ell (\text{LP})$ and $Q_\ell (\text{HP})$ are the low pressure and high pressure line Q 's possible. The accuracy to which $(\nu_m (\text{LP}) - \nu_m (\text{HP}))$ can be measured can be taken as the stability of the masers over the time of measurements. If a stability of 2×10^{-15} is achieved we thus have, from the line Q measurements reported here, a calculated tuning accuracy of about 4×10^{-15} .

ELECTRONIC CONTROLS

The following electronic systems are integral parts of the masers: 1) Power supplies, 2) VacIon control, 3) Hydrogen pressure control, 4) Magnetic field control, 5) Low frequency oscillator for the measurement of transitions between the Zeeman levels and subsequently for the determination of the magnetic induction at the site of the storage bulb, 6) Varactor control, 7) 100 MHz power oscillator to excite the hydrogen plasma in the dissociator, 8) Temperature regulators.

The design of these various controls has been made along the lines of established technology and published data in this field [11,12,13,14].

Their detailed description will be given somewhere else. It is necessary here only to mention that great care was taken in their construction in order to produce stable units. For example the temperature regulators are themselves regulated in temperature. The varactor control uses a Kelvin-Varley divider. The power sources are regulated at their input to each unit. We expect by means of these techniques to minimize external perturbations on the controls and unwanted perturbations on the maser frequency itself.

THE RECEIVER AND PHASE-LOCKED-LOOP

A receiver has been designed to detect the maser signal at 1.4 GHz and to phase-lock a basic quartz crystal oscillator to that signal. The frequency of the oscillator has been chosen as 100 MHz for reason of good phase stability at low cost. The design of that receiver is shown in Figure 10. It has been mounted as a breadboard and tests on its dynamic behaviour are being made. A final report will be given later.

CONCLUSION

In this paper we have described the construction of two hydrogen masers and have given experimental results on the operation of one of them. From the preliminary results obtained it is expected that the frequency stability will still be mainly affected by the thermal stability of the cavity. The magnetic field and the barometric pressure fluctuations should not affect the maser at the stability level above a few parts in 10^{15} which is our goal for averaging times of several hours.

ACKNOWLEDGEMENTS

We would like to thank MM. Roger Blier and Yvon Chalifour for their competent technical assistance. We would also like to thank Mr. Julien Morasse who has contributed greatly through his competence in the mechanical design of the masers. This program of research is sponsored by the National Sciences and Engineering Research Council of Canada and the Ministère de l'Éducation de la Province de Québec.

REFERENCES

- [1] Kleppner, D., Goldenberg, H.M. and Ramsey, N.F., Phys. Rev. 126, 603-15, 1962.
- [2] Kleppner, D., Berg, H.C., Crampton, S.B., Ramsey, N.F., Vessot, R.F.C., Peters, H.E., and Vanier, J., J. Phys. Rev. A. 138, 972-83, 1965.
- [3] Vanier, J. and Larouche, R., Metrologia 14, 31-37, 1978.
- [4] Vanier, J. and Vessot, R.F.C., App. Phys. Letters 4, 122-23, 1964.
- [5] Morris, D., IEEE Trans. on Instr. and Meas., 339-342, 1978.

- [6] Kuhnle, P.F., Proc. of the 11th PTTI Applications and Planning Meeting, 197-213, 1979.
- [7] Allegheny, Ludlum, Brachenridge Penn.
- [8] Gubser, D.E., Wolf, S.A., Cox, J.E., Rev. Sci. Instr. 50, 751-756, 1979.
- [9] Viennet, J., Petit, P., Audoin, C., J. of Phys. E. Scientific Inst. 6, 257-261, 1973.
- [10] Petit, P., Viennet, J., Barillet, R., Desaintfuscien, M., Audoin, C., Metrologia 10, 61, 1964.
- [11] Vessot, R.F.C., Levine, M., Final Report Contract J.P.L. 9548118 Grant NSG 8052, 1977.
- [12] Petit, P., Viennet, J., Barillet, R., Desaintfuscien, M., Audoin, C., Metrologia 10, 61, 1974.
- [13] Reinhardt, V.S., Rueger, L.J., Space Electronics Systems Group, Report S3 LJR 002, September 1979.
- [14] Beverini, N. and Vanier, J., IEEE Trans. on Instr. and Meas., IM-28, 100-104, 1979.

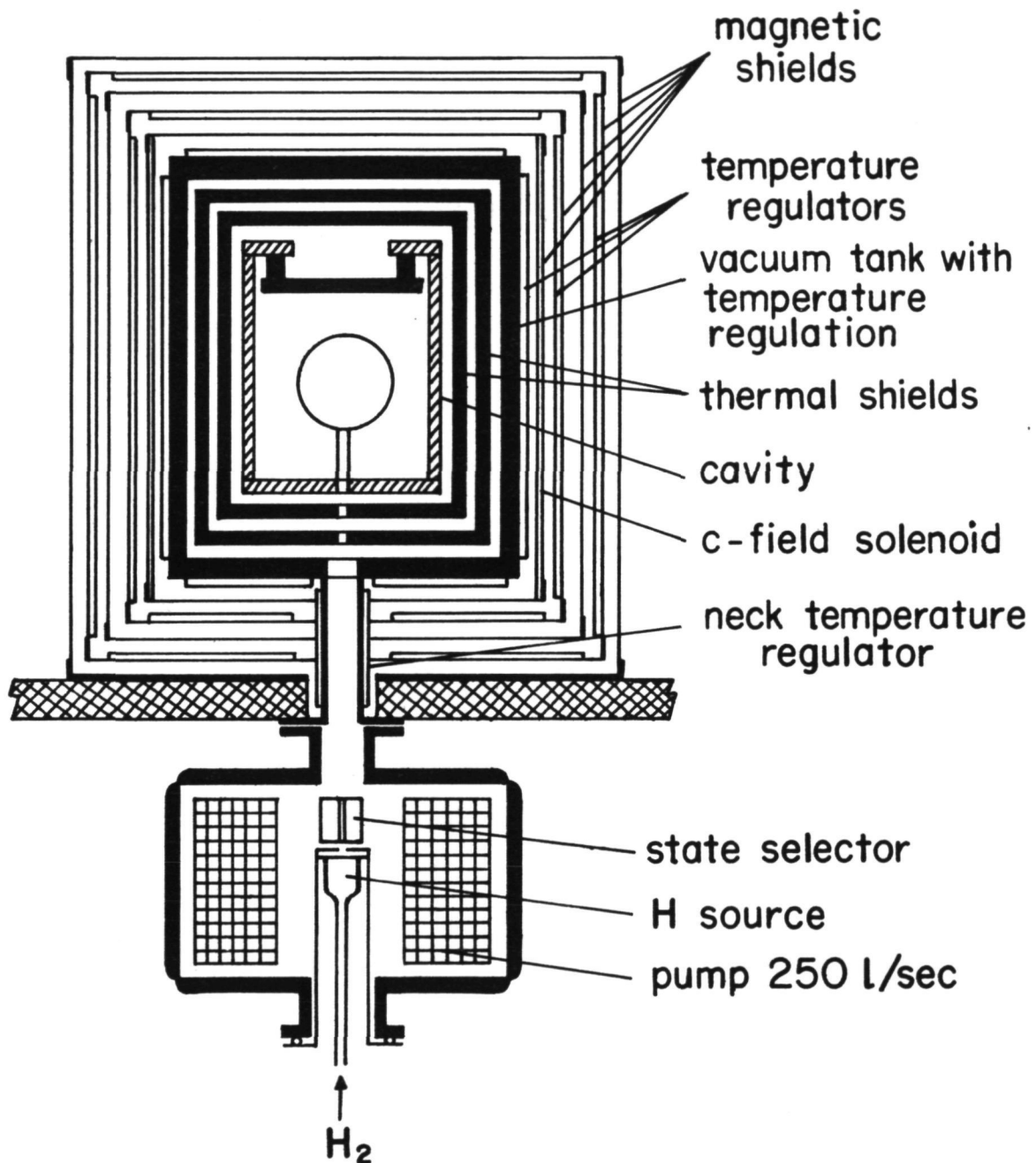


Figure 1 : Schematic drawing giving the main concepts used in the maser design.

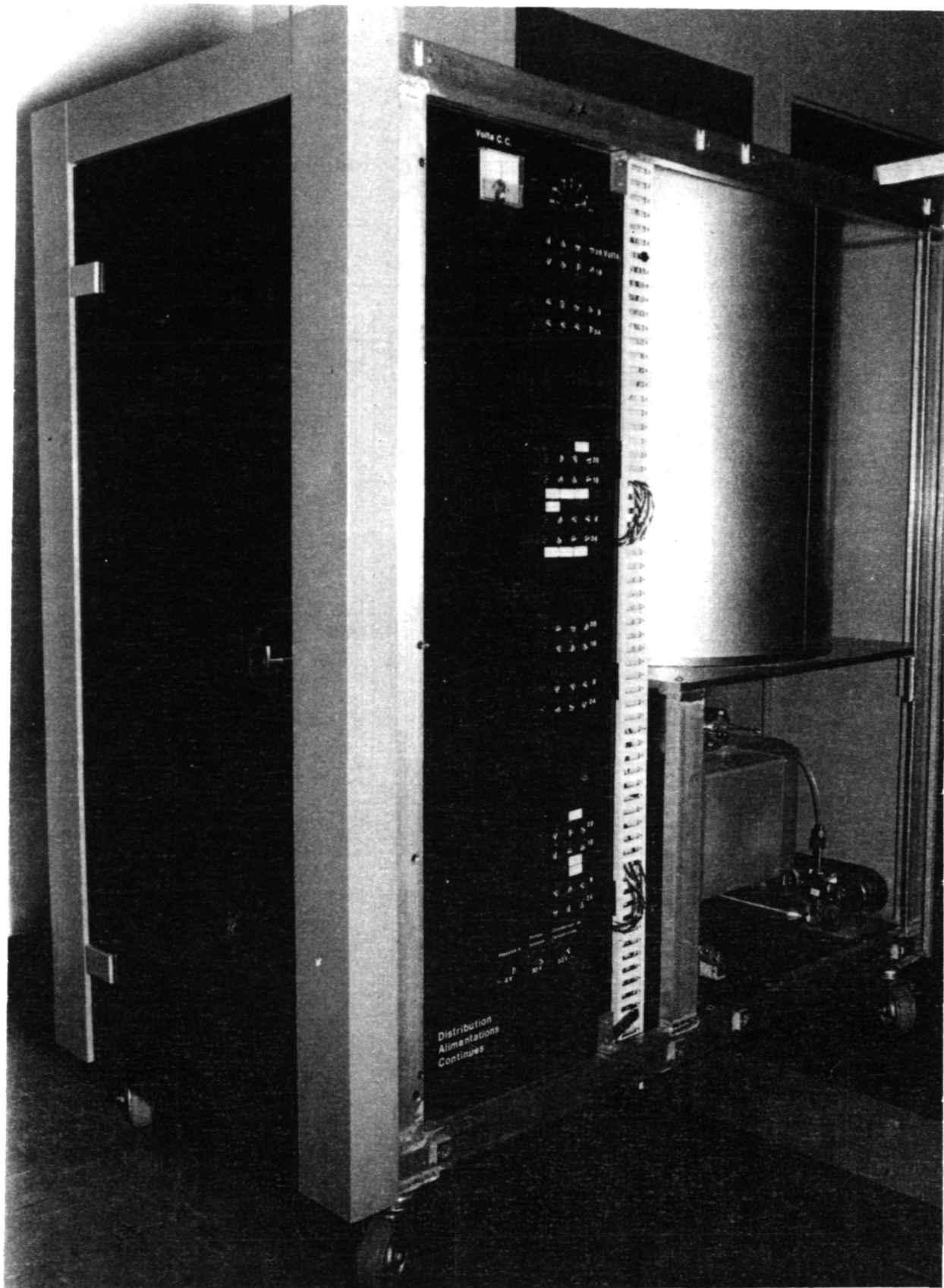


Figure 2 : Photograph of one of the masers.

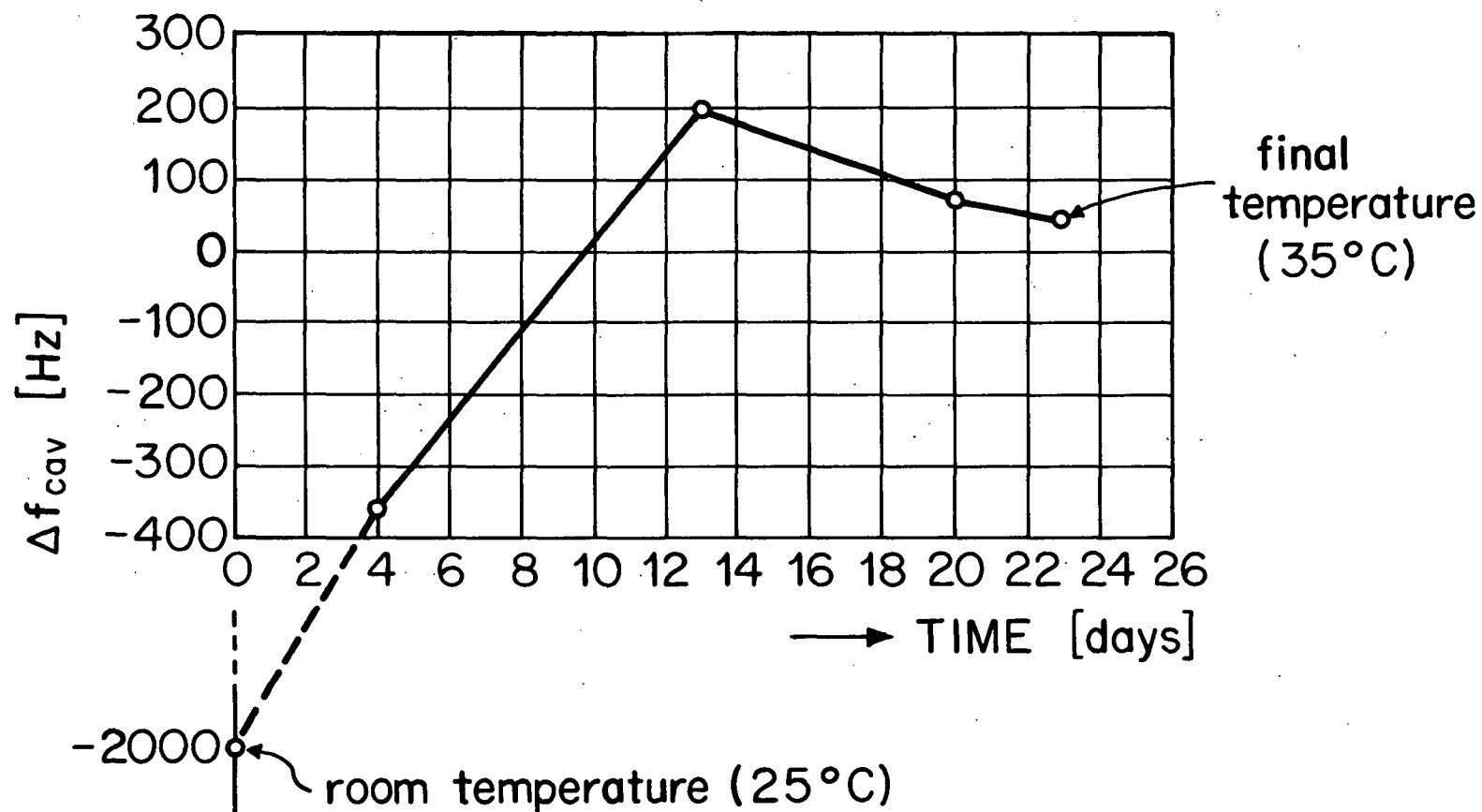


Figure 3 : Variation of the cavity resonance frequency after a step function variation of the temperature has been applied to the vacuum enclosure.

TRANSVERSE SHIELDING FACTOR S_T [dB]

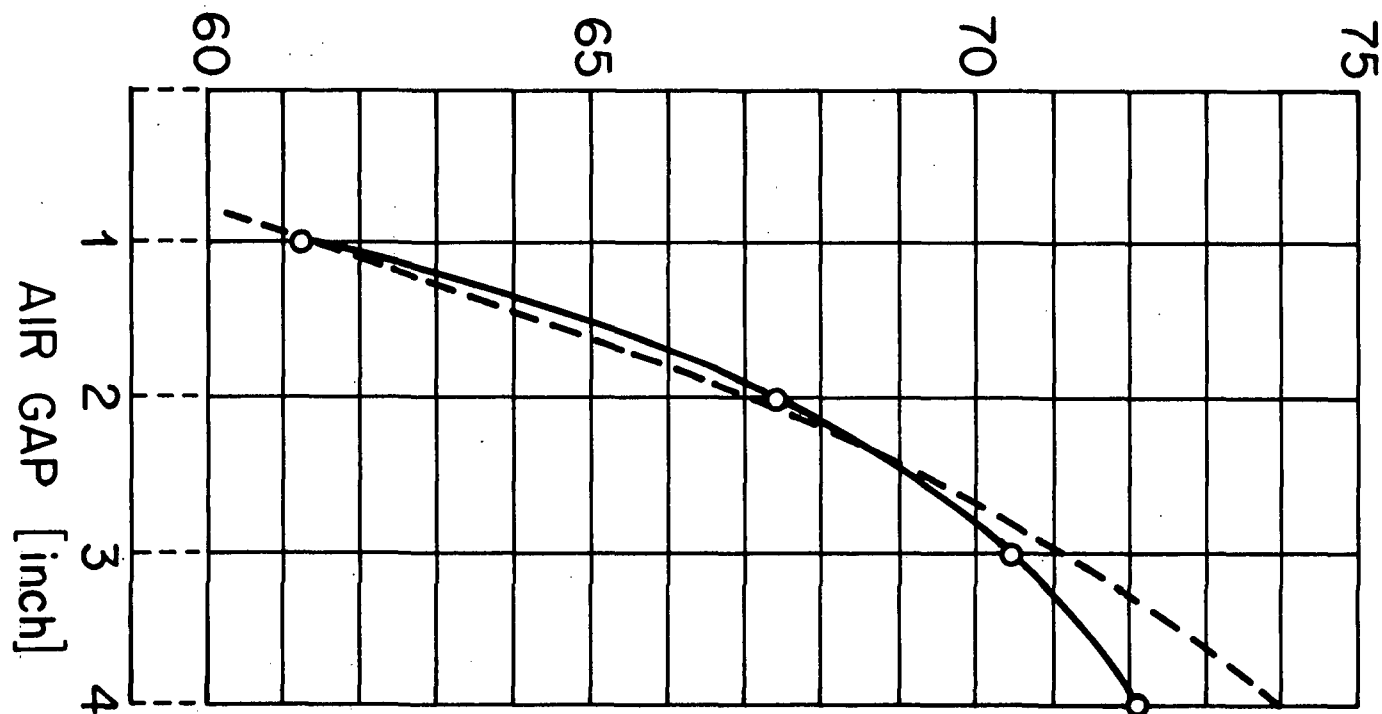


Figure 4 : Shielding factor as a function of the air gap ($B_{ext}=10^{-4}T$);
solid line: experimental; dotted line: theoretical.

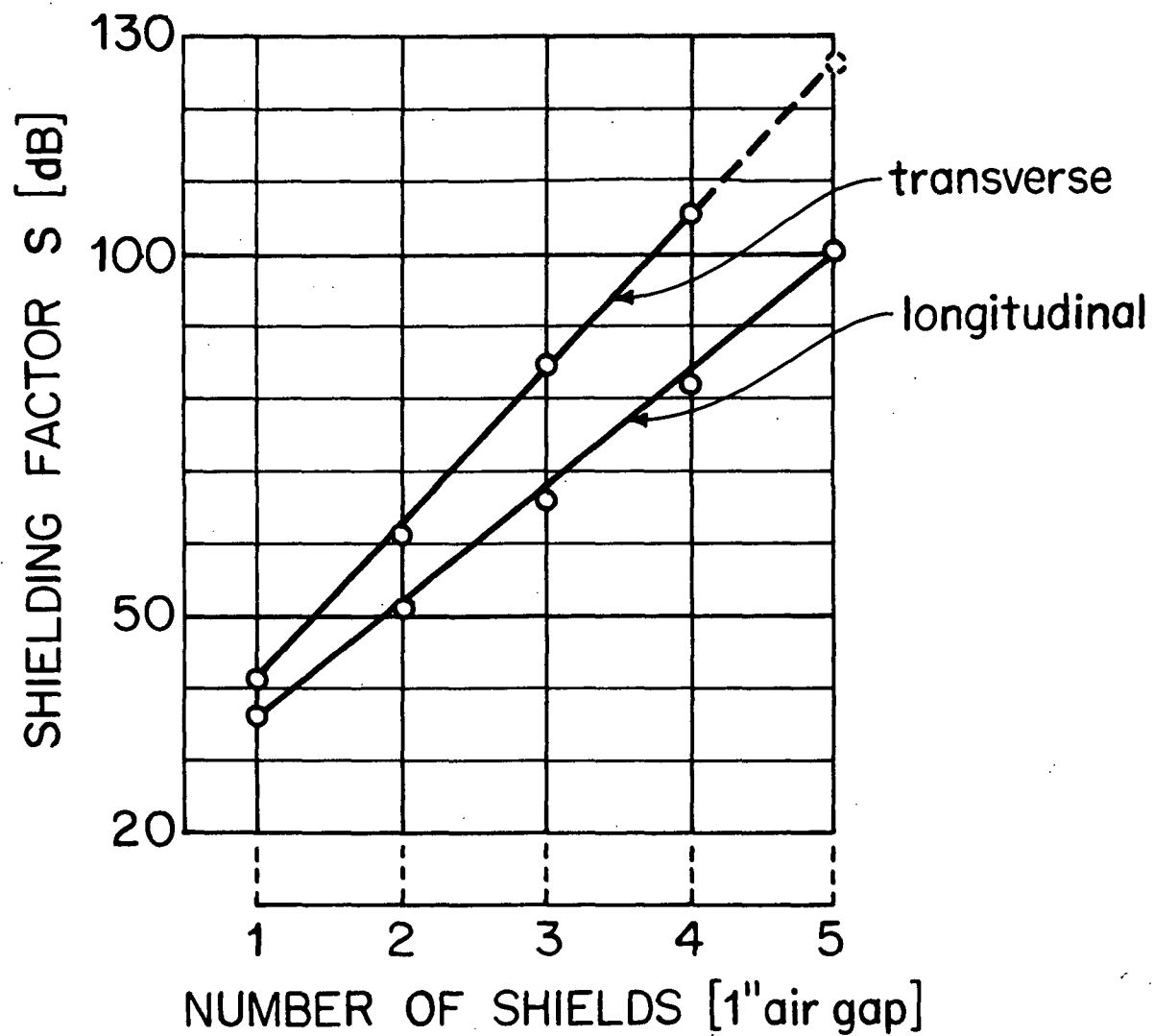


Figure 5 : Graph showing the increase in shielding factor with the number of concentric shields used.

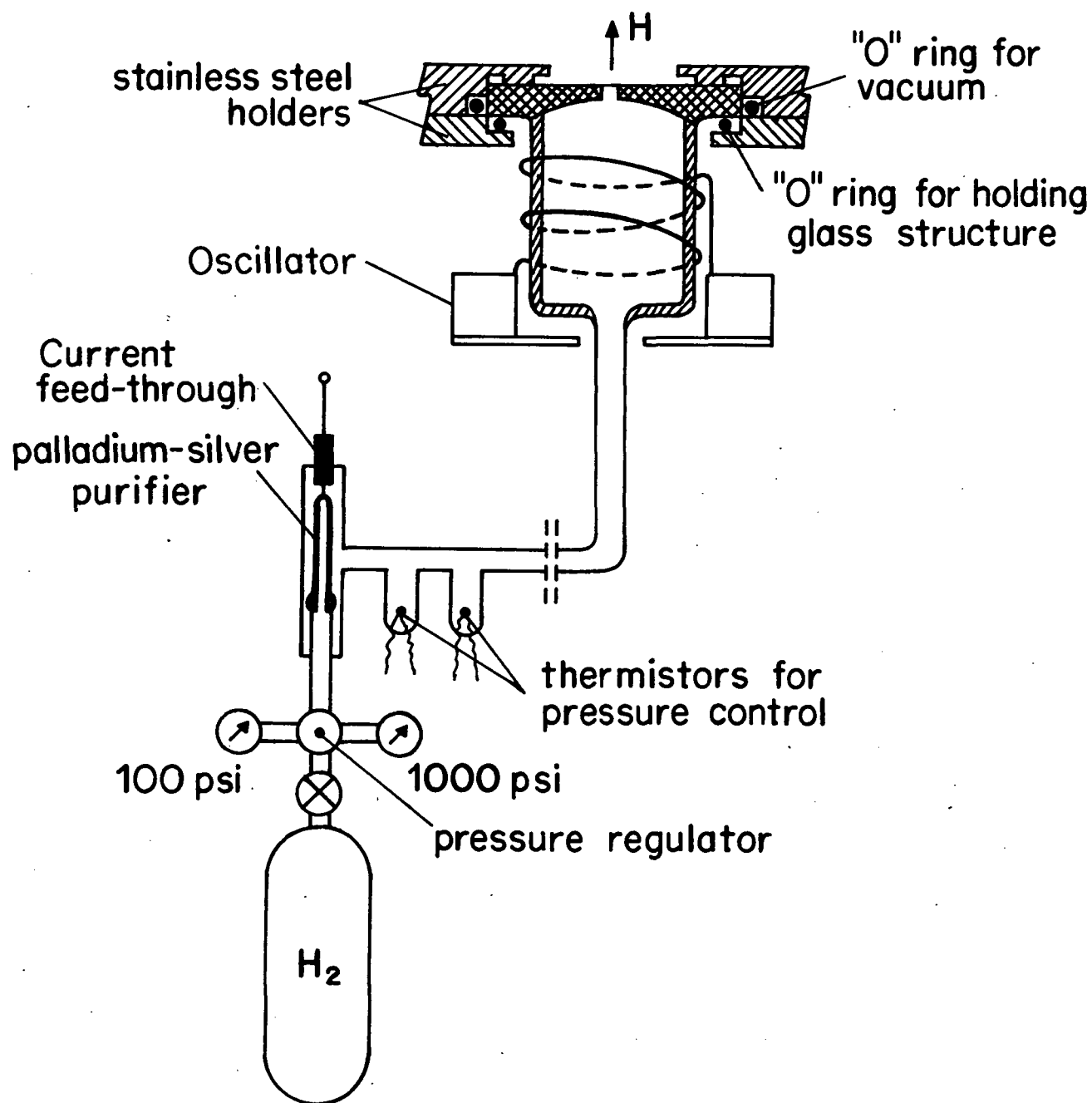


Figure 6 : Block diagram of the hydrogen source and the pressure control.

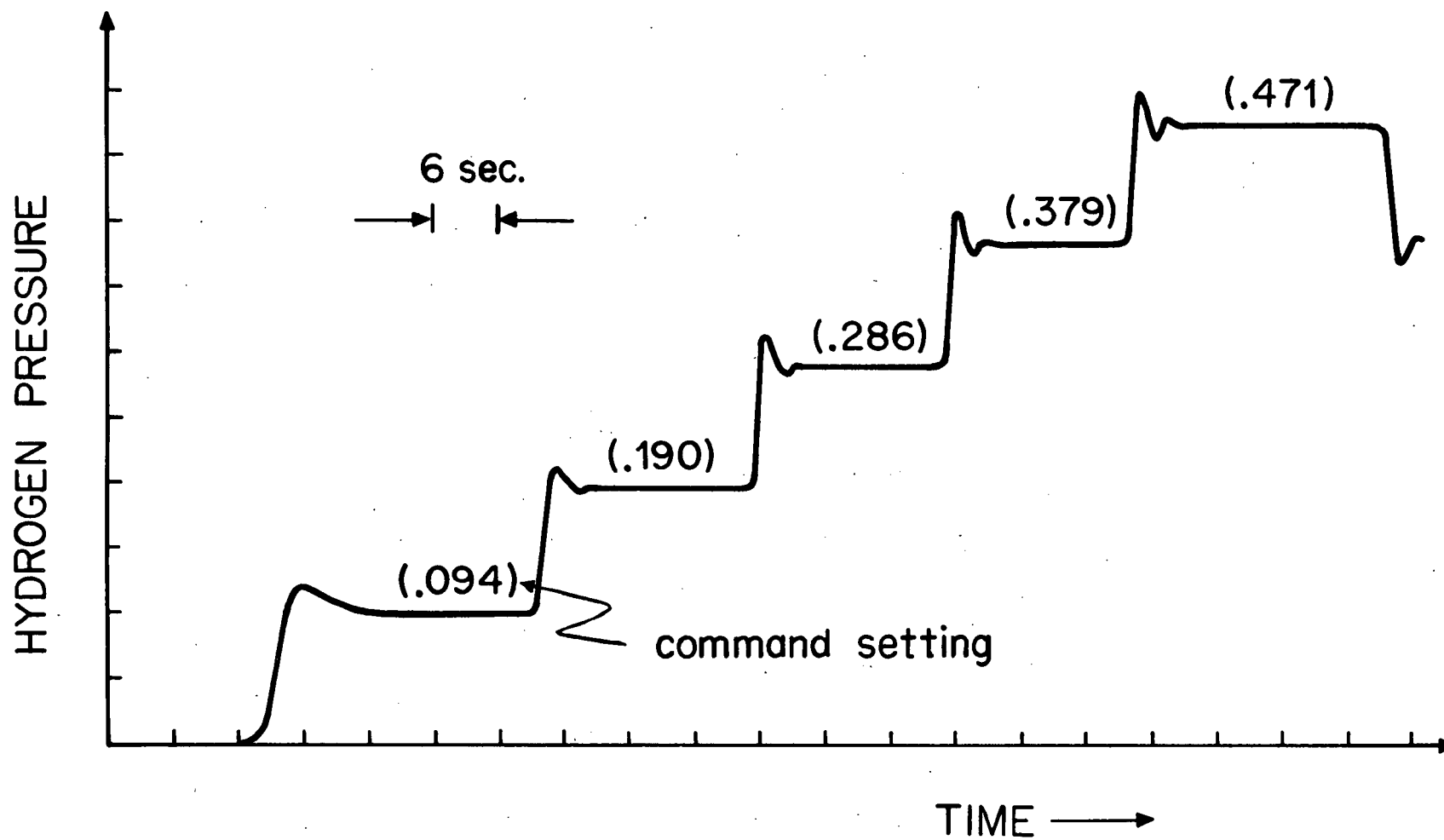


Figure 7 : Response of the pressure control system to a step function command.

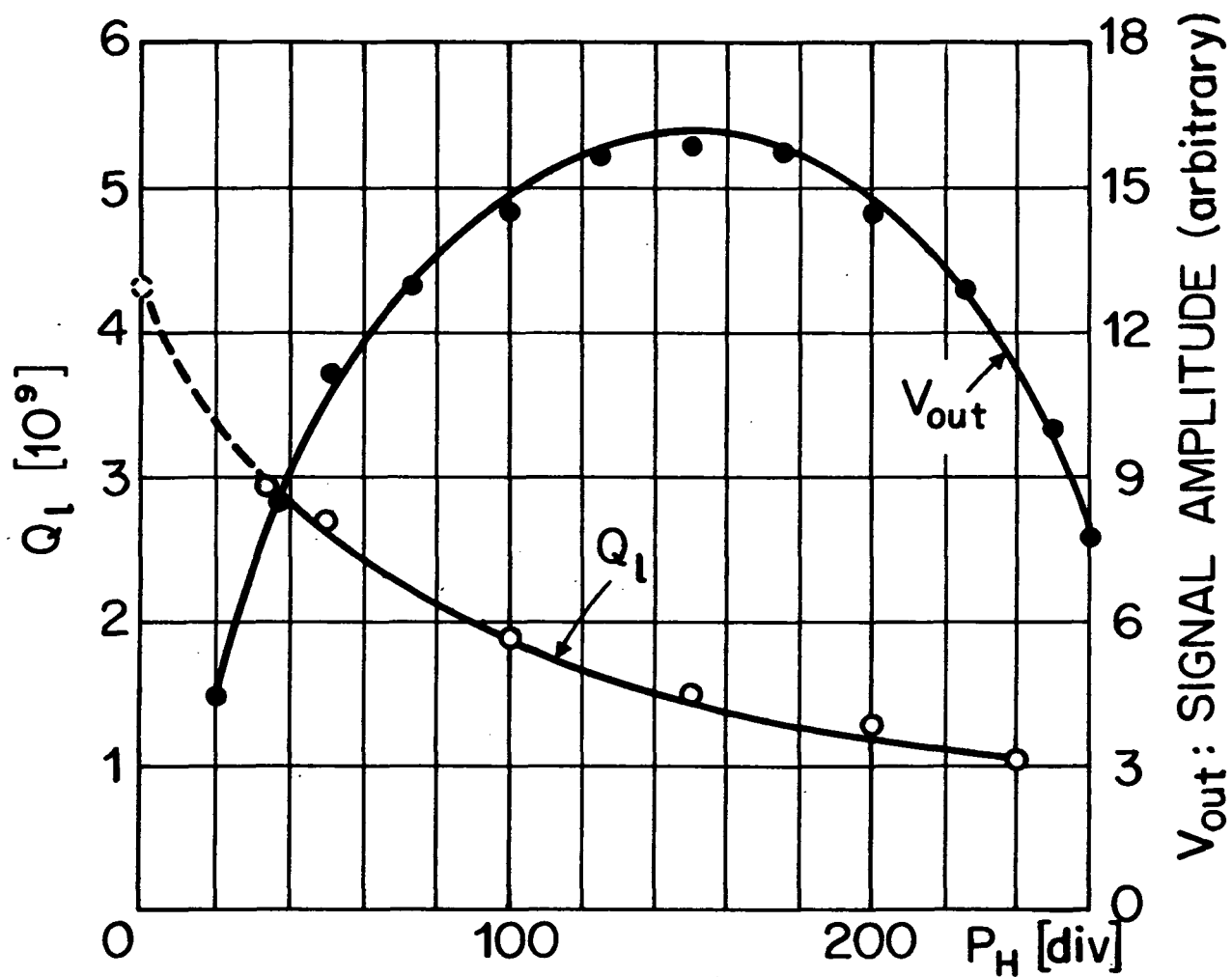


Figure 8 : Signal output of the maser and atomic line Q as a function of hydrogen pressure.

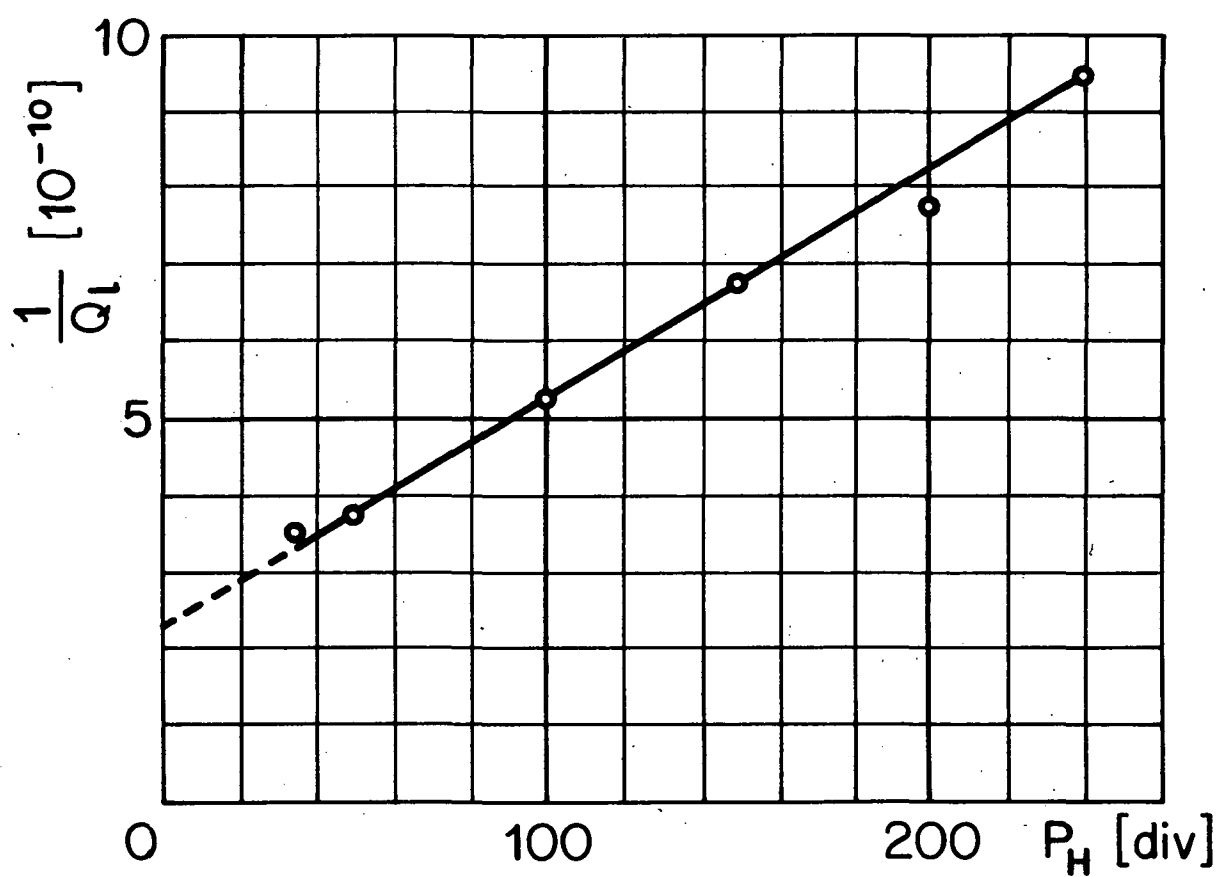


Figure 9 : Inverse of the line Q as a function of hydrogen pressure.

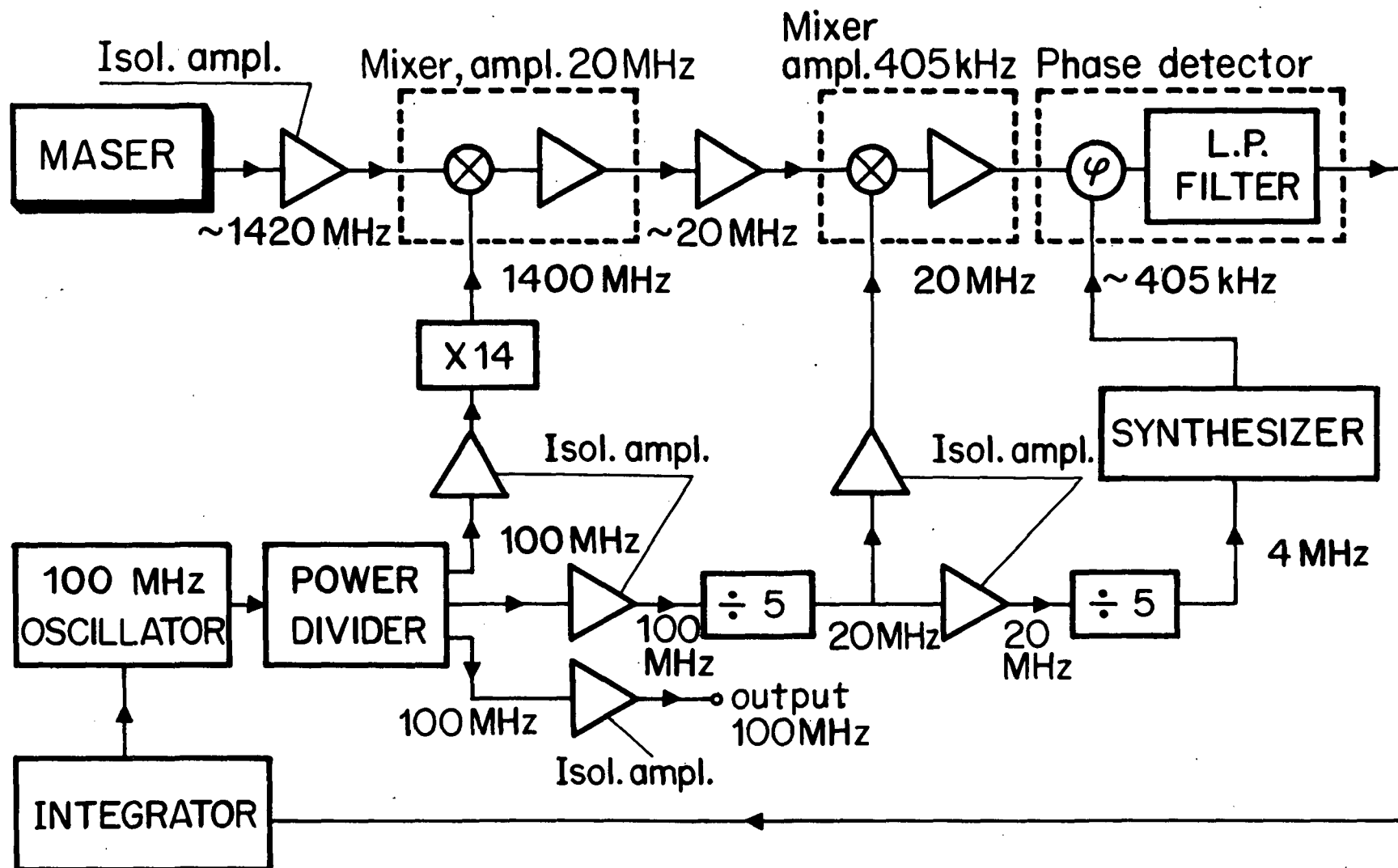


Figure 10 : Block diagram of the 100 MHz phase-locked-loop system for the hydrogen maser.

QUESTIONS AND ANSWERS

MR. DAVID HOWE, National Bureau of Standards

It was a very interesting experiment that you have set-up, Dr. Vanier, but I have a couple of questions with regard to the human factor with five shields. Was that a calculation or was that experimental?

DR. VANIER:

Oh, experimental.

MR. HOWE:

Okay, and what guarantee do you have that there are no residuals after degaussing? For example, creep will change that frequency, long-term --

DR. VANIER:

It does not, I have no guarantee of that.

MR. HOWE:

What kind of sensor are you using to determine the temperature? What accuracy is that sensor over long-term?

DR. VANIER:

The sensor, itself?

MR. HOWE:

Yes.

DR. VANIER:

For the magnetic field?

MR. HOWE:

No, I am sorry, for the temperature?

DR. VANIER:

It is standard; I can give you the company.

MR. HOWE:

And, was that an all glass thing?

DR. VANIER:

Yes. This was not really a problem here. When we say we want stability over let's say 1,000 seconds. We don't want stability over a year, we want to tune the maser all the time.

MR. HOWE:

I understand that, but maybe I don't understand. So, what you are saying is that you use the pressure method of tuning.

DR. VANIER:

We use the spin exchange broadening method of tuning, you have to. You could not rely on any temperature stability of the order of magnitude required here.

MR. HOWE:

I agree.

DR. VANIER:

To measure the wall shift on a long-term basis.

MR. HOWE:

Fine, that was a misunderstanding on my part.

And, last; at what level does the spin exchange come in with this method of tuning? In other words, with pressure modulation do you --

DR. VANIER:

You mean the spin exchange shift itself?

MR. HOWE:

Yes.

DR. VANIER:

Well, I think that we have shown that in the past a long time ago and of course there are small effects, second order effects, but

we have shown that the spin exchange tuning technique, the broadening technique used cancels exactly within the first order the spin exchange shift.

The cavity is mistuned by this process in such a way that the spin exchange shift is canceled, which you don't have in other types of tuning. Yes, that is the whole secret; I think that we have shown that a long time ago, to a great accuracy.

MR. HOWE:

My problem is being able to separate out the --

DR. VANIER:

In the passive time.

MR. HOWE:

Yes.

DR. VANIER:

Oh, in the passive time then you don't use spin exchange broadening to change the maser, in that case you use spin exchange exactly -- you can prove mathematically and it works out in practice that once you have found that point where your frequency is independent of pressure it is a simple point.

DR. REINHARDT, NASA/Goddard

Are you setting up any devices to measure magnetic shift and anomalous spin exchange shifts, because they can be on the order of several parts in 10^{13} .

DR. VANIER:

You are talking about ϵ_M or ϵ_H ?

DR. REINHARDT:

Yes.

DR. VANIER:

No, not yet. I am not there yet.

DR. REINHARDT:

But, are you going to?

DR. VANIER:

Yes, we think that we will be able to do that, yes.

DR. REINHARDT:

Okay.

DR. VANIER:

But, I will talk to you about it.

SOME NEW RESULTS ON THE FREQUENCY CHARACTERISTICS
OF QUARTZ CRYSTALS IRRADIATED BY IONIZING
AND PARTICLE RADIATIONS

Harish Bahadur and R. Parshad,
National Physical Laboratory,
Hillside Road, New Delhi,
110 012 (India)

ABSTRACT

Investigations on the frequency behavior of AT-cut quartz crystals irradiated by X -, γ -rays and fast neutrons have been carried out. Initial instability in frequency for γ - and neutron irradiated crystals has been found. All the different radiations first give a negative frequency shift at lower doses which are followed by positive frequency shift for increased doses. An explanation of the results in terms of the fundamental crystal structure consideration is offered. Applications of the frequency results for radiation hardening are proposed.

INTRODUCTION

To date, radiation effects in quartz crystals is a widely studied subject. The major stimulus in the area has been largely due to the use of quartz crystals as essential electronic components for various types of communication, time and frequency standardization and other scientific and industrial uses. It is expected that with an increased understanding of the relationship of various structural properties and radiation effects, the performance characteristics of quartz material can be greatly improved according to requirements.

Due to the development of high stability quartz crystals, it is becoming possible to disseminate time and frequency signals by using quartz crystal oscillators in flying clocks, satellites etc.(1). However, for the purpose of dissemination to be achieved, it would become necessary to harden the quartz crystals against natural ionizing (X- or γ -rays) and particle (protons, neutrons, α -particles etc.)

radiations present in space. Alternatively, the effects on frequency characteristics of quartz crystals exposed to the radiation environment can be allowed for if the frequency characteristics of irradiated crystals are properly understood. All this indicates the need to study the effect of ionizing and particle radiations on the frequency and structural characteristics of quartz crystals.

A number of papers (2-19) have appeared on the radiation effects on the frequency characteristics of quartz crystals. The frequency changes due to irradiation by fast neutrons are permanent positive frequency offsets. The change in frequency due to ionizing radiations is of two kinds; transient and permanent. King and Sander (20-24) have extensively studied the transient frequency changes in quartz resonators. The transient frequency shift has been found to last for about 15 minutes in natural crystals and for a greater time (~ 1 hour) in synthetic crystals and is due to the temporary removal of H^+ ions from Al^{3+} -centers in the quartz lattice under the influence of irradiation and their back diffusion after the termination of irradiation. Bahadur and Parshad (25) have recently given a simple method to demonstrate the transient frequency shifts in X- or Gamma-irradiated quartz crystal resonators. The permanent frequency change in the quartz crystals has been found to be due to the drift of the alkali ions, freed from their charge compensating positions as a result of irradiation, to ion traps in the c-axis. The alkali ions can be brought back to the Al^{3+} -centers only by heating the quartz crystals (say at $200^\circ C$). The permanent frequency change in natural quartz due to irradiation with ionizing rays is negative and in the synthetic crystals it is positive. In the case of swept crystals (H^+ ions replacing the alkali ions in the quartz lattice), there is almost negligible change of frequency(8). However, for reasons being investigated perfect radiation insensitivity (radiation hardening) has not yet been achieved (26,27).

This paper presents and discusses some new results obtained on the frequency characteristics of quartz crystals irradiated by X-, γ -rays and fast neutrons. Some limited data on the subject has been published earlier (28).

EXPERIMENTAL

The quartz crystals used for the investigations were of two types; one, rectangular AT-cut plates of dimensions $3.8 \times 2.8 \times 0.04 \text{ cm}^3$ capable of vibrating in their fundamental thickness-shear mode in the frequency region of 1.87 MHz

and the others AT-circular beveled centrally plated disks of frequency around 5 and 10 MHz. The precision in the frequency measurement was ± 1 Hz as the frequencies were measured digitally.

The radiations used were X-rays (30 kV, 12 ma, Cu target, white radiations), γ -rays (^{60}Co , 1000 Ci, 1.25 MeV average energy) and fast neutrons ($^{241}\text{Am-Be}$). Neutron irradiation was done by two different $^{241}\text{Am-Be}$ sources (half life 433 years). One of the sources, following the well known α -n reaction, emitted neutron flux of 2.67×10^7 neutrons/sec/cm². The associated γ -dose rate was feeble (~ 0.25 mR/sec at one meter from the source). The other $^{241}\text{Am-Be}$ source emitted fast neutrons with average energy of 4.5 MeV and a flux of 10^7 neutrons/sec/cm². The strength of this source was 5 Ci having $5 \times 3.7 \times 10^{10}$ disintegrations per second and 40% of these disintegrations were accompanied by emission of 60 keV γ -rays and 13% (of disintegrations) by emission of 100 keV γ -rays. Other γ -energies were quite low. It may be noted here that 60 keV and 100 keV γ -energies are not considerable enough to cause nuclear displacements in the lattice, the main effect being due to neutrons. The γ -rays would in fact act like X-rays for their frequency effects.

Irradiation with Ionizing Radiations

The results of X- and γ -irradiation were of the same broad pattern with regard to the permanent frequency offset. However, for γ -irradiation there was observed a period of initial unstable oscillations when the irradiated crystals were first incorporated in the self-oscillating circuit. Fig. 1 depicts a typical result for a natural crystal exposed to 2000 Rads and allowed to oscillate. This instability in the initial oscillations was to a large extent independent of time of idle keeping of the crystal after the termination of irradiation and before the generation of oscillations. For X-irradiation, no such instability of oscillations was noticed, the change in the frequency offset being only steady.

The nature of steady frequency offset for both X- and γ -rays was such that for lower doses the frequency decreased and with continued irradiation, the frequency, after reaching a negative limit started increasing to a value even greater than that of the virgin crystal. Many natural crystals were investigated for this behavior. Figs. 2 and 3 depict the plot of steady frequency change versus irradiation dose for two crystals. It was observed that different

crystal specimens, yielded, for the same accumulated irradiation dose, different magnitude of frequency offsets. This of-course indicates, as is widely accepted to be the case, individual variations in the lattice characteristics of the crystal by way of impurity concentration, crystal imperfections etc. Table (I) depicts the frequency offsets for a set of three different crystals which were uniformly irradiated by ^{60}Co with a dose of 48 kRads. Fundamental and third overtone steady frequencies for virgin and irradiated crystals are listed. It can be seen that the offsets in the frequencies of irradiated crystals with regard to those of virgin crystals are always positive. Table (II) depicts the results for a set of four crystals uniformly irradiated with a dose of 5 MRads. The post-irradiation frequencies mentioned are those which were measured after the crystals were allowed to oscillate and their initial instability was culminated by the mechanical oscillations themselves.

Still higher doses (~ 7.5 MRads) were given to different specimens and it was noticed that for prolonged irradiation, the relative change in the magnitude of frequencies were, in an apparent unexpected manner, much less than the values obtained for relatively lower doses. Also, it would be significant to mention here that the darkening in the crystals irradiated with doses of 7.5 MRads was relatively less than what was induced by 5 MRads, as observed visually. This phenomenon may be attributed to what is called 'radiation bleaching'. Fig.4 depicts the initial frequency instability character for a crystal of 1.87 MHz after it was irradiated with a dose of 7.5 MRads and made to oscillate. The pre-irradiation frequency for this specimen was 1869293 Hz and after 7.5 MRads irradiation the frequency upturned to 1.870031 Hz (a positive offset of 738 Hz). Two other such crystals were irradiated with the same dose. Fig.5 depicts the initial frequency instability character for one of the crystals. The pre-irradiation virgin frequency for this crystal was 1870190 Hz and the post-irradiation frequency was 1870397 Hz (a positive offset of 207 Hz). For the other crystal the pre-irradiation frequencies for fundamental and third overtone modes were 1870160 Hz and 5605502 Hz respectively. Upon irradiation, these frequencies changed to 1870450 Hz and 5605963 Hz for the two modes. The total offset for the fundamental mode was thus +290 Hz while for the third overtone it was +461 Hz. A crystal of 5 HMz (AT-cut) drawn from Bharat Electronics Ltd., Bangalore, India was also investigated for its frequency behavior for heavy irradiation. Fig.6 depicts the frequency instability character in the initial period of oscillations after irradiation.

TABLE (I)

Pre- and post-irradiation steady frequencies of three different quartz crystals oscillated in fundamental and third overtone modes. Each crystal was irradiated uniformly by dose of 48 kRads.

Crystal No.	Pre-irradiation Fundamental Frequencies (Hz)	Pre-irradiation Third Overtone Frequencies (Hz)	Post-irradiation Fundamental Frequencies (Hz)	Post-irradiation Third Overtone Frequencies (Hz)
1	1869451	5605051	1870558	5605421
2	1869381	5604527	1870521	5604927
3	1870206	5602694	1871059	5603927

TABLE (II)

Pre- and post-irradiation steady frequencies of four different quartz crystals after irradiating each crystal uniformly by a dose of 5 MRads using ^{60}Co (Average energy = 1.25 MeV).

Crystal No.	Frequencies of the virgin quartz crystals (Hz)	Post-irradiation Frequencies (Hz)	Permanent offset in frequency (Hz)
1	1750058	1751089	1031
2	1870659	1870949	290
3	1749946	1750742	796
4	1870164	1871256	1092

The frequency of this particular crystal specimen while it was virgin was 4997578 Hz and upon irradiation with a dose of 7.5 MRads, the frequency became 4997811 Hz, thus with a net change in frequency of +233 Hz.

Irradiation with Fast Neutrons

Different virgin quartz crystals, after their frequencies were measured, were given varying accumulated doses of neutrons and their post-irradiation frequency behavior was recorded. Like the case of γ -irradiation, the results fall in two broad classifications. Firstly, following the termination of irradiation, the crystals when put into oscillations (the fundamental mode being used) showed an initial instability for some time when the oscillation frequency was unstable and afterwards the frequency was stabilized. This initial instability also was found to be independent of the time of idle keeping of the quartz crystals spaced between the termination of irradiation and generation of mechanical oscillations. This region of frequency instability in terms of time required for stabilization and the frequency changes again depended upon individual specimen and accumulated dose. The steady frequency offset due to neutron irradiation was the value which the crystals attained after culminating the region of frequency instability. These results resemble the irradiation-frequency character due to γ -rays. However, the distinct results with neutrons and gamma irradiation are the manner in which the frequency stabilizes and is described below.

A crystal was irradiated with a dose of 4×10^{10} nvt. It was observed that as the crystal started oscillating, there was a region of unstable frequency which persisted for a period of about an hour. The frequency, during this time, approached towards the pre-irradiation value. After the region of frequency instability was over the frequency offset at a value which was almost that for the virgin crystal. The maximum frequency drift during this period of stabilization was about 50 Hz. Another crystal specimen was irradiated with a dose of 7×10^{10} nvt and its frequency behavior is shown in fig.7. In this case the frequency changed by an extent of the order of 90 Hz and after about an hour and half the frequency was stabilized. In this case also, it was found that there was hardly any steady offset within the limit of accuracy of experimental observation. A third crystal was given the dose of 9.2×10^{10} nvt. This crystal showed a steady offset of about -50 Hz, the frequency stabilizing after about an hour long mechanical oscillations of the crystal. The maximum frequency drift was of the order

of 45 Hz in the region of initial frequency instability. Fig.8 depicts the oscillation characteristics of a neutron-irradiated crystal with a dose of 16×10^{10} nvt. The steady frequency offset in this case was of the order of 110 Hz and the frequency instability region extended for about an hour with a maximum frequency drift of about -90 Hz. With prolonged irradiation, it was found that the extent of steady offset was increasingly negative. A different crystal was exposed to 20.7×10^{10} nvt. The frequency offset was about -200 Hz. The instability continued for about two hours in this case with a maximum frequency drift of the order of 250 Hz (Fig.9).

It may be seen from Figs.7 to 9 that during the course of culmination of region of frequency instability after neutron irradiation, the frequency of oscillations tends always towards the value of the frequency of the virgin crystals and in most cases, in the region of unstable frequency, there is a linear variation of frequency with time. This character is different from that existing for γ -irradiation. There, in the region of culmination of initial frequency instability the frequency variations were up and down before the frequencies got stabilized.

A crystal was irradiated in stages and its frequency character was observed. Fig.10 depicts the plot of steady frequency offsets when accumulated doses were given to the crystal, these doses corresponding to the points A,B,C,D,E and F. At the point A, the accumulated dose given to the crystal was 2×10^{10} nvt. It can be seen that there was not much change of frequency at this stage. As the irradiation proceeded to 20×10^{10} nvt (point B) the frequency decreased by a negative offset of about 100 Hz. With further irradiation up to 36×10^{10} nvt (point C), it may be seen that the frequency decreased still further. As the irradiation was still advanced to 60×10^{10} nvt (point D), the net frequency change started upturning and with 80×10^{10} nvt (point E), the frequency was at a value higher than that of the virgin crystal. With still prolonged irradiation of 4×10^{11} nvt (point F) the frequency continued to increase. This observation (increase of frequency with neutron irradiation) fits well with those reported in literature (29-31).

Two crystals were irradiated by fast neutrons with a dose of 2×10^{12} nvt. Fig.11 depicts the post-irradiation oscillation character, for one of the crystals. The character broadly resembles the one reported in the preceding paragraphs. The crystal required about 40 minutes of mechanical oscillations for the region of initial frequency instability

to be culminated. It is significant to mention here that in the specimens irradiated by γ -rays or neutrons, the region of frequency instability could be largely reduced or even eliminated if the crystals were warmed to about 100°C for a period of 20-25 minutes. The crystal of which the frequency character is shown in Fig.11 had its frequency 1869981 Hz when it was in the virgin state and after being irradiated by fast neutrons with a dose of 2×10^{12} nvt the steady frequency of the quartz crystal became 1870288 Hz. It can thus be seen that in this case the net frequency change was positive by 307 Hz. The other specimen, irradiated with the same dose (2×10^{12} nvt), also took about 40 minutes for the frequency to stabilize. During this period the maximum frequency change was about 13 Hz. The pre- and post-irradiation frequencies were 1870007 and 1870218 Hz respectively showing a net positive change of 211 Hz. This crystal was given further irradiation of 6×10^{12} nvt. The steady frequency for this crystal after the second irradiation was 1870377 Hz.

A crystal which was given a dose of 8×10^{12} nvt at a stretch showed the frequency character depicted in Fig.12. The crystal required about half an hour for the culmination of initial frequency instability. The virgin crystal oscillated at the frequency of 1870037 Hz while after the neutron irradiation of 8×10^{12} nvt, the steady frequency value was 1870331 Hz. Thus a net positive steady frequency change of about 300 Hz was caused by neutron irradiation.

SUMMARY OF RESULTS

From the foregoing, it can be seen that the following experimental results about the irradiation characteristics of quartz crystals have been obtained.

- (1) The initial frequency instability is caused by γ - and neutron irradiation but not by X-irradiation.
- (2) For low doses of neutron, X- and γ -irradiation, the steady frequency shift is negative. For the higher doses, the frequency shift becomes positive for the three different kinds of irradiation. In between, a stage would of-course be reached when there is no resultant frequency shift due to irradiation.

DISCUSSION OF RESULTS

Before proceeding further, it should be mentioned that while the negative frequency shift for ionizing radiations has been observed by a number of workers (2-4,6,8), the positive frequency shift has earlier been observed only in

a few investigations (30,32). Again, while the positive frequency shifts by neutron irradiation is already known (29-31), the negative frequency shift for low enough doses of neutrons was not observed before.

In the following we will attempt to explain the above results in terms of the lattice structure of the quartz crystals.

Initial Frequency Instability

The neutron and γ -irradiation cause nuclear displacements. While the displacements caused by neutrons are straightforward knock-on processes, those caused by γ -rays are by indirect mechanism through the high energy Compton electrons released by γ -rays causing Coulombic interaction with the nuclei. In the case of X-rays there will be no nuclear displacement caused since the Compton electrons do not have sufficient energy to penetrate the electron cloud of atoms.

It is our opinion that, among the atomic displacements caused by appropriate radiations, a fraction of these are indeed very near the equilibrium atomic positions and hence the atoms so displaced can be brought back to the original positions by very low activation energies supplied by vibrations themselves or by warming.

Steady Frequency Shifts by Ionizing Radiations

The negative frequency shifts are now well known to be caused by the generation of A-centers from their precursors the Al^{3+} -centers, by ionization of electrons of one or more O-atoms bonded with Al^{3+} . Regarding the positive frequency shift there is no mechanism yet propounded.

We believe that the crystal defects are the source of positive frequency shift in two different ways. When the defects are created due to heavy γ -bombardment or neutrons, a positive frequency shift is produced. Also, these defects, whichever of them are electron traps, will give additional positive frequency shift when electrons are trapped therein. Apart from these crystal defects other impurity centers, except the Al^{3+} like the alkali ions trapped in the c-axis at Ge, Ti or other trapping sites will also give a positive frequency shift when populated by trapped electrons. Incidentally, some of these crystal defects on trapping of electrons will form color centers which apart from giving the optical absorption, also give, unlike the case of A-centers, EPR at room temperature. In our observations, we recorded a number of these paramagnetic resonances both sharp and broad

(33). In our opinion, these EPR resonances are good evidence for the presence of the crystal defects giving the positive frequency shift. As to why the crystal defects when produced should give a positive frequency shift may be seen in the following way. These defects disrupt the otherwise perfect atomic arrangement in the crystal, making it more difficult than before, due to the additional potential barriers created by the defects, for atomic displacements to take place, particularly under a shear stress. Thus, with increase of shear modulus of rigidity, the frequency of the AT-cut and other resonators should increase. A support to this argument is provided by the fact that hardness of the crystals was found to increase as a result of γ - and neutron irradiation. Hardness would of-course increase when it becomes more difficult for the atoms to make transverse displacements due to the hindering potential barriers caused by these defects.

As to why the electron trapping of the defects should cause positive frequency shift, i.e. an increase of elasticity is not clear at this stage. Probably, the trapped electrons contribute to extra electrical forces leading to the increased elastic moduli. At any rate, the fact that electron trapping at the defects causes a positive frequency shift is supported by the following experimental observations.* Quartz crystals were irradiated with ultra-violet light ($\sim 3650 \text{ \AA}$). In all the cases a positive frequency shift, unaccompanied by any initial negative frequency shift was recorded. The uv light would of-course not be able to form A-centers (which would yield a negative frequency shift), but would be able to fill atleast some of the other crystal defects with electrons ionized off from atoms by uv radiations. Thus, it follows that the electron trapping of crystal defects causes a positive frequency shift.

The role of crystal defects in causing positive frequency shift is also supported by the fact that all those crystals which gave the positive shift were not optically clear quartz, this fact indicating the presence of defects and other impurities in the lattice which become color centers. Optically clear quartz, did not, in accordance with earlier results of Capone *et.al.*(8), King (4) and Frondel (1,2) give positive frequency shift.

With all the above in view, the following seems to be taking place by γ -irradiation of quartz crystals.

In the early stages of γ -irradiation, the ionization of the Al^{3+} -centers, due to their higher cross section,

*Details of this work will be published separately.

takes place predominantly giving rise to negative frequency shift. With continued irradiation, crystal defects and other impurity centers having a lesser cross section get increasingly trapped with the electrons, all this producing the turn over of frequency shift observed. For higher doses of γ -irradiation, the magnitude of positive frequency shift is all the greater due to the generation of defects by γ -rays themselves.

Steady Frequency Shifts due to Neutron Irradiation

The role of crystal defects in causing a positive frequency shift straightforwardly explains the effect of higher doses of neutrons in causing the frequency increase.

Regarding the effect of low doses of neutron irradiation causing the negative frequency shift, no straightforward fundamental explanation can be given at the present. However, the decrease of frequency is in accordance with the observation of expansion of the quartz lattice under neutron irradiation (34). The expansion would lead to decrease of interatomic forces and the associated moduli of elasticity.

At the higher neutron doses, the lattice expansion no doubt takes place increasingly but the role of expansion in causing the decrease of frequency seems to be exceeded (atleast for reasonable neutron doses used for obtaining frequency offsets) by the role of defects, so generated by neutrons, in causing the frequency shift. That the role of defects on the elastic moduli particularly the shear modulus is preponderant is shown by the increase of hardness by neutron irradiation referred to above.

APPLICATIONS

The present work, apart from giving explanations for some of the frequency effects of irradiation, also indicates applications towards radiation hardening of crystals, this radiation hardening making it possible to use quartz crystals in space satellites to generate precise frequencies and time intervals. It is clear that at the extreme of the negative frequency shift the differential of the frequency shift with continued irradiation vanishes. It follows that the crystal will assume radiation hardness for some range of irradiation dose if the crystal has already been irradiated enough for obtaining the maximum of the negative frequency shift. This technique would apply both for γ -

and neutron irradiation with the greater returns for neutron irradiation since for this no other technique has yet been developed. In contrast, for γ -irradiation the method of using vacuum swept crystals (35) for satisfactory radiation hardening (though not perfect) has already been established.

ACKNOWLEDGMENTS

For this work, the generous help of Dr. A. Nagaratnam of Inst. Nuclear Medicine and Allied Sciences, New Delhi, Dr. J. Bahadur of Nuclear Research Laboratory of I.A.R.I., New Delhi, Dr. L.M. Tiwari of I.I.T, New Delhi and Dr. M.G. Shahani of B.A.R.C., Bombay in various facets of irradiation is gratefully acknowledged. H. Bahadur thanks the Department of Atomic Energy, Govt. of India for the award of research fellowship.

REFERENCES

1. J.C. King, "Hardening quartz resonators to ionizing radiation -a review" Proc. Int. Conf. Evaluation of Space Environment on Materials, Centre Spatial de Toulouse, June 17-21, 1974.
2. C. Frondel, Am. Miner. 30, 416 (1945).
3. C. Frondel, Am. Miner. 30, 432 (1945).
4. J.C. King, Bell System Tech. Jour. 38, 573 (1959).
5. R.A. Poll and S.L. Ridgway, IEEE Trans. Nucl. Sc. NS-13, 130 Dec'(1966).
6. D.B. Fraser, Jour. Appl. Phys. 35, 2913 (1963).
7. D.B. Fraser, Physical Acoustics (Ed. W.P. Mason), Academic Press, New York, 5, 59 (1968).
8. B.R. Capone, A. Kahan, R.N. Brown and J.R. Buckmelter IEEE Trans. Nucl.Sc. NS-17, 217 (1970).
9. T.M. Flanagan and T.E. Wrobel, IEEE Trans. Nucl. Sc. NS-16, 130 Dec'(1969).
10. E.P EerNisse, "Radiation Effects in Swept and Unswept Optical Grade Synthetic Quartz AT- Resonators" Tech. Memo. Sandia Laboratories, SC-TM-70-417, July 1970.
11. B. Capone, A. Kahan and B. Sawyer, Proc. Annual Frequency Control Symposium, US Army Electronics Command, Atlantic City, New Jersey, 25, 109 (1971).

12. A. Kahan, B.R. Capone and R.N. Brown, "Radiation Hardness of Electrodiffused (Swept) Electronic Grade Quartz", Tech. Memo. LQ-16 Air Force Cambridge Research Laboratories, Bedford, Mass. 16 March 1973.
13. J.C. King (Ed.), Radiation Effects in Quartz Crystals, Radiation Effects, 26, No.4 (1975).
14. T. Aoki, K. Norisawa and M. Sakisaka, Japanese Jour. Applied Physics, 15, 2131 (1976).
15. T. Aoki, K. Norisawa and M. Sakisawa, Japanese Jour. Applied Physics, 15, 749 (1976).
16. Paul Pellegrini, F. Euler, A. Kahan, T.M. Flanagan and T.F. Wrobel, IEEE Trans. Nucl. Sc. NS-25, 1267, Dec'1978.
17. F. Euler, P.Ligor, A. Kahan, P.Pellegrini, T.M. Flanagan, and T.F. Wrobel, Proc. Annual Frequency Control Symp., US Army Electronics Command, Atlantic City, New Jersey 32, 24 (1978).
18. H.G. Lipson, F. Euler and P.A. Ligor, Proc. Annual Frequency Control Symposium, US Army Electronics Command, Atlantic City, New Jersey, 33, 122 (1979).
19. F. Euler, H.G. Lipson and P.A. Ligor, Proc. Annual Frequency Control Symposium, US Army Electronics Command, Atlantic City, New Jersey, 34, (1980).
20. J.C. King and H.H. Sander, IEEE Trans. Nucl. Sc. NS-19, 23 (1972).
21. E.F. Hartman and J.C. King, Proc. Annual Frequency Control Symposium, US Army Electronics Command, Atlantic City, New Jersey, 27, 124 (1973).
22. J.C. King and H.H. Sander, Radiation Effects, 26, 203 (1975).
23. E.F. Hartman and J.C. King, Radiation Effects, 26, 219 (1975).
24. J.C. King and H.H. Sander, IEEE Trans. Nucl. Sc., NS-20, 117 (1973).
25. Harish Bahadur and R. Parshad, Rev. Scientific Instruments - in press.
26. T.J. Young, D.R. Koehler and R.A. Adams, Proc. Annual Frequency Control Symposium, US Army Electronics Command, Atlantic City, New Jersey, 32, 34 (1978).
27. D.R. Koehler, Proc. Annual Frequency Control Symposium, US Army Electronics Command, New Jersey, 33, (1979).

28. Harish Bahadur and R. Parshad, Indian Jour. Physics, 53(A), 239 (1979).
29. J.C. King and D.B. Fraser, Proc. Annual Frequency Control Symposium, US Army Electronics Command, Atlantic City, New Jersey, 16, 7 (1962).
30. F.B. Johnson and R.S. Pease, Phil. Mag. 45, 651 (1954).
31. J.C. King, "Final Report on Fundamental Studies of the Properties of Natural and Synthetic Quartz Crystals", 15 Jan., 1960, (Contract DA 36-039 Sc- 64586).
32. R.B. Belser and W.H. Hicklin, Proc. Annual Frequency Control Symposium, US Army Electronics Command, New Jersey, 16, 110 (1962).
33. Harish Bahadur, S.K. Gupta and R. Parshad, Proc. 1980 Nuclear Physics and Solid State Physics Symposium, Deptt. Atomic Energy, India - in press.
34. M. Wittels, Phys. Rev. 89, 656 (1953).
35. J.C. King, U.S. Patent no. 3,932,777, Jan. 13, (1976).

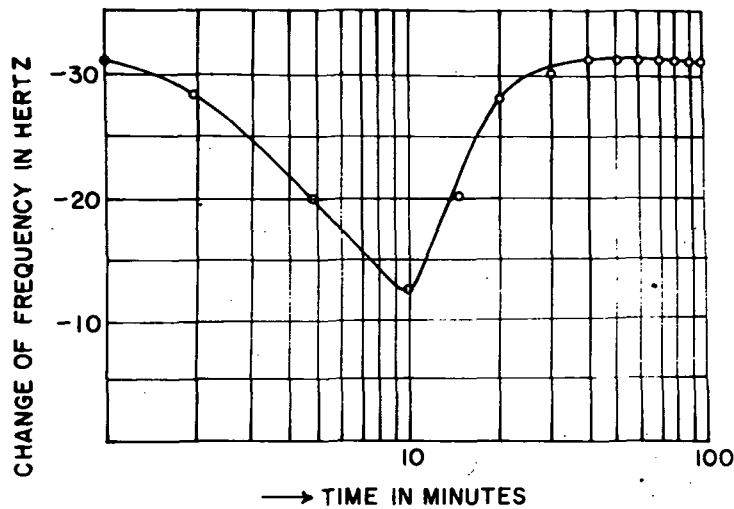


Fig.1. Frequency behavior of a quartz crystal (AT-cut, 1.87 MHz) after irradiation with gamma rays (dose = 2000 Rads; using ^{60}Co) and allowed to oscillate.

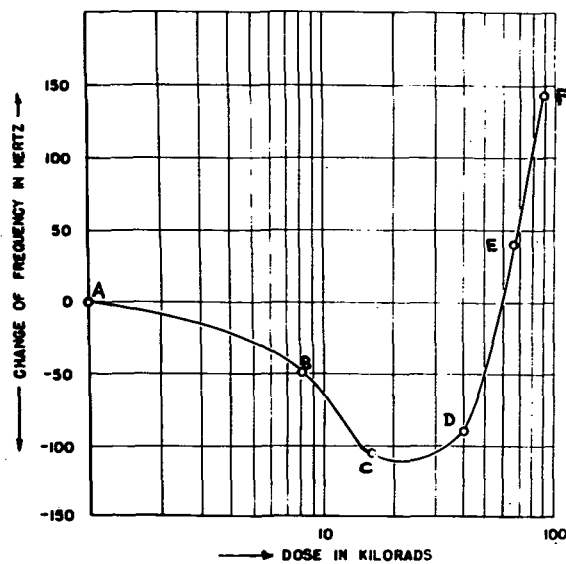


Fig.2 Steady frequency offsets of a natural AT-cut quartz crystal irradiated in stages A, B,....E. Accumulated doses at B = 8,000 Rads, at C = 16,000 Rads, at D = 40,000 Rads, at E = 64,000 Rads and at F = 88,000 Rads.

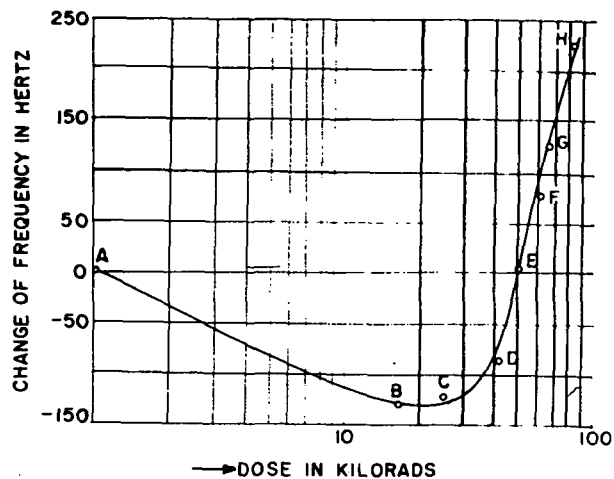


Fig.3 Steady frequency offsets of a natural quartz crystal (AT-cut, 1.87 MHz) irradiated by gamma rays in stages A,B,C----H (using ^{60}Co). Accumulated doses at A =8000 Rads, at B=16,000 Rads, at C=40,000 Rads, at D=64,000 Rads, at E=88,000 Rads, at F=112,000 Rads, at G=136,000 Rads, and at H=160,000 Rads.

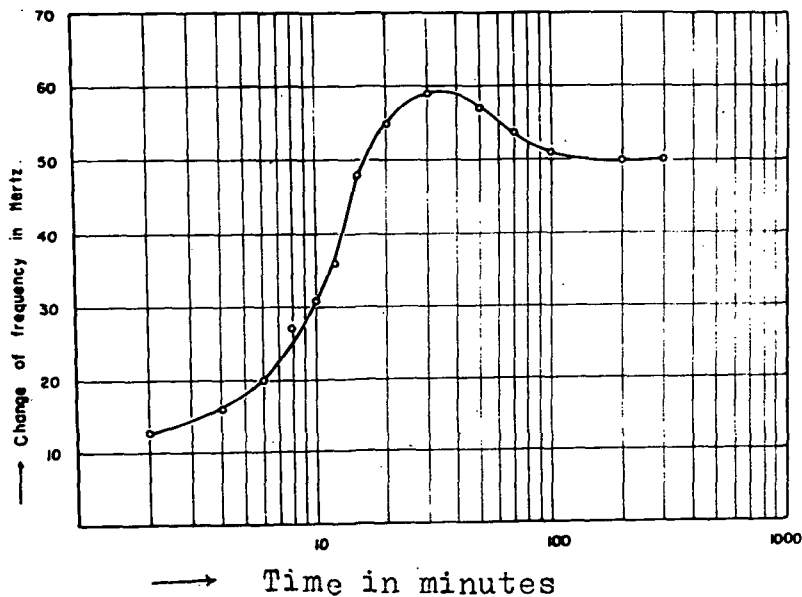


Fig.4 Frequency behavior of a natural AT-cut (1.87 MHz) quartz crystal after being irradiated by gamma rays (dose = 7.5 MRads) and allowed to oscillate.

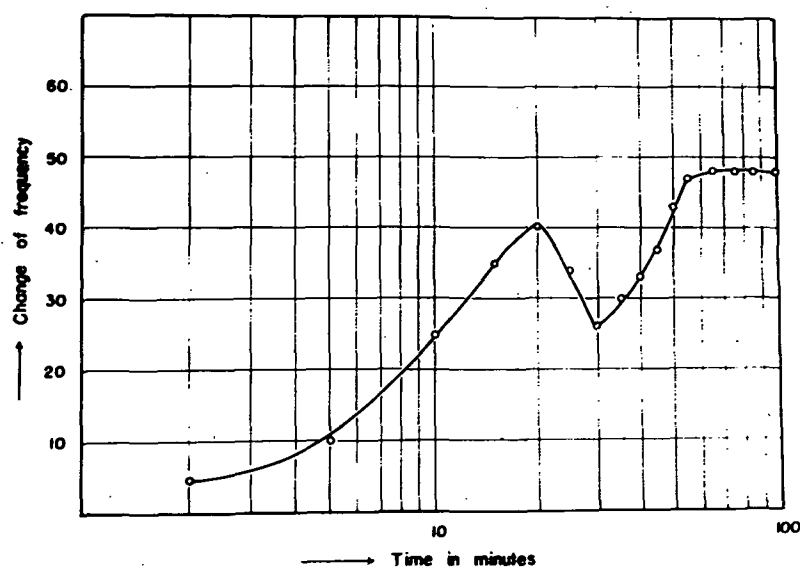


Fig.5 Initial frequency instability characteristics of a natural AT-cut quartz crystal (1.87 MHz) after irradiation by gamma rays (dose = 7.5 MRads) using ^{60}Co and allowed to oscillate.

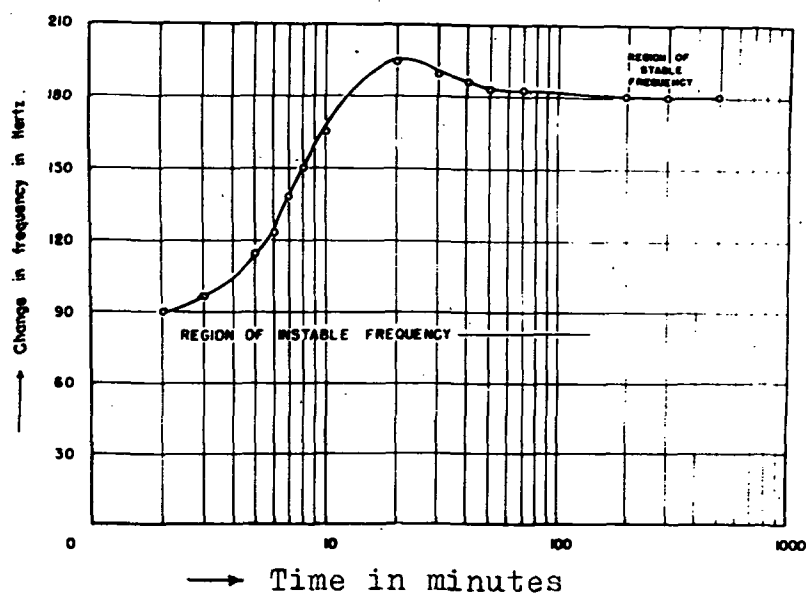


Fig.6 Initial frequency instability characteristics of a natural AT-cut (5 MHz) quartz crystal after irradiation by gamma rays (dose = 7.5 MRads) using ^{60}Co and allowed to oscillate.

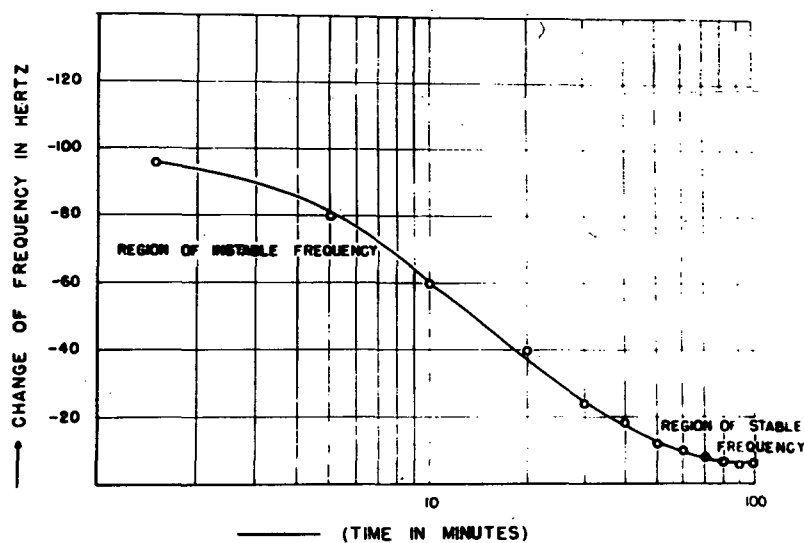


Fig- 7 Frequency stability characteristic of a quartz crystal, irradiated by hot neutrons with a dose of 7×10^{10} nvt, after setting it into oscillations.

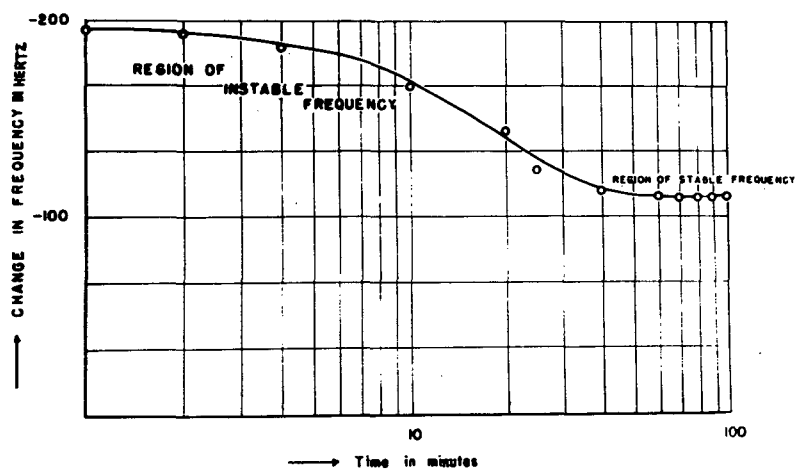


Fig. 8 Frequency behavior of a natural AT-cut quartz crystal (1.87 MHz) irradiated by fast neutrons with a dose of 16×10^{10} nvt and allowed to oscillate.

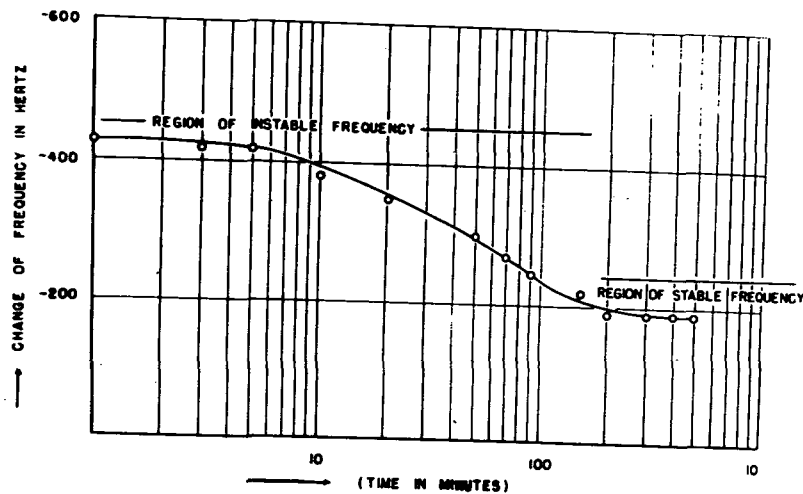


Fig. 9 Frequency behavior of a natural AT-cut quartz crystal (1.87 MHz) irradiated by fast neutrons with a dose of 20.7×10^{10} nvt and allowed to oscillate.

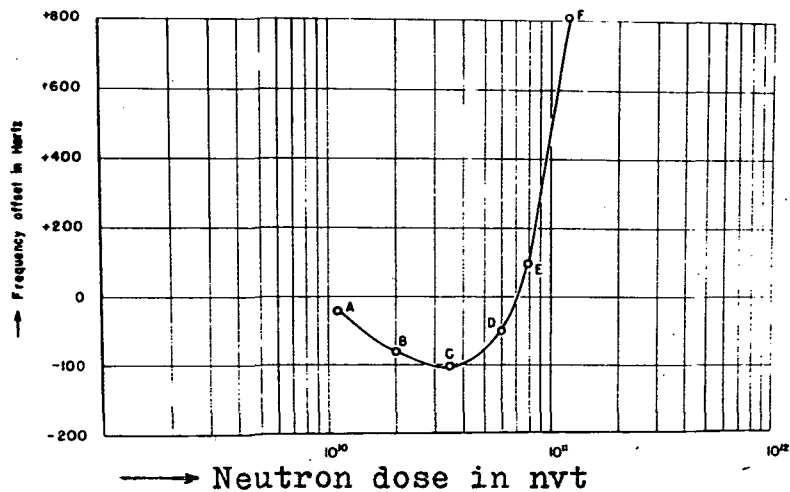


Fig. 10

Steady frequency offsets of a quartz crystal of 1.87 MHz irradiated at different accumulated neutron doses, using $^{241}\text{Am}-\text{Be}$, after the temporary frequency instability has been removed. Doses at A = 2×10^{10} nvt, B = 20×10^{10} nvt, C = 36×10^{10} nvt, D = 60×10^{10} nvt, E = 80×10^{10} nvt, F = 4×10^{11} nvt.

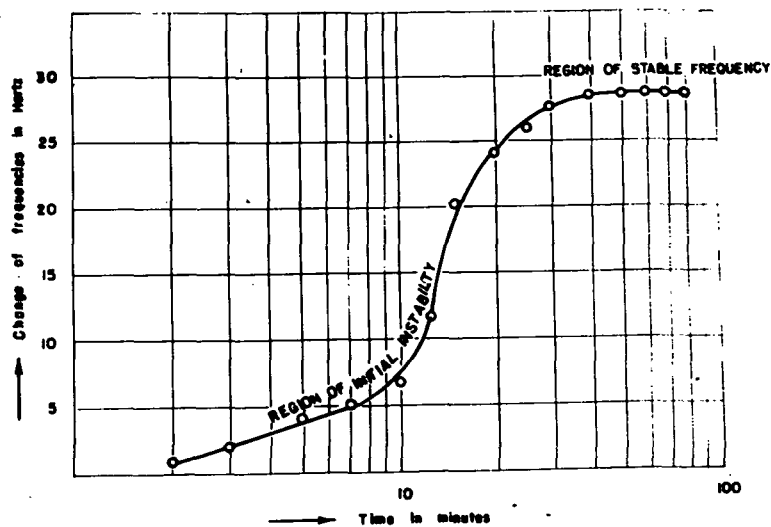


Fig- 11 Frequency behavior of a natural AT-cut (1.87 MHz) quartz crystal with time after irradiation with fast neutrons with accumulated dose of 2×10^{12} nvt using $^{241}\text{Am} - \text{Be}$.

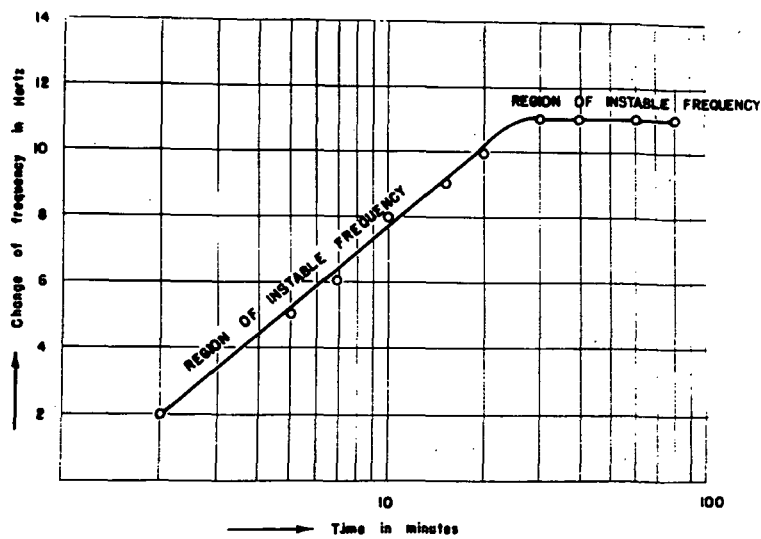


Fig- 12 Frequency behavior of a natural AT-cut (1.87 MHz) quartz crystal with time after irradiation by fast neutrons with accumulated dose of 8×10^{12} nvt using $^{241}\text{Am} - \text{Be}$.

Page Intentionally Left Blank

PRECISE T & F INTERCOMPARISON VIA VLF PHASE MEASUREMENTS

A.Sen Gupta, G.K.Goel and B.S.Mathur
Time and Frequency Section
National Physical Laboratory, Hillside Road,
New Delhi-110012, India.

ABSTRACT

The Indian subcontinent does not fall in the groundwave range of any LORAN-C transmission. As such, at present the only alternative technique in this region for convenient and routine T & F intercomparison is via VLF phase measurements. At NPL, New Delhi, continuous phase recording of the 16 kHz transmissions from GBR (UK) is being made. In addition the published midday phase data of GBR from several laboratories-NPL (UK), RGO(UK), PTB (FRG) and USNO (USA) - are being received regularly. In the present paper we discuss T & F intercomparisons between the local time scale, UTC (India), at NPL and those at the above mentioned laboratories, using the VLF phase data. A major factor which limits the accuracy of long term comparison is the seasonal variation in the VLF propagation delay over long paths. It is shown that by taking into account the seasonal propagation delay variations in a semiempirical way the accuracy of T & F comparisons can be considerably improved. In fact over a one year period accuracy of few parts in 10^{14} in frequency and 1-2 μ sec in time have been obtained.

The relative frequency offset difference between UTC (India) and UTC (PTB) evaluated in the present work as $(7.0 \pm 0.1) \times 10^{-13}$ agrees very well with that obtained via the satellite experiment described in a companion paper.

INTRODUCTION

The National Physical Laboratory (NPL), New Delhi, India has the statutory obligation of maintaining the India

Standards of time and Frequency. This is being achieved at present with the help of two commercial cesium clocks: NPL-1 (Oscilloquartz Model 3200) and NPL-2 (Hewlett Packard Model 5061A with option 004). A time scale, UTC (India), is being maintained using the NPL-1. One of major problems being faced by us at NPL is that of a regular time and frequency transfer link between UTC (India) with those of the other international timekeeping laboratories. The Indian subcontinent does not fall in the groundwave range of any LORAN-C transmitter thus prohibiting the use of this technique.

The first serious attempt in having an accurate link was made in May-June, 1979, when a two way satellite time transfer experiment was performed between NPL and PTB, West Germany (Mathur et al, 1980 and references there in). With the help of this experiment UTC (India) was synchronised with UTC (PTB). From July, 1979 onwards we are continuously tracking the phase of 15 kHz transmissions from GBR (UK). The choice of this station was dictated by the fact that; (a) the received signal strength at our location is very good so that a precise phase tracking is possible and (b) there are several timekeeping laboratories which track this station and publish their data. We are regularly receiving the GBR phase data from PTB (FRG), USNO (USA), NPL (UK) and RGO (UK). Utilizing the VLF data it has been possible to establish a fairly precise link between UTC (India) and UTC of the abovementioned laboratories as will be described in the subsequent sections.

A confirmation of the accuracy of the VLF links was made possible with a portable clock trip from USNO in September, 1980. This is described briefly in a separate subsection.

THE TECHNIQUE

The VLF time transfer technique has been described by Becker et al (1969). This basically consists of recording the time difference between the 1 pps of the local time scale and some specified phase (generally the positive zero crossing) of the received VLF signal appearing just subsequently. This measurement is referred to as the 'phase time', or simply 'phase' of the received signal relative to the local time scale. The recording is done at the local noon over the path mid point when VLF propagation conditions are most stable. Subtracting the daily values of phase measurements recorded at two laboratories

gives the difference between their time scales. This difference is ambiguous to an additive constant which involves the difference between the propagation delays over the two paths. While this ambiguity is immaterial for frequency comparison between the two time scales it has to be eliminated if a time comparison is desired. Elimination of the additive constant can be achieved by an initial calibration with the help of either a portable clock or two way satellite experiment.

A major factor which degrades precision and accuracy of the VLF time transfer is the non constancy of the propagation delay. There is a day to day jitter in the propagation delay because of the normal variability of the ionospheric D-region. This is more pronounced during winter than during summer, as will be shown in the next section (see also Belrose, 1968). The jitter evidently reduces the precision of the link. Sudden ionospheric disturbances (SID) due to solar flares may occasionally cause path anomalies, but these generally last for short durations and can be isolated by careful inspection of the data (Reeder, 1971).

In addition, over long paths there are also systematic seasonal variations in the propagation delay which can some times be as large as 15 μ sec (Iijima et al, 1968; Swanson & Kugel, 1972). If these are not taken into account then they may introduce significant inaccuracy in the time and frequency comparisons. The seasonal variation in the propagation delay occurs mainly due to variations in the D-region ionization. This consists of two parts, namely (a) seasonal variation of the Solar Zenith angle at the mid path noon and (b) variations in the mesospheric neutral atmospheric constituents, which are to some extent related to meteorological phenomena (Belrose 1968). Of the above, only the first part, (a), can be modeled with definiteness. It has been shown by Swanson & Kugel (1972) to be of the form $M(1 - \cos \chi)$, where, $\cos \chi$ is the average of the cosine of the solar zenith angle χ over the path at the midday. M is an empirical constant dependent on the propagation path and to some extent on the solar activity.

THE DATA

(a) NPL (India) data : The midday phase observations of the 16 kHz GBR signal relative to UTC (India) recorded daily between 08-30 to 09-30 UT are shown in Fig.1(a) for the

period 10th July, 1979 to 10th July, 1980. Twice during the one year time the NPL-1 underwent discontinuities in operation for short periods. Once during 23-25 August, 1979 and again during 30 August - 7 September, 1980. In both cases it was possible to restart UTC (India) by synchronizing NPL-1 with NPL-2 and giving suitable time corrections (of 1.3 and 5.5 μ sec respectively). The time corrections were determined from the intercomparison data between these two clocks which was taken periodically throughout.

We observe the following features in Fig.1(a). The day to day variability is much smaller in summer than in winter. The rms jitter in summer is less than 1 μ sec while in winter it is about 2.5 μ sec. There is a gradual drift in the phase data arising due to a relative frequency offset between UTC (India) and the transmitted frequency of GBR. This drift is modulated by a seasonal variation in the propagation delay. As mentioned in the earlier section, the Solar Zenith angle related seasonal variation of the form $M(1-\cos\chi)$ can be modelled and eliminated. To determine $\cos\chi$ we follow Iijima et al (1968). We divide the propagation path (6700km) into 10 equal segments and determine $\cos\chi$ at the midpoint of each. The average of these values gives $\overline{\cos\chi}$ over the path. To determine the value of M we take help of the observed diurnal variation of phase delay. It has been shown by Swanson and Kugel (1972) that around midpath noon, the temporal variation of phase delay is also of the form $M(1-\cos\chi)$. We thus make comparisons between the temporal variation of the observed phase delay and that of the calculated factor $M(1-\cos\chi)$ by varying M. The value of M which gives best agreement between the forms of the two variations is selected. Utilising the whole years data the best value of $M=12.5\pm1$ was obtained. In Figs.2 and 3 we have shown as illustrations the observed diurnal phase for groups of 15 days in April and June and the calculated $M(1-\cos\chi)$. The good agreement between the two is evident. Adopting the above value of M the calculated seasonal variation of $M(1-\cos\chi)$ at the midpath noon for the full year is shown in Fig.1(b). This shows an annual variation with a summer to winter phase retardation of 7 μ sec. On subtracting out this seasonal variation from the observed data in Fig.1(a) we get the resultant variations as shown in Fig.4(a). The phase drift now appears more regular but there still persist some short period variations during the period September, 1979 to February, 1980 with peak amplitudes of 2-3 μ sec.

(b) PTB data: The midday phase observations of GBR relative to UTC(PTB) is shown in Fig.4(b). This path is only 790 km long and the solar zenith angle related seasonal variation in the phase delay is not expected to be significant. It is not apparent in the data also. During the period from September '79 to February '80, the nature of variations in the PTB data are very much similar to NPL (India) data in Fig.4 (a). It is notable in this connection that GBR-PTB path is almost overlapping with 1/8 of the GBR-NPL (India) path. This indicates the possibility that the shorter period variations mentioned above are arising from this portion of the path.

(c) RGO data: The midday phase variation of GBR relative to UTC (RGO) is shown in Fig.4(c). In this case also the path length being very short (180km) seasonal variations are almost absent.

(d) USNO data : The midday phase variations of GBR relative to UTC (USNO) are shown in Fig.5(a). The propagation path in this case is long (5800 km) and so the solar zenith angle related seasonal variation is significant. As we do not have the diurnal phase variation for this station it is not possible to determine M as was done earlier for NPL data. In absence of anything better we have just adopted the same value of $M=12.5$ and calculated the variation of midday values of $M(1-\cos\alpha)$. This is shown in Fig 5(b). Subtracting variations in Fig 5(b) from those in Fig 5(a) we get the resultant as shown in Fig 5(c). In this case also during September 1979 to February 1980, we observe anomalous variations of similar nature as in PTB and NPL (India) data. But these variations are of larger magnitude (~ 12 μ sec peak to peak)

(e) NPL (UK) data : The midday phase observation of GBR relative to UTC (NPL,UK) showed occasional jumps of 5,10 and 15 μ sec over the whole year. These were most probably due to some equipment malfunction. Thus the data from this station have not been used.

RESULTS AND DISCUSSION

For intercomparison between UTC (India) and UTC of the other laboratories, the individual phase data in Figs 4(b), 4(c) and 5(c) have to be subtracted from Fig 4(a). In Fig 6 we have shown : (a) UTC (India)-UTC (PTB), (b) UTC (India)- UTC(RGO) and (c) UTC (India)-UTC(USNO). It is clear that of the three links the one with PTB has the

minimum jitter and anomalies due to propagation variations. In Fig.6 we have drawn regression lines through the points which represent the overall drift rates. The slope of these straight lines give the relative frequency offset, S , between UTC (India) and the other UTC scales. Following results are obtained.

$$S_{\text{India,PTB}} = (7.0 \pm 0.1) \times 10^{-13}$$

$$S_{\text{India,RGO}} = (7.3 \pm 0.2) \times 10^{-13}$$

$$S_{\text{India,USNO}} = (6.9 \pm 0.2) \times 10^{-13}$$

The value of $S_{\text{India,PTB}}$ obtained above is in fairly good agreement with a value of $(7.1 \pm 0.5) \times 10^{-13}$ obtained via the satellite experiment (Mathur et al, 1980) during May-June, 1979. This indicates that the UTC (India) has been maintaining a fairly constant rate. The relative offset with the other two laboratories are also consistent (within the uncertainties) with LORAN-C links connecting these. LORAN-C link results have been calculated as follows :

$$S_{\text{PTB,USNO}} = 0.4 \times 10^{-13}$$

$$S_{\text{PTB,RGO}} = 0.0 \times 10^{-13}$$

To get an idea of the precision of the frequency transfer estimates we have made some computations of the variance, σ_y , on the India-PTB link which is the best of the three links. We get the following values :

$$\sigma_y (\tau = 1 \text{ day}) = 2 \times 10^{-11}$$

$$\sigma_y (\tau = 10 \text{ days}) = 3 \times 10^{-12}$$

$$\sigma_y (\tau = 30 \text{ days}) = 2 \times 10^{-13}$$

$$\sigma_y (\tau = 100 \text{ days}) = 1 \times 10^{-13}$$

The σ_y estimate on the other two links are some what higher than the above.

The graphs in Fig.6 have not been given in absolute terms i.e., the origins of the graphs are not shown. Absolute calibrations is necessary for actual time transfer between UTC (India) and other UTC scales. As mentioned earlier this was performed by the satellite experiment in May-June, 1979. As a result of this experiment it was found that

on 29 June '79 UTC (India)-UTC(PTB) = (2.7 ± 0.1) μ sec. The VLF observations were started on 10 July onwards (as the GBR transmission was off for a month before this). Thus in Fig 6(a) we assign a value of 2.7 μ sec to the ordinate where the regression line crosses the abscissa on 29 June '79. Since the difference between UTC (PTB) and UTC (RGO) and UTC(USNO) are known from the LORAN-C links it is possible to calibrate the other two graphs also.

PORTABLE CLOCK TRIP

A portable clock trip from the USNO was made during 18-21, September, 1980. This made it possible to evaluate the accuracy of the time transfer accuracy of the VLF link. In Fig. 7 we have shown the results of only one link UTC(India)-UTC(PTB) extended upto the end of September '80. There are two crosses in Fig. 7 on 29 June '79 representing the satellite experiment time transfer and on 20 September '80 representing the portable clock result. The discrepancy between results of the portable clock and the regression line predicted by the VLF data is only 1.5 μ sec which is quite small.

CONCLUSION

In this paper we have discussed a VLF time and frequency intercomparison link between UTC (India) and UTC of PTB, RGO and USNO. It is clear that the India-PTB link is the best of the three. It has been shown that by taking due account of the seasonal variations over long paths it is possible to achieve frequency intercomparison to a few parts in 10^{14} over one year period. Time transfer can be achieved to an accuracy of 1-2 μ sec.

We realise, however, that this accuracy level is still not acceptable to BIH for inclusion of UTC (India) in the international UTC coordinated by them. In fact a similar problem must be faced by many other remote timekeeping laboratories which are not covered by LORAN-C groundwaves or regular portable clock trips.

Our future plans in improving our links with the international time keeping community are : (a) reception of more VLF stations possibly OMEGA(JAPAN, Liberia, La Reunion), (b) having regular portable clock trips, (c) using the NNSS satellite signals and (d) using some geostationary satellite links on a regular basis.

ACKNOWLEDGEMENTS

We are highly thankful to Prof.G.Becker of PTB, West Germany who was with us at the begining of the VLF experiment and gave us very useful suggestions. We thankfully acknowledge the receipt of the VLF phase data from PTB, RGO, NPL and USNO. Thanks are also due to the other members of time and frequency group for their help and cooperation.

REFERENCES

1. Becker, G., Fisher, B, Kramer, G, Methods and results of international VLF time comparison (In Germany Proc. Colloque International de Chronometric, Pris, 1969.
2. Mathur, B.S., Banerjee, P., Sood, P.C., Mithlesh Saxena, Kumar, Nand and Suri, A.K., Precise T & F Intercomparison between NPL, India and PTB, Federal Republic of Germany via Satellite Symphonie-1, XII Annual PTTI Applic.& Plan.Meeting, Dec.2-4,1980.
3. Belrose, J.S., Low and Very Low Frequency Radio wave propagation, AGARD Lecture series XXIX,1969.
4. Reder, F.N., VLF Propagation Observed During Low and High Solar Activity, Progress in Radio Science :1966-1969, Vol. 2, USRI-Belgium, 1971.
5. Swanson, E.R. and Kugel, C.P., OMEGA VLF Timing, NELC Tech. Rep. No. 1740 (Revision-1), June 1972.
6. Iijima, S., Torao, M. and Fujiwara, K., Phase Variations of VLF wave GBR and GBZ as received, Annals of Tokyo Astron. Observatory Vol. XI, No.1, 1968.

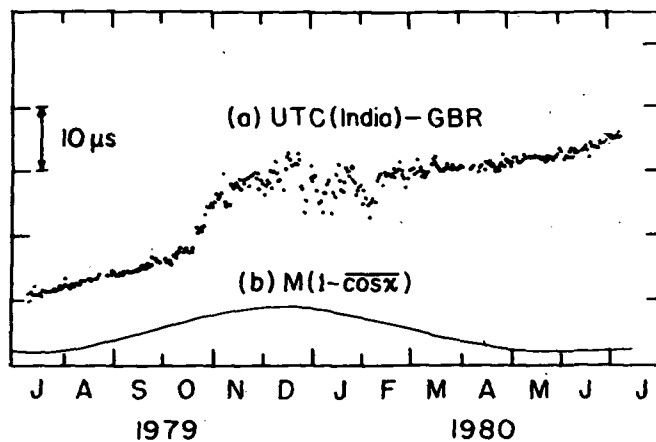


Fig.1 (a) Daily values of GBR phase relative to UTC(India).
 (b) Calculated seasonal variation factor $M(1-\cos\chi)$ for GBR-NPL path.

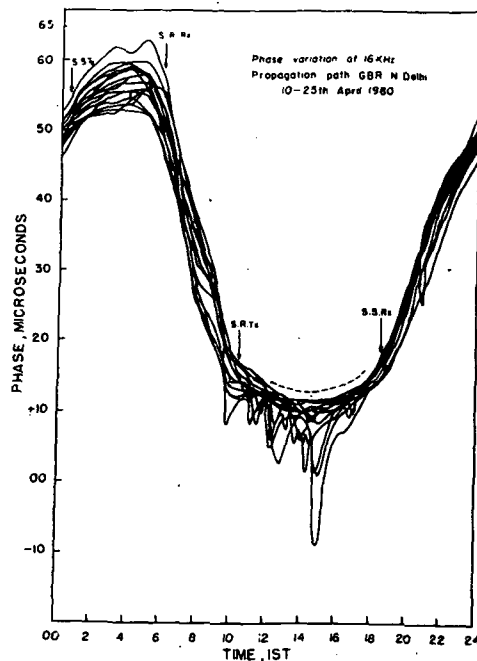


Fig. 2 Diurnal variation of GBR phase for 15 days in April 1980 compared with the variation of $M(1-\cos\chi)$ (dotted line) around midday.

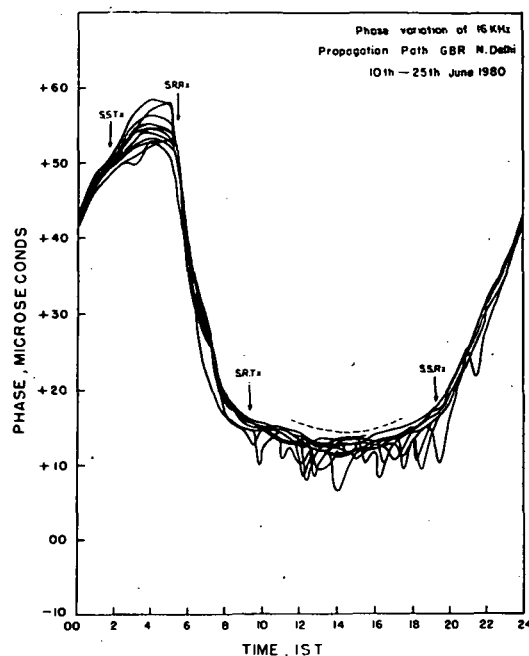


Fig. 3 Same as in Fig.2 for 15 days in June'80.

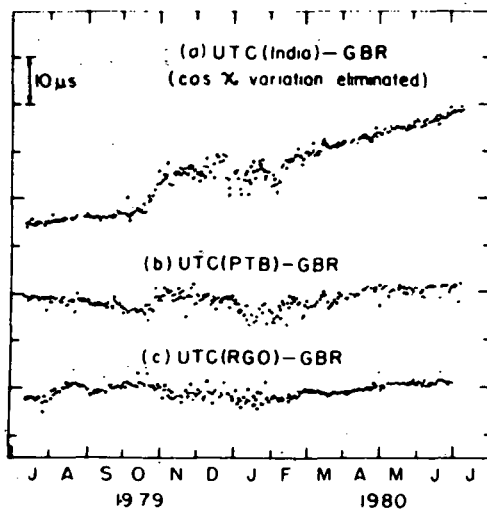


Fig.4 (a) GBR phase relative to UTC(India) corrected for solar zenith angle variations. (b) GBR phase relative to UTC(PTB). (c) GBR phase relative to UTC (RGO).

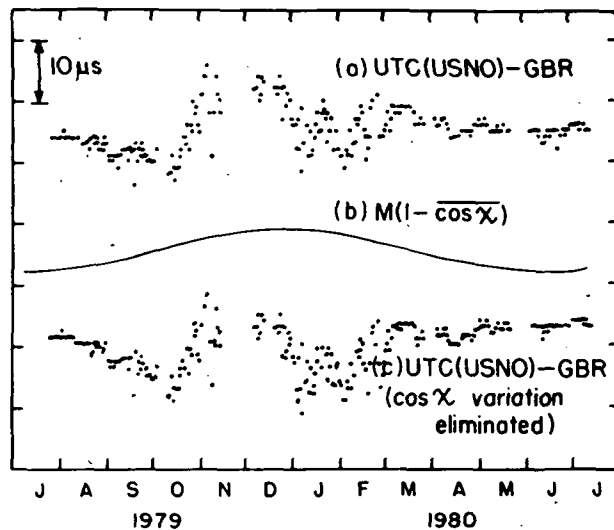


Fig. 5 (a) GBR phase relative to UTC(USNO). (b) Calculated seasonal variation factor $M(1 - \cos \chi)$ for GBR-USNO path. (c) GBR phase relative to UTC(USNO) corrected for solar zenith angle variations.

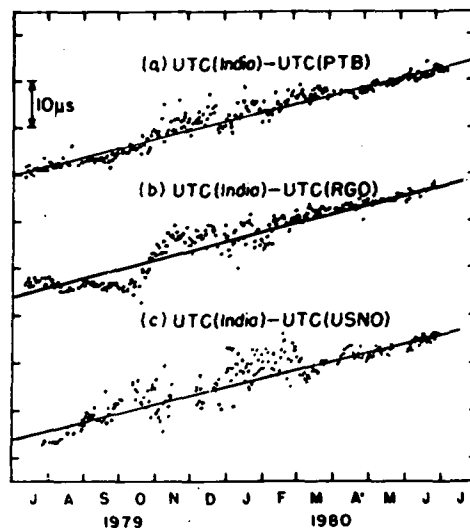


Fig. 6 (a) UTC (India) - UTC (PTB). (b) UTC (India)-UTC (RGO). (c) UTC (India) - UTC (USNO).

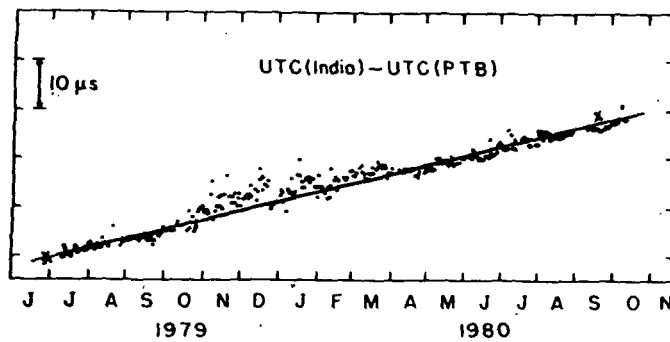


Fig.7 UTC (India)- UTC (PTB). The two crosses shown- on 29 June'79 represents the satellite time transfer and on 20 Sept'80 represents the portable clock check.

PRECISE T & F INTERCOMPARISON BETWEEN NPL, INDIA
AND PTB, FEDERAL REPUBLIC OF GERMANY
VIA SATELLITE SYMPHONIE-1

B.S.Mathur, P.Banerjee, P.C.Sood, Mithlesh Saxena,
Nand Kumar and A.K.Suri
Time and Frequency Section
National Physical Laboratory, Hillside Road,
New Delhi-110012, India.

ABSTRACT

In this paper we report a T & F intercomparison experiment between the National Physical Laboratory (NPL), New Delhi, India and Physikalisch-Technische Bundesanstalt (PTB), Federal Republic of Germany, carried out from May 16 to June 29, 1979. The participating earth stations were New Delhi, India and Raisting, FRG. The NPL clock was placed at New Delhi Earth Station and the Raisting Clock was calibrated with PTB/Primary standard via LORAN-C and travelling clocks. The random uncertainty of time comparisons, represented by two sample Allan Variance σ (30 seconds), was less than 10 nanoseconds. The relative frequency difference between the NPL and Raisting Clocks, $\Delta_{\text{NPL,RAIS}}$, as measured over the 44 days period was found to be -15.7×10^{-13} . The relative frequency difference between PTB Primary Standard and Raisting Clock, $\Delta_{\text{PTB,RAIS}}$, during this period, was measured to be -22.8×10^{-13} . The relative frequency difference between NPL clock and PTB Primary Standard, $\Delta_{\text{NPL,PTB}}$, thus, is $+7.1 \times 10^{-13}$.

The clock rate (UTC, India) evaluated in the present work as $+7.1 \pm 0.5 \times 10^{-13}$, agrees very well with that obtained via VLF phase measurements over one year period described in a companion paper and with USNO travelling clock time comparisons made in September, 1980.

INTRODUCTION

The French-German Satellite Symphonie-1 was made available for Indian Telecommunication experiments from June 1977 to June 1979. It was parked over the equator at 49°E longitude. This group has earlier^(1,2), in 10th and 11th PTTI Meetings, reported Clock Synchronisation and Time Dissemination Experiments in India by means of satellite Symphonie. In this paper we report a simultaneous two way mode time and frequency comparison experiment⁽³⁾ by means of satellite symphonie between the atomic clocks at the National Physical Laboratory (NPL), New Delhi and the time scale of Physikalisch-Teschnische Bundesantalt (PTB), Federal Republic of Germany. This experiment was performed over a 44 days period, from May 16 to 23 and then again from June 28 to 29, 1979. The main objectives were: to synchronise UTC (NPL) to that of UTC (PTB) and to find out the relative frequency difference of NPL clocks, $S_{\text{NPL,PTB}}$, with respect of PTB Primary Standard.

The earth stations which participated in the experiments were New Delhi earth station (DES) where one of the NPL cesium clocks, oscilloquartz Model 3200, hence forth called NPL-1, was kept and the Raisting earth station (RES). The other cesium clock at NPL, HP Model 5061A with option 004 hence forth called NPL-2 which participated in the experiments and was at a different location was intercompared with NPL-1 by regular rubidium clock transportations. The Cesium clock at Raisting earth station (HP Model 5061A with option 004) was calibrated with PTB, Primary Standard via LORAN-C and travelling clocks.

The theory and the measurement uncertainties of a simultaneous two way mode time transfer are well known⁽⁴⁾ and will not be described. Only the experimental details and the results will be discussed.

DETAILS OF THE EXPERIMENTAL SET UP AT DES

The experimental set up at NPL is shown in Fig.1. It is similar to the one used by Hubner and Hetzel⁽⁵⁾ for time comparisons performed by means of the satellite Symphonie between Raisting (FRG) and Pleumeur-Bodou (France). The 1 PPS pulse from NPL-1 was placed on TV synch pulse as the picture signal (wave form of the signal shown in Fig.1). To have identical signal pattern throughout the duration of

the experiment a perfect phase and frequency synchronisation between 1 PPS of Cs clock and TV sync pulse is required. To achieve this, frequency of TV synch pulse generator was locked to that of Cs clock and a definite phase relation with 1 PPS of Cs clock was maintained.

As is clear from Fig.1 the 1 PPS of NPL Cs clock was directly fed to "START" port of the time interval counter and the signal was received from Raisting (Similar type of pulse as shown in Fig.1) was directly used to "STOP" the time interval counter.

Initially the data was taken once every second with a time interval counter (HP 5248 L/M) of 10 nanoseconds resolution as it could be interfaced with the available printer (HP 5050B). Later, in view of the better measurement uncertainties, a counter (HP 5345A) with 2 nanoseconds resolution was used and the data was taken once every 30 seconds. The counter used at Raisting had a 1 nanosecond resolution.

RESULTS

Fig.2 shows a 30 minutes section of measurement values, as obtained once every 30 seconds in New Delhi and Raisting. The data was taken once every 30 seconds for about an hour on each day. In Fig.2 the satellite motion has been eliminated by plotting first difference and only the deviations from the straight line have been shown.

The random uncertainty for the upper curve, which is the half difference of the measured values at New Delhi and Raisting is ± 4 nanoseconds. The mean half difference of the measured values at New Delhi and Raisting along with standard deviation and Allan Variance ($\tau = 30$ seconds) are given in Table 1. Typical values of random uncertainties are in the range of ± 3 to ± 10 nanoseconds. In two cases, values of even about ± 70 nanoseconds were found. The reasons for this large uncertainty could not be ascertained.

The NPL-1, which was used in direct measurements with Raisting, experienced a phase angle shift during the two sets of data in May and June and a phase shift correction of 564 ns with an estimated uncertainty of 20 ns, based on the relative frequency difference of two NPL cesium clocks, SNPL-1, NPL-2, was applied to the second set data of June. SNPL-1, NPL-2, measured by regular rubidium clock transportations during the experiment was found to be 22 ns/day, with NPL-2 running faster than NPL-1.

The daily mean half difference of the measured values at New Delhi and Raisting T (NPL-1 -Raisting) are plotted in Fig.3. The slope of this curve gives the relative frequency difference between NPL-1 and Raisting clock, $\Delta_{\text{NPL,RAIS}}$, as measured over the 44 days period. The value in this case is found to be $-15.7 \pm 0.4 \times 10^{-13}$. In Fig.3 an expanded view of first set of data is shown. The uncertainty shown is the uncertainty of the slope of inclination of the regression line through the two sets of data points. The time comparisons T(Raisting-UTC,PTB) between Raisting clock and PTB primary standard during the above measurement period is plotted in Fig.4. The slope of the curve gives the relative frequency difference $\Delta_{\text{PTB,RAIS}}$. The data for this curve was made available through the courtesy of PTB and is tabulated in Table 2. Points on Fig.4 represent measurements via LORAN-C and points with circle represent measurements via travelling clock. $\Delta_{\text{PTB,RAIS}}$ from Fig.4 is found to be $-22.8 \pm 0.3 \times 10^{-13}$. From Figs. 3 and 4 the relative frequency difference between NPL clock and PTB primary standard $\Delta_{\text{NPL,PTB}}$ ($\Delta_{\text{NPL,RAIS}} - \Delta_{\text{PTB,RAIS}}$), thus, is $+ 7.1 \pm 0.5 \times 10^{-13}$.

CONCLUSIONS

The time comparison made with U.S. Naval Observatory travelling Clock brought to New Delhi in September 1980 agreed with the initial NPL-1 clock setting with respect to PTB to within a small fraction of a microsecond and with the NPL-PTB relative frequency difference, $\Delta_{\text{NPL,PTB}}$, of $+ 7.1 \times 10^{-13}$ to within few parts in 10^{-14} , with those measured by means of satellite symphonie.

Similarly, $\Delta_{\text{NPL,PTB}}$ reported in this paper is in good agreement with the relative frequency difference $\Delta_{\text{NPL,PTB}}$ $7.0 \pm 0.1 \times 10^{-13}$ evaluated from VLF phase measurements over one year period and described in a companion paper.

With this paper we conclude a series of time transfer and time comparison experiments by means of satellite symphonie which were initiated in April 1978 and were reported in tenth and eleventh PTTI Meetings. The future plans on time dissemination via satellites include some more experiments with Indian experimental satellite APPLE (to be launched in mid 1981), a time dissemination service via operational Indian domestic satellite INSAT to be launched in late 1981, involvement in IASSO/SIRIO-2 experiments and possibilities of international time comparisons via some common view satellites.

The intercalibrations between PTB and Raisting clocks were made via LORAN-C and travelling clocks. Four time comparisons were made during this period via travelling clocks with an estimated uncertainty of ± 50 ns. The LORAN-C measurements were more uncertain than these.

A basic limitation, contributing maximum uncertainty, of a two-way time transfer via satellite is the precise measurement of individual path delay of transmitter and receiver. At New Delhi no attempts were made to measure individual path delay of transmitter and receiver. Only combined loop delay consisting of transmitter, test loop translator (a replica of transponder on satellite) and receiver was measured. This gave a value of 1900 ± 10 nanoseconds. PTB has communicated separate measurements on path delay of transmitter and receiver at Raisting earth station. These, including filter delays, are :

Transmitter (Raisting) :	956 ns
Receiver (Raisting) :	954 ns
Total	<hr/> :1910 ns

It may be seen that total path delays encountered at New Delhi and Raisting are same with transmitter and receiver contributing half of the total delay.

A clock transport between NPL and PTB during the experiment was not possible for financial reasons and the uncertainty of time comparisons could not be ascertained. However, based on equality of path delays at Raisting and New Delhi, with transmitter and receiver delay being almost equal, one could infer 100 nanoseconds as the upper limit for accuracy uncertainty of time comparisons. These include time transfer uncertainty between PTB and Raisting (~ 50 ns), time transfer uncertainty between NPL-1 and NPL-2 (~ 20 ns) and uncertainty in path delays (~ 100 ns).

The Relativistic Correction⁽⁶⁾ due to earth's rotation for the NPL-PTB time comparison experiment is calculated to be $+ 179.5$ ns. This value should be added to column 3 (mean value) of Table 1 to get the true value for the time difference between Raisting and NPL. It is a significant contribution in view of the precision of less than 10 ns achieved in the experiment. However, in absence of travelling clock time comparison, this could not be verified.

ACKNOWLEDGEMENTS

First of all we will like to thank Prof.G.Becker of Physikalische-Teschnische Bundesanstalt for agreeing to do the experiment and for allowing us to publish the results. We are grateful to Mr.B.Fisher and Dr.P.Hetzel for their help in the successful completion of the experiment and for supplying us the PTB-Raisting data used in this experiment. Without Mr.J.Jahreis at the Raisting earth station and Mr.M.L.Hasiya at New Delhi earth station the experiment was just not possible. We are thankful to other staff members at New Delhi earth station for their most valuable suggestions and to Dr.A.Sen Gupta of NPL for his careful study of the manuscript of this paper and valuable suggestions.

We express our gratitude to STEP Management Board and Symphonie Utilisation Group for their approval and assistance for the experiment.

Finally, it is always a great pleasure to acknowledge the advise and encouragement received from Dr.A.R.Verma, Director, National Physical Laboratory, New Delhi, India.

REFERENCES

1. Somayaajulu, Y.V., Mathur, B.S., Jain, C.L., Banerjee, P., Garg, S.C., Singh, L., Sood, P.C., and Tyagi, T.R., "Clock Synchronisation Experiments in India Using Symphonie Satellite" Proc. Tenth PTTI Meeting, November, 1978.
2. Mathur, B.S., Banerjee, P., Sood, P.C., Saxena, Mithlesh, Nand Kumar, Suri, A.K., Jain, C.L. and Kumar, K., "A Study of Time Dissemination Via Satellite in India" Proc. Eleventh PTTI Meeting, November, 1979.
3. Becker, G., Fisher, B., Hetzel, P., Mathur, B.S., "Time and Frequency Comparisons by means of Symphonie" Paper presented at Seminar on Symphonie held at Berlin in February, 1980.

4. Brunet, M., "Two-way Time Transfers Between National Research Council (Ottawa) and Paris Observatory via The Symphonie Satellite", Paper presented at Seminar on Symphonie held at Berlin in February, 1980.
5. Hubner, U., Hetzel, P., "Zweiweg-Zeitvergleich mit dem Satelliten Symphonie", Kleinheubacher Berichte Vol. 21, pp 459-468, 1978.
6. Mathur, B.S., Saxena, G.M., "Relativistic Correction for the NPL (India) - PTB (West Germany) clock Synchronisation Experiments", Indian Journal of Pure and Applied Physics, Vol.18, No.8, pp. 601-603, 1980 and Private Communication with PTB.

Table 1
TIME COMPARISONS BETWEEN RAISTING'S CLOCK AND
UTC(PTB) VIA LORAN-C AND TRAVELLING CLOCK.

Date	MJD	T(Raisting-UTC (PTB) by clock transportation (us)	T(Raisting-UTC (PTB) via LORAN-C (us)
14.05.79	44007	0,367	
16.05.79	44009		0,060
17.05.79	44010		0,304
18.05.79	44011		0,497
21.05.79	44014		1,092
22.05.79	44015		1,415
23.05.79	44016		1,527
30.05.79	44023		2,955
31.05.79	44024		3,034
01.06.79	44025		3,350
06.06.79	44030	4,113	4,136
07.06.79	44031		4,342
08.06.79	44032		4,709
09.06.79	44033		4,752
13.06.79	44042		6,519
19.06.79	44043		6,680
20.06.79	44044		6,903
21.06.79	44045		7,153
28.06.79	44052		8,469
29.06.79	44053	8,705	8,730

Table 2

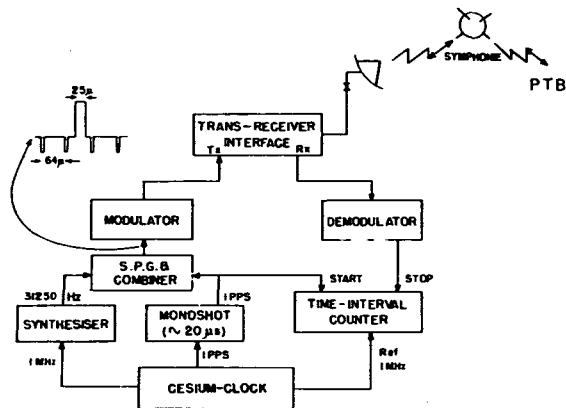
TIME COMPARISONS, STANDARD DEVIATION AND
ALLAN VARIANCE BETWEEN RAISTING'S CLOCK
AND NPL-1 VIA SATELLITE SYMPHONIE

Date	MJD	Mean Value	Standard Deviation	Allan Variance = 30 Sec.
		* **		***
May 16'79	44009	- 6.0 ns	20.2 ns	4.4 ns
May 17'79	44010	+104.7ns	10.96 ns	10.6 ns
May 18'79	44011	+263.7ns	7.92 ns	10.3 ns
May 21'79	44014	+698.8ns	4.24 ns	3.8 ns
May 22'79	44015	+746.9ns	62.52 ns	65.1 ns
May 23'79	44016	+951.5ns	7.91 ns	2.8 ns
June 28'79	44052	+5067.0 ns	88.4 ns	60.5 ns
June 29'79	44053	+5401.2 ns	8.5 ns	4.78ns

* Positive sign indicates Raistings 1 PPS coming earlier than NPL 1 PPS.

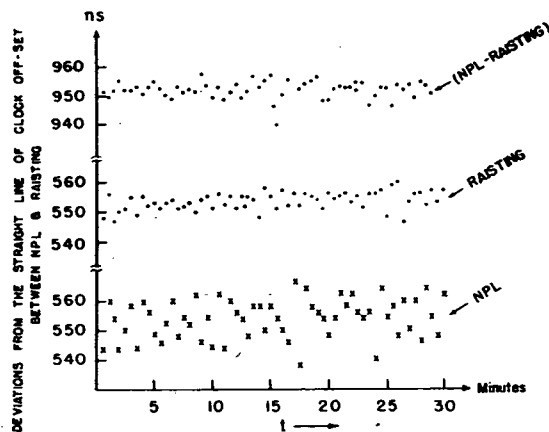
** NPL Time was off by 436.2943 us and was set after the experiment on May 16'79.

*** For limited number of observations.



EXPERIMENTAL SET-UP OF NPL-PTB CLOCK SYNCHRONISATION
EXPERIMENT (MAY-JUNE, 1979)

S.P.G. = Synch pulse generator
Fig. 1



NPL-PTB CLOCK SYNCHRONISATION EXPERIMENT MAY-JUNE, 1979.

Fig.2 : Deviations from the straight line of
Clock off-set between NPL and Raisting.

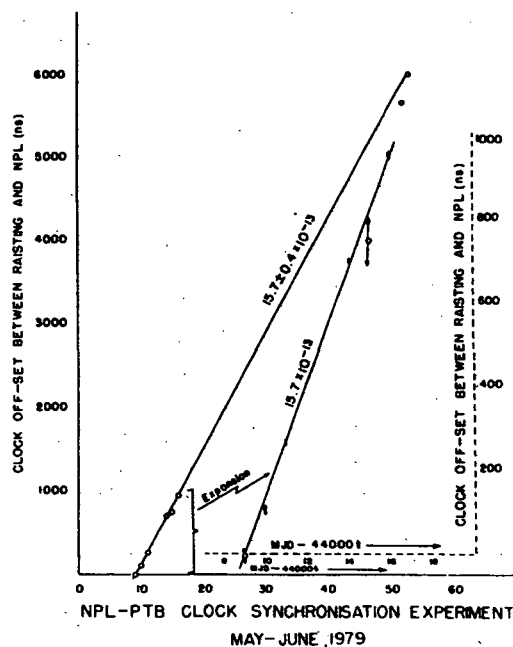


Fig.3 : Clock off-set between NPL and Raisting (SNPL,RAIS).

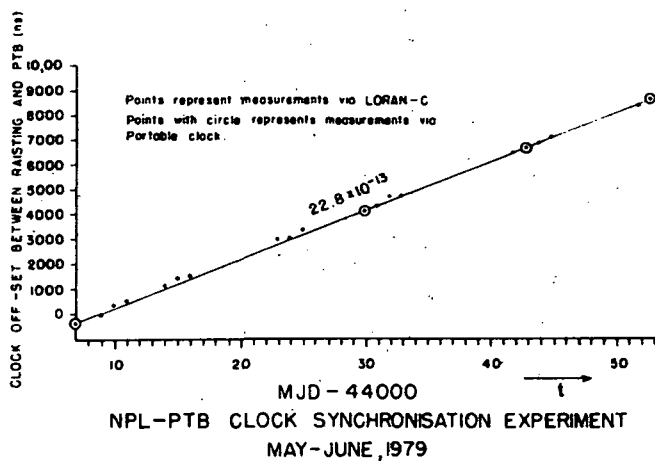


Fig. 4: Clock off-set between PTB and Raisting (SPTB,RAIS)..

S.No.	Date	Mean Jullian Day MJD	Mean Value	Standard Deviation	Allan Variance $\tau = 30$ Sec.
1.	MAY 16'79	44009	* -6.0 ns	20.2 ns	* * *
2.	MAY 17'79	44010	+104.7 ns	10.96 ns	10.6 ns
3.	MAY 18'79	44011	+263.7 ns	7.92 ns	10.3 ns
4.	MAY 21'79	44014	+698.8 ns	4.24 ns	3.8 ns
5.	MAY 22'79	44015	+746.9 ns	62.52 ns	65.1 ns
6.	MAY 23'79	44016	+951.5 ns	7.91 ns	2.8 ns
7.	JUNE 28'79	44052	+5067.0 ns	88.4 ns	60.5 ns
8.	JUNE 29'79	44053	+5401.2 ns	8.5 ns	4.78 ns

* Positive sign indicates Raistings lpps coming earlier than NPL lpps.

* * NPL Time was off by 436.2943 μ s and was set after
the experiment on May 16'79.

* * * For limited number of observations.

Figure 5. NPL (New Delhi)--PTB (West Germany) Clock Synchronization Experiments via Satellite Symphony-I

12TH ANNUAL PRECISE TIME AND TIME INTERVAL
REGISTRATION

William A. Adams
NASA
4814 Nantucket Rd.
College Park, MD 20740

David W. Allan
NBS
325 Broadway
Boulder, CO 80303

Ralph T. Allen
NAVELEX
Code 51022
Washington, DC

Carroll O. Alley
Univ. of Maryland
Dept. of Physics & Astronomy
College Park, MD 20742

Heinz W. Badura
Efratom California Inc.
18851 Bardeen Ave.
Irvine, CA 92715

Frederick J. Bailey III
U.S. Air Force/ESMC/RSL
R.R. 3, Box 613
Merritt Island, FL 32952

P. Banerjee
National Physical Laboratory
Hillside Rd.
New Delhi, India 110 012

John A. Bangert
Defense Mapping Agency
Attn. GSGC
6500 Brookes Lane
Washington, DC 20315

James F. Barnaba
Newark AFB, Ohio
Newark, Ohio 43055

James A. Barnes
National Bureau of Standards
Boulder, CO 80302

Charles A. Bartholomew
NRL
Code 7960
Washington, DC 20375

John C. Bear
General Dynamics - Pomona Division
1675 West Mission Boulevard
Pomona, CA 91766

Christian J. Beauvy
C.E.P.E.
101 Rue du President Roosevelt
Sartrouville, France 78500

Roger E. Beehler
National Bureau of Standards
325 Broadway
Boulder, CO 80303

Henry M. Beisner
IBM
18100 Frederick Pike
Gaithersburg, MD 20760

Henri-Claude Berard
C.E.P.E.
101 Rue du President Roosevelt
Sartrouville, France 78500

Alex Bezat
Honeywell
1625 Zarthan Ave.
Minneapolis, MN

Eric L. Blomberg
KERNCO
28 Harbor St.
Danvers, MA 01923

Jack C. Bowerman
NAVELEX
Code 46014
Washington, DC 20360

James R. Bowser
VITRO Laboratories Division
Automation Industries, Inc.
14000 Georgia Ave.
Silver Spring, MD 20910

William R. Brookes
Dept. Energy Mines & Resources
13 Wedgewood CRES
Ottawa, Ontario, Canada K1B 4B5

Thomas O. Brooks
JPL
4800 Oak Grove Drive
Pasadena, CA 91103

Ellis H. Bryant, Jr.
The Weatherchron Company
4881 Powers Ferry Rd., N. W.
Atlanta, GA 30327

James A. Buisson
Naval Research Lab
Washington, DC 20375

Giovanni Busca
ASULAB
6 Max Meuron
Neuchatel, Switzerland

Robert W. Camp
CINOX
4914 Gray Rd.
Cincinnati, OH 45232

Richard J. Carlson
Communications Security Est.
Dept. National Defence
101 Colonel By Drive
Ottawa, Ontario, Canada K1A 0K2

Roy E. Cashion
S.N., Inc.
621 Lostrand Ln.
Rockville, MD 20760

L. Charron
U.S. Naval Observatory
Washington, DC 20390

Andrew R. Chi
GSFC
Code 810
Greenbelt, MD 20771

R. Clarke
U.S. Naval Observatory
Washington, DC 20390

Robert J. Coates
GSFC
Code 904
Greenbelt, MD 20771

Richard C. Coffin
Jet Propulsion Lab
4800 Oak Grove Dr.
Pasadena, CA 91214

Maurice J. Coileman
DMAHTC
6500 Brooks Ln.
Washington, DC 20315

Jimmie B. Collie
NESEC Portsmouth
Naval Observatory
34th & Mass. Ave., N.W.
Washington, DC 20390

Richard C. Collum
ISOTEMP Research, Inc.
916 Preston Ave.
Charlottesville, VA 22901

Michael A. V. Cruz
Navy Primary Standards Laboratory
NARF North Island
San Diego, CA 92135

Henry W. Czubak
U.S. Army Satellite
Communications Agency
Fort Monmouth, NJ 07703

Peter R. Dachel
BFEL
Rt. 108
Columbia, MD 21045

Fredrick Danzy
NRL
4555 Overlook Ave., S. W.
Washington, DC 20375

Charles L. Daves, Jr.
Hughes Aircraft Company
P.O. Box N
Aurora, CO 80041

Walter N. Dean
Verdes Engineering Co.
26619 Shorewood Rd.
Rancho Palos Verdes, CA 90274

Rudolf Decher
NASA-MSFC
Huntsville, AL 35812

B. Louis Decker
DMA Aerospace Center
402 Devon Court
Ballwin, MO 63011

Bearl F. Dennison
Hughes Aircraft Coi.
P.O. Box N
Aurora, CO 80041

Lawrence Doepke
DMAAC
9418 Oakwood Manor
St. Louis, MO 63126

Robert W. Donaldson
Westinghouse Electric Corp.
P.O. Box 1897, MS935
Baltimore, MD 21203

Bill J. Duncan
NASA-MSFC
Rt. 7
Fayetteville, TN 37334

Peter J. Dunn
EALA WASC
6807 Kenilworth Ave.
Riverdale, MD

Reginald J. Dunn
Office of Naval Attache
Embassy of Australia
1601 Massachusetts Ave.
Washington, DC 20036

Mary S. Ealum
Defense Mapping Agency
Aerospace Center
7014 Christopher Dr.
St. Louis, MO 63129

Richard L. Ealum
7014 Christopher Dr.
St. Louis, MO 63129

Warren E. Edwall
RCA 1901 North Moore St.
Arlington, VA 22209

Richard A. Eichinger
Bendix
9250 Route 108
Columbia, MD

James H. Ewing
Gawer-Knoop Co.
9209 Wendell St.
Silver Spring, MD 20901

Patrick J. Fell
NSWC
Code K-12
Dahlgren, VA 22448

Theodore D. Finsod
Navy Astronautics Group
SPM 3324
Point Mugu, CA 93042

George T. Fouratt
I.T.T.
VAFB P.O. Box 1886
CA 93437

Charles H. Fourtner
Bendix Field Eng.
Jet Propulsion Lab
551 Agnes Dr.
Barstow, CA 92311

Hugo Fruehauf
Efratom California, Inc.
18851 Bardeen Ave.
Irvine, CA 92715

Larry M. Galloway
AGMC Newark AFS
Newark, OH 43055

Davis R. Gamble, Jr.
Defense Communications
Engineering Center
1860 Wiehle Ave.
Reston, VA 22090

Virgil F. Gardner
NASA/GSFC
1109 Montrose Ave.
Laurel, MD 20810

Michel P. Geesen
Electronique Marcel Dassault
55 Quai Carnot
St. Cloud, France 92214

Robert M. Glasmeier
Aerospace Guidance and
Meteorology Center
Newark AF Station MLTS
Newark, OH 43055

Seymour Goldberg
EG&G, Inc.
35 Congress St.
Salem, MA 01970

Richard L. Greenspan
C.S. Draper Lab, Inc.
555 Technology Square
Cambridge, MA 02139

R. G. Hall
U.S. Naval Observatory
Washington, DC 20390

Tadayoshi Hara
International Latitude
Observatory of Mizusawa
Mizusawa-shi, Iwate-Ken, 023, Japan

Samuel N. Harmatuk
1575 Odell St.
Bronx, NY 10462

Daniel J. Healey, III
Westinghouse Electric Corp.
P.O. Box 746
Baltimore, MD 21203

Marlyn L. Hed
TRW-DSSG
One Space Park S/534
Redondo Beach, CA 90278

Helmut Hellwig
Frequency and Time Systems, Inc.
34 Tozer Rd.
Beverly, MA 01915

Robert J. Hesselberth
Spectracom Corp
320 N. Washington St.
Rochester, NY 14625

Henry R. Heuerman
Defense Mapping Agency
Hydrographic Topographic Ctr.
1500 Brookes Ln.
Washington, DC 20315

Raymond J. Hibbs
NASA-GSFC Code 814
Greenbelt, MD 20771

Norman Houlding
MITRE Corp.
P.O. Box 208
Bedford, MA 01730

David A. Howe
NBS
2145 Goddard Pl.
Boulder, CO 80303

Edward A. Imbier
Smithsonian Institution
60 Garden St.
Cambridge, MA 02138

Harold W. Jackson
Bendix Corporation
1300 E. Joppa Rd.
Baltimore, Md. 21204

Peter S. Jaworski
U.S. Army Satellite
Communications Agency
11 Irma Pl.
Oceanport, NJ 07757

Alain R. Jendly
Oscilloquartz SA
16 Brevards
Neuchatel, Switzerland

Charles J. Jensik
DIEZO Crystal co.
100 K St.
Carlisle, PA 17013

A. Johnson
U.S. Naval Observatory
Washington, DC 20390

Donald E. Johnson
BFEC Jet Propulsion Laboratory
Oak Grove Dr.
Pasadena, CA 91010

W. Klepczynski
U.S. Naval Observatory
Washington, DC 20390

Peter Kartaschoff
Swiss Post Office
R. & D. Division
Technical Center
Bern, Switzerland CH 3029

William w. Kellogg
Lockheed Missiles and Space Company
Building 154
Sunnyvale, CA 94088

Robert H. Kern
KERNCO, Inc.
28 Harbor St.
Danvers, MA 01923

Henry I. Kin
1842 EEG/EETSA
Scott AFB, IL 62225

Frank K. Koide
Rockwell International
3370 Miraloma Ave.
Mail Code HC02
Anaheim, CA 92803

Robert M. Kovacs
KENTRON Int., Inc.
P.O. Box 1207
APO San Francisco, CA 96555

Paul F. Kuhnle
Jet Propulsion Laboratory
4800 Oak Grove Dr.
Pasadena, CA 91103

Algie L. Lance
TRW-DSSG
One Space Park
Redondo Beach, CA 90278

J. M. Landers
Data Time, Inc.
12600 Viewside Dr.
Gaithersburg, Md. 20760

Eric L. Lasley
General Dynamics
2017 Pintosco Court
Carlsbad, CA 92008

Jean-Daniel Lavanceau
LT International, Inc.
4907 Asbury Ln.
Bethesda, MD 20014

David Lerner, Engineer
Current Designs Corporation
210 East 86 St.
New York, NY 10028

Sigfrido M. Leschiutta
Istituto Elettrotecnico Nazionale
91 Strada Delle Caccie
Torino, Italy 10135

Vestal R. Lester
Hughes Aircraft Co.
19631 Strathern St.
Reseda, CA 91335

Martin W. Levine
Frequency & Time Systems, Inc.
34 Tozer Rd.
Beverly, MA 01915

Dean L. Lindstrom
Hughes Aircraft Co.
P.O. Box 92919
Los Angeles, CA 90009

C. Lukae
U.S. Naval Observatory
Washington, DC 20390

George F. Lutes
Jet Propulsion Laboratory, 238/420
4800 Oak Grove Dr.
Pasadena, CA 91103

John V. LuValle
Jet Propulsion Laboratory
4800 Oak Grove
Pasadena, CA 91103

Donald W. Lynch
NRL Code 7960
Washington, DC 20375

George A. Madrid
Jet Propulsion Lab
4800 Oak Grove
Pasadena, CA 91103

George J. Maki
1417 Pacific Ave.
Santa Barbara, CA 93109

John C. Mankins
JPL/Bendix Field Engineering
4800 Oak Grove Dr.
Pasadena, CA 91103

Thomas B. McCaskill
NRL Code 7966
4555 Overlook Ave., SW
Washington, DC 20375

Raullo J. McConahy
Applied Physics Lab/
Johns Hopkins Univ.
Johns Hopkins Rd.
Laurel, MD 20810

Arthur O. McCoubrey
National Bureau of Standards
Gaithersburg, MD 20760

John S. McNabb
TRAK Systems
4722 Eisenhower Blvd.
Tampa, FL 33614

John E. McKeever
U.S. Coast Guard Hdqs.
G-EEE-4/TP64
2100 2nd St., S.W.
Washington, DC

Marvin Meirs
Frequency Electronics, Inc.
3 Delaware Dr.
New Hyde Park, NY 11040

Edwin E. Mengel
Johns Hopkins Applied Physics Lab
Johns Hopkins Rd.
Laurel, Md. 20810

Richard E. Miller
MOXON, Inc.
2222 Mickelson Dr.
Irvine, CA 92715

Gills Missouri
HYDRO Quebec
1800 Montee Ste. Julie
Varenes PQ Canada JOL2PC

Donald H. Mitchell
KENTRON International, Inc.
Yuma Proving Grounds
P.O. Box 4819
Yuma, AZ 85364

Billy B. Moon
U.S. Air Force, PTTI Training
17124 E. Brown Circle
Aurora, CO 80013

Derek Morris
Physics Division
National Research Council
Montreal Rd.
Ottawa, Ontario Canada K1A 0R6

Ivan I. Mueller
Ohio State University
Dept. of Geodetic Science
1958 Neil Ave.
Columbus, OH 43210

Francis H. Mullen
Frequency & Time Systems, Inc.
34 Tozer Rd.
Beverly, MA 01915

Leonardo L. Mureddu
Stazione Astronomica
Internazionale Di Latitudine
72 Via Ospedale
Cagliari, Italy 09100

James A. Murray
Naval Research Lab.
Code 7962
Washington, DC 20375

James P. Murphy
NASA Headquarters
Washington, DC 20546

Joseph Murphy
Westinghouse Elec.
1013 Beulah Rd.
Pittsburgh, PA 15235

Robert Naber
Navy Astronautics Group
Code SPM213
Point Mugu, CA 93042

Frank J. Narr
VITRO Laboratories
14000 Georgia Ave.
Silver Spring, MD 20910

Lawrence W. Nelson
General Electric
901 Broad St.
Utica, NY 13323

Klemens Nottarp
Institut Fur Angewandte Geodasie
Satellitenbeobachtung
Station Wettzell
D-8493 Kotzting
F.R. Germany

Orville Jay Oaks, Jr.
Naval Research Lab
4555 Overlook Ave., S.W.
Washington, DC 20375

John T. O'Hara
Marktron, Inc.
57 W. Timonium Rd.
Timonium, MD 21093

George W. Oja
Navy Metrology Engineering Center
P.O. Box 2436
Pomona, CA 91769

William W. Orr
BURTEK, Inc.
221 S. 85th E. Ave.
Tulsa, OK 74112

Terry N. Osterdock
Hewlett Packard Co.
5301 Stevens Creek Blvd.
Santa Clara, CA 95050

Eugene J. O'Sullivan
MITRE Corporation
P.O. Box 208
Bedford, MA 01730

Xiaspli Pan
Shaanxi Astronomical Observatory
P.O. Box 18, Lintong, Xian,
Shaanxi Province
People's Republic of China

Ken Putkovich
U.S. Naval Observatory
Washington, DC 20390

James A. Pearson
The Aerospace Corporation
P.O. Box 92957
Los Angeles, CA 90009

Harry E. Peters
Sigma Tau Standards Corporation
Box 1877, 1014 Huckabee Ln.
Tuscaloosa, AL 35403

H. E. Petrey
Def. Map. Agy.
6424 No. 54 Ave.
St. Petersburg, FL 33709

Edward A. Pettit
Eastern Space & Missile Center
Range Systems Management
U.S. Air Force
Patrick Air Force Base, FL 32925

David H. Phillips
NRL Code 7526
Washington, DC 20375

Alvin B. Plaughter
NASA-GSFC
GSFC Bldg. 12, Room H106
Greenbelt, MD 20705

James W. Porter
AUSTRON, Inc.
1915 Kramer Ln.
Austin, TX 78758

H. R. Potts
Bendix Field Eng. Co.
9250 Rt. 108
Columbia, MD 21227

George E. Price
AUSTRON, Inc.
1915 Kramer Ln.
Austin, TX 78758

Gerard L. Punt
Interstate Electronics
707 E. Vermont Ave.
Anaheim, CA 92803

Eduardo J. Ramon
Observatorio Naval (Argentina)
2099 Espana
Buenos Aires, Argentina 1107

James R. Ransom
Westinghouse Electric Co.
107 E. Susquehanna Ave.
Towson, MD 21204

Victor S. Reinhardt
NASA
GSFC, Code 814
Greenbelt, MD 20771

William J. Riley
EG&G, Inc.
35 Congress St.
Salem, MA 01970

Ronald C. Roloff
Bendix
81005 McKenstry Dr.
Laurel, MD 20810

Michael W. Rowan
MITRE Corp.
Batterey Humphrey
San Diego, CA 92153

Lauren J. Rueger
Applied Physics Laboratory
Johns Hopkins University
Johns Hopkins Rd.
Laurel, MD 20810

David C. Sayers
Lockheed Missiles & Space Company
P.O. Box 6429 NSBS Bangor
Bremerton, WS 98315

Wolfgang Schulter
Institut Fur Angewandte Geodasie
G. Weinbergstrasse
Frankfurt/M-Sindlingen
F.R. Germany D6230

David C. Scull
U.S. Coast Guard OMEGA
2112 Wittington Bl.
Alexandria, Va. 22308

Malvin C. Schwalje
Frequency & Time Systems, Inc.
34 Tozer Rd.
Beverly, MA 01915

Gunter Seeber, Professor
Theoretische Geodasie
Univ. Hannover
G. Nienburgerstrasse
Hannover, F.R. Germany D-3000

Hermann Seeger, Professor
Geodatisches Institut
Univ. Bonn
17, Nussallee
Bonn, F.R. Germany D-5400

Bernard Serene
European Space Agency
18 Ave E. Belin
31055 Toulouse, Cedex

David B. Shaffer
Phoenix Corp.
C/O Code 945 NASA/GSFC
Greenbelt, MD 21401

Leonard F. Shepard
Time System Technology, Inc.
52 Morris Ave.
Lake Grove, NY 11755

Alexander Skopetz
NASA/GSFC
11911 Galaxy Ln
Bowie, MD 20715

James A. Slater
Defense Mapping Agency
6500 Brookes Ln.
Washington, DC

Arthur E. Smith
Code 3412.3
DATA Collection Div.
Range Inst. System Dept.
Pt. Mugu, CA 93042

William E. Smith
Efratom California, Inc.
18851 Bardeen Ave.
Irvine, CA 92715

Frade Victorio Souza
Naval Observatory Argentina
2099 Espana Av.
Buenos Aires, Argentina 1107

Gary L. Spradlin
JPL
4800 Oak Grove Dr.
Pasadena, CA 91003

Robert B. Stitt
EG&G, Inc.
35 Congress St.
Salem, MA 01970

P. Schumacher
Observatoire De Neuchatel
58 Rue De L'Observatoire
Neuchatel C.H.-2000 Switzerland

Charles S. Stone
Brightline Corporation
P.O. Box 1016
Cedar Park, TX 78613

Harris A. Stover
DCEC
1860 Wiehle Ave.
Reston, VA 22090

John T. Strain
Frequency Electronics
Suite 210, 13975 Conn. Ave.
Silver Spring, Md. 20906

Edmund P. Sullivan
EG&G, Inc.
35 Congress St.
Salem, MA 01970

Richard L. Sydnor
Jet Propulsion Lab
4800 Oak Grove Dr.
Pasadena, CA 91109

Arthur C. Taber
S.F. State University
560 Rockdale Drive
San Francisco, CA 94127

Philip E. Talley
The Aerospace Corp.
550 Margo Avenue
Long Beach, CA 90803

Douglas M. Tennant
USAF/Space Division
13020 Kornblum #11
Hawthorne, CA 90250

Harold L. Theiss
NASA Headquarters
Washington, DC

Mr. J. W. Tomlin
Hughes Aircraft Company
Space and Communications Group
P.O. Box 92919 - Airport Station
Los Angeles, CA 90009

Jimmie L. Toms
Austron Navigation, Inc.
1800 Old Meadow Road, Suite 102
McLean, VA 22102

Glen E. Treankler
U.S. Air Force
2400 El Segundo Boulevard
El Segundo, CA 90007

James E. Trimm
Dynalectron Corporation
P.O. Drawer R
Holloman AFB, NM 88330

Emanuel Tward
JPL
4800 Oak Grove Drive
Pasadena, CA 91103

Kenneth M. Uglow
P.O. Box 2260
Sarasota, FL 33578

John L. VanGroos
True Time Instruments
3243 Santa Rosa Avenue
Santa Rosa, CA

Petr Vanicek
University of New Brunswick
Department of Surveying, U.N.B.
Fredericton, N.B., Canada E3B 5A3

Robert J. Van Wechel
Interstate Electronics Corp.
1001 E. Ball Road
Anaheim, CA 92803

Jacques Vanier
Electrical Engineering Dept.
Laval University
Quebec, Canada G1K 7P4

Lester B. Veenstra
Comsat Laboratory
22300 Comsat Drive
Clarksburg, MD 20734

Robert F.C. Vessot
Smithsonian Astrophysical Observatory
60 Garden Street
Cambridge, Mass. 02138

John R. Vig
USAERADCOM, ET&D Lab., ATTN: DELET-MQ
Fort Monmouth, New Jersey 07703

Charles H. Volk
Aerospace Corporation
P.O. Box 92957, MS A6-1667
Los Angeles, CA 90009

E. S. Walker
Hughes Aircraft Co.
P.O. Box "N"
Aurora, Colorado 80014

William C. Walker
Pan Am World Airways
Bldg. 989, MU 840
Patrick AFB, Florida 32925

Pekka T. Wallin
Tech. Research Centre of Finland
Electrical Engineering Laboratory
OTAKAARI 5
02150 ESP00 15 Finland

Harry T. M. Wang
Hughes Research Laboratories
3011 Malibu Canyon Road
Malibu, CA 90265

Samuel C. Ward
Caltech Jet Propulsion Laboratory
4800 Oak Grove Drive
Pasadena, CA 91103

S. Clark Wardrip
NASA/GSFC
Code 814.2
Greenbelt, Maryland 20715

David H. Weber
Naval Electronic Systems Command
Washington, D. C.

Robert M. Weigand
The MITRE Corporation
P.O. Box 208
Bedford, Mass. 01730

Joseph D. White
NRL
4555 Overlook Avenue, Code 7962
Washington, D. C. 20375

Fletcher D. Wicker
The Aerospace Corporation
El Segundo Boulevard
El Segundo, CA

Phillip C. Wildhagen
Aerospace Corporation
Box 92957, 120-2210
Los Angeles, CA 90009

Warren L. Wilson
Fairchild Test Systems
707 Spindrift Drive
San Jose, CA 95134

David H. Winfield
IBM
21 Firstfield Road
Gaithersburg, MD 20760

G. Winkler
U.S. Naval Observatory
Washington, DC 20390

Stuart A. Wolf
Naval Research Lab.
Washington, DC 20375

Dr. William H. Wooden
DMAHTC
9950 Cherry Tree Lane
Silver Spring, MD 20901

Raymond F. Woolley
Sperry Systems Management
4700A Boston Way
Lanham, MD 20801

Sien-Chong Wu
Jet Propulsion Laboratory
4800 Oak Grove Drive
Pasadena, CA 91109

Nicholas F. Yannoni
Rome Ai Development Center
Hanscom AFB
Bedford, MA 01731

Shuhua Ye
Shanghai Observatory, Shanghai,
The People's Republic of China
Rm 810 Forum Apt.
11801 Rockville Pike
Rockville, MD 20852

Thomas P. Yunck
JPL 264/738
4800 Oak Grove Drive
Pasadena, CA 91020

Bruce V. Zieminski
TV Audio Support Activity
Sacramento Army Depot
Sacramento, CA 95823

Samuel H. Zingales
The Mitre Corporation
P.O. Box 208
Bedford, MA 01730

BIBLIOGRAPHIC DATA SHEET

1. Report No. CP 2175	2. Government Accession No.	3. Recipient's Catalog No.	
4. Title and Subtitle Proceedings of the Twelfth Annual Precise Time and Time Interval (PTTI) Applications Planning Meeting December 2-4, 1980		5. Report Date March 1981	
		6. Performing Organization Code 814.2	
7. Author(s) Schuyler C. Wardrip, Editor		8. Performing Organization Report No.	
9. Performing Organization Name and Address Goddard Space Flight Center Greenbelt, Md. 20770		10. Work Unit No.	
		11. Contract or Grant No.	
		13. Type of Report and Period Covered	
12. Sponsoring Agency Name and Address Naval Electronics Systems Command NASA Goddard Space Flight Center Naval Observatory		14. Sponsoring Agency Code	
Naval Research Laboratory National Bureau of Standards Defense Communications Agency			
15. Supplementary Notes			
16. Abstract These proceedings contain the papers presented at the Twelfth Annual Precise Time and Time Interval (PTTI) Applications and Planning Meeting, including questions and answers following presentations. The purpose of the meeting was to give PTTI managers, systems engineers, and program planners a transparent view of the state-of-the-art, an opportunity to express needs, a view of important future trends, and a review of relevant past accomplishments; to provide PTTI users with new and useful applications, procedures, and techniques; to allow the PTTI researcher to better assess fruitful directions for research efforts.			
17. Key Words (Selected by Author(s)) Time, Time transfer, Time dissemination, time measurement, Hydrogen masers, masers.		18. Distribution Statement Unclassified Unlimited STAR Category 36	
19. Security Classif. (of this report) Unclassified	20. Security Classif. (of this page) Unclassified	21. No. of Pages to come	22. Price*

WSMC/PMET AFL 2827
TECHNICAL LIBRARY
VANDENBERG AFB, CA 93437

DATE DUE

TK Precise Time and Time
7878.2 Interval (PTTI)
P7 Applications and
1980 Planning Meeting
 (12th: 1980: Green-
 belt, Md.)

OEMCO

U. S. AIR FORCE

National Aeronautics and
Space Administration
Washington, D.C.
20546

Official Business

Penalty for Private Use, \$300

SPECIAL FOURTH CLASS MAIL
BOOK

Postage and Fees Paid
National Aeronautics and
Space Administration
NASA-451



NASA

POSTMASTER: If Undeliverable (Section 158
Postal Manual) Do Not Return
